Synthesis and Reactivity of Heavy Pnictogenyltrielanes stabilized by N-heterocyclic Carbenes

Dissertation

zur Erlangung des

Doktorgrades der Naturwissenschaften

(*Dr. rer. nat.*)

der Fakultät für Chemie und Pharmazie

der Universität Regensburg

vorgelegt von

Robert Szlosek

aus Regensburg

August, 2024

Diese Arbeit wurde angeleitet von Prof. Dr. Manfred Scheer.

Promotionsgesuch eingereicht am: 05. August 2024

Tag der mündlichen Prüfung: 20. September 2024

Vorsitzender: Prof. Dr. Rainer Müller

Prüfungsausschuss: Prof. Dr. Manfred Scheer

Prof. Dr. Nikolaus Korber

Dr. Katja Dettmer-Wilde

Universität Regensburg

Eidesstattliche Erklärung

Ich erkläre hiermit an Eides statt, dass ich die vorliegende Arbeit ohne zulässige Hilfe Dritter und ohne Benutzung anderer als der angegebenen Hilfsmittel angefertigt habe; die aus anderen Quellen direkt oder indirekt übernommenen Daten und Konzepte sind unter Angabe der Literaturzitate gekennzeichnet. Die Arbeit wurde bisher weder im In- noch im Ausland in gleicher oder ähnlicher Form einer anderen Prüfungsbehörde vorgelegt.

_____

Robert Szlosek

To my family:

Sujuan, Ramón, Erich

and my dear Lisa

This thesis was elaborated within the period from April 2020 till August 2024 in the Institute of Inorganic Chemistry at the University of Regensburg under supervision of Prof. Dr. Manfred Scheer.

Parts of this work have already been published or submitted:

(* = Co-First authorship: these authors contributed equally to this work)

R. Szlosek,* M. T. Ackermann,* C. Marquardt, M. Seidl, A. Y. Timoshkin, M. Scheer, *Chem. Eur. J.* **2023**, *29*, e202202911.

R. Szlosek, M. A. K. Weinhart, G. Balázs, M. Seidl, L. Zimmermann, M. Scheer, *Chem. Eur. J.* **2023**, *29*, e202300340.

R. Szlosek, M. Seidl, G. Balázs, M. Scheer, *Chem. Eur. J.* **2023**, *29*, e202301752.

M. T. Ackermann, R. Szlosek, C. Riesinger, M. Seidl, A. Y. Timoshkin, E. Rivard, M. Scheer, *Chem. Eur. J.* **2024**, *30*, e202303680.

R. Szlosek, A. S. Niefanger, G. Balázs, M. Seidl, A. Y. Timoshkin, M. Scheer, *Chem. Eur. J.* **2024**, *30*, e202303603.

R. Szlosek, C. Marquardt, O. Hegen, G. Balázs, C. Riesinger, A. Y. Timoshkin, M. Scheer, *in revision.*

"Do or do not. There is no try."

Master Yoda *– Star Wars Ep. V*

Preface

During the period of this work, several parts have already been published (*vide supra*). These are reproduced in the present document and reprinted each with the permission of the scientific publisher.

The specific author contributions to each topic are listed in a separate section at the end of each chapter which accurately describe the involvement of all given authors to the topics.

To ensure a uniform design of this thesis, the chapter are grouped into “Introduction”, “Results and Discussion”, “Conclusion”, “References”, “Supporting Information” and “Author Contributions”. In each chapter, the same formatting is applied, and the compound enumeration begins anew, though small deviations of the format are present due to different journal requirements or author contributions. A separate chapter concludes all information of each chapter separately at the end of this work.

Table of Contents

1 Introduction 1

1.1 Applications of 13/15 Compounds 1

1.2 Properties and Electronic Structure of molecular 13/15 Compounds 3

1.3 Reactivity of Pnictogenylboranes and heavier Congeners 5

1.4 N-Heterocyclic Carbenes and their Applications 9

1.5 References 11

2 Research Objectives 15

3 Coordination of Pnictogenylboranes towards Tl(I) salts and a Tl-mediated P-P coupling 17 .....

3.1 Introduction 18

3.2 Results and Discussion 19

3.3 Conclusion 27

3.4 References 27

3.5 Supporting Information 29

3.5.1 Experimental Section 29

3.5.2 NMR Data 36

3.5.3 X-ray powder diffraction data 52

3.5.4 Crystallographic Data 53

3.5.5 Computational Data 62

3.5.6 References 71

3.6 Author Contributions 72

4 NHC-stabilized Tripentelyltrielanes 73

4.1 Introduction 74

4.2 Results and Discussion 75

4.3 Conclusion 83

4.4 References 83

4.5 Supporting Information 86

4.5.1 General Information 86

4.5.2 Experimental Details 86

4.5.3 NMR Data 92

4.5.4 Crystallographic Data 105

4.5.5 Computational Data 112

4.5.6 References 120

4.6 Author contributions....121

5 A general Pathway towards NHC·GaH_2(OTf) adducts – The key for the Synthesis of NHC-stabilized cationic 13/15 Chain Compounds of Gallium....123

5.1 Introduction....124

5.2 Results and Discussion....125

5.3 Conclusion....133

5.4 References....133

5.5 Supporting Information....136

5.5.1 General Information....136

5.5.2 Experimental Details....136

5.5.3 NMR Data....144

5.5.4 Crystallographic Data....172

5.5.5 Computational Details....179

5.5.6 References....190

5.6 Author Contributions....191

6 Characterization of the Ligand Properties of Donor stabilized Pentelyltrielanes....193

6.1 Introduction....194

6.2 Results and Discussion....195

6.3 Conclusion....202

6.4 References....203

6.5 Supporting Information....206

6.5.1 General Information....206

6.5.2 Experimental Details....206

6.5.3 NMR Data....219

6.5.4 Crystallographic Data....266

6.5.5 Computational Details....276

6.5.6 References....306

6.6 Author Contributions....306

7 The parent GaH_2SbH_2 monomer stabilized by a N-heterocyclic carbene....307

7.1 Introduction....308

7.2 Results and Discussion....309

7.3 Conclusion....313

7.4 References....313

7.5 Supporting Information....315

7.5.1 General Information ... 315
7.5.2 Experimental Details ... 315
7.5.3 NMR Data ... 319
7.5.4 Crystallographic Data ... 324
7.5.5 Computational Details ... 326
7.5.6 References ... 332
7.6 Author Contributions ... 333
8 Synthesis of Bismuthanyl-substituted monomeric Triel Hydrides ... 335
8.1 Introduction ... 336
8.2 Results and Discussion ... 338
8.3 Conclusion ... 341
8.4 References ... 342
8.5 Supporting Information ... 345
8.5.1 General Information ... 345
8.5.2 Experimental Details ... 345
8.5.3 NMR Data ... 352
8.5.4 Mass spectra ... 364
8.5.5 Crystallographic Data ... 367
8.5.6 Computational Details ... 373
8.5.7 References ... 383
8.6 Author Contributions ... 384
9 NHC-stabilized Mixed Group 13/14/15 Element Hydrides ... 385
9.1 Introduction ... 386
9.2 Results and Discussion ... 387
9.3 Conclusion ... 393
9.4 References ... 394
9.5 Supporting Information ... 396
9.5.1 Experimental section ... 396
9.5.2 NMR data ... 400
9.5.3 Crystallographic data ... 421
9.5.4 Molecular structures ... 423
9.5.5 Computational details ... 426
9.5.6 References ... 441
9.6 Author Contributions ... 442

10 Electrophilic functionalization of Donor stabilized Phosphanylboranes – a new Pathway towards heavy 13/14/15 parent hydride containing Compounds 443

10.1 Introduction.....444

10.2 Results and Discussion.....445

10.3 Conclusion.....450

10.4 References.....450

10.5 Supporting Information.....453

10.5.1 General Information.....453

10.5.2 Experimental Details.....454

10.5.3 NMR Data.....462

10.5.4 Crystallographic Data.....497

10.5.5 References.....505

10.6 Author Contributions.....505

11 Thesis Treasury.....507

11.1 Synthesis and Reactivity of an NHC stabilized Triphosphanylborane.....507

11.2 Deprotonation of parent Phosphanylboranes.....514

11.3 Synthesis of an NHC stabilized Phosphanylborane Au(I) complex.....518

12 Conclusion.....524

12.1 Coordination of Pnictogenylboranes Towards Tl(I) Salts and a Tl-mediated P-P coupling 524

12.2 NHC-Stabilized Parent Tripentelyltrielanes.....525

12.3 A general Pathway towards NHC·GaH_2(OTf) adducts – The key for the Synthesis of NHC-stabilized cationic 13/15 Chain Compounds of Gallium.....526

12.4 Characterization of the Ligand Properties of Donor stabilized Pnictogenyltrielanes.....527

12.5 The parent GaH_2SbH_2 monomer stabilized by a N-heterocyclic carbene.....529

12.6 Synthesis of Bismuthanyl-substituted monomeric Triel Hydrides.....530

12.7 Electrophilic Functionalization of Donor stabilized Phosphanylboranes.....531

13 Appendices.....534

13.1 Alphabetic List of Abbreviations.....534

13.2 Acknowledgements.....538

1 Introduction

1.1 Applications of 13/15 Compounds

The chemistry of compounds made up by elements of groups 13 and 15 has thrived within the last decades. Besides the academic interest in creating new inorganic materials and exploring their properties, the investigations and research in the realm of 13/15 chemistry also emerge from a large interest for industrial applications of these compounds.[1] Most importantly, materials consisting of groups 13 and 15 play a large role in semiconductors (or as still often labelled as III-V semiconductors according to their respective main group numbers). Semiconductors in general are solid state materials, which have the characteristic property of a small band gap between the valence band and the conduction band.[1–4] By thermal excitation, electrons possess enough energy to overcome the band gap, thus the material displays conducting capabilities at elevated temperatures (cf. Figure 1.1).[5] Semiconductors are typically used in electronics, ranging from photovoltaics, sensors to optical devices and many more, with an estimated sales volume of 553 billion USD worldwide.[1]

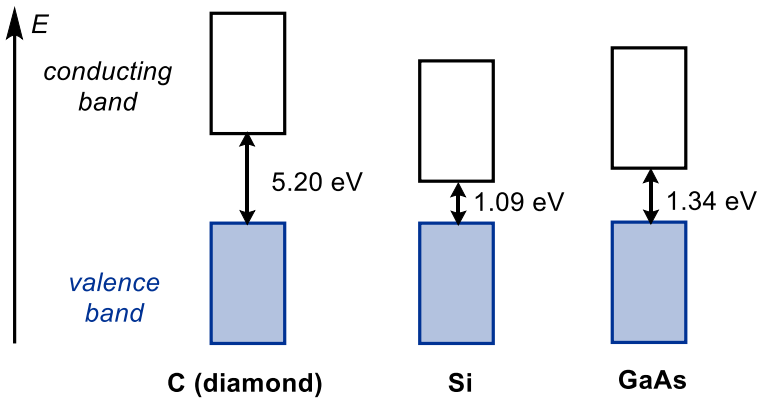

Figure 1.1: Schematic qualitative visualization of band gaps E_G of carbon (diamond), silicon and galliumarsenide.[6,7]

While silicon still plays the most prominent part in semiconductor applications,[1] III-V compounds such as, e.g., GaAs (band gap of E_G = 1.34 eV)[7] have gained more and more attention over the last years. Especially, the mobility of electrons in GaAs is much larger as in silicon and thus making it appealing for fast responding devices.[7,8] Additionally, GaAs is also more interesting for optical devices such as light-emitting diodes (LEDs) due to a fully allowed electronic transition from the valence to the conducting band. The emitted wavelength depends on the band gap energy E_G (equation 1), which is controlled by the stoichiometric composition of the semiconductor material.[4] For $GaAs_{1-x}P_x$, the band gap lies between 2.26 eV (x = 1) to 1.44 eV (x = 0) corresponding to λ_{max} in the range of 550-860 nm.[4]

$$\lambda_{max} = \frac{hc}{E_G} \tag{1}$$

Furthermore, elements of groups 13/15 are important dopants for *n*- or *p*-semiconductors.[8,9] Other important III-V combinations consist of InSb, InAs, InP, GaP, GaSb and AlSb.[10] On the other side, while silicon materials suffer from inferior properties, its abundancy, high stability of its oxides and effective growing of large stable single-crystals by the Czochralski method, it still remains the most important element for semiconductors.[3]

The industrial synthesis of III-V semiconductors relies usually on a process named chemical vapour deposition (CVD).[3,11] During this process, two reactants are brought together at elevated temperatures in the gas phase which deposits the desired material on a cooler surface. When these precursors include organometallic compounds, the process is labelled as metal-organic chemical vapour deposition (MOCVD). An impressive illustration is the preparation of GaAs layers: At 700-900 °C, $GaMe_3$ and AsH_3 are combined which results in the deposition of GaAs layers under release of methane (Scheme 1.1).[3,8,12]

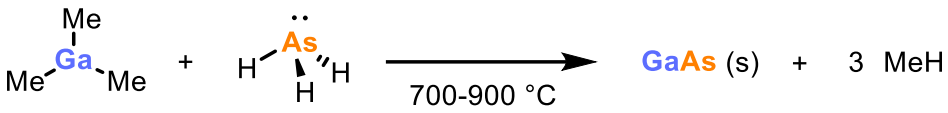

Scheme 1.1: Industrial synthesis of GaAs by MOCVD.

While being very effective, the reactants used in this process are highly volatile, pyrophoric ($GaMe_3$) or extremely toxic (AsH_3). Thus, a demand for other precursors suitable for this process exists. Based on the lability of group 13 donor acceptor adducts,[13] it could be shown that the corresponding amine adducts of group 13 such as, e.g. Quin·GaH_3 (Quin = quinuclidine), can be used as Ga sources just as well.[14] Additionally, an important discovery could be achieved that both elements to be deposited can be bound molecularly in a single CVD precursor (single-source precursor).[15]

Moreover, 13/15 compounds are investigated as potential hydrogen-storage materials.[16–18] With dihydrogen emerging as a green fuel nowadays, the demand for storage has increased accordingly. As an abundant and clean energy carrier, hydrogen fulfils many desirable properties to be used in e.g. fuel cells.[19] The most important methods for hydrogen storage consist of physical ways, sorbents, metal hydrides and main group hydrides.[16,17] In particular, B-N compounds possess a high gravimetric capacity and are of special interest in this field, although the undesirable formation of boron nitrides often hinders reversible dihydrogen binding (cf. Scheme 1.2).[8,16,18] All these applications require a fundamental and thorough understanding of molecular 13/15 chemistry. Especially, the focus lies on preparing and studying the lightweight parent compounds as candidates for CVD or hydrogen-storage materials and examining their structural and electronic properties.

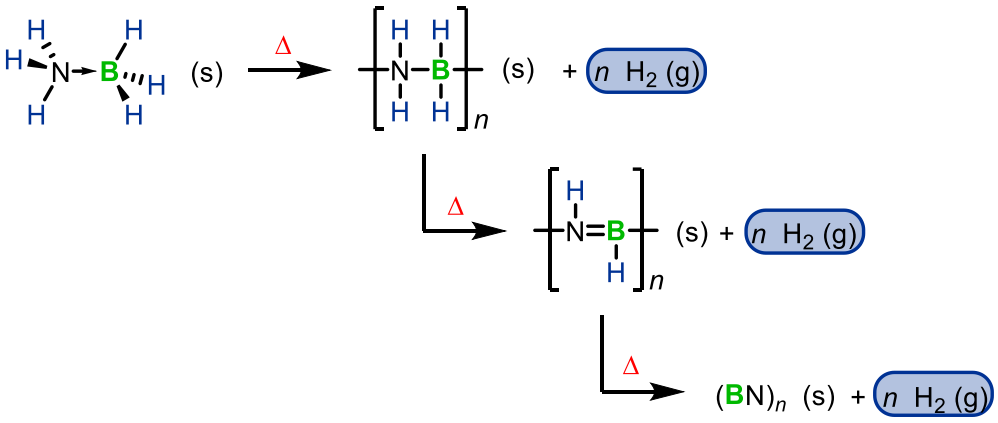

Scheme 1.2: Thermal dehydrogenation steps of $H_3N{\cdot}BH_3$ as an example for hydrogen release of 13/15 parent compounds.

1.2 Properties and Electronic Structure of molecular 13/15 Compounds

The discovery of $H_3N{\cdot}BF_3$ in 1809 by Gay-Lussac marked the beginning of the chemistry of 13/15 compounds.[20] With the combination of a group 13 and a group 15 element, these compounds are isoelectronic towards hydrocarbon compounds and can thus be considered as their inorganic equivalents. This observation is in line with Hoffmann's well-established principle of isolobality (Figure 1.2), which states that two molecular fragments can formally be exchanged if there is a similarity in number, symmetry, energy and form of the frontier molecular orbitals and as well as the number of electrons residing therein.[21] Over the past years, many important milestones have been achieved by chemists. Most notably are the early reports of the adducts $H_3P{\cdot}BCl_3$, $Me_3N{\cdot}BH_3$ and the benzene analogue borazine $B_3N_3H_6$ by Burg and Schlesinger in 1937.[22] When examined more closely, the similarities as well as the differences between 13/15 parent monomers and their organic counterparts become evident: being isoelectronic, the structural features of 13/15 parent compounds are very similar to their organic analogues (e.g. $d_{BN}(H_3B{\cdot}NH_3)$ = 1.58 Å, $d_{CC}(H_3C\text{-}CH_3)$ = 1.54 Å)[6]. However, the bonds between the triel and the pnictogen are polarized towards the more electronegative element, leading to a substantial change in reactivity and physical properties.[6,23] Taking borazine as an example, this becomes especially evident: formally isoelectronic to benzene, the compound could be described as being aromatic in nature, but this has been the subject of many theoretical studies.[24,25,26] By now, it is widely believed that aromaticity in borazine is questionable.[26] The first, purely inorganic benzene derivative displaying full delocalization of six π-electrons, namely $(BCl)_2(BPMe_3)_2(NMes)_2$ has only recently been synthesized with significant changes to the core borazine motif and with substituents attached to each ring position.[24]

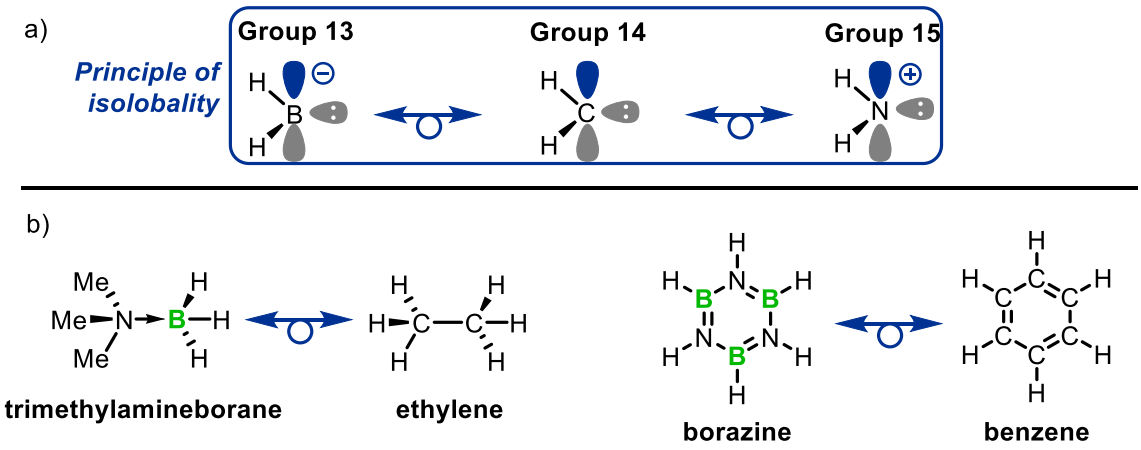

Figure 1.2: a) Isolobal relationship between $\{EH_2\}$ fragments of groups 13-15; b) selected examples of group 13/15 compounds and their organic counterparts.

More general, the structure of 13/15 compounds strongly varies and depends on the substituents at the respective triel and pnictogen atoms (Figure 1.3).[27,28] Sterically more encumbering substituents, such as cyclohexyl or *tert*-butyl substituents favour smaller oligomers, while smaller substituents (e.g. methyl residues) lead to larger adduct formation. Hence, 13/15 compounds display an extraordinary diversity of structural motifs, including hyper-coordinated moieties (Figure 1.3, **B**) and cage compounds (Figure 1.3, **H**). Apart from these examples, other oligomers are usually made up by regular 2c-2e σ-bonds, as to be predicted (Figure 1.3, **A**, **C**-**G**). Since many of these compounds display high sensitivity towards air, progress in this field can largely be attributed to the development of inert gas techniques such as

developed by Schlenk.[28,29] This is especially relevant for the heavier 13/15 element combinations, which partially display dramatic sensitivity towards air, temperature and light.[23]

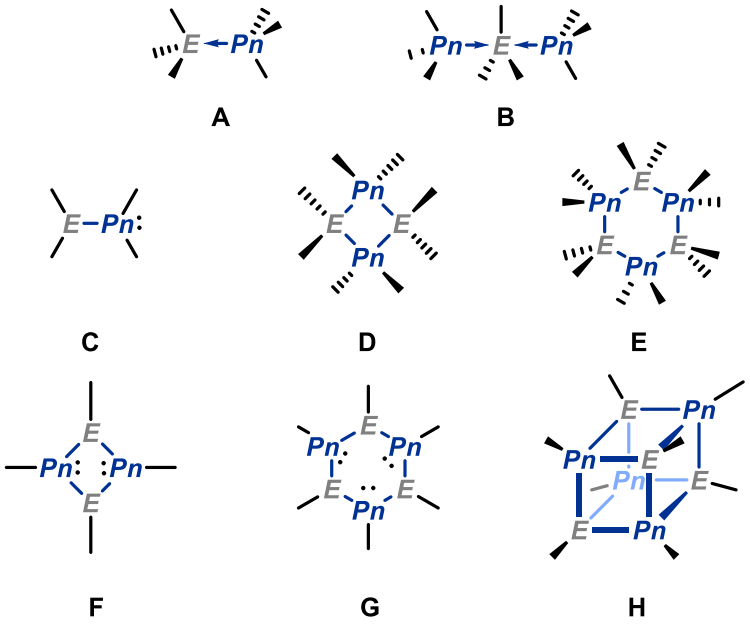

Figure 1.3: Overview of selected structural geometries of 13/15 compounds (*E* = triel, *Pn* = pnictogen).[28]

The chemistry of the parent pnictogenyltrielanes is significantly impacted by the tendency towards spontaneous oligo- or polymerization, even at low temperatures (cf. Figure 1.4).[30,31] This intermolecular reaction pathway can be avoided by kinetic stabilization of the monomer. Bulky residues at the pnictogen or the triel impose a steric hinderance (Figure 1.4, type **A**),[32] while simultaneous stabilization by a Lewis acid (LA) and a Lewis base (LB, Figure 1.4, type **B**) provide electronic saturation of the molecule.[33] In the past, it could also be shown that stabilization by Lewis base only is also possible (Figure 1.4, type **C**).[34–36] Regarding stabilization by just a Lewis acid (type **D**), the synthesis of this motif has not been accomplished, so far, although theoretically plausible as predicted by quantum chemical calculations.[37] When comparing different phosphanyltrielane analogues of ethylene (cf. Figure 1.5), the electronic properties can be illustrated by quantum chemical calculations. The phosphanyltrielanes can be described as stronger donors and better π-acceptors due to the strong bond polarization.

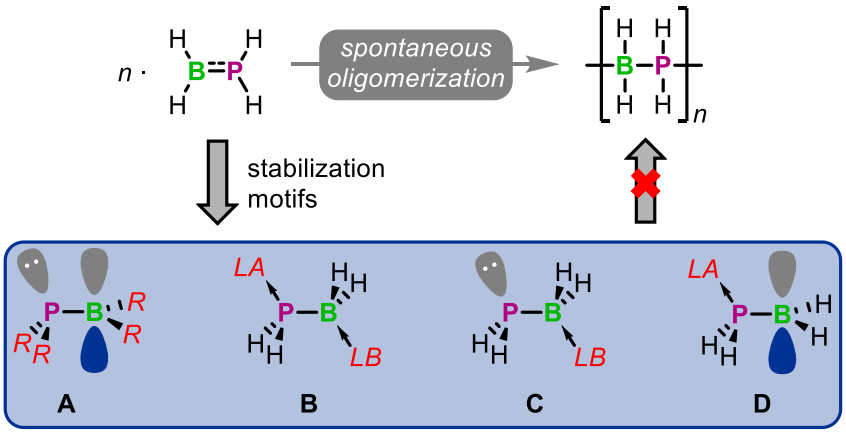

Figure 1.4: Overview of stabilization motifs of parent pnictogenyltrielanes as exemplified for phosphanylboranes: A) stabilization by bulky organic residues, B) simultaneous stabilization by Lewis acid (LA) and Lewis base (LB), C) stabilization by Lewis base only, D) stabilization by Lewis acid only.

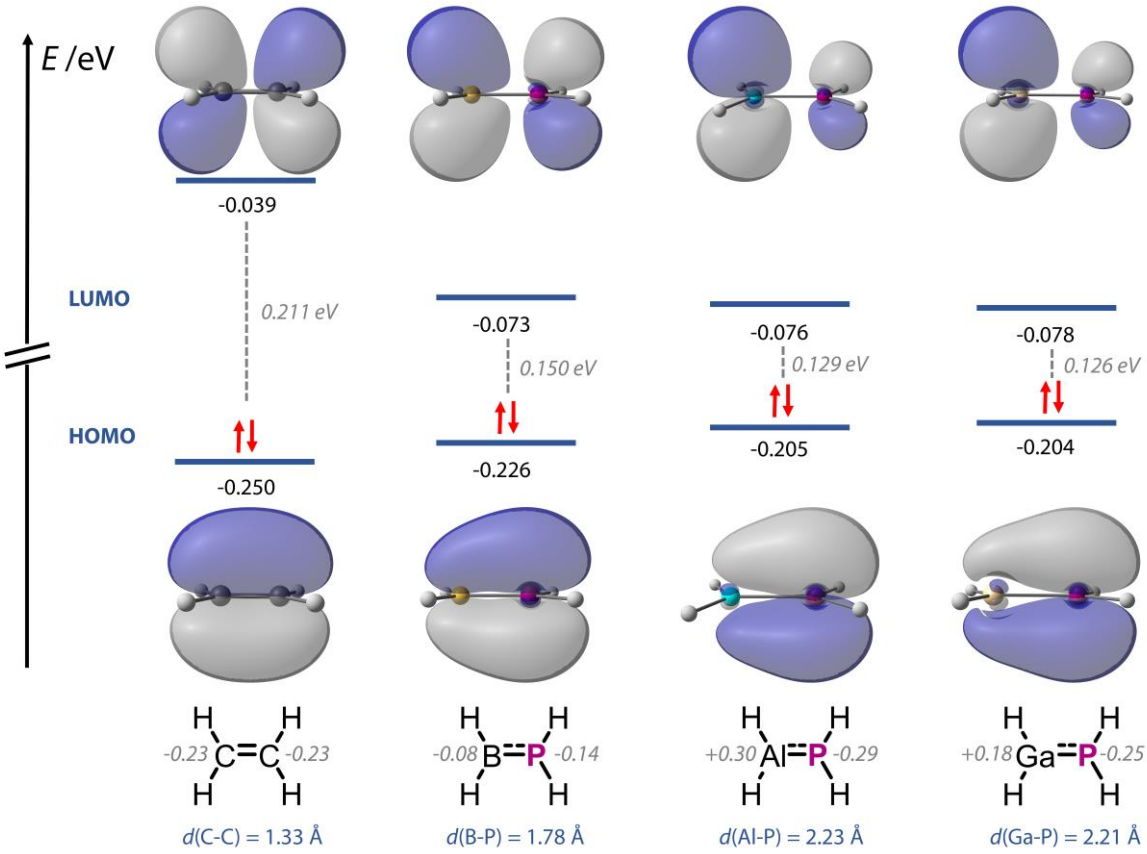

Figure 1.5: Calculated frontier Kohn-Sham orbitals of ethylene and its pnictogenylborane analogues (BP86-D4/def2-TZVP level of theory; isosurfaces drawn with a contour value of 0.075). Triel-pnictogen bond distances are given as predicted by the quantum chemical calculations. Mulliken atomic charges are displayed as grey numbers.

Simultaneously, the bond strength decreases when moving down the periodic tables due to poorer orbital overlap and decreased efficiency of *s*-*p* orbital mixing (hybridization defect). Thus, going from B to Ga results in increasing bond polarity and longer bond distances, though the Al and Ga containing compounds show similar atomic charges and bond distances due to *d*-block contraction.[6] This can also be seen by the HOMO having an increasing contribution from the P atom while the LUMO is largely comprised by the triel *p*-orbital. Moreover, the enhanced donor and acceptor capabilities explain the tendency of these ethylene analogues towards spontaneous oligomerization. Once stabilized by a suitable LA/LB combination or just a LB, the monomers display a fascinating variety of reactivity as described in the next chapter.

1.3 Reactivity of Pnictogenylboranes and heavier Congeners

The reactivity of pnictogenylboranes has been explored in detail in numerous previous studies (Scheme 1.3). Specifically, Lewis base stabilized 13/15 monomers have shown a remarkable range of reactivity. The molecules possess two reactive sites at both ends (displacement of the Lewis base, pnictogen lone pair) which can be exploited. Most notable, it could be demonstrated that catenation reactions are possible in various ways, either cationic, neutral, or anionic.[38,39,40,41]

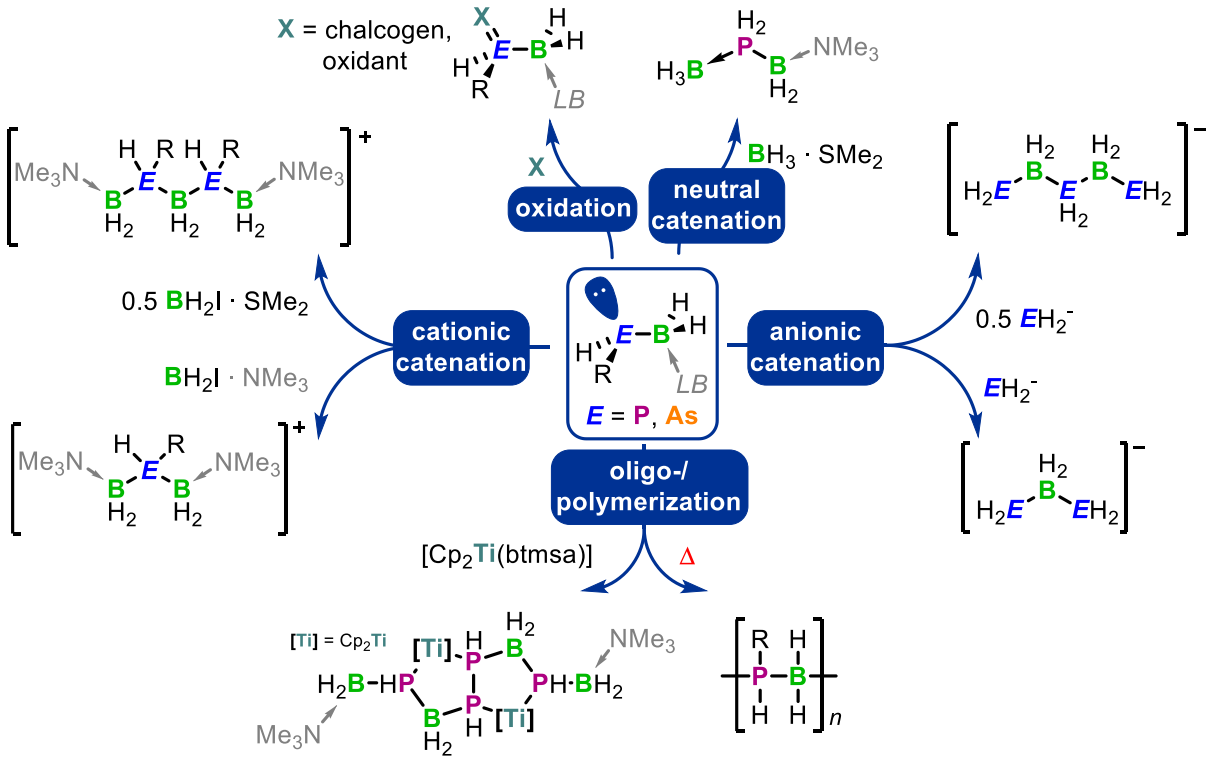

Scheme 1.3: Overview of conversions of Lewis base stabilized pnictogenylboranes (***E*** = P, As; btmsa = bis(trimethylsilyl)acetylene).

Depending on the stoichiometry and the reagents, controlled reaction outcomes have been achieved, leading to three or five-membered 13/15 chain structures. It could also be shown that even longer chain compounds such as $[Me_3N{\cdot}BH_2PH^tBu(BH_2PH_2)_2BH_2PH^tBuBH_2{\cdot}NMe_3]I$ are accessible.[42] Furthermore, the pnictogenylboranes reacted with chalcogens or suitable group 16 oxidants with selective oxidation of the pnictogen lone pair.[39,43] The Lewis base stabilized pnictogenylborane monomers also serve as excellent sources towards inorganic 13/15 oligo- and polymers as the oligomerization can be conveniently be induced by thermal or catalytic pathways.[38,44] In analogy to phosphines, pnictogenylboranes also act as capable ligands in coordination chemistry.

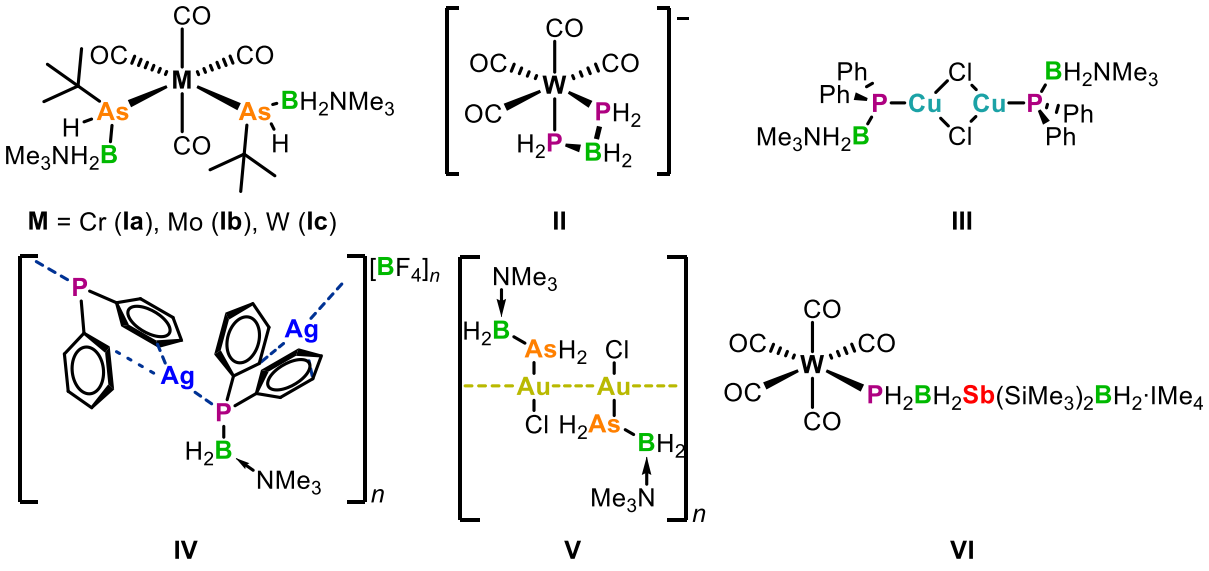

Figure 1.6: Selected examples for the coordination chemistry of pnictogenylboranes (IMe_4 = 1,3,4,5-Tetramethylimidazolin-2-ylidene).

Numerous complexes have been described in the literature, ranging from classic transition metal carbonyl complexes (Figure 1.6, **I**, **II**, **VI**) to coinage metal salts (Figure 1.6, **III**-**V**).[38,41,45,46] Based on aurophilic interactions, Au(I) complexes of donor stabilized pnictogenylboranes (e.g. Figure 1.6, **V**) have displayed interesting luminescent properties, making them promising candidates for optical applications.[45] All reactivity studies, so far, have focussed on the lighter pnictogenylboranes, which, compared to their heavier congeners. The question remains if the Lewis base stabilized heavier 13/15 compounds follow the same reaction principles as their borane counterparts or display changed patterns of reactivity. Simultaneously, it is not entirely clear so far, how exchanging boron for heavier group 13 elements affects the donor properties of Lewis base stabilized pnictogenyltrielanes. In fact, even a comparison of pnictogenylboranes towards regular phosphines has never been drawn in the past and such an investigation would fill an important gap in the literature around this class of compounds.

Most recently, novel Lewis base stabilized 13/14/15 combinations including germanium could be prepared starting from IDipp·GeH_2BH_3 (IDipp = 1,3-Bis-(2,6-diisopropylphenyl)-imidazolin-2-ylidene).[31,47] A triflation by addition of methyltriflate led to IDipp·GeH_2BH_2(OTf) under extrusion of methane (Scheme 1.4), which serves as a versatile synthon towards the formation of cationic 13/14/15 hydride chain compounds due to the facile substitution of the triflate anion.[48] Reactions with Lewis base stabilized pnictogenylboranes led to the formation of four-membered cationic (parent) 13/14/15 chain compounds (Scheme 1.4, bottom), whereas the addition of phosphines or arsines resulted in three-membered chain compounds (Scheme 1.4, right). The addition of PH_3 also led to the respective cationic chain compound, despite the weak nucleophilicity of PH_3, as was identified by multinuclear NMR spectroscopy. Furthermore, based on early results IDipp·GeH_2BH_2(OTf) could also potentially serve as suitable platform towards salt metathesis.[49] Investigations on the preparation and stability of NHC (NHC = N-heterocyclic carbene) stabilized Ge materials are especially attractive, as Rivard and co-workers could demonstrate the thermolytic deposition of nanodimensional Ge thin films of variable thickness from the dissolved adducts as an important proof of concept.[50] All the abovementioned chain compounds feature germanium directly bound to an NHC. Mixed 13/14/15 materials that feature a terminal tetrel at the chain structure are, however, not reported. The same accounts for other elements of group 14. It would be desirable to prepare and characterize novel mixed 13/14/15 combinations and explore their chemical and physical properties, especially towards the deposition of thin layers.

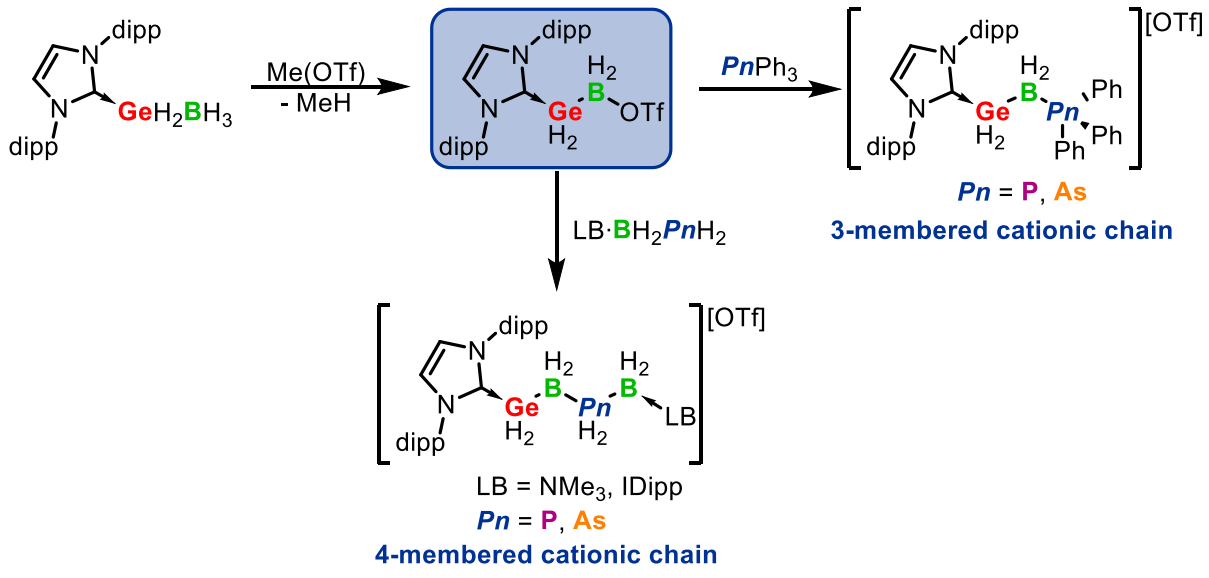

Scheme 1.4: Selected examples for the formation of parent cationic 13/14/15 chain compounds starting from IDipp·GeH_2BH_3.

While the reactivity of Lewis base stabilized pnictogenylboranes has been investigated in many facets, the chemistry of the heavier congeners is barely explored. Owed to the decreasing bond energy between the heavy pnictogens and triels, the synthesis is hampered especially due to the high sensitivity towards air and temperature.[34,35,51] The heaviest reported combinations of donor stabilized parent group 13/15 monomers currently consists of the stibanylboranes $IMe_4{\cdot}BH_2SbH_2$, $IMe_4{\cdot}BH_2Sb(SiMe_3)_2$ and the arsanylgallanes and alanes $IDipp{\cdot}EH_2AsH_2$ (E = Al, Ga; IDipp = 1,3-Bis-(2,6-diisopropylphenyl)-imidazolin-2-ylidene, IMe_4 = 1,3,4,5-Tetramethylimidazolin-2-ylidene).[34,35,52] All these compounds are highly sensitive towards air and decompose at room temperature. The stibanylboranes will also decompose visibly when exposed to light. Furthermore, a di-substitution pattern could first be realized by double salt metathesis leading to $IDipp{\cdot}EH(PnH_2)_2$.[35] This class of compound represents the first branched parent pnictogenyltrielanes and should in principle offer the possibility for chelation of suitable metal centres, and branched catenation by reaction with main group electrophiles, which remains to be explored. Based on preliminary results, a $LB{\cdot}E(PnH_2)_3$ motif should be accessible as well but has so far not been reported in the literature.[53] These tripentelyltrielanes would provide even more options for investigations on reactivity. Especially, it is worth investigating whether these compounds could act as tridentate ligands in coordination chemistry or as platforms for building branched 13/15 compounds, as well. The preliminary results indicate that at least the triphosphanylgallane $IDipp{\cdot}Ga(PH_2)_3$ exists as a stable compound, but other 13/15 combinations for this type of compounds yet have to be discovered.

Regarding NHC stabilized 13/15 compounds, von Hänisch and co-workers could also prove in several studies that the ring opening of oligomeric silylphosphanylgallanes by addition of NHCs provides a reliable synthetic access towards these type of compounds.[54] Reports on 13/15 molecular combinations including indium, however, are still scarce throughout the literature. To this date, no 13/15 combinations of indium stabilized only by a Lewis base are known and thus remain a valuable synthetic target, especially with NHCs as potent stabilization platforms for stable monomeric indium 13/15 compounds. In 2019, the isolation of the β-diketiminate (Nacnac) stabilized $(Dipp_2Nacnac)In(PH_2)_2$ could be achieved, though, besides the compounds $(Dipp_2Nacnac)E(PnH_2)_2$ (E = Al, Ga; *Pn* = P, As).[55] In general, Nacnac stabilized low valent group 13 elements in oxidation state +I also provide a highly reactive platform for oxidative additions that can be used for the preparation of 13/15 or even 13/14/15 element combinations. For example, reactions of $(Dipp_2Nacnac)Ga$ with PH_3, AsH_3 and *in situ* generated SbH_3 leads to the parent addition products $(Dipp_2Nacnac)GaHPnH_2$ (*Pn* = P, As, Sb; Figure 1.7, **IX**).[56] In a separate study, von Hänisch and co-workers could also add $MeBiH_2$ to $(Dipp_2Nacnac)Ga$ by the same strategy (Figure 1.7, **X**).[57] Similarly, reactions with silylphosphines also resulted in the corresponding oxidative addition reactions (Figure 1.7, **XI**).[58] As a side note, von Hänisch and co-workers could also show that the deprotonation of *in situ* prepared SbH_3 in the presence of crown ethers affords the parent isolable $[M(crown)][SbH_2]$ (M = alkali metal) salts, that show great potential for salt metathesis reaction as a stable $[SbH_2]^-$ carrier.[59] In contrast, non-coordinated $KSbH_2$ is of very limited practical use due to decomposition occurring at temperatures above -78 °C, thus marking the discovery of the stable $[M(crown)][SbH_2]$ salts as a major breakthrough in the field.[60] The chemistry of β-diketiminate stabilized low valent group 13 elements further extends as a key stabilizing factor for Ga=*Pn* multiple bonded species. Pioneering works by S. Schulz and co-workers have explored the synthesis and reactivity of these rare moieties resulting in a library of important discoveries, such as gallapnictenes and distibiranes (Figure 1.7, **XII**, **XIII**).[61] Another important contribution to be mentioned is the preparation of a phosphanyl-phosphagallene by Goicoechea and co-workers, which is capable of small molecule activation such as dihydrogen, ammonia or carbon dioxide (Figure 1.7, **XIV**).[62] While the stabilization by β-diketiminates has many unique features, the ligand occupies two binding sites at the central atom and increases its oxidation state by +I. In contrast, strong σ-donors such as NHCs do not change the oxidation state and only bind to the central atom by one binding site, allowing more versatility of the bound

substituents. In combination with a much higher adduct stabilization than from, e.g., tertiary amines, NHC stabilized 13/15 compounds have emerged as a new generation of compounds within this field based on their unique steric and electronic features as explained within the next section.[34,35]

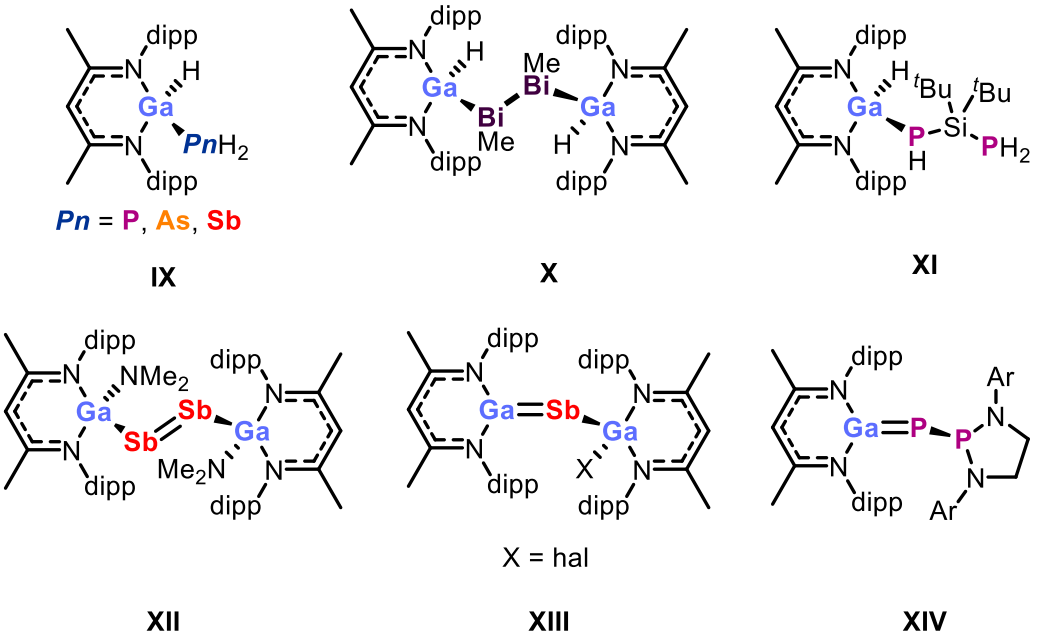

Figure 1.7: Selected examples of β-diketiminate stabilized 13/15 gallanes and gallenes.

1.4 N-Heterocyclic Carbenes and their Applications

Since their first discovery by Wanzlick and Öfele and later the isolation by Arduengo,[63,64] N-heterocyclic carbenes (NHCs) have emerged as one of the most important 2-electron σ-donors in transition metal and main group chemistry.[65–67] NHCs can be defined as heterocyclic systems containing one carbene atom and at least one nitrogen atom.[65,67] The electronic ground state of NHCs resides in a singlet state due to its cyclic structure, thus providing the compounds with strong σ-donating capabilities.[67,68] The singlet state itself is further stabilized by the withdrawing inductive effect (-I) of the electronegative heteroatom and a donating mesomeric effect (+M) of electron density from the nitrogen lone pairs into the unoccupied *p*-orbital of the carbene C atom (Figure 1.8).

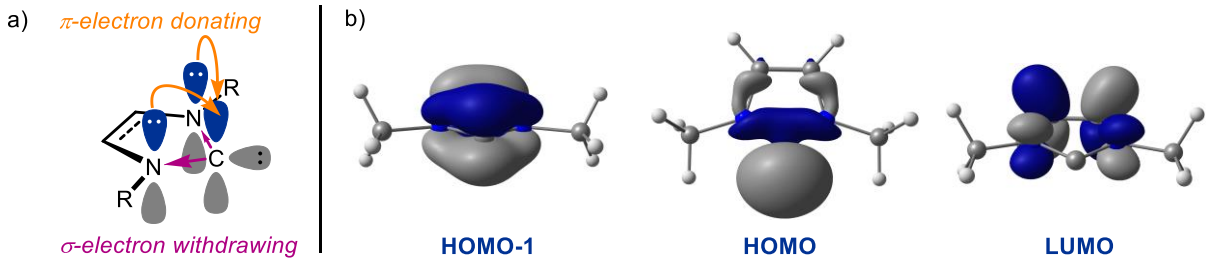

Figure 1.8: a) Schematic representation of electronic effects within NHCs; b) depiction of calculated frontier Kohn-Sham molecular orbitals of 1,3-Dimethyl-imidazolin-2-ylidene (BP86-D4/def2-SVP).

NHCs allow for plenty of options for modification of the steric and electronic properties of the compounds. The four main influencing factors are the embedded heteroatoms, the backbone structure, the

substituents bound to the heteroatoms and the overall ring size.[67] The classic NHCs as described by Arduengo are (aromatic) imidazolylidenes (Figure 1.9, **I**).[64,69] Saturation of the NHC backbone leads to imidazolinylidenes (Figure 1.9, **II**), which slightly changes the donor strength and mode of reactivity as the saturated backbone becomes less prone to undergo side reactions. Alternative heteroatoms within the ring are also accessible (Figure 1.9, **III**), as well as ring structures containing more than two heteroatoms (Figure 1.9, **IV**). Furthermore, NHCs exist as annelated ring systems (Figure 1.9, **V**). In addition, the library of cyclic(alkyl)(amino) carbenes (CAACs, Figure 1.9, **VI**) by Bertrand and co-workers display even stronger σ-donor and π-acceptor capabilities and have been studied intensively in the past.[70] NHCs are also known to undergo transformation to "abnormal" NHCs (Figure 1.9, **VII**) under certain conditions.[71] A relatively new class of NHCs are N,N'-diamidocarbenes (DACs, Figure 1.9, **VIII**), which possess a higher electrophilic character and thus different reactivity patterns.[72]

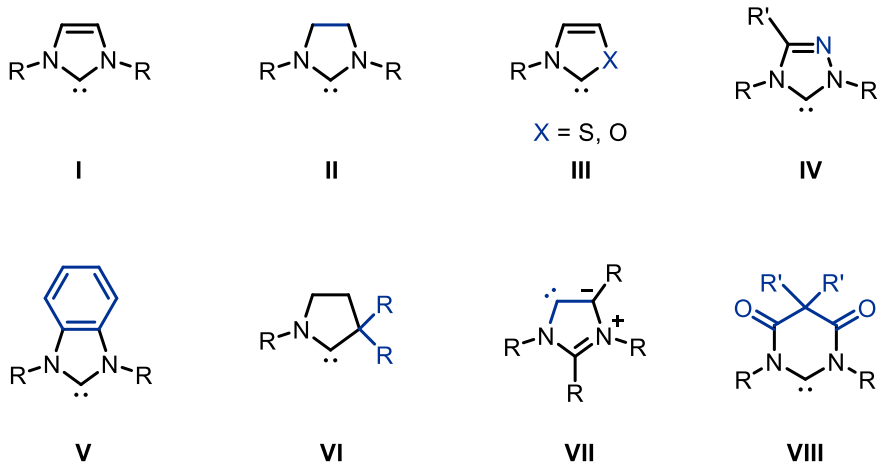

Figure 1.9: Depiction of selected commonly used classes of NHCs.[67,73]

Over the years, NHCs have proven themselves as essential tools in main group chemistry, transition metal catalysis and organocatalysis.[65,66,74,75] Coordination to *p*-block elements results in the stabilization of reactive species which otherwise might be too difficult to handle, small molecule activation, and adducts to be used as frustrated Lewis pairs or reagents in organic synthesis.[67,76] NHC transition metal complexes serve as platforms for organometallic materials[77] such as metal-organic frameworks,[78] metallopharmaceuticals[79] and especially homogeneous catalysis including efficient cross-couplings, olefin metathesis and asymmetric catalysis.[73,80,81] The most famous example is represented by the second generation of Grubbs type catalysts containing NHC bound ruthenium centres, drastically outperforming the first-generation ruthenium phosphine complexes in catalytic performance in nearly every aspect.[81,82] However recently, with the Nobel Prize in 2021 being awarded to the development of (asymmetric) organocatalysis,[83] the interest in organocatalysis has increased significantly, as well. In contrast to homogeneous transition metal catalysis with NHCs, the underlying mechanisms for organocatalytic applications of NHCs are vastly different. As opposed to classical transition metal catalysis, organocatalysis relies on much more abundant organic compounds instead of expensive and rare transition metals, making the field also highly attractive for industrial applications.

In general, NHC catalysis is governed by their strong σ-donor and moderate π-acceptor capabilities, which dictates the modes of action (Scheme 1.5):[74] After addition to carbonyl groups (Scheme 1.5, top), enamine/Michael type reactivity (Scheme 1.5, left) is observed by reaction with electrophiles or internal elimination of a leaving group. Based on the π-acceptor property of NHCs, α-acidic deprotonation, or elimination/substitution of the NHC can also occur (Scheme 1.5, middle), releasing the catalyst. In other

cases, the NHC influences the reaction by standing as a bystander in hydride transfer or nucleophilic attacks in α-position (Scheme 1.5, right).

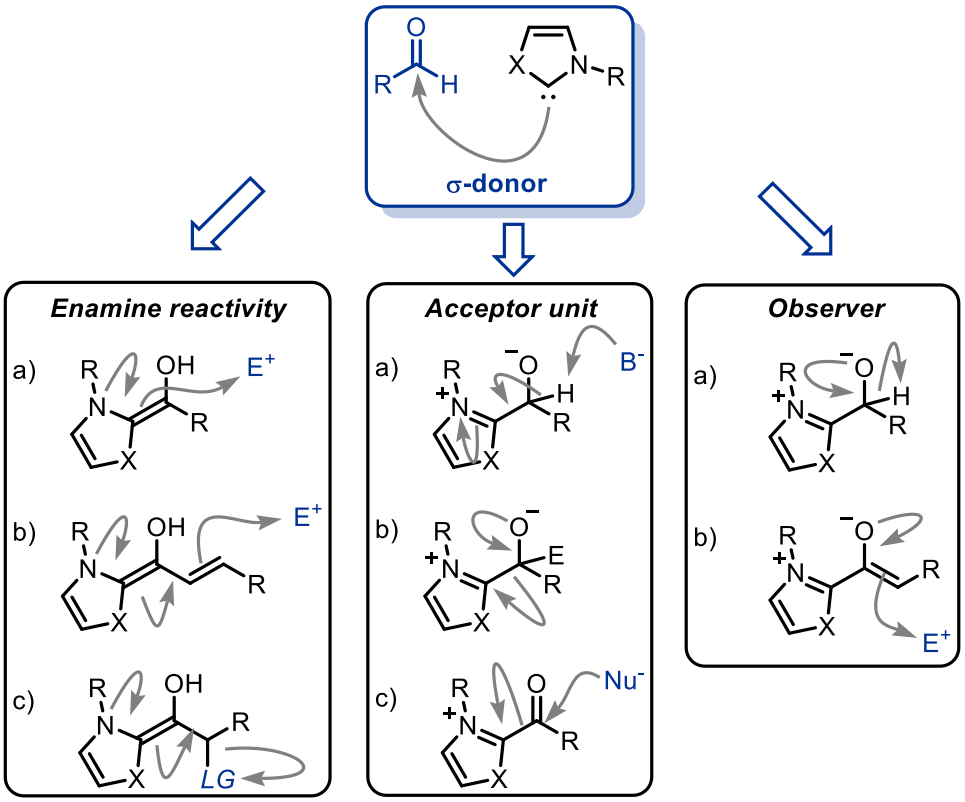

Scheme 1.5: Common modes of action in for NHCs in organocatalysis.[74] Enamine reactivity: a) attack on electrophile, b) conjugate attack on electrophile, c) elimination of internal leaving group; acceptor unit: a) deprotonation of α-acidic proton, b) leaving group by internal elimination, c) leaving group by external attack; observer unit: a) hydride transfer, b) classic enolate behaviour.

All these properties and mechanisms mentioned in the aforementioned sections make NHCs highly potent candidates for investigations in the field of 13/15 compounds and their further applications. Especially, studies on the heavier 13/15 congeners and their reactivity are very scarce, so far. The question remains if the use of NHCs enables the isolation of heavy 13/15 parent monomers beyond gallium and arsenic which are otherwise not accessible and if so, which chemical and physical properties these compound exhibit.

1.5 References

[1] H. Sicius in *Handbuch der chemischen Elemente* (Hrsg.: H. Sicius), Springer Berlin Heidelberg, Berlin, Heidelberg, **2020**, S. 1–6.

[2] J. Smoliner, *Was Studierende der Physik und Elektrotechnik wissen sollten,* 2. Aufl., Springer Spektrum, Berlin, Heidelberg, **2020**.

[3] P. Y. Yu, M. Cardona, *Fundamentals of semiconductors. Physics and materials properties ; with 52 tables and 116 problems,* 3. Aufl., Springer, Berlin, Heidelberg, **2005**.

[4] A. R. West, *Solid state chemistry and its applications,* 1. Aufl., Wiley, Chichester, West Sussex, **2013**.

[5] M. Binnewies, M. Finze, M. Jäckel, P. Schmidt, H. Willner, G. Rayner-Canham, *Allgemeine und anorganische Chemie,* 3. Aufl., Springer Spektrum, Berlin, **2016**.

[6] A. F. Holleman, E. Wiberg, *Lehrbuch der anorganischen Chemie,* 102. Aufl., de Gruyter, Berlin, **2008**.

[7] E. Riedel, H.-J. Meyer, *Allgemeine und anorganische Chemie,* 12. Aufl., de Gruyter, Berlin, Boston, **2019**.
[8] C. E. Housecroft, A. Sharpe, *Inorganic Chemistry,* 4. Aufl., Pearson, New York, **2012**.
[9] A. C. Jones, P. O'Brien, *CVD of Compound Semiconductors: Precursor Synthesis Development and Applications*, VCH, Weinheim, **1996**.
[10] H. Ibach, H. Lüth, *Festkörperphysik. Einführung in die Grundlagen ; mit 18 Tafeln und 104 Übungen,* 7. Aufl., Springer, Berlin, Heidelberg, **2009**.
[11] a) G. B. Stringfellow, *Rep. Prog. Phys.* **1982**, *45*, 469–525; b) M. R. Leys, *Chemtronics* **1987**, *2*, 155–164.
[12] C. Elschenbroich, *Organometallchemie,* 6. Aufl., Teubner, Wiesbaden, **2008**.
[13] A. Y. Timoshkin, *Chem. Eur. J.* **2024**, *30*, e202302457.
[14] a) J. S. Foord, T. J. Whitaker, E. N. Downing, D. O'Hare, A. C. Jones, *Appl. Phys. Lett.* **1993**, *63*, 1270–1272; b) S. Marchant, C. Y. Tang, A. J. Downs, T. M. Greene, H.-J. Himmel, S. Parsons, *Dalton Trans.* **2005**, 3281–3290.
[15] a) A. H. Cowley, R. A. Jones, *Angew. Chem. Int. Ed.* **1989**, *28*, 1208-1215; *Angew. Chem.* **1989**, *101*, 1235-1243; b) J. F. Janik, R. L. Wells, V. G. Young, A. L. Rheingold, I. A. Guzei, *J. Am. Chem. Soc.* **1998**, *120*, 532–537; c) S. M. Stuczynski, R. L. Opila, P. Marsh, J. G. Brennan, M. L. Steigerwald, *Chem. Mater.* **1991**, *3*, 379–381.
[16] C. W. Hamilton, R. T. Baker, A. Staubitz, I. Manners, *Chem. Soc. Rev.* **2009**, *38*, 279–293.
[17] R. Hoffmann, *J. Chem. Phys.* **1964**, *40*, 2474–2480.
[18] I. P. Jain, P. Jain, A. Jain, *J. Alloys Compd.* **2010**, *503*, 303–339.
[19] S. Satyapal, J. Petrovic, C. Read, G. Thomas, G. Ordaz, *Catal. Today* **2007**, *120*, 246–256.
[20] J. Gay-Lussac, J. Thenard, *Mem. Phys. Chim. Soc. d'Arcueil* **1809**, *2*, 210–211.
[21] R. Hoffmann, *Angew. Chem. Int. Ed. Engl.* **1982**, *21*, 711–724.
[22] a) A. Besson, *Comptes Rendus* **1890**, 516; b) A. B. Burg, H. I. Schlesinger, *J. Am. Chem. Soc.* **1937**, *59*, 780–787; c) A. Stock, E. Pohland, *Chem. Ber.* **1926**, *59*, 2210–2215.
[23] K. Knabel, I. Krossing, H. Nöth, H. Schwenk-Kircher, M. Schmidt-Amelunxen, T. Seifert, *Eur. J. Inorg. Chem.* **1998**, *1998*, 1095–1114.
[24] K. Ota, R. Kinjo, *Angew. Chem. Int. Ed.* **2020**, *59*, 6572–6575.
[25] a) D. Benker, T. M. Klapötke, G. Kuhn, J. Li, C. Miller, *Heteroatom Chem.* **2005**, *16*, 311–315; b) D. L. Coopera, S. C. Wright, J. Gerratt, P. A. Hyams, M. Raimondi, *J. Chem. Soc., Perkin Trans. 2* **1989**, 719; c) I. Fernández, G. Frenking, *Faraday Discuss.* **2007**, *135*, 403-421; d) P. W. Fowler, E. Steiner, *J. Phys. Chem. A* **1997**, *101*, 1409–1413; e) B. Kiran, A. K. Phukan, E. D. Jemmis, *Inorg. Chem.* **2001**, *40*, 3615–3618; f) P. v. R. Schleyer, H. Jiao, N. J. R. E. van Hommes, V. G. Malkin, O. L. Malkina, *J. Am. Chem. Soc.* **1997**, *119*, 12669–12670; g) J. J. Torres-Vega, A. Vásquez-Espinal, J. Caballero, M. L. Valenzuela, L. Alvarez-Thon, E. Osorio, W. Tiznado, *Inorg. Chem.* **2014**, *53*, 3579–3585.
[26] R. Islas, E. Chamorro, J. Robles, T. Heine, J. C. Santos, G. Merino, *Struct. Chem.* **2007**, *18*, 833–839.
[27] S. Schulz, *Coord. Chem. Rev.* **2001**, *215*, 1–37.
[28] S. Schulz, *Adv. Organomet. Chem.* **2003**, *49*, 225–317.
[29] a) W. Schlenk, A. Thal, *Ber. Dtsch. Chem. Ges.* **1913**, *46*, 2840–2854; b) S. Herzog, J. Dehnert, *Z. Chem.* **1964**, *4*, 1–11; c) W. Schlenk, J. Holtz, *Ber. Dtsch. Chem. Ges.* **1917**, *50*, 262–274; d) T. T. Tidwell, *Angew. Chem. Int. Ed.* **2001**, *40*, 331–337.
[30] a) J.-M. Denis, H. Forintos, H. Szelke, L. Toupet, T.-N. Pham, P.-J. Madec, A.-C. Gaumont, *Chem. Comm.* **2003**, 54–55; b) P. P. Power, *Chem. Rev.* **1999**, *99*, 3463–3503; c) A. Y. Timoshkin, *Coord. Chem. Rev.* **2005**, *249*, 2094–2131.
[31] A. M. Belousova, A. Y. Timoshkin, *J. Phys. Chem. A* **2023**, *127*, 7353–7363.
[32] X. Feng, M. M. Olmstead, P. P. Power, *Inorg. Chem.* **1986**, *25*, 4615–4616.
[33] a) U. Vogel, P. Hoemensch, K.-C. Schwan, A. Y. Timoshkin, M. Scheer, *Chem. Eur. J.* **2003**, *9*, 515–519; b) U. Vogel, A. Y. Timoshkin, M. Scheer, *Angew. Chem. Int. Ed.* **2001**, *40*, 4409–4412; c) A. V. Pomogaeva, A. S. Lisovenko, A. Y. Timoshkin, *Russ. J. Gen. Chem.* **2023**, *93*, 900–908; d) T. I. Demirer, B. Morgenstern, D. M. Andrada, *Eur. J. Inorg. Chem.* **2022**, e202200477.
[34] M. A. K. Weinhart, A. S. Lisovenko, A. Y. Timoshkin, M. Scheer, *Angew. Chem. Int. Ed.* **2020**, *59*, 5541-5545; *Angew. Chem.* **2020**, *132*, 5586-5590.
[35] M. A. K. Weinhart, M. Seidl, A. Y. Timoshkin, M. Scheer, *Angew. Chem.* **2021**, *133*, 3850–3855; *Angew. Chem. Int. Ed.* **2021**, *60*, 3806–3811.
[36] K.-C. Schwan, A. Y. Timoskin, M. Zabel, M. Scheer, *Chem. Eur. J.* **2006**, *12*, 4900–4908.
[37] A. V. Pomogaeva, A. S. Lisovenko, A. S. Zavgorodnii, A. Y. Timoshkin, *J. Comput. Chem.* **2023**, *44*, 218–228.
[38] F. Lehnfeld, M. Seidl, A. Y. Timoshkin, M. Scheer, *Eur. J. Inorg. Chem.* **2022**, *3*, e202100930.
[39] O. Hegen, A. V. Virovets, A. Y. Timoshkin, M. Scheer, *Eur. J. Inorg. Chem.* **2018**, *24*, 16521-16525.
[40] a) C. Marquardt, A. Adolf, A. Stauber, M. Bodensteiner, A. V. Virovets, A. Y. Timoshkin, M. Scheer, *Chem. Eur. J.* **2013**, *19*, 11887–11891; b) C. Marquardt, T. Kahoun, J. Baumann, A. Y. Timoshkin, M. Scheer, *Z. Anorg. Allg. Chem.* **2017**, *643*, 1326–1330; c) C. Marquardt, C. Thoms, A. Stauber, G. Balázs, M. Bodensteiner, M. Scheer, *Angew. Chem. Int. Ed.* **2014**, *53*, 3727–3730; d) C. Marquardt, G. Balázs, J. Baumann, A. V. Virovets, M. Scheer, *Chem. Eur. J.* **2017**, *23*, 11423–11429;

e) C. Marquardt, T. Kahoun, A. Stauber, G. Balázs, M. Bodensteiner, A. Y. Timoshkin, M. Scheer, *Angew. Chem. Int. Ed.* **2016**, *55*, 14828–14832.

[41] M. Elsayed Moussa, T. Kahoun, M. T. Ackermann, M. Seidl, M. Bodensteiner, A. Y. Timoshkin, M. Scheer, *Organometallics* **2022**, *41*, 1572–1578.

[42] C. Marquardt, *PhD thesis* **2015**, Universität Regensburg.

[43] a) F. Lehnfeld, M. Seidl, A. Timoshkin, M. Scheer, *Eur. J. Inorg. Chem.* **2023**, *26*, e202300338; b) C. Marquardt, O. Hegen, T. Kahoun, M. Scheer, *Chem. Eur. J.* **2017**, *23*, 4397–4404.

[44] a) M. Bodensteiner, A. Y. Timoshkin, E. V. Peresypkina, U. Vogel, M. Scheer, *Chem. Eur. J.* **2013**, *19*, 957–963; b) M. Bodensteiner, U. Vogel, A. Y. Timoshkin, M. Scheer, *Angew. Chem. Int. Ed.* **2009**, *48*, 4629–4633; c) J. Braese, F. Lehnfeld, V. T. Annibale, T. Oswald, R. Beckhaus, I. Manners, M. Scheer, *Chem. Eur. J.* **2023**, *29*, e202301741; d) C. Marquardt, T. Jurca, K.-C. Schwan, A. Stauber, A. V. Virovets, G. R. Whittell, I. Manners, M. Scheer, *Angew. Chem. Int. Ed.* **2015**, *54*, 13782–13786; e) C. Thoms, C. Marquardt, A. Y. Timoshkin, M. Bodensteiner, M. Scheer, *Angew. Chem. Int. Ed.* **2013**, *52*, 5150–5154; f) A. V. Butlak, I. V. Kazakov, A. Stauber, O. Hegen, M. Scheer, A. V. Pomogaeva, A. Y. Timoshkin, *Eur. J. Inorg. Chem.* **2019**, *2019*, 3885–3891; g) C. Marquardt, O. Hegen, A. Vogel, A. Stauber, M. Bodensteiner, A. Y. Timoshkin, M. Scheer, *Chem. Eur. J.* **2018**, *24*, 360–363.

[45] J. Braese, A. Schinabeck, M. Bodensteiner, H. Yersin, A. Y. Timoshkin, M. Scheer, *Chem. Eur. J.* **2018**, *24*, 10073–10077.

[46] a) M. Elsayed Moussa, J. Braese, C. Marquardt, M. Seidl, M. Scheer, *Eur. J. Inorg. Chem.* **2020**, *26*, 2501–2505; b) M. Elsayed Moussa, C. Marquardt, O. Hegen, M. Seidl, M. Scheer, *New J. Chem.* **2021**, *45*, 14916–14919; c) K.-C. Schwan, A. Adolf, M. Bodensteiner, M. Zabel, M. Scheer, *Z. Anorg. Allg. Chem.* **2008**, *634*, 1383–1387; d) O. Hegen, C. Marquardt, A. Y. Timoshkin, M. Scheer, *Angew. Chem. Int. Ed.* **2017**, *56*, 12783–12787.

[47] a) E. Rivard, *Dalton Trans.* **2014**, *43*, 8577–8586; b) A. Sidiropoulos, C. Jones, A. Stasch, S. Klein, G. Frenking, *Angew. Chem. Int. Ed.* **2009**, *48*, 9701–9704; c) A. V. Pomogaeva, A. M. Belousova, I. V. Kazakov, A. Y. Timoshkin, *Inorg. Chim. Acta* **2024**, *559*, 121785.

[48] a) M. T. Ackermann, M. Seidl, F. Wen, M. J. Ferguson, A. Y. Timoshkin, E. Rivard, M. Scheer, *Chem. Eur. J.* **2022**, *28*, e20210370; b) M. T. Ackermann, M. Seidl, R. Grande, Y. Zhou, M. J. Ferguson, A. Y. Timoshkin, E. Rivard, M. Scheer, *Chem. Sci.* **2023**, *14*, 2313–2317.

[49] M. T. Ackermann, *PhD thesis* **2022**, Universität Regensburg.

[50] J. Sinclair, G. Dai, R. McDonald, M. J. Ferguson, A. Brown, E. Rivard, *Inorg. Chem.* **2020**, *59*, 10996–11008.

[51] a) A. Y. Timoshkin, G. Frenking, *Inorg. Chem.* **2003**, *42*, 60–69; b) A. V. Pomogaeva, M. Scheer, A. Y. Timoshkin, *Chem. Eur. J.* **2018**, *24*, 17046–17054.

[52] a) C. Marquardt, O. Hegen, M. Hautmann, G. Balázs, M. Bodensteiner, A. V. Virovets, A. Y. Timoshkin, M. Scheer, *Angew. Chem. Int. Ed.* **2015**, *54*, 13122–13125; b) A. V. Pomogaeva, A. Y. Timoshkin, *J. Phys. Chem. A* **2021**, *125*, 3415–3424.

[53] M. A. K. Weinhart, *PhD thesis* **2020**, Universität Regensburg.

[54] a) M. Kapitein, M. Balmer, C. von Hänisch, *Z. Anorg. Allg. Chem.* **2016**, *642*, 1275–1281; b) M. Kapitein, M. Balmer, L. Niemeier, C. von Hänisch, *Dalton Trans.* **2016**, *45*, 6275–6281; c) M. Balmer, M. Kapitein, C. von Hänisch, *Dalton Trans.* **2017**, *46*, 7074–7081.

[55] B. Li, S. Bauer, M. Seidl, A. Y. Timoshkin, M. Scheer, *Chem. Eur. J.* **2019**, *25*, 13714–13718.

[56] S. Schneider, S. Ivlev, C. von Hänisch, *Chem. Comm.* **2021**, *57*, 3781–3784.

[57] S. Schneider, C. von Hänisch, *Chem. Commun.* **2022**, *58*, 1522–1525.

[58] S. Schneider, C. Hänisch, *Eur. J. Inorg. Chem.* **2021**, *2021*, 4655–4660.

[59] a) K. Dollberg, S. Schneider, R.-M. Richter, T. Dunaj, C. von Hänisch, *Angew. Chem. Int. Ed.* **2022**, *61*, e202213098; b) K. Dollberg, S. Schneider, C. von Hänisch, *Synlett* **2023**, *34*, 1777–1780; c) J. Du, K. Dollberg, J. A. Seed, A. J. Wooles, C. von Hänisch, S. T. Liddle, *Nature Chem.* **2024**.

[60] E. Amberger, H. Boeters, *Angew. Chem. Int. Ed. Engl.* **1963**, *2*, 686.

[61] a) A. Bücker, C. Wölper, G. Haberhauer, S. Schulz, *Chem. Comm.* **2022**, *58*, 9758–9761; b) C. Ganesamoorthy, C. Helling, C. Wölper, W. Frank, E. Bill, G. E. Cutsail, S. Schulz, *Nat. Comm.* **2018**, *9*, 87; c) S. Ghosh, E. Glöckler, C. Wölper, J. Linders, N. Janoszka, A. H. Gröschel, S. Schulz, *Eur. J. Inorg. Chem.* **2022**, *2022*; d) C. Helling, C. Ganesamoorthy, C. Wölper, S. Schulz, *Dalton Trans.* **2022**, *51*, 2050–2058; e) C. Helling, C. Wölper, Y. Schulte, G. E. Cutsail III, S. Schulz, *Inorg. Chem.* **2019**, *58*, 10323–10332; f) C. Helling, C. Wölper, S. Schulz, *J. Am. Chem. Soc.* **2018**, *140*, 5053–5056; g) C. Helling, C. Wölper, S. Schulz, *Eur. J. Inorg. Chem.* **2020**, *2020*, 4225–4235; h) C. Helling, C. Wölper, S. Schulz, *Dalton Trans.* **2020**, *49*, 11835–11842; i) J. Krüger, C. Ganesamoorthy, L. John, C. Wölper, S. Schulz, *Chem. Eur. J.* **2018**, *24*, 9157–9164; j) J. Krüger, C. Wölper, G. Haberhauer, S. Schulz, *Inorg. Chem.* **2022**, *61*, 597–604; k) J. Krüger, C. Wölper, S. Schulz, *Angew. Chem. Int. Ed.* **2021**, *60*, 3572–3575; l) B. Li, B. L. Geoghegan, H. M. Weinert, C. Wölper, G. E. Cutsail, S. Schulz, *Chem. Comm.* **2022**, *58*, 4372–4375; m) B. Li, C. Wölper, G. Haberhauer, S. Schulz, *Angew. Chem. Int. Ed.* **2021**, *133*, 2014–2019; n) J. Schoening, L. John, C. Wölper, S. Schulz, *Dalton Trans.* **2019**, *48*, 17729–17734; o) M. K. Sharma, P. Dhawan, C. Helling, C. Wölper, S. Schulz, *Chem. Eur. J.* **2022**, *28*, e202200444; p) M. K. Sharma, C. Wölper, G.

Haberhauer, S. Schulz, *Angew. Chem. Int. Ed.* **2021**, *60*, 6784–6790; q) M. K. Sharma, C. Wölper, S. Schulz, *Dalton Trans.* **2022**, *51*, 1612–1616; r) H. M. Weinert, C. Wölper, S. Schulz, *Chem. Sci.* **2022**, *13*, 3775–3786.

[62] a) D. W. N. Wilson, J. Feld, J. M. Goicoechea, *Angew. Chem. Int. Ed.* **2020**, *132*, 21100–21104; b) J. Feld, D. W. N. Wilson, J. M. Goicoechea, *Angew. Chem. Int. Ed.* **2021**, *60*, 22057–22061.

[63] a) H.-W. Wanzlick, H.-J. Schönherr, *Angew. Chem. Int. Ed. Engl.* **1968**, *7*, 141–142; b) K. Öfele, *J. Organomet. Chem.* **1968**, *12*, P42-P43.

[64] A. J. Arduengo, R. L. Harlow, M. Kline, *J. Am. Chem. Soc.* **1991**, *113*, 361–363.

[65] V. Nesterov, D. Reiter, P. Bag, P. Frisch, R. Holzner, A. Porzelt, S. Inoue, *Chem. Rev.* **2018**, *118*, 9678–9842.

[66] C. Romain, S. Bellemin-Laponnaz, S. Dagorne, *Coord. Chem. Rev.* **2020**, *422*, 213411.

[67] M. N. Hopkinson, C. Richter, M. Schedler, F. Glorius, *Nature* **2014**, *510*, 485–496.

[68] a) S. P. Nolan (Hrsg.) *N-heterocyclic carbenes. Effective tools for organometallic synthesis*, Wiley-VCH, Weinheim, **2014**; b) D. J. Nelson, S. P. Nolan, *Chem. Soc. Rev.* **2013**, *42*, 6723–6753; c) S. Díez-González (Hrsg.) *ISSN*, *v.27*, Royal Society of Chemistry, Cambridge, **2017**.

[69] A. J. Arduengo, R. Krafczyk, R. Schmutzler, H. A. Craig, J. R. Goerlich, W. J. Marshall, M. Unverzagt, *Tetrahedron* **1999**, *55*, 14523–14534.

[70] a) V. Lavallo, Y. Canac, C. Präsang, B. Donnadieu, G. Bertrand, *Angew. Chem. Int. Ed.* **2005**, *44*, 5705–5709; b) R. Jazzar, M. Soleilhavoup, G. Bertrand, *Chem. Rev.* **2020**, *120*, 4141–4168; c) S. Kumar Kushvaha, A. Mishra, H. W. Roesky, K. Chandra Mondal, *Chem. Asian J.* **2022**, *17*, e202101301; d) M. Melaimi, R. Jazzar, M. Soleilhavoup, G. Bertrand, *Angew. Chem. Int. Ed.* **2017**, *56*, 10046–10068; e) U. S. D. Paul, U. Radius, *Eur. J. Inorg. Chem.* **2017**, *2017*, 3362–3375; f) M. Soleilhavoup, G. Bertrand, *Acc. Chem. Res.* **2015**, *48*, 256–266.

[71] a) E. Aldeco-Perez, A. J. Rosenthal, B. Donnadieu, P. Parameswaran, G. Frenking, G. Bertrand, *Science* **2009**, *326*, 556–559; b) O. Schuster, L. Yang, H. G. Raubenheimer, M. Albrecht, *Chem. Rev.* **2009**, *109*, 3445–3478.

[72] J. P. Moerdyk, D. Schilter, C. W. Bielawski, *Acc. Chem. Res.* **2016**, *49*, 1458–1468.

[73] S. Díez-González, N. Marion, S. P. Nolan, *Chem. Rev.* **2009**, *109*, 3612–3676.

[74] A. T. Biju, N. Kuhl, F. Glorius, *Acc. Chem. Res.* **2011**, *44*, 1182–1195.

[75] D. Enders, O. Niemeier, A. Henseler, *Chem. Rev.* **2007**, *107*, 5606–5655.

[76] N. Kuhn, A. Al-Sheikh, *Coord. Chem. Rev.* **2005**, *249*, 829–857.

[77] L. Mercs, M. Albrecht, *Chem. Soc. Rev.* **2010**, *39*, 1903–1912.

[78] K. Oisaki, Q. Li, H. Furukawa, A. U. Czaja, O. M. Yaghi, *J. Am. Chem. Soc.* **2010**, *132*, 9262–9264.

[79] K. M. Hindi, M. J. Panzner, C. A. Tessier, C. L. Cannon, W. J. Youngs, *Chem. Rev.* **2009**, *109*, 3859–3884.

[80] a) F. Glorius (Hrsg.) *Topics in Organometallic Chemistry*, Springer Berlin Heidelberg, **2007**; b) F. Glorius in *Topics in Organometallic Chemistry* (Hrsg.: F. Glorius), Springer Berlin Heidelberg, **2007**, S. 1–20; c) W. A. Herrmann, *Angew. Chem. Int. Ed.* **2002**, *41*, 1290–1309; d) W. A. Herrmann, M. Elison, J. Fischer, C. Köcher, G. R. J. Artus, *Angew. Chem. Int. Ed. Engl.* **1995**, *34*, 2371–2374; e) R. H. Grubbs, T. M. Trnka in *Ruthenium in Organic Synthesis* (Hrsg.: S.-I. Murahashi), Wiley-VCH Verlag GmbH & Co. KGaA, Weinheim, FRG, **2004**, S. 153–177; f) Y. Li, F. Kwong, W. Yu, A. Chan, *Coord. Chem. Rev.* **2007**, *251*, 2119–2144; g) C. Chen, F.-S. Liu, M. Szostak, *Chem. Eur. J.* **2021**, *27*, 4478–4499; h) A. Jayaraj, A. V. Raveedran, A. T. Latha, D. Priyadarshini, P. C. A. Swamy, *Coord. Chem. Rev.* **2023**, *478*, 214922; i) F. Wang, L. Liu, W. Wang, S. Li, M. Shi, *Coord. Chem. Rev.* **2012**, *256*, 804–853.

[81] T. Weskamp, W. C. Schattenmann, M. Spiegler, W. A. Herrmann, *Angew. Chem. Int. Ed. Engl.* **1998**, *37*, 2490–2493.

[82] a) P. Schwab, R. H. Grubbs, J. W. Ziller, *J. Am. Chem. Soc.* **1996**, *118*, 100–110; b) M. S. Sanford, M. Ulman, R. H. Grubbs, *J. Am. Chem. Soc.* **2001**, *123*, 749–750; c) S. H. Hong, M. W. Day, R. H. Grubbs, *J. Am. Chem. Soc.* **2004**, *126*, 7414–7415; d) B. F. Straub, *Angew. Chem. Int. Ed.* **2005**, *44*, 5974–5978; e) M. Scholl, T. M. Trnka, J. P. Morgan, R. H. Grubbs, *Tetrahedron Lett.* **1999**, *40*, 2247–2250; f) M. Scholl, S. Ding, C. W. Lee, R. H. Grubbs, *Org. Lett.* **1999**, *1*, 953–956; g) J. Huang, E. D. Stevens, S. P. Nolan, J. L. Petersen, *J. Am. Chem. Soc.* **1999**, *121*, 2674–2678.

[83] I. Hargittai, *Struct. Chem.* **2022**, *33*, 303–305.

2 Research Objectives

This work focusses on the synthesis and reactivity of donor stabilized monomeric pentelyltrielanes containing heavy group 13 elements such as Al, Ga and In on one side, and heavy group 15 elements ranging from phosphorus to bismuth on the other side. Although the chemistry of donor stabilized pnictogenylboranes has been established for years, containing nearly all elements from group 15, the chemistry of the heavier homologs has been in focus only very recently, based on the weak bonding between the heavy group 13 and the group 15 elements.

Based on previous results, a trifold substitution pattern for 13/15 compounds $D{\cdot}\mathrm{E}(Pn\mathrm{H}_2)_3$ (D = donor, E = triel, Pn = pnictogen) is achievable, though so far only known for IDipp·$\mathrm{Ga}(\mathrm{PH}_2)_3$. Key aim of this work is to extend this pattern to other combinations of 13/15 compounds. In this context, the following tasks will be addressed:

- Synthesis and characterization of the whole series of branched IDipp·$\mathrm{E}(Pn\mathrm{H}_2)_3$ with E = B, Al, Ga, In and Pn = P, As
- Investigations on their reactivity such as a possible coordination behaviour or further catenation

The reactivity of the heavier pentelyltrielanes NHC·$\mathrm{EH}_2Pn\mathrm{H}_2$ is so far barely known. In analogy to the reactivity of pnictogenylboranes, cationic chain elongation with a group 13 fragment is desirable, which should give cationic 13/15/13 structural motifs of the heavier homologs. Therefore, it is investigated if the synthesis of these elongated cationic chains is possible, despite the low bonding energies between group 13 and 15 elements:

- Synthesis and characterization of three-membered mixed 13/15 chain compounds $[D{\cdot}\mathrm{GaH}_2Pn\mathrm{H}_2\mathrm{BH}_2{\cdot}D]^+$
- Variation of the attached donor molecules D
- Introduction of organic groups and variation of the central chain motif

Despite being known for decades, donor stabilized pnictogenylboranes have never been classified regarding their donor properties. Thus, a comparison between these classes of compounds including the heavier 13/15 homologs and a comparison with regular phosphines is a desired aim of this work. Specifically, the following methods are applied to categorize the group 13/15 compounds:

- By reaction with $\mathrm{Ni(CO)_4}$, the Tolman Electronic Parameters (TEPs) and Tolman Cone Angles (TCAs) of the compounds are evaluated and the products are characterized according to their steric demand and donor strength.
- The electronic situation is evaluated by quantum chemical calculations.
- With the TEPs and TCAs at hand, a direct comparison towards phosphines as well as superbasic phosphines can be drawn.

With the determination of electronic and steric properties at hand, a suitable reaction scope for extended functionalization of pnictogenylboranes can be set up. Cationic functionalization of donor stabilized pnictogenylboranes has so far been limited to few group 13 and 14 electrophiles. By generating group 13-17 electrophiles *in situ*, the functionalization of pnictogenyboranes could be generalized by reaction with other electrophiles from the *p*-block. The focus lies on obtaining cationic 13/15/14 chain compounds, that contain the heavier group 14 elements as terminal functional groups and exploring their reactivity.

The chemistry of 13/15 compounds containing antimony has been limited due to the extraordinary sensitivity of the compounds towards air, light and temperature. Especially, the parent monomers are difficult to synthesize and characterize. Von Hänisch and co-workers synthesized the novel stibanide reagent K(18c6)SbH_2, which opens up the possibility to directly prepare the parent stibanyltrielanes in one-step salt metathesis reactions, which otherwise might not be obtainable. Thus, this work also considers the exploration of K(18c6)SbH_2 as a useful synthon for the preparation of parent stibanyltrielanes by salt metathesis reactions or anionic 13/15 catenation.

Moreover, the behaviour of donor stabilized phosphanylboranes as Brønsted acids and bases has so far been limited due to decomposition of the substrates upon (de-)protonation. Possibly, with more robust Donor molecules such as NHCs stabilizing the 13/15 monomers, this type of chemistry could be enabled, leading to $[NHC{\cdot}BH_2PH_3]^+$ or $[NHC{\cdot}BH_2PH]^-$, respectively. Hence, these types of conversions are targeted and if successful, the reactivity of these highly reactive moieties is explored.

3 Coordination of Pnictogenylboranes towards Tl(I) salts and a Tl-mediated P-P coupling

R. Szlosek,[+] M. T. Ackermann,[+] C. Marquardt, M. Seidl, A. Y. Timoshkin and M. Scheer

+ These authors contributed equally to this manuscript.

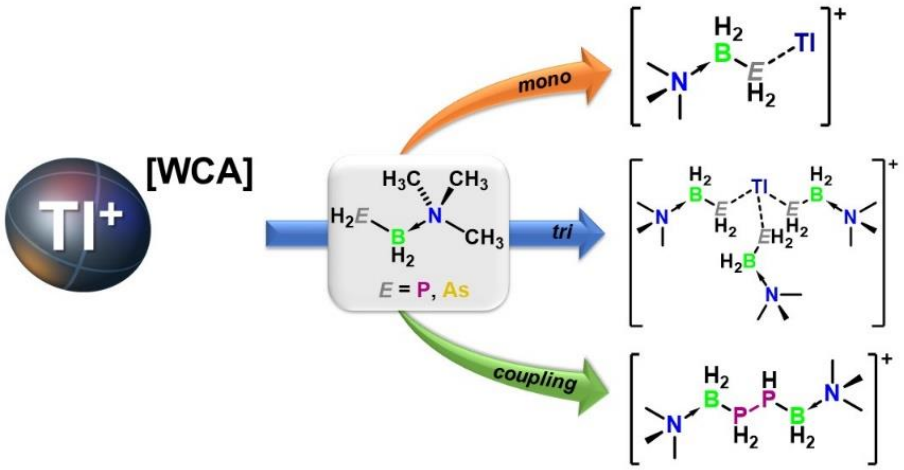

Abstract: The coordination chemistry of only Lewis-base (LB)-stabilized pnictogenylboranes $EH_2BH_2{\cdot}NMe_3$ (E = P, As) towards Tl(I) salts has been studied. The reaction of $Tl[BAr^{Cl}]$ (BAr^{Cl} = $[B(3,5\text{-}C_6H_3Cl_2)_4]^-$) with the corresponding pnictogenylborane results in the formation of $[Tl(EH_2BH_2{\cdot}NMe_3)][BAr^{Cl}]$ (**1a**: E = P; **1b**: E = As). Whereas the Tl(I) ion in **1a/b** is monocoordinated, the exchange of the weakly coordinating anion (WCA) in the Tl(I) salt leads to the formation of a trigonal pyramidal coordination mode at the Tl atom by coordination of three equivalents of $EH_2BH_2{\cdot}NMe_3$ in $[Tl(EH_2BH_2{\cdot}NMe_3)_3][WCA]$ (**2a**: E = P, WCA = TEF^{Cl}; **2b**: E = As, WCA = TEF) (TEF = $[Al\{OC(CF_3)_3\}_4]^-$, TEF^{Cl} = $[Al\{(OC(CF_3)_2(CCl_3)\}_4]^-$). Furthermore, by using two equivalents of $PH_2BH_2{\cdot}NMe_3$, a Tl(I)-mediated P-P coupling takes place in CH_2Cl_2 as solvent resulting in $[Me_3N{\cdot}H_2PH_2PHBH_2{\cdot}NMe_3][WCA]$ (WCA = TEF, **3a**; BAr^{Cl}, **3b**; TEF^{Cl}, **3c**). In contrast, for the arsenic derivatives **1b** and **2b**, no coupling reaction is observed. The underlying chemical processes are elucidated by quantum chemical computations.

3.1 Introduction

The very weak interactions of weakly coordinating anions (WCAs) with their corresponding cations allows to study the pseudo gas phase coordination chemistry of naked cations in the condensed phase, such as monocationic group 13 elements.[1] The first structurally characterized Tl(I)-arene complex was reported in 1985 by Schmidbauer and coworkers.[2] Following this discovery, Tl(I) coordination chemistry received little attention for almost 20 years during which rarely new developments were reported. The years after 2000 marked a turning point in this field of chemistry, as several new Tl(I) complexes were described by different groups. In 2005, Power and coworkers reported on $Tl_2[Ar_2P_4]$ complexes resulting from the reaction between P_4 and $[TlAr_2]$ (Ar = 2,6- diisopropylphenyl).[3] Bochmann and coworkers reported on the first examples of Tl(I)-arene and Tl(I)-diethylether complexes in which no predominant bonding between the employed WCA ($[H_2N\text{-}B(C_6F_5)_3]^-$) and the complex cations $[Tl(arene)_n]^+$ and $[Tl(Et_2O)_4]^+$, respectively, exists.[4] Those missing interactions simplify investigations on the coordination chemistry of the Tl^+ ion. Additionally, the groups of Mindiola and Ozerov prepared a PNP pincer complex of Tl (Figure 3.1, **I**) by reaction of Li(PNP) with Tl(OTf).[5] Simultaneously, our group was able to report the first coordination compounds composed of organometallic polyphosphorus (P_n) complexes and Tl(I) (Figure 3.1, **II**).[6] Previous results have already demonstrated that organometallic P_n ligand complexes represent excellent building blocks for supramolecular assemblies.[7] Subsequently, by using the WCA $[Al\{OC(CF_3)_3\}_4]^-$ (TEF),[8] our group was able to expand the coordination chemistry of P_n ligand complexes from monovalent transition metals (Cu, Ag) to monovalent group 13 metals (Ga, In, Tl).[9] Hereby, several coordination compounds as well as one-dimensional coordination polymers have been obtained.

Moreover, for the first time, Krossing and coworkers introduced the synthesis of univalent gallium and indium phosphine complexes $[M(PR_3)_n]^+$ (M = Ga, In, Tl; Figure 3.1: **IIIa**, **IIIb**).[10,11] The obtained complexes reveal a trigonal-pyramidal coordination at the group 13 metal atom in the solid state for PPh_3, while the increased steric bulk of P^tBu_3 leads to carbene-analogous bis-phosphine complexes.

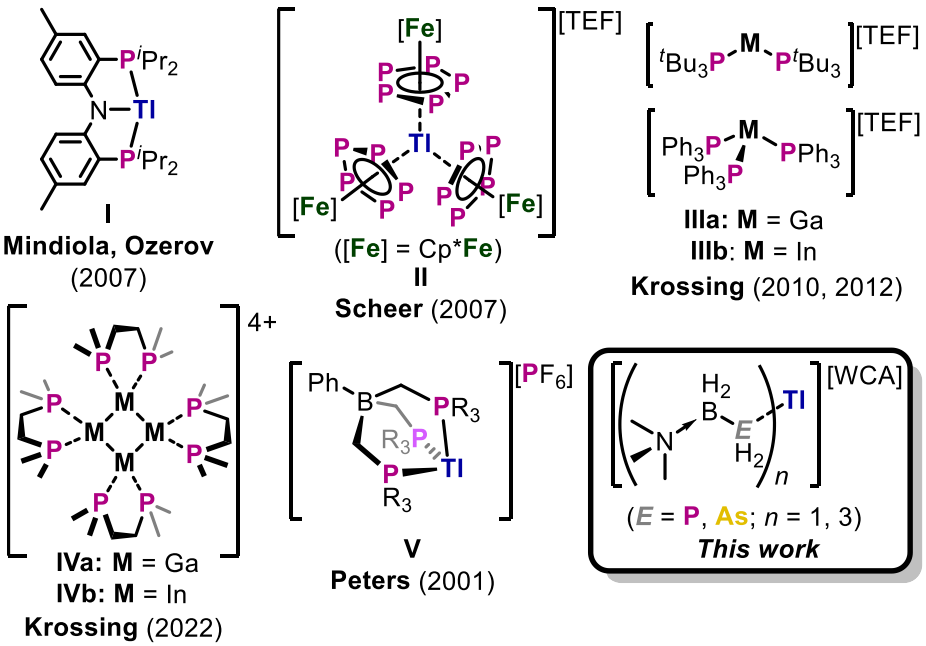

Figure 3.1: Examples of phosphorus-based coordination compounds with low-valent group 13 salts of weakly coordinating anions.

Very recently, Krossing and coworkers also reported on bis(dimethylphosphino)ethane stabilized indium and gallium tetracationic salts (Figure 3.1, **IVa, IVb**).[12] In contrast, no monovalent thallium phosphine complexes have been reported so far. Given the fact that Tl(I) can be considered a rather soft metal, it seems surprising that the number of Tl(I) phosphine adducts is very limited, despite phosphines being very suitable ligands in principle. The first structurally characterized homoleptic phosphine adduct of Tl(I) supported by a tris(phosphino)borate was reported in 2001 by Peters and Botley (Figure 3.1, **V**).[13] Since then, hardly any new Tl(I) phosphine adducts have been published to our knowledge.
Our group has an interest in the synthesis and reactivity of only LB-stabilized 13/15 monomers such as pnictogenylboranes $EH_2BH_2{\cdot}NMe_3$ (E = P, As),[14,15] which are excellent building blocks for the formation of group 13/15 oligomeric and polymeric compounds.[16] In addition, pnictogenylboranes turned out to be excellent donors for transition metal and main group Lewis acids.[14,15,17–20] While cluster formation was observed for reactions with Cu(I) complexes,[18,20] coordination towards Au(I) centers afforded complexes with aurophilic interactions acting as blue-green light emitters.[19] The reaction of phosphanylborane with the early transition metal compound [Cp_2Ti(btmsa)] (btmsa = bis(trimethylsilyl)acetylene) results in dehydrocoupling leading to oligomeric chains stabilized in the coordination sphere of titanium.[21] Therefore, the question arises whether coordination complexes of the main group element Tl(I) with pnictogenylboranes including unknown monocoordinated complexes are achievable and, if so, whether subsequent reactions will occur.
Herein, we report on the synthesis of new Tl(I) salts, the first pnictogenylborane Tl(I) coordination compounds and an unprecedented Tl(I)-mediated P-P coupling. Moreover, the synthesis of novel Tl[WCA] salts and an improved synthetic route of NMe_3-stabilized parent pnictogenylboranes are presented.

3.2 Results and Discussion

To start off our investigations, we evaluated suitable Tl[WCA] salts in the literature. Tl[TEF][22] synthesized earlier by Krossing and coworkers was considered to be an appropriate reagent for our purposes. However, we decided to introduce a larger variety in the substrate scope by having slightly more differences in the steric and the electronic nature of the used WCA. Thus, we prepared Tl[BAr^{Cl}] (BAr^{Cl}=[B(3,5-$C_6H_3Cl_2)_4$]$^-$) and Tl[TEF^{Cl}] (TEF^{Cl}=[Al{(OC(CF_3)$_2$(CCl_3)}$_4$]$^-$) by sonication of a suspension of Na[BAr^{Cl}] or Li[TEF^{Cl}] with TlF in CH_2Cl_2 for 24 h [Eq. (1)]. After subsequent filtration of NaF/LiF, the Tl(I) salts can be isolated as microcrystalline powders and recrystallized for improved purity. Both compounds are obtained as colorless solids in good yields that can be stored under an inert atmosphere for months.

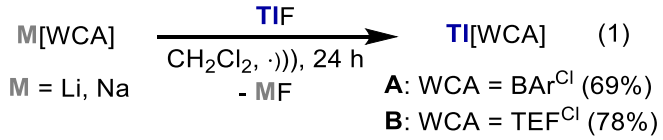

Tl[BAr^{Cl}] (**A**) shows a sharp singlet in the $^{11}B\{^1H\}$ NMR spectrum at -6.39 ppm (CD_3CN) and Tl[TEF^{Cl}] (**B**) a sharp singlet in the $^{19}F\{^1H\}$ NMR spectrum at -68.6 ppm (CD_2Cl_2). **A** and **B** crystallize from CH_2Cl_2/*n*-hexane as colorless plates and blocks in the space groups $P2_1/n$ and *Pbcn*, respectively, and the molecular structures in the solid state were elucidated by single crystal X-ray diffraction (Figure 3.2). The asymmetric units show Tl^+ loosely coordinated to their respective WCA by weak interactions with either aryl groups or halide atoms. The ESI-MS spectra of **A** and **B** show intact [BAr^{Cl}]$^-$ and [TEF^{Cl}]$^-$ anions in the gas phase at *m*/*z* = 594.8 and 1164.5, respectively.

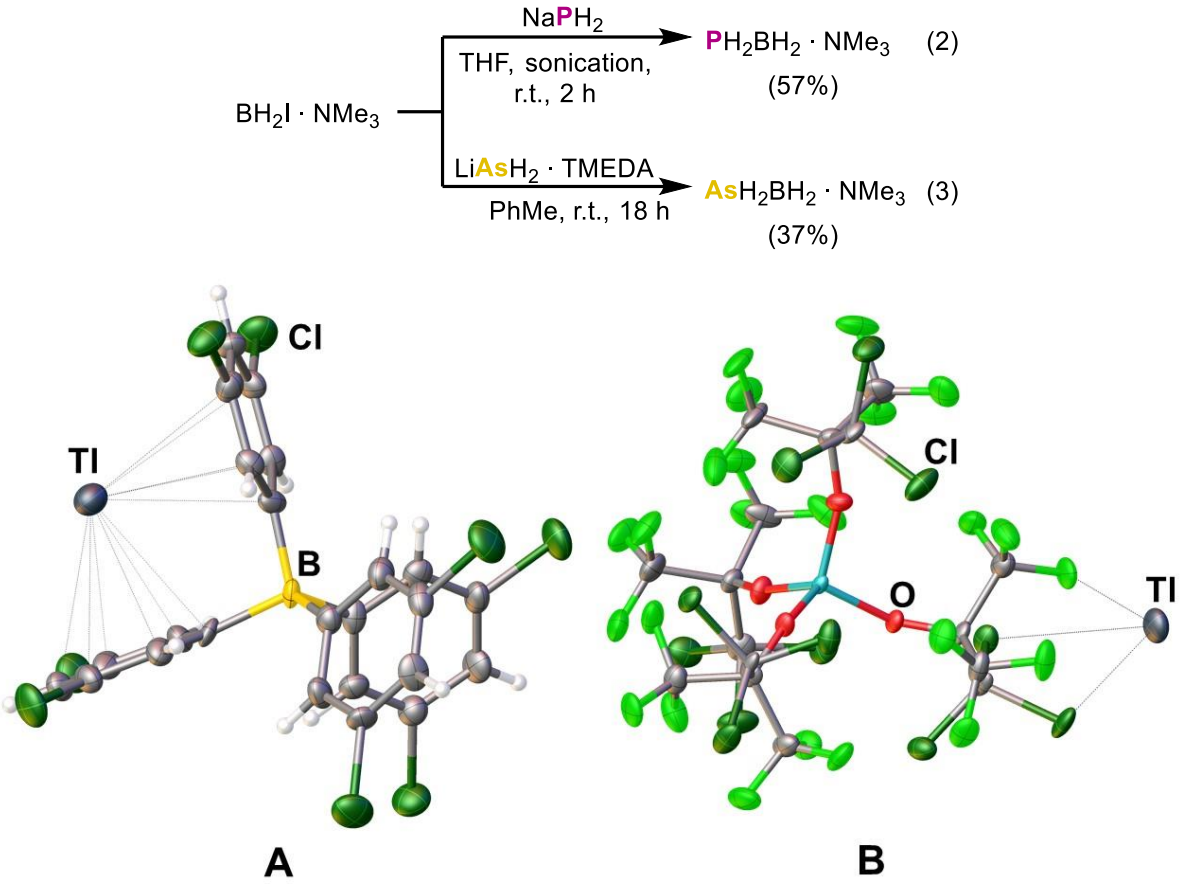

Figure 3.2: Molecular structures of **A** and **B** in the solid state. Anisotropic displacement ellipsoids are shown at 50% probability.

Then, we set out to react **A**, **B** and Tl[TEF] with Lewis base stabilized phosphanyl and arsanylboranes $EH_2BH_2{\cdot}NMe_3$ (E=P, As), which by themselves are usually obtained by salt metathesis of $(Me_3Si)_2ELi{\cdot}THF$ with $BH_2Cl{\cdot}NMe_3$ followed by treatment with MeOH. To avoid this time-consuming and expensive synthetic route, we devised a new, simpler and robust approach of these compounds. By directly employing $NaPH_2$ and $LiAsH_2{\cdot}TMEDA$ in salt metathesis reactions with $BH_2I{\cdot}NMe_3$ [Eqs. (2) and (3)], both arsanyl- and phosphanylboranes $EH_2BH_2{\cdot}NMe_3$ could conveniently be prepared in one-step reactions in yields of 57% (E = P) and 37% (E = As), respectively. With now plentiful starting material available, we performed coordination attempts with Tl[WCA] by adding the pnictogenylboranes either neat or in a solution of toluene to a solution (WCA=TEF, TEF^{Cl}) or suspension (WCA=BAr^{Cl}) of Tl[WCA] in dichloromethane. Reactions of **A** with the corresponding pnictogenylboranes $EH_2BH_2{\cdot}NMe_3$ (E = P, As) in a stoichiometry of 1:1 lead to the monovalent coordination compounds $[Tl(EH_2BH_2{\cdot}NMe_3)][BAr^{Cl}]$ (**1a**: E = P; **1b**: E = As) [Eq. (4)]. Even if the amount of pnictogenylborane was increased, the only isolable products are **1a** and **1b**.

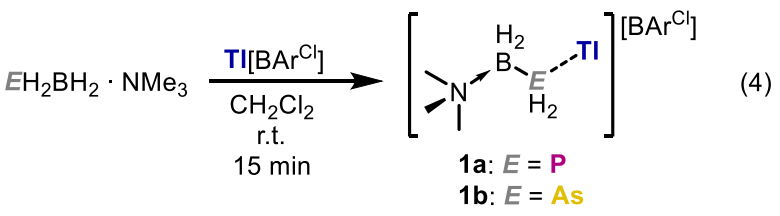

(4)

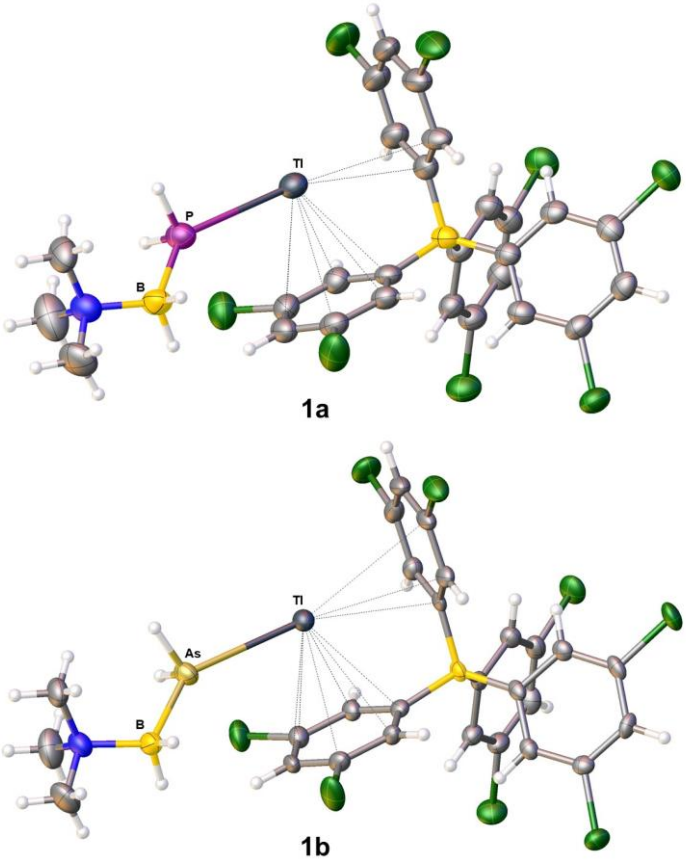

Figure 3.3: Molecular structures of **1a** and **1b** in the solid state. Anisotropic displacement ellipsoids are shown at 50% probability. Selected bond lengths [Å] and angles [°]: **1a**: N-B 1.628(10), B-P 1.960(8), P-Tl 3.0419(15), N-B-P 115.6(5), B-P-Tl 138.6(3). **1b**: N-B 1.616(11), B-As 2.072(9), As-Tl 3.1193(8), N-B-As 115.4(5), B-As-Tl1 143.4(3).

The products are obtained as colorless solids in yields of 80% (**1a**) and 72% (**1b**), respectively, that are stable under inert conditions at room temperature for months. In the ESI-MS spectrum, the molecular ion peaks of **1a** and **1b** were detected at m/z = 310.1 and 354.0, respectively. **1a** displays a significantly downfield shifted triplet in the ^{31}P NMR spectrum at -132.0 ppm ($^{1}J_{HP}$ = 175 Hz, CD_2Cl_2) and a broadened triplet at -8.4 ppm ($^{1}J_{BH}$ = 100 Hz) for the {BH_2} unit in the ^{11}B NMR spectrum, as well as a nonet at -7.1 ppm ($^{1}J_{BH}$ = 3 Hz) from [BAr^{Cl}]$^-$. **1b** shows a broadened triplet at -6.3 ppm ($^{1}J_{BH}$ = 100 Hz, CD_2Cl_2) and a nonet at -7.1 ppm ($^{1}J_{BH}$=3 Hz) in the ^{11}B NMR spectrum. Both **1a** and **1b** crystallize in the monoclinic space group $P2_1/c$ as clear colorless needles and blocks, respectively, from CH_2Cl_2/*n*-hexane (Figure 3.3). The molecular structures show linear coordination modes of one molecule of a pnictogenylborane towards Tl^+ with a bond length of 3.0419(15) Å (E = P) or 3.1193(8) Å (E = As), respectively. The As-Tl distance is slightly elongated compared to the P-Tl bond, as the atomic radius of As is larger. The N-B [**1a**: 1.628(10) Å, **1b**: 1.616(11) Å] and B-E [**1a**: 1.960(8) Å, **1b**: 2.072(9) Å] bonds are within the range of classic single bonds.[14,15] In both compounds, the Tl^+ ion is loosely coordinated by the anion throughout simultaneous interaction with two aryl groups of [BAr^{Cl}]$^-$ in the solid state. These compounds represent the first monovalent phosphine Tl(I) complexes.

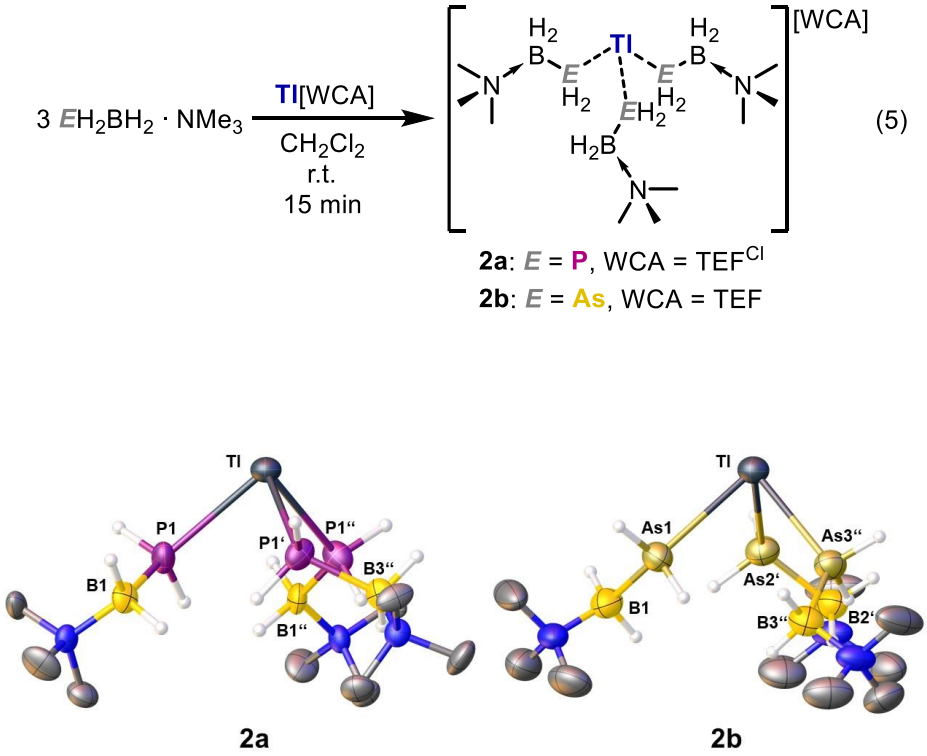

Figure 3.4: Molecular structures of **2a** and **2b** in the solid state. Anisotropic displacement ellipsoids are shown at 50% probability level. Counter ions and hydrogen atoms bound to carbon are omitted for clarity. Selected bond lengths [Å] and angles [°] (primes indicate symmetry-generated parts): **2a**: Tl-P1 2.989(4), P1-B1 1.961(18), P1-Tl-P1' 84.23(5). **2b**: Tl-As1 3.1158(12), As1-B1 2.084(12), As1-Tl-As1' 125.8(4).

After the successful synthesis of **1a** and **1b**, we wondered if it is possible to coordinate several molecules of pnictogenylborane simultaneously to the Tl(I) ion. Therefore, we exchanged $[BAr^{Cl}]^-$ for the even weaker coordinating $[TEF]^-$ and $[TEF^{Cl}]^-$ anions to loosen the ion pair between Tl^+ and the WCA and hence facilitate the coordination of multiple ligands [Eq. (5)]. When three equivalents of $EH_2BH_2{\cdot}NMe_3$ are added to a suspension of the Tl[WCA] salts in CH_2Cl_2, the threefold coordinated Tl(I) pnictogenylborane compounds $[Tl(EH_2BH_2{\cdot}NMe_3)_3][WCA]$ (**2a**: E = P, WCA = TEF^{Cl}; **2b**: E = As, WCA = TEF) are obtained as colorless solids in excellent yields between 74 and 80% [Eq. (5)]. In contrast to the reactions with the $[BAr^{Cl}]^-$ salts (see above), only intractable product mixtures were formed when one equivalent of $EH_2BH_2{\cdot}NMe_3$ was added to the $[TEF]^-$ and $[TEF^{Cl}]^-$ Tl(I) salts. Both **2a** and **2b** can be stored at room temperature under inert atmosphere for months. The ESI-MS spectra of **2a** and **2b** show fragment ion peaks of $[Tl(PH_2BH_2{\cdot}NMe_3)_2]^+/[Tl(PH_2BH_2{\cdot}NMe_3)]^+$ (m/z = 415.1, 310.0) and $[Tl(AsH_2BH_2{\cdot}NMe_3)]^+$ (m/z = 354.0) instead of the molecular ion peaks for **2a** and **2b** due to fragmentation. **2a** displays a broadened triplet in the ^{31}P NMR spectrum at -166.7 ppm ($^1J_{HP}$ = 175 Hz, CD_2Cl_2) and a strongly broadened triplet in the ^{11}B NMR spectrum at -8.0 ppm ($^1J_{HB}$ = 103 Hz, CD_2Cl_2). Similarly, **2b** shows a broadened triplet in the ^{11}B NMR spectrum at -6.5 ppm ($^1J_{BH}$ = 111 Hz, CD_2Cl_2). Single crystals of **2a** and **2b** suitable for diffraction experiments were grown by layering CH_2Cl_2 solutions with *n*-hexane (Figure 3.4). For both compounds, the cation directly resides on a threefold screw axis parallel to the *c* axis in the crystal lattice, resulting in the three coordination arms at Tl^+ to be symmetry equivalent. The interactions between Tl^+ and the WCAs as seen in **1a** and **1b** are not present in this case. **2a** crystallizes in the trigonal space group *R3c* as clear colorless needles. The molecular structure shows a trigonal pyramidal coordination mode of three phosphanylborane molecules to Tl^+ (Figure 3.4, left). The P-Tl bonds are equidistant with 3.002(3) Å and are close to the P-In bonds in $[In(PPh_3)_3]^+$ [2.9645(12)–3.0314(11) Å] due to

similar atomic radii (In: 1.67 Å, Tl: 1.70 Å).[23] They are also slightly elongated compared to $[PhB(CH_2P^iPr_2)_3Tl]^+$ [2.8936(8)–2.9206(9) Å]. The P-B bond length of 1.961(18) Å resembles a classic P-B single bond [cf. $PH_2BH_2{\cdot}NMe_3$: 1.976(2) Å].[15] The P-Tl-P bond angles lie between 82.24(12)° and 86.13(11)° and are considerably smaller than in $[In(PPh_3)_3]^+$ [92.11(3)–95.72(3)°][10] owing to the more pronounced inert pair effect of thallium compared to indium. The P-Tl-P bond angles are also larger in comparison to $[PhB(CH_2PPh_2)_3Tl]^+$ [75.25(2)–77.72(2)°], as the scorpionate ligand introduces a higher steric strain in the backbone of the complex. **2b** crystallizes in the trigonal space group *P*31*c* as clear colorless blocks (Figure 3.4, right). The molecular structure reveals a trigonal pyramidal coordination mode of the three arsanylborane molecules to Tl^+. The As-Tl bonds are equidistant with 3.1158(12) Å, which are elongated compared to **2a** due to the increased atomic radius of As. This is also accompanied by identical As-Tl-As angles of 81.51(4)°, which are slightly shorter than the P-Tl-P angles within **2a**. Accompanying DFT studies (M06-2X/def2-TZVPP, cf. Supporting Information)[24–26] show that the formation of all these complexes is exothermic and exergonic for both phosphanyl- and arsanylborane. The formation of a tight ion pair of $[Tl(EH_2BH_2{\cdot}NMe_3)]^+$ with $[BAr^{Cl}]^-$ is exothermic by 317 kJ mol^{-1} (E = P) and 321 kJ mol^{-1} (E = As), respectively.

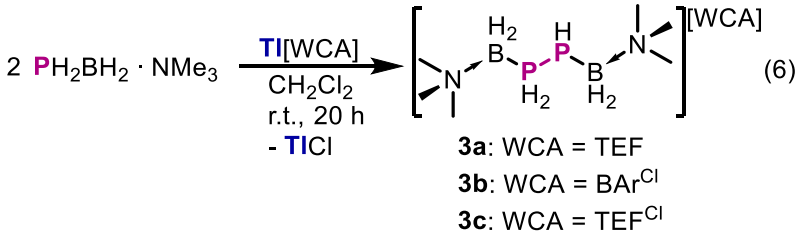

(6)

Although **2b** is stable in solution, according to NMR spectroscopy, **2a** is prone to a side reaction by involvement of CH_2Cl_2 as solvent, which then was investigated thoroughly. The combination of two equivalents of $PH_2BH_2{\cdot}NMe_3$ and a solution of Tl[TEF] in CH_2Cl_2, leads to a white solid which precipitates out of the reaction mixture after stirring overnight [Eq. (6)]. The powder was separated by filtration and identified as TlCl by X-ray powder diffraction (cf. Supporting Information). The soluble product was identified as $[Me_3N{\cdot}BH_2PH_2PHBH_2{\cdot}NMe_3][TEF]$ (**3a**) by multinuclear NMR spectroscopy, featuring a Tl(I)-mediated P-P bond formation. Although Tl(I) salts were used as promotors in Suzuki cross couplings previously, a similar Tl(I) coupling reaction with solvent involvement (see below) has not yet been reported to our knowledge.[27] The $^{31}P\{^1H\}$ NMR spectrum (Figure 3.5) of **3a** shows a broadened doublet of multiplets at -91.3 ppm (^{31}P NMR: broadened and superimposed doublet of triplets, $^1J_{PH}$ = 357 Hz) and a doublet -199.6 ppm (^{31}P NMR: broadened and overlain doublet of doublets, $^1J_{PH}$ = 228 Hz) with coupling constants of $^1J_{PP}$ = 255 Hz and $^1J_{BP}$ = 32 Hz which overall correspond to a $\{PH_2\text{-}PH\}$ structure motif. Furthermore, the coupling between the two signals in the $^{31}P\{^1H\}$ spectrum was confirmed by $^{31}P,^{31}P$ COSY NMR (Figure 3.6). The $^{11}B\{^1H\}$ NMR spectrum of **3a** shows two broadened doublets at -10.7 ppm ($^1J_{BP}$ = 55 Hz) and -6.5 ppm ($^1J_{BP}$ = 32 Hz). These signals are split up upon proton coupling into a very broad triplet ($^1J_{BH}$=120 Hz) and a triplet of doublets ($^1J_{BH}$ = 127 Hz), respectively, thus confirming two separated $\{BH_2\}$ moieties bound to one P atom each. The ESI-MS spectrum of a solution of **3a** shows the molecular ion peak at *m/z* = 209 for $[Me_3N{\cdot}BH_2PH_2PHBH_2{\cdot}NMe_3]^+$ and several fragment peaks at *m/z* = 149 ($[Me_3N{\cdot}H_2BH_2P\text{-}PHBH_2]^+$), 135 ($[Me_3N{\cdot}H_2BH_2P\text{-}PH]^+$) and 104 ($[Me_3N{\cdot}H_2BPH]^+$).

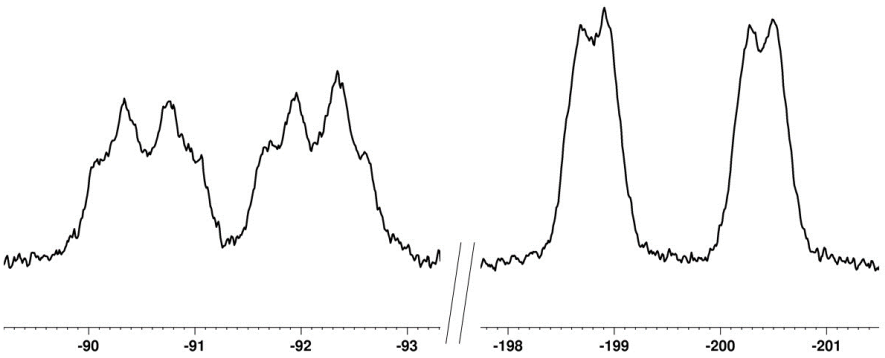

Figure 3.5: Sections of the $^{31}P\{^{1}H\}$ NMR spectrum of **3a** (298 K, CD_2Cl_2).

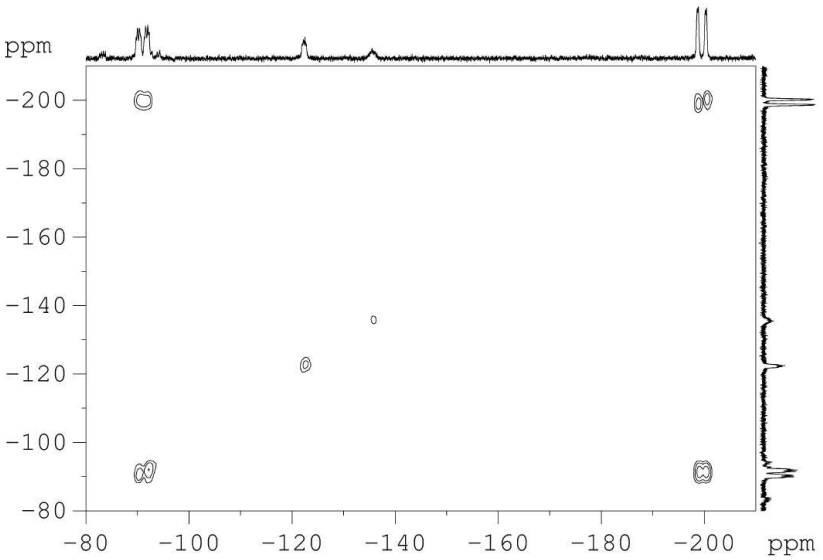

Figure 3.6: ^{31}P, ^{31}P COSY NMR spectrum of **3a** highlighting the coupling between the two signals (298 K, CD_2Cl_2).

Although the compound could be crystallized by solvent diffusion, crystallographic characterization was unsuccessful, as only the anion of **3a** can be refined properly. Analogous reactions [Eq. (6)] with **A** and **B** led to the same results (**3b**, **3c**) as could easily be confirmed by NMR spectroscopy. Still, even with different WCAs, the crystallographic determination of the solid state structure of $[Me_3N{\cdot}BH_2PH_2\text{-}PHBH_2{\cdot}NMe_3]^+$ was unfortunately not possible. To further investigate the influence of the solvent, CH_2Cl_2 was exchanged for 1,2-difluorobenzene and the reaction was repeated. No precipitate was observed in this case after prolonged stirring. According to $^{31}P\{^{1}H\}$ NMR spectroscopy data, the P-P coupling was indeed prevented and instead a highly broadened singlet at -143.0 ppm ($w_{1/2}$ = 69 Hz) was found. As the chemical shift for this species lies in between **1a** (-132.0 ppm) and **2a** (-166.3 ppm), it seems likely that the twofold coordinated compound $[Tl(PH_2BH_2{\cdot}NMe_3)_2]^+$ was formed. Unfortunately, the structure determination by X-ray crystallography was not possible due to the poor diffraction of any grown crystalline samples. The ESI-MS spectrum of this solution shows the coordination compounds $[Tl(PH_2BH_2{\cdot}NMe_3)]^+$ (m/z = 310.09) and $[Tl(PH_2BH_2{\cdot}NMe_3)_2]^+$ (m/z = 415.2). Interestingly, the molecular ion peak of the coupling product **3a** can also be detected at m/z = 209.20, which is probably a result of fragmentation and recombination in the mass spectrometer as no sign of **3a** was detected in the NMR spectra. Other test reactions with different Tl^+ salts (e. g. $Tl[PF_6]$) were unsuccessful, highlighting the importance of the employed WCAs in this coupling reaction.

In this context, we wondered if it might be possible to induce the P-P coupling with an abstracting agent other than Tl^+. Thus, we exposed two equivalents of phosphanylborane to $[Ph_3C][TEF]$[28] in CH_2Cl_2 [Eq. (7)]. The ^{31}P NMR spectrum of the reaction mixture shows several broadened signals, including unreacted $Me_3N{\cdot}BH_2PH_2$, the known cationic 13/15/13 chain compound $[Me_3N{\cdot}BH_2PH_2BH_2{\cdot}NMe_3]^+$ (135.5 ppm, t, $^1J_{HP}$ = 354 Hz)[29] and a very sharp triplet at -70.0 ppm ($^1J_{HP}$ = 192 Hz), which is very likely caused by a $\{PH_2\}$ moiety that is not bound to a boron nucleus such as Ph_3CPH_2. After work-up and crystallization from CH_2Cl_2/*n*-hexane, a clean inseparable mixture of the compound $[Me_3N{\cdot}BH_2PH_2BH_2{\cdot}NMe_3]^+$ and another ionic product remained, which could be identified as $[Me_3N{\cdot}BH_2PH_2CPh_3][TEF]$ (**4**) by Xray structure analysis (see below).

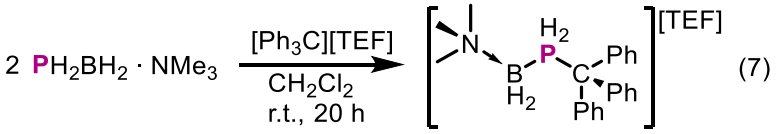

4

The NMR data of the crystals also show that **4** represents the minor part of the crystalline product (~34%), which is less than in the reaction mixture (~71%). Overall, these observations indicate that **4** decomposes slowly in solution in the presence of an excess of phosphanylborane to give *in situ* $[Me_3N{\cdot}BH_2][TEF]$, which is easily attacked by $Me_3N{\cdot}BH_2PH_2$. Hence, the P-P coupling observed previously remains unique to reactions with Tl[WCA], so far. The ESI-MS spectrum of the crystals of **4** shows the molecular ion peaks of $[Me_3N{\cdot}BH_2PH_2CPh_3]^+$ (m/z = 348.2), $[Ph_3C]^+$ (m/z = 243.1) and $[Me_3N{\cdot}BH_2PH_2BH_2{\cdot}NMe_3]^+$ (m/z = 177.2). Single crystals of **4** suitable for single crystal X-ray diffraction experiments were grown by layering a solution of **4** in CH_2Cl_2 with *n*-hexane at 8°C (Figure 3.7).

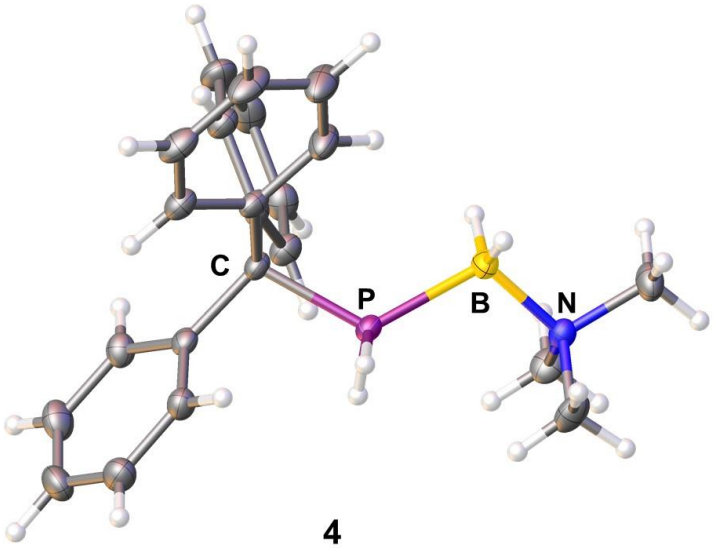

4

Figure 3.7: Molecular structure of **4** in the solid state. Anisotropic displacement ellipsoids are shown at 50% probability level. The counter ion is omitted for clarity. Selected bond lengths [Å] and angles [°]: N-B 1.603(3), B-P 1.977(2), P-C 1.8842(19), N-B-P 110.80(14), B-P-C 120.87(9).

The compound crystallizes as large clear colorless prisms in the monoclinic space group *C*2/*c*. The CPBN chain adopts a zigzag geometry with all bond distances (cf. Figure 3.7) within regular single bond lengths for the respective interelement bonding and a CP-BN torsion angle of -155.7365(7)°. The substituents on the core motif are arranged in regular tetrahedral geometries.

To gain insight into this reaction behavior, quantum chemical calculations on possible reaction pathways were performed (M06-2X/def2-TZVPP).[24–26] Initially, a stepwise mechanism was considered

starting with proton abstraction from $PH_2BH_2{\cdot}NMe_3$ by for example $[CH_2Cl]^+$, potentially leading to in situ formed $[PHBH_2{\cdot}NMe_3]^+$ or $[PH_2BH{\cdot}NMe_3]^+$ which could then undergo addition to a second molecule of phosphanylborane (Scheme 3.1, black pathway). Upon geometry optimization, the structures of $[EHBH_2{\cdot}NMe_3]^+$ (E = P, As, C_S point group) turned out to be transition states with respect to the H atom transfer from B to the P center. Optimization without symmetry constraints results in asymmetric $[EH_2BH{\cdot}NMe_3]^+$ cations which are by 148 kJ mol^{-1} (E = P) and 84 kJ mol^{-1} (E = As) lower in energy than corresponding $[EHBH_2{\cdot}NMe_3]^{+\neq}$ transition states. Therefore, two types of addition products were considered: one containing an E-E bond, formally originating from the nucleophilic attack of $EH_2BH_2{\cdot}NMe_3$ at the $[EHBH_2{\cdot}NMe_3]^{+\neq}$ cation and the alternative isomer with a second E-B bond, originating from the nucleophilic attack at the $[EH_2BH{\cdot}NMe_3]^+$ cation. Optimized structures and relative energies of isomers are given in the Supporting Information. It turned out that both isomers (indicated as EE-isomer and EB-isomer) are true minima on the potential energy surface and, in case of E = P, the PB-isomer is by 6.3 kJ mol^{-1} lower in energy than the PP-isomer. In contrast, for E = As, the AsAs-isomer is by 15.8 kJ mol^{-1} lower in energy than the AsB-isomer due to the weaker donor ability of As compared to P. The calculated results for a stepwise mechanism oppose the experimental findings, as exclusively the PP-isomer was observed and the coupling did not take place in case of $AsH_2BH_2{\cdot}NMe_3$, even though the process is exergonic.

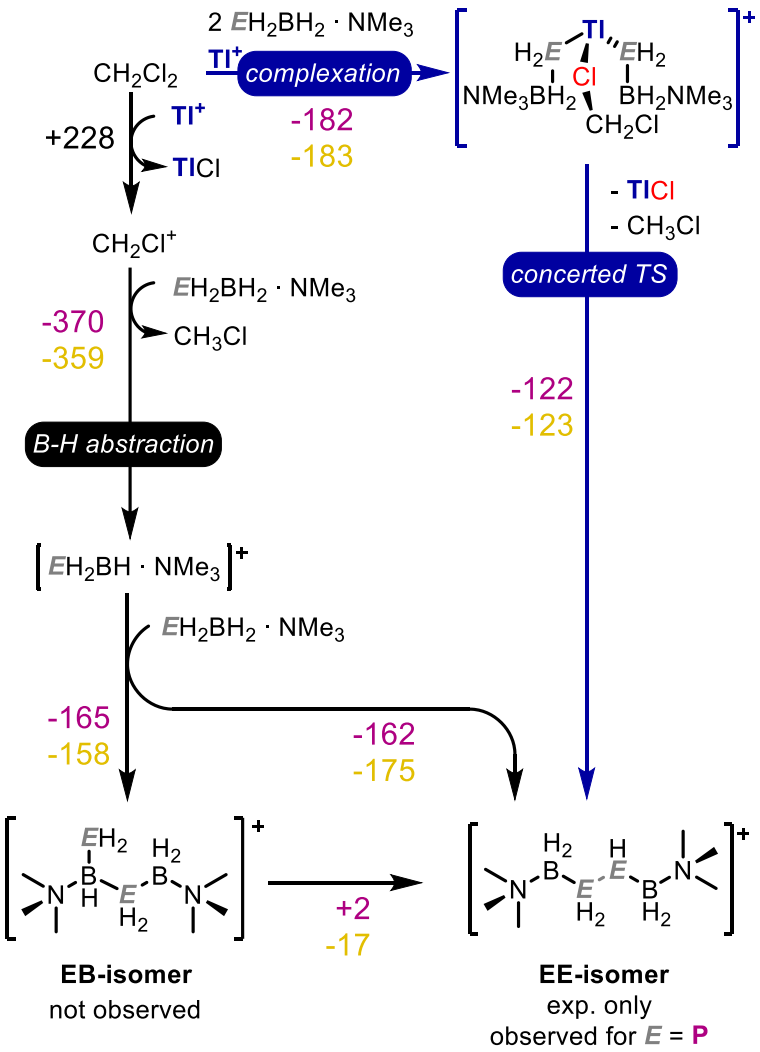

Scheme 3.1: Schematic representation of possible mechanisms towards the coupling of pnictogenylboranes by H-atom abstraction (black arrows) or complexation (blue arrows) (M06-2X/def2-TZVPP). Values represent calculated reaction Gibbs Free Energies $\Delta_R G°_{298}$ in kJ mol^{-1} (yellow: E = As, purple: E = P).

This finding suggests that more likely a complex, concerted mechanism at the Tl^+ ion takes place rather than the calculated stepwise formation. One possibility is the simultaneous coordination in situ of two pnictogenylboranes and one molecule of CH_2Cl_2 (Scheme 3.1, blue pathway), forming the complex $[Tl(EH_2BH_2{\cdot}NMe_3)_2(CH_2Cl_2)]^+$ which then undergoes the coupling reaction in case of E = P. And indeed, the formation of $[Tl(EH_2BH_2{\cdot}NMe_3)_2(CH_2Cl_2)]^+$ is exergonic in both cases. Even the pathway leading to the coupling products is predicted to be highly exergonic at room temperature. Although it was not possible to locate the corresponding transition states, it is likely that the activation barrier for the P-P coupling is low enough to proceed smoothly, while any As-As coupling is kinetically hindered in contrast. Moreover, the formation of $[Tl(EH_2BH_2{\cdot}NMe_3)_2(CH_2Cl_2)]^+$ is likely to be prevented when a stronger coordinating anion such as $[PF_6]^-$ is used, which could explain the absence of the P-P coupling in this case.[30]

3.3 Conclusion

In summary, we were able to synthesize unprecedented coordination products of pnictogenylboranes and Tl(I) salts of weakly coordinating anions. At a stoichiometry of 1:1, the monovalent complexes $[Tl(EH_2BH_2{\cdot}NMe_3)][BAr^{Cl}]$ (**1a**: E = P; **1b**: E = As) were obtained and fully characterized, which represent unprecedented examples of monovalent Tl(I) phosphine/arsine complexes. By variation of the anion towards even looser interactions with the cation, we were also able to isolate and characterize the threefold coordinated Tl(I) compounds $[Tl(EH_2BH_2{\cdot}NMe_3)_3][WCA]$ (**2a**: E = P, WCA = TEF^{Cl}; **2b**: E = As, WCA = TEF). Surprisingly, when two equivalents of phosphanylborane were used for those reactions, an intriguing coupling reaction involving CH_2Cl_2 took place under elimination of TlCl, leading to $[Me_3N{\cdot}BH_2PH_2PHBH_2{\cdot}NMe_3][WCA]$ (WCA = TEF, **3a**; BAr^{Cl}, **3b**; TEF^{Cl}, **3c**) as characterized by multinuclear NMR spectroscopy. The coupling reaction itself does not take place when CH_2Cl_2 as solvent is replaced with a different solvent such as 1,2-difluorobenzene. Reaction with the H-atom abstractor $[Ph_3C][TEF]$ exclusively led to the coordination compound $[Me_3N{\cdot}BH_2PH_2CPh_3][TEF]$ (**4**), representing a unique cationic 13/15/14 chain compound. Computational studies on the P-P coupling reaction show that, very likely, a sophisticated concerted mechanism takes place, as stepwise H-atom abstraction would rather lead to a different isomer with the formation of an additional P-B bond. During these investigations, the synthesis of novel Tl[WCA] salts $Tl[BAr^{Cl}]$ (**A**) and $Tl[TEF^{Cl}]$ (**B**) was developed and the synthetic approach towards the Lewis base-stabilized pnictogenylboranes $EH_2BH_2{\cdot}NMe_3$ (E =P, As) was further improved by using reactions of $NaPH_2$ and $LiAsH_2{\cdot}TMEDA$ with $IBH_2{\cdot}NMe_3$, enabling future investigations on the reactivity of these compounds on a much broader scale.

3.4 References

[1] a) T. A. Engesser, M. R. Lichtenthaler, M. Schleep, I. Krossing, *Chem. Soc. Rev.* **2016**, *45*, 789–899; b) I. Krossing, I. Raabe, *Angew. Chem.* **2004**, *116*, 2116–2142; *Angew. Chem. Int. Ed.* **2004**, *43*, 2066-2090; c) I. Krossing, I. Raabe, *Angew. Chem. Int. Ed.* **2004**, *43*, 2066–2090; *Angew. Chem.* **2004**, *116*, 2116; d) I. Krossing, I. Raabe, *Chem. Eur. J.* **2004**, *10*, 5017–5030; e) I. Krossing, A. Reisinger, *Coord. Chem. Rev.* **2006**, *250*, 2721–2744; f) I. M. Riddlestone, A. Kraft, J. Schaefer, I. Krossing, *Angew. Chem. Int. Ed.* **2018**, *57*, 13982–14024; g) M. R. Rosenthal, *J. Chem. Educ.* **1973**, *50*, 331–335; h) S. H. Strauss, *Chem. Rev.* **1993**, *93*, 927–942.

[2] H. Schmidbaur, W. Bublak, J. Riede, G. Müller, *Angew. Chem. Int. Ed.* **1985**, *24*, 414–415.

[3] a) A. R. Fox, R. J. Wright, E. Rivard, P. P. Power, *Angew. Chem. Int. Ed.* **2005**, *44*, 7729–7733; b) R. J. Wright, A. D. Phillips, S. Hino, P. P. Power, *J. Am. Chem. Soc.* **2005**, *127*, 4794–4799.

[4] a) Y. Sarazin, D. L. Hughes, N. Kaltsoyannis, J. A. Wright, M. Bochmann, *J. Am. Chem. Soc.* **2007**, *129*, 881–894; b) Y. Sarazin, N. Kaltsoyannis, J. A. Wright, M. Bochmann, *Organometallics* **2007**, *26*, 1811–1815.

[5] J. C. DeMott, F. Basuli, U. J. Kilgore, B. M. Foxman, J. C. Huffman, O. V. Ozerov, D. J. Mindiola, *Inorg. Chem.* **2007**, *46*, 6271–6276.

[6] S. Welsch, L. J. Gregoriades, M. Sierka, M. Zabel, A. V. Virovets, M. Scheer, *Angew. Chem. Int. Ed.* **2007**, *46*, 9323–9326; *Angew. Chem.* **2007**, *119*, 9483-9487.

[7] a) E. V. Peresypkina, A. V. Virovets, M. Scheer, *Coord. Chem. Rev.* **2021**, *446*, 213995; b) J. Bai, A. V. Virovets, M. Scheer, *Science* **2003**, *300*, 781–783; c) A. V. Virovets, E. Peresypkina, M. Scheer, *Chem. Rev.* **2021**, *121*, 14485–14554.

[8] I. Krossing, *Chem. Eur. J.* **2001**, *7*, 490–502.

[9] a) M. Fleischmann, S. Welsch, H. Krauss, M. Schmidt, M. Bodensteiner, E. V. Peresypkina, M. Sierka, C. Gröger, M. Scheer, *Chem. Eur. J.* **2014**, *20*, 3759–3768; b) S. Welsch, M. Bodensteiner, M. Dušek, M. Sierka, M. Scheer, *Chem. Eur. J.* **2010**, *16*, 13041–13045.

[10] A. Higelin, U. Sachs, S. Keller, I. Krossing, *Chem. Eur. J.* **2012**, *18*, 10029–10034.

[11] J. M. Slattery, A. Higelin, T. Bayer, I. Krossing, *Angew. Chem. Int. Ed.* **2010**, *49*, 3228–3231; *Angew. Chem.* **2010**, *122*, 3297-3301.

[12] A. Barthélemy, H. Scherer, I. Krossing, *Chem. Eur. J.* **2022**, *28*, e202201369.

[13] T. A. Betley, J. C. Peters, *Inorg. Chem.* **2003**, *42*, 5074–5084.

[14] C. Marquardt, A. Adolf, A. Stauber, M. Bodensteiner, A. V. Virovets, A. Y. Timoshkin, M. Scheer, *Chem. Eur. J.* **2013**, *19*, 11887–11891.

[15] K.-C. Schwan, A. Y. Timoskin, M. Zabel, M. Scheer, *Chem. Eur. J.* **2006**, *12*, 4900–4908.

[16] a) M. Bodensteiner, A. Y. Timoshkin, E. V. Peresypkina, U. Vogel, M. Scheer, *Chem. Eur. J.* **2013**, *19*, 957–963; b) C. Marquardt, T. Jurca, K.-C. Schwan, A. Stauber, A. V. Virovets, G. R. Whittell, I. Manners, M. Scheer, *Angew. Chem. Int. Ed.* **2015**, *54*, 13782–13786; *Angew. Chem.* **2015**, *127*, 13986-13991; c) C. Thoms, C. Marquardt, A. Y. Timoshkin, M. Bodensteiner, M. Scheer, *Angew. Chem.* **2013**, *125*, 5254–5259; *Angew. Chem. Int. Ed.* **2013**, *52*, 5150-5154.

[17] a) A. Adolf, M. Zabel, M. Scheer, *Eur. J. Inorg. Chem.* **2007**, *2007*, 2136–2143; b) C. Marquardt, T. Kahoun, J. Baumann, A. Y. Timoshkin, M. Scheer, *Z. Anorg. Allg. Chem.* **2017**, *643*, 1326–1330; c) M. Elsayed Moussa, C. Marquardt, O. Hegen, M. Seidl, M. Scheer, *New J. Chem.* **2021**, *45*, 14916–14919; d) F. Lehnfeld, M. Seidl, A. Y. Timoshkin, M. Scheer, *Eur. J. Inorg. Chem.* **2022**, *2022*, e202100930.

[18] K.-C. Schwan, A. Adolf, M. Bodensteiner, M. Zabel, M. Scheer, *Z. Anorg. Allg. Chem.* **2008**, *634*, 1383–1387.

[19] J. Braese, A. Schinabeck, M. Bodensteiner, H. Yersin, A. Y. Timoshkin, M. Scheer, *Chem. Eur. J.* **2018**, 10073–10077.

[20] M. Elsayed Moussa, J. Braese, C. Marquardt, M. Seidl, M. Scheer, *Eur. J. Inorg. Chem.* **2020**, *2020*, 2501–2505.

[21] C. Thoms, C. Marquardt, A. Y. Timoshkin, M. Bodensteiner, M. Scheer, *Angew. Chem. Int. Ed.* **2013**, *52*, 5150–5154; *Angew. Chem.* **2013**, *125*, 5254-5259.

[22] M. Gonsior, I. Krossing, N. Mitzel, *Z. Anorg. Allg. Chem.* **2002**, 1821–1830.

[23] A. F. Holleman, E. Wiberg, N. Wiberg, *Lehrbuch der Anorganischen Chemie,* 102. Aufl., W. De Gruyter, Berlin, New York, **2007**.

[24] Gaussian 16, Revision C.01, M. J. Frisch, G. W. Trucks, H. B. Schlegel, G. E. Scuseria, M. A. Robb, J. R. Cheeseman, G. Scalmani, V. Barone, G. A. Petersson, H. Nakatsuji, X. Li, M. Caricato, A. V. Marenich, J. Bloino, B. G. Janesko, R. Gomperts, B. Mennucci, H. P. Hratchian, J. V. Ortiz, A. F. Izmaylov, J. L. Sonnenberg, D. Williams-Young, F. Ding, F. Lipparini, F. Egidi, J. Goings, B. Peng, A. Petrone, T. Henderson, D. Ranasinghe, V. G. Zakrzewski, J. Gao, N. Rega, G. Zheng, W. Liang, M. Hada, M. Ehara, K. Toyota, R. Fukuda, J. Hasegawa, M. Ishida, T. Nakajima, Y. Honda, O. Kitao, H. Nakai, T. Vreven, K. Throssell, J. A. Montgomery, Jr., J. E. Peralta, F. Ogliaro, M. J. Bearpark, J. J. Heyd, E. N. Brothers, K. N. Kudin, V. N. Staroverov, T. A. Keith, R. Kobayashi, J. Normand, K. Raghavachari, A. P. Rendell, J. C. Burant, S. S. Iyengar, J. Tomasi, M. Cossi, J. M. Millam, M. Klene, C. Adamo, R. Cammi, J. W. Ochterski, R. L. Martin, K. Morokuma, O. Farkas, J. B. Foresman, and D. J. Fox, Gaussian, Inc., Wallingford CT, **2016**.

[25] F. Weigend, R. Ahlrichs, *Phys. Chem. Chem. Phys.* **2005**, *7*, 3297–3305.

[26] Y. Zhao, D. G. Truhlar, *Theor. Chem. Acc.* **2008**, *120*, 215–241.

[27] a) S. A. Frank, H. Chen, R. K. Kunz, M. J. Schnaderbeck, W. R. Roush, *Org. Lett.* **2000**, *2*, 2691–2694; b) M. Sato, N. Miyaura, A. Suzuki, *Chem. Lett.* **1989**, *18*, 1405–1408.

[28] I. Krossing, H. Brands, R. Feuerhake, S. Koenig, *J. Fluor. Chem.* **2001**, *112*, 83–90.

[29] C. Marquardt, C. Thoms, A. Stauber, G. Balázs, M. Bodensteiner, M. Scheer, *Angew. Chem. Int. Ed.* **2014**, *53*, 3727–3730.

[30] A different pathway to the P-P coupling could potentially proceed via *β*-hydrogen elimination from $[Tl(PH_2BH_2{\cdot}NMe_3)_2][WCA]$ leading to *in situ* formed $TlH(PH_2BH_2{\cdot}NMe_3)$. Subsequent reactivity with $PH_2BH_2{\cdot}NMe_3$ could then lead to **3a**-**3c**.

3.5 Supporting Information

3.5.1 Experimental Section

General Information: All reactions were performed under an atmosphere of dry argon using standard glove box and Schlenk techniques. All solvents are degassed and purified by standard procedures. Prior to use, solvents were purified using an MBraun SPS-800 solvent purification system and degassed at room temperature. The NMR spectra were recorded on a Bruker Avance 400 spectrometer (^{1}H: 400.13 MHz, ^{31}P: 161.976 MHz, ^{11}B: 128.378 MHz) with δ [ppm] referenced to external $SiMe_4$ (^{1}H), H_3PO_4 (^{31}P), $BF_3 \cdot Et_2O$ (^{11}B). Mass spectra were recorded on a ThermoQuest Finnigan TSQ 7000 (ESI-MS) or a Waters/Micromass ESI LCT-TOF spectrometer (ESI-MS) by the in-house facility. Elemental analyses were determined with a Vario micro cube apparatus by the in-house facility.

The compounds $Li[TEF^{Cl}]$[1], $IBH_2 \cdot NMe_3$,[2] $NaPH_2$,[3] $LiAsH_2(tmeda)$[4] and $Na[BAr^{Cl}]$[5] were prepared according to literature procedures. $[Ph_3C][TEF]$[6] and Tl[TEF][7] were provided by the Scheer group (special thanks to Christoph Riesinger; both compounds were prepared according to the given literature procedures). The improved synthesis of $H_2PH_2B \cdot NMe_3$ was performed with $IBH_2 \cdot NMe_3$ instead of $ClBH_2 \cdot NMe_3$, due to easier availability and improved reaction behaviour compared to $ClBH_2 \cdot NMe_3$.

3.5.1.1 Synthesis of $H_2PBH_2 \cdot NMe_3$

A solution of $IBH_2 \cdot NMe_3$ (9.950 g, 50.00 mmol) in 20 mL tetrahydrofuran is added to a suspension of $NaPH_2$ (2.800 g, 50.00 mmol) in 20 mL toluene at -80 °C. The suspension is sonicated for two hours, and the resulting mixture is filtered over diatomaceous earth. Afterwards, all volatiles are removed in vacuo. By using a condensation bridge, $H_2PBH_2 \cdot NMe_3$ is condensed at 65-70 °C under reduced pressure. $H_2PBH_2 \cdot NMe_3$ forms an emulsion with *n*-hexane. The product can be isolated by decanting the supernatant at 0 °C. Further purification could be achieved by repeated crystallization from *n*-hexane. Yield of $H_2PBH_2 \cdot NMe_3$: 3.010 g (57%). Analytical data agree with the previously published results.[8]

3.5.1.2 Synthesis of $H_2AsBH_2 \cdot NMe_3$

A solution of $IBH_2 \cdot NMe_3$ (120 mg, 0.60 mmol) in 5 mL toluene is added to a suspension of $LiAsH_2 \cdot TMEDA$ in 5 mL toluene at room temperature. The solution is stirred for 18 hours, then all volatiles are removed in vacuo. By using a condensation bridge, $H_2AsBH_2 \cdot NMe_3$ is condensed at 45-50 °C under reduced pressure ($1 \cdot 10^{-3}$ mbar). Further purification could be achieved by crystallization from *n*-hexane at -30 °C. Yield of crystalline $H_2AsBH_2 \cdot NMe_3$: 33 mg (37%). Analytical data agree with the previously published results.[9]

3.5.1.3 Synthesis of Tl[BAr^{Cl}] (A)

A suspension of Na[BAr^{Cl}] (432 mg, 0.70 mmol) and TlF (156 mg, 0.70 mmol) in 50 mL CH_2Cl_2 was sonicated for 24 h. Afterwards the reaction mixture was filtered over diatomaceous earth. Subsequently, all volatiles were removed under reduced pressure, the remaining white solid washed with *n*-hexane (3x10 mL) and dried under vacuum. Tl[BAr^{Cl}] (**A**) was obtained as a crystalline solid of colorless needles at room temperature. Crystals suitable for single crystal X-ray structure analysis have been obtained by storing of a concentrated solution of **A** in CH_2Cl_2 at room temperature. Yield of **A**: 384 mg (69%).

^{1}H NMR (CD_3CN, 25 °C): δ = 6.98-7.09 (m).

^{11}B NMR (CD_3CN, 25 °C): δ = -6.4 (n, $^3J_{B,H}$ = 3 Hz).

^{11}B{^{1}H} NMR (CD_3CN, 25 °C): δ = -6.4 (s).

ESI-MS (MeCN): *m/z* = 594.8 (100%, [BAr^{Cl}]$^-$).

Elemental analysis (%) calculated for $C_{24}H_{12}BCl_8Tl(CH_2Cl_2)_{0.5}$ (**A**$(CH_2Cl_2)_{0.5}$): C: 34.96, H: 1.56; found: C: 34.80, H: 1.78.

3.5.1.4 Synthesis of Tl[TEF^{Cl}] (B)

A suspension of Li[TEF^{Cl}] (1.00 g, 0.86 mmol) and TlF (192 mg, 0.86 mmol) in 50 mL CH_2Cl_2 was sonicated for 24 h. Afterwards, the reaction mixture was filtered over diatomaceous earth. Subsequently, all volatiles were removed under reduced pressure, the remaining white solid washed with *n*-hexane (3x10 mL) and dried under vacuum. Tl[TEF^{Cl}] (**1**) was obtained as a white powder at room temperature. Single crystals of **B** suitable for X-ray diffractions have been obtained by dissolving a small amount of **B** in CH_2Cl_2 and layering the solution with sixfold amount of *n*-hexane and storing at -28 °C. Yield of **B**: 911 mg (78%).

^{19}F NMR (CD_2Cl_2, 25 °C): δ = –68.6 (s).

^{19}F{^{1}H} NMR (CD_2Cl_2, 25 °C): δ = –68.6 (s).

ESI-MS (MeCN): *m/z* = 1164.5 (100%, [TEF^{Cl}]$^-$).

Elemental analysis (%) calculated for $C_{16}AlCl_{12}F_{24}O_4Tl$: C: 14.04; found: C: 14.10.

3.5.1.5 Synthesis of [Tl(H_2PBH_2·NMe_3)][BAr^{Cl}] (1a)

To a solution of 80 mg (0.10 mmol) Tl[BAr^{Cl}] (**A**) in 5 mL of CH_2Cl_2, 11 mg (0.10 mmol) H_2P-BH_2·NMe_3 were added at room temperature. The mixture was stirred for 15 min and filtered. Subsequently, the solution was layered by the sixfold amount of *n*-hexane. [Tl(H_2PBH_2·NMe_3)][BAr^{Cl}] (**1a**) crystallized at -28 °C as colourless rods. The crystals were separated and washed with *n*-hexane (3×5 mL). Yield of [Tl(H_2PBH_2·NMe_3)][BAr^{Cl}] (**1a**): 74 mg (80%).

^{1}H NMR (CD_2Cl_2, 25 °C): δ = 1.95 (m, 2H, BH_2), 2.48 (d, $^{1}J_{H,P}$ = 175 Hz, 2H, PH_2), 2.63 (s, 9H, NMe_3), 7.07 (m, 3H, *p*-H, Ar), 7.21 (m, 9H, *o*-H, Ar).

^{31}P NMR (CD_2Cl_2, 25 °C): δ = -132.0 (t, $^{1}J_{H,P}$ = 175 Hz, br).

^{31}P{^{1}H} NMR (CD_2Cl_2, 25 °C): δ = -132.0 (s, br).

^{11}B NMR (CD_2Cl_2, 25 °C): δ = -8.4 (t, $^{1}J_{B,H}$ = 100 Hz), -7.1 (n, $^{3}J_{B,H}$ = 3 Hz, $[BAr^{Cl}]^-$).

^{11}B{^{1}H} NMR (CD_2Cl_2, 25 °C): δ = -8.4 (s), -7.1 (s, $[BAr^{Cl}]^-$).

ESI-MS (MeCN): *m/z* = 310.1 (50%, $[Tl(H_2PBH_2{\cdot}NMe_3)]^+$), 205.0 (5%, $[Tl]^+$).

Elemental analysis (%) calculated for $C_{24}H_{12}BCl_8Tl(CH_2Cl_2)_{0.5}$ (**A**$(CH_2Cl_2)_{0.5}$): C: 34.96, H: 1.56; found: C: 34.80, H: 1.78.

3.5.1.6 Synthesis of $[Tl(H_2AsBH_2{\cdot}NMe_3)][BAr^{Cl}]$ (1b)

To a solution of 80 mg (0.10 mmol) $Tl[BAr^{Cl}]$ (**A**) in 5 mL of CH_2Cl_2, 15 mg (0.10 mmol) H_2As-$BH_2{\cdot}NMe_3$ were added at room temperature. The mixture was stirred for 15 min and filtered. Subsequently the solution was layered by the sixfold amount of *n*-hexane. $[Tl(H_2AsBH_2{\cdot}NMe_3)][BAr^{Cl}]$ (**1b**) crystallized at -28 °C as colourless needles. The crystals were separated and washed with *n*-hexane (3×5 mL). Yield of $[Tl(H_2AsBH_2{\cdot}NMe_3)][BAr^{Cl}]$ (**1b**): 69 mg (72%).

^{1}H NMR (CD_2Cl_2, 25 °C): δ = 1.18 (m, 2H, AsH_2), 2.36 (q, $^{1}J_{B,H}$ = 110 Hz, 2H, BH_2), 2.68 (s, 9H, NMe_3), 7.08 (m, 3H, *p*-H, Ar), 7.21 (m, 9H, *o*-H, Ar).

^{11}B NMR (CD_2Cl_2, 25 °C): δ = -6.3 (t, $^{1}J_{B,H}$ = 110 Hz), -7.1 (n, $^{3}J_{B,H}$ = 3 Hz, $[BAr^{Cl}]^-$).

^{11}B{^{1}H} NMR (CD_2Cl_2, 25 °C): δ = -6.3 (s), -7.1 (s, $[BAr^{Cl}]^-$).

ESI-MS (MeCN): *m/z* = 354.0 (30%, $[Tl(H_2AsBH_2{\cdot}NMe_3)]^+$), 205.0 (5%, $[Tl]^+$).

Elemental analysis (%) calculated for $C_{27}H_{25}B_2Cl_8NAsTl$: C 34.21, H 2.66 N 1.48; found: C 34.63, H 2.77, N 1.30.

3.5.1.7 Synthesis of $[Tl(H_2PBH_2{\cdot}NMe_3)_3][TEF^{Cl}]$ (2a)

To a solution of 137 mg (0.10 mmol) $Tl[TEF^{Cl}]$ (**B**) in 5 mL of CH_2Cl_2 32 mg (0.30 mmol), $H_2PBH_2{\cdot}NMe_3$ were added at room temperature. The mixture was stirred for 15 min and filtered. Subsequently, the solution was layered by the sixfold amount of *n*-hexane. $[Tl(H_2PBH_2{\cdot}NMe_3)_3][TEF^{Cl}]$ (**2a**) crystallized at -28 °C as colourless needles. The crystals were separated and washed with *n*-hexane (3×5 mL). Yield of $[Tl(H_2PBH_2{\cdot}NMe_3)_3][TEF^{Cl}]$ (**2a**): 151 mg (90%).

^{1}H NMR (CD_2Cl_2, 25 °C): δ = 2.03 (d, $^{1}J_{H,P}$ = 220 Hz, 2H, PH_2), 2.15 (m, 2H, BH_2), 2.68 (s, 9H, NMe_3).

^{31}P NMR (CD_2Cl_2, 25 °C): δ = -166.7 (t, $^{1}J_{H,P}$ = 220 Hz, br).

$^{31}P\{^{1}H\}$ NMR (CD_2Cl_2, 25 °C): δ = -166.3 (s, br).

^{11}B NMR (CD_2Cl_2, 25 °C): δ = -8.0 (t, $^{1}J_{B,H}$ = 103 Hz).

$^{11}B\{^{1}H\}$ NMR (CD_2Cl_2, 25 °C): δ = -8.0 (s).

ESI-MS (MeCN): *m/z* = 415.1 (45%, $[Tl(H_2PBH_2{\cdot}NMe_3)_2]^+$), 310.0 (60%, $[Tl(H_2PBH_2{\cdot}NMe_3)]^+$), 205.0 (2%, $[Tl]^+$).

Elemental analysis (%) calculated for $C_{25}H_{39}AlB_3Cl_{12}F_{24}N_3O_4P_3Tl$: C 17.83, H 2.33, N 2.5; found: C 18.05, H 2.39, N 2.41.

3.5.1.8 Synthesis of $[Tl(H_2AsBH_2{\cdot}NMe_3)_3][TEF]$ (2b)

To a solution of 117 mg (0.10 mmol) Tl[TEF] in 5 mL of CH_2Cl_2 45 mg (0.30 mmol) $H_2AsBH_2{\cdot}NMe_3$ were added at room temperature. The mixture was stirred for 15 min and filtered. Subsequently the solution was layered by the sixfold amount of *n*-hexane. $[Tl(H_2AsBH_2{\cdot}NMe_3)_3][TEF]$ (**2b**) crystallized at -28 °C as colourless needles. The crystals were separated and washed with *n*-hexane (3×5 mL). Yield of $[Tl(H_2AsBH_2{\cdot}NMe_3)_3][TEF]$ (**2b**): 120 mg (74%).

^{1}H NMR (CD_2Cl_2, 25 °C): δ = 1.30 (m, 2H, AsH_2), 2.43 (q, $^{1}J_{B,H}$ = 111 Hz, 2H, BH_2), 2.72 (s, 9H, NMe_3).

^{19}F NMR (CD_2Cl_2, 25 °C): δ = -75.6 (s).

$^{19}F\{^{1}H\}$ NMR (CD_2Cl_2, 25 °C): δ = –75.6 (s).

^{11}B NMR (CD_2Cl_2, 25 °C): δ = -6.5 (t, $^{1}J_{B,H}$ = 111 Hz).

$^{11}B\{^{1}H\}$ NMR (CD_2Cl_2, 25 °C): δ = -6.5 (s).

ESI-MS (MeCN): *m/z* = 354.0 (100%, $[Tl(H_2AsBH_2{\cdot}NMe_3)]^+$), 205.0 (75%, $[Tl]^+$).

Elemental analysis (%) calculated for $C_{25}H_{39}AlAs_3B_3F_{36}N_3O_4Tl$: C 18.56, H 2.43, N 2.60; found: C 18.77, H 2.39, N 2.44.

3.5.1.9 Synthesis of $[Me_3N{\cdot}H_2BH_2P\text{-}PHBH_2{\cdot}NMe_3][TEF]$ (3a)

To a solution of 117 mg (0.10 mmol) Tl[TEF] in 5 mL of CH_2Cl_2 21 mg (0.20 mmol) $PH_2BH_2{\cdot}NMe_3$ were added at room temperature. The mixture was stirred for 20 h upon which TlCl precipitated. After filtration over a celite pad, the threefold amount of *n*-pentane was added and the mixture stored at -28 °C. $[Me_3N{\cdot}H_2BH_2P–PHBH_2{\cdot}NMe_3][TEF]$ crystallizes at -28°C as colourless needles. The crystals were separated and washed with *n*-hexane (3×5 mL). Yield of $[Me_3N{\cdot}H_2BH_2P–PHBH_2{\cdot}NMe_3][TEF]$ (**3a**): 35 mg (30%).

^{1}H NMR (CD_2Cl_2, 25 °C): due to strongly broadened signals and extensive amount of overlap throughout the entire spectrum, no clear assignment of signals was possible.

^{31}P NMR (CD_2Cl_2, 25 °C): δ = -91.3 (dm, br and overlain, $^1J_{P,H} \approx 357$ Hz, PH_2), -199.6 (dd ("pseudo-triplet"), br and overlain, $^1J_{P,H} \approx 255$ Hz, PH).

^{31}P{^{1}H} NMR (CD_2Cl_2, 25 °C): δ = -91.3 (dm, br, $^1J_{P,P}$ = 255 Hz, br, PH_2), -199.6 (dd, br, $^1J_{P,P}$ = 255 Hz, $^1J_{P,B}$ = 32 Hz, br, PH).

^{11}B NMR (CD_2Cl_2, 25 °C): δ = -10.7 (t, br, $^1J_{B,H}$ = 119 Hz, $^1J_{B,P}$ = 55 Hz, BH_2), -6.5 (t, very br, $^1J_{B,H}$ = 113 Hz, BH_2).

^{11}B{^{1}H} NMR (CD_2Cl_2, 25 °C): δ = -10.7 (d, br, $^1J_{B,P}$ = 55 Hz, BH_2), -6.5 (d, br, $^1J_{B,P}$ = 25 Hz, BH_2).

^{19}F NMR (CD_2Cl_2, 25 °C): δ = -75.6 (s).

^{19}F{^{1}H} NMR (CD_2Cl_2, 25 °C): δ = –75.6 (s).

ESI-MS (CH_2Cl_2, pos. mod.): *m/z* = 209 (100%, $[Me_3N{\cdot}H_2BH_2P–PHBH_2{\cdot}NMe_3]^+$), 149 (30%, $[Me_3N{\cdot}H_2BH_2P–PHBH_2]^+$), 135 (15%, $[Me_3N{\cdot}H_2BH_2P–PH]^+$), 104 (7%, $[Me_3N{\cdot}H_2BPH]^+$).

ESI-MS (CH_2Cl_2, neg. mod.): *m/z* = 967 (100%, $[TEF]^-$).

Elemental analysis (%) calculated for $C_{22}H_{25}AlP_2B_2F_{36}N_2O_4$: C 22.47, H 2.13, N 2.38; found: C 22.84, H 1,97, N 2.52.

3.5.1.10 Synthesis of $[Me_3N{\cdot}H_2BH_2P\text{-}PHBH_2{\cdot}NMe_3][BAr^{Cl}]$ (3b)

To a suspension of $Tl[BAr^{Cl}]$ (78 mg, 0.10 mmol) in a small amount of CH_2Cl_2, $PH_2BH_2 \cdot NMe_3$ (stock solution: 0.5 M in toluene, 0.4 mL, 0.20 mmol) was added *via* syringe. The mixture was stirred for 20 h upon which TlCl precipitated. After filtration over a celite pad, the solution was layered by the sixfold amount of *n*-pentane. $[Me_3N{\cdot}H_2BH_2P–PHBH_2{\cdot}NMe_3][BAr^{Cl}]$ crystallizes at 8 °C as colourless blocks. The crystals were separated, washed with *n*-hexane (3×5 mL) and dried *in vacuo*. Yield of $[Me_3N{\cdot}H_2BH_2P–PHBH_2{\cdot}NMe_3][BAr^{Cl}]$: 23 mg (29%).

^{1}H NMR (CD_2Cl_2, 25 °C): due to strongly broadened signals and extensive amount of overlap throughout the entire spectrum, no clear assignment of signals was possible.

^{31}P NMR (CD_2Cl_2, 25 °C): δ = -90.8 (dt, br and overlain, $^1J_{P,H} \approx 348$ Hz, PH_2), -199.2 (dd ("pseudo-triplet"), br and overlain, $^1J_{P,H} \approx 237$ Hz, PH).

^{31}P{^{1}H} NMR (CD_2Cl_2, 25 °C): δ = -90.8 (dm, br, $^1J_{P,P}$ = 259 Hz, br, PH_2), –199.2 (d, br, $^1J_{P,P}$ = 259 Hz, br, PH).

^{11}B NMR (CD_2Cl_2, 25 °C): δ = -10.7 (t, very br, $^1J_{B,H}$ = 121 Hz, BH_2), -7.2 (n, $^3J_{B,H}$ = 2.74 Hz, $[BAr^{Cl}]^-$), -6.5 (t, very br, $^1J_{B,H} \approx 111$ Hz, BH_2).

^{11}B{^{1}H} NMR (CD_2Cl_2, 25 °C): δ = -10.7 (d, br, $^1J_{B,P}$ = 59 Hz, BH_2), -7.2 (s, $[BAr^{Cl}]^-$), -6.5 (m, very br).

ESI-MS (CH_2Cl_2, pos. mod.): *m/z* = 209.17 (100%, $[Me_3N{\cdot}H_2BH_2P–PHBH_2{\cdot}NMe_3]^+$),

ESI-MS (CH_2Cl_2, neg. mod.): *m/z* = 594.85 (100%, $[BAr^{Cl}]^-$).

Elemental analysis (%) calculated for $C_{30}H_{37}Cl_8B_3N_2P_2$: C: 44.84, H: 4.64, N: 3.49; found: C: 44.82, H: 4.56, N: 2.89.

3.5.1.11 Synthesis of $[Me_3N{\cdot}H_2BH_2P\text{-}PHBH_2{\cdot}NMe_3][TEF^{Cl}]$ (3c)

To a solution of 136 mg (0.1 mmol) $Tl[TEF^{Cl}]$ in CH_2Cl_2, $PH_2BH_2{\cdot}NMe_3$ (stock solution: 0.5 M in toluene, 0.4 mL, 0.2 mmol) was added *via* syringe. The mixture was stirred for 20 h at room temperature upon which TlCl precipitated. Then, the solution was filtered over a celite pad. After several attempts, a few single crystals could be obtained by layering a solution of **3c** in CH_2Cl_2 with *n*-hexane. Alternatively, precipitation from the CH_2Cl_2 solution gave a very small of amount of $[Me_3N{\cdot}H_2BH_2P–PHBH_2{\cdot}NMe_3][TEF^{Cl}]$ as a colourless powder (yield < 10%, owed due to poor overall solubility).

^{1}H NMR (CD_2Cl_2, 25 °C): due to strongly broadened signals and extensive amount of overlap throughout the entire spectrum, no clear assignment of signals was possible.

^{31}P NMR (CD_2Cl_2, 25 °C): δ = -90.7 (dt, br and overlain, $^1J_{P,H} \approx 357$ Hz, PH_2), -199.4 (dd ("pseudo-triplet"), br and overlain, $^1J_{P,H} \approx 255$ Hz, PH).

^{31}P{^{1}H} NMR (CD_2Cl_2, 25 °C): δ = -90.7 (dm, br, $^1J_{P,P}$ = 255 Hz, br, PH_2), -199.4 (dd, br, $^1J_{P,P}$ = 255 Hz, $^1J_{B,P}$ = 31 Hz, br, PH).

^{11}B NMR (CD_2Cl_2, 25 °C): δ = -10.7 (t, br, $^1J_{B,H}$ = 119 Hz, $^1J_{B,P}$ = 55 Hz, BH_2), -6.5 (t, very br, $^1J_{B,H}$ = 113 Hz, BH_2).

^{11}B{^{1}H} NMR (CD_2Cl_2, 25 °C): δ = -10.7 (d, br, $^1J_{B,P}$ = 55 Hz, BH_2), -6.5 (d, br, $^1J_{B,P}$ = 31 Hz, BH_2).

Elemental analysis (%): could not be successfully performed, as it was not possible to obtain high purity samples of **3c**.

3.5.1.12 Synthesis of $[Me_3N{\cdot}BH_2PH_2CPh_3][TEF^{Cl}]$ (4)

To a solution of 121 mg (0.1 mmol) $[Ph_3C][TEF]$ in CH_2Cl_2, $PH_2BH_2{\cdot}NMe_3$ (stock solution: 0.5 M in toluene, 0.4 mL, 0.2 mmol) was added *via* syringe. The solution immediately changed its colour from yellowish to colourless. After stirring for 16 hours at room temperature, the solution was layered with *n*-hexane and left in the refrigerator at 8 °C. **4** crystallized as large colourless needles/prisms together with $[Me_3N{\cdot}BH_2PH_2BH_2{\cdot}NMe_3][TEF]$ (ratio 0.52:1), suitable for X-ray diffraction experiments. Yield of the crystalline mixture: 70 mg.

^{1}H NMR (CD_2Cl_2, 25 °C): the signals are strongly overlain by signals from $[Me_3N{\cdot}BH_2PH_2BH_2{\cdot}NMe_3]$ and due to strong line broadening caused by quadrupolar moments and similar chemical shifts, no unambiguous assignment of signals was possible.

^{31}P NMR (CD_2Cl_2, 25 °C): δ = –35.8 (m, br).

^{31}P{^{1}H} NMR (CD_2Cl_2, 25 °C): δ = –35.8 (s, br).

^{11}B NMR (CD_2Cl_2, 25 °C): δ = –11.6 (td, br, $^1J_{B,H}$ = 112 Hz, $^1J_{B,P}$ = 60 Hz, BH_2).

^{11}B{^{1}H} NMR (CD_2Cl_2, 25 °C): δ = –11.6 (d, br, $^{1}J_{B,P}$ = 60 Hz, BH_2).

^{19}F NMR (CD_2Cl_2, 25 °C): δ = –75.6 (s).

ESI-MS (1,2-difluorobenzene, pos. mod.): *m/z* = 177.20 (100%, $[Me_3N{\cdot}BH_2PH_2BH_2{\cdot}NMe_3]^+$), 243.14 (30%, $[CPh_3]^+$), 348.22 (75%, $[Me_3N{\cdot}BH_2PH_2CPh_3]^+$).

Elemental analysis (%) calculated for 0.52 × **4** + 1 × [$Me_3N \cdot BH_2PH_2BH_2 \cdot NMe_3$][TEF] ($Al_{1.52}O_{6.08}C_{41.76}F_{54.72}H_{38.56}B_{2.52}N_{2.52}P_{1.52}$): C: 27.44, H: 2.13, N: 1.93; found: C: 28.02, H: 2.05, N: 1.94. *Note: ratio according to ^{31}P NMR signal integration gives 0.5234 to 1.000, as well.*

3.5.1.13 Reaction of $PH_2BH_2{\cdot}NMe_3$ with Tl[TEF] in 1,2-difluorobenzene

To a solution of 117 mg (0.1 mmol) Tl[TEF] in 1,2-difluorobenzene, $PH_2BH_2{\cdot}NMe_3$ (stock solution: 0.5 M in toluene, 0.4 mL, 0.2 mmol) was added *via* syringe. After stirring for 16 hours at room temperature, the solution was layered with *n*-hexane and left in the refrigerator at 8 °C. The product of the reaction crystallized as large colourless needles, which were unfortunately not suitable for X-ray diffraction experiments, due to weak diffraction below *d* = 1.12 Å. Crystalline yield of unidentified product: 37 mg.

^{1}H NMR (CD_2Cl_2, 25 °C): δ = 4.00 (q, $^{1}J_{B,H}$ = 114 Hz, overlain by multiple signals, BH_2), 4.51 (s, overlain by several signal, NMe_3). The signal for the {PH_2} moiety is likely overlain by the massive {BH_2} quartet and cannot be identified.

^{31}P NMR (CD_2Cl_2, 25 °C): δ = –146.9 (m, br).

^{31}P{^{1}H} NMR (CD_2Cl_2, 25 °C): δ = –146.9 (s, br).

^{11}B NMR (CD_2Cl_2, 25 °C): δ = –6.5 (t, br, $^{1}J_{B,H}$ = 108 Hz, BH_2).

^{11}B{^{1}H} NMR (CD_2Cl_2, 25 °C): δ = –6.5 (m, br, BH_2).

^{19}F NMR (CD_2Cl_2, 25 °C): δ = –73.9 (s).

ESI-MS (1,2-difluorobenzene, pos. mod.): *m/z* = 209.20 (38%, $[Me_3N{\cdot}H_2BH_2P{-}PHBH_2{\cdot}NMe_3]^+$), 310.09 (100%, $[Tl(PH_2BH_2{\cdot}NMe_3)]^+$), 415.20 (21%, $[Tl(PH_2BH_2{\cdot}NMe_3)_2]^+$).

Elemental analysis (%): was not performed, as it was not possible to unambiguously determine the product of the reaction, as structural determination by X-ray crystallography was not possible and the mass spectrum indicates a large degree of fragmentation upon ionization.

3.5.2 NMR Data

Tl[BAr^{Cl}]

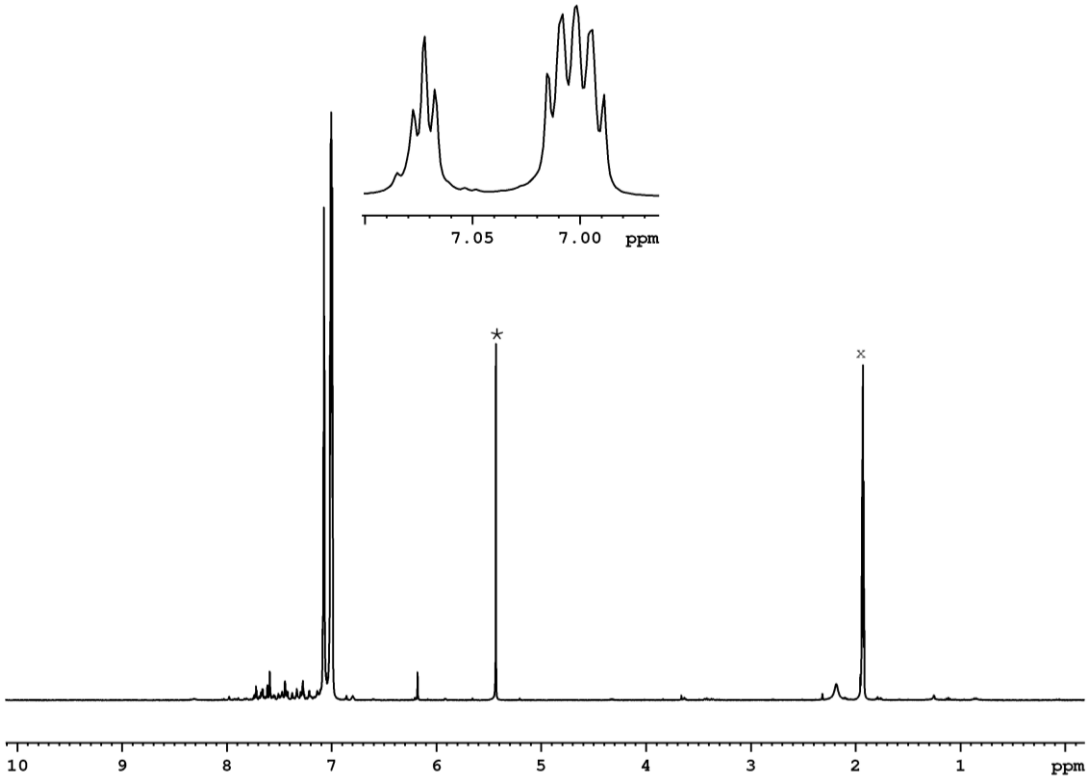

Figure S 3.1: ^{1}H NMR spectrum of Tl[BAr^{Cl}] (**A**) in CD_3CN. * = solvent (CH_2Cl_2). ^{x} = solvent (CD_3CN).

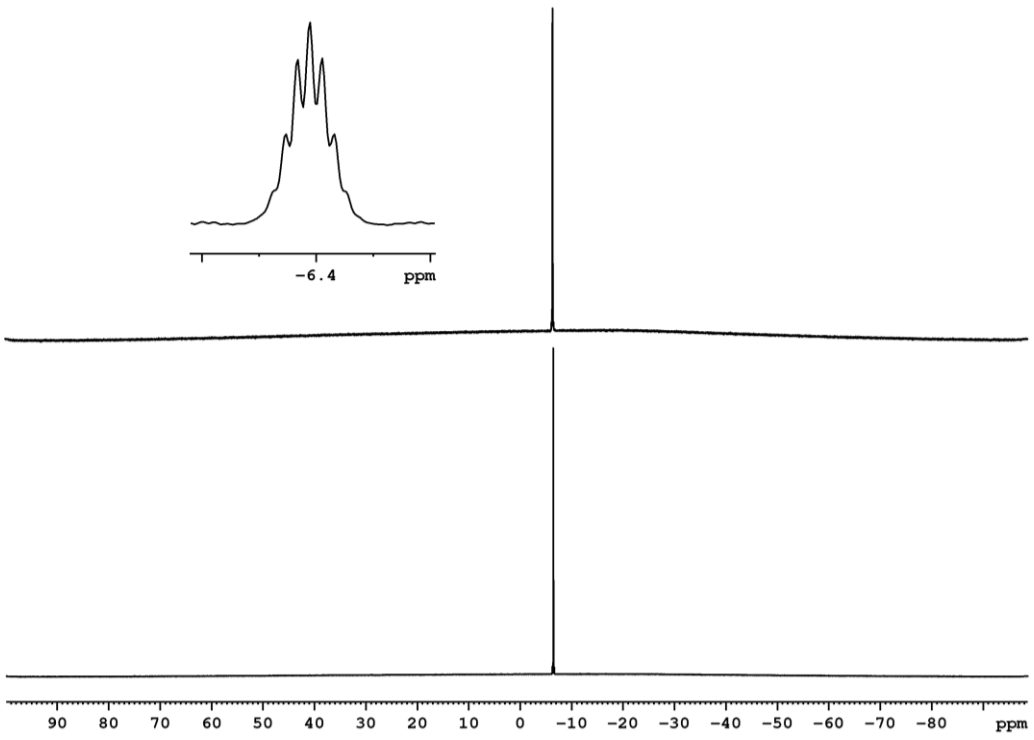

Figure S 3.2: ^{11}B{^{1}H} (bottom) and ^{11}B (top) NMR spectrum of Tl[BAr^{Cl}] (**A**) in CD_3CN.

Tl[TEF^{Cl}]

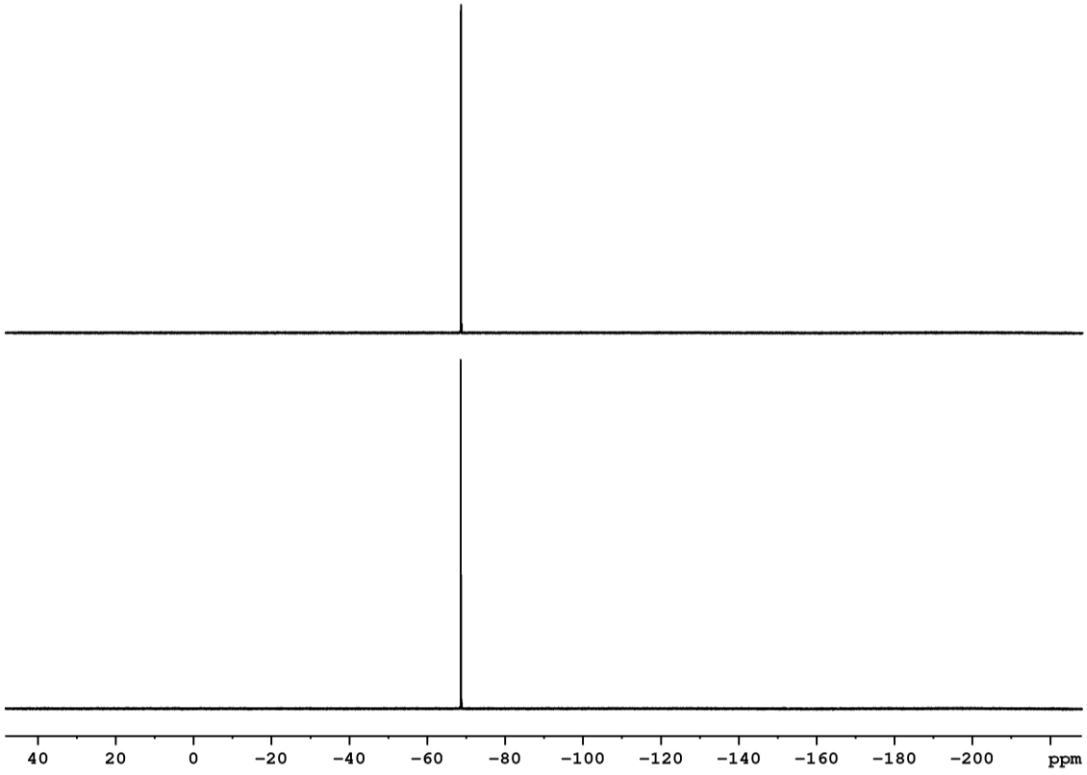

Figure S 3.3: $^{19}F\{^{1}H\}$ (bottom) and ^{19}F (top) NMR spectra of Tl[TEF^{Cl}] (**B**) in CD_2Cl_2.

[Tl(H_2PBH_2·NMe_3)][BAr^{Cl}]

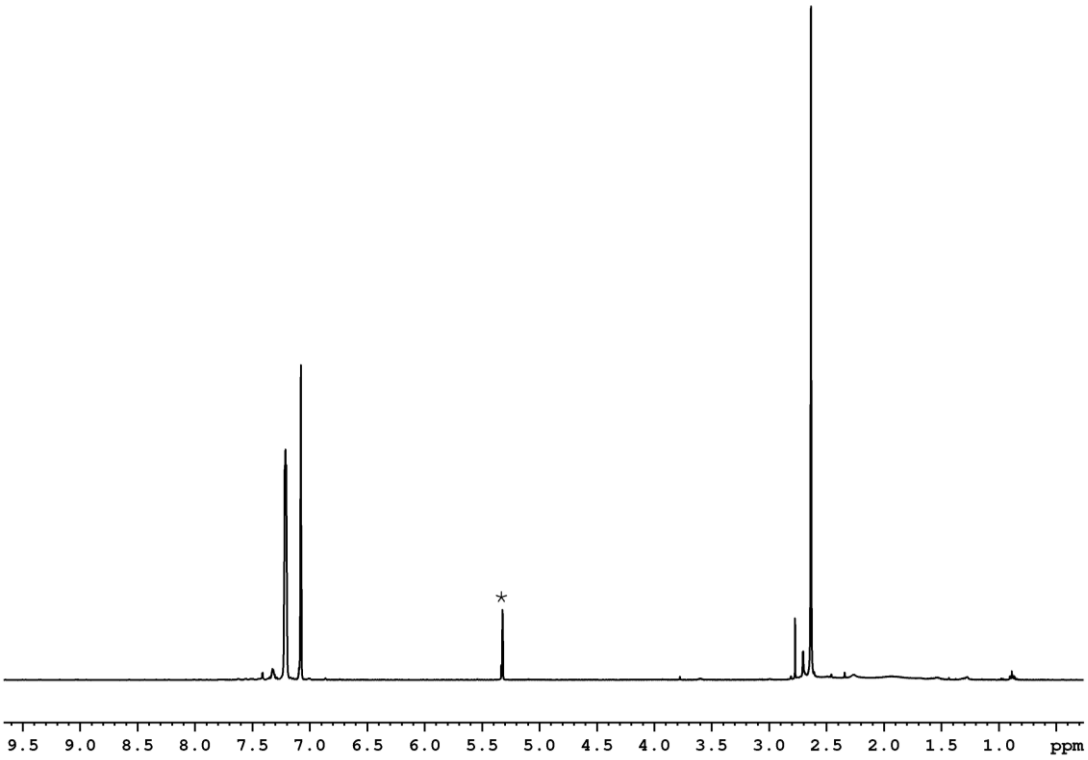

Figure S 3.4: ^{1}H NMR spectrum of [Tl(H_2PBH_2·NMe_3)][BAr^{Cl}] (**1a**) in CD_2Cl_2. * = solvent (CD_2Cl_2).

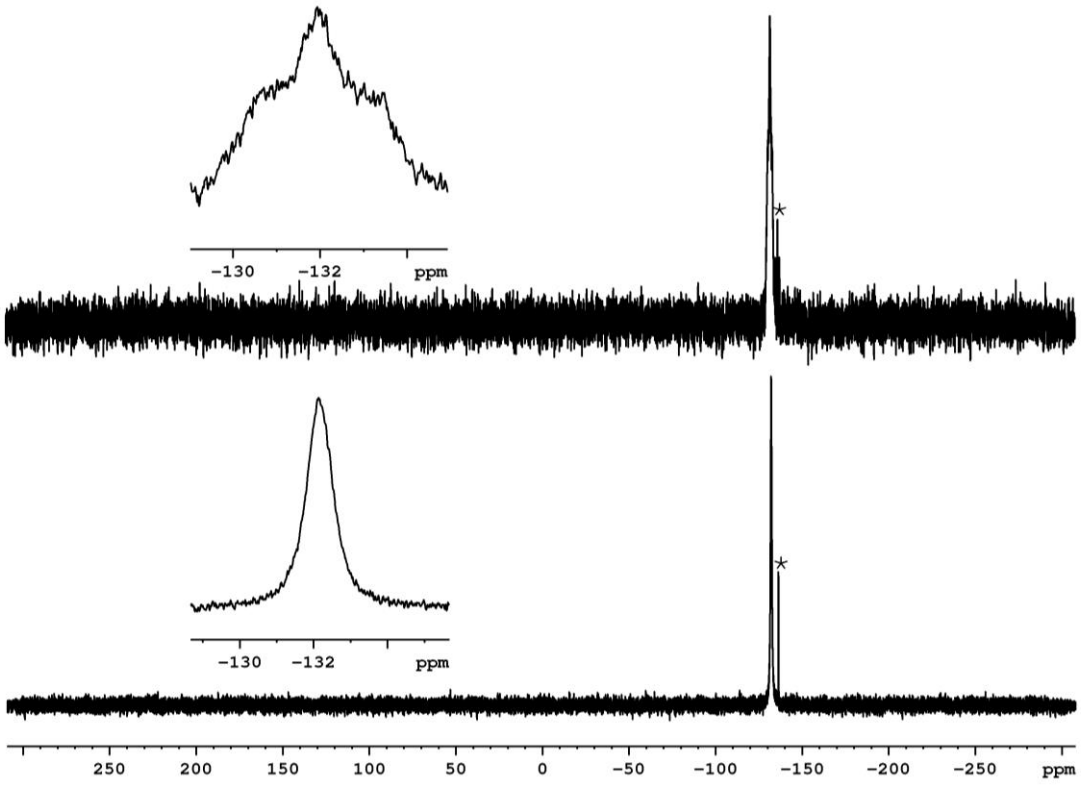

Figure S 3.5: $^{31}P\{^{1}H\}$ (bottom) and ^{31}P (top) NMR spectra of $[Tl(H_2PBH_2{\cdot}NMe_3)][BAr^{Cl}]$ (**1a**) in CD_2Cl_2. * = unidentified side product.

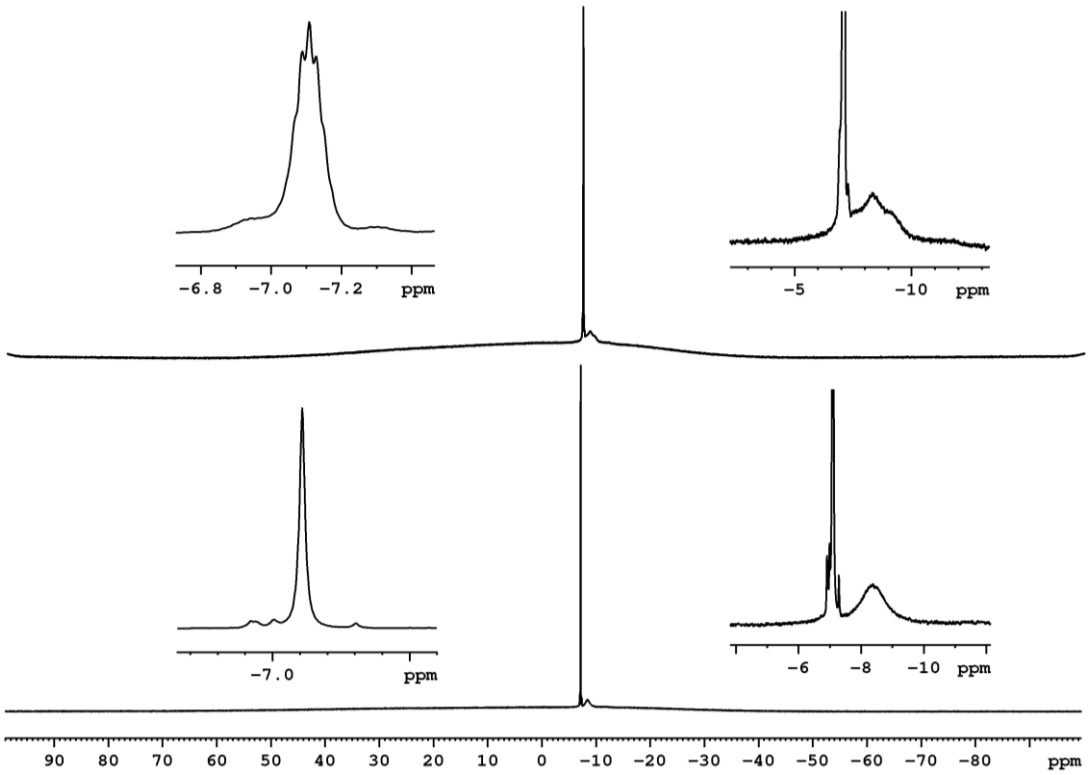

Figure S 3.6: $^{11}B\{^{1}H\}$ (bottom) and ^{11}B (top) NMR spectra of $[Tl(H_2PBH_2{\cdot}NMe_3)][BAr^{Cl}]$ (**1a**) in CD_2Cl_2.

[Tl(H$_2$AsBH$_2$·NMe$_3$)][BAr^{Cl}]

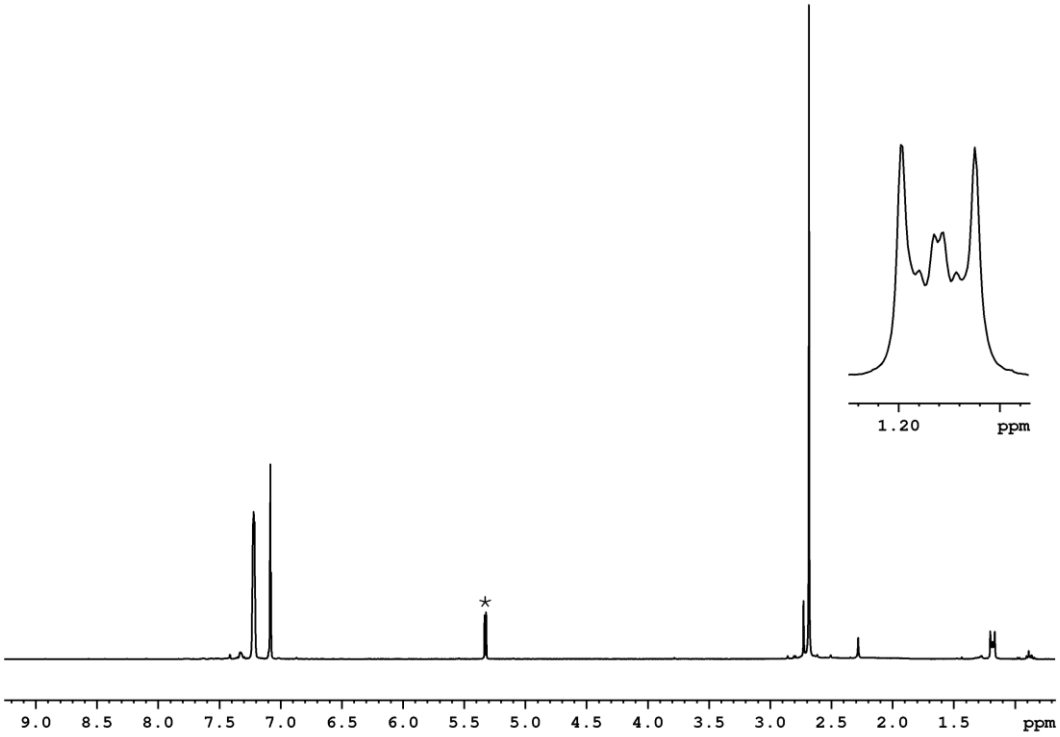

Figure S 3.7: ^{1}H NMR spectrum of [Tl(H$_2$AsBH$_2$·NMe$_3$)][BAr^{Cl}] (**1b**) in CD_2Cl_2. * = solvent (CD_2Cl_2).

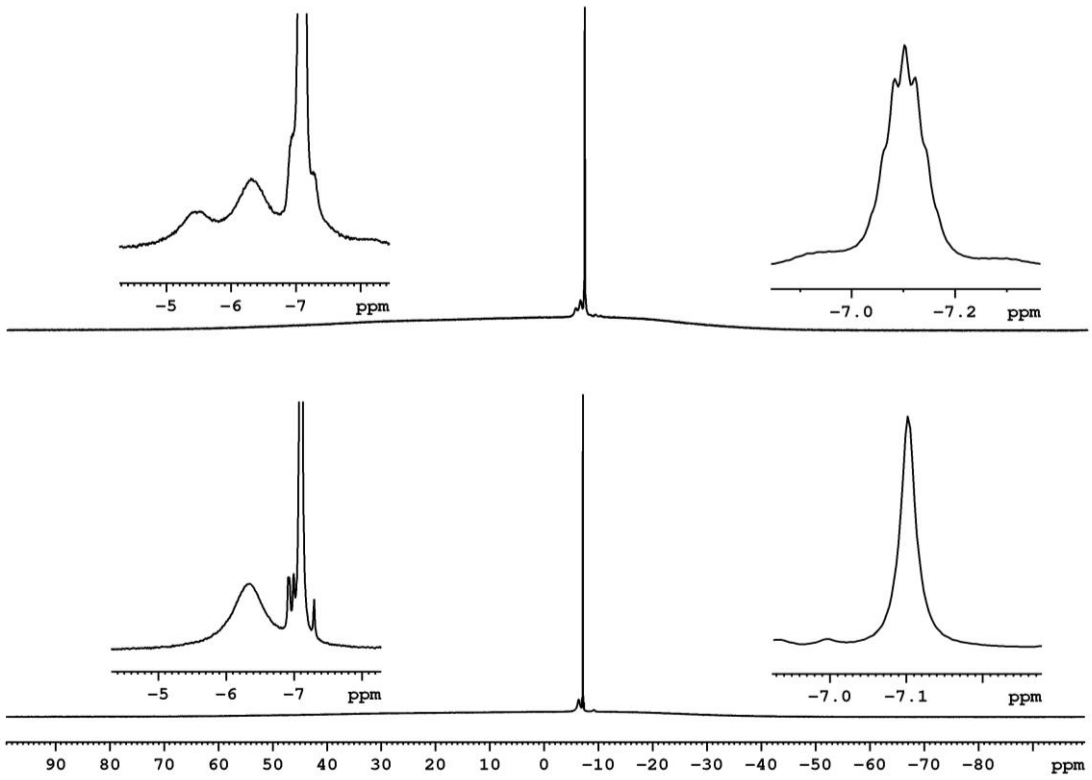

Figure S 3.8: ^{11}B{^{1}H} (bottom) and ^{11}B (top) NMR spectra of [Tl(H$_2$AsBH$_2$·NMe$_3$)][BAr^{Cl}] (**1b**) in CD_2Cl_2.

[Tl(H$_2$PBH$_2$·NMe$_3$)$_3$][TEF^{Cl}]

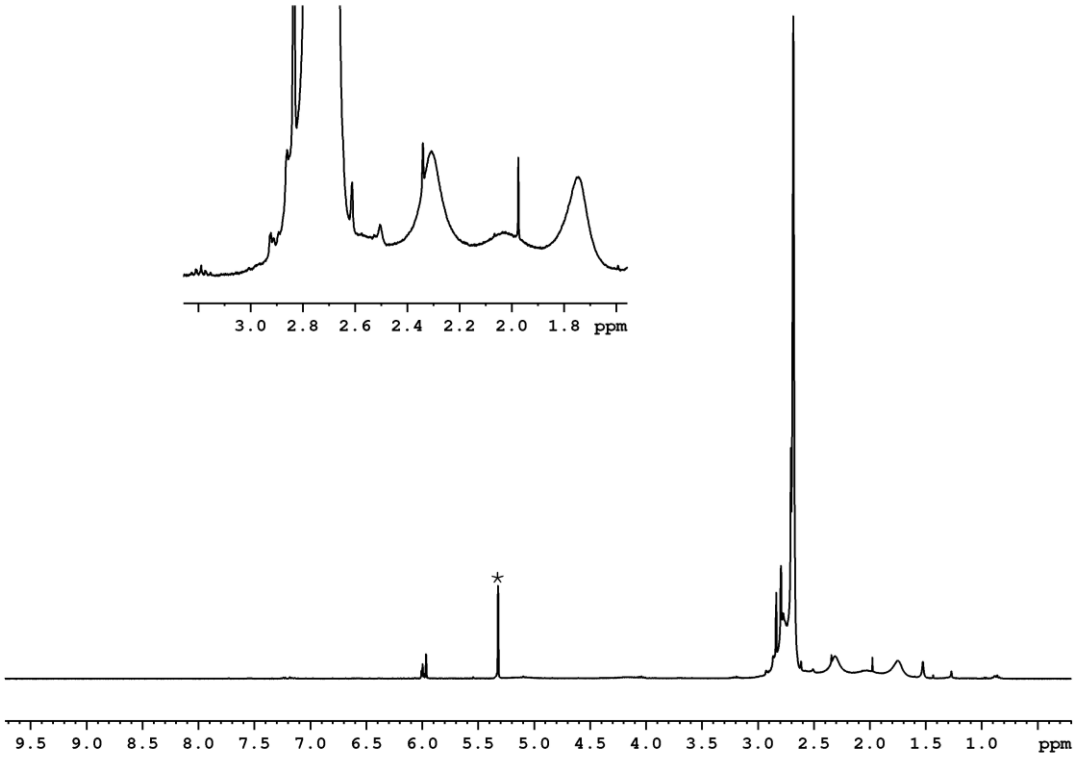

Figure S 3.9: ^{1}H NMR spectrum of [Tl(H$_2$PBH$_2$·NMe$_3$)$_3$][TEF^{Cl}] (**2a**) in CD_2Cl_2. * = solvent (CD_2Cl_2).

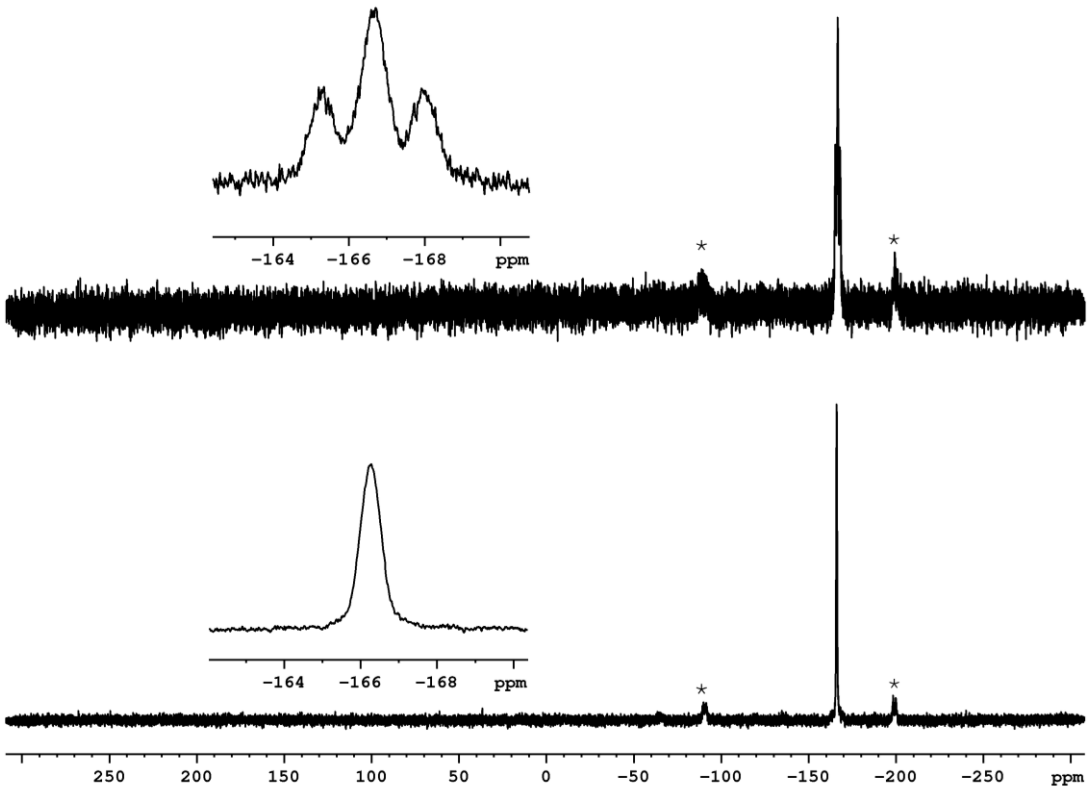

Figure S 3.10: ^{31}P{^{1}H} (bottom) and ^{31}P (top) NMR spectra of [Tl(H$_2$PBH$_2$·NMe$_3$)$_3$][TEF^{Cl}] (**2a**) in CD_2Cl_2. * = subsequent reaction product.

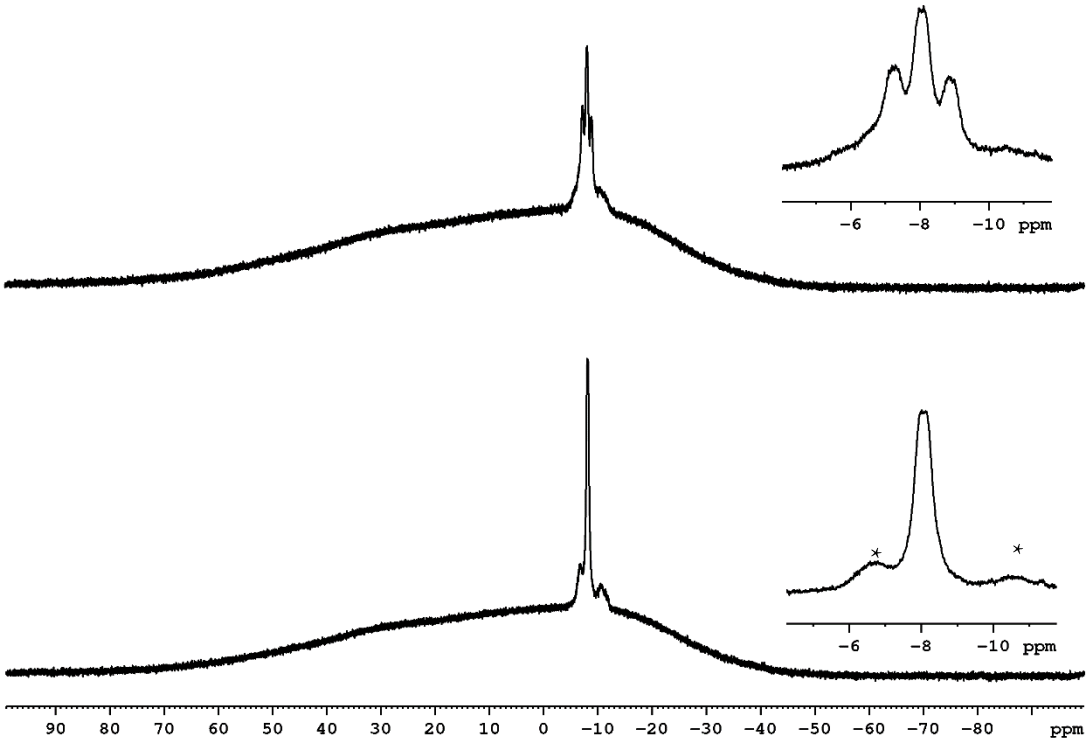

Figure S 3.11: $^{11}B\{^{1}H\}$ (bottom) and ^{11}B (top) NMR spectra of $[Tl(H_2PBH_2{\cdot}NMe_3)_3][TEF^{Cl}]$ (**2a**) in CD_2Cl_2 (* = unidentified impurity.

$[Tl(H_2AsBH_2{\cdot}NMe_3)_3][TEF]$

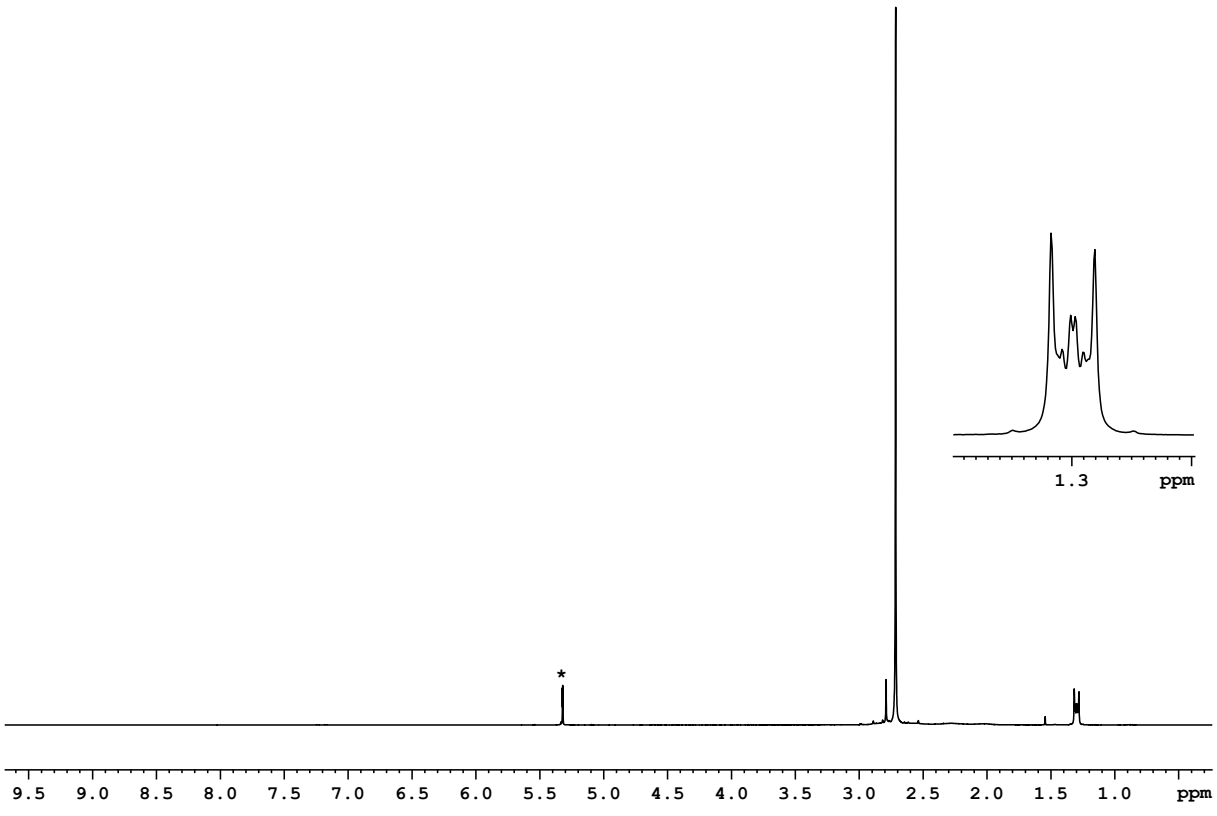

Figure S 3.12: ^{1}H NMR spectrum of $[Tl(H_2AsBH_2{\cdot}NMe_3)_3][TEF]$ (**2b**) in CD_2Cl_2. * = solvent (CD_2Cl_2).

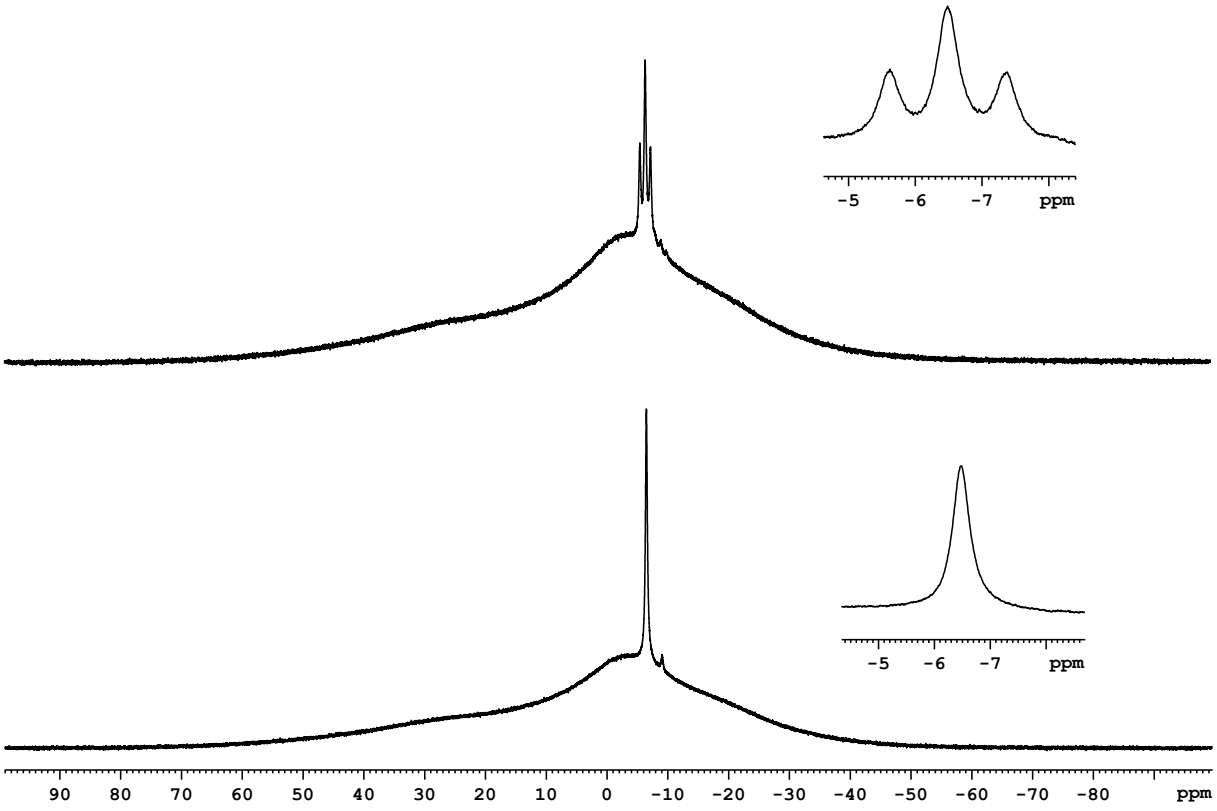

Figure S 3.13: $^{11}B\{^{1}H\}$ (bottom) and ^{11}B (top) NMR spectra of $[Tl(H_2AsBH_2{\cdot}NMe_3)_3][TEF]$ (**2b**) in CD_2Cl_2.

$[Me_3N{\cdot}H_2BH_2P\text{-}PHBH_2{\cdot}NMe_3][TEF]$

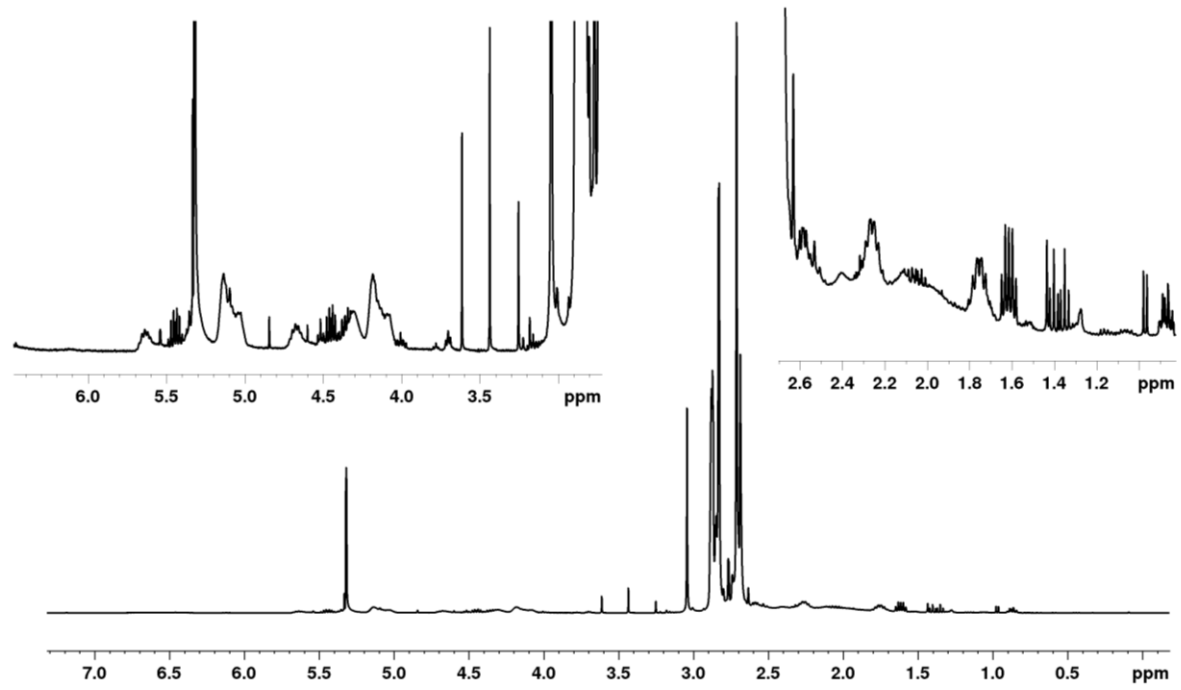

Figure S 3.14: ^{1}H NMR spectrum of $[Me_3N{\cdot}H_2BH_2P\text{-}PHPH_2BH_2{\cdot}NMe_3][TEF]$ (**3a**) in CD_2Cl_2.

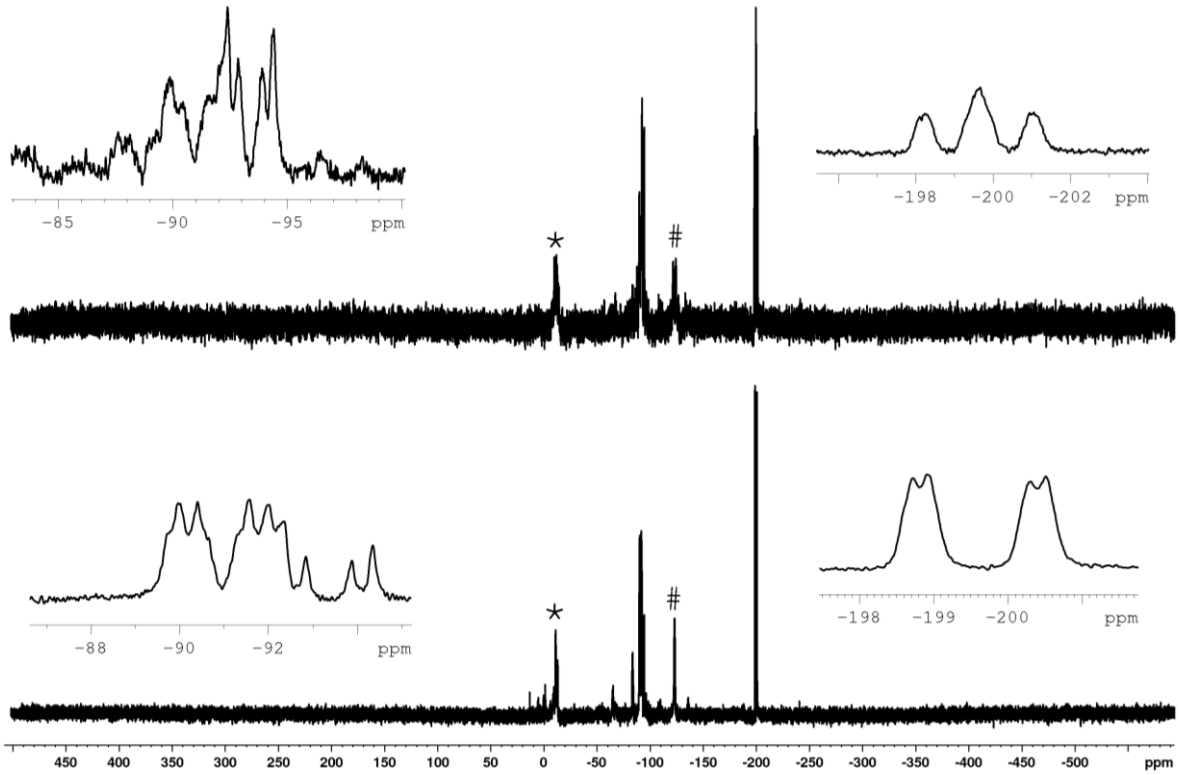

Figure S 3.15: $^{31}P\{^{1}H\}$ (bottom) and ^{31}P (top) NMR spectrum of $[Me_3N{\cdot}H_2BH_2P\text{-}PHPH_2BH_2{\cdot}NMe_3][TEF]$ (**3a**) in CD_2Cl_2 (* = unidentified impurity, # = $[Tl(PH_2BH_2{\cdot}NMe_3)]^+$).

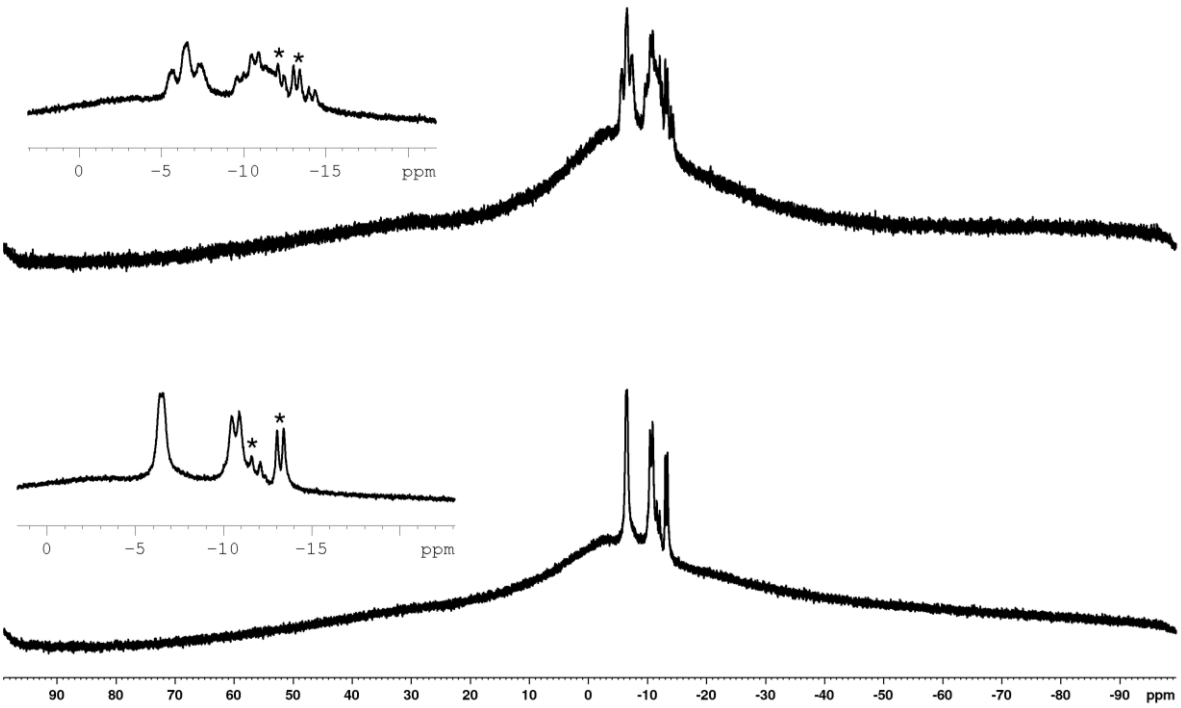

Figure S 3.16: $^{11}B\{^{1}H\}$ (bottom) and ^{11}B (top) NMR spectrum of $[Me_3N{\cdot}H_2BH_2P\text{-}PHPH_2BH_2{\cdot}NMe_3][TEF]$ (**3a**) in CD_2Cl_2 (* = unidentified impurities).

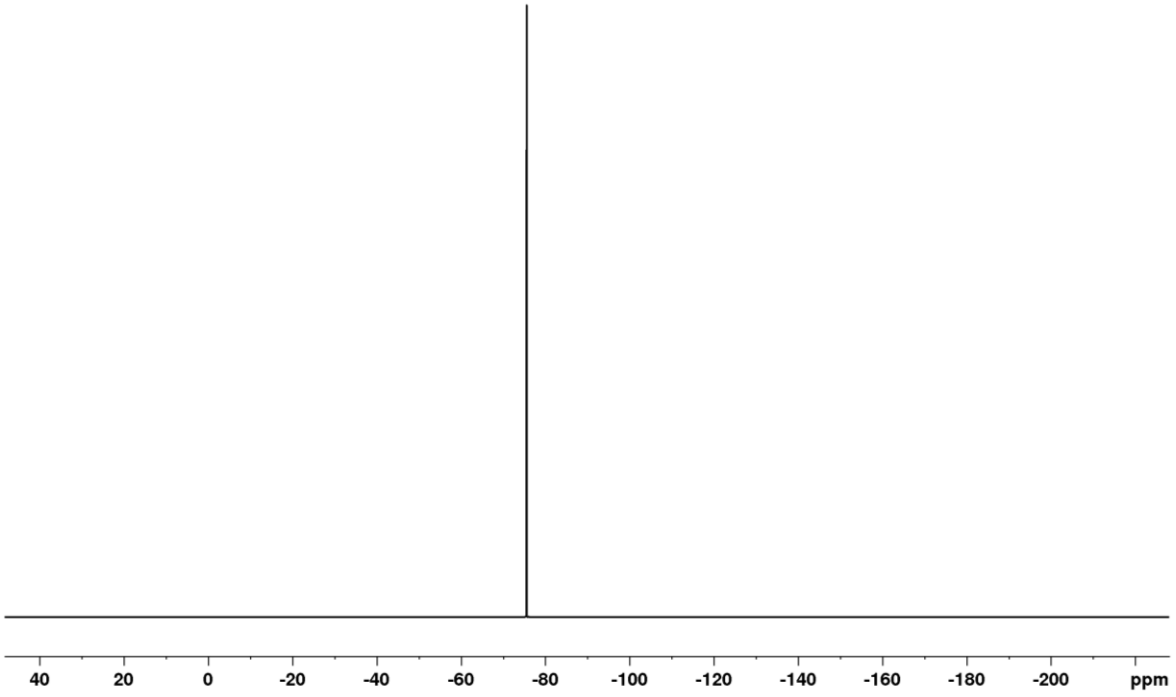

Figure S 3.17: $^{19}F\{^{1}H\}$ NMR spectrum of $[Me_3N{\cdot}H_2BH_2P\text{-}PHPH_2BH_2{\cdot}NMe_3][TEF]$ (**3a**) in CD_2Cl_2.

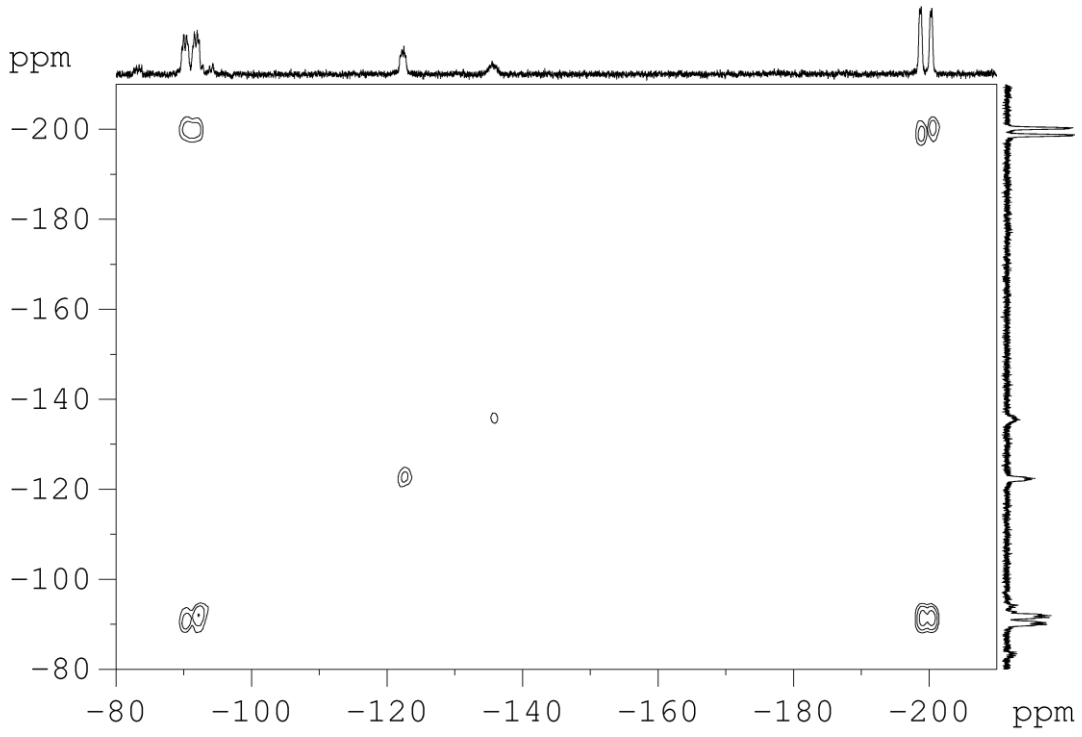

Figure S 3.18: ^{31}P, ^{31}P COSY NMR spectrum of $[Me_3N{\cdot}H_2BH_2P\text{-}PHPH_2BH_2{\cdot}NMe_3][TEF]$ (**3a**) in CD_2Cl_2.

[$Me_3N{\cdot}H_2BH_2P$-$PHBH_2{\cdot}NMe_3$][BAr^{Cl}]

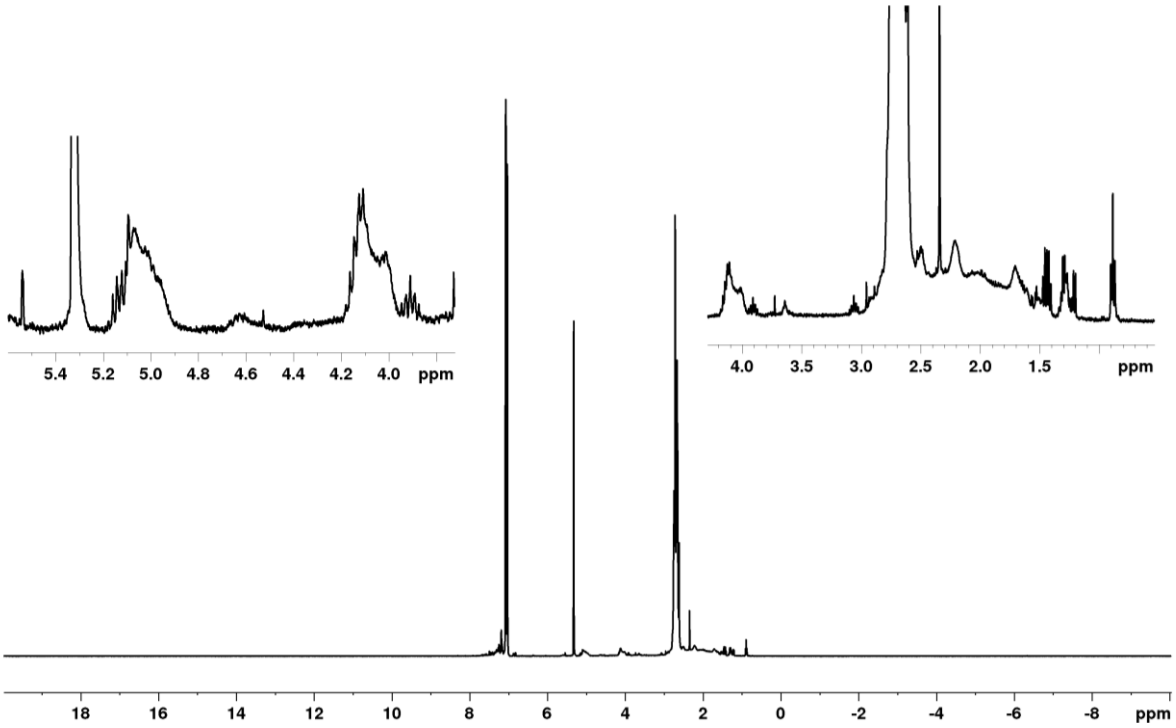

Figure S 3.19: ^{1}H NMR spectrum of [$Me_3N{\cdot}H_2BH_2P$-$PHPH_2BH_2{\cdot}NMe_3$][BAr^{Cl}] (**3b**) in CD_2Cl_2. * = solvent (CD_2Cl_2).

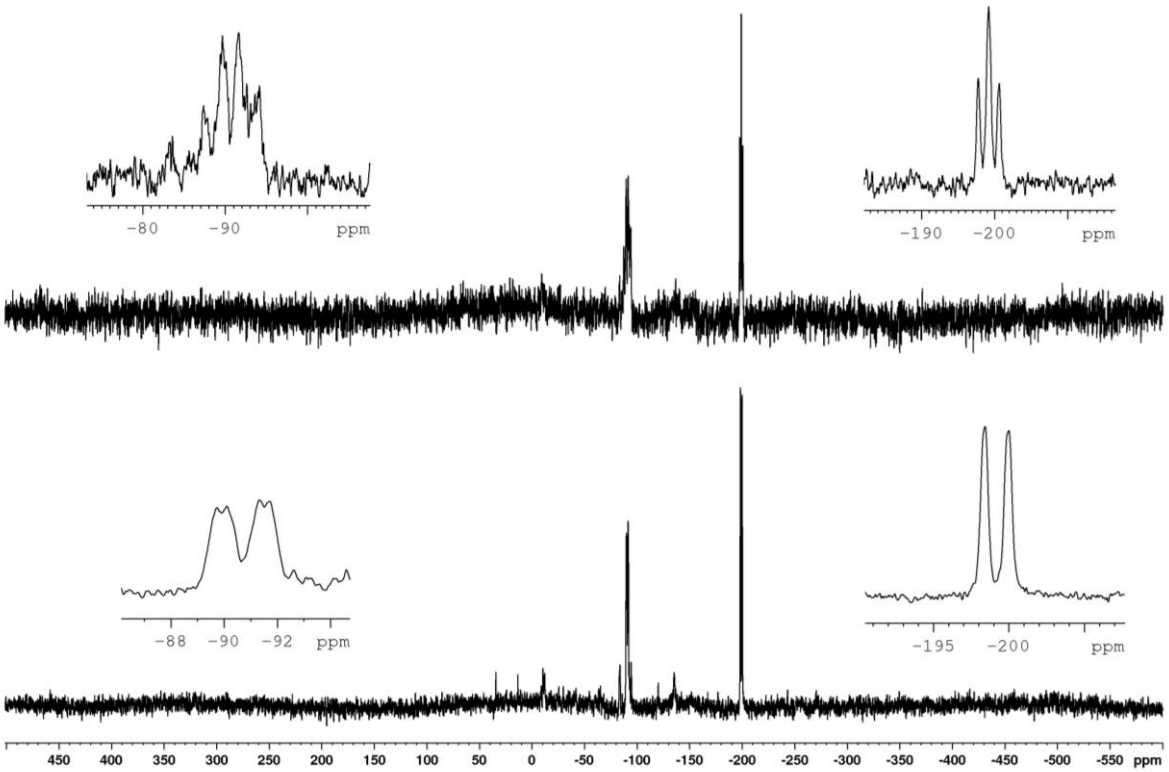

Figure S 3.20: $^{31}P\{^{1}H\}$ (bottom) and ^{31}P (top) NMR spectrum of [$Me_3N{\cdot}H_2BH_2P$-$PHPH_2BH_2{\cdot}NMe_3$][BAr^{Cl}] (**3b**) in CD_2Cl_2.

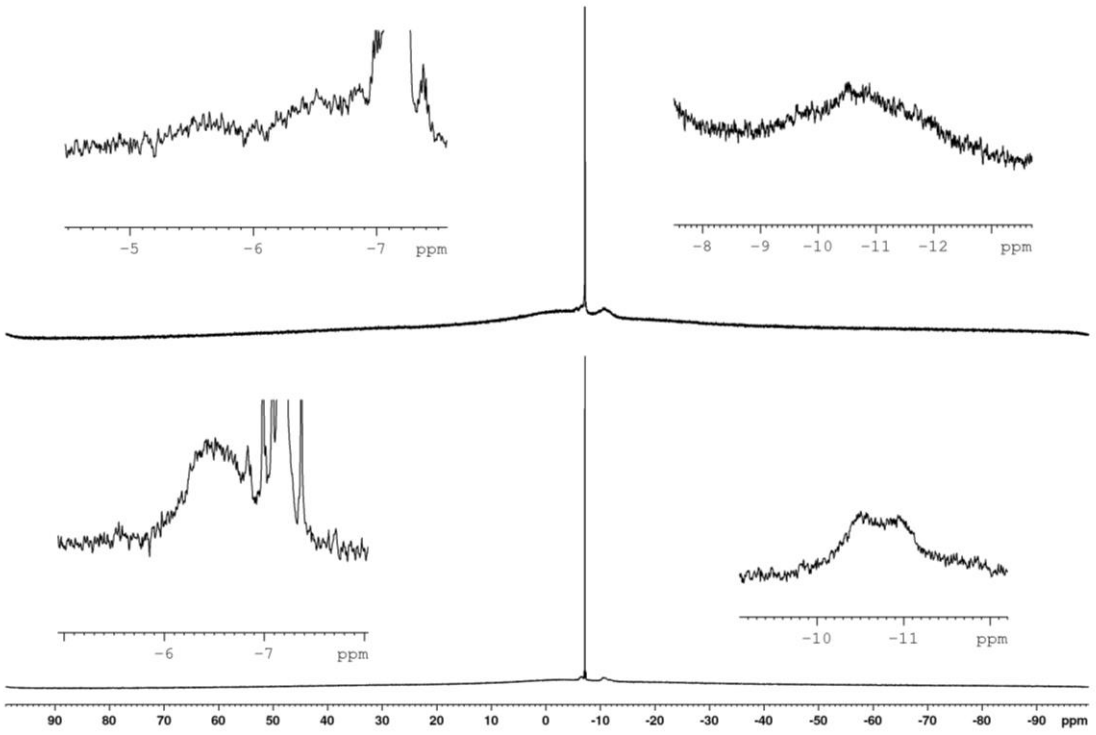

Figure S 3.21: $^{11}B\{^{1}H\}$ (bottom) and ^{11}B (top) NMR spectrum of $[Me_3N{\cdot}H_2BH_2P\text{-}PHPH_2BH_2{\cdot}NMe_3][BAr^{Cl}]$ (**3b**) in CD_2Cl_2.

$[Me_3N{\cdot}H_2BH_2P\text{-}PHBH_2{\cdot}NMe_3][TEF^{Cl}]$

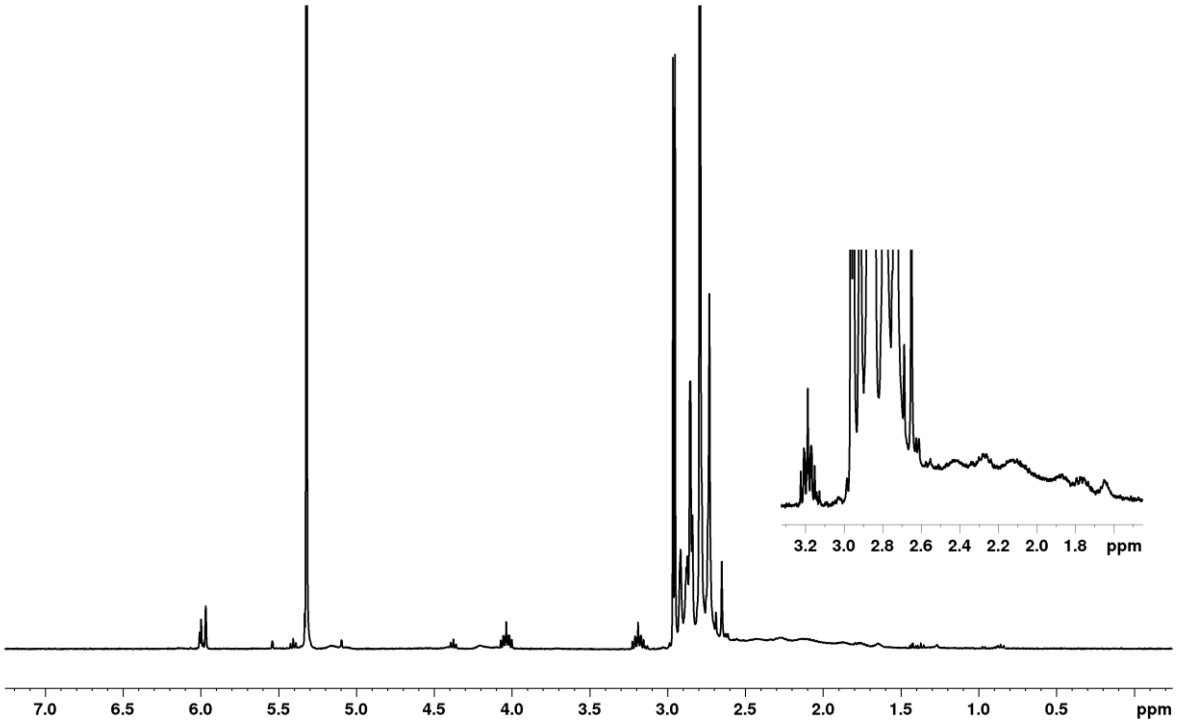

Figure S 3.22: ^{1}H NMR spectrum of $[Me_3N{\cdot}H_2BH_2P\text{-}PHPH_2BH_2{\cdot}NMe_3][TEF^{Cl}]$ (**3c**) in CD_2Cl_2. * = solvent (CD_2Cl_2).

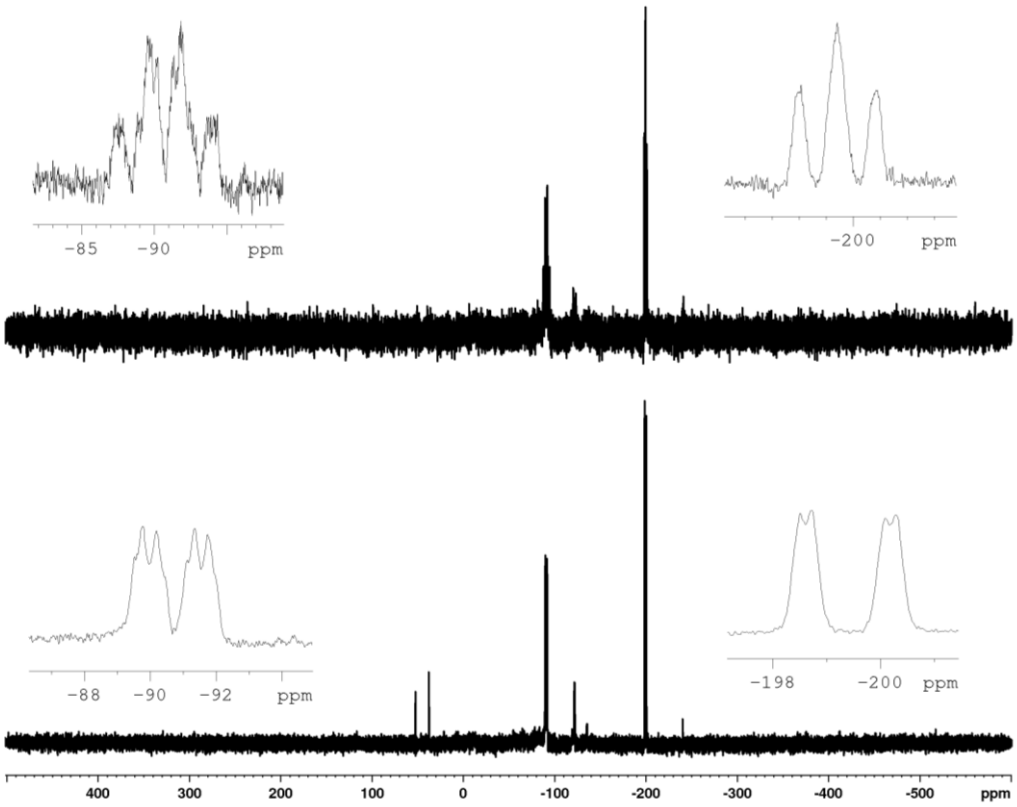

Figure S 3.23: $^{31}P\{^{1}H\}$ (bottom) and ^{31}P (top) NMR spectrum of $[Me_3N{\cdot}H_2BH_2P\text{-}PHPH_2BH_2{\cdot}NMe_3][TEF^{Cl}]$ (**3c**) in CD_2Cl_2.

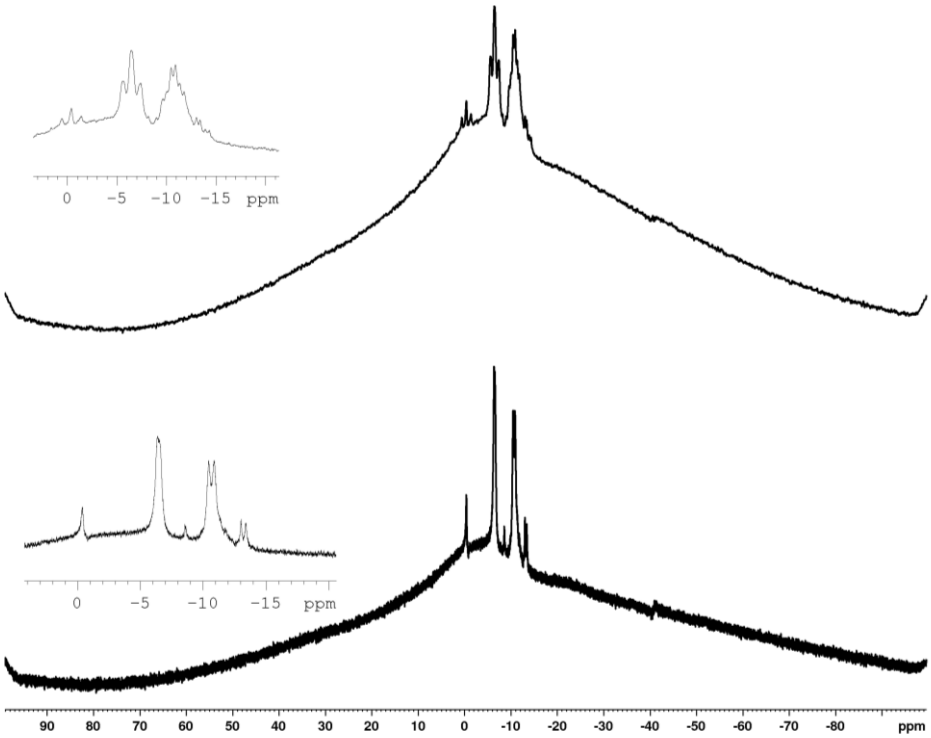

Figure S 3.24: $^{11}B\{^{1}H\}$ (bottom) and ^{11}B (top) NMR spectrum of $[Me_3N{\cdot}H_2BH_2P\text{-}PHPH_2BH_2{\cdot}NMe_3][TEF^{Cl}]$ (**3c**) in CD_2Cl_2.

[$Me_3N{\cdot}BH_2PH_2CPh_3$][TEF]

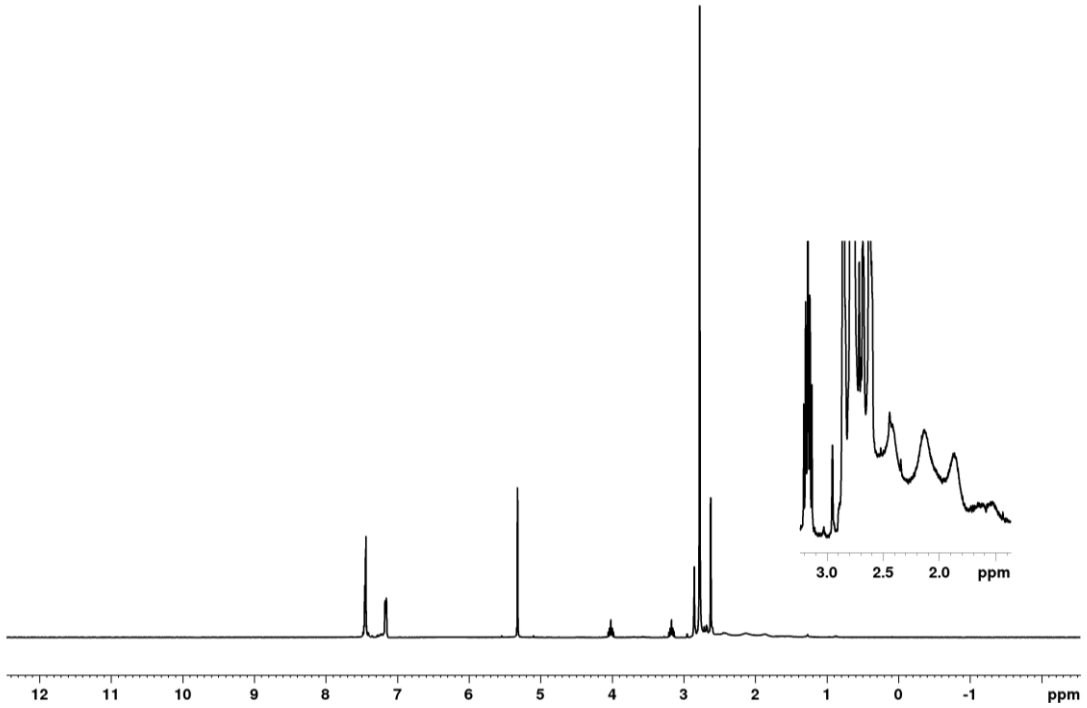

Figure S 3.25: ^{1}H NMR spectrum of [$Me_3N{\cdot}BH_2PH_2CPh_3$][TEF] (**4**) (+ [$Me_3N{\cdot}BH_2PH_2BH_2{\cdot}NMe_3]^+$) in CD_2Cl_2.

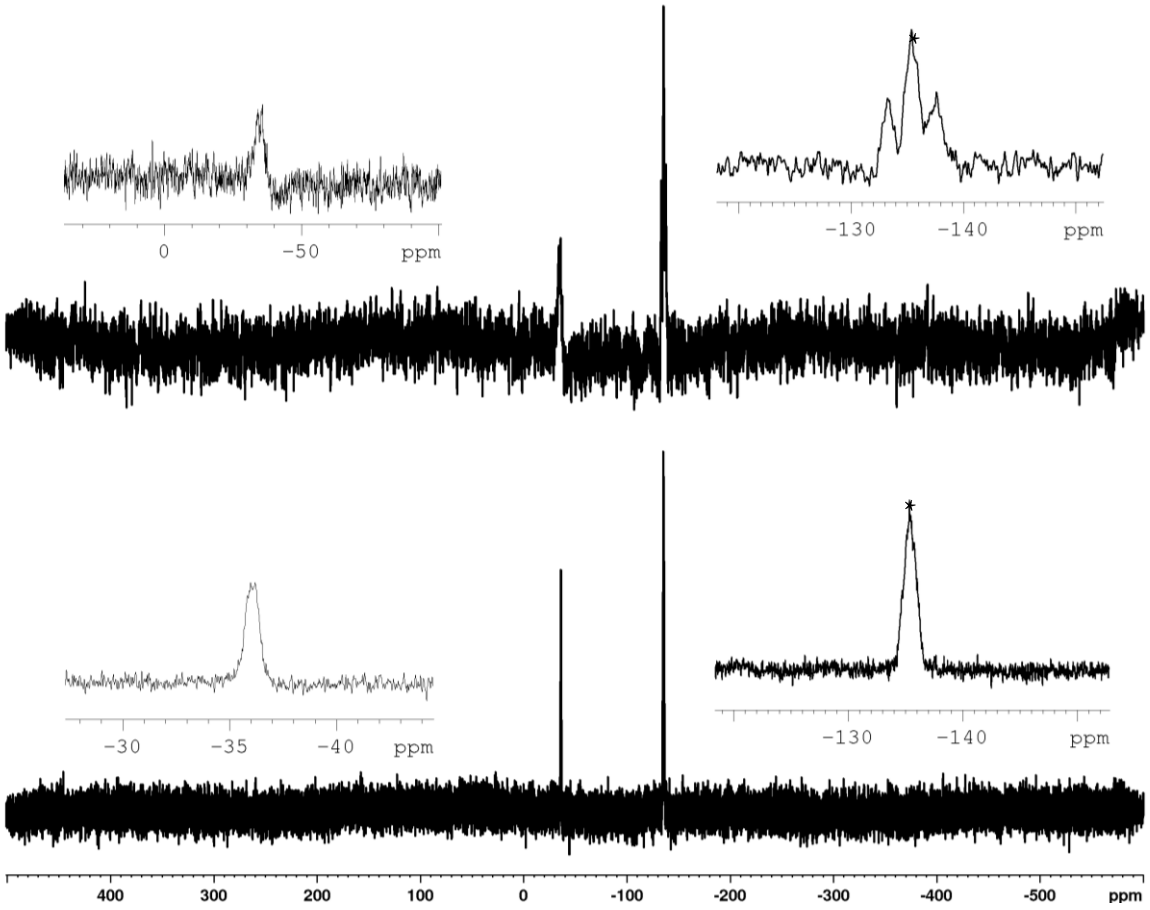

Figure S 3.26: $^{31}P\{^{1}H\}$ (bottom) and ^{31}P (top) NMR spectrum of [$Me_3N{\cdot}BH_2PH_2CPh_3$][TEF] (**4**) (+ [$Me_3N{\cdot}BH_2PH_2BH_2{\cdot}NMe_3]^+$, *) in CD_2Cl_2.

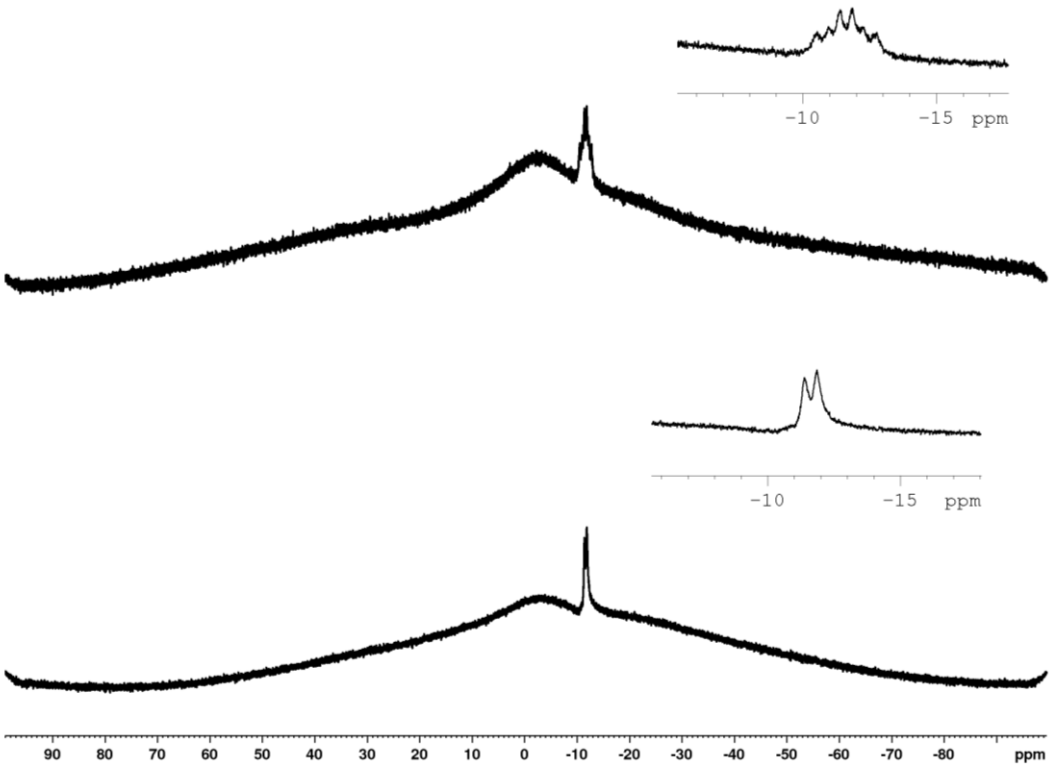

Figure S 3.27: $^{11}B\{^{1}H\}$ (bottom) and ^{11}B (top) NMR spectrum of $[Me_3N{\cdot}BH_2PH_2CPh_3][TEF]$ (**4**) (+ $[Me_3N{\cdot}BH_2PH_2BH_2{\cdot}NMe_3]^+$) in CD_2Cl_2.

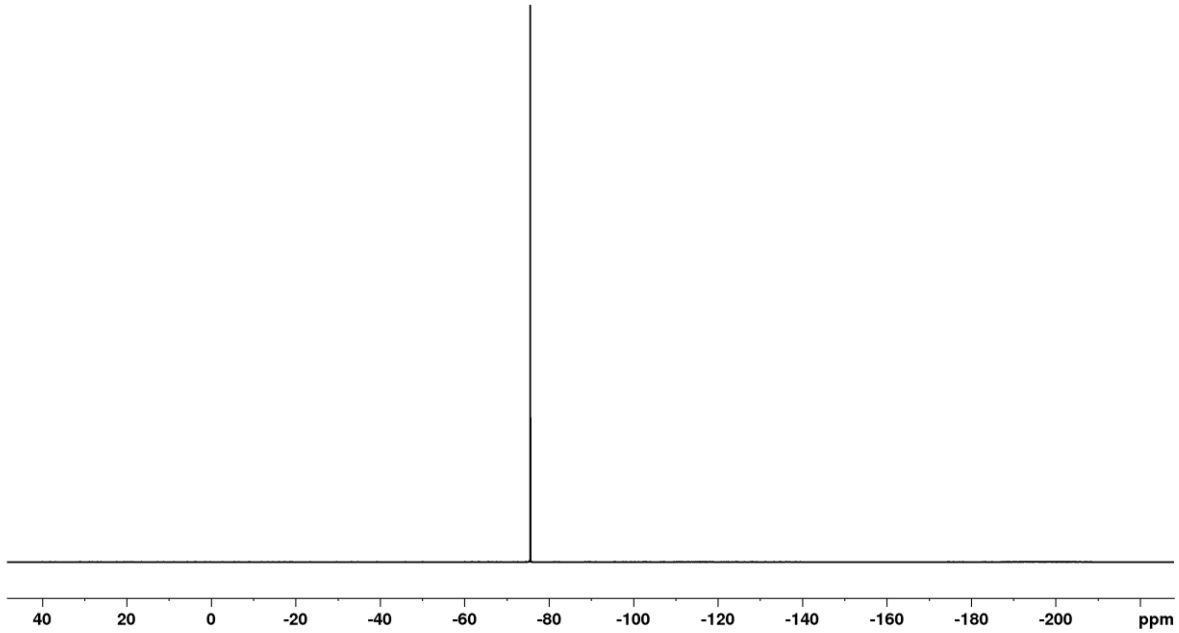

Figure S 3.28: ^{19}F NMR spectrum of $[Me_3N{\cdot}BH_2PH_2CPh_3][TEF]$ (**4**) (+ $[Me_3N{\cdot}BH_2PH_2BH_2{\cdot}NMe_3]^+$) in CD_2Cl_2.

Reaction of $PH_2BH_2{\cdot}NMe_3$ with Tl[TEF] in 1,2-difluorobenzene

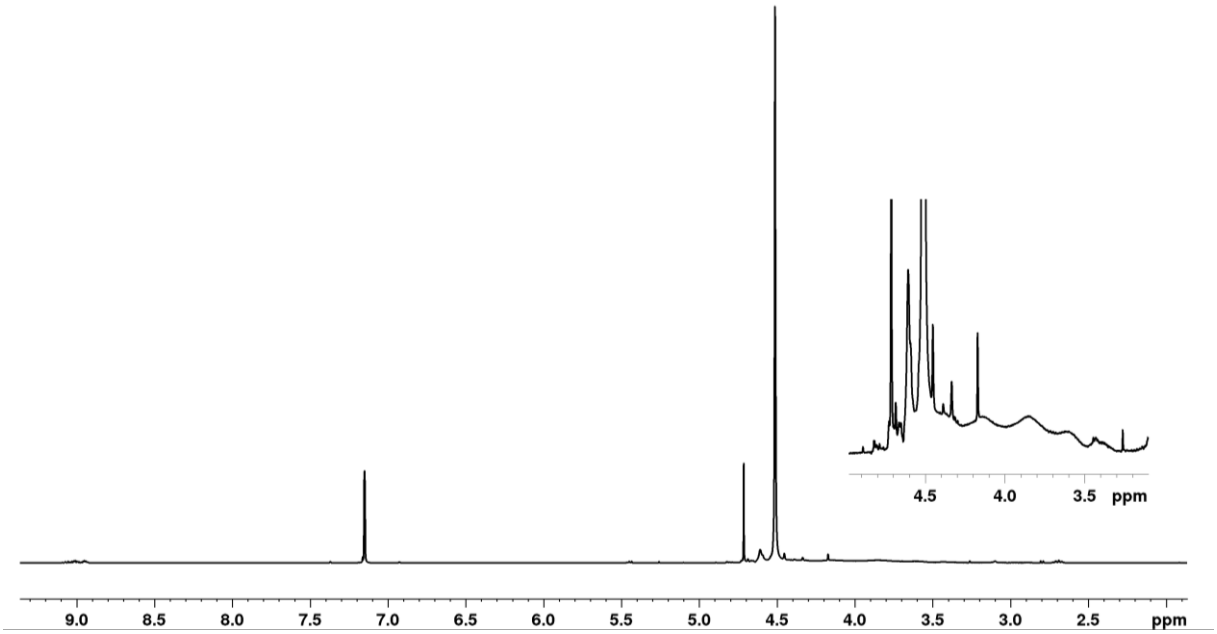

Figure S 3.29: ^{1}H NMR spectrum of spectrum of the crystals resulting from the reaction of 2 $PH_2BH_2{\cdot}NMe_3$ with Tl[TEF] in 1,2-difluorobenzene (298 K, CD_2Cl_2).

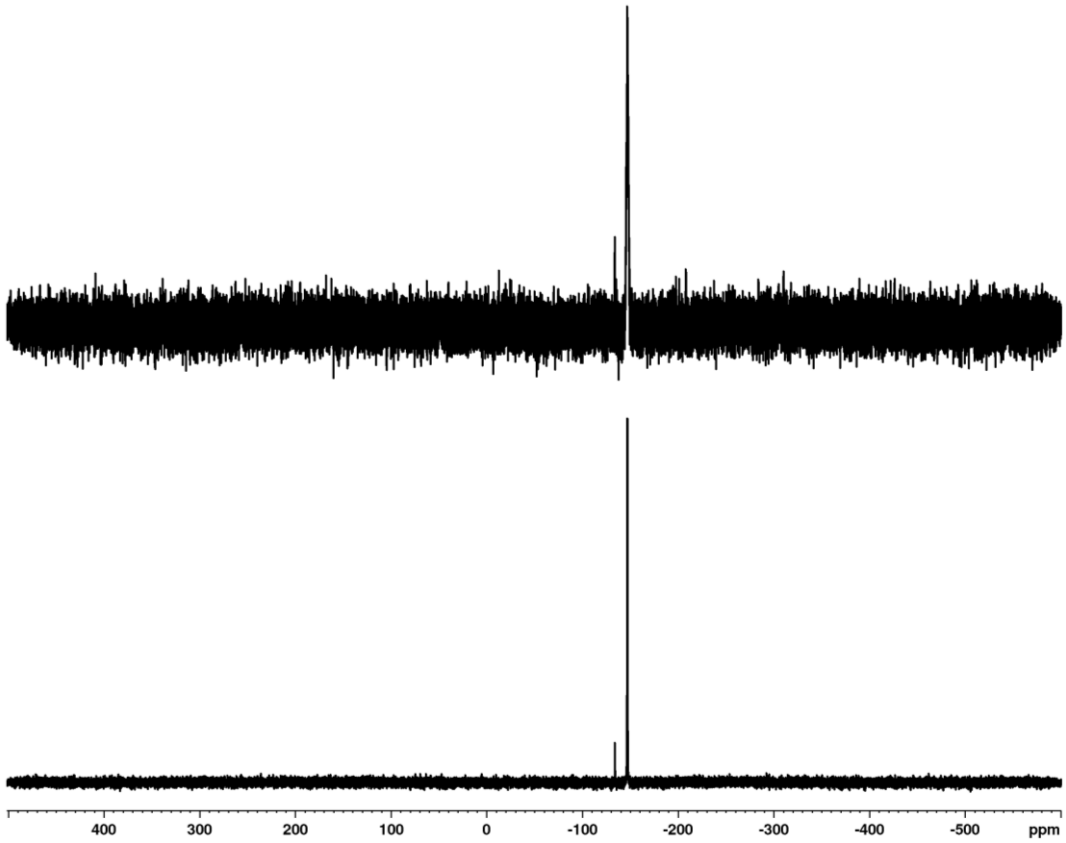

Figure S 3.30: $^{31}P\{^{1}H\}$ (bottom) and ^{31}P (top) NMR spectrum of the crystals resulting from the reaction of 2 $PH_2BH_2{\cdot}NMe_3$ with Tl[TEF] in 1,2-difluorobenzene (298 K, CD_2Cl_2).

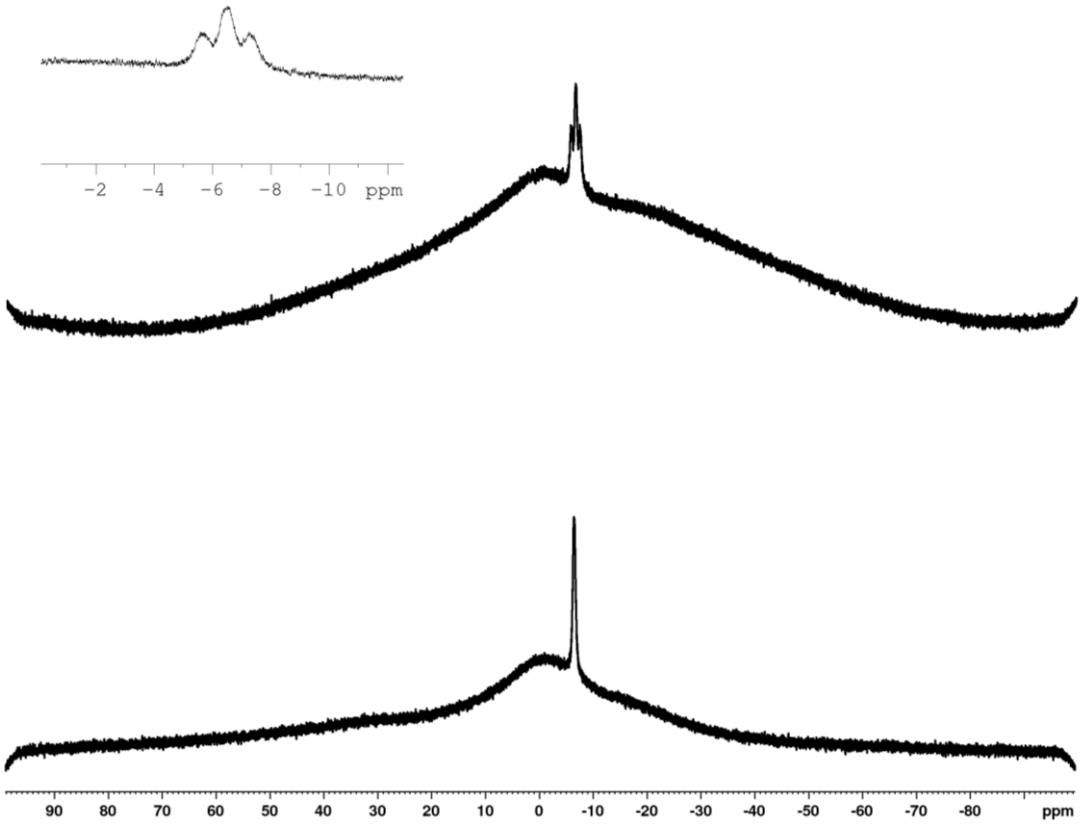

Figure S 3.31: $^{11}B\{^{1}H\}$ (bottom) and ^{11}B (top) NMR spectrum of the crystals resulting from the reaction of 2 $PH_2BH_2{\cdot}NMe_3$ with Tl[TEF] in 1,2-difluorobenzene (298 K, CD_2Cl_2).

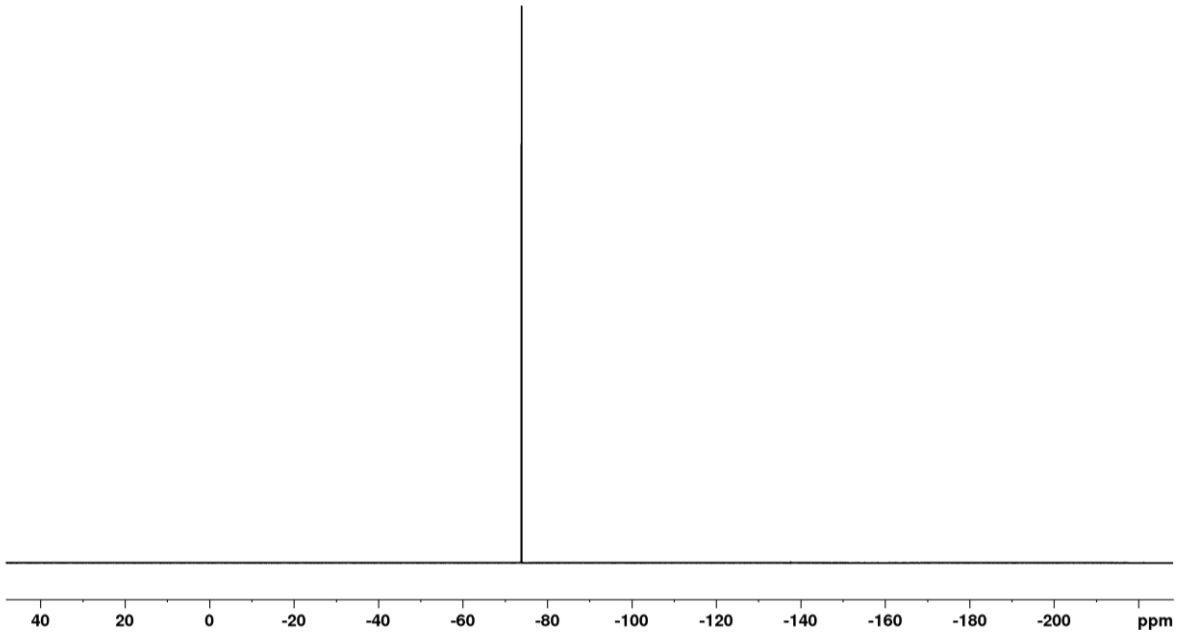

Figure S 3.32: ^{19}F spectrum of the crystals resulting from the reaction of 2 $PH_2BH_2{\cdot}NMe_3$ with Tl[TEF] in 1,2-difluorobenzene (298 K, CD_2Cl_2).

3.5.3 X-ray powder diffraction data

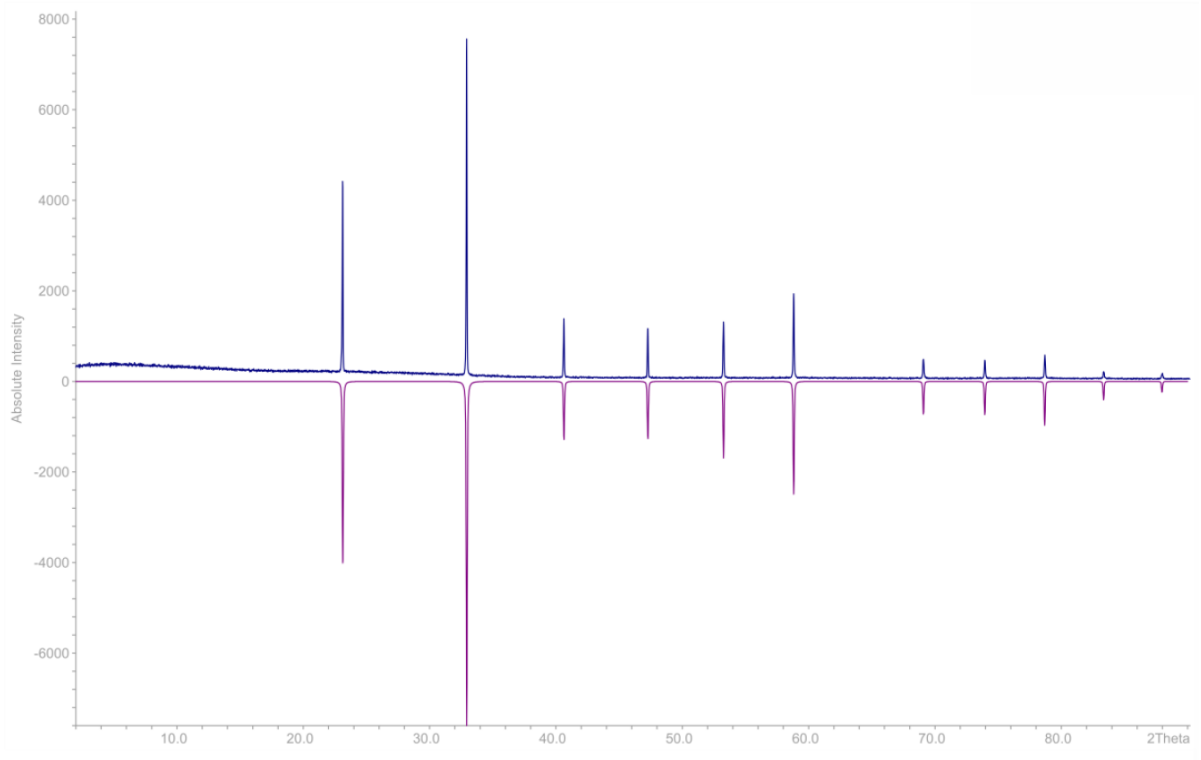

Figure S 3.33: X-ray powder diffraction pattern of the precipitated powder (top) vs. theoretical pattern of TlCl (bottom). The measurements were carried out with a STOE Stadi P diffractometer with monochromatic CuK_{α}-radiation (λ = 1.540598 Å, Ge monochromator) and a Mythen 1 K detector at 293 K.

3.5.4 Crystallographic Data

Single crystal X-ray structure determination: Single-crystal X-ray diffraction data were collected on a Xcalibur Gemini Ultra diffractometer (*Oxford Diffraction*, AtlasS2 CCD detector; **1b**, **2a**, **2b**), a GV50 diffractometer (*Rigaku*, TitanS2 CCD detector; **A**, **B, 4**) or a XtaLAB Synergy R DW system (*Rigaku*, HyPix-Arc 150 detector; **1a**). Crystals were selected under mineral oil and mounted on MiTeGen MicroLoops. Data were collected using Cu-K_α radiation (λ = 1.54178 Å). Data reduction, scaling and absorption corrections were performed using CrysAlisPro (*Rigaku*). Using Olex2, all structures were solved with ShelXT and a least-square refinement in F^2 was carried out with ShelXL. All non-hydrogen atoms were refined anisotropically. Unless noted otherwise, the hydrogen atoms at the carbon atoms were located in idealized positions and refined isotropically according to the riding model.

Figures were created with Olex2.

Crystallographic data and details of the experiments are given in Table S 3.1, Table S 3.2 and Table S 3.3.

CIF files with comprehensive information on the details of the diffraction experiments and full tables of bond lengths and angles are deposited in the Cambridge Crystallographic Data Centre under the deposition codes CCDC 2194092-2194098. These data can be obtained free of charge at www.ccd.cam.ac.uk/conts/retrieving.html (or from the Cambridge Crystallographic Data Centre, 12 Union Road, Cambridge CB2 1EZ, UK; Fax: + 44-1223-336-033; e-mail: deposit@ccdc.cam.ac.uk).

Table S 3.1: Crystallographic data for compounds **A**, **B**, and **1a**.

Compound	**A**	**B**	**1a**
Internal naming	MA32	MA27	RS500
CCDC number	2194092	2194093	2194094
Formula	$C_{25}H_{14}BCl_{10}Tl$	$AlC_{16}Cl_{12}F_{24}O_4Tl$	$C_{27.75}H_{26.5}B_2Cl_{9.5}NPTl$
$D_{calc.}$/ g cm^{-3}	1.968	2.672	1.802
m/mm^{-1}	18.786	19.641	15.848
Formula Weight	884.04	1368.91	967.73
Colour	clear colourless	clear colourless	clear colourless
Shape	plate-shaped	block-shaped	block-shaped
Size/mm^3	0.18×0.07×0.02	0.15×0.10×0.10	0.46×0.15×0.09
T/K	122.97(19)	122.99(14)	100.00(10)
Crystal System	monoclinic	orthorhombic	monoclinic
Space Group	$P2_1/n$	$Pbcn$	$P2_1/c$
a/Å	11.8526(5)	15.1473(5)	12.8644(2)
b/Å	15.4245(7)	15.4398(5)	15.7972(3)
c/Å	16.5523(9)	14.5515(4)	17.9464(3)
a/°	90	90	90
b/°	99.676(5)	90	102.0262(18)
g/°	90	90	90
V/Å^3	2983.0(2)	3403.18(18)	3567.06(11)
Z	4	4	4
Z'	1	0.5	1
Wavelength/Å	1.54184	1.54184	1.54184
Radiation type	Cu K_a	Cu K_a	Cu K_a
Q_{min}/°	3.944	4.089	3.513
Q_{max}/°	67.075	74.869	75.128
Measured Refl's.	14841	12510	33746
Indep't Refl's	5261	3333	7183
Refl's I≥2 s(I)	2885	2917	5918
R_{int}	0.1313	0.1229	0.0363
Parameters	398	354	401
Restraints	147	39	12
Largest Peak	2.047	4.126	1.292
Deepest Hole	-2.352	-2.585	-1.838
GooF	0.883	1.086	1.068
wR_2 (all data)	0.1649	0.1988	0.1437
wR_2	0.1549	0.1893	0.1375
R_1 (all data)	0.1107	0.0738	0.0584
R_1	0.0668	0.0682	0.0495

Table S 3.2: Crystallographic data for compounds **1b**, **2a** and **2b**.

Compound	**1b**	**2a**	**2b**
Internal naming	MA43	MA28	1
CCDC number	2194095	2194096	2194097
Formula	$C_{28}H_{27}AsB_2Cl_{10}NTl$	$C_{25}H_{39}AlB_3Cl_{12}F_{24}N_3O_4P_3Tl$	$C_{25}H_{39}AlAs_3B_3F_{36}N_3O_4Tl$
D_{calc}/ g cm^{-3}	1.897	1.93	2.062
m/mm^{-1}	16.575	12.438	9.788
Formula Weight	1032.91	1683.68	1618.13
Colour	clear colourless	clear colourless	clear colourless
Shape	needle-shaped	needle-shaped	block-shaped
Size/mm^3	0.73×0.07×0.05	0.20×0.05×0.02	0.40×0.20×0.14
T/K	123(1)	123	123.05(10)
Crystal System	monoclinic	trigonal	trigonal
Flack Parameter	-	-0.035(12)	-0.058(5)
Hooft Parameter	-	-0.022(9)	-0.039(2)
Space Group	$P2_1/c$	$R3c$	$P31c$
a/Å	12.9362(4)	29.8494(9)	16.92690(10)
b/Å	15.9544(5)	29.8494(9)	16.92690(10)
c/Å	17.8864(7)	33.8004(12)	10.50350(10)
a/°	90	90	90
b/°	101.535(4)	90	90
g/°	90	120	120
V/Å^3	3617.0(2)	26081.0(18)	2606.27(4)
Z	4	18	2
Z'	1	1	0.333333
Wavelength/Å	1.54184	1.54184	1.54178
Radiation type	Cu K_a	CuK_a	Cu K_a
Q_{min}/°	3.487	4.306	3.014
Q_{max}/°	66.711	66.184	66.513
Measured Refl's.	17547	26015	46858
Indep't Refl's	6272	8320	3069
Refl's I≥2 s(I)	5193	6872	3022
R_{int}	0.052	0.0806	0.0495
Parameters	435	694	356
Restraints	60	25	184
Largest Peak	1.592	0.847	0.605
Deepest Hole	-1.307	-1.121	-0.952
GooF	1.075	1.018	1.051
wR_2 (all data)	0.1229	0.1014	0.0848
wR_2	0.1159	0.0944	0.0845
R_1 (all data)	0.0593	0.0646	0.0322
R_1	0.0476	0.0479	0.0318

Table S 3.3: Crystallographic data for compound **4**.

Compound	**4**
Internal naming	RS556
CCDC number	2194098
Formula	$C_{38}H_{28}AlBF_{36}NO_4P$
$D_{calc.}$/ g cm^{-3}	1.778
m/mm^{-1}	2.352
Formula Weight	1315.37
Colour	clear colourless
Shape	prism-shaped
Size/mm^3	0.56×0.17×0.15
T/K	123.00(10)
Crystal System	monoclinic
Space Group	$C2/c$
a/Å	39.5094(5)
b/Å	12.2858(2)
c/Å	20.6645(3)
a/°	90
b/°	101.590(2)
g/°	90
V/Å^3	9826.1(3)
Z	8
Z'	1
Wavelength/Å	1.54184
Radiation type	Cu K_a
Q_{min}/°	4.245
Q_{max}/°	66.723
Measured Refl's.	38452
Indep't Refl's	8665
Refl's I≥2 s(I)	7457
R_{int}	0.0508
Parameters	758
Restraints	0
Largest Peak	0.255
Deepest Hole	-0.328
GooF	1.027
wR_2 (all data)	0.095
wR_2	0.0886
R_1 (all data)	0.0432
R_1	0.0356

3.5.4.1 Crystal Structures

Tl[BAr^{Cl}] (A) · CH_2Cl_2

A crystallized from CH_2Cl_2 at room temperature as clear colourless plate-shaped crystals in the monoclinic space group $P2_1/n$. The structure of **A** in the solid state is shown in Figure S 3.34.

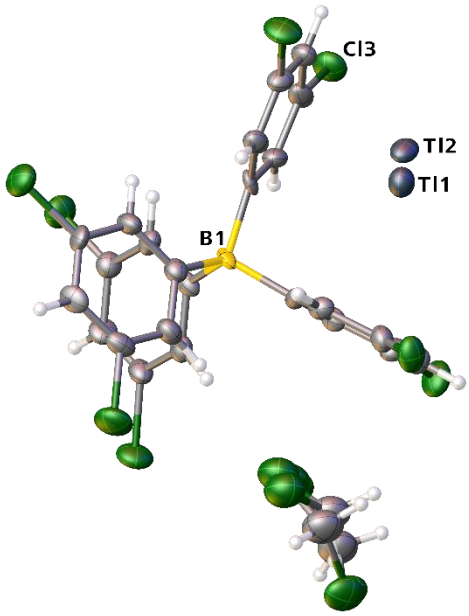

Figure S 3.34: Molecular structure of **A** in the solid state. Anisotropic displacement ellipsoids are shown at 50% probability.

The asymmetric unit contains one molecule of **A** and one molecule of CH_2Cl_2 distributed over three positions with occupancies of 0.47, 0.36 and 0.17. These atoms were refined with the restraints SADI and SIMU. The Tl^+ ion is disordered over two positions with occupancies of 0.974 and 0.026 and was refined with the SIMU restraint.

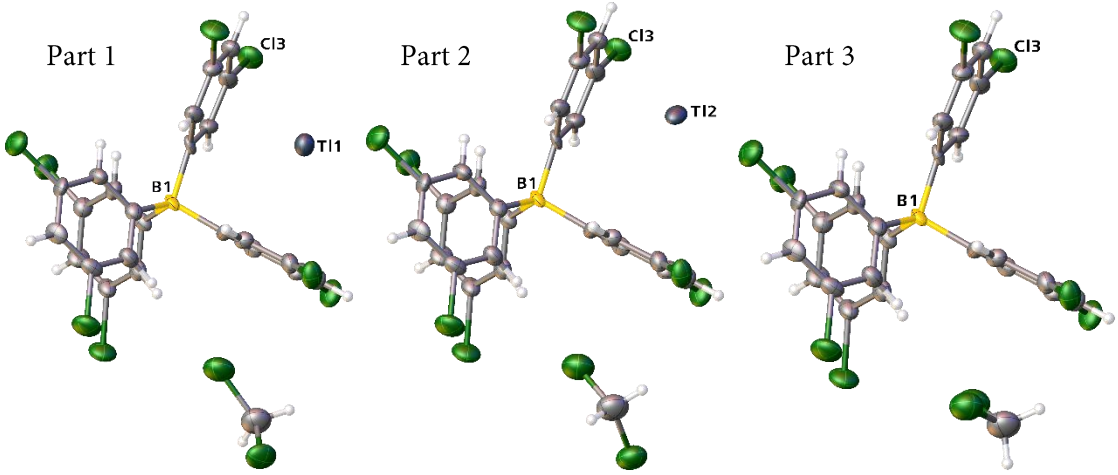

Figure S 3.35: Individual parts of the solid-state structure of **A**.

Tl[TEF^{Cl}] (B)

B crystallized from a CH_2Cl_2 solution layered with six times the amount of *n*-hexane at -28 °C as clear colourless block-shaped crystals in the orthorhombic space group *Pbcn*. The structure of **B** is shown in Figure S 3.36.

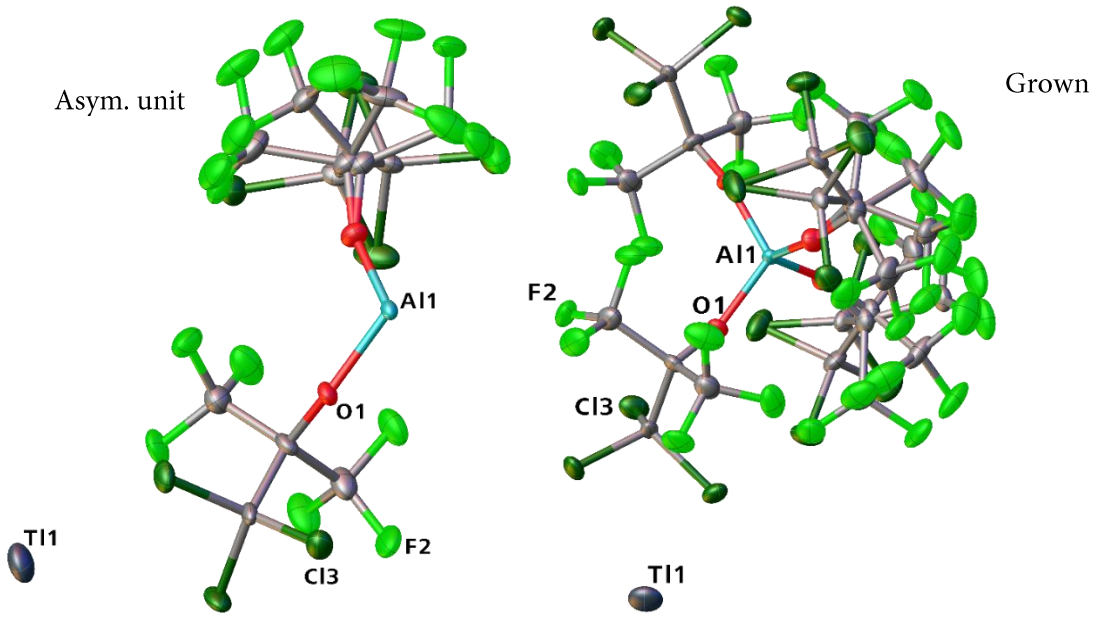

Figure S 3.36: Molecular structure of **B** in the solid state. Anisotropic displacement ellipsoids are shown at 50% probability.

The asymmetric unit contains 0.5 molecules of **B**. One $\{C(CF_3)_2CCl_3\}$ branch is disordered by rotation and was refined with SADI, SIMU and ISOR restraints.

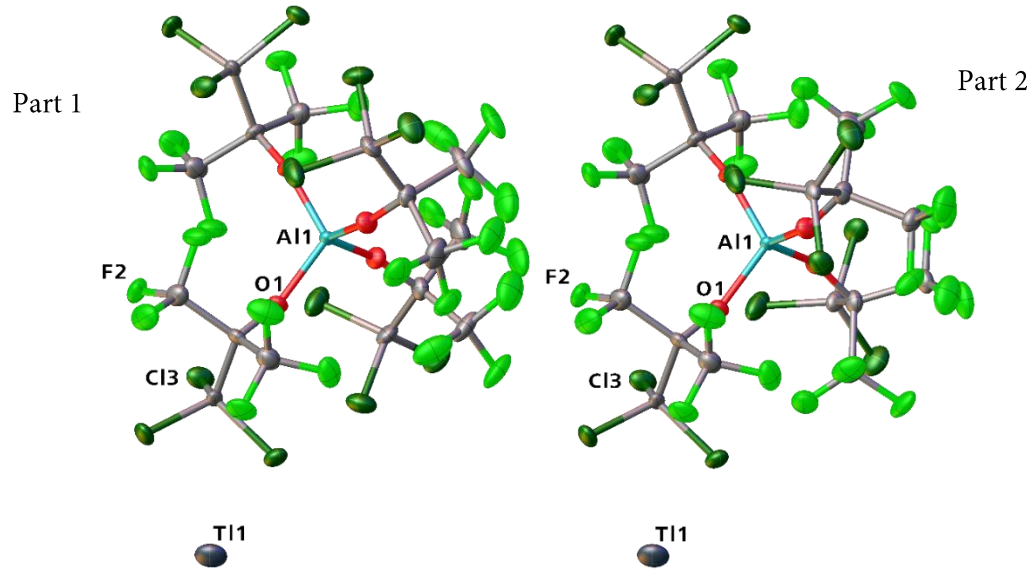

Figure S 3.37: Grown individual parts of the structure of **B** in the solid state.

[Tl(H$_2$PBH$_2$·NMe$_3$)][BAr^{Cl}] (1a) · CH$_2$Cl$_2$

1a crystallized from a CH_2Cl_2 solution layered with six times the amount of *n*-hexane at -28 °C as clear colourless block-shaped crystals in the monoclinic group $P2_1/c$. The structure of **1a** is shown in Figure S 3.38.

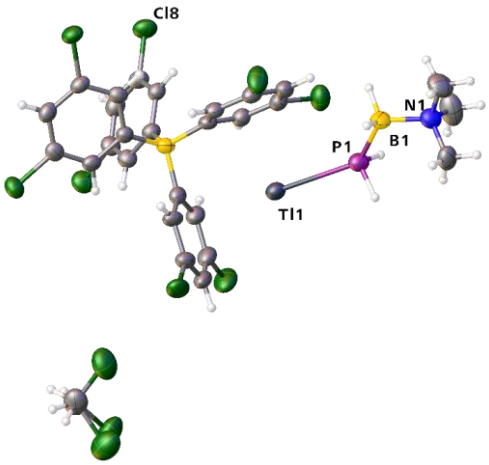

Figure S 3.38: Molecular structure of **1a** in the solid state. Anisotropic displacements ellipsoids are shown at 50% probability. Selected bond lengths [Å] and angles [°]: N1-B1 1.628(10), B1-P1 1.960(8), P1-Tl1 3.0419(15), N1-B1-P1 115.6(5), B1-P1-Tl1 138.6(3).

The asymmetric unit contains one molecule of **1a** and one molecule of CH_2Cl_2 with disorder at one {CH_2Cl} branch. This was refined with the SIMU restraint.

[Tl(H$_2$AsBH$_2$·NMe$_3$)][BAr^{Cl}] (1b) · CH$_2$Cl$_2$

1b crystallized from a CH_2Cl_2 solution layered with six times the amount of *n*-hexane at -28 °C as clear colourless needle-shaped crystals in the monoclinic group $P2_1/c$. The structure of **1b** is shown in Figure S 3.39.

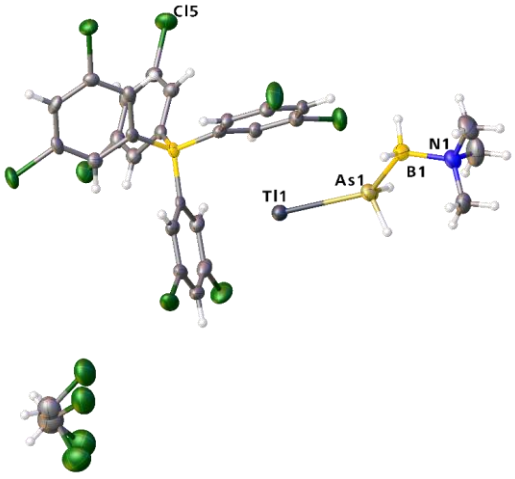

Figure S 3.39: Molecular structure of **1b** in the solid state. Anisotropic displacement ellipsoids are shown at 50% probability. Selected bond lengths [Å] and angles [°]: N1-B1 1.616(11), B1-As1 2.072(9), As1-Tl1 3.1193(8), N1-B1-As1 115.4(5), B1-As1-Tl1 143.4(3).

The asymmetric unit contains one molecule of **1b** and one disordered molecule of CH_2Cl_2. This was refined by applying SADI and SIMU restraints.

$[Tl(H_2PBH_2{\cdot}NMe_3)_3][TEF^{Cl}]$ (2a)

2a crystallized from a CH_2Cl_2 solution layered with six times the amount of *n*-hexane at -28 °C as clear colourless needle-shaped crystals in the trigonal group *R*3*c*. The structure of **2a** is shown in Figure S 3.40.

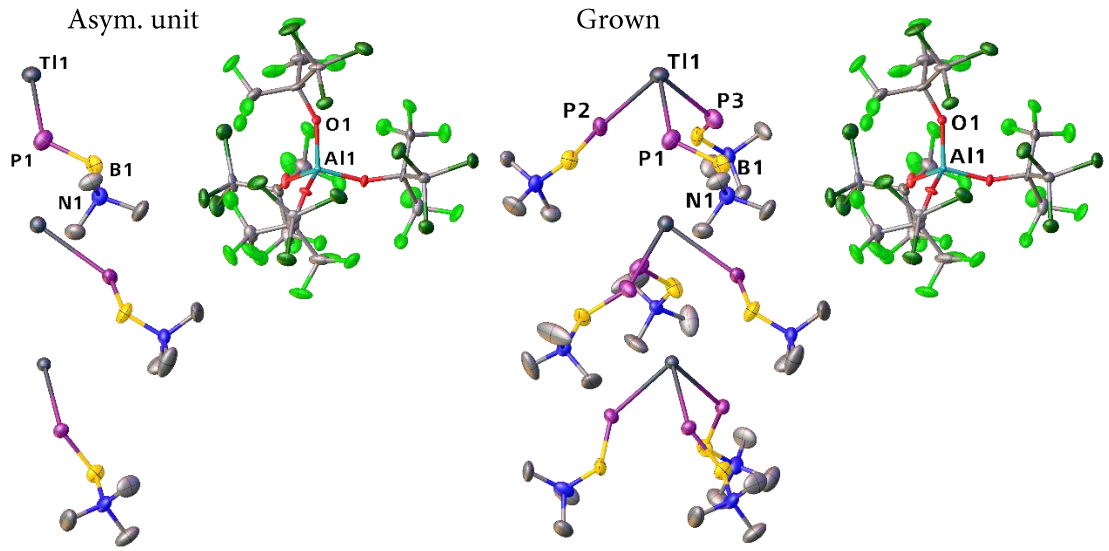

Figure S 3.40: Molecular structure of 2a in the solid state. Anisotropic displacement ellipsoids are shown at 50% probability level. Hydrogen atoms are omitted for clarity. Selected bond lengths [Å] and angles [°]: N1-B1 1.58(2), B1-P1 1.961(18), P1-Tl1 2.989(4), P1-Tl1-P2 84.235, B1-P1-Tl1 119.4(5).

The asymmetric unit contains one molecule of **2a** (the cation is distributed along three symmetry equivalent positions with an occupation of 0.33 each). The $[TEF^{Cl}]^-$ anion was refined by applying ISOR and SIMU restraints.

$[Tl(H_2AsBH_2{\cdot}NMe_3)_3][TEF]$ (2b)

2b crystallized from a CH_2Cl_2 solution layered with six times the amount of *n*-hexane at -28 °C as clear colourless block-shaped crystals in the trigonal group *P*31*c*. The structure of **2b** is shown in Figure S 3.41.

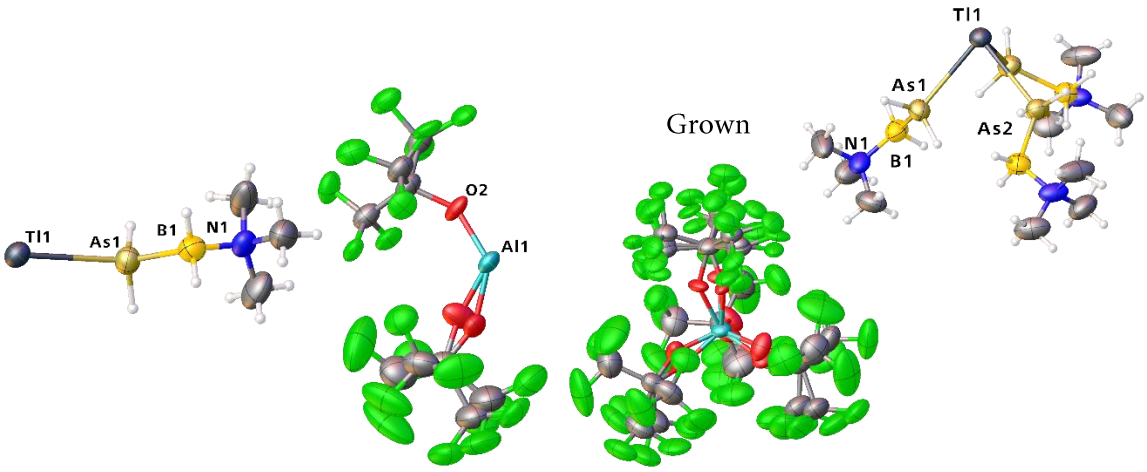

Figure S 3.41: Molecular structure of **2b** in the solid state. Anisotropic displacement ellipsoids are shown at 50% probability level. Selected bond lengths [Å] and angles [°]: N1-B1 1.593(15), B1-As1 2.084(12), As1-Tl1 3.1158(12), As1-Tl1-As2 81.507, N1-B1-As1 117.1(8), B1-As1-Tl1 125.8(4).

The asymmetric unit contains 1/3 molecule of $[Tl(H_2AsBH_2 \cdot NMe_3)_3]^+$ and 1/2 $[TEF]^-$. The anion is disordered in several $\{C(CF_3)_3\}$ branches and was refined by applying DFIX, SADI and SIMU restraints.

$[Me_3N{\cdot}BH_2PH_2CPh_3][TEF]$ (4)

4 crystallized from a CH_2Cl_2 solution layered with three times the amount of *n*-hexane at 8 °C as clear colourless prism-shaped crystals in the trigonal group *C2/c*. The structure of **4** is shown in Figure S 3.42.

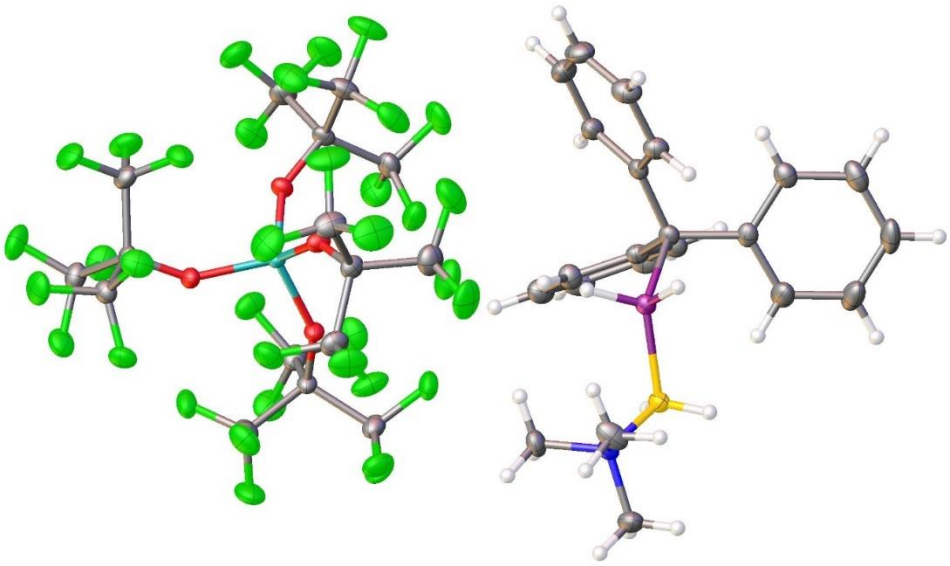

Figure S 3.42: Molecular structure of **2b** in the solid state. Anisotropic displacement ellipsoids are shown at 50% probability level. Selected bond lengths [Å] and angles [°]: N-B 1.603(3), B-P 1.977(2), P-C 1.8842(19), N-B-P 110.80(14), B-P-C 120.87(9).

The asymmetric unit contains molecule of $[Me_3N \cdot BH_2PH_2CPh_3][TEF]$ without any incorporated solvent molecules. Unusually, the $[TEF]^-$ anion does not display disorder in its $\{C(CF_3)_3\}$ branches.

3.5.5 Computational Data

All computations have been carried out using Gaussian 16 program package.[9] The geometries of the compounds have been fully optimized with M06-2X high-nonlocality functional with the double amount of nonlocal exchange (2X)[10] with all electron def2-TZVPP basis set (ECP on Tl).[11] Basis sets were obtained from the EMSL basis set exchange database.[12] All structures correspond to minima on their respective potential energy surfaces (PES) or transition states (TS) as verified by the subsequent vibrational analysis.

Table S 3.4: Reaction energies $\Delta E°_0$, standard enthalpies $\Delta H°_{298}$, Gibbs energies $\Delta G°_{298}$ (kJ mol^{-1}) and standard entropies $\Delta S°_{298}$ (J mol^{-1} K^{-1}) for the considered gas phase processes (M06-2X/def2-TZVPP level of theory).

Process	$\Delta E°_0$	$\Delta H°_{298}$	$\Delta S°_{298}$	$\Delta G°_{298}$
Coordination at Tl$^+$				
$Tl^+ + PH_2BH_2NMe_3 = Tl(PH_2BH_2NMe_3)^+$	-158.3	-154.9	-93.4	-127.0
$Tl^+ + AsH_2BH_2NMe_3 = Tl(AsH_2BH_2NMe_3)^+$	-151.7	-149.0	-82.4	-124.5
$Tl^+ + 3\ PH_2BH_2NMe_3 = Tl(PH_2BH_2NMe_3)_3^+$	-365.9	-351.4	-426.8	-224.1
$Tl^+ + 3\ AsH_2BH_2NMe_3 = Tl(AsH_2BH_2NMe_3)_3^+$	-352.4	-342.3	-406.2	-221.2
$Tl(PH_2BH_2NMe_3)^+ + 2\ PH_2BH_2NMe_3 = Tl(PH_2BH_2NMe_3)_3^+$	-207.7	-196.5	-333.4	-97.1
$Tl(AsH_2BH_2NMe_3)^+ + 2\ AsH_2BH_2NMe_3 = Tl(AsH_2BH_2NMe_3)_3^+$	-200.7	-193.3	-323.8	-96.7
Abstraction processes				
$CH_2Cl_2 + Tl^+ = TlCl + CH_2Cl^+$	248.5	240.8	43.0	228.0
$CH_2Cl^+ + PH_2BH_2NMe_3 = CH_3Cl + PH_2BHNMe_3^+$	-378.2	-370.2	-1.4	-369.8
$CH_2Cl^+ + AsH_2BH_2NMe_3 = CH_3Cl + AsH_2BHNMe_3^+$	-362.8	-356.0	9.1	-358.7
Overall reaction equations for abstractions				
$CH_2Cl_2 + Tl^+ + PH_2BH_2NMe_3 = TlCl + PH_2BHNMe_3^+ + CH_3Cl$	-129.7	-129.4	41.6	-141.8
$CH_2Cl_2 + Tl^+ + AsH_2BH_2NMe_3 = TlCl + AsH_2BHNMe_3^+ + CH_3Cl$	-114.2	-115.2	52.1	-130.7
$CH_2Cl_2 + TlPH_2BH_2NMe_3^+ = TlCl + PH_2BHNMe_3^+ + CH_3Cl$	28.6	25.5	135.0	-14.8
$CH_2Cl_2 + TlAsH_2BH_2NMe_3^+ = TlCl + AsH_2BHNMe_3^+ + CH_3Cl$	37.5	33.9	134.5	-6.2
Addition processes				
$PH_2BHNMe_3^+ + PH_2BH_2NMe_3 = NMe_3BH_2PHPH_2BH_2NMe_3^+$	-226.1	-212.7	-169.1	-162.3
$AsH_2BHNMe_3^+ + AsH_2BH_2NMe_3 = NMe_3BH_2AsHAsH_2BH_2NMe_3^+$	-251.5	-237.8	-155.5	-191.5
$PH_2BHNMe_3^+ + PH_2BH_2NMe_3 = NMe_3BH(PH_2)PH_2BH_2NMe_3^+$	-232.3	-221.5	-191.0	-164.5
$AsH_2BHNMe_3^+ + AsH_2BH_2NMe_3 = NMe_3BH(AsH_2)AsH_2BH_2NMe_3^+$	-219.4	-210.7	-176.7	-158.0
Overall reaction equations for the coupling				
$CH_2Cl_2 + Tl^+ + 2\ PH_2BH_2NMe_3 = TlCl + CH_3Cl + NMe_3BH_2PHPH_2BH_2NMe_3^+$	-355.7	-342.1	-127.5	-304.1
$CH_2Cl_2 + Tl^+ + 2\ AsH_2BH_2NMe_3 = TlCl + CH_3Cl + NMe_3BH_2AsHAsH_2BH_2NMe_3^+$	-349.4	-338.7	-109.5	-306.1
$CH_2Cl_2 + Tl^+ + 2\ PH_2BH_2NMe_3 = TlCl + CH_3Cl + NMe_3BH(PH_2)PH_2BH_2NMe_3^+$	-362.0	-350.9	-149.4	-306.3
$CH_2Cl_2 + Tl^+ + 2\ AsH_2BH_2NMe_3 = TlCl + CH_3Cl + NMe_3BH(AsH_2)AsH_2BH_2NMe_3^+$	-333.6	-325.9	-124.6	-288.8
Comparison of Isomers				
PP isomer = PB isomer	-6.3	-8.8	-21.9	-2.2
PP isomer = PAs isomer	15.8	12.8	-15.2	17.3

Table S 3.5: Total energies E^o_0, sum of electronic and thermal enthalpies H^o_{298} (Hartree) and standard entropies S^o_{298} (cal mol^{-1}K^{-1}) (M06-2X/def2-TZVPP level of theory)

Compound	E^o_0	H^o_{298}	S^o_{298}
Tl^+	-172.1863631	-172.184003	41.857
TlCl	-632.6766656	-632.672278	61.281
CH_3Cl	-500.0991075	-500.057198	55.872
CH_2Cl_2	-959.6959285	-959.661608	64.459
$PH_2BHNMe_3^+$	-542.2163585	-542.049912	88.211
$PHBH_2NMe_3^+$ (TS)	-542.1598498		
$AsH(\mu\text{-}H)BHNMe_3^+$ intermediate	-2436.747016	-2436.582939	89.764
$AsH_2BHNMe_3^+$	-2436.753237	-2436.588393	91.211
$AsHBH_2NMe_3^+$ (TS)	-2436.721184		
$PH_2BH_2NMe_3$	-543.0604496	-542.884487	89.108
$AsH_2BH_2NMe_3$	-2437.603211	-2437.428384	89.607
$Tl(PH_2BH_2NMe_3)^+$	-715.3070976	-715.127484	108.647
$Tl(AsH_2BH_2NMe_3)^+$	-2609.847367	-2609.669156	111.769
$Tl(PH_2BH_2NMe_3)_3^+$	-1801.507091	-1800.971300	207.173
$Tl(AsH_2BH_2NMe_3)_3^+$	-7485.130231	-7484.599536	213.591
$[Tl(PH_2BH_2NMe_3)_2(CH_2Cl_2)]^+$	-2218.1206481	-2217.726543	195.130
$[Tl(AsH_2BH_2NMe_3)_2(CH_2Cl_2)]^+$	-6007.203286	-6006.812742	199.674
$Tl(PH_2BH_2NMe_3)^+$ $[B(C_6H_3Cl_2)_4]^-$ ion pair	-5343.775713	-5343.270983	273.782
$Tl(AsH_2BH_2NMe_3)^+$ $[B(C_6H_3Cl_2)_4]^-$ ion pair	-7238.317465	-7237.814517	277.166
$NMe_3BH_2PHPH_2BH_2NMe_3^+$ (*PP isomer*)	-1085.362907	-1085.01541	136.894
$NMe_3BH_2PH_2BH(PH_2)NMe_3^+$ (*PB isomer*)	-1085.365297	-1085.018752	131.66
$NMe_3BH_2AsHAsH_2BH_2NMe_3^+$ (*AsAs isomer*)	-4874.446006	-4874.101905	142.215
$NMe_3BH_2AsH_2BH(AsH_2)NMe_3^+$ (*AsB isomer*)	-4874.439996	-4874.097038	138.59
$[B(C_6H_3Cl_2)_4]^-$ D_{2d} 2im	-4628.347953		
$Tl(PH_2BH_2NMe_3)^+$ $[B(C_6H_3Cl_2)_4]^-$	-5343.775713	-5343.270983	273.782
$Tl(AsH_2BH_2NMe_3)^+$ $[B(C_6H_3Cl_2)_4]^-$	-7238.317465	-7237.814517	277.166

Table S 3.6: Optimized geometries of theoretically studied compounds. Cartesian *xyz* coordinates in Ångströms (M06-2X/def2-TZVPP level of theory).

TlCl

81	0.000000000	0.000000000	0.439484000
17	0.000000000	0.000000000	-2.094011000

CH_3Cl

6	0.000000000	0.000000000	-1.122263000
17	0.000000000	0.000000000	0.654901000
1	0.000000000	1.028669000	-1.466578000
1	0.890854000	-0.514335000	-1.466578000
1	-0.890854000	-0.514335000	-1.466578000

CH_2Cl_2

1	-0.894735000	0.000000000	1.373540000
6	0.000000000	0.000000000	0.764057000
1	0.894735000	0.000000000	1.373540000
17	0.000000000	1.468108000	-0.215630000
17	0.000000000	-1.468108000	-0.215630000

$CHCl_2^+$

6	0.000000000	0.000000000	-1.034614000
17	0.000000000	0.000000000	0.549419000
1	0.000000000	0.950228000	-1.566219000
1	0.000000000	-0.950228000	-1.566219000

$[PH_2BHNMe_3]^+$

7	-0.808545000	0.009322000	-0.009886000
6	-1.496647000	0.522106000	1.222326000
6	-0.655720000	-1.470871000	0.097788000
6	-1.644722000	0.332275000	-1.213110000
1	-1.805710000	1.405798000	-1.256652000
1	-2.595959000	-0.187976000	-1.117334000
1	-1.125784000	-0.005798000	-2.107982000
1	-0.032546000	-1.704013000	0.958555000
1	-0.196160000	-1.848062000	-0.811703000
1	-1.639811000	-1.916661000	0.225187000
1	-1.639890000	1.595117000	1.130171000
1	-0.880359000	0.297776000	2.090532000
1	-2.458380000	0.019871000	1.310585000
15	2.184891000	0.029513000	0.090357000
1	2.965962000	0.835957000	-0.746623000
5	0.514549000	0.784738000	-0.151853000
1	0.360870000	1.954229000	-0.224570000
1	2.143993000	-1.178934000	-0.619076000

$[PHBH_2NMe_3]^+$ (TS)

7	-0.680965000	0.391647000	0.000000000
6	-1.193955000	-0.303079000	1.213321000
6	-1.193955000	-0.303079000	-1.213321000
6	-1.193955000	1.794552000	0.000000000
1	-0.828669000	2.302646000	0.888481000
1	-2.282433000	1.774902000	0.000000000
1	-0.828669000	2.302646000	-0.888481000
1	-0.861173000	-1.339514000	-1.202905000
1	-0.812099000	0.200010000	-2.098220000
1	-2.282156000	-0.274836000	-1.211736000
1	-0.812099000	0.200010000	2.098220000
1	-0.861173000	-1.339514000	1.202905000
1	-2.282156000	-0.274836000	1.211736000
15	1.855710000	-1.150165000	0.000000000
1	3.090571000	-0.468791000	0.000000000
5	0.896637000	0.445180000	0.000000000
1	1.349587000	1.035980000	0.962621000
1	1.349587000	1.035980000	-0.962621000

$AsH(\mu\text{-}H)BHNMe_3^+$ intermediate

7	-1.360853000	0.012279000	-0.000104000
6	-2.009967000	0.198518000	1.338973000
6	-1.182300000	-1.445955000	-0.253423000
6	-2.254475000	0.583363000	-1.057456000
1	-2.410945000	1.639471000	-0.857612000
1	-3.203802000	0.051221000	-1.036032000
1	-1.780946000	0.455210000	-2.028384000
1	-0.580727000	-1.878821000	0.541400000
1	-0.689681000	-1.585926000	-1.213438000
1	-2.161288000	-1.920274000	-0.273313000
1	-2.173114000	1.259299000	1.510455000
1	-1.357034000	-0.208818000	2.107527000
1	-2.960398000	-0.331687000	1.337605000
33	1.721780000	-0.047668000	0.016029000
1	2.396532000	1.310827000	0.014216000
5	-0.041045000	0.832051000	0.053152000
1	-0.219161000	1.997338000	0.123976000
1	0.733481000	0.523447000	-1.188950000

$[AsH_2BHNMe_3]^+$

7	1.390931000	-0.008849000	-0.013813000
6	2.023636000	-0.531171000	1.244843000
6	1.237660000	1.471491000	0.095863000
6	2.275772000	-0.327255000	-1.183098000
1	2.441697000	-1.399996000	-1.222655000
1	3.220426000	0.196509000	-1.049491000
1	1.791337000	0.012298000	-2.096611000
1	0.587513000	1.701730000	0.937038000
1	0.806057000	1.852764000	-0.825413000
1	2.218448000	1.913881000	0.256612000
1	2.173993000	-1.603082000	1.150863000
1	1.368809000	-0.314318000	2.086669000
1	2.979097000	-0.027324000	1.379886000
33	-1.731890000	-0.013996000	0.048227000
1	-2.426707000	-0.870576000	-0.979664000
5	0.076404000	-0.786309000	-0.202851000
1	0.251243000	-1.949706000	-0.316178000
1	-1.600505000	1.264783000	-0.747238000

$[AsHBH_2NMe_3]^+$ (TS)

7	-1.355313000	-0.121689000	0.000000000
6	-1.355313000	-0.983743000	1.212617000
6	-1.355313000	-0.983743000	-1.212617000
6	-2.604065000	0.699083000	0.000000000
1	-2.612473000	1.325261000	0.887903000
1	-3.467529000	0.036002000	0.000000000
1	-2.612473000	1.325261000	-0.887903000
1	-0.470603000	-1.617985000	-1.204817000
1	-1.350307000	-0.351754000	-2.096995000
1	-2.244928000	-1.611233000	-1.211082000
1	-1.350307000	-0.351754000	2.096995000
1	-0.470603000	-1.617985000	1.204817000
1	-2.244928000	-1.611233000	1.211082000
33	1.721529000	0.116059000	0.000000000
1	2.302322000	1.518417000	0.000000000
5	-0.130176000	0.881090000	0.000000000
1	-0.131201000	1.591916000	0.979675000
1	-0.131201000	1.591916000	-0.979675000

$PH_2BH_2NMe_3$

6	-2.026841000	-0.895701000	0.000174000
1	-1.988047000	-1.524631000	0.885419000
1	-1.987999000	-1.525110000	-0.884735000
1	-2.942620000	-0.301916000	-0.000018000
6	-0.895123000	0.848520000	1.204626000
1	-1.823015000	1.422718000	1.215491000
1	-0.041839000	1.520076000	1.194811000
1	-0.838937000	0.211259000	2.083766000
6	-0.895466000	0.848486000	-1.204637000
1	-1.823119000	1.423085000	-1.215005000
1	-0.840072000	0.211173000	-2.083774000
1	-0.041892000	1.519680000	-1.195356000
7	-0.846872000	-0.003969000	-0.000009000
15	2.246072000	-0.092694000	-0.000003000
1	2.121831000	0.864133000	1.035954000
1	2.121962000	0.864403000	-1.035917000
5	0.489123000	-0.964222000	-0.000178000
1	0.389855000	-1.626536000	-1.002876000
1	0.389874000	-1.626861000	1.002259000

$AsH_2BH_2NMe_3$

6	-2.605091000	-0.895985000	-0.000507000
1	-2.567778000	-1.525180000	0.884537000
1	-2.567608000	-1.524448000	-0.886072000
1	-3.519184000	-0.299764000	-0.000350000
6	-1.473553000	0.847686000	1.205212000
1	-2.404029000	1.417485000	1.214983000
1	-0.622489000	1.521830000	1.194969000
1	-1.415045000	0.210727000	2.084391000
6	-1.473226000	0.848626000	-1.204561000
1	-2.403828000	1.418225000	-1.214282000
1	-1.414196000	0.212372000	-2.084219000
1	-0.622334000	1.522972000	-1.193437000
7	-1.422630000	-0.005410000	-0.000004000
33	1.772472000	-0.048733000	0.000018000
1	1.584268000	0.991585000	1.102542000
1	1.584464000	0.991277000	-1.103000000
5	-0.096625000	-0.967750000	-0.000163000
1	-0.185461000	-1.626891000	-1.003723000
1	-0.185589000	-1.627341000	1.003046000

$[Tl(PH_2BH_2NMe_3)]^+$

6	-4.377847000	1.470803000	0.000808000
1	-4.109530000	2.038322000	-0.885926000
1	-4.109840000	2.037036000	0.888458000
1	-5.446543000	1.258681000	0.000474000
6	-3.996156000	-0.579825000	-1.209171000
1	-5.072388000	-0.748406000	-1.212838000
1	-3.479591000	-1.536088000	-1.199953000
1	-3.705968000	-0.014668000	-2.091185000
6	-3.996385000	-0.581481000	1.208037000
1	-5.072671000	-0.749708000	1.211465000
1	-3.705995000	-0.017725000	2.090869000
1	-3.480158000	-1.537905000	1.197405000
7	-3.618584000	0.191031000	-0.000001000
15	-0.779295000	-0.916602000	0.000038000
1	-1.049740000	-1.795954000	-1.062578000
1	-1.050081000	-1.796576000	1.062050000
81	2.042841000	0.100536000	-0.000001000
5	-2.056545000	0.575256000	0.000385000
1	-1.831664000	1.198599000	1.002587000
1	-1.831401000	1.199518000	-1.001281000

$[Tl(AsH_2BH_2NMe_3)]^+$

6	-4.587966000	1.503951000	-0.001379000
1	-4.364834000	2.088153000	-0.889753000
1	-4.363816000	2.090836000	0.884968000
1	-5.636138000	1.207060000	-0.000338000
6	-4.045096000	-0.513178000	-1.207830000
1	-5.105899000	-0.761200000	-1.213091000
1	-3.457936000	-1.427584000	-1.194693000
1	-3.794931000	0.069397000	-2.090684000
6	-4.044262000	-0.509796000	1.210293000
1	-5.104968000	-0.758207000	1.216728000
1	-3.793931000	0.075385000	2.091375000
1	-3.456762000	-1.423997000	1.199484000
7	-3.728962000	0.287443000	0.000013000
33	-0.728040000	-0.665031000	-0.000067000
1	-0.980465000	-1.641158000	-1.129770000
1	-0.980814000	-1.639100000	1.131261000
81	2.251142000	0.151386000	0.000011000
5	-2.210297000	0.807924000	-0.001296000
1	-2.028793000	1.434474000	1.003547000
1	-2.029720000	1.432098000	-1.007780000

$[Tl(PH_2BH_2NMe_3)_3]^+$

6	3.195527000	1.988414000	-3.096183000
1	2.743932000	1.082302000	-3.491937000
1	4.151061000	1.745370000	-2.640215000

1	3.336443000	2.715666000	-3.896011000
6	1.020648000	2.937403000	-2.696157000
1	1.204173000	3.699129000	-3.454306000
1	0.343165000	3.321304000	-1.938051000
1	0.579263000	2.052731000	-3.148332000
6	2.942654000	3.754114000	-1.482105000
1	3.199390000	4.449525000	-2.281209000
1	3.840157000	3.449371000	-0.949399000
1	2.254554000	4.229184000	-0.789177000
7	2.299135000	2.550400000	-2.057848000
15	1.074698000	1.937084000	0.662668000
1	0.000000000	2.741164000	0.232975000
1	1.840907000	2.979833000	1.221757000
81	0.000000000	0.000000000	2.815601000
5	2.064180000	1.390918000	-0.941340000
1	3.156386000	1.038347000	-0.576148000
1	1.448260000	0.513794000	-1.492892000
6	0.124253000	-3.761615000	-3.096183000
1	-0.434665000	-2.917466000	-3.491937000
1	-0.563996000	-4.467609000	-2.640215000
1	0.683614000	-4.247278000	-3.896011000
6	2.033542000	-2.352609000	-2.696157000
1	2.601453000	-2.892408000	-3.454306000
1	2.704751000	-1.957841000	-1.938051000
1	1.488086000	-1.528022000	-3.148332000
6	1.779831000	-4.425470000	-1.482105000
1	2.253707000	-4.995515000	-2.281209000
1	1.067165000	-5.050359000	-0.949399000
1	2.535304000	-4.067093000	-0.789177000
7	1.059144000	-3.266309000	-2.057848000
15	1.140216000	-1.899258000	0.662668000
1	2.373918000	-1.370582000	0.232975000
1	1.660158000	-3.084188000	1.221757000
5	0.172480000	-2.483091000	-0.941340000
1	-0.678959000	-3.252684000	-0.576148000
1	-0.279171000	-1.511127000	-1.492892000
6	-3.319780000	1.773201000	-3.096183000
1	-2.309267000	1.835164000	-3.491937000
1	-3.587065000	2.722240000	-2.640215000
1	-4.020058000	1.531612000	-3.896011000
6	-3.054190000	-0.584794000	-2.696157000
1	-3.805626000	-0.806720000	-3.454306000
1	-3.047916000	-1.363462000	-1.938051000
1	-2.067349000	-0.524709000	-3.148332000
6	-4.722485000	0.671357000	-1.482105000
1	-5.453097000	0.545990000	-2.281209000
1	-4.907321000	1.600988000	-0.949399000
1	-4.789858000	-0.162091000	-0.789177000
7	-3.358278000	0.715909000	-2.057848000
15	-2.214913000	-0.037827000	0.662668000
1	-2.373918000	-1.370582000	0.232975000
1	-3.501064000	0.104355000	1.221757000
5	-2.236660000	1.092174000	-0.941340000
1	-2.477427000	2.214337000	-0.576148000
1	-1.169089000	0.997333000	-1.492892000

$[Tl(AsH_2BH_2NMe_3)_3]^+$

6	3.175895000	1.972537000	-3.343311000
1	2.715546000	1.063843000	-3.722633000
1	4.145415000	1.734395000	-2.915293000
1	3.290013000	2.697884000	-4.149050000
6	1.012328000	2.921529000	-2.883782000
1	1.175122000	3.685269000	-3.644538000
1	0.354158000	3.300902000	-2.106678000
1	0.561734000	2.036743000	-3.326487000
6	2.968520000	3.741997000	-1.726736000
1	3.207493000	4.430963000	-2.536771000
1	3.877488000	3.438120000	-1.213393000
1	2.298323000	4.222449000	-1.020208000
7	2.308396000	2.535876000	-2.279938000
33	1.122981000	1.962383000	0.578118000
1	0.000000000	2.882699000	0.132333000
1	2.003812000	3.071245000	1.128333000
81	0.000000000	0.000000000	2.825723000
5	2.110436000	1.377657000	-1.162337000
1	3.208220000	1.023882000	-0.823565000
1	1.462823000	0.505342000	-1.680214000
6	0.120320000	-3.736674000	-3.343311000
1	-0.436458000	-2.883653000	-3.722633000
1	-0.570678000	-4.457232000	-2.915293000
1	0.691430000	-4.198177000	-4.149050000
6	2.023954000	-2.337466000	-2.883782000
1	2.603976000	-2.860320000	-3.644538000
1	2.681586000	-1.957161000	-2.106678000
1	1.483005000	-1.504848000	-3.326487000
6	1.756404000	-4.441813000	-1.726736000
1	2.233580000	-4.993252000	-2.536771000
1	1.038755000	-5.077063000	-1.213393000
1	2.507587000	-4.101631000	-1.020208000
7	1.041935000	-3.267068000	-2.279938000
33	1.137983000	-1.953721000	0.578118000
1	2.496491000	-1.441350000	0.132333000
1	1.657870000	-3.270974000	1.128333000
5	0.137868000	-2.516520000	-1.162337000
1	-0.717402000	-3.290341000	-0.823565000
1	-0.293773000	-1.519513000	-1.680214000
6	-3.296214000	1.764137000	-3.343311000
1	-2.279088000	1.819810000	-3.722633000
1	-3.574737000	2.722838000	-2.915293000
1	-3.981442000	1.500293000	-4.149050000
6	-3.036282000	-0.584062000	-2.883782000
1	-3.779098000	-0.824949000	-3.644538000
1	-3.035744000	-1.343742000	-2.106678000
1	-2.044738000	-0.531896000	-3.326487000
6	-4.724925000	0.699816000	-1.726736000
1	-5.441073000	0.562288000	-2.536771000
1	-4.916243000	1.638944000	-1.213393000
1	-4.805910000	-0.120818000	-1.020208000
7	-3.350332000	0.731192000	-2.279938000
33	-2.260964000	-0.008662000	0.578118000
1	-2.496491000	-1.441350000	0.132333000
1	-3.661682000	0.199729000	1.128333000
5	-2.248304000	1.138863000	-1.162337000
1	-2.490818000	2.266459000	-0.823565000
1	-1.169050000	1.014171000	-1.680214000

[Tl(PH$_2$BH$_2$NMe$_3$)][B(C$_6$H$_3$Cl$_2$)$_4$] ion pair

81	-1.782527000	1.552560000	-0.013484000
15	-4.904238000	0.521689000	-0.354173000
1	-5.818095000	1.255570000	-1.140069000
1	-4.544886000	-0.379085000	-1.382725000
7	-7.044448000	-1.592152000	0.181577000
6	-7.895968000	-0.973365000	-0.857373000
1	-8.393914000	-0.106774000	-0.429035000
1	-8.634015000	-1.696432000	-1.205736000
1	-7.270878000	-0.656319000	-1.687269000
5	-6.044802000	-0.508009000	0.873956000
1	-5.350657000	-1.139881000	1.625175000
1	-6.743373000	0.286664000	1.445341000
6	-6.285402000	-2.715486000	-0.412956000
1	-6.976427000	-3.433472000	-0.855628000
1	-5.705058000	-3.197235000	0.370055000
1	-5.612741000	-2.332421000	-1.175650000
6	-7.915429000	-2.127023000	1.255494000
1	-8.508281000	-1.313007000	1.662724000
1	-7.286796000	-2.539557000	2.039960000
1	-8.567323000	-2.901159000	0.849314000
17	5.988168000	1.360014000	2.916696000
17	3.455069000	-3.225791000	4.122482000
17	5.358397000	0.085953000	-3.980463000
17	3.158595000	-4.646396000	-2.688751000
17	-2.635414000	-2.434234000	-2.011001000
17	0.742761000	4.667981000	1.839045000
17	-2.393324000	-1.097796000	3.190137000
17	0.144796000	3.533721000	-3.378976000
6	2.784809000	-0.444989000	1.307781000
6	2.699908000	-1.583627000	2.112791000
1	1.931854000	-2.326685000	1.938678000
6	3.823492000	0.450715000	1.577046000
1	3.955150000	1.338274000	0.970528000
6	1.344298000	2.262057000	0.757622000
1	1.619377000	1.986071000	1.767932000
6	-0.432338000	-1.387808000	-0.839644000
1	0.007814000	-1.463437000	-1.825928000
6	0.326768000	-0.903060000	0.233894000
6	1.459523000	1.331058000	-0.282693000
6	2.616496000	-0.943367000	-1.237478000
6	-0.309790000	-0.835027000	1.481516000
1	0.228695000	-0.464637000	2.345397000
6	1.079503000	1.759080000	-1.562871000
1	1.144211000	1.079510000	-2.403753000
6	0.882823000	3.550937000	0.520182000
6	2.534647000	-2.321091000	-1.459524000
1	1.878645000	-2.937067000	-0.856786000
6	4.620971000	-0.903458000	3.418173000
1	5.317799000	-1.075529000	4.224237000
6	4.714129000	0.219116000	2.612088000
6	3.509619000	-0.221384000	-2.032630000
1	3.634444000	0.845007000	-1.893116000
6	-1.632490000	-1.232359000	1.638786000
6	3.296900000	-2.931961000	-2.440720000
6	0.512623000	3.972399000	-0.749155000
1	0.163846000	4.978426000	-0.927765000
6	3.601091000	-1.797833000	3.143128000
6	-1.747563000	-1.797096000	-0.659970000
6	4.172851000	-2.213501000	-3.237460000
1	4.762302000	-2.696361000	-4.001788000
6	4.264837000	-0.851362000	-3.009008000
6	0.620886000	3.051227000	-1.782013000
6	-2.376588000	-1.723940000	0.573978000
1	-3.402195000	-2.035037000	0.708160000
5	1.821296000	-0.248962000	0.006390000

[Tl(AsH$_2$BH$_2$NMe$_3$)][B(C$_6$H$_3$Cl$_2$)$_4$] ion pair

81	-1.541128000	1.564882000	-0.046945000
33	-4.806487000	0.574877000	-0.035309000
1	-5.864456000	1.422290000	-0.727114000
1	-4.428468000	-0.171599000	-1.313559000
7	-6.887718000	-1.799397000	0.124593000
6	-7.775013000	-1.052417000	-0.794039000
1	-8.325689000	-0.310856000	-0.220356000
1	-8.466284000	-1.743095000	-1.277727000
1	-7.169015000	-0.550760000	-1.542928000
5	-5.965034000	-0.809186000	1.021636000
1	-5.232207000	-1.517987000	1.655138000
1	-6.709538000	-0.161976000	1.705602000
6	-6.061408000	-2.747517000	-0.657210000
1	-6.708524000	-3.418943000	-1.222235000
1	-5.443549000	-3.320998000	0.029423000
1	-5.422145000	-2.190835000	-1.336632000
6	-7.727109000	-2.575220000	1.070525000
1	-8.366577000	-1.887117000	1.615891000
1	-7.075904000	-3.091345000	1.770631000
1	-8.332289000	-3.295177000	0.518753000
17	6.146348000	1.276474000	3.012923000
17	3.586426000	-3.327669000	4.084220000
17	5.654076000	0.068468000	-3.889547000
17	3.304981000	-4.633776000	-2.762875000
17	-2.459152000	-2.320766000	-2.094232000
17	0.924361000	4.622054000	1.902962000
17	-2.231172000	-1.127179000	3.138842000
17	0.474194000	3.598064000	-3.352656000
6	2.965622000	-0.487927000	1.317308000
6	2.865917000	-1.643130000	2.096891000
1	2.099057000	-2.380425000	1.894855000
6	4.001329000	0.399716000	1.621249000
1	4.143799000	1.299975000	1.036330000
6	1.543099000	2.234752000	0.790139000
1	1.787019000	1.936084000	1.802087000
6	-0.242847000	-1.349492000	-0.881474000
1	0.202532000	-1.404965000	-1.866832000
6	0.515178000	-0.901693000	0.208836000
6	1.682507000	1.323794000	-0.265613000
6	2.822268000	-0.953159000	-1.236107000
6	-0.130732000	-0.850934000	1.452809000
1	0.405674000	-0.506599000	2.328649000
6	1.343599000	1.780656000	-1.547096000
1	1.428532000	1.118120000	-2.399596000
6	1.097048000	3.531576000	0.566027000

6	2.710909000	-2.322543000	-1.492901000
1	2.026336000	-2.935856000	-0.920097000
6	4.767868000	-0.994456000	3.445503000
1	5.451650000	-1.184937000	4.258581000
6	4.875712000	0.144381000	2.664796000
6	3.751209000	-0.235674000	-1.993842000
1	3.899864000	0.823496000	-1.825207000
6	-1.458881000	-1.237350000	1.592417000
6	3.480024000	-2.929594000	-2.471400000
6	0.766633000	3.981001000	-0.704938000
1	0.429215000	4.992717000	-0.872914000
6	3.750430000	-1.880728000	3.136289000
6	-1.565436000	-1.744277000	-0.720632000
6	4.391712000	-2.215429000	-3.230685000
1	4.986772000	-2.695271000	-3.992561000
6	4.512706000	-0.861635000	-2.967625000
6	0.899570000	3.080392000	-1.752901000
6	-2.199937000	-1.697577000	0.511742000
1	-3.228480000	-2.004936000	0.633622000
5	2.020881000	-0.264629000	0.006680000

$[NMe_3BH_2PHPH_2BH_2NMe_3]^+$ (PP isomer)

7	-3.728358000	0.161522000	-0.074351000
6	-4.074878000	-0.253193000	1.306895000
6	-4.046119000	-0.942653000	-1.010898000
6	-4.551906000	1.344615000	-0.435019000
1	-4.296081000	2.164518000	0.230706000
1	-5.608478000	1.096872000	-0.335174000
1	-4.328988000	1.627542000	-1.459935000
1	-3.494810000	-1.833875000	-0.716373000
1	-3.753289000	-0.646786000	-2.015104000
1	-5.114231000	-1.156212000	-0.980817000
1	-3.859179000	0.569905000	1.982830000
1	-3.476601000	-1.117606000	1.583896000
1	-5.133023000	-0.508711000	1.356552000
5	-2.180341000	0.599975000	-0.196470000
1	-1.975582000	1.419277000	0.661158000
1	-2.004525000	1.007699000	-1.310321000
15	-0.974972000	-0.954955000	0.195451000
15	0.789086000	0.289275000	0.288724000
1	-0.626932000	-1.392810000	-1.101004000
1	0.804639000	0.794750000	1.594298000
1	0.581450000	1.469877000	-0.442026000
5	2.377949000	-0.734326000	-0.231724000
1	2.385021000	-1.688187000	0.491007000
7	3.769265000	0.044089000	-0.085334000
1	2.199318000	-0.995684000	-1.387271000
6	4.054027000	0.408044000	1.325078000
6	3.814175000	1.265618000	-0.926514000
6	4.828855000	-0.892563000	-0.554492000
1	4.801979000	-1.789109000	0.058463000
1	5.800587000	-0.407655000	-0.468623000
1	4.630318000	-1.154472000	-1.590082000
1	3.312091000	1.124076000	1.671105000
1	5.044170000	0.856986000	1.393262000
1	4.010046000	-0.489709000	1.936023000
1	3.077753000	1.979596000	-0.564455000
1	3.587658000	0.995109000	-1.954527000
1	4.805656000	1.713072000	-0.867737000

$[NMe_3BH_2PH_2BH(PH_2)NMe_3]^+$ (PB isomer)

7	-2.750396000	-0.543739000	-0.076884000
6	-2.605987000	-2.000265000	-0.327155000
6	-3.863262000	-0.041834000	-0.935354000
6	-3.123640000	-0.335242000	1.345818000
1	-2.306390000	-0.663103000	1.984247000
1	-4.018966000	-0.911932000	1.574408000
1	-3.318475000	0.721622000	1.511929000
1	-3.620314000	-0.246002000	-1.974512000
1	-3.972820000	1.028611000	-0.787142000
1	-4.782675000	-0.555151000	-0.657244000
1	-1.902000000	-2.422729000	0.385282000
1	-2.241564000	-2.149463000	-1.340803000
1	-3.572794000	-2.486569000	-0.204573000
5	-1.404251000	0.258080000	-0.481473000
1	-1.264230000	0.146048000	-1.665867000
15	-1.537779000	2.165746000	0.012571000
15	0.238566000	-0.487318000	0.283338000
1	-0.874930000	2.140508000	1.261708000
1	0.419687000	-1.852693000	-0.008234000
1	0.167921000	-0.565404000	1.683808000
5	1.776876000	0.604614000	-0.281611000
1	1.622866000	0.807963000	-1.451942000
7	3.205339000	-0.091627000	-0.065485000
1	1.732083000	1.586862000	0.398981000
6	3.400618000	-1.251326000	-0.970242000
6	3.406835000	-0.523073000	1.339035000
6	4.230260000	0.937959000	-0.396612000
1	4.063118000	1.283889000	-1.413063000
1	5.222989000	0.498425000	-0.306830000
1	4.124716000	1.771082000	0.292178000
1	2.662032000	-2.015913000	-0.743796000
1	4.399798000	-1.661553000	-0.828274000
1	3.277575000	-0.918114000	-1.996996000
1	2.720839000	-1.335935000	1.568134000
1	3.210474000	0.319504000	1.997530000
1	4.430704000	-0.870093000	1.472912000
1	-0.408114000	2.590492000	-0.711411000

$[NMe_3BH_2AsHAsH_2BH_2NMe_3]^+$ (AsAs isomer)

7	-3.829446000	-0.393534000	0.141565000
6	-4.281489000	0.236406000	-1.123065000
6	-4.149903000	0.503132000	1.277660000
6	-4.568189000	-1.671430000	0.321908000
1	-4.321029000	-2.335889000	-0.501520000
1	-5.639588000	-1.473120000	0.335154000
1	-4.258953000	-2.124974000	1.259320000
1	-3.673966000	1.469167000	1.119667000
1	-3.772733000	0.056710000	2.194279000
1	-5.228683000	0.641998000	1.344336000
1	-4.046938000	-0.430188000	-1.948636000
1	-3.762869000	1.181802000	-1.261574000
1	-5.355856000	0.412796000	-1.079405000

5	-2.260875000	-0.755085000	0.106192000
1	-2.061122000	-1.403710000	-0.885285000
1	-1.990047000	-1.316296000	1.129404000
33	-1.082608000	1.010537000	-0.094259000
33	0.891212000	-0.328084000	-0.337843000
1	-0.726188000	1.244713000	1.368724000
1	0.920902000	-0.712494000	-1.794707000
1	0.630544000	-1.677755000	0.288879000
5	2.576141000	0.689455000	0.348746000
1	2.609098000	1.680655000	-0.317126000
7	3.953569000	-0.103159000	0.187560000
1	2.356563000	0.865486000	1.510682000
6	4.263105000	-0.404394000	-1.232269000
6	3.968896000	-1.363007000	0.971733000
6	5.014077000	0.799098000	0.720957000
1	5.015555000	1.717898000	0.141231000
1	5.980710000	0.303246000	0.641594000
1	4.792057000	1.024785000	1.760318000
1	3.527757000	-1.105146000	-1.620592000
1	5.254965000	-0.849094000	-1.302657000
1	4.227256000	0.519117000	-1.803941000
1	3.228712000	-2.049233000	0.566839000
1	3.729863000	-1.135904000	2.007318000
1	4.955859000	-1.819354000	0.906959000

$[NMe_3BH_2AsH_2BH(AsH_2)NMe_3]^+$ (AsB isomer)

7	-2.602053000	-0.991794000	-0.135310000
6	-2.356008000	-2.421985000	-0.457603000
6	-3.772635000	-0.541270000	-0.945364000
6	-2.955421000	-0.879555000	1.303620000
1	-2.100765000	-1.175012000	1.907694000
1	-3.800036000	-1.531995000	1.520944000
1	-3.223674000	0.150301000	1.527020000
1	-3.535734000	-0.665081000	-1.998505000
1	-3.972744000	0.505110000	-0.734301000
1	-4.638350000	-1.146870000	-0.681581000
1	-1.595217000	-2.817351000	0.209949000
1	-2.018812000	-2.497480000	-1.488384000
1	-3.278702000	-2.985119000	-0.324636000
5	-1.335706000	-0.077819000	-0.537383000
1	-1.192181000	-0.158171000	-1.721154000
33	-1.604559000	1.923640000	0.020421000
33	0.472719000	-0.722691000	0.251153000
1	-0.833049000	1.882715000	1.336335000
1	0.784612000	-2.179819000	-0.038417000
1	0.414687000	-0.800396000	1.758928000
5	1.994932000	0.560687000	-0.380648000
1	1.826262000	0.683324000	-1.558451000
7	3.477459000	0.018772000	-0.118273000
1	1.833933000	1.555004000	0.260911000
6	3.786573000	-1.187366000	-0.925468000
6	3.720549000	-0.271716000	1.315994000
6	4.396714000	1.113826000	-0.541232000
1	4.208411000	1.343471000	-1.586436000
1	5.427726000	0.788991000	-0.407102000
1	4.197196000	1.992839000	0.065061000
1	3.140921000	-2.004299000	-0.614298000
1	4.827531000	-1.470091000	-0.773248000
1	3.611457000	-0.961945000	-1.973917000
1	3.114946000	-1.122989000	1.619007000
1	3.446167000	0.601300000	1.902750000
1	4.773157000	-0.507159000	1.468359000
1	-0.409618000	2.414621000	-0.772904000

$[Tl(PH_2BH_2NMe_3)][B(C_6H_3Cl_2)_4]$

81	-1.782527000	1.552560000	-0.013484000
15	-4.904238000	0.521689000	-0.354173000
1	-5.818095000	1.255570000	-1.140069000
1	-4.544886000	-0.379085000	-1.382725000
7	-7.044448000	-1.592152000	0.181577000
6	-7.895968000	-0.973365000	-0.857373000
1	-8.393914000	-0.106774000	-0.429035000
1	-8.634015000	-1.696432000	-1.205736000
1	-7.270878000	-0.656319000	-1.687269000
5	-6.044802000	-0.508009000	0.873956000
1	-5.350657000	-1.139881000	1.625175000
1	-6.743373000	0.286664000	1.445341000
6	-6.285402000	-2.715486000	-0.412956000
1	-6.976427000	-3.433472000	-0.855628000
1	-5.705058000	-3.197235000	0.370055000
1	-5.612741000	-2.332421000	-1.175650000
6	-7.915429000	-2.127023000	1.255494000
1	-8.508281000	-1.313007000	1.662724000
1	-7.286796000	-2.539557000	2.039960000
1	-8.567323000	-2.901159000	0.849314000
17	5.988168000	1.360014000	2.916696000
17	3.455069000	-3.225791000	4.122482000
17	5.358397000	0.085953000	-3.980463000
17	3.158595000	-4.646396000	-2.688751000
17	-2.635414000	-2.434234000	-2.011001000
17	0.742761000	4.667981000	1.839045000
17	-2.393324000	-1.097796000	3.190137000
17	0.144796000	3.533721000	-3.378976000
6	2.784809000	-0.444989000	1.307781000
6	2.699908000	-1.583627000	2.112791000
1	1.931854000	-2.326685000	1.938678000
6	3.823492000	0.450715000	1.577046000
1	3.955150000	1.338274000	0.970528000
6	1.344298000	2.262057000	0.757622000
1	1.619377000	1.986071000	1.767932000
6	-0.432338000	-1.387808000	-0.839644000
1	0.007814000	-1.463437000	-1.825928000
6	0.326768000	-0.903060000	0.233894000
6	1.459523000	1.331058000	-0.282693000
6	2.616496000	-0.943367000	-1.237478000
6	-0.309790000	-0.835027000	1.481516000
1	0.228695000	-0.464637000	2.345397000
6	1.079503000	1.759080000	-1.562871000
1	1.144211000	1.079510000	-2.403753000
6	0.882823000	3.550937000	0.520182000
6	2.534647000	-2.321091000	-1.459524000
1	1.878645000	-2.937067000	-0.856786000
6	4.620971000	-0.903458000	3.418173000
1	5.317799000	-1.075529000	4.224237000

6	4.714129000	0.219116000	2.612088000
6	3.509619000	-0.221384000	-2.032630000
1	3.634444000	0.845007000	-1.893116000
6	-1.632490000	-1.232359000	1.638786000
6	3.296900000	-2.931961000	-2.440720000
6	0.512623000	3.972399000	-0.749155000
1	0.163846000	4.978426000	-0.927765000
6	3.601091000	-1.797833000	3.143128000
6	-1.747563000	-1.797096000	-0.659970000
6	4.172851000	-2.213501000	-3.237460000
1	4.762302000	-2.696361000	-4.001788000
6	4.264837000	-0.851362000	-3.009008000
6	0.620886000	3.051227000	-1.782013000
6	-2.376588000	-1.723940000	0.573978000
1	-3.402195000	-2.035037000	0.708160000
5	1.821296000	-0.248962000	0.006390000

$[Tl(AsH_2BH_2NMe_3)][B(C_6H_3Cl_2)_4]$

81	-1.541128000	1.564882000	-0.046945000
33	-4.806487000	0.574877000	-0.035309000
1	-5.864456000	1.422290000	-0.727114000
1	-4.428468000	-0.171599000	-1.313559000
7	-6.887718000	-1.799397000	0.124593000
6	-7.775013000	-1.052417000	-0.794039000
1	-8.325689000	-0.310856000	-0.220356000
1	-8.466284000	-1.743095000	-1.277727000
1	-7.169015000	-0.550760000	-1.542928000
5	-5.965034000	-0.809186000	1.021636000
1	-5.232207000	-1.517987000	1.655138000
1	-6.709538000	-0.161976000	1.705602000
6	-6.061408000	-2.747517000	-0.657210000
1	-6.708524000	-3.418943000	-1.222235000
1	-5.443549000	-3.320998000	0.029423000
1	-5.422145000	-2.190835000	-1.336632000
6	-7.727109000	-2.575220000	1.070525000
1	-8.366577000	-1.887117000	1.615891000
1	-7.075904000	-3.091345000	1.770631000
1	-8.332289000	-3.295177000	0.518753000
17	6.146348000	1.276474000	3.012923000
17	3.586426000	-3.327669000	4.084220000
17	5.654076000	0.068468000	-3.889547000
17	3.304981000	-4.633776000	-2.762875000
17	-2.459152000	-2.320766000	-2.094232000
17	0.924361000	4.622054000	1.902962000
17	-2.231172000	-1.127179000	3.138842000
17	0.474194000	3.598064000	-3.352656000
6	2.965622000	-0.487927000	1.317308000
6	2.865917000	-1.643130000	2.096891000
1	2.099057000	-2.380425000	1.894855000
6	4.001329000	0.399716000	1.621249000
1	4.143799000	1.299975000	1.036330000
6	1.543099000	2.234752000	0.790139000
1	1.787019000	1.936084000	1.802087000
6	-0.242847000	-1.349492000	-0.881474000
1	0.202532000	-1.404965000	-1.866832000
6	0.515178000	-0.901693000	0.208836000
6	1.682507000	1.323794000	-0.265613000
6	2.822268000	-0.953159000	-1.236107000
6	-0.130732000	-0.850934000	1.452809000
1	0.405674000	-0.506599000	2.328649000
6	1.343599000	1.780656000	-1.547096000
1	1.428532000	1.118120000	-2.399596000
6	1.097048000	3.531576000	0.566027000
6	2.710909000	-2.322543000	-1.492901000
1	2.026336000	-2.935856000	-0.920097000
6	4.767868000	-0.994456000	3.445503000
1	5.451650000	-1.184937000	4.258581000
6	4.875712000	0.144381000	2.664796000
6	3.751209000	-0.235674000	-1.993842000
1	3.899864000	0.823496000	-1.825207000
6	-1.458881000	-1.237350000	1.592417000
6	3.480024000	-2.929594000	-2.471400000
6	0.766633000	3.981001000	-0.704938000
1	0.429215000	4.992717000	-0.872914000
6	3.750430000	-1.880728000	3.136289000
6	-1.565436000	-1.744277000	-0.720632000
6	4.391712000	-2.215429000	-3.230685000
1	4.986772000	-2.695271000	-3.992561000
6	4.512706000	-0.861635000	-2.967625000
6	0.899570000	3.080392000	-1.752901000
6	-2.199937000	-1.697577000	0.511742000
1	-3.228480000	-2.004936000	0.633622000
5	2.020881000	-0.264629000	0.006680000

$[Tl(PH_2BH_2NMe_3)_2(CH_2Cl_2)]^+$

17	-1.117106000	1.486318000	3.336087000
17	-0.930251000	-1.262738000	2.335903000
81	0.155051000	-2.489920000	-0.416376000
6	-0.220639000	0.373011000	2.320086000
1	0.792132000	0.289236000	2.695815000
1	-0.249873000	0.731748000	1.299220000
6	3.115376000	3.929667000	-0.470883000
1	2.558559000	4.200086000	0.421843000
1	2.484395000	4.062103000	-1.345332000
1	4.008884000	4.547498000	-0.556946000
6	4.365164000	2.324494000	0.817886000
1	5.228347000	2.985803000	0.748084000
1	4.700031000	1.292336000	0.868603000
1	3.784656000	2.564161000	1.705168000
6	4.279767000	2.143619000	-1.588950000
1	5.146405000	2.798461000	-1.675025000
1	3.639104000	2.257925000	-2.459390000
1	4.610106000	1.111852000	-1.512215000
7	3.505951000	2.499685000	-0.376573000
15	2.328140000	-0.305057000	-0.081011000
1	3.173488000	-0.546139000	1.021284000
1	3.246137000	-0.717447000	-1.068464000
5	2.136077000	1.643562000	-0.261814000
1	1.510715000	1.839598000	-1.271436000
1	1.568543000	2.040228000	0.721927000
6	-3.591249000	3.320832000	0.107307000
1	-2.688079000	3.901151000	0.273332000
1	-3.876442000	2.829109000	1.033440000
1	-4.396433000	3.967754000	-0.240203000

6	-2.889113000	2.949094000	-2.170347000
1	-3.657433000	3.653730000	-2.487652000
1	-2.740563000	2.197965000	-2.941452000
1	-1.953879000	3.472966000	-1.988966000
6	-4.556546000	1.518607000	-1.165054000
1	-5.339871000	2.196887000	-1.502234000
1	-4.857458000	1.032021000	-0.241178000
1	-4.370862000	0.768848000	-1.928673000
7	-3.310705000	2.281911000	-0.917660000
15	-1.467900000	-0.097274000	-1.471012000
1	-0.942379000	0.505358000	-2.630310000
1	-2.583805000	-0.696262000	-2.090415000
5	-2.143541000	1.341570000	-0.316338000
1	-2.593236000	0.818953000	0.668026000
1	-1.204788000	2.058954000	-0.083817000

$[Tl(AsH_2BH_2NMe_3)_2(CH_2Cl_2)]^+$

17	-1.054457000	1.709591000	3.375831000
17	-0.843420000	-1.069065000	2.470339000
81	0.185217000	-2.557441000	-0.169084000
6	-0.166864000	0.580100000	2.370544000
1	0.857253000	0.527451000	2.716395000
1	-0.231212000	0.901170000	1.337319000
6	3.147931000	4.113326000	0.077905000
1	3.131543000	4.116919000	1.164059000
1	2.177015000	4.421842000	-0.299281000
1	3.923569000	4.785642000	-0.287682000
6	4.756223000	2.320351000	0.120388000
1	5.511411000	3.030387000	-0.215221000
1	4.993096000	1.329067000	-0.255032000
1	4.720979000	2.300015000	1.206451000
6	3.458430000	2.736813000	-1.874462000
1	4.202168000	3.453880000	-2.220564000
1	2.474193000	3.013023000	-2.243924000
1	3.715187000	1.743364000	-2.230207000
7	3.427069000	2.730762000	-0.392980000
33	2.334178000	-0.232906000	-0.293418000
1	3.733644000	-0.697311000	0.063391000
1	2.548780000	-0.272709000	-1.797274000
5	2.244525000	1.799114000	0.186003000
1	1.208242000	2.199834000	-0.273790000
1	2.298389000	1.871371000	1.382707000
6	-4.000650000	3.189027000	0.272188000
1	-3.160276000	3.873129000	0.347210000
1	-4.175732000	2.727987000	1.240476000
1	-4.891769000	3.721719000	-0.058928000
6	-3.385649000	2.755163000	-2.020117000
1	-4.239784000	3.359100000	-2.325160000
1	-3.202765000	1.978584000	-2.757943000
1	-2.501691000	3.380720000	-1.924544000
6	-4.834927000	1.222744000	-0.840774000
1	-5.699985000	1.794506000	-1.175383000
1	-5.037869000	0.771801000	0.126752000
1	-4.607662000	0.446019000	-1.565129000
7	-3.664996000	2.123696000	-0.709969000
33	-1.546823000	-0.145017000	-1.319486000
1	-1.032074000	0.563571000	-2.558689000
1	-2.706434000	-0.832110000	-2.019800000
5	-2.380024000	1.351369000	-0.121613000
1	-2.723019000	0.820071000	0.896802000
1	-1.510557000	2.167414000	0.028403000

3.5.6 References

[1] X. Zheng, Z. Zhang, G. Tan, X. Wang, *Inorg. Chem.* **2016**, *55*, 1008–1010; 1008–1010.

[2] C. Marquardt, C. Thoms, A. Stauber, G. Balázs, M. Bodensteiner, M. Scheer, *Angew. Chem. Int. Ed.* **2014**, *53*, 3727–3730.

[3] G. Brauer, *Handbuch der präparativen Anorganischen Chemie*, F. Enke Verlag, Stuttgart, **1978**.

[4] T. J. Hadlington, T. Szilvási, M. Driess, *J. Am. Chem. Soc.* **2019**, *141*, 3304–3314; 3304–3314.

[5] R. Anulewicz-Ostrowska, T. Klis, D. Krajewski, B. Lewandowski, J. Serwatowski, *Tetrahedron Lett.* **2003**, *44*, 7329–7331; 7329–7331.

[6] I. Krossing, H. Brands, R. Feuerhake, S. Koenig, *J. Fluor. Chem.* **2001**, *112*, 83–90; 83–90.

[7] M. Gonsior, I. Krossing, *Z. Anorg. Allg. Chem.* **2002**, *628*, 1821–1830; 1821–1830.

[8] K.-C. Schwan, A. Y. Timoskin, M. Zabel, M. Scheer, *Chem. Eur. J.* **2006**, *12*, 4900–4908; 4900–4908.

[9] C. Marquardt, A. Adolf, A. Stauber, M. Bodensteiner, A. V. Virovets, A. Y. Timoshkin, M. Scheer, *Chem. Eur. J.* **2013**, *19*, 11887–11891; 11887–11891.

[10] Gaussian 16, Revision C.01, M. J. Frisch, G. W. Trucks, H. B. Schlegel, G. E. Scuseria, M. A. Robb, J. R. Cheeseman, G. Scalmani, V. Barone, G. A. Petersson, H. Nakatsuji, X. Li, M. Caricato, A. V. Marenich, J. Bloino, B. G. Janesko, R. Gomperts, B. Mennucci, H. P. Hratchian, J. V. Ortiz, A. F. Izmaylov, J. L. Sonnenberg, D. Williams-Young, F. Ding, F. Lipparini, F. Egidi, J. Goings, B. Peng, A. Petrone, T. Henderson, D. Ranasinghe, V. G. Zakrzewski, J. Gao, N. Rega, G. Zheng, W. Liang, M. Hada, M. Ehara, K. Toyota, R. Fukuda, J. Hasegawa, M. Ishida, T. Nakajima, Y. Honda, O. Kitao, H. Nakai, T. Vreven, K. Throssell, J. A. Montgomery, Jr., J. E. Peralta, F. Ogliaro, M. J. Bearpark, J. J. Heyd, E. N. Brothers, K. N. Kudin, V. N. Staroverov, T. A. Keith, R. Kobayashi, J. Normand, K. Raghavachari, A. P. Rendell, J. C. Burant, S. S. Iyengar,

J. Tomasi, M. Cossi, J. M. Millam, M. Klene, C. Adamo, R. Cammi, J. W. Ochterski, R. L. Martin, K. Morokuma, O. Farkas, J. B. Foresman, and D. J. Fox, Gaussian, Inc., Wallingford CT, **2016**.

[11] Y. Zhao, D. G. Truhlar, *Theor. Chem. Acc.* **2008**, *120*, 215–241; 215–241.

[12] F. Weigend, R. Ahlrichs, *Phys. Chem. Chem. Phys.* **2005**, *7*, 3297–3305; 3297–3305.

[13] a) D. Feller, *J. Comp. Chem.* **1996**, *17*, 1571–1586; 1571–1586; b) K. L. Schuchardt, B. T. Didier, T. Elsethagen, L. Sun, V. Gurumoorthi, J. Chase, J. Li, T. L. Windus, *J. Chem. Inf. Model.* **2007**, *47*, 1045–1052; 1045–1052; c) B. P. Pritchard, D. Altarawy, B. Didier, T. D. Gibson, T. L. Windus, *J. Chem. Inf. Model.* **2019**, *59*, 4814–4820; 4814–4820.

3.6 Author Contributions

- R. Szlosek* – writing of the first paper draft and the final manuscript, experimental work (reproductions of all compounds, acquisition of analytical data, X-ray data of **1a**, synthesis and characterization of **4**), quantum chemical calculations)
- M. T. Ackermann* – writing of the original introduction, syntheses of compounds **1a/b**
- C. Marquardt – experimental work (original preparation and characterization of **2a/b**; first observation of P-P coupling products **3a/b** and subsequent investigations incl. NMR and powder X-ray diffraction studies)
- M. Seidl – finalization of single-crystal of X-ray diffraction data
- Y. Timoshkin – quantum chemical calculations, acquisition of funding, co-writing of final manuscript
- M. Scheer – project supervision, acquisition of funding, co-writing of final manuscript

(* = equal contribution)

4 NHC-stabilized Tripentelyltrielanes

R. Szlosek, M. A. K. Weinhart, G. Balázs, M. Seidl, L. Zimmermann and M. Scheer

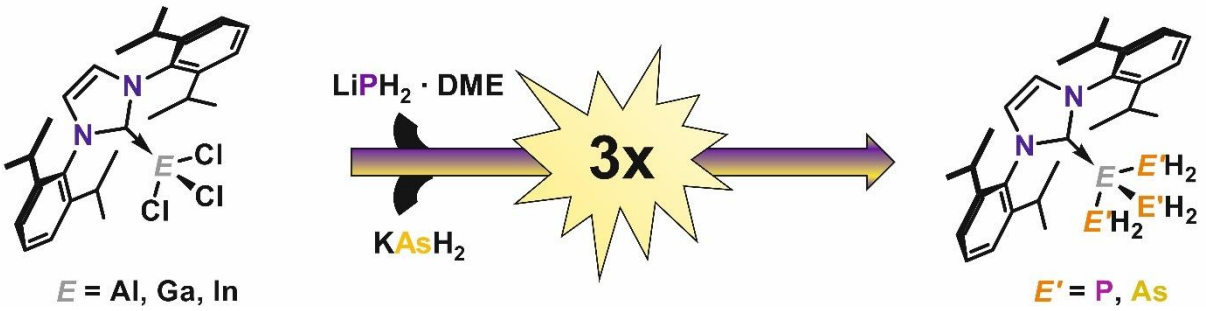

Abstract: A missing family of the extremely air sensitive tripentelyltrielanes was discovered. Their stabilisation was achieved by using the bulky NHC IDipp (NHC = N-heterocyclic carbene, IDipp = 1,3-bis(2,6-diisopropylphenyl)-imidazolin-2-ylidene). The tripentelylgallanes and tripentelylalanes IDipp·Ga$(PH_2)_3$ (**1a**), IDipp·Ga$(AsH_2)_3$ (**1b**), IDipp·Al$(PH_2)_3$ (**2a**) and IDipp·Al$(AsH_2)_3$ (**2b**) were synthesised by salt metathesis of IDipp·ECl_3 (E = Al, Ga, In) with alkali metal pnictogenides such as $NaPH_2$/$LiPH_2$·DME and $KAsH_2$, respectively. Moreover, the detection of the first NHC-stabilised tripentelylindiumane IDipp·In$(PH_2)_3$ (**3**) was possible by multinuclear NMR spectroscopy. Initial investigations of the coordination ability of these compounds resulted in the successful isolation of the coordination compound [IDipp·Ga$(PH_2)_2(\mu_3$-$PH_2\{HgC_6F_4\}_3)$] (**4**) by reaction of **1a** with $(HgC_6F_4)_3$. The compounds were characterised by multinuclear NMR spectroscopy as well as single crystal X-ray diffraction studies. Supporting computational studies highlight the electronic features of the products.

4.1 Introduction

Hydrocarbon compounds are the most basic materials used as fuels and for the production of specialised chemicals. However, already hundreds of years ago, chemists discovered the inorganic equivalents made up by elements of the groups 13 and 15, forming the so-called group 13/15 compounds. Starting with the preparation of $H_3N{\cdot}BF_3$ by Gay-Lussac in 1809, many milestone discoveries such as borazine $B_3N_3H_6$ and $Me_3N{\cdot}BH_3$ followed.[1] Although isoelectronic towards their organic counterparts, these compounds differ drastically from them in terms of reactivity and physical properties due to their different bond polarity. In the last years, the focus has more and more shifted towards the heavier homologues, mainly phosphorus/arsenic on the group 15 side and aluminium/gallium on the group 13 side, partially owing to practical applications of 13/15 compounds such as GaAs in the semiconductor industry.[2,3] The demand for stable precursor compounds of this type has increased accordingly, for their use in, for example MOCVD processes (metal–organic chemical vapor deposition).[2,4]

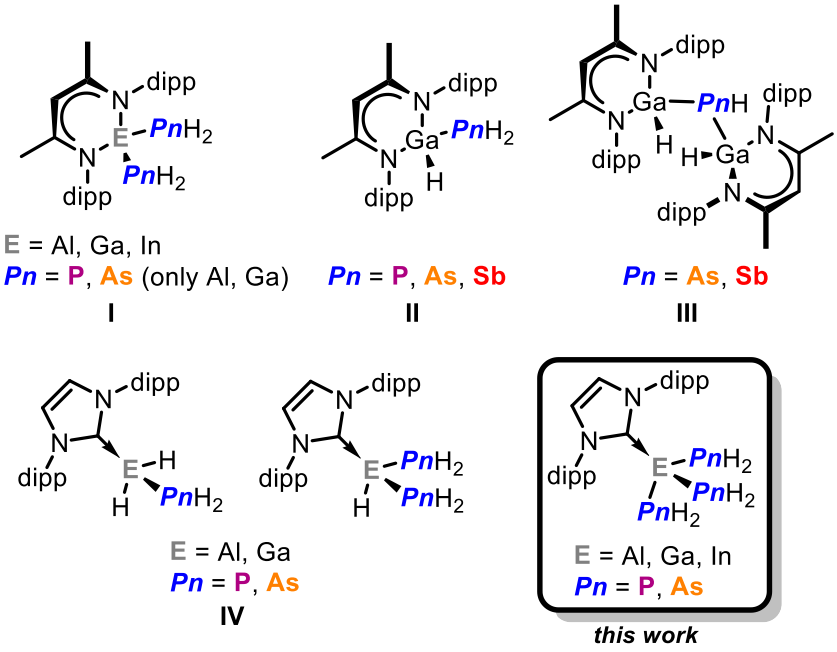

Figure 4.1: Examples for donor-stabilised parent pentelyltrielanes of Al, Ga and In (dipp = 2,6-diisopropylphenyl).

Several stabilisation strategies for the parent 13/15 monomers H_2E-PnH_2 (E = Al/Ga, *Pn* = P, As) or disubstituted HE-$(PnH_2)_2$ compounds are known today, usually involving the use of donor molecules or a combination with a suitable Lewis acid.[5] Most examples include borane compounds, although simultaneous stabilisation of GaH_2PH_2 and AlH_2PH_2 by $\{W(CO)_5\}$ and NMe_3 was already reported several years ago.[6] When no additional Lewis acid is provided, the most common examples for the stabilisation of the parent monomers of the heavier homologues of group 13 are provided by *β*-diketiminates (Nacnac, Figure 4.1, **I**, **II** and **III**) or N-heterocyclic carbenes (NHC) (Figure 4.1, **IV**). In particular, by employing the bulky NHC 1,3-bis-(2,6-diisopropylphenyl)-imidazolin-2-ylidene (IDipp),[7] our group synthesised the first examples of the stable mono- and disubstituted compounds IDipp·EH_2PnH_2 and IDipp·$EH(PnH_2)_2$ (E = Al, Ga; *Pn* = P, As).[8,9] Recently, especially *β*-diketiminates have been experiencing a tremendous gain in popularity in the field of group 13/15 element chemistry.[10] Pioneering works by S. Schulz *et al.* investigated the synthesis, characterisation and reactivity of Ga = *Pn* (*Pn* = P, As, Sb) multiple bonded species stabilised by Nacnac systems, resulting in a fascinating variety of structural motifs ranging from gallapnictenes to distibiranes.[11] Goicoechea *et al.* showed the successful synthesis of (Nacnac)-stabilised phosphanyl-phosphagallene and demonstrated its reactivity as a frustrated Lewis pair by conversions with H_2 and CO_2.[12] Furthermore, (Nacnac)E*Pn*H_2 (E = Ga, Al, In; *Pn* = P, As, Sb)

and (Nacnac)E(PnH_2)$_2$ were reported by our own group as well as by the von Hänisch group.[13,14] Von Hänisch *et al.* were also able to synthesise neutral 13/(15/14)/13 chain compounds by oxidative addition of (Nacnac)GaHPnH_2 or silyl(di)phosphanes with (Nacnac)Ga.[14,15]

In view of tripentelyltrielanes E(PnH_2)$_3$, however, only tris(dialkylphosphanyl)boranes B(PR_2)$_3$ are known so far, as the strong bonds between phosphorus and boron in combination with bulky organic residues keep the molecules together as monomers despite lacking external stabilisation.[16] Still, the parent compound B(PH_2)$_3$ currently remains unknown. The same accounts for reports on tripentelyltrielanes of the heavier group 13 homologues, which is not surprising given the highly labile nature of the bonding between the heavier group 13 and group 15 elements.[17] As the β-diketiminate ligand occupies two binding sites on the group 13 element, a tripentelyltrielane pattern is difficult to achieve by stabilisation from Nacnac substituents only. One possibility is provided by a strong 2-electron donor such as a NHC,[18] a cyclic (alkyl)(amino)carbene (CAAC)[19] or a tertiary amine.[20] But no such adducts have been reported to our knowledge to this date.

Herein we report the synthesis and characterisation of the first monomeric parent tripentelyltrielanes stabilised by the Lewis base IDipp. These include the elements Al, Ga and In on the group 13 and P and As on the group 15 side. Moreover, the first results of the reactivity of these compounds are presented and specific electronic features are discussed, highlighted by quantum chemical calculations.

4.2 Results and Discussion

As shown in previous work both experimentally and theoretically, hydrogen elimination from a mixture of PH_3 or AsH_3 and IDipp·EH_3 (E = Al, Ga) does not lead all the way to the desired tripentelyltrielane, but instead ends at the first or second substitution step, respectively, as the intermediates become less and less prone to hydrogen elimination after each substitution step.[8,9] Therefore, salt metathesis provides a better synthetic pathway towards these 13/15-compounds. Thus, the reactions of IDipp·$GaCl_3$[21] with 3.5 equivalents of $LiPH_2$·DME[22] and $KAsH_2$[23] [Equation (1)] were performed.

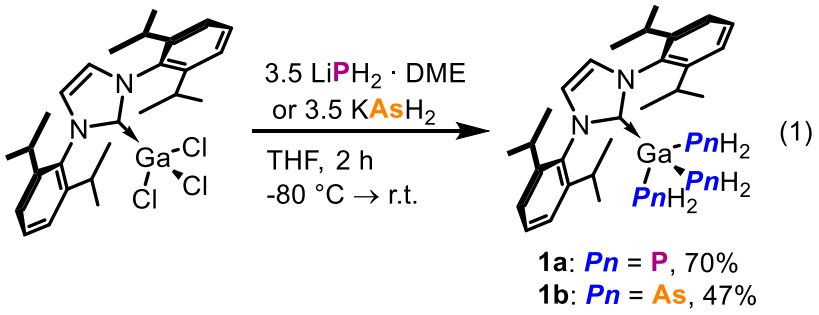

That way, the NHC-stabilised parent tripentelylgallanes IDipp·Ga(PH_2)$_3$ (**1a**) and IDipp·Ga(AsH_2)$_3$ (**1b**) were obtained analytically pure in good isolated yields of 70% and 47%, respectively. Alternatively, **1a** can also be synthesised by using $NaPH_2$[23] instead of $LiPH_2$·DME, however with slightly lowered yields. Both products are colourless solids that display high sensitivity towards air and decompose slowly at room temperature. Thus, they can be stored for at least several months under an inert atmosphere at -30 °C. Simultaneously with presenting the salt metathesis in Equation (1), we investigated a possible one-pot reaction of formally generating [M(PnH_2)$_3$]$_n$ (M = Ga, Al; *Pn* = P, As) *in situ* and then adding the NHC to the reaction mixture in a simple one-pot reaction to break up the oligomers into NHC-stabilised monomers. Although possible, the route in Equation (1) proved to be far cleaner and higher yielding (cf. Supporting Information). The $^{31}P\{^1H\}$ NMR spectrum of **1a** shows a singlet at -231.7 ppm

that is split into a triplet in the ^{31}P NMR spectrum ($^{1}J_{HP}$ = 173 Hz). This concurs with a doublet in the ^{1}H NMR spectrum at 0.99 ppm (6 H, $^{1}J_{HP}$ = 173 Hz). The ^{1}H NMR spectrum of **1b** displays a distinct sharp singlet at 0.75 ppm for the AsH_2 moieties bound to Ga (6 H). Attempts to obtain LIFDI-MS data were unsuccessful due to the rapid decomposition of **1a** and **1b** upon ionisation, leading only to fragment peaks of $[IDipp\text{-}H]^+$ at m/z = 398.29. In case of **1b**, a fragment peak of $[IDipp{\cdot}Ga(AsH_2)_2]^+$ was detected at m/z = 611.09. The purity of **1a** and **1b** was confirmed by elemental analysis. Single crystals of **1a/b** were obtained from a saturated *n*-hexane solution at -28°C as small colourless needles and examined by single crystal X-ray structure determination (Figure 4.2).

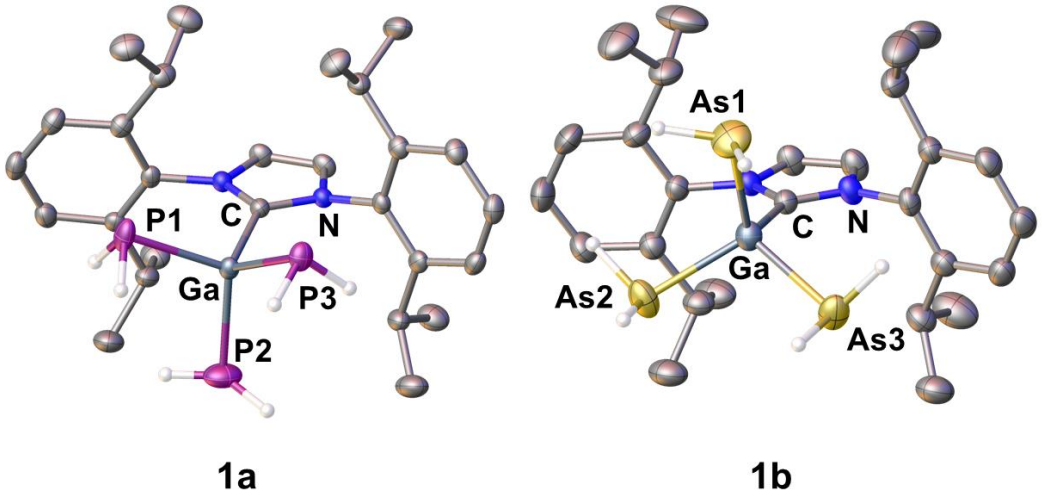

Figure 4.2: Molecular structure of **1a** and **1b** in the solid state. Anisotropic displacement ellipsoids are shown at 50% probability level. Disordered parts and hydrogen atoms bound to carbon atoms are omitted for clarity. Selected bond lengths [Å] and angles [°]: **1a**: C-Ga 2.064(9), Ga-P1 2.3514(7), Ga-P2 2.3554(8), Ga-P3 2.3609(7), C-Ga-P1 109.67(6), C-Ga-P2 105.68(7), C-Ga-P3 110.85(6), P1-Ga-P3 105.41(3), P1-Ga-P2 115.31(3), P2-Ga-P3 109.99(3). **1b**: C-Ga 2.068(3), Ga-As1 2.4526(8), Ga-As2 2.4634(9), Ga-As3 2.4583(8), C-Ga-As1 109.30(9), C-Ga-As2 108.75(10), C-Ga-As3 107.2(1), As1-Ga-As3 110.22(3), As1-Ga-As2 111.83(3), As2-Ga-As3 109.40(3).

1a and **1b** crystallise in the monoclinic space group $P2_1/c$. The Ga-P and Ga-As bond distances of 2.3608(8)–2.3649(9) Å (Ga-P) and 2.4437(7)–2.4550(7) Å (Ga-As) are within the range of Ga-P and Ga-As single bonds (cf. $IDipp{\cdot}GaH_2PH_2$: 2.3373(6) Å, $IDipp{\cdot}GaH_2AsH_2$: 2.4503(12) Å).[8,9] The central {$CGaP_3$} and {$CGaAs_3$} units adopt tetrahedral geometries with P-Ga-P and Al-Ga-As bond angles of 109.86(13)°-110.87(14)° (P-Ga-P) and 109.40(3)°–111.83(3)° (As- Ga-As), respectively.

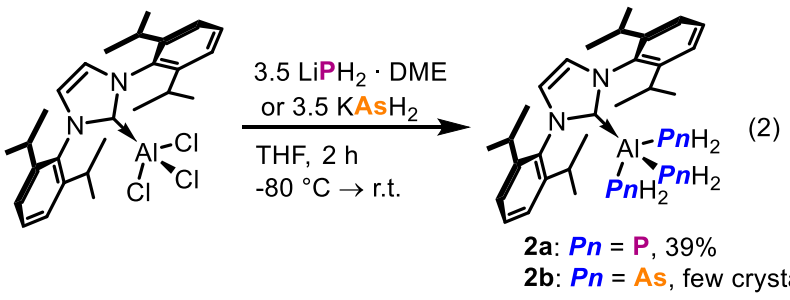

After the successful synthesis of the gallium compounds, we turned our attention to aluminium, which displays even greater sensitivity towards decomposition in this type of compounds.[8,9] In addition to the apparent sensitivity, the weak bonding between the pnictogen atoms and aluminium complicate this

chemistry further. Nevertheless, the salt elimination reactions of IDipp·$AlCl_3$ with $LiPH_2$·DME and $KAsH_2$ were carried out (equation (2)), yielding the novel branched compounds IDipp·$Al(PH_2)_3$ (**2a**) and IDipp·$Al(AsH_2)_3$ (**2b**). The tripentelylalanes are obtained as colourless solids (**2a**: 39%; **2b**: few crystals) that show extreme sensitivity towards air, and crystalline samples of **2a** and **2b** also decompose quickly in degassed mineral oil or perfluorinated oil. **2a** and **2b** are also rather unstable at room temperature in both solution and in the solid state and decompose fast and quantitatively under release of IDipp and PH_3 or AsH_3, respectively. The $^{31}P\{^1H\}$ NMR spectrum of a freshly prepared solution of **2a** at room temperature (C_6D_6) displays a sharp singlet at -252.0 ppm split into a triplet ($^1J_{HP}$ = 175 Hz) in the ^{31}P NMR spectrum. This coincides with a broadened doublet in the ^1H NMR spectrum at 0.66 ppm ($^1J_{HP}$ = 175 Hz, 6 H). The synthesis of **2b** is accompanied by several side products that were impossible to be separated or washed away due to a solubility that is very similar to that of the product. Separation of crystals under the microscope was not possible due to the fast thermal decomposition of **2b**. All variations of the reaction conditions (temperature, addition of reagents, stoichiometry) did not prevent the formation of these side products. Attempts to obtain MS data were unsuccessful due to the rapid decomposition of **2a** and **2b** upon ionisation, leading only to fragment peaks of $[IDipp\text{-}H]^+$ at m/z = 389.28. However, despite the extraordinary sensitivity of **2a** and **2b**, by quick and careful manipulation, it was also possible to determine the structures of **2a** and **2b** by single-crystal X-ray structure analysis (Figure 4.3).

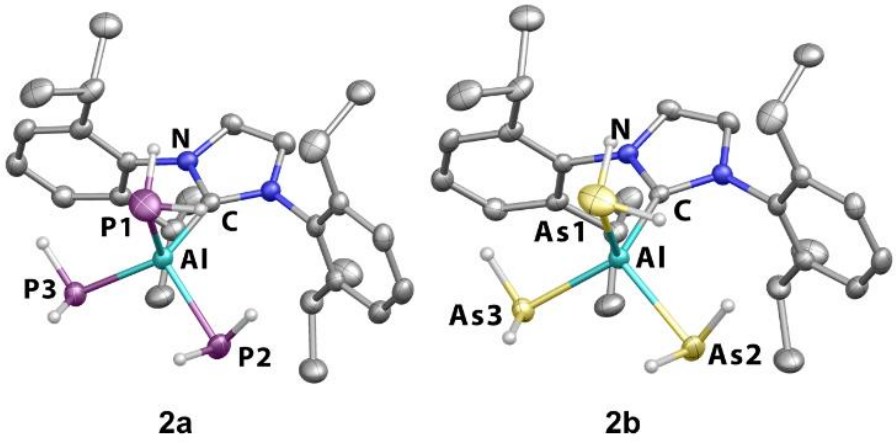

Figure 4.3: Molecular structure of **2a** and **2b** in the solid state. Anisotropic displacement ellipsoids are shown at 50% probability level. Hydrogen atoms bound to carbon atoms are omitted for clarity. Selected bond lengths [Å] and angles [°]: **2a**: C-Al 2.0672(19), Al-P1 2.3672(8), Al-P2 2.3720(8), Al-P3 2.3616(8), C-Al-P1 107.94(6), C-Al-P2 111.23(5), C-Al-P3 109.50(6), P1-Al-P3 115.24(3), P1-Al-P2 108.43(3), P2-Al-P3 104.49(3). **2b**: C-Al 2.063(3), Al-As1 2.4631(9), Al-As2 2.4638(9), Al-As3 2.4583(9), C-Al-As1 108.48(8), C-Al-As2 111.10(8), C-Al-As3 110.21(8), As1-Al-As3 114.43(3), As1-Al-As2 108.39(4), As2-Al-As3 104.18(3).

2a and **2b** crystallise as small, clear, colourless needles from saturated *n*-hexane solutions at -28 °C in the monoclinic space group $P2_1/c$. The Al-P and Al-As bond lengths of 2.3616(8)–2.3720(8) Å (P-Al) and 2.4583(9)–2.4638(9) Å (As-Al) are within the range of Al-P and Al-As single bonds, respectively (cf. IDipp·AlH_2PH_2: 2.3131(10) Å, IDipp·$AlH(AsH_2)_2$: 2.46 Å).[8,9] The P-Al-P and As-Al-As bond angles lie between 104.49(3)°–115.24(3)° (P-Al-P) and 104.18(3)°–114.43(3)° (As-Al-As) and reveal tetrahedral geometries at the {$CAlP_3$} and {$CAlAs_3$} units. Overall, the structural parameters of **2a/b** are almost identical to **1a/b**, as the *d*-block contraction of gallium causes a bonding feature that is very similar to that of its aluminium counterparts. In all the above-mentioned reactions, an excess amount of $LiPH_2$·DME/$NaPH_2$ or $KAsH_2$ was necessary to ensure the completeness of the reaction, as otherwise a mixture of IDipp·$ECl_{3-x}(PnH_2)_x$ (E = Ga, Al; *Pn* = P, As) is formed, according to NMR data. However, we observed that this causes the partial NHC substitution by the pnictogenide reagent, as a lot of

unbound IDipp is obtained, as identified by ^{1}H NMR spectroscopy. This prompted us to take a closer look at the reaction mixtures. And indeed, NMR spectroscopic investigations on the reaction between IDipp·$AlCl_3$ and $NaPH_2$ show the formation of $[Al(PH_2)_4]^-$ by a strongly broadened triplet of multiplets in the ^{31}P NMR spectrum at -247.5 ppm which explains the lowered yields of these reactions in general. Moreover, the controlled substitution of one or two chlorides from IDipp·$GaCl_3$ was also tested, which unfortunately resulted in inseparable mixtures of IDipp·$GaCl_{3-x}(PH_2)_x$ in all attempts.
Furthermore, the question came up whether a similar reaction pattern is also possible with the even heavier group 13 homologues. Hence, it was tested to perform the triple salt metathesis reaction on a suitable NHC·$InCl_3$ precursor. Since IDipp·$InCl_3$ (**A**) has not been described in literature, it was synthesised by direct synthesis from IDipp and $InCl_3$ [Equation (3)]. A is obtained as a white-greyish solid that can be stored under an inert atmosphere at room temperature for at least several months.

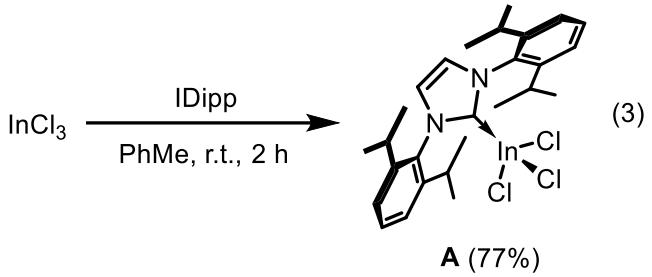

A (77%) (3)

The ^{1}H NMR spectrum of A shows a characteristic set of signals for IDipp adducts with two separate doublets at 1.18 ppm and 1.38 ppm for the diastereotopic isopropyl CH_3 protons (cf. detailed data in the Supporting Information). Crystals suitable for single crystal X-ray structure determination were grown by slow evaporation of a solution of **A** in CH_2Cl_2. The molecular structure in the solid state (Figure 4.4) shows a tetrahedral geometry at the {CInCl3} unit with Cl-In-Cl bond angles between 105.37(8)° and 115.16(8)°. The In-Cl bonds lie between 2.3557(3)–2.3689(9) Å and are significantly shorter than the In-Br bonds in IDipp·$InBr_3$ (2.500 Å).

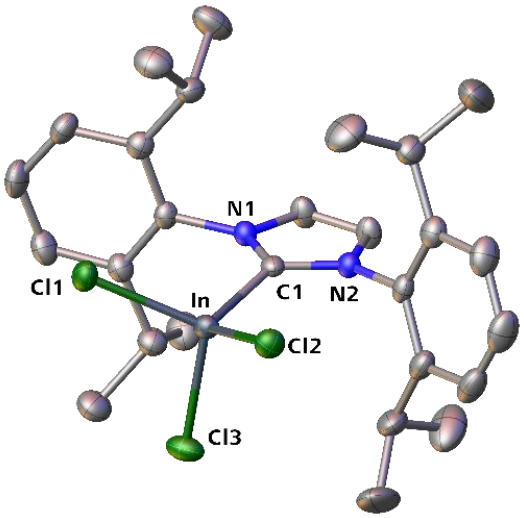

Figure 4.4: Molecular structure of **A** in the solid state. Anisotropic displacement ellipsoids are shown at 50% probability level. Hydrogen atoms are omitted for clarity. Selected bond lengths [Å] and angles [°]: C1-In 2.187(3), In-Cl1 2.3585(8), In-Cl2 2.3557(8), In-Cl3 2.3689(9), C1-In-Cl1 115.16(8), C1-In-Cl2 113.84(8), C1-In-Cl3 105.37(8).

With a suitable precursor at hand, the analogous salt metathesis reactions with $LiPH_2$·DME and $KAsH_2$ were investigated. To prevent decomposition by reduction towards an In(I) species, these reactions were performed under exclusion of light and careful temperature monitoring. Solid $LiPH_2$·DME was added to a solution of **A** at -80 °C and the solution was allowed to reach 0 °C over the course of three hours

[Equation (4)]. After work-up by extraction with toluene, small amounts of IDipp·In(PH_2)$_3$ (**3**) could be obtained and characterised by multinuclear NMR spectroscopy. Despite several washing steps with cold *n*-hexane (-60 °C), unbound IDipp could not be completely separated from the final product.

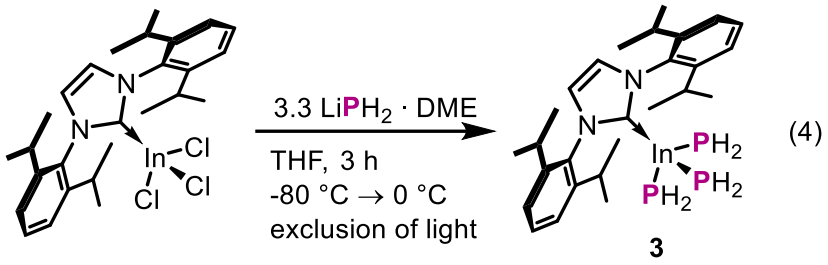

(4)

3 was obtained by this reaction in very small amounts as colourless solids that decompose at room temperature and under ambient light. The reaction suffers from significant product loss due to decomposition by thermal pathways and especially IDipp substitution, as the IDipp-In bond is comparably weak and causes the release of large amounts of unbound IDipp. The $^{31}P\{^1H\}$ NMR spectrum of **3** in C_6D_6 shows a sharp singlet at -264.7 ppm (^{31}P NMR: triplet, $^1J_{HP}$ =167 Hz) for the {PH_2} moieties besides a small amount of PH_3 as the result of decomposition already at r. t. (Figure 4.5). The ^1H NMR spectrum shows a characteristic doublet at 0.65 ppm for the {PH_2} protons ($^1J_{HP}$=167 Hz) with an integral ratio of overall 6 protons (Figure 4.6), thus confirming the existence of **3**.

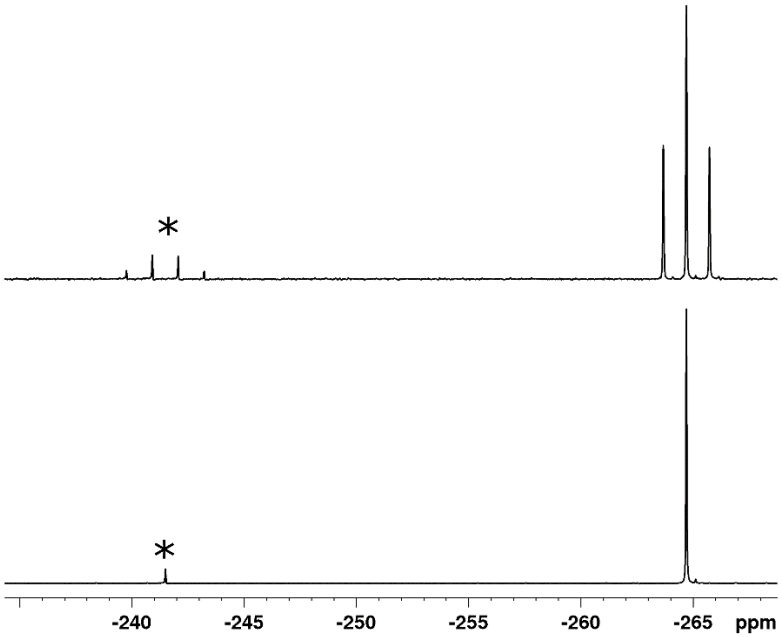

Figure 4.5: ^{31}P NMR (top) and $^{31}P\{^1H\}$ NMR (bottom) spectra of 3 (298 K, * = PH_3 resulting from sample decomposition).

When using $KAsH_2$ in the reaction (equation 4), it could be visually confirmed that a reaction is taking place by precipitation of solid KCl, accompanied by a slight colour change of the solution. However, despite all our efforts, the presence of IDipp·In(AsH_2)$_3$ could not be confirmed by ^1H NMR spectroscopy, which always showed the presence of a product mixture. It was also not possible to grow crystals of any of the products for identification purposes, as the inseparable mixture decomposes quickly at -30 °C already under exclusion of light. However, according to DFT calculations (B3LYP-D4/def2-TZVP),[24–28,29] IDipp·In(AsH_2)$_3$ indeed represents a minimum on the potential energy surface that unfortunately still remains experimentally elusive.

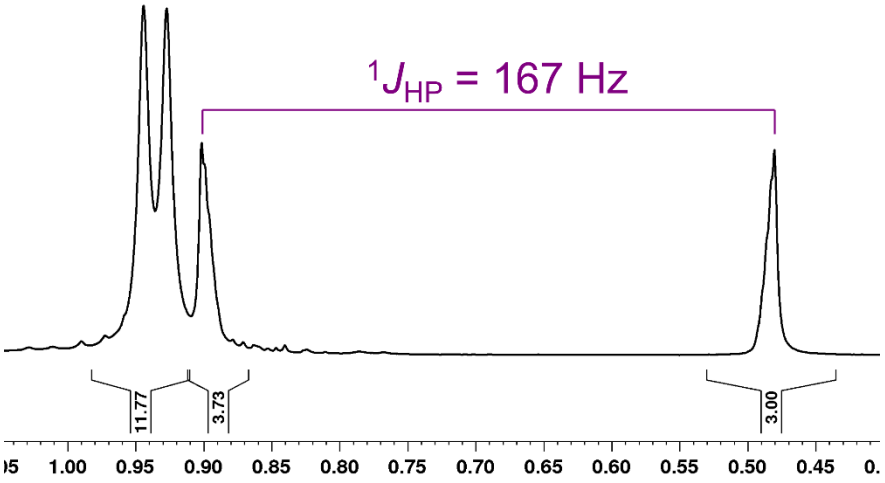

Figure 4.6: Section of the ^{1}H NMR spectrum of **3** revealing a doublet for the PH_2 protons (C_6D_6, 298 K).

The electronic structure and nature of bonding within the synthesised compounds was evaluated by NBO[30] analysis, employing density functional theory. NPA charge analysis (TPSSh/def2-TZVP)[28,31] revealed the polar nature of the interatomic bonds, which is largest for the triphosphanyl and triarsanylalane (Figure 4.7a). The *Wiberg Bond Indices* for the pnictogen-triel bonds lie between 0.79–0.85 (**1a**), 0.80–0.84 (**1b**), 0.74–0.78 (**2a**), and 0.76–0.81 (**2b**). These combined DFT analyses indicate polarised albeit weak single bonds for these compounds.

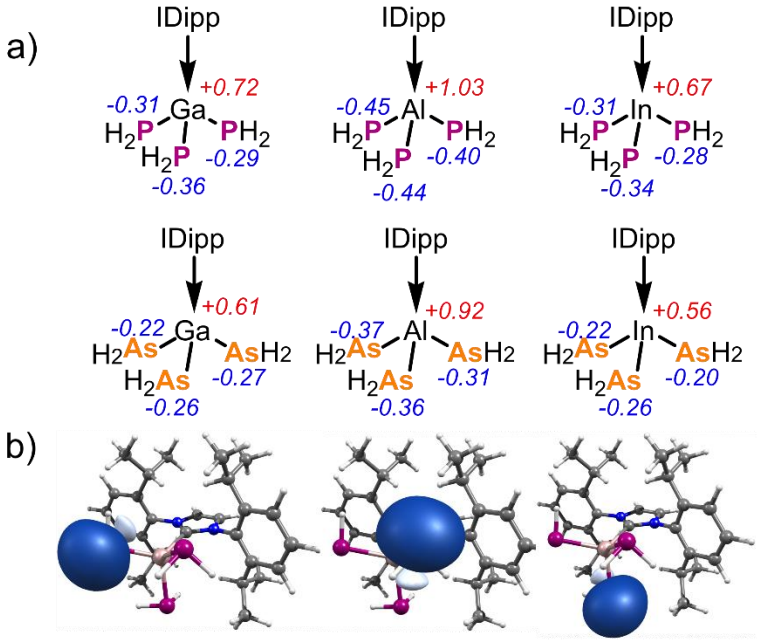

Figure 4.7: a) Calculated Natural Charges for NHC-stabilised tripentelyltrielanes of heavy group 13 elements (TPSSh/def2-TZVP // B3LYP-D4/def2-TZVP level of theory). b) Depiction of calculated lone pair orbitals of **1a** (NBO).

As evident from NBO calculations, localised lone pairs can be assigned to all pnictogen atoms within these compounds (Figure 4.7b). Therefore, we assumed that the synthesised tripentelyltrielanes would display a versatile coordination chemistry as mono- or multidentate ligands towards main group elements and transition metals despite their high sensitivity. Due to displaying the best availability and stability, **1a** was used as the reagent of choice for the following coordination attempts. Thus, reactions with many main group electrophiles and transition metal complexes such as $BH_3{\cdot}SMe_2$, $AlMe_3$,

$Me(SO_3CF_3)$, AuCl(tht) (tht = tetrahydrothiophene), $[W(MeCN)_3(CO)_3]$, $[W(CO)_4(nbd)]$ (nbd = norbornadiene), $[Pt(PhCN)_2Cl_2]$, transition metal salts of weakly coordinating anions and many more were performed.

Unfortunately, most of these reactions led to either intractable mixtures or the breakage of one or more Ga-P bonds rather than coordination. As the Ga-P bonds seemed particularly sensitive to classic coordination chemistry, we targeted to synthesise a more softly bound metal complex. Therefore, the trimeric *o*-perfluorophenylenemercury $(HgC_6F_4)_3$[32] was chosen as a Lewis-acidic compound known to be available for weak interactions. $(HgC_6F_4)_3$ has been a subject of many studies of coordination chemistry and has shown versatile coordination modes, covalent as well as noncovalent.[33,34] When a solution of **1a** in 1,2-difluorobenzene is added to a suspension $(HgC_6F_4)_3$ in 1,2-difluorobenzene, the immediate formation of a clear red solution is observed [Equation (5)]. The $^{31}P\{^1H\}$ spectrum of this reaction solution showed a slightly broadened singlet at -220.7 ppm, which is shifted downfield by roughly +12 ppm compared to the starting material and is indicative of a dynamic coordination of **1a** to $(HgC_6F_4)_3$.

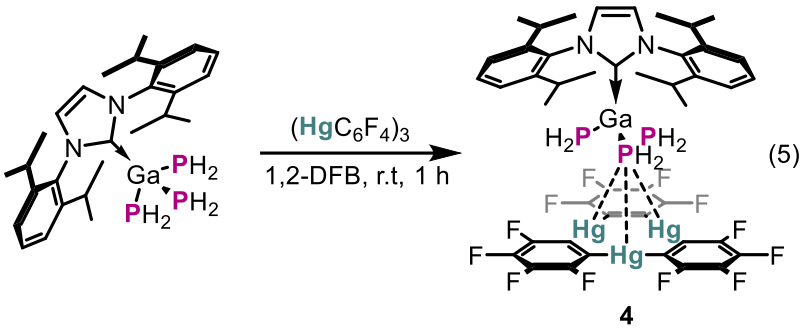

(5)

4

After work-up, the colourless coordination compound [IDipp·$Ga(PH_2)_2(\mu_3\text{-}PH_2\{HgC_6F_4\}_3)$] (**4**) could be crystallised within a unidentifiable mixture of red-brown amorphous solids as clear colourless plates (Figure 4.8). **4** displays a high sensitivity towards air and decomposes at room temperature releasing PH_3. Low temperature NMR experiments to determine the dynamic binding situation failed as dissolving the compound in CD_2Cl_2 leads exclusively to unbound **1a**, because the excess of CD_2Cl_2 causes the replacement of IDipp·$Ga(PH_2)_3$, likely to be resulting in the complex $(HgC_6F_4)_3\cdot CD_2Cl_2$.[34] Other solvents such as THF-d_8 are deemed unsuitable due to the poor solubility of **4** as well as the possible coordination of THF towards $(HgC_6F_4)_3$. DFT calculations (PWPB95-D4/def2-TZVPP//BP86-D4/def2-TZVP, CPCM = CH_2Cl_2)[26–28,35,36,37] suggest that the dissociation process of the adduct **4** into **1a** and $(HgC_6F_4)_3$ is slightly exergonic by -1.06 kcal mol^{-1} at 298 K, further indicating the facile dissociation of **4**. Single crystals suitable for X-ray structure determination were grown by layering a solution of **4** in 1,2-difluorobenzene with *n*-hexane at -30 °C. **4** crystallises in the monoclinic space group $P2_1/n$ as clear colourless plates (Figure 4.8). Its crystal structure shows one molecule of IDipp·$Ga(PH_2)_3$ coordinated to the mercury ring system by one $\{PH_2\}$ arm. The P-Hg distances are very long and lie between 3.18109(13)–3.3168(13) Å. These distances are well below the sum of the Van der Waals radii of P and Hg (3.6 Å) and are indicative of at least weak attractive forces.

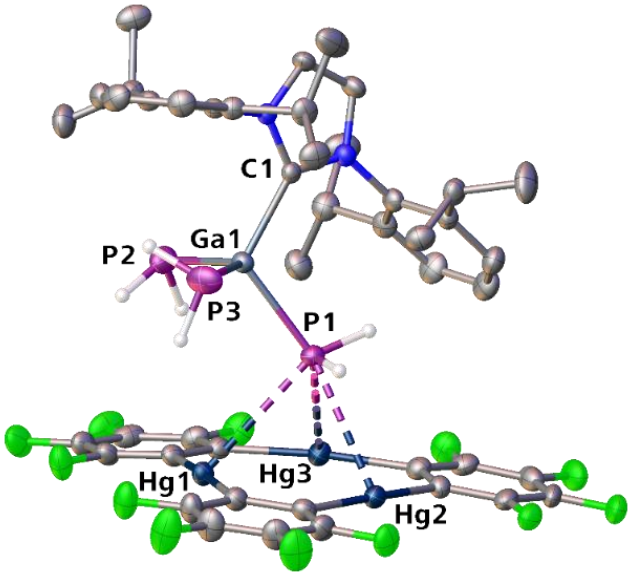

Figure 4.8: Molecular structure of **4** in the solid state. Anisotropic displacement ellipsoids are shown at 50% probability level. Hydrogen atoms bound to carbon are omitted for clarity. Selected bond lengths [Å] and angles [°]: P1-Hg1 3.2547(13), P1-Hg2 3.1809(13), P1-Hg3 3.3169(13), Hg1-Hg2 3.5697(4), Hg2-Hg3 3.6002(4), Hg1-Hg3 3.5579(5, C1-Ga1 2.064(5), Ga1-P1 2.3809(14), Ga1-P2 2.3719(15), Ga1-P3 2.3310(15), C1-Ga1-P1 113.95(13), C1-Ga1-P2 105.74(12), C1-Ga1-P3 109.32(13), P1-Hg1-Hg2 55.33(2), P1-Hg2-Hg3 58.17(2), P1-Hg3-Hg2 56.38(2), Hg1-Hg2-Hg3 59.498(6), Hg2-Hg3-Hg1 59.823(6), Hg3-Hg1-Hg2 60.679(6).

Furthermore, the Ga-P_{Hg} bond is slightly elongated with 2.3809(14) Å and the $C_{Carbene}$-Ga-P_{Hg} bond angle is slightly widened towards 113.95(13)°. The lengthening of the Ga-P bond upon coordination might explain the pronounced instability and hence easy decomposition of the coordination compounds of **2a** (see above).

The loose coordination mode of the ligand raised the question as to whether the bonding situation could still be described by covalent bonds or not. Therefore, quantum chemical calculations were performed (ZORA-B3LYP-D4/ZORA-def2-TZVPP (SARC on Hg)[24–28,38] //BP86-D4/def2-SVP[26–28,35,36] level of theory, Figure 9). The calculated structure is in good agreement with the solid-state structure. The *Wiberg Bond Indices* for the P-Hg bonds lie between 0.0243–0.0264 and do not indicate covalent bonding between these atoms. This is further supported by an *atoms-in-molecules* analysis[39] with no bond-critical points being found along the P-Hg coordination paths. By a *non-covalent interaction* analysis (NCI), a surface of the reduced density gradient between the three Hg atoms and the phosphorus atom indicates strong electrostatic interactions (Figure 4.9, right).[40] Furthermore, an NBO analysis (TPSSh/def2-TZVPP)[28,31] shows that the lone pair (orbital contributions from P: *s* 0.42, *p* 0.58) of the respective phosphorus atom points directly towards the centre of the mercury ring system (Figure 4.9, left). Overall, the applied computational methods suggest an electrostatic attraction based on the interactions of the three mercury atoms with the electron density around an occupied, nearly sp^2-hybridised orbital of the phosphorus atom.

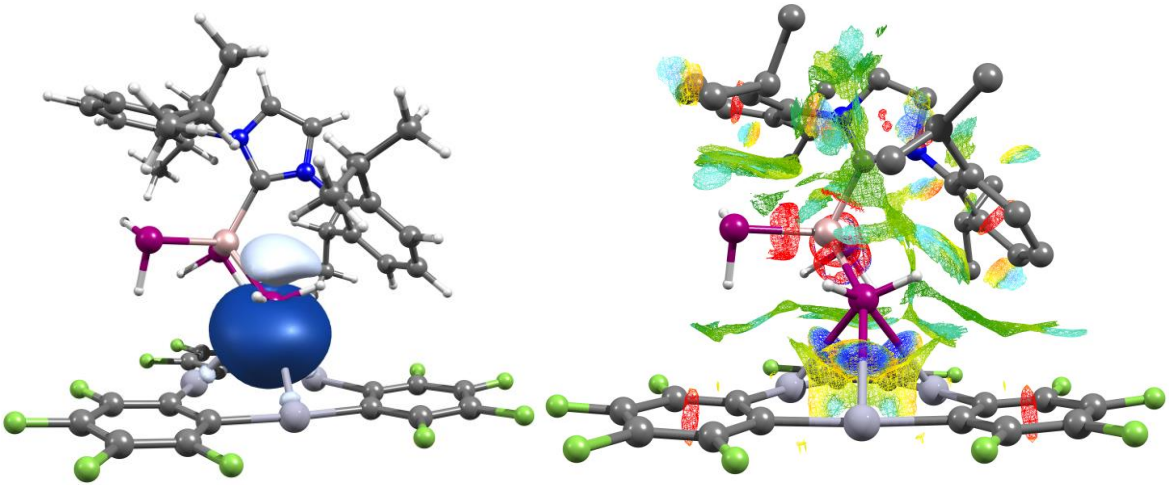

Figure 4.9 Occupied lone pair orbital (NBO) within **4** coordinating towards the $\{Hg\}_3$ unit (left) and plot of the calculated reduced density gradient of [IDipp·Ga$(PH_2)_2(\mu_3$-$PH_2\{HgC_6F_4\}_3)$] (right). Hydrogen atoms bound to carbon are omitted for clarity. The lined surfaces show regions of weak interactions within the molecule. Colour scheme: blue (strong electrostatic interaction), green (Van der Waals interaction), red (strong repulsion).

4.3 Conclusion

In summary, we were able to complete the series of NHC-stabilised pentelylgallanes and alanes by synthesizing the first branched tripnictogenyl-substituted NHC adducts IDipp·Ga$(PH_2)_3$ (**1a**), IDipp·Ga$(AsH_2)_3$ (**1b**), IDipp·Al$(PH_2)_3$ (**2a**) and IDipp·Al$(AsH_2)_3$ (**2b**) by triple salt metathesis reactions. All these products decompose at ambient temperatures under strictly inert conditions and display extraordinary sensitivity towards air. In addition, the first NHC-stabilised triphosphanylindiumane IDipp·In$(PH_2)_3$ (**3**) was accessible by this pathway, as evident from its NMR spectroscopic features. Investigations on the reactivity of these compounds proved difficult due to very weak bonding between the group 13 and group 15 elements, resulting in bond cleavage in most cases. However, coordination towards $(HgC_6F_4)_3$ could be realised in [IDipp·Ga$(PH_2)_2(\mu_3$-$PH_2\{HgC_6F_4\}_3)$] (**4**) where one arm of the ligand is simultaneously coordinated to three Hg atoms by weak interaction. Electronic structure calculations confirm mainly electrostatic bonding within **4** and point out the highly polarised bonding between the group 15 and 13 elements in the obtained NHC-stabilised tripentelyltrielanes. In view of the instability of the presented compounds, these could not act as multidentate ligands so far, as bond breakage was observed. By decreasing the size of the NHC and using alkylated compounds instead of the parent compounds, this reaction behaviour might be improved. Future studies will also investigate catenation with suitable electrophiles and the use of these compounds as single-source precursors in chemical vapor deposition processes (CVD) towards the synthesis of thin layers of 13/15 materials.

4.4 References

[1] a) A. B. Burg, H. I. Schlesinger, *J. Am. Chem. Soc.* **1937**, *59*, 780–787; b) J. Gay-Lussac, J. Thenard, *Mem. Phys. Chim. Soc. d'Arcueil* **1809**, *2*, 210–211; c) A. Stock, E. Pohland, *Chem. Ber.* **1926**, *59*, 2210–2215.

[2] C. E. Housecroft, A. Sharpe, *Inorganic Chemistry*, 4. Aufl., Pearson, New York, **2012**, p. 859-860.

[3] S. Schulz, *Adv. Organomet. Chem.* **2003**, *49*, 225–317.

[4] a) A. C. Jones, P. O'Brien, *CVD of Compound Semiconductors: Precursor Synthesis Development and Applications*, VCH, Weinheim, **1996**; b) M. R. Leys, *Chemtronics* **1987**, *2*, 155–164; c) G. B. Stringfellow, *Rep. Prog. Phys.* **1982**, *45*, 469–525; d) R. A. Fischer, J. Weiß, *Angew. Chem. Int. Ed.* **1999**, *38*, 2830-2850; *Angew. Chem.* **1999**, *111*, 3002-3022; e) J. D. Masuda, A. J. Hoskin, T. W. Graham, C. Beddie, M. C. Fermin, N. Etkin, D. W. Stephan, *Chem. Eur. J.* **2006**, *12*, 8696–8707; f) R. D. Wells, W. L. Gladfelter, *J. Cluster Sci.* **1997**, *8*, 217–238; g) T. J. Clark, K. Lee, I. Manners, *Chem. Eur. J.* **2006**, *12*, 8634–8648; h) B. Neumüller, E. Iravani, *Coord. Chem. Rev.* **2004**, *248*, 817–834; i) S. Schulz, *Coord. Chem. Rev.* **2001**, *215*, 1–37; j) A. Y. Timoshkin, *Coord. Chem. Rev.* **2005**, *249*, 2094–2131; k) A. Staubitz, A. Presa Soto, I. Manners, *Angew. Chem. Int. Ed.* **2008**, *47*, 6212–6215; *Angew. Chem.* **2008**, *120*, 6308–6311.

[5] a) A. Adolf, M. Zabel, M. Scheer, *Eur. J. Inorg. Chem.* **2007**, *2007*, 2136–2143; b) C. A. Jaska, A. J. Lough, I. Manners, *Inorg. Chem.* **2004**, *43*, 1090–1099; c) M. Bodensteiner, A. Y. Timoshkin, E. V. Peresypkina, U. Vogel, M. Scheer, *Chem. Eur. J.* **2013**, *19*, 957–963; d) K.-C. Schwan, A. Y. Timoskin, M. Zabel, M. Scheer, *Chem. Eur. J.* **2006**, *12*, 4900–4908; e) C. Marquardt, A. Adolf, A. Stauber, M. Bodensteiner, A. V. Virovets, A. Y. Timoshkin, M. Scheer, *Chem. Eur. J.* **2013**, *19*, 11887–11891; f) U. Vogel, P. Hoemensch, K.-C. Schwan, A. Y. Timoshkin, M. Scheer, *Chem. Eur. J.* **2003**, *9*, 515–519.

[6] U. Vogel, A. Y. Timoshkin, M. Scheer, *Angew. Chem. Int. Ed.* **2001**, *40*, 4409–4412.

[7] A. J. Arduengo, R. Krafczyk, R. Schmutzler, H. A. Craig, J. R. Goerlich, W. J. Marshall, M. Unverzagt, *Tetrahedron* **1999**, *55*, 14523–14534.

[8] M. A. K. Weinhart, A. S. Lisovenko, A. Y. Timoshkin, M. Scheer, *Angew. Chem. Int. Ed.* **2020**, *59*, 5541-5545; *Angew. Chem.* **2020**, *132*, 5586-5590.

[9] M. A. K. Weinhart, M. Seidl, A. Y. Timoshkin, M. Scheer, *Angew. Chem.* **2021**, *133*, 3850–3855; *Angew. Chem. Int. Ed.* **2021**, *60*, 3806–3811.

[10] F. Dankert, C. Hering-Junghans, *Chem. Comm.* **2022**, *58*, 1242–1262.

[11] a) M. K. Sharma, P. Dhawan, C. Helling, C. Wölper, S. Schulz, *Chem. Eur. J.* **2022**, *28*, e202200444; b) M. K. Sharma, C. Wölper, G. Haberhauer, S. Schulz, *Angew. Chem. Int. Ed.* **2021**, *60*, 6784–6790; c) A. Bücker, C. Wölper, G. Haberhauer, S. Schulz, *Chem. Comm.* **2022**, *58*, 9758–9761; d) C. Helling, C. Wölper, S. Schulz, *J. Am. Chem. Soc.* **2018**, *140*, 5053–5056; e) C. Helling, C. Wölper, Y. Schulte, G. E. Cutsail III, S. Schulz, *Inorg. Chem.* **2019**, *58*, 10323–10332; f) C. Ganesamoorthy, C. Helling, C. Wölper, W. Frank, E. Bill, G. E. Cutsail, S. Schulz, *Nat. Comm.* **2018**, *9*, 87; g) S. Ghosh, E. Glöckler, C. Wölper, J. Linders, N. Janoszka, A. H. Gröschel, S. Schulz, *Eur. J. Inorg. Chem.* **2022**, *2022*; h) C. Helling, C. Ganesamoorthy, C. Wölper, S. Schulz, *Dalton Trans.* **2022**, *51*, 2050–2058; i) C. Helling, C. Wölper, S. Schulz, *Eur. J. Inorg. Chem.* **2020**, *2020*, 4225–4235; j) C. Helling, C. Wölper, S. Schulz, *Dalton Trans.* **2020**, *49*, 11835–11842; k) J. Krüger, C. Wölper, G. Haberhauer, S. Schulz, *Inorg. Chem.* **2022**, *61*, 597–604; l) J. Krüger, C. Ganesamoorthy, L. John, C. Wölper, S. Schulz, *Chem. Eur. J.* **2018**, *24*, 9157–9164; m) J. Krüger, C. Wölper, S. Schulz, *Angew. Chem. Int. Ed.* **2021**, *60*, 3572–3575; n) B. Li, B. L. Geoghegan, H. M. Weinert, C. Wölper, G. E. Cutsail, S. Schulz, *Chem. Comm.* **2022**, *58*, 4372–4375; o) B. Li, C. Wölper, G. Haberhauer, S. Schulz, *Angew. Chem. Int. Ed.* **2021**, *133*, 2014–2019; p) J. Schoening, L. John, C. Wölper, S. Schulz, *Dalton Trans.* **2019**, *48*, 17729–17734; q) M. K. Sharma, C. Wölper, S. Schulz, *Dalton Trans.* **2022**, *51*, 1612–1616; r) H. M. Weinert, C. Wölper, S. Schulz, *Chem. Sci.* **2022**, *13*, 3775–3786.

[12] D. W. N. Wilson, J. Feld, J. M. Goicoechea, *Angew. Chem. Int. Ed.* **2020**, *132*, 21100–21104.

[13] B. Li, S. Bauer, M. Seidl, A. Y. Timoshkin, M. Scheer, *Chem. Eur. J.* **2019**, *25*, 13714–13718.

[14] S. Schneider, S. Ivlev, C. von Hänisch, *Chem. Comm.* **2021**, *57*, 3781–3784.

[15] a) N. J. Hardman, B. E. Eichler, P. P. Power, *Chem. Comm.* **2000**, 1991–1992; b) S. Schneider, C. Hänisch, *Eur. J. Inorg. Chem.* **2021**, *2021*, 4655–4660.

[16] A. Ordyszewska, N. Szynkiewicz, J. Chojnacki, R. Grubba, *Inorg. Chem.* **2022**, *61*, 4361–4370.

[17] A. Y. Timoshkin, G. Frenking, *Inorg. Chem.* **2003**, *42*, 60–69.

[18] A. J. Arduengo, R. L. Harlow, M. Kline, *J. Am. Chem. Soc.* **1991**, *113*, 361–363.

[19] V. Lavallo, Y. Canac, C. Präsang, B. Donnadieu, G. Bertrand, *Angew. Chem. Int. Ed.* **2005**, *44*, 5705–5709.

[20] a) D. F. Shriver, A. E. Shirk, J. A. Dilts, *Inorg. Synth.* **1977**, *17*, 42–45; b) G. W. Schaeffer, E. R. Anderson, *J. Am. Chem. Soc.* **1949**, *71*, 2143–2145; c) J. K. Ruff, M. F. Hawthorne, *J. Am. Chem. Soc.* **1960**, *82*, 2141–2144.

[21] N. Marion, E. C. Escudero-Adán, J. Benet-Buchholz, E. D. Stevens, L. Fensterbank, M. Malacria, S. P. Nolan, *Organometallics* **2007**, *26*, 3256–3259.

[22] H. Schäfer, G. Fritz, W. Hölderich, *Z. Anorg. Allg. Chem.* **1977**, *428*, 222–224.

[23] G. Brauer, *Handbuch der Präparativen Anorganischen Chemie,* 3. Aufl., **1975**, Vol. 1, p. 516-517.

[24] A. D. Becke, *J. Chem. Phys.* **1993**, *98*, 5648–5652.

[25] C. Lee, W. Yang, R. G. Parr, *Phys. Rev. B* **1988**, *37*, 785–789.

[26] E. Caldeweyher, C. Bannwarth, S. Grimme, *J. Chem. Phys.* **2017**, *147*, 34112.

[27] E. Caldeweyher, S. Ehlert, A. Hansen, H. Neugebauer, S. Spicher, C. Bannwarth, S. Grimme, *J. Chem. Phys.* **2019**, *150*, 154122.

[28] F. Weigend, R. Ahlrichs, *Phys. Chem. Chem. Phys.* **2005**, *7*, 3297-305.

[29] a) F. Neese, *WIREs Comput. Mol. Sci.* **2012**, *2*, 73–78; b) F. Neese, *WIREs Comput. Mol. Sci.* **2018**, *8*, e1327; c) F. Neese, *WIREs Comput. Mol. Sci.* **2022**, *12*, e1606; d) F. Neese, F. Wennmohs, U. Becker, C. Riplinger, *J. Chem. Phys.* **2020**, *152*, 224108.
[30] A. E. Reed, L. A. Curtiss, F. Weinhold, *Chem. Rev.* **1988**, *88*, 899–926.
[31] V. N. Staroverov, G. E. Scuseria, J. Tao, J. P. Perdew, *J. Chem. Phys.* **2003**, *119*, 12129–12137.
[32] P. Sartori, A. Golloch, *Chem. Ber.* **1968**, *101*, 2004–2009.
[33] a) M. Fleischmann, C. Heindl, M. Seidl, G. Balázs, A. V. Virovets, E. V. Peresypkina, M. Tsunoda, F. P. Gabbaï, M. Scheer, *Angew. Chem. Int. Ed.* **2012**, *51*, 9918–9921; b) M. Fleischmann, J. S. Jones, G. Balázs, F. P. Gabbaï, M. Scheer, *Dalton Trans.* **2016**, *45*, 13742–13749; c) O. Loveday, J. Jover, J. Echeverría, *Inorg. Chem.* **2022**, *61*, 12526–12533; d) M. Tsunoda, M. Fleischmann, J. S. Jones, N. Bhuvanesh, M. Scheer, F. P. Gabbaï, *Dalton Trans.* **2016**, *45*, 5045–5051.
[34] M. Fleischmann, J. S. Jones, F. P. Gabbaï, M. Scheer, *Chem. Sci.* **2015**, *6*, 132–139.
[35] A. D. Becke, *Phys. Rev. A* **1988**, *38*, 3098–3100.
[36] J. P. Perdew, *Phys. Rev. B* **1986**, *33*, 8822–8824.
[37] a) V. Barone, M. Cossi, *J. Phys. Chem. A* **1998**, *102*, 1995–2001; b) L. Goerigk, S. Grimme, *J. Chem. Theory Comput.* **2011**, *7*, 291–309.
[38] a) D. A. Pantazis, X.-Y. Chen, C. R. Landis, F. Neese, *J. Chem. Theory Comput.* **2008**, *4*, 908–919; b) E. van Lenthe, J. G. Snijders, E. J. Baerends, *J. Chem. Phys.* **1996**, *105*, 6505–6516.
[39] R. F. W. Bader, *Acc. Chem. Res.* **1985**, *18*, 9–15.
[40] a) T. Lu, F. Chen, *J. Comput. Chem.* **2012**, *33*, 580–592; b) A. Otero-de-la-Roza, E. R. Johnson, J. Contreras-García, *Phys. Chem. Chem. Phys.* **2012**, *14*, 12165–12172; c) J. Contreras-García, E. R. Johnson, S. Keinan, R. Chaudret, J.-P. Piquemal, D. N. Beratan, W. Yang, *J. Chem. Theory Comput.* **2011**, *7*, 625–632.

4.5 Supporting Information

4.5.1 General Information

4.5.1.1 Working Techniques

All working steps were carried out under argon inert gas atmosphere using standard Schlenk and glovebox techniques. Glassware was dried in an oven at 170 °C and pre-conditioned in vacuum ($p < 10^{-3}$ mbar, 650 °C) shortly before use. The protective gas was cleansed from traces of H_2O and O_2 by passing it through a BASF R 3-11 ($CuO/MgSiO_3$) catalyst, concentrated H_2SO_4, Orange Gel and Sicapent® supported on pumice stone. Prior to use, solvents were purified using an MBraun SPS-800 solvent purification system, degassed by freeze-pump-thaw cycles and stored over activated molecular sieves for at least 48 hours. C_6D_6 was dried over Na/K alloy, distilled, degassed by freeze-pump-thaw cycles and stored over activated molecular sieves (4 Å). Elemental Analysis (CHN) was performed by the in-house facility. All mass spectra were recorded on a Jeol AccuTOF GCX mass spectrometer (LIFDI-MS) by the in-house facility.
IDipp,[1] IDipp·$GaCl_3$,[2] $KAsH_2$,[3] $LiPH_2$·DME[4] and $NaPH_2$[3] were prepared according to literature procedures. $GaCl_3$ and $AlCl_3$ were purchased from Sigma Aldrich and purified by sublimation prior to use. *Ortho*-perfluoromercuryphenylene $(HgC_6F_4)_3$[5] was provided by the Scheer group.

4.5.1.2 Spectroscopic Analysis

All NMR spectra were recorded on a BRUKER Avance 400 (frequencies: ^{1}H: 400.13 MHz, ^{13}C: 100.61 MHz, ^{31}P: 161.98 MHz, ^{19}F: 376.50 MHz) or Avance 300 (^{1}H: 300.13 MHz) spectrometers. Substances of reference are $Si(CH_3)_4$ (^{1}H, ^{13}C, internal standard), 85 % H_3PO_4 (^{31}P), $CFCl_3$ (^{19}F). Chemical shifts δ are presented in ppm referring to the external standards and coupling constants J are given in Hz without consideration of absolute signs. IR spectra were recorded in the solid state on a ThermoScientific Nicolet iS5 spectrometer with an ATR element equipped with a diamond crystal.

4.5.2 Experimental Details

4.5.2.1 Synthesis of IDipp·$InCl_3$ (A)

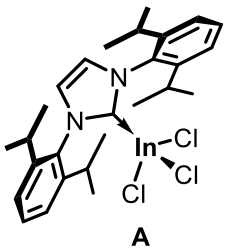

A

A mixture of $InCl_3$ (353 mg, 1.6 mmol) and IDipp (621 mg, 1.6 mmol) was dissolved in diethylether and stirred for 2 h at room temperature, resulting in a white-greyish suspension. The solvent was removed *in vacuo*, the remaining solids washed with *n*-hexane and the product dried *in vacuo* (749 mg, 77 %). Crystals suitable for X-ray single crystal diffraction experiments were obtained by slow evaporation of a solution of **A** in dichloromethane.

^{1}H NMR (400.30 MHz, CD_2Cl_2, 298 K): 1.18 (d, 12 H, 4 × ^{i}Pr-CH_3, $^3J_{HH}$ = 6.93 Hz), 1.38 (d, 12 H, 4 × ^{i}Pr-CH_3, $^3J_{HH}$ = 6.93 Hz), 2.51 (sep, 4 H, 4 × ^{i}Pr-C*H*, $^3J_{HH}$ = 6.83 Hz), 7.39 (d, 4 H, 4 × aryl-C$_{meta}$*H*, $^3J_{HH}$ = 7.86 Hz), 7.46 (s, 2 H, NC*H*C*H*N), 7.60 (t, 2 H, 2 × aryl-C$_{para}$H, $^3J_{HH}$ = 7.86 Hz).

^{13}C{^{1}H} NMR (100.61 MHz, CD_2Cl_2, 298 K): 22.5 (s, ^{i}Pr-*C*H$_3$), 25.6 (s, ^{i}Pr-*C*H$_3$), 29.1 (s, *C*H(CH$_3$)$_2$), 124.6 (s, *Ar*), 124.9 (s, *Ar*), 126.7 (s, *Ar*), 131.8 (s, NCH), 145.7 (s, *Ar*).

Elemental Analysis ($C_{27}H_{42}InN_2Cl_3$) **[%]:** calcd. C 53.18, H 5.95, N 4.59; found C 54.12, H 6.36, N 4.61.

(1) Synthesis of IDipp·$AlCl_3$ (B)

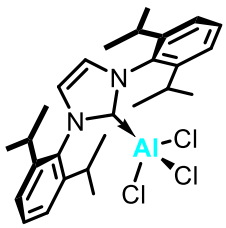

B

A solid mixture of IDipp (583 mg, 1.5 mmol) and $AlCl_3$ (200 mg, 1.5 mmol) was suspended in toluene and the reaction mixture stirred for three hours at room temperature, yielding a beige suspension. The solvent was removed in vacuo and the remainders washed twice with diethylether. The product was then dried *in vacuo* and obtained as a white powder (550 mg, 70 %). *Note: stirring for too long will cause side reactions, eventually leading to the precipitation of unidentified black solids.*

^{1}H NMR (400.30 MHz, CD_2Cl_2, 298 K): 1.15 (d, 12 H, 4 × ^{i}Pr-CH_3, $^3J_{HH}$ = 6.78 Hz), 1.36 (d, 12 H, 4 × ^{i}Pr-CH_3, $^3J_{HH}$ = 6.78 Hz), 2.54 (sep, 4 H, 4 × ^{i}Pr-CH, $^3J_{HH}$ = 6.78 Hz), 7.34 (d overlaid by s, 6 H, NCHCHN and 4 × aryl-C$_{meta}H$, $^3J_{HH}$ = 8.02 Hz), 7.55 (t, 2 H, 2 × aryl-C$_{para}$H, $^3J_{HH}$ = 8.02 Hz). The NMR data is in good agreement with literature values. [18]

^{13}C{^{1}H} NMR (100.61 MHz, CD_2Cl_2, 298 K): 22.2 (s, ^{i}Pr-CH_3), 25.6 (s, ^{i}Pr-CH_3), 29.0 (s, $CH(CH_3)_2$), 124.1 (s, *Ar*), 125.0 (s, *Ar*), 126.7 (s, *Ar*), 131.2 (s, NCH), 145.8 (s, *Ar*). The NMR data is in good agreement with literature values. [18]

4.5.2.2 Synthesis of IDipp·$Ga(PH_2)_3$ (1a)

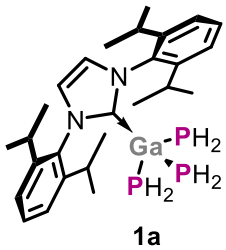

1a

$LiPH_2$·DME (357 mg, 3.08 mmol) was suspended in THF and cooled to -80 °C. Then, IDipp·$GaCl_3$ (497 mg, 0.88 mmol) was dissolved in THF and slowly added to the $LiPH_2$·DME suspension. After stirring for 20 min, the mixture was allowed to warm up to room temperature over the course of two hours, yielding a slightly cloudy yellowish solution. All volatiles were removed *in vacuo*, the product extracted with toluene and filtered through a P4 glass frit. The frit was washed once with additional toluene and the filtrate collected. After removal of solvent *in vacuo*, the product was washed twice with cold *n*-hexane (-50 °C) and dried *in vacuo*, yielding **1a** as a microcrystalline white powder (342 mg, 70 %). Crystals suitable for X-ray single crystal diffraction experiments were obtained by storing a saturated solution of **1a** in *n*-hexane at -28 °C overnight. **1a** decomposes slowly at room temperature and needs to be stored at low temperatures under inert conditions.

^{1}H NMR (400.30 MHz, C_6D_6, 298 K): 0.97 (d, 12 H, 4 × ^{i}Pr-CH_3, $^3J_{HH}$ = 6.87 Hz), 0.99 (dm, 6 H, $^1J_{PH}$ =173.1 Hz, $^4J_{HH}$ = 2.55 Hz, 3 × PH_2) 1.50 (d, 12 H, 4 × ^{i}Pr-CH_3, $^3J_{HH}$ = 6.87 Hz), 2.79 (sep, 4 H, 4 × ^{i}Pr-CH, $^3J_{HH}$ = 6.87 Hz), 6.47 (s, 2 H, NCHCHN), 7.14 (d, 4 H, 4 × aryl-C$_{meta}H$, $^3J_{HH}$ = 7.65 Hz), 7.26 (t, 2 H, 2 × aryl-C$_{para}$H, $^3J_{HH}$ = 7.65 Hz).

^{13}C{^{1}H} NMR (100.61 MHz, C_6D_6, 298 K): 22.8 (s, ^{i}Pr-CH_3), 25.7 (s, ^{i}Pr-CH_3), 28.8 (s, $CH(CH_3)_2$), 124.5 (s, *Ar*), 124.9 (s, *Ar*), 131.1 (s, NCH), 134.2 (s, *Ar*), 145.5 (s, *Ar*).

^{31}P{^{1}H} NMR (161.98 MHz, C_6D_6, 298 K): -231.74 (s).

^{31}P NMR (161.98 MHz, C_6D_6, 298 K): -231.74 (t, $^1J_{HP}$ = 173.1 Hz).

IR (ATR) ν (cm^{-1}): 2961, 2925, 2866, 2288 (PH), 1592, 1559, 1463, 1402, 1387, 1364, 1326, 1256, 1206, 1108, 1061, 946, 936, 902, 765, 757, 638, 435.

LIFDI-MS (*m/z*): 389.2877 $[IDipp\text{-}H]^+$ (100 %). Does not show a molecular ion peak due to decomposition during the ionization process.

Elemental Analysis ($C_{27}H_{42}GaN_2P_3$) **[%]:** calcd. C 58.19, H 7.60, N 5.03; found C 58.60, H 7.50, N 5.05.

4.5.2.3 Synthesis of IDipp·Ga(AsH$_2$)$_3$ (1b)

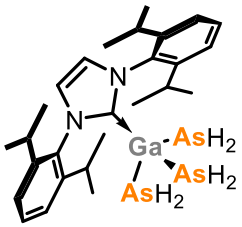

1b

$KAsH_2$ (292 mg, 2.52 mmol) was suspended in THF and cooled to -80 °C. Then, IDipp·$GaCl_3$ (395 mg, 0.70 mmol) was dissolved in THF and slowly added to the $KAsH_2$ suspension. After stirring for 20 min, the mixture was allowed to warm up to room temperature over the course of four hours, yielding a yellowish suspension. The solvent was removed *in vacuo*, the product was extracted with toluene and filtered through a P4 glass frit. After *in vacuo* removal of solvent, the product was washed twice with cold *n*-hexane (-50 °C) and dried *in vacuo*, yielding **1b** as a white powder (227 mg, 47 %). Crystals suitable for X-ray single crystal diffraction experiments were obtained by storing a saturated solution of **1b** in *n*-hexane at -28 °C overnight.

^{1}H NMR (400.30 MHz, C_6D_6, 298 K): 0.75 (s, 6 H, 3 × AsH_2), 0.93 (d, 12 H, 4 × ^{i}Pr-CH_3, $^3J_{HH}$ = 6.88 Hz), 1.46 (d, 12 H, 4 × ^{i}Pr-CH_3, $^3J_{HH}$ = 6.88 Hz), 2.73 (sep, 4 H, 4 × ^{i}Pr-CH, $^3J_{HH}$ = 6.88 Hz), 6.43 (s, 2 H, NCHCHN), 7.11 (d, 4 H, 4 × aryl-C$_{meta}H$, $^3J_{HH}$ = 7.79 Hz), 7.23 (t, 2 H, 2 × aryl-C$_{para}$H, $^3J_{HH}$ = 7.79 Hz).

^{13}C{^{1}H} NMR (100.61 MHz, C_6D_6, 298 K): 22.9 (s, ^{i}Pr-CH_3), 25.7 (s, ^{i}Pr-CH_3), 28.8 (s, $CH(CH_3)_2$), 124.6 (s, *Ar*), 125.0 (s, *Ar*), 131.2 (s, NCH), 134.3 (s, *Ar*), 145.5 (s, *Ar*).

IR ν (ATR, cm^{-1}): 2962, 2922, 2867, 2070 (AsH), 1587, 1554, 1528, 1452, 1383, 1362, 1324, 1230, 1205, 1105, 1059, 945, 801, 754.

LIFDI-MS (*m/z*): 389.2952 $[IDipp\text{-}H]^+$ (100 %), 611.0851 $[IDipp{\cdot}Ga(AsH_2)_2]^+$ (56 %). Does not show a molecular ion peak due to decomposition during the ionization process.

Elemental Analysis ($C_{27}H_{42}As_3GaN_2$) **[%]:** calcd. C 47.06, H 6.14, N 4.07; found C 46.72, H 6.14, N 3.85.

4.5.2.4 Synthesis of IDipp·Al(PH$_2$)$_3$ (2a)

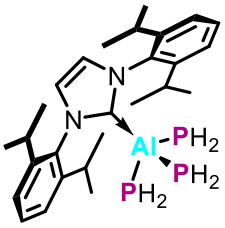

2a

$LiPH_2$·DME (84 mg, 0.72 mmol) was suspended in THF and cooled to -80 °C. Then, IDipp·$AlCl_3$ (104 mg, 0.2 mmol) was dissolved in THF and slowly added to the $LiPH_2$·DME suspension. After stirring for 20 min, the mixture was allowed to warm up to room temperature over the course of two hours, yielding a yellowish suspension. All volatiles were removed *in vacuo*, the product extracted with toluene and filtered through a P4 glass frit. After removal of solvent *in vacuo*, the product was washed once with cold *n*-hexane (-50 °C) and dried *in vacuo*, yielding **2a** as a microcrystalline white powder (40 mg, 39 %). Crystals suitable for X-ray single crystal diffraction experiments were obtained by storing a saturated solution of **2a** in *n*-hexane at -28 °C overnight. **2a** is

an extremely air sensitive compound that needs to be stored under an inert atmosphere at low temperatures.

^{1}H NMR (400.30 MHz, C_6D_6, 298 K): 0.66 (d, broad, 6 H, 4 × PH_2, $^{1}J_{HP}$ = 174.5 Hz), 0.93 (d, 12 H, 4 × ^{i}Pr-CH_3, $^{3}J_{HH}$ = 6.76 Hz), 1.47 (d, 12 H, 4 × ^{i}Pr-CH_3, $^{3}J_{HH}$ = 6.76 Hz), 2.73 (sep, 4 H, 4 × ^{i}Pr-CH, $^{3}J_{HH}$ = 6.76 Hz), 6.44 (s, 2 H, NCHCHN), 7.10 (d, 4 H, 4 × aryl-C$_{meta}H$, $^{3}J_{HH}$ = 7.71 Hz), 7.23 (t, 2 H, 2 × aryl-C$_{para}$H, $^{3}J_{HH}$ = 7.71 Hz).

^{31}P{^{1}H} NMR (161.98 MHz, C_6D_6, 298 K): -251.95 (s).

^{31}P NMR (161.98 MHz, C_6D_6, 298 K): -251.95 (t, $^{1}J_{HP}$ = 174.5 Hz).

^{13}C{^{1}H} NMR (100.61 MHz, C_6D_6, 298 K): 22.7 (q, ^{i}Pr-CH_3), 25.8 (^{i}Pr-CH_3), 28.8 ($CH(CH_3)_2$), 124.5 (*Ar*), 125.0 (*Ar*), 131.2 (NCH), 134.1 (*Ar*), 145.5 (*Ar*).

IR *ν* (ATR, cm^{-1}): 2960, 2920, 2865, 2067 (PH), 1459, 1387, 1364, 1325, 1206, 1111, 1061, 936, 801, 767, 757, 635, 524, 440.

LIFDI-MS (*m*/*z*): 389.2797 [IDipp-H]$^{+}$ (100 %). Does not show a molecular ion peak due to decomposition during the ionization process.

Elemental Analysis ($C_{27}H_{42}AlN_2P_3$) **[%]:** calcd. C 63.03, H 8.23, N 5.44; found C 64.18, H 8.24, N 5.30.

4.5.2.5 Synthesis of IDipp·Al(AsH$_2$)$_3$ (2b)

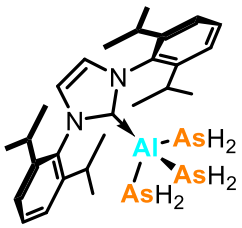

2b

IDipp·$AlCl_3$ (156 mg, 0.3 mmol) was dissolved in THF and cooled to -80 °C. Then, solid $KAsH_2$ (125 mg, 1.08 mmol) was added to the solution. After stirring for 20 min, the mixture was allowed to warm up to room temperature over the course of one hour, yielding a yellowish suspension. The solvent was removed *in vacuo*, the product extracted with toluene and filtered through a P4 glass frit. After removal of solvent *in vacuo*, the product was washed once with cold *n*-hexane (-40 °C) and dried *in vacuo*, yielding a microcrystalline white powder, that contains **2b** alongside unidentified impurities (104 mg). Crystals of **2b** suitable for X-ray single crystal diffraction experiments were obtained by storing a saturated solution of this mixture in *n*-hexane at -28 °C overnight. **2b** is extremely sensitive towards air and decomposes quickly at ambient temperatures under deposition of gray solids and needs to be stored at low temperatures.

^{1}H NMR (400.30 MHz, C_6D_6, 298 K): despite numerous attempts, impurities as a result from side reactions and thermal decomposition could neither be prevented nor separated from **2b**. The NMR data shows several overlayed signals, which cannot be interpreted clearly (cf. Figure S 4.19).

LIFDI-MS (*m*/*z*): 389.2774 [IDipp-H]$^{+}$ (100 %). Does not show a molecular ion peak due to decomposition during the ionization process.

Elemental Analysis ($C_{27}H_{42}As_3AlN_2$) **[%]:** Elemental analysis could not be carried out as it was not possible to isolate pure **2b**.

4.5.2.6 Synthesis of IDipp·In(PH$_2$)$_3$ (3)

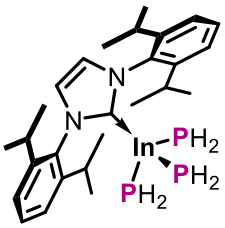

3

This experiment was performed under exclusion of light and careful monitoring of the reaction temperature at all times.

IDipp·InCl$_3$ (183 mg, 0.3 mmol) was dissolved in THF and cooled to about -80 °C. Then, solid LiPH$_2$·DME (122 mg, 1.05 mmol) was added to the solution. The reaction mixture was slowly warmed to 0 °C, yielding a cloudy yellowish solution (all following working steps were carried out at temperatures between -30 °C and -20 °C). All volatiles were then removed *in vacuo*, the product extracted with toluene and filtered through a P4 glass frit. After removal of solvent *in vacuo*, the product was washed twice with cold *n*-hexane (*T* = -60 °C) and dried *in vacuo*, yielding **3** as microcrystalline white crumbs (2 mg, 1 %). **3** is an extremely sensitive compound that is best stored under exclusion of light at maximum -30 °C. **3** decomposes rapidly under release of IDipp and PH$_3$ (cf. NMR data).

^{1}H NMR (400.30 MHz, C$_6$D$_6$, 298 K): 0.65 (d, 6 H, 3 × PH$_2$, $^1J_{PH}$ = 166.9 Hz), 0.90 (d, 12 H, 4 × ^{i}Pr-C*H*$_3$, $^3J_{HH}$ = 6.80Hz), 1.38 (d, 12 H, 4 × ^{i}Pr-C*H*$_3$, $^3J_{HH}$ = 6.80 Hz), 2.66 (sep, 4 H, 4 × ^{i}Pr-C*H*, $^3J_{HH}$ = 6.80 Hz), 6.42 (s, 2 H, NC*HCH*N), 7.11 (d, 4 H, 4 × aryl-C$_{meta}$*H*, $^3J_{HH}$ = 7.71 Hz), 7.23 (t, 2 H, 2 × aryl-C$_{para}$H, $^3J_{HH}$ = 7.71 Hz).

^{31}P{^{1}H} NMR (161.98 MHz, C$_6$D$_6$, 298 K): -264.70 (s).

^{31}P NMR (161.98 MHz, C$_6$D$_6$, 298 K): -264.70 (t, $^1J_{HP}$ = 166.9 Hz).

Elemental Analysis (C$_{27}$H$_{42}$InN$_2$P$_3$) **[%]:** Elemental analysis was not carried out as it was not possible to completely separate IDipp resulting from rapid thermal decomposition from the product.

4.5.2.7 Synthesis of [IDipp·Ga(PH$_2$)$_2$(μ_3-PH$_2${HgC$_6$F$_4$}$_3$)] (4)

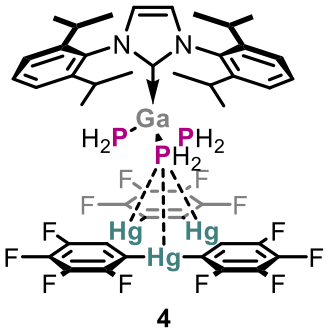

4

$Hg_3C_{18}F_{12}$ (105 mg, 0.1 mmol) was suspended in 1,2-difluorobenzene. A solution of IDipp·Ga(PH$_2$)$_3$ (56 mg, 0.1 mmol) in 1,2-difluorobenzene was added to the suspension at room temperature. A reaction was immediately observed as the suspension clarified and the solution took on an orange-red colour. Subsequently, the reaction mixture was stirred at room temperature of one hour. Crystals suitable for X-ray single crystal diffraction experiments were obtained by layering the solution of **4** in with *n*-hexane (-30 °C) (96 mg, contaminated with inseparable orange-brown amorphous solids). **4** is highly sensitive towards air and decomposes at room temperature under release of PH$_3$.

^{1}H NMR (400.30 MHz, C$_6$D$_6$-capillary/1,2-difluorobenzene, 298 K): 0.88 (dm, 6 H, 3 × PH$_2$), 1.18 (d, 12 H, 4 × ^{i}Pr-C*H*$_3$, $^3J_{HH}$ = 7.07 Hz), 1.39 (d, 12 H, 4 × ^{i}Pr-CH$_3$, $^3J_{HH}$ = 7.07 Hz), 2.78 (sep, 4 H, 4 × ^{i}Pr-C*H*, $^3J_{HH}$ = 7.07 Hz), 6.8-7.2 (solvent signals).

$^{31}P\{^{1}H\}$ NMR (161.98 MHz, C_6D_6-capillary/1,2-difluorobenzene, 298 K): -220.74 (s, broad, $w_{1/2}$ = 27 Hz)

^{31}P NMR (161.98 MHz, C_6D_6-capillary/1,2-difluorobenzene, 298 K): -220.74 (t, $^{1}J_{HP}$ = 186.5 Hz, broad, $w_{1/2}$ = 30 Hz)

$^{19}F\{^{1}H\}$ NMR (376.50 MHz, C_6D_6-capillary/1,2-difluorobenzene, 298 K): -114.01 (s, *o*-F), -157.82 (m, *m*-F)

Elemental Analysis ($C_{45}H_{41}P_3GaN_2F_{12}Hg_3$) **[%]:** Elemental analysis could not be carried out as it was not possible to isolate pure **4**.

4.5.3 NMR Data

4.5.3.1 IDipp·$InCl_3$ (A)

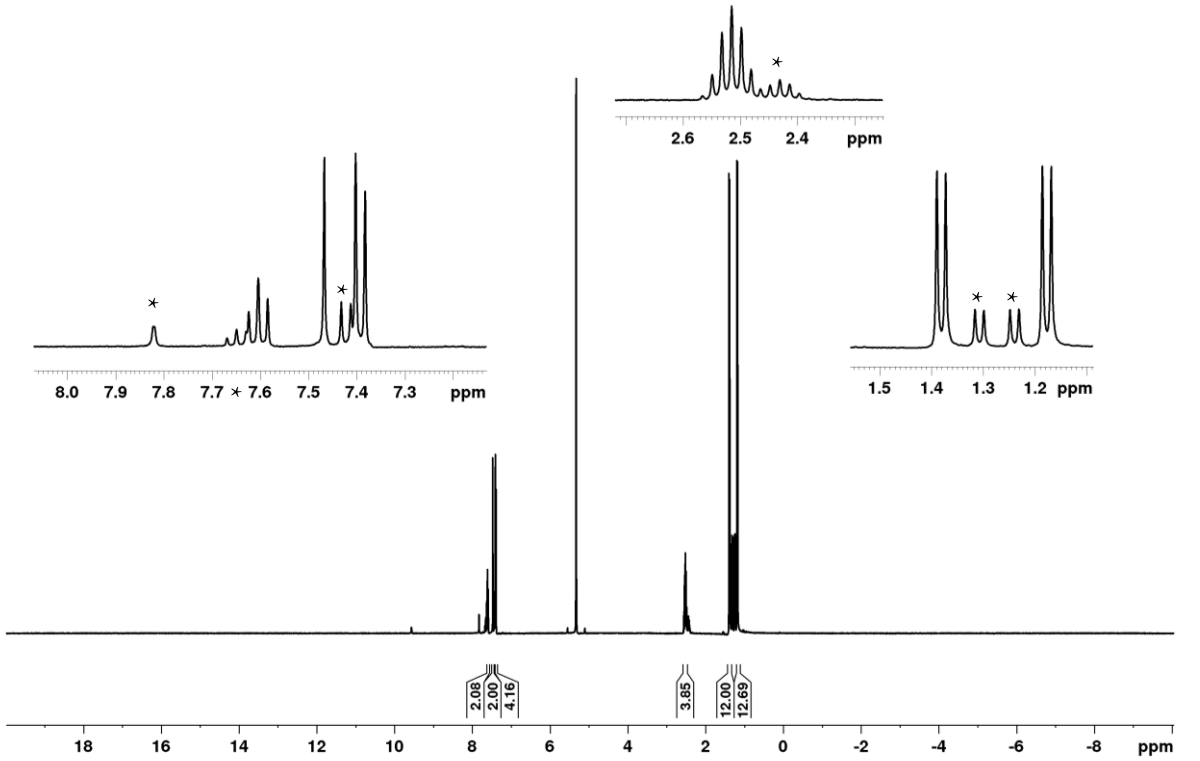

Figure S 4.1: ^{1}H NMR spectrum of IDipp·$InCl_3$ in CD_2Cl_2 at 298 K (* = $[IDipp\text{-}H]^+$).

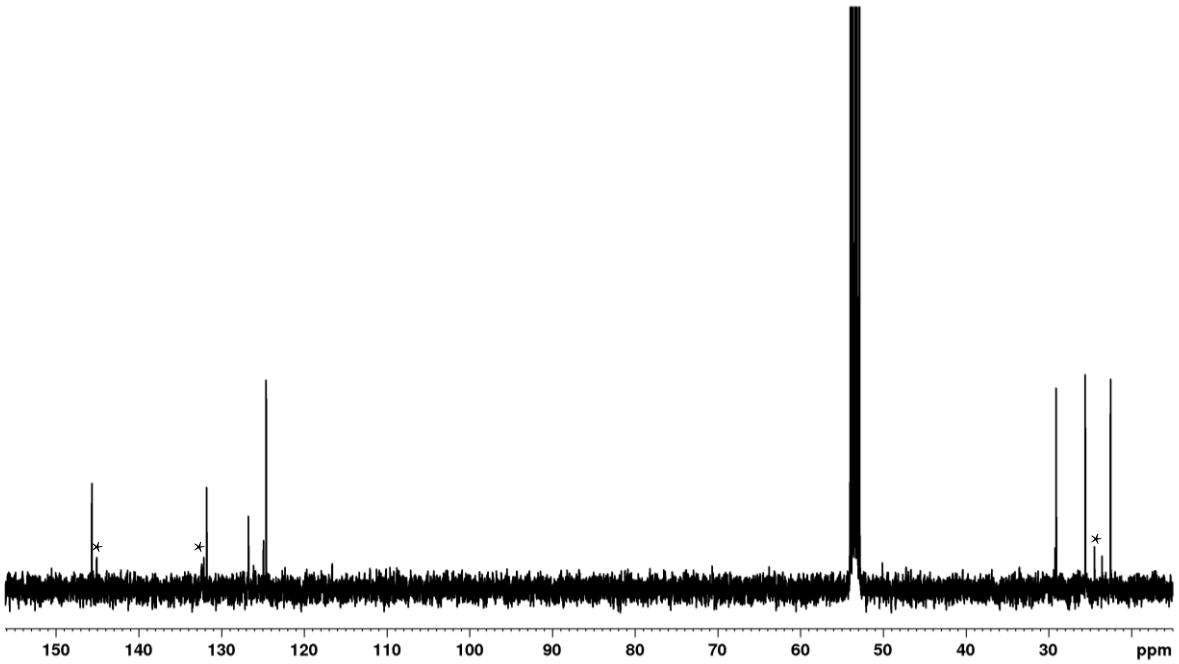

Figure S 4.2: $^{13}C\{^{1}H\}$ NMR spectrum of IDipp·$AlCl_3$ in CD_2Cl_2 at 298 K (* = $[IDipp\text{-}H]^+$).

4.5.3.2 IDipp·$AlCl_3$ (B)

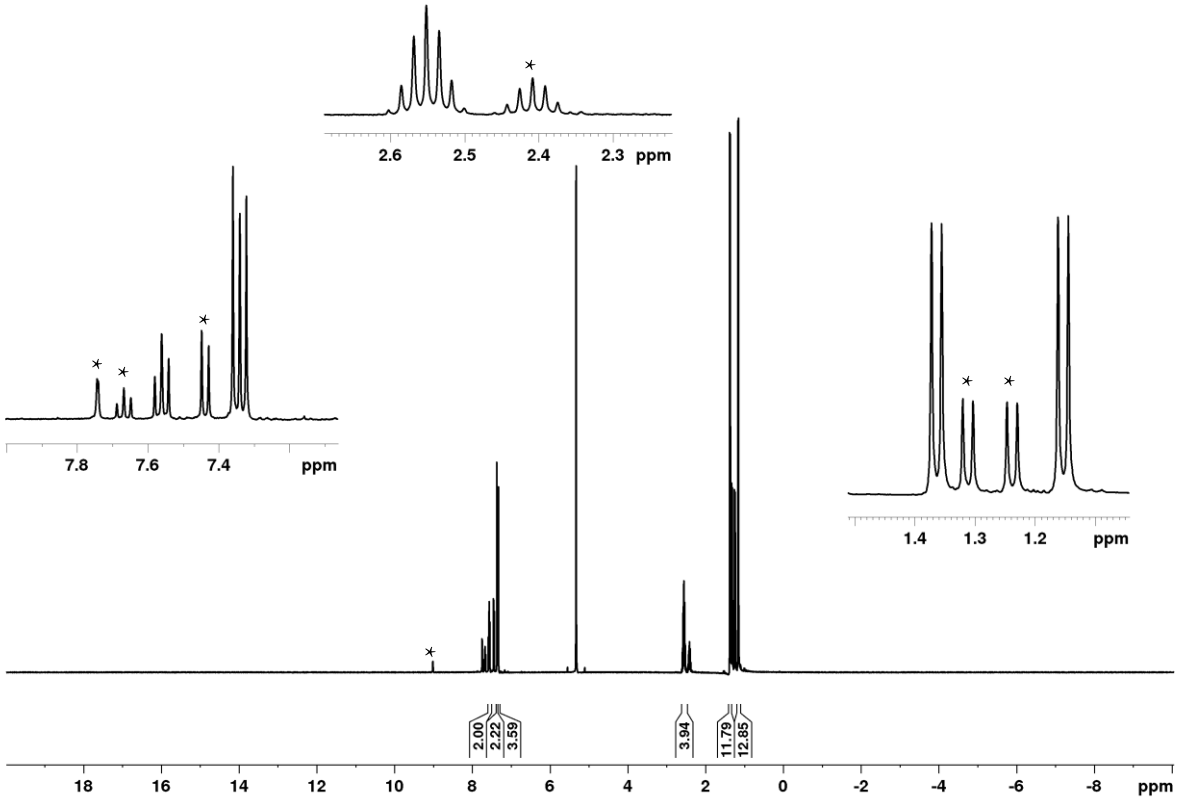

Figure S 4.3: ^{1}H NMR spectrum of IDipp·$AlCl_3$ in CD_2Cl_2 at 298 K (* = $[IDipp\text{-}H]^+$).

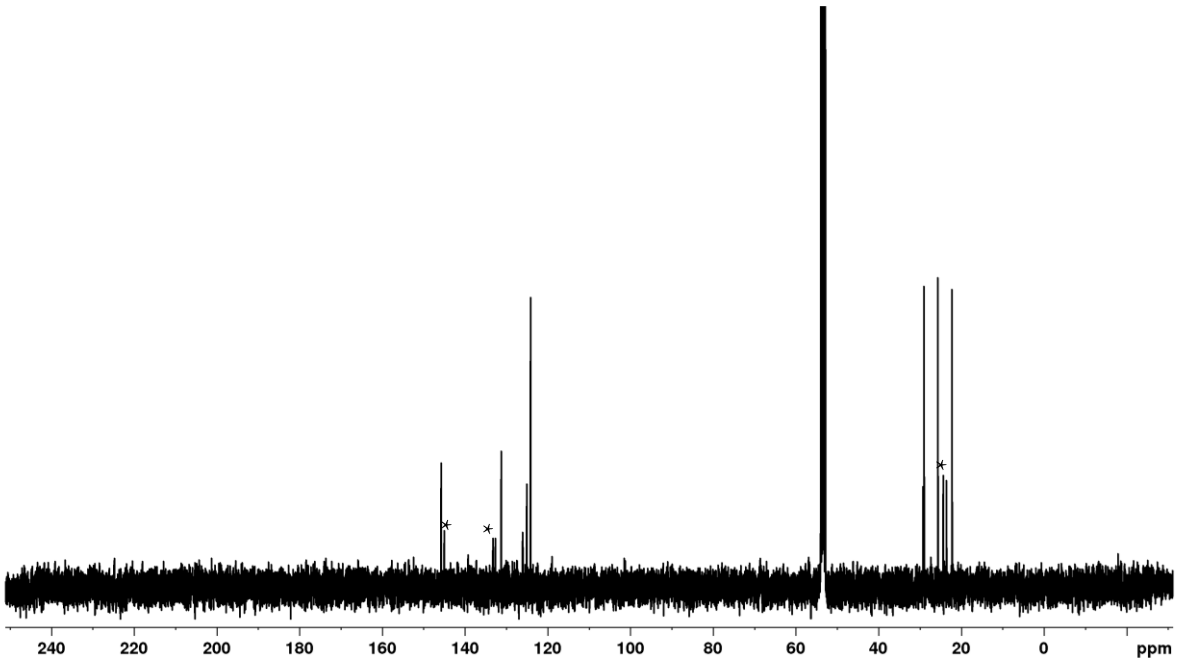

Figure S 4.4: $^{13}C\{^{1}H\}$ NMR spectrum of IDipp·$AlCl_3$ in CD_2Cl_2 at 298 K (* = $[IDipp\text{-}H]^+$).

4.5.3.3 IDipp·Ga(PH$_2$)$_3$ (1a)

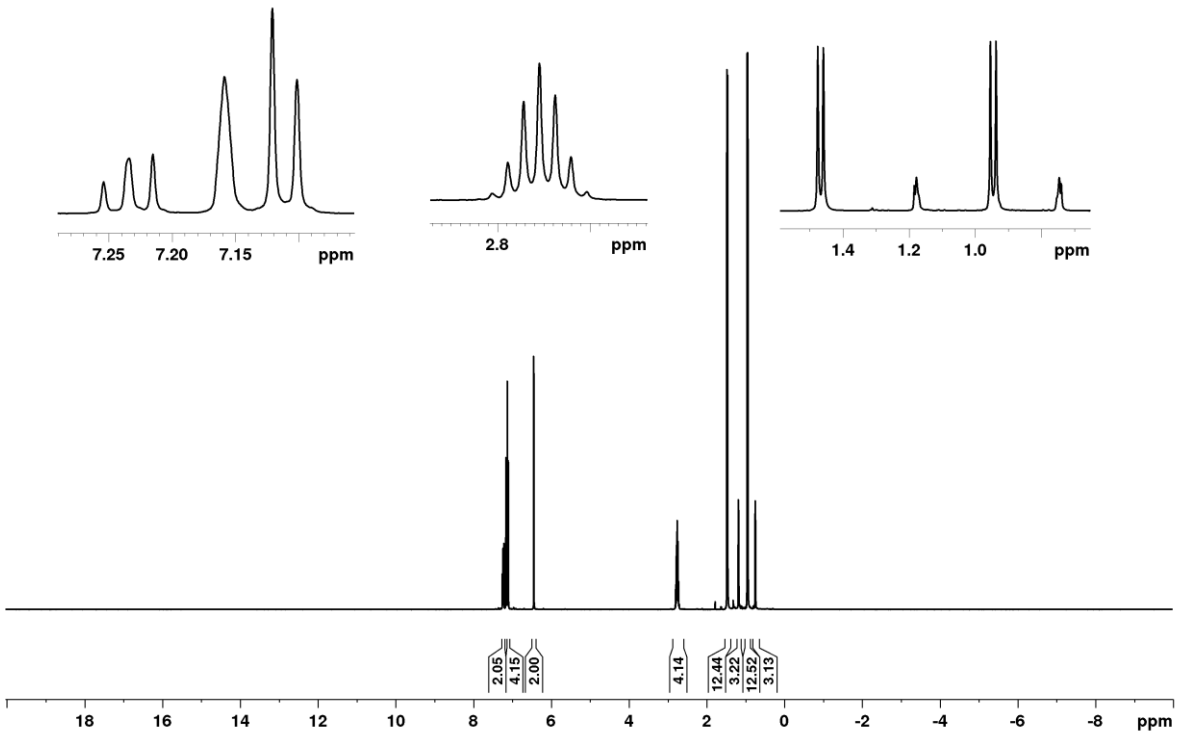

Figure S 4.5: ^{1}H NMR spectrum of IDipp·Ga(PH$_2$)$_3$ in C_6D_6 at 298 K.

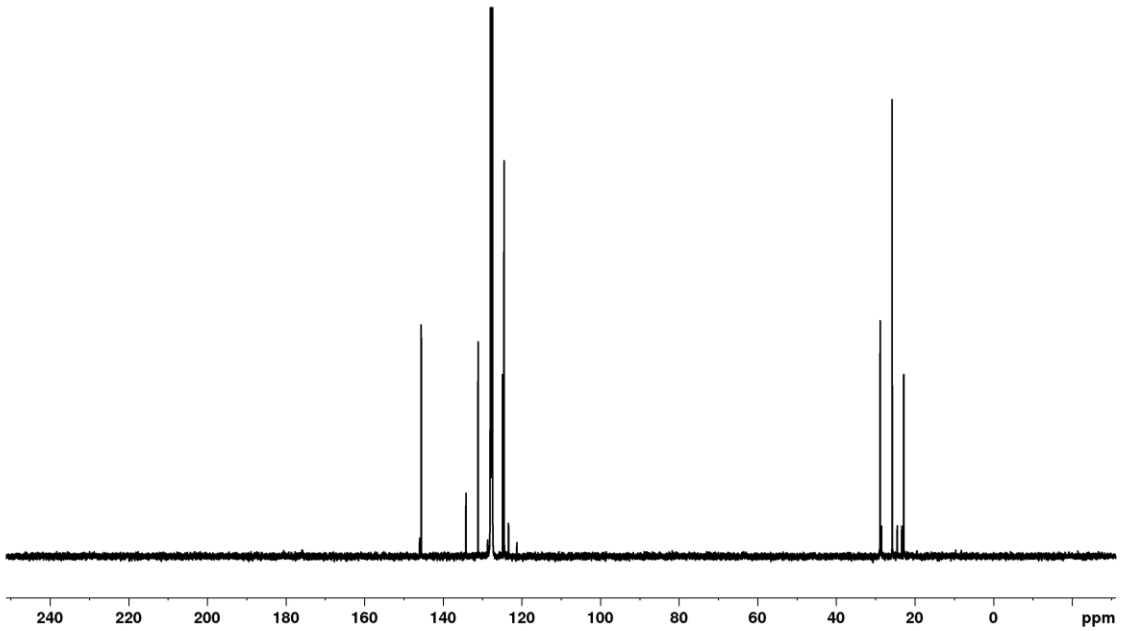

Figure S 4.6: ^{13}C{^{1}H] NMR spectrum of IDipp·Ga(PH$_2$)$_3$ in C_6D_6 at 298 K.

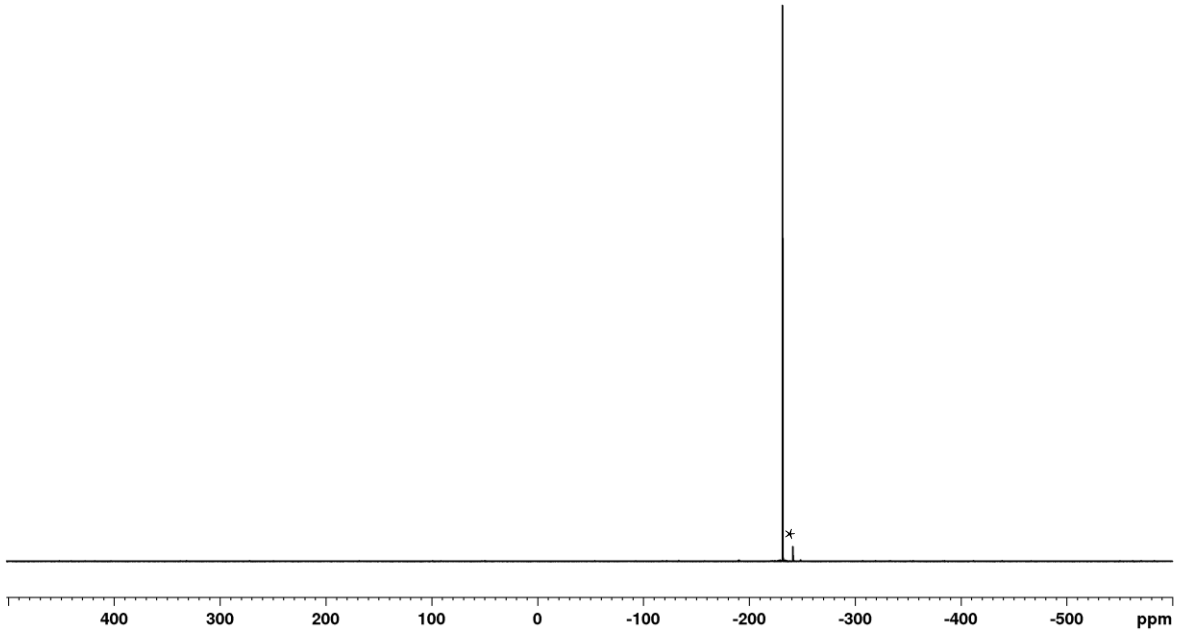

Figure S 4.7: $^{31}P\{^{1}H\}$ NMR spectrum of IDipp·Ga$(PH_2)_3$ in C_6D_6 at 298 K (* = PH_3).

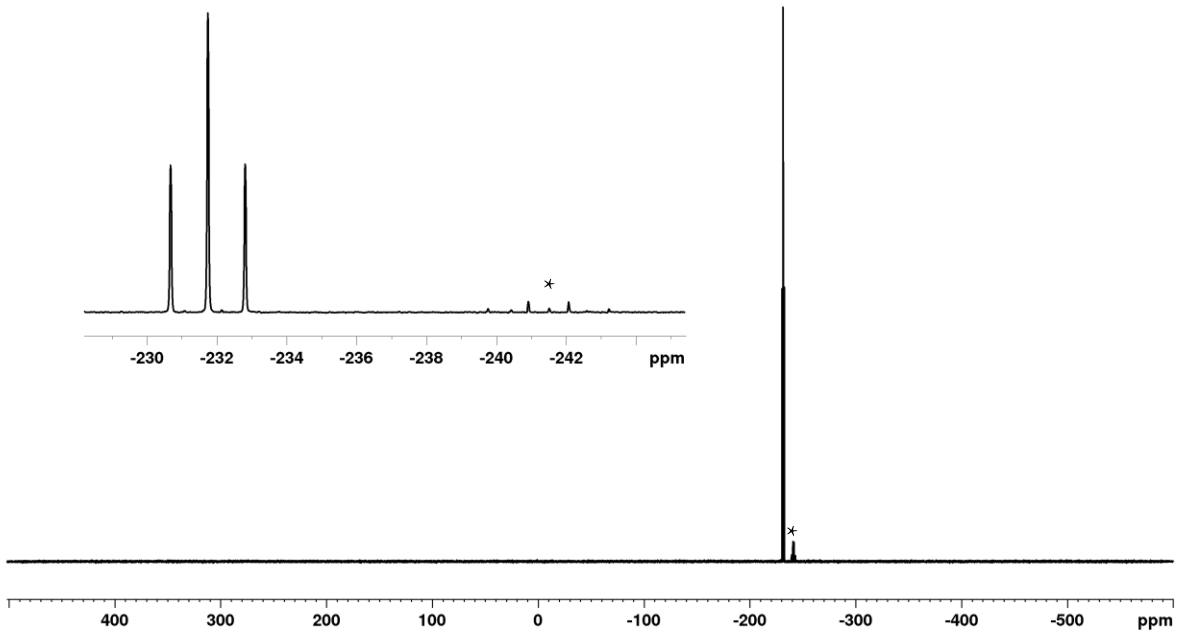

Figure S 4.8: ^{31}P NMR spectrum of IDipp·Ga$(PH_2)_3$ in C_6D_6 at 298 K (* = PH_3).

4.5.3.4 In situ ^{31}P NMR spectra after addition of $NaPH_2$ to $GaCl_3$

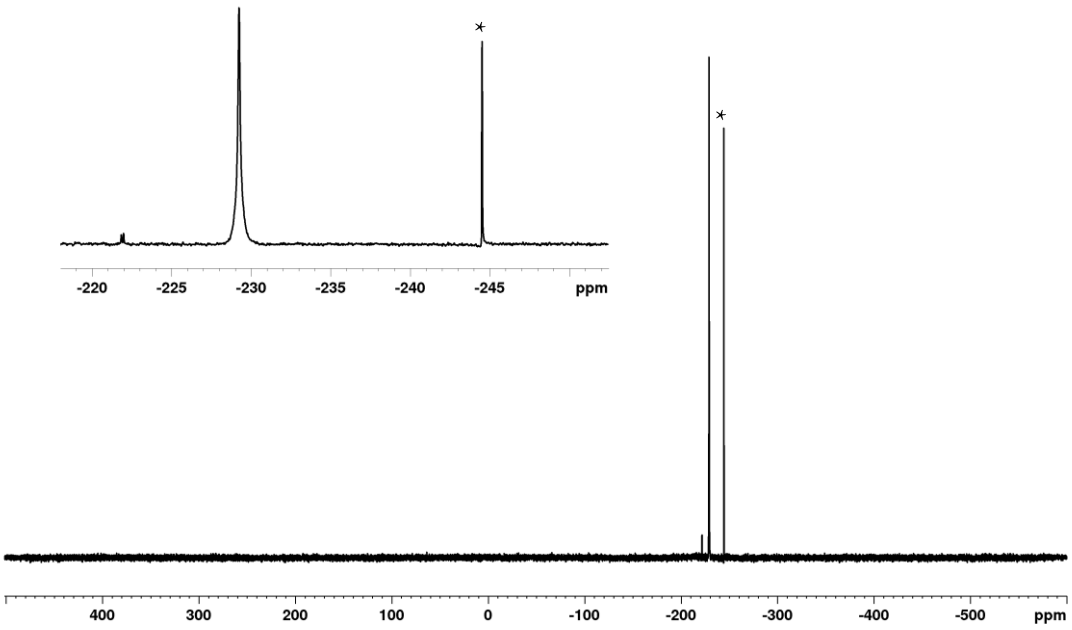

Figure S 4.9: *In situ* $^{31}P\{^1H\}$ NMR spectrum of the reaction between 3 eq. $NaPH_2$ and $GaCl_3$ (THF/-C_6D_6-cap.; * = PH_3).

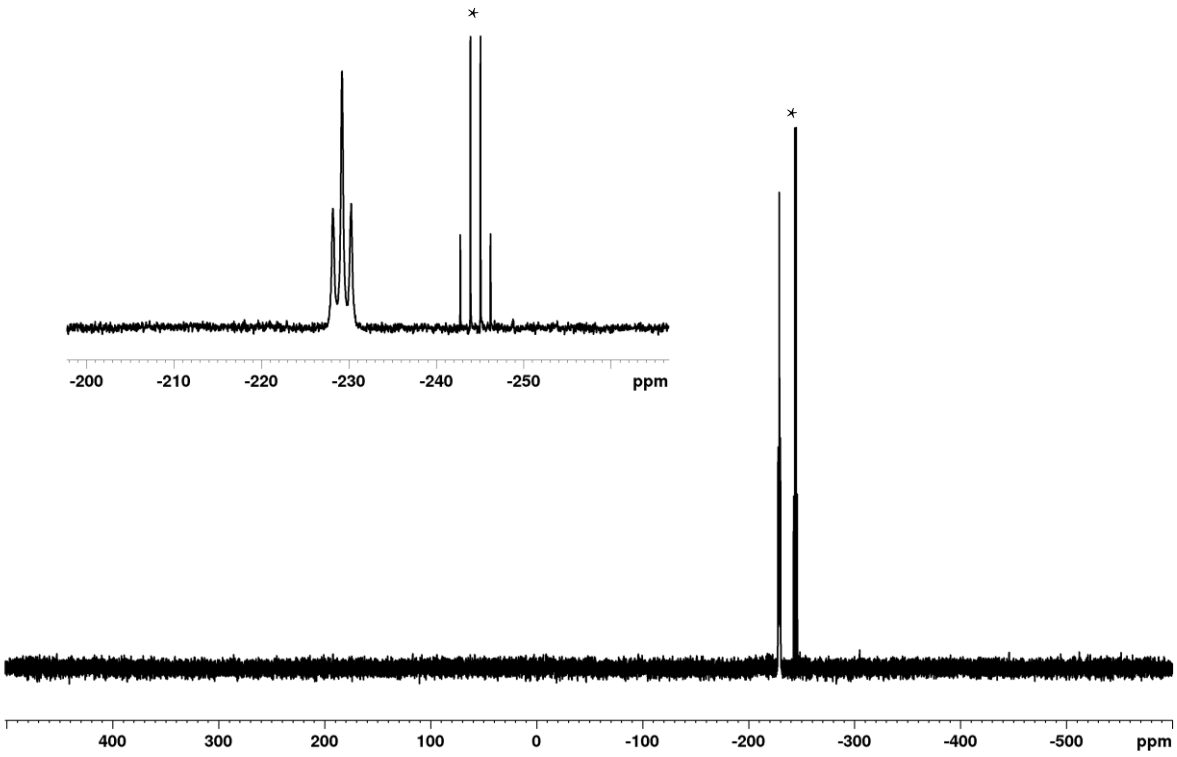

Figure S 4.10: *In situ* $^{31}P\{^1H\}$ NMR spectrum of the reaction between $NaPH_2$ and $GaCl_3$ (THF/C_6D_6-cap.; * = PH_3).

4.5.3.5 IDipp·Ga(AsH$_2$)$_3$ (1b)

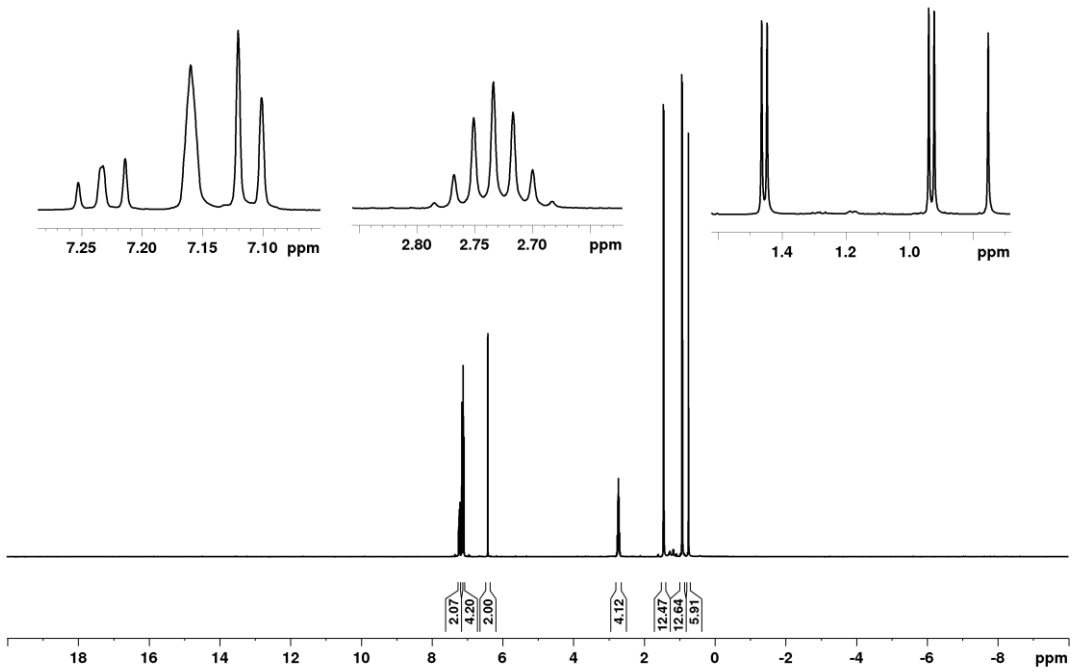

Figure S 4.11: ^{1}H NMR spectrum of IDipp·Ga(AsH$_2$)$_3$ in C_6D_6 at 298 K.

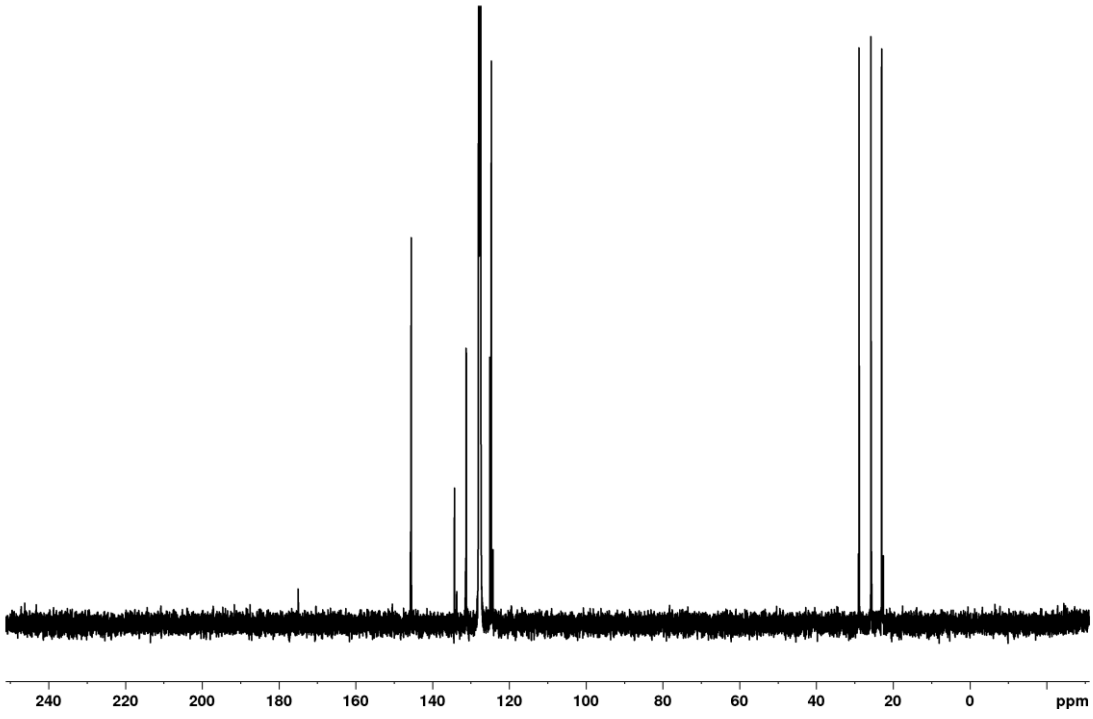

Figure S 4.12: ^{13}C{^{1}H} NMR spectrum of IDipp·Ga(AsH$_2$)$_3$ in C_6D_6 at 298 K.

4.5.3.6 IDipp·Al(PH$_2$)$_3$ (2a)

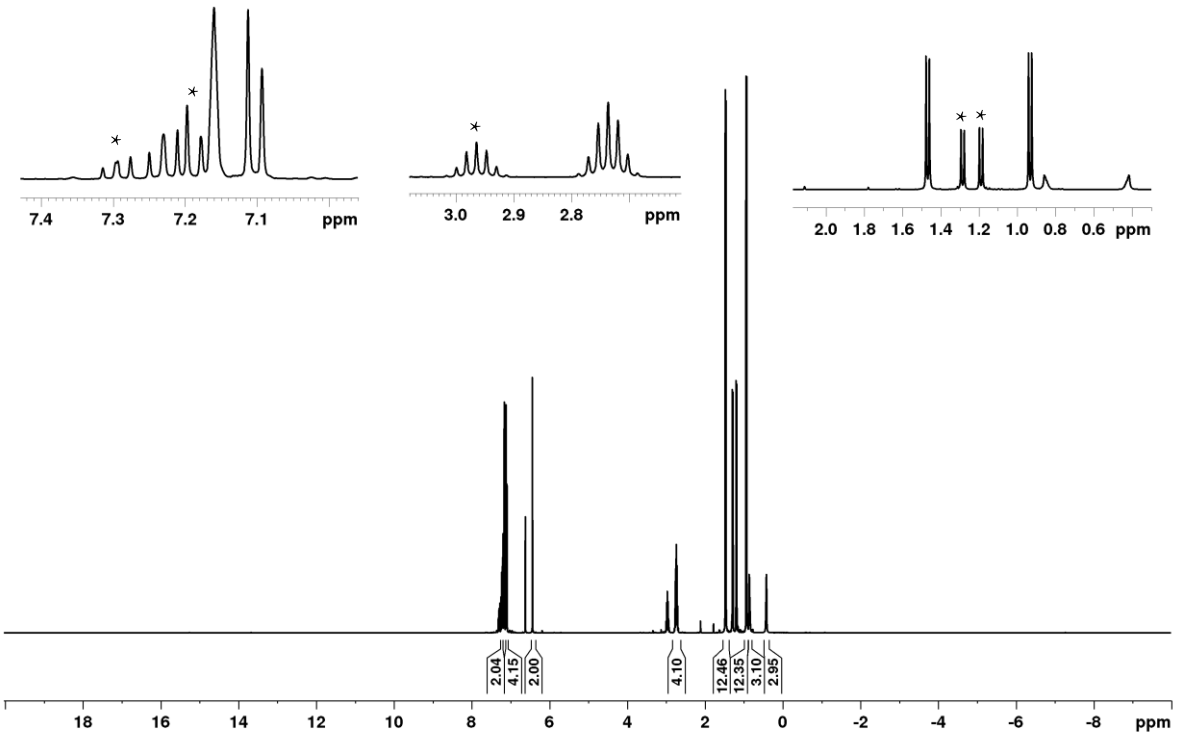

Figure S 4.13: ^{1}H NMR spectrum of IDipp·Al(PH$_2$)$_3$ in C$_6$D$_6$ at 298 K (* = IDipp).

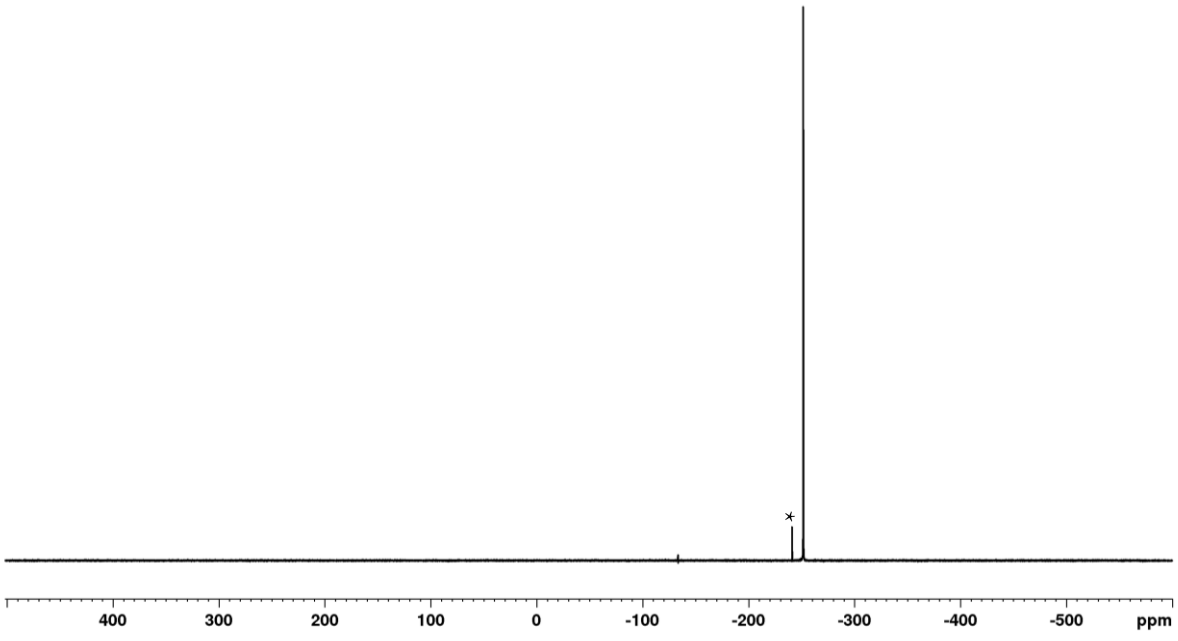

Figure S 4.14: ^{31}P{^{1}H} NMR spectrum of IDipp·Al(PH$_2$)$_3$ in C$_6$D$_6$ at 298 K (* = PH$_3$).

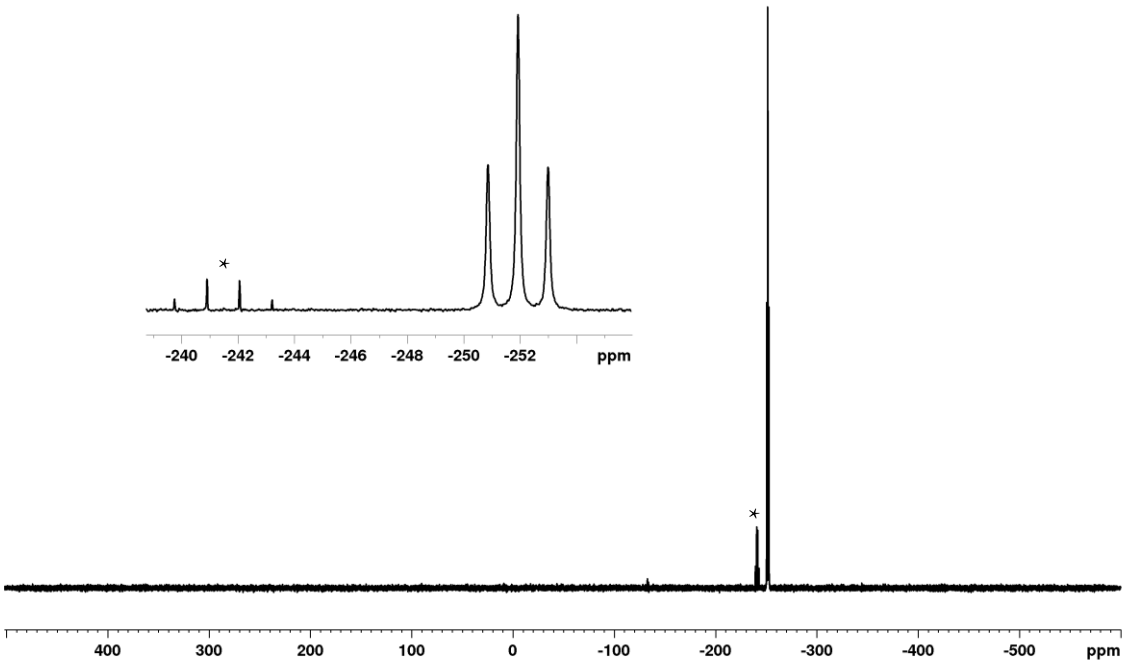

Figure S 4.15: ^{31}P NMR spectrum of IDipp·Al$(PH_2)_3$ in C_6D_6 at 298 K (* = PH_3).

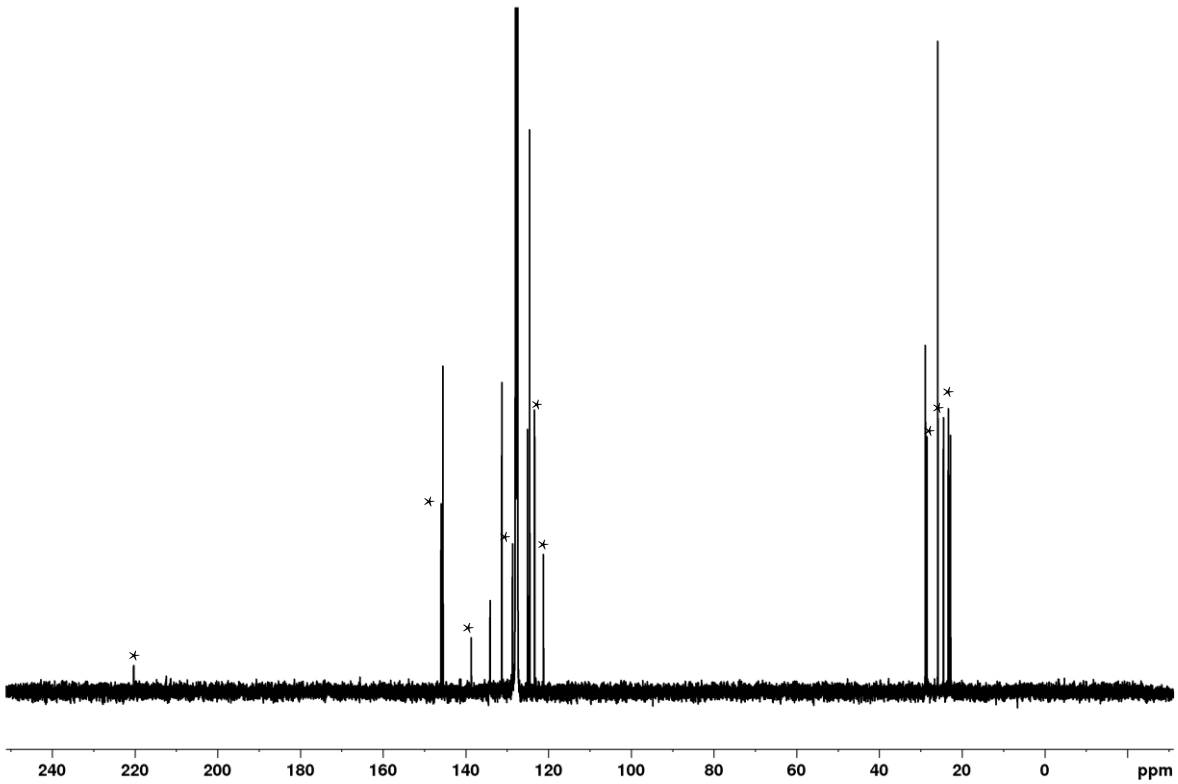

Figure S 4.16: $^{13}C\{^1H\}$ NMR spectrum of IDipp·Al$(PH_2)_3$ in C_6D_6 at 298 K (* = IDipp).

4.5.3.7 *In situ* NMR spectra of formation of 2a

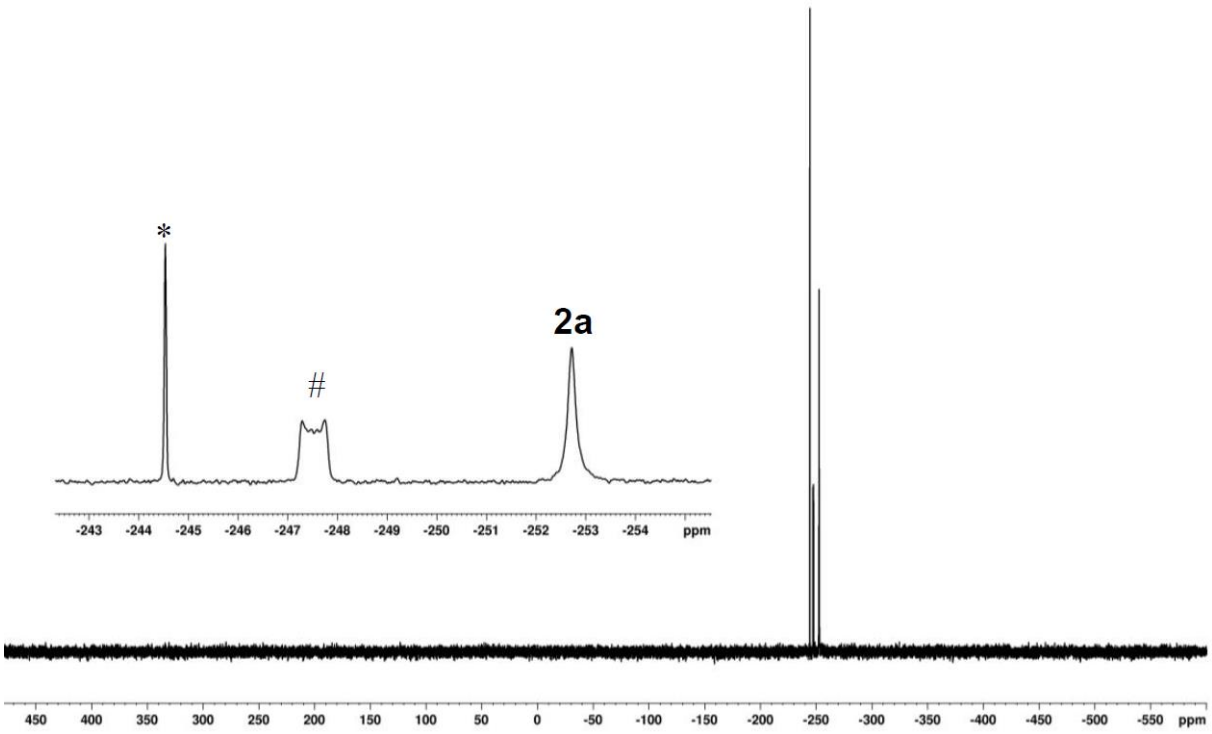

Figure S 4.17: *In situ* $^{31}P\{^{1}H\}$ NMR spectrum taken from the reaction mixture of **2a** in THF (C_6D_6-capillary) at 298 K (* = PH_3, # = $[Al(PH_2)_4]^-$).

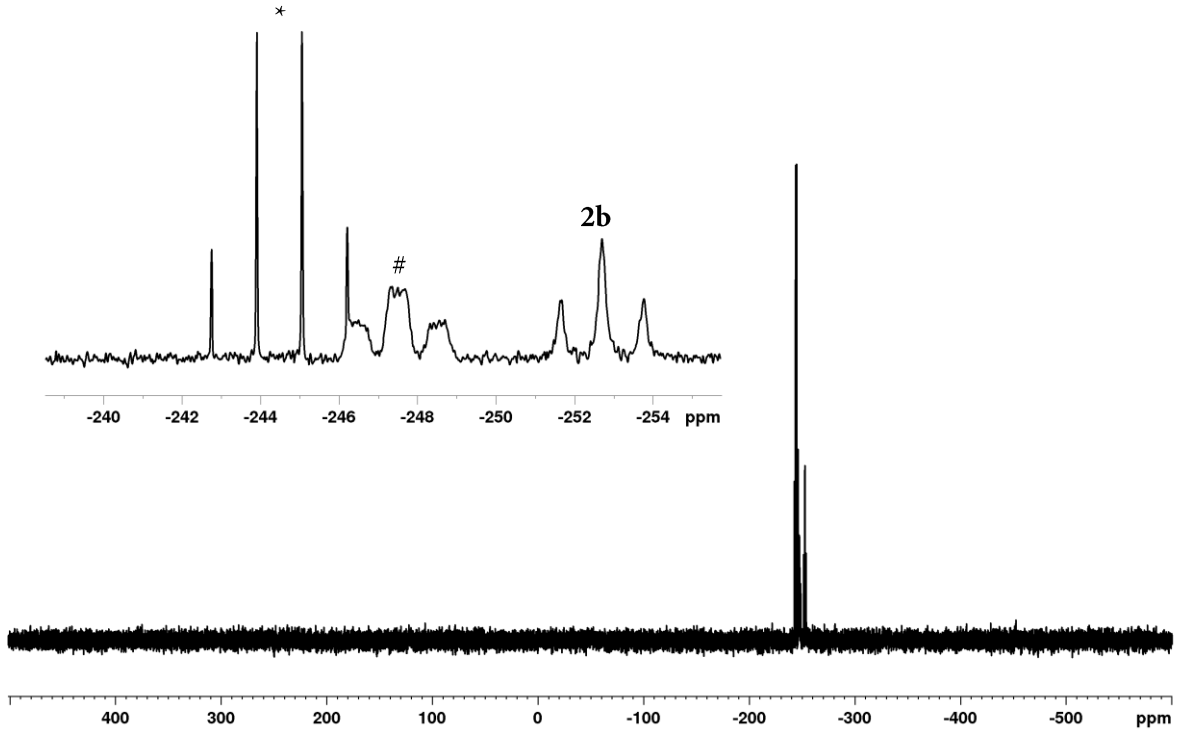

Figure S 4.18: *In situ* ^{31}P NMR spectrum taken from the reaction mixture of **2b** in THF (C_6D_6-capillary) at 298 K (* = PH_3, # = $[Al(PH_2)_4]^-$).

4.5.3.8 Mixture containing IDipp·Al(AsH$_2$)$_3$ (2b)

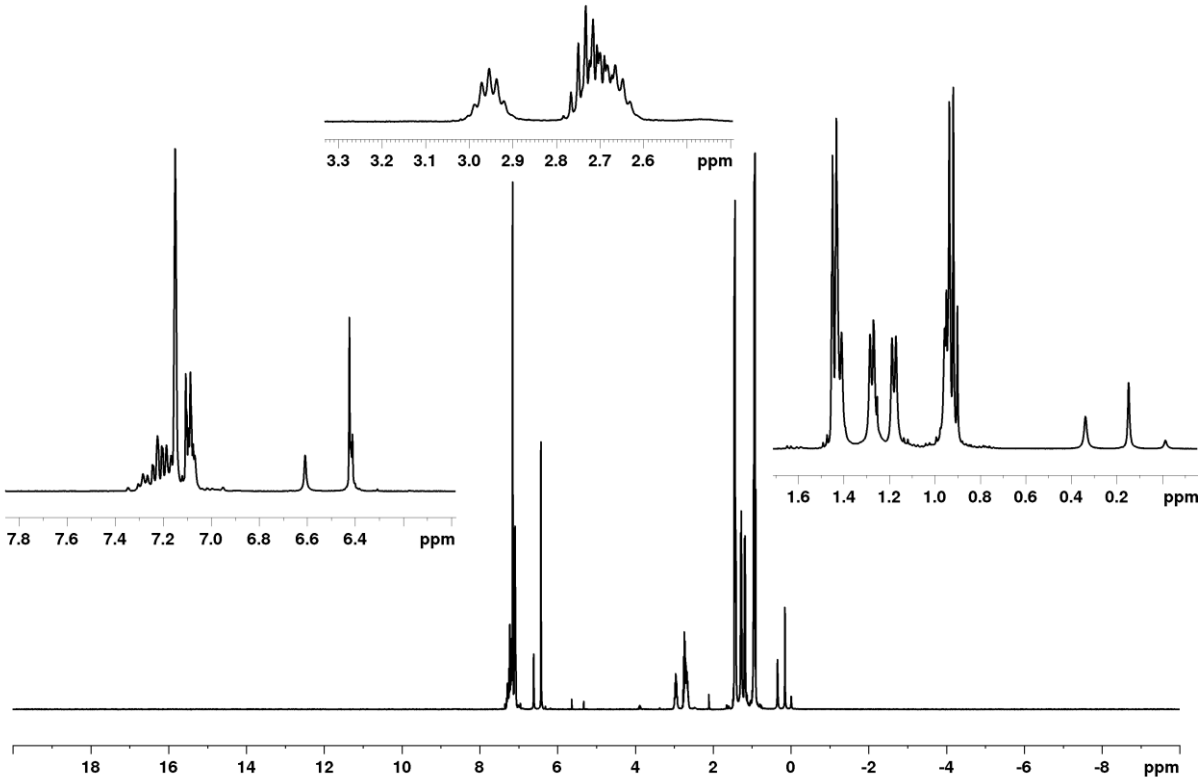

Figure S 4.19: ^{1}H NMR spectrum of the mixture containing IDipp·Al(AsH$_2$)$_3$ in C_6D_6 at 298 K.

4.5.3.9 IDipp·In(PH$_2$)$_3$ (3)

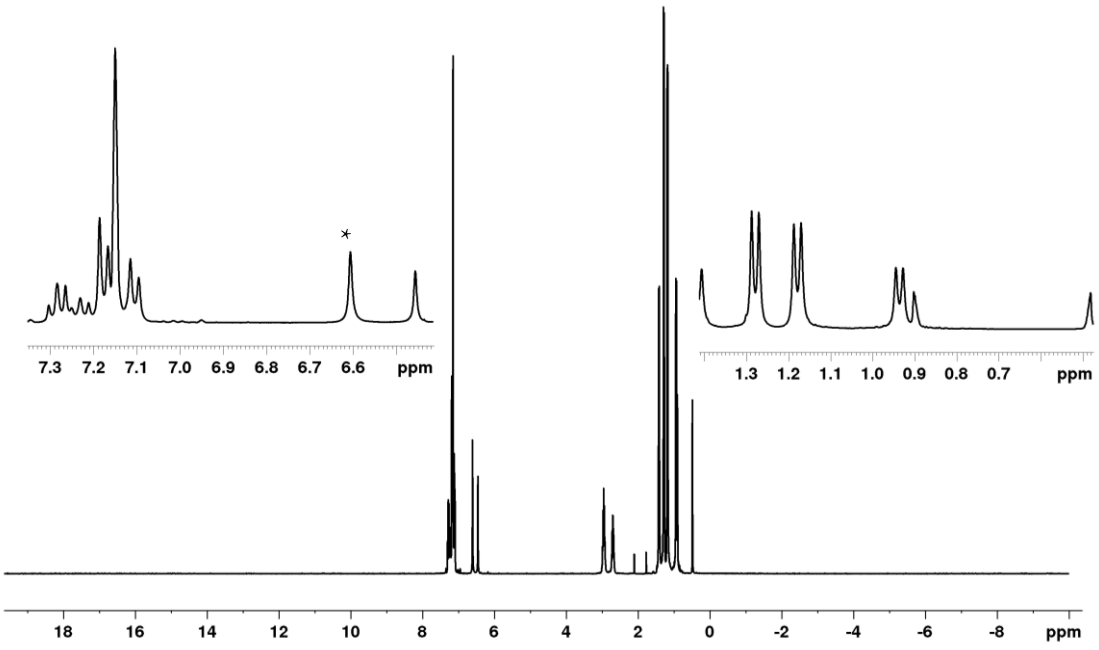

Figure S 4.20: ^{1}H NMR spectrum of IDipp·In(PH$_2$)$_3$ in C_6D_6 at 298 K (* = IDipp).

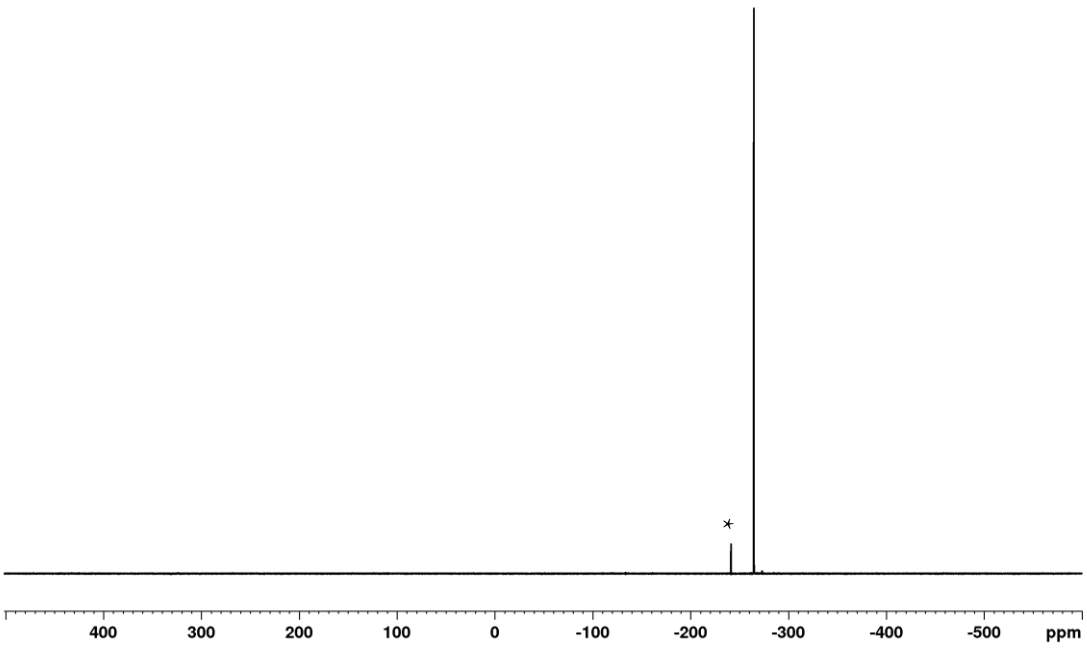

Figure S 4.21: $^{31}P\{^{1}H\}$ NMR spectrum of IDipp·In$(PH_2)_3$ in C_6D_6 at 298 K (* = PH_3).

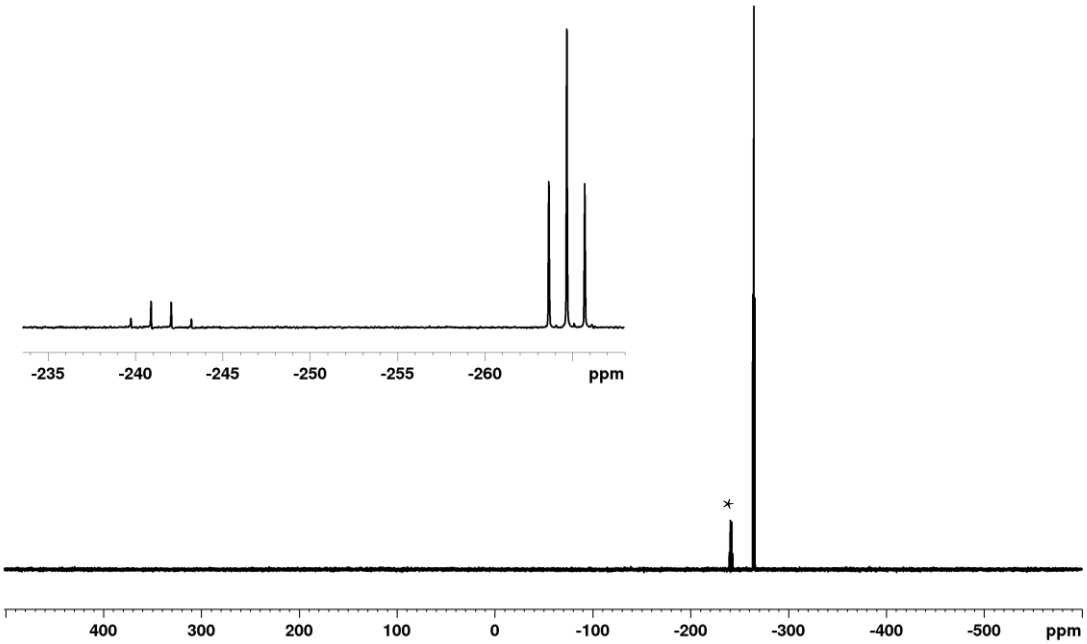

Figure S 4.22: ^{31}P NMR spectrum of IDipp·In$(PH_2)_3$ in C_6D_6 at 298 K (* = PH_3).

4.5.3.10 Mixture containing [IDipp·Ga(PH$_2$)$_2$(μ_3-PH$_2${HgC$_6$F$_4$}$_3$)] (4)

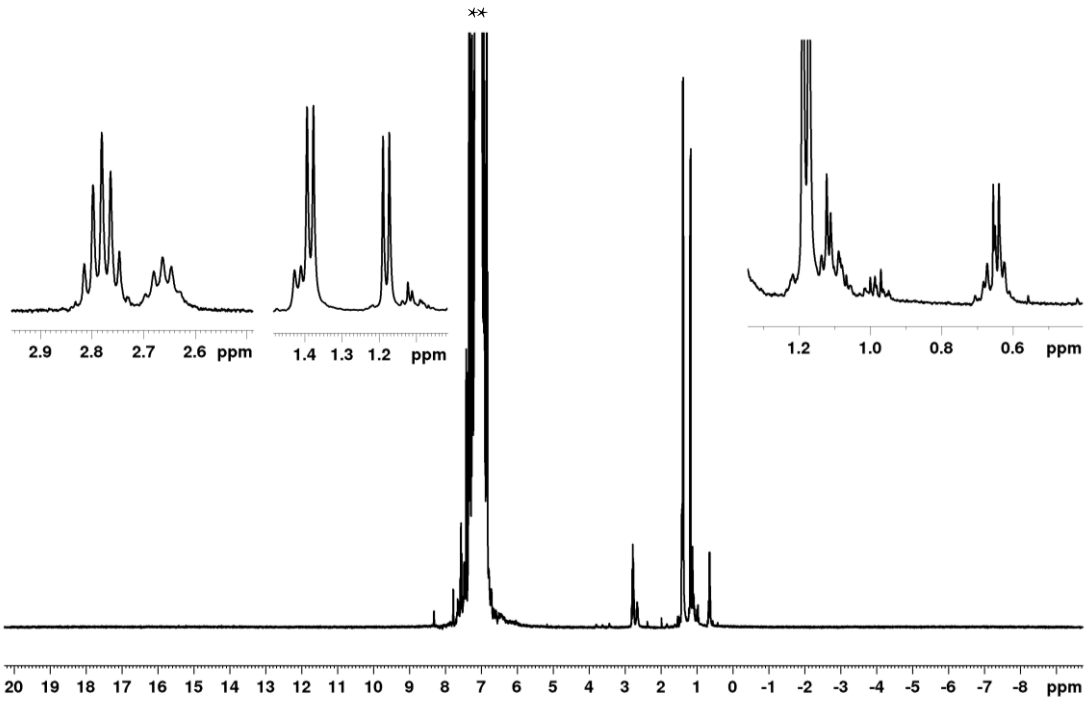

Figure S 4.23: ^{1}H NMR spectrum of the mixture containing [IDipp·Ga(PH$_2$)$_2$(μ_3-PH$_2${HgC$_6$F$_4$}$_3$)] in 1,2-difluorobenzene (C$_6$D$_6$-capillary) at 298 K (* = solvent signals).

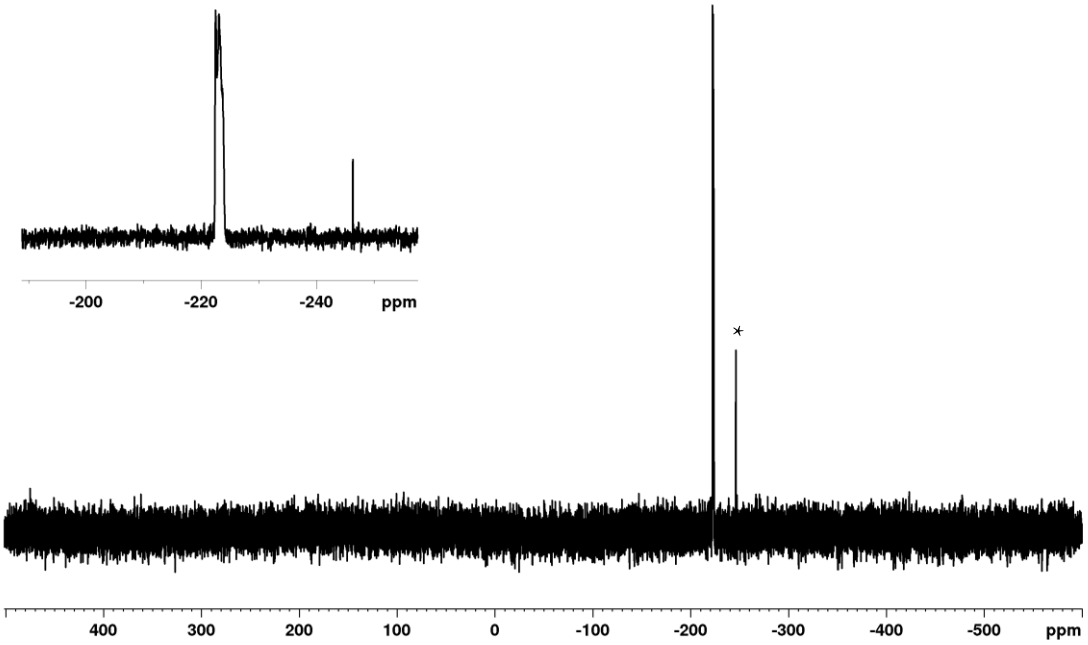

Figure S 4.24: ^{31}P{^{1}H} NMR spectrum of the mixture containing [IDipp·Ga(PH$_2$)$_2$(μ_3-PH$_2${HgC$_6$F$_4$}$_3$)] in 1,2-difluorobenzene (C$_6$D$_6$-capillary) at 298 K (* = PH$_3$).

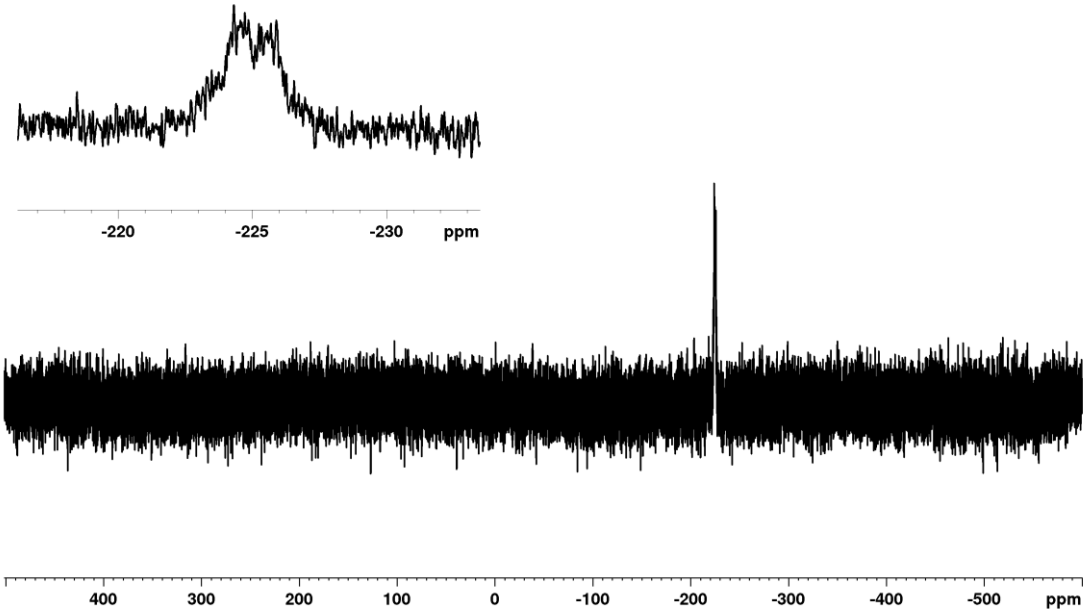

Figure S 4.25: ^{31}P NMR spectrum of the mixture containing [IDipp·Ga(PH_2)$_2$(μ_3-PH_2{HgC_6F_4}$_3$)] in 1,2-difluorobenzene (C_6D_6-capillary) at 298 K.

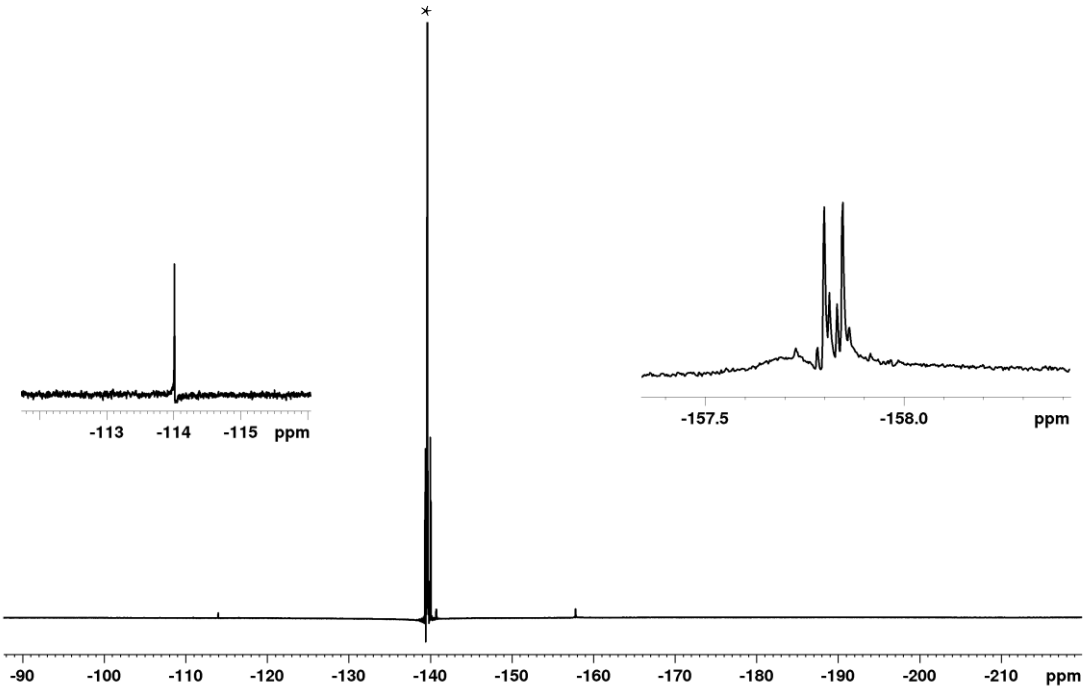

Figure S 4.26: $^{19}F\{^1H\}$ NMR spectrum of the mixture containing [IDipp·Ga(PH_2)$_2$(μ_3-PH_2{HgC_6F_4}$_3$)] in 1,2-difluorobenzene (C_6D_6-capillary) at 298 K (* = solvent signal). Due to the overwhelming intensity of the solvent peak compared to all other peaks, completely satisfactory phase correction by zeroth and first order corrections, while still maintaining a clear view of the less intense signals, was not possible.

4.5.4 Crystallographic Data

Single crystal X-ray structure determination: Single crystal X-ray diffraction data were collected on a GV50 diffractometer (*Rigaku*, TitanS2 CCD detector; **1a**) or a XtaLAB Synergy R DW system (*Rigaku*, HyPix-Arc 150 detector; **A**, **1b**, **2a**, **2b**, **4**) Crystals were selected under degassed mineral oil and mounted on MiTeGen MicroLoops. Data were collected using Cu-K_α (λ = 1.54178 Å, **A**-**2b**) or Mo-K_α (λ = 0.71073 Å, **4**) radiation. Data reduction, scaling and absorption corrections were performed using CrysAlisPro (*Rigaku*). Using Olex2, all structures were solved with ShelXT and a least-square refinement in F^2 was carried out with ShelXL. All non-hydrogen atoms were refined anisotropically. Unless noted otherwise, the hydrogen atoms at the carbon atoms were located in idealized positions and refined isotropically according to the riding model. Figures were created with Olex2.[7] Crystallographic data and details of the experiments are given in Table S 4.1 and Table S 4.2.

CIF files with comprehensive information on the details of the diffraction experiments and full tables of bond lengths and angles are deposited in the Cambridge Crystallographic Data Centre under the deposition codes CCDC 2218931 (**A**), 2218932 (**1a**) 2218933 (**1b**), 2218934 (**2a**), 2218935 (**2b**), 2218936 (**4**). These data can be obtained free of charge at www.ccdc.cam.ac.uk/conts/retrieving.html (or from the Cambridge Crystallographic Data Centre, 12 Union Road, Cambridge CB2 1EZ, UK; Fax: +44-1223-336-033; e-mail: deposit@ccdc.cam.ac.uk).

Table S 4.1: Crystallographic data for compounds **A**, **1a** and **1b**.

Compound	A	1a	1b
Formula	$C_{54}H_{72}Cl_6In_2N_4$	$C_{21.6}H_{33.6}Ga_{0.8}N_{1.6}P_{2.4}$	$C_{27}H_{41.7}As_{2.95}GaN_2$
$D_{calc.}$/ g cm^{-3}	1.392	1.208	1.453
μ/mm^{-1}	9.146	2.823	4.777
Formula Weight	1219.49	445.80	685.06
Colour	clear colourless	clear colourless	clear colourless
Shape	block-shaped	block-shaped	needle-shaped
Size/mm^3	0.90×0.53×0.20	0.13×0.11×0.07	0.29×0.05×0.04
T/K	100.00(10)	122.97(11)	123.01(10)
Crystal System	monoclinic	monoclinic	monoclinic
Space Group	$P2_1/n$	$P2_1/c$	$P2_1/c$
a/Å	17.98870(10)	17.9958(3)	18.2144(2)
b/Å	16.34500(10)	17.8852(3)	17.94110(10)
c/Å	20.35500(10)	20.8635(4)	20.9648(3)
α/°	90	90	90
β/°	103.5410(10)	114.089(2)	113.911(2)
γ/°	90	90	90
V/Å^3	5818.52(6)	6130.3(2)	6263.03(15)
Z	4	10	8
Z'	1	2.5	2
Wavelength/Å	1.54184	1.54184	1.54184
Radiation type	Cu Kα	Cu K$_a$	Cu K$_a$
Θ_{min}/°	2.954	2.690	2.654
Θ_{max}/°	74.795	73.898	74.367
Measured Refl's.	66188	34752	63689
Indep't Refl's	11731	11922	12565
Refl's I≥2 σ(I)	11305	10902	10358
R_{int}	0.0565	0.0258	0.0561
Parameters	612	669	701
Restraints	0	79	102
Largest Peak	2.113	0.794	1.043
Deepest Hole	-1.599	-0.448	-1.496
GooF	1.069	1.153	1.103
wR_2 (all data)	0.1294	0.0987	0.1357
wR_2	0.1282	0.0965	0.131
R_1 (all data)	0.0481	0.0425	0.0565
R_1	0.0469	0.0387	0.0472

Table S 4.2: Crystallographic data for compounds **2a**, **2b** and **4**.

Compound	2a	2b	4
Formula	$C_{27}H_{42}AlN_2P_3$	$C_{27}H_{42}AlAs_3N_2$	$C_{45}H_{42}F_{12}GaHg_3N_2P_3$
$D_{calc.}$/ g cm^{-3}	1.112	1.374	2.193
μ/mm^{-1}	2.169	4.21	10.185
Formula Weight	514.51	646.36	1603.2
Colour	clear colourless	clear colourless	clear colourless
Shape	needle-shaped	block-shaped	plate-shaped
Size/mm^3	0.20×0.08×0.07	0.20×0.06×0.05	0.20×0.11×0.05
T/K	123.01(10)	123.01(10)	123.00(10)
Crystal System	monoclinic	monoclinic	monoclinic
Space Group	$P2_1/c$	$P2_1/c$	$P2_1/n$
a/Å	18.0033(2)	18.2079(2)	10.8118(2)
b/Å	17.90170(10)	17.91740(10)	24.9724(6)
c/Å	20.8213(2)	20.9450(2)	17.9886(4)
α/°	90	90	90
β/°	113.7010(10)	113.8440(10)	91.420(2)
γ/°	90	90	90
V/Å^3	6144.49(11)	6249.85(11)	4855.37(18)
Z	8	8	4
Z'	2	2	1
Wavelength/Å	1.54184	1.54184	0.71073
Radiation type	Cu Kα	Cu Kα	Mo Kα
Θ_{min}/°	2.68	2.653	2.222
Θ_{max}/°	75.779	73.982	30.551
Measured Refl's.	64637	54165	42875
Indep't Refl's	12462	12316	14528
Refl's I≥2 σ(I)	9821	10333	11186
R_{int}	0.0394	0.0351	0.0477
Parameters	663	656	621
Restraints	36	67	6
Largest Peak	0.335	1.35	3.275
Deepest Hole	-0.406	-1.068	-1.498
GooF	1.04	1.023	0.997
wR_2 (all data)	0.1156	0.0997	0.0971
wR_2	0.1077	0.0956	0.0906
R_1 (all data)	0.0601	0.0492	0.0577
R_1	0.0435	0.0392	0.0386

4.5.4.1 Crystal Structures

IDipp·$InCl_3$ (A)

A crystallized by slow evaporation of CH_2Cl_2 solution as clear colourless block-shaped crystals in the monoclinic space group $P2_1/n$. The structure of **A** in the solid state is shown in Figure S 4.27.

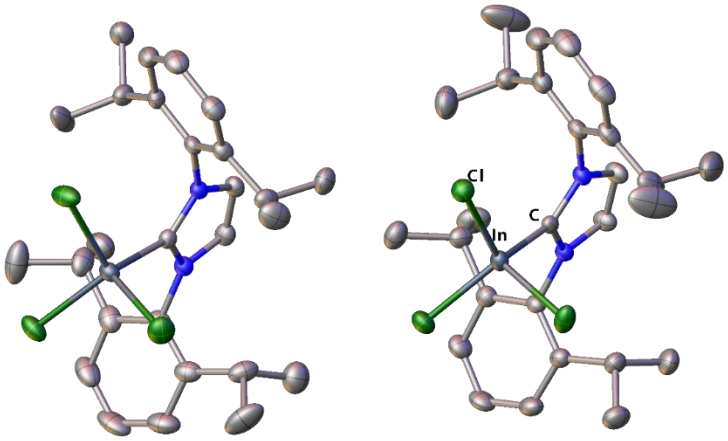

Figure S 4.27: Molecular structure of **A** in the solid state (asymmetric unit). Anisotropic displacement ellipsoids are shown at 50% probability level. Hydrogen atoms are omitted for clarity. Selected bond lengths [Å] and angles [°]: C-In 2.187(3), In-Cl 2.3557(8), C-In-Cl 113.84(4).

The asymmetric unit contains two molecules of **A** and was refined without further restraints or constraints.

IDipp·$Ga(PH_2)_3$ (1a)

1a crystallized from a saturated *n*-hexane solution at -28 °C as clear colourless block-shaped crystals in the monoclinic space group $P2_1/c$. The structure of **1a** in the solid state is shown in Figure S 4.28.

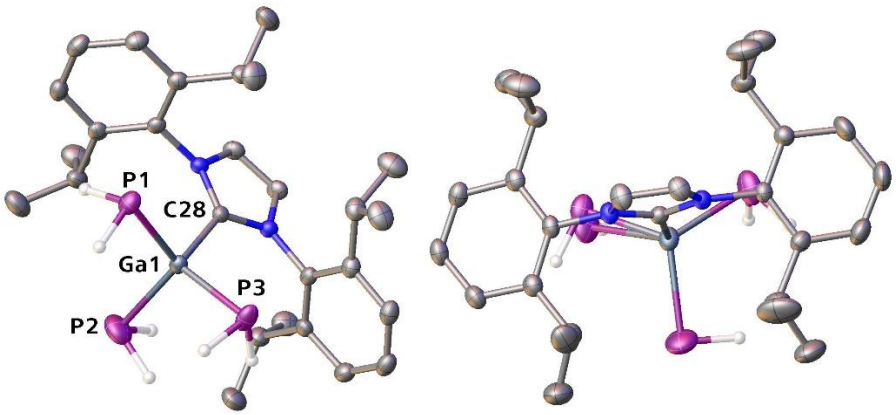

Figure S 4.28: Molecular structure of **1a** in the solid state (asymmetric unit). Anisotropic displacement ellipsoids are shown at 50% probability level. Hydrogen atoms bound to carbon are omitted for clarity. Selected bond lengths [Å] and angles [°]: C28-Ga1 2.069(2), Ga1-P1 2.3514(7), Ga-P2 2.3555(8), Ga-P3 2.3609(8), C28-Ga-P1 109.67(6), C28-Ga-P2 105.68(7), C28-Ga-P3 110.85(6).

The asymmetric unit contains two molecules of **1a**. Hydrogen atoms bound to P atoms were refined by applying SADI, DANG and DFIX restraints. One P atom position displays positional disorder and was refined by applying SIMU and SADI restraints.

IDipp·Ga(AsH$_2$)$_3$ (1b)

1b crystallized from a saturated *n*-hexane solution at -28 °C as clear colourless needle-shaped crystals in the monoclinic space group $P2_1/c$. The structure of **1b** in the solid state is shown in Figure S 4.29.

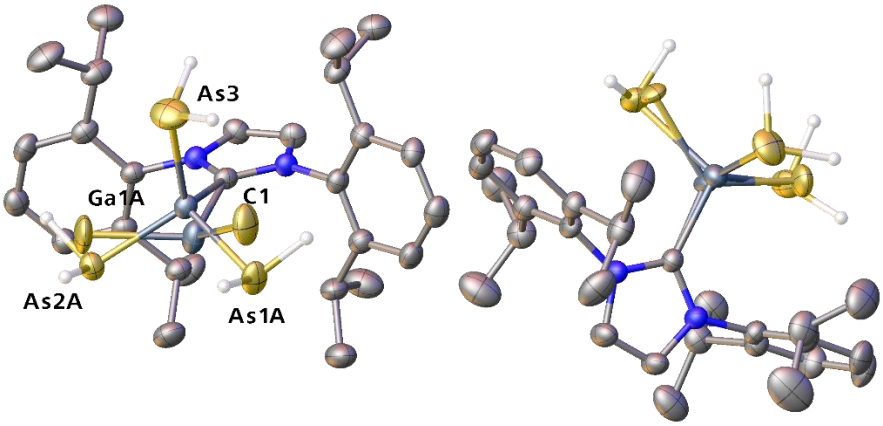

Figure S 4.29: Molecular structure of **1b** in the solid state (asymmetric unit). Anisotropic displacement ellipsoids are shown at 50% probability level. Hydrogen atoms bound to carbon are omitted for clarity. Selected bond lengths [Å] and angles [°]: C1-Ga1A 2.081(3), Ga1A-As1A 2.4550(7), Ga1A-As2A 2.4433(7), Ga1A-As3 2.4509(8), C1-Ga1A-As1A 110.64(9), C1-Ga1A-As2A 110.61(9), C1-Ga1A-As3 107.35(9).

The asymmetric unit contains two molecules of **1b**. Both display small disorder (occ. 0.05 each) in the {Ga(AsH$_2$)$_3$} units, which could partially be refined by DANG, SIMU, DFIX and SADI restraints.

IDipp·Al(PH$_2$)$_3$ (2a)

2a crystallized from a saturated *n*-hexane solution at -28 °C as clear colourless needle-shaped crystals in the monoclinic space group $P2_1/c$. The structure of **2a** in the solid state is shown in Figure S 4.30.

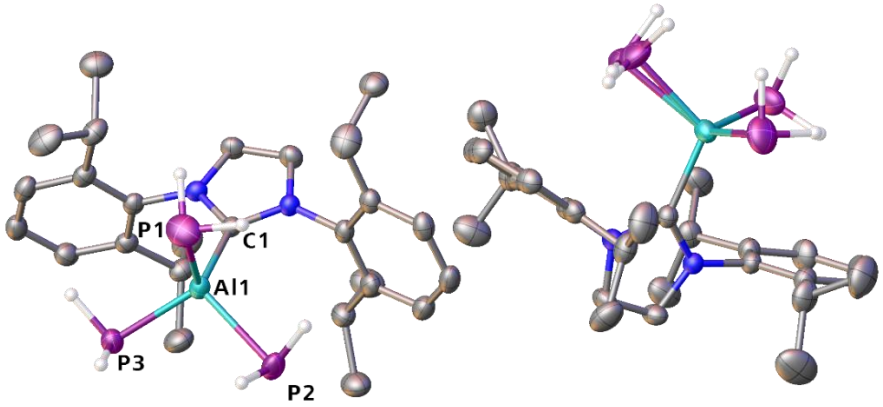

Figure S 4.30: Molecular structure of **2a** in the solid state (asymmetric unit). Anisotropic displacement ellipsoids are shown at 50% probability level. Hydrogen atoms bound to carbon are omitted for clarity. Selected bond lengths [Å] and angles [°]: C1-

Al1 2.0672(19), Al1-P1 2.3672(8), Al1-P2 2.3720(8), Al1-P3 2.3616(8), C1-Al1-P1 107.94(6), C1-Al1-P2 111.23(5), C1-Al1-P3 109.50(6).

The asymmetric unit contains two molecules of **2a**. One moiety displays disorder in one {PH_2} branch, which was refined by applying SADI, DANG and DFIX restraints.

IDipp·Al(AsH_2)$_3$ (2b)

2b crystallized from a saturated *n*-hexane solution at -28 °C as clear colourless needle-shaped crystals in the monoclinic space group $P2_1/c$. The structure of **2b** in the solid state is shown in Figure S 4.31.

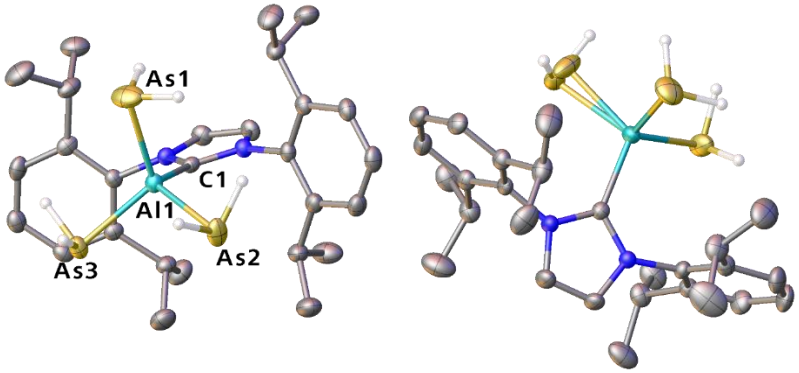

Figure S 4.31: Molecular structure of **2b** in the solid state (asymmetric unit). Anisotropic displacement ellipsoids are shown at 50% probability level. Hydrogen atoms bound to carbon are omitted for clarity. Selected bond lengths [Å] and angles [°]: C1-Al1 2.063(3), Al1-As1 2.4631(9), Al1-As2 2.4638(9), Al1-As3 2.4583(9), C1-Al1-As1 108.48(8), C1-Al1-P2 111.10(8), C1-Al1-P3 110.21(8).

The asymmetric unit contains two molecules of **2b**. One moiety displays disorder in one {AsH_2} group, which was refined by applying SIMU, SADI, DFIX and DANG restraints.

[IDipp·Ga(PH_2)$_2$(μ_3-PH_2{HgC_6F_4}$_3$)] (4)

4 crystallized by diffusion of *n*-hexane into a 1,2-difluorobenzene solution of 4 at -28 °C as clear colourless plate-shaped crystals in the monoclinic space $P2_1/n$. The structure of **4** is shown in Figure S 4.32.

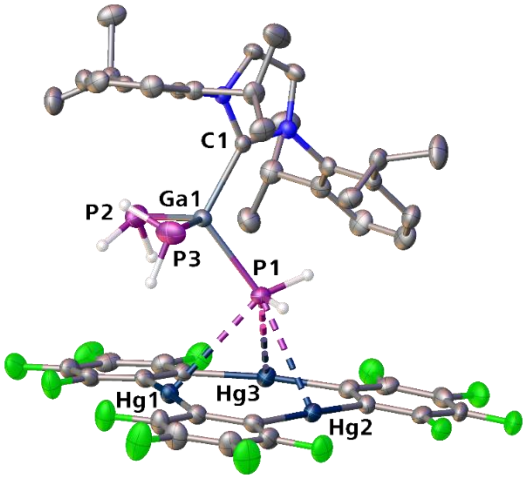

Figure S 4.32: Molecular structure of **4** in the solid state (asymmetric unit). Anisotropic displacement ellipsoids are shown at 50% probability level. Hydrogen atoms bound to carbon are omitted for clarity. Selected bond lengths [Å] and angles [°]: P1-Hg1 3.2544(13), P1-Hg2 3.1809(13), P1-Hg3 3.3168(13), C1-Ga1 2.064(5), Ga1-P1 2.3809(14), Ga1-P2 2.3719(15), Ga1-P3 2.3310(15), C1-Ga1-P1 113.95(13), C1-Ga1-P2 105.74(12), C1-Ga1-P3 109.32(13), P1-Hg1-Hg2 55.33(2), P1-Hg2-Hg3 58.17(2), P1-Hg3-Hg2 56.38(2).

The asymmetric unit contains one molecule of **4**. Hydrogen atoms bound to P atoms were refined by applying DFIX restraints.

4.5.5 Computational Data

4.5.5.1 General Information

Quantum chemical calculations were performed using ORCA version 4.2.1 developed by Neese *et al.*[8] Images of calculated structures were generated with ChemCraft.[9] Molecular geometries were optimized at the B3LYP-D4/def2-TZVP level of theory.[10–14] Subsequent analytical frequency analysis was carried out in order to determine the nature of stationary points on the potential energy surface. The RIJCOSX approximation was applied to enhance the calculation speed.[15] *Natural Bond Orbital* analysis (NBO 6.0)[16] was carried out with ORCA 4.2.1 at the TPSSh/def2-TZVP[14,17] level of theory and used to describe electronic densities and to calculate the *Wiberg Bond Index* matrix (WBI).[18] The molecular structure of **4** was optimized at the ZORA-BP86-D4/def2-SVP[12,19–22] level of theory followed by a single-point calculation at the ZORA-B3LYP-D4/def2-TZVPP (SARC-ZORA-TZVPP on Hg)[10,12,13,21,22] level of theory.

Dissociation energies of $(HgC_6F_4)_3$ adducts: Molecular geometries were optimized at the BP86-D4/def2-TZVP (CPCM = CH_2Cl_2)[14,19,20,23] level of theory. Subsequent numerical frequency analysis was carried out in order to determine the nature of stationary points on the potential energy surface. Electronic energies were refined by single point calculations at the PWPB95-D4/def2-TZVPP (CPCM = CH_2Cl_2)[14,23,24] level of theory. *Non-Covalent Interaction* Analysis (NCI, Figure S 4.33)[25] was performed using Multiwfn[26] and visualization of resulting .cube files with ChemCraft.[9]

4.5.5.2 NCI analysis of [IDipp·Ga$(PH_2)_2(\mu_3$-$PH_2\{HgC_6F_4\}_3)$]

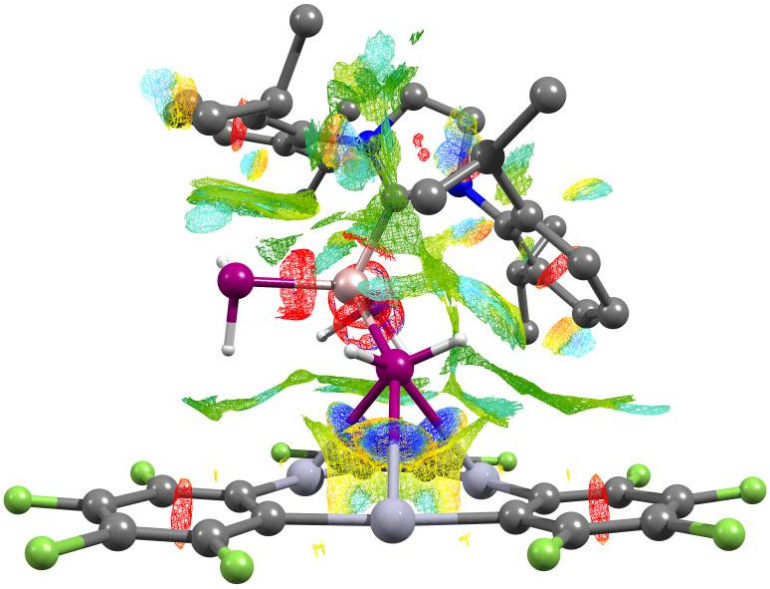

Figure S 4.33: Plot of the calculated reduced density gradient of [IDipp·Ga$(PH_2)_2(\mu_3$-$PH_2\{HgC_6F_4\}_3)$]. Hydrogen atoms bound to carbon have been omitted for clarity. The lined surfaces show regions of weak interactions within the molecule. Color scheme: blue (strong attractive interaction), green (Van der Waals interaction), red (strong repulsion e.g., by steric strain). Besides a view on the Van der Waals contacts of the $\{PH_2\}$ groups to the NHC aryl residues, a clear visualization of the attractive forces between one $\{PH_2\}$ arm and $(HgC_6F_4)_3$ is obtained (blue spots between the cyclic system and the $\{PH_2\}$ groups).

4.5.5.3 Cartesian Coordinates of optimized Structures

IDipp·Ga(PH$_2$)$_3$

C	0.68851377775924	0.26044499478641	-2.05289574243330
C	-0.65909287512274	0.29938251767885	-2.04708264101008
N	-1.05784326160560	0.05295542381987	-0.74727048523817
C	0.01324104621290	-0.12819583107252	0.06243863012490
N	1.08391339124790	-0.01120858249159	-0.75623876498279
H	1.39857341133460	0.38572758616511	-2.84855660184074
H	-1.36680566829945	0.46448611238106	-2.83741633095286
C	2.45999244108872	-0.24279188486493	-0.40093181329807
C	2.91844069839975	-1.56753784917383	-0.36200027234385
C	3.28095650535638	0.85861387120417	-0.15432455995536
C	4.26556485422274	-1.76258390694112	-0.07899669564790
C	4.62280646543051	0.60565275620608	0.12486648404151
C	5.11045371979467	-0.68852601881749	0.15769431988790
H	4.66057522283348	-2.76672564194419	-0.02633269316261
H	5.29005079333013	1.43200905195390	0.32763437761548
C	-2.43801035464398	-0.14735651850887	-0.38416855219277
C	-2.95152182172245	-1.44747788721750	-0.47867870710688
C	-4.29601471730341	-1.62493542992368	-0.16711405112340
C	-5.08519371392203	-0.55422844943448	0.21832673201806
H	-4.72738505122878	-2.61491833115528	-0.21352905627284
C	-4.54807540897339	0.72019582535035	0.29712287038617
H	-5.17676330102093	1.54367060355659	0.60523621555292
C	-3.20936568252908	0.95478715102451	-0.00575613592233
C	-2.10695140496785	-2.61674321645569	-0.95137286928892
H	-1.06066139993839	-2.36172265783053	-0.78668325169859
C	-2.30041961465267	-2.84025078956997	-2.45946242615149
C	-2.37614736734832	-3.91021455956508	-0.17724811795086
H	-2.29520098646963	-3.74803721842902	0.89708229759346
H	-3.36807845198315	-4.31239930430851	-0.39326478602171
H	-1.64967915267184	-4.67102801877613	-0.47085452358876
H	-3.33688830252115	-3.10749072233149	-2.67737378834512
H	-1.66086557325727	-3.65324420434964	-2.80970155932176
H	-2.05700107973888	-1.94855086772677	-3.03816317394490
C	-2.64020732851700	2.35911155377089	0.03097015113781
H	-1.55962176216481	2.27907733076224	0.15071588895823
C	-2.90884281985998	3.08141151387251	-1.29871395534022
C	-3.16868012735242	3.18680552732401	1.20563181140964
H	-4.22554437297179	3.43243618362719	1.08218959736246
H	-3.04175060946030	2.66377544092195	2.15261550199076
H	-2.61987014537250	4.12729210546490	1.27224971430794
H	-2.48576071754362	2.54230915100730	-2.14743761025600
H	-2.47111068011838	4.08183946662699	-1.28351986059915
H	-3.98273342331330	3.18402644346607	-1.47075968092853
C	1.99469932880658	-2.74502024087646	-0.62340863786854
H	1.01282729443107	-2.48189788993600	-0.22753848616214
C	1.84518653587730	-3.01187106786379	-2.12992280781783
C	2.42542666142956	-4.03008435713917	0.08743344144892
H	3.33137950290337	-4.45322397168317	-0.35185971306544
H	2.60447940747996	-3.86306424467604	1.14900816074343
H	1.63891641978725	-4.78055678851452	-0.00826176119583
H	1.45747367663825	-2.14748822071124	-2.66670933578576
H	1.15938252439709	-3.84448257650876	-2.30062820905183
H	2.81116079973542	-3.27574548840112	-2.56665748331275
C	2.76048750637230	2.28175195110930	-0.20145585823377
H	1.67353607556675	2.24355134772598	-0.12556196267951
C	3.26195825321410	3.12539404530393	0.97459536365497
C	3.11715111952090	2.94929780714408	-1.53788630362409
H	4.20059091527829	3.01505745843976	-1.66073819910832
H	2.72036671577328	2.39256500861925	-2.38818418478684
H	2.71044321273386	3.96200582358976	-1.57906224995369
H	3.06451007120182	2.63273393059918	1.92557534107170
H	2.75219273257541	4.09031590319096	0.98439855142554
H	4.33363660515065	3.32142259672210	0.90418451902157
H	-6.12672343499036	-0.71532927403651	0.46628801949543
H	6.15453805286014	-0.86572980286729	0.38287058494931
Ga	-0.02055150821024	-0.20680390810035	2.15593763546470
P	-0.13403322271288	2.10155103071025	2.82741836852334
H	0.20705981985654	2.68960517446074	1.57918508728515
H	1.20365026984436	2.15148175960109	3.30005865165334
P	-1.90304767520028	-1.51275087602993	2.79234415037315
H	-2.87608317499023	-0.48391182710637	2.71353740505890
H	-1.65966640595793	-1.30491398505315	4.17618259383022
P	1.87512455975914	-1.14569601566788	3.23329806514444
H	2.87693048550895	-0.55565991881116	2.42407521712513
H	1.90721772394372	-2.38344562831611	2.54202047190986

IDipp·Ga(AsH$_2$)$_3$

Ga	4.04363450476608	9.10530574724033	16.31285818096600
As	6.44325892509682	8.72697246869493	16.83482849823060
As	3.93561279271675	11.07960977771280	14.80918272263040
As	2.63339736532066	9.35529849514954	18.37139338578280
N	3.58679352487097	6.11819222329048	15.63452614453720
N	2.28670110347416	7.35055704718969	14.45638757662250
C	3.30335504287381	7.41103663711277	15.34775280906360
C	1.71310162285942	8.46395826232908	13.74408282650250
C	4.71511302920461	5.64674304545960	16.39626557033050
C	5.92241819575319	5.45089441567787	15.71292701856330
C	0.48885116513179	8.97872312417971	14.17727808151860
C	2.74635938458217	5.26435071998410	14.94593255804260
H	2.81959958645551	4.19717197884244	15.03899458482700

C	4.54884853533498	5.36015471287151	17.75332477981380
C	1.92895303763051	6.03924019433254	14.20472978958380
H	1.14324291810571	5.78611958694150	13.51832553958660
C	2.39281823691121	8.94478382358632	12.61461864048440
C	6.05937742888875	5.71398770856056	14.22436387211890
H	5.25740144848647	6.38865517619684	13.92783705034570
C	-0.07178569258061	10.00910608619690	13.42563206266060
H	-1.01516539099856	10.43933064335260	13.73170830587300
C	0.56798810167963	10.49989152349680	12.30099368771170
H	0.12001712094769	11.30710836531430	11.73540226293120
C	6.99509137526538	4.95224742688622	16.44587264290970
H	7.94826496901113	4.80046051685961	15.95897372472630
C	5.65367265084298	4.86162581300319	18.43859514853600
H	5.56999327432719	4.63733305344561	19.49267918716930
C	1.78837069943256	9.97665027360205	11.90393447807100
H	2.28435171128311	10.38842146841930	11.03720319127020
C	3.21739333281497	5.54152561175557	18.45329282784600
H	2.63409440550585	6.26289223979568	17.88118035838380
C	-0.22926240881426	8.43543501149988	15.39716446550640
H	0.50623776739872	7.92201954657850	16.01740538594620
C	6.86275884294793	4.66080745033830	17.79337412122980
H	7.71205072726414	4.28199637356695	18.34773887430730
C	3.71831032780555	8.35611218420097	12.16123611865930
H	4.26033478928759	8.04601139461754	13.05536035841560
C	5.88372951869814	4.40848476242895	13.43331167157630
H	5.93751633670260	4.60270969499954	12.36002085253160
H	4.92418384082763	3.93358268745663	13.64141028626540
H	6.67148347572525	3.69606582022073	13.68817949795960
C	-1.30379265993306	7.41567759713827	14.99009343753770
H	-1.79712728300460	7.00865867552416	15.87532995895510
H	-0.88335356399858	6.58137916988747	14.42741676707660
H	-2.06579552322082	7.88729791103031	14.36536082000630
C	7.37678684153056	6.39793824763088	13.84826734274160
H	7.36016998826074	6.66975061936993	12.79072955356130
H	8.23327775283691	5.73761925553693	13.99835328482080
H	7.53481182972765	7.30161889645989	14.43594943770850
C	4.61578036172760	9.35741552940985	11.43034598463890
H	4.21702081032601	9.61731726665035	10.44725460734680
H	5.60017883143656	8.91336675483013	11.27116874424470
H	4.74417441063814	10.27171684430330	12.00870928620640
C	2.43351909924507	4.22034602521257	18.47083522677970
H	2.26009543044764	3.83872998052002	17.46349606460270
H	1.46200777576078	4.36068297394299	18.94949929028220
H	2.97880787050589	3.45527616094381	19.02827766429760
C	3.49699178994620	7.11290480899874	11.28475875647960
H	2.92970381594276	6.33890828333605	11.79997719297660
H	4.45636024129896	6.68243528027430	10.98964093531330
H	2.95393522064852	7.38084641039464	10.37550079584400
C	3.36459704482718	6.09968247135603	19.87136252258610
H	3.81185549304632	5.36882697184190	20.54833261600850
H	2.38376858883057	6.35979694512943	20.27171726178480
H	3.97796545306497	7.00027976286427	19.88453682689190
C	-0.84571754836841	9.54243375901445	16.25729192947650
H	-1.69534551764189	10.01503285372540	15.76033917317120
H	-0.11318503126472	10.31219255935670	16.49544704852300
H	-1.20828808012660	9.12287872020484	17.19716237728440
H	6.51978635647682	10.06578069461080	17.56599161472470
H	6.19468814496630	7.96350304445419	18.13090552623520
H	4.32845100489277	11.99673545744470	15.96600122428740
H	2.44890557522908	11.34087703472000	15.02564577718800
H	1.77534360599425	10.46206509018410	17.76882063409510
H	1.58965424611169	8.29245485030844	18.02170117628010

IDipp·Al(PH$_2$)$_3$

P	3.34589768029132	8.69364015593504	2.39031745060679
Al	5.65318877831580	9.04600001764505	2.83688134515572
P	5.75912058012908	10.91516832726230	4.30264514942767
P	7.01763795333597	9.28335525413397	0.87642519725580
N	7.39792018823220	7.29325216967698	4.68067305258739
N	6.06558276083026	6.07285396206000	3.52833261126611
C	6.37696568137921	7.36500307701275	3.79286513175938
C	8.00141211884691	8.40629990696568	5.36947692695680
C	3.71773961549197	5.44496457569934	3.41918404832108
C	4.94003581187674	5.61287735161240	2.75459087190098
C	7.72760396632030	5.97995946128644	4.95096962642175
H	8.51099698724444	5.71979991790413	5.63732872737960
C	6.89012738626644	5.21174216436923	4.22416362473933
H	6.79566876997010	4.14517379983253	4.14432142219102
C	7.35818105061913	8.89721650343337	6.51498835868301
C	9.21492698201946	8.91260307152673	4.89545183865183
C	4.02284190232355	4.82785136785540	0.70218195656801
H	4.12102041694175	4.59182571001393	-0.34820625188361
C	2.65035386713568	4.95693412175596	2.67189293968200
H	1.68622093808495	4.82679236685202	3.14275463073947
C	5.12490026179426	5.31122956772528	1.40295562510284
C	2.80015224245832	4.65286405598626	1.32887414438799
H	1.95382778716270	4.28361772442518	0.76354976660396
C	9.79668233619991	9.95208840908326	5.61734333537212
H	10.73128428193840	10.37773542915750	5.27975877118044
C	3.55901270963066	5.73046466096207	4.90160019997699
H	4.34378081833392	6.42808606476880	5.19307324687751
C	9.18989179493202	10.45647968375200	6.75503030216181
H	9.65450930246592	11.27046696502360	7.29704572489695
C	7.98420195174388	9.93611122359186	7.19652937916800
H	7.51501868683788	10.35570927727200	8.07449344246628

C	6.05291240829351	8.30803523267221	7.02156676881475
H	5.50030517878925	7.94058519945357	6.15641138835265
C	9.90254924934496	8.34396627986442	3.66902643123603
H	9.14533204679877	7.84682408336290	3.06177822145801
C	6.47242187336243	5.45312048665919	0.72382319459558
H	7.07649817880394	6.14076279736165	1.31560875754387
C	3.75161651443120	4.44343550602155	5.71913425085871
H	3.68221893554285	4.65731775644109	6.78784447109897
H	4.72169383406561	3.98197062970654	5.53163876473962
H	2.97962422576195	3.71194872562726	5.46987870345304
C	10.95327230024780	7.29704254813489	4.07038238764500
H	11.42648796818200	6.87261013411356	3.18231078239152
H	10.51634221170770	6.47714062708988	4.64126193169912
H	11.73372178542250	7.75149813031379	4.68493954041553
C	6.31871250788876	7.11546634813849	7.95437503252390
H	6.86948129438797	7.44006912804385	8.84023077145433
H	6.89800667101579	6.33172911384636	7.46704730977761
H	5.37528388787204	6.67626079753100	8.28587126655460
C	2.22394870097698	6.39376823017813	5.25121514551047
H	1.38370731910756	5.71016542777248	5.11288640801294
H	2.05467563271427	7.27944297942067	4.63975579031248
H	2.22723790121139	6.69172147182334	6.30179759130125
C	5.15056288271491	9.33073277301340	7.71607556283961
H	4.17773263057079	8.87873004136891	7.91884794457524
H	4.99649991903713	10.20835362618700	7.08929914106021
H	5.56313314865136	9.65046199090707	8.67554837574530
C	6.36675939004785	6.04234802489660	-0.68556895569534
H	5.88383256787625	5.34941661996887	-1.37756247010647
H	7.36348853764325	6.25354340835290	-1.07569139837671
H	5.80633993895229	6.97688596210811	-0.68713483733801
C	7.20231606815232	4.10149005155179	0.69485401441780
H	7.34145379178745	3.69531592459581	1.69811251489036
H	8.18706706569369	4.20976735764203	0.23526873280270
H	6.63641694151502	3.36913189480494	0.11462080942482
C	10.54184321320050	9.42552864562765	2.79341862973591
H	11.41657010936870	9.86947171256703	3.27296286036830
H	9.83432825052260	10.22120389209920	2.56491578541416
H	10.87309199551020	8.99010649457111	1.84924356796179
H	3.50784167992284	7.95978095822633	1.18656995582725
H	7.13610497189574	11.20280952066960	4.11503555239571
H	5.33632685149429	11.80412161746690	3.27604163296508
H	3.22766138780846	9.94393296696920	1.72356851079840
H	7.92486845032213	8.21478611130458	1.11259152415717
H	7.88200397222879	10.24973242694200	1.45050503978134

IDipp·Al(AsH$_2$)$_3$

As	6.44033071578293	8.74140121125434	16.81382399560530
As	3.93636635815336	11.06330785169270	14.79287784349540
As	2.62702412979484	9.33266362827653	18.36263397338170
Al	4.03667285533276	9.09611880357638	16.30441160233750
N	3.60640664680969	6.12018435138033	15.63809083824620
N	2.30056394381596	7.34381219284805	14.45691931074970
C	3.31442222359981	7.41400703179452	15.35401614981420
C	5.94574481885730	5.46214567389665	15.73121665488950
C	0.49085961246670	8.95994262223432	14.17280942919830
C	1.71741796316531	8.45004490314797	13.73947110792060
C	2.77464912738688	5.26193008163281	14.94734150688380
H	2.85492256122139	4.19531535198863	15.04041218489890
C	4.73193049112864	5.64979663312234	16.40642276790060
C	6.09306797408741	5.72941086239953	14.24416240414220
H	5.30304690183699	6.41825104275625	13.94727836437060
C	4.55512791232472	5.35085879342841	17.75970083943230
C	1.95385593729300	6.03146683004392	14.20375249051180
H	1.17224234311014	5.77308810375226	13.51468571729230
C	-0.07688285653849	9.98338054160769	13.41710877800860
H	-1.02146180541157	10.41053481239990	13.72365535405790
C	2.38899349729337	8.92496859482048	12.60253463374880
C	0.55678365390303	10.47093385420670	12.28755947261390
H	0.10330549502604	11.27319678850450	11.71934647246710
C	6.87306091246479	4.66598138590551	17.81546130326210
H	7.72003701605194	4.28916613570936	18.37468779239720
C	7.01468031954199	4.96526874128791	16.47055834173140
H	7.97255720526891	4.82105849525308	15.99089672154390
C	5.65733350968782	4.85482925949760	18.45126465815360
H	5.56546412644687	4.62205898081823	19.50282721242980
C	-0.22390687063252	8.41688694950315	15.39488276934770
H	0.51508186127786	7.91382354580137	16.01937341560020
C	3.21567817803760	5.51165209936956	18.44981831340220
H	2.62575602284280	6.22629935587948	17.87604954071210
C	1.77716178081401	9.94984878710762	11.88806061048740
H	2.26741726245657	10.35751362124910	11.01612090090730
C	3.71164509525911	8.33556297180699	12.14204882634620
H	4.25557705565225	8.01653484614030	13.03180764406170
C	-1.28781379297049	7.38462389717240	14.99104650304940
H	-2.05293054110827	7.84555328338118	14.36217963221410
H	-1.77903213609830	6.97789428560788	15.87757254225670
H	-0.85838517574975	6.55118634021956	14.43389203078140
C	5.90060553382330	4.42970617951720	13.44691430332490
H	5.96233805057501	4.62763921086142	12.37473509804090
H	4.93341686724860	3.96787138213110	13.64805214395770
H	6.67678995128491	3.70494849446520	13.70244929575300
C	-0.85315204134178	9.52195499418049	16.24824584271770
H	-0.12958026877250	10.30130952189810	16.48262459016830
H	-1.21148281675810	9.10369380384753	17.19026666363750
H	-1.70772901397150	9.98219341444229	15.74817655591930

C	3.48275634712762	7.09925873114603	11.25760837485520
H	2.91385378965042	6.32408298682544	11.76946082446890
H	4.43943703598185	6.66697153082454	10.95653808622720
H	2.93780351471188	7.37554338006813	10.35202909828040
C	7.42306469347728	6.39218585456878	13.87435385708870
H	8.26704057361851	5.71486090115878	14.01955779150240
H	7.59687455392975	7.28889532301484	14.46819734106200
H	7.41207469404966	6.67171987745038	12.81879525251740
C	2.45149727592804	4.17874788054460	18.45706191365520
H	2.29198051938390	3.79729420085704	17.44734905865660
H	1.47419824164464	4.30313250510686	18.92825077145250
H	3.00360939784359	3.42025174465889	19.01671282851390
C	4.60994789889148	9.33935917158845	11.41531999743420
H	4.20910359954366	9.60655233356743	10.43509354834270
H	5.59279374065685	8.89391745657232	11.25041894336890
H	4.74185747752290	10.24967581072160	11.99916722116760
C	3.34350854758566	6.06666993397907	19.87117022684610
H	3.79691884573542	5.34015707374234	20.54868607147950
H	2.35573078287214	6.31003990018792	20.26485503312140
H	3.94252454427294	6.97669383174074	19.89277236350000
H	6.20170814907108	7.96612252889938	18.10468554915790
H	6.49312301926470	10.07974567482200	17.54883899325090
H	4.32706447279390	11.97511803630200	15.95531924667940
H	2.44870458203103	11.32476496087370	15.00075749958950
H	1.75521159382608	10.42689375611020	17.75789174217720
H	1.59963351681310	8.25252407084805	18.02036322142800

[IDipp·Ga(PH$_2$)$_2$(μ_3-PH$_2${HgC$_6$F$_4$}$_3$)]

Ga	5.13867614929554	6.19459503736944	9.23842075022658
P	4.21605843471425	8.34357057755243	8.74106577290005
P	7.45287941881763	5.91455657981940	8.73380587155392
P	4.50111240518655	5.87458086299050	11.49888163093320
N	4.27597663726326	3.42253359425217	8.31402500787371
N	4.01702675032537	4.81921504666645	6.68167467436918
C	4.32105387652516	4.75219412919839	8.01112079071072
C	3.95261741391630	2.66651306840580	7.19362012724689
H	3.85691126433511	1.57863055635287	7.23691129881211
C	4.39779421496520	2.88638697297356	9.65041667824936
C	6.83711625155512	2.28290036886912	9.12008410834048
H	6.70589433010156	3.08673731075710	8.36522055277015
C	4.80553567401573	6.74178360482688	5.34750884729476
C	6.23212285737550	6.21185916184704	5.38289462367930
H	6.36888708673476	5.67278717099925	6.34578539606157
C	3.25909544538800	2.95762026853847	10.49378767328300
C	3.38437017622543	2.40068987540764	11.77935718173960
H	2.53144791262371	2.44340423168302	12.47037215083240
C	4.48002435228122	7.93380784675694	4.67331045260538
H	5.27287107666502	8.52722240037301	4.19857772963902
C	5.69506914369089	1.78040729284564	11.34737058966400
H	6.63681950114153	1.33533588371011	11.69918358942020
C	3.74055356391151	6.03722543273343	5.95637632648485
C	3.78900627673138	3.55036240456071	6.15979568004038
H	3.51018554932787	3.39902035823101	5.11355801195679
C	5.63074315244451	2.32276828280186	10.04928558945250
C	7.28522860655164	7.32494542182034	5.33205558572987
H	7.32336831963369	7.82460254889181	4.34274589835551
H	8.29316322516858	6.91228841141488	5.53318621089599
H	7.09005241693087	8.10043992481240	6.09715213754134
C	2.12477290460633	7.66179380953440	5.21137129114088
H	1.09187430720407	8.03648184132853	5.15595590433710
C	2.39450397616331	6.46935568202985	5.91181147778379
C	4.58459307611615	1.81284227918772	12.19884591071210
H	4.65950490614896	1.38911408279507	13.21186497073410
C	1.27040009699921	5.72239245870197	6.62199390127116
H	1.67208648239686	4.75449373514628	6.98424266900891
C	1.95049729051357	3.58841157315220	10.02586054718090
H	2.21737552828268	4.41663788177536	9.33627808307579
C	1.13236900025817	4.21094800995397	11.16637124687080
H	0.71442772995683	3.44050642630071	11.84737348139960
H	0.27245751371711	4.77297512425968	10.74941207587100
H	1.75094276063457	4.91306803840650	11.75997623994960
C	8.15467768372938	2.57760079676211	9.85500252786433
H	8.08664578664797	3.50872228920364	10.45087493909170
H	8.97648445421491	2.71019364608533	9.12379263828382
H	8.44464547869283	1.75058746895333	10.53622565690530
C	3.15406901873960	8.38235095775840	4.59603239813338
H	2.92621061938415	9.30603422894973	4.04650378907208
C	0.78972810707415	6.50115947536152	7.86128120683822
H	0.38318966752635	7.49527560673488	7.58224607015257
H	1.61809480996848	6.66841056080198	8.57706155311798
H	-0.01186822563573	5.94237014071520	8.38594756283326
C	6.91372382850773	0.93404991377819	8.37552655330594
H	7.03955604091504	0.09406122179238	9.09030428476673
H	7.77673587210262	0.92144886080449	7.67864003596398
H	5.99941703723459	0.73113700664359	7.78291688745586
C	1.10004177084702	2.57272992260004	9.23369887816710
H	1.64221458524926	2.15797377225180	8.36153596769765
H	0.17343602859632	3.05239619777615	8.85619695361259
H	0.80222997213610	1.72205312354149	9.88138583631741
C	0.10744161168131	5.39467807546195	5.66833734513710
H	-0.65861916312268	4.78444337288604	6.18888110998653
H	0.45560510230757	4.82597051593281	4.78229449060108
H	-0.39648325396859	6.31250024783432	5.30146919594570
C	6.45814017985413	5.18628320622426	4.25216182695537
H	5.75412585618522	4.33295779040666	4.31783403882016

H	7.48789105611655	4.77745590840002	4.30151477765346
H	6.32278117512529	5.66065509351551	3.25796975843888
F	5.21759967343494	11.24226486871290	4.32487159379599
F	0.82198870507954	12.33570958364180	7.41448330510536
F	2.89785997654480	12.05973039815630	3.16718331254059
F	0.70996519652388	12.63792974415010	4.70794788652814
C	3.10042007939822	11.62203832787650	7.30484604565623
C	4.24084564729185	11.34657777676730	6.50656390672400
C	1.93075670411675	12.07089887937820	6.68637189931233
C	4.16102840430428	11.53239769156070	5.12649546102083
C	2.97631535992101	11.96034603356810	4.50332481255728
C	1.84887777903759	12.24135914347500	5.29188087770188
Hg	6.06914683220777	9.78131674253470	10.88368469859560
Hg	3.08885412000830	11.23973416645120	9.37961647527491
Hg	6.02233575267957	10.60058506620100	7.34506585546309
F	0.95263787420194	11.57701117577480	11.72333575582860
F	5.35798220796351	9.15876739171304	13.91556376686900
F	8.97568215633798	8.65565663576462	11.53003262857300
F	8.93717272181349	9.99156436154128	6.21560099399601
F	11.16401941176280	8.90056264646624	7.33979880224015
F	11.18369850323430	8.23765912396839	9.99520344558248
F	3.13573995600207	9.60515763165131	15.43396902680710
F	0.94264128551947	10.81883618346940	14.34000217828270
C	3.18005716029348	10.76021567925720	11.42966887880490
C	7.76130962381874	9.89436274659784	8.29557076173871
C	4.32005893852091	10.13549216688710	11.99955365822200
C	7.77511783672863	9.55921515564386	9.67399995617644
C	4.28850109034874	9.75966421382686	13.34447644132080
C	2.05991275254231	10.98893437899270	12.23313839159410
C	8.91527741883917	9.68610786983878	7.53582160570107
C	8.93698534365349	9.01886989359172	10.22738308447920
C	10.08903943805040	8.78724920339634	9.45497499987104
C	3.15637583416499	9.98184119918334	14.14892466222540
C	2.02987765978709	10.60566345806270	13.58667967845880
C	10.07818055803800	9.12464322372571	8.09133662951336
H	7.87638875793718	6.30946179639339	10.05033955785450
H	7.62462087001672	7.23299195746219	8.19694113300573
H	5.56756375632355	4.96219403070263	11.82250902036940
H	5.24994968689906	7.02796767671051	11.93673789736950
H	3.02099466412116	8.19206043861688	9.52224147066742
H	3.56266082158038	8.21487311107470	7.47629807905137

CH_2Cl_2

C	-1.34292475835301	-0.00010267007051	-1.95511789546184
H	-0.83928119322184	-0.96584242939915	-1.88156865167754
H	-0.64979435069589	0.84156357910837	-1.90038223427288
Cl	-2.17304235656859	0.07043648550616	-3.53991110992854
Cl	-2.48359360516067	0.13435588685513	-0.58163375465919

$(HgC_6F_4)_3$

F	5.25754342840472	11.37304155919630	4.35102656256346
F	0.79524859766299	12.22474840193130	7.40406017899526
F	2.98665450549258	12.33634802587720	3.22174342266874
F	0.75977124416408	12.76148715118590	4.74654312524485
C	3.07455472128269	11.50371183250160	7.29907881774840
C	4.22864885611820	11.28323306724700	6.50895472973257
C	1.93080213292935	11.99710826894650	6.68510642968375
C	4.17151609563383	11.56933688575900	5.15126151545254
C	3.01801529457392	12.06542098822250	4.54213013283611
C	1.88204478654660	12.28240273216610	5.31989763135411
Hg	6.07163629473479	9.82777692675265	10.87908609825760
Hg	3.05490524042916	11.10368393271280	9.35215804165719
Hg	6.00307805604957	10.54676048840300	7.33630926215640
F	0.86754516878610	11.32288247380740	11.66097653805560
F	5.44264504671592	9.40448733993310	13.97235425100870
F	8.99423510341544	8.73084736383440	11.54564302798700
F	8.88443434080244	9.83609428155426	6.18619872347599
F	11.13912368188470	8.86620276576193	7.34002925653785
F	11.19268822609380	8.31359450586690	10.01509834565560
F	3.21531793762975	9.80299178311320	15.46717774631900
F	0.93114095321331	10.76025062143430	14.31281052602640
C	3.15086726851859	10.65916215238780	11.39385774856910
C	7.71842374811467	9.80470855079227	8.27539702323372
C	4.33393322427620	10.16321203985100	11.99234560933100
C	7.74637337460344	9.52031265381406	9.66220841132103
C	4.32774598786366	9.88562958836651	13.35305712000250
C	2.03007097217269	10.84892702691960	12.19178855571470
C	8.86425238384541	9.57723005412583	7.52441469775876
C	8.91880587210314	9.02302351189888	10.21627127393910
C	10.06601120957240	8.79716383255325	9.45421137108512
C	3.19728334894160	10.07988976807320	14.14778439076590
C	2.03224824509907	10.56805766246790	13.55885494927290
C	10.03869665532500	9.07863452654133	8.08953596458827

$CH_2Cl_2 \cdot (HgC_6F_4)_3$

Cl	-12.31978039423930	-5.94516902798692	11.33704274771290
Cl	-10.21740462754470	-7.44530875568094	9.87035980616765
C	-11.84232499363440	-6.69150892068821	9.78657245665617
H	-12.56297730411520	-7.47600996781899	9.54816553196653
H	-11.80108923791040	-5.90360960745544	9.03062424240610
Hg	-6.65595210649557	-6.32272186351145	10.06068795701080
Hg	-8.88704787263530	-5.21487953293745	7.44805100647555
Hg	-9.28728863075901	-3.96945463558883	10.81089801033740
F	-7.95337611196893	-6.64232300999145	4.75653095517355
F	-5.96068148406917	-8.39738997273105	4.20278032328968
F	-4.27748060715368	-9.24440908543469	6.18161132876915
F	-4.58030188455826	-8.33727535731285	8.71948838760208

F	-11.76211465856240	-1.96355899215938	10.77331697223980
F	-13.49149216264080	-1.21455406244563	8.82323546236748
F	-13.22504379067460	-2.19886325768926	6.28880428626553
F	-11.22461493470900	-3.93276609213740	5.69572764762974
F	-5.13245474281612	-6.91828667816059	12.79571306240970
F	-5.49009702784437	-6.02313947370711	15.33075009467460
F	-7.48079206877858	-4.23929543718165	15.89703244161480
F	-9.11847970113221	-3.34321743394212	13.92961625620170
C	-6.45343513956777	-6.98920146234520	8.08860099788820
C	-7.32505534251788	-6.55094672308357	7.06355877269637
C	-7.13781350858497	-7.03550224345798	5.77600375460177
C	-6.12175384571927	-7.93868594425301	5.46045199741417
C	-5.26321947617715	-8.37063665965901	6.46975522376008
C	-5.44435570501216	-7.88692374769868	7.76624604270010
C	-10.41192176668410	-3.87117868979607	7.94499446958486
C	-10.54997686677210	-3.36135896705703	9.25804421011125
C	-11.58570034388910	-2.47576596818463	9.52331602722540
C	-12.49186103404290	-2.07392318381480	8.54122857277714
C	-12.35631659304730	-2.57647481022865	7.24816184739915
C	-11.31714802150200	-3.46601888560806	6.97280841583296
C	-7.98868515774727	-4.67024568180450	12.28994258313770
C	-6.95852898016397	-5.59459135556964	11.99653042852990
C	-6.13849463050972	-6.02860470650673	13.02964697515890
C	-6.29792362867575	-5.58594018562799	14.34351916541730
C	-7.31333897115778	-4.67613867858728	14.63240537878980
C	-8.14057664598509	-4.23382094215508	13.59917616000240

IDipp-Ga(PH_2)$_3$ (BP86-D4/def2-TZVP, CPCM = CH_2Cl_2)

C	0.69232024541579	0.20948595243359	-2.08463819017089
C	-0.66747146279364	0.23739624743986	-2.08282719281500
N	-1.06556700693966	0.02750438806501	-0.77212622469911
C	0.00981677787268	-0.12700419172956	0.04858090875499
N	1.08791696068308	-0.01606812310470	-0.77515263569400
H	1.40776613824913	0.31770963441548	-2.88968164834782
H	-1.38196135920654	0.37594477008974	-2.88440211472035
C	2.45919513747065	-0.24101010752928	-0.38791691959347
C	2.93058083274031	-1.56800190237326	-0.39018965782363
C	3.25649018005347	0.86474599537288	-0.05023503992192
C	4.26912214944287	-1.76826695786543	-0.03448586167434
C	4.58728260893713	0.60651478388723	0.30433438182908
C	5.08787016617680	-0.69383946387388	0.31055618779289
H	4.67438280593071	-2.77986665023113	-0.01628792685080
H	5.23931576641099	1.43474903279286	0.58166765828567
C	-2.44257446616398	-0.15620344551806	-0.38482779707534
C	-2.96622987515668	-1.46177070412648	-0.44324892457628
C	-4.31428258058055	-1.62385533577573	-0.10113276443185
C	-5.09263199133717	-0.53236782278249	0.27945440675937
H	-4.75841294249872	-2.61916520222686	-0.12941884254959
C	-4.54136002919721	0.74719788464388	0.32489161280993
H	-5.16378508873514	1.59019058725029	0.62553086668998
C	-3.19900873247124	0.96587871556091	-0.00978700712523
C	-2.13217061903275	-2.64133818895787	-0.91358377179141
H	-1.07207551631012	-2.37101449387001	-0.80265727629283
C	-2.39036436955434	-2.91096056786986	-2.40808420363436
C	-2.36116240469074	-3.91183534765599	-0.08489548962946
H	-2.20399605475325	-3.71803390396239	0.98503390169821
H	-3.37874325245926	-4.30710594493352	-0.21935796515453
H	-1.65805220018922	-4.69371067464965	-0.40599840963659
H	-3.43903661262030	-3.20349449885982	-2.56950332331850
H	-1.74711893947069	-3.72911661059234	-2.76367807833534
H	-2.18744057582236	-2.02326865520721	-3.02284278773122
C	-2.60923717210439	2.36401104905318	-0.01024024321459
H	-1.51463893835945	2.26826512569180	0.04767681130395
C	-2.94469963845917	3.08327585397644	-1.33038425917917
C	-3.06392732309825	3.19715860725431	1.19494932326146
H	-4.13771822450954	3.42990613065296	1.14600343151216
H	-2.86730150616105	2.67317680430829	2.14081964578552
H	-2.51872465526533	4.15140735129128	1.21560523413180
H	-2.58110206030031	2.52103860047946	-2.20179664023701
H	-2.48301038577118	4.08142301335737	-1.34862297498335
H	-4.03329381082410	3.20613497098712	-1.43595029849181
C	2.04091721364573	-2.73316029634679	-0.79143017663073
H	1.00331159427520	-2.45945984792775	-0.54675614332589
C	2.11923737783967	-2.97555330655568	-2.31141597166886
C	2.35387247316013	-4.03053085860328	-0.03619268334276
H	3.33436168007359	-4.44071761946997	-0.31922316569538
H	2.34706318925793	-3.87751652436505	1.05179946040517
H	1.59665064739416	-4.78901339967294	-0.27997385704291
H	1.85017854405139	-2.07949996747046	-2.88566358844734
H	1.43429273380017	-3.78537261735677	-2.60216925023586
H	3.14045237397872	-3.26961708552960	-2.59779256871996
C	2.71851653952403	2.28367645908006	-0.10310421869635
H	1.62875945192522	2.23379682314911	0.04540411950767
C	3.29287293099892	3.18185982865605	0.99955185714595
C	2.98066275223611	2.90731755680850	-1.48768938619705
H	4.06258347140703	2.97671186472887	-1.67739809063766
H	2.53291793149862	2.31490430381992	-2.29676585277499
H	2.55851332694842	3.92197615915295	-1.53344211706829
H	3.18341169169678	2.72195083276307	1.99096136931345
H	2.76052365295463	4.14351964603600	1.00921814209623
H	4.35892556524648	3.39614729203047	0.83397584337175
H	-6.14020825278851	-0.68068577135291	0.54676064768043
H	6.12666620032935	-0.87319477493523	0.59290105777660
Ga	-0.03054860029655	-0.20192526330095	2.10287406250495
P	-0.03474658159214	2.06503079884392	2.89298330509565

H	0.07528515660019	2.71952436156848	1.62712557356574
H	1.37634980177064	2.11475730458835	3.11957648353248
P	-1.95671029524414	-1.39633450822296	2.83423950433984
H	-2.90325281560530	-0.34506849872175	2.63057459030987
H	-1.72474686852686	-1.02371343811039	4.19866145609961
P	1.81132193894912	-1.23150183004993	3.19308813567463
H	2.84473809215168	-0.64935008138631	2.39944440898318
H	1.81408610779234	-2.45587424715545	2.45818715216566

[IDipp·Ga(PH$_2$)$_2$(μ_3-PH$_2${HgC$_6$F$_4$}$_3$)]

(BP86-D4/def2-TZVP, CPCM = CH$_2$Cl$_2$)

Ga	5.27791324028630	6.15773919359910	9.07447531924880
P	4.27335486750120	8.29863585259970	8.81389477074640
P	7.50748307292680	6.02300542121380	8.23985374815930
P	5.11363220143760	5.78722711658240	11.41106638320580
N	4.29656741803010	3.39954299553860	8.24145771755320
N	3.81337986673090	4.82559739119380	6.69936095229410
C	4.31215823190200	4.72915081561410	7.96153905949130
C	3.79668948197050	2.67200584010030	7.17212870259570
H	3.69214779715910	1.59496201886040	7.20801080884070
C	4.60649601623490	2.83461503290700	9.53254948469540
C	6.93897633977990	2.26425910938180	8.65657101001200
H	6.68663661433020	3.05186866489510	7.93017346422130
C	4.37786950362650	6.77775160932520	5.30735645166860
C	5.78552199088500	6.25322263430460	5.09382441156570
H	6.08024656925730	5.70254442428590	6.00256214698700
C	3.59874267846560	2.86671759999920	10.51816326364040
C	3.89804421422140	2.27563372494980	11.75109798953910
H	3.14998162555950	2.28104659923670	12.54346784669180
C	3.95721309490950	7.98470386537210	4.73682400854390
H	4.65979623030780	8.57409826600590	4.15005425449340
C	6.12063105145650	1.69410241191130	10.99308898448490
H	7.09378888029000	1.24638342634220	11.19569206088070
C	3.43016716302090	6.06196139456860	6.06054494138520
C	3.49069715967370	3.57280380976620	6.19880514328930
H	3.05647587879300	3.44446238218410	5.21504493802020
C	5.87603860261460	2.27205821740740	9.74017141483480
C	6.81337016478550	7.36804373800110	4.87287954920780
H	6.67695859262940	7.85796334350220	3.89781099309270
H	7.82840061174810	6.94809339134030	4.89466787366780
H	6.74751339180550	8.13921370009900	5.65364981459860
C	1.73854247097770	7.71071380034520	5.65755584393480
H	0.72309583100120	8.08614068157990	5.79165757402500
C	2.10572749209260	6.49365577673570	6.24788515596500
C	5.14172298166620	1.69019808274160	11.98409401499110
H	5.35344359184040	1.23668026191320	12.95383127166040
C	1.09027117994180	5.70562647597780	7.05800380614530
H	1.56629725285070	4.78016223553170	7.40924534649270
C	2.23437889012720	3.48140847201370	10.24982656061780
H	2.37204816371190	4.28318482562140	9.50880873837450
C	1.60290582945930	4.12589792143260	11.48937947685560
H	1.31924290033510	3.37477354476270	12.24120695100230
H	0.68789907516850	4.66066780680740	11.19766060267980
H	2.29058557513840	4.84433052132200	11.95636587485170
C	8.33471550741470	2.58475632752960	9.20799242766440
H	8.33186155931380	3.52195572499030	9.78152574727540
H	9.04648847080160	2.69692474824120	8.37804343520250
H	8.70735515189110	1.78152543213740	9.86037536359550
C	2.65362254771210	8.44797631232390	4.91177349430520
H	2.34990168472400	9.39264180191580	4.46033783057670
C	0.63509657409630	6.48303151947000	8.30265913766040
H	0.14536908067510	7.42859146728990	8.02687770473300
H	1.48786146707610	6.71876432653140	8.95387405841970
H	-0.08330773699730	5.88343866110140	8.88020288112200
C	6.94406591332500	0.91558449735120	7.91305129196810
H	7.20133803453520	0.09698450857600	8.60228727095260
H	7.68892973500470	0.92933490950650	7.10388223785160
H	5.96336573822160	0.68989514281970	7.47196059450610
C	1.27937795107350	2.43639228512860	9.64153503570340
H	1.68569389102260	1.99341464467770	8.72261375647690
H	0.31355336633280	2.90241047922320	9.39723630265760
H	1.09650816814490	1.62299883680250	10.36002387334130
C	-0.10650334062000	5.29148091162770	6.18555631959820
H	-0.80387619670610	4.67392227146850	6.76997931678180
H	0.22192819418100	4.70900763479200	5.31277002020230
H	-0.65741875975980	6.17096447575520	5.82087849238180
C	5.81698513744850	5.25151568233200	3.92354459679120
H	5.13469912639830	4.40706624223960	4.08998318847180
H	6.83261314561180	4.84932020364800	3.79622369829310
H	5.52278156235050	5.74845882868650	2.98673888883600
F	6.25724516324150	11.12480136502020	4.52254102574180
F	1.34108849102210	12.31669882806840	6.61388546994230
F	4.28216049192190	12.07065993076980	2.92493969688960
F	1.82816829727380	12.66873749275020	3.96883496466120
C	3.56288644038640	11.50678043693460	6.98545989180720
C	4.83256812415340	11.19791327971170	6.44489799273030
C	2.58272535243400	12.00479453002750	6.14055364777830
C	5.04882677444980	11.40619519486370	5.09150544178270
C	4.05507045820410	11.89826122084490	4.24430061924080
C	2.80426049470800	12.20249938895900	4.77661631437280
Hg	5.73015979735760	9.86710011783560	11.13953598386400
Hg	3.14391636211710	11.19904556120410	9.02077396128960
Hg	6.37532623281980	10.43973442996410	7.64950661915710
F	0.61059194275120	11.78849923350270	10.89388404855430

F	4.50819770500790	9.65361194123570	14.09175164600520	C	9.14292667169810	9.48152309971800	8.44027929897140
F	8.42997906330690	8.70454172996230	12.41239547241880	C	8.63251346395570	8.96941029932900	11.08919125638920
F	9.44011586590240	9.71092678663530	7.12800228905530	C	9.89868840258050	8.68399131279580	10.57609855855150
F	11.37556794754510	8.67027167964800	8.71921208695280	C	2.33203693979580	10.50221281523380	13.81685785579780
F	10.86730262725470	8.15800056537220	11.35500003562290	C	1.34122825320780	11.04748189365890	13.00352893441280
F	2.08432563342330	10.29621359869790	15.12772215253800	C	10.15848651462340	8.94684261366060	9.23290065772940
F	0.14046537028180	11.36560834471180	13.53220323964090	H	8.08926000260670	6.50619751101590	9.45271083602280
C	2.83134069354050	10.91399366995680	11.07917342518410	H	7.49903312504210	7.31798229493210	7.64631761600360
C	7.87667801611800	9.74673867131890	8.93899775893940	H	6.14832286691340	4.80280459195680	11.48612601210680
C	3.83900875443580	10.36363119535680	11.90614767788010	H	6.01967486910180	6.86538914388700	11.67912221420040
C	7.61558515804790	9.49026689932910	10.30366879668700	H	3.07873826896100	8.04697123672890	9.54906866844430
C	3.56650920039110	10.17518362276290	13.25289268214520	H	3.65729971919800	8.22890846536360	7.53749804197380
C	1.61168340029520	11.24777947623240	11.64864507388800				

4.5.6 References

[1] A. J. Arduengo, R. Krafczyk, R. Schmutzler, H. A. Craig, J. R. Goerlich, W. J. Marshall, M. Unverzagt, *Tetrahedron* **1999**, *55*, 14523–14534.

[2] N. Marion, E. C. Escudero-Adán, J. Benet-Buchholz, E. D. Stevens, L. Fensterbank, M. Malacria, S. P. Nolan, *Organometallics* **2007**, *26*, 3256–3259.

[3] R. Klement, G. Brauer, *Handbuch der Präparativen Anorganischen Chemie*, Ferdinand Elke Verlag, Stuttgart, **1987**.

[4] H. Schäfer, G. Fritz, W. Hölderich, *Z. anorg. allg. Chem.* **1977**, 222.

[5] P. Sartori, A. Golloch, *Chem. Ber.* **1968**, *101*, 2004–2009.

[6] V. N. Mikhaylov, I. V. Kazakov, T. N. Parfeniuk, O. V. Khoroshilova, M. Scheer, A. Y. Timoshkin, I. A. Balova, *Dalton Trans.* **2021**, *50*, 2872–2879.

[7] O. V. Dolomanov, L. J. Bourhis, R. J. Gildea, J. A. K. Howard, H. Puschmann, *J. Appl. Crystallogr.* **2009**, *42*, 339–341.

[8] a) F. Neese, *Wiley Interdiscp. Rev.-Comput. Mol. Sci.* **2012**, *2*, 73–78; b) F. Neese, *Wiley Interdiscp. Rev.-Comput. Mol. Sci.* **2018**, *8*; c) F. Neese, F. Wennmohs, U. Becker, C. Riplinger, *J. Chem. Phys.* **2020**, *152*, 224108.

[9] "Chemcraft - Graphical program for visualization of quantum chemistry computations", https://www.chemcraftprog.com/index.html, **2017**.

[10] A. D. Becke, *J. Chem. Phys.* **1993**, 5648–5652.

[11] E. Caldeweyher, C. Bannwarth, S. Grimme, *J. Chem. Phys.* **2017**, *147*, 34112.

[12] E. Caldeweyher, S. Ehlert, A. Hansen, H. Neugebauer, S. Spicher, C. Bannwarth, S. Grimme, *J. Chem. Phys.* **2019**, *150*, 154122.

[13] C. Lee, W. Yang, R. Parr, *Phys. Rev. B* **1988**, 785–789.

[14] F. Weigend, R. Ahlrichs, *Phys. Chem. Chem. Phys.* **2005**, *7*, 3297–3305.

[15] F. Neese, F. Wennmohs, A. Hansen, U. Becker, *Chem. Phys.* **2009**, *356*, 98–109.

[16] E. D. Glendening, C. R. Landis, F. Weinhold, *J. Comput. Chem.* **2013**, *34*, 1429–1437.

[17] a) V. N. Staroverov, G. E. Scuseria, *J. Chem. Phys.* **2003**, 12129; b) J. Tao, J. P. Perdew, V. N. Staroverov, G. E. Scuseria, *Phys. Rev. Lett.* **2003**, *91*, 146401.

[18] A. E. Reed, L. A. Curtiss, F. Weinhold, *Chem. Rev.* **1988**, 899–926.

[19] A. D. Becke, *Phys. Rev. A* **1988**, *38*, 3098–3100.

[20] J. P. Perdew, *Phys. Rev. B* **1986**, *33*, 8822–8824.

[21] D. A. Pantazis, X.-Y. Chen, C. R. Landis, F. Neese, *J. Chem. Theory Comput.* **2008**, *4*, 908–919.

[22] E. van Lenthe, J. G. Snijders, E. J. Baerends, *J. Chem. Phys.* **1996**, *105*, 6505–6516.

[23] V. Barone, M. Cossi, *J. Phys. Chem. A* **1998**, *102*, 1995–2001.

[24] L. Goerigk, S. Grimme, *J. Chem. Theory Comput.* **2011**, *7*, 291–309.

[25] a) J. Contreras-García, E. R. Johnson, S. Keinan, R. Chaudret, J.-P. Piquemal, D. N. Beratan, W. Yang, *J. Chem. Theory Comput.* **2011**, *7*, 625–632; b) A. Otero-de-la-Roza, E. R. Johnson, J. Contreras-García, *Phys. Chem. Chem. Phys.* **2012**, *14*, 12165–12172.

[26] T. Lu, F. Chen, *J. Comput. Chem.* **2012**, *33*, 580–592.

4.6 Author contributions

- R. Szlosek – writing of the original draft, all experimental work including reproduction of **1a**, quantum chemical calculations, acquisition of X-ray data
- M. A. K. Weinhart – original discovery of **1a** and acquisition of the corresponding single-crystal X-ray diffraction data
- G. Balázs – project management, conceptualization
- M. Seidl – finalization of single-crystal X-ray diffraction data
- L. Zimmermann – acquisition of all IR data
- M. Scheer – project supervision, acquisition of funding, co-writing of final manuscript

5 A general Pathway towards NHC·GaH$_2$(OTf) adducts – The key for the Synthesis of NHC-stabilized cationic 13/15 Chain Compounds of Gallium

R. Szlosek, M. Seidl, G. Balázs and M. Scheer

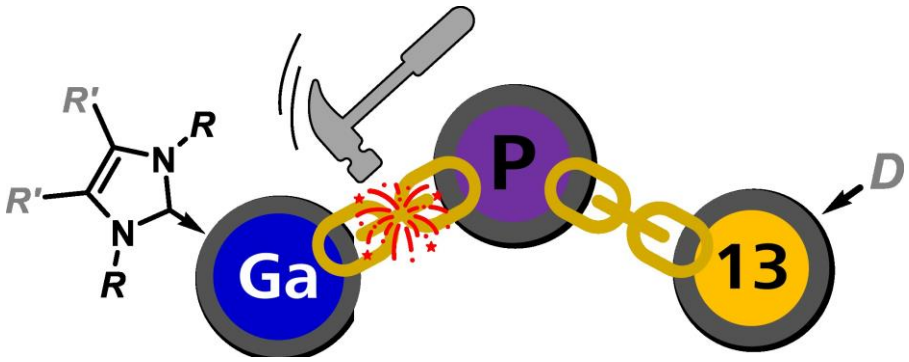

Abstract: A general pathway towards NHC (NHC = N-heterocyclic carbene)-stabilized galliummonotriflates NHC·GaH$_2$(OTf) (NHC = IDipp, **1a**; IPr$_2$Me$_2$, **1b**; IMes, **1c**; IDipp = 1,3-bis(2,6-diisopropylphenyl)-imidazolin-2-ylidene, IPr$_2$Me$_2$ = 1,3-bis-(diisopropyl)-4,5-dimethyl-imidazolin-2-ylidene, IMes = 1,3-bis(2,4,6-trimethylphenyl)-imidazolin-2-ylidene) is reported. Quantum chemical calculations give detailed insight into the underlying reaction pathway. The obtained NHC·GaH$_2$(OTf) compounds were employed in reactions with donor-stabilized pnictogenylboranes to synthesize the elusive cationic parent 13/15/13 chain compounds [IDipp·GaH$_2$ER$_2$E'H$_2$·D][OTf] (**3a**: D = IDipp, E = P, E' = B, R = H; **3b**: D = NMe$_3$, E = P, E' = B, R = H, **3c**: D = NMe$_3$, E = P, E' = B, R = Ph, **3d**: D = IDipp, E = P, E' = Ga, R = H). Supporting computational studies highlight the electronic features of the products.

5.1 Introduction

Semiconductor materials such as GaAs represent the backbone of almost all modern digital devices. In industry, thin layers of, for example, GaAs are obtained by metal–organic chemical vapor deposition (MOCVD) from $GaMe_3$ and AsH_3.[1] With the rapidly increasing demand for smaller and more powerful electronics, the research for suitable 13/15 compounds as useful precursor compounds has expanded. The first milestones in this field were, however, already set a long time ago, starting with compounds such as $H_3N{\cdot}BF_3$, borazine and $Me_3N{\cdot}BH_3$.[2] Compared to their organic counterparts, the 13/15 compounds differ in terms of their reactivity and physical properties due to polarized bonding. The chemistry of 13/15 compounds was especially pushed by the concept of single-source precursors in the late 20th century, where a group 13 and a group 15 element are fixed in a single compound that can then be used for MOCVD processes.[3] Of special interest are the parent hydrogen-bearing compounds that are isoelectronic to their organic counterparts (i. e., $H_2E\text{-}MH_2 \rightarrow H_2C{=}CH_2$, $HE{=}MH \rightarrow HC{\equiv}CH$; E=triel, M=pnictogen) and are lighter in molecular weight and thus, more volatile than their alkyl-substituted versions. Besides possessing a well-defined stoichiometry for controlled deposition, the atomic diversity of 13/15 substrates is beneficial for achieving unusual materials. Besides applications for the semiconductor industry, 13/15 compounds are also considered as candidates for lightweight hydrogen storage materials.[4]

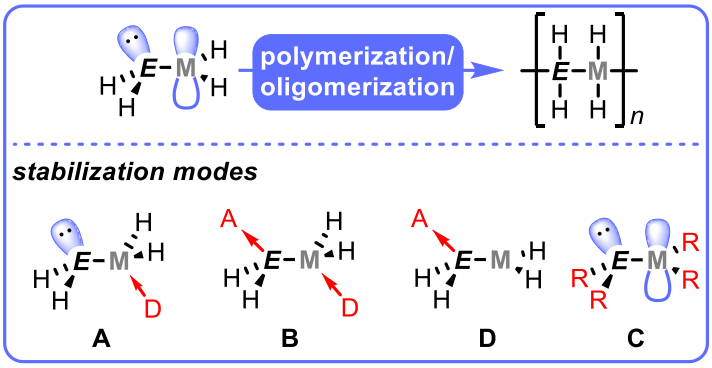

Figure 5.1: Different stabilization modes of 13/15 monomeric compounds (E = group 15 element, M = group 13 element): A) stabilization by only a single donor, B) stabilization by simultaneous donor and acceptor interaction, C) stabilization by acceptor only, D) stabilization by bulky organic residues.

Typical 13/15 monomers are prone to undergoing spontaneous head-to-tail oligo- or polymerization and thus require additional stabilization (Figure 5.1).[5] The easiest way to achieve this, is by a donor system such as tertiary amines, *β*-diketiminates (Nacnac) or *N*-heterocyclic carbenes (NHC, type **A**). Especially with NHCs and Nacnac donor systems, a huge variety of 13/15 compounds was enabled ranging from the parent phosphanyl, arsanyl and stibanyl gallanes to phosphanyl phosphagallenes and many other spectacular results.[6] Also, simultaneous stabilization by an acceptor and a donor attached to the monomer has been used in the past for the stabilization of parent phosphanylalanes (type **B**).[7] Although plausible, stabilization by a single acceptor only (type **C**) has not been realized experimentally so far. Furthermore, bulky organic residues play a crucial role in the stabilization of the said monomers and other low-valent group 13 species, especially with emphasis on their versatile use as Frustrated Lewis Pairs (FLPs) in synthesis and catalysis.[8] In the past, our group showed that trimethylaminestabilized pnictogenylboranes can be functionalized with neutral,[9,10,11] anionic[12] or cationic fragments,[9,10,13–15] leading to elongated chain-like 13/15 monomers (Figure 5.2). In the latter case, three- or even five-membered chain compounds could be obtained by reaction of $NMe_3{\cdot}BH_2EH_2$ with $BH_2I{\cdot}NMe_3$ or 0.5 $BH_2I{\cdot}SMe_2$, respectively (E = P, As).[14,15] Besides these catenation reactions, controlled oligo/polymerization,[10,16] coordination[10,17] and oxidation capabilities of Lewis base-stabilized pnictogenylboranes

could also be demonstrated.[9,18] In all of these reactions, boron was used as group 13 element because of the high stability of the resulting products.

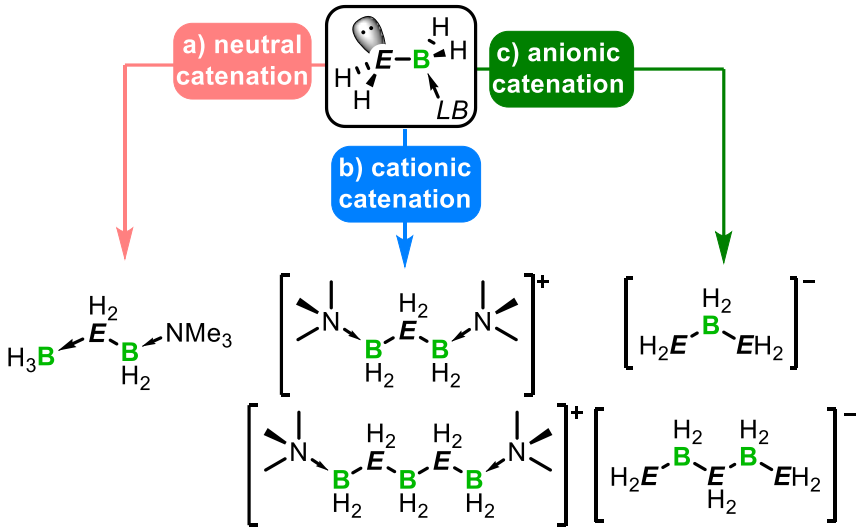

Figure 5.2: Overview of *catena* extensions of Lewis base-stabilized parent pnictogenylborane monomers (E = P, As, LB = Lewis base). Description of depicted pathways: a) reaction with neutral group 13 sources such as BH_3·SMe_2, b) reaction with suitable $[BH_2]^+$ synthons such as Me_3N·BH_2I or Me_2S·BH_2I, c) reaction with group 15 $[EH_2]^-$ sources such as $NaPH_2$ or $KAsH_2$.

However, analogous parent chain compounds with the heavier group 13 homologues are unknown so far. Investigations on these compounds are hampered by the intrinsically low bond energies between the heavy group 13 elements and phosphorus or arsenic, often resulting in the extreme sensitivity of such products towards air and thermal decomposition already at room temperature.[19–21] Furthermore, the needed monomers themselves are difficult to generate in larger quantities, which are necessary for in-depth studies.[19,20] Thus, the question arises as to whether especially charged 13/15 chain compounds including group 13 elements heavier than boron are accessible at all, despite the low tendency to form stable bonds, and which donors would be suitable to keep the core motifs intact. Herein, the preparation of novel NHC-stabilized galliummonotriflates is reported, which were used for the synthesis of unprecedented cationic 13/15/13 chains with {GaH_2} links, stabilized by two separate donor systems.

5.2 Results and Discussion

First, the reactivity of NHC-stabilized phosphanylgallane IDipp·GaH_2PH_2 with suitable group 13 electrophiles which could enable cationic catenation was investigated. Therefore, reactions with BH_2I·NMe_3 were attempted (Scheme 5.1). However, no reaction was observed, since the nucleophilicity of IDipp·GaH_2PH_2 is too low to substitute iodide from BH_2I·NMe_3. Even if iodide was replaced by the superior leaving group triflate, no reaction took place. Then, reactions of BH_2Cl·NMe_3 in the presence of halide abstractors such as $AlCl_3$ and Tl[TEF] (TEF=[Al{$OC(CF_3)_3$}$_4$]$^-$) were attempted,[22] which, unfortunately, led to the decomposition of the starting material, presumably via cleavage of the Ga-P bond. The introduction of alkyl groups at the phosphorus atom did not provide steps forward towards the desired reactivity.

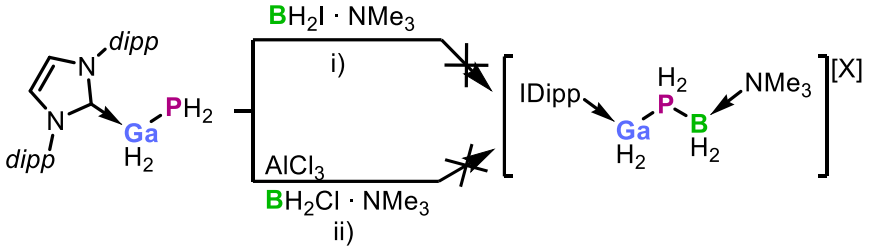

Scheme 5.1: Attempted cationic catenations of IDipp·GaH$_2$PH$_2$ with BH$_2$I·NMe$_3$ and BH$_2$Cl·NMe$_3$/AlCl$_3$ (X = I, AlCl$_4$). Reaction conditions: i) Et$_2$O, -80 °C → r.t., 16 h, ii) CH$_2$Cl$_2$, -80 °C → r.t., 2 h.

A different approach to the targeted products could be realized by reversing the reaction principle and combining donor-stabilized phosphanylboranes *D*·BH$_2$PH$_2$ with a [NHC·GaH$_2$]$^+$ synthon such as IDipp·GaH$_2$I described by Radius *et al.*[23] According to preliminary NMR data, these reactions showed full conversion of the starting material (see Supporting Information). However, it was not possible to grow single crystals for X-ray structure determination for an unambiguous proof of connectivity. Thus, as an alternative, we targeted the introduction of a different leaving group such as triflate ([OTf]$^-$ = [SO$_3$CF$_3$]$^-$) at the Ga atom. Interestingly, such starting materials have not been described in literature. The addition of Me(OTf) to a solution of NHC·GaH$_3$ (NHC = IDipp (1,3-Bis-(2,6-diisopropylphenyl)-imidazolin-2-ylidene, **1a**), IMes (1,3-Bis-(2,4,6-trimethylphenyl)-imidazolin-2-ylidene, **1b**), IPr$_2$Me$_2$ (1,3-Bis-(diisopropyl)-4,5-dimethylimidazolin-2-ylidene, **1c**)) in toluene results in a visible extrusion of methane and the precipitation of the unprecedented galliummonotriflates NHC·GaH$_2$(OTf) (Scheme 5.2a). After work-up, the compounds are obtained as air sensitive colourless solids in isolated yields between 77–88% that can be stored for months under an inert atmosphere at -30°C.

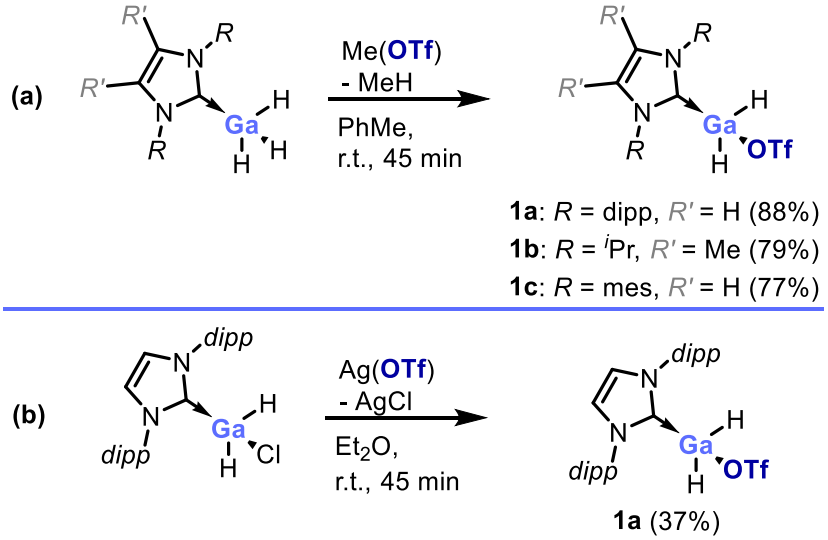

Scheme 5.2: Synthesis of NHC-stabilized galliummonotriflates by elimination of methane (a) or salt metathesis with Ag(OTf) (b). Isolated yields are given in parentheses.

Alternatively, by reacting IDipp·GaH$_2$Cl with Ag(OTf) (Scheme 5.2b), similar products can also be synthesized by salt metathesis, which gives somewhat lowered yields and needs an additional filtration step. The ^{1}H NMR spectra of **1a–c** show characteristic, broadened singlets for the GaH$_2$ unit at 4.88 ppm (**1a**, C$_6$D$_6$, 2 H), 4.22 ppm (**1b**, CD$_2$Cl$_2$, 2 H), and 5.62 ppm (**1c**, C$_6$D$_6$, 2 H), besides the characteristic signals of the corresponding NHC moieties. The ^{19}F{^{1}H} NMR spectra of all three compounds show a singlet between -77.3 and -77.6 ppm for bound [OTf]$^-$ moieties, which is slightly shifted downfield compared

to the unbound $[OTf]^-$ anion (-79 ppm, cf. Supporting Information). The mass spectra reveal peaks of $[IDipp{\cdot}GaH_2]^+$ at m/z = 459.25 (**1a**, LIFDI-MS), $[IPr_2Me_2{\cdot}GaH_2]^+$ at m/z = 253.11 (**1b**, ESI-MS), and $[IMes{\cdot}GaH_2]^+$ at m/z = 375.31 (**1c**, ESI-MS). Single crystals of **1a** were grown by slow evaporation of a concentrated solution in benzene and of **1b** by cooling a saturated solution in toluene to -28°C overnight. Unfortunately, all attempts at crystallizing **1c** have failed so far. **1c** can be readily isolated as a microcrystalline powder though.

1a crystallizes in the acentric orthorhombic space group $P2_12_12_1$ as clear colourless block-shaped crystals (Figure 5.3; Flack parameter: -0.016(8)). The asymmetric unit shows one formula unit of IDipp·GaH_2(OTf). The triflate group is arranged almost perpendicular to the $\{CGaH_2\}$ part with a $C_{carbene}$-Ga-O angle of 99.27(9)°, indicative of weak bonding towards the gallium atom with a long Ga-OTf distance of 1.991(2) Å. This distance is also well above the sum of covalent radii of a Ga-O single bond (1.87 Å),[24] underlining this weak interaction. Overall, the structure is more resembling of a $[IDipp{\cdot}GaH_2]^+$ ion with a loose interaction of the triflate ion.

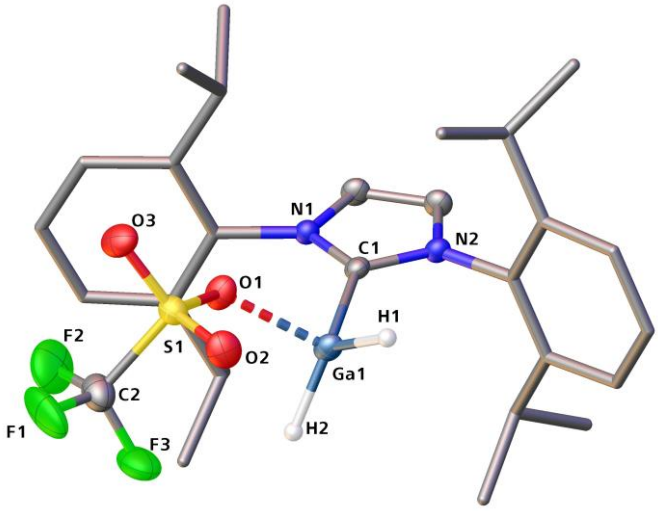

Figure 5.3: Molecular structure of **1a** in the solid state. Anisotropic displacement ellipsoids are shown at 50% probability level. Hydrogen atoms bound to carbon are omitted for clarity. Dipp groups are displayed as a stick model for improved clarity. Selected bond lengths [Å] and angles [°]: N1-C1 1.350(3), N2-C1 1.347(3), C1-Ga1 2.039(3), Ga1-H1 1.51(4), Ga-H2 1.49(4), Ga1-O1 1.991(2), O1-S1 1.4781(19), S1-O2 1.427(2), S1-O3 1.427(2), S1-C2 1.822(3), C2-F1 1.328(4), C2-F2 1.318(4), C2-F3 1.327(4), N1-C1-Ga1 130.94(19), N2-C1-Ga1 123.62(18), C1-Ga1-O1 99.27(9), C1-Ga1-H1 113.5(14), C1-Ga-H2 113.7(14), H1-Ga1-H2 123(2), Ga1-O1-S1 127.35(12).

1b crystallizes in the orthorhombic space group *Pbca* as clear colourless prism-shaped crystals. The asymmetric unit shows one formula unit of $IPr_2Me_2{\cdot}GaH_2$(OTf). When grown, the crystal structure reveals a one-dimensional polymeric network with μ_2-bridging triflates as a zigzag chain (Figure 5.4). The NHC units are oriented perpendicular to each other around the main $\{GaOTf\}_\infty$ strand. The O-Ga distance is extremely long and lies between 2.3777(15)–2.2533(15) Å but still well below the sum of the van der Waals radii (3.39 Å). The O-Ga-O angle of 174.64(5)° is close to 180° and together with a $C_{carbene}$-Ga-O angle of 86.10(7)–88.54(7)° highlights the slightly distorted trigonal bipyramidal structure. Overall, all this nicely illustrates the influence of the sterics of the NHC on the molecular structure of these adducts, as the larger NHCs in, for example, **1a** prevent the formation of polymeric structures.

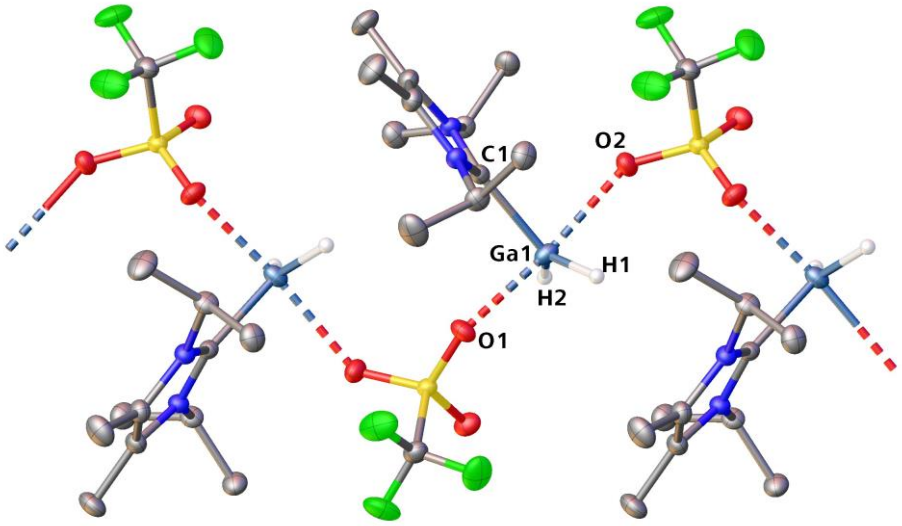

Figure 5.4: 1D polymeric structure of **1b** in the solid state. Anisotropic displacement ellipsoids are shown at 50% probability level. Hydrogen atoms bound to carbon are omitted for clarity. Selected bond lengths [Å] and angles [°]: C1-Ga1 2.0281(19), Ga1-H1 1.46(2), Ga1-H2 1.46(3), Ga1-O2 2.3777(15), Ga1-O1 2.2533(15), C1-Ga1-O1 88.54(7), C1-Ga1-O2 86.10(7), H1-Ga1-H2 126.8(13), C1-Ga1-H1 117.0(9), C1-Ga1-H2 115.8(10), O1-Ga1-O2 174.64(5).

Interestingly, several similar reactions are described in the literature. Rivard and co-workers reacted IMes·GaH$_3$ with Me(OTf) in CH_2Cl_2 over the course of 16 h and observed exclusively di-triflation leading to IMes·GaH(OTf)$_2$.[25] On the other hand, Radius and coworkers could selectively synthesize NHC·GaH$_2$I by the analogous reaction of NHC·GaH$_3$ with a large excess of MeI in toluene.[23] To compare our results with the results achieved by the Rivard and Radius groups, experimental and theoretical investigations were performed. As MeI displays a slightly lower reactivity than Me(OTf) and thus slower reaction progress, the sequential iodination of IDipp ·GaH$_3$ with MeI was chosen as a model system as this allowed for easier reaction monitoring. First, the influence of the solvent used was tested. The reaction of IDipp·GaH$_3$ in the presence of an excess amount of MeI in CH_2Cl_2 or toluene (30-45 min) at room temperature in both cases yields exclusively the monoiodinated product according to ^{1}H NMR spectroscopy, upon which the influence of the solvent regarding the product formation could be excluded. When the stirring time is increased to 16 h however, full conversion towards di-iodinated IDipp·GaHI$_2$ is observed by ^{1}H NMR spectroscopy (Eq. (1), Figure 5.5). This result indicates that the first reaction step happens almost instantaneously, which then deactivates the hydrides bound to the gallium atom and hence drastically slows down the reaction rate for the second reaction with MeI. It was also tested, if full conversion to IDipp·GaI$_3$ is possible by reacting IDipp·GaH$_3$ with an excess amount of MeI in boiling toluene overnight. According to ^{1}H NMR spectroscopy, no gallium hydride peak is found anymore (see Supporting Information), which indicates full conversion of the starting material as well as the intermediates. However, the spectrum clearly shows a product mixture of several species, which might be the result of ongoing side reactions.

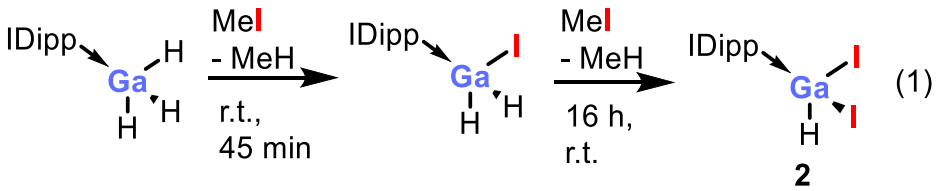

To further probe our assumptions, we performed quantum chemical calculations at the robust DLPNO-CCSD(T)/def2-QZVP//B3LYP-D4/def2-TZVP[26,27,28] level of theory on the model reaction of

IPr$_2$Me$_2$·GaH$_3$ in three subsequent iodination steps (see Supporting Information). The calculated reaction pathway shows that all three iodination steps are exergonic and therefore show favourable thermodynamics. Most importantly though, the second transition state lies +3.42 kcal mol^{-1} higher in energy than the first. According to the transition state theory by Eyring and Polanyi,[29] the first iodination is faster compared to the second by $k_1 = 325 \times k_2$ at $T = 298$ K, which agrees with the observed reactivity. For the still bulkier IDipp or IMes, an even more pronounced difference in reaction rates could be expected.

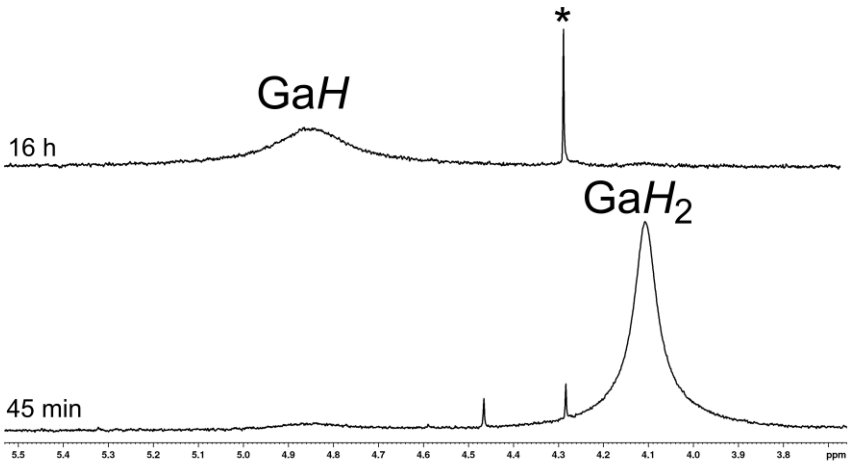

Figure 5.5: Comparison of sections of the ^{1}H NMR spectra of the reaction of exc. MeI with IDipp · GaH$_3$ after 45 min and after 16 h (C_6D_6, 298 K, * = unidentified impurity).

With the novel NHC-stabilized galliummonotriflates at hand, it was then possible to address the question as to whether reactions of pnictogenylboranes lead to new cationic 13/15 chain compounds containing gallium. Therefore, IDipp·BH$_2$PH$_2$ was reacted with **1a** by stirring for 30 min at room temperature in *o*-difluorobenzene (Eq. (2)).[32] NMR spectroscopic monitoring revealed full conversion of the starting material after this time (see Supporting Information). By layering the solution with *n*-hexane at -30°C, large single crystals of the unprecedented 13/15 cationic chain compound [IDipp·GaH$_2$PH$_2$BH$_2$·IDipp][OTf] (**3a**) were obtained (Figure 5.6). Characteristic NMR spectroscopic data are summarized in Table 5.1. Note that all signals in the ^{31}P and ^{11}B NMR spectra appear strongly broadened due to quadrupolar relaxation induced by the boron and gallium nuclei ($\omega_{1/2} > 100$ Hz). **3a** also shows a characteristic doublet in the ^{1}H NMR spectrum for the {GaH$_2$} unit with a coupling constant of $^2J_{HP} = 38$ Hz. The molecular ion peak for **3a** is detected in the ESI-MS spectrum at $m/z = 893.53$.

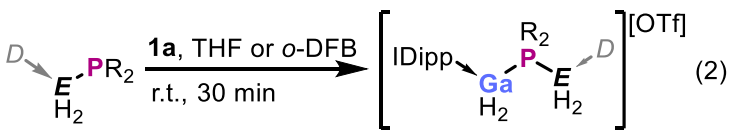

(2)

3a: *D* = IDipp, ***E*** = **B**, R = H, 46%
3b: *D* = NMe$_3$, ***E*** = **B**, R = H, 42%
3c: *D* = NMe$_3$, ***E*** = **B**, R = Ph, 72%
3d: *D* = IDipp, ***E*** = **Ga**, R = H, 50%

Table 5.1: Heteronuclear NMR chemical shifts and signal multiplicities of compounds **3a**-**d** [ppm] (298 K).[33]

NMR spectrum	**3a** (CD_2Cl_2)	**3b** (CD_2Cl_2)	**3c** (CD_2Cl_2)	**3d** (*o*-DFB)
$^{31}P\{^1H\}$	-168.2, s, br	-176.5, s, br	-39.9, s, br	-220.0, s
^{31}P	-168.2, t, br	-176.5, t, br	-39.9, s, br	-220.0, t(qt)
$^{11}B\{^1H\}$	-35.0, s, br	-11.3, s, br	-7.6, s, br	-
^{11}B	-35.0, s, br	-11.3, s, br	-7.6, s, br	-
$^{19}F\{^1H\}$	-79.1, s	-79.1, s	-78.7, s	-78.6, s

3a crystallizes in the monoclinic space group $P2_1/c$ as clear colourless blocks (Figure 5.6, top left), which are highly air- and temperature-sensitive. The asymmetric unit shows one molecule of **3a**, which is disordered at all chain atom positions (see Supporting Information). The core chain motif shows Ga-P and B-P bond distances of the range of classic single bonds with 2.379(7) Å (Ga-P, cf. IDipp·GaH$_2$PH$_2$: 2.3373(6) Å) and 1.949(10) Å (P-B, cf. Me$_3$N·BH$_2$PH$_2$: 1.976(2) Å). The Ga-P-B angle of 103.8(3)° is considerably smaller compared to the B-P-B angle within [Me$_3$N·BH$_2$PH$_2$BH$_2$·NMe$_3$]$^+$ (107.5(8)°) as a result of the steric influence of the attached IDipp moieties. The chain itself reveals a nearly antiperiplanar zigzag conformation with a torsion angle of -165.9(5)° (C1-B1-P1-Ga1).

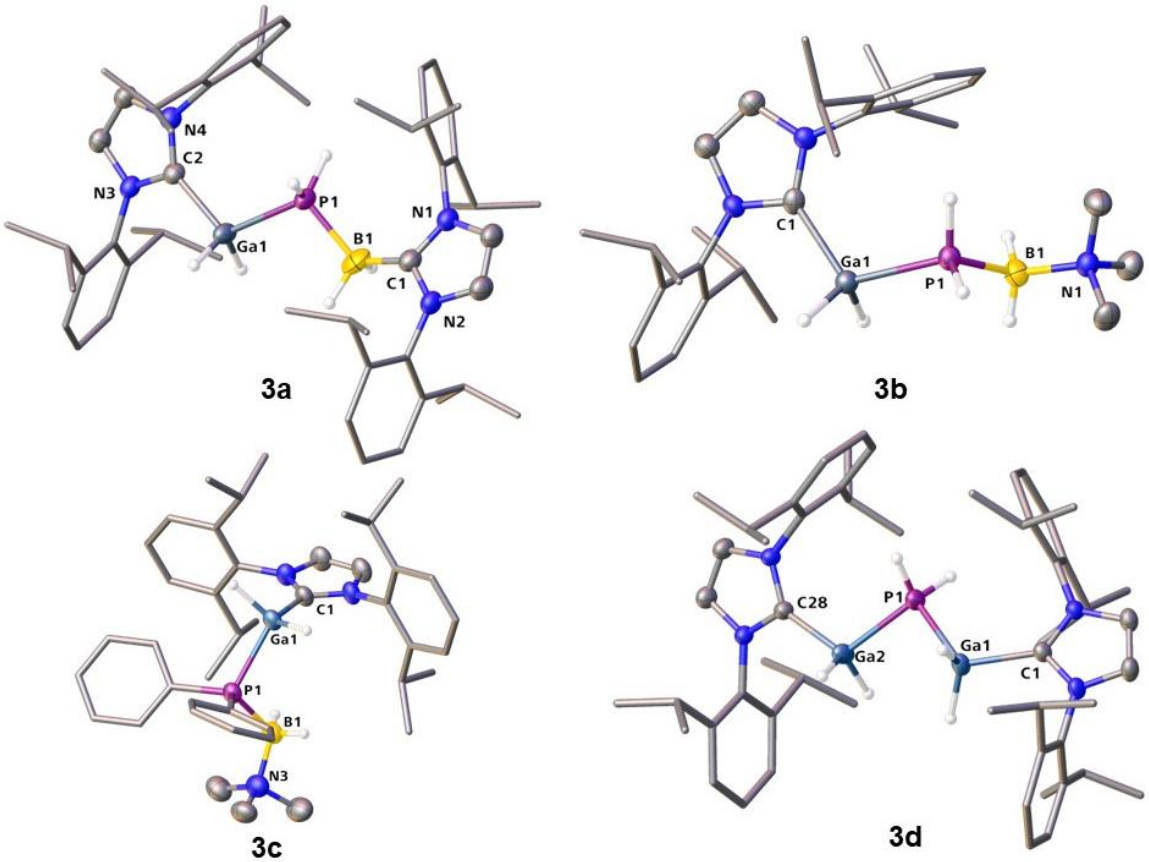

Figure 5.6: Molecular structures of **3a**-**d** in the solid state. Anisotropic displacement ellipsoids are shown at 50% probability level. Hydrogen atoms bound to carbon and the triflate anions are omitted for clarity. Dipp groups are displayed as a stick model for improved clarity. Selected bond lengths [Å] and angles [°]: 3a: N1-C1 1.347(4), N2-C1 1.354(4), C1-B1 1.601(11), B1-P1 1.949(10), P1-Ga1 2.3731(15), Ga1-C2 2.055(3), C2-N3 1.355(3), C2-N4 1.343(3), N1-C1-B1 127.5(4), N2-C1-B1 127.2(4), C1-B1-P1 119.6(5), B1-P1-Ga1 103.8(3), P1-Ga1-C2 114.40(8), Ga1-C2-N3 120.92(19), Ga1-C2-N4 134.3(2). 3b: C1-

Ga1 2.054(7), Ga1-P1 2.4002(16), P1-B1 1.959(8), B1-N1 1.597(9), C1-Ga1-P1 111.62(17), Ga1-P1-B1 111.5(2), P1-B1-N1 116.2(5). 3c: C1-Ga1 2.044(2), Ga1-P1 2.4007(7), P1-B1 1.965(3), B1-N3 1.612(4), C1-Ga1-P1 114.15(7), Ga1-P1-B1 106.99(9), P1-B1-N3 120.1(2). 3d: C1-Ga1 2.032(3), Ga1-P1 2.3831(10), P1-Ga2 2.3658(10), Ga2-C28 2.032(3), C1-Ga1-P1 112.85(10), Ga1-P1-Ga2 100.61(4), P1-Ga2-C28 113.95(10).

Despite observing the formation of a stable, though highly air-sensitive chain compound, which decomposes slowly at room temperature, the question arose if the simultaneous stabilization by two bulky donors imposes a necessary requirement to keep the central structural motif intact or if the steric demand can be further reduced. Thus, $PH_2BH_2{\cdot}NMe_3$ was reacted with **1a** by stirring in *o*-difluorobenzene at room temperature for 30 min (Eq. (2)). By subsequent layering with *n*-hexane at -30°C, clear colourless plates of [IDipp·GaH$_2$PH$_2$BH$_2$·NMe$_3$][OTf] (**3b**) were obtained. **3b** shows a drastically higher sensitivity towards air than **3a** and decomposes faster at room temperature. Characteristic heteronuclear NMR data for **3b** are given in Table 5.1. Additionally, the ^{1}H NMR spectrum shows a broadened doublet at 3.60 ppm for the {GaH$_2$} unit ($^2J_{HP}$ = 33 Hz) and a doublet of multiplets for the {PH$_2$} protons between 1.50 and 2.30 ppm ($^1J_{HP}$ = 322 Hz). In the ESI-MS spectrum, the molecular ion peak of [IDipp·GaH$_2$PH$_2$BH$_2$·NMe$_3$]$^+$ was detected at *m*/*z* = 564.48. **3b** crystallizes in the monoclinic space group *Cc* as clear colourless plates (Flack parameter: -0.01(3), Figure 5.6, top right)). The asymmetric unit contains one molecule of **3b** and does not show any disorder at the chain positions, in contrast to **3a** (cf. Supporting Information). The Ga-P distance is slightly elongated towards 2.400(15) Å compared to **3a** and is indicative of a weakened Ga-P bond. The B-P bond within **3b** is 1.960(8) Å long and has thus almost the same length as the B-P bond in **3a**. The Ga-P-B angle of 111.5(2) Å is significantly larger than that in **3a**, indicating the weaker steric influence of the NMe$_3$ group compared to IDipp in **3a**. Furthermore, the central chain is arranged in an antiperiplanar conformation with a Ga1-P1-B1-N1 torsion angle of -175.0(4)°.

Judging by the crystal structures of the parent compounds **3a** and **3b**, it could be assumed that the sterical arrangement should leave enough space to include organic residues at the chain motif. To test this hypothesis, **1a** was reacted with $NMe_3{\cdot}BH_2PPh_2$ in *o*-difluorobenzene (Eq. (2)). By subsequent layering with *n*-hexane at -30°C, large colourless crystals were obtained, which were identified as the desired chain compound [IDipp·GaH$_2$PPh$_2$BH$_2$·NMe$_3$][OTf] (**3c**) by multinuclear NMR spectroscopy, ESI-MS and X-ray crystallography (Figure 5.6, bottom left). Just as **3a** and **3b**, **3c** displays high sensitivity towards air and decomposes at room temperature. **3c** shows characteristic, strongly broadened signals (see Table 5.1) in both ^{31}P and ^{11}B NMR spectra due to quadrupolar relaxation. The ^{1}H NMR spectrum features a broadened doublet at 3.92 ppm for the {GaH$_2$} unit ($^2J_{HP}$ = 38 Hz). In the ESI-MS spectrum, the molecular ion peak of [IDipp·GaH$_2$PPh$_2$BH$_2$·NMe$_3$]$^+$ was detected at *m*/*z* = 716.34. **3c** crystallizes in the triclinic space group *P*-1 as clear colourless blocks (Figure 5.6). Overall, the bond lengths are very similar to those in **3b** (Ga-P: 2.4010(7) Å, P-B: 1.963(3) Å, B-N: 1.611(4) Å) and all within the range of single bonds. The same accounts for the corresponding bond angles (Ga-P-B: 107.03(9)°, P-B-N: 120.24(19)°). The chain motif is arranged in near perfect antiperiplanar conformation with a Ga1-P1-B1-N1 dihedral angle of 175.7(2)°.

Seeing how well the NHC-stabilized galliummonotriflates underwent nucleophilic substitution, it could be questioned whether NHC-stabilized phosphanylgallane IDipp·GaH$_2$PH$_2$ as an even weaker donor would also undergo such a transformation. Although such a symmetric species would impose a certain stability, the low Ga-P bonding energy might prevent the isolation of the desired cationic chain compound. Thus, a mixture of **1a** and IDipp·GaH$_2$PH$_2$ in *o*-difluorobenzene was stirred for 30 min and the reaction mixture layered with *n*-hexane at -30°C (Eq. (2)). That way, highly air-sensitive crystals of [IDipp·GaH$_2$PH$_2$GaH$_2$·IDipp][OTf] (**3d**) were obtained after two weeks, which decompose at room temperature (Figure 6). **3d** represents the first example of the parent 2e-donor stabilized 13/15 cationic chain compound including only heavy group 13 elements. **3d** displays extreme lability and immediately

converts back to the starting materials when dissolved in THF or CH_2Cl_2. However, **3d** is stable in *o*-difluorobenzene, indicating that the IDipp·GaH_2PH_2 unit is easily replaced by other donor molecules. The ^{31}P NMR spectrum of **3d** in a solution of 1,2-difluorobenzene (C_6D_6-capillary, r.t.) shows a triplet of quintets at -220.0 ppm with coupling constants of $^1J_{HP}$ = 278 Hz and $^2J_{HP}$ = 45 Hz. In the ESI-MS spectrum, strong fragmentation together with the release of methane is observed, leading to a molecular ion peak of {[IDipp·$GaH_2PH_2GaH_2$·IDipp]$^+$ - CH_4} diminished by methane at *m*/*z* = 937.50. **3d** crystallizes as clear irregular blocks in the acentric orthorhombic space group *Pna*2$_1$ (Figure 5.6, bottom right; Flack parameter -0.044(15)). The structure in the solid state adapts a slightly distorted arrangement with a highly bent central Ga1-P-Ga2 bond angle of 100.61(4)°. The Ga-P bond lengths of 2.3658(9) Å and 2.3831(10) Å are slightly asymmetric due to steric reasons and within the range of single bonds. The C1-Ga1-P1-Ga1 torsion angle of 147.76(11)° reveals an anticlinal conformation.

To further examine the bonding situation of the obtained chain compounds, quantum chemical computations were performed (Table 5.2). According to NPA charge analysis[30] (TPSSh/def2-TZVP//B3LYP-D4/def2-TZVP),[27,28,31] the central chain motifs display a large degree of polarization. Compound **3a**, for example, bears a total charge of +0.43 for the entire {$GaH_2PH_2BH_2$} core structure and thus highlights the electron deficiency compensated by the two donors. **3c–d** show a similar trend (Table 5.2), though the phenyl rings at **3c** overall reduce the positive charge on the chain structure. Furthermore, the H atoms at Ga also display a considerably hydridic character in contrast to the H atoms at B. The Wiberg Bond Indices (WBI) for all P-B and P-Ga bonds describe single bonds between the atom pairs, although the WBIs remain significantly lower for the P-Ga bonding due to the weak bond strengths, which also explains the thermal instability of **3a–d**. The NBO analysis also shows, that the core motifs are made up by regular 2c–2e σ-bonds between the pnictogen and the triel atoms with the main contribution coming from the pnictogen (see Supporting Information).

Table 5.2: Calculated Natural Charges *q*, Wiberg Bond Indices (WBI) and sum of charges of the central {$GaH_2PR_2EH_2$} chain motif *Q*(chain) for compounds **3a**-**d** as calculated by NBO computations.

Calc. property	**3a**	**3b**	**3c**	**3d**
q(Ga)	+0.64	+0.67	+0.65	+0.64
q(P)	+0.22	+0.17	+0.73	-0.18
q(B)	-0.51	-0.24	-0.23	-
q(H_P)	+0.24	+0.29	-	+0.46
q(H_{Ga})	-0.24	-0.23	-0.24	-0.24
q(H_B)	+0.04	+0.01	-0.01	-
Q(Chain)	+0.43	+0.74	+0.23	+1.06
WBI (Ga-P)	0.67	0.64	0.62	0.69
WBI (P-B)	0.96	1.00	0.97	-

5.3 Conclusion

In summary, the novel NHC- stabilized galliummonotriflates IDipp·GaH_2(OTf) (**1a**), IPr_2Me_2·GaH_2(OTf) (**1b**), and IMes·GaH_2(OTf) (**1c**) were synthesized in high yields. **1c** adapts a one-dimensional polymeric structure in the solid state compared to **1a**, which does not show an oligomerized structure. Our experimental investigations demonstrate that the degree of substitution of such triflation or iodination reactions can be easily controlled via the reaction time. This is further supported by quantum chemical computations, which indicate that the second reaction step proceeds much slower due to a higher activation barrier. By reacting different donor-stabilized pnictogenylboranes with IDipp·GaH_2(OTf) (**1a**), the unprecedented, extremely air-sensitive parent Ga/15/13 chain compounds [IDipp·$GaH_2PH_2BH_2$·IDipp][OTf] (**3a**), [IDipp·$GaH_2PH_2BH_2$·NMe_3][OTf] (**3b**) and [IDipp·$GaH_2PPh_2BH_2$·NMe_3][OTf] (**3c**) were synthesized and comprehensively characterized. All obtained products show pronounced instability at room temperature. By reacting **1a** with IDipp·GaH_2PH_2, it was also possible to synthesize the first cationic 13/15 three-membered parent chain compound that only contains heavy group 13 homologues, [IDipp·$GaH_2PH_2GaH_2$·IDipp][OTf] (**3d**), which, besides the aforementioned sensitivity towards air and temperature, is also only stable in *o*-difluorobenzene. Quantum chemical calculations highlight the strongly polarized bonding situation along the central chain motifs.

5.4 References

[1] a) C. E. Housecroft, A. Sharpe, *Inorganic Chemistry*, 4. Aufl., Pearson, New York, **2012**; b) A. C. Jones, P. O'Brien, *CVD of Compound Semiconductors: Precursor Synthesis Development and Applications*, VCH, Weinheim, **1996**; c) M. R. Leys, *Chemtronics* **1987**, *2*, 155–164; d) G. B. Stringfellow, *Rep. Prog. Phys.* **1982**, *45*, 469–525; e) R. A. Fischer, J. Weiß, *Angew. Chem. Int. Ed.* **1999**, *38*, 2830-2850; *Angew. Chem.* **1999**, *111*, 3002-3022; f) J. D. Masuda, A. J. Hoskin, T. W. Graham, C. Beddie, M. C. Fermin, N. Etkin, D. W. Stephan, *Chem. Eur. J.* **2006**, *12*, 8696–8707; g) R. D. Wells, W. L. Gladfelter, *J. Cluster Sci.* **1997**, *8*, 217–238.

[2] a) A. B. Burg, H. I. Schlesinger, *J. Am. Chem. Soc.* **1937**, *59*, 780–787; b) J. Gay-Lussac, J. Thenard, *Mem. Phys. Chim. Soc. d'Arcueil* **1809**, *2*, 210–211; c) A. Stock, E. Pohland, *Chem. Ber.* **1926**, *59*, 2210–2215.

[3] a) A. H. Cowley, R. A. Jones, *Angew. Chem. Int. Ed.* **1989**, *28*, 1208-1215; *Angew. Chem.* **1989**, *101*, 1235-1243; b) J. F. Janik, R. L. Wells, V. G. Young, A. L. Rheingold, I. A. Guzei, *J. Am. Chem. Soc.* **1998**, *120*, 532–537; c) S. M. Stuczynski, R. L. Opila, P. Marsh, J. G. Brennan, M. L. Steigerwald, *Chem. Mater.* **1991**, *3*, 379–381.

[4] a) C. W. Hamilton, R. T. Baker, A. Staubitz, I. Manners, *Chem. Soc. Rev.* **2009**, *38*, 279–293; b) R. Hoffmann, *J. Chem. Phys.* **1964**, *40*, 2474–2480; c) A. Staubitz, A. P. M. Robertson, M. E. Sloan, I. Manners, *Chem. Rev.* **2010**, *110*, 4023–4078.

[5] a) J.-M. Denis, H. Forintos, H. Szelke, L. Toupet, T.-N. Pham, P.-J. Madec, A.-C. Gaumont, *Chem. Comm.* **2003**, 54–55; b) P. P. Power, *Chem. Rev.* **1999**, *99*, 3463–3503.

[6] a) M. Kapitein, M. Balmer, L. Niemeier, C. von Hänisch, *Dalton Trans.* **2016**, *45*, 6275–6281; b) M. Kapitein, M. Balmer, C. von Hänisch, *Z. Anorg. Allg. Chem.* **2016**, *642*, 1275–1281; c) O. Lemp, M. Balmer, K. Reiter, F. Weigend, C. von Hänisch, *Chem. Commun.* **2017**, *53*, 7620–7623; d) D. W. N. Wilson, W. K. Myers, J. M. Goicoechea, *Dalton Trans.* **2020**, *49*, 15249–15255; e) A. K. Swarnakar, C. Hering-Junghans, K. Nagata, M. J. Ferguson, R. McDonald, N. Tokitoh, E. Rivard, *Angew. Chem. Int. Ed.* **2015**, *54*, 10666–10669; f) A. Heilmann, J. Hicks, P. Vasko, J. M. Goicoechea, S. Aldridge, *Angew. Chem. Int. Ed.* **2020**, *132*, 4927–4931; g) J. Hicks, P. Vasko, J. M. Goicoechea, S. Aldridge, *Nature* **2018**, *557*, 92–95; h) D. W. N. Wilson, J. Feld, J. M. Goicoechea, *Angew. Chem. Int. Ed.* **2020**, *132*, 21100–21104; i) A. Bücker, C. Wölper, G. Haberhauer, S. Schulz, *Chem. Comm.* **2022**, *58*, 9758–9761; j) C. Ganesamoorthy, C. Helling, C. Wölper, W. Frank, E. Bill, G. E. Cutsail, S. Schulz, *Nat. Comm.* **2018**, *9*, 87; k) S. Ghosh, E. Glöckler, C. Wölper, J. Linders, N. Janoszka, A. H. Gröschel, S. Schulz, *Eur. J. Inorg. Chem.* **2022**, *2022*; l) C. Helling, C. Ganesamoorthy, C. Wölper, S. Schulz, *Dalton Trans.* **2022**, *51*, 2050–2058; m) C. Helling, C. Wölper, S. Schulz, *J. Am. Chem. Soc.* **2018**, *140*, 5053–5056; n) C. Helling, C. Wölper, Y. Schulte, G. E. Cutsail III, S. Schulz, *Inorg. Chem.* **2019**, *58*, 10323–10332; o) C. Helling, C. Wölper, S. Schulz, *Eur. J. Inorg. Chem.* **2020**, *2020*, 4225–4235; p) C. Helling, C. Wölper, S. Schulz, *Dalton Trans.* **2020**, *49*, 11835–11842; q)

J. Krüger, C. Ganesamoorthy, L. John, C. Wölper, S. Schulz, *Chem. Eur. J.* **2018**, *24*, 9157–9164; r) J. Krüger, C. Wölper, G. Haberhauer, S. Schulz, *Inorg. Chem.* **2022**, *61*, 597–604; s) J. Krüger, C. Wölper, S. Schulz, *Angew. Chem. Int. Ed.* **2021**, *60*, 3572–3575; t) B. Li, C. Wölper, G. Haberhauer, S. Schulz, *Angew. Chem. Int. Ed.* **2021**, *133*, 2014–2019; u) B. Li, B. L. Geoghegan, H. M. Weinert, C. Wölper, G. E. Cutsail, S. Schulz, *Chem. Comm.* **2022**, *58*, 4372–4375; v) J. Schoening, L. John, C. Wölper, S. Schulz, *Dalton Trans.* **2019**, *48*, 17729–17734; w) M. K. Sharma, C. Wölper, G. Haberhauer, S. Schulz, *Angew. Chem. Int. Ed.* **2021**, *60*, 6784–6790; x) M. K. Sharma, P. Dhawan, C. Helling, C. Wölper, S. Schulz, *Chem. Eur. J.* **2022**, *28*, e202200444; y) M. K. Sharma, C. Wölper, S. Schulz, *Dalton Trans.* **2022**, *51*, 1612–1616; z) H. M. Weinert, C. Wölper, S. Schulz, *Chem. Sci.* **2022**, *13*, 3775–3786; aa) S. Schneider, C. Hänisch, *Eur. J. Inorg. Chem.* **2021**, *2021*, 4655–4660.

[7] a) A. Adolf, M. Zabel, M. Scheer, *Eur. J. Inorg. Chem.* **2007**, *2007*, 2136–2143; b) C. A. Jaska, A. J. Lough, I. Manners, *Inorg. Chem.* **2004**, *43*, 1090–1099; c) U. Vogel, P. Hoemensch, K.-C. Schwan, A. Y. Timoshkin, M. Scheer, *Chem. Eur. J.* **2003**, *9*, 515–519; d) U. Vogel, A. Y. Timoshkin, M. Scheer, *Angew. Chem. Int. Ed.* **2001**, *40*, 4409–4412.

[8] a) J. A. Bailey, M. F. Haddow, P. G. Pringle, *Chem. Comm.* **2014**, *50*, 1432–1434; b) J. A. Bailey, M. Ploeger, P. G. Pringle, *Inorg. Chem.* **2014**, *53*, 7763–7769; c) J. A. Bailey, P. G. Pringle, *Coord. Chem. Rev.* **2015**, *297*, 77–90; d) J. M. Breunig, A. Hübner, M. Bolte, M. Wagner, H.-W. Lerner, *Organometallics* **2013**, *32*, 6792–6799; e) T. Chen, E. N. Duesler, H. Nöth, R. T. Paine, *J. Organomet. Chem.* **2000**, *614-615*, 99–106; f) T. Chen, J. Jackson, S. A. Jasper, E. N. Duesler, H. Nöth, R. T. Paine, *J. Organomet. Chem.* **1999**, *582*, 25–31; g) F. Dankert, C. Hering-Junghans, *Chem. Comm.* **2022**, *58*, 1242–1262; h) D. Dou, G. W. Linti, T. Chen, E. N. Duesler, R. T. Paine, H. Nöth, *Inorg. Chem.* **1996**, *35*, 3626–3634; i) S. J. Geier, T. M. Gilbert, D. W. Stephan, *Inorg. Chem.* **2011**, *50*, 336–344; j) S. J. Geier, T. M. Gilbert, D. W. Stephan, *J. Am. Chem. Soc.* **2008**, *130*, 12632–12633; k) M. Kaaz, J. Bender, D. Förster, W. Frey, M. Nieger, D. Gudat, *Dalton Trans.* **2014**, *43*, 680–689; l) M. A. Mardones, A. H. Cowley, L. Contreras, R. A. Jones, *J. Organomet. Chem.* **1993**, *455*, C1-C2; m) K. M. Simpson, R. W. Gedridge, JR., K. T. Higa, *J. Organomet. Chem.* **1993**, *456*, 31–34; n) A. M. Spokoyny, C. D. Lewis, G. Teverovskiy, S. L. Buchwald, *Organometallics* **2012**, *31*, 8478–8481; o) A. Tsurusaki, T. Sasamori, A. Wakamiya, S. Yamaguchi, K. Nagura, S. Irle, N. Tokitoh, *Angew. Chem. Int. Ed.* **2011**, *123*, 11132–11135; p) N. E. Stubbs, T. Jurca, E. M. Leitao, C. H. Woodall, I. Manners, *Chem. Commun.* **2013**, *49*, 9098–9100.

[9] O. Hegen, A. V. Virovets, A. Y. Timoshkin, M. Scheer, *Eur. J. Inorg. Chem.* **2018**, *24*, 16521-16525.

[10] F. Lehnfeld, M. Seidl, A. Y. Timoshkin, M. Scheer, *Eur. J. Inorg. Chem.* **2022**, *3*, e202100930.

[11] a) C. Marquardt, A. Adolf, A. Stauber, M. Bodensteiner, A. V. Virovets, A. Y. Timoshkin, M. Scheer, *Chem. Eur. J.* **2013**, *19*, 11887–11891; b) C. Marquardt, T. Kahoun, J. Baumann, A. Y. Timoshkin, M. Scheer, *Z. Anorg. Allg. Chem.* **2017**, *643*, 1326–1330; c) K.-C. Schwan, A. Y. Timoskin, M. Zabel, M. Scheer, *Chem. Eur. J.* **2006**, *12*, 4900–4908.

[12] a) M. Elsayed Moussa, T. Kahoun, M. T. Ackermann, M. Seidl, M. Bodensteiner, A. Y. Timoshkin, M. Scheer, *Organometallics* **2022**, *41*, 1572–1578; b) C. Marquardt, T. Kahoun, A. Stauber, G. Balázs, M. Bodensteiner, A. Y. Timoshkin, M. Scheer, *Angew. Chem. Int. Ed.* **2016**, *55*, 14828–14832.

[13] M. T. Ackermann, M. Seidl, F. Wen, M. J. Ferguson, A. Y. Timoshkin, E. Rivard, M. Scheer, *Chem. Eur. J.* **2022**, *28*, e20210370.

[14] C. Marquardt, G. Balázs, J. Baumann, A. V. Virovets, M. Scheer, *Chem. Eur. J.* **2017**, *23*, 11423–11429.

[15] C. Marquardt, C. Thoms, A. Stauber, G. Balázs, M. Bodensteiner, M. Scheer, *Angew. Chem. Int. Ed.* **2014**, *53*, 3727–3730.

[16] a) M. Bodensteiner, A. Y. Timoshkin, E. V. Peresypkina, U. Vogel, M. Scheer, *Chem. Eur. J.* **2013**, *19*, 957–963; b) M. Bodensteiner, U. Vogel, A. Y. Timoshkin, M. Scheer, *Angew. Chem. Int. Ed.* **2009**, *48*, 4629–4633; c) C. Marquardt, T. Jurca, K.-C. Schwan, A. Stauber, A. V. Virovets, G. R. Whittell, I. Manners, M. Scheer, *Angew. Chem. Int. Ed.* **2015**, *54*, 13782–13786; d) C. Thoms, C. Marquardt, A. Y. Timoshkin, M. Bodensteiner, M. Scheer, *Angew. Chem. Int. Ed.* **2013**, *52*, 5150–5154; e) C. Marquardt, O. Hegen, A. Vogel, A. Stauber, M. Bodensteiner, A. Y. Timoshkin, M. Scheer, *Chem. Eur. J.* **2018**, *24*, 360–363.

[17] a) J. Braese, A. Schinabeck, M. Bodensteiner, H. Yersin, A. Y. Timoshkin, M. Scheer, *Chem. Eur. J.* **2018**; b) M. Elsayed Moussa, J. Braese, C. Marquardt, M. Seidl, M. Scheer, *Eur. J. Inorg. Chem.* **2020**, *26*, 2501–2505; c) M. Elsayed Moussa, C. Marquardt, O. Hegen, M. Seidl, M. Scheer, *New J. Chem.* **2021**, *45*, 14916–14919; d) K.-C. Schwan, A. Adolf, M. Bodensteiner, M. Zabel, M. Scheer, *Z. Anorg. Allg. Chem.* **2008**, *634*, 1383–1387.

[18] C. Marquardt, O. Hegen, T. Kahoun, M. Scheer, *Chem. Eur. J.* **2017**, *23*, 4397–4404.

[19] M. A. K. Weinhart, A. S. Lisovenko, A. Y. Timoshkin, M. Scheer, *Angew. Chem. Int. Ed.* **2020**, *59*, 5541-5545; *Angew. Chem.* **2020**, *132*, 5586-5590.

[20] M. A. K. Weinhart, M. Seidl, A. Y. Timoshkin, M. Scheer, *Angew. Chem.* **2021**, *133*, 3850–3855; *Angew. Chem. Int. Ed.* **2021**, *60*, 3806–3811.

[21] A. Y. Timoshkin, G. Frenking, *Inorg. Chem.* **2003**, *42*, 60–69.

[22] M. Gonsior, I. Krossing, *Z. Anorg. Allg. Chem.* **2002**, *628*, 1821–1830.

[23] A. Hock, L. Werner, M. Riethmann, U. Radius, *Eur. J. Inorg. Chem.* **2020**, *42*, 4015–4023.

[24] P. Pyykkö, M. Atsumi, *Chem. Eur. J.* **2009**, *15*, 12770–12779.

[25] A. K. Swarnakar, M. J. Ferguson, R. McDonald, E. Rivard, *Dalton Trans.* **2017**, *46*, 1406–1412.

[26] a) A. D. Becke, *J. Chem. Phys.* **1993**, *98*, 5648–5652; b) C. Lee, W. Yang, R. G. Parr, *Phys. Rev. B* **1988**, *37*, 785–789; c) Y. Guo, C. Riplinger, U. Becker, D. G. Liakos, Y. Minenkov, L. Cavallo, F. Neese, *J. Chem. Phys.* **2018**, *148*, 11101; d) V. Ásgeirsson, B. O. Birgisson, R. Bjornsson, U. Becker, F. Neese, C. Riplinger, H. Jónsson, *J. Chem. Theory Comput.* **2021**, *17*, 4929–4945; e) F. Weigend, R. Ahlrichs, *Phys. Chem. Chem. Phys.* **2005**, *7*, 3297-305; f) F. Neese, *WIREs Comput. Mol. Sci.* **2012**, *2*, 73–78; g) F. Neese, *WIREs Comput. Mol. Sci.* **2018**, *8*, e1327; h) F. Neese, *WIREs Comput. Mol. Sci.* **2022**, *12*, e1606; i) F. Neese, F. Wennmohs, U. Becker, C. Riplinger, *J. Chem. Phys.* **2020**, *152*, 224108.

[27] E. Caldeweyher, C. Bannwarth, S. Grimme, *J. Chem. Phys.* **2017**, *147*, 34112.

[28] E. Caldeweyher, S. Ehlert, A. Hansen, H. Neugebauer, S. Spicher, C. Bannwarth, S. Grimme, *J. Chem. Phys.* **2019**, *150*, 154122.

[29] a) M. G. Evans, M. Polanyi, *Trans. Faraday. Soc.* **1935**, *31*, 875–894; b) H. Eyring, *J. Chem. Phys.* **1935**, *3*, 107–115.

[30] A. E. Reed, L. A. Curtiss, F. Weinhold, *Chem. Rev.* **1988**, *88*, 899–926.

[31] a) A. D. Becke, *Phys. Rev. A* **1988**, *38*, 3098–3100; b) J. P. Perdew, *Phys. Rev. B* **1986**, *33*, 8822–8824; c) V. N. Staroverov, G. E. Scuseria, J. Tao, J. P. Perdew, *J. Chem. Phys.* **2003**, *119*, 12129–12137.

[32] Given yields refer to the isolated amounts of product at room temperature.

[33] NMR samples were prepared quickly at room temperature and measured directly after sample preparation.

5.5 Supporting Information

5.5.1 General Information

5.5.1.1 Working Techniques

All working steps were carried out under argon inert gas atmosphere using standard Schlenk and glovebox techniques. Glassware was dried in an oven at 170 °C and pre-conditioned in vacuum (< 10^{-3} mbar, 650 °C) shortly before use. The protective gas was cleansed from traces of H_2O and O_2 by passing it through a BASF R 3-11 (CuO/$MgSiO_3$) catalyst, concentrated H_2SO_4, Orange Gel and Sicapent® supported on pumice stone. Prior to use, solvents were purified using an MBraun SPS-800 solvent purification system, degassed by freeze-pump-thaw cycles and stored over molecular sieves for at least 48 hours. C_6D_6 was dried over Na/K, distilled, degassed at room temperature and stored over molecular sieves (4 Å). CD_2Cl_2 was dried over CaH_2, distilled, and degassed by freeze-pump-thaw. 1,2-difluorobenzene was dried over CaH_2, distilled, and degassed at room temperature. Elemental Analysis (CHNS) was performed by the in-house facility. Mass spectra were recorded on a Jeol AccuTOF GCX mass spectrometer (LIFDI-MS) or ThermoQuest Finnigan TSQ 7000 (ESI-MS) mass spectrometer by the in-house facility or on a Waters Micromass LCT ESI-TOF mass spectrometer at the Scheer group.

IDipp,[1] IDipp·GaH_3,[2] IPrMe·GaH_3,[2] IDipp·GaH_2Cl,[3] and IDipp·GaH_2PH_2[3] were prepared according to literature procedures. Me(OTf) and MeI were purchased from Sigma Aldrich/Merck and used as received. BH_3·SMe_2 was purchased from ABCR and used as received. Me_3N·BH_2PH_2[4] and Me_3N·BH_2PPh_2[5] were provided by the Scheer group (Dr. Matthias T. Ackermann). IDipp·BH_2PH_2 was prepared by salt metathesis as follows (alternatively, donor exchange from Me_3N·BH_2PH_2 with IDipp can be used, as described by the literature).[6] IDipp·BH_2I was prepared by a slightly adapted literature procedure, as follows.

5.5.1.2 Spectroscopic Analysis

All NMR spectra were recorded on a BRUKER Avance 400 (frequencies: ^{1}H: 400.13 MHz, ^{31}P: 161.98 MHz, ^{19}F: 376.50 MHz, ^{11}B: 128.43, ^{13}C: 100.61) or Avance 300 (^{1}H: 300.13 MHz) spectrometers. Substances of reference are $Si(CH_3)_4$ (^{1}H, ^{13}C), 85 % H_3PO_4 (^{31}P), $BF_3 \cdot Et_2O$ (^{11}B) and $CFCl_3$ (^{19}F). Chemical shifts δ are presented in ppm referring to the external standards and coupling constants J are given in Hz without consideration of absolute signs.

5.5.2 Experimental Details

5.5.2.1 Synthesis of IDipp·BH_3

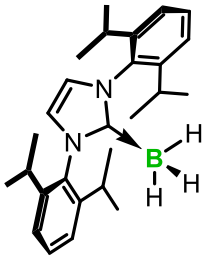

A Schlenk tube was charged with IDipp (4.2 g, 10.808 mmol) and the solids dissolved in toluene. Then, neat BH_3·SMe_2 (1.0 mL, 10.808 mmol) was added *via* syringe. The mixture was stirred for two hours at room temperature and then all volatiles were removed in vacuo, yielding IDipp·BH_3 as a white powder (4.043 g, 93%).

^{1}H NMR (400.30 MHz, C_6D_6, 298 K): 7.25 (t, 2 H, 2 × aryl-C_{para}H, $^3J_{HH}$ = 7.78 Hz), 7.12 (d, 4 H, 4 × aryl-$C_{meta}H$, $^3J_{HH}$ = 7.78 Hz), 6.33 (s, 2 H, NC*H*C*H*N), 2.71 (sep, 4 H,

4 × ^{i}Pr-C*H*, $^{3}J_{HH}$ = 7.17 Hz), 1.39 (d, 12 H, 4 × ^{i}Pr-CH$_3$, $^{3}J_{HH}$ = 7.17 Hz), 1.33 (q, broad and superimposed, $^{1}J_{HB}$ = 86 Hz, B*H*$_3$), 1.09 (d, 12 H, 4 × ^{i}Pr-C*H*$_3$, $^{3}J_{HH}$ = 7.17 Hz)

^{11}B{^{1}H} NMR (128.43 MHz, C$_6$D$_6$, 298 K): -35.6 (s, broad)

^{11}B NMR (128.43 MHz, C$_6$D$_6$, 298 K): -35.6 (q, broad, $^{1}J_{HB}$ = 86 Hz)

The NMR data are consistent with the literature values.[7]

5.5.2.2 Synthesis of IDipp·BH$_2$I

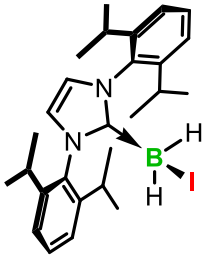

A Schlenk tube was charged with IDipp·BH$_3$ (1.640 g, 4.095 mmol) and the solids dissolved in benzene. Then, solid I$_2$ (519 mg, 2.05 mmol) was added under a stream of argon in portions. The yellow-orange suspension was stirred overnight at room temperature. Subsequently, all volatiles were removed *in vacuo* and the remaining solids washed several times with cold toluene (-30 °C). The final product was dried *in vacuo*, yielding a slightly yellowish powder (1.026 g, 47%).

^{1}H NMR (400.30 MHz, CD$_2$Cl$_2$, 298 K): 7.57 (t, 2 H, 2 × aryl-C$_{para}$H, $^{3}J_{HH}$ = 7.85 Hz), 7.38 (d, 4 H, 4 × aryl-C$_{meta}$*H*, $^{3}J_{HH}$ = 7.85 Hz), 7.22 (s, 2 H, NC*H*C*H*N), 2.62 (sep, 4 H, 4 × ^{i}Pr-C*H*, $^{3}J_{HH}$ = 6.91 Hz), 1.85 (m, very broad, 2 H, B*H*$_2$) 1.39 (d, 12 H, 4 × ^{i}Pr-CH$_3$, $^{3}J_{HH}$ = 6.91 Hz), 1.18 (d, 12 H, 4 × ^{i}Pr-C*H*$_3$, $^{3}J_{HH}$ = 6.91 Hz)

^{11}B{^{1}H} NMR (128.43 MHz, CD$_2$Cl$_2$, 298 K): -32.4 (s, very broad)

^{11}B NMR (128.43 MHz, CD$_2$Cl$_2$, 298 K): -32.4 (m, very broad)

The NMR data are consistent with the literature values.[8]

5.5.2.3 Synthesis of IDipp·BH$_2$PH$_2$

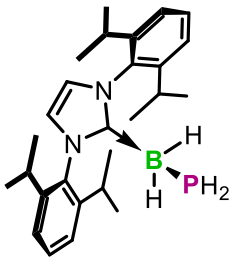

IDipp·BH$_2$I (1.030 g, 1.946 mmol) was dissolved in tetrahydrofuran and cooled to -80 °C. Then, solid NaPH$_2$ (142 mg, 2.5 mmol) was added to the solution and the mixture stirred for two hours at room temperature, yielding an opaque solution. After removing all volatiles in vacuo, the product was extracted with toluene and filtered over a P4 glass frit packed with Celite. After collecting the solution, the solvent was removed in vacuo, yielding IDipp·BH$_2$PH$_2$ as a clean white powder (737 mg, 87%).

^{1}H NMR (400.30 MHz, C$_6$D$_6$, 298 K): 7.27 (t, 2 H, 2 × aryl-C$_{para}$H, $^{3}J_{HH}$ = 7.65 Hz), 7.14 (d, 4 H, 4 × aryl-C$_{meta}$*H*, $^{3}J_{HH}$ = 7.65 Hz), 6.46 (s, 2 H, NC*H*C*H*N), 2.82 (sep, 4 H, 4 × ^{i}Pr-C*H*, $^{3}J_{HH}$ = 6.83 Hz), 1.91 (q, very broad, superimposed, 2 H, B*H*$_2$, $^{1}J_{HB}$ = 91 Hz), 1.42 (d, 12 H, 4 × ^{i}Pr-CH$_3$, $^{3}J_{HH}$ = 6.91 Hz), 1.31 (dm, 2 H, superimposed, P*H*$_2$, $^{1}J_{HB}$ = 182 Hz) 1.07 (d, 12 H, 4 × ^{i}Pr-C*H*$_3$, $^{3}J_{HH}$ = 6.91 Hz)

^{31}P{^{1}H} NMR (161.98 MHz, C$_6$D$_6$, 298 K): -212.6 (s, very broad)

^{31}P NMR (161.98 MHz, C$_6$D$_6$, 298 K): -212.6 (t, very broad, $^{1}J_{HP}$ = 182 Hz)

^{11}B{^{1}H} NMR (128.43 MHz, C_6D_6, 298 K): -34.0 (s, very broad)

^{11}B NMR (128.43 MHz, C_6D_6, 298 K): -34.0 (t, very broad, $^1J_{HB}$ = 91 Hz)

The NMR data are consistent with the literature values.[6]

5.5.2.4 Reaction of IDipp·BH$_2$PH$_2$ with IDipp·GaH$_2$I

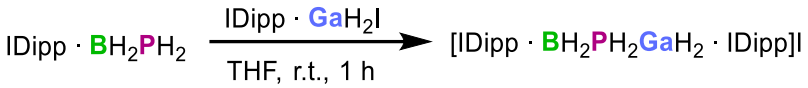

A clear solution of IDipp·BH$_2$PH$_2$ (65 mg, 0.15 mmol) in tetrahydrofuran was added to a clear solution of IDipp·GaH$_2$I (88 mg, 0.15 mmol) in tetrahydrofuran and the mixture stirred at room temperature for one hour. The solvent was removed in vacuo, leaving a white-foamy residue. The solids were washed with diethylether and dried *in vacuo*. Crystallization attempts by solvent diffusion or cooling did not prove successful.

^{1}H NMR (400.30 MHz, CD_2Cl_2, 298 K): due to the presence of several side products and strong signal overlap as well as strongly broadened signals, unambiguous assignment of the signals was not possible.

^{31}P{^{1}H} NMR (161.98 MHz, CD_2Cl_2, 298 K): -168.2 (s, broad)

^{11}B{^{1}H} NMR (128.43 MHz, CD_2Cl_2, 298 K): -35.0 (s, broad)

5.5.2.5 Synthesis of IDipp·GaH$_2$(OTf) (1a)

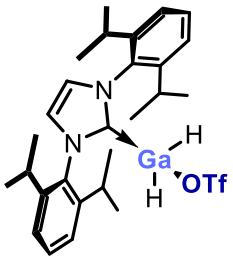

Pathway A: Reduction of Me(OTf)

Me(OTf) (0.5 mL, excess) was added to a clear solution of IDipp·GaH$_3$ (500 mg, 1.08 mmol) in toluene *via* syringe. The solution started bubbling and instantly became cloudy as the product was formed, which is less soluble toluene owed to its increased polarity. After stirring for 45 min at room temperature, all volatiles were removed *in vacuo*, yielding **1a** as a pure white powder (580 mg, 88 %). Single crystals suitable for X-ray diffraction experiments were obtained by slow evaporation of a concentrated benzene solution of **1a**.

Pathway B: Salt metathesis with Ag(OTf)

A solution of Ag(OTf) (52 mg, 0.2 mmol) in diethylether was added to a solution of IDipp·GaH$_2$Cl (100 mg, 0.2 mmol) in diethylether. Upon addition, the mixture instantly turned black. After stirring for 30 min at room temperature, the suspension was filtered through a P3 glass frit. The solution was collected, and the solvent removed in vacuo, yielding **1a** as a white powder (45 mg, 37 %).

^{1}H NMR (400.30 MHz, C_6D_6, 298 K): 7.22 (t, 2 H, 2 × aryl-C$_{para}$H, $^3J_{HH}$ = 7.84 Hz), 7.05 (d, 4 H, 4 × aryl-C$_{meta}$H, $^3J_{HH}$ = 7.84 Hz), 6.36 (s, 2 H, NC*H*C*H*N), 4.88 (s, broad, 2 H, GaH$_2$), 2.44 (sep, 4 H, 4 × ^{i}Pr-C*H*, $^3J_{HH}$ = 6.87 Hz), 1.30 (d, 12 H, 4 × ^{i}Pr-CH$_3$, $^3J_{HH}$ = 6.90 Hz), 0.93 (d, 12 H, 4 × ^{i}Pr-C*H*$_3$, $^3J_{HH}$ = 6.90 Hz)

^{13}C{^{1}H} NMR (100.61 MHz, C_6D_6, 298 K): 22.5 (s, ^{i}Pr-CH_3), 24.9 (s, ^{i}Pr-CH_3), 28.8 (s, $CH(CH_3)_2$), 124.3 (s, *Ar*), 124.4 (s, *Ar*), 131.3 (s, NCH), 132.6 (s, *Ar*), 144.8 (s, *Ar*)

^{19}F{^{1}H} NMR (376.50 MHz, C_6D_6, 298 K): -77.3 (s)

LIFDI-MS (*m/z*): 389.2983 [IDipp-H]$^+$ (100 %), 459.2505 [IDippGaH$_2$]$^+$ (48 %)

Elemental Analysis ($C_{28}H_{38}GaF_3N_2O_3S$) **[%]:** calcd. C 55.19, H 6.29, N 4.60, S 5.26; found C 55.37, H 5.98, N 4.57, S 5.00.

5.5.2.6 Synthesis of IPr$_2$Me$_2$·GaH$_2$(OTf) (1b)

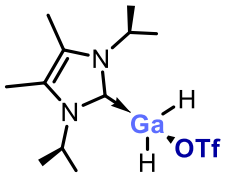

Me(OTf) (0.3 mL, excess) was added to a clear solution of IPr$_2$Me$_2$·GaH$_3$ (208 mg, 0.82 mmol) in toluene *via* syringe. The solution started bubbling extensively and gradually turned cloudy. After stirring for 45 min at room temperature, all volatiles were removed *in vacuo*, yielding **1b** as a white powder (260 mg, 79 %). Large single crystals suitable for X-ray diffraction experiments were obtained by storing a saturated toluene solution of **1b** at -28 °C.

^{1}H NMR (400.30 MHz, C_6D_6, 298 K): 5.62 (s, broad, 2 H, GaH_2), 5.08 (sep, 2 H, $^3J_{HH}$ = 6.91 Hz, 2 × iPrC*H*), 1.38 (s, 6 H, NC(CH_3C(CH_3)N), 1.07 (d, 12 H, $^3J_{HH}$ = 6.91 Hz, *i*Pr(CH$_3$)$_2$)

^{13}C{^{1}H} NMR (100.61 MHz, C_6D_6, 298 K): 9.3 (2 × NCCH_3), 21.0 (s, ^{i}Pr-CH_3), 52.68 (s, $CH(CH_3)_2$), 126.5 (s, NCCH_3)

^{19}F{^{1}H} NMR (376.50 MHz, C_6D_6, 298 K): -77.6 (s)

ESI-MS (*m/z*): 181.1588 [IPr$_2$Me$_2$-H]$^+$ (100 %), 253.2505 [IPr$_2$Me$_2$-GaH$_2$]$^+$ (15 %), 431.2325 [(IPr$_2$Me$_2$)$_2$-GaH$_2$]$^+$ (75%)

Elemental Analysis ($C_{12}H_{22}GaF_3N_2O_3S$) **[%]:** calcd. C 35.93, H 5.53, N 6.98, S 7.99; found C 34.97, H 5.14, N 6.42, S 7.85.

5.5.2.7 Synthesis of IMes·GaH$_2$(OTf) (1b)

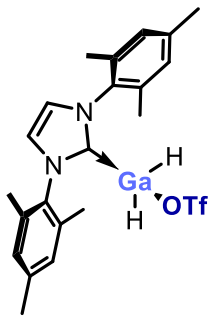

Me(OTf) (0.13 mL, excess) was added to a clear solution of IMes·GaH$_3$ (152 mg, 0.5 mmol) in dichloromethane *via* syringe. After stirring for 30 min at room temperature, all volatiles were removed *in vacuo*, yielding **3** as a white powder that was washed with *n*-hexane and dried *in vacuo* (202 mg, 77 %).

^{1}H NMR (400.30 MHz, C_6D_6, 298 K): 6.70 (s, 4 H, 4 x aryl-C$_{meta}$*H*), 5.92 (s, 2 H, NC*H*C*H*N), 4.81 (s, broad, 2 H, GaH$_2$), 2.04 (s, 6 H, aryl-C$_{para}$*H*), 1.89 (s, 12 H, 4 x aryl-C$_{ortho}$CH_3)

^{13}C{^{1}H} NMR (100.61 MHz, C_6D_6, 298 K): 16.9 (s, CH_3), 20.7 (s, CH_3), 123.1 (s, *Ar*), 129.3 (s, NCH), 133.2 (s, *Ar*), 134.4 (s, *Ar*), 140.2 (s, *Ar*)

^{19}F{^{1}H} NMR (376.50 MHz, C$_6$D$_6$, 298 K): -77.5 (s)

ESI-MS (*m/z*, 1,2-difluorobenzene, pos. mod.): 305.2955 [IMes-H]$^+$ (100%), 375.3099 [IMes · GaH$_2$]$^+$ (4%)

Elemental Analysis (C$_{22}$H$_{26}$GaF$_3$N$_2$O$_3$S) **[%]:** calcd. C 50.31, H 4.99, N 5.33; found C 51.59, H 5.16, N 5.39.

5.5.2.8 Synthesis of IDipp·GaHI$_2$ (2)

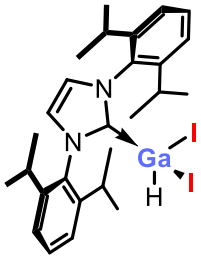

MeI (0.2 mL, excess) was added to a solution of IDipp·GaH$_3$ (200 mg, 0.43 mmol) in dichloromethane *via* syringe, which instantly turned cloudy under visible extrusion of methane gas. After stirring for 68 h at room temperature, all volatiles were removed and IDipp·GaHI$_2$ was obtained as a white powder (207 mg, 68 %).

^{1}H NMR (400.30 MHz, C$_6$D$_6$, 298 K): 7.23 (t, 2 H, 2 × aryl-C$_{para}$H, $^3J_{HH}$ = 7.71 Hz), 7.08 (d, 4 H, 4 × aryl-C$_{meta}$*H*, $^3J_{HH}$ = 7.71 Hz), 6.45 (s, 2 H, NC*H*C*H*N), 4.86 (s, broad, 1 H, Ga*H*), 2.72 (sep, 4 H, 4 × ^{i}Pr-C*H*, $^3J_{HH}$ = 6.52 Hz), 1.45 (d, 12 H, 4 × ^{i}Pr-CH$_3$, $^3J_{HH}$ = 6.52 Hz), 0.95 (d, 12 H, 4 × ^{i}Pr-C*H*$_3$, $^3J_{HH}$ = 6.90 Hz)

^{13}C{^{1}H} NMR (100.61 MHz, C$_6$D$_6$, 298 K): 22.9 (s, ^{i}Pr-*C*H$_3$), 25.6 (s, ^{i}Pr-C*H*$_3$), 28.8 (s, *C*H(CH$_3$)$_2$), 124.4 (s, *Ar*), 124.9 (s, *Ar*), 131.3 (s, NCH), 133.2 (s, *Ar*), 145.4 (s, *Ar*)

Elemental Analysis (C$_{27}$H$_{37}$GaN$_2$I$_2$) **[%]:** calcd. for: 1 × **2** + 0.3 × C$_{27}$H$_{38}$GaIN$_2$ (IDipp · GaI$_3$) C 43.69, H 4.99, N 3.77; found C 43.36, H 5.13, N 3.74.

5.5.2.9 Synthesis of [IDipp·GaH$_2$PH$_2$BH$_2$·IDipp][OTf] (3a)

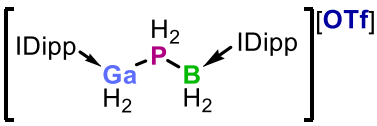

A solution of IDipp·BH$_2$PH$_2$ (43 mg, 0.1 mmol) in tetrahydrofuran was added to a solution of IDipp·GaH$_2$(OTf) (61 mg, 0.1 mmol) in tetrahydrofuran and the mixture stirred at room temperature for one hour. The colourless solution was layered with a THF/*n*-hexane mixture (1:1) and then additional *n*-hexane and left for crystallization at -30 °C. **3a** is obtained as large colourless blocks after two weeks, which are washed multiple times with *n*-hexane (r.t.) and dried *in vacuo* (48 mg, 46%). **3a** is sensitive to air and decomposes at room temperature. The product contains considerable amounts of [IDipp-H][OTf] from thermal decomposition, that could not be separated.

^{1}H NMR (400.30 MHz, CD$_2$Cl$_2$, 298 K): 1.11 (4 × overlapping doublets, 48 H, ^{i}Pr-C*H*$_3$), 1.18 (dm, very broad, 2 H, P*H*$_2$, $^1J_{HP}$ = 323 Hz), 2.30 (sep, 8 H, 4 × ^{i}Pr-C*H*, $^3J_{HH}$ = 7.16 Hz), 3.23 (d, broad, 2 H, GaH$_2$, $^2J_{HP}$ = 38 Hz), 7.18 (s, 2 H, NC*H*C*H*N), 7.24 (d, 4 H, 4 × aryl-C$_{meta}$*H*, $^3J_{HH}$ = 7.84 Hz), 7.31 (d, 4 H, 4 × aryl-C$_{meta}$*H*, $^3J_{HH}$ = 7.84 Hz), 7.34 (s, 2 H, NC*H*C*H*N), 7.49 (t, 2 H, 2 × aryl-C$_{para}$H, $^3J_{HH}$ = 7.84 Hz), 7.56 (t, 2 H, 2 × aryl-C$_{para}$H, $^3J_{HH}$ = 7.84 Hz). *The {BH$_2$} protons cannot be detected, as it the signal is likely too broadened and disappears within the spectral noise. For ^{1}H,^{1}H COSY NMR spectrum: cf. section "NMR Data".*

^{31}P{^{1}H} NMR (161.98 MHz, CD$_2$Cl$_2$, 298 K): -168.2 (s, broad)

^{31}P NMR (161.98 MHz, CD$_2$Cl$_2$, 298 K): -168.2 (t, broad, $^1J_{HP}$ = 323 Hz)

^{11}B{^{1}H} NMR (128.43 MHz, CD_2Cl_2, 298 K): -35.0 (s, very broad)

^{11}B NMR (128.43 MHz, CD_2Cl_2, 298 K): -35.0 (s, very broad)

^{19}F{^{1}H} NMR (376.50 MHz, CD_2Cl_2, 298 K): -79.1 (s)

ESI-MS (1,2-difluorobenzene, pos. mod.): *m*/*z* = 389.30 (100%, [IDipp-H]$^+$), 893.53 (19%, [IDipp·GaH$_2$PH$_2$BH$_2$·IDipp]$^+$)

Elemental Analysis ($C_{55}H_{78}GaBF_3N_4P_3O_3S$) **[%]:** could not be performed, as it was not possible to separate [IDipp-H]$^+$ from **3a**.

5.5.2.10 Synthesis of [IDipp·GaH$_2$PH$_2$BH$_2$·NMe$_3$][OTf] (3b)

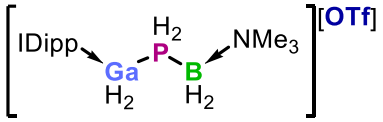

IDipp·GaH$_2$(OTf) (65 mg, 0.19 mmol) was dissolved in 1,2-difluorobenzene in a Schlenk tube. Then, PH$_2$BH$_2$·NMe$_3$ (0.5 M stock solution in toluene; 0.3 mL, 0.15 mmol) was added via syringe. The clear colourless mixture was stirred for 30 min at room temperature. Subsequently, the solution was layered with *n*-hexane and left at -30 °C for crystallization. **3b** crystallized as thin colourless plates. The crystals were washed multiple times with *n*-hexane (r.t.) and dried *in vacuo* (30 mg, 42%).

^{1}H NMR (400.30 MHz, CD_2Cl_2, 298 K): 1.20 (d, superimposed, 4 × ^{i}Pr-C*H*$_3$, $^3J_{HH}$ = 6.90 Hz), 1.28 (d, superimposed, 4 × ^{i}Pr-C*H*$_3$, $^3J_{HH}$ = 6.90 Hz), 1.50+2.30 (dm, broad and partially superimposed, 2 H, P*H*$_2$, $^1J_{HP}$ = 322 Hz), 2.47 (sep, 4 H, 4 × ^{i}Pr-C*H*, $^3J_{HH}$ = 6.90 Hz), 2.56 (s, 9 H, N(C*H*$_3$)$_3$), 3.60 (d, broad, 2 H, Ga*H*$_2$, $^2J_{HP}$ ≈ 33 Hz), 7.40 (d, superimposed, 4 × aryl-C$_{meta}$*H*, $^3J_{HH}$ = 7.92 Hz), 7.50 (s, 4 H, NC*H*$_2$C*H*$_2$N), 7.60 (t, 2 H, 2 × aryl-C$_{para}$H, $^3J_{HH}$ = 7.92 Hz). *The {BH$_2$} protons cannot be detected, as it the signal is likely too broadened and superimposed.*

^{31}P{^{1}H} NMR (161.98 MHz, CD_2Cl_2, 298 K): -176.5 (s, broad)

^{31}P NMR (161.98 MHz, CD_2Cl_2, 298 K): -176.5 (t, broad, $^1J_{HP}$ = 322 Hz)

^{11}B{^{1}H} NMR (128.43 MHz, CD_2Cl_2, 298 K): -8.2 (s, broad)

^{11}B NMR (128.43 MHz, CD_2Cl_2, 298 K): -8.2 (t, broad, $^1J_{HB}$ = 110 Hz)

^{19}F{^{1}H} NMR (376.50 MHz, CD_2Cl_2, 298 K): -79.0 (s)

ESI-MS (1,2-difluorobenzene, pos. mod.): *m*/*z* = 389.4161 (85%, [IDipp-H]$^+$), 564.4757 (100%, [IDipp·GaH$_2$PH$_2$BH$_2$·NMe$_3$]$^+$)

Elemental Analysis ($C_{30}H_{48}BF_3GaN_3O_3PS$) **[%]:** could not be performed, as it was not possible to isolate an analytically pure sample of **3b**.

5.5.2.11 Synthesis of [IDipp·GaH$_2$PPh$_2$BH$_2$·NMe$_3$][OTf] (3c)

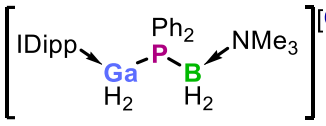

IDipp·GaH$_2$(OTf) (76 mg, 0.12 mmol) and Me$_3$N·BH$_2$PPh$_2$ (26 mg, 0.12 mmol) were weighed together into a Schlenk tube. Then, the mixture was dissolved in 1,2-difluorobenzene and stirred at room temperature for one hour. Subsequently, the solution was layered with *n*-hexane and left at -30 °C for crystallization. **3c** crystallized as clear colourless prisms. The crystals were washed once with toluene (r.t.) and twice with *n*-hexane (r.t.) and finally dried *in vacuo* (77 mg, 72%).

^{1}H NMR (400.30 MHz, CD$_2$Cl$_2$, 298 K): 1.08 (d, 12 H, 4 × ^{i}Pr-C*H*$_3$, $^3J_{HH}$ = 6.77 Hz), 1.12 (d, 12 H, 4 × ^{i}Pr-C*H*$_3$, $^3J_{HH}$ = 6.77 Hz), 2.38 (s, 9 H, N(C*H*$_3$)$_3$), 2.49 (sep, 4 H, 4 × ^{i}Pr-C*H*, $^3J_{HH}$ = 6.77 Hz), 3.92 (d, 2 H, Ga*H*$_2$, $^2J_{HP}$ = 38 Hz), 7.18-7.26 (m, 8 H, 2 × phenyl-C$_{ortho/meta}$*H*), 7.27 (d, 4 H, 4 × aryl-C$_{meta}$*H*, $^3J_{HH}$ = 7.92 Hz), 7.31-7.40 (m, 2 H, 2 × phenyl-C$_{para}$*H*), 7.44 (s, 4 H, NC*H*$_2$C*H*$_2$N), 7.52 (t, 2 H, 2 × aryl-C$_{para}$H, $^3J_{HH}$ = 7.92 Hz). *The {BH$_2$} protons cannot be detected, as it the signal is likely too broadened and superimposed.*

^{31}P{^{1}H} NMR (161.98 MHz, CD$_2$Cl$_2$, 298 K): -39.9 (s, broad)

^{31}P NMR (161.98 MHz, CD$_2$Cl$_2$, 298 K): -39.9 (s, broad)

^{11}B{^{1}H} NMR (128.43 MHz, CD$_2$Cl$_2$, 298 K): -7.6 (s, broad)

^{11}B NMR (128.43 MHz, CD$_2$Cl$_2$, 298 K): -7.6 (s, broad)

^{19}F{^{1}H} NMR (376.50 MHz, CD$_2$Cl$_2$, 298 K): -78.7 (s)

ESI-MS (1,2-difluorobenzene, pos. mod.): *m/z* = 258.14 (37%, [HPPh$_2$BH$_3$·NMe$_3$]$^+$), 329.24 (< 1%, [Me$_3$N·BH$_2$PPh$_2$BH$_2$·NMe$_3$]$^+$), 389.30 (100%, [IDipp-H]$^+$), 716.34 (< 1%, [IDipp·GaH$_2$PPh$_2$BH$_2$·NMe$_3$]$^+$)

Elemental Analysis (C$_{43}$H$_{59}$BF$_3$GaN$_3$O$_3$PS) **[%]:** could not be performed as it was not possible to isolate an analytically pure sample of **3c**.

5.5.2.12 Synthesis of [IDipp · GaH$_2$PH$_2$GaH$_2$ · IDipp][OTf] (3d)

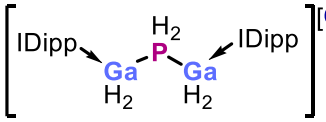

IDipp · GaH$_2$(OTf) (73 mg, 0.12 mmol) and IDipp · GaH$_2$PH$_2$ (59 mg, 0.12 mmol) were weighed together into a Schlenk tube. Then, the mixture was dissolved in 1,2-difluorobenzene and stirred at room temperature for 30 min. Subsequently, the solution was layered with *n*-hexane and left at -30 °C for crystallization. **3d** crystallized as clear colourless blocks. The crystals were washed multiple times with *n*-hexane (r.t.) and dried *in vacuo* (55 mg, 50%). **3d** is unstable in most organic solvents except for 1,2-difluorobenzene and decomposes at room temperature under release of PH$_3$.

^{1}H NMR (400.30 MHz, 1,2-difluorobenzene/C$_6$D$_6$-capillary, 298 K): due to inseparable impurities/decomposition products, no clear assignment of signals was possible due to signal overlap.

^{31}P{^{1}H} NMR (161.98 MHz, 1,2-difluorobenzene/C$_6$D$_6$-capillary, 298 K): -220.0 (s)

^{31}P NMR (161.98 MHz, 1,2-difluorobenzene/C_6D_6-capillary, 298 K): -220.0 (t(quin.), $^1J_{HP}$ = 278 Hz, $^2J_{HP}$ = 45 Hz)

^{19}F{^{1}H} NMR (376.50 MHz, 1,2-difluorobenzene/C_6D_6-capillary, 298 K): -78.6 (s)

ESI-MS (1,2-difluorobenzene, pos. mod.): *m*/*z* = 389.3794 (100%, $[IDipp\text{-}H]^+$), 937.5032 (1%, $[IDipp{\cdot}GaH_2PH_2GaH_2{\cdot}IDipp]^+ - CH_4$)

Elemental Analysis ($C_{55}H_{78}F_3Ga_2N_4O_3PS$) [%]: could not be performed, as it was not possible to isolate an analytically pure sample of **3d**.

5.5.3 NMR Data

5.5.3.1 IDipp·BH$_3$

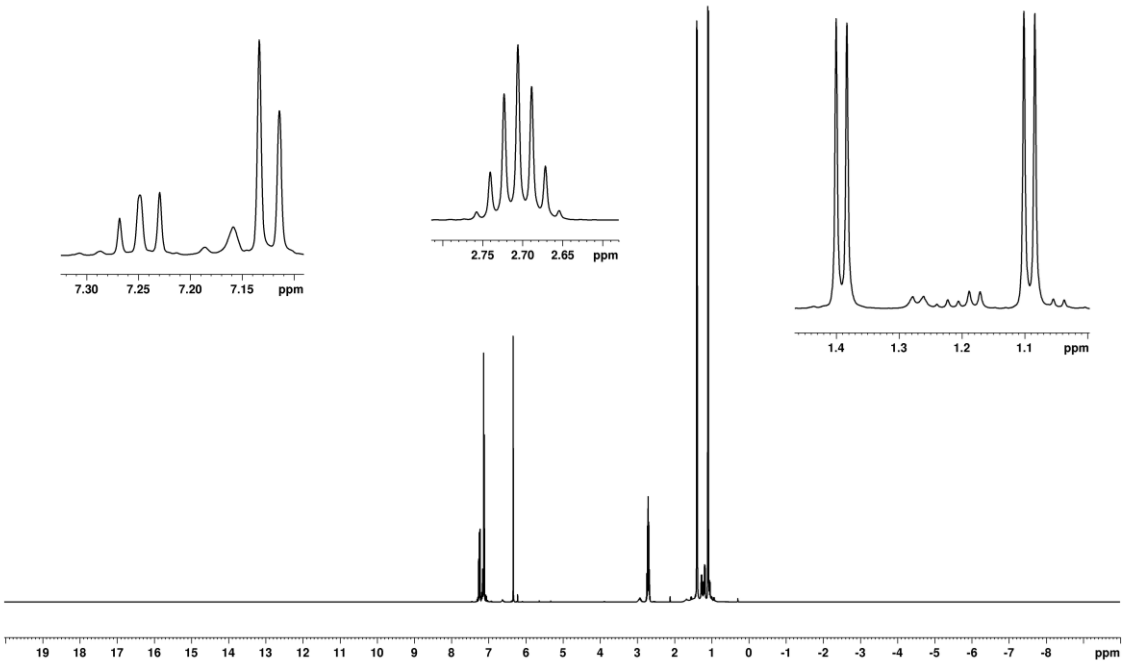

Figure S 5.1: ^{1}H NMR spectrum of IDipp·BH$_3$ (C_6D_6, 298 K).

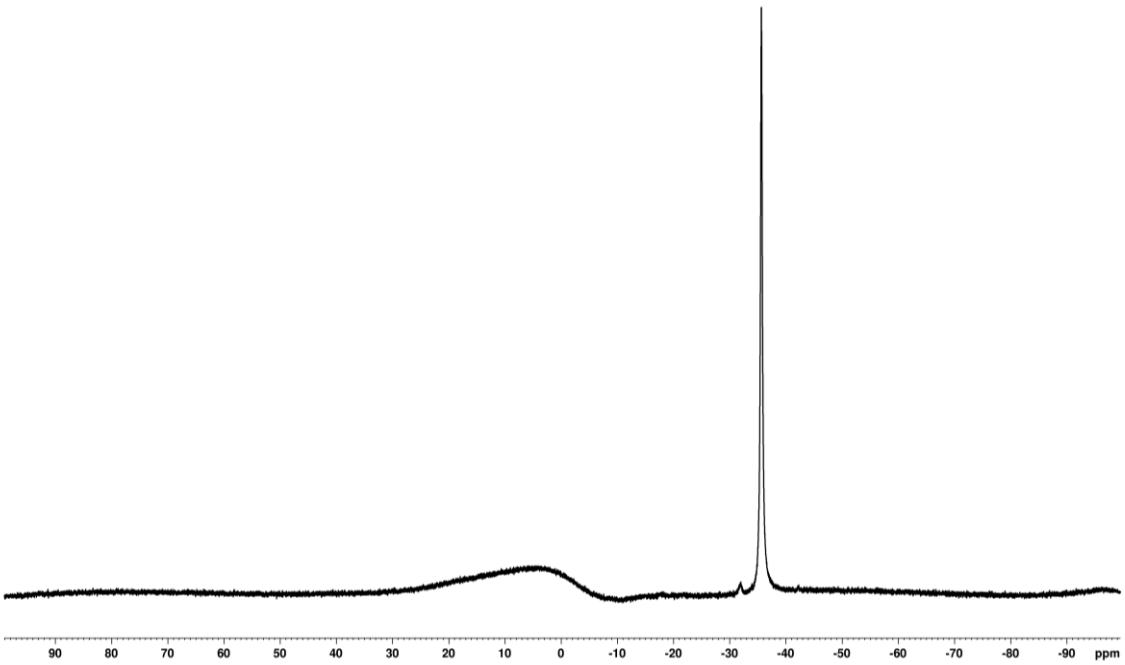

Figure S 5.2: ^{11}B{^{1}H} NMR spectrum of IDipp·BH$_3$ (C_6D_6, 298 K).

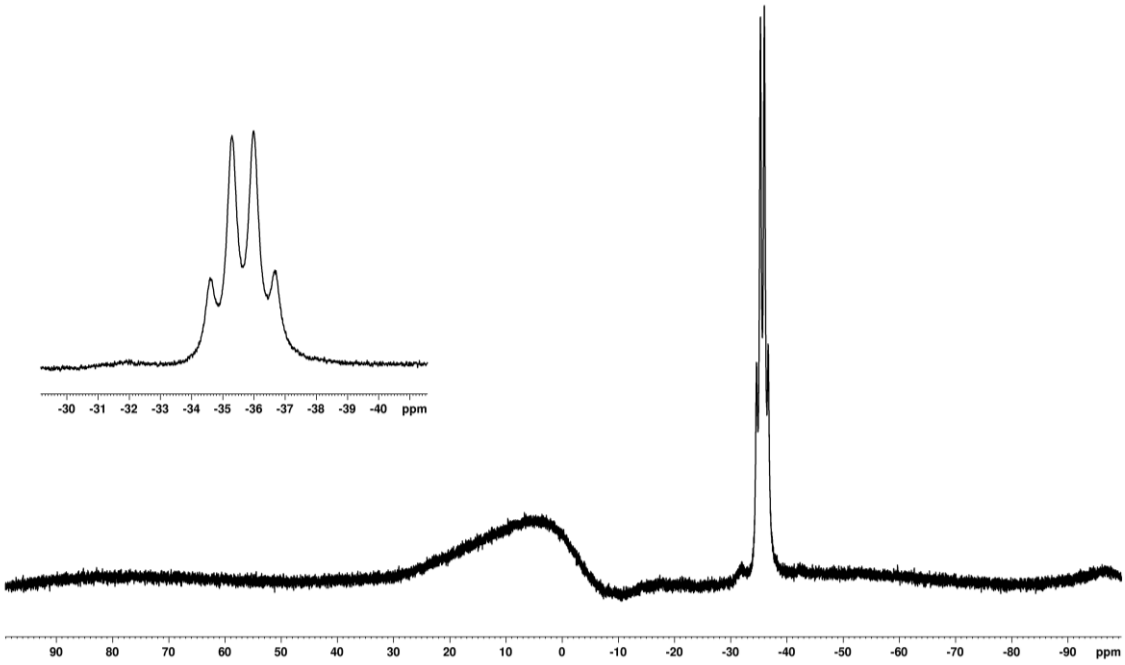

Figure S 5.3: ^{11}B NMR spectrum of IDipp·BH_3 (C_6D_6, 298 K).

5.5.3.2 IDipp·BH_2I

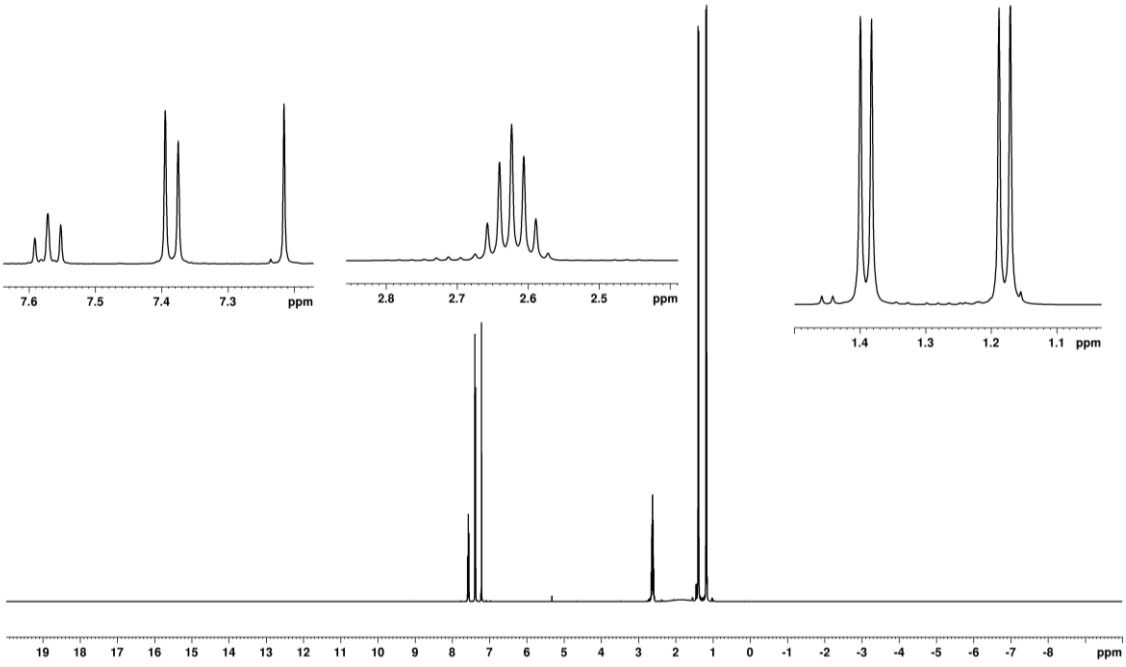

Figure S 5.4: ^{1}H NMR spectrum of IDipp·BH_2I (CD_2Cl_2, 298 K).

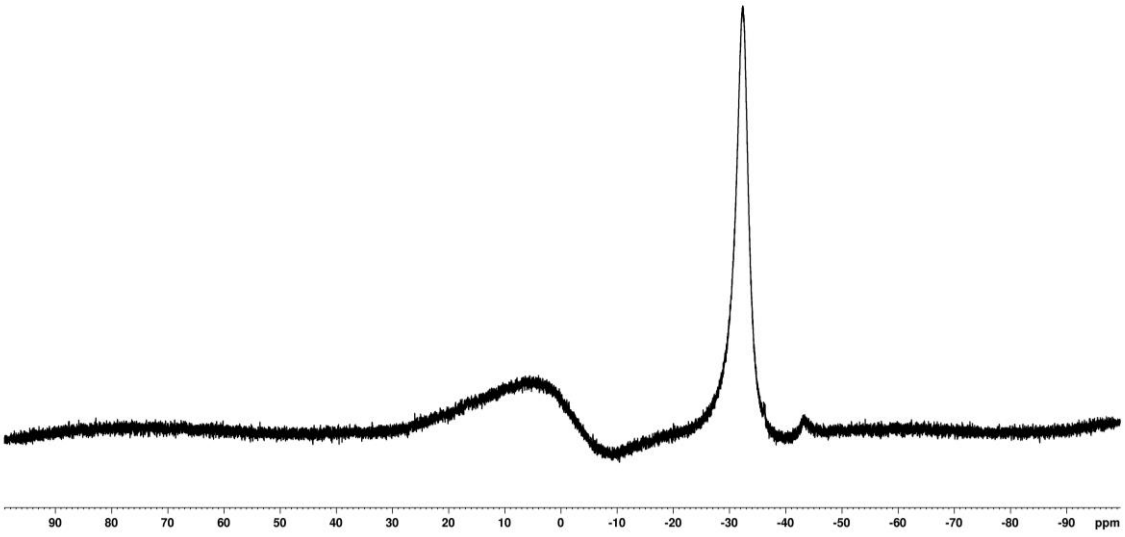

Figure S 5.5: $^{11}B\{^1H\}$ NMR spectrum of IDipp·BH_2I (CD_2Cl_2, 298 K).

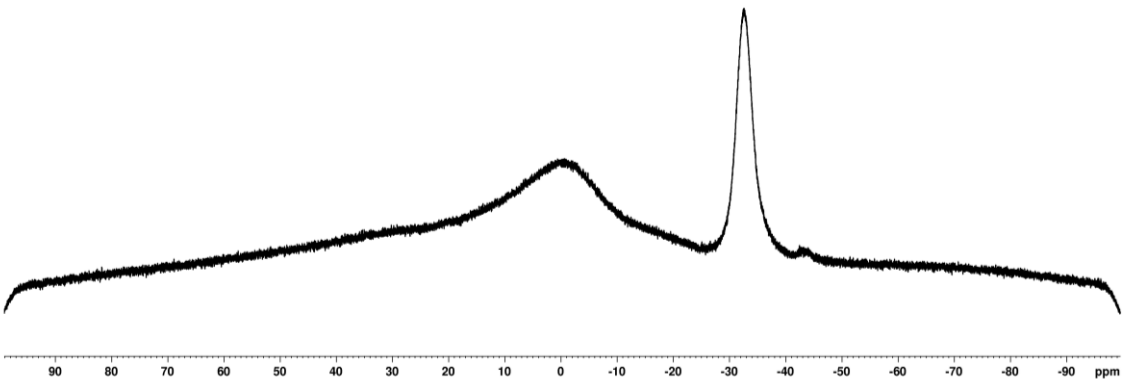

Figure S 5.6: ^{11}B NMR spectrum of IDipp·BH_2I (CD_2Cl_2, 298 K).

5.5.3.3 Reaction of IDipp·BH$_2$PH$_2$ with IDipp·GaH$_2$I

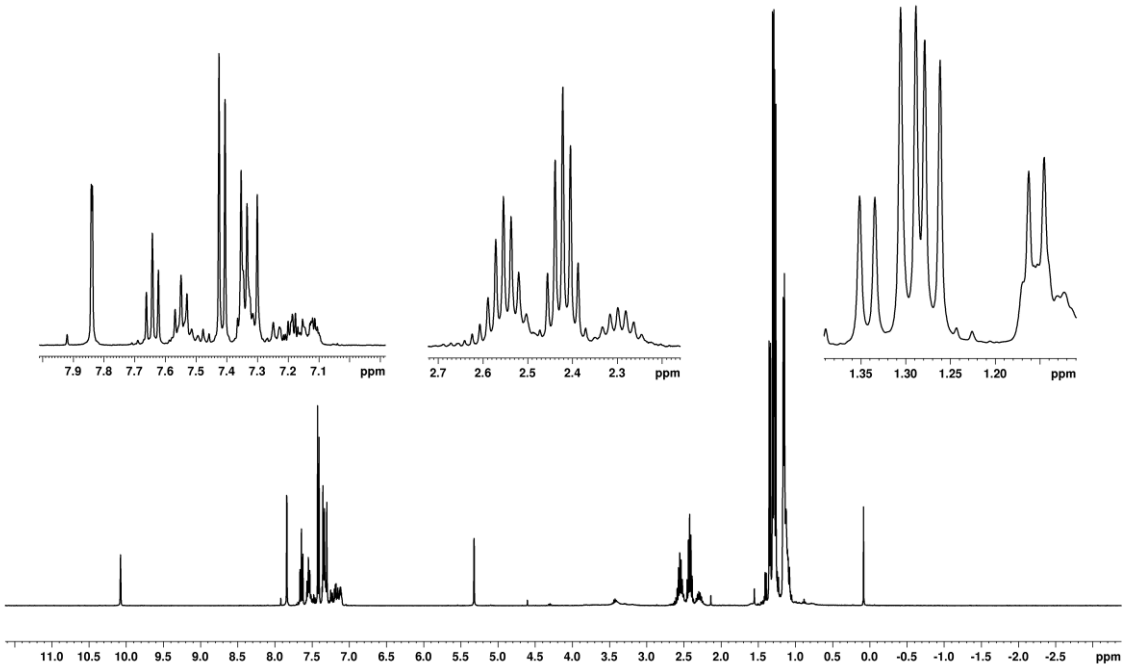

Figure S 5.7: ^{1}H NMR spectrum of the reaction between IDipp·BH$_2$PH$_2$ and IDipp·GaH$_2$I (CD$_2$Cl$_2$, 298 K).

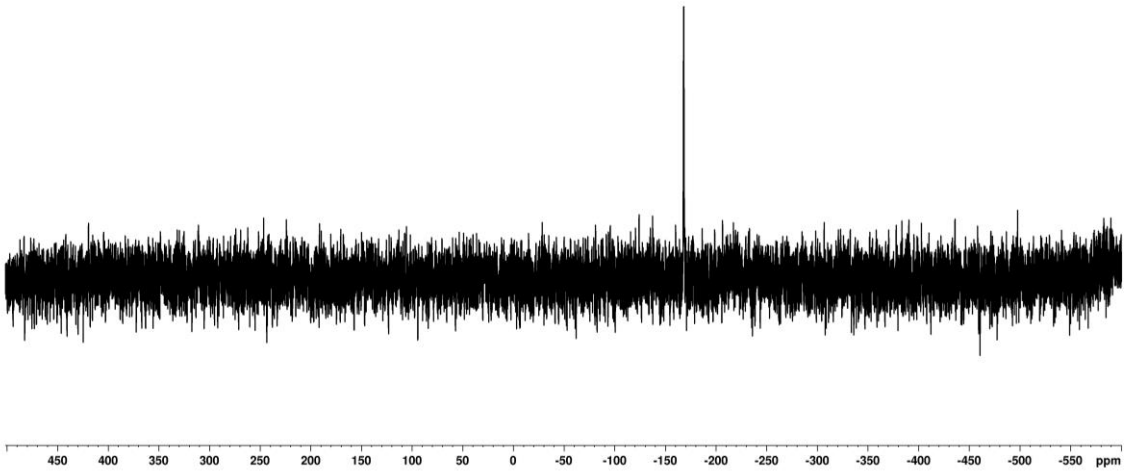

Figure S 5.8: ^{31}P{^{1}H} NMR spectrum of the reaction between IDipp·BH$_2$PH$_2$ and IDipp·GaH$_2$I (CD$_2$Cl$_2$, 298 K).

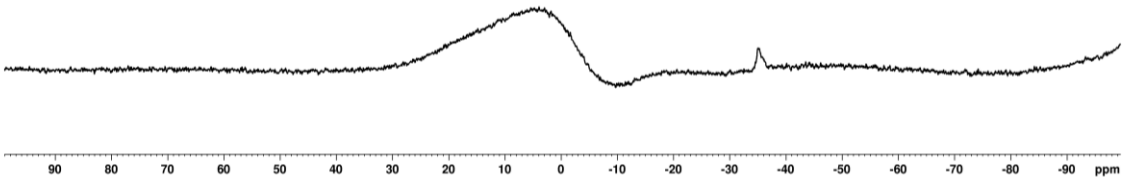

Figure S 5.9: $^{11}B\{^1H\}$ NMR spectrum of the reaction between IDipp·BH_2PH_2 and IDipp·GaH_2I (CD_2Cl_2, 298 K).

5.5.3.4 IDipp·BH_2PH_2

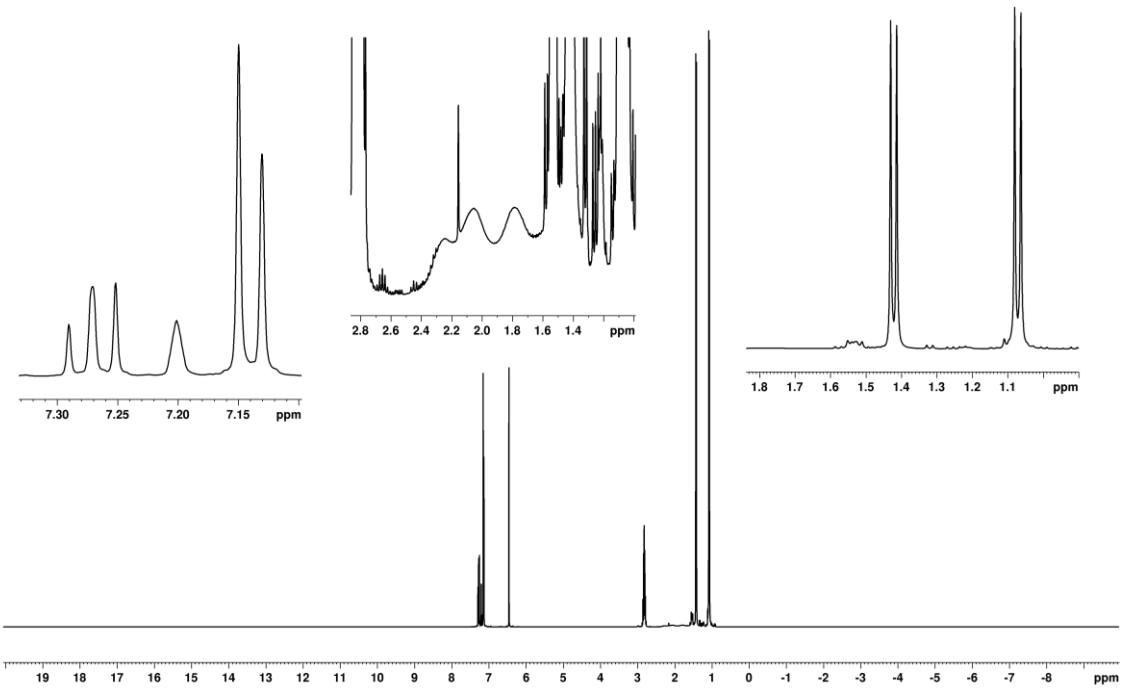

Figure S 5.10: ^1H NMR spectrum of IDipp·BH_2PH_2 (C_6D_6, 298 K).

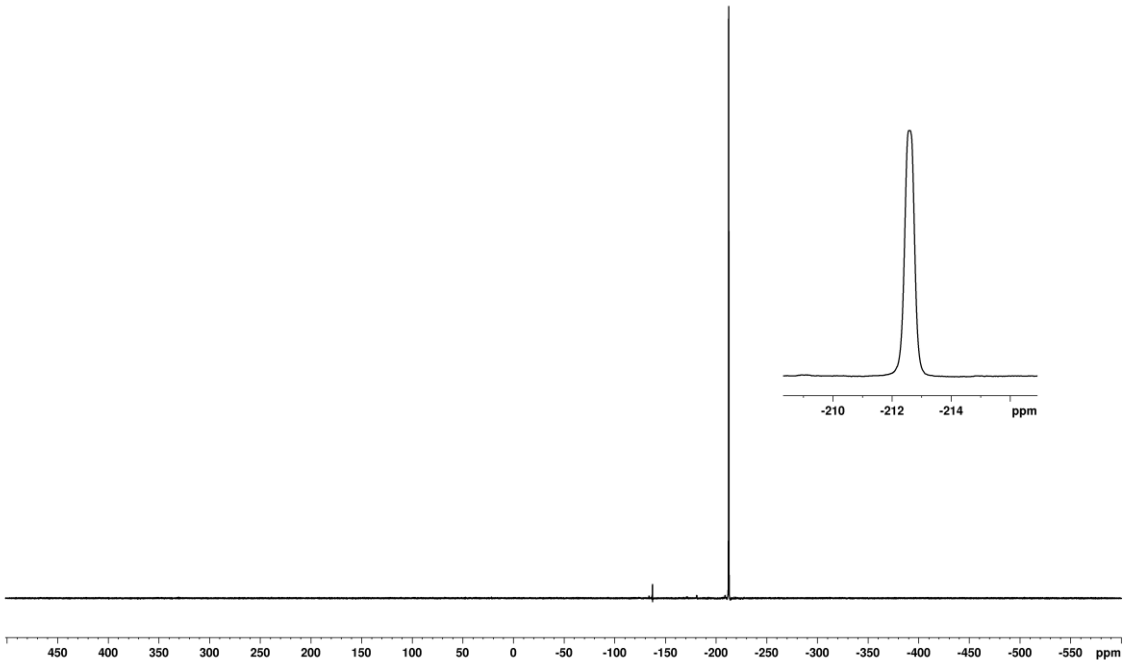

Figure S 5.11: $^{31}P\{^1H\}$ NMR spectrum of IDipp·BH_2PH_2 (C_6D_6, 298 K).

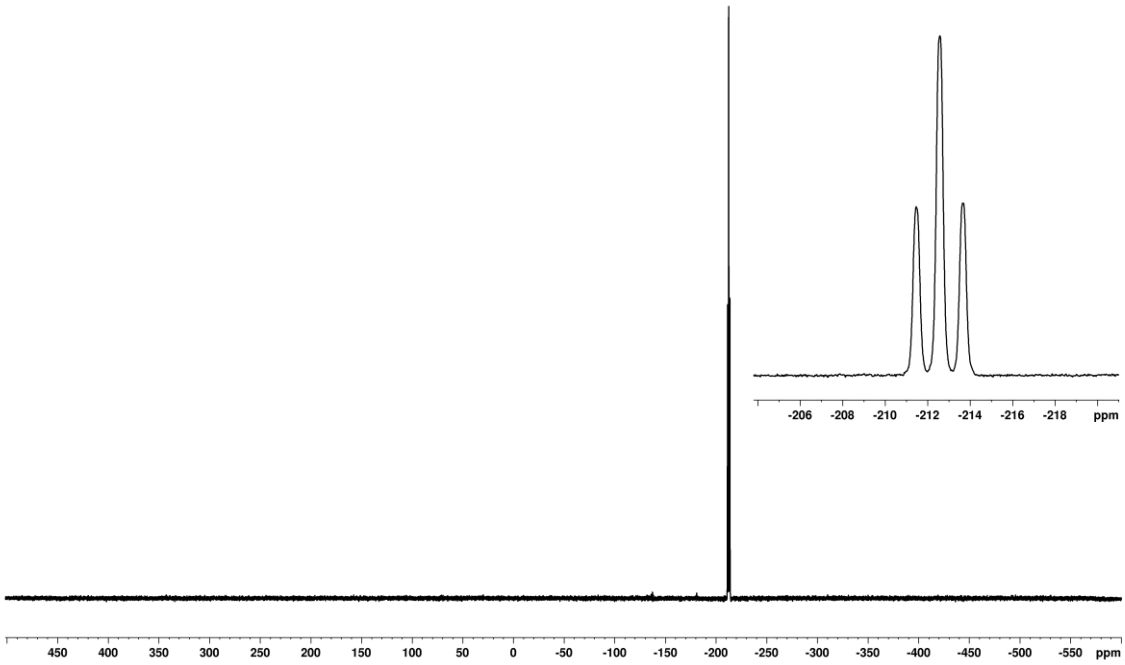

Figure S 5.12: ^{31}P NMR spectrum of IDipp·BH_2PH_2 (C_6D_6, 298 K).

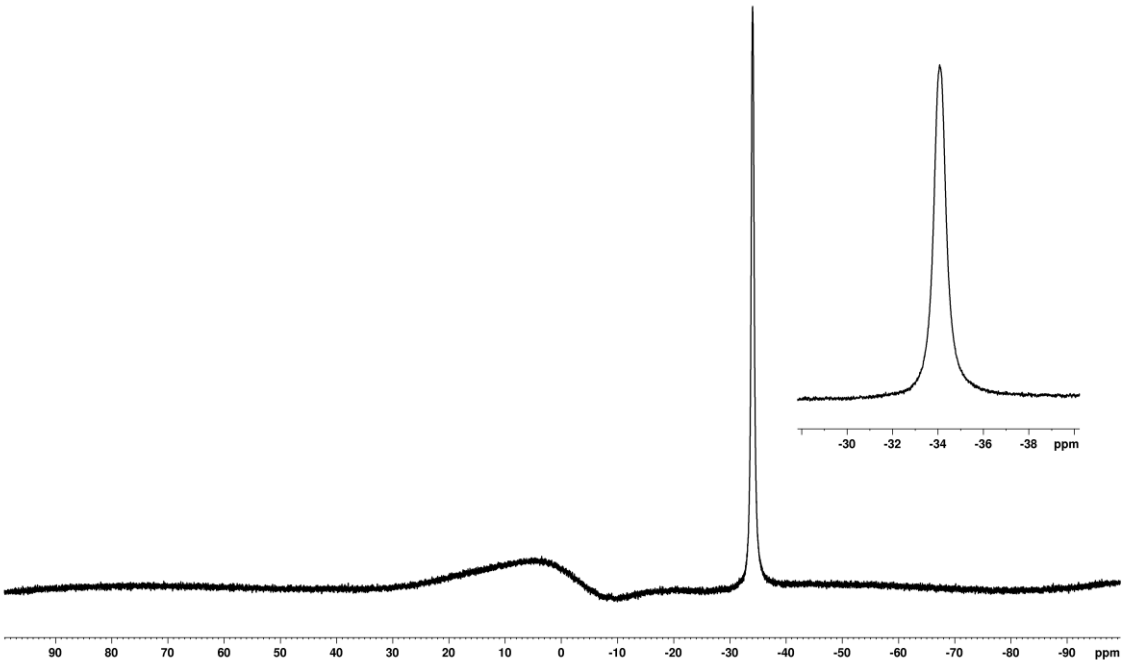

Figure S 5.13: $^{11}B\{^1H\}$ NMR spectrum of IDipp·BH_2PH_2 (C_6D_6, 298 K).

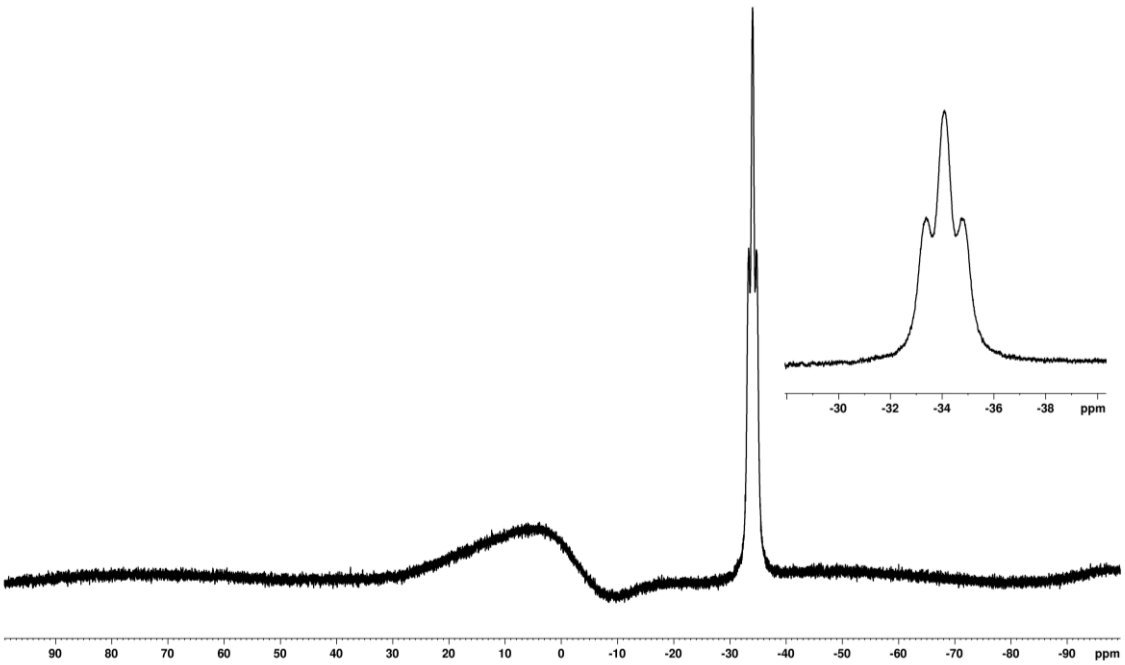

Figure S 5.14: ^{11}B NMR spectrum of IDipp·BH_2PH_2 (C_6D_6, 298 K).

5.5.3.5 IDipp·GaH$_2$(OTf)

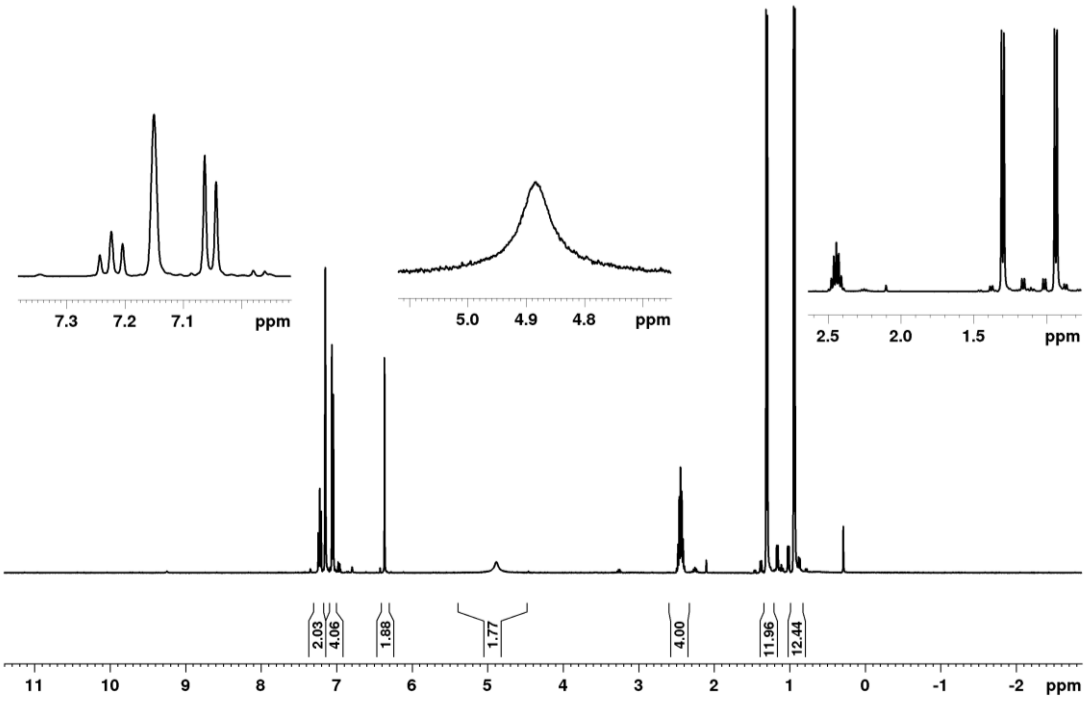

Figure S 5.15: ^{1}H NMR spectrum of IDipp·GaH$_2$(OTf) (C_6D_6, 298 K).

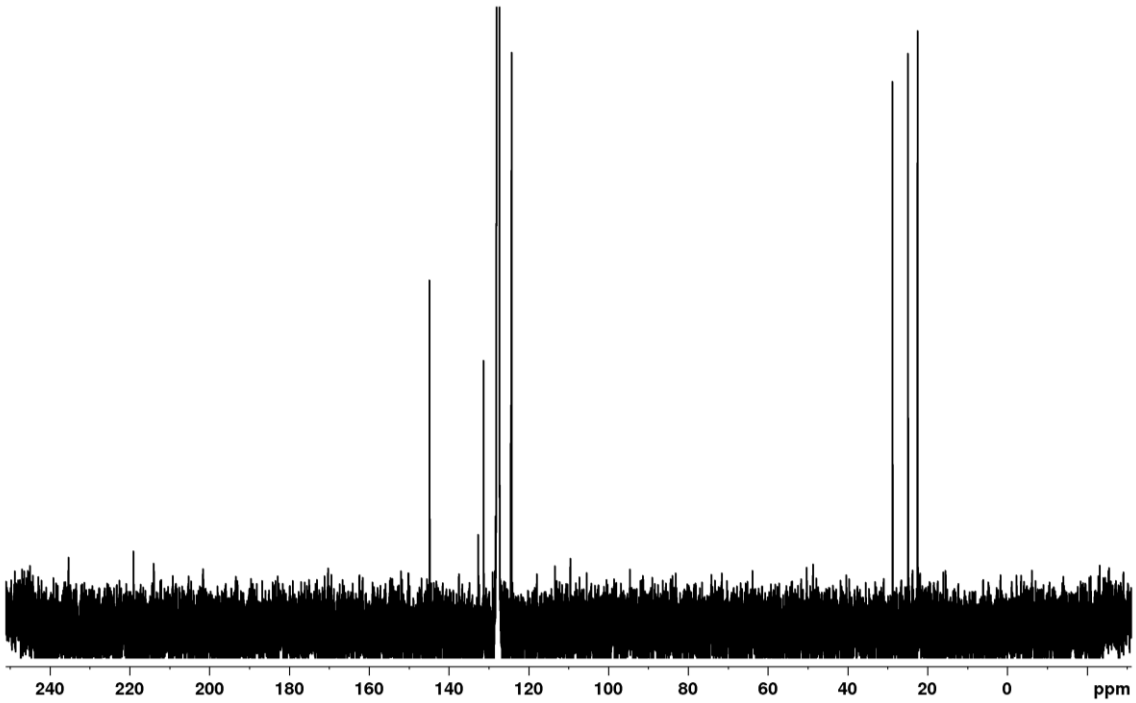

Figure S 5.16: ^{13}C{^{1}H} NMR spectrum of IDipp·GaH$_2$(OTf) (C_6D_6, 298 K).

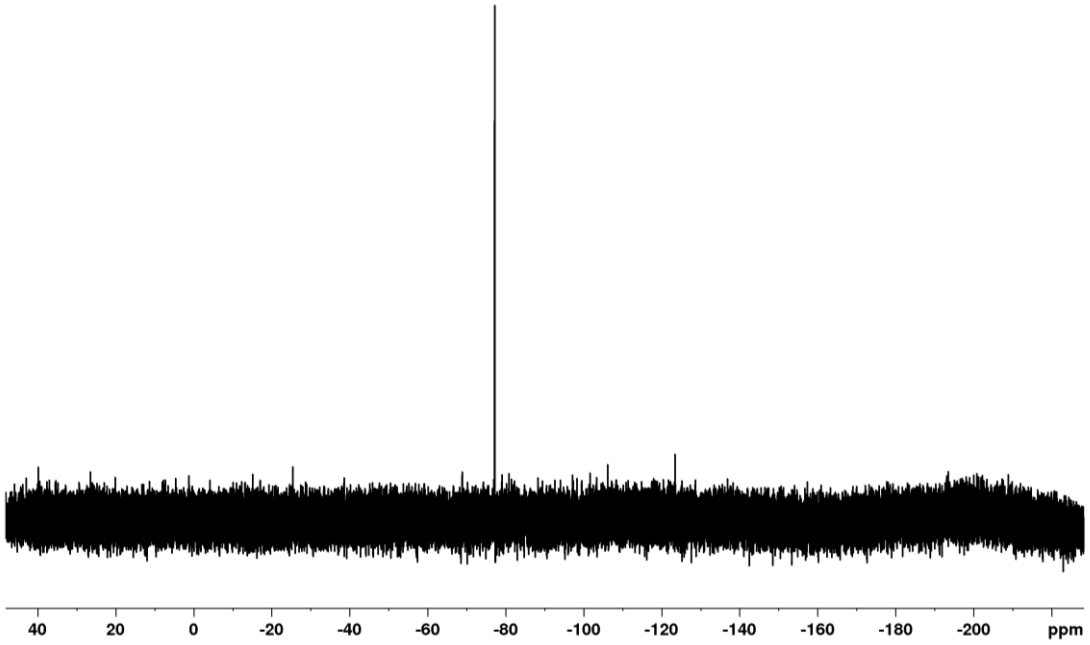

Figure S 5.17: $^{19}F\{^1H\}$ NMR spectrum of IDipp·GaH_2(OTf) (C_6D_6, 298 K).

5.5.3.6 IPr_2Me_2·GaH_2(OTf)

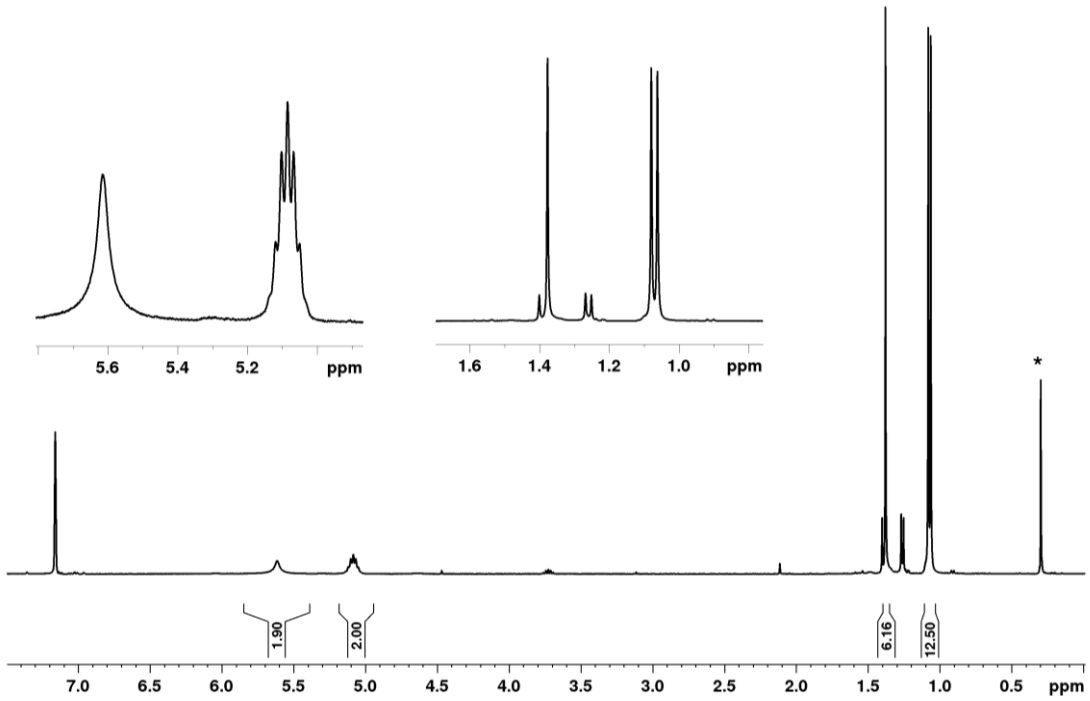

Figure S 5.18: ^1H NMR spectrum of IPr_2Me_2·GaH_2(OTf) (C_6D_6, 298 K; * = unidentified impurity)

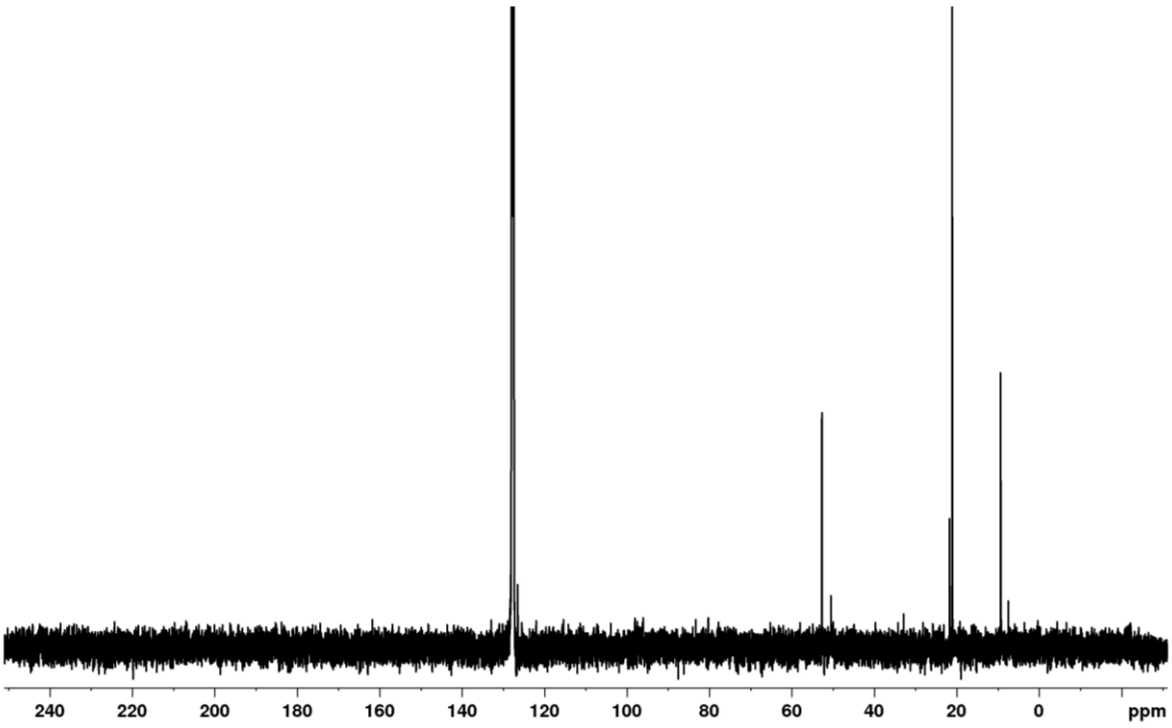

Figure S 5.19: $^{13}C\{^1H\}$ NMR spectrum of IPr_2Me_2·GaH_2(OTf) (C_6D_6, 298 K).

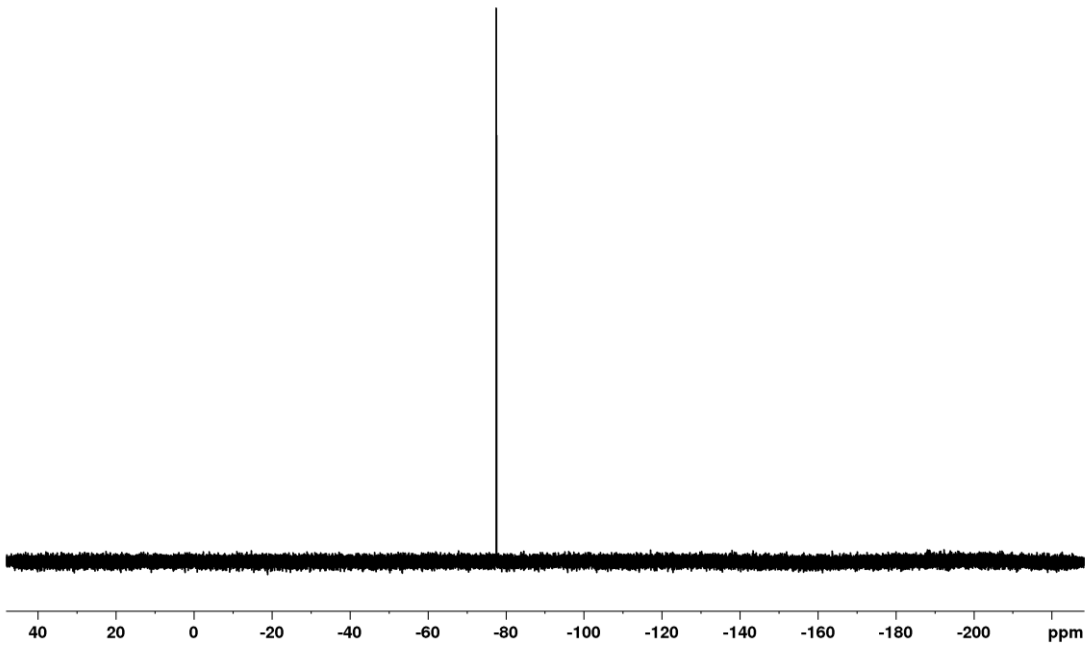

Figure S 5.20: $^{19}F\{^1H\}$ NMR spectrum of IPr_2Me_2·GaH_2(OTf) (C_6D_6, 298 K).

5.5.3.7 IMes·GaH$_2$(OTf)

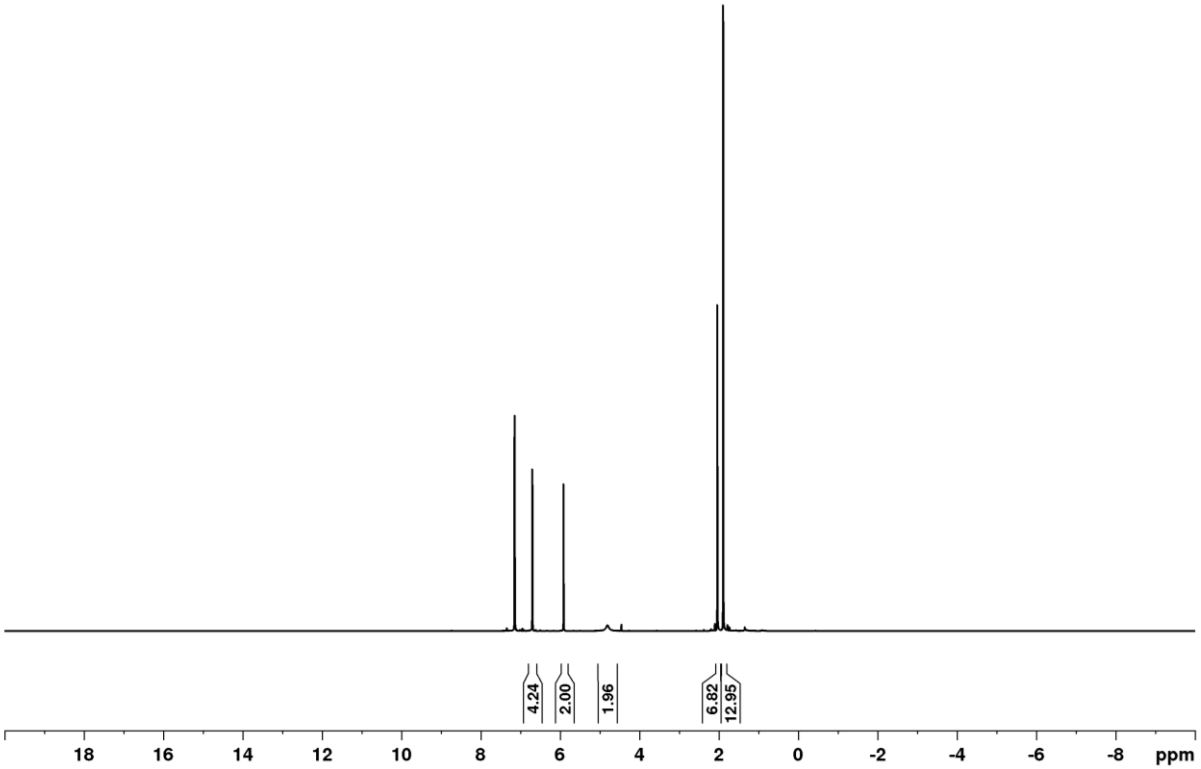

Figure S 5.21: ^{1}H NMR spectrum of IMes·GaH$_2$(OTf) (C_6D_6, 298 K).

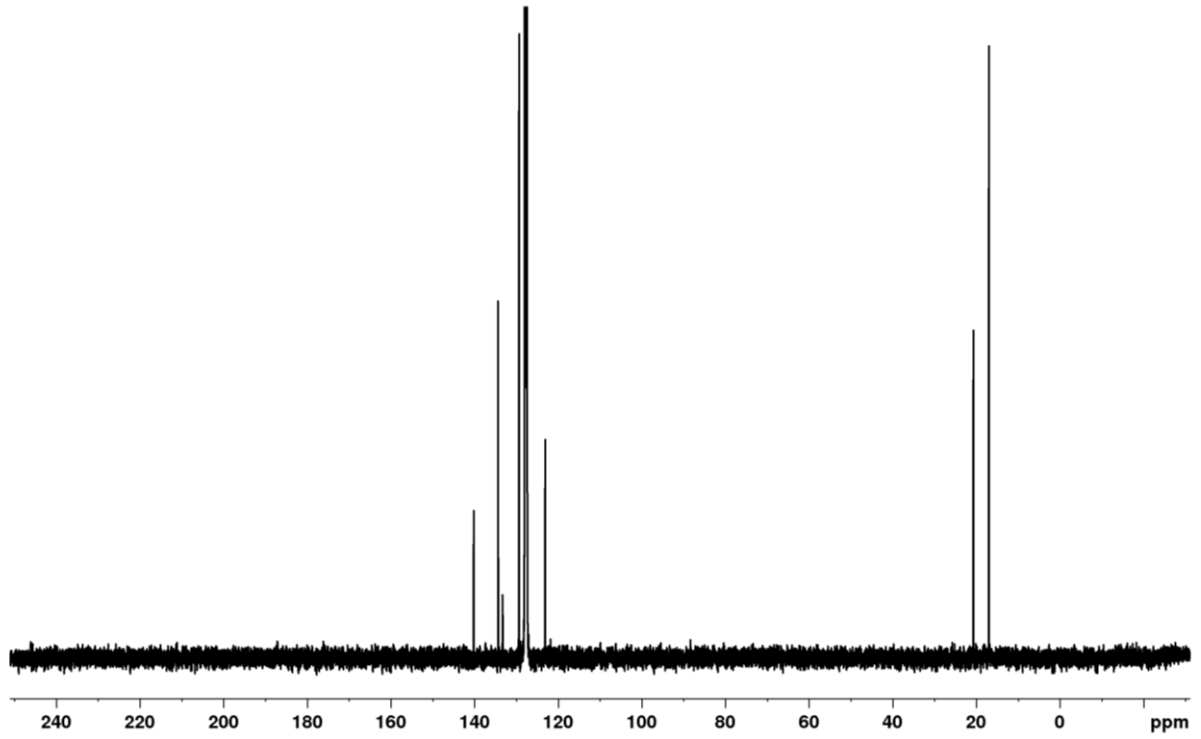

Figure S 5.22: ^{13}C{^{1}H} NMR spectrum of IMes·GaH$_2$(OTf) (C_6D_6, 298 K).

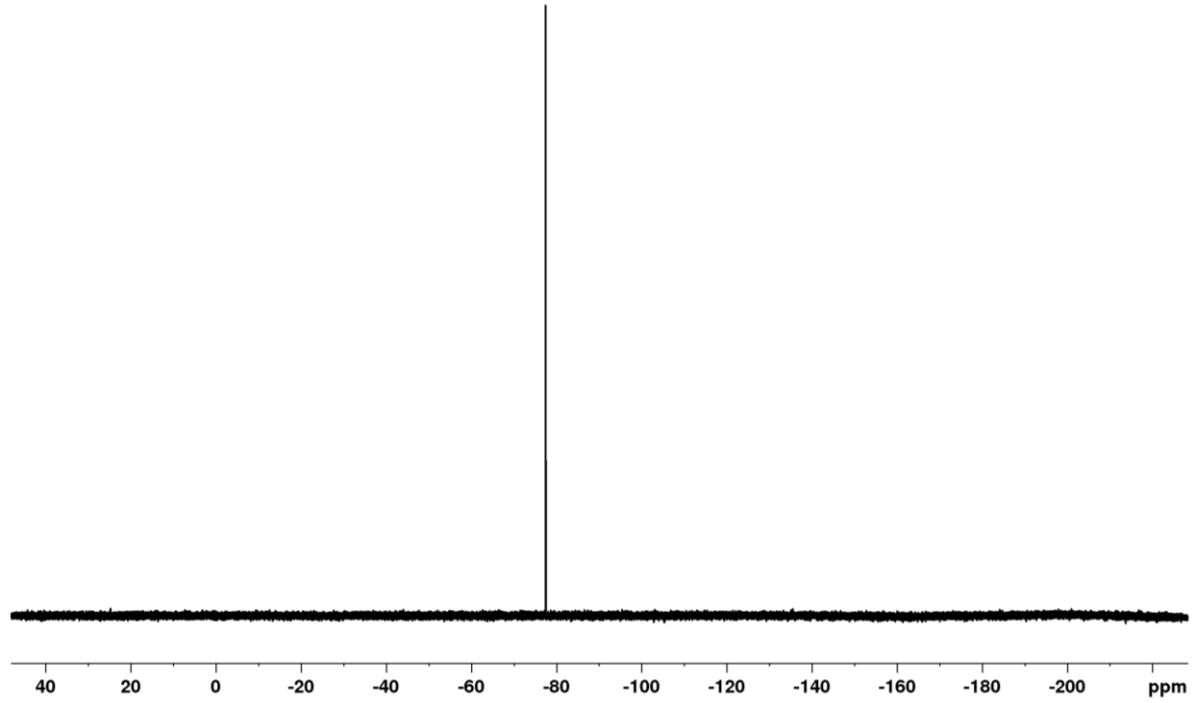

Figure S 5.23: $^{19}F\{^{1}H\}$ NMR spectrum of IMes·GaH$_2$(OTf) (C_6D_6, 298 K).

5.5.3.8 IDipp·GaHI$_2$

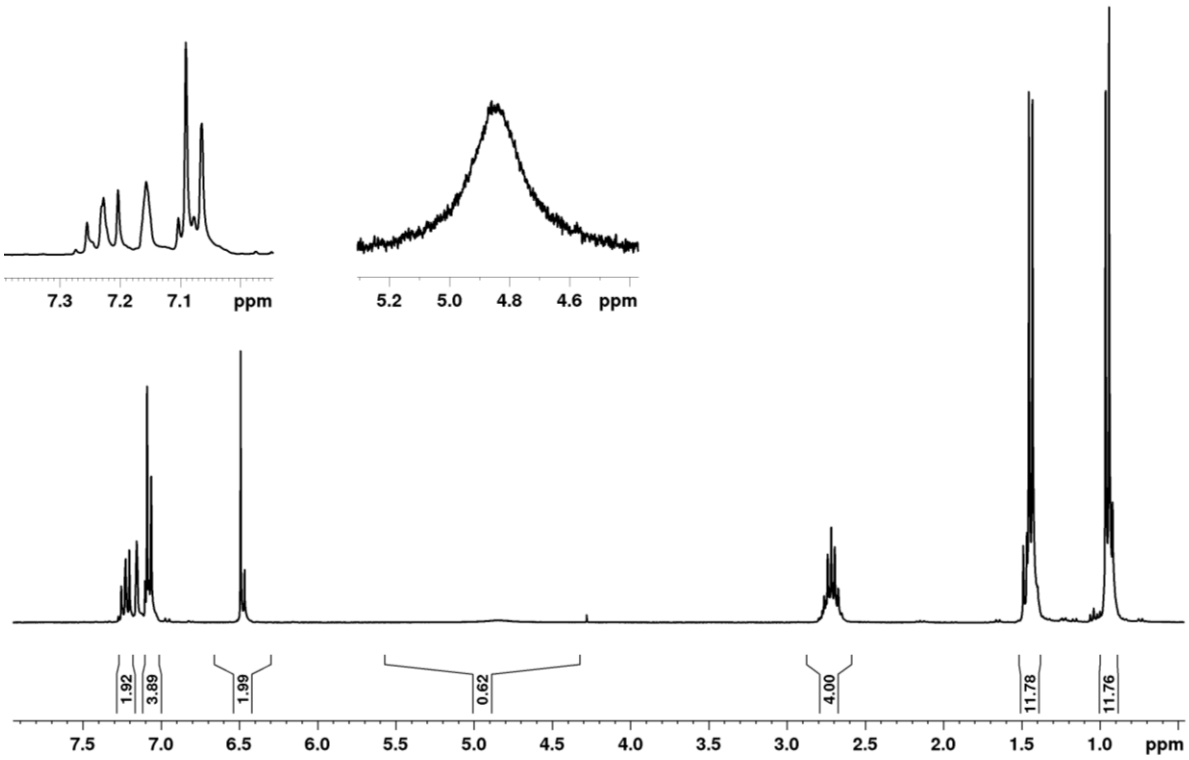

Figure S 5.24: ^{1}H NMR spectrum of IDipp·GaHI$_2$ (C_6D_6, 298 K).

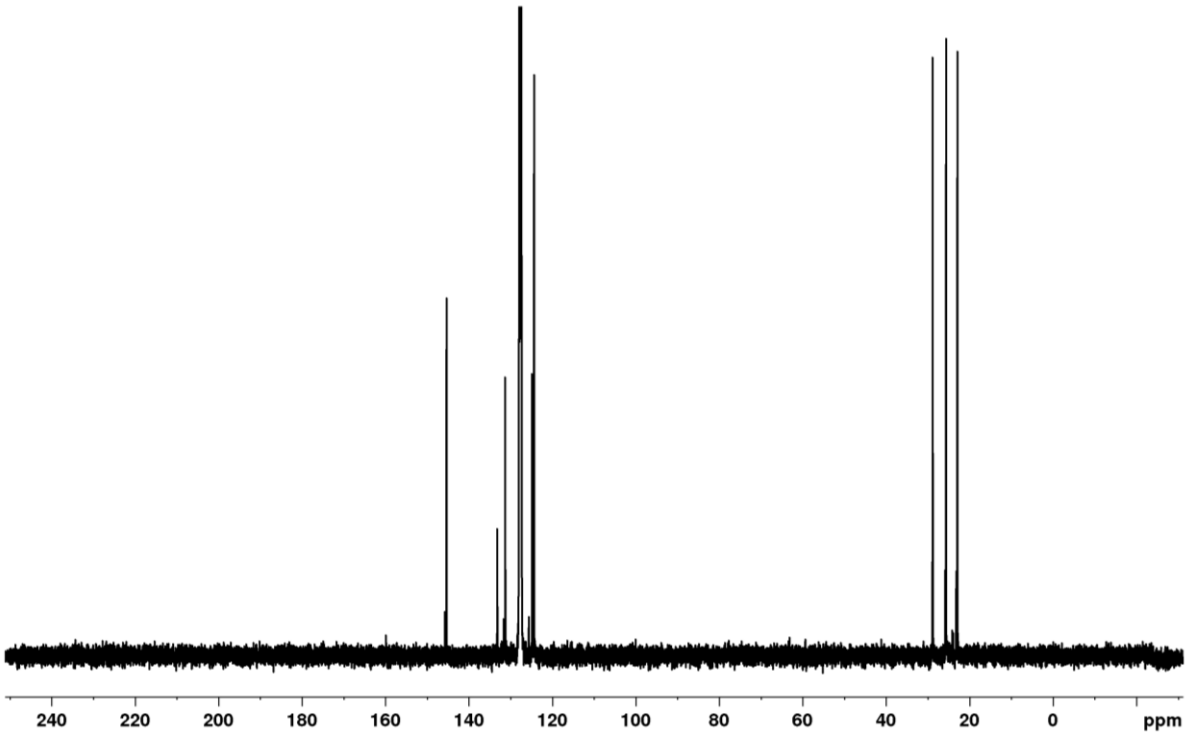

Figure S 5.25: $^{13}C\{^1H\}$ NMR spectrum of IDipp·$GaHI_2$ (C_6D_6, 298 K).

5.5.3.9 Reaction of IDipp·GaH_3 with excess MeI (reflux)

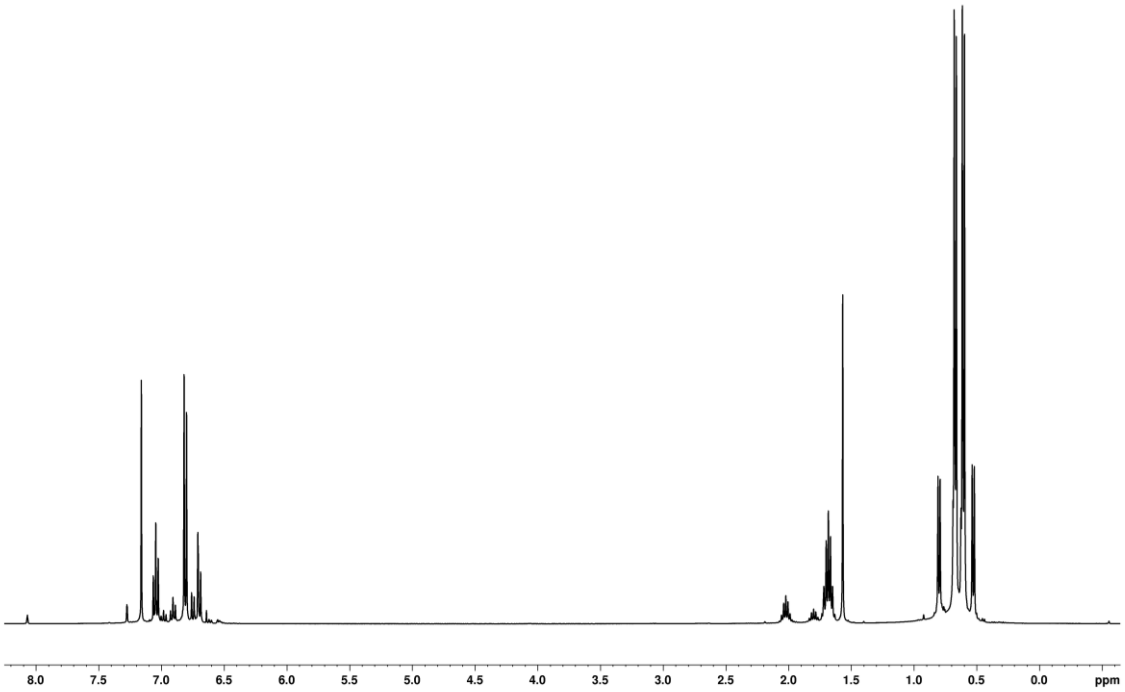

Figure S 5.26: ^1H NMR spectrum after boiling IDipp·GaH_3 with an excess amount of MeI in toluene overnight ($CDCl_3$, 298 K).

5.5.3.10 Reaction mixture containing 3a after 30 min

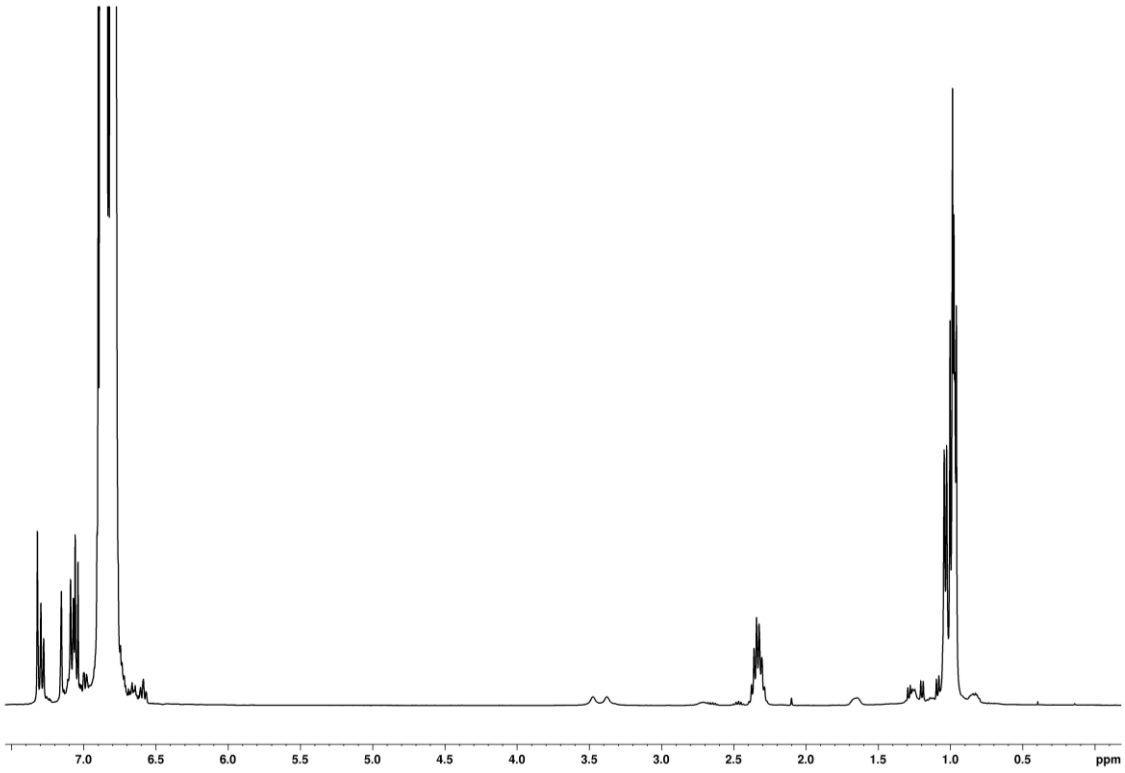

Figure S 5.27: Section of the ^{1}H NMR spectrum of the reaction mixture containing **3a** after 30 min showing full conversion of the starting material (298 K, 1,2-difluorobenzene/C_6D_6-capillary).

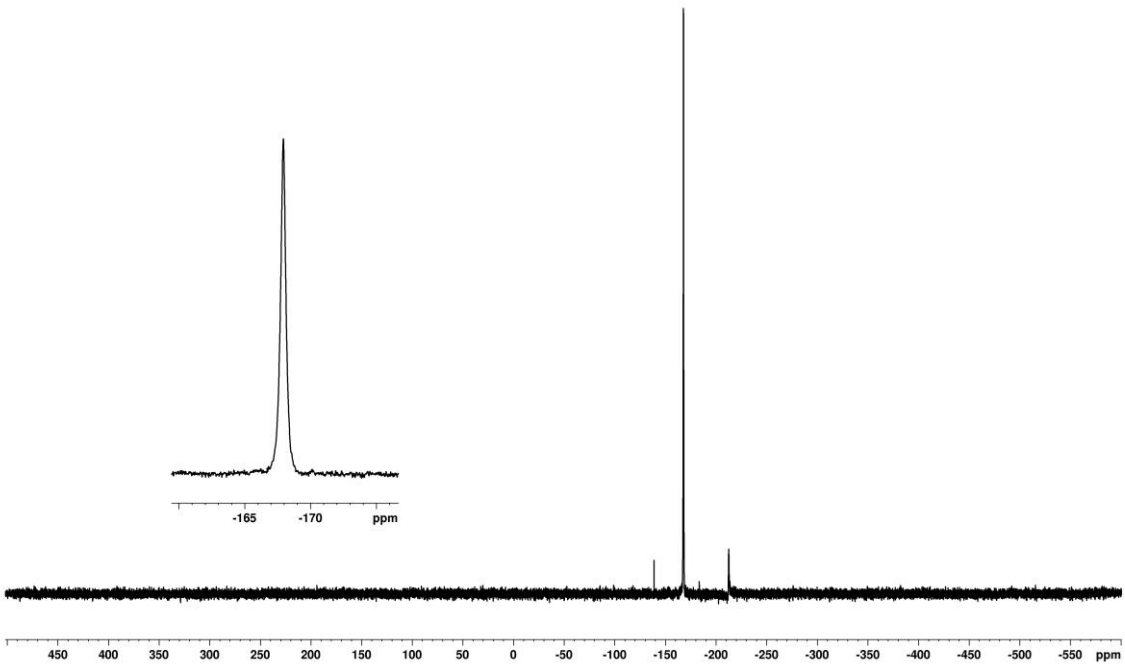

Figure S 5.28: Section of the $^{31}P\{^{1}H\}$ NMR spectrum of the reaction mixture containing **3a** after 30 min showing full conversion of the starting material (298 K, 1,2-difluorobenzene/C_6D_6-capillary).

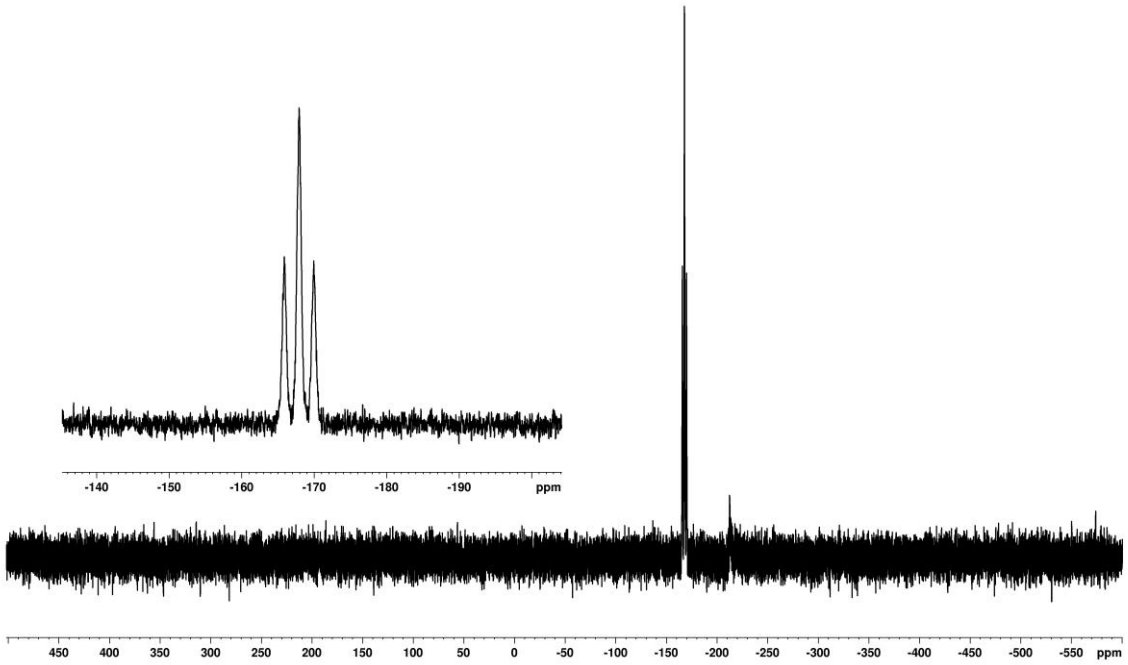

Figure S 5.29: ^{31}P NMR spectrum of the reaction mixture containing **3a** after 30 min (298 K, 1,2-difluorobenzene/C_6D_6-capillary).

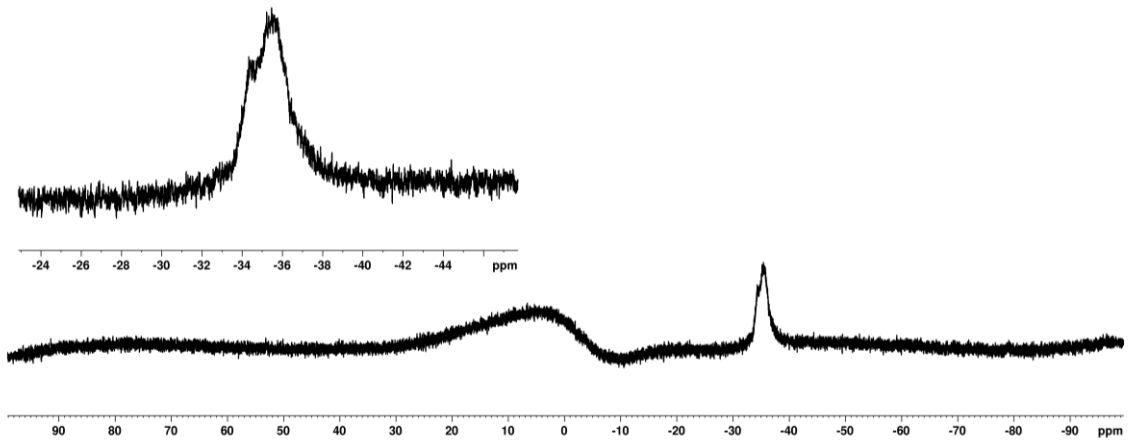

Figure S 5.30: $^{11}B\{^1H\}$ NMR spectrum of the reaction mixture containing **3a** after 30 min (298 K, 1,2-difluorobenzene/C_6D_6-capillary).

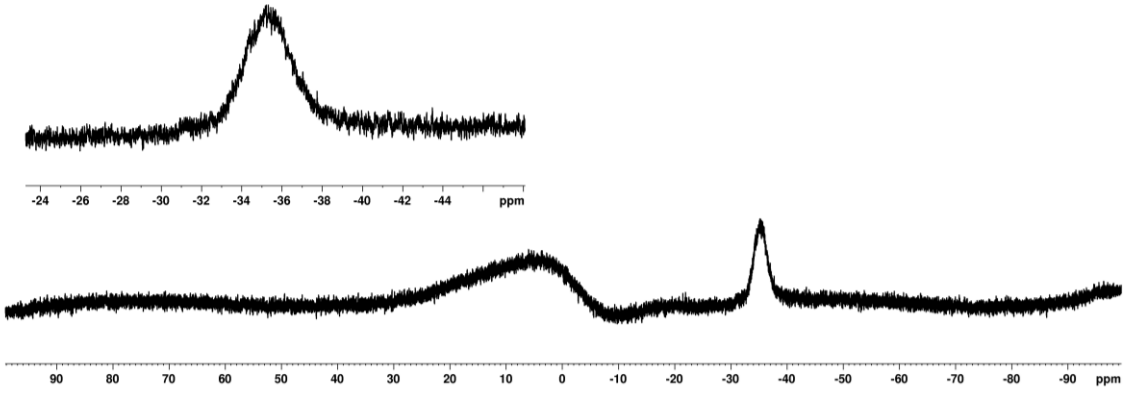

Figure S 5.31: ^{11}B NMR spectrum of the reaction mixture containing **3a** after 30 min (298 K, 1,2-difluorobenzene/C_6D_6-capillary).

5.5.3.11 [IDipp·$GaH_2PH_2BH_2$·IDipp][OTf]

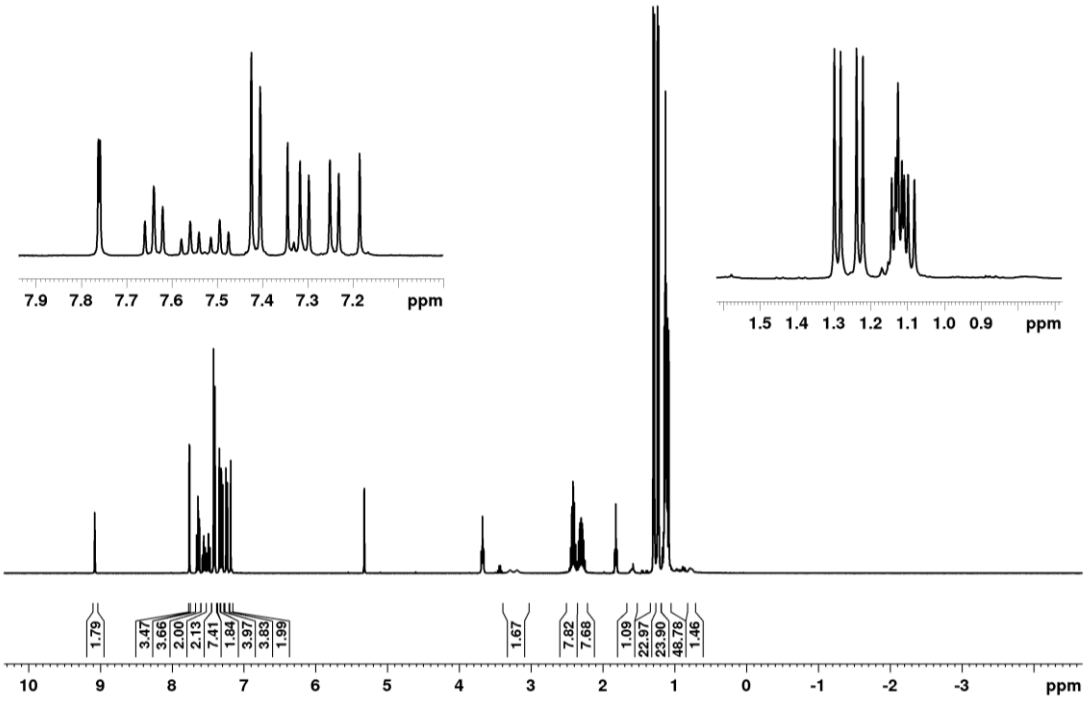

Figure S 5.32: ^{1}H NMR spectrum of [IDipp·$GaH_2PH_2BH_2$·IDipp][OTf] (CD_2Cl_2, 298 K).

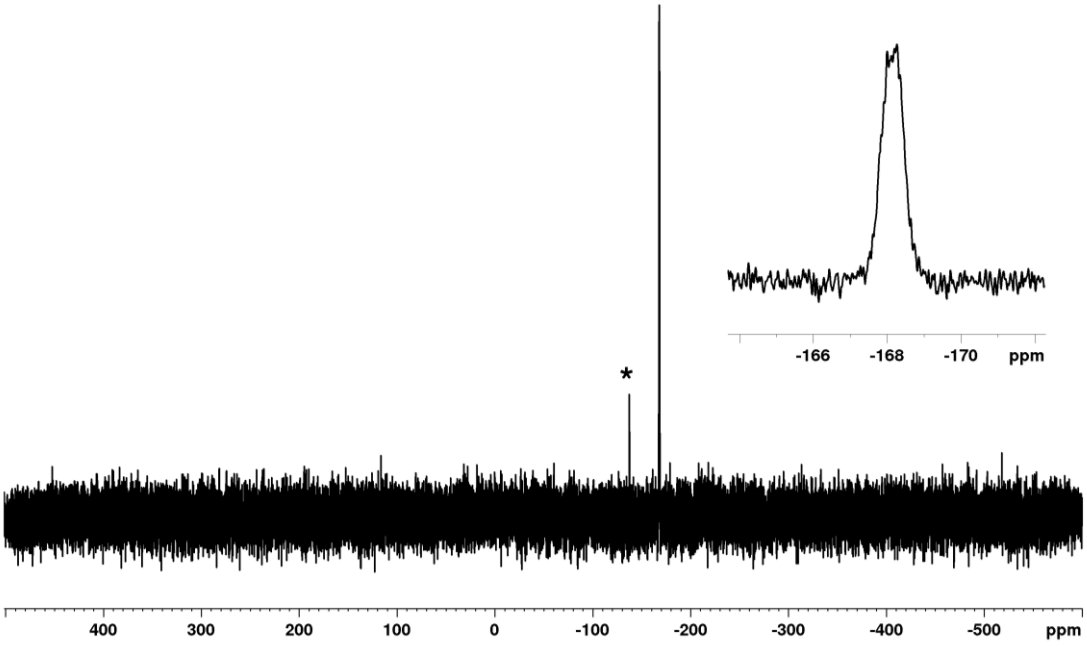

Figure S 5.33: $^{31}P\{^1H\}$ NMR spectrum of [IDipp · $GaH_2PH_2BH_2$ · IDipp][OTf] (CD_2Cl_2, 298 K; * = unidentified impurity).

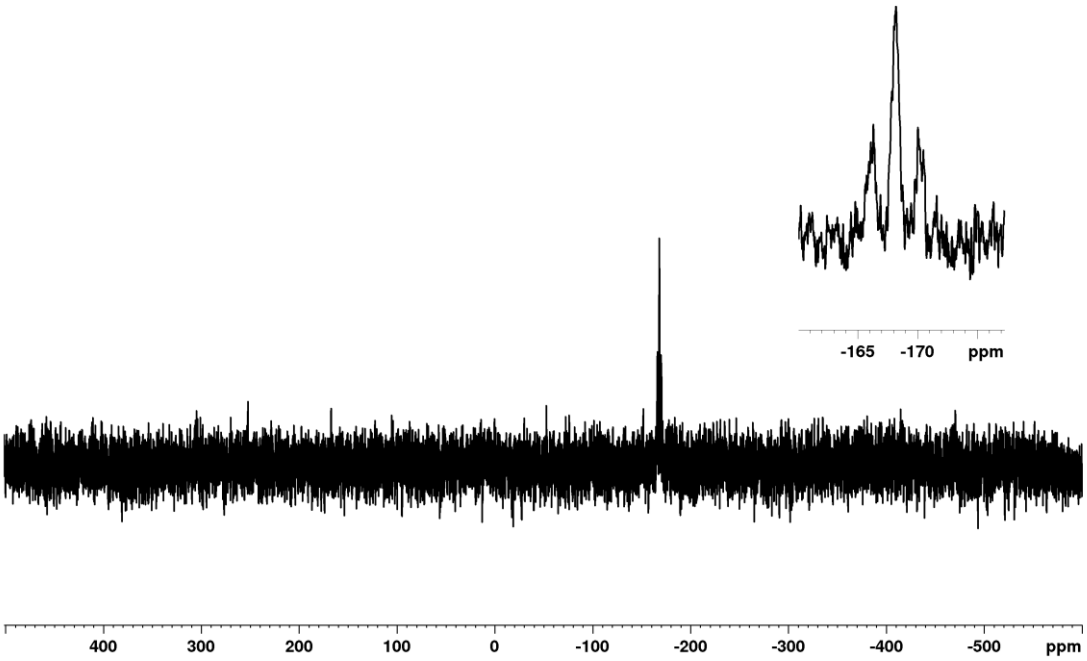

Figure S 5.34: ^{31}P NMR spectrum of [IDipp·$GaH_2PH_2BH_2$·IDipp][OTf] (CD_2Cl_2, 298 K).

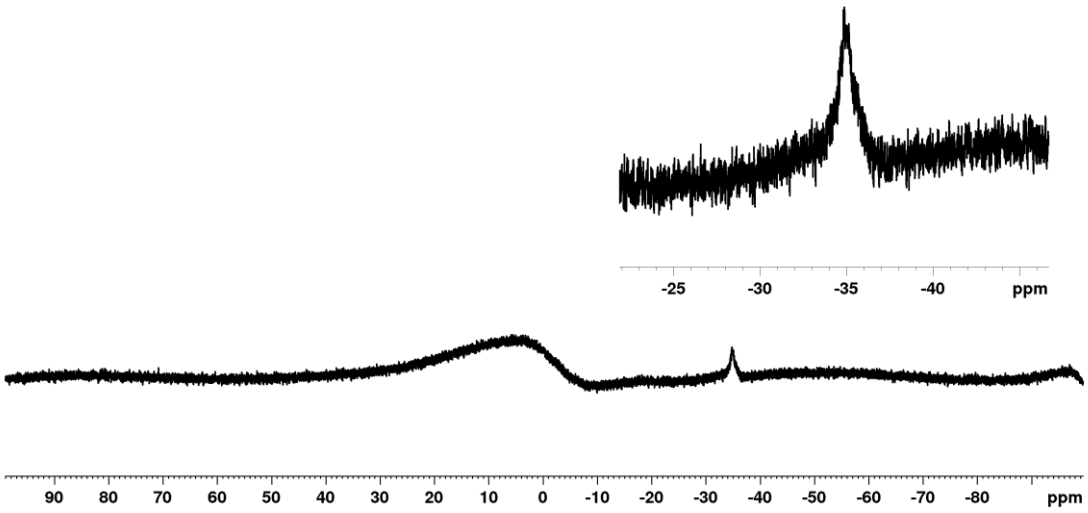

Figure S 5.35: $^{11}B\{^1H\}$ NMR spectrum of [IDipp·$GaH_2PH_2BH_2$·IDipp][OTf] (CD_2Cl_2, 298 K).

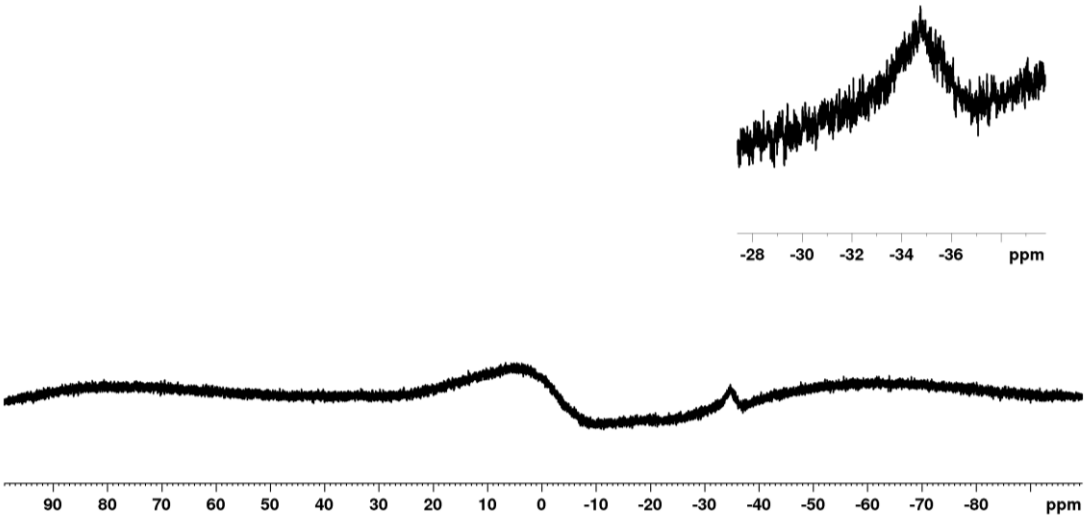

Figure S 5.36: ^{11}B NMR spectrum of [IDipp·$GaH_2PH_2BH_2$·IDipp][OTf] (CD_2Cl_2, 298 K).

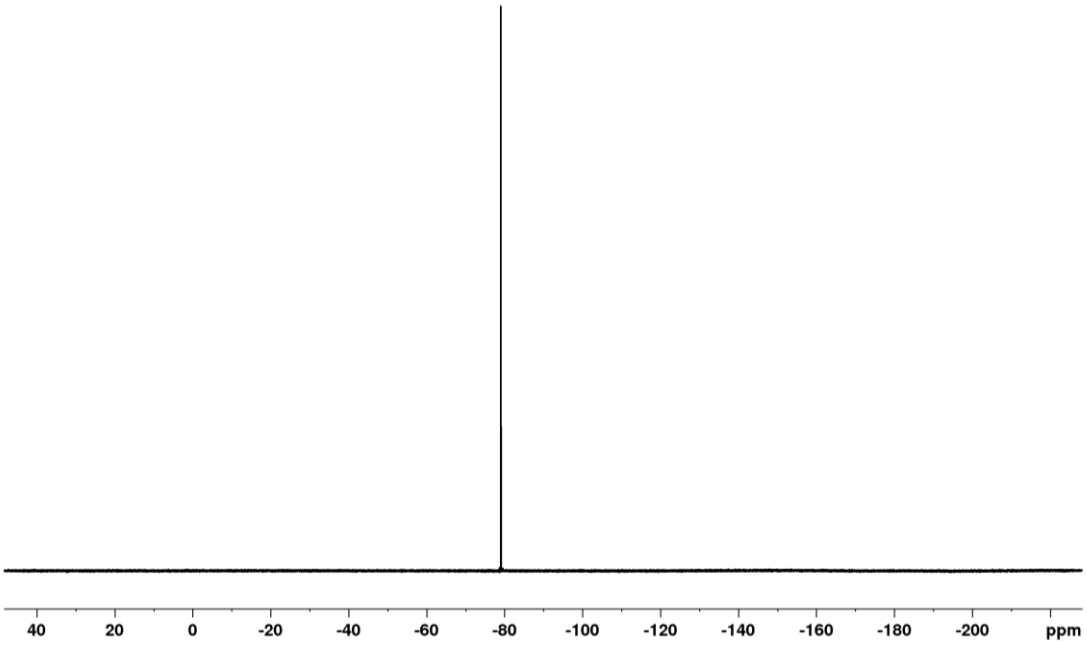

Figure S 5.37: $^{19}F\{^1H\}$ NMR spectrum of [IDipp·$GaH_2PH_2BH_2$·IDipp][OTf] (CD_2Cl_2, 298 K).

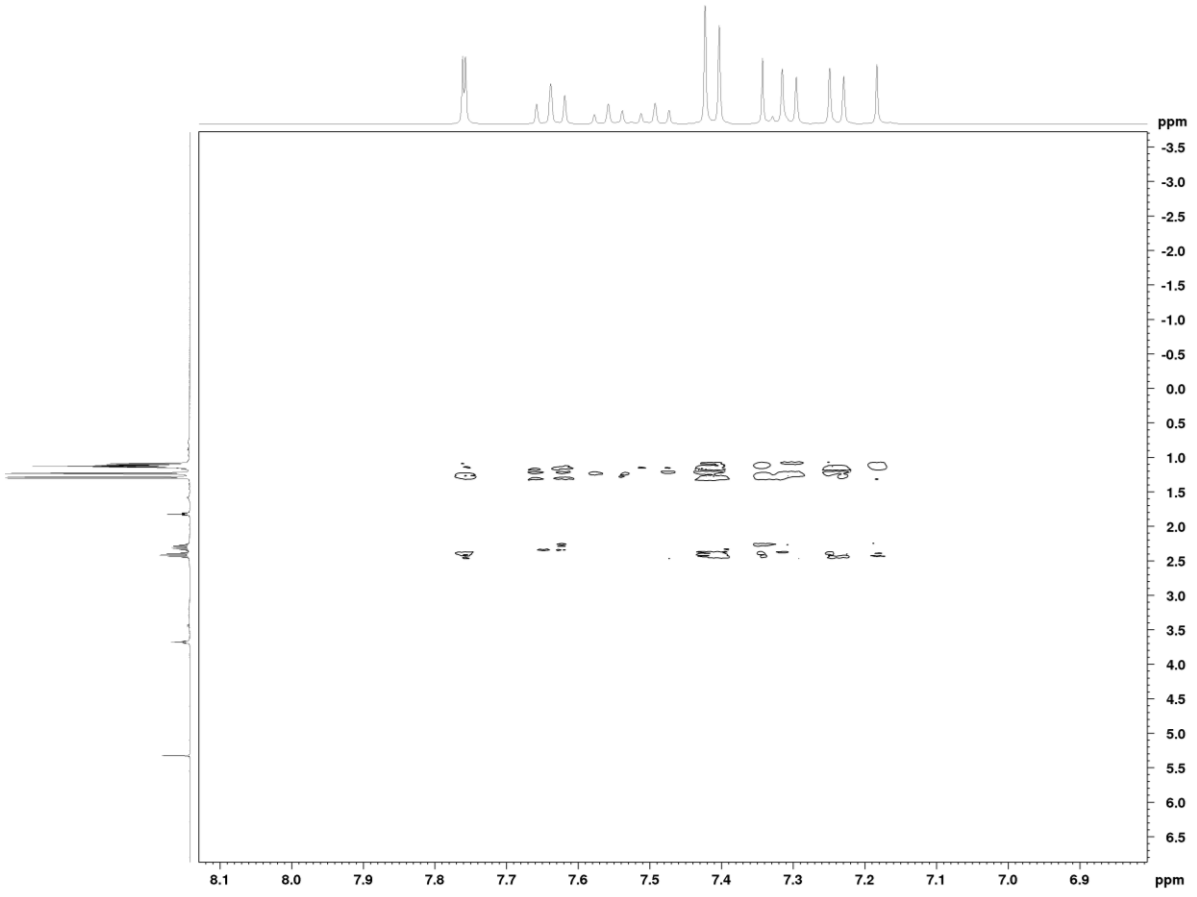

Figure S 5.38: Section of the ^1H, ^1H COSY NMR spectrum of [IDipp·$GaH_2PH_2BH_2$·IDipp][OTf] (CD_2Cl_2, 298 K, zoomed).

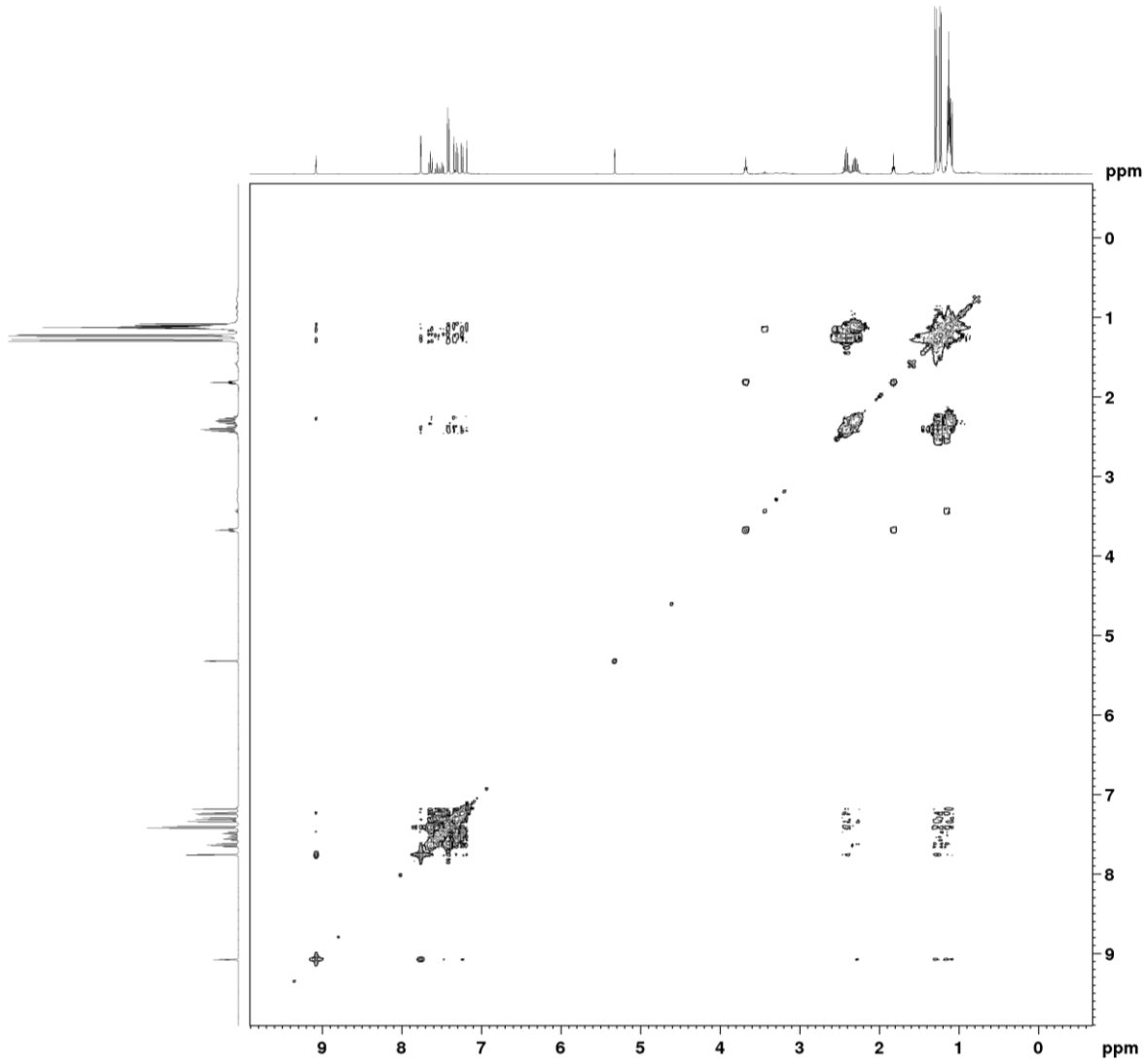

Figure S 5.39: ^{1}H, ^{1}H COSY NMR spectrum of [IDipp·$GaH_2PH_2BH_2$·IDipp][OTf] (CD_2Cl_2, 298 K, full view).

5.5.3.12 [IDipp·$GaH_2PH_2BH_2$·NMe_3][OTf]

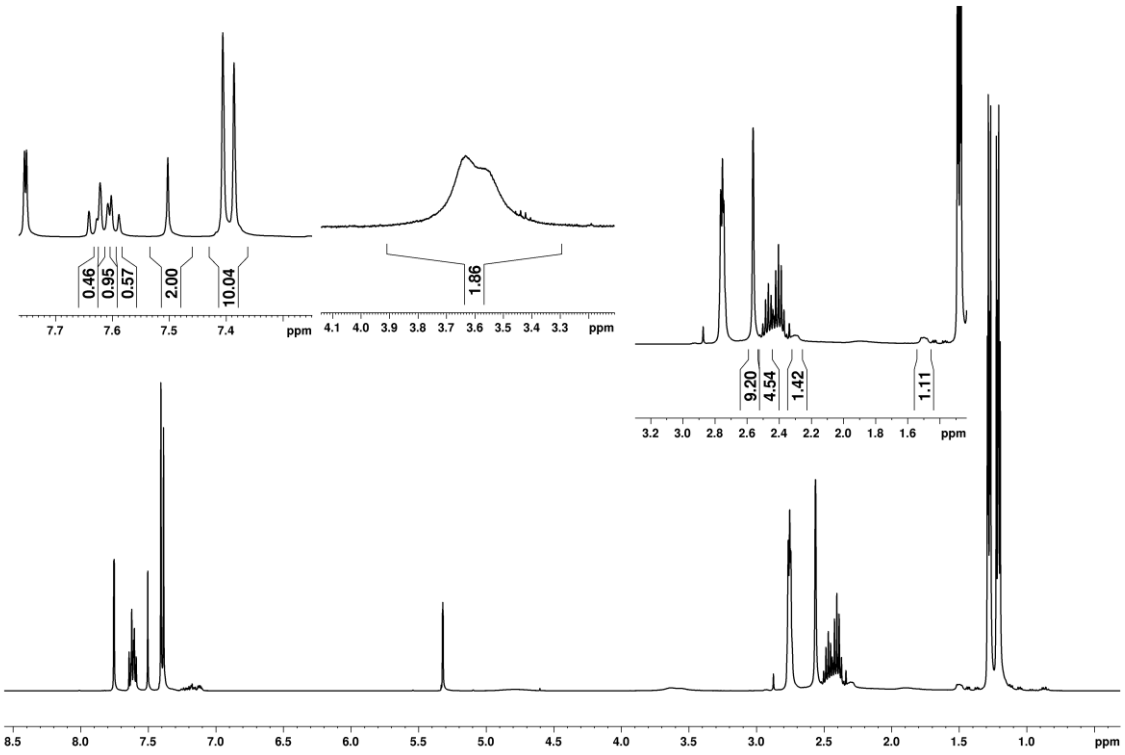

Figure S 5.40: ^{1}H NMR spectrum of [IDipp·$GaH_2PH_2BH_2$·NMe_3][OTf] (CD_2Cl_2, 298 K).

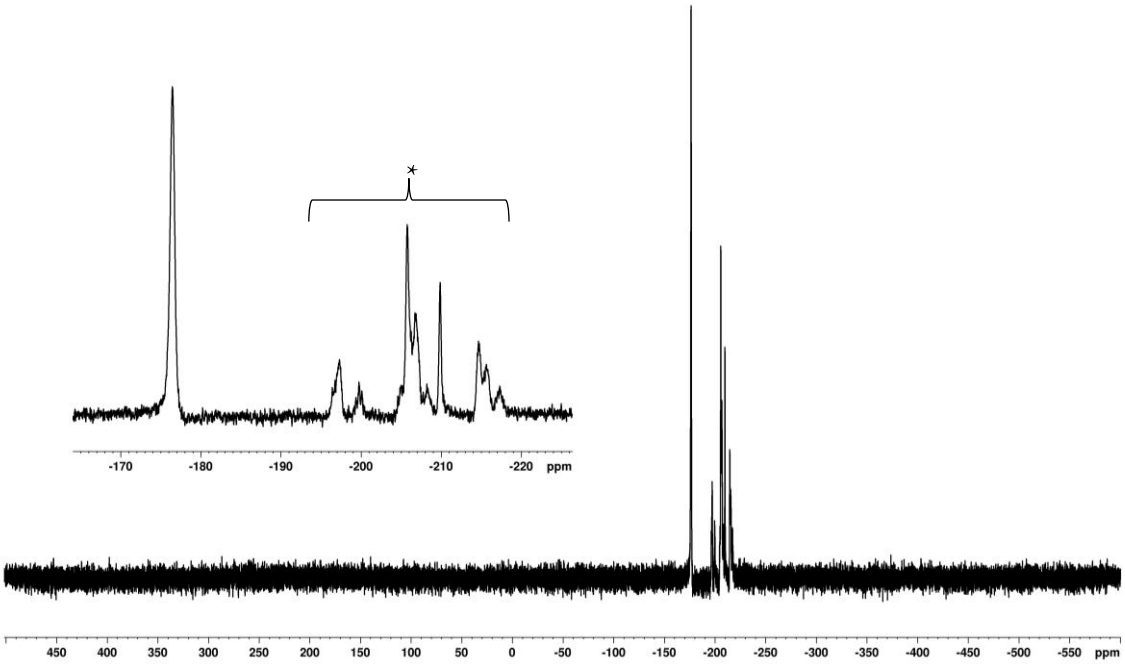

Figure S 5.41: $^{31}P\{^{1}H\}$ NMR spectrum of [IDipp·$GaH_2PH_2BH_2$·NMe_3][OTf] (CD_2Cl_2, 298 K, * = unidentified impurities).

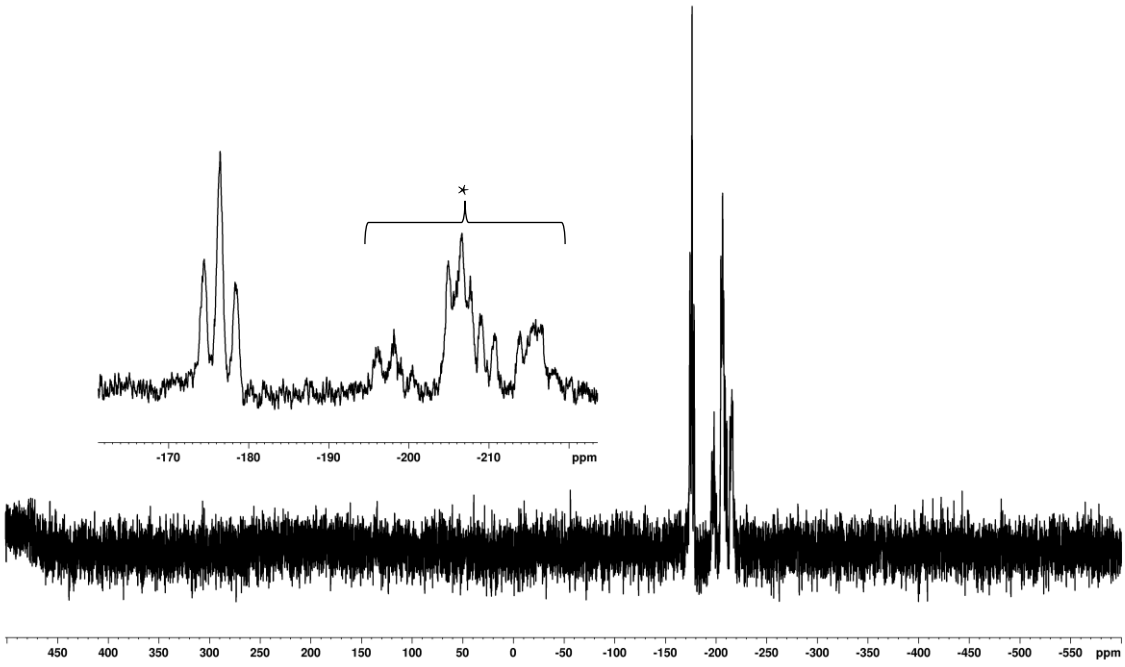

Figure S 5.42: ^{31}P NMR spectrum of [IDipp·$GaH_2PH_2BH_2$·NMe_3][OTf] (CD_2Cl_2, 298 K, * = unidentified impurities).

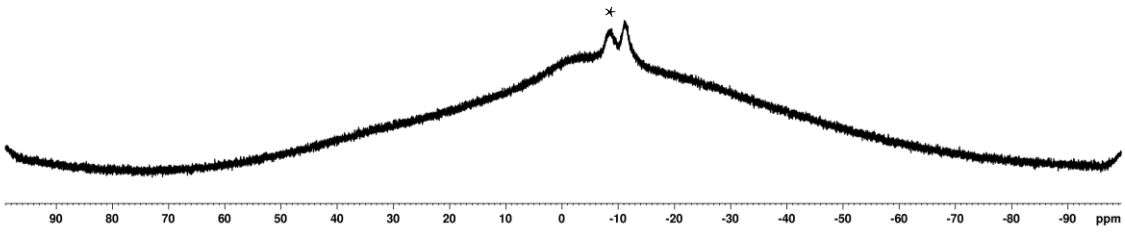

Figure S 5.43: $^{11}B\{^1H\}$ NMR spectrum of [IDipp·$GaH_2PH_2BH_2$·NMe_3][OTf] (CD_2Cl_2, 298 K, * = unidentified impurity).

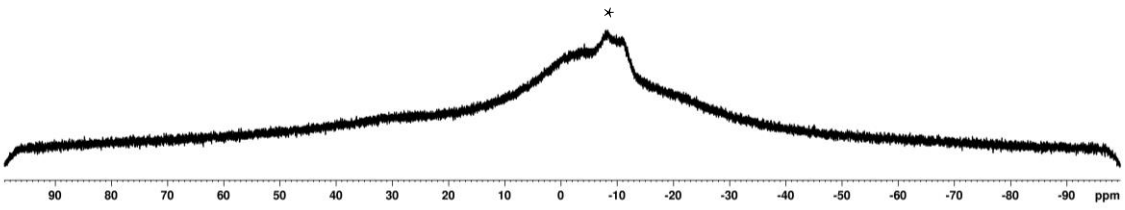

Figure S 5.44: ^{11}B NMR spectrum of [IDipp·$GaH_2PH_2BH_2$·NMe_3][OTf] (CD_2Cl_2, 298 K, * = unidentified impurity).

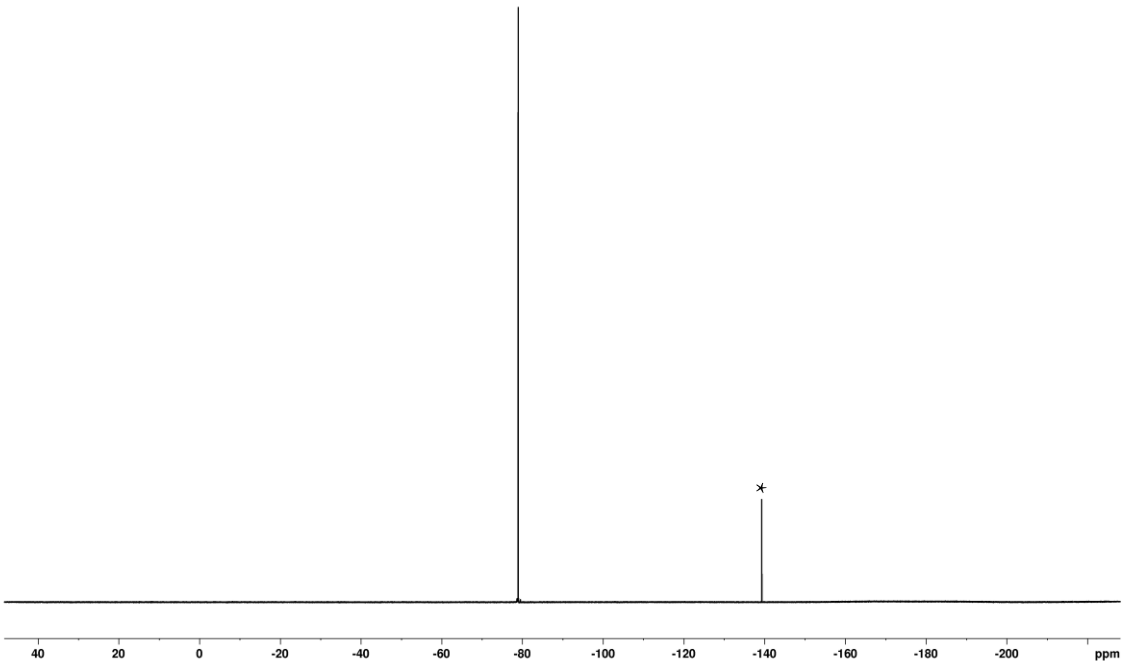

Figure S 5.45: $^{19}F\{^1H\}$ NMR spectrum of [IDipp·$GaH_2PH_2BH_2$·NMe_3][OTf] (CD_2Cl_2, 298 K, * = residual 1,2-difluorobenzene).

5.5.3.13 [IDipp·GaH$_2$PPh$_2$BH$_2$·NMe$_3$][OTf]

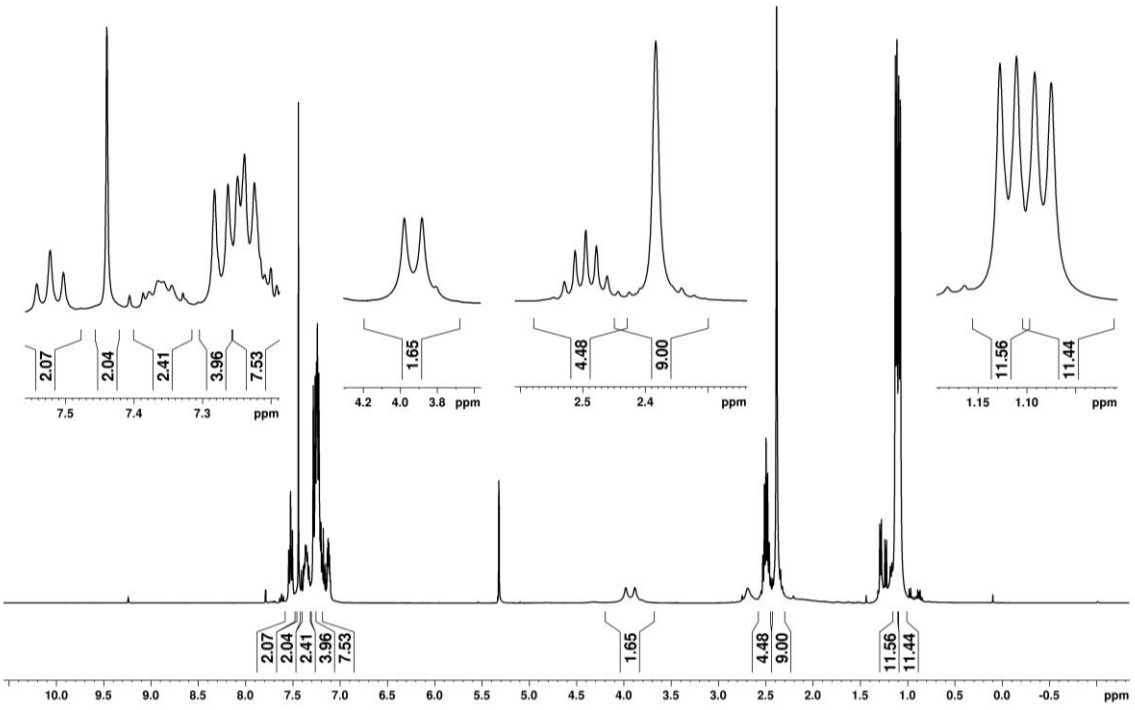

Figure S 5.46: ^{1}H NMR spectrum of [IDipp · GaH$_2$PPh$_2$BH$_2$ · NMe$_3$][OTf] (CD$_2$Cl$_2$, 298 K).

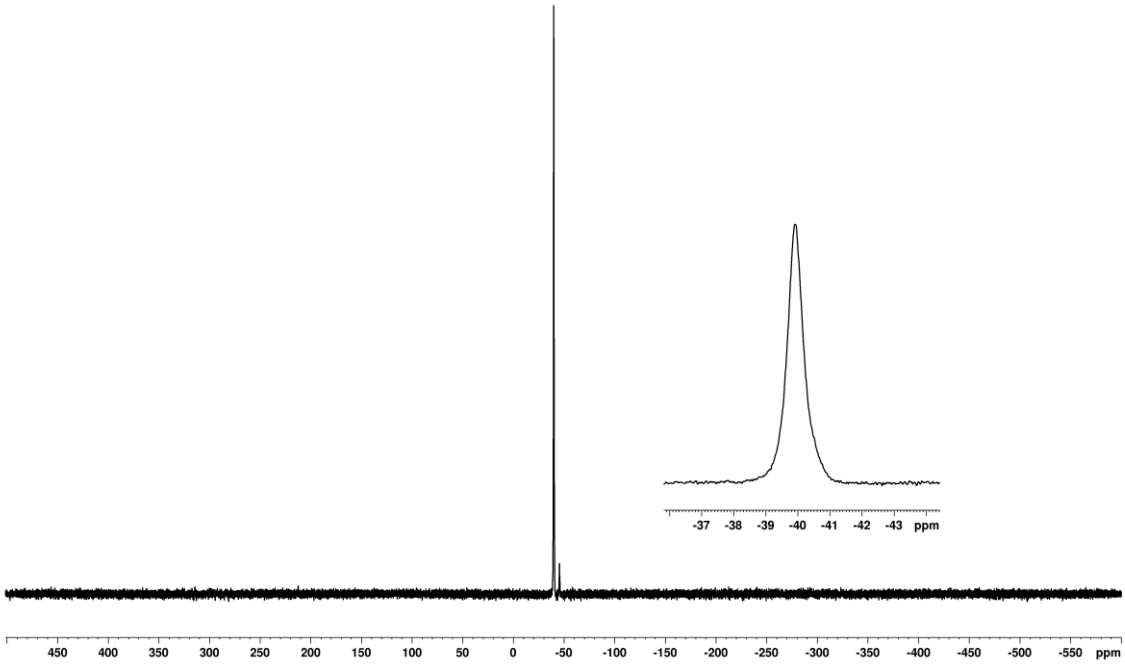

Figure S 5.47: ^{31}P{^{1}H} NMR spectrum of [IDipp·GaH$_2$PPh$_2$BH$_2$·NMe$_3$][OTf] (CD$_2$Cl$_2$, 298 K).

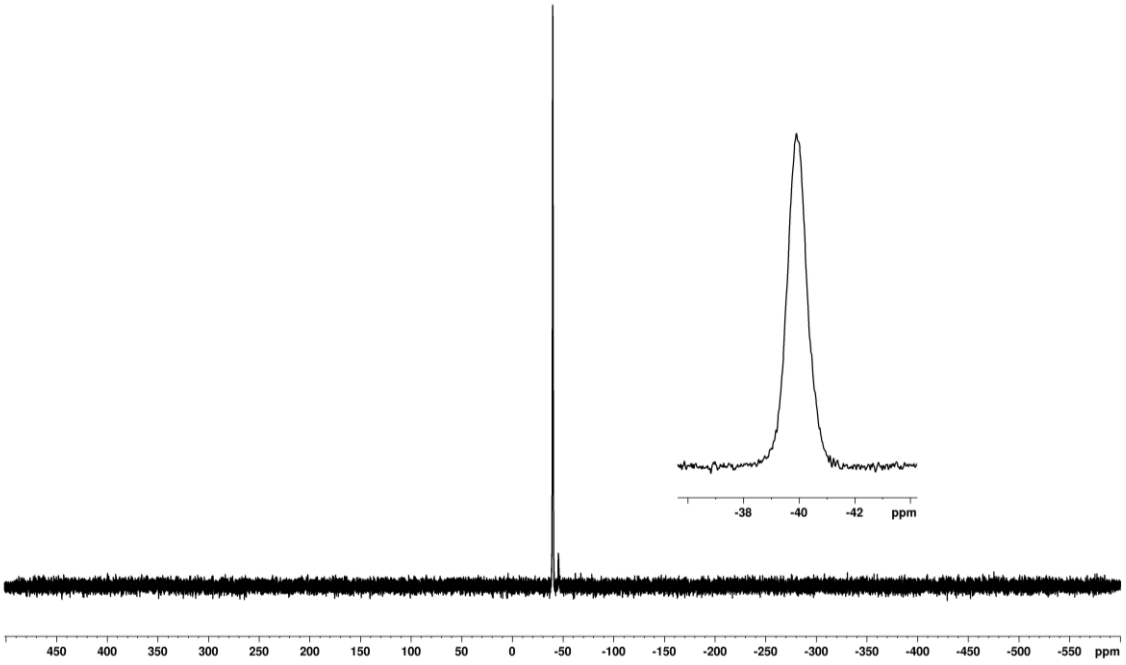

Figure S 5.48: ^{31}P NMR spectrum of [IDipp·$GaH_2PPh_2BH_2$·NMe_3][OTf] (CD_2Cl_2, 298 K).

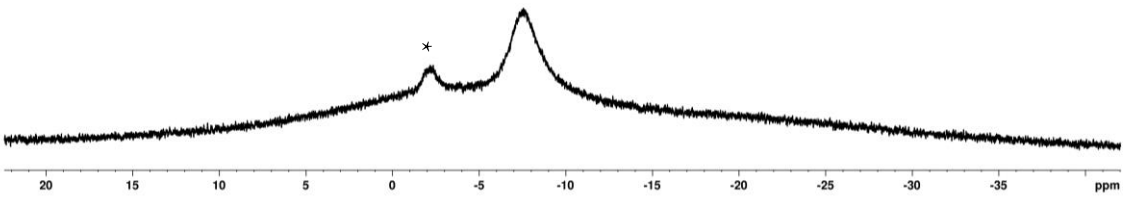

Figure S 5.49: $^{11}B\{^1H\}$ NMR spectrum of [IDipp·$GaH_2PPh_2BH_2$·NMe_3][OTf] (CD_2Cl_2, 298 K, * = unidentified impurity).

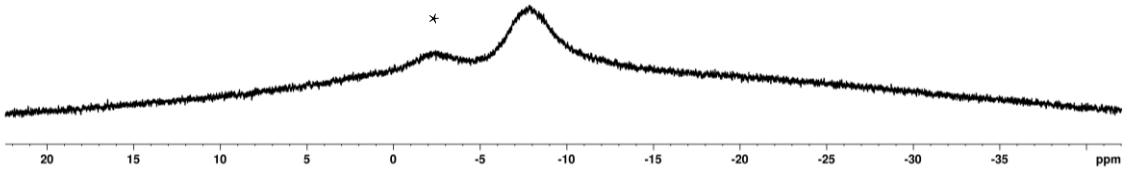

Figure S 5.50: ^{11}B NMR spectrum of [IDipp·$GaH_2PPh_2BH_2$·NMe_3][OTf] (CD_2Cl_2, 298 K, * = unidentified impurity).

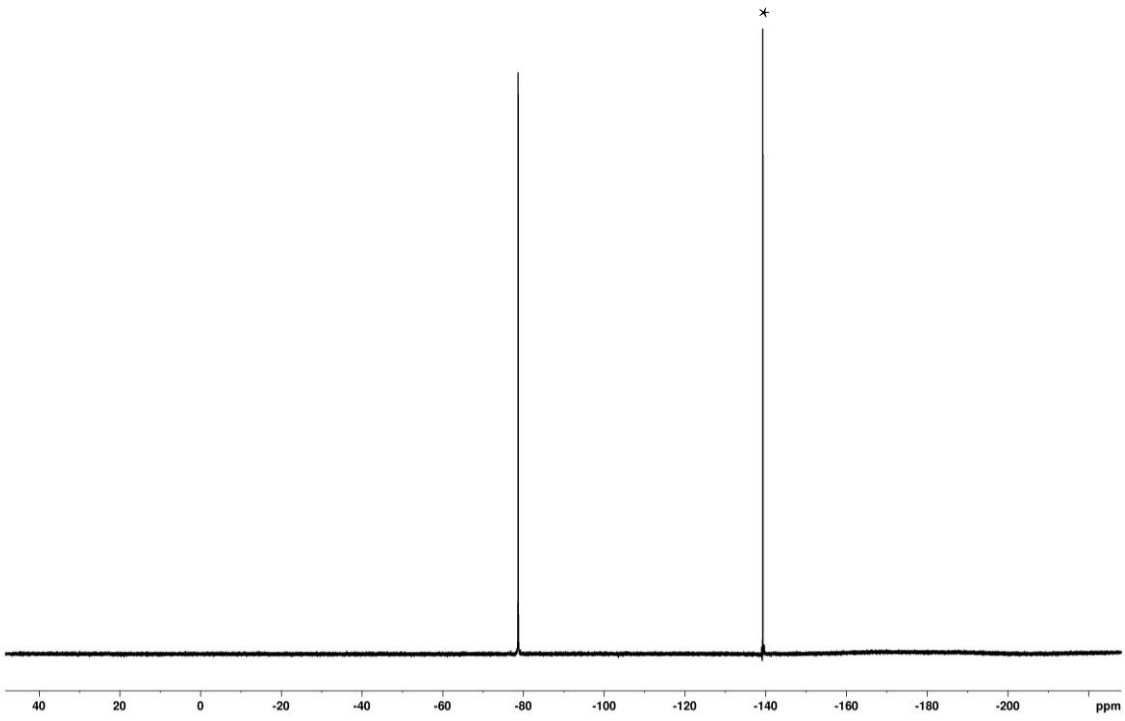

Figure S 5.51: $^{19}F\{^1H\}$ NMR spectrum of [IDipp·$GaH_2PPh_2BH_2$·NMe_3][OTf] (CD_2Cl_2, 298 K, * = residual 1,2-difluorobenzene).

5.5.3.14 [IDipp·$GaH_2PH_2GaH_2$·IDipp][OTf]

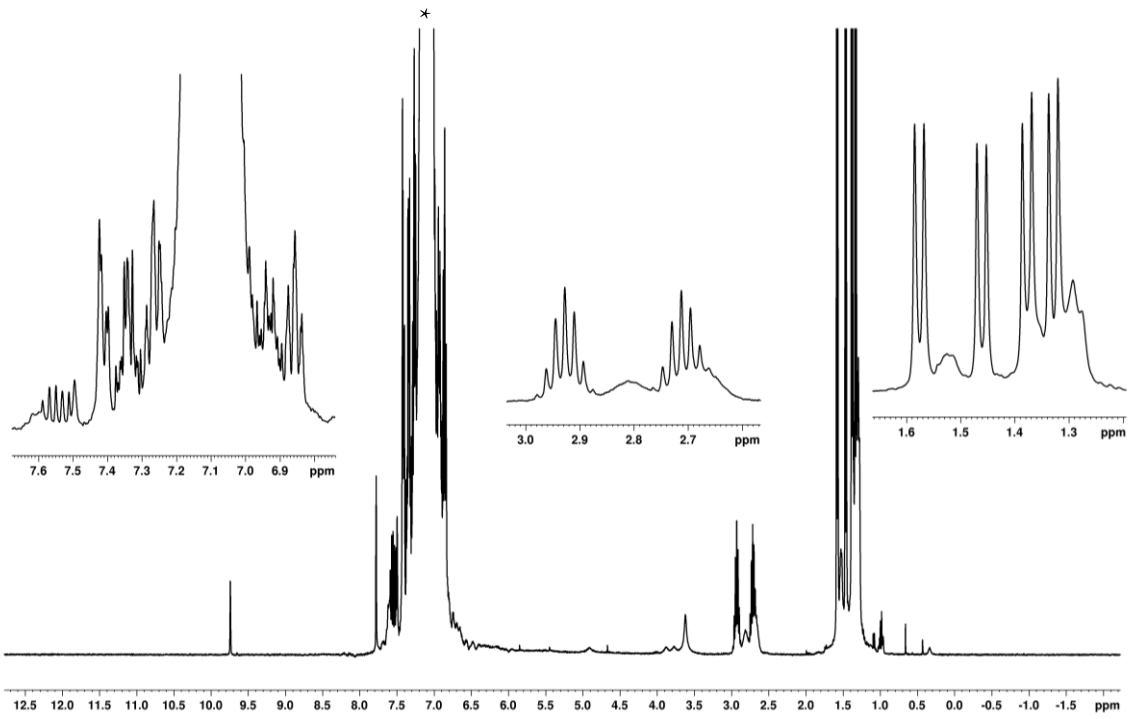

Figure S 5.52: ^{1}H NMR spectrum of [IDipp·$GaH_2PH_2GaH_2$·IDipp][OTf] (1,2-difluorobenzene/C_6D_6-capillary, 298 K; * = solvent signal).

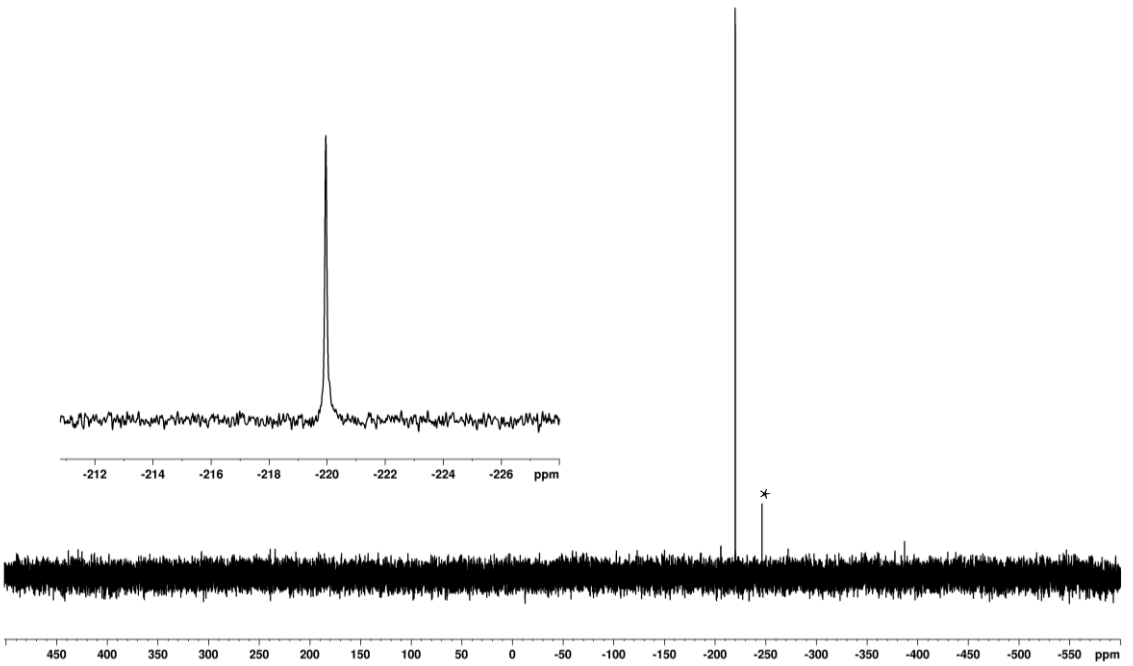

Figure S 5.53: $^{31}P\{^{1}H\}$ NMR spectrum of [IDipp·$GaH_2PH_2GaH_2$·IDipp][OTf] (1,2-difluorobenzene/C_6D_6-capillary, 298 K; * = PH_3).

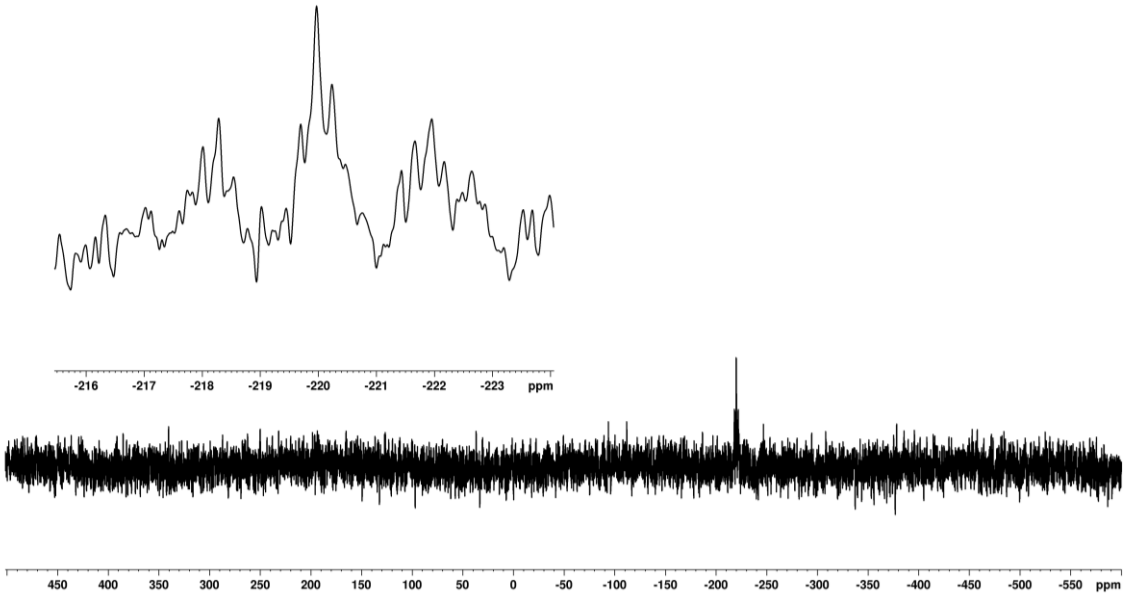

Figure S 5.54: ^{31}P NMR spectrum of [IDipp·GaH$_2$PH$_2$GaH$_2$·IDipp][OTf] (1,2-difluorobenzene/C$_6$D$_6$-capillary, 298 K).

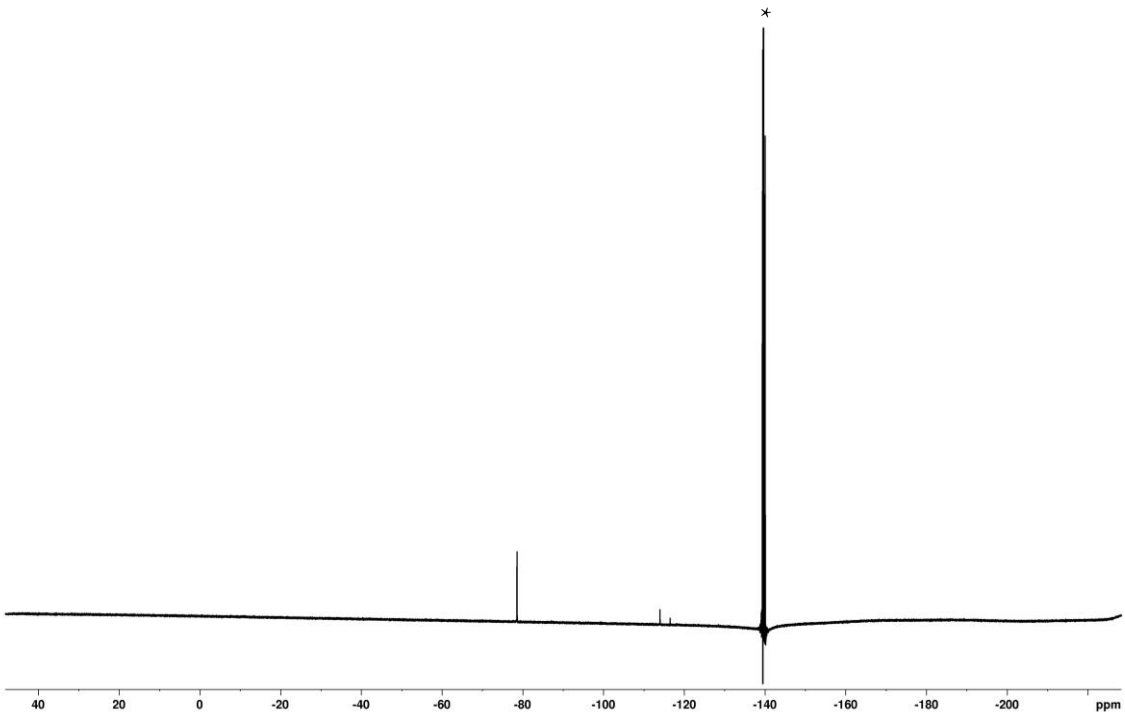

Figure S 5.55: ^{19}F{^{1}H} NMR spectrum of [IDipp·GaH$_2$PH$_2$GaH$_2$·IDipp][OTf] (CD$_2$Cl$_2$, 298 K, * = 1,2-difluorobenzene). Due to the strong intensity of the solvent signal, completely satisfactory phase correction while maintaining a clear view at the product signal was not possible.

5.5.4 Crystallographic Data

Single Crystal X-ray structure determination: Single-crystal X-ray diffraction data sets were collected using an Oxford Diffraction GV50 diffractometer (**1a**, **1b**) or a XtaLAB Synergy R, DW system diffractometer (**3a**, **3b, 3c, 3d**) equipped with a HyPix-Arc 150 detector operating at T = 123.01(10) K. Crystals were selected under mineral oil or perfluorinated Fomblin. Data reduction, scaling and absorption corrections were performed using CrysAlisPro (Rigaku, V1.171.41.90a, 2020). A gaussian absorption correction was performed using CrysAlisPro 1.171.41.90a (Rigaku Oxford Diffraction, 2020). Numerical absorption correction based on gaussian integration over a multifaceted crystal model. Empirical absorption correction using spherical harmonics, implemented in SCALE3 ABSPACK scaling algorithm. Using Olex2,[9] the structures were solved with ShelXT[10] and a least-squares refinement on $F2$ was carried out with ShelXL.[11] All non-hydrogen atoms were refined anisotropically. The hydrogen atoms at the carbon atoms have been located in idealized positions and refined isotropically according to the riding model. Figures were created with Olex2.

CCDC 2263441-2263446 contain the supplementary crystallographic data for this paper. These data can be obtained free of charge at www.ccdc.cam.ac.uk/conts/retrieving.html (or from the Cambridge Crystallographic Data Centre, 12 Union Road, Cambridge CB2 1EZ, UK; Fax: +44-1223-336-033; e-mail: deposit@ccdc.cam.ac.uk).

Table S 5.1: Crystallographic data for compounds **1a**, **1b** and **3**.

Compound	**1a**	**1b**	**3a**
CCDC	2263441	2263442	2263443
Formula	$C_{28}H_{38}F_3GaN_2O_3S$	$C_{12}H_{22}F_3GaN_2O_3S$	$C_{61.8}H_{91.6}BF_3GaN_4O_{4.7}PS$
Dcalc	1.301	1.573	1.188
μ/mm^{-1}	2.245	3.78	1.552
Formula Weight	609.38	401.09	1166.35
Colour	clear colourless	clear colourless	clear colourless
Shape	block-shaped	prism-shaped	block
Size/mm^3	0.90×0.21×0.14	0.40×0.23×0.16	0.80×0.46×0.39
T/K	122.97(13)	123.02(10)	122.99(10)
Crystal System	orthorhombic	orthorhombic	monoclinic
Flack Parameter	-0.016(8)	-	-
Hooft Parameter	-0.022(6)	-	-
Space Group	$P2_12_12_1$	*Pbca*	$P2_1/c$
a/Å	10.69340(10)	10.27220(10)	10.4802(2)
b/Å	15.04970(10)	15.9010(2)	32.9221(5)
c/Å	19.32810(10)	20.7392(3)	18.9856(3)
α/°	90	90	90
β/°	90	90	95.209(2)
γ/°	90	90	90
V/Å^3	3110.52(4)	3387.50(7)	6523.55(19)
Z	4	8	4
Z'	1	1	1
Wavelength/Å	1.54184	1.54184	1.54184
Radiation type	Cu K_a	Cu K_α	Cu K_α
Θ_{min}/°	3.722	4.264	2.684
Θ_{max}/°	66.539	66.788	73.247
Measured Refl's.	23444	13814	37837
Indep't Refl's	5457	2997	12469
Refl's I≥2 σ(I)	5373	2920	10492
R_{int}	0.0377	0.0297	0.0394
Parameters	359	213	816
Restraints	0	0	59
Largest Peak	0.226	0.321	0.796
Deepest Hole	-0.404	-0.586	-0.662
GooF	1.039	1.071	1.07
wR_2 (all data)	0.0697	0.0872	0.1859
wR_2	0.0692	0.0866	0.1801
R_1 (all data)	0.0271	0.0319	0.0744
R_1	0.0263	0.0313	0.0646

Table S 5.2: Crystallographic data for compounds **3b**, **3c** and **3d**.

Compound	**3b**	**3c**	**3d**
CCDC	2263444	2263445	2263446
Formula	$C_{31}H_{51}BF_3GaN_3O_3PS$	$C_{52}H_{65}BF_6GaN_3O_3PS$	$C_{55}H_{78}F_3Ga_2N_4O_3PS$
Dcalc	1.290	1.295	1.241
μ/mm^{-1}	2.373	1.895	2.123
Formula Weight	714.30	1037.63	1102.68
Colour	clear colourless	clear colourless	clear colourless
Shape	plate-shaped	prism-shaped	irregular-shaped
Size/mm^3	0.34×0.19×0.02	0.34×0.14×0.11	0.62×0.25×0.14
T/K	123.01(10)	123.00(10)	122.99(10)
Crystal System	monoclinic	triclinic	orthorhombic
Flack Parameter	-0.01(3)	-	-0.044(15)
Hooft Parameter	-0.030(12)	-	-0.038(8)
Space Group	*Cc*	*P*-1	$Pna2_1$
a/Å	9.6198(2)	12.5731(4)	19.9415(2)
b/Å	32.4795(6)	12.9043(3)	26.8997(2)
c/Å	11.9750(3)	16.7258(4)	11.00220(10)
α/°	90	97.653(2)	90
β/°	100.490(2)	97.452(2)	90
γ/°	90	92.488(2)	90
V/Å^3	3679.01(14)	2661.73(12)	5901.80(9)
Z	4	2	4
Z'	1	1	1
Wavelength/Å	1.54184	1.54184	1.54184
Radiation type	Cu K_a	Cu K_a	Cu K_a
Θ_{min}/°	2.721	2.691	3.964
Θ_{max}/°	75.348	75.578	75.334
Measured Refl's.	31348	52707	46819
Indep't Refl's	6003	10795	11174
Refl's I≥2 σ(I)	5377	8830	10397
R_{int}	0.0924	0.0450	0.0544
Parameters	426	822	735
Restraints	6	553	100
Largest Peak	0.722	0.989	0.491
Deepest Hole	-1.276	-0.664	-0.506
GooF	1.101	1.080	1.046
wR_2 (all data)	0.1496	0.1525	0.1143
wR_2	0.1372	0.1459	0.1121
R_1 (all data)	0.0597	0.0652	0.0445
R_1	0.0517	0.0539	0.0413

5.5.4.1 Crystal structures

IDipp·GaH$_2$(OTf) (1a)

1a crystallized by slow evaporation of a benzene solution at room temperature as clear colourless block-shaped crystals in the orthorhombic space group $P2_12_12_1$. The structure of **1a** in the solid state is shown in Figure S 5.56.

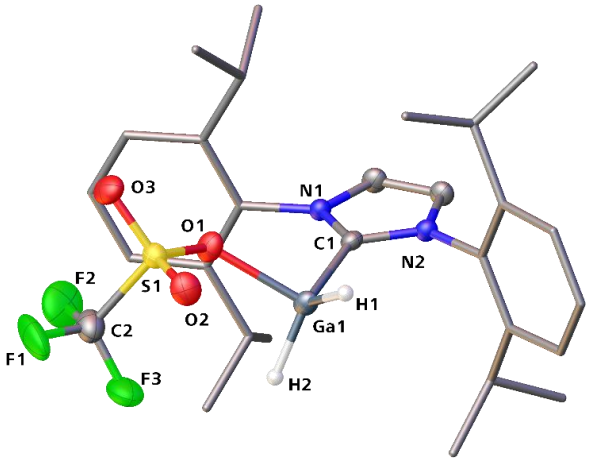

Figure S 5.56: Molecular structure of 1a in the solid state. Anisotropic displacement ellipsoids are shown at 50% probability level. Hydrogen atoms bound to carbon are omitted for clarity. Dipp moieties are displayed in a stick model for overall clarity. Selected bond lengths [Å] and angles [°]: N1-C1 1.350(3), N2-C1 1.347(3), C1-Ga1 2.039(3), Ga1-H1 1.51(4), Ga-H2 1.49(4), Ga1-O1 1.991(2), O1-S1 1.4781(19), S1-O2 1.427(2), S1-O3 1.427(2), S1-C2 1.822(3), C2-F1 1.328(4), C2-F2 1.318(4), C2-F3 1.327(4), N1-C1-Ga1 130.94(19), N2-C1-Ga1 123.62(18), C1-Ga1-O1 99.27(9), C1-Ga1-H1 113.5(14), C1-Ga-H2 113.7(14), H1-Ga1-H2 123(2), Ga1-O1-S1 127.35(12).

The asymmetric unit contains one molecule of **1a** and was refined without further restrains/constraints. H-atoms bound to Ga were refined freely.

IPr$_2$Me$_2$·GaH$_2$(OTf) (1b)

1b crystallized from a saturated toluene solution at -28 °C as clear colourless prism-shaped crystals in the orthorhombic space group *Pbca*. The structure of **1b** in the solid state is shown in Figure S 5.57.

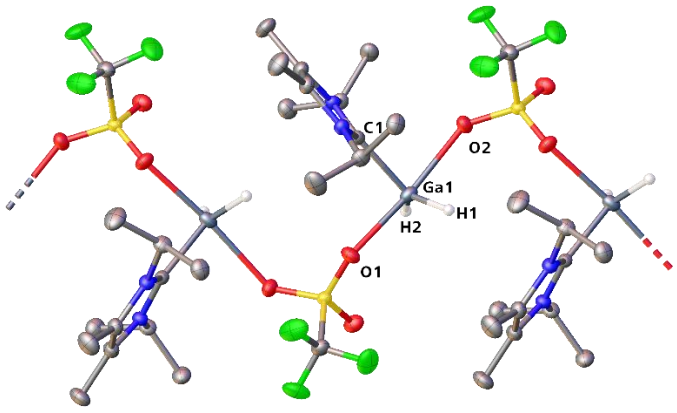

Figure S 5.57: Grown molecular structure of **1b** in the solid state. Anisotropic displacement ellipsoids are shown at 50% probability level. Hydrogen atoms bound to carbon are omitted for clarity. Selected bond lengths [Å] and angles [°]: C1-Ga1

2.0281(19), Ga1-H1 1.46(2), Ga1-H2 1.46(3), Ga1-O2 2.3777(15), Ga1-O1 2.2533(15), C1-Ga1-O1 88.54(7), C1-Ga1-O2 86.10(7), H1-Ga1-H2 126.8(13), C1-Ga1-H1 117.0(9), C1-Ga1-H2 115.8(10), O1-Ga1-O2 174.64(5).

The asymmetric unit (Figure S 5.58) contains one monomeric unit of **1b** and was refined without further restrains/constraints. H-atoms bound to Ga were refined freely. The grown structure reveals a one-dimensional polymeric arrangement of monomers.

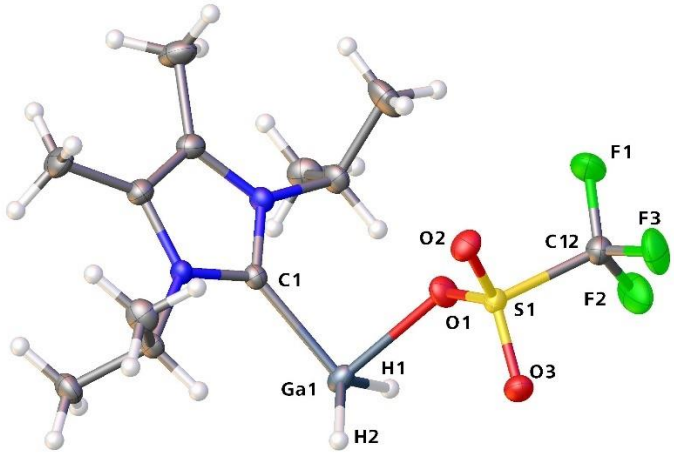

Figure S 5.58: Molecular structure of **1b** in the solid state (asymmetric unit). Anisotropic displacement ellipsoids are shown at 50% probability level. Selected bond lengths [Å] and angles [°]: C1-Ga1 2.0281(19), Ga1-H1 1.46(2), Ga1-H1 1.46(2), Ga1-H2 1.46(3), Ga1-O1 2.2533(15), O1-S2 1.4499(15), S1-O2 1.4458(15), S1-O3 1.4351(16), S1-C12 1.828(2), C12-F1 1.325(3), C12-F2 1.320(3), C12-F3 1.331(3), C1-Ga1-O1 88.54(7), Ga1-O1-S1 131.96(9), H1-Ga1-H2 126.8(13), C1-Ga1-H1 117.0(9), C1-Ga1-H2 115.8(10).

[IDipp·GaH$_2$PH$_2$BH$_2$·IDipp][OTf] (3a) · 2 THF

3a crystallized by layering a THF solution with a THF/*n*-hexane interphase and an *n*-hexane phase at -30 °C as clear colourless blocks in the monoclinic space group $P2_1/c$. The structure of **3a** in the solid state is shown in Figure S 5.59.

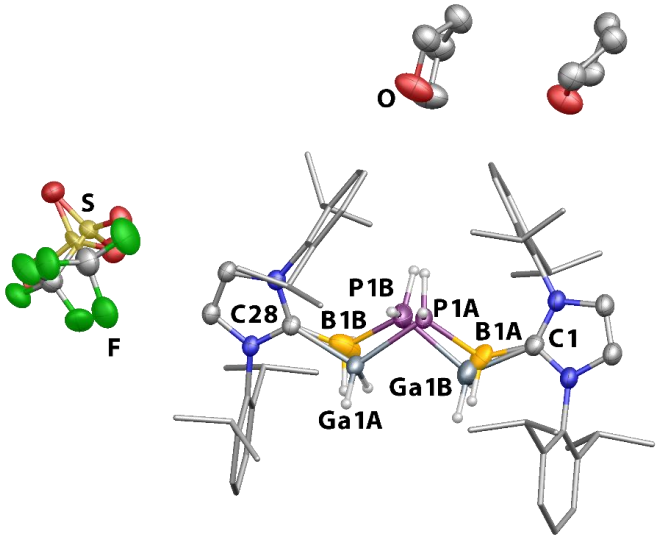

Figure S 5.59: Molecular structure of **3a** in the solid state. Anisotropic displacement ellipsoids are shown at 50% probability level. Hydrogen atoms bound to carbon are omitted for clarity. Dipp moieties are displayed in a stick model for improved overall clarity. Selected bond lengths [Å] and angles [°]: Ga1A-C28 2.055(3), Ga1A-P1A 2.3731(15), P1A-B1A 1.949(10), B1A-

C1 1.601(11), C28-B1B 1.591(10), C1-Ga1B 2.057(4), Ga1B-P1B 2.379(7), B1B-P1B 2.071(19), C28-Ga1A-P1A 114.40(8), B1A-P1A-Ga1A 103.8(3), C1-B1A-P1A 119.6(5), C1-Ga1B-P1B 111.4(2), C28-B1B-P1B 115.3(10), B1B-P1BGa1B 102.7(4).

The asymmetric unit of **3a** contains one formula unit of the title compound and 2 molecules of THF (occ. 0.85). The central chain motif is disordered in all three positions, as well as the triflate anion. For a satisfactory structure model, SADI, SIMU, DFIX and AFIX restraints have been applied to model the disordered parts.

[IDipp·GaH$_2$PH$_2$BH$_2$·NMe$_3$][OTf] (3b) · THF

3b crystallized by layering a 1,2-difluorobenzene solution with *n*-hexane at -30 °C as clear colourless plates in the monoclinic space group *Cc*. The structure of **3b** in the solid state is shown in Figure S 5.60.

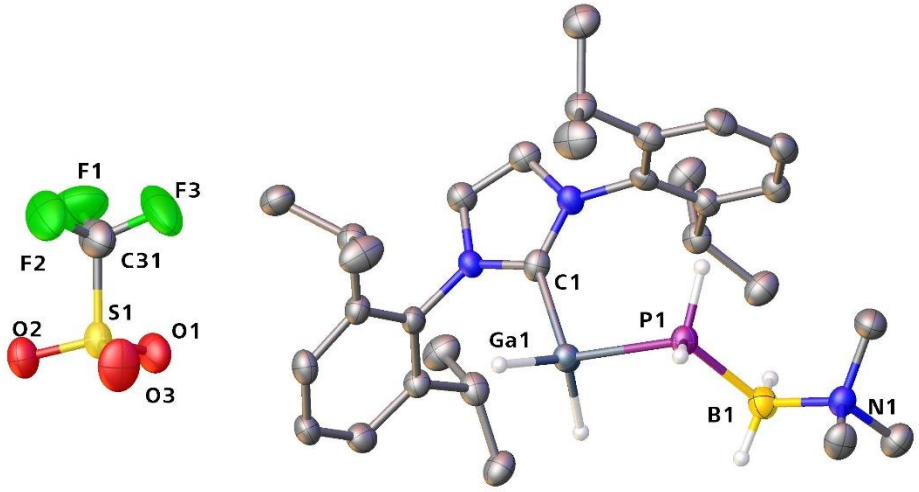

Figure S 5.60: Molecular structure of **3b** in the solid state. Anisotropic displacement ellipsoids are shown at 50% probability level. Hydrogen atoms bound to carbon are omitted for clarity. Selected bond lengths [Å] and angles [°]: C1-Ga1 2.054(7), Ga1-P1 2.4002(16), P1-B1 1.959(8), B1-N1 1.597(9), C1-Ga1-P1 111.62(17), Ga1-P1-B1 111.5(2), P1-B1-N1 116.2(5).

The asymmetric unit of **3b** contains one formula unit of the title compound. Hydrogen atoms bound to Ga, P, and B were restrained by DFIX restraints.

[IDipp·GaH$_2$PPh$_2$BH$_2$·NMe$_3$][OTf] (3c) · 1.5 C$_6$F$_2$H$_4$

3c crystallized by layering a 1,2-difluorobenzene solution with *n*-hexane at -30 °C as clear colourless blocks in the triclinic space group $P\bar{1}$. The structure of **3c** in the solid state is shown in Figure S 5.61.

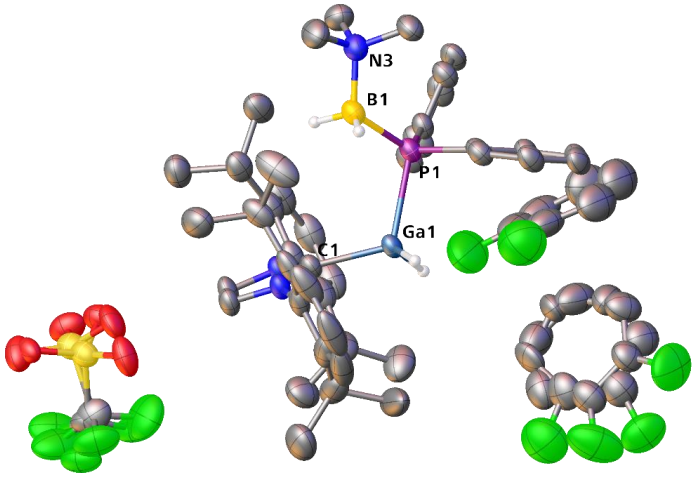

Figure S 5.61: Molecular structure of **3c** in the solid state. Anisotropic displacement ellipsoids are shown at 50% probability level. Hydrogen atoms bound to carbon are omitted for clarity. Selected bond lengths [Å] and angles [°]: C1-Ga1 2.044(2), Ga1-P1 2.4007(7), P1-B1 1.965(3), B1-N3 1.612(4), C1-Ga1-P1 114.15(7), Ga1-P1-B1 106.99(9), P1-B1-N3 120.1(2).

The asymmetric unit of **3c** contains one formula unit of the title compound. Hydrogen atoms bound to Ga, P, and B were restrained by SADI, DFIX and DANG restraints. The triflate anion and one 1,2-difluorobenzene molecule display positional disorder and were modelled with SADI, DFIX, SIMU, RIGU and DANG restraints.

[IDipp·GaH$_2$PH$_2$GaH$_2$·IDipp][OTf] (3d)

3d crystallized by layering a 1,2-difluorobenzene solution with *n*-hexane at -30 °C as a clear colourless irregular in the orthorhombic space group *Pna*2$_1$. The structure of **3d** in the solid state is shown in Figure S 5.62.

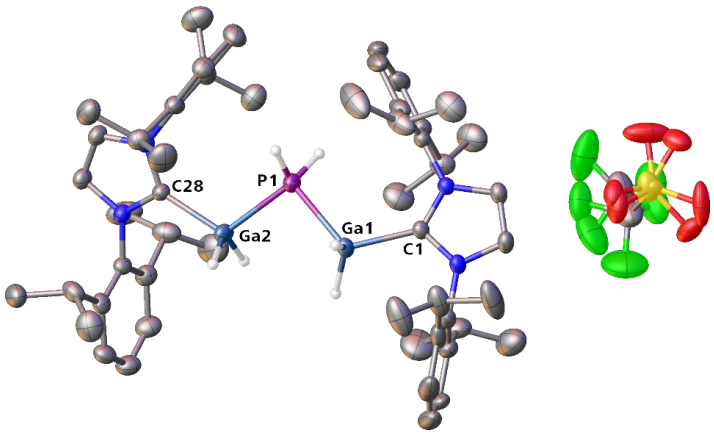

Figure S 5.62: Molecular structure of **3d** in the solid state. Anisotropic displacement ellipsoids are shown at 50% probability level. Hydrogen atoms bound to carbon are omitted for clarity. Selected bond lengths [Å] and angles [°]: C1-Ga1 2.032(3), Ga1-P1 2.3831(10), P1-Ga2 2.3658(10), Ga2-C28 2.032(3), C1-Ga1-P1 112.85(10), Ga1-P1-Ga2 100.61(4), P1-Ga2-C28 113.95(10).

The asymmetric unit of **3d** contains one formula unit of the title compound. Hydrogen atoms bound to Ga and P were restrained by SADI, DFIX and DANG restraints. The triflate anion displays positional disorder and was modelled with SADI, DFIX, and SIMU restraints.

5.5.5 Computational Details

5.5.5.1 General Information

Quantum chemical calculations were performed using ORCA version 4.2.1 and version 5.0.3.[12] developed by Neese *et al.* Images of calculated structures were generated with ChemCraft.[13] Molecular geometries were optimized at the B3LYP-D4/def2-TZVP[14,15] level of theory. Subsequent analytical frequency analysis was carried out in order to determine the nature of stationary points on the potential energy surface. The RIJCOSX approximation was applied to enhance the calculation speed.[16] *Natural Bond Orbital* analysis (NBO 6.0)[17] was carried out at the TPSSh/def2-TZVP[15,18] level of theory and used to describe electronic densities and to calculate the *Wiberg Bond Index* matrix (WBI). Electronic energies were refined by single point calculations at the DLPNO-CCSD(T)/def2-QZVP[15,19] level of theory. Approximate transition states were found using the *Nudged Elastic Band* method (NEB-CI)[20] as implemented in ORCA followed by a geometry optimization and frequency analysis of the saddle point.

5.5.5.2 Stepwise Iodination of $IPr_2Me_2 \cdot GaH_3$

Thermodynamic characteristics for the stepwise iodination of $IPr_2Me_2{\cdot}GaH_3$ were calculated at the above-mentioned level of theory and are given in Table S 5.3 and visualized in Figure S 5.63.

Table S 5.3: Gibbs' Free Energy values ΔG_R for the stepwise gas phase iodination of $IPr_2Me_2{\cdot}GaH_3$ with MeI (DLPNO-CCSD(T)/def2-QZVP // B3LYP-D4/def2-TZVP).

Reaction	ΔG_R /kcal mol^{-1}
$IPr_2Me_2{\cdot}GaH_3$ + MeI → $IPr_2Me_2{\cdot}GaH_2I$ + MeH	-49.32
$IPr_2Me_2{\cdot}GaH_3$ + MeI → $[IPr_2Me_2{\cdot}GaH_3 \cdot MeI]^{\neq}$	+58.90
$IPr_2Me_2{\cdot}GaH_2I$ + MeI → $IPr_2Me_2{\cdot}GaHI_2$ + MeH	-45.66
$IPr_2Me_2{\cdot}GaHI_2$ + MeI → $[IPr_2Me_2{\cdot}GaH_2I \cdot MeI]^{\neq}$	+62.32
$IPr_2Me_2{\cdot}GaHI_2$ + MeI → $IPr_2Me_2{\cdot}GaI_3$ + MeH	-41.13
$IPr_2Me_2{\cdot}GaHI_2$ + MeI → $[IPr_2Me_2{\cdot}GaHI_2 \cdot MeI]^{\neq}$	+62.96

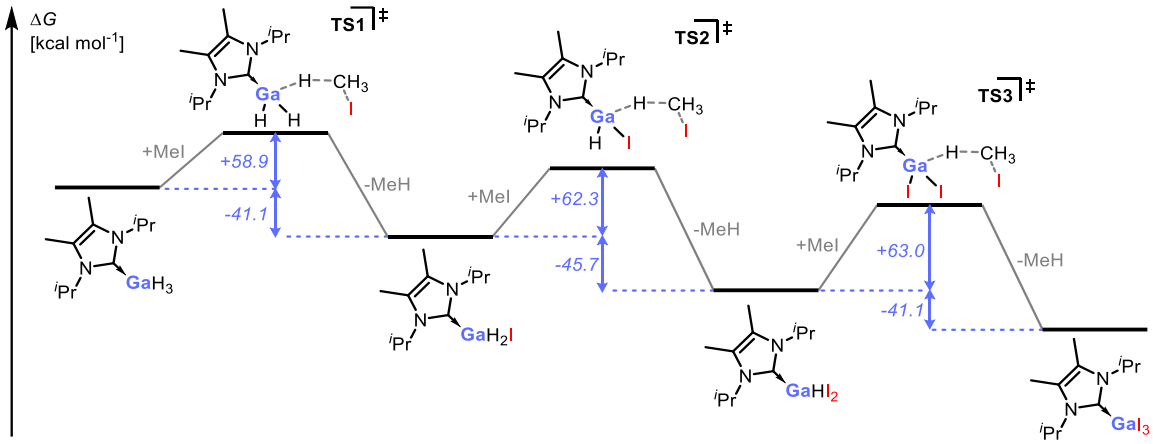

Figure S 5.63: Calculated reaction pathway of the gas-phase stepwise iodination of IPr$_2$Me$_2$·GaH$_3$ with MeI (DLPNO-CCSD(T)/def2-QZVP // B3LYP-D4/def2-TZVP). Gibbs' Free Energy values ΔG are given in [kcal mol^{-1}]. Transition state geometries are given alongside the coordinates of the optimized structures (vide infra).

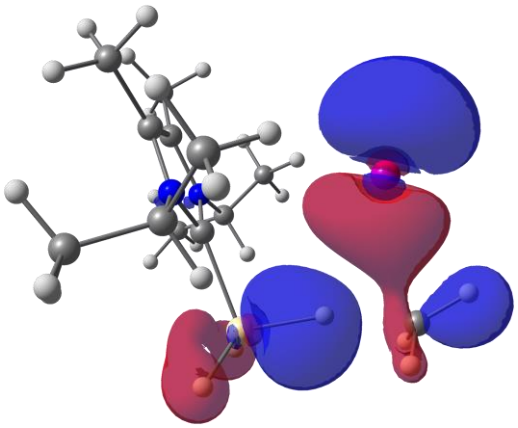

Figure S 5.64: Depiction of the HOMO of TS1 showing the decisive orbital interactions during the transition state.

5.5.5.3 Natural Bonding Orbitals along the chain structures of 3a-d

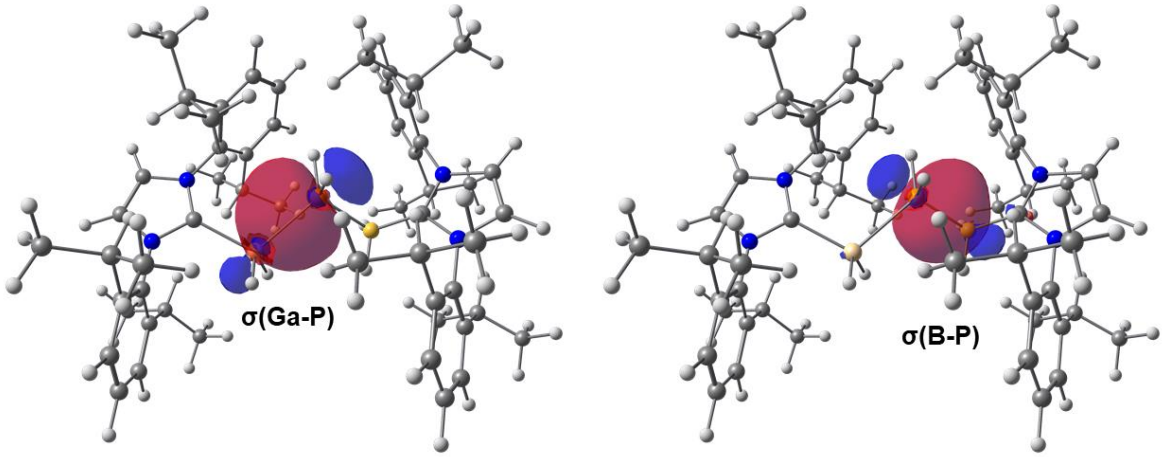

Figure S 5.65: NBOs of the σ(E-P) bonds (E = Ga, B) within **3a**. Individual contributions: σ(Ga-P): Ga 22.52% (0.16 s, 0.83 p, 0.01 d), P 77.48% (0.30 s, 0.70 p); σ(B-P): B 41.33% (0.22 s, 0.78 p), P 58.67% (0.30 s, 0.69 p, 0.01 d).

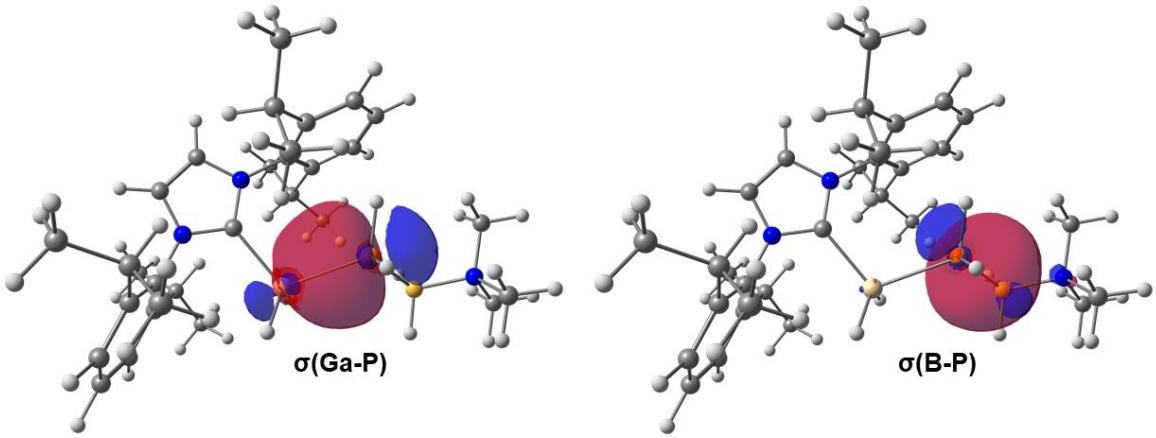

Figure S 5.66: NBOs of the σ(E-P) bonds (E = Ga, B) within **3b**. Individual contributions: σ(Ga-P): Ga 20.79% (0.15 s, 0.85 p), P 79.21% (0.31 s, 0.69 p); σ(B-P): B 41.12% (0.24 s, 0.75 p, 0.01 d), P 58.88% (0.30 s, 0.70 p).

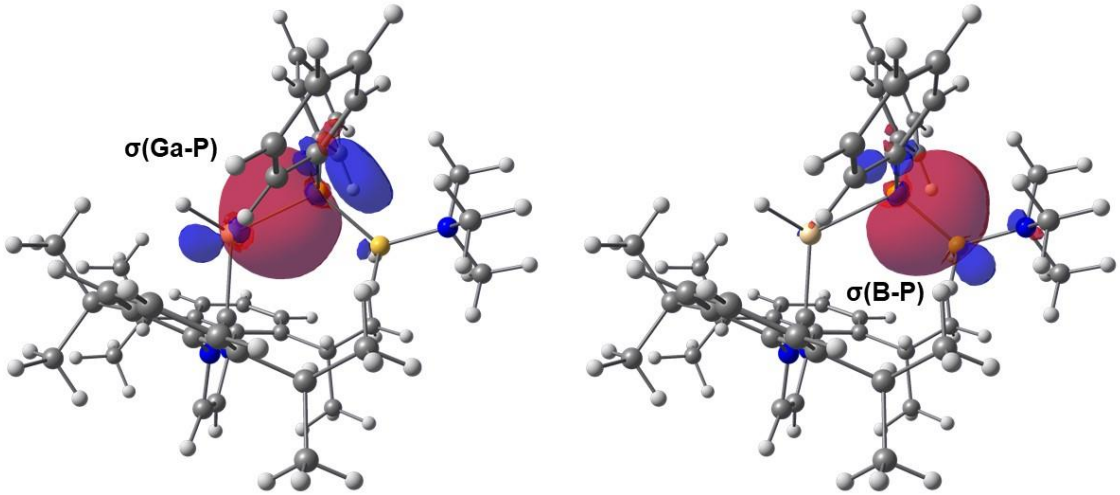

Figure S 5.67: NBOs of the σ(E-P) bonds (E = Ga, B) within **3c**. Individual contributions: σ(Ga-P): Ga 22.30% (0.17 s, 0.83 p), P 77.70% (0.26 s, 0.74 p); σ(B-P): B 42.34% (0.25 s, 0.74 p, 0.01 d), P 57.66% (0.30 s, 0.69 p, 0.01 d).

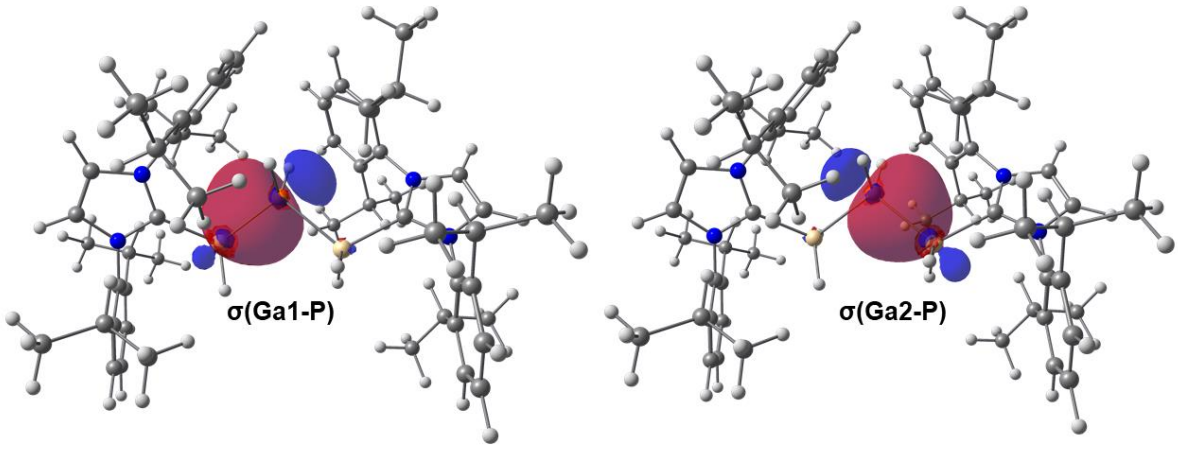

Figure S 5.68: NBOs of the σ(E-P) bonds (E = Ga, B) within **3d**. Individual contributions: σ(Ga1-P): Ga 22.77% (0.17 s, 0.83 p), P 77.23% (0.30 s, 0.70 p); σ(Ga2-P): Ga2 22.82% (0.17 s, 0.83 p), P 77.18% (0.30 s, 0.69 p, 0.01 d).

5.5.5.4 Cartesian Coordinates of optimized Structures

CH_3I

C	-1.7522019650587	-3.1115521509370	-0.1061589326247
I	-0.7041354484760	-4.9914633201838	0.0444315848676
H	-1.0121018814531	-2.3216882249215	-0.0455094441152
H	-2.4521586665231	-3.0634518656273	0.7203087247657
H	-2.2651532844891	-3.1017681523305	-1.0611898608933

CH_4

C	-1.6371513205950	-3.3179818359325	-0.0896211824087
H	-1.1078707401570	-4.2672249009859	-0.0135771267184
H	-0.9221412187653	-2.4979272803882	-0.0322745783325
H	-2.3521572061242	-3.2343572755230	0.7281715295742
H	-2.1664307603586	-3.2724324211705	-1.0408165701146

IPr_2Me_2·GaH_3

C	0.5509777992028	0.0622846932408	-0.0938701064902
C	-0.5317005577344	-0.7345632114602	-0.3100964561064
N	-0.8644345276500	-0.5919678035436	-1.6553674214286
C	-0.0239433152444	0.2693826043179	-2.2651620035902
N	0.8400231228810	0.6729152290636	-1.3106526870432
Ga	0.0484697649074	0.9014770755000	-4.2729783870775
H	1.4911672645702	0.4053120148399	-4.7377494401080
H	-1.1738355266081	0.1947450784915	-5.0058424853082
H	-0.0689248301599	2.4870389070509	-4.1448463537206
C	-1.2392180278415	-1.6141546800961	0.6615165723452
H	-0.8862511793190	-1.4064337198092	1.6698381622310
H	-2.3168793584991	-1.4521220644845	0.6564085381259
H	-1.0627495555861	-2.6727629763700	0.4616945703803
C	1.2978361010249	0.2814849874042	1.1760129007499
H	2.3747850038210	0.1824311404364	1.0420041895796
H	1.1063490049140	1.2692961050181	1.5996712538838
H	0.9940041224529	-0.4581263743798	1.9143388760558
C	-1.9948361986895	-1.2088623218188	-2.3771911030567
H	-1.8229773482998	-0.9158651884802	-3.4111122853973
C	-3.3276378956708	-0.6035056658171	-1.9465998878744
C	-1.9676207553730	-2.7326214169938	-2.3163559620716
H	-0.9748913494557	-3.1122807912080	-2.5619098537941
H	-2.2614278541315	-3.1238511451547	-1.3427276931892
H	-2.6686341730171	-3.1268219079410	-3.0535115197930
H	-3.5937894338890	-0.8612951747929	-0.9206998448791
H	-4.1201987230562	-0.9745799868391	-2.5983543484324
H	-3.2984265605566	0.4828931064181	-2.0358676333814
C	1.9545186880773	1.5896240811875	-1.6242836502720
H	1.7294302373588	1.9339923695968	-2.6314096664754
C	3.2843738273870	0.8445476882170	-1.6764875626512
C	1.9733839939728	2.8203678465649	-0.7236767601810
H	0.9821252187959	3.2716118214645	-0.6653375855011
H	2.3217075441591	2.6019801092625	0.2851242700679
H	2.6521196267228	3.5585041067638	-1.1530553811404
H	3.5865708789977	0.4642356550590	-0.6996416292361
H	4.0654608159157	1.5210272102905	-2.0269722010877
H	3.2217993436205	0.0107049520009	-2.3756026341325

IPr_2Me_2·GaH_2I

C	0.5074809561655	0.1333708987863	-0.0797313238687
C	-0.5985220798171	-0.6335025355928	-0.2930906553869
N	-0.9698722006614	-0.4330712706396	-1.6176467244987
C	-0.1210376912331	0.4248659883998	-2.2195205002318
N	0.7802170192885	0.7782435941946	-1.2805164174412
Ga	-0.0576776652385	0.9051487357307	-4.2374151500820
I	1.5547868244236	-1.0668564068824	-4.9473847500697
H	-1.4788436976623	0.6866827338623	-4.8805626173149
H	0.6795191190211	2.2845367497953	-4.4265794901868
C	-1.3235851285700	-1.4945824543906	0.6814404834151
H	-0.7119516456041	-1.6384617248276	1.5701057664281
H	-2.2662297242504	-1.0459846818981	1.0017202512829
H	-1.5458355108095	-2.4800564691831	0.2747830266660
C	1.2727566611140	0.3130344507237	1.1848026817183
H	2.3474173332107	0.2265396443952	1.0328228532349
H	1.0784505137418	1.2842073475078	1.6448041172684
H	0.9814876328231	-0.4517880138493	1.9021866789793
C	-2.0535036318295	-1.1114765407272	-2.3611482273823
H	-2.0654394106108	-0.6000353883897	-3.3208004566828
C	-3.4210725353308	-0.9019444836284	-1.7185134559115
C	-1.7109121935848	-2.5750176855086	-2.6236730527654
H	-0.7391014988092	-2.6564449939252	-3.1105143743152
H	-1.7000818904035	-3.1699181265664	-1.7095359579812
H	-2.4605075119652	-3.0042709750910	-3.2902877871004
H	-3.5547425185207	-1.4836857936791	-0.8074340245764
H	-4.1914161916623	-1.2163470241860	-2.4239285940403
H	-3.5866034071070	0.1517478933722	-1.4887467327550
C	1.9328024330034	1.6515257115223	-1.5913553525941
H	1.7256280587945	2.0005386828136	-2.6003248670946
C	3.2358127161665	0.8588331247442	-1.6373445642023
C	1.9892622780550	2.8802617610984	-0.6894867781353
H	1.0186545870257	3.3766506148107	-0.6461237746828
H	2.3077501969574	2.6448817349375	0.3252946289714
H	2.7094823818059	3.5869367090674	-1.1039333501718
H	3.5418435140803	0.5011859909797	-0.6536486768736
H	4.0307002307006	1.5021508591517	-2.0178980315782
H	3.1396088652928	0.0081436960716	-2.3115680100406

IPr^{Me2}·$GaHI_2$

C	0.5707909095300	0.0225478837764	-0.1095923868505
C	-0.5210981289166	-0.7674216613703	-0.3142710656477
N	-0.8549718792666	-0.6384030898613	-1.6570310974453
C	-0.0076824121804	0.2137931356405	-2.2694226707354
N	0.8690373508020	0.6159276229583	-1.3296980677282
Ga	-0.1367795875857	0.8653759430063	-4.2237175660451
I	2.1491709442918	0.3060428082660	-5.3051872934551
H	-1.3172699933175	0.1996304104155	-5.0110720857373
I	-0.5044657448031	3.4212246555956	-3.9400150306971
C	-1.2369682550763	-1.6263154274940	0.6695256056221
H	-0.9127218566833	-1.3772678913644	1.6777826955469
H	-2.3161616033502	-1.4826905156220	0.6323341913805
H	-1.0363912270479	-2.6874161393809	0.5103576583953
C	1.3118563161742	0.2508343697824	1.1616914919599
H	2.3848209761275	0.1071730731690	1.0448064029065
H	1.1511266730381	1.2573333334798	1.5508556887949
H	0.9702409903108	-0.4540797026453	1.9167366585672
C	-2.0006520095588	-1.2519738191878	-2.3625870068646
H	-1.8182852744135	-1.0165823456211	-3.4081906542946
C	-3.3127407264113	-0.5810867559823	-1.9679720590434
C	-2.0209508653104	-2.7720778079270	-2.2389109667192
H	-1.0366922354424	-3.1928185341749	-2.4486537397351
H	-2.3471047709634	-3.1133650242444	-1.2577371569364
H	-2.7198050873737	-3.1726148929058	-2.9743354488446
H	-3.5815477363336	-0.7727207760860	-0.9287011486373
H	-4.1176565176664	-0.9644238028331	-2.5967234919991
H	-3.2508530753736	0.4973139099830	-2.1172160047622
C	1.9928539618231	1.5344967338959	-1.6301303372825
H	1.8300320639377	1.8199063684851	-2.6653736460560
C	3.3353940793596	0.8149708138180	-1.5653611699249
C	1.9328540639308	2.8100050096290	-0.7984146935682
H	0.9368246247312	3.2497060229824	-0.8388487241812
H	2.2169037398262	2.6488791250248	0.2409575070536
H	2.6298232550873	3.5328541155472	-1.2237845038524
H	3.6226297648295	0.5531639310334	-0.5468626368672
H	4.1058680547171	1.4725666247978	-1.9694243717275
H	3.3172964065580	-0.0864453515858	-2.1765660845887

IPr^{Me2}·GaI_3

C	0.9397074162054	0.2574169781647	0.1378736624805
C	-0.1475056255876	-0.5406373707843	-0.0560985423069
N	-0.4940362056580	-0.4210505302233	-1.3947097113701
C	0.3384784860308	0.4367001329362	-2.0177819820136
N	1.2245114428210	0.8481897056773	-1.0853667765667
Ga	0.2901268422303	1.1688095446062	-3.9541059319802
I	2.5254607934120	0.4723799347184	-5.0309643615948
I	-1.6203047350959	0.3682923895982	-5.4893274339788
I	0.0119853602370	3.7186824513295	-3.6481230631940
C	-0.8522933412600	-1.3949666807938	0.9397643915429
H	-0.5406510596428	-1.1182149130506	1.9447159860070
H	-1.9333509479692	-1.2743386811314	0.8909198113390
H	-0.6281742515479	-2.4542508863747	0.8029697384498
C	1.6820839254829	0.4973219889725	1.4065390757101
H	2.7576226590151	0.3833807242330	1.2847560890820
H	1.4953155315779	1.4964555871916	1.8031818255781
H	1.3629547237084	-0.2221711829946	2.1574985745138
C	-1.6272490991396	-1.0790624756083	-2.0789803306312
H	-1.4560504819016	-0.8723432719750	-3.1302287210042
C	-2.9537103444887	-0.4286868674186	-1.7044843571893
C	-1.6119914837655	-2.5958331102675	-1.9235720075115
H	-0.6141028561100	-2.9971895510893	-2.1053583752497
H	-1.9540736478881	-2.9300641708218	-0.9454462844926
H	-2.2829898188275	-3.0225238029827	-2.6699983042946
H	-3.2266477269496	-0.6051500639852	-0.6633688478529
H	-3.7431062055895	-0.8404072272144	-2.3342116557168
H	-2.9157160317521	0.6467381077700	-1.8790315950832
C	2.3640310580357	1.7480676359534	-1.3852551592130
H	2.2046619599876	2.0500840565954	-2.4158913757508
C	3.6921117709406	1.0004354419846	-1.3359577270445
C	2.3377098061525	3.0171886139256	-0.5418341022821
H	1.3469279203821	3.4697849269392	-0.5542162090986
H	2.6445305661398	2.8436644696947	0.4886419820080
H	3.0328770529198	3.7352253672230	-0.9779253502073
H	3.9803173375783	0.7232652747369	-0.3221774029034
H	4.4728026505732	1.6467467364256	-1.7386053157472
H	3.6527793297432	0.1052985030396	-1.9549284174328

TS1

C	0.7051714012007	-0.1802141106987	1.6657615989222
C	-0.2799888128425	-1.0886116407910	1.4129579226638
N	-0.9278927806362	-0.6592279026264	0.2641184977035
C	-0.3767287079833	0.4852709693166	-0.1874866945648
N	0.6281077912030	0.7754740876925	0.6632306497488
Ga	-0.9808423712673	1.5860337200845	-1.8274389194173
H	-0.0671245238822	0.8380241406660	-3.0166008870984
H	-2.5173253216002	1.3115781294862	-2.1026690844198
H	-0.5018671336315	3.0870937093051	-1.6628793724607
C	-0.6182703388904	-2.3127217566895	2.1905830761018
H	-0.1710800827695	-2.2521557018717	3.1815311636614
H	-1.6926739205298	-2.4317208565982	2.3238578267860
H	-0.2380381714695	-3.2180506958584	1.7142321698549
C	1.6897964657570	-0.1842708582090	2.7829754907819
H	2.6717021828068	-0.5363616736716	2.4620036671479
H	1.8168734114354	0.8039405967979	3.2227587814500
H	1.3456289159439	-0.8508567186510	3.5721772309067

C	-2.0376920786641	-1.3287079227554	-0.4456541548144
H	-2.1066133720033	-0.7881552979990	-1.3862393597762
C	-3.3590712410298	-1.1352157254135	0.2910194237038
C	-1.7216431397140	-2.7836077262225	-0.7785868076176
H	-0.7263507113214	-2.8695013659925	-1.2149691762100
H	-1.7929577675843	-3.4384505403427	0.0888637826132
H	-2.4452619964218	-3.1370817489680	-1.5145758767435
H	-3.3692630260596	-1.6354395449928	1.2603060291457
H	-4.1720558405244	-1.5503305720590	-0.3066779646042
H	-3.5591184834135	-0.0743658127537	0.4447234873827
C	1.5130747933739	1.9419445158425	0.4638992169950
H	1.2436882272564	2.3048402596216	-0.5245892074653
C	2.9870639317479	1.5509090651953	0.4203152880448
C	1.1956287654536	3.0524803106966	1.4601161716593
H	0.1421852244872	3.3282897791101	1.4021056236951
H	1.4236455572715	2.7655215945991	2.4874418912099
H	1.7907395601955	3.9352281256609	1.2211794164892
H	3.3914941615142	1.3242041838399	1.4059518809173
H	3.5580333408512	2.3890709101615	0.0182020281115
H	3.1368913967457	0.6938233349297	-0.2365153190862
H	1.3315185587251	-0.3463136085276	-4.9298027051034
C	0.6503560789434	0.3524402510280	-4.4771300335971
H	0.9958627493519	1.3746859014744	-4.5033610446042
H	-0.3788095628894	0.1982659897402	-4.7633961787044
I	1.8232068708635	-1.2977577935563	-2.5417395294089

TS2

C	0.5939641031956	-0.2815498757979	1.6838200951385
C	-0.6169716941462	-0.9098960999734	1.6966773555846
N	-1.0901554872358	-0.8830295614079	0.3910629558340
C	-0.2074321413361	-0.2529791542450	-0.4091351682302
N	0.8264236750161	0.1064794086683	0.3708654562855
Ga	-0.5305712364435	0.2384414759597	-2.3791358023956
H	0.5446053358194	1.4081653894918	-2.9082394607393
H	-0.7333680933275	-1.0168109473995	-3.2998042184567
I	-2.6432738812325	1.7861072152504	-2.2227920817688
C	-1.3415294667039	-1.4922964233654	2.8600352621362
H	-0.6731171004683	-1.5524499816069	3.7163924729713
H	-2.1986688711554	-0.8819157124530	3.1503770729059
H	-1.7040460629040	-2.4996264717210	2.6597194748540
C	1.5220380112815	-0.0398103423240	2.8228685495969
H	2.4028665854232	-0.6822143242696	2.7765443839342
H	1.8659955223617	0.9931809698576	2.8555823354051
H	1.0117964845263	-0.2429609943044	3.7622611012066
C	-2.3265962966252	-1.4987362178725	-0.1379540807634
H	-2.3675926898044	-1.1614222673470	-1.1715670233062
C	-3.5815023437218	-0.9727610198876	0.5478453820154
C	-2.2204512406018	-3.0205900251605	-0.1563083671899
H	-1.3184651701375	-3.3371818248293	-0.6810078061091
H	-2.2079033400829	-3.4493830387717	0.8459206218504
H	-3.0817992546626	-3.4340222313391	-0.6825768565919
H	-3.7025456298534	-1.3634260727437	1.5572111391672
H	-4.4515719081725	-1.2798614145439	-0.0334520000340
H	-3.5725598076214	0.1162287984570	0.5793406346419
C	1.9987779120675	0.8342414972518	-0.1677937758100
H	1.8700375248570	0.7940310972879	-1.2485654516197
C	3.3159629392623	0.1325441407898	0.1367390791467
C	1.9801306467848	2.3031983534840	0.2339427873108
H	1.0204056622791	2.7589863124621	-0.0124289066664
H	2.1692337197276	2.4459378695270	1.2988399124935
H	2.7580775767969	2.8242176309080	-0.3242863584075
H	3.6513020143082	0.2882673263324	1.1616014620039
H	4.0741453634174	0.5375417462032	-0.5339162240690
H	3.2421658983710	-0.9393183245186	-0.0532031410045
H	1.4710608762734	3.5743129250443	-3.8685543972275
C	0.7042561031583	2.8419311607886	-3.6886326676766
H	-0.0082386332799	3.1325397991920	-2.9289225969467
H	0.2730966372513	2.4156367381291	-4.5826452820554
I	3.2820177573381	1.6602524707967	-3.6167258674142

TS3

C	0.4577581375950	-0.2750219692532	1.8216332121380
C	-0.7384072329060	-0.9202567042158	1.6957461913563
N	-1.1104412408301	-0.8124721577320	0.3623939629056
C	-0.1793406971089	-0.1167665114619	-0.3178994104342
N	0.7835467770127	0.2067952610701	0.5610309527372
Ga	-0.2985634213239	0.4354768362594	-2.2819970949847
H	0.7811827616591	1.5241763301907	-2.9696874734066
I	-0.1861691081606	-1.7036580663466	-3.6984382175852
I	-2.5028372744036	1.7961717462175	-2.4973938501602
C	-1.5389076765369	-1.5913185749668	2.7569446783317
H	-0.9507090336575	-1.6647811059511	3.6690705442789
H	-2.4472392159984	-1.0342014630578	2.9923769997492
H	-1.8315928280455	-2.6020887691513	2.4768924485261
C	1.2909078730167	-0.1049998947100	3.0441936526657
H	2.1775109079752	-0.7409042555183	3.0258326133070
H	1.6221689256055	0.9242666143157	3.1731026129359
H	0.7098050245548	-0.3723478686145	3.9244614328222
C	-2.2933693118323	-1.4132053493762	-0.2965083586101
H	-2.2416190583356	-1.0465340823551	-1.3184861857394
C	-3.6033803843470	-0.9062196900314	0.2930781103125
C	-2.1838577891403	-2.9328309707824	-0.3585502757223
H	-1.2291800116458	-3.2316867116039	-0.7902072056751
H	-2.2952977768382	-3.4006154108256	0.6195169714061
H	-2.9753718635471	-3.3173359799102	-1.0027053100775
H	-3.8121159336637	-1.3282960429431	1.2752423324207

H	-4.4181998849576	-1.1944466955595	-0.3717876968075
H	-3.6004579573519	0.1813186430329	0.3608994408132
C	1.9832552860880	0.9804628153073	0.1648029501329
H	1.9268156098682	1.0342502452332	-0.9226548639288
C	3.2789481895145	0.2515718860129	0.4953722618191
C	1.9332374719026	2.4096562236628	0.6887444994258
H	0.9873496547382	2.8860576292238	0.4283323722109
H	2.0642258709433	2.4618221627715	1.7703146858224
H	2.7373828155494	2.9771350324343	0.2201107271023
H	3.5358886885010	0.3099555486368	1.5526888015111
H	4.0833957260023	0.7173247583258	-0.0743965442552
H	3.2254520420767	-0.7969340153289	0.1996203445687
H	1.6270359591855	3.2405255006507	-4.5723021070961
C	0.9233771247502	2.5039506793636	-4.2274607783232
H	0.0231547719070	2.9358517987284	-3.8085970824408
H	0.7764358720082	1.6768459225747	-4.9084817858043
I	3.5082222101767	2.0533066556835	-3.1548485582485

[IDipp·GaH$_2$PH$_2$BH$_2$·IDipp]$^+$

Ga	3.2268160100896	14.0760399662812	4.0918649129593
H	4.7912998862828	14.2051535998431	4.1083167064354
H	2.3069148589297	15.2542878313275	3.6227857059357
P	2.7925534712644	12.3487591923769	2.4522265303906
H	2.7960887908028	11.0070798192243	2.8616674909579
H	1.4670480780966	12.4427655282547	1.9905994002015
B	4.0949350681435	12.6619959628394	1.0281546802627
H	4.2457263936509	13.8501916943604	1.0093478195111
H	5.0818301835583	12.1023277705934	1.4256089779208
N	2.6365344242144	12.2672465334059	6.5570419012304
N	2.5659904476429	14.3577367720441	7.0106148863822
N	3.5851462357586	10.8803606417215	-0.8599518258663
N	3.3809958999412	12.9296825466540	-1.4693620118384
C	2.7053562980680	13.4880497392655	5.9917120975040
C	3.6718203793454	12.1498089671662	-0.4077924985505
C	2.4121800602740	13.6914741317910	8.2087432563893
H	2.2837636889635	14.2133170928216	9.1390753871695
C	1.3584455300220	16.4264876624270	6.5824669604789
C	2.5714184923954	15.7894341681883	6.8600826451169
C	2.4598010135362	12.3704573778197	7.9239816881351
H	2.3780662380765	11.5038785106666	8.5542265742608
C	3.7885281158173	16.4653332729917	6.9920609569512
C	3.2519449849028	10.8670452852462	-2.2006194173345
H	3.1464956988668	9.9510519779329	-2.7507646921767
C	2.6916819512999	11.0234217206205	5.8398813224209
C	3.8162656807943	9.6997628189717	-0.0733497127670
C	2.5731607407962	18.5160381494369	6.5871358125694
H	2.5736520992192	19.5934729084451	6.4824027707177
C	3.4134064213700	14.3684648435430	-1.4820372013977
C	5.0848068677997	15.7451522778633	7.3124614577310
H	4.9367103311338	14.6799396507674	7.1287862771061
C	5.1376594061426	9.3091167375698	0.1690969325645
C	1.4785120520517	10.3946098291565	5.5336106689719
C	0.1401966490757	11.0263238565569	5.8780252590299
H	0.2826113008715	11.6644669640126	6.7514324019864
C	3.4812081604631	17.1087775576454	-1.5400504265709
H	3.5071876816541	18.1906918631977	-1.5646174457610
C	3.9413710782798	10.5060851967992	5.4880156074428
C	0.0528808893734	15.6673088214304	6.4398506911713
H	0.2759665194077	14.6001332486916	6.4401500053980
C	1.3870570693058	17.8119563289040	6.4520393086437
H	0.4713042499465	18.3472223059884	6.2397014521720
C	2.7055029339312	8.9758983069327	0.3748849219622
C	3.1192074682263	12.1558888365355	-2.5822716171721
H	2.8776783118675	12.5938021870469	-3.5330430351852
C	3.9529945239507	9.2933095587010	4.8017127882960
H	4.8954499979215	8.8566396869943	4.5027001261462
C	4.5976195359964	14.9920709129273	-1.8839110038494
C	3.7599229442014	17.8503320554730	6.8509009633740
H	4.6765731668019	18.4157494148760	6.9476525162404
C	1.5494278052242	9.1811091051878	4.8565227355814
H	0.6403011090195	8.6537768258192	4.6059759566646
C	4.6050386406676	16.3845246021542	-1.9041343967172
H	5.5024612399790	16.9091735052896	-2.2031999102893
C	2.2668707248314	15.0665238324591	-1.0949493413200
C	2.9541964467390	7.8003920091413	1.0777978226021
H	2.1232949154466	7.2011837181283	1.4245904120030
C	6.3236230099511	10.0722908370958	-0.3896799459812
H	5.9890644756303	11.0727909764191	-0.6591016230558
C	5.3283851160580	8.1354925324577	0.8943749753850
H	6.3335526798059	7.7937473447096	1.0994864599612
C	1.2807839529579	9.4064682579342	0.0748631011221
H	1.3027178418764	10.4486683081515	-0.2484509375386
C	5.2394453844777	11.1956175342574	5.8621484125685
H	5.0184402620950	12.2363850037390	6.0981854369210
C	2.3255366463920	16.4565694428111	-1.1388050494911
H	1.4597030415485	17.0378581376115	-0.8524005993291
C	5.8498738406292	14.2106556479018	-2.2365669931524
H	5.5863430979329	13.1551220647191	-2.3146719612479
C	2.7729016076528	8.6362385466037	4.4982328252352
H	2.8063485933843	7.6924510020940	3.9730739000727
C	-0.8698961167733	15.9412752323844	7.6353688886375
H	-1.1445439638932	16.9966190606634	7.6865192042995
H	-0.3881516830610	15.6782182870655	8.5790411166081
H	-1.7898977066635	15.3594441145182	7.5498995425546
C	4.2504321563029	7.3850655711131	1.3361146856239

H	4.4235635935800	6.4653213045600	1.8809356346350
C	6.2424800338106	16.1937849484835	6.4147029692025
H	6.5170732116589	17.2341244024341	6.5962709799608
H	5.9883111876095	16.0843918030413	5.3603182761141
H	7.1257020798909	15.5847665135618	6.6160176300833
C	5.4378663878692	15.9129833334529	8.7977678070273
H	6.3480023715983	15.3607422822340	9.0397264693824
H	4.6383182881633	15.5479095133771	9.4450322509817
H	5.6065235383359	16.9639492543865	9.0408806600534
C	0.6919548794582	8.5730044812891	-1.0733952758398
H	1.2987597035963	8.6400365945377	-1.9767882794160
H	-0.3156550642009	8.9146403967635	-1.3176885766367
H	0.6325426809316	7.5191741847950	-0.7940615709746
C	0.3710309661068	9.3361788679521	1.3059147870394
H	0.2119998932362	8.3069025512302	1.6320541481861
H	-0.6084100906850	9.7559214965772	1.0691882567594
H	0.7886820959532	9.8912808955128	2.1442589661458
C	0.9965048546369	14.3578426860327	-0.6661020874385
H	1.2463023687119	13.3177478131756	-0.4511499114823
C	6.4272887390020	14.6263202157892	-3.5942435276531
H	5.6841387771892	14.5337371012412	-4.3883502601425
H	7.2790265271936	13.9934819224124	-3.8502000437127
H	6.7786403849338	15.6593747672676	-3.5849008735357
C	-0.6464133750091	15.9764853079968	5.1109063016134
H	-1.5372968637746	15.3546901718599	5.0022918078183
H	0.0148006580719	15.7829211944150	4.2659008275411
H	-0.9661800669063	17.0185670830369	5.0579674962858
C	-0.9324516997872	9.9991612877545	6.2499862599886
H	-1.2345792319602	9.3949839737205	5.3927415831536
H	-1.8249494118496	10.5112588797946	6.6126434748056
H	-0.5871022427918	9.3240301035338	7.0344296904418
C	-0.3440956481322	11.9271081951062	4.7311288868345
H	0.3739082329408	12.7142565728617	4.5022032026735
H	-1.2903580174290	12.4030438499223	4.9950800063124
H	-0.5039791965518	11.3420824804338	3.8230571986010
C	6.8308908156808	9.3929467559710	-1.6708926416788
H	7.1872692536189	8.3820169131556	-1.4625983792602
H	7.6584200728932	9.9601156040514	-2.1013310102486
H	6.0436175397359	9.3200419974430	-2.4235539661221
C	5.8358771473417	10.5525308799380	7.1231079848843
H	5.1374239524832	10.5919537879163	7.9609981334012
H	6.7496210487860	11.0707602625491	7.4198645061717
H	6.0841357753346	9.5040438449924	6.9454055871510
C	7.4520461520365	10.2445794692636	0.6309237283013
H	7.0856752264060	10.7050054160708	1.5487243564018
H	8.2300624616224	10.8884590924667	0.2176195162422
H	7.9212070726167	9.2928240096582	0.8865349483845
C	6.2517275918575	11.2083745290432	4.7127226490020
H	6.6075008005965	10.2050321436545	4.4723562408214
H	7.1216502377717	11.8039883313335	4.9932891774889
H	5.8254943671822	11.6466596928145	3.8101734943217
C	6.8965646570172	14.3356028764851	-1.1197066714466
H	7.2257543770315	15.3707438652591	-1.0079302535543
H	7.7741828932742	13.7290526515777	-1.3535642222966
H	6.4948295484248	14.0068039909556	-0.1611226129252
C	-0.0325668686676	14.3544917580527	-1.8055765006245
H	-0.9344057534382	13.8149605894021	-1.5086615435909
H	0.3670784923809	13.8786074212730	-2.7028762129653
H	-0.3212782362030	15.3734678425423	-2.0709257081889
C	0.4019884636226	14.9519963743677	0.6155197394099
H	0.0117919511966	15.9575657541087	0.4502943621996
H	1.1432719860178	15.0108612289138	1.4129859230144
H	-0.4300229707592	14.3361429014267	0.9636105195108

[IDipp·$GaH_2PH_2BH_2$·NMe_3]$^+$

Ga	2.2606509193144	13.5404574518526	5.9987571791562
P	2.8895340024345	11.7425455810508	7.5371058322958
N	1.4849902685414	9.6505753386905	9.2380669140247
N	3.7637624082252	14.7042819845725	3.6803011920190
N	4.3808128053763	12.6636720955590	3.8807361139530
C	1.2504795854400	17.4116976815621	3.6494255814755
H	0.2705669481903	17.6257551273924	3.2458471441779
C	1.8905643078789	18.3654574853258	4.4256443818296
H	1.4050075448800	19.3131711330816	4.6198547612211
C	3.7905157579198	16.9019732177106	4.7255549354570
C	3.1189873221668	15.9674844316490	3.9325530113212
C	3.6260287173046	13.6176319614623	4.4627316236170
C	3.1447792407189	18.1131205465383	4.9580465523797
H	3.6264570393548	18.8667315977517	5.5665534443100
C	1.8506884929023	16.1838950186916	3.3834634099853
C	5.8421884086561	9.7630118178977	5.6332207795157
H	6.7228195652390	9.4989177223588	6.2013716422969
C	5.1630295139884	16.6377380006153	5.3150106763519
H	5.4411395848369	15.6077808234714	5.0884546896029
C	5.7098557867307	11.0531180233237	5.1247548752770
C	4.8584149938286	8.8084150980879	5.4185344904965
H	4.9849107845563	7.8093382236167	5.8166679161941
C	4.5503148671716	11.3316170884922	4.3918052242301
C	3.7244306830407	9.1183953596797	4.6844159570191
H	2.9755101650305	8.3576676397948	4.5145496279067
C	2.3470702857326	10.7055072234621	3.2678759445862
H	2.1899766613547	11.7837707018968	3.2804336996875
C	6.7541872729888	12.1200608642091	5.4068981888394
H	6.7176201196448	12.8495633203833	4.5966773347923
C	3.5451138517485	10.3905679339734	4.1442287317355

C	-0.3133652554519	14.9674598055682	2.8552270727090
H	-0.9011551476674	15.8613071330009	2.6409625098357
H	-0.4384227411676	14.7200050792705	3.9095822648003
H	-0.7350464860353	14.1531542297089	2.2632877309725
C	1.0485804979262	10.0656518494573	3.7640305036974
H	1.0695382954529	8.9776686968408	3.6772277921442
H	0.2116735496417	10.4204774935384	3.1610456204075
H	0.8455908550708	10.3268198001559	4.8025563285279
C	0.1308241788525	9.0931389953494	9.5354596097552
H	0.2165775882738	8.2919460528175	10.2700173912185
H	-0.3019311193263	8.7108650685945	8.6149141941947
H	-0.4995923267998	9.8886958338766	9.9232746766199
C	1.1645880098543	15.1581961883252	2.5002706370958
H	1.6535046396170	14.1947081757244	2.6536059820183
C	2.0708645546171	10.1741846721659	10.5031918670132
H	1.4489485819810	10.9872290203505	10.8689684384230
H	3.0735402488051	10.5462843634323	10.3097134152232
H	2.1168732451566	9.3787672920271	11.2472274045045
C	2.6445876516939	10.2972548878515	1.8161211520739
H	3.5348615408412	10.7973430106471	1.4314030123975
H	1.8053679927025	10.5573283959664	1.1686595739817
H	2.8082610012447	9.2201657915944	1.7418420799350
C	2.3446636630539	8.5556141303803	8.7094476114045
H	2.4015187647852	7.7452809046739	9.4365473113818
H	3.3424300689486	8.9402313700843	8.5155428690136
H	1.9155368888022	8.1906615477105	7.7799241676462
C	4.5961214424513	14.4397676062485	2.6131869759732
H	4.8323247728063	15.1849126779633	1.8760538007132
C	6.4263775575977	12.8709871517895	6.7070329903339
H	5.4456605666370	13.3451936511667	6.6663978739331
H	7.1663030539631	13.6516942472927	6.8911076114384
H	6.4391968863295	12.1892446116367	7.5603869983823
C	4.9849886701296	13.1504780395296	2.7370183173871
H	5.6313982242004	12.5422382976115	2.1311927810267
C	1.3342574354554	15.5300321259811	1.0194874960370
H	0.8564452559908	16.4874987242936	0.8029317665977
H	0.8773658516287	14.7726928853595	0.3796093526995
H	2.3869638104893	15.6156203429548	0.7440459419186
C	5.1609803943763	16.7764331323141	6.8423354573078
H	6.1385129089955	16.5056680502429	7.2461760730848
H	4.4084594819849	16.1300059968223	7.2949412470376
H	4.9510703430944	17.8019106388345	7.1508121421016
C	8.1821086524718	11.5687543528626	5.4437227938072
H	8.3513978204350	10.9272485790632	6.3103183574883
H	8.8939514687975	12.3926290838794	5.5105296118670
H	8.4138538263334	10.9933590072752	4.5462299674155
C	6.2195542238664	17.5464440884354	4.6721252941904
H	6.0115842298766	18.5983842705551	4.8759327135097
H	6.2490226312454	17.4185513326344	3.5883695375284
H	7.2110139459828	17.3193123359132	5.0687799294297
B	1.2772838510937	10.8224925346963	8.1421435038182
H	3.8524645598710	10.8299561267997	7.0815809972937
H	0.8021645503084	10.3183644596189	7.1632558271964
H	3.5989502841318	12.2906308063082	8.6232460914524
H	0.5684549363987	11.6594908285585	8.6275629269493
H	2.3570418527665	14.8229097177472	6.8869721199087
H	0.9139998642216	13.0358340123403	5.3734204294223

[IDipp·GaH$_2$PPh$_2$BH$_2$·NMe$_3$]$^+$

Ga	1.7374057734756	8.3615973560638	3.7069402985098
P	3.5054337930096	7.0075694203524	2.7282503606049
N	0.5943571068014	7.5792369713592	6.4218523695154
N	2.3282943583915	8.8066370316741	6.7218394243968
N	4.9213526012594	4.3072961087123	3.2900235760548
C	1.6051722960115	8.1885385742732	5.7610997312460
C	2.7702577076633	6.6704546412194	1.0940772378894
C	-0.5575972220240	6.9584201540453	5.8128422177841
C	2.9603972283616	7.5403058991859	0.0186741506996
H	3.6165439533448	8.3938182145010	0.1178938118156
C	1.8811568172528	5.6025971290687	0.9481182153784
H	1.6843163177638	4.9463696117459	1.7845747746299
C	5.0236819548016	7.9608851393226	2.4102107839534
C	1.4426439603099	6.2434129932517	-1.3306968975673
H	0.9331378296737	6.0754719148511	-2.2705515862010
C	-0.5690625415777	5.5725443189718	5.6228716200869
C	1.7710925202579	8.5926103730778	7.9668475678565
H	2.1924284266609	9.0156313796904	8.8591660326702
C	4.7381578619249	9.1820412041106	6.7924236207840
C	3.2132383176032	11.0030549402698	6.1351940602554
C	5.8983750274786	7.6288709921844	1.3697341089622
H	5.6468942823079	6.8350878440138	0.6787105044769
C	3.4586508672468	9.6771946773760	6.5201385481845
C	5.3555176356039	9.0188919541955	3.2550130056854
H	4.6804708845279	9.3144633535488	4.0444406882887
C	7.0827807616661	8.3279351883872	1.1915062999586
H	7.7457704809699	8.0639929477447	0.3775166404960
C	4.9784710977935	7.7467483280039	7.2205892636116
H	4.1060267528473	7.1580584382692	6.9317364280950
C	0.6789095351314	7.8224467298659	7.7769798977027
H	-0.0521633855960	7.4483020260444	8.4689779709148
C	1.2268526035868	5.3881375748193	-0.2560753854374
H	0.5417583141651	4.5556298583783	-0.3535590811783
C	7.4131521988292	9.3696226355937	2.0531385575055
H	8.3361096130286	9.9171314967118	1.9124323424994
C	0.5887422866180	4.6936074540477	6.0603735319867

H	1.5080177804203	5.2735785673562	5.9529425670739
C	2.3053483413748	7.3224716766658	-1.1869370428289
H	2.4661660624763	8.0034435595984	-2.0127585739431
C	-1.6255347992493	7.7917928594142	5.4685071989969
C	6.5467758454236	9.7136369944576	3.0814161201477
H	6.7858569328041	10.5318769946784	3.7465093999567
C	5.8039835693649	10.0721939400432	6.6816583981640
H	6.8084673633615	9.7318740573005	6.8908953385595
C	4.7499134497184	3.8949407691948	1.8696340910168
H	4.9001535475690	4.7516084998549	1.2209728353031
H	3.7416119415607	3.5177068709275	1.7272468614181
H	5.4739702087193	3.1176785155951	1.6240277333323
C	1.8096956160762	11.5412488078255	5.9267423061300
H	1.1691840925297	10.7085174025292	5.6413417128020
C	6.3064357870407	4.8225958769473	3.4874756034327
H	7.0252420569883	4.0578926964727	3.1915814870648
H	6.4412000276102	5.0690827529449	4.5357566471002
H	6.4537579163029	5.7147365159561	2.8884095437771
C	4.3180491247991	11.8420760310952	6.0183804995167
H	4.1757793363561	12.8707107571253	5.7196373135415
C	-1.7119102798761	5.0246842003657	5.0474240018424
H	-1.7683746942193	3.9592021356622	4.8776133200928
C	6.1928849097825	7.1294679318043	6.5199017744837
H	7.1280108046969	7.5762513914796	6.8608919174945
H	6.1336762915385	7.2540350245805	5.4396292436385
H	6.2445919034426	6.0628677495032	6.7473578306229
C	5.1387324797913	7.6464264062513	8.7452762957987
H	5.2851230245405	6.6073985872830	9.0470341085975
H	4.2655782398322	8.0278721946220	9.2743396815933
H	6.0052586887734	8.2200863512470	9.0802015277817
C	5.5967458077021	11.3863705177715	6.2988810970891
H	6.4376828888320	12.0638056375574	6.2198035826674
C	4.7491154016673	3.1008609996208	4.1523623802328
H	3.7619250766523	2.6811262663940	3.9817050982820
H	4.8381973622201	3.3978155945759	5.1940945478431
H	5.5152432638785	2.3638745105049	3.9092271751435
C	-1.6117745261589	9.2902899372469	5.7081108634022
H	-0.6403080534964	9.5672822180850	6.1158262822546
C	-2.7431710693242	7.1909229584926	4.8944905852031
H	-3.5888544613800	7.8018861666647	4.6084674621288
C	0.7417679378707	3.4339594131371	5.2041481625935
H	1.6694787739687	2.9232943079008	5.4669350010052
H	0.7704053636551	3.6701480704560	4.1404709062024
H	-0.0720138264160	2.7272862203853	5.3752083071453
B	3.8010516873693	5.3800767160154	3.7657450642602
C	0.4462364260456	4.2964652838525	7.5392229868112
H	-0.4731782875717	3.7286519631413	7.6959952173877
H	0.4186370692402	5.1637978955119	8.1974289654462
H	1.2860353011671	3.6710025640714	7.8493343042391
C	1.2618715075279	12.1217073166357	7.2403687548915
H	1.2576192744405	11.3818926097404	8.0417726298491
H	0.2372163327210	12.4720246772004	7.1017321914574
H	1.8659921683221	12.9693020291753	7.5702572327144
C	-2.7858134066748	5.8240172429960	4.6842230930124
H	-3.6626309911552	5.3744089614643	4.2361472232106
C	1.7181521956680	12.5708963436144	4.7986184483685
H	2.2261550748140	13.5029070858057	5.0522011222031
H	0.6718204775481	12.8162509746422	4.6103931319445
H	2.1445341900605	12.1828810050470	3.8735854201743
C	-2.6622439130663	9.6870892659252	6.7541805154951
H	-2.6085015988752	10.7579370426734	6.9594685748507
H	-2.5094010546142	9.1528939176177	7.6938205400584
H	-3.6724318777026	9.4644770571050	6.4060718621054
C	-1.7953861449010	10.0789395016374	4.4057120423894
H	-2.7793383455940	9.9024063312022	3.9679881532139
H	-1.0467990307121	9.8028121214190	3.6629272669438
H	-1.7085638297754	11.1498190189428	4.5992107334051
H	2.1348871722625	9.8379813788929	3.3596380524621
H	0.4623964119387	7.6807659253799	3.1088252672748
H	2.7467235874433	4.8159424640698	3.7480939493961
H	4.0989460776820	5.7336594937133	4.8720913706184

[IDipp·$GaH_2PH_2GaH_2$·IDipp]$^+$

Ga	11.9799847915786	4.4812895356355	11.1162426739545
Ga	14.9207851038965	4.7582832219456	13.5733165086549
P	14.3664087170526	4.7746633323712	11.2384520287140
C	15.5501852995212	4.8673678982240	18.1877627142228
H	14.9649794715179	4.2859417064814	18.9001108043145
C	8.3815692504699	4.0668937603403	10.2362824054658
N	17.7887644837728	3.6139999074720	13.0861012928870
C	11.1996644050014	5.6512878843654	9.6280189558265
N	17.4960187833726	4.3932928530143	15.0692020350823
C	16.8829197847508	4.2533288855419	13.8674674017370
C	16.8770949954210	5.0267019468889	16.2074906006362
C	16.8502282314754	2.0778328086262	11.4363106434352
C	18.0962439727992	4.0981504941010	10.7174312302855
C	13.1714426585132	6.3398706515881	8.3059707682928
C	13.8718069814631	7.5029428412050	8.6718767575472
C	15.7015253191309	6.2391415837308	18.3792423993138
H	15.2383147652352	6.7190213397609	19.2423183960231
C	18.8140182691402	5.3915512498329	11.0746309065395
H	19.3320115988062	5.2353670863753	12.0340410363475
C	10.7869372219819	6.8953612241209	7.7859382600638
H	11.0371949104483	7.4554452890109	6.8938212193513
C	15.2443964632421	7.5262042979926	8.3978903015259

H	15.8289821534718	8.4095423220115	8.6538074199440	H	7.0185363099217	2.6110386384785	11.0551672040864
C	13.1871575797462	8.6513562511710	9.3967801215231	C	17.0053480212134	1.9731435172182	17.7798517835597
H	12.1243047812541	8.6462743980369	9.1103386068399	H	18.0395799151243	2.2783361136382	17.5660886841027
N	9.8662461047905	5.8629129447365	9.4982205877822	H	16.9301419467880	0.8883326744944	17.6175497645052
C	17.5708394120951	3.2512122190774	11.7107896195176	H	16.8122517603667	2.1722732167845	18.8441252316831
C	18.7697232407382	3.8516379279404	15.0457416488968	C	14.8297218536551	0.7944439562984	12.2680304566332
H	19.4183986803842	3.8688266335315	15.9121026035871	H	14.7341922822891	0.1526957201328	11.3805048468359
C	9.5889061828122	6.6249647918907	8.3765294894661	H	14.1903262989977	1.6760190782700	12.1224850149316
H	8.5782786958735	6.9039878761187	8.1075642019067	H	14.4317286351067	0.2333271628762	13.1245357122072
N	11.7587149562457	6.2921827301161	8.5712641089108	C	13.2509922488711	8.4375184700084	10.9217989026302
C	16.1341691999657	4.2243259384936	17.0905103510244	H	12.7797474902765	7.4934251723350	11.2282835420778
C	17.7996396275238	6.5331689393758	11.2798559624262	H	12.7340686457566	9.2546687351186	11.4442685613094
H	17.2348580054504	6.7117732800967	10.3538307087691	H	14.2945512109449	8.4205199421264	11.2692085848407
H	18.3180689675325	7.4632576082304	11.5531939057243	C	7.7954472323209	3.3927559906358	7.8912393507053
H	17.0760898023386	6.3019812663094	12.0729189230465	H	6.7939315226970	3.0485614076103	8.1880281264261
C	17.0327292611454	6.4148392420792	16.3547493456325	H	8.1105665852586	2.8089131172955	7.0144574882033
C	15.9950994002022	2.7243854880029	16.8936682881642	H	7.7095592623484	4.4450630287097	7.5855069180940
H	16.2357884402717	2.4970530707619	15.8435536247127	C	14.5636945369195	2.2285422380992	17.1399423680678
C	16.6776977492307	1.7419640243344	10.0871543033645	H	14.2661502056777	2.3430587060759	18.1921482297086
H	16.1309646877698	0.8360020181889	9.8253095034703	H	14.4896350403959	1.1594082442659	16.8957397939541
C	13.7522256092098	10.0248469553988	9.0141799165414	H	13.8436976977479	2.7732541767478	16.5145741551976
H	14.7789196071705	10.1627969068852	9.3832878562372	C	17.1827221054446	-0.0435027459184	12.7369566895164
H	13.1399694502926	10.8195072442537	9.4622336717016	H	16.7952068999887	-0.6686104623804	13.5539086651079
H	13.7590978431055	10.1721436794215	7.9252399500539	H	18.2143190405608	0.2426839549743	12.9867260022267
C	18.9554287303707	3.3542387443947	13.7905797746950	H	17.2170780054595	-0.6592814664425	11.8260532975764
H	19.7977236651116	2.8469302071022	13.3373058275354	C	17.0421692907601	8.4807132789166	14.8905451272316
C	17.8921881408009	3.7148591525998	9.3883280245836	H	16.0669284135161	8.1884960056508	14.4774109001637
H	18.2942220939728	4.3295499650424	8.5843437667282	H	17.6059540190694	9.0113237132202	14.1097292657118
C	16.2884283734311	1.1923814795970	12.5345957258481	H	16.8666077037143	9.1941192620925	15.7085151709720
H	16.2961676035199	1.7650052872301	13.4735637315113	C	8.7963665880243	3.2153909558868	9.0482321445131
C	17.8276167490146	7.2493219249060	15.3653597921115	H	9.7770886865800	3.5746348582544	8.6991572000944
H	18.0194058272983	6.6314179889777	14.4755301981440	C	8.5192389793250	6.1935985212695	11.5048294677575
C	13.7739032133281	5.2166985323015	7.7154978812586	C	13.6711510738528	2.6760154656657	7.6406621864216
C	12.9685853452382	3.9963332974351	7.3017741038598	H	14.5988349695403	2.5471849673438	7.0650789220874
H	12.0224391358715	4.0044635320766	7.8624893346311	H	13.0142356517478	1.8299069940158	7.3965075880754
C	8.8884597580395	5.3636407778709	10.4335444627037	H	13.9159646887331	2.6164509182791	8.7095851986470
C	17.1974178981526	2.5471269942088	9.0775908631160	C	15.8740824074566	6.4342675624110	7.8020987715431
H	17.0640381259037	2.2578753921183	8.0346298195137	H	16.9428413123770	6.4788485594898	7.5891379097542
C	16.4298606687718	7.0043619800171	17.4712442599934	C	12.6211551414184	4.0789308186016	5.8041869122741
H	16.5261503665744	8.0791742027696	17.6275041956613	H	12.0729087603784	5.0018029260711	5.5681911368515
C	19.1896919688978	7.6440288736344	15.9620000108800	H	11.9951023117917	3.2256717341747	5.5068756902980
H	19.0576846061468	8.2660665293581	16.8591797232791	H	13.5331097374569	4.0635714272094	5.1893116674709
H	19.7797618216670	8.2195343219560	15.2341829078181	C	19.8788104135970	5.7953818345898	10.0480361064010
H	19.7735268492873	6.7591096526286	16.2528703800731	H	20.5878153797730	4.9794520124393	9.8506213272664
C	15.1504445766188	5.2919831547943	7.4719193976580	H	20.4472354781477	6.6587257842060	10.4200898839416
H	15.6583331033910	4.4465035904141	7.0094616736033	H	19.4291273218368	6.0945334922161	9.0898891835816
C	7.4397438585503	3.6101105226716	11.1646287094935	C	7.0353022187698	4.4123877927081	12.2301082065076

H	6.2990738622668	4.0355069817681	12.9412200098078	H	10.4675747753484	6.9746689516099	13.2953197045456
C	8.9674712845899	1.7342618799424	9.4081627073691	C	8.0488956322405	8.6619092623637	11.4100807636155
H	8.0095638932533	1.2635543927456	9.6715107739716	H	7.6423011204680	8.5686586295340	10.3928111461799
H	9.6591369940746	1.6082193390344	10.2520312787292	H	8.4849398912050	9.6658347996608	11.5145403668540
H	9.3720302995032	1.1837402435954	8.5471513704096	H	7.2068683853365	8.5847651352099	12.1130976688485
C	7.5701617682197	5.6867465723741	12.3995440524504	C	9.1053272646610	7.5812278030342	11.6984390097496
H	7.2512338809580	6.2959831471033	13.2459650038349	H	9.9220212163458	7.7118925302101	10.9727089079887
H	14.8427234855230	5.9546310874190	10.6238594990976	H	11.4465570346870	5.0310686813200	12.4886328450500
H	15.0276885705059	3.8178366095820	10.4342973138105	H	11.7739421087163	2.9703969278073	10.7125670019366
C	9.7161458787346	7.7509679692945	13.0977143635673	H	14.6860118694469	6.2474692324080	14.0259489459694
H	8.9488382167679	7.6938849638028	13.8830317050785	H	14.0728906166706	3.5799596909073	14.1867450229540
H	10.2009892513007	8.7341180379148	13.1822725722587				

5.5.6 References

[1] A. J. Arduengo, R. Krafczyk, R. Schmutzler, H. A. Craig, J. R. Goerlich, W. J. Marshall, M. Unverzagt, *Tetrahedron* **1999**, *55*, 14523–14534.

[2] A. Hock, L. Werner, C. Luz, U. Radius, *Dalton Trans.* **2020**, *49*, 11108–11119.

[3] M. A. K. Weinhart, A. S. Lisovenko, A. Y. Timoshkin, M. Scheer, *Angew. Chem. Int. Ed.* **2020**, *59*, 5541–5545; *Angew. Chem.* **2020**, *132*, 5586-5590.

[4] K.-C. Schwan, A. Y. Timoskin, M. Zabel, M. Scheer, *Chem. Eur. J.* **2006**, *12*, 4900–4908.

[5] C. Marquardt, T. Jurca, K.-C. Schwan, A. Stauber, A. V. Virovets, G. R. Whittell, I. Manners, M. Scheer, *Angew. Chem. Int. Ed.* **2015**, *54*, 13782–13786.

[6] C. Marquardt, O. Hegen, A. Vogel, A. Stauber, M. Bodensteiner, A. Y. Timoshkin, M. Scheer, *Chem. Eur. J.* **2018**, *24*, 360–363.

[7] Y. Wang, B. Quilian, P. Wei, C. S. Wannere, Y. Xie, R. B. King, H. F. Schaefer, P. v. R. Schleyer, G. H. Robinson, *J. Am. Chem. Soc.* **2007**, *129*, 12412–12413.

[8] J. Monot, A. Solovyev, H. Bonin-Dubarle, É. Derat, D. P. Curran, M. Robert, L. Fensterbank, M. Malacria, E. Lacôte, *Angew. Chem. Int. Ed.* **2010**, *122*, 9352–9355.

[9] O. V. Dolomanov, L. J. Bourhis, R. J. Gildea, J. A. K. Howard, H. Puschmann, *J. Appl. Crystallogr.* **2009**, *42*, 339–341.

[10] G. M. Sheldrick, *Acta Cryst. A* **2015**, *71*, 3–8.

[11] G. M. Sheldrick, *Acta Cryst. C* **2015**, *71*, 3–8.

[12] a) F. Neese, *WIREs Comput. Mol. Sci.* **2012**, *2*, 73–78; b) F. Neese, *WIREs Comput. Mol. Sci.* **2018**, *8*, e1327; c) F. Neese, *WIREs Comput. Mol. Sci.* **2022**, *12*, e1606; d) F. Neese, *J. Comput. Chem.* **2022**, *1*, 1–16; e) F. Neese, F. Wennmohs, U. Becker, C. Riplinger, *J. Chem. Phys.* **2020**, *152*, 224108.

[13] "Chemcraft - graphical software for visualization of quantum chemistry computations. https://www.chemcraftprog.com".

[14] a) A. D. Becke, *J. Chem. Phys.* **1993**, *98*, 5648–5652; b) C. Lee, W. Yang, R. G. Parr, *Phys. Rev. B* **1988**, *37*, 785–789; c) E. Caldeweyher, C. Bannwarth, S. Grimme, *J. Chem. Phys.* **2017**, *147*, 34112; d) E. Caldeweyher, S. Ehlert, A. Hansen, H. Neugebauer, S. Spicher, C. Bannwarth, S. Grimme, *J. Chem. Phys.* **2019**, *150*, 154122.

[15] F. Weigend, R. Ahlrichs, *Phys. Chem. Chemical Phys.* **2005**, *7*, 3297–3305.

[16] a) F. Neese, *J. Comput. Chem.* **2003**, *24*, 1740–1747; b) F. Neese, F. Wennmohs, A. Hansen, U. Becker, *Chem. Phys.* **2009**, *356*, 98–109.

[17] A. E. Reed, L. A. Curtiss, F. Weinhold, *Chem. Rev.* **1988**, *88*, 899–926.

[18] V. N. Staroverov, G. E. Scuseria, J. Tao, J. P. Perdew, *J. Chem. Phys.* **2003**, *119*, 12129–12137.

[19] Y. Guo, C. Riplinger, U. Becker, D. G. Liakos, Y. Minenkov, L. Cavallo, F. Neese, *J. Chem. Phys.* **2018**, *148*, 11101.

[20] V. Ásgeirsson, B. O. Birgisson, R. Bjornsson, U. Becker, F. Neese, C. Riplinger, H. Jónsson, *J. Chem. Theory Comput.* **2021**, *17*, 4929–4945.

5.6 Author Contributions

- R. Szlosek – writing of original draft, experimental work, quantum chemical calculations
- M. Seidl – finalization of single-crystals X-ray diffraction data
- G. Balázs – project management, conceptualization
- M. Scheer – project supervision, acquisition of funding, co-writing of final manuscript

6 Characterization of the Ligand Properties of Donor stabilized Pentelyltrielanes

R. Szlosek, A. S. Niefanger, G. Balázs, M. Seidl, A. Y. Timoshkin and M. Scheer

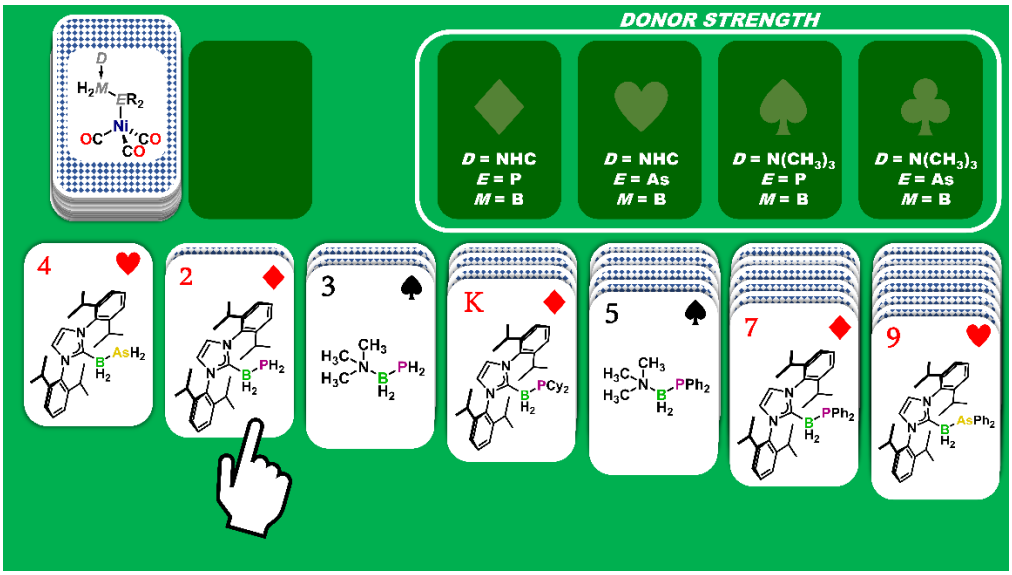

Abstract: A general synthesis and the characterization of novel alkyl-substituted NHC-stabilized pnictogenylboranes NHC·BH_2ER_2 (NHC = N-heterocyclic carbene, E = P, As; R_2 = Me_2, Ph_2, ^tBuH, Cy_2, $(SiMe_3)_2$) are reported. These compounds were reacted with $Ni(CO)_4$ to the corresponding complexes of the type [(NHC·BH_2ER_2)$Ni(CO)_3$] to determine their donor strength by Tolman Electronic Parameters (TEPs) and their steric demand as ligands compared to classical phosphines, superbasic phosphines and other commonly applied donor systems. The results show that the NHC-stabilized pnictogenyltrielanes can be considered as being highly basic, while their steric influence depends strongly on the organic residues as well as the donor attached to the {BH_2} moiety. Although weaker than commonly used superbasic phosphines, the donor strength of pnictogenyltrielanes in general can be classified as of similar strength as NHCs. The steric and electronic properties can easily be modified by alkyl substitution as evident from the TEP trends.

6.1 Introduction

Phosphines and especially trivalent phosphorus ligands have become ubiquitous compounds in synthetic chemistry and homogeneous catalysis.[1,2] Compared to amines or arsines, phosphines offer versatile advantages that make them ideal ligands in many cases. By strong σ-donation and moderate π-acceptor abilities, the soft phosphines bind excellently to soft metal centers and their ligand properties can readily be modified by adjusting the attached organic residues.[1] In that regard, chiral phosphines play a significant role especially in asymmetric catalysis, as the high inversion barrier prevents their racemization.[1,3] Furthermore, the highly abundant ^{31}P nucleus allows for facile reaction monitoring by NMR spectroscopy.[4] The sterics and electronics of phosphines can easily be modified by varying the organic substituents. Although disputed nowadays,[5] the traditional and still highly relevant classification of donor strength is represented by the Tolman Electronic Parameter (TEP), formally introduced by C. Tolman as the magnitude of the A_1 vibration mode in $[Ni(CO)_3L]$.[6,7,8] Due to the dangerous toxicity of the required $Ni(CO)_4$, alternative carbonyl complexes of Rh, Cr, Au and Ir were used in the past.[9] Today, however, computational methods are able to provide reliable theoretical values for any ligands by frequency analysis of the respective carbonyl complexes.[10]

In many applications, phosphines were replaced by N-heterocyclic carbenes (NHCs)[11] or cyclic (alkyl)(amino)carbenes (CAACs)[12] as stronger σ-donors.[13] However, during more recent years, new and highly basic classes of phosphines have been developed that are often referred to as "superbasic phosphines".[14] An overview of selected examples of mono-substituted "superbasic" phosphines is given in Figure 6.1. In general, electron-donating substituents are introduced to increase the basicity of the P atom.[15,16]

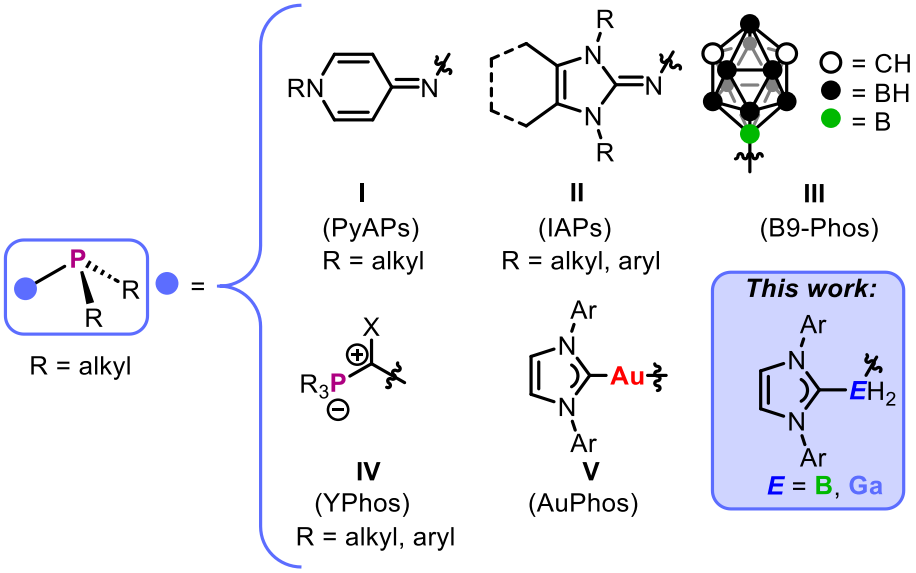

Figure 6.1: Selected examples of mono-substituted "superbasic" phosphines $(L)PR_2$.

Most commonly, amine- or imine-based substituents are used (e.g. PyAPs **I**, IAPs **II**),[17–20] but it is also possible to increase the basicity with e.g. carborane residues (B9-Phos, **III**).[21] Furthermore, the Gessner group developed phosphines carrying an ylidic substituent (YPhos, **IV**), finding broad application as ligands in transition metal-catalyzed cross coupling reactions.[22] Alternatively, [(NHC)Au]-substituted terminal phosphines were developed by the groups of Toste, Bergman, Corrigan and Liu (AuPhos, **V**).[23,24] Based on a π-repulsion between d_{Au} and p_P orbitals, AuPhos ligands are highly electron-rich and can be further tuned regarding the steric and electronic nature at the NHC or by having multiple

[(NHC)Au] substituents surrounding the P atom.[23] The *d-p* repulsion is further enhanced as NHCs only show comparatively low π-acceptor capabilities. Significant contributions to the field of superbasic phosphines were also made by the Dielmann group who developed several novel types of superbasic phosphines including pyridinylidenaminophosphines (PyAPs, **I**),[20] imidazolin-2-ylidenaminophosphines (IAPs, **II**),[17–19] 1,2,5 trimethylpyrrolyl-phosphines $P(tmp)_3$[25] and tris(1,1,3,3-tetramethylguanidinyl)-phosphine $P(tmg)_3$.[26] These compounds have shown remarkable reactivity and basicity while still being easy to access in larger quantities. Typically, these superbasic phosphines are used as ligands in catalysis including reactions such as hydroaminations, coupling reactions, decarbonylations, and many more.[14,27] As shown by Dielmann and co-workers, however, by the splitting of CO_2, the superbasic phosphines are powerful enough to activate small molecules.[19]

A different class of phosphines is represented by phosphines containing a $\{D{\cdot}BH_2\}$ (D = NHC, NMe_3) residue, namely phosphanylboranes.[28–31] The same accounts for the heavier homolog containing arsenic $D{\cdot}BH_2AsR_2$.[32–34] In recent years, the stabilization of 13/15 monomers containing the heavy group 13 homologs Ga, Al and In by an NHC could be reported in several studies as well.[35,36] These monomers have been the subject of numerous studies and proved to be suitable building blocks towards 13/15 oligo- and polymeric compounds induced by thermal or transition metal-catalyzed pathways.[37] Furthermore, the reactivity towards main group electrophiles, nucleophiles and transition metals was extensively investigated, as well as the oxidation of the pnictogen atom with chalcogens.[28,29,31–33,38]

Despite known for almost two decades, neither a clear determination of the electronic and steric properties of these 13/15 compounds nor a comparison towards classic phosphines and modern superbasic phosphines have been reported so far. Herein, we report the first systematic study of the donor strength and steric demand of NHC- and NMe_3-stabilized pnictogenyltrielanes by the evaluation of the TEPs of the corresponding Ni carbonyl complexes which have been synthesized by the reactions with $Ni(CO)_4$. Furthermore, a general synthetic access towards E-alkyl (E = P, As)-substituted NHC-stabilized pnictogenylboranes $NHC{\cdot}BH_2ER_2$ is described, and the effects of the substitution are discussed.

6.2 Results and Discussion

Prior to the determination of TEPs, a suitable substrate scope was needed. As the NHC-stabilized 13/15 monomers display the highest stability and accessibility, these compounds were chosen as the first candidates for the reactions with $Ni(CO)_4$. However, with substituted $NHC{\cdot}BH_2ER_2$ (E = P, As; R = alkyl) not reported in the literature, the aim was to synthesize a broad scope of alkyl-substituted NHC-stabilized pnictogenylboranes. By salt metathesis reactions of $NHC{\cdot}BH_2I$ with alkalimetalphosphanides and arsanides, several novel NHC-stabilized pnictogenylboranes were obtained in moderate to good yields (eq. 1). Surprisingly, in these reactions, the choice of solvent played a crucial role, when, for example, tetrahydrofuran was used instead of Et_2O under the same reaction conditions, only intractable product mixtures were obtained as oily residues. Therefore, Et_2O is necessary to isolate the pure products.

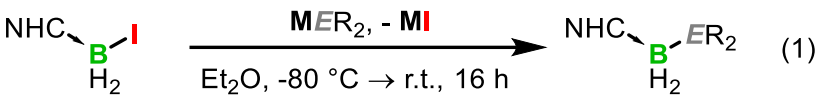

(1)

1a: NHC = SIDipp, *E* = P, R = H (62%)
1b: NHC = IDipp, *E* = P, R = Ph (72%)
1c: NHC = IDipp, *E* = P, R = Me (57%)
1d: NHC = IDipp, *E* = P, R_2 = H^{t}Bu (54%)
1e: NHC = IDipp, *E* = P, R = Cy (60%)
1f: NHC = IDipp, *E* = P, R = $SiMe_3$ (15%)
2: NHC = IDipp, *E* = As, R = Ph (37%)

Compounds **1a**-**2** were obtained as colorless to yellowish solids which could be stored under an inert atmosphere for at least several months without any signs of decomposition. Characteristic heteronuclear NMR data are summarized in Table 6.1. It was possible to crystallize compounds **1a**, **1d**, **1e** and **2** as single crystals suitable for X-ray diffraction studies and determine their solid-state structure (Figure 6.2, top row). The B-E bond lengths lie within the range of regular single bonds and the bond angles reveal (pseudo)tetrahedral geometries at the atoms of the element 13/15 core motifs. Remarkably, **1d**, containing a chiral P atom, crystallizes as a racemic mixture with both (*R*/*S*) enantiomers present in the asymmetric unit (cf. Supporting Information).

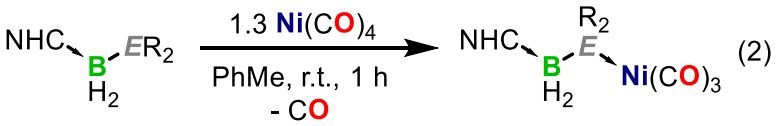

(2)

3a: NHC = SIDipp, *E* = P, R = H (28%)
3b: NHC = IDipp, *E* = P, R = Ph (39%)
3c: NHC = IDipp, *E* = P, R = Me (29%)
3d: NHC = IDipp, *E* = P, R_2 = H^{t}Bu (54%)
3e: NHC = IDipp, *E* = P, R = Cy (55%)
3f: NHC = IDipp, *E* = P, R = $SiMe_3$ (25%)
3g: NHC = IDipp, *E* = P, R = H (24%)
4a: NHC = IDipp, *E* = As, R = H (49%)
4b: NHC = IDipp, *E* = As, R = Ph (24%)

Following the successful synthesis of suitable substrates, reactions with $Ni(CO)_4$ were carried out to prepare the corresponding [(NHC·BH_2ER_2)$Ni(CO)_3$] complexes and determine the TEPs. Thus, $Ni(CO)_4$ was added to solutions of **1a**-**2** in toluene and the solutions stirred for one hour (eq. 2). According to NMR spectroscopic investigations of the reaction mixtures, full conversion is already achieved after one hour in all cases. Noteworthily, no evidence of sequential CO substitutions at $Ni(CO)_4$ can be found, as no product mixtures are observed, which can largely be attributed to the bulkiness of IDipp preventing a second substitution step of CO. After work-up, the complexes **3a**-**4** were isolated in moderate yields as brown powders. The brown color can likely be attributed to the presence of Ni nanoparticles which could not be fully separated by filtration.[45] Characteristic heteronuclear NMR data are summarized in Table 6.2.

Table 6.1: Heteronuclear NMR chemical shifts [ppm], coupling constants [Hz] and signal multiplicities of compounds 1a-f and 2 (298 K, C_6D_6; s = singlet, d = doublet, t = triplet, q = quartet, m = multiplet, br = broad).

Entry	$^{31}P\{^{1}H\}$ NMR	^{31}P NMR	$^{11}B\{^{1}H\}$ NMR	^{11}B NMR
1a	-213.2 (s, br)	-213.2 (t, br)	-34.3 (s, br)	-34.3 (t, br)
1b	-38.1 (m, br)	-38.1 (m, br)	-26.9 (s, br)	-26.9 (t, br)
1c	-104.0 (q, br)	-104.0 (q, br)	-24.8 (d, br)	-24.8 (td, br)
1d	-67.3 (s, br)	-67.3 (d, br)	-33.0 (s, br)	-33.0 (t, br)
1e	-37.8 (m, br)	37.8 (m, br)	-30.0 (s, br)	-30.0 (t, br)
1f	-265.0 (s, br)	-265.0 (s, br)	-33.3 (s, br)	-33.3 (t, br)
2	-	-	-26.7 (s, br)	-26.7 (t, br)

Compounds **3a**-**3h** show a characteristic large downfield shift in the $^{31}P\{^{1}H\}/^{31}P$ NMR spectra compared to their uncoordinated counterparts. Furthermore, it was possible to crystallize compounds **3a**, **3g** and **4a** and determine their structure by single-crystal X-ray structure determination (Figure 6.2, bottom row). The compounds crystallized from Et_2O/*n*-hexane (**3a, 3g**) or toluene/*n*-hexane (**4a**) mixtures at *T* = -30 °C as clear colorless blocks (**3a**, **3g**) or plates in the monoclinic space group $P2_1/c$. All structures show a regular tetrahedral coordination of the Ni atom by three CO molecules and one pnictogenylborane. All bonds within the compounds are within the expected range of the respective single bonds.

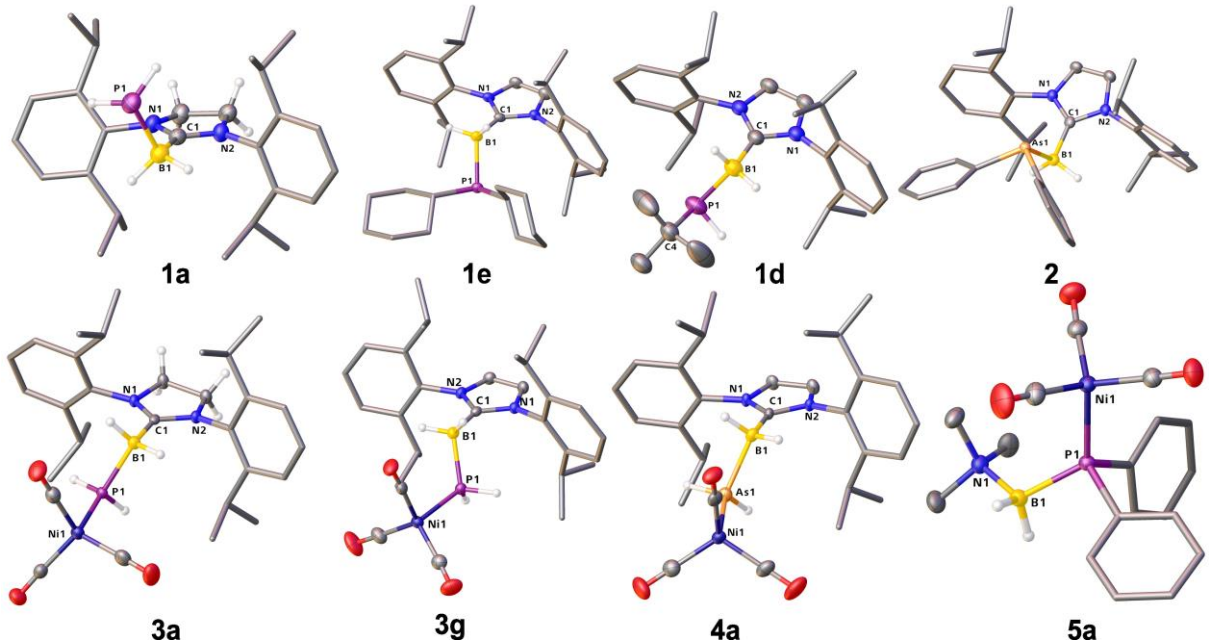

Figure 6.2: Molecular structures of **1a**, **1e**, **1d**, **2** and **3a**, **3g**, **4a**, **5a** in the solid state. Anisotropic displacement ellipsoids are shown at 50% probability level. Hydrogen atoms bound to carbon are omitted for clarity. Dipp groups are displayed as stick models for clarity. Selected bond lengths [Å] and angles [°]: **1a**: N1-C1 1.356(6), N2-C1 1.340(6), C1-B1 1.579(8), B1-P1 2.038(6), N1-C1-N2 108.6(4), C1-B1-P1 111.6(4); **1e**: N1-C1 1.361(2), N2-C1 1.362(2), C1-B1 1.605(2), B1-P1 1.9944(19), N1-C1-N2 104.12(14), N1-C1-B1 126.97(15), N2-C1-B1 128.69(14), C1-B1-P1 115.45(12); **1d** (only one enantiomer shown): N1-C1 1.360(4), N2-C1 1.360(4), C1-B1 1.596(4), B1-P1 1.993(3), P1-C4 1.867(4), N1-C1-N2 104.2(2), N1-C1-B1 126.7(3), N2-C1-B1 128.9(3), C1-B1-P1 112.3(2), B1-P1-C4 102.85(15); **2**: N1-C1 1.3556(17), N2-C1 1.3594(16), C1-B1 1.5957(19), B1-As1 2.1109(14), N1-C1-N2 104.19(11), N1-C1-B1 128.64(11), N2-C1-B1 127.16(11), C1-B1-P1 108.94(9); **3a**: N1-C1 1.344(2), N2-C1 1.336(2), C1-B1 1.598(2), B1-P1 1.966(2), P1-Ni 2.2500(5), N1-C1-N2 104.19(11), N1-C1-B1 126.87(14), N2-C1-B1 124.32(14), C1-B1-P1 111.70(11), B1-P1-Ni1 115.56(6); **4a**: N1-C1 1.359(4), N2-C1 1.355(4), C1-B1 1.597(4), B1-As1 2.072(4),

As1-Ni 2.3445(6), N1-C1-N2 105.1(2), N1-C1-B1 128.6(2), N2-C1-B1 126.3(3), C1-B1-As1 113.3(2), B1-As1-Ni1 116.03(10); **3g**: N1-C1 1.356(2), N2-C1 1.360(2), C1-B1 1.597(2), B1-P1 1.966(2), P1-Ni 2.2605(5), N1-C1-N2 104.21(14), N1-C1-B1 128.96(14), N2-C1-B1 126.82(14), C1-B1-P1 114.48(12), B1-P1-Ni1 115.59(6); **5a**: N1-B1 1.611(2), B1-P1 1.977(2), P1-Ni1 2.2581(5), N1-B1-P1 116.21(12), B1-P1-Ni1 121.12(6).

Table 6.2: Heteronuclear NMR chemical shifts and multiplicities of compounds **3a**-**5c** [ppm] (298 K, C_6D_6; d = doublet, t = triplet, q = quartet, m = multiplet, br = broad).

Entry	$^{31}P\{^1H\}$ NMR	^{31}P NMR	$^{11}B\{^1H\}$ NMR	^{11}B NMR
3a	-164.5 (q, br)	-164.5 (tq, br)	-32.2 (d, br)	-32.2 (td, br)
3b	-11.1 (q, br)	-11.1 (m, br)	-26.8 (m, br)	-26.8 (br)
3c	-68.9 (m, br)	-68.9 (m, br)	-24.8 (d, br)	-24.8 (dt, br)
3d	-38.7 (q, br)	-38.7 (dm, br)	-30.4 (d, br)	-30.4 (dt, br)
3e	-37.8 (m, br)	-37.8 (m, br)	-30.0 (s, br)	-30.0 (t, br)
3f	-241.8 (m, br)	-241.8 (m, br)	-33.2 (m, br)	-33.2 (m, br)
3g	-163.5 (q, br)	-163.5 (tq, br)	-32.2 (d, br)	-32.2 (m, br)
4a	-	-	-32.0 (s, br)	-32.0 (t, br)
4b	-	-	-26.9 (s, br)	-26.9 (t, br)
5a	-20.7 (q, br)	-20.7 (m, br)	-4.09 (d, br)	-4.09 (m, br)
5b	-47.2 (q, br)	-47.2 (dm, br)	-7.3 (d, br)	-7.3 (td, br)
5c	-155.6 (q, br)	-155.6 (tq, br)	-7.8 (d)	-7.8 (d, br)

To address the influence of the donor molecule attached to boron, the same reactions were performed with the NMe_3-stabilized compounds $Me_3N{\cdot}BH_2PR_2$ (R_2 = Ph_2, H^{t}Bu, H_2). As NMe_3 significantly decreases the steric bulk of the reactants, the reaction principle was reversed by adding the phosphanylboranes dropwise to solutions of $Ni(CO)_4$ (eq. 3). After 10 min, all volatiles were removed and the reaction outcomes investigated by multinuclear NMR spectroscopy. The reactions showed full conversion and small amounts of the inseparable side products $[(Me_3N{\cdot}BH_2PR_2)_xNi(CO)_{4-x}]$ (x = 2, 3; cf. Supporting Information). After filtration, **5a**-**c** were obtained as brown solids or oils in moderate yields, respectively. Characteristic heteronuclear NMR data for **5a**-**c** are given in Table 6.2.

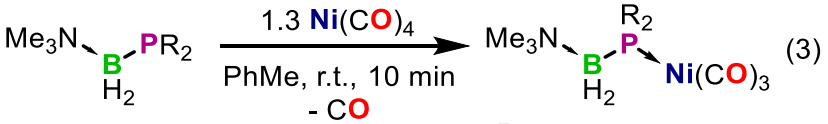

5a: R = Ph (51%)
5b: R_2 = H^{t}Bu (94%)
5c: R = H (62%)

Compound **5a** also crystallized from a saturated toluene solution at -30 °C as colorless blocks suitable for X-ray structure determination (Figure 6.2). **5a** crystallizes in the monoclinic space group $P2_1/n$. The solid-state structure of **5a** shows a tetrahedral coordination of the phosphanylborane to the {$Ni(CO)_3$} unit with a B-P-Ni angle of 121.12(6)°. The bond lengths of 2.2581(5) Å (P-Ni) and 1.977(2) (B-P) lie within the range of usual single bonds.

In this context, the question arose if it was also possible to synthesize the corresponding Ni complex of NHC-stabilized phosphanylgallanes and determine the donor strength, despite the high sensitivity of the compound due to the lability of the Ga-P bond. Thus, freshly prepared IDipp·GaH_2PH_2[36] was

reacted with $Ni(CO)_4$ (eq. 4). The reaction mixture showed full conversion already after 10 minutes with a downfield shift of the ^{31}P resonance signal of +55 ppm. After work-up, [(IDipp·GaH_2PH_2)$Ni(CO)_3$] (**6**) is obtained in moderate yields as a brown powder. **6** represents the first example of a coordination compound of the highly unstable parent compound IDipp·GaH_2PH_2. The ^{31}P NMR spectrum of **6** shows a distinct sharp triplet of triplets at -222.5 ppm ($^1J_{HP}$ = 172 Hz, $^3J_{HP}$ = 19 Hz) that merges into a singlet in the $^{31}P\{^1H\}$ NMR spectrum.

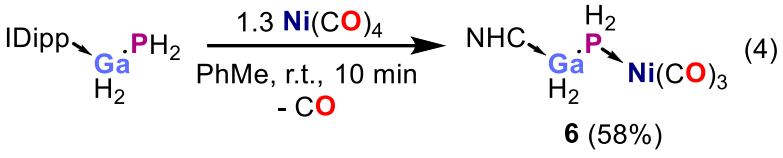

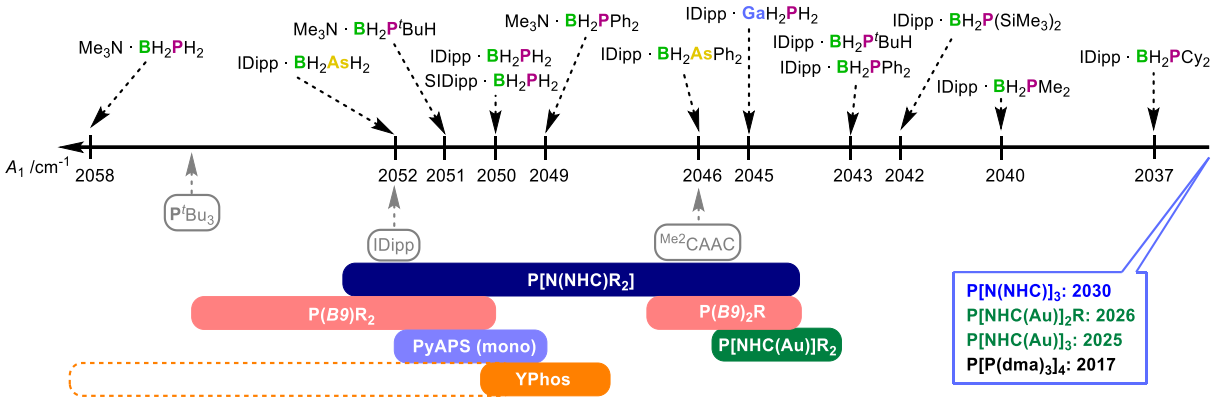

Figure 6.3: Schematic representation of the determined TEPs [cm^{-1}] in this work and comparison to selected phosphines and NHCs. TEPs were determined by the magnitude of the A_1 vibration mode in the corresponding IR spectra (ATR diamond crystal). TEPs of substance classes are represented by averaged areas. As the YPhos ligand system can vary strongly depending on the substituents, the region of the highest donor strength is given in bold print.

After the successful synthesis of the complexes **3a-5a**, IR spectra of the solid products were recorded to evaluate the TEPs and compare the donor strength of the different compounds by evaluating the A_1 vibration modes (Figure 6.3). In line with regular phosphines, the alkyl substituents on the pnictogen atom generally increase the donor strength. Compared to their substituted counterparts, the parent compounds reveal the weakest donor strength of the herein investigated compounds. Moreover, the group 13 element also strongly influences the donor strength with e.g. phosphanylgallanes, as they ge-nerally are stronger donors than phosphanylboranes (cf: **6**: 2045 cm^{-1}, **3g**: 2050 cm^{-1}). Just as arsines and phosphines, arsanylboranes show higher TEPs and can be considered slightly weaker donors than the respective phosphanylboranes (**4a**: 2052 cm^{-1}, **3g**: 2050 cm^{-1}). In general, exchanging NMe_3 for a stronger donor such as an NHC increases the overall donor strength, as the 13/15 monomer becomes more electron-rich (cf. **5c**: 2059 cm^{-1} → **3g**: 2050 cm^{-1}).

With the common trend towards donor strength based on the composition of the 13/15 monomer now established, a comparison towards classic phosphines and other commonly used 2e-σ-donors is now addressed. All compounds **3a**-**5b** (except for **5c**) show lower TEPs and thus higher donor strength than regular phosphines PR_3 (cf. P^tBu_3: 2056 cm^{-1}), even the measured arsanylboranes. Based on the magnitude of the measured TEPs, a donor strength similar to that of NHCs can be attributed to **3a**-**5c** with some of them being significantly stronger donors. Although modern superbasic phosphines such as Sundermayer's phosphazenylphosphines (2017 cm^{-1}),[16] Dielmann's tris(imidzalolin-2-ylidenamino)phosphine (2030 cm^{-1}),[19] Liu's AuPhos ligands P[(NHC)Au]$_2$R (2026 cm^{-1}) and P[(NHC)Au]$_3$ (2025 cm^{-1}) commonly achieve higher donor strengths,[23] a remarkable value for the pnictogenyltrielanes is set by IDipp·BH_2PCy_2 (**3e**) with a TEP of 2037 cm^{-1}, which is comparable to $P(NIMes)_2{}^iPr$ (2039 cm^{-1}),[17] and $P(tmg)_3$ (2037 cm^{-1})[26] making **3e** the strongest donor within the herein presented series of

pnictogenyltrielanes.[39] This is especially intriguing, as **3e** displays such a high donor strength while having only one {NHC·BH_2} unit attached, which greatly simplifies the synthesis of **3e**.

Table 6.3: Calculated averaged TCA [°][40] and percent buried volumes %V_{bur} [%][41,42] from the solid-state structures of **3a**, **3g**, **4a** and **5a** and comparison to selected phosphines.[62] %V_{bur} values of **3a**, **3g**, **4a** and **4g** were calculated from the solid-state structures (r = 3.5 Å, bond radii scaled by 1.17).

	3a	**3g**	**4a**	**5a**	**PH_3**[8]	**PMe_3**[8]	**$PMePh_2$**[8]
TCA	94	95	93	135	87	118	136
%V_{bur}	22.5	23.0	14.8	31.0	-	22.2	-
	PCy_3[6a]		**P(tmp)$_3$**[25]		**P(9-*m*Cb)^{t}Bu$_2$**[21]		**P(NI^{i}Pr)$_3$**[19]
TCA	170		163		178		178
%V_{bur}	31.8		36.1		41.8		38.7

With the solid-state structures of [(SIDipp·BH_2PH_2)Ni(CO)$_3$] (**3a**), [(IDipp·BH_2PH_2)Ni(CO)$_3$] (**3g**), [(IDipp·BH_2AsH_2)Ni(CO)$_3$] (**4a**) and [(Me_3N·BH_2PPh_2)Ni(CO)$_3$] (**5a**) at hand, it was also possible to calculate the Tolman Cone Angles (TCAs) and percent buried volumes (%V_{bur})[41,42] directly from them to evaluate the steric demand of the ligands (Table 6.3).[40] The TCAs for the parent phosphanyl- and arsanylboranes (**3a**, **3g**, **4a**) are only slightly larger than the value of PH_3 and thus show that the steric demand at the pnictogen atom is comparatively low. The TCA for **5a** (135°) is comparable to the one for $PMePh_2$ (136°). This is further supported by comparably low %V_{bur} values for all compounds. Thus, the pnictogenyltrielanes can be considered as significantly stronger donors than regular phosphines while being sterically less hindered at the pnictogen atom. In comparison, other superbasic phosphines of comparable donor strength such as P(tmp)$_3$, P(9-*m*Cb)^{t}Bu$_2$ and P(NI^{i}Pr)$_3$ reveal a higher steric demand (cf. Table 6.3).

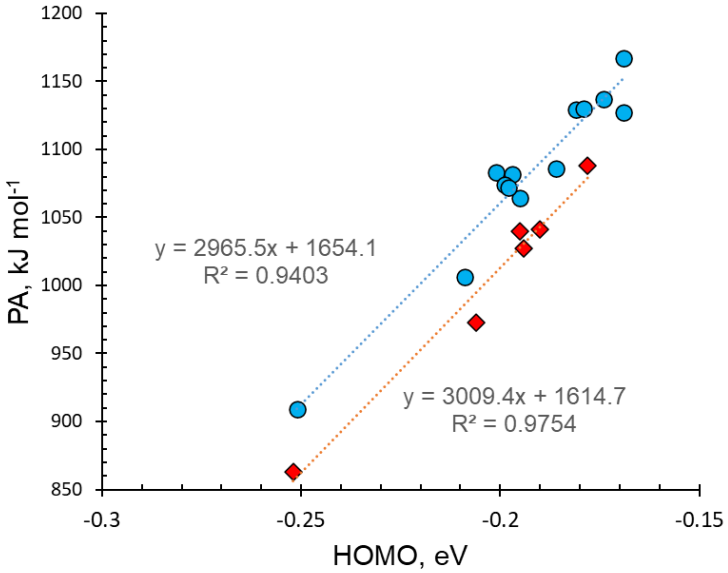

Figure 6.4: Correlation between the HOMO energy of the ligand **L** [eV] and PA [kJ mol^{-1}]. Blue: P-containing **L**; red: As-containing **L**.

To further investigate the electronic properties of the compounds, quantum chemical calculations were performed (B3LYP/def2-TZVP level of theory).[43] The prominent values of computationally considered ligands **L** are summarized in Table 6.4. There are satisfactory correlations between E_{HOMO}, $\Delta\nu$(CO) and

proton affinity (PA) values (Figures 6.4-6.6). In contrast, there is no correlation between the charges on the P and As atoms and the PA values and dissociation enthalpies $\Delta_{diss}H°_{298}$ and $pK_{diss(298)}$ values for the studied complexes.

Table 6.4: Proton affinities (PA), HOMO energies (E_{HOMO}), Mulliken charges on the donor atom q(P/As), the shift in the symmetric stretching CO vibration upon complex formation with {Ni(CO)$_3$} ($\Delta\nu$(CO) with respect to free CO), dissociation enthalpies ($\Delta_{diss}H°_{298}$), dissociation constants ($pK_{diss(298)}$) and the donor-acceptor bond distance (R(Ni-P/As)) for complexes of ligands L with {Ni(CO)$_3$} (B3LYP/def2-TZVP level of theory).

L	PA /kJ mol^{-1}	E_{HOMO} /eV	q(P/As)	$\Delta\nu$(CO) /cm^{-1}	$\Delta_{diss}H°_{298}$ /kJ mol^{-1}	$pK_{diss(298)}$	$R_{Ni-P/As}$ /Å
$Me_3CCH_2PH_2$	909	-0.251	-0.068	70.8	53.9	2.01	2.2769
$Me_3N{\cdot}BH_2PH_2$	1006	-0.209	-0.297	84.1	74.5	4.54	2.3179
$Me_3N{\cdot}BH_2PH^tBu$	1064	-0.195	-0.216	90.7	69.1	3.18	2.3500
$Me_3N{\cdot}BH_2PPh_2$	1086	-0.186	-0.104	89.8	74.6	3.47	2.3390
$SIDipp{\cdot}BH_2PH_2$	1083	-0.201	-0.217	89.0	78.4	6.33	2.3058
$IDipp{\cdot}BH_2PH_2$	1082	-0.197	-0.217	89.7	79.6	6.05	2.3057
$IDipp{\cdot}AlH_2PH_2$	1074	-0.199	-0.310	87.4	70.1	4.96	2.3252
$IDipp{\cdot}GaH_2PH_2$	1072	-0.198	-0.345	86.9	67.2	4.24	2.3191
$IDipp{\cdot}BH_2PH^tBu$	1129	-0.181	-0.156	99.8	66.5	1.50	2.3311
$IDipp{\cdot}BH_2PPh_2$	1137	-0.174	-0.061	98.3	50.9	-1.51	2.3320
$IDipp{\cdot}BH_2PMe_2$	1127	-0.169	-0.015	102.9	80.4	4.15	2.3260
$IDipp{\cdot}BH_2PCy_2$	1167	-0.169	-0.030	105.9	51.8	0.34	2.3591
$IDipp{\cdot}BH_2P(SiMe_3)_2$	1130	-0.179	-0.283	103.3	43.7	-2.53	2.4156
$Me_3CCH_2AsH_2$	863	-0.252	-0.005	70.9	43.1	-0.50	2.4168
$Me_3N{\cdot}BH_2AsH_2$	973	-0.206	-0.221	84.8	63.8	3.18	2.4412
$Me_3N{\cdot}BH_2AsH^tBu$	1027	-0.194	-0.107	90.9	64.9	3.03	2.4636
$Me_3N{\cdot}BH_2AsPh_2$	1041	-0.190	0.066	88.9	68.5	3.51	2.4488
$IDipp{\cdot}BH_2AsH_2$	1040	-0.195	-0.166	89.7	64.2	3.68	2.4341
$IDipp{\cdot}BH_2AsPh_2$	1088	-0.178	0.172	96.3	45.2	-1.96	2.4529

When considering $Me_3N{\cdot}BH_2PH_2$ and $Me_3N{\cdot}BH_2AsH_2$ with the isoelectronic carbon compounds neopentylphosphine and neopentylarsine ($Me_3CCH_2PH_2$ and $Me_3CCH_2AsH_2$), the higher HOMO energy of the {$Me_3N{\cdot}BH_2$} derivative leads to much larger PA (by 97 and 110 kJ mol^{-1}), which is also reflected in the Tolman electronic parameter (Table 6.4). The substitution of the H atom in the EH_2 group by ^{t}Bu and two hydrogen atoms by two phenyl substituents further increases the HOMO energy and the PA by 58-82 kJ mol^{-1} for E = P and 54-68 kJ mol^{-1} for E = As. Despite the PA of the $Me_3N{\cdot}BH_2EPh_2$ derivatives being larger than the PA of $Me_3N{\cdot}BH_2EH^tBu$, the Tolman electronic parameter is smaller for E = P and As, which may be attributed to the steric demand of tertiary phosphines and arsines. Replacing NMe_3 by an NHC generally increases the PA by 51-77 kJ mol^{-1}; the values of the PA for SIDipp and IDipp are very close. The substitution of the boron atom in $IDipp{\cdot}BH_2PH_2$ by aluminium and gallium leads to a decrease of the PA by 8-10 kJ mol^{-1}. Overall, the computed order of the PA of the studied phosphines is: $Me_3CCH_2PH_2 < Me_3N{\cdot}BH_2PH_2 < Me_3N{\cdot}BH_2PH^tBu < IDipp{\cdot}GaH_2PH_2 < IDipp{\cdot}AlH_2PH_2 < IDipp{\cdot}BH_2PH_2 < SIDipp{\cdot}BH_2PH_2 < Me_3N{\cdot}BH_2PPh_2 < IDipp{\cdot}BH_2PMe_2 < IDipp{\cdot}BH_2PH^tBu < IDipp{\cdot}BH_2P(SiMe_3)_2 < IDipp{\cdot}BH_2PPh_2 < IDipp{\cdot}BH_2PCy_2$, with the NHC-stabilized phosphanylboranes displaying the highest PA. The computed order of the PA of the studied arsines reveals an analogous trend in this regard: $Me_3CCH_2AsH_2 < Me_3N{\cdot}BH_2AsH_2 < Me_3N{\cdot}BH_2AsH^tBu < IDipp{\cdot}BH_2AsH_2 < Me_3N{\cdot}BH_2AsPh_2 < IDipp{\cdot}BH_2AsPh_2$.

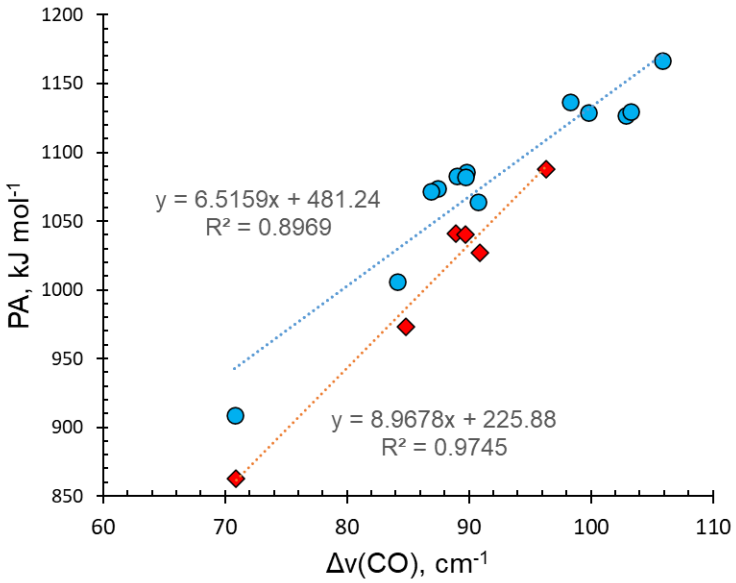

Figure 6.5: Correlation between the Tolman electronic parameter of the ligands **L** Δν(CO) [cm^{-1}] and the PA (in kJ mol^{-1}). Blue: P containing **L**; red: As containing **L**.

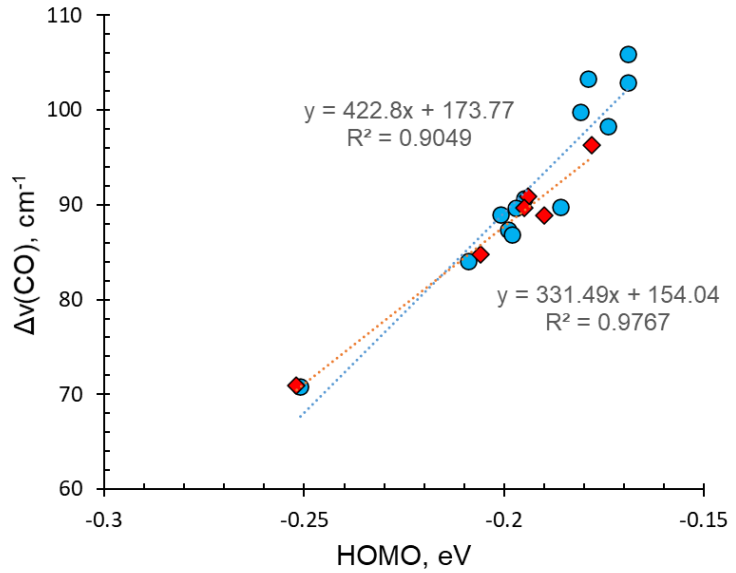

Figure 6.6: Correlation between the HOMO energy of the ligands **L** [eV] and the Tolman electronic parameter Δν(CO) [cm^{-1}]. Blue: P containing **L**; red: As containing **L**.

6.3 Conclusion

In summary, we expanded the range of NHC-stabilized pnictogenylboranes by synthesizing novel compounds of the type NHC·BH_2ER_2 (**1a**: NHC = SIDipp, ER_2 = PH_2; **1b**: NHC = IDipp, ER_2 = PPh_2; **1c**: NHC = IDipp, ER_2 = PMe_2; **1d**: NHC = IDipp, ER_2 = PH^tBu; **1e**: NHC = IDipp, ER_2 = PCy_2; **1f**: NHC = IDipp, ER_2 = $P(SiMe_3)_2$, **2**: NHC = IDipp, ER_2 = $AsPh_2$). The convenient general synthetic procedure allows for easy fine tuning of the donor properties of the compounds. Alongside the respective parent compounds, these compounds were reacted with $Ni(CO)_4$ to give the mono-substitution complexes [(NHC·BH_2ER_2)$Ni(CO)_3$] (**3a**: NHC = SIDipp, ER_2 = PH_2; **3b**: NHC = IDipp, ER_2 = PPh_2; **3c**: NHC = IDipp, ER_2 = PMe_2; **3d**: NHC = IDipp, ER_2 = PH^tBu; **3e**: NHC = IDipp, ER_2 = PCy_2; **3f**: NHC = IDipp,

ER_2 = $P(SiMe_3)_2$, **3g**: NHC = IDipp, ER_2 = PH_2; **4a**: NHC = IDipp, ER_2 = PH_2; **4b**: NHC = IDipp, ER_2 = $AsPh_2$). Similarly, the reaction of IDipp·GaH_2PH_2 with $Ni(CO)_4$ yielded the unprecedented complex [$Ni(CO)_3$(IDipp·GaH_2PH_2)] (**6**) which represents the first example of stable coordination of IDipp·GaH_2PH_2 to a metal center. Analogous reactions of $Me_3N{\cdot}BH_2PR_2$ yielded the corresponding compounds [($Me_3N{\cdot}BH_2PR_2$)$Ni(CO)_3$] (**5a**: R_2 = Ph_2; **5b**: R_2 = H^{t}Bu, **5c**: R_2 = H_2). Evaluation of the Tolman Electronic Parameters and percent buried volumes %V_{bur} showed that **3a**-**5c** can in general be considered as of similar donor strength as NHCs, albeit weaker than modern superbasic phosphines. **3a**-**5c** reveal similar trends compared to phosphines, with the alkyl substitution strongly increasing the donor strength. Exchanging boron for gallium increases the donor strength, while replacing phosphorus with arsenic decreases it accordingly. Analysis of the Tolman Cone Angles revealed the steric demand of the pnictogen atoms within the pnictogenyltrielanes to be comparatively low, with the parent compounds exhibiting a similar steric demand at the pnictogen atom as to PH_3. Quantum chemical calculations highlight the electronic nature and explain the observed trends in donor strength by examining the theoretical TEPs and comparison with the proton affinities.

6.4 References

[1] J. F. Hartwig, *Organotransition Metal Chemistry. From bonding to catalysis*, University Science Books, Sausalito, California, **2010**.

[2] a) S. L. Buchwald, C. Mauger, G. Mignani, U. Scholz, *Adv. Synth. Catal.* **2006**, *348*, 23–39; b) R. Dorel, C. P. Grugel, A. M. Haydl, *Angew. Chem. Int. Ed.* **2019**, *58*, 17118–17129; c) N. Miyaura, K. Yamada, A. Suzuki, *Tetrahedron Letters* **1979**, *20*, 3437–3440; d) J. P. Wolfe, S. Wagaw, S. L. Buchwald, *J. Am. Chem. Soc.* **1996**, *118*, 7215–7216; e) P. Ruiz-Castillo, S. L. Buchwald, *Chem. Rev.* **2016**, *116*, 12564–12649.

[3] a) G. Erre, S. Enthaler, K. Junge, S. Gladiali, M. Beller, *Coord. Chem. Rev.* **2008**, *252*, 471–491; b) T. Hayashi, *Acc. Chem. Res.* **2000**, *33*, 354–362; c) I. G. Rios, A. Rosas-Hernandez, E. Martin, *Molecules* **2011**, *16*, 970–1010; d) Y. Xiao, Z. Sun, H. Guo, O. Kwon, *Beilstein J. Org. Chem.* **2014**, *10*, 2089–2121.

[4] O. Kühl, *Phosphorus-31 NMR Spectroscopy*, Springer Berlin Heidelberg, Berlin, Heidelberg, **2009**.

[5] D. Setiawan, R. Kalescky, E. Kraka, D. Cremer, *Inorg. Chem.* **2016**, *55*, 2332–2344.

[6] a) C. A. Tolman, *Chem. Rev.* **1977**, *77*, 313–348; b) W. Strohmeier, F.-J. Müller, *Chem. Ber.* **1967**, *100*, 2812–2821.

[7] H. Clavier, S. P. Nolan, *Chem. Commun.* **2010**, *46*, 841–861.

[8] C. A. Tolman, *J. Am. Chem. Soc.* **1970**, *92*, 2953–2956.

[9] a) Y. Canac, C. Lepetit, M. Abdalilah, C. Duhayon, R. Chauvin, *J. Am. Chem. Soc.* **2008**, *130*, 8406–8413; b) A. R. Chianese, X. Li, M. C. Janzen, J. W. Faller, R. H. Crabtree, *Organometallics* **2003**, *22*, 1663–1667; c) A. Fürstner, M. Alcarazo, H. Krause, C. W. Lehmann, *J. Am. Chem. Soc.* **2007**, *129*, 12676–12677; d) R. A. Kelly III, H. Clavier, S. Giudice, N. M. Scott, E. D. Stevens, J. Bordner, I. Samardjiev, C. D. Hoff, L. Cavallo, S. P. Nolan, *Organometallics* **2008**, *27*, 202–210; e) M. Mayr, K. Wurst, K.-H. Ongania, M. R. Buchmeiser, *Chem. Eur. J.* **2004**, *10*, 1256–1266.

[10] a) G. A. Ardizzoia, S. Brenna, *Phys. Chem. Chem. Phys.* **2017**, *19*, 5971–5978; b) R. Kalescky, E. Kraka, D. Cremer, *Inorg. Chem.* **2014**, *53*, 478–495; c) T. R. Kégl, R. M. B. Carrilho, T. Kégl, *J. Organomet. Chem.* **2020**, *924*, 121462; d) T. R. Kégl, N. Pálinkás, L. Kollár, T. Kégl, *Molecules* **2018**, *23*, 3176; e) O. Kuhl, *Chem. Rev.* **2005**, *249*, 693–704; f) R. Tonner, G. Frenking, *Organometallics* **2009**, *28*, 3901–3905.

[11] A. J. Arduengo, R. L. Harlow, M. Kline, *J. Am. Chem. Soc.* **1991**, *113*, 361–363.

[12] V. Lavallo, Y. Canac, C. Präsang, B. Donnadieu, G. Bertrand, *Angew. Chem. Int. Ed.* **2005**, *44*, 5705–5709.

[13] a) F. Wang, L. Liu, W. Wang, S. Li, M. Shi, *Coord. Chem. Rev.* **2012**, *256*, 804–853; b) M. S. Sanford, M. Ulman, R. H. Grubbs, *J. Am. Chem. Soc.* **2001**, *123*, 749–750; c) A. Jayaraj, A. V. Raveedran, A. T. Latha, D. Priyadarshini, P. C. A. Swamy, *Coord. Chem. Rev.* **2023**, *478*, 214922; d) S. H. Hong, M. W. Day, R. H. Grubbs, *J. Am. Chem. Soc.* **2004**, *126*, 7414–7415; e) R. H. Grubbs, T. M. Trnka in *Ruthenium in Organic Synthesis* (Hrsg.: S.-I. Murahashi), Wiley-VCH Verlag GmbH & Co. KGaA, Weinheim, FRG, **2004**, S. 153–177; f) C. Chen, F.-S. Liu, M. Szostak, *Chem. Eur. J.* **2021**, *27*, 4478–4499.

[14] R. F. Weitkamp, B. Neumann, H.-G. Stammler, B. Hoge, *Chem. Eur. J.* **2021**, *27*, 10807–10825.

[15] a) J. Tang, J. Dopke, J. G. Verkade, *J. Am. Chem. Soc.* **1993**, *115*, 5015–5020; b) Z. Thammavongsy, I. M. Kha, J. W. Ziller, J. Y. Yang, *Dalton Trans.* **2016**, *45*, 9853–9859; c) J. Münchenberg, H. Thönnessen, P. G. Jones, R. Schmutzler, *Phosphorus Sulfur Silicon Relat. Elem.* **1997**, *123*, 57–74; d) M. Freytag, V. Plack, P. G. Jones, R. Schmutzler, *Z. Naturforsch. B* **2004**, *59*, 499–502.
[16] S. Ullrich, B. Kovačević, X. Xie, J. Sundermeyer, *Angew. Chem. Int. Ed.* **2019**, *58*, 10335–10339.
[17] T. Witteler, H. Darmandeh, P. Mehlmann, F. Dielmann, *Organometallics* **2018**, *37*, 3064–3072.
[18] M. A. Wünsche, P. Mehlmann, T. Witteler, F. Buß, P. Rathmann, F. Dielmann, *Angew. Chem. Int. Ed.* **2015**, *54*, 11857–11860.
[19] P. Mehlmann, C. Mück-Lichtenfeld, T. T. Y. Tan, F. Dielmann, *Chem. Eur. J.* **2017**, *23*, 5929–5933.
[20] P. Rotering, L. B. Wilm, J. A. Werra, F. Dielmann, *Chem. Eur. J.* **2020**, *26*, 406–411.
[21] J. Schulz, R. Clauss, A. Kazimir, S. Holzknecht, E. Hey-Hawkins, *Angew. Chem. Int. Ed.* **2023**, *62*, e202218648.
[22] a) H. Darmandeh, J. Löffler, N. V. Tzouras, B. Dereli, T. Scherpf, K.-S. Feichtner, S. Vanden Broeck, K. van Hecke, M. Saab, C. S. J. Cazin et al., *Angew. Chem. Int. Ed.* **2021**, *60*, 21014–21024; b) J. Handelmann, C. N. Babu, H. Steinert, C. Schwarz, T. Scherpf, A. Kroll, V. H. Gessner, *Chem. Sci.* **2021**, *12*, 4329–4337; c) X.-Q. Hu, D. Lichte, I. Rodstein, P. Weber, A.-K. Seitz, T. Scherpf, V. H. Gessner, L. J. Gooßen, *Org. Lett.* **2019**, *21*, 7558–7562; d) Z. Hu, X.-J. Wei, J. Handelmann, A.-K. Seitz, I. Rodstein, V. H. Gessner, L. J. Gooßen, *Angew. Chem. Int. Ed.* **2021**, *60*, 6778–6783; e) S. Lapointe, A. Sarbajna, V. H. Gessner, *Acc. Chem. Res.* **2022**, *55*, 770–782; f) J. Löffler, R. M. Gauld, K.-S. Feichtner, I. Rodstein, J.-A. Zur, J. Handelmann, C. Schwarz, V. H. Gessner, *Organometallics* **2021**, *40*, 2888–2900; g) L. T. Scharf, I. Rodstein, M. Schmidt, T. Scherpf, V. H. Gessner, *ACS Catal.* **2020**, *10*, 999–1009; h) T. Scherpf, C. Schwarz, L. T. Scharf, J.-A. Zur, A. Helbig, V. H. Gessner, *Angew. Chem. Int. Ed.* **2018**, *57*, 12859–12864; i) T. Scherpf, H. Steinert, A. Großjohann, K. Dilchert, J. Tappen, I. Rodstein, V. H. Gessner, *Angew. Chem.* **2020**, *132*, 20777–20784; j) J. Tappen, I. Rodstein, K. McGuire, A. Großjohann, J. Löffler, T. Scherpf, V. H. Gessner, *Chem. Eur. J.* **2020**, *26*, 4281–4288; k) P. Weber, T. Scherpf, I. Rodstein, D. Lichte, L. T. Scharf, L. J. Gooßen, V. H. Gessner, *Angew. Chem. Int. Ed.* **2019**, *58*, 3203–3207; l) O. Planas, V. Peciukenas, M. Leutzsch, N. Nöthling, D. A. Pantazis, J. Cornella, *J. Am. Chem. Soc.* **2022**, *144*, 14489–14504; m) T. Scherpf, H. Steinert, A. Großjohann, K. Dilchert, J. Tappen, I. Rodstein, V. H. Gessner, *Angew. Chem. Int. Ed.* **2020**, *59*, 20596–20603.
[23] R. Wei, S. Ju, L. L. Liu, *Angew. Chem. Int. Ed.* **2022**, *61*, e202205618.
[24] a) M. W. Johnson, S. L. Shevick, F. D. Toste, R. G. Bergman, *Chem. Sci.* **2013**, *4*, 1023–1027; b) B. Khalili Najafabadi, J. F. Corrigan, *Can. J. Chem.* **2016**, *94*, 593–598; c) L. Liu, D. A. Ruiz, F. Dahcheh, G. Bertrand, R. Suter, A. M. Tondreau, H. Grützmacher, *Chem. Sci.* **2016**, *7*, 2335–2341.
[25] J. A. Werra, K. Wurst, L. B. Wilm, P. Löwe, M. B. Röthel, F. Dielmann, *Organometallics* **2023**, *42*, 597–605.
[26] F. Buß, M. B. Röthel, J. A. Werra, P. Rotering, L. F. B. Wilm, C. G. Daniliuc, P. Löwe, F. Dielmann, *Chem. Eur. J.* **2022**, *28*, e202104021.
[27] F. Buß, M. Das, D. Janssen-Müller, A. Sietmann, A. Das, L. F. B. Wilm, M. Freitag, M. Seidl, F. Glorius, F. Dielmann, *Chem. Commun.* **2023**, *59*, 12019–12022.
[28] K.-C. Schwan, A. Y. Timoskin, M. Zabel, M. Scheer, *Chem. Eur. J.* **2006**, *12*, 4900–4908.
[29] U. Vogel, P. Hoemensch, K.-C. Schwan, A. Y. Timoshkin, M. Scheer, *Chem. Eur. J.* **2003**, *9*, 515–519.
[30] A. Adolf, M. Zabel, M. Scheer, *Eur. J. Inorg. Chem.* **2007**, *2007*, 2136–2143.
[31] C. Marquardt, T. Kahoun, J. Baumann, A. Y. Timoshkin, M. Scheer, *Z. Anorg. Allg. Chem.* **2017**, *643*, 1326–1330.
[32] C. Marquardt, A. Adolf, A. Stauber, M. Bodensteiner, A. V. Virovets, A. Y. Timoshkin, M. Scheer, *Chem. Eur. J.* **2013**, *19*, 11887–11891.
[33] O. Hegen, A. V. Virovets, A. Y. Timoshkin, M. Scheer, *Eur. J. Inorg. Chem.* **2018**, *24*, 16521-16525.
[34] F. Lehnfeld, M. Seidl, A. Y. Timoshkin, M. Scheer, *Eur. J. Inorg. Chem.* **2022**, *3*, e202100930.
[35] a) B. Li, S. Bauer, M. Seidl, A. Y. Timoshkin, M. Scheer, *Chem. Eur. J.* **2019**, *25*, 13714–13718; b) R. Szlosek, M. A. K. Weinhart, G. Balázs, M. Seidl, L. Zimmermann, M. Scheer, *Chem. Eur. J.* **2023**, *29*, e202300340; c) M. A. K. Weinhart, M. Seidl, A. Y. Timoshkin, M. Scheer, *Angew. Chem.* **2021**, *133*, 3850–3855; *Angew. Chem. Int. Ed.* **2021**, *60*, 3806–3811.
[36] M. A. K. Weinhart, A. S. Lisovenko, A. Y. Timoshkin, M. Scheer, *Angew. Chem. Int. Ed.* **2020**, *59*, 5541-5545; *Angew. Chem.* **2020**, *132*, 5586-5590.
[37] a) C. Thoms, C. Marquardt, A. Y. Timoshkin, M. Bodensteiner, M. Scheer, *Angew. Chem. Int. Ed.* **2013**, *52*, 5150–5154; b) C. Marquardt, T. Jurca, K.-C. Schwan, A. Stauber, A. V. Virovets, G. R. Whittell, I. Manners, M. Scheer, *Angew. Chem. Int. Ed.* **2015**, *54*, 13782–13786; c) M. Bodensteiner, U. Vogel, A. Y. Timoshkin, M. Scheer, *Angew. Chem. Int. Ed.* **2009**, *48*, 4629–4633; d) M. Bodensteiner, A. Y. Timoshkin, E. V. Peresypkina, U. Vogel, M. Scheer, *Chem. Eur. J.* **2013**, *19*, 957–963; e) C. Marquardt, O. Hegen, A. Vogel, A. Stauber, M. Bodensteiner, A. Y. Timoshkin, M. Scheer, *Chem. Eur. J.* **2018**, *24*, 360–363; f) A. M. Belousova, A. Y. Timoshkin, *J. Phys. Chem. A* **2023**, *127*, 7353–7363; g) J. Braese, F. Lehnfeld, V. T. Annibale, T. Oswald, R. Beckhaus, I. Manners, M. Scheer, *Chem. Eur. J.* **2023**, *29*, e202301741.
[38] a) F. Lehnfeld, M. Seidl, A. Y. Timoshkin, M. Scheer, *Eur. J. Inorg. Chem.* **2022**, *3*, e202100930; b) C. Marquardt, T. Kahoun, A. Stauber, G. Balázs, M. Bodensteiner, A. Y. Timoshkin, M. Scheer, *Angew. Chem. Int. Ed.* **2016**, *55*, 14828–14832; c) M. Elsayed Moussa, T. Kahoun, M. T. Ackermann, M. Seidl, M. Bodensteiner, A. Y. Timoshkin, M. Scheer,

Organometallics **2022**, *41*, 1572–1578; d) J. Braese, A. Schinabeck, M. Bodensteiner, H. Yersin, A. Y. Timoshkin, M. Scheer, *Chem. Eur. J.* **2018**; e) M. Elsayed Moussa, J. Braese, C. Marquardt, M. Seidl, M. Scheer, *Eur. J. Inorg. Chem.* **2020**, *26*, 2501–2505; f) M. Elsayed Moussa, C. Marquardt, O. Hegen, M. Seidl, M. Scheer, *New J. Chem.* **2021**, *45*, 14916–14919; g) K.-C. Schwan, A. Adolf, M. Bodensteiner, M. Zabel, M. Scheer, *Z. Anorg. Allg. Chem.* **2008**, *634*, 1383–1387; h) R. Szlosek, M. T. Ackermann, C. Marquardt, M. Seidl, A. Y. Timoshkin, M. Scheer, *Chem. Eur. J.* **2023**, *29*, e202202911; i) M. T. Ackermann, M. Seidl, F. Wen, M. J. Ferguson, A. Y. Timoshkin, E. Rivard, M. Scheer, *Chem. Eur. J.* **2022**, *28*, e20210370; j) M. T. Ackermann, M. Seidl, R. Grande, Y. Zhou, M. J. Ferguson, A. Y. Timoshkin, E. Rivard, M. Scheer, *Chem. Sci.* **2023**, *14*, 2313–2317; k) C. Marquardt, G. Balázs, J. Baumann, A. V. Virovets, M. Scheer, *Chem. Eur. J.* **2017**, *23*, 11423–11429; l) C. Marquardt, C. Thoms, A. Stauber, G. Balázs, M. Bodensteiner, M. Scheer, *Angew. Chem. Int. Ed.* **2014**, *53*, 3727–3730; m) C. Marquardt, O. Hegen, T. Kahoun, M. Scheer, *Chem. Eur. J.* **2017**, *23*, 4397–4404; n) F. Lehnfeld, M. Seidl, A. Timoshkin, M. Scheer, *Eur. J. Inorg. Chem.* **2023**, e202300338.

[39] a) R. Dorta, E. D. Stevens, N. M. Scott, C. Costabile, L. Cavallo, C. D. Hoff, S. P. Nolan, *J. Am. Chem. Soc.* **2005**, *127*, 2485–2495; b) U. S. D. Paul, C. Sieck, M. Haehnel, K. Hammond, T. B. Marder, U. Radius, *Chem. Eur. J.* **2016**, *22*, 11005–11014.

[40] T. E. Müller, D. M. P. Mingos, *Transition Met. Chem.* **1995**, *20*, 533–539.

[41] L. Falivene, R. Credendino, A. Poater, A. Petta, L. Serra, R. Oliva, V. Scarano, L. Cavallo, *Organometallics* **2016**, *35*, 2286–2293.

[42] L. Falivene, Z. Cao, A. Petta, L. Serra, A. Poater, R. Oliva, V. Scarano, L. Cavallo, *Nat. Chem.* **2019**, *11*, 872–879.

[43] a) A. D. Becke, *J. Chem. Phys.* **1993**, *98*, 5648–5652; b) C. Lee, W. Yang, R. G. Parr, *Phys. Rev. B* **1988**, *37*, 785–789; c) F. Weigend, R. Ahlrichs, *Phys. Chem. Chem. Phys.* **2005**, *7*, 3297-305.

[44] a) A. J. Arduengo, R. Krafczyk, R. Schmutzler, H. A. Craig, J. R. Goerlich, W. J. Marshall, M. Unverzagt, *Tetrahedron* **1999**, *55*, 14523–14534; b) R. Szlosek, M. Seidl, G. Balázs, M. Scheer, *Chem. Eur. J.* **2023**, *29*, e202301752; c) O. V. Dolomanov, L. J. Bourhis, R. J. Gildea, J. A. K. Howard, H. Puschmann, *J. Appl. Crystallogr.* **2009**, *42*, 339–341; d) G. M. Sheldrick, *Acta Cryst. C* **2015**, *71*, 3–8; e) G. M. Sheldrick, *Acta Cryst. A* **2015**, *71*, 3–8; f) Gaussian 09, Revision E.01, M. J. Frisch, G. W. Trucks, H. B. Schlegel, G. E. Scuseria, M. A. Robb, J. R. Cheeseman, G. Scalmani, V. Barone, G. A. Petersson, H. Nakatsuji, X. Li, M. Caricato, A. Marenich, J. Bloino, B. G. Janesko, R. Gomperts, B. Mennucci, H. P. Hratchian, J. V. Ortiz, A. F. Izmaylov, J. L. Sonnenberg, D. Williams-Young, F. Ding, F. Lipparini, F. Egidi, J. Goings, B. Peng, A. Petrone, T. Henderson, D. Ranasinghe, V. G. Zakrzewski, J. Gao, N. Rega, G. Zheng, W. Liang, M. Hada, M. Ehara, K. Toyota, R. Fukuda, J. Hasegawa, M. Ishida, T. Nakajima, Y. Honda, O. Kitao, H. Nakai, T. Vreven, K. Throssell, J. A. Montgomery, Jr., J. E. Peralta, F. Ogliaro, M. Bearpark, J. J. Heyd, E. Brothers, K. N. Kudin, V. N. Staroverov, T. Keith, R. Kobayashi, J. Normand, K. Raghavachari, A. Rendell, J. C. Burant, S. S. Iyengar, J. Tomasi, M. Cossi, J. M. Millam, M. Klene, C. Adamo, R. Cammi, J. W. Ochterski, R. L. Martin, K. Morokuma, O. Farkas, J. B. Foresman, and D. J. Fox, Gaussian, Inc., Wallingford CT, 2016; g) National InstituteRelease 22, May 2022, NIST Standard Reference Database 101, Internet: https://cccbdb.nist.gov/vibscalejust.asp of Standards and Technology, Computational Chemistry Comparison and Benchmark DataBase.

[45] Further attempts by the amalgamation of the Ni particles by treating the solutions with elemental Hg followed by filtration did not provide a complete separation of the Ni particles either.

6.5 Supporting Information

6.5.1 General Information

6.5.1.1 Working Techniques

All working steps were carried out under argon inert gas atmosphere using standard Schlenk and glovebox techniques. Glassware was dried in an oven at 150 °C and pre-conditioned in vacuum ($p < 10^{-3}$ mbar, 650 °C) shortly before use. The protective gas was cleansed from traces of H_2O and O_2 by passing it through a BASF R 3-11 ($CuO/MgSiO_3$) catalyst, concentrated H_2SO_4, Orange Gel and Sicapent® supported on pumice stone. Prior to use, solvents were purified using an MBraun SPS-800 solvent purification system, degassed by freeze-pump-thaw cycles, and stored over molecular sieves for at least 48 hours. C_6D_6 was dried over Na/K, distilled, degassed at room temperature, and stored over molecular sieves (4 Å). CD_2Cl_2 was dried over CaH_2, distilled, and degassed by freeze-pump-thaw. Elemental Analysis (CHN) was performed by the in-house facility. Mass spectra were recorded on a Jeol AccuTOF GCX mass spectrometer (FD-MS, LIFDI-MS) by the in-house facility.

SIDipp,[1] IDipp·BH_2PH_2,[2] IDipp·BH_2AsH_2,[3] IDipp·GaH_2PH_2[4] and $Me_3N{\cdot}BH_2PPh_2$[5], KBn,[6] $NaPH_2$,[7] $NaPPh_2$ (stock solution),[5] $KAsPh_2$[8] and $LiPMe_2$[9] into were prepared according to literature procedures. $BH_3{\cdot}SMe_2$ was purchased from ABCR and used as received. $Me_3N{\cdot}BH_2PH_2$[10] was provided by the Scheer group (Dr. Matthias T. Ackermann).

6.5.1.2 Spectroscopic Analysis

All NMR spectra were recorded on a BRUKER Avance 400 (frequencies: ^{1}H: 400.13 MHz, ^{31}P: 161.98 MHz, ^{19}F: 376.50 MHz, ^{11}B: 128.43, ^{13}C: 100.61) or Avance 300 (^{1}H: 300.13 MHz) spectrometers. Substances of reference are $Si(CH_3)_4$ (^{1}H), 85 % H_3PO_4 (^{31}P) and $BF_3{\cdot}Et_2O$ (^{11}B). Chemical shifts δ are presented in ppm referring to the external standards and coupling constants J are given in Hz without consideration of absolute signs. IR spectra were recorded in the solid state using a ThermoFisher Nicolet iS5 FT-IR spectrometer on a Diamond ATR crystal.

6.5.2 Experimental Details

6.5.2.1 Preparation of $KPCy_2$

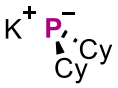

KBn (664 mg, 5.1 mmol) was suspended in diethylether and cooled to -80 °C. Then, a solution of Cy_2PH (1.113 g, 5.6 mmol, 1.1 eq.) in diethylether was added dropwise to the bright-red suspension and the mixture stirred using a glass stirring bar. After continuous stirring for 2.5 hours, a yellow-brown suspension was obtained. The solids were isolated by filtration over a P4 glass frit and washed three times with diethylether. After drying *in vacuo*, the $KPCy_2$ could be isolated as yellowish solids (830 mg, 63%).

$^{31}P\{^{1}H\}$ NMR (161.98 MHz, THF/C_6D_6-cap., 298 K): δ = -12.9 (s).

^{31}P NMR (161.98 MHz, THF/C_6D_6-cap., 298 K): δ = -12.9 (s).

6.5.2.2 Preparation of KP^{t}BuH

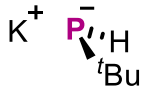

KBn (2.6 g, 20 mmol) was suspended in diethylether. Then, neat ^{t}BuPH$_2$ (2.6 mL, 20.4 mmol, 1 eq.) was added slowly *via* syringe to the bright-red suspension and the mixture stirred using a glass stirring bar. After continuous stirring for 2.5 hours, a beige suspension was obtained. After removing all volatiles *in vacuo*, the KP^{t}BuH could be isolated as brownish solids (2.013 g, 79%).

$^{31}P\{^{1}H\}$ NMR (161.98 MHz, THF/C_6D_6-cap., 298 K): δ = -55.9 (s).

^{31}P NMR (161.98 MHz, THF/C_6D_6-cap., 298 K): δ = -55.9 (d(decet), $^1J_{PH}$ = 145 Hz, $^3J_{PH}$ = 145 Hz).

6.5.2.3 Synthesis of SIDipp·BH$_2$I

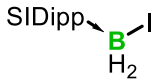

A Schlenk tube was charged with SIDipp·BH$_3$ (722 mg, 1.78 mmol) and the solids suspended in a small amount of benzene and placed in a water bath (r.t.). Then, solid I$_2$ (227 mg, 0.89 mmol, 0.5 eq.) was added under a stream of argon. The reaction mixture was stirred overnight at room temperature, resulting in a cloudy solution. Then, all volatiles were removed *in vacuo* yielding SIDipp·BH$_2$I as a yellowish powder (835 mg, 88%).

^{1}H NMR (400.30 MHz, CD_2Cl_2, 298 K): 0.7-1.7 (m, very broad and superimposed by multiple signals, B*H*$_2$), 1.20 (d, 12 H, 4 × ^{i}Pr-C*H*$_3$, $^3J_{HH}$ = 7.03 Hz), 1.33 (d, 12 H, 4 × ^{i}Pr-C*H*$_3$, $^3J_{HH}$ = 7.03 Hz), 3.03 (sep, 4 H, 4 × ^{i}Pr-C*H*, $^3J_{HH}$ = 7.03 Hz), 3.99 (s, 4 H, NC*H*$_2$C*H*$_2$N), 7.19 (d, 4 H, 4 × aryl-C$_{meta}$*H*, $^3J_{HH}$ = 7.75 Hz), 7.36 (t, 2 H, 2 × aryl-C$_{para}$H, $^3J_{HH}$ = 7.75 Hz).

$^{11}B\{^{1}H\}$ NMR (128.38 MHz, CD_2Cl_2, 298 K): -33.6 (s, very broad).

^{11}B NMR (128.38 MHz, CD_2Cl_2, 298 K): -33.6 (s, very broad).

LIFDI-MS (*m/z*): 391.31 [SIDipp-H]$^+$ (100%, complete decomposition upon ionization).

Elemental Analysis ($C_{27}H_{40}BIN_2$) **[%]:** calc. C 61.15, H 7.60, N 5.28; found C 60.72, H 7.65, N 5.09. The found values differ slightly due to the presence of trace amounts of inseparable SIDipp·BHI$_2$ (cf. NMR data).

6.5.2.4 Synthesis of SIDipp·BH$_2$PH$_2$ (1a)

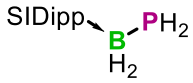

SIDipp·BH$_2$I (885 mg, 1.67 mmol) was dissolved in tetrahydrofuran and cooled to -80 °C. Then, solid NaPH$_2$ (140 mg, 2.5 mmol, 1.5 eq.) was added. The reaction mixture was stirred for 5 hours at room temperature. Then, all volatiles were removed in

vacuo and the product extracted with toluene and filtered over a P3 glass frit covered with Celite. The solvent was removed *in vacuo* from the filtrate, yielding SIDipp·BH_2PH_2 as yellowish solids (452 mg, 62%).

^{1}H NMR (400.30 MHz, C_6D_6, 298 K): 1.20 (d, 12 H, 4 × ^{i}Pr-CH_3, $^3J_{HH}$ = 6.98 Hz), 1.60/1.15 (m, broad and superimposed, 2 H, $^1J_{HP}$ = 181 Hz, PH_2), 1.49 (d, 12 H, 4 × ^{i}Pr-CH_3, $^3J_{HH}$ = 6.98 Hz), 3.27 (sep, 4 H, 4 × ^{i}Pr-CH, $^3J_{HH}$ = 6.98 Hz), 3.5 (s, 4 H, NCH_2CH_2N), 7.14 (d, 4 H, 4 × aryl-C$_{meta}H$, $^3J_{HH}$ = 7.82 Hz), 7.26 (t, 2 H, 2 × aryl-C$_{para}$H, $^3J_{HH}$ = 7.82 Hz). Signals of {BH_2} could not be reliably assigned due to superimposing signals and severe line broadening between 2.0 and 1.2 ppm.

^{31}P{^{1}H} NMR (161.98 MHz, C_6D_6, 298 K): δ = -213.2 (s, broad).

^{31}P NMR (161.98 MHz, C_6D_6, 298 K): δ = -213.2 (t, $^1J_{HP}$ = 181 Hz, broad).

^{11}B{^{1}H} NMR (128.38 MHz, C_6D_6, 298 K): -34.3 (s, broad).

^{11}B NMR (128.38 MHz, C_6D_6, 298 K): -34.3 (t, broad, $^1J_{BH}$ = 91 Hz).

LIFDI-MS (*m/z*): 436.31 $[M]^+$ (100%), 817.64 $[IDipp{\cdot}BH(PH_2)_2BH_2{\cdot}IDipp]^+$ (17%).

Elemental Analysis ($C_{29.97}H_{46.73}B_{1.11}N_{2.22}P_{1.22}$) **[%]:** calc. C 73.77; H 9.65, N 6.37 (SIDipp·BH_2PH_2 + 0.11 SIDipp·$BH(PH_2)_2$; cf. NMR data and section 6.5.2.3); found C 73.43, H 9.56, N 6.23.

6.5.2.5 Synthesis of IDipp·BH_2PPh_2 (1b)

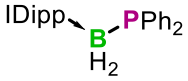

IDipp·BH_2I (500 mg, 0.95 mmol) was dissolved in diethylether and cooled to -80 °C. Then, a solution of $NaPPh_2$ (1.0 mL, 1.0 mmol, 1.0 M in THF, 1.1 eq.) was added *via* syringe, and the reaction mixture stirred overnight at room temperature, resulting in a yellow suspension. After removing all volatiles *in vacuo*, the product was extracted with toluene and filtered through a P3 glass frit covered with Celite. The solution was collected, and the solvent removed *in vacuo*, yielding an oily residue. Washing steps with *n*-hexane and further drying *in vacuo* yielded IDipp·BH_2PPh_2 as a colourless powder (401 mg, 72%).

^{1}H NMR (400.30 MHz, C_6D_6, 298 K): 1.02 (d, 12 H, 4 × ^{i}Pr-CH_3, $^3J_{HH}$ = 6.88 Hz), 1.29 (d, 12 H, 4 × ^{i}Pr-CH_3, $^3J_{HH}$ = 6.88 Hz), 2.28 (q, broad, 2 H, BH_2, $^1J_{BH}$ = 105 Hz), 2.81 (sep, 4 H, 4 × ^{i}Pr-CH, $^3J_{HH}$ = 6.88 Hz), 6.41 (s, 2 H, NCHCHN), 6.90-7.00 (m, 6 H, 2 × phenyl-C$_{meta/para}H$), 7.14 (d, 4 H, 4 × aryl-C$_{meta}H$, $^3J_{HH}$ = 7.65 Hz), 7.26 (t, 2 H, 2 × aryl-C$_{para}$H, $^3J_{HH}$ = 7.65 Hz), 7.28-7.31 (m, 4 H, 2 × phenyl-C$_{ortho}H$).

^{31}P{^{1}H} NMR (161.98 MHz, C_6D_6, 298 K): δ = -38.1 (m, broad).

^{31}P NMR (161.98 MHz, C_6D_6, 298 K): δ = -38.1 (m, broad).

^{11}B{^{1}H} NMR (128.38 MHz, C_6D_6, 298 K): -26.9 (s, broad).

^{11}B NMR (128.38 MHz, C_6D_6, 298 K): -26.9 (t, broad, $^1J_{BH}$ = 105 Hz).

LIFDI-MS (*m/z*): 586.36 $[M]^+$ (100%).

Elemental Analysis ($C_{39}H_{48}BPN_2$) **[%]:** calc. C 79.85; H 8.25, N 4.78; found C 79.72, H 8.56, N 4.59.

6.5.2.6 Synthesis of IDipp·BH_2PMe_2 (1c)

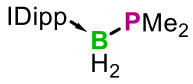

IDipp·BH_2I (212 mg, 0.4 mmol) was dissolved in diethylether and cooled to -80 °C. Then, solid $LiPMe_2$ (55 mg, 0.8 mmol, 2 eq.) was added, and the reaction mixture stirred overnight at room temperature, resulting in an off-white suspension. After removing all volatiles *in vacuo*, the product was extracted with *n*-hexane and filtered through a P3 glass frit covered with Celite. The solution was collected, and the solvent removed *in vacuo*, yielding IDipp·BH_2PMe_2 as a colourless powder (106 mg, 57 %).

^{1}H NMR (400.30 MHz, C_6D_6, 298 K): 0.89 (d, 6 H, P(CH_3)$_2$, $^2J_{HP}$ = 1.68 Hz) 1.04 (d, 12 H, 4 × ^{i}Pr-CH_3, $^3J_{HH}$ = 6.82 Hz), 1.46 (d, 12 H, 4 × ^{i}Pr-CH_3, $^3J_{HH}$ = 6.82 Hz), 1.67 (q, broad and superimposed, 2 H, BH_2, $^1J_{HB}$ = 89 Hz), 2.85 (sep, 4 H, 4 × ^{i}Pr-CH, $^3J_{HH}$ = 6.82 Hz), 6.34 (s, 2 H, NC*H*C*H*N), 7.11 (d, 4 H, 4 × aryl-C$_{meta}$*H*, $^3J_{HH}$ = 7.70 Hz), 7.21 (t, 2 H, 2 × aryl-C$_{para}$H, $^3J_{HH}$ = 7.70 Hz).

^{31}P{^{1}H} NMR (161.98 MHz, C_6D_6, 298 K): δ = -104.0 (q, broad, $^1J_{BP}$ = 46 Hz).

^{31}P NMR (161.98 MHz, C_6D_6, 298 K): δ = -104.0 (q, broad, $^1J_{BP}$ = 46 Hz).

^{11}B{^{1}H} NMR (128.38 MHz, C_6D_6, 298 K): -24.8 (d, broad, $^1J_{BP}$ = 46 Hz).

^{11}B NMR (128.38 MHz, C_6D_6, 298 K): -24.8 (td, broad, $^1J_{BP}$ = 46 Hz, $^1J_{BH}$ = 89 Hz).

LIFDI-MS (*m/z*): 389.29 [IDipp-H]$^+$ (17%), 863.64 [IDipp·$BH_2PMe_2BH_2$·IDipp]$^+$ (100%). Complete sample decomposition upon ionization.

Elemental Analysis ($C_{29}H_{44}BN_2P$) [%]: calcd. C 75.32, H 9.59, N 6.06; found C 75.12, H 9.93, N 6.09.

6.5.2.7 Synthesis of IDipp·BH_2PH^tBu (1d)

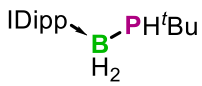

IDipp·BH_2I (500 mg, 0.95 mmol) was dissolved in diethylether and cooled to -80 °C. Then, solid K^{t}BuH (121 mg, 0.945 mmol, 1 eq.) was added, and the reaction mixture stirred overnight at room temperature, resulting in a greenish suspension. After removing all volatiles *in vacuo*, the product was extracted with *n*-hexane and filtered through a P3 glass frit covered with Celite. The yellowish solution was collected, and the solvent removed *in vacuo*, yielding IDipp · BH_2PH^tBu as a colourless powder (249 mg, 54%). Single crystals suitable for X-ray structure determination could be obtained by storing a solution of IDipp·BH_2PH^tBu in *n*-hexane at -30 °C.

^{1}H NMR (400.30 MHz, C_6D_6, 298 K): 1.02 (d, 6 H, 2 × ^{i}Pr-CH_3, $^3J_{HH}$ = 6.98 Hz), 1.06 (d, 6 H, 2 × ^{i}Pr-CH_3, $^3J_{HH}$ = 6.98 Hz), 1.20 (d, 9 H, C(CH_3)$_3$, $^3J_{HP}$ = 10.58 Hz) 1.44 (d, 6 H, 4 × ^{i}Pr-CH_3, $^3J_{HH}$ = 6.98 Hz), 1.50 (d, 6 H, 4 × ^{i}Pr-CH_3, $^3J_{HH}$ = 6.98 Hz), 1.97 (m, broad and superimposed, 2 H, BH_2), 2.00 (dt, superimposed, ~ 1 H, P*H*, $^1J_{HP}$ = 182.04 Hz, $^3J_{HH}$ = 9.05 Hz), 2.74 (sep, 2 H, 2 × ^{i}Pr-CH, $^3J_{HH}$ = 6.98 Hz), 2.88 (sep, 2 H, 2 × ^{i}Pr-CH, $^3J_{HH}$ = 6.98 Hz), 6.38 (s, 4 H, NCH_2CH_2N), 6.90-7.00 (m, 6 H, 2 × phenyl-C$_{meta/para}$*H*), 7.10 (d, 4 H, 4 × aryl-C$_{meta}$*H*, $^3J_{HH}$ = 7.85 Hz), 7.21 (t, 2 H, 2 × aryl-C$_{para}$H, $^3J_{HH}$ = 7.85 Hz).

^{31}P{^{1}H} NMR (161.98 MHz, C_6D_6, 298 K): δ = -67.3 (s, broad).

^{31}P NMR (161.98 MHz, C_6D_6, 298 K): δ = -67.3 (d, broad, $^{1}J_{PH}$ = 184 Hz).

^{11}B{^{1}H} NMR (128.38 MHz, C_6D_6, 298 K): -33.0 (s, broad).

^{11}B NMR (128.38 MHz, C_6D_6, 298 K): -33.0 (t, broad, $^{1}J_{BH}$ = 91 Hz).

LIFDI-MS (*m*/*z*): 389.29 $[IDipp\text{-}H]^+$ (100%, complete decomposition upon ionization).

Elemental Analysis ($C_{31}H_{48}BN_2P$) [%]: calcd. C 75.91, H 9.86, N 5.71; found. C 75.58, H 9.36, N 5.72.

6.5.2.8 Synthesis of IDipp·BH$_2$PCy$_2$ (1e)

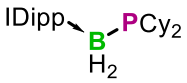

IDipp·BH_2I (300 mg, 0.57 mmol) was dissolved in diethylether and cooled to -80 °C. Then, solid $KPCy_2$ (201 mg, 0.85 mmol, 1.5 eq.) was added, and the reaction mixture stirred overnight at room temperature, resulting in an orange suspension. After removing all volatiles *in vacuo*, the product was extracted with *n*-hexane and filtered through a P3 glass frit covered with Celite. The solution was collected, and the solution concentrated *in vacuo*. By storing the saturated solution at -30 °C, single crystals suitable for X-ray structure determination could be obtained (204 mg, 60%).

^{1}H NMR (400.30 MHz, C_6D_6, 298 K): 1.05 (d, 12 H, 4 × ^{i}Pr-CH_3, $^{3}J_{HH}$ = 6.91 Hz), 1.19 (m , 11 H, Cy), 1.49 (d, 12 H, 4 × ^{i}Pr-CH_3, $^{3}J_{HH}$ = 6.91 Hz), 1.68 (m, 11 H, Cy), 2.83 (sep, 4 H, 4 × ^{i}Pr-CH, $^{3}J_{HH}$ = 6.91 Hz), 6.42 (s, 2 H, NC*H*C*H*N), 7.14 (d, 4 H, 4 × aryl-C$_{meta}H$, $^{3}J_{HH}$ = 7.78 Hz), 7.27 (t, 2 H, 2 × aryl-C$_{para}$H, $^{3}J_{HH}$ = 7.78 Hz). {BH_2} protons could not be unambiguously located due to signal overlap.

^{31}P{^{1}H} NMR (161.98 MHz, C_6D_6, 298 K): δ = -37.8 (m, broad).

^{31}P NMR (161.98 MHz, C_6D_6, 298 K): δ = -37.8 (m, broad).

^{11}B{^{1}H} NMR (128.38 MHz, C_6D_6, 298 K): -30.0 (s, broad).

^{11}B NMR (128.38 MHz, C_6D_6, 298 K): -30.0 (t, broad, $^{1}J_{BH}$ = 101 Hz).

LIFDI-MS (*m*/*z*): 630.45 $[(Cy_2P)BH_2]_3^+$ (100%).

6.5.2.9 Synthesis of IDipp·BH$_2$P(SiMe$_3$)$_2$ (1f)

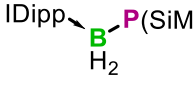

IDipp·BH_2I (500 mg, 0.95 mmol) was dissolved in diethylether and cooled to -80 °C. Then, solid $KP(SiMe_3)_2$ (205 mg, 1.0 mmol, 1.1 eq.) was added, and the reaction mixture stirred overnight at room temperature, resulting in a white suspension. After removing all volatiles *in vacuo*, the product was extracted with *n*-hexane and filtered through a P3 glass frit covered with Celite. The solution was collected, and the solvent removed *in vacuo*, IDipp·$BH_2P(SiMe_3)_2$ as a colourless powder (80 mg, 15%).

^{1}H NMR (400.30 MHz, C_6D_6, 298 K): 0.17 (d, 18 H, 2 × Si(CH_3)$_3$, $^{2}J_{HP}$ = 3.54 Hz), 1.02 (d, 12 H, 4 × ^{i}Pr-CH_3, $^{3}J_{HH}$ = 6.56 Hz), 1.49 (d, 12 H, 4 × ^{i}Pr-CH_3, $^{3}J_{HH}$ = 6.56 Hz), 1.52 (q, superimposed, broad, 2 H, BH_2,

$^{1}J_{BH} \approx$ 100 Hz), 2.80 (sep, 4 H, 4 × ^{i}Pr-C*H*, $^{3}J_{HH}$ = 6.56 Hz), 6.34 (s, 2 H, NC*H*C*H*N), 7.14 (d, 4 H, 4 × aryl-C$_{meta}$*H*, $^{3}J_{HH}$ = 8.13 Hz), 7.26 (t, 2 H, 2 × aryl-C$_{para}$H, $^{3}J_{HH}$ = 8.13 Hz).

^{31}P{^{1}H} NMR (161.98 MHz, C_6D_6, 298 K): δ = -265.0 (s, broad).

^{31}P NMR (161.98 MHz, C_6D_6, 298 K): δ = -265.0 (s, broad).

^{11}B{^{1}H} NMR (128.38 MHz, C_6D_6, 298 K): -33.3 (s, broad).

^{11}B NMR (128.38 MHz, C_6D_6, 298 K): -33.3 (t, broad, $^{1}J_{BH}$ = 98 Hz).

LIFDI-MS (*m*/*z*): 389.29 [IDipp-H]$^{+}$ (58%). 835.63 [IDipp·$BH_2PH_2BH_2$·IDipp]$^{+}$ (100%). Complete sample decomposition upon ionization.

Elemental Analysis ($C_{33}H_{56}BN_2PSi_2$) [%]: due to the presence of trace amounts $HP(SiMe_3)_2$ and inseparable IDipp·BH_2PH_2, satisfactory elemental analysis was not possible.

6.5.2.10 Synthesis of IDipp·BH_2AsPh_2 (2)

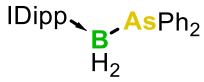

IDipp·BH_2I (212 mg, 0.4 mmol) was dissolved in diethylether and cooled to -80 °C. Then, solid $KAsPh_2$ (161 mg, 0.6 mmol, 1.5 eq.) was added, and the reaction mixture stirred overnight at room temperature, resulting in a yellow suspension. After removing all volatiles *in vacuo*, the product was extracted with toluene and filtered through a P3 glass frit covered with Celite. The colourless solution was collected, and the solvent removed *in vacuo*. The resulting oily residue was washed twice with *n*-hexane and the final product dried *in vacuo*, yielding IDipp·BH_2AsPh_2 as a colourless powder (94 mg, 37%). Single crystals of IDipp·BH_2AsPh_2 suitable for X-ray structure determination could be obtained by storing IDipp·BH_2AsPh_2 in a mixture of toluene/*n*-hexane at -30 °C.

^{1}H NMR (400.30 MHz, C_6D_6, 298 K): 1.09 (d, 12 H, 4 × ^{i}Pr-CH_3, $^{3}J_{HH}$ = 6.95 Hz), 1.29 (d, 12 H, 4 × ^{i}Pr-CH_3, $^{3}J_{HH}$ = 6.95 Hz), 2.28 (q, broad, 2 H, BH_2, $^{1}J_{BH} \approx$ 100 Hz), 2.89 (sep, 4 H, 4 × ^{i}Pr-C*H*, $^{3}J_{HH}$ = 6.95 Hz), 6.50 (s, 2 H, NC*H*C*H*N), 6.98-7.08 (m, 6 H, 2 × phenyl-C$_{meta/para}$*H*), 7.14 (d, 4 H, 4 × aryl-C$_{meta}$*H*, $^{3}J_{HH}$ = 7.68 Hz), 7.29 (t, 2 H, 2 × aryl-C$_{para}$H, $^{3}J_{HH}$ = 7.68 Hz), 7.45-7.49 (m, 4 H, 2 × phenyl-C$_{ortho}$*H*).

^{11}B{^{1}H} NMR (128.38 MHz, C_6D_6, 298 K): -26.7 (s, broad).

^{11}B NMR (128.38 MHz, C_6D_6, 298 K): -26.7 (t, broad, $^{1}J_{BH}$ = 99 Hz).

LIFDI-MS (*m*/*z*): 630.31 [M]$^{+}$ (100%).

Elemental Analysis ($C_{39}H_{48}BN_2As$) [%]: calcd. C 74.29, H 7.67, N 4.44; found C 74.41, H 7.72, N 4.31.

6.5.2.11 General Procedure for the Synthesis of [(NHC·BH_2ER_2)Ni(CO)$_3$]

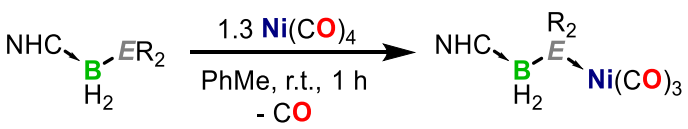

The corresponding pnictogenylborane NHC·BH_2ER_2 was dissolved in a small amount of toluene. Then, $Ni(CO)_4$ (1.3 eq., 0.81 M stock solution in toluene) was added *via* syringe and the mixture stirred for one hour at room temperature. After removing all volatiles *in vacuo*, the residue was dissolved in diethylether and filtered through a cannula wrapped with a glass fibre filter. Subsequently, the solvent was removed *in vacuo* to yield the corresponding complexes as brownish solids. *Note: the work-up of the reaction mixture results in Ni nanoparticles, which could not be completely separated by multiple filtration steps or amalgamation (treatment of the solutions with elemental Hg and subsequent filtration) which did not allow for satisfying elemental analyses of the final products.*

6.5.2.12 [(SIDipp·BH_2PH_2)$Ni(CO)_3$] (3a)

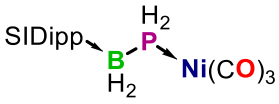

The complex was prepared according to the given general procedure. Reagents: SIDipp·BH_2PH_2 (65 mg, 0.18 mmol); $Ni(CO)_4$ (0.22 mL, 0.81 M stock solution in toluene, 0.18 mmol, 1 eq.). Yield: 24 mg, 28%, brownish solids.

^{1}H NMR (400.30 MHz, C_6D_6, 298 K): 1.07 (d, 12 H, 4 × ^{i}Pr-C*H*$_3$, $^3J_{HH}$ = 6.84 Hz), 1.36 (d, 12 H, 4 × ^{i}Pr-C*H*$_3$, $^3J_{HH}$ = 6.84 Hz), 1.40 (q, very broad, B*H*$_2$, superimposed by multiple signals), 2.00/2.68 (dm, 2 H, P*H*$_2$, $^2J_{HP}$ = 275 Hz) 3.01 (sep, 4 H, 4 × ^{i}Pr-C*H*, $^3J_{HH}$ = 6.84 Hz), 3.33 (s, 4 H, NC*H*$_2$C*H*$_2$N), 7.00 (d, 4 H, 4 × aryl-C$_{meta}$*H*, $^3J_{HH}$ = 7.78 Hz), 7.13 (dd, 2 H, superimposed with solvent signal, 2 × aryl-C$_{para}$H, $^3J_{HH}$ = 7.78 Hz).

^{31}P{^{1}H} NMR (161.98 MHz, C_6D_6, 298 K): -164.5 (q, broad, $^1J_{PB}$ = 55 Hz).

^{31}P NMR (161.98 MHz, C_6D_6, 298 K): -164.5 (tq, broad, $^1J_{HP}$ = 273 Hz, $^1J_{PB}$ = 55 Hz).

^{11}B{^{1}H} NMR (128.38 MHz, C_6D_6, 298 K): -32.2 (d, $^1J_{PB}$ = 55 Hz).

^{11}B NMR (128.38 MHz, C_6D_6, 298 K): -32.2 (td, broad, $^1J_{PB}$ = 55 Hz, $^1J_{HB}$ ≈ 114 Hz).

IR (ATR) *ν* (cm^{-1}): 2966, 2928, 2868, 2414 (B-H), 2390 (B-H), 2348 (P-H), 2330 (P-H), 2052 (C-O), 1960 (C-O), 1590.

6.5.2.13 [(IDipp·BH_2PPh_2)$Ni(CO)_3$] (3b)

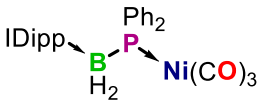

The complex was prepared according to the given general procedure. Reagents: IDipp·BH_2PPh_2 (88 mg, 0.15 mmol); $Ni(CO)_4$ (0.22 mL, 0.81 M stock solution in toluene, 0.18 mmol, 1.3 eq.). Yield: 43 mg, 39%, brownish solids.

^{1}H NMR (400.30 MHz, C_6D_6, 298 K): 0.94 (d, 12 H, 4 × ^{i}Pr-C*H*$_3$, $^3J_{HH}$ = 6.70 Hz), 1.34 (d, 12 H, 4 × ^{i}Pr-C*H*$_3$, $^3J_{HH}$ = 6.70 Hz), 2.54 (q, broad and superimposed with sep signal, ~ 2 H, B*H*$_2$), 2.77 (sep, superimposed with BH_2 signal, 4 H, 4 × ^{i}Pr-C*H*, $^3J_{HH}$ = 6.70 Hz), 6.35 (s, 2 H, NC*H*C*H*N), 6.84 (m, superimposed, phenyl-C$_{meta}$-*H*), 6.93 (d, 6 H, superimposed, 4 × aryl-C$_{meta}$*H* + 2 × phenyl-C$_{para}$-*H*, $^3J_{HH}$ = 7.70 Hz), 7.06 (t, 2 × aryl-C$_{para}$H, $^3J_{HH}$ = 7.70 Hz), 7.51 (t, 4 H, phenyl-C$_{ortho}$*H*, $^3J_{HH}$ = 8.19 Hz).

^{31}P{^{1}H} NMR (161.98 MHz, C_6D_6, 298 K): -11.1 (q, broad, $^1J_{PB}$ ≈ 84 Hz).

^{31}P NMR (161.98 MHz, C_6D_6, 298 K): -11.1 (m, broad).

^{11}B{^{1}H} NMR (128.38 MHz, C_6D_6, 298 K): -26.8 (m, broad).

^{11}B NMR (128.38 MHz, C_6D_6, 298 K): -26.8 (m, broad).

IR (ATR) *ν* (cm^{-1}): 2968, 2927, 2869, 2412 (B-H), 2382 (B-H), 2043 (C-O), 1944 (C-O), 1583, 1561.

LIFDI-MS (*m/z*): 586.4 (100%, [IDipp·BH_2PPh_2]$^+$, complete decomposition upon ionization).

6.5.2.14 [(IDipp·BH_2PMe_2)Ni(CO)$_3$] (3c)

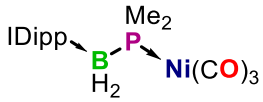

The complex was prepared according to the given general procedure. Reagents: IDipp·BH_2PMe_2 (51 mg, 0.11 mmol); $Ni(CO)_4$ (0.16 mL, 0.81 M stock solution in toluene, 0.13 mmol, 1.3 eq.). Yield: 19 mg, 29%, brownish solids.

^{1}H NMR (400.30 MHz, C_6D_6, 298 K): 0.80 (d, 6 H, P(CH_3)$_2$, $^{2}J_{HP}$ = 6.89 Hz) 1.01 (d, 12 H, 4 × ^{i}Pr-CH_3, $^{3}J_{HH}$ = 6.65 Hz), 1.43 (d, 12 H, 4 × ^{i}Pr-CH_3, $^{3}J_{HH}$ = 6.65 Hz), 1.56 (q, broad and superimposed, 2 H, BH_2, $^{1}J_{HB} \approx$ 100 Hz), 2.79 (sep, 4 H, 4 × ^{i}Pr-CH, $^{3}J_{HH}$ = 6.65 Hz), 6.36 (s, 2 H, NCHCHN), 7.07 (d, 4 H, 4 × aryl-C$_{meta}H$, $^{3}J_{HH}$ = 7.68 Hz), 7.17 (t, superimposed by solvent signal, 2 H, 2 × aryl-C$_{para}$H, $^{3}J_{HH}$ = 7.68 Hz).

^{31}P{^{1}H} NMR (161.98 MHz, C_6D_6, 298 K): -68.9 (m, broad).

^{31}P NMR (161.98 MHz, C_6D_6, 298 K): -68.9 (m, broad).

^{11}B{^{1}H} NMR (128.38 MHz, C_6D_6, 298 K): -24.8 (d, broad, $^{1}J_{PB}$ = 62 Hz).

^{11}B NMR (128.38 MHz, C_6D_6, 298 K): -24.8 (dt (superimposed), broad, $^{1}J_{HB}$ = 90 Hz).

IR (ATR) *ν* (cm^{-1}): 2960, 2921, 2852, 2395 (B-H), 2290 (B-H), 2040 (C-O), 1951 (C-O), 1591, 1534.

6.5.2.15 [(IDipp·BH_2PH^tBu)Ni(CO)$_3$] (3d)

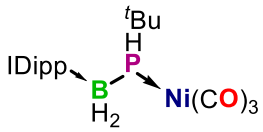

The complex was prepared according to the given general procedure. Reagents: IDipp·BH_2PH^tBu (74 mg, 0.15 mmol); $Ni(CO)_4$ (0.22 mL, 0.81 M stock solution in toluene, 0.18 mmol, 1.3 eq.). Yield: 25 mg, 26%, brownish solids.

^{1}H NMR (400.30 MHz, C_6D_6, 298 K): 0.97 (d, 6 H, superimposed, 2 × ^{i}Pr-CH_3, $^{3}J_{HH}$ = 6.61 Hz), 0.98 (d, 6 H, superimposed, 2 × ^{i}Pr-CH_3, $^{3}J_{HH}$ = 6.61 Hz), 1.05 (d, ~ 9 H, superimposed, C(CH_3)$_3$, $^{3}J_{HP}$ = 13.16 Hz), 1.40 (d, ~ 6 H, superimposed, 2 × ^{i}Pr-CH_3, $^{3}J_{HH}$ = 6.61 Hz), 1.48 (d, ~ 6 H, superimposed, 2 × ^{i}Pr-CH_3, $^{3}J_{HH}$ = 6.61 Hz), 1.85 (m, ~ 2 H, very broad and superimposed, BH_2), 2.58 (sep, 2 H, 2 × ^{i}Pr-CH, $^{3}J_{HH}$ = 6.61 Hz), 2.90 (sep, 2 H, 2 × ^{i}Pr-CH, $^{3}J_{HH}$ = 6.61 Hz), 6.36 (s, 2 H, NCHCHN), 7.05 (d, 2 H, 2 × aryl-C$_{meta}H$, $^{3}J_{HH}$ = 8.26 Hz), 7.10 (d, 2 H, 2 × aryl-C$_{meta}H$, $^{3}J_{HH}$ = 8.26 Hz),7.18 (t, 2 H, 2 × aryl-C$_{para}$H, $^{3}J_{HH}$ = 8.26 Hz). {PH_2} protons could not be unambiguously located due to signal broadening and superposition.

^{31}P{^{1}H} NMR (161.98 MHz, C_6D_6, 298 K): -38.7 (q, broad, $^{1}J_{PB}$ = 70 Hz).

^{31}P NMR (161.98 MHz, C_6D_6, 298 K): -38.7 (dm, broad, $^{1}J_{PH}$ = 273 Hz).

^{11}B{^{1}H} NMR (128.38 MHz, C_6D_6, 298 K): -30.4 (d, broad, $^{1}J_{PB} \approx$ 70 Hz).

^{11}B NMR (128.38 MHz, C_6D_6, 298 K): -30.4 (dt, superimposing, broad, $^{1}J_{HB} \approx$ 95 Hz).

IR (ATR) ν (cm^{-1}): 2965, 2927, 2866, 2390 (B-H), 2366 (B-H), 2043 (C-O), 1946 (C-O), 1590, 1562, 1459.

6.5.2.16 [(IDipp·BH$_2$PCy$_2$)Ni(CO)$_3$] (3e)

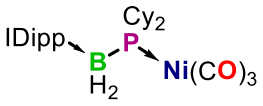

The complex was prepared according to the given general procedure. Reagents: IDipp·BH$_2$PCy$_2$ (90 mg, 0.15 mmol); Ni(CO)$_4$ (0.22 mL, 0.81 M stock solution in toluene, 0.18 mmol, 1.3 eq.). Yield: 61 mg, 55%, brownish solids.

^{1}H NMR (400.30 MHz, C_6D_6, 298 K): 1.05 (d, 12 H, 4 × ^{i}Pr-CH_3, $^{3}J_{HH}$ = 6.93 Hz), 1.19 (m, 11 H, P(C$_6H_{11}$)), 1.49 (d, 12 H, 4 × ^{i}Pr-CH_3, $^{3}J_{HH}$ = 6.93 Hz), 1.68 (m, 11 H, superimposed, P(C$_6H_{11}$)), 2.83 (sep, 4 H, 4 × ^{i}Pr-CH, $^{3}J_{HH}$ = 6.93 Hz), 6.43 (s, 2 H, NCHCHN), 7.14 (d, 4 H, 4 × aryl-C$_{meta}H$, $^{3}J_{HH}$ = 7.72 Hz), 7.69 (t, 2 × aryl-C$_{para}$H, $^{3}J_{HH}$ = 7.72 Hz). {BH$_2$} cannot be unambiguously assigned due to broadened and overlapping signals.

^{31}P{^{1}H} NMR (161.98 MHz, C_6D_6, 298 K): -37.8 (m, broad).

^{31}P NMR (161.98 MHz, C_6D_6, 298 K): -37.8 (m, broad).

^{11}B{^{1}H} NMR (128.38 MHz, C_6D_6, 298 K): -30.0 (s, very broad,).

^{11}B NMR (128.38 MHz, C_6D_6, 298 K): -30.0 (t, broad, $^{1}J_{HB} \approx$ 103 Hz).

IR (ATR) ν (cm^{-1}): 2963, 2914, 2847, 2433 (B-H), 2400 (B-H), 2037 (C-O), 1948 (C-O), 1592, 1563.

6.5.2.17 [(IDipp·BH$_2$P(SiMe$_3$)$_2$)Ni(CO)$_3$] (3f)

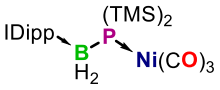

The complex was prepared according to the given general procedure. Reagents: IDipp·BH$_2$P(SiMe$_3$)$_2$ (77 mg, 0.13 mmol); Ni(CO)$_4$ (0.20 mL, 0.81 M stock solution in toluene, 0.16 mmol, 1.3 eq.). Yield: 23 mg, 25%, brownish solids.

^{1}H NMR (400.30 MHz, C_6D_6, 298 K): 0.08 (d, 18 H, 2 × Si(CH_3)$_3$, $^{3}J_{HP}$ = 4.27 Hz), 0.96 (d, partially superimposed, ~ 12 H, 4 × ^{i}Pr-CH_3, $^{3}J_{HH}$ = 6.83 Hz), 1.49 (d, ~ 12 H, 4 × ^{i}Pr-CH_3, $^{3}J_{HH}$ = 6.83 Hz), 1.84 (m, broad and superimposed, 2 H, BH_2), 2.93 (sep, superimposed, ~ 4 H, 4 × ^{i}Pr-CH, $^{3}J_{HH}$ = 6.83 Hz), 6.38 (s, 2 H, NCHCHN), 7.12 (d, superimposed, ~ 4 H, 4 × aryl-C$_{meta}H$, $^{3}J_{HH}$ = 7.72 Hz), 7.22 (t, superimposed, ~ 2 H, 2 × aryl-C$_{para}$H, $^{3}J_{HH}$ = 7.72 Hz).

^{31}P{^{1}H} NMR (161.98 MHz, C_6D_6, 298 K): -241.8 (m, broad).

^{31}P NMR (161.98 MHz, C_6D_6, 298 K): -241.8 (m, broad).

^{11}B{^{1}H} NMR (128.38 MHz, C_6D_6, 298 K): -33.2 (m, very broad).

^{11}B NMR (128.38 MHz, C_6D_6, 298 K): -33.2 (m, very broad).

IR (ATR) ν (cm^{-1}): 2964, 2933, 2869, 2417 (B-H), 2386 (B-H), 2041 (C-O), 1952 (C-O), 1592, 1567.

6.5.2.18 [(IDipp·BH_2PH_2)Ni(CO)$_3$] (3g)

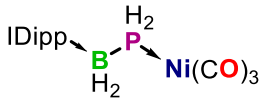

The complex was prepared according to the given general procedure. Reagents: IDipp·BH_2PH_2 (65 mg, 0.15 mmol); Ni(CO)$_4$ (0.22 mL, 0.81 M stock solution in toluene, 0.18 mmol, 1.3 eq.). Yield: 14 mg, 24%, off-white powder.

^{1}H NMR (400.30 MHz, C_6D_6, 298 K): 0.97 (d, 12 H, 4 × ^{i}Pr-C*H*$_3$, $^3J_{HH}$ = 7.09 Hz), 1.29 (d, 12 H, 4 × ^{i}Pr-C*H*$_3$, $^3J_{HH}$ = 7.09 Hz), 1.84 (q, broad and superimposed with PH_2 signal, B*H*$_2$, $^1J_{HB} \approx$ 100 Hz), 2.57 (sep, 4 H, 4 × ^{i}Pr-C*H*, $^3J_{HH}$ = 7.09 Hz), 2.33 (dm, 2 H, $^1J_{PH}$ = 272.9 Hz, P*H*$_2$), 6.30 (d, 4 H, 4 × aryl-C$_{meta}$*H*, $^3J_{HH}$ = 7.90 Hz), 7.03 (s, 2 H, NC*H*C*H*N), 7.18 (t, superimposed with solvent signal, 2 × aryl-C$_{para}$H, $^3J_{HH}$ = 7.96 Hz).

^{31}P{^{1}H} NMR (161.98 MHz, C_6D_6, 298 K): -163.5 (q, broad, $^1J_{PB}$ = 60 Hz).

^{31}P NMR (161.98 MHz, C_6D_6, 298 K): -163.5 (tq, broad, $^1J_{HP}$ = 273 Hz, $^1J_{PB}$ = 60 Hz).

^{11}B{^{1}H} NMR (128.38 MHz, C_6D_6, 298 K): -32.2 (d, $^1J_{PB}$ = 60 Hz).

^{11}B NMR (128.38 MHz, C_6D_6, 298 K): -32.2 (m, broad).

IR (ATR) ν (cm^{-1}): 2961, 2926, 2867, 2413 (B-H), 2362 (B-H), 2337 (P-H), 2311 (P-H), 2050 (C-O), 1954 (C-O).

6.5.2.19 [(IDipp·BH_2AsPh_2)Ni(CO)$_3$] (4a)

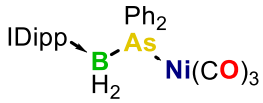

The complex was prepared according to the given general procedure. Reagents: IDipp·BH_2AsPh_2 (76 mg, 0.12 mmol); Ni(CO)$_4$ (0.18 mL, 0.81 M stock solution in toluene, 0.15 mmol, 1.3 eq.). Yield: 22 mg, 24%, brownish solids.

^{1}H NMR (400.30 MHz, C_6D_6, 298 K): 0.97 (d, 12 H, 4 × ^{i}Pr-C*H*$_3$, $^3J_{HH}$ = 6.67 Hz), 1.36 (d, 12 H, 4 × ^{i}Pr-C*H*$_3$, $^3J_{HH}$ = 6.67 Hz), 2.50 (q, very broad and superimposed, 2 H, B*H*$_2$, $^1J_{HB} \approx$ 110 Hz), 2.79 (sep, superimposed, 4 H, 4 × ^{i}Pr-C*H*, $^3J_{HH}$ = 6.67 Hz), 6.33 (s, 2 H, NC*H*C*H*N), 6.86 (m, superimposed 4 H, phenyl-C$_{meta}$H), 6.94 (d, 4 H, 4 × aryl-C$_{meta}$*H*, $^3J_{HH}$ = 7.24 Hz), 7.06 (2 × superimposing t, 4 H, 2 × aryl-C$_{para}$H + 2 × phenyl-C$_{para}$H, $^3J_{HH}$ = 7.72 Hz), 7.47 (d, 4 × phenyl-C$_{ortho}$*H*, 4 H, $^3J_{HH}$ = 5.67 Hz).

^{11}B{^{1}H} NMR (128.38 MHz, C_6D_6, 298 K): -26.9 (s, broad).

^{11}B NMR (128.38 MHz, C_6D_6, 298 K): -26.9 (t, broad, $^1J_{HB}$ = 103 Hz).

IR (ATR) ν (cm^{-1}): 2964, 2926, 2869, 2420 (B-H), 2385 (B-H), 2046 (C-O), 1951 (C-O).

LIFDI-MS (*m*/*z*): 630.3 (100%, [IDipp·BH_2AsPh_2]$^+$, complete decomposition upon ionization).

6.5.2.20 [(IDipp·BH_2AsH_2)$Ni(CO)_3$] (4b)

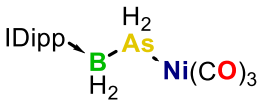

The complex was prepared according to the given general procedure. Reagents: IDipp·BH_2AsH_2 (72 mg, 0.15 mmol), $Ni(CO)_4$ (0.22 mL, 0.81 M stock solution in toluene, 0.18 mmol, 1.3 eq.). Yield: 46 mg, 49%, brownish solids.

^{1}H NMR (400.30 MHz, C_6D_6, 298 K): 0.96 (d, 12 H, 4 × ^{i}Pr-CH_3, $^3J_{HH}$ = 6.00 Hz), 1.30 (d, 12 H, 4 × ^{i}Pr-CH_3, $^3J_{HH}$ = 6.00 Hz), 2.16-1.12 (q, very broad, BH_2, superimposed by multiple signals), 2.58 (sep, 4 H, 4 × ^{i}Pr-CH, $^3J_{HH}$ = 6.00 Hz), 6.31 (s, 2 H, NCHCHN), 7.03 (d, 4 H, 4 × aryl-C$_{meta}H$, $^3J_{HH}$ = 7.18 Hz), 7.18 (t, partially superimposed by solvent signal, 2 H, 2 × aryl-C$_{para}$H, $^3J_{HH}$ = 7.18 Hz). AsH_2 protons could not be unambiguously located due to the appearance of strongly overlapping and broadened signals.

^{11}B{^{1}H} NMR (128.38 MHz, C_6D_6, 298 K): -32.0 (s, broad).

^{11}B NMR (128.38 MHz, C_6D_6, 298 K): -32.0 (t, broad, $^1J_{HB} \approx$ 106 Hz).

IR (ATR) ν (cm^{-1}): 2962, 2926, 2868, 2429 (B-H), 2382 (B-H), 2146 (As-H), 2116 (As-H), 2050 (C-O), 1969 (C-O), 1591, 1562.

FD-MS (*m/z*): 620.3 ([M]$^+$, 40%), 478.4 ([IDipp·BH_2AsH_2]$^+$, 100%), 401.4 ([IDipp·BH_2]$^+$, 62%).

6.5.2.21 Synthesis of [(IDipp·GaH_2PH_2)$Ni(CO)_3$] (6)

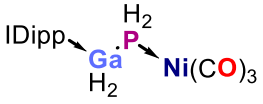

A batch of freshly prepared IDipp·GaH_2PH_2 (61 mg, 0.12 mmol) was dissolved in toluene. Then, $Ni(CO)_4$ (0.18 mL, 0.81 M stock solution in toluene, 0.15 mmol, 1.3 eq.) was added *via* syringe. After stirring at room temperature for 15 min, all volatiles were removed *in vacuo*. Subsequently the residue was dissolved in diethylether and filtered through a cannula wrapped with a glass fibre filter. Removing all volatiles *in vacuo* yielded the corresponding complex as a black-brown residue (46 mg, 58%).

^{1}H NMR (400.30 MHz, C_6D_6, 298 K): 0.96 (d, 12 H, 4 × ^{i}Pr-CH_3, $^3J_{HH}$ = 6.94 Hz), 1.29 (d, 12 H, 4 × ^{i}Pr-CH_3, $^3J_{HH}$ = 6.94 Hz), 1.64/0.97 (dm, PH_2, 2 H, $^1J_{HP}$ = 274 Hz), 2.50 (sep, 4 H, 4 × ^{i}Pr-CH, $^3J_{HH}$ = 6.94 Hz), 4.00 (d, broad, 2 H, GaH_2, $^2J_{HP}$ = 41 Hz), 6.41 (s, 2 H, NCHCHN), 7.04 (d, 4 H, 4 × aryl-C$_{meta}H$, $^3J_{HH}$ = 7.78 Hz), 7.19 (t, 2 × aryl-C$_{para}$H, $^3J_{HH}$ = 7.78 Hz).

^{31}P{^{1}H} NMR (161.98 MHz, C_6D_6, 298 K): -222.5 (s).

^{31}P NMR (161.98 MHz, C_6D_6, 298 K): -222.5 (tt, $^1J_{HP}$ = 274 Hz, $^3J_{HP}$ = 41 Hz).

IR (ATR) ν (cm^{-1}): 2963, 2926, 2869, 2045 (C-O), 1955 (C-O), 1784, 1594, 1557.

LIFDI-MS (*m/z*): 389.3 ([IDipp-H]$^+$, 100%; complete decomposition upon ionization).

6.5.2.22 General Procedure for the Synthesis of [(Me$_3$N·BH$_2$PR$_2$)Ni(CO)$_3$]

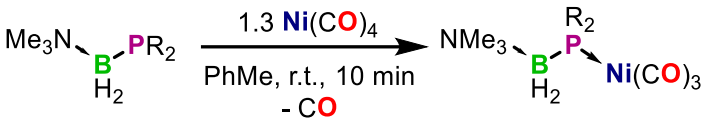

The corresponding pnictogenylborane Me$_3$N·BH$_2$ER$_2$ was dissolved in a small amount of toluene. In parallel, Ni(CO)$_4$ (1.3 eq., 0.81 M stock solution in toluene) was diluted in a separate Schlenk tube in toluene. Then, the pnictogenylborane was added dropwise to the Ni(CO)$_4$ solution and the mixture stirred for 10 min at room temperature. After removing all volatiles *in vacuo*, the residue was dissolved in diethylether and filtered through a cannula wrapped with a glass fibre filter. Subsequently, the solvent was removed *in vacuo* to isolate the corresponding complexes. *Note: the work-up of the reaction mixture results in Ni nanoparticles, which could not be completely separated by multiple filtration steps or amalgamation which did not allow for satisfying elemental analyses of the final products.*

6.5.2.23 [(Me$_3$N·BH$_2$PPh$_2$)Ni(CO)$_3$] (5a)

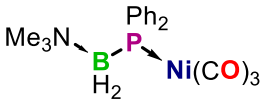

The complex was prepared according to the given general procedure. Reagents: Me$_3$N·BH$_2$PPh$_2$ (51 mg, 0.15 mmol), Ni(CO)$_4$ (0.30 mL, 0.81 M stock solution in toluene, 0.24 mmol, 1.6 eq.). Yield: 41 mg, 51%, brownish oil.

^{1}H NMR (400.30 MHz, C$_6$D$_6$, 298 K): 1.82 (s, 9 H, N(C*H*$_3$)$_3$), 2.80 (q, br, 2 H, $^1J_{HB}$ ≈ 131 Hz, B*H*$_2$), 7.02 (m, br, 2 H, 2 × phenyl-C$_{para}$-H), 7.12 (m, br, 4 H, 4 × phenyl-C$_{meta}$-H), 7.84 (t, 4 H, $^3J_{HH}$ = 8.75 Hz, 4 × phenyl-C$_{ortho}$-H).

^{31}P{^{1}H} NMR (161.98 MHz, C$_6$D$_6$, 298 K): -20.7 (q, broad, $^1J_{PB}$ ≈ 76 Hz).

^{31}P NMR (161.98 MHz, C$_6$D$_6$, 298 K): -20.7 (m, broad).

^{11}B{^{1}H} NMR (128.38 MHz, C$_6$D$_6$, 298 K): -4.09 (d, broad, $^1J_{PB}$ ≈ 76 Hz).

^{11}B NMR (128.38 MHz, C$_6$D$_6$, 298 K): -4.09 (m, very broad, $^1J_{HB}$ ≈ 131 Hz).

IR (ATR) *ν* (cm^{-1}): 2938, 2923, 2853, 2433 (B-H), 2386 (B-H), 2049 (C-O), 1950 (C-O), 1582, 1566.

6.5.2.24 [(Me$_3$N·BH$_2$PH^{t}Bu)Ni(CO)$_3$] (5b)

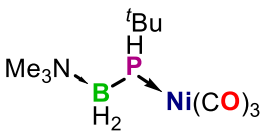

The complex was prepared according to the given general procedure. Reagents: Me$_3$N·BH$_2$PH^{t}Bu (32 mg, 0.20 mmol), Ni(CO)$_4$ (0.30 mL, 0.81 M stock solution in toluene, 0.24 mmol, 1.2 eq.). Yield: 57 mg, 94%, brownish oil.

^{1}H NMR (400.30 MHz, C$_6$D$_6$, 298 K): 1.29 (d, 9 H, C(C*H*$_3$)$_3$, $^3J_{HP}$ = 13.45 Hz), 1.89 (s, 9 H, N(C*H*$_3$)$_3$), 2.45 (q, broad and superimposed, 2 H, B*H*$_2$, $^1J_{HB}$ = 106.84 Hz) 2.73/3.42 (dq, 1 H, P*H*, $^1J_{HP}$ = 271.37 Hz, $^2J_{HB}$ = 4.24 Hz).

$^{31}P\{^{1}H\}$ NMR (161.98 MHz, C_6D_6, 298 K): -47.2 (q, broad, $^{1}J_{PB}$ = 66 Hz).

^{31}P NMR (161.98 MHz, C_6D_6, 298 K): -47.2 (dm, broad, $^{1}J_{HP}$ = 273 Hz).

$^{11}B\{^{1}H\}$ NMR (128.38 MHz, C_6D_6, 298 K): -7.3 (d, $^{1}J_{PB}$ = 66 Hz).

^{11}B NMR (128.38 MHz, C_6D_6, 298 K): -7.3 (td, broad, $^{1}J_{PB}$ = 66 Hz, $^{1}J_{HB} \approx$ 107 Hz).

IR (ATR) ν (cm^{-1}): 2859, 2392, 2051 (C-O), 1955 (C-O), 1808, 1483.

6.5.2.25 [($Me_3N{\cdot}BH_2PH_2$)Ni(CO)$_3$] (5c)

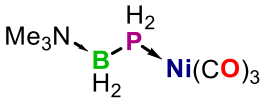

The complex was prepared according to the given general procedure. Reagents: $Me_3N{\cdot}BH_2PH_2$ (0.3 mL, 0.5 M stock solution in toluene, 0.15 mmol), $Ni(CO)_4$ (0.30 mL, 0.81 M stock solution in toluene, 0.18 mmol, 1.3 eq.). Yield: 23 mg, 62%, brownish oil.

^{1}H NMR (400.30 MHz, C_6D_6, 298 K): 2.01 (s, 9 H , $N(CH_3)_3$), 2.60 (q, very broad and superimposed, $^{1}J_{HB} \approx$ 110 Hz, BH_2), 2.52/3.20 (dm, 2 H, $^{1}J_{HP}$ = 266 Hz, PH_2).

$^{31}P\{^{1}H\}$ NMR (161.98 MHz, C_6D_6, 298 K): -155.6 (q, broad, $^{1}J_{PB}$ = 58 Hz).

^{31}P NMR (161.98 MHz, C_6D_6, 298 K): -155.6 (tq, broad, $^{1}J_{HP}$ = 266 Hz, $^{1}J_{PB}$ = 58 Hz).

$^{11}B\{^{1}H\}$ NMR (128.38 MHz, C_6D_6, 298 K): -7.8 (d, $^{1}J_{PB}$ = 58 Hz).

^{11}B NMR (128.38 MHz, C_6D_6, 298 K): -7.8 (td, broad, $^{1}J_{PB}$ = 58 Hz, $^{1}J_{HB}$ = 110 Hz).

IR (ATR) ν (cm^{-1}): 2943, 2920, 2857, 2377 (B-H), 2293 (P-H), 2059 (C-O), 1887 (C-O), 1481.

6.5.3 NMR Data

6.5.3.1 $KPCy_2$

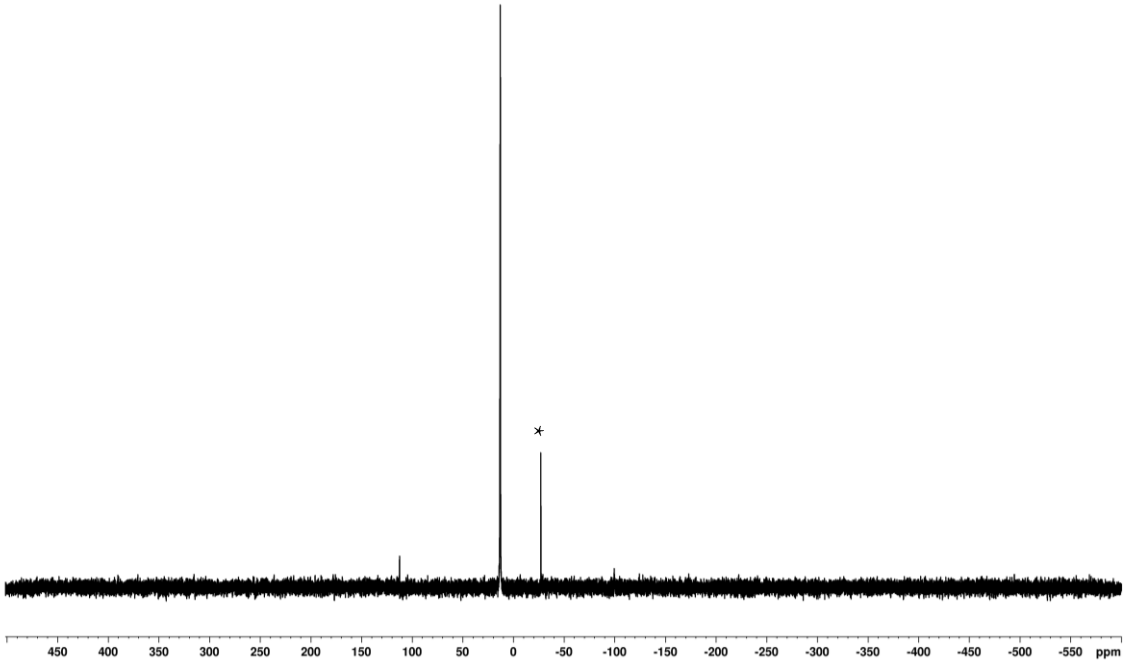

Figure S 6.1: $^{31}P\{^{1}H\}$ NMR spectrum of $KPCy_2$ (THF/C_6D_6-cap., 298 K, * = $HPCy_2$ from sample decomposition).

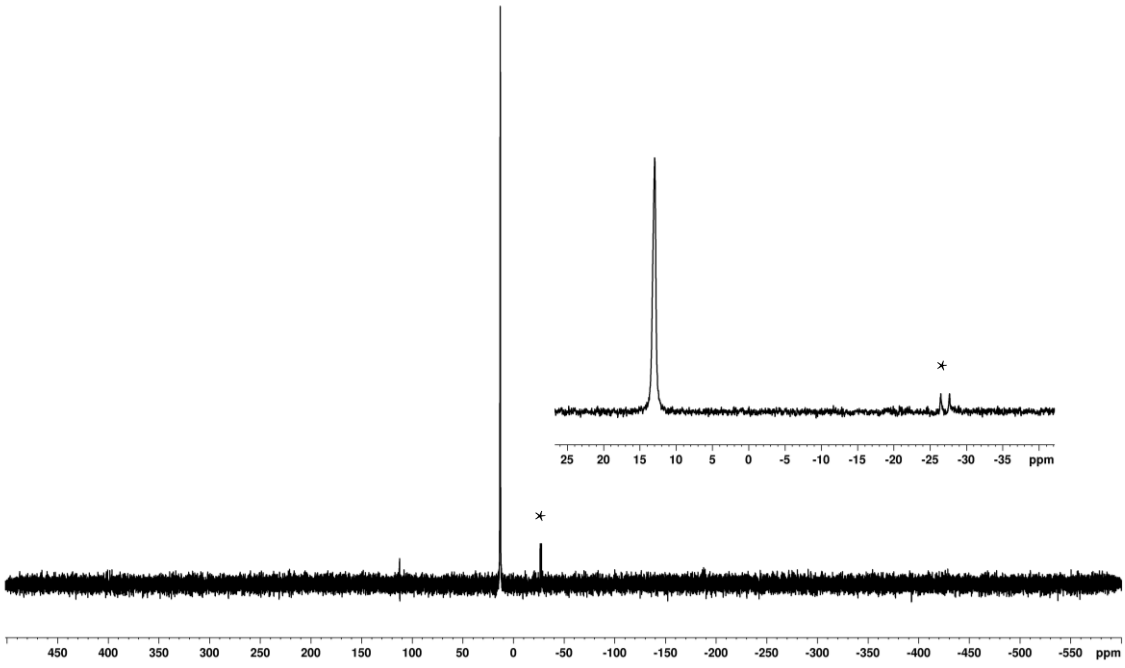

Figure S 6.2: ^{31}P NMR spectrum of $KPCy_2$ (THF/C_6D_6-cap., 298 K, * = $HPCy_2$ from sample decomposition).

6.5.3.2 KP*t*BuH

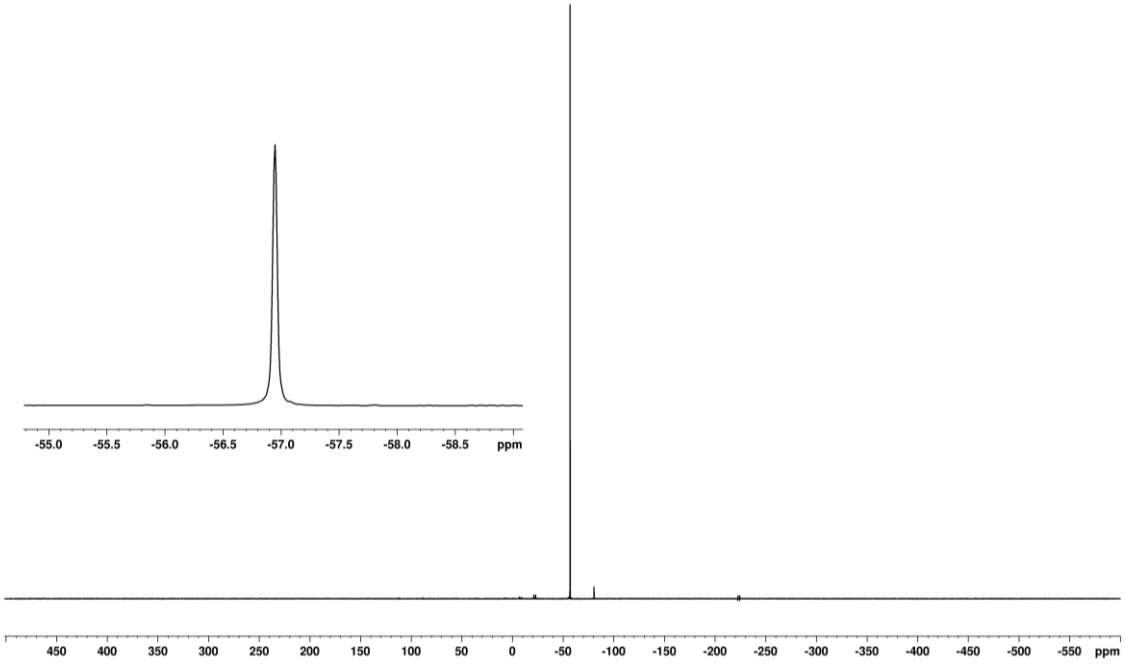

Figure S 6.3: $^{31}P\{^{1}H\}$ NMR spectrum of KP^{t}BuH (THF/C_6D_6-cap., 298 K).

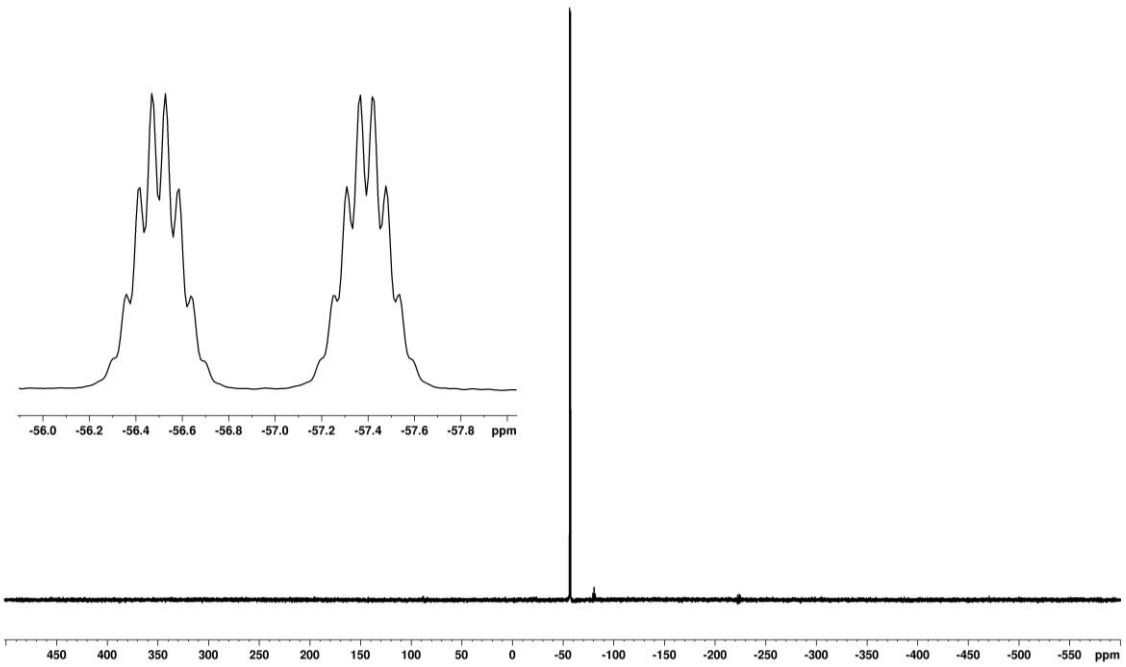

Figure S 6.4: ^{31}P NMR spectrum of KP^{t}BuH (THF/C_6D_6-cap., 298 K).

6.5.3.3 SIDipp·BH_2I

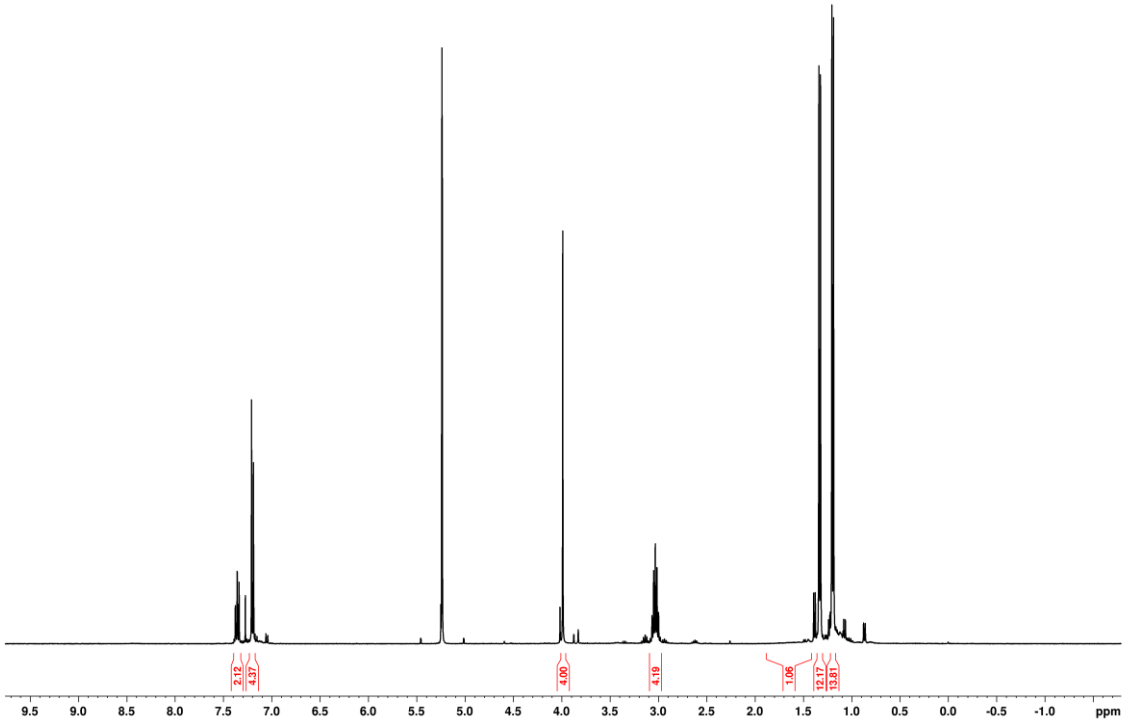

Figure S 6.5: ^{1}H NMR spectrum of SIDipp·BH_2I (CD_2Cl_2, 298 K).

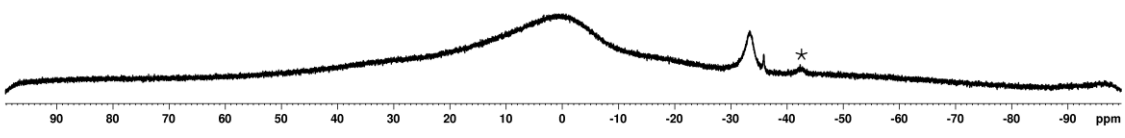

Figure S 6.6: $^{11}B\{^{1}H\}$ NMR spectrum of SIDipp·BH_2I (CD_2Cl_2, 298 K; * = SIDipp·BHI_2).

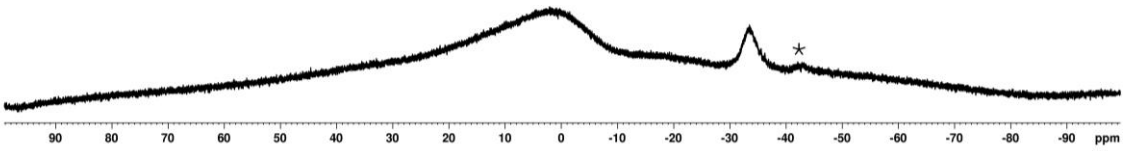

Figure S 6.7: ^{11}B NMR spectrum of SIDipp·BH_2I (CD_2Cl_2, 298 K; * = SIDipp·BHI_2).

6.5.3.4 SIDipp·BH_2PH_2

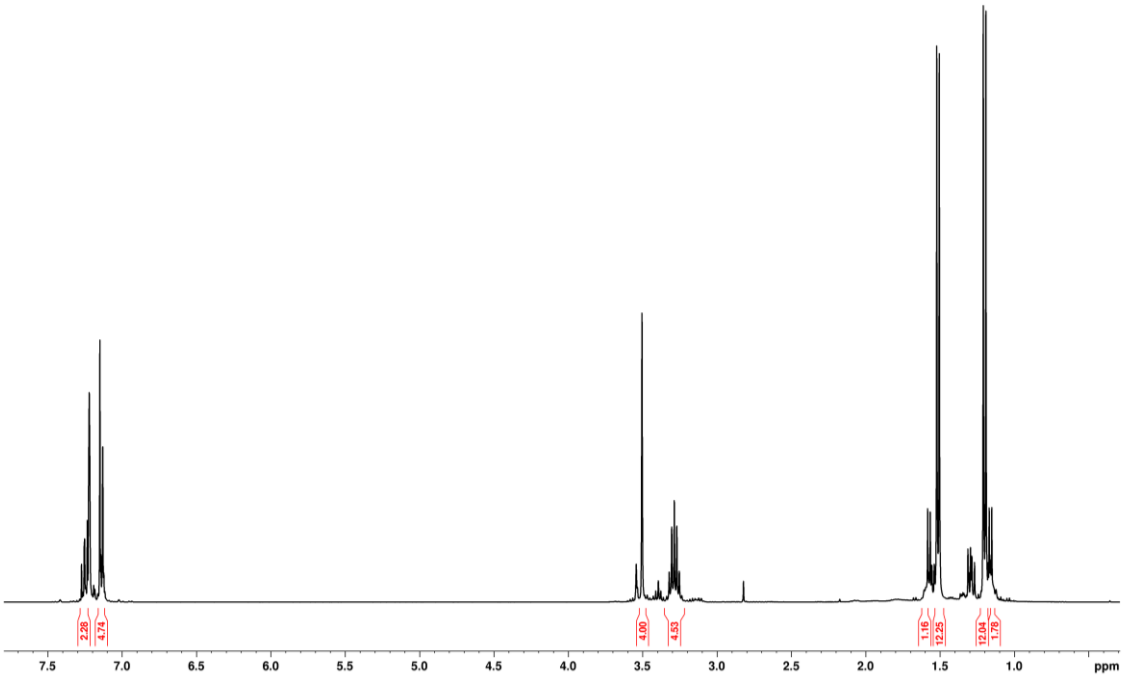

Figure S 6.8: ^1H NMR spectrum of SIDipp·BH_2PH_2 (C_6D_6, 298 K).

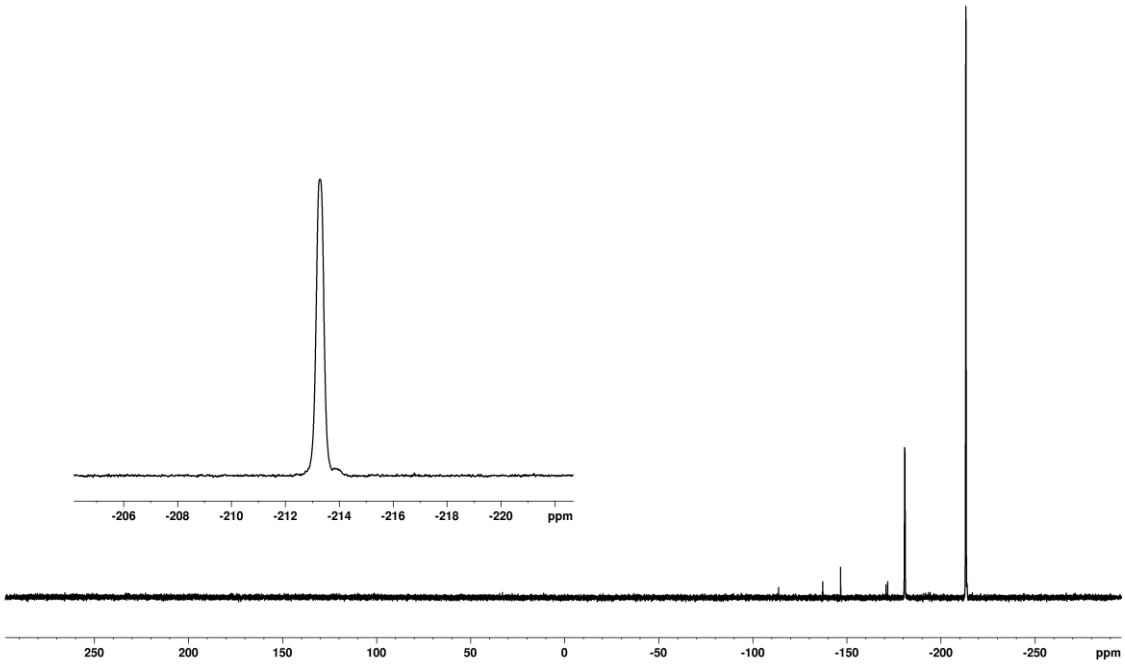

Figure S 6.9: $^{31}P\{^{1}H\}$ NMR spectrum of SIDipp·BH_2PH_2 (C_6D_6, 298 K).

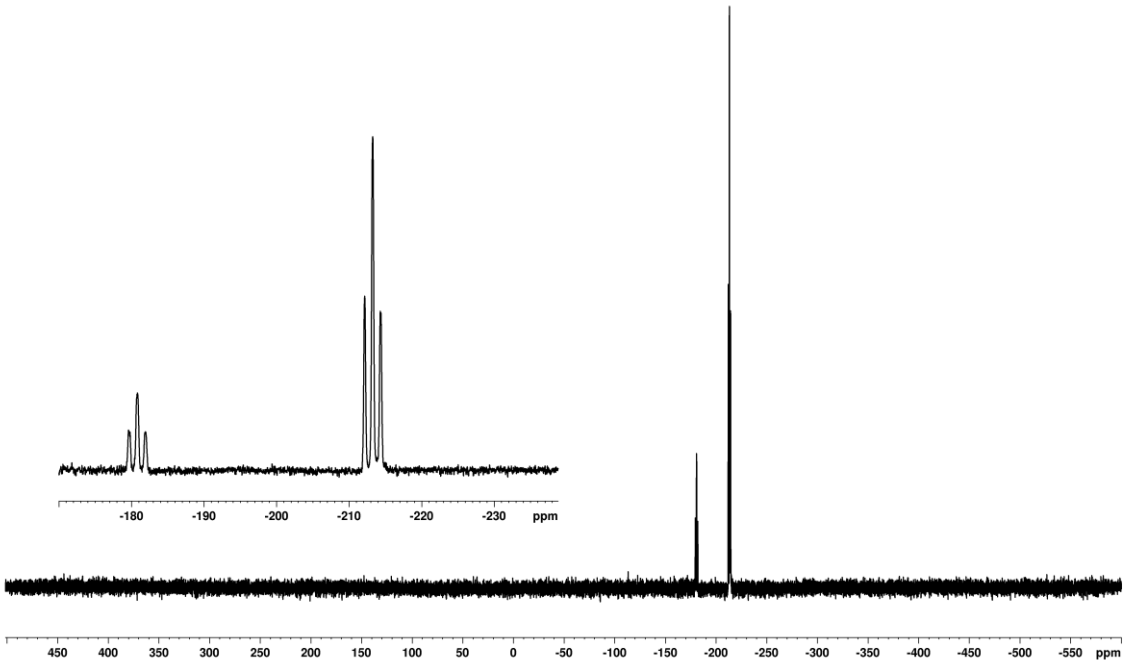

Figure S 6.10: ^{31}P NMR spectrum of SIDipp·BH_2PH_2 (C_6D_6, 298 K).

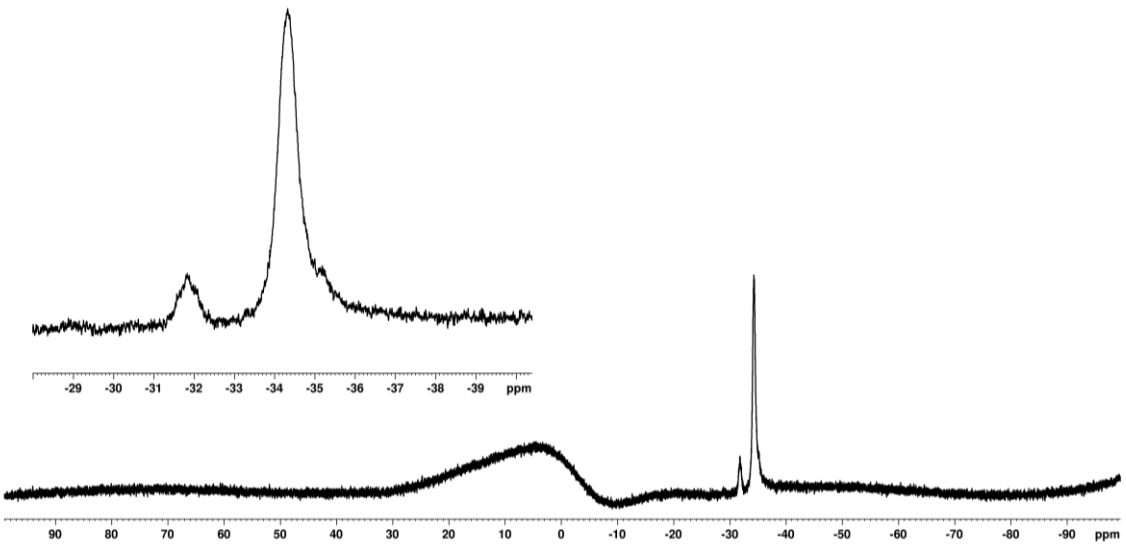

Figure S 6.11: $^{11}B\{^{1}H\}$ NMR spectrum of SIDipp·BH_2PH_2 (C_6D_6, 298 K).

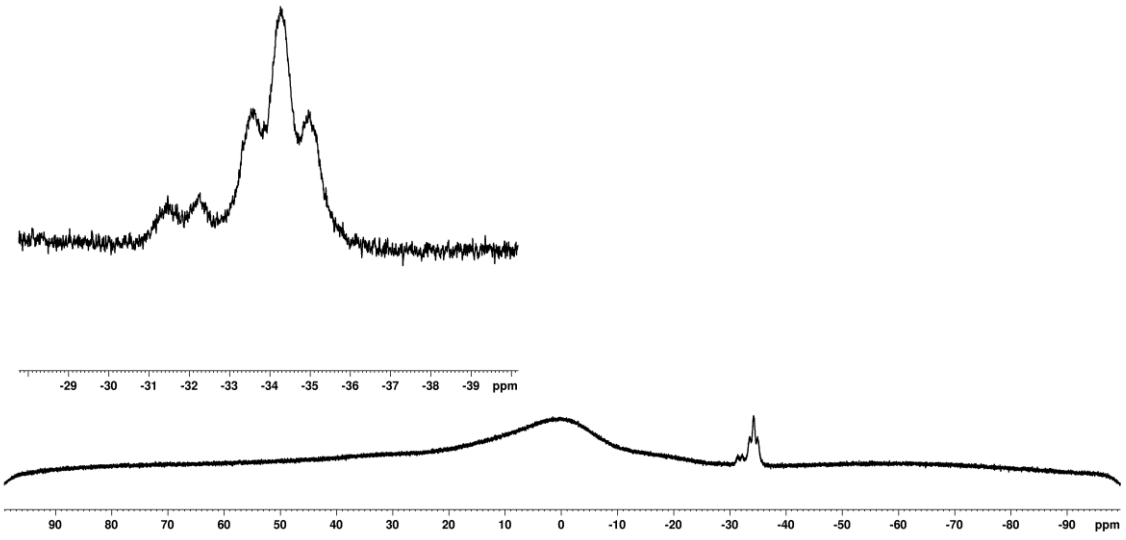

Figure S 6.12: ^{11}B NMR spectrum of SIDipp·BH_2PH_2 (C_6D_6, 298 K).

6.5.3.5 IDipp·BH_2PPh_2

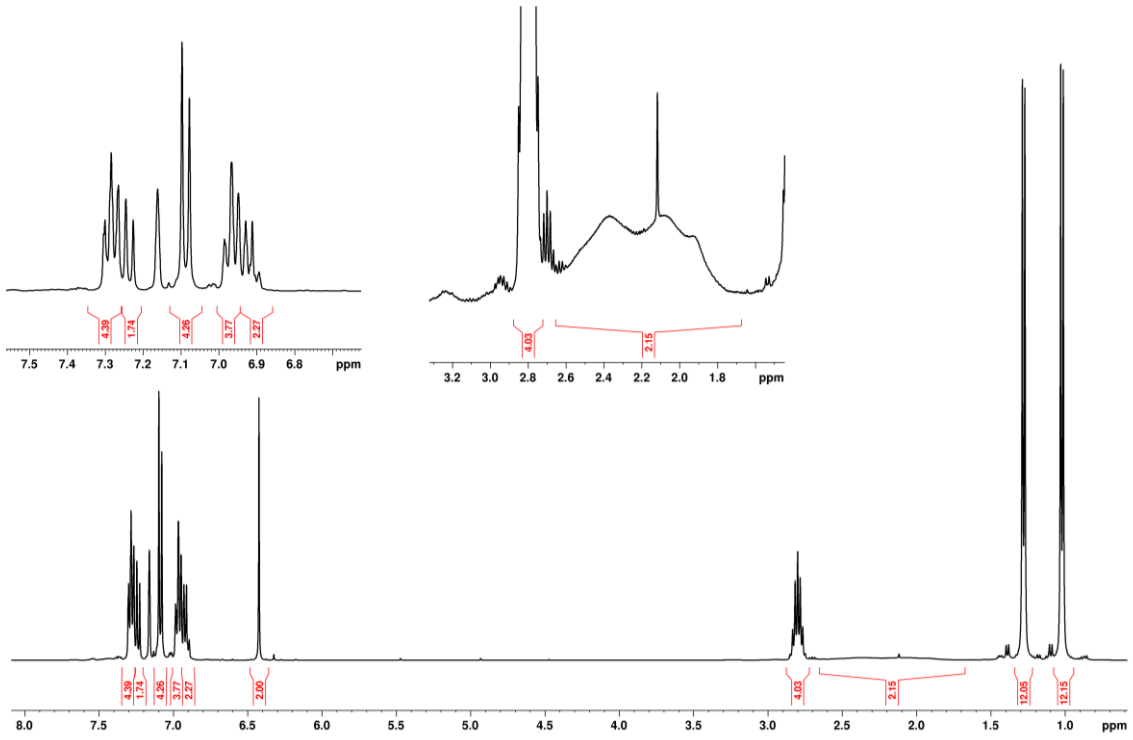

Figure S 6.13: ^{1}H NMR spectrum of IDipp·BH_2PPh_2 (C_6D_6, 298 K).

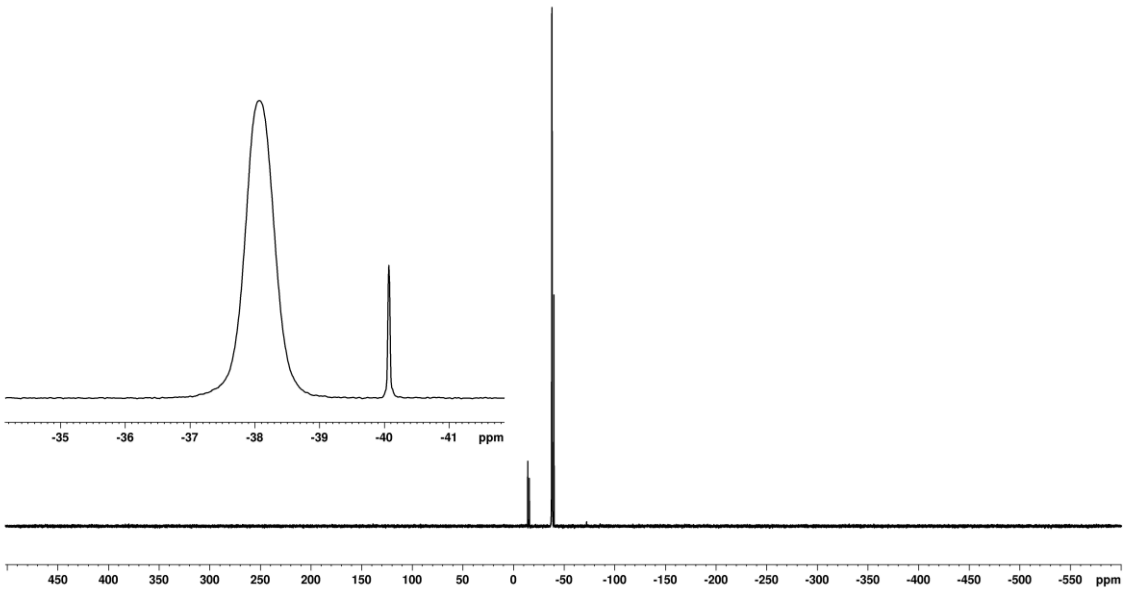

Figure S 6.14: $^{31}P\{^{1}H\}$ NMR spectrum of IDipp·BH_2PPh_2 (C_6D_6, 298 K).

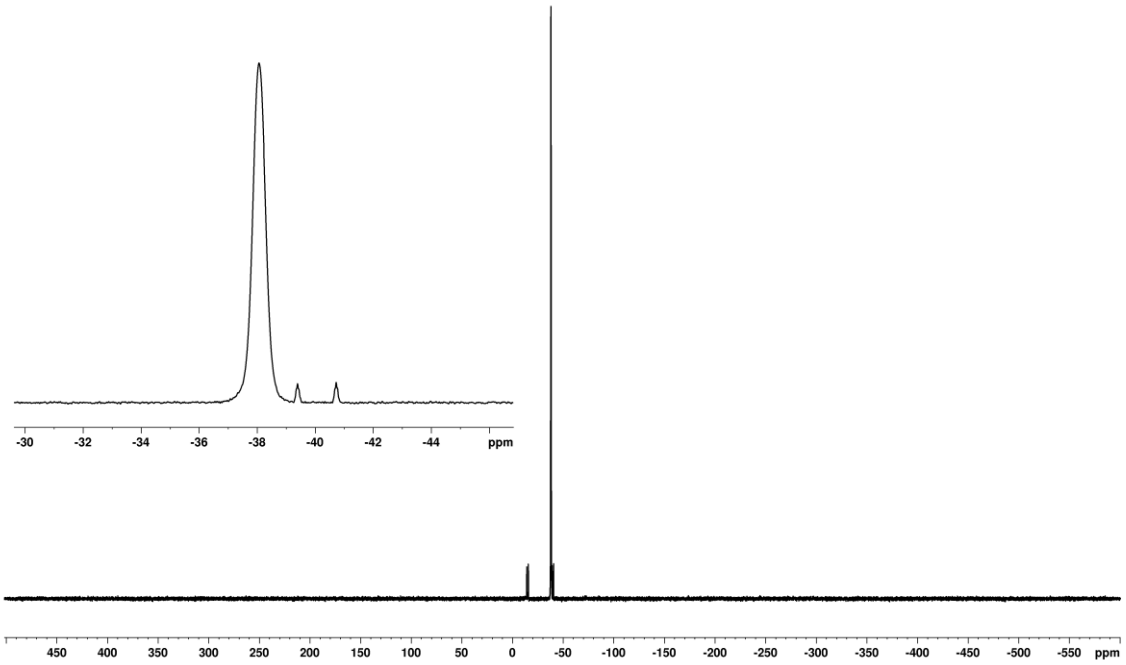

Figure S 6.15: ^{31}P NMR spectrum of IDipp·BH_2PPh_2 (C_6D_6, 298 K).

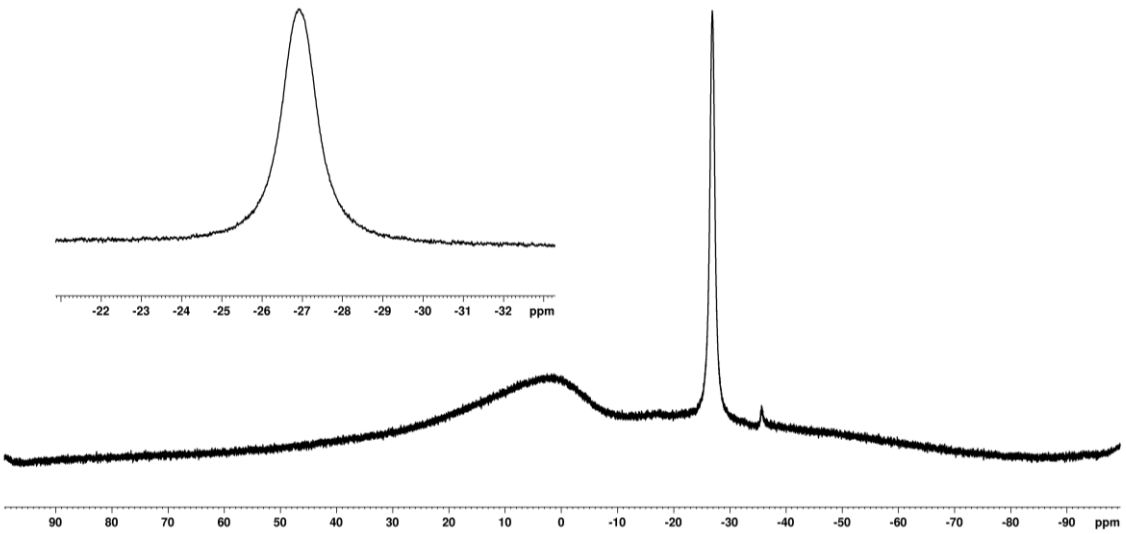

Figure S 6.16: $^{11}B\{^1H\}$ NMR spectrum of IDipp·BH_2PPh_2 (C_6D_6, 298 K).

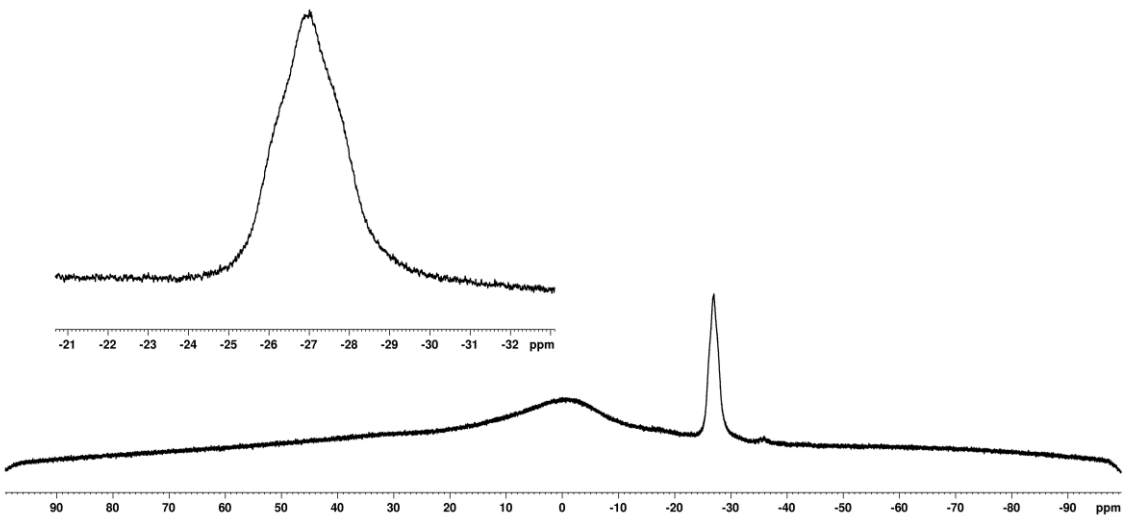

Figure S 6.17: ^{11}B NMR spectrum of IDipp·BH_2PPh_2 (C_6D_6, 298 K).

6.5.3.6 IDipp·BH_2PMe_2

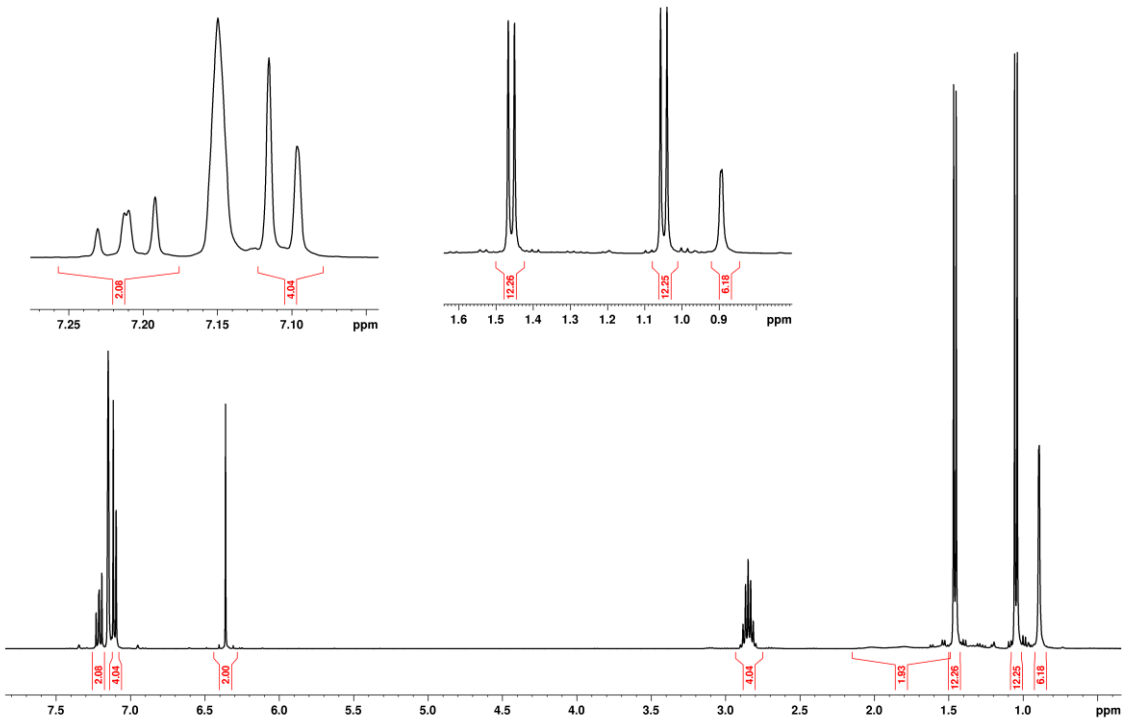

Figure S 6.18: ^{1}H NMR spectrum of IDipp·BH_2PMe_2 (C_6D_6, 298 K).

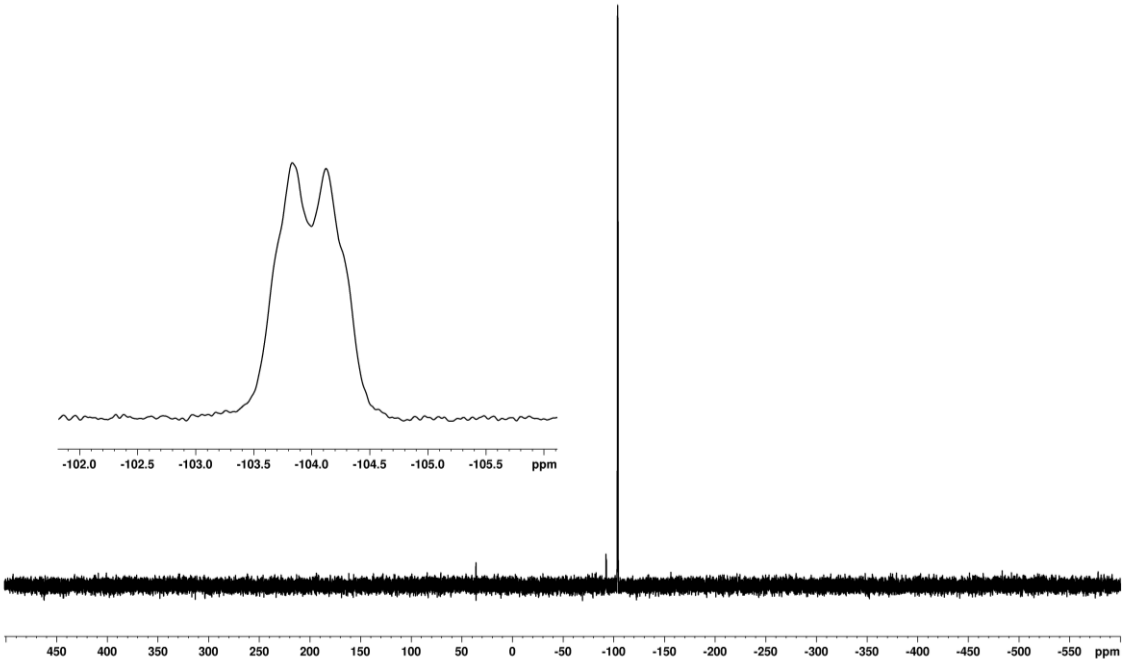

Figure S 6.19: $^{31}P\{^{1}H\}$ NMR spectrum of IDipp·BH_2PMe_2 (C_6D_6, 298 K).

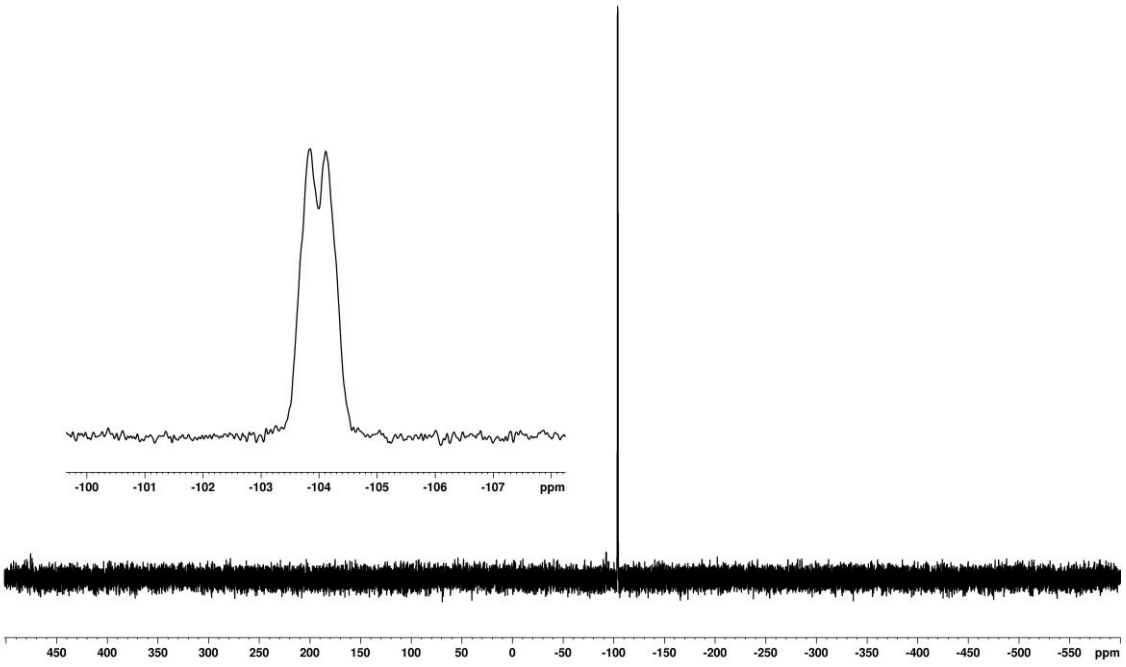

Figure S 6.20: ^{31}P NMR spectrum of IDipp·BH_2PMe_2 (C_6D_6, 298 K).

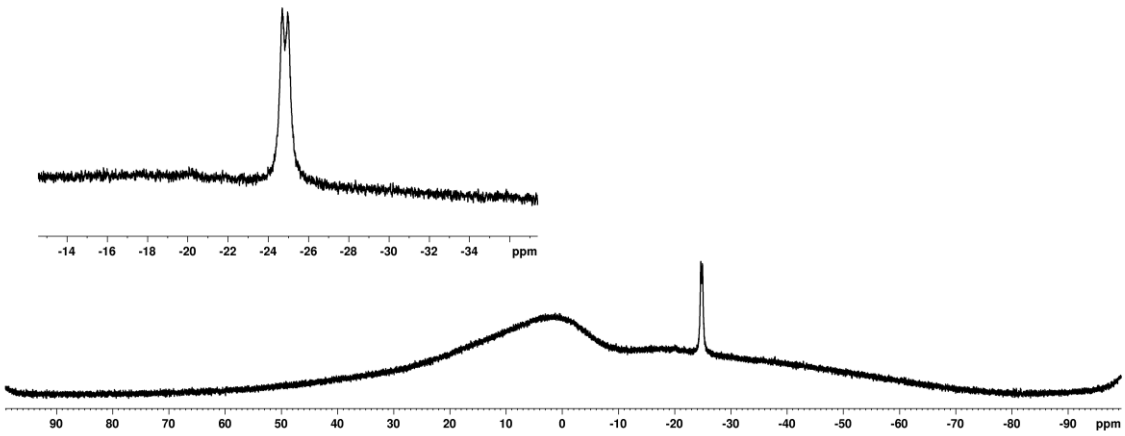

Figure S 6.21: $^{11}B\{^{1}H\}$ NMR spectrum of IDipp·BH_2PMe_2 (C_6D_6, 298 K).

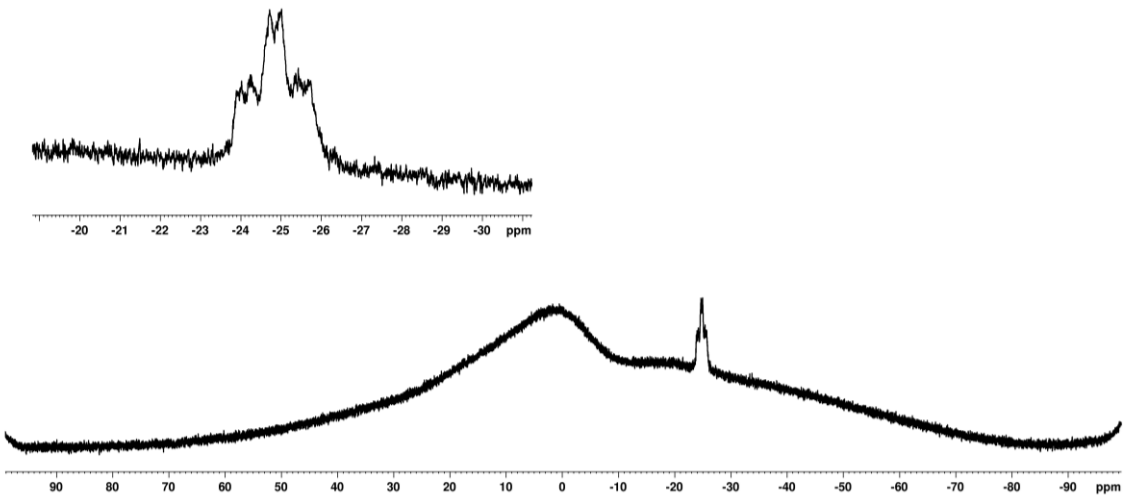

Figure S 6.22: ^{11}B NMR spectrum of IDipp·BH_2PMe_2 (C_6D_6, 298 K).

6.5.3.7 IDipp·BH_2AsPh_2

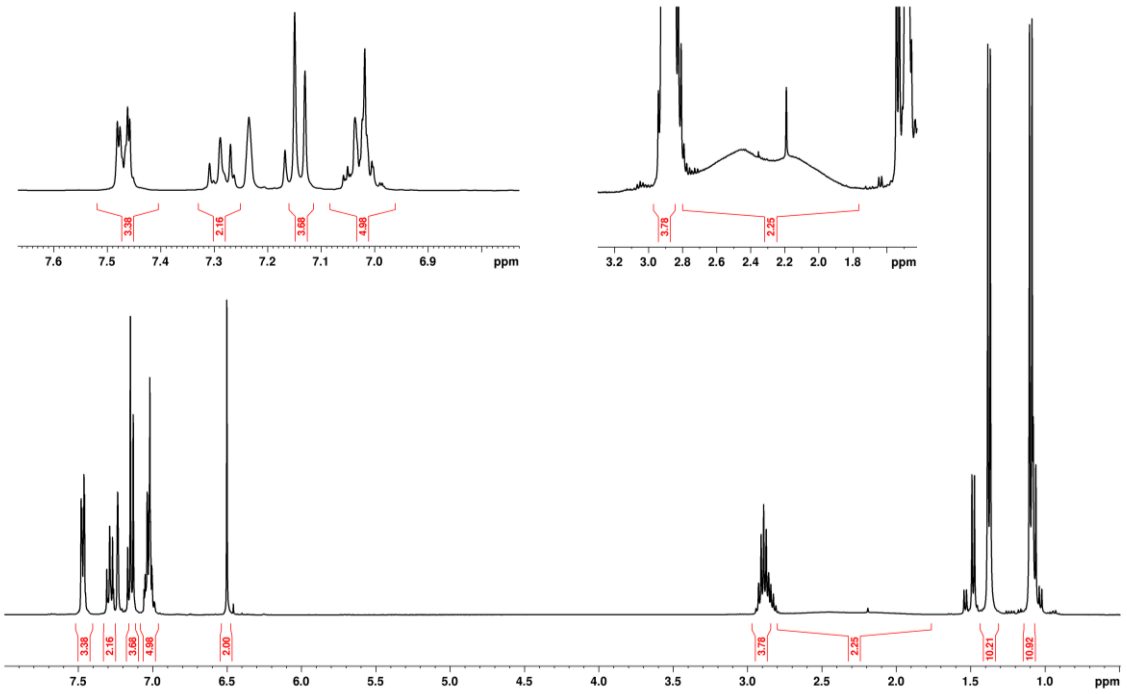

Figure S 6.23: ^{1}H NMR spectrum of IDipp·BH_2AsPh_2 (C_6D_6, 298 K).

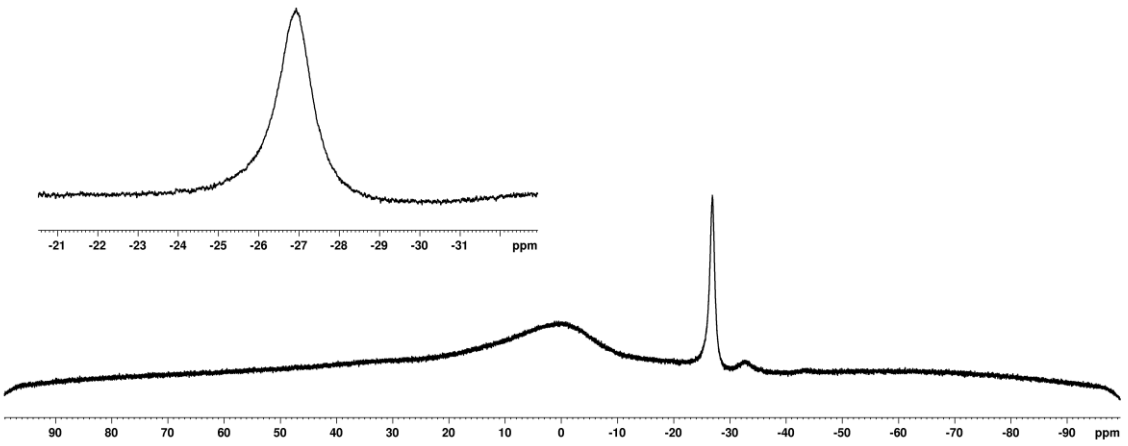

Figure S 6.24: $^{11}B\{^{1}H\}$ NMR spectrum of IDipp·BH_2AsPh_2 (C_6D_6, 298 K).

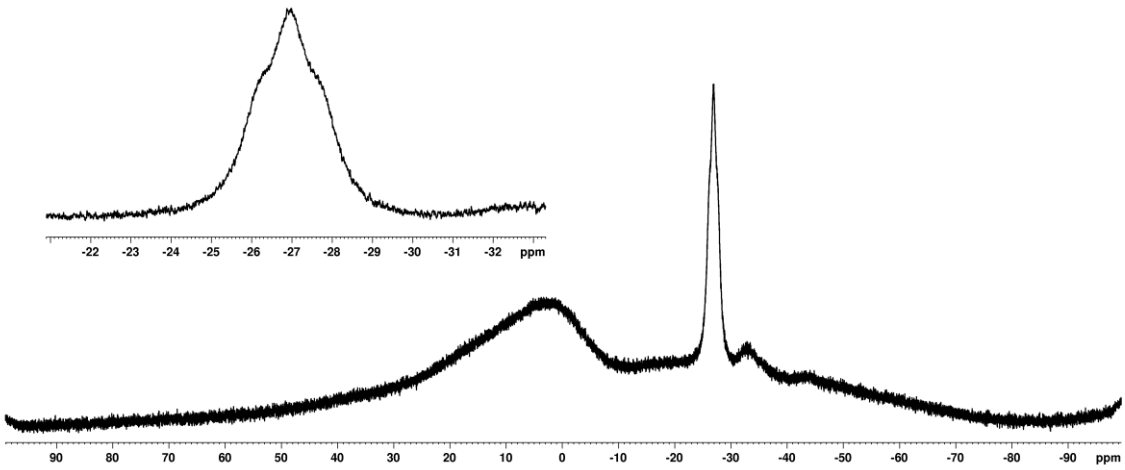

Figure S 6.25: ^{11}B NMR spectrum of IDipp·BH_2AsPh_2 (C_6D_6, 298 K).

6.5.3.8 IDipp·BH_2PH^tBu

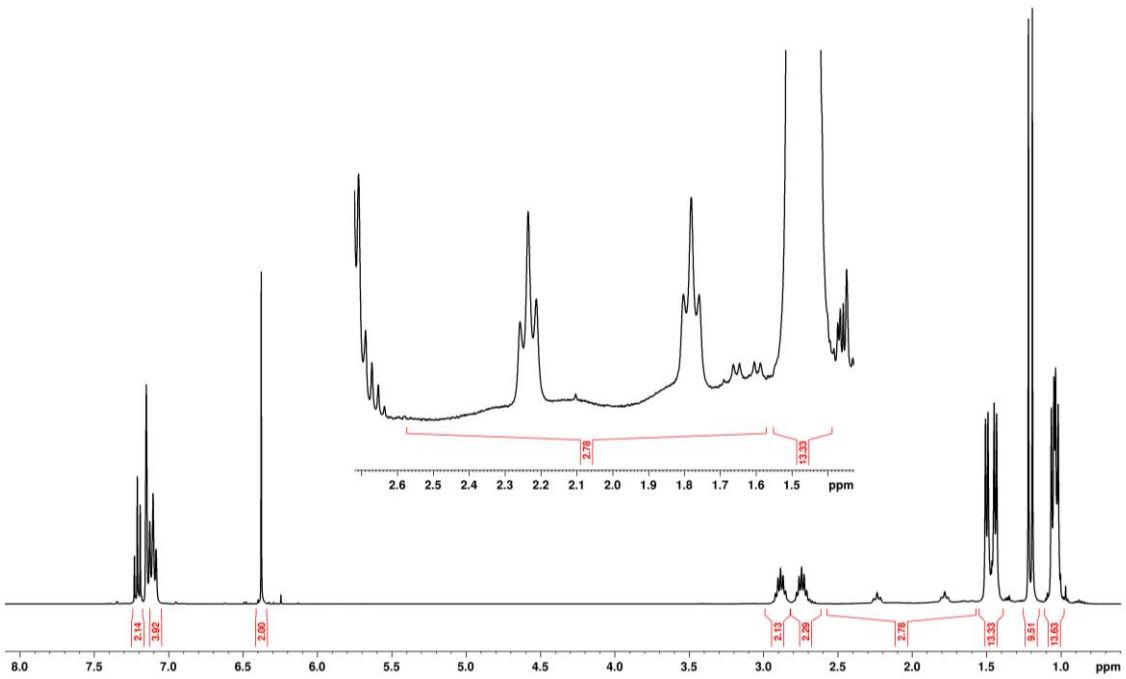

Figure S 6.26: ^1H NMR spectrum of IDipp·BH_2PH^tBu (C_6D_6, 298 K).

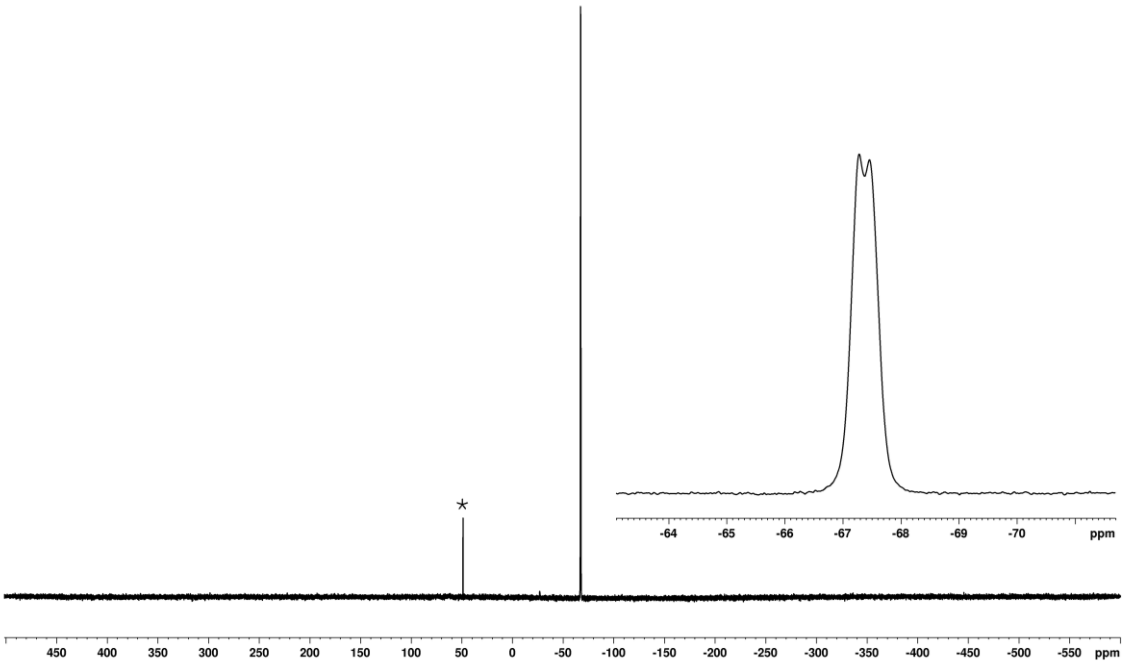

Figure S 6.27: $^{31}P\{^{1}H\}$ NMR spectrum of IDipp·BH_2PH^tBu (C_6D_6, 298 K; * = unidentified impurity).

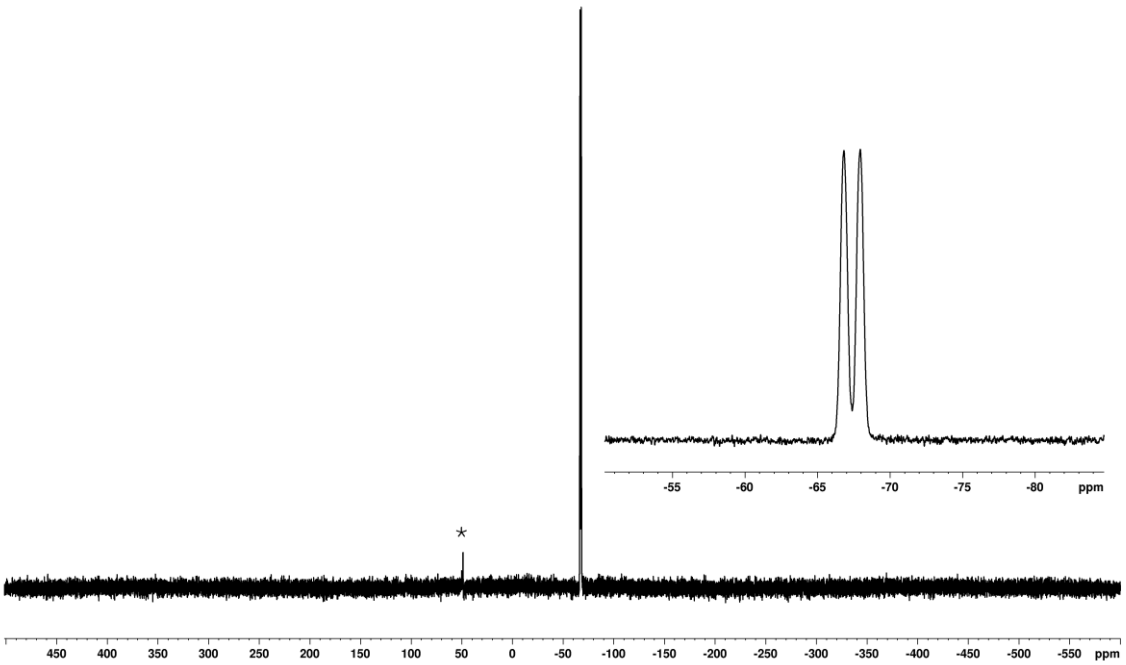

Figure S 6.28: ^{31}P NMR spectrum of IDipp·BH_2PH^tBu (C_6D_6, 298 K; * = unidentified impurity).

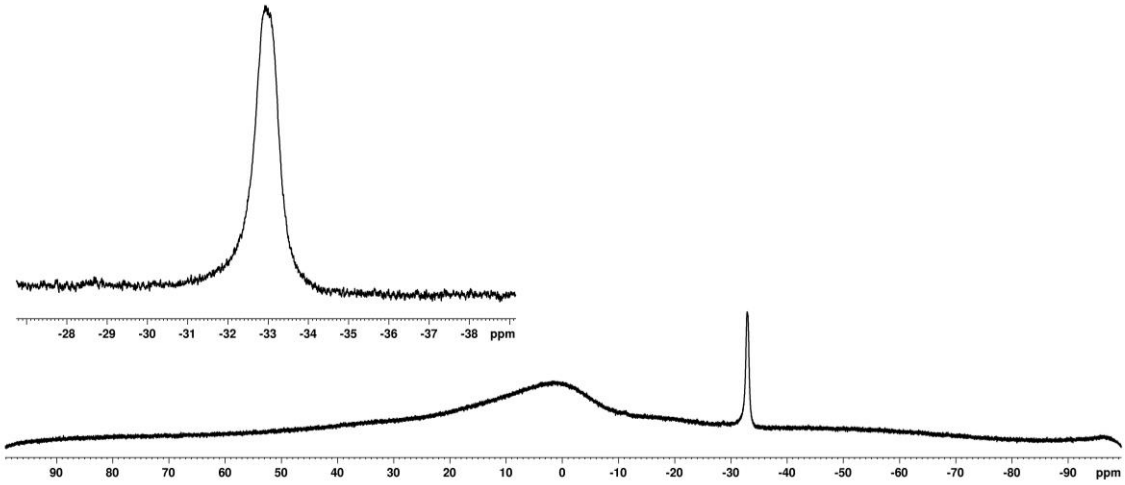

Figure S 6.29: $^{11}B\{^{1}H\}$ NMR spectrum of IDipp·BH_2PH^tBu (C_6D_6, 298 K).

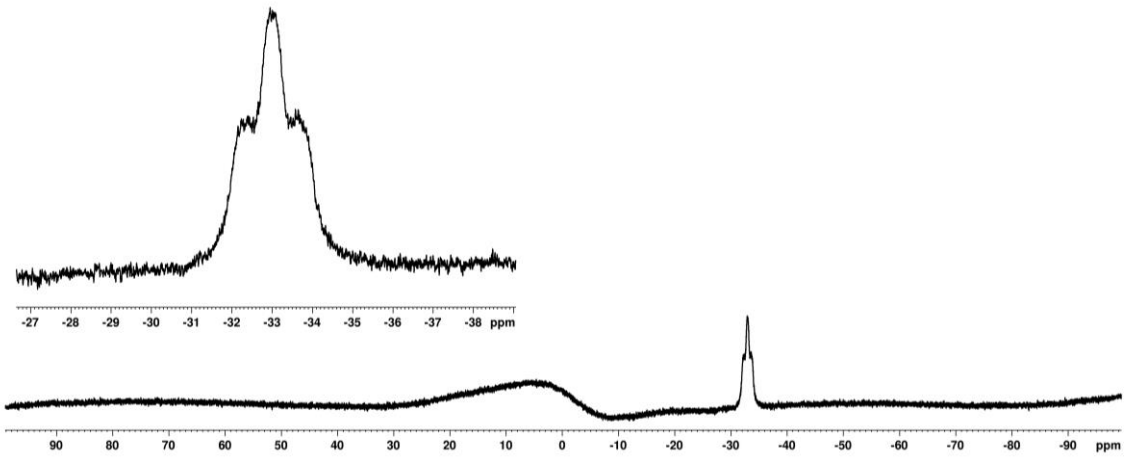

Figure S 6.30: ^{11}B NMR spectrum of IDipp·BH_2PH^tBu (C_6D_6, 298 K).

6.5.3.9 IDipp·BH_2PCy_2

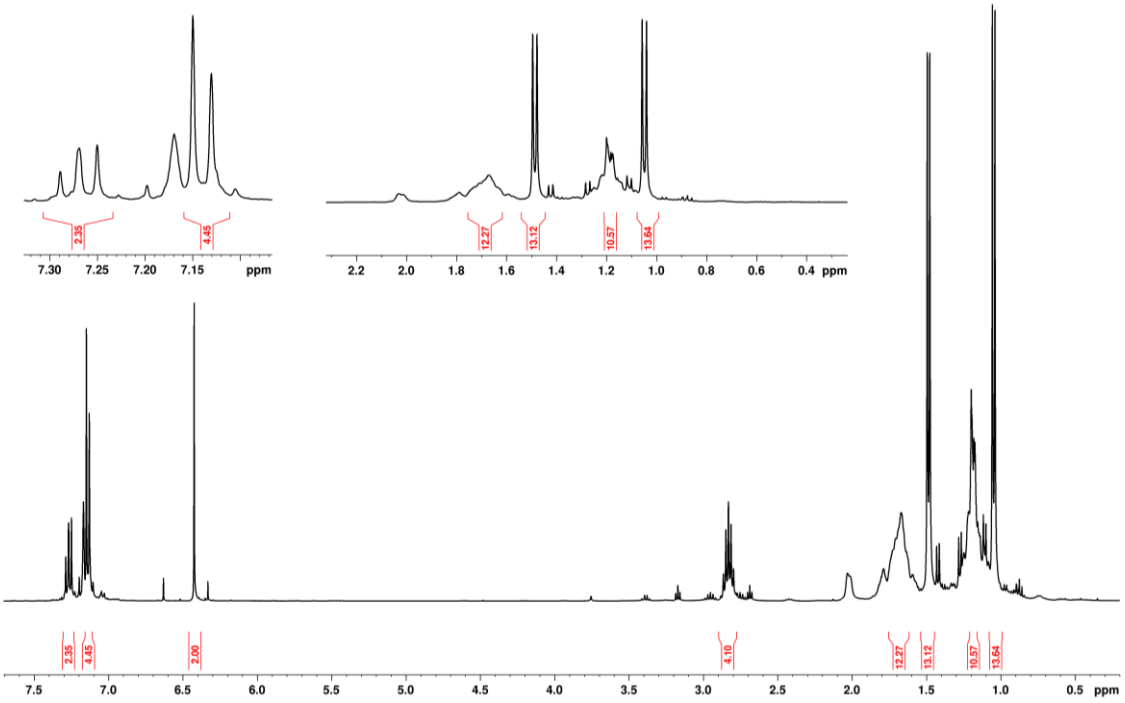

Figure S 6.31: ^{1}H NMR spectrum of IDipp·BH_2PCy_2 (C_6D_6, 298 K).

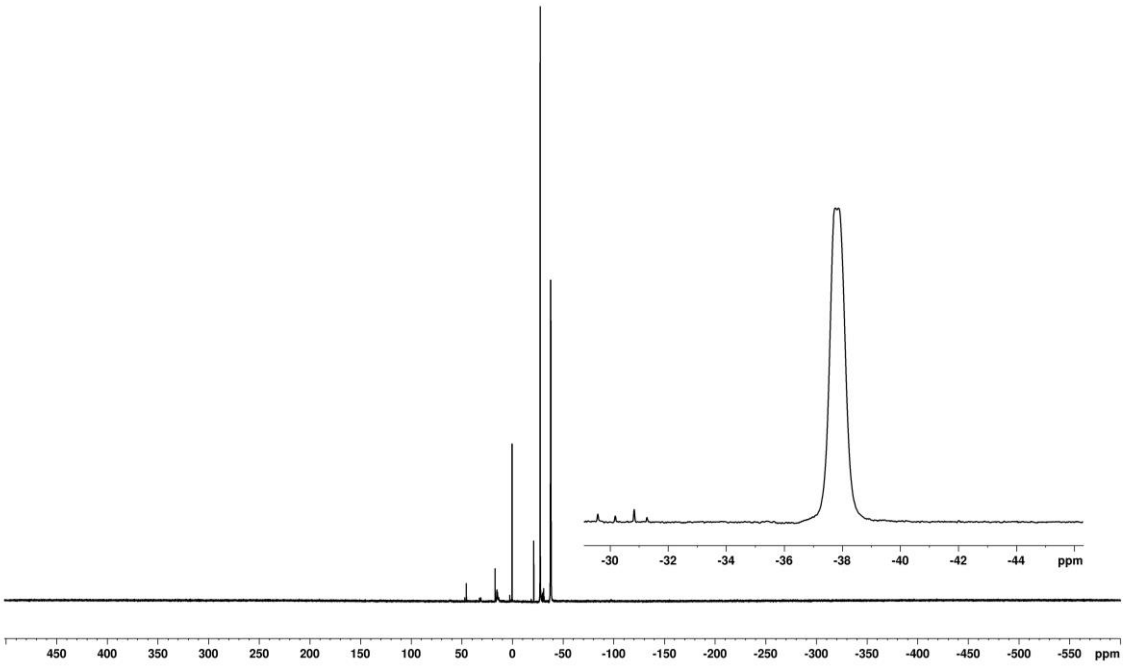

Figure S 6.32: $^{31}P\{^{1}H\}$ NMR spectrum of IDipp·BH_2PCy_2 (C_6D_6, 298 K).

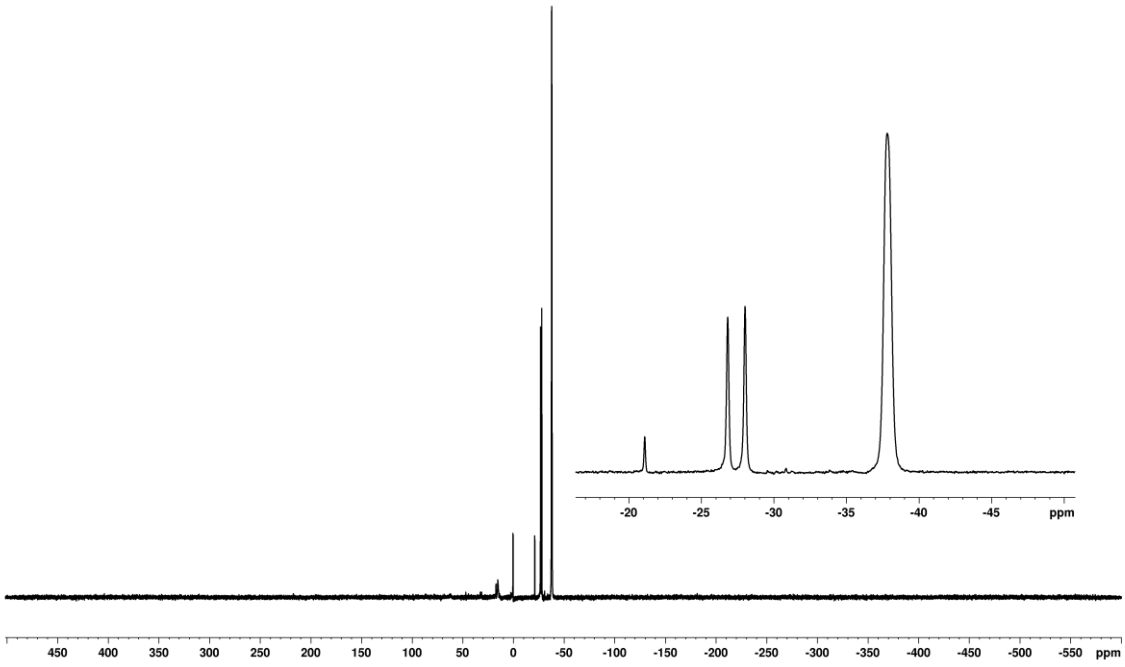

Figure S 6.33: ^{31}P NMR spectrum of IDipp·BH_2PCy_2 (C_6D_6, 298 K).

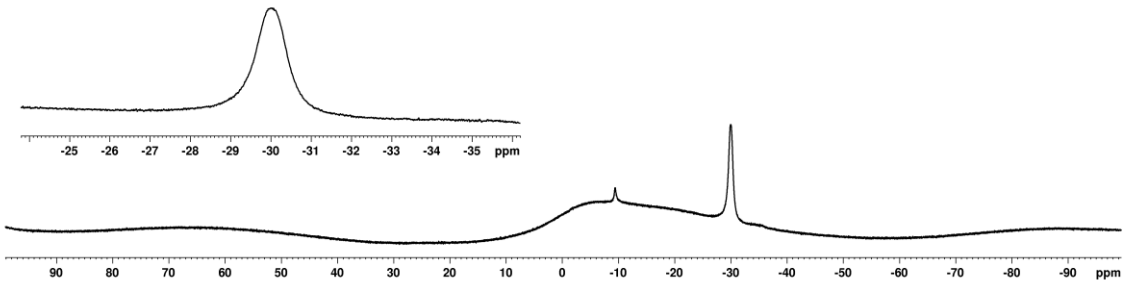

Figure S 6.34: $^{11}B\{^1H\}$ NMR spectrum of IDipp·BH_2PCy_2 (C_6D_6, 298 K).

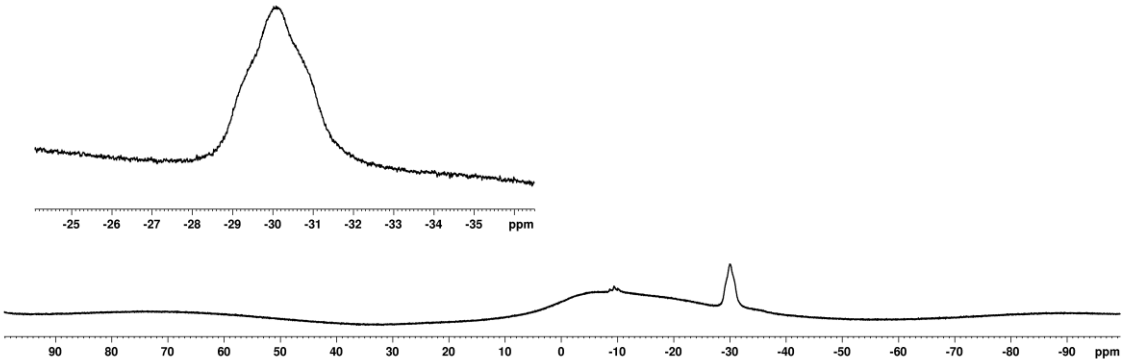

Figure S 6.35: ^{11}B NMR spectrum of IDipp·BH_2PCy_2 (C_6D_6, 298 K).

6.5.3.10 IDipp·$BH_2P(SiMe_3)_2$

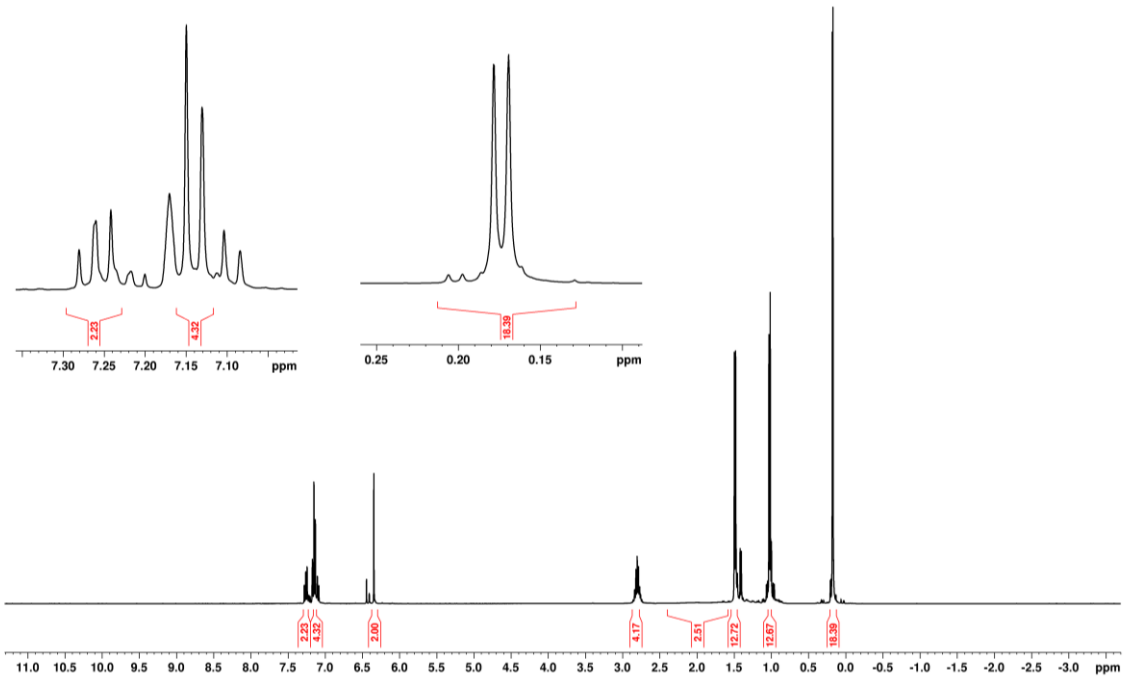

Figure S 6.36: ^1H NMR spectrum of IDipp·$BH_2P(SiMe_3)_2$ (C_6D_6, 298 K).

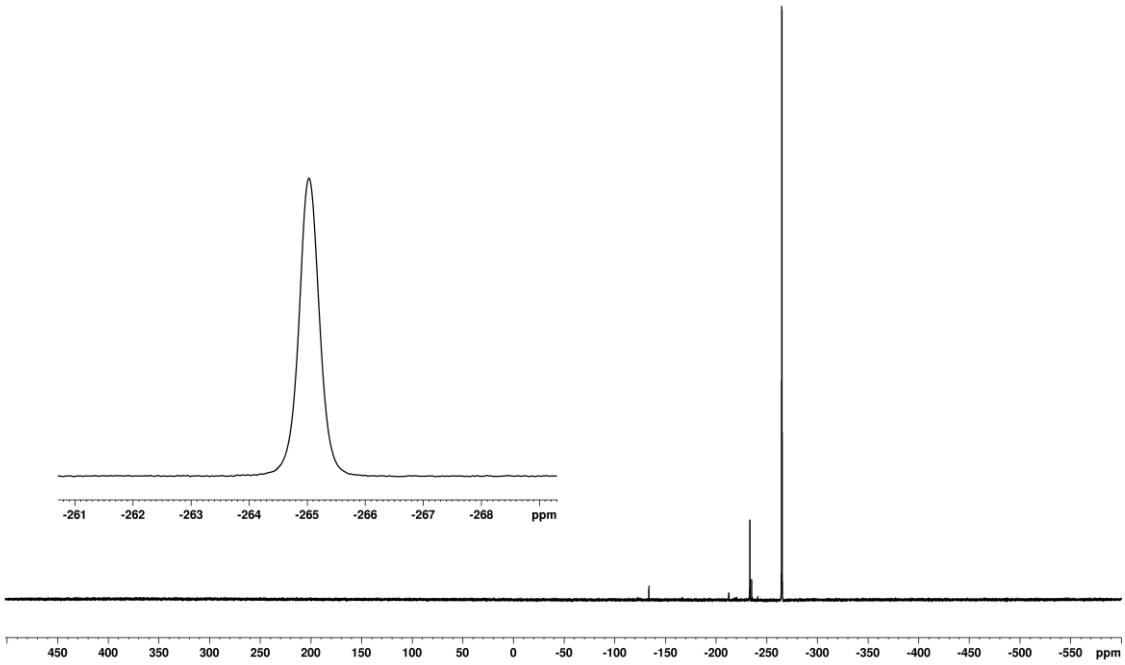

Figure S 6.37: $^{31}P\{^{1}H\}$ NMR spectrum of IDipp·$BH_2P(SiMe_3)_2$ (C_6D_6, 298 K).

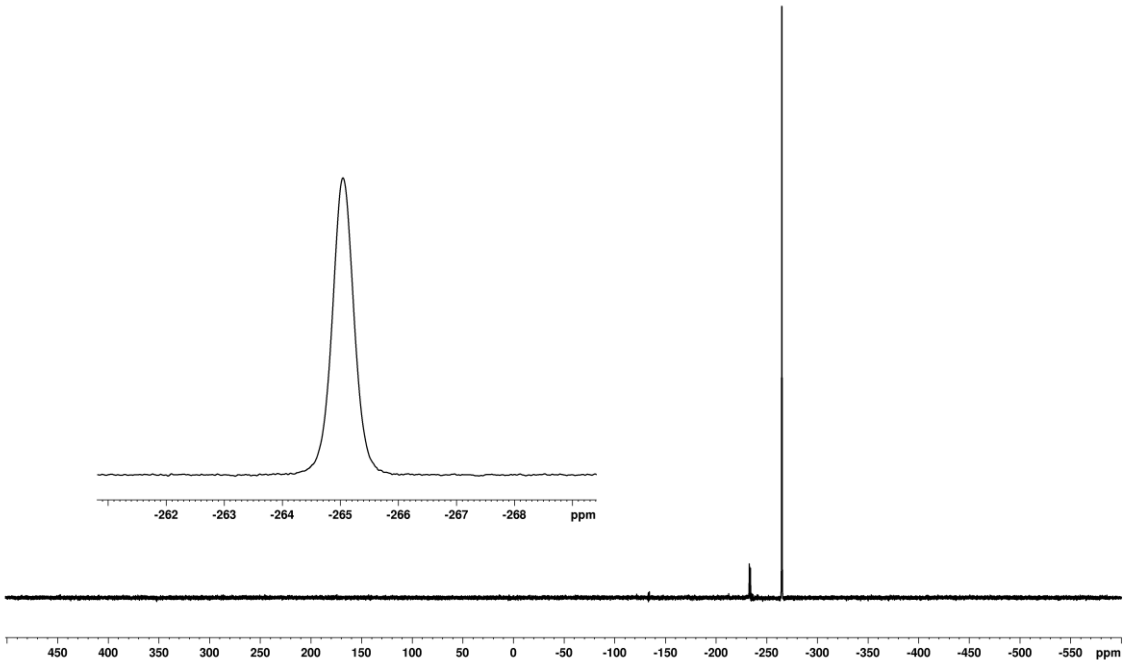

Figure S 6.38: ^{31}P NMR spectrum of IDipp·$BH_2P(SiMe_3)_2$ (C_6D_6, 298 K).

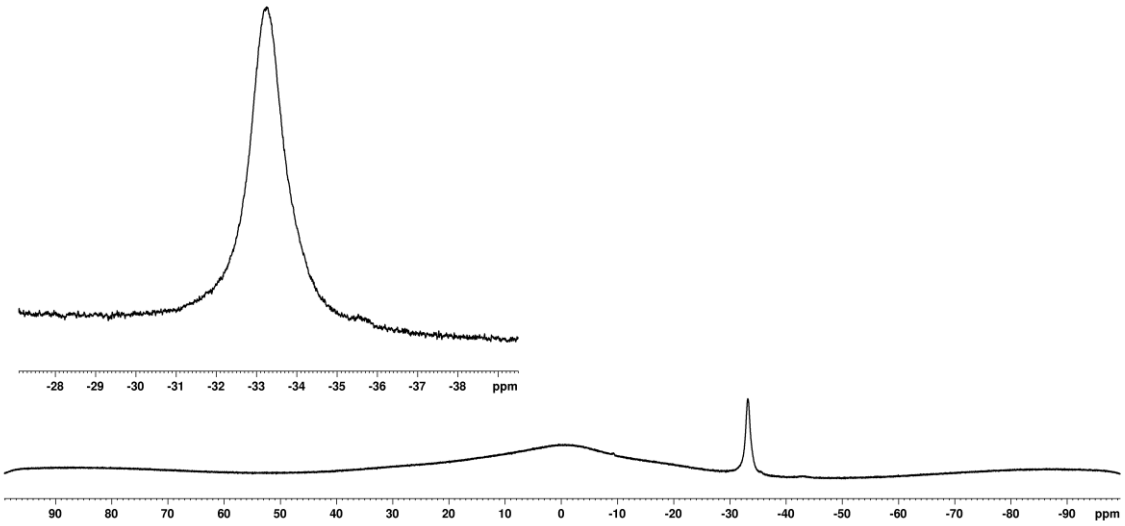

Figure S 6.39: $^{11}B\{^{1}H\}$ NMR spectrum of IDipp·$BH_2P(SiMe_3)_2$ (C_6D_6, 298 K).

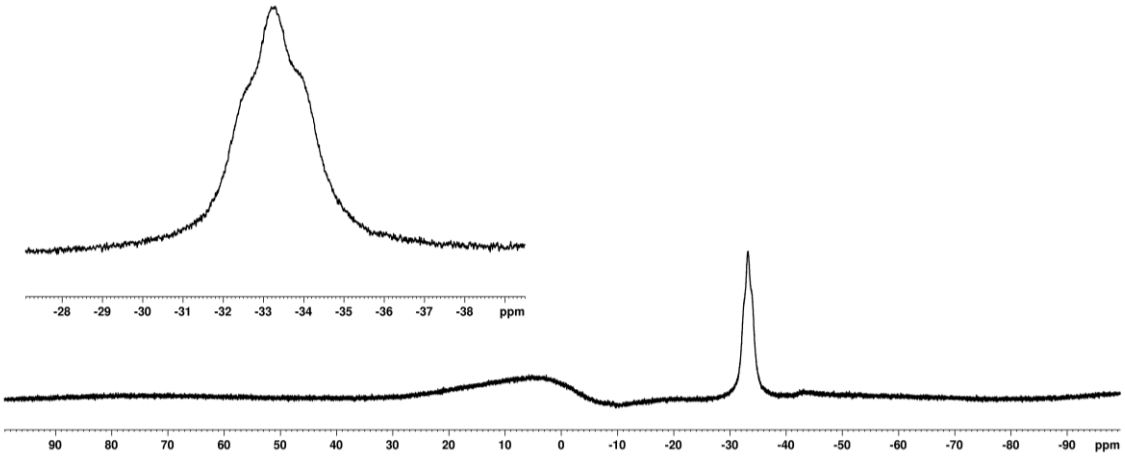

Figure S 6.40: ^{11}B NMR spectrum of IDipp·$BH_2P(SiMe_3)_2$ (C_6D_6, 298 K).

6.5.3.11 [(IDipp·BH_2PPh_2)Ni(CO)$_3$]

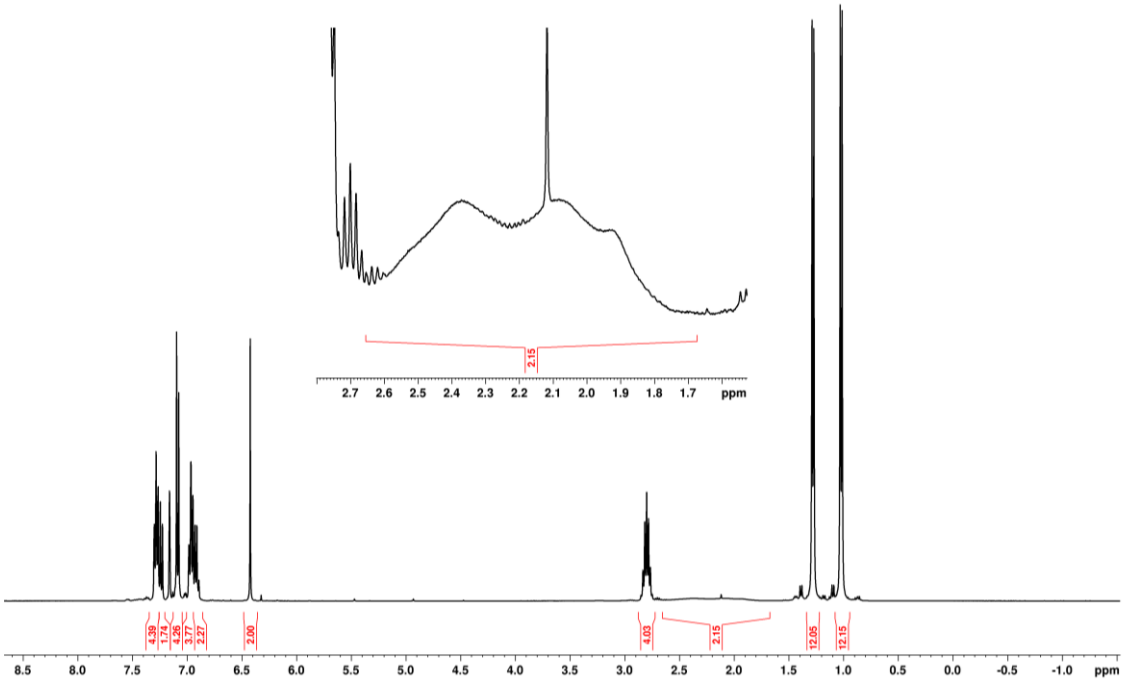

Figure S 6.41: ^{1}H NMR spectrum of [(IDipp·BH_2PPh_2)Ni(CO)$_3$] (C_6D_6, 298 K).

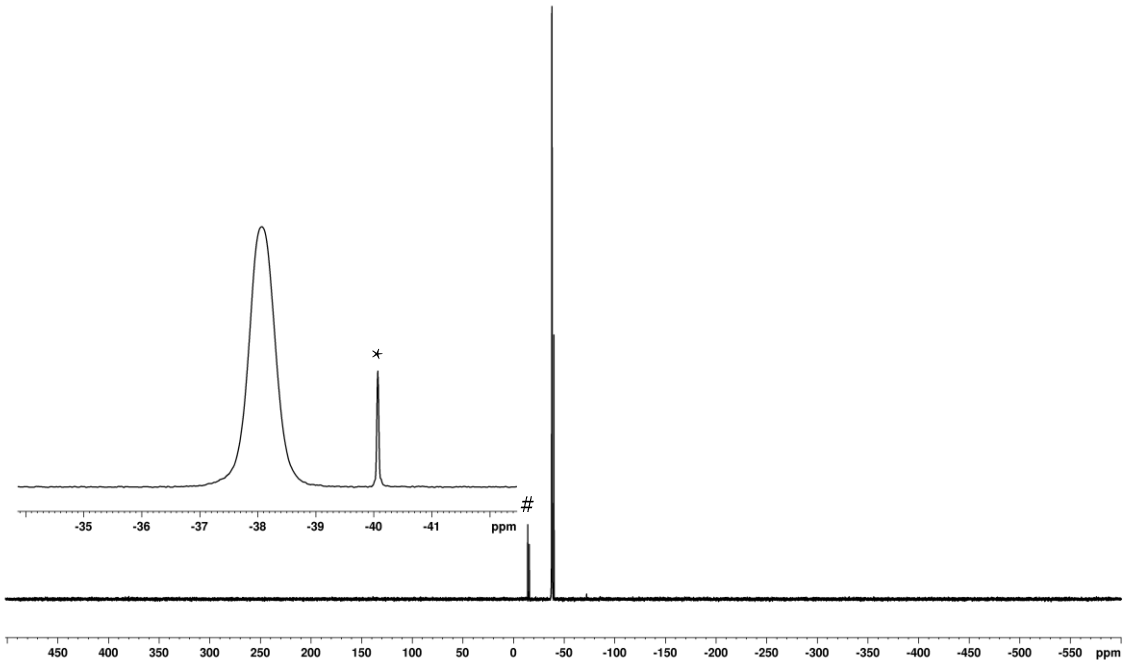

Figure S 6.42: ^{31}P{^{1}H} NMR spectrum of [(IDipp·BH_2PPh_2)Ni(CO)$_3$] (C_6D_6, 298 K; * = $HPPh_2$, # = unidentified impurity).

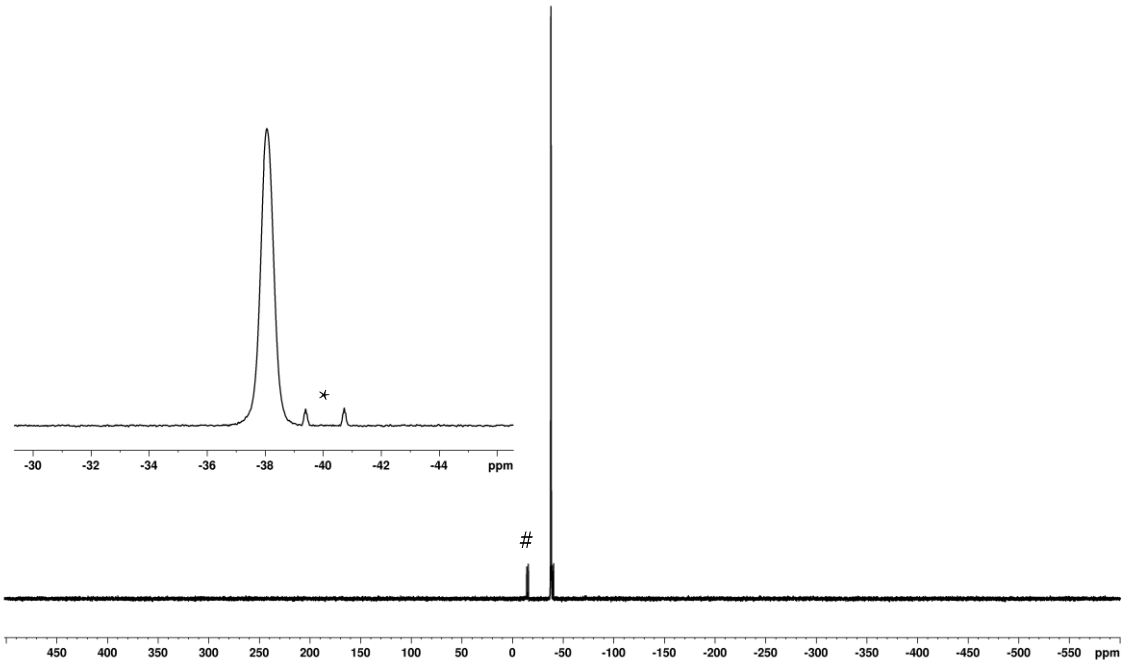

Figure S 6.43: ^{31}P NMR spectrum of [(IDipp·BH_2PPh_2)Ni$(CO)_3$] (C_6D_6, 298 K; * = $HPPh_2$, # = unidentified impurity).

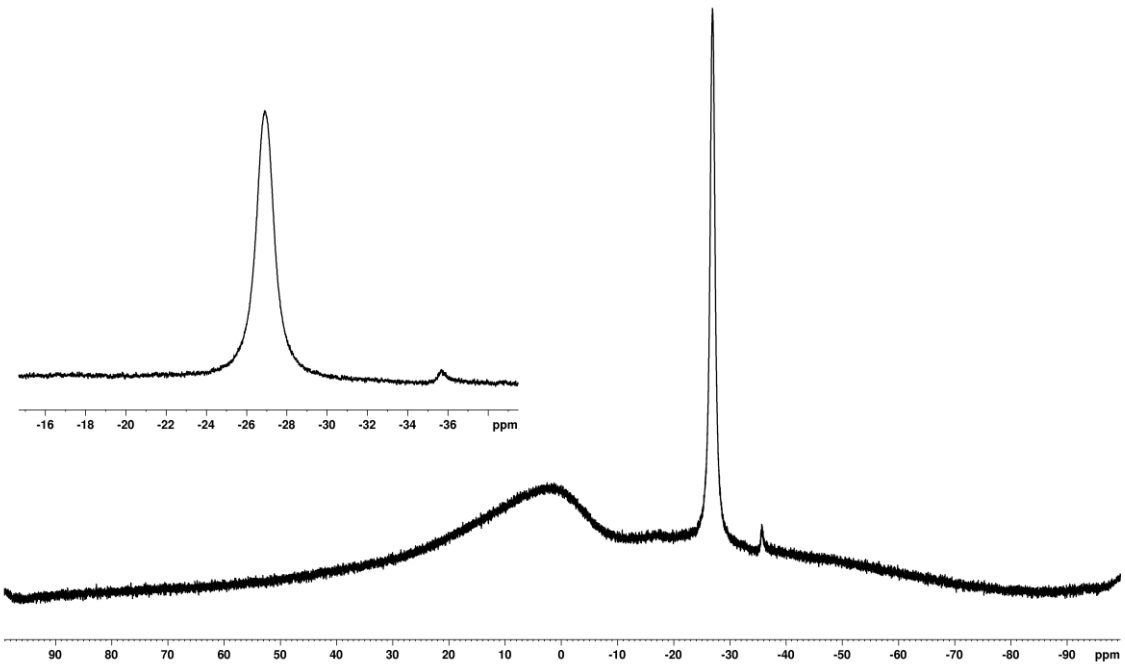

Figure S 6.44: $^{11}B\{^1H\}$ NMR spectrum of [(IDipp·BH_2PPh_2)Ni$(CO)_3$] (C_6D_6, 298 K).

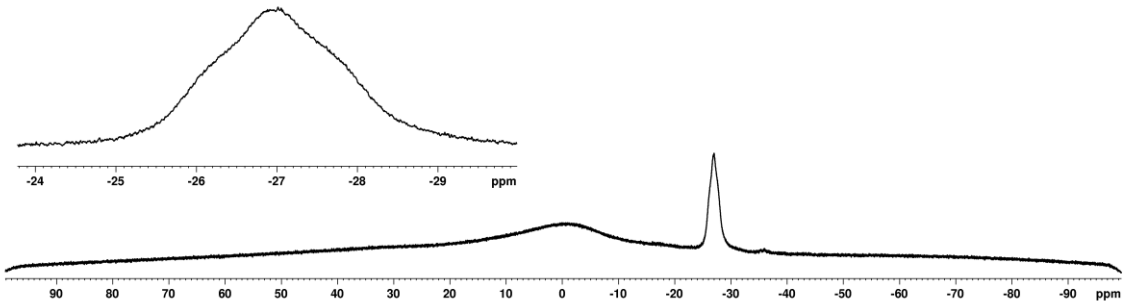

Figure S 6.45: ^{11}B NMR spectrum of [(IDipp·BH_2PPh_2)Ni(CO)$_3$] (C_6D_6, 298 K).

6.5.3.12 [(IDipp·BH_2PMe_2)Ni(CO)$_3$]

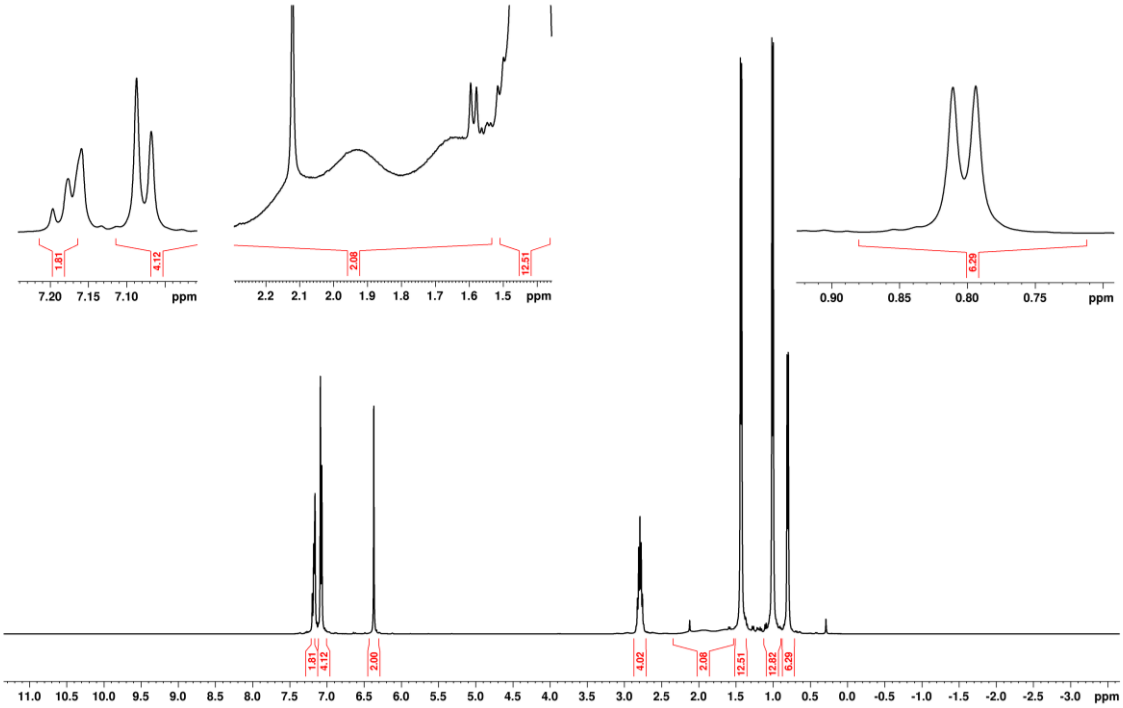

Figure S 6.46: ^{1}H NMR spectrum of [(IDipp·BH_2PMe_2)Ni(CO)$_3$] (C_6D_6, 298 K).

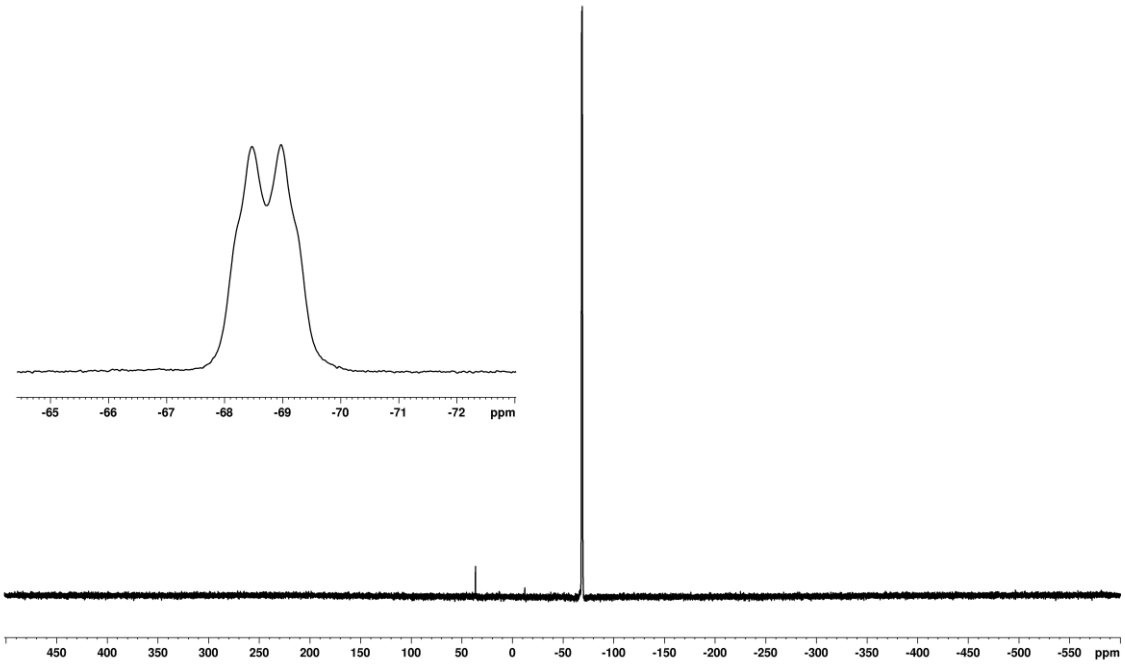

Figure S 6.47: $^{31}P\{^{1}H\}$ NMR spectrum of [(IDipp·BH_2PMe_2)Ni$(CO)_3$] (C_6D_6, 298 K).

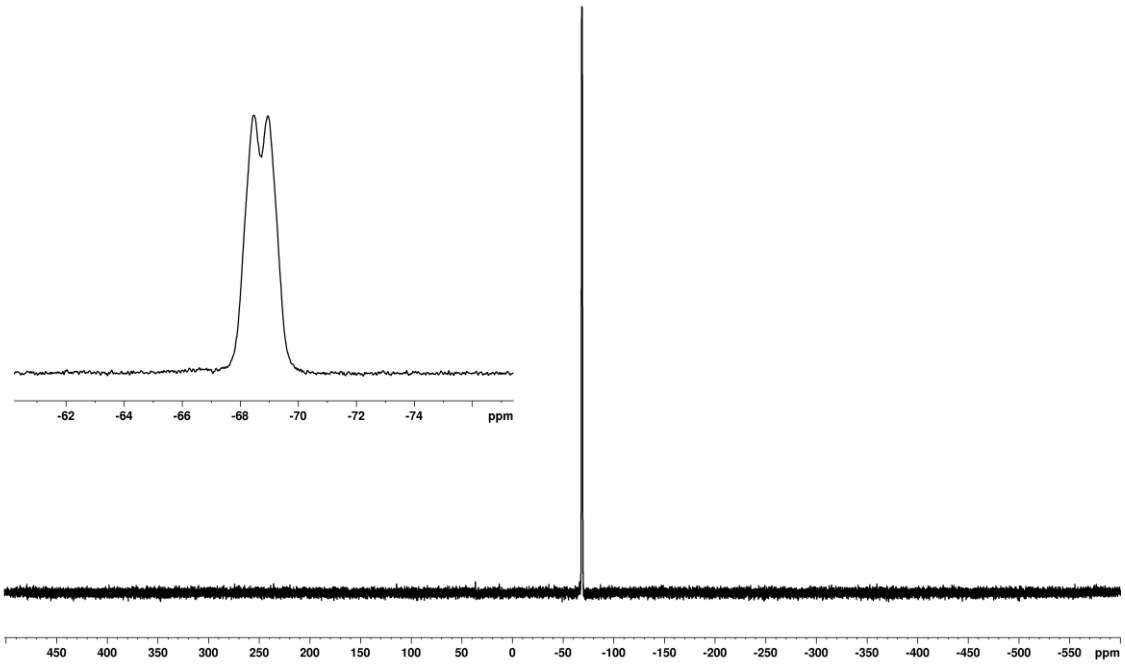

Figure S 6.48: ^{31}P NMR spectrum of [(IDipp·BH_2PMe_2)Ni$(CO)_3$] (C_6D_6, 298 K).

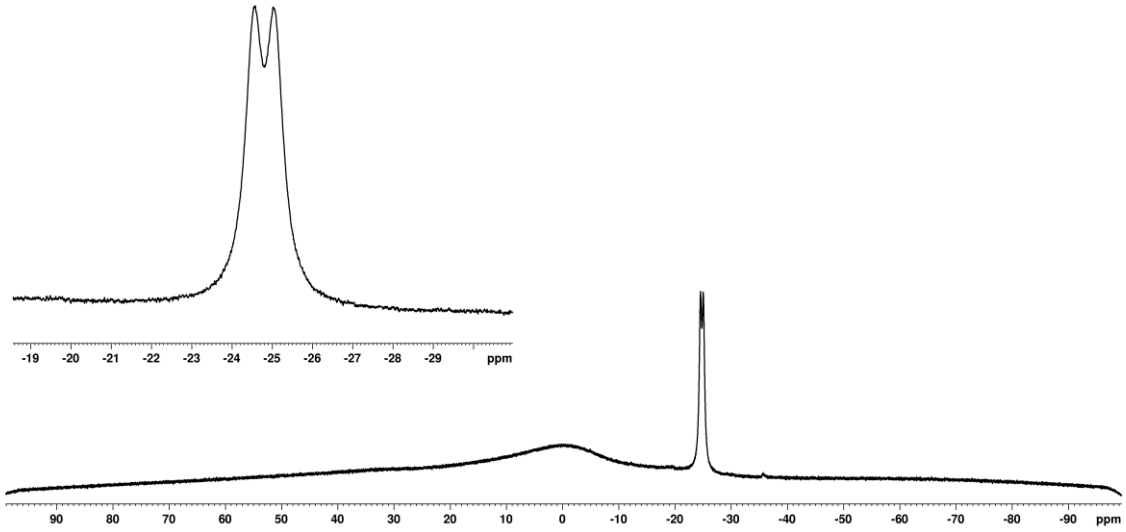

Figure S 6.49: $^{11}B\{^{1}H\}$ NMR spectrum of $[(IDipp{\cdot}BH_2PMe_2)Ni(CO)_3]$ (C_6D_6, 298 K).

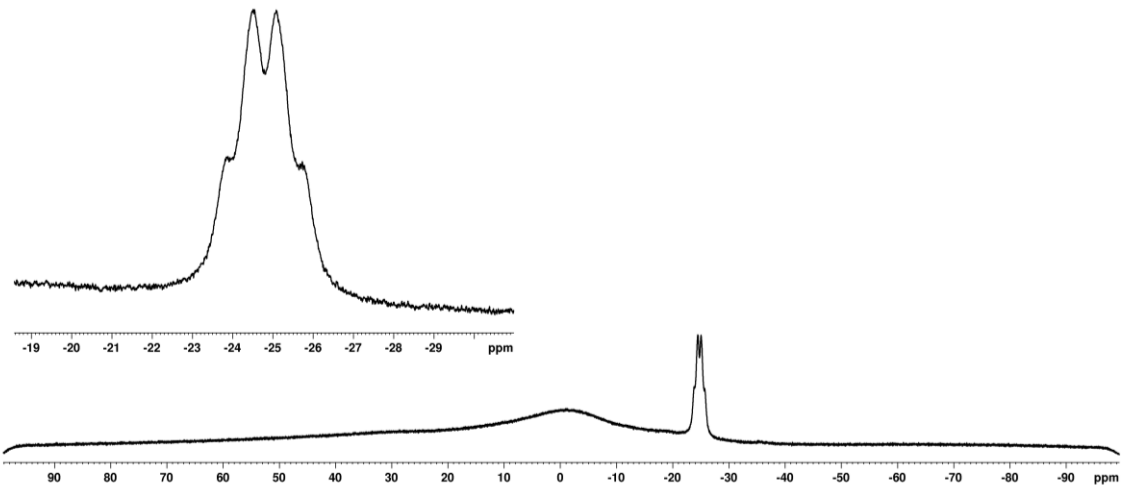

Figure S 6.50: ^{11}B NMR spectrum of $[(IDipp{\cdot}BH_2PMe_2)Ni(CO)_3]$ (C_6D_6, 298 K).

6.5.3.13 [(IDipp·BH_2PH^tBu)Ni$(CO)_3$]

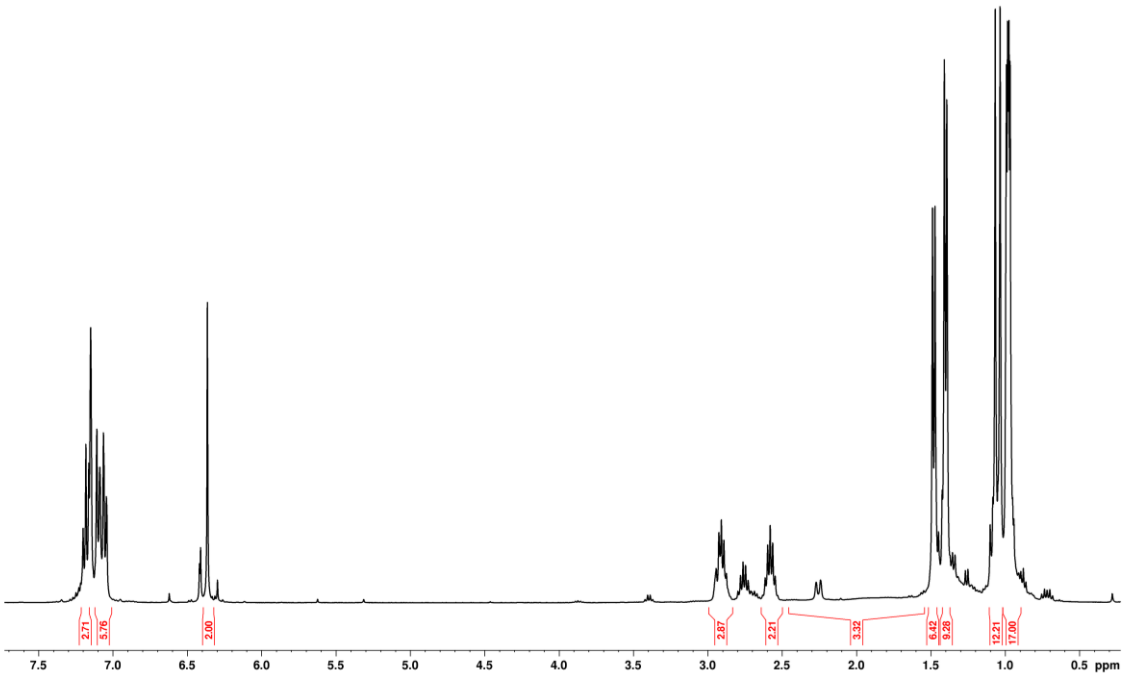

Figure S 6.51: ^{1}H NMR spectrum of [(IDipp·BH_2PH^tBu)Ni$(CO)_3$] (C_6D_6, 298 K). Note: the deviating integral values in the aliphatic region are caused by signal overlap.

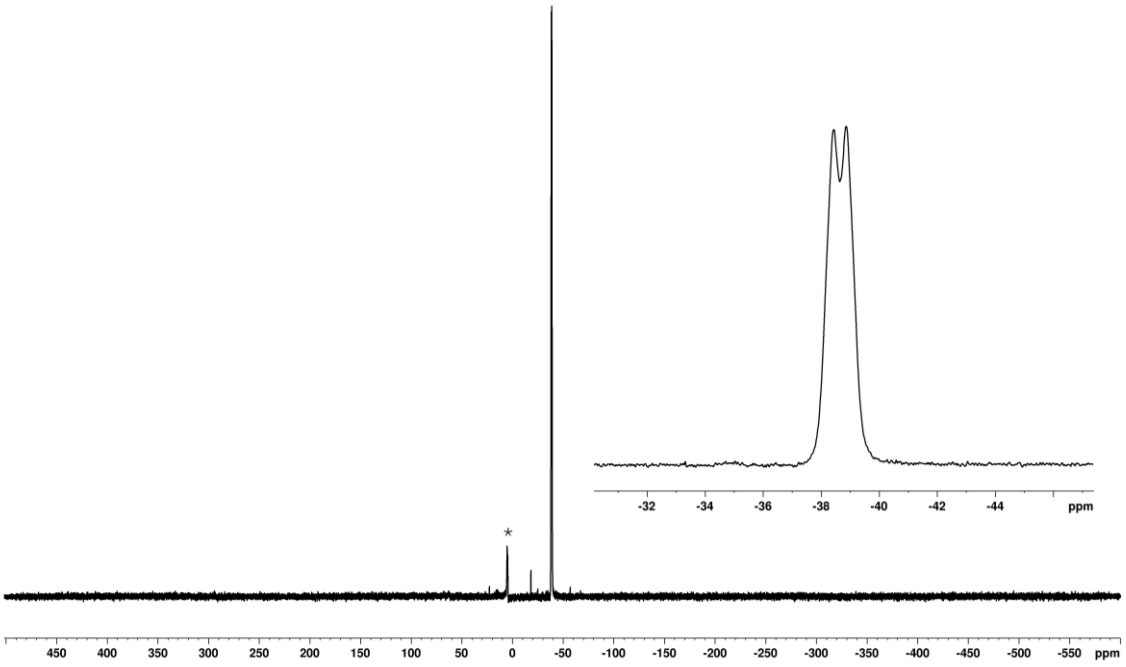

Figure S 6.52: $^{31}P\{^1H\}$ NMR spectrum of [(IDipp·BH_2PH^tBu)Ni$(CO)_3$] (C_6D_6, 298 K; * = unidentified impurity).

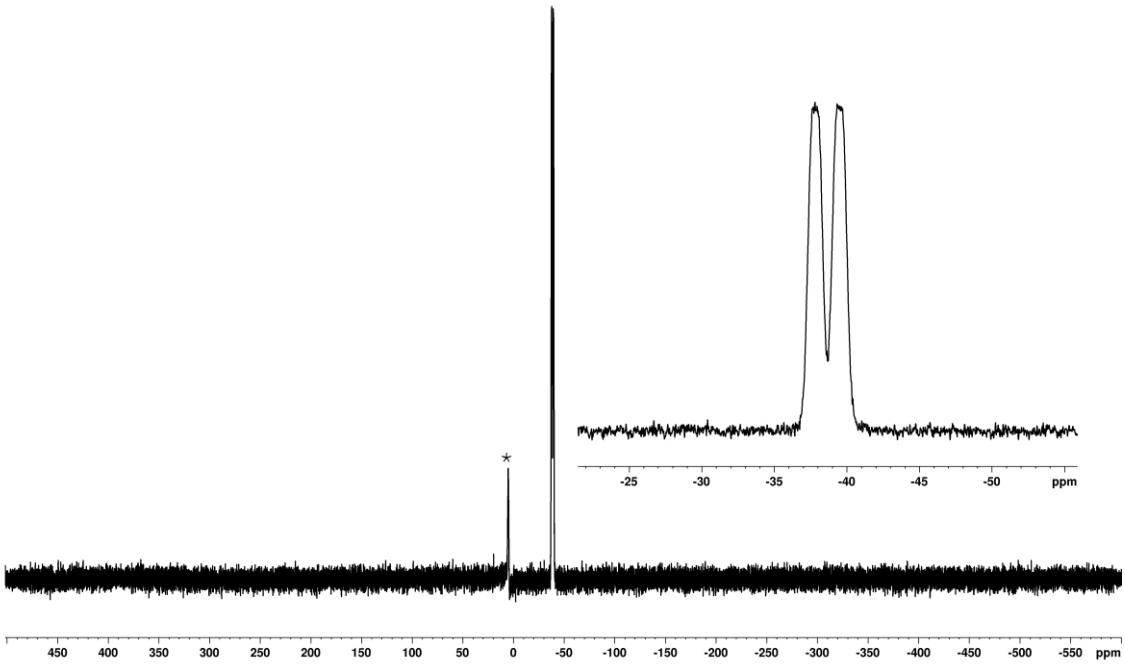

Figure S 6.53: ^{31}P NMR spectrum of [(IDipp·BH_2PH^tBu)Ni$(CO)_3$] (C_6D_6, 298 K; * = unidentified impurity).

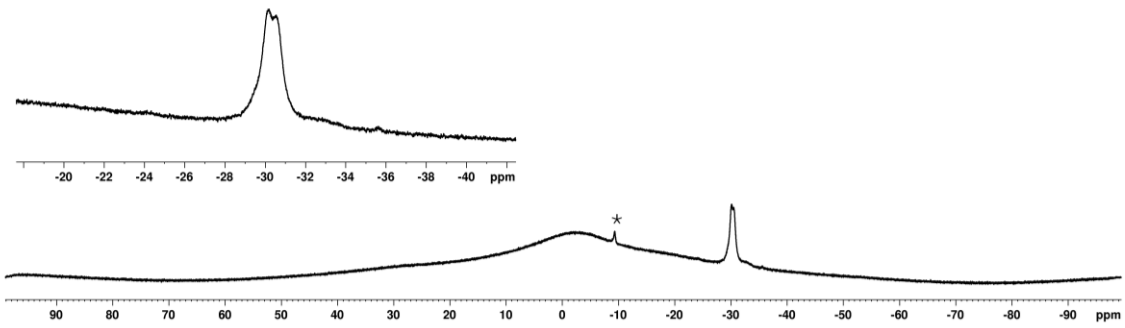

Figure S 6.54: $^{11}B\{^1H\}$ NMR spectrum of [(IDipp·BH_2PH^tBu)Ni$(CO)_3$] (C_6D_6, 298 K; * = unidentified impurity).

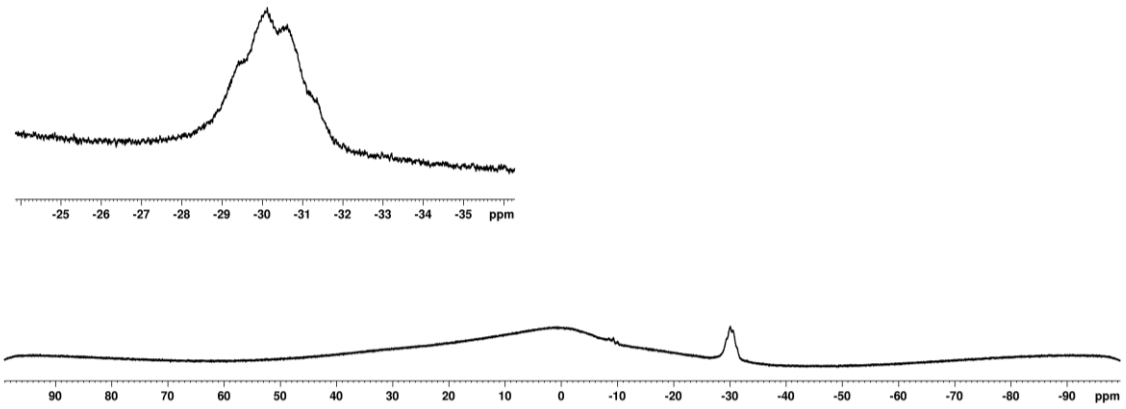

Figure S 6.55: ^{11}B NMR spectrum of [(IDipp·BH_2PH^tBu)Ni(CO)$_3$] (C_6D_6, 298 K).

6.5.3.14 [(IDipp·BH_2PCy_2)Ni(CO)$_3$]

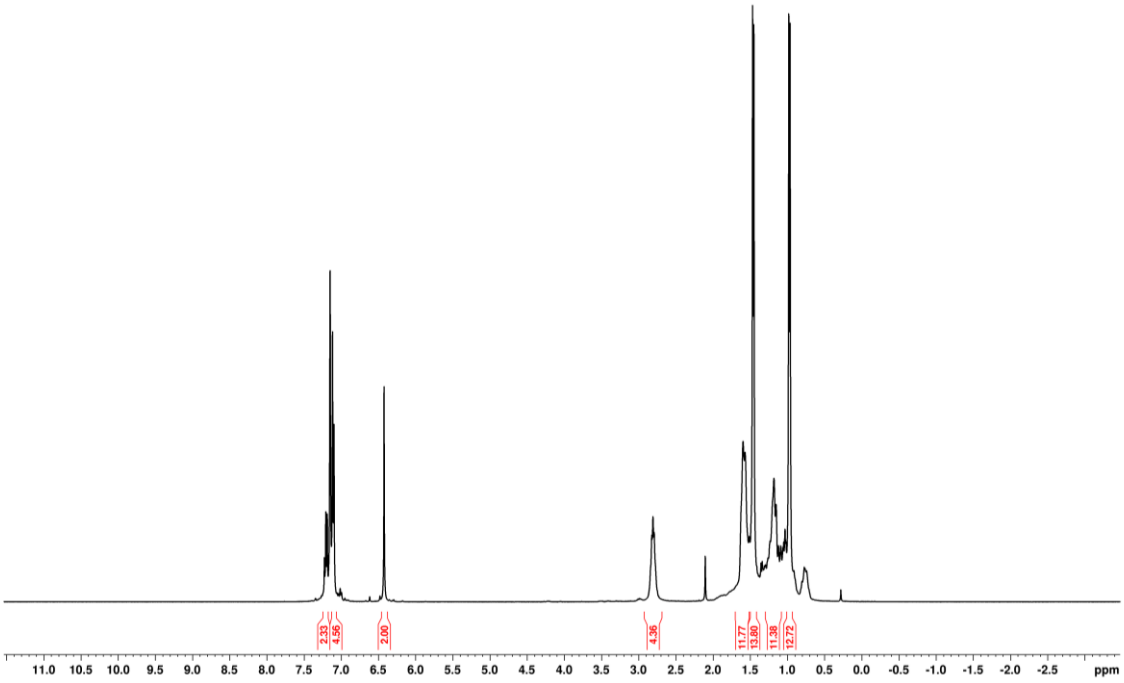

Figure S 6.56: ^{1}H NMR spectrum of [(IDipp·BH_2PCy_2)Ni(CO)$_3$] (C_6D_6, 298 K).

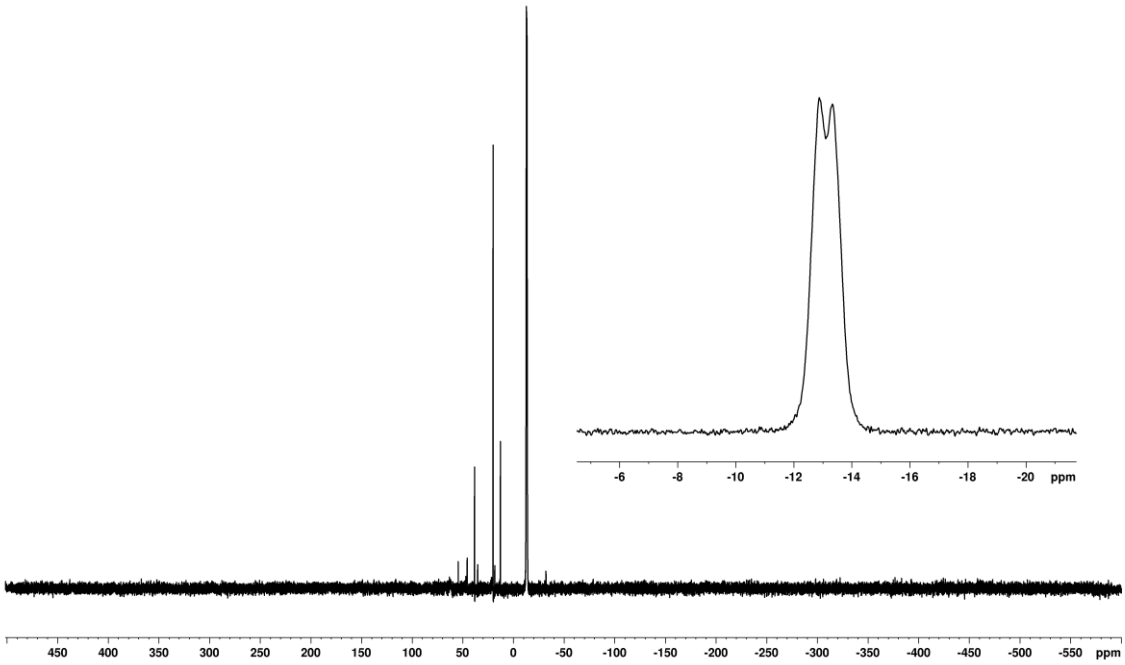

Figure S 6.57: $^{31}P\{^{1}H\}$ NMR spectrum of $[(IDipp{\cdot}BH_2PCy_2)Ni(CO)_3]$ (C_6D_6, 298 K).

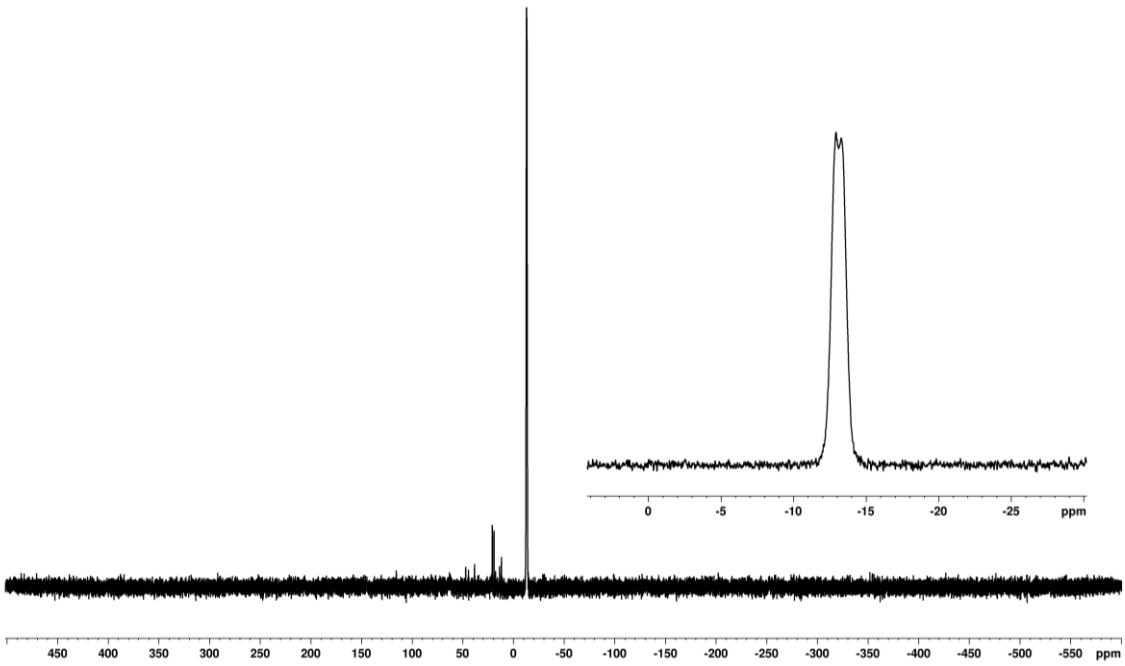

Figure S 6.58: ^{31}P NMR spectrum of $[(IDipp{\cdot}BH_2PCy_2)Ni(CO)_3]$ (C_6D_6, 298 K).

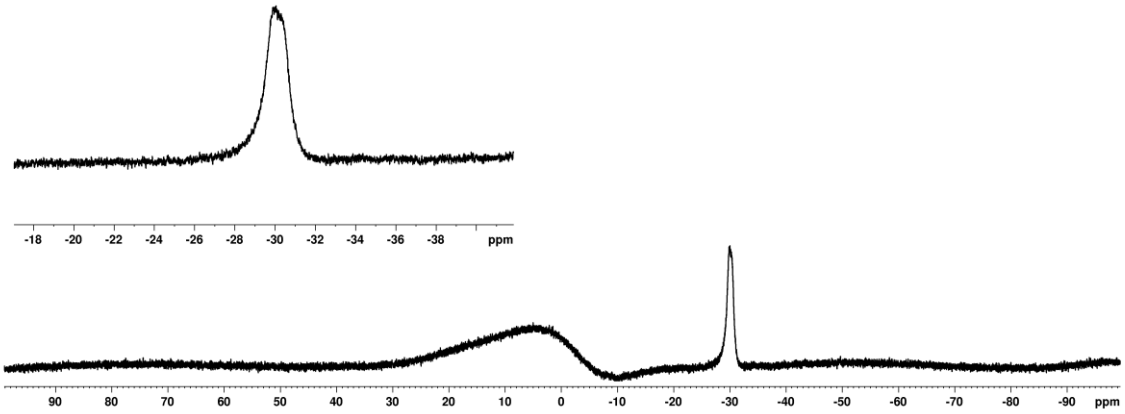

Figure S 6.59: $^{11}B\{^{1}H\}$ NMR spectrum of [(IDipp·BH_2PCy_2)Ni(CO)$_3$] (C_6D_6, 298 K).

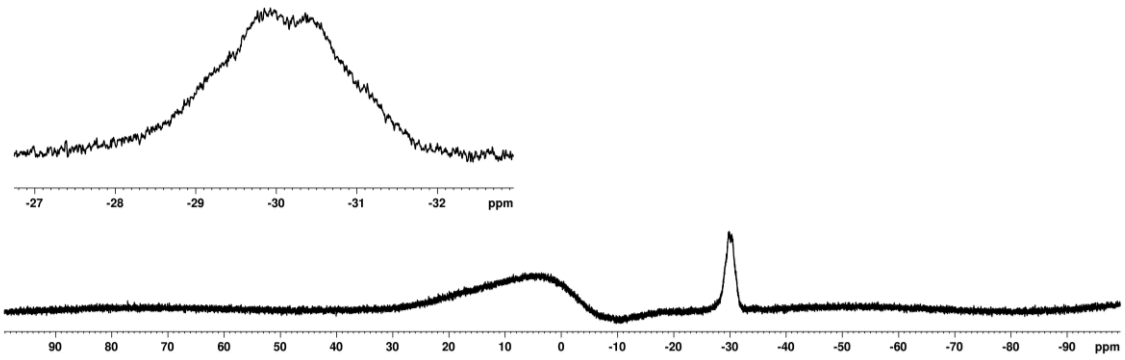

Figure S 6.60: ^{11}B NMR spectrum of [(IDipp·BH_2PCy_2)Ni(CO)$_3$] (C_6D_6, 298 K).

6.5.3.15 [(IDipp·$BH_2P(SiMe_3)_2$)$Ni(CO)_3$]

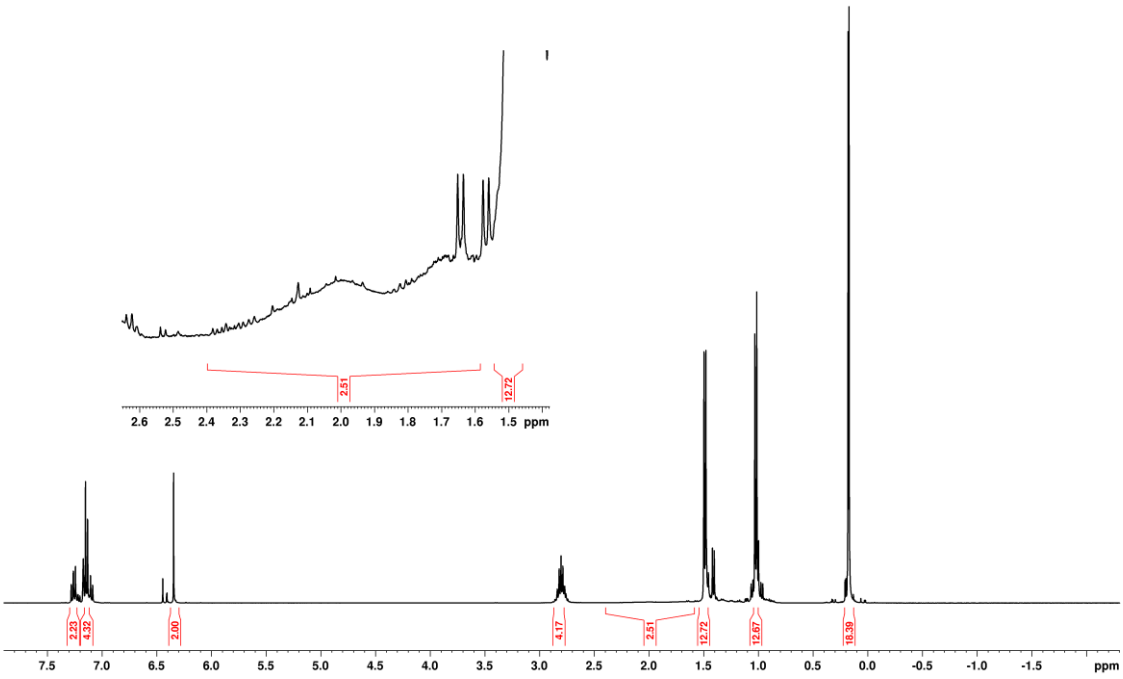

Figure S 6.61: ^1H NMR spectrum of [(IDipp·$BH_2P(SiMe_3)_2$)$Ni(CO)_3$] (C_6D_6, 298 K).

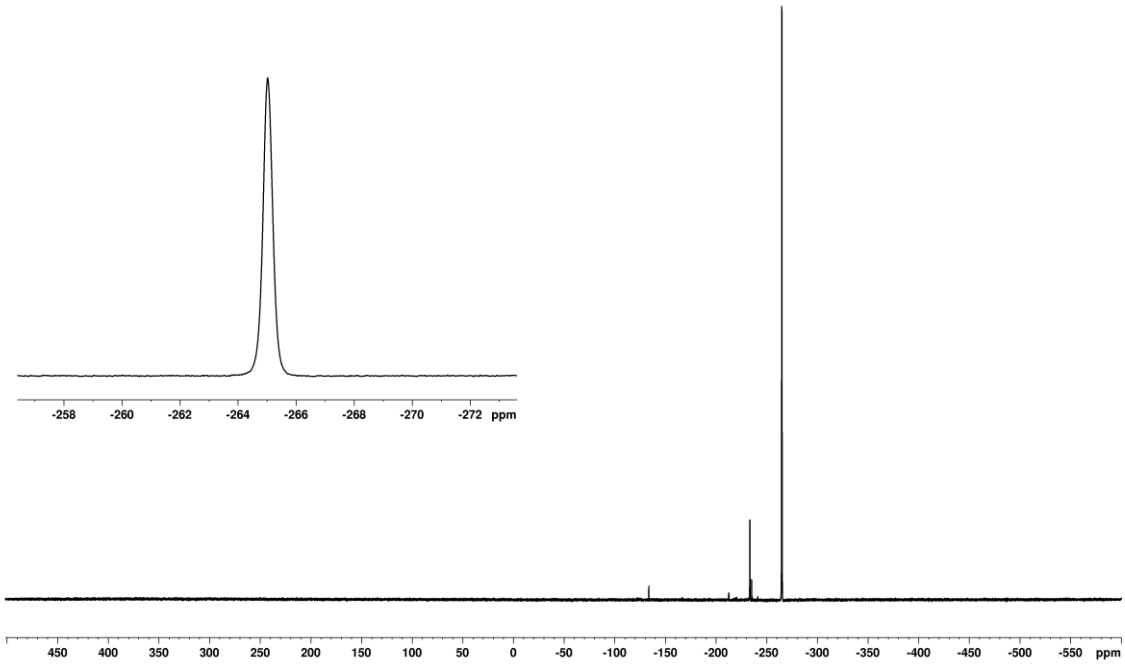

Figure S 6.62: $^{31}P\{^1H\}$ NMR spectrum of [(IDipp·$BH_2P(SiMe_3)_2$)$Ni(CO)_3$] (C_6D_6, 298 K).

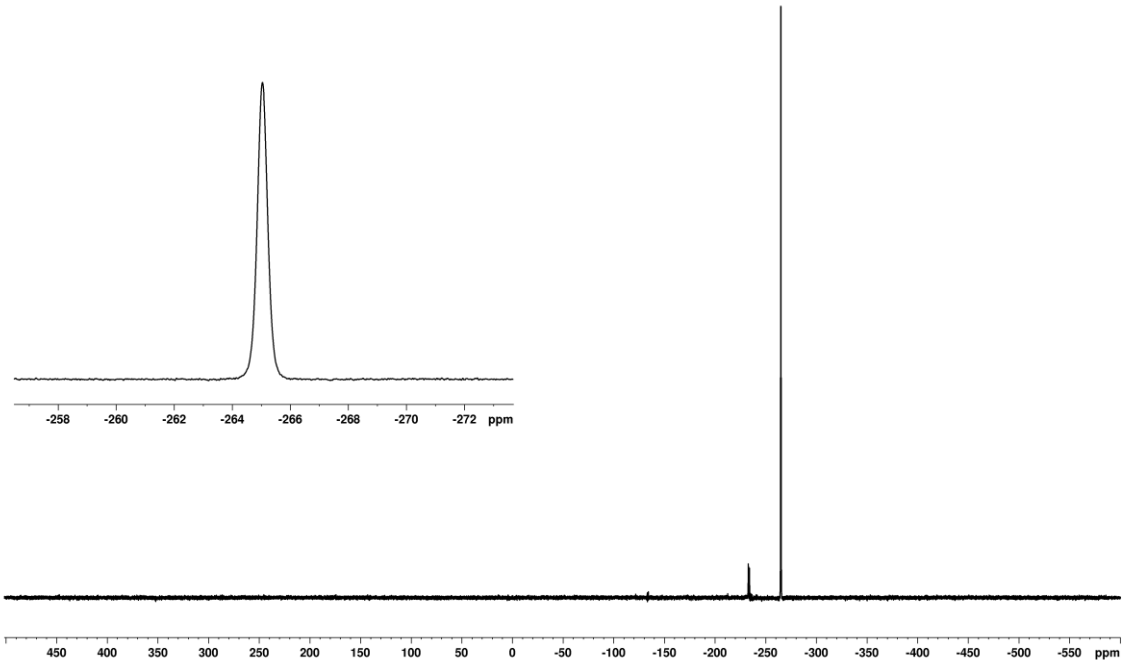

Figure S 6.63: ^{31}P NMR spectrum of [(IDipp·$BH_2P(SiMe_3)_2$)Ni$(CO)_3$] (C_6D_6, 298 K).

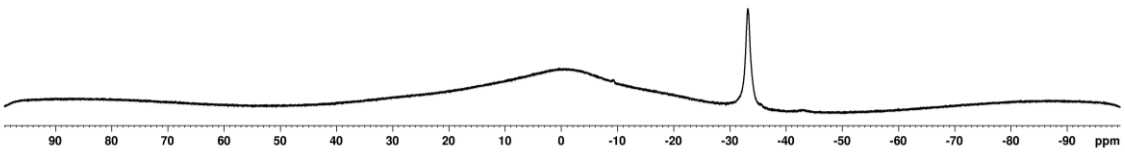

Figure S 6.64: $^{11}B\{^1H\}$ NMR spectrum of [(IDipp·$BH_2P(SiMe_3)_2$)Ni$(CO)_3$] (C_6D_6, 298 K).

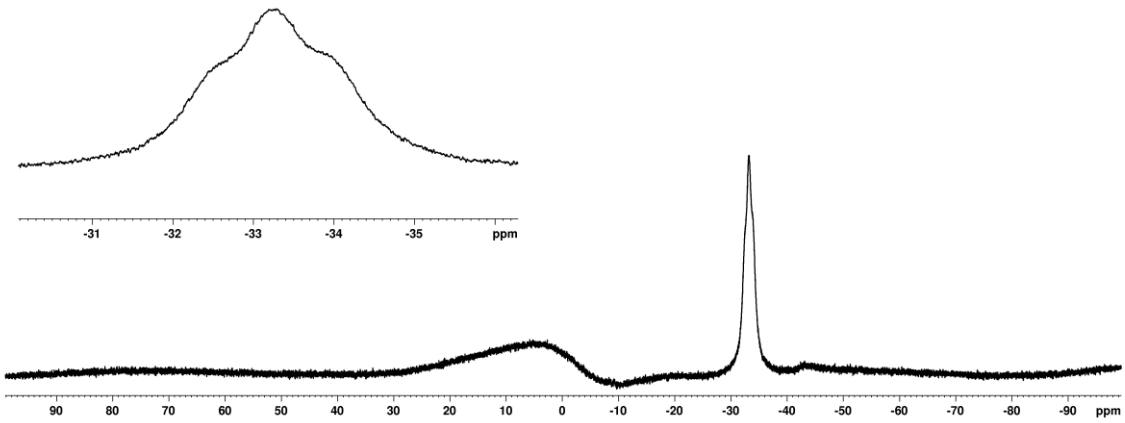

Figure S 6.65: ^{11}B NMR spectrum of [(IDipp·$BH_2P(SiMe_3)_2$)Ni$(CO)_3$] (C_6D_6, 298 K).

6.5.3.16 [(IDipp·BH_2AsPh_2)Ni$(CO)_3$]

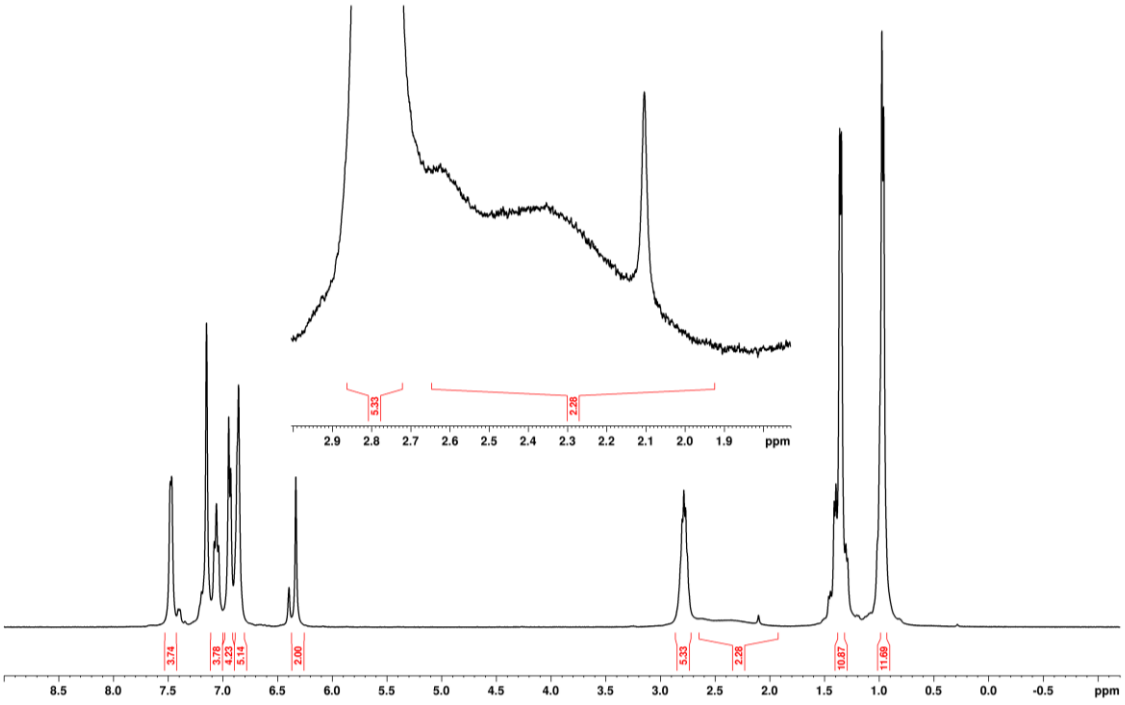

Figure S 6.66: ^{1}H NMR spectrum of [(IDipp·BH_2AsPh_2)Ni$(CO)_3$] (C_6D_6, 298 K).

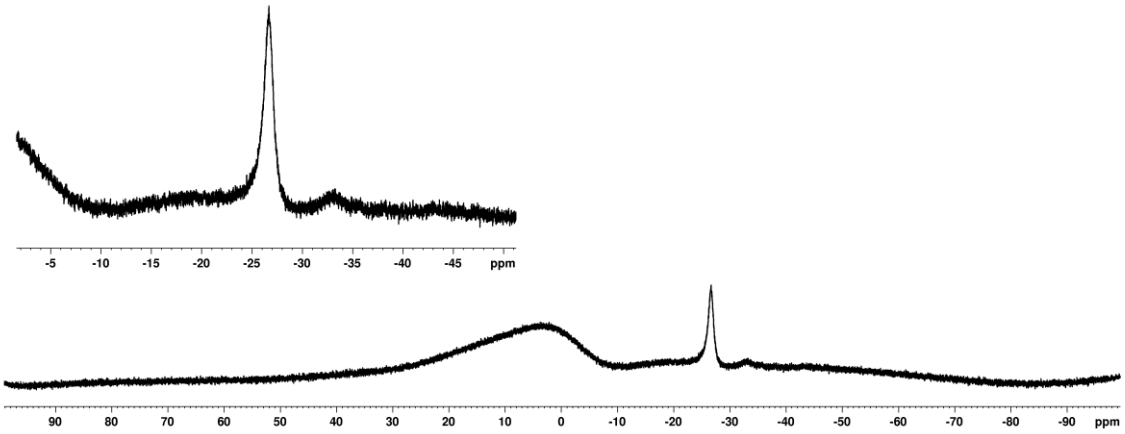

Figure S 6.67: $^{11}B\{^{1}H\}$ NMR spectrum of [(IDipp·BH_2AsPh_2)Ni$(CO)_3$] (C_6D_6, 298 K).

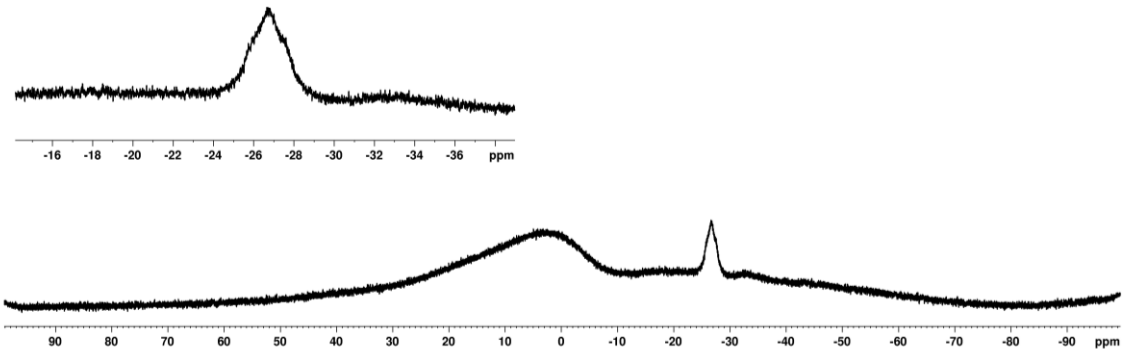

Figure S 6.68: ^{11}B NMR spectrum of [(IDipp·BH_2AsPh_2)Ni$(CO)_3$] (C_6D_6, 298 K).

6.5.3.17 [(IDipp·BH_2AsH_2)Ni(CO)$_3$]

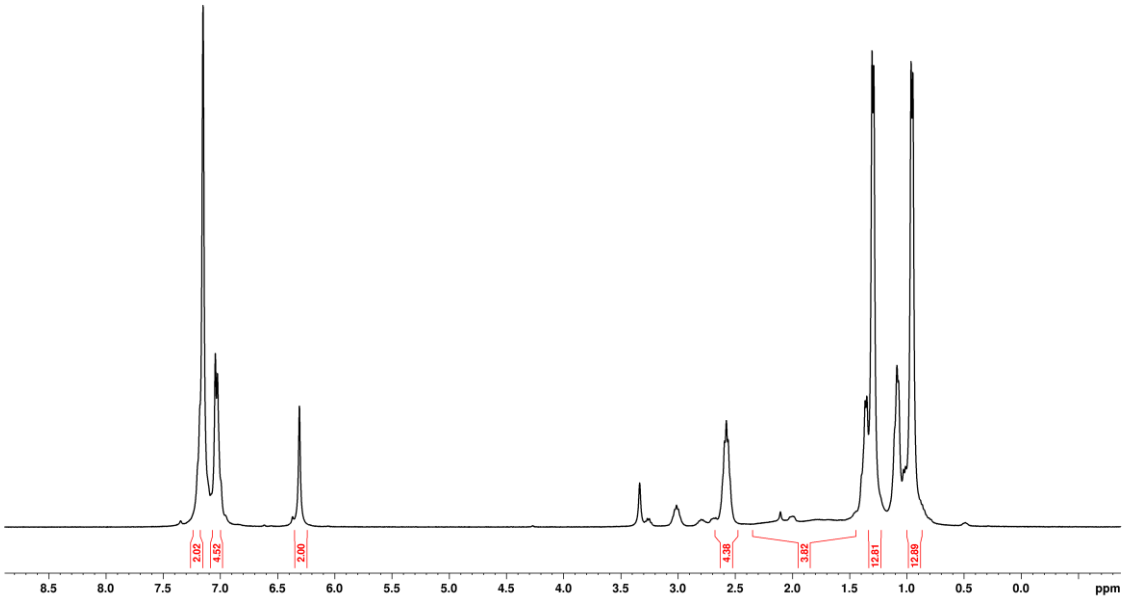

Figure S 6.69: ^{1}H NMR spectrum of [(IDipp·BH_2AsH_2)Ni(CO)$_3$] (C_6D_6, 298 K).

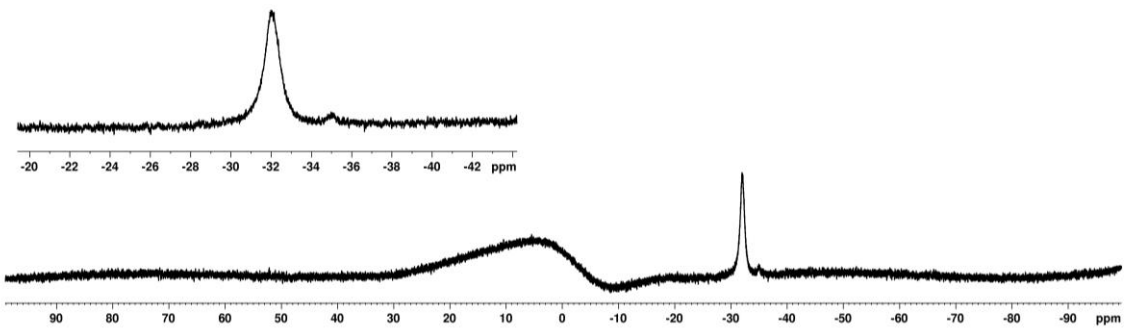

Figure S 6.70: ^{11}B{^{1}H} NMR spectrum of [(IDipp·BH_2AsH_2)Ni(CO)$_3$] (C_6D_6, 298 K).

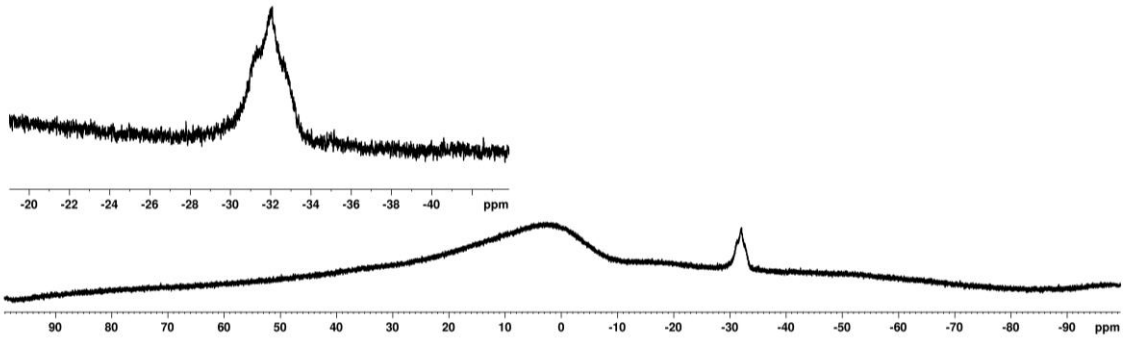

Figure S 6.71: ^{11}B NMR spectrum of [(IDipp·BH_2AsH_2)Ni(CO)$_3$] (C_6D_6, 298 K).

6.5.3.18 [(IDipp·GaH_2PH_2)Ni(CO)$_3$]

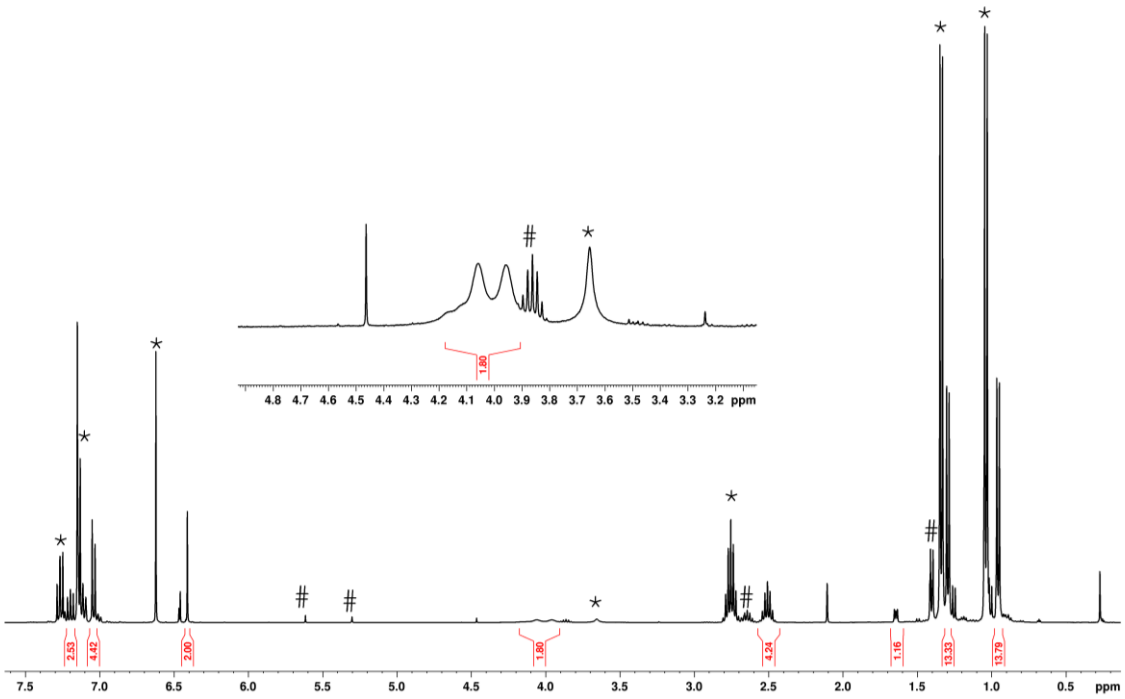

Figure S 6.72: ^{1}H NMR spectrum of [(IDipp·GaH_2PH_2)Ni(CO)$_3$] (C_6D_6, 298 K; # = IDipp-H_2, * = IDipp·GaH_3).

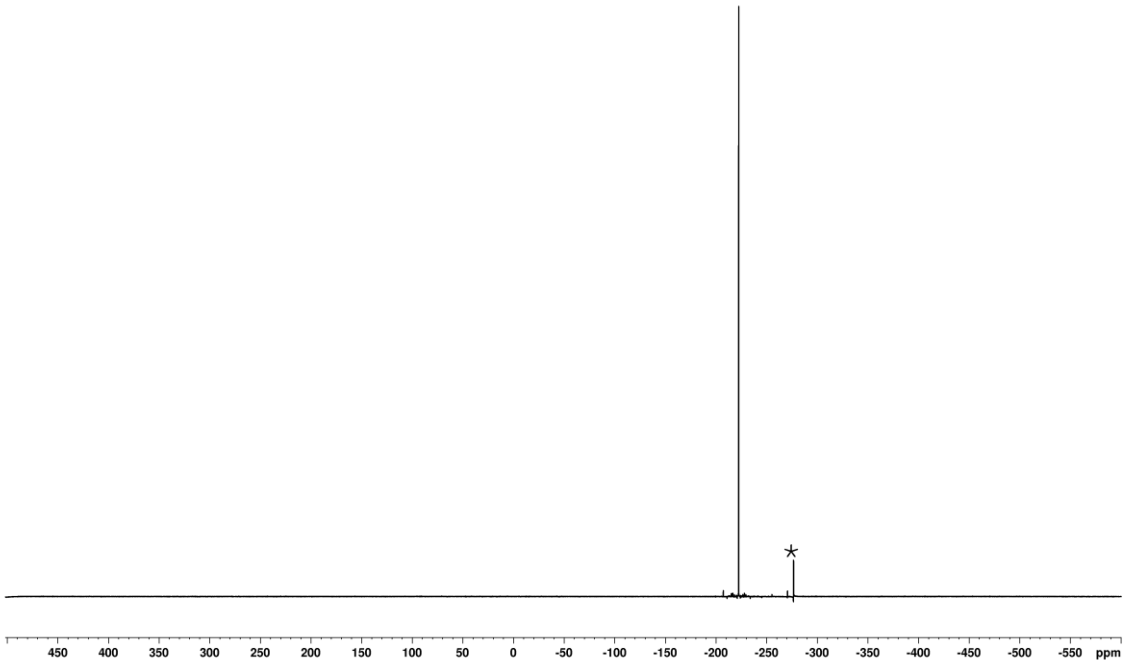

Figure S 6.73: $^{31}P\{^{1}H\}$ NMR spectrum of [(IDipp·GaH_2PH_2)Ni(CO)$_3$] (C_6D_6, 298 K; * = IDipp·GaH_2PH_2).

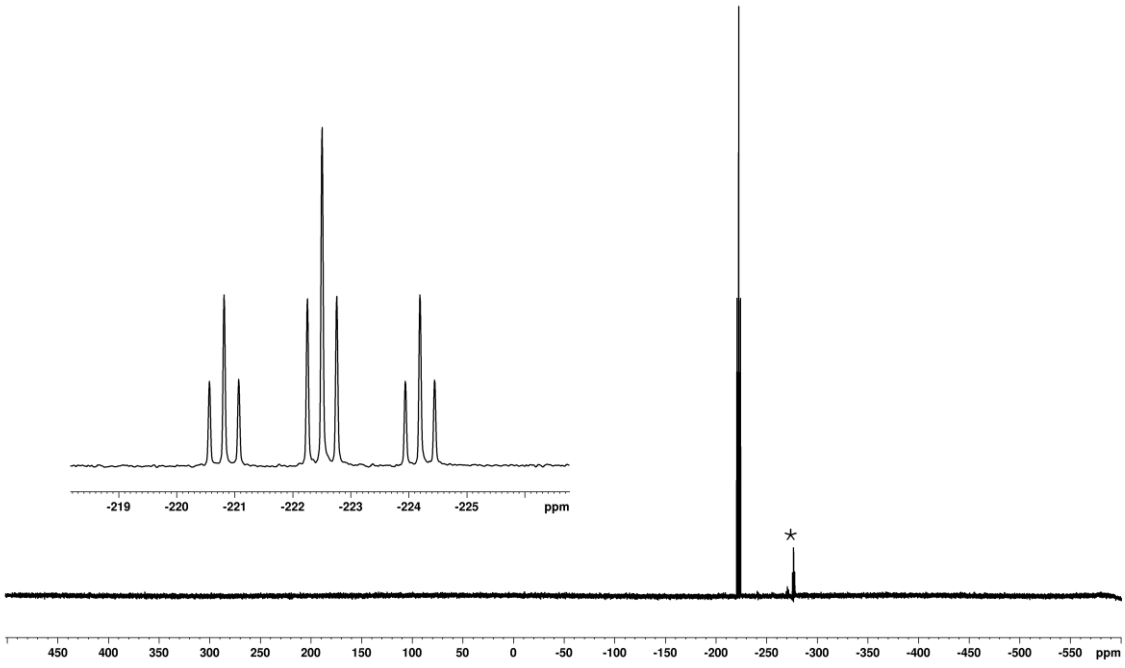

Figure S 6.74: ^{31}P NMR spectrum of [(IDipp·GaH_2PH_2)Ni(CO)$_3$] (C_6D_6, 298 K; * = IDipp·GaH_2PH_2).

6.5.3.19 [(Me$_3$N·BH$_2$PPh$_2$)Ni(CO)$_3$]

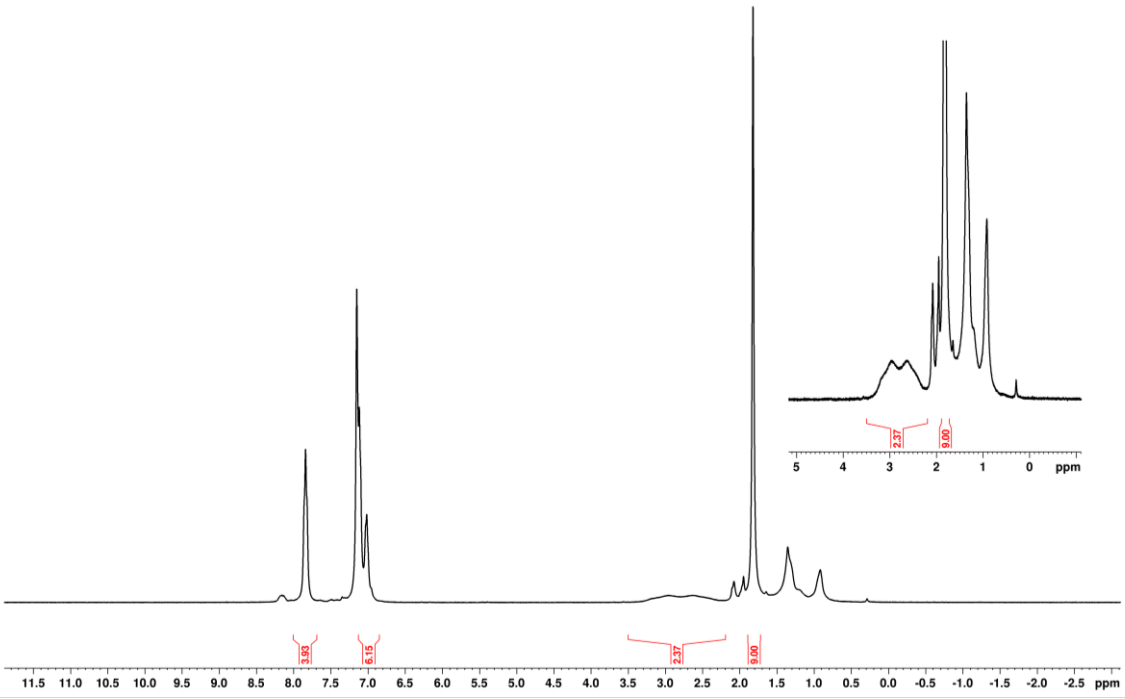

Figure S 6.75: ^{1}H NMR spectrum of [(Me$_3$N·BH$_2$PPh$_2$)Ni(CO)$_3$] (C$_6$D$_6$, 298 K).

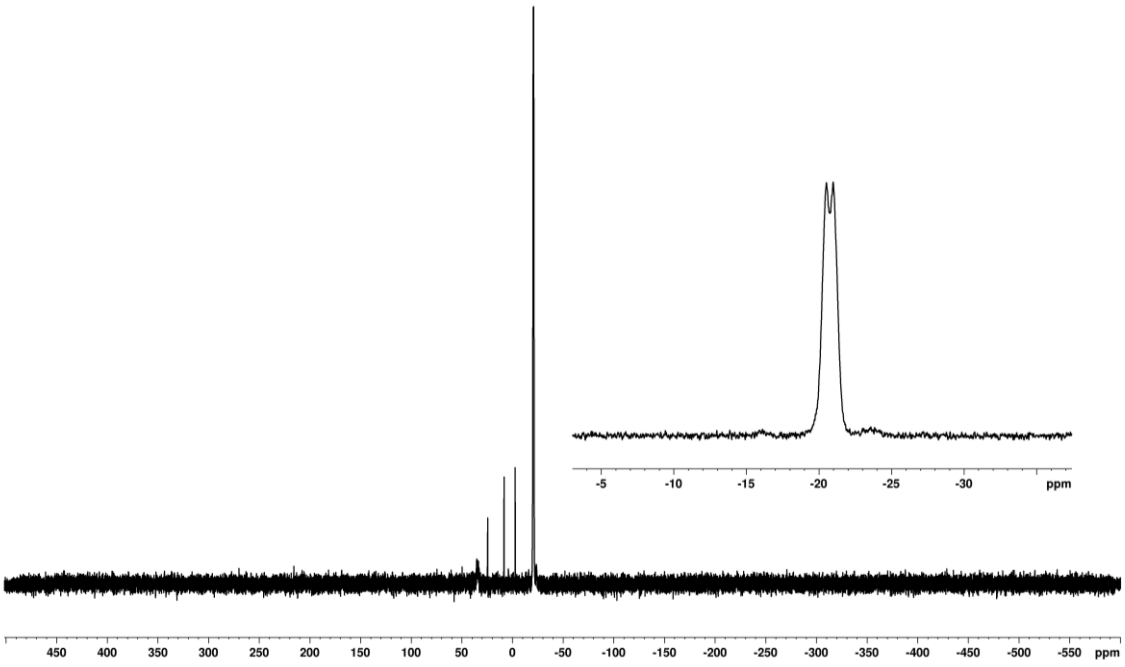

Figure S 6.76: ^{31}P{^{1}H} NMR spectrum of [(Me$_3$N·BH$_2$PPh$_2$)Ni(CO)$_3$] (C$_6$D$_6$, 298 K).

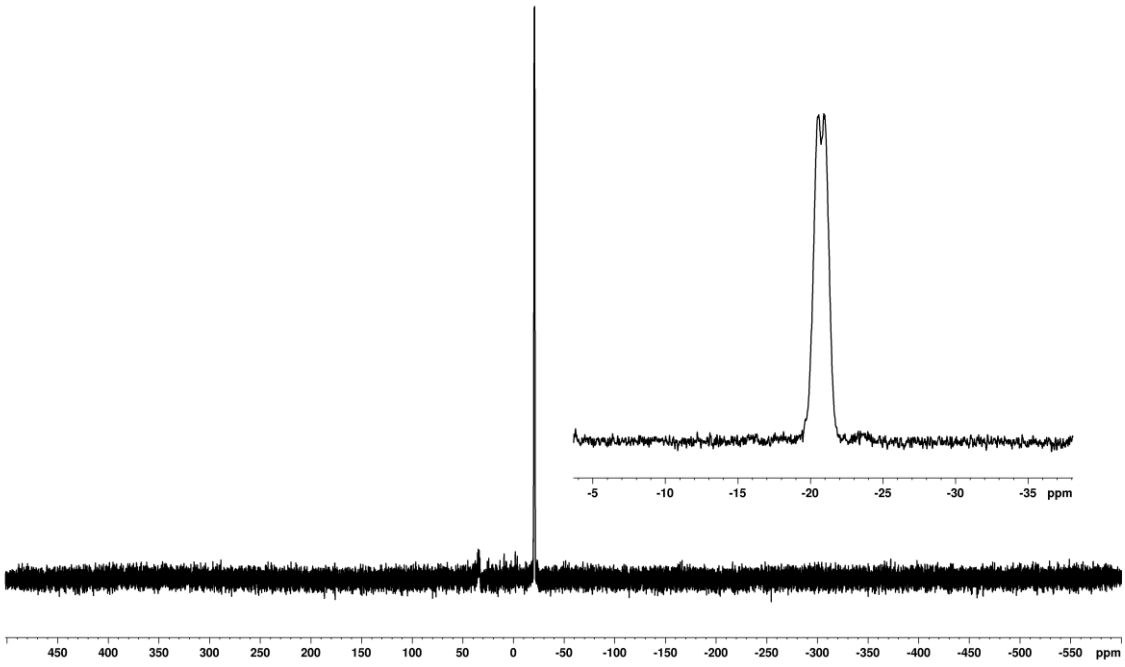

Figure S 6.77: ^{31}P NMR spectrum of $[(Me_3N{\cdot}BH_2PPh_2)Ni(CO)_3]$ (C_6D_6, 298 K).

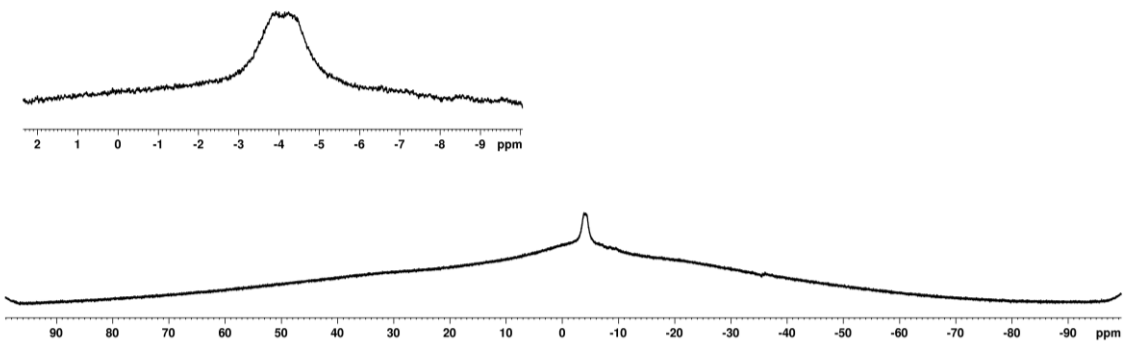

Figure S 6.78: $^{11}B\{^1H\}$ NMR spectrum of $[(Me_3N{\cdot}BH_2PPh_2)Ni(CO)_3]$ (C_6D_6, 298 K).

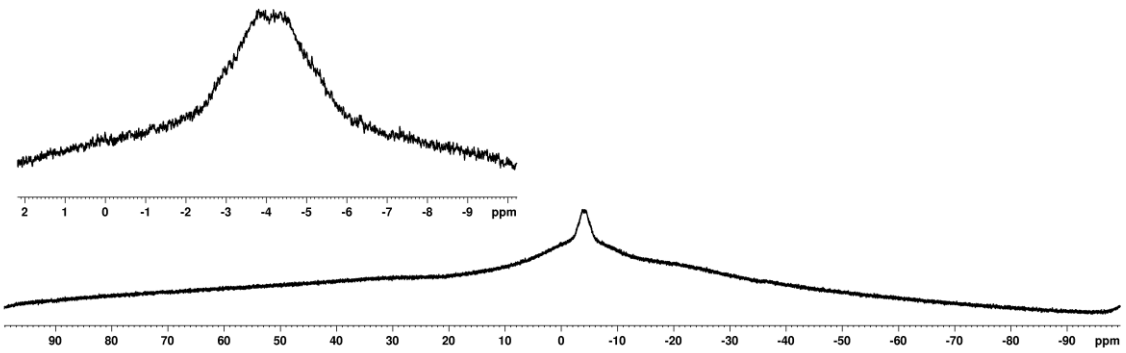

Figure S 6.79: ^{11}B NMR spectrum of $[(Me_3N{\cdot}BH_2PPh_2)Ni(CO)_3]$ (C_6D_6, 298 K).

6.5.3.20 $[(Me_3N{\cdot}BH_2PH_2)Ni(CO)_3]$

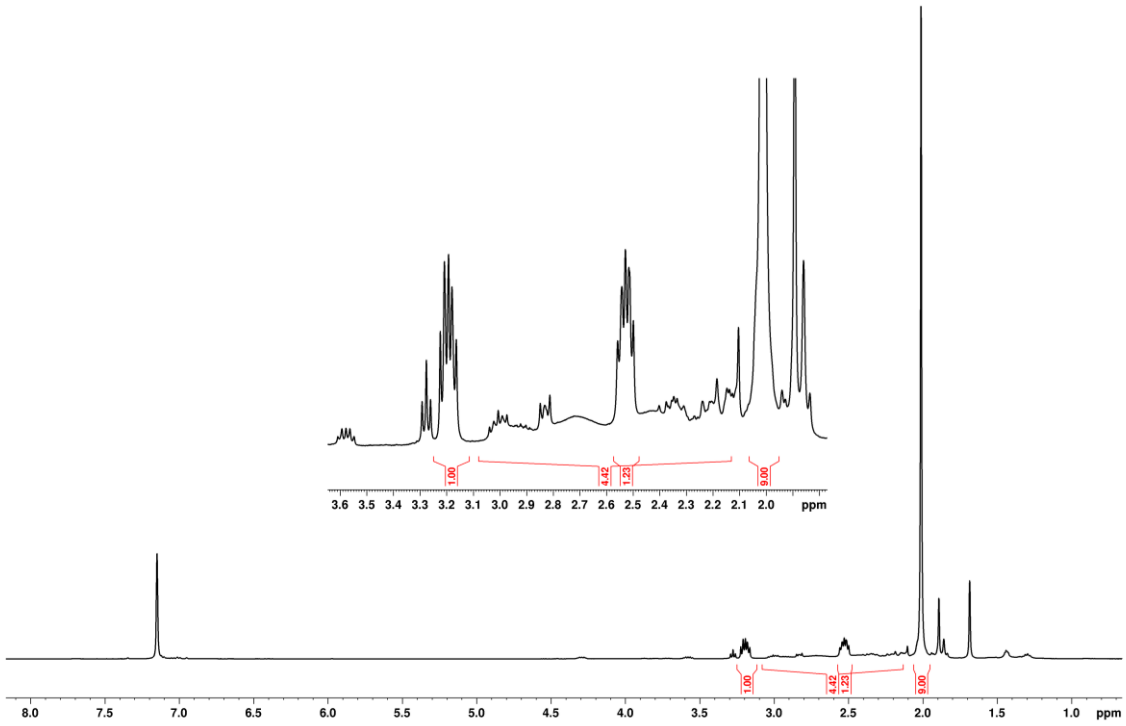

Figure S 6.80: ^{1}H NMR spectrum of $[(Me_3N{\cdot}BH_2PH_2)Ni(CO)_3]$ (C_6D_6, 298 K).

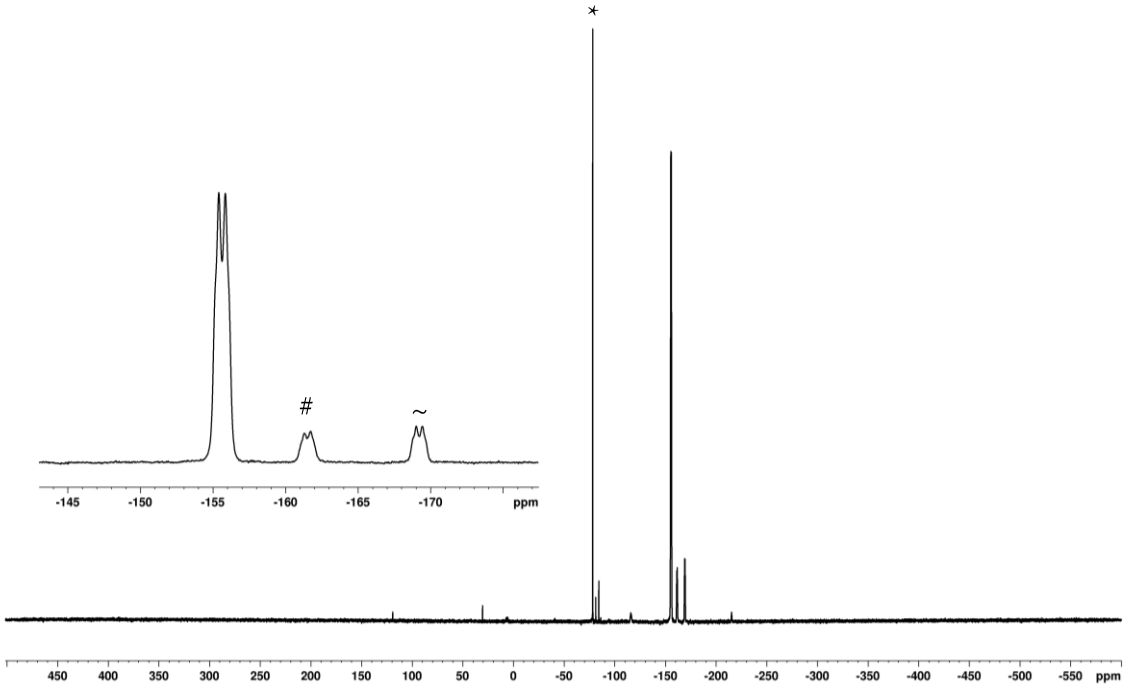

Figure S 6.81: $^{31}P\{^{1}H\}$ NMR spectrum of $[(Me_3N{\cdot}BH_2PH_2)Ni(CO)_3]$ (C_6D_6, 298 K, * = unidentified side product, # = $[(Me_3N{\cdot}BH_2PH_2)_2Ni(CO)_2]$, ~ = $[(Me_3N{\cdot}BH_2PH_2)_3Ni(CO)]$).

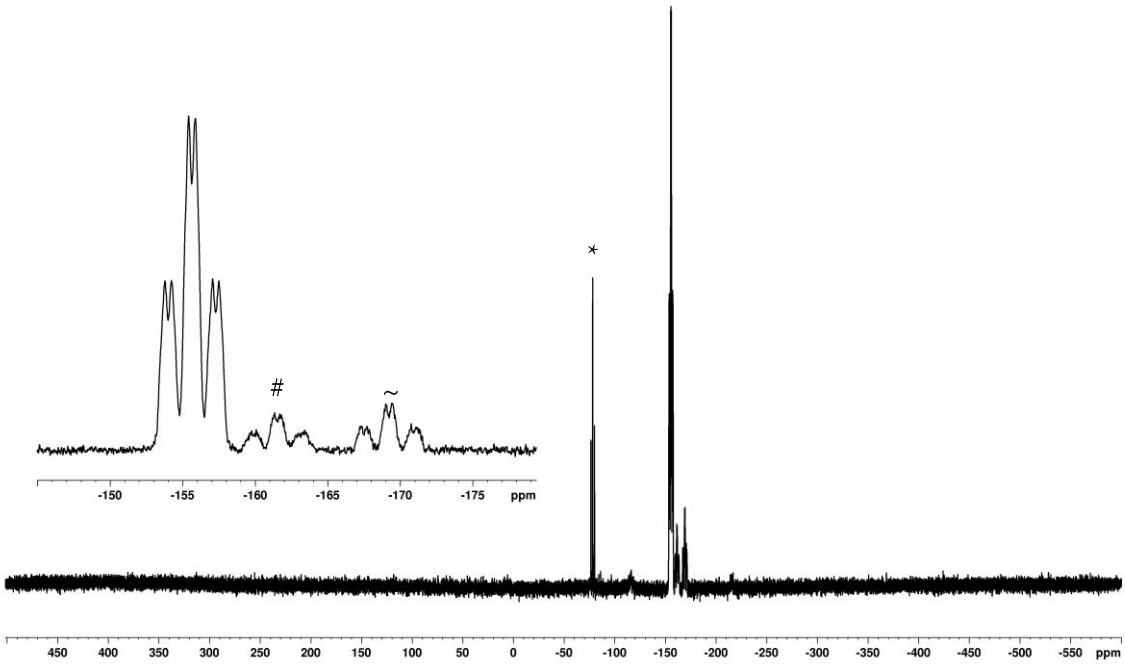

Figure S 6.82: ^{31}P NMR spectrum of $[(Me_3N{\cdot}BH_2PH_2)Ni(CO)_3]$ (C_6D_6, 298 K, * = unidentified side product, # = $[(Me_3N{\cdot}BH_2PH_2)_2Ni(CO)_2]$, ~ = $[(Me_3N{\cdot}BH_2PH_2)_3Ni(CO)]$).

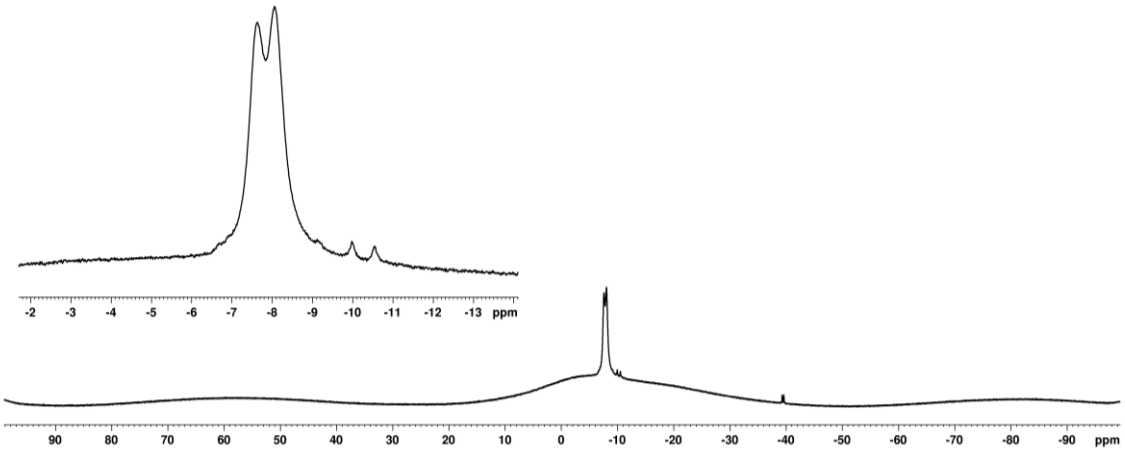

Figure S 6.83: $^{11}B\{^{1}H\}$ NMR spectrum of $[(Me_3N{\cdot}BH_2PH_2)Ni(CO)_3]$ (C_6D_6, 298 K).

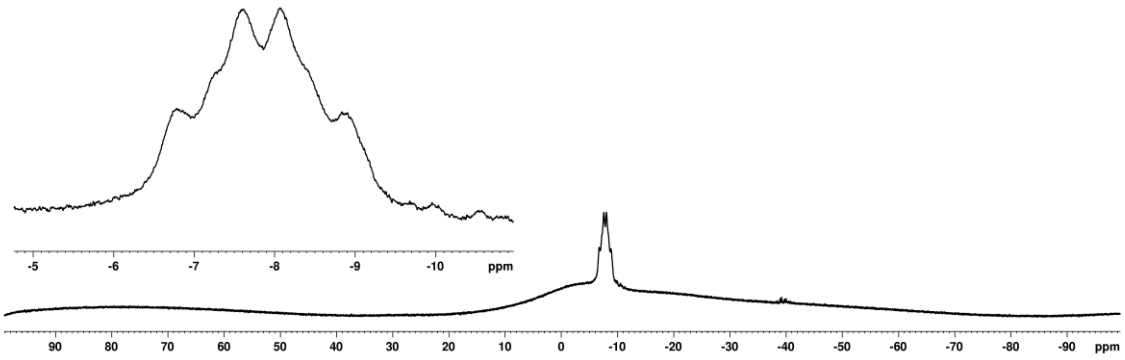

Figure S 6.84: ^{11}B NMR spectrum of $[(Me_3N{\cdot}BH_2PH_2)Ni(CO)_3]$ (C_6D_6, 298 K).

6.5.3.21 [(Me$_3$N·BH$_2$PH^{t}Bu)Ni(CO)$_3$]

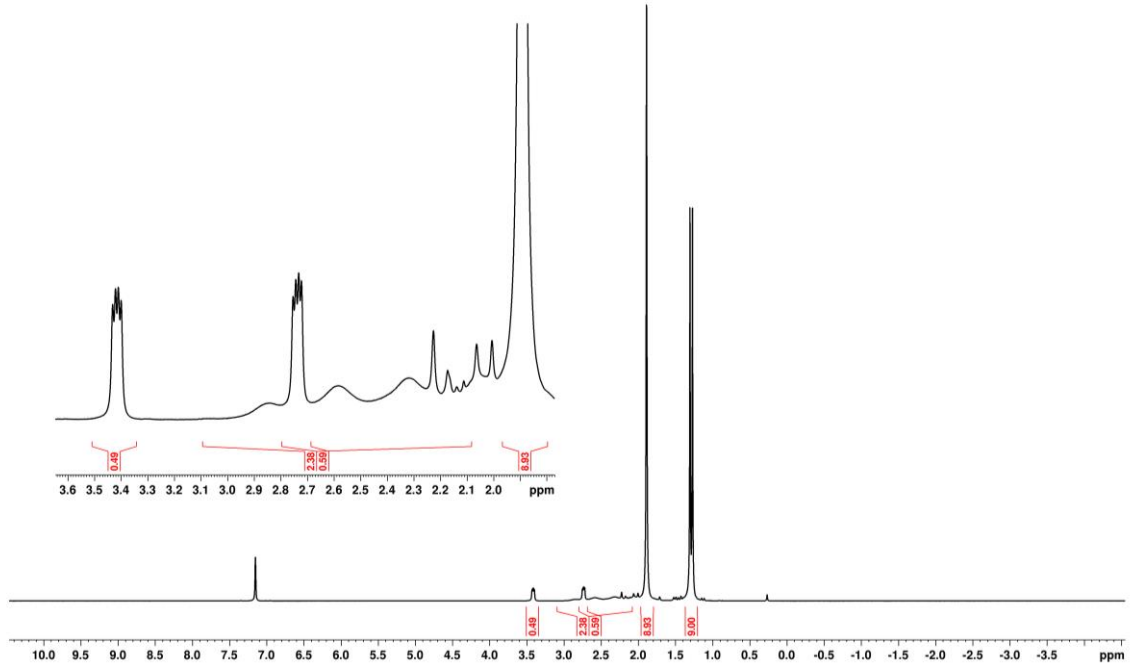

Figure S 6.85: ^{1}H NMR spectrum of [(Me$_3$N·BH$_2$PH^{t}Bu)Ni(CO)$_3$] (C$_6$D$_6$, 298 K).

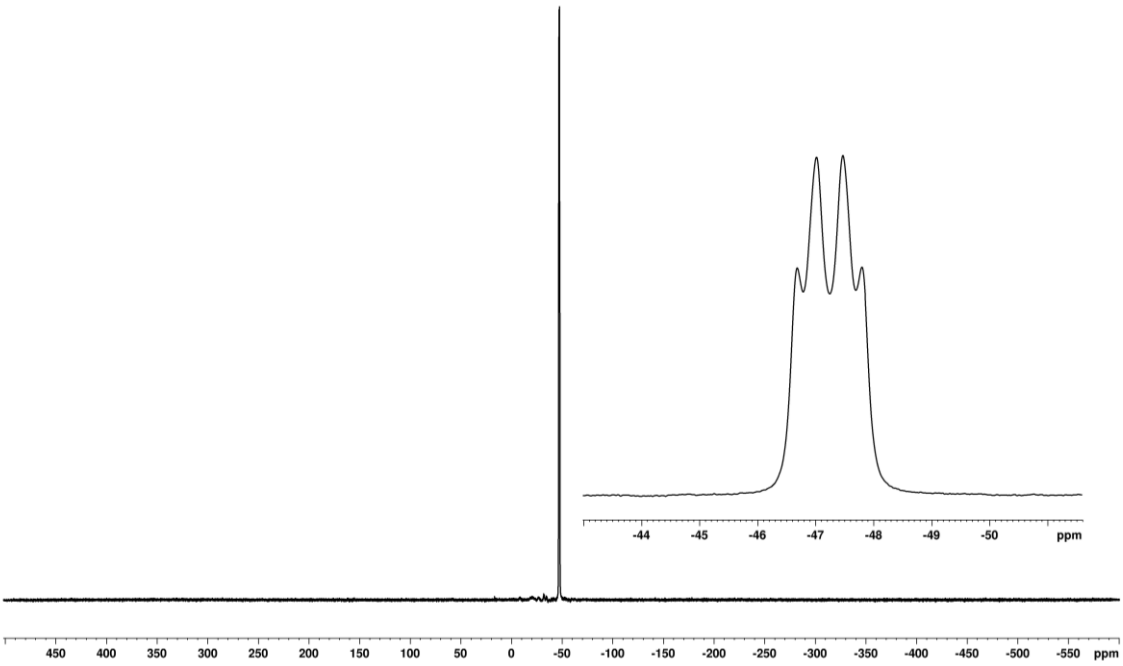

Figure S 6.86: ^{31}P{^{1}H} NMR spectrum of [(Me$_3$N·BH$_2$PH^{t}Bu)Ni(CO)$_3$] (C$_6$D$_6$, 298 K).

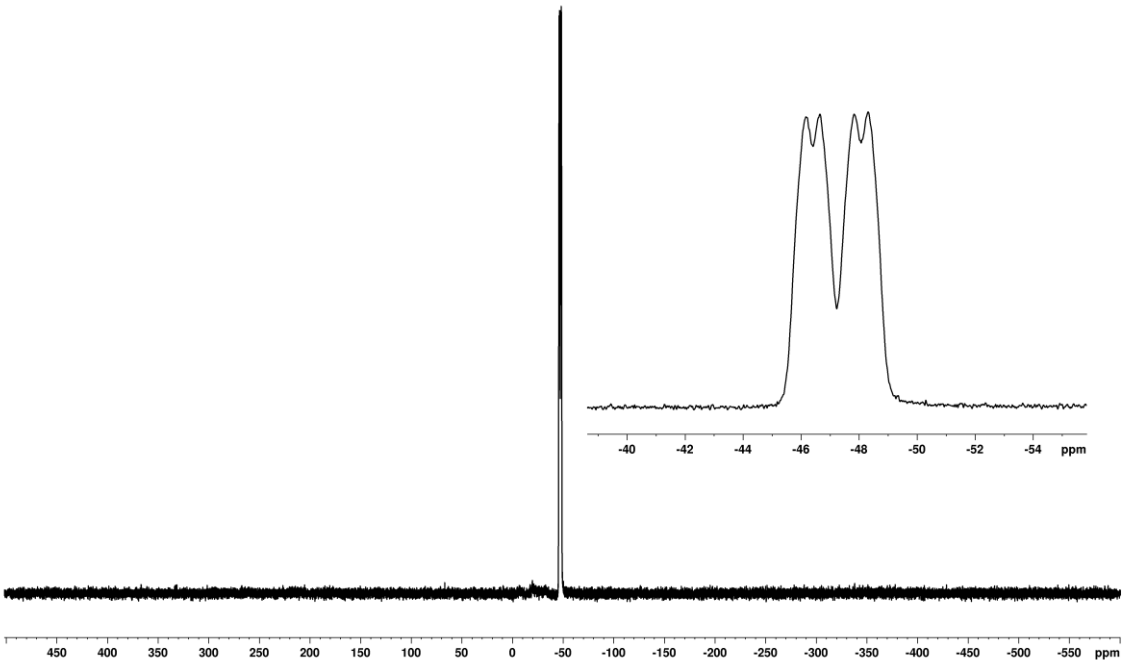

Figure S 6.87: ^{31}P NMR spectrum of [($Me_3N{\cdot}BH_2PH^tBu$)Ni(CO)$_3$] (C_6D_6, 298 K).

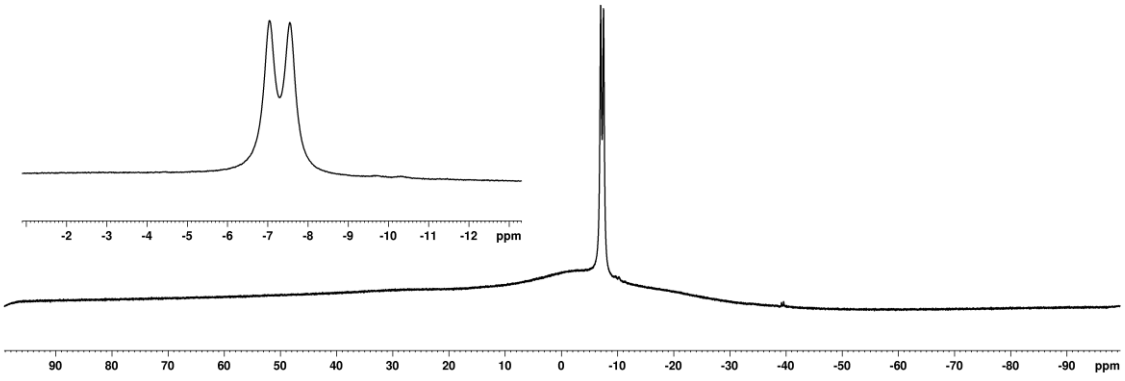

Figure S 6.88: $^{11}B\{^1H\}$ NMR spectrum of [($Me_3N{\cdot}BH_2PH^tBu$)Ni(CO)$_3$] (C_6D_6, 298 K).

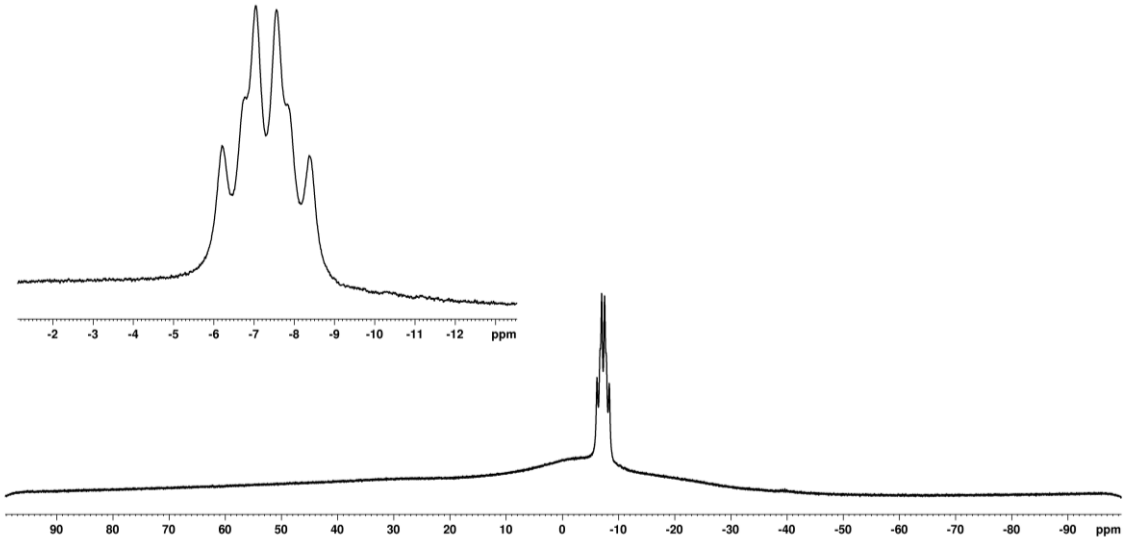

Figure S 6.89: ^{11}B NMR spectrum of [($Me_3N{\cdot}BH_2PH^tBu$)Ni(CO)$_3$] (C_6D_6, 298 K).

6.5.3.22 [(IDipp·BH_2PH_2)Ni(CO)$_3$]

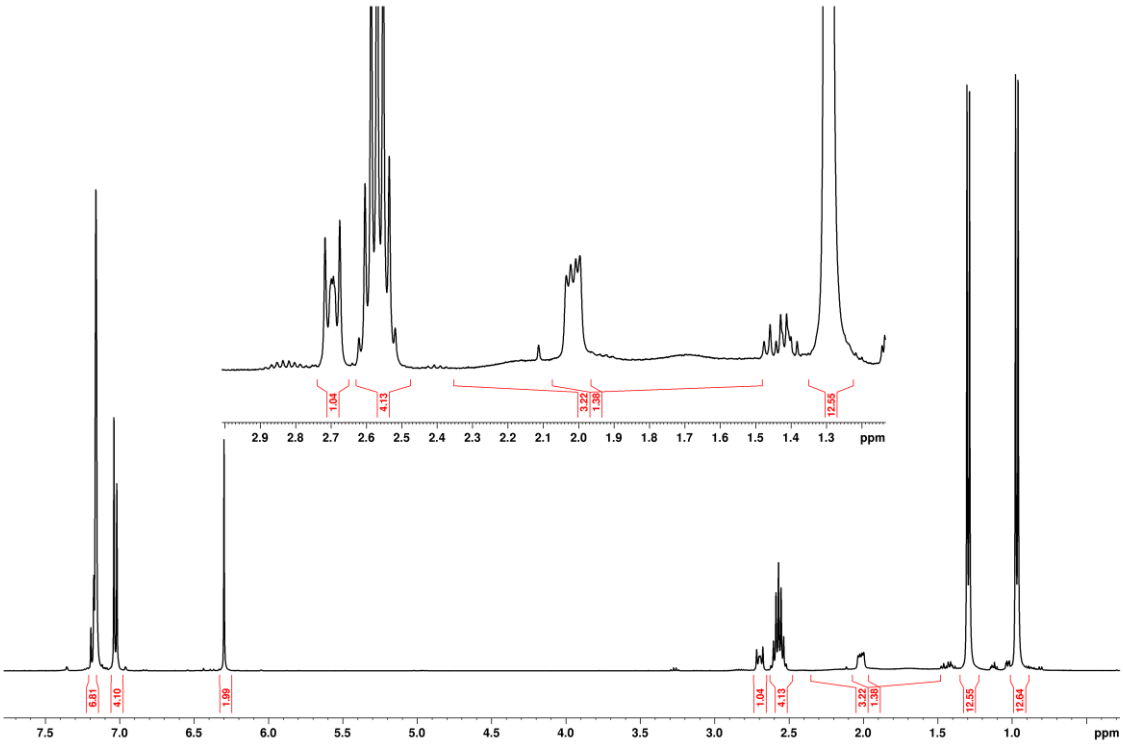

Figure S 6.90: ^{1}H NMR spectrum of [(IDipp·BH_2PH_2)Ni(CO)$_3$] (C_6D_6, 298 K).

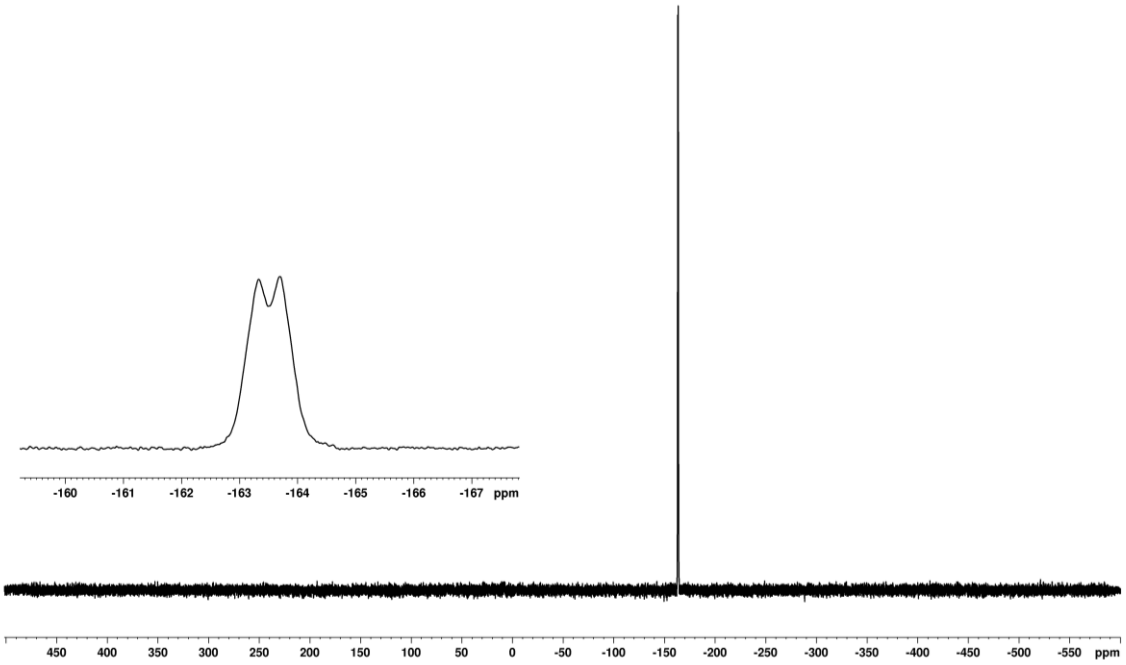

Figure S 6.91: $^{31}P\{^{1}H\}$ NMR spectrum of [(IDipp·BH_2PH_2)Ni$(CO)_3$] (C_6D_6, 298 K).

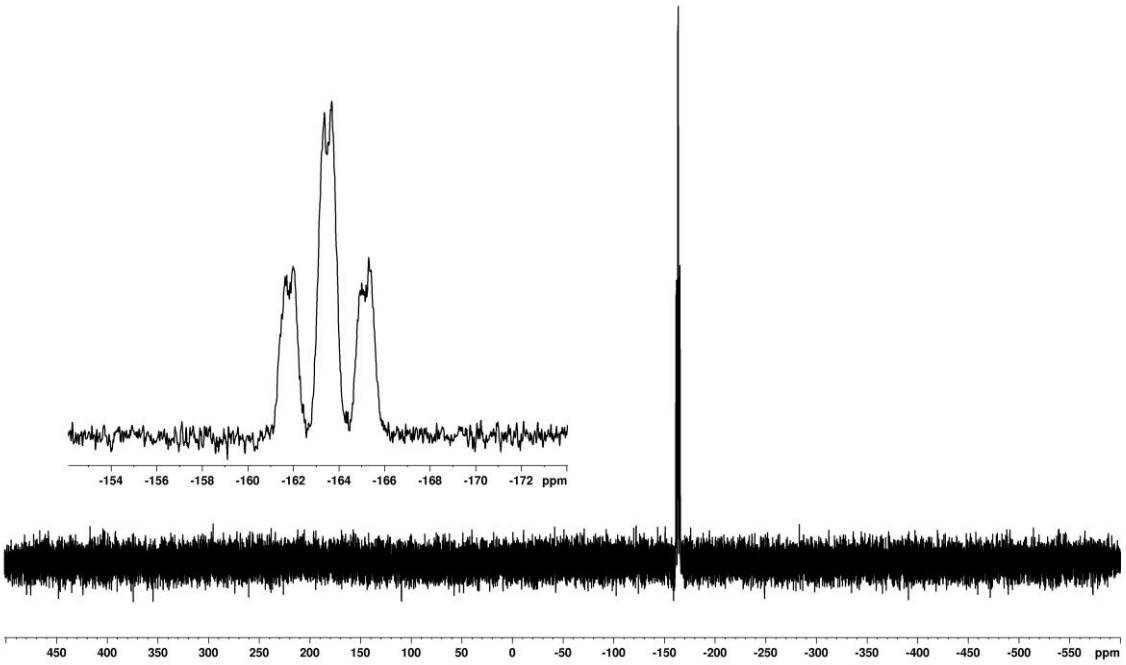

Figure S 6.92: ^{31}P NMR spectrum of [(IDipp·BH_2PH_2)Ni$(CO)_3$] (C_6D_6, 298 K).

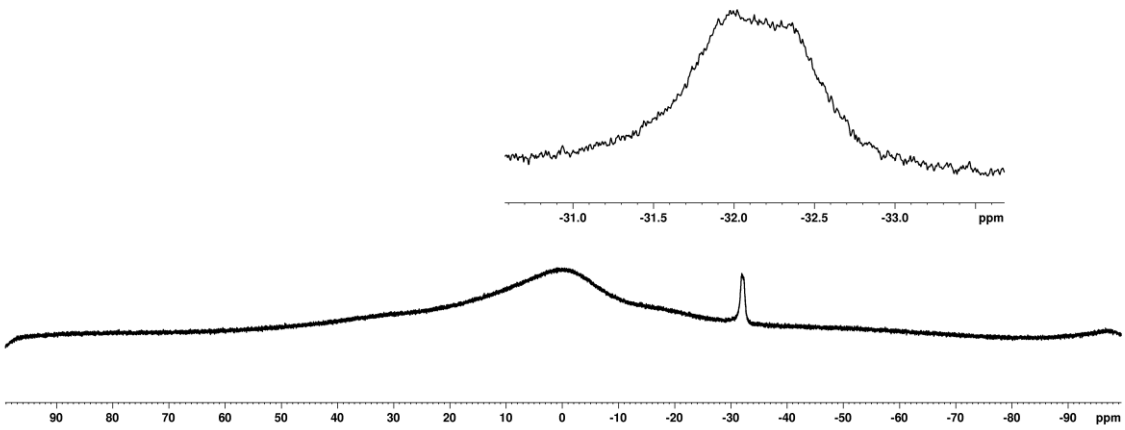

Figure S 6.93: $^{11}B\{^{1}H\}$ NMR spectrum of $[(IDipp{\cdot}BH_2PH_2)Ni(CO)_3]$ (C_6D_6, 298 K).

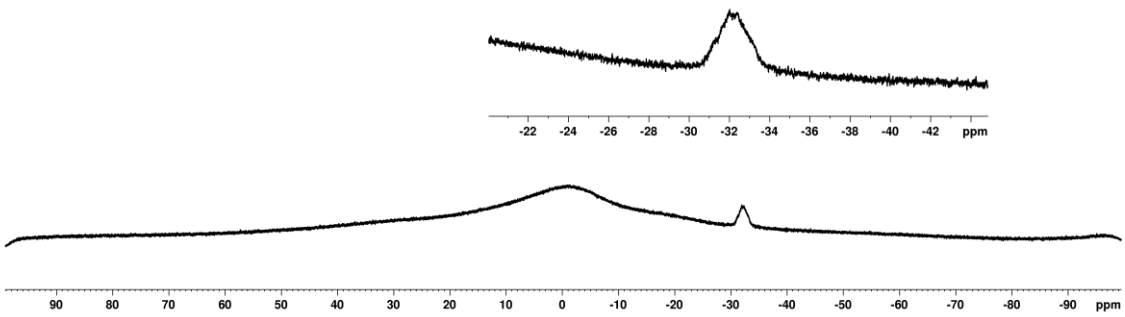

Figure S 6.94: ^{11}B NMR spectrum of $[(IDipp{\cdot}BH_2PH_2)Ni(CO)_3]$ (C_6D_6, 298 K).

6.5.4 Crystallographic Data

Single Crystal X-ray structure determination: Single-crystal X-ray diffraction data sets were collected using an Oxford Diffraction GV50 diffractometer (**1a, 1e, 1d, 2, 3g, 4a, 5a**) or a XtaLAB Synergy R, DW system diffractometer (**3a**) equipped with a HyPix-Arc 150 detector operating at T = 123.01(10) K. Crystals were selected under mineral oil or perfluorinated Fomblin. Data reduction, scaling and absorption corrections were performed using CrysAlisPro (Rigaku, V1.171.41.90a, 2020). A gaussian absorption correction was performed using CrysAlisPro 1.171.41.90a (Rigaku Oxford Diffraction, 2020). Numerical absorption correction based on gaussian integration over a multifaceted crystal model. Empirical absorption correction using spherical harmonics, implemented in SCALE3 ABSPACK scaling algorithm. Using Olex2,[11] the structures were solved with ShelXT[12] and a least-squares refinement on $F2$ was carried out with ShelXL.[13] All non-hydrogen atoms were refined anisotropically. The hydrogen atoms at the carbon atoms have been located in idealized positions and refined isotropically according to the riding model. Figures were created with Olex2.

CCDC 2304605-2304612 contain the supplementary crystallographic data for this paper. These data can be obtained free of charge at www.ccdc.cam.ac.uk/conts/retrieving.html (or from the Cambridge Crystallographic Data Centre, 12 Union Road, Cambridge CB2 1EZ, UK; Fax: +44-1223-336-033; e-mail: deposit@ccdc.cam.ac.uk).

Table S 6.1: Crystallographic data for compounds **1a**, **1e** and **1d**.

Compound	1a	1e	1d
CCDC	2304605	2304606	2304607
Formula	$C_{27}H_{42}BN_2P$	$C_{39}H_{60}BN_2P$	$C_{31}H_{48}BN_2P$
Dcalc	1.076	1.097	1.024
μ/mm^{-1}	0.998	0.862	0.891
Formula Weight	436.40	598.67	490.49
Colour	clear colourless	clear colourless	clear colourless
Shape	block-shaped	plate-shaped	block-shaped
Size/mm^3	0.18×0.12×0.04	0.31×0.15×0.08	0.39×0.13×0.09
T/K	122.99(10)	122.99(10)	123.00(10)
Crystal System	monoclinic	triclinic	orthorhombic
Flack Parameter	0.38(2)	-	0.020(6)
Hooft Parameter	-0.045(6)	-	0.019(5)
Space Group	$P2_1$	P-1	$P2_12_12_1$
a/Å	12.32610(10)	9.4332(2)	12.33520(10)
b/Å	41.7286(4)	10.2234(2)	13.93740(10)
c/Å	15.73960(10)	20.2077(4)	18.5128(2)
α/°	90	86.640(2)	90
β/°	93.3810(10)	82.968(2)	90
γ/°	90	69.537(2)	90
V/Å^3	8081.59(11)	1811.85(7)	3182.73(5)
Z	12	2	4
Z'	6	1	1
Wavelength/Å	1.54184	1.54184	1.54184
Radiation type	Cu K_a	Cu K_a	Cu K_a
Θ_{min}/°	2.812	4.410	3.970
Θ_{max}/°	74.293	66.724	73.584
Measured Refl's.	99281	27043	51648
Indep't Refl's	30988	6390	6350
Refl's I≥2 σ(I)	25884	5675	5797
R_{int}	0.0318	0.0594	0.0311
Parameters	1797	404	341
Restraints	32	18	3
Largest Peak	0.381	0.627	0.376
Deepest Hole	-0.414	-0.487	-0.470
GooF	1.068	0.983	1.047
wR_2 (all data)	0.1506	0.1372	0.1421
wR_2	0.1404	0.1305	0.1377
R_1 (all data)	0.0648	0.0555	0.0542
R_1	0.0532	0.0495	0.0496

Table S 6.2: Crystallographic data for compounds **2**, **3a** and **3g**.

Compound	**2**	**3a**	**3g**
CCDC	2304608	2304609	2304610
Formula	$C_{39}H_{48}AsBN_2$	$C_{30}H_{42}BN_2NiO_3P$	$C_{30}H_{40}BN_2NiO_3P$
Dcalc	1.191	1.243	1.235
μ/mm^{-1}	1.503	1.637	1.632
Formula Weight	630.52	579.14	577.13
Colour	clear colourless	clear colourless	clear colourless
Shape	block-shaped	block-shaped	block-shaped
Size/mm^3	0.36×0.14×0.09	0.60×0.23×0.14	0.56×0.14×0.09
T/K	122.99(10)	293(2)	123.00(10)
Crystal System	monoclinic	monoclinic	monoclinic
Space Group	$P2_1/n$	$P2_1/n$	$P2_1/n$
a/Å	12.90820(10)	10.94040(10)	9.23570(10)
b/Å	16.28200(10)	19.2660(2)	21.9447(3)
c/Å	16.85270(10)	14.8049(2)	15.3910(2)
α/°	90	90	90
β/°	96.7920(10)	97.4670(10)	95.7680(10)
γ/°	90	90	90
V/Å^3	3517.10(4)	3094.08(6)	3103.57(7)
Z	4	4	4
Z'	1	1	1
Wavelength/Å	1.54184	1.54184	1.54184
Radiation type	Cu K_a	Cu K_a	Cu K_a
Θ_{min}/°	3.788	3.786	4.029
Θ_{max}/°	75.419	66.755	66.698
Measured Refl's.	32335	25653	29906
Indep't Refl's	7134	5460	5468
Refl's I≥2 σ(I)	6763	5109	4866
R_{int}	0.0203	0.0510	0.0670
Parameters	404	367	367
Restraints	0	0	0
Largest Peak	0.241	0.403	0.321
Deepest Hole	-0.335	-0.590	-0.436
GooF	1.021	1.030	1.042
wR_2 (all data)	0.0633	0.1131	0.1020
wR_2	0.0626	0.1108	0.0977
R_1 (all data)	0.0270	0.0421	0.0421
R_1	0.0256	0.0401	0.0372

Table S 6.3: Crystallographic data for compounds **4a** and **5a**.

Compound	**4a**	**5a**
CCDC	2304611	2304612
Formula	$C_{30}H_{40}AsBN_2NiO_3$	$C_{18}H_{21}BNO_3PNi$
Dcalc	1.319	1.340
μ/mm^{-1}	2.311	2.301
Formula Weight	621.08	399.85
Colour	clear colourless	clear colourless
Shape	plate-shaped	block-shaped
Size/mm^3	0.42×0.13×0.04	0.70×0.39×0.21
T/K	293(2)	123.00(10)
Crystal System	monoclinic	monoclinic
Space Group	$P2_1/n$	$P2_1/n$
a/Å	9.2013(2)	8.70460(10)
b/Å	22.1748(4)	22.9175(3)
c/Å	15.4086(3)	10.06020(10)
a/°	90	90
b/°	95.791(2)	99.0630(10)
g/°	90	90
V/Å^3	3127.88(11)	1981.83(4)
Z	4	4
Z'	1	1
Wavelength/Å	1.54184	1.54184
Radiation type	Cu K_a	Cu K_a
Q_{min}/°	3.505	3.858
Q_{max}/°	66.753	66.754
Measured Refl's.	31856	15230
Indep't Refl's	5512	3498
Refl's I≥2 *s*(I)	4791	3378
R_{int}	0.0756	0.0475
Parameters	367	238
Restraints	0	0
Largest Peak	0.555	0.372
Deepest Hole	-0.941	-0.292
GooF	1.038	1.068
wR_2 (all data)	0.1391	0.0938
wR_2	0.1312	0.0930
R_1 (all data)	0.0558	0.0343
R_1	0.0484	0.0334

6.5.4.1 Crystal structures

SIDipp·BH_2PH_2 (1a)

1a crystallized by from a concentrated *n*-hexane solution at -30 °C as clear colourless block-shaped crystals in the monoclinic space group $P2_1$. The structure of **1a** in the solid state is shown in Figure S 6.95. The asymmetric unit contains 6 molecules of **1a**. Hydrogen atoms bound to B and P were refined by applying DFIX and DANG restraints.

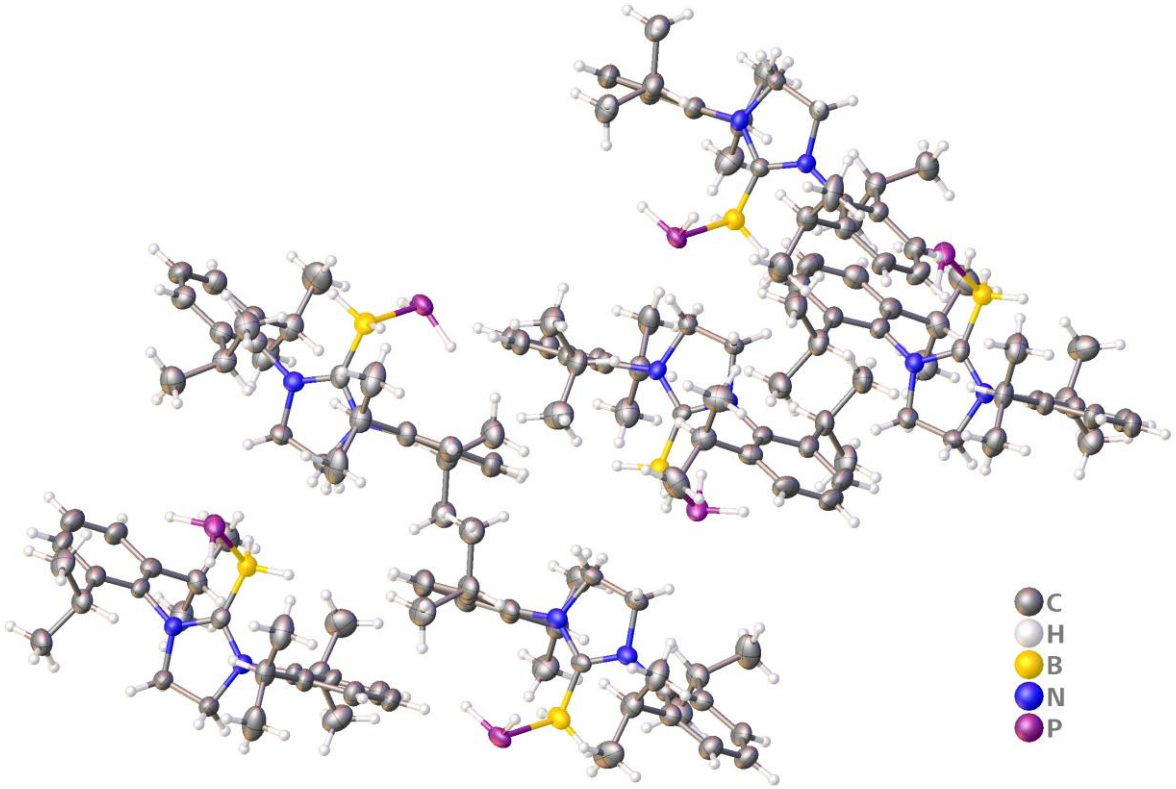

Figure S 6.95: Structure of **1a** in the solid state (asymmetric unit). Anisotropic displacement ellipsoids are displayed with 50% probability.

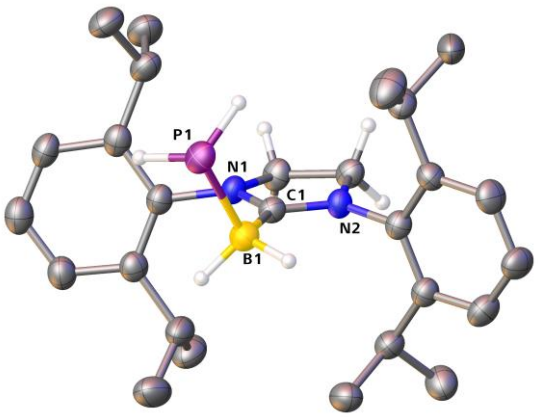

Figure S 6.96: Molecular structure of **1a** in the solid state (individual molecule). Anisotropic displacement ellipsoids are displayed with 50% probability. Hydrogen atoms bound to Dipp moieties are omitted for clarity. Selected bond lengths [Å] and angles [°]: N1-C1 1.356(6), N2-C1 1.340(6), C1-B1 1.579(8), B1-P1 2.038(6), N1-C1-N2 108.6(4), C1-B1-P1 111.6(4).

IDipp·BH_2PCy_2 (1e)

1e crystallized by from a concentrated *n*-hexane solution at -30 °C as clear colourless plate-shaped crystals in the triclinic space group *P*-1. The structure of **1e** in the solid state is shown in Figure S 6.97.

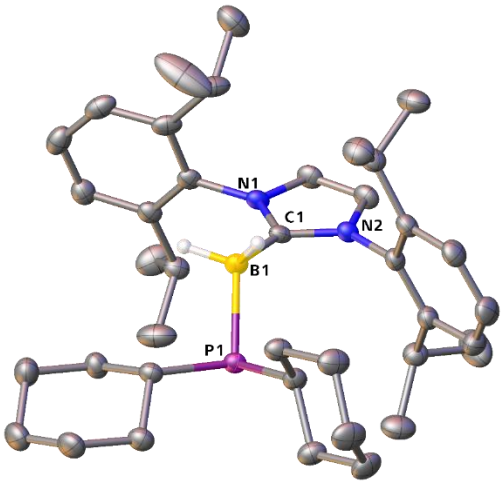

Figure S 6.97: Molecular structure of **1e** in the solid state. Anisotropic displacement ellipsoids are shown at 50% probability level. Hydrogen atoms bound to carbon are omitted for clarity. Selected bond lengths [Å] and angles [°]: N1-C1 1.361(2), N2-C1 1.362(2), C1-B1 1.605(2), B1-P1 1.9944(19), N1-C1-N2 104.12(14), N1-C1-B1 126.97(15), N2-C1-B1 128.69(14), C1-B1-P1 115.45(12).

The asymmetric unit contains one molecule of **1e** and was refined without further restrains/constraints. H-atoms bound to B were refined freely.

IDipp·BH_2PH^tBu (1d)

1d crystallized by from a concentrated *n*-hexane solution at -30 °C as clear colourless block-shaped crystals in the orthorhombic space group $P2_12_12_1$. The structure of **1d** in the solid state is shown in Figure S 6.98.

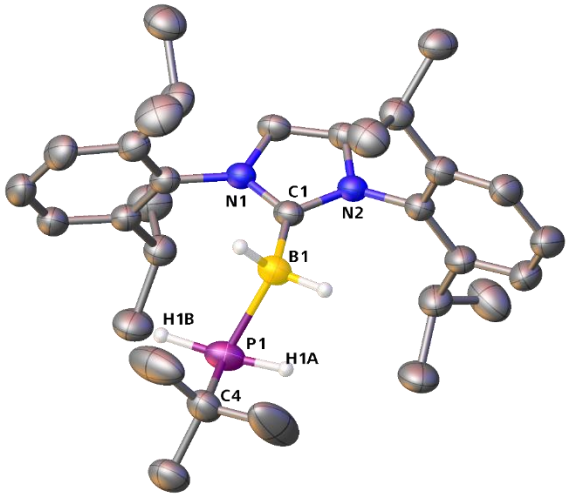

Figure S 6.98: Molecular structure of **1d** in the solid state. Anisotropic displacement ellipsoids are shown at 50% probability level. Hydrogen atoms bound to carbon are omitted for clarity. Selected bond lengths [Å] and angles [°]: N1-C1 1.360(4), N2-

C1 1.360(4), C1-B1 1.596(4), B1-P1 1.993(3), P1-C4 1.867(4), N1-C1-N2 104.2(2), N1-C1-B1 126.7(3), N2-C1-B1 128.9(3), C1-B1-P1 112.3(2), B1-P1-C4 102.85(15).

The asymmetric unit contains one molecule of 1**d** as a racemic mixture between the (*R*) and (*S*) isomer (occ. 0.5 each). This disorder was refined by DFIX, SADI and SIMU restraints.

IDipp·BH_2AsPh_2 (2)

2 crystallized from a *n*-hexane/toluene mixture (1:1) at -30 °C as clear colourless block-shaped crystals in the orthorhombic space group $P2_1/n$. The structure of **2** in the solid state is shown in Figure S 6.99.

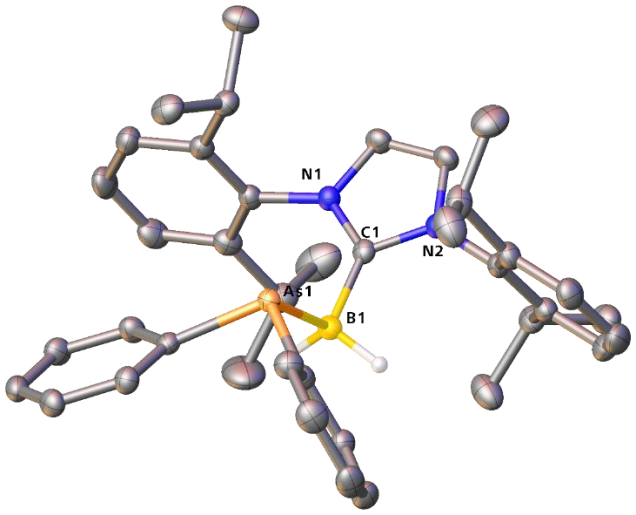

Figure S 6.99: Molecular structure of **2** in the solid state. Anisotropic displacement ellipsoids are shown at 50% probability level. Hydrogen atoms bound to carbon are omitted for clarity. Selected bond lengths [Å] and angles [°]: N1-C1 1.3556(17), N2-C1 1.3594(16), C1-B1 1.5957(19), B1-As1 2.1109(14), N1-C1-N2 104.19(11), N1-C1-B1 128.64(11), N2-C1-B1 127.16(11), C1-B1-P1 108.94(9).

The asymmetric unit contains one molecule of **2** and was refined without further restrains/constraints. H-atoms bound to B were refined freely.

[(SIDipp·BH_2PH_2)$Ni(CO)_3$] (3a)

3a crystallized from a Et_2O/*n*-hexane mixture (2:1) at -30 °C as clear colourless block-shaped crystals in the monoclinic space group $P2_1/n$. The structure of **3a** in the solid state is shown in Figure S 6.100.

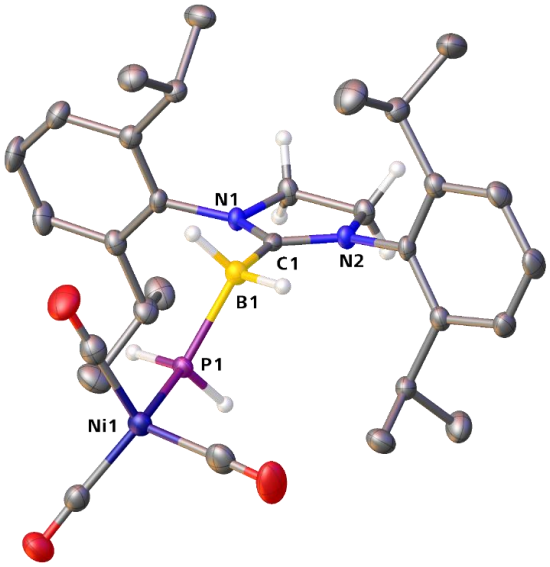

Figure S 6.100: Molecular structure of **3a** in the solid state. Anisotropic displacement ellipsoids are shown at 50% probability level. Hydrogen atoms bound to carbon are omitted for clarity. Dipp moieties are displayed in a stick model for improved overall clarity. Selected bond lengths [Å] and angles [°]: N1-C1 1.344(2), N2-C1 1.336(2), C1-B1 1.598(2), B1-P1 1.966(2), P1-Ni 2.2500(5), N1-C1-N2 104.19(11), N1-C1-B1 126.87(14), N2-C1-B1 124.32(14), C1-B1-P1 111.70(11), B1-P1-Ni1 115.56(6).

The asymmetric unit contains one molecule of **3a** and was refined without further restrains/constraints. H-atoms bound to B and P were refined freely.

[(IDipp·BH_2AsH_2)$Ni(CO)_3$] (4a)

4a crystallized from a toluene/*n*-hexane mixture (1:2) at -30 °C as clear colourless block-shaped crystals in the monoclinic space group $P2_1/n$. The structure of **4a** in the solid state is shown in Figure S 6.101.

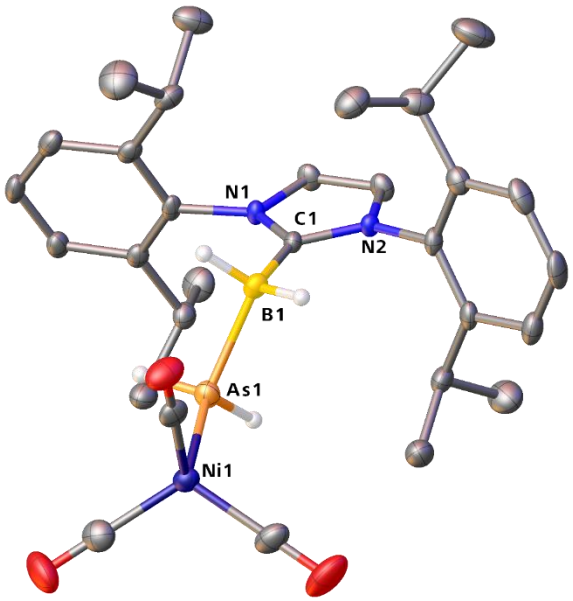

Figure S 6.101: Molecular structure of **4a** in the solid state. Anisotropic displacement ellipsoids are shown at 50% probability level. Hydrogen atoms bound to carbon are omitted for clarity. Selected bond lengths [Å] and angles [°]: N1-C1 1.359(4), N2-

C1 1.355(4), C1-B1 1.597(4), B1-As1 2.072(4), As1-Ni 2.3445(6), N1-C1-N2 105.1(2), N1-C1-B1 128.6(2), N2-C1-B1 126.3(3), C1-B1-As1 113.3(2), B1-As1-Ni1 116.03(10).

The asymmetric unit contains one molecule of **4a** and was refined without further restrains/constraints. H-atoms bound to B and As were refined freely.

[(IDipp·BH_2PH_2)$Ni(CO)_3$] (4g)

4g crystallized from a Et_2O/*n*-hexane mixture (2:1) at -30 °C as clear colourless plate-shaped crystals in the monoclinic space group $P2_1/n$. The structure of **4g** in the solid state is shown in Figure S 6.102.

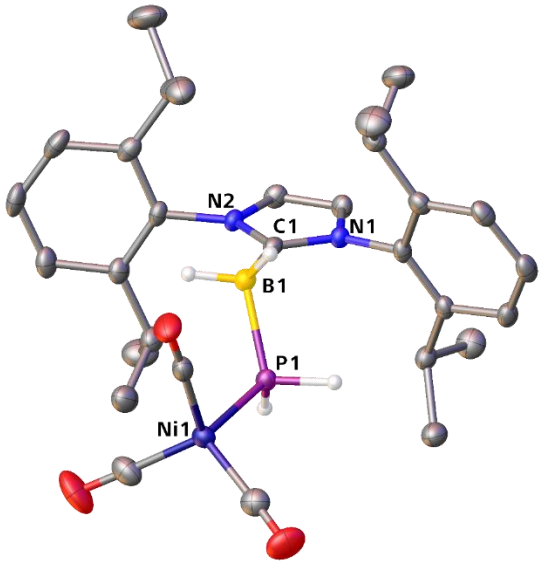

Figure S 6.102: Molecular structure of **4g** in the solid state. Anisotropic displacement ellipsoids are shown at 50% probability level. Hydrogen atoms bound to carbon are omitted for clarity. Selected bond lengths [Å] and angles [°]: N1-C1 1.356(2), N2-C1 1.360(2), C1-B1 1.597(2), B1-P1 1.966(2), P1-Ni 2.2605(5), N1-C1-N2 104.21(14), N1-C1-B1 128.96(14), N2-C1-B1 126.82(14), C1-B1-P1 114.48(12), B1-P1-Ni1 115.59(6).

The asymmetric unit contains one molecule of **4g** and was refined without further restrains/constraints. H-atoms bound to B and P were refined freely.

[(Me_3N·BH_2PPh_2)$Ni(CO)_3$] (5a)

5a crystallized from a saturated toluene solution at -30 °C as clear colourless block-shaped crystals in the monoclinic space group $P2_1/n$. The structure of **5a** in the solid state is shown in Figure S 6.103.

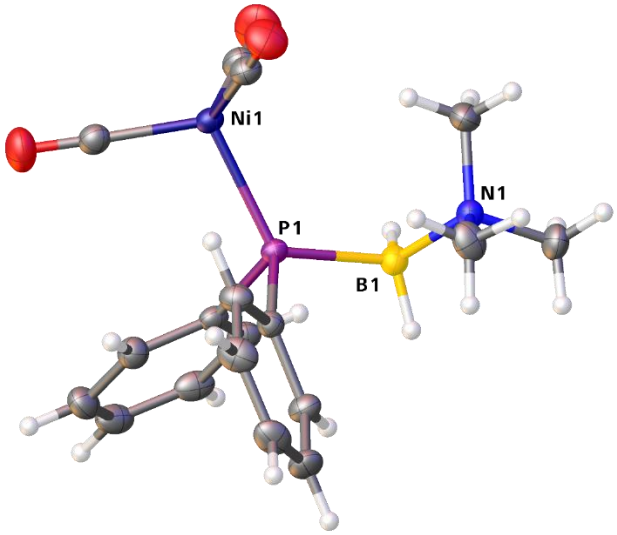

Figure S 6.103: Molecular structure of **5a** in the solid state. Anisotropic displacement ellipsoids are shown at 50% probability level. Hydrogen atoms bound to carbon are omitted for clarity. Selected bond lengths [Å] and angles [°]: N1-B1 1.611(2), B1-P1 1.977(2), P1-Ni1 2.2581(5), N1-B1-P1 116.21(12), B1-P1-Ni1 121.12(6).

The asymmetric unit contains one molecule of **5a** and was refined without further restrains/constraints. H-atoms bound to B were refined freely.

6.5.5 Computational Details

6.5.5.1 General Information

The geometries of the compounds have been fully optimized with gradient-corrected density functional theory (DFT) in form of Becke's three-parameter hybrid method B3LYP with def2-TZVP all electron basis set.[14] The Gaussian 09 program package was used throughout.[15] All structures correspond to minima on their respective potential energy surfaces as verified by the computation of the second derivatives. Computed harmonic vibrational frequencies ω were scaled by 0.965.[16]

6.5.5.2 Harmonic vibrational frequencies

Table S 6.4: Computed harmonic vibrational frequencies of the A_1 mode of the {Ni(CO)$_3$} vibration in the complex (ω(CO)$_{unscaled}$), the frequency scaled by the factor 0.965 (ν(CO)$_{scaled}$), the experimental values ν(CO)$_{exp}$, and the computed shift in the stretching CO vibration upon complex formation $\Delta\nu$(CO), cm^{-1} with respect to free CO (B3LYP/def2-TZVP level of theory).

Compound	ω(CO)$_{unscaled}$	ν(CO)$_{scaled}$	ν(CO)$_{exp}$	$\Delta\nu$(CO)
CO	2214.1	2136.6	2143	
[Ni(CO)$_4$]	2190.5	2113.9	2128	
Ni(CO)$_3$	2177.2	2101.0		
[Ni(CO)$_3$PH$_2$CH$_2$CMe$_3$]	2140.8	2065.8		70.8
[Ni(CO)$_3$AsH$_2$CH$_2$CMe$_3$]	2140.7	2065.8		70.9
[Ni(CO)$_3$PH$_2$BH$_2$NMe$_3$]	2127.0	2052.5	2051	84.1
[Ni(CO)$_3$AsH$_2$BH$_2$NMe$_3$]	2126.3	2051.9		84.8
[Ni(CO)$_3$PH$_2$BH$_2$·SIDipp]	2121.9	2047.7	2052	89.0
[Ni(CO)$_3$PH$_2$BH$_2$·IDipp]	2121.2	2047.0	2050	89.7
[Ni(CO)$_3$AsH$_2$BH$_2$·IDipp]	2121.2	2047.0	2046	89.7
[Ni(CO)$_3$PH$_2$AlH$_2$·IDipp]	2123.6	2049.2		87.4
[Ni(CO)$_3$PH$_2$GaH$_2$·IDipp]	2124.1	2049.7	2045	86.9
[Ni(CO)$_3$PH^{t}BuBH$_2$·NMe$_3$]	2120.2	2046.0	2051	90.7
[Ni(CO)$_3$AsH^{t}BuBH$_2$·NMe$_3$]	2119.9	2045.7		90.9
[Ni(CO)$_3$PH^{t}BuBH$_2$·IDipp]	2110.7	2036.8	2043	99.8
[Ni(CO)$_3$PMe$_2$BH$_2$·IDipp]	2107.6	2033.8	2040	102.9
[Ni(CO)$_3$PPh$_2$BH$_2$·NMe$_3$]	2121.1	2046.9	2049	89.8
[Ni(CO)$_3$AsPh$_2$BH$_2$·NMe$_3$]	2122.0	2047.7		88.9
[Ni(CO)$_3$PPh$_2$BH$_2$·IDipp]	2112.3	2038.4	2048	98.3
[Ni(CO)$_3$AsPh$_2$BH$_2$·IDipp]	2114.4	2040.4	2046	96.3
[Ni(CO)$_3$PCy$_2$BH$_2$·IDipp]	2104.4	2030.7	2037	105.9
[Ni(CO)$_3$P(SiMe$_3$)$_2$BH$_2$·IDipp]	2107.1	2033.3	2041	103.3

6.5.5.3 Thermodynamic data

Table S 6.5: Total energies E^{o}_{0}, sum of electronic and thermal enthalpies H^{o}_{298} (Hartree) and standard entropies S^{o}_{298} (cal mol^{-1}K^{-1}) (B3LYP/def2-TZVP level of theory).

Compound	E^{o}_{0}	H^{o}_{298}	S^{o}_{298}
H^+	0.0000000	0.00236	26.014
CO	-113.3625260	-113.354177	47.19
$[Ni(CO)_4]$	-1961.9723579	-1961.929657	99.564
$Ni(CO)_3$	-1848.5782113	-1848.546078	90.204
$PH_2CH_2CMe_3$	-539.8183704	-539.641571	88.363
$[HPH_2CH_2CMe_3]^+$	-540.1646582	-539.976857	91.295
$[Ni(CO)_3PH_2CH_2CMe_3]$	-2388.4221893	-2388.210236	140.23
$AsH_2CH_2CMe_3$	-2434.3521330	-2434.177315	92.109
$[HAsH_2CH_2CMe_3]^+$	-2434.6808524	-2434.495838	94.12
$[Ni(CO)_3AsH_2CH_2CMe_3]$	-4282.9494542	-4282.739796	145.51
$PH_2BH_2{\cdot}NMe_3$	-543.2072707	-543.033402	90.168
$[HPH_2BH_2{\cdot}NMe_3]^+$	-543.5905207	-543.405126	90.583
$[Ni(CO)_3PH_2BH_2{\cdot}NMe_3]$	-2391.8169967	-2391.607838	141.44
$AsH_2BH_2{\cdot}NMe_3$	-2437.7419648	-2437.569754	92.641
$[HAsH_2BH_2{\cdot}NMe_3]^+$	-2438.1126660	-2437.929922	94.614
$[Ni(CO)_3AsH_2BH_2{\cdot}NMe_3]$	-4286.3473875	-4286.140123	146.273
$PH_2BH_2{\cdot}SIDipp$	-1530.3496192	-1529.6797	214.017
$[HPH_2BH_2{\cdot}SIDipp]^+$	-1530.7619823	-1530.080198	215.965
$[Ni(CO)_3PH_2BH_2{\cdot}SIDipp]$	-3378.9606000	-3378.255631	270.343
$PH_2BH_2{\cdot}IDipp$	-1529.1483650	-1528.502554	214.333
$[HPH_2BH_2{\cdot}IDipp]^+$	-1529.5606364	-1528.902938	216.472
$[Ni(CO)_3PH_2BH_2{\cdot}IDipp]$	-3377.7601002	-3377.078931	268.444
$AsH_2BH_2{\cdot}IDipp$	-3423.6858746	-3423.041669	216.883
$[HAsH_2BH_2{\cdot}IDipp]^+$	-3424.0818235	-3423.426868	220.48
$[Ni(CO)_3AsH_2BH_2{\cdot}IDipp]$	-5272.2913971	-5271.612198	272.443
$PH_2AlH_2{\cdot}IDipp$	-1746.7471010	-1746.108693	221.897
$[HPH_2AlH_2{\cdot}IDipp]^+$	-1747.1562956	-1746.50643	228.02
$[Ni(CO)_3PH_2AlH_2{\cdot}IDipp]$	-3595.3549799	-3594.681461	278.624
$PH_2GaH_2{\cdot}IDipp$	-3429.1837944	-3428.545409	225.463
$[HPH_2GaH_2{\cdot}IDipp]^+$	-3429.5921954	-3428.942307	228.762
$[Ni(CO)_3PH_2GaH_2{\cdot}IDipp]$	-5277.7905914	-5277.117067	281.224
$PH^tBuBH_2{\cdot}NMe_3$	-700.5182701	-700.225202	115.986
$[HPH^tBuBH_2{\cdot}NMe_3]^+$	-700.9236920	-700.619014	119.944
$[Ni(CO)_3PH^tBuBH_2{\cdot}NMe_3]$	-2549.1260969	-2548.797595	165.366
$AsH^tBuBH_2{\cdot}NMe_3$	-2595.0529878	-2594.761085	118.706
$[HAsH^tBuBH_2{\cdot}NMe_3]^+$	-2595.4441471	-2595.141912	125.164
$[Ni(CO)_3AsH^tBuBH_2{\cdot}NMe_3]$	-4443.6587042	-4443.33187	170.757
$PH^tBuBH_2{\cdot}IDipp$	-1686.4588909	-1685.693809	239.447
$[HPH^tBuBH_2{\cdot}IDipp]^+$	-1686.8890249	-1686.111995	242.76
$[Ni(CO)_3PH^tBuBH_2{\cdot}IDipp]$	-3535.0658463	-3534.265202	283.213
$PMe_2BH_2{\cdot}IDipp$	-1607.8109006	-1607.103788	227.491

$[HPMe_2BH_2{\cdot}IDipp]^+$	-1608.2400000	-1607.529956	232.803
$[Ni(CO)_3PMe_2BH_2{\cdot}IDipp]$	-3456.4230813	-3455.68049	272.214
$PPh_2BH_2{\cdot}NMe_3$	-1005.4753650	-1005.126894	142.073
$[HPPh_2BH_2{\cdot}NMe_3]^+$	-1005.8890100	-1005.528689	142.287
$[Ni(CO)_3PPh_2BH_2{\cdot}NMe_3]$	-2854.0849977	-2853.701379	188.379
$AsPh_2BH_2{\cdot}NMe_3$	-2900.0076291	-2899.660074	143.959
$[HAsPh_2BH_2{\cdot}NMe_3]^+$	-2900.4039378	-2900.045682	147.478
$[Ni(CO)_3AsPh_2BH_2{\cdot}NMe_3]$	-4748.6146087	-4748.23223	195.318
$PPh_2BH_2{\cdot}IDipp$	-1991.4140251	-1990.593535	261.948
$[HPPh_2BH_2{\cdot}IDipp]^+$	-1991.8469617	-1991.014484	263.698
$[Ni(CO)_3PPh_2BH_2{\cdot}IDipp]$	-3840.0148129	-3839.158996	304.461
$AsPh_2BH_2{\cdot}IDipp$	-3885.9488842	-3885.12917	265.557
$[HAsPh_2BH_2{\cdot}IDipp]^+$	-3886.3633001	-3885.532782	267.175
$[Ni(CO)_3AsPh_2BH_2{\cdot}IDipp]$	-5734.547239	-5733.692478	310.546
$PCy_2BH_2{\cdot}IDipp$	-1998.6591450	-1997.697832	260.966
$[HPCy_2BH_2{\cdot}IDipp]^+$	-1999.1035915	-1998.129105	270.359
$[Ni(CO)_3PCy_2BH_2{\cdot}IDipp]$	-3847.2616210	-3846.263637	311.197
$P(SiMe_3)_2BH_2{\cdot}IDipp$	-2346.6626899	-2345.79343	281.366
$[HP(SiMe_3)_2BH_2{\cdot}IDipp]^+$	-2347.0930042	-2346.213084	286.107
$[Ni(CO)_3P(SiMe_3)_2BH_2{\cdot}IDipp]$	-4195.2608571	-4194.35615	324.947

6.5.5.4 Coordinates of optimized structures

Table S 6.6: Optimized geometries of computationally studied compounds. xyz coordinates are given in /Å (B3LYP/def2-TZVP).

CO			
8	0.000000000	0.000000000	0.482096000
6	0.000000000	0.000000000	-0.642794000
$[Ni(CO)_4]$			
28	0.000000000	0.000000000	0.000000000
8	1.719569000	1.719569000	1.719569000
8	-1.719569000	-1.719569000	1.719569000
8	1.719569000	-1.719569000	-1.719569000
6	1.064557000	1.064557000	1.064557000
6	-1.064557000	-1.064557000	1.064557000
6	1.064557000	-1.064557000	-1.064557000
6	-1.064557000	1.064557000	-1.064557000
8	-1.719569000	1.719569000	-1.719569000
$Ni(CO)_3$			
28	0.000000000	0.000000000	0.000512000
8	0.000539000	2.952936000	-0.000716000
8	2.557048000	-1.476935000	-0.000716000
8	-2.557588000	-1.476001000	-0.000716000
6	0.000000000	1.816414000	0.000157000
6	1.573060000	-0.908207000	0.000157000
6	-1.573060000	-0.908207000	0.000157000
$PH_2CH_2CMe_3$			
15	2.085002000	-0.003706000	0.112391000
6	-0.823273000	0.000155000	-0.001262000
6	-0.828573000	1.510739000	-0.279881000
1	-1.764350000	1.961449000	0.058488000
1	-0.725910000	1.716357000	-1.348367000
1	-0.014083000	2.020375000	0.240145000
6	-0.936401000	-0.247121000	1.510670000
1	-0.098917000	0.192066000	2.055068000
1	-0.955149000	-1.317043000	1.733204000
1	-1.857327000	0.190484000	1.902840000
6	-2.029420000	-0.644809000	-0.704720000
1	-2.967320000	-0.227591000	-0.330210000
1	-2.052670000	-1.724068000	-0.535198000
1	-1.995308000	-0.475686000	-1.783657000
6	0.459857000	-0.651493000	-0.569447000
1	0.458270000	-0.571425000	-1.658070000
1	0.448323000	-1.719257000	-0.331320000
1	2.275833000	1.078269000	-0.785840000
1	2.920449000	-0.873167000	-0.635108000
$[HPH_2CH_2CMe_3]^+$			
15	-2.012757000	-0.024920000	-0.000029000
6	0.861083000	0.013705000	0.000001000
6	0.909930000	0.886394000	1.261660000
1	1.854840000	1.428373000	1.301711000
1	0.837232000	0.287690000	2.172210000
1	0.119161000	1.642256000	1.280714000
6	0.910367000	0.887367000	-1.260973000
1	0.119821000	1.643458000	-1.279525000
1	0.837626000	0.289402000	-2.172009000
1	1.855445000	1.429090000	-1.300489000
6	2.048759000	-0.964521000	-0.000160000
1	2.985471000	-0.406361000	0.000252000
1	2.042974000	-1.603577000	-0.885221000
1	2.042604000	-1.604263000	0.884406000
6	-0.417164000	-0.876240000	-0.000565000

1	-0.442703000	-1.526456000	0.879739000
1	-0.442645000	-1.525498000	-0.881566000
1	-2.213067000	0.788113000	1.118813000
1	-3.070990000	-0.940009000	-0.001716000
1	-2.212264000	0.791351000	-1.116657000

$[Ni(CO)_3PH_2CH_2CMe_3]$

28	1.448962000	0.000307000	-0.099458000
15	-0.277346000	0.050000000	1.384261000
8	3.877941000	-0.007272000	1.593657000
8	1.264906000	-2.486502000	-1.696017000
6	-2.887744000	-0.002521000	0.020840000
8	1.308223000	2.444932000	-1.761751000
6	-2.995134000	-1.510123000	0.293531000
1	-3.695264000	-1.973809000	-0.404431000
1	-3.356042000	-1.707442000	1.306211000
1	-2.034934000	-2.016265000	0.172772000
6	2.939769000	-0.004990000	0.947243000
6	1.322343000	-1.528701000	-1.081004000
6	-2.340524000	0.232810000	-1.394261000
1	-1.346910000	-0.195840000	-1.522509000
1	-2.275182000	1.299929000	-1.619050000
1	-2.999399000	-0.223699000	-2.136076000
6	-4.289421000	0.624698000	0.120227000
1	-4.958532000	0.189979000	-0.625599000
1	-4.252244000	1.702771000	-0.052722000
1	-4.731138000	0.456811000	1.105349000
6	1.352935000	1.503775000	-1.120499000
6	-2.002068000	0.689929000	1.085180000
1	-2.515171000	0.663282000	2.049514000
1	-1.880584000	1.744510000	0.821401000
1	-0.567142000	-1.149804000	2.069732000
1	-0.007703000	0.812438000	2.541649000

$AsH_2CH_2CMe_3$

33	1.655750000	-0.006590000	0.060077000
6	-1.369247000	-0.000695000	-0.002735000
6	-1.362875000	1.532584000	-0.094608000
1	-2.281273000	1.948743000	0.325690000
1	-1.289298000	1.865547000	-1.132815000
1	-0.525422000	1.966629000	0.456578000
6	-1.442804000	-0.431436000	1.470009000
1	-0.589769000	-0.062515000	2.042524000
1	-1.460038000	-1.520553000	1.559931000
1	-2.350261000	-0.044380000	1.939158000
6	-2.607233000	-0.539680000	-0.741957000
1	-3.526693000	-0.157412000	-0.291592000
1	-2.644933000	-1.630974000	-0.704055000
1	-2.599765000	-0.241038000	-1.792918000
6	-0.118911000	-0.592937000	-0.684346000
1	-0.131147000	-0.372491000	-1.751722000
1	-0.124211000	-1.680243000	-0.577072000
1	1.824773000	1.218477000	-0.837088000
1	2.464699000	-0.879347000	-0.897319000

$[HAsH_2CH_2CMe_3]^+$

33	-1.603541000	-0.014275000	-0.001092000
6	1.384070000	0.014522000	0.000017000
6	1.383023000	0.927952000	1.233250000
1	2.315548000	1.490092000	1.283680000
1	1.293408000	0.357869000	2.160593000
1	0.577358000	1.668494000	1.203143000
6	1.457906000	0.847400000	-1.286942000
1	0.648405000	1.579332000	-1.359311000
1	1.432426000	0.217337000	-2.178441000
1	2.389527000	1.412769000	-1.311923000
6	2.591462000	-0.941593000	0.064609000
1	3.516470000	-0.364123000	0.062831000
1	2.617833000	-1.613974000	-0.794814000
1	2.578038000	-1.546169000	0.973329000
6	0.140088000	-0.901913000	-0.008526000
1	0.101693000	-1.545638000	0.873194000
1	0.107274000	-1.538151000	-0.895425000
1	-1.895684000	0.728385000	1.262753000
1	-2.704764000	-1.017517000	-0.144362000
1	-1.799974000	0.964173000	-1.113656000

$[Ni(CO)_3AsH_2CH_2CMe_3]$

28	-1.582294000	0.266884000	-0.003427000
33	0.293836000	-1.256568000	-0.000559000
8	-3.955007000	-1.495569000	0.113184000
8	-1.382537000	1.981278000	2.398263000
6	2.962209000	0.219341000	0.002299000
8	-1.471144000	1.798239000	-2.530727000
6	3.052054000	0.029199000	1.523621000
1	3.703266000	0.786392000	1.965135000
1	3.461457000	-0.951572000	1.778329000
1	2.075822000	0.121814000	2.004784000
6	-3.029775000	-0.832269000	0.069132000
6	-1.436199000	1.313724000	1.476100000
6	2.344892000	1.588638000	-0.316366000
1	1.338194000	1.686398000	0.091267000
1	2.285792000	1.752995000	-1.394858000
1	2.954123000	2.389010000	0.108981000
6	4.381879000	0.164740000	-0.591977000
1	5.001243000	0.965244000	-0.181116000
1	4.359889000	0.283476000	-1.677689000
1	4.870542000	-0.786139000	-0.367005000
6	-1.494283000	1.200185000	-1.560820000
6	2.151914000	-0.919572000	-0.650189000
1	2.679524000	-1.867649000	-0.536008000
1	2.043279000	-0.733506000	-1.721067000
1	0.622839000	-1.980810000	1.292897000
1	0.085018000	-2.527177000	-0.805819000

$PH_2BH_2{\cdot}NMe_3$

15	2.148911000	0.047295000	0.096758000
7	-0.850670000	-0.009510000	-0.007823000
6	-0.835849000	1.432806000	-0.364840000
1	-1.749394000	1.918295000	-0.014982000
1	-0.757203000	1.525315000	-1.445565000
1	0.027453000	1.904422000	0.099804000
6	-0.914248000	-0.149191000	1.471382000
1	-0.016682000	0.283871000	1.906163000
1	-0.954945000	-1.206694000	1.721164000
1	-1.800558000	0.358388000	1.857934000
6	-2.056044000	-0.642859000	-0.602943000
1	-2.961008000	-0.176205000	-0.206836000
1	-2.049340000	-1.703142000	-0.363723000
1	-2.019201000	-0.525625000	-1.682772000
5	0.487821000	-0.779663000	-0.627314000
1	0.365538000	-0.683374000	-1.821691000
1	0.395901000	-1.914255000	-0.228737000
1	2.646423000	0.709306000	-1.054530000
1	2.991785000	-1.079375000	-0.047867000

$[HPH_2BH_2{\cdot}NMe_3]^+$

15	2.159477000	0.010281000	-0.000020000
7	-0.895128000	0.005758000	-0.000003000
6	-0.986294000	-0.854509000	1.220991000
1	-1.937527000	-1.384746000	1.225029000
1	-0.911444000	-0.227217000	2.105445000
1	-0.177169000	-1.582229000	1.217734000
6	-0.986757000	-0.854099000	-1.221257000

1	-0.177369000	-1.581519000	-1.218783000
1	-0.912660000	-0.226457000	-2.105524000
1	-1.937814000	-1.384651000	-1.224894000
6	-2.065365000	0.952426000	0.000363000
1	-2.989840000	0.376762000	0.000098000
1	-2.015509000	1.577706000	-0.886892000
1	-2.015555000	1.576968000	0.888139000
5	0.411014000	0.922846000	-0.000099000
1	0.461843000	1.573617000	1.003593000
1	0.461834000	1.573518000	-1.003856000
1	2.531764000	-0.787567000	1.093380000
1	3.136867000	1.012444000	-0.000327000
1	2.531751000	-0.788290000	-1.092913000

$[Ni(CO)_3PH_2BH_2{\cdot}NMe_3]$

28	1.452215000	0.055634000	0.119490000
15	-0.197777000	-0.666826000	-1.339321000
8	3.933136000	-0.280963000	-1.463543000
8	0.950243000	2.892904000	0.756190000
7	-2.878544000	-0.023741000	-0.036074000
8	1.388523000	-1.748699000	2.460728000
6	-2.796102000	1.344878000	-0.614934000
1	-3.401168000	2.037047000	-0.027032000
1	-3.157849000	1.315165000	-1.639960000
1	-1.761448000	1.678058000	-0.606161000
6	2.981994000	-0.150412000	-0.848881000
6	1.139570000	1.791267000	0.512453000
6	-2.328499000	-0.008749000	1.348911000
1	-1.275793000	0.257411000	1.311967000
1	-2.429317000	-1.003486000	1.775196000
1	-2.874667000	0.714281000	1.957114000
6	-4.309982000	-0.432158000	0.025429000
1	-4.862547000	0.250083000	0.674135000
1	-4.369469000	-1.445123000	0.415000000
1	-4.727342000	-0.413255000	-0.977755000
6	1.408688000	-1.053268000	1.555266000
5	-2.099689000	-1.114781000	-0.979098000
1	-2.711302000	-1.153128000	-2.014828000
1	-2.119706000	-2.155255000	-0.374086000
1	-0.251741000	0.120441000	-2.513170000
1	0.145998000	-1.872785000	-1.984786000

$AsH_2BH_2{\cdot}NMe_3$

33	1.704370000	0.026158000	0.055443000
7	-1.408394000	-0.011617000	-0.007744000
6	-1.379531000	1.347233000	-0.609252000
1	-2.277980000	1.902615000	-0.331734000
1	-1.322211000	1.249464000	-1.690619000
1	-0.499707000	1.877220000	-0.251756000
6	-1.442140000	0.105062000	1.474641000
1	-0.540583000	0.609496000	1.812873000
1	-1.470928000	-0.894079000	1.902334000
1	-2.323848000	0.668760000	1.786402000
6	-2.640235000	-0.712521000	-0.459827000
1	-3.526685000	-0.162468000	-0.135461000
1	-2.648348000	-1.713722000	-0.036783000
1	-2.624301000	-0.788382000	-1.543730000
5	-0.109040000	-0.903514000	-0.513600000
1	-0.242397000	-1.004275000	-1.704354000
1	-0.197432000	-1.950529000	0.076270000
1	2.051276000	0.699615000	-1.271368000
1	2.554338000	-1.196671000	-0.252853000

$[HAsH_2BH_2NMe_3]^+$

33	-1.710413000	-0.007534000	-0.000008000
7	1.451663000	-0.004529000	-0.000010000
6	1.523999000	0.857663000	1.220798000
1	2.463674000	1.408079000	1.224602000
1	1.462135000	0.229001000	2.105219000
1	0.699073000	1.567098000	1.216787000
6	1.525362000	0.855297000	-1.222404000
1	0.699439000	1.563576000	-1.221611000
1	1.466231000	0.224787000	-2.105683000
1	2.464279000	1.407021000	-1.225330000
6	2.642825000	-0.926963000	0.001560000
1	3.554076000	-0.330748000	0.000403000
1	2.606989000	-1.554016000	-0.885144000
1	2.607139000	-1.550821000	0.890520000
5	0.177896000	-0.960907000	0.000062000
1	0.126948000	-1.593480000	1.011250000
1	0.127224000	-1.593905000	-1.010848000
1	-2.143692000	0.839049000	1.164353000
1	-2.750361000	-1.086101000	-0.000092000
1	-2.143749000	0.839340000	-1.164128000

$[Ni(CO)_3AsH_2BH_2{\cdot}NMe_3]$

28	1.560663000	0.316599000	0.002744000
33	-0.216936000	-1.356593000	-0.003393000
8	4.015806000	-1.302727000	-0.331962000
8	1.068743000	2.099726000	-2.294299000
7	-2.940254000	0.198165000	0.009874000
8	1.450313000	1.652218000	2.635028000
6	-2.847854000	0.313773000	-1.471835000
1	-3.409846000	1.184340000	-1.813705000
1	-3.253469000	-0.589576000	-1.920966000
1	-1.806081000	0.424537000	-1.762229000
6	3.069352000	-0.680556000	-0.203161000
6	1.251453000	1.406248000	-1.403066000
6	-2.328527000	1.403857000	0.638191000
1	-1.274898000	1.450945000	0.376339000
1	-2.423954000	1.321147000	1.717719000
1	-2.838071000	2.302731000	0.287306000
6	-4.379426000	0.140964000	0.394851000
1	-4.883520000	1.057184000	0.081849000
1	-4.450106000	0.027930000	1.473536000
1	-4.839436000	-0.719682000	-0.083225000
6	1.483008000	1.128290000	1.620640000
5	-2.241962000	-1.179342000	0.546221000
1	-2.865683000	-2.087147000	0.068137000
1	-2.278443000	-1.135582000	1.746479000
1	-0.287631000	-2.127163000	-1.311612000
1	0.096111000	-2.566511000	0.851430000

$PH_2BH_2{\cdot}SIDipp$

15	-0.394006000	-1.534318000	2.741865000
7	-1.056243000	0.008761000	-0.594467000
7	1.131686000	-0.057489000	-0.593240000
6	0.040156000	0.024761000	0.192080000
6	-0.716507000	0.033151000	-2.027555000
1	-0.989700000	1.000662000	-2.456755000
1	-1.256117000	-0.739870000	-2.570536000
6	-2.933984000	1.412715000	0.153231000
6	3.117604000	1.285701000	-0.091406000
6	2.512807000	0.019925000	-0.200037000
6	-2.098146000	2.683454000	0.094346000
1	-1.055265000	2.395707000	-0.027780000
6	-3.260956000	-0.993914000	-0.224515000
6	-4.280296000	1.508097000	0.503689000
1	-4.689694000	2.471191000	0.778864000
6	-4.600506000	-0.837099000	0.127705000
1	-5.257992000	-1.696381000	0.114554000
6	-3.311024000	-2.697103000	-2.084783000
1	-4.397258000	-2.809175000	-2.065668000
1	-2.885962000	-3.636983000	-2.444639000

1	-3.079349000	-1.918410000	-2.813502000
6	2.624838000	-2.547468000	-0.153808000
1	1.545353000	-2.421123000	-0.243218000
6	4.475013000	1.338069000	0.219244000
1	4.960278000	2.300263000	0.321698000
6	-2.428913000	0.143235000	-0.187539000
6	3.246939000	-1.165433000	-0.020456000
6	-5.106773000	0.397302000	0.498711000
1	-6.148753000	0.494939000	0.777212000
6	0.795116000	-0.199520000	-2.018088000
1	1.066285000	-1.196097000	-2.373742000
1	1.342426000	0.531092000	-2.613703000
6	5.215007000	0.181667000	0.404127000
1	6.268671000	0.244651000	0.646234000
6	2.870281000	-3.416462000	1.088594000
1	3.929245000	-3.653390000	1.209247000
1	2.330477000	-4.361408000	0.997976000
1	2.528169000	-2.919560000	1.995852000
6	-2.772158000	-2.362788000	-0.680950000
1	-1.683209000	-2.326970000	-0.733388000
6	2.908702000	3.402724000	-1.466221000
1	3.935304000	3.725210000	-1.281112000
1	2.304782000	4.299099000	-1.623999000
1	2.907046000	2.825575000	-2.393394000
6	2.324876000	3.426006000	0.998591000
1	1.896856000	2.859097000	1.824877000
1	1.722415000	4.325078000	0.849299000
1	3.329010000	3.744936000	1.286330000
6	-2.493341000	3.539306000	-1.122495000
1	-3.524260000	3.889843000	-1.038076000
1	-2.413320000	2.979306000	-2.056481000
1	-1.847399000	4.417202000	-1.197140000
6	3.123263000	-3.266521000	-1.419281000
1	2.936531000	-2.680403000	-2.321423000
1	2.623852000	-4.231483000	-1.531944000
1	4.198274000	-3.452120000	-1.366766000
6	4.604046000	-1.055003000	0.282362000
1	5.190328000	-1.952559000	0.430945000
5	0.091605000	0.143909000	1.776323000
6	-3.136977000	-3.491071000	0.294666000
1	-2.770472000	-3.283957000	1.298552000
1	-2.692846000	-4.430562000	-0.041602000
1	-4.216732000	-3.643169000	0.348993000
6	-2.181051000	3.512525000	1.383763000
1	-1.498378000	4.362933000	1.324843000
1	-1.903862000	2.915490000	2.251627000
1	-3.184613000	3.911288000	1.545005000
6	2.353508000	2.586301000	-0.287957000
1	1.320320000	2.335134000	-0.526457000
1	-0.715218000	0.953189000	2.158751000
1	1.209459000	0.433686000	2.114495000
1	0.003493000	-2.549214000	1.825602000
1	-1.763340000	-1.651761000	2.388619000

$[HPH_2BH_2{\cdot}SIDipp]^+$

15	-1.365293000	-0.341337000	2.763170000
7	-0.965468000	0.006645000	-0.719720000
7	1.223659000	-0.030868000	-0.632662000
6	0.103297000	0.022689000	0.083203000
6	-0.578999000	0.003532000	-2.147560000
1	-0.922462000	0.923406000	-2.622027000
1	-1.039015000	-0.837618000	-2.662809000
6	-2.906544000	1.363329000	-0.070934000
6	3.279655000	1.145438000	0.005102000
6	2.581726000	-0.065607000	-0.144394000
6	-2.145631000	2.666956000	-0.275828000
1	-1.103658000	2.425358000	-0.489146000
6	-3.101225000	-1.091945000	-0.230206000
6	-4.239328000	1.408607000	0.338521000
1	-4.701130000	2.365770000	0.541262000
6	-4.428887000	-0.981796000	0.183326000
1	-5.037725000	-1.872392000	0.263944000
6	-3.148454000	-2.882573000	-1.995344000
1	-4.223907000	-3.049732000	-1.913430000
1	-2.691106000	-3.813909000	-2.333704000
1	-2.994279000	-2.127343000	-2.767693000
6	2.452535000	-2.637982000	-0.088655000
1	1.418781000	-2.421501000	-0.364892000
6	4.605291000	1.075978000	0.431367000
1	5.170653000	1.989448000	0.560081000
6	-2.343426000	0.095313000	-0.316926000
6	3.181387000	-1.314570000	0.097212000
6	-4.990108000	0.251333000	0.476849000
1	-6.022954000	0.312327000	0.795183000
6	0.950933000	-0.098450000	-2.082248000
1	1.331646000	-1.037442000	-2.484778000
1	1.454767000	0.719795000	-2.594892000
6	5.215209000	-0.140815000	0.688486000
1	6.246053000	-0.169792000	1.017413000
6	2.406075000	-3.456629000	1.211195000
1	3.404588000	-3.763117000	1.526238000
1	1.816108000	-4.363692000	1.065580000
1	1.962077000	-2.885346000	2.027686000
6	-2.553480000	-2.453797000	-0.640582000
1	-1.473359000	-2.360962000	-0.767758000
6	3.331834000	3.163994000	-1.513790000
1	4.383457000	3.380375000	-1.318767000
1	2.838683000	4.107808000	-1.754206000
1	3.288301000	2.523565000	-2.396944000
6	2.709765000	3.440554000	0.922696000
1	2.231387000	2.987966000	1.791891000
1	2.195593000	4.377001000	0.698157000
1	3.735754000	3.689463000	1.197910000
6	-2.698865000	3.430768000	-1.492357000
1	-3.733340000	3.737615000	-1.328857000
1	-2.675820000	2.822426000	-2.398323000
1	-2.109773000	4.331409000	-1.673504000
6	3.069741000	-3.464789000	-1.228996000
1	3.082849000	-2.911780000	-2.170153000
1	2.502926000	-4.384974000	-1.383185000
1	4.099292000	-3.744586000	-1.000315000
6	4.509327000	-1.321271000	0.519781000
1	5.000004000	-2.265049000	0.718430000
5	0.154026000	0.187890000	1.674248000
6	-2.790291000	-3.552115000	0.405904000
1	-2.343285000	-3.305566000	1.370168000
1	-2.345422000	-4.489413000	0.068592000
1	-3.852575000	-3.737690000	0.568997000
6	-2.152799000	3.563053000	0.971444000
1	-1.559118000	4.460224000	0.789878000
1	-1.726876000	3.054934000	1.837782000
1	-3.161636000	3.887212000	1.230989000
6	2.664022000	2.504851000	-0.295129000
1	1.611402000	2.353883000	-0.541721000
1	0.272913000	1.352687000	1.956449000
1	1.037490000	-0.454666000	2.167432000
1	-1.748079000	-1.689180000	2.778380000
1	-2.597695000	0.318360000	2.665991000
1	-1.016143000	-0.129469000	4.103735000

$[Ni(CO)_3PH_2BH_2{\cdot}SIDipp]$

28	3.157542000	-2.343647000	-0.732869000

15	1.753162000	-0.787264000	0.227381000
7	-0.760144000	1.918266000	0.525938000
7	-2.146741000	0.225930000	0.539356000
8	5.512474000	-2.451682000	1.049400000
8	3.759266000	-1.262530000	-3.417895000
8	1.641489000	-4.879381000	-0.824305000
6	-0.928796000	0.636524000	0.151560000
6	0.370372000	2.771424000	0.269553000
6	-1.983828000	2.490530000	1.117256000
1	-2.404781000	3.238368000	0.441442000
1	-1.766019000	2.977494000	2.065273000
6	0.533763000	3.349149000	-1.003941000
6	-2.770607000	-1.049977000	0.304910000
6	-3.524096000	-1.229036000	-0.868921000
6	-4.178809000	-2.446765000	-1.043746000
1	-4.756026000	-2.615625000	-1.943816000
6	-2.680786000	-2.049961000	1.288182000
6	-2.886576000	1.265263000	1.274342000
1	-3.015085000	0.967567000	2.317074000
1	-3.875719000	1.406824000	0.839426000
6	-0.447647000	3.135239000	-2.148034000
1	-1.099695000	2.303992000	-1.883793000
6	1.239814000	3.075527000	1.336448000
6	-1.884016000	-1.875929000	2.572686000
1	-1.333680000	-0.936876000	2.501134000
6	-4.100850000	-3.447470000	-0.088893000
1	-4.614978000	-4.387456000	-0.245708000
6	1.036370000	2.541976000	2.749160000
1	0.272737000	1.763889000	2.705154000
6	1.621756000	4.199906000	-1.197530000
1	1.778511000	4.646948000	-2.170094000
6	-3.359832000	-3.247022000	1.063804000
1	-3.301273000	-4.037397000	1.800721000
6	0.243245000	2.754358000	-3.464811000
1	0.853849000	3.571497000	-3.853771000
1	-0.506148000	2.519111000	-4.223346000
1	0.880945000	1.880260000	-3.338583000
6	4.605979000	-2.416343000	0.354654000
6	0.529365000	3.651689000	3.688949000
1	1.287267000	4.426818000	3.820256000
1	0.299149000	3.241505000	4.674767000
1	-0.368567000	4.139431000	3.305527000
6	-0.845227000	-2.990984000	2.763847000
1	-1.321975000	-3.960059000	2.922207000
1	-0.226260000	-2.782722000	3.638962000
1	-0.189861000	-3.078313000	1.897882000
6	2.304568000	3.939012000	1.085857000
1	2.992527000	4.181613000	1.885101000
6	2.224981000	-3.897895000	-0.790139000
6	-3.639285000	-0.161651000	-1.946576000
1	-3.061726000	0.705003000	-1.624497000
6	3.526847000	-1.681553000	-2.381180000
6	-1.331334000	4.380291000	-2.345809000
1	-1.862029000	4.653256000	-1.431343000
1	-2.073223000	4.200916000	-3.127211000
1	-0.732413000	5.242743000	-2.645901000
6	2.502307000	4.490074000	-0.169248000
1	3.341581000	5.151430000	-0.344638000
6	2.299490000	1.898001000	3.339353000
1	2.680927000	1.102945000	2.700762000
1	2.075687000	1.468407000	4.318137000
1	3.096713000	2.630027000	3.480411000
5	0.084962000	-0.272871000	-0.685643000
6	-2.809493000	-1.784619000	3.798127000
1	-3.541284000	-0.980543000	3.696646000
1	-2.227215000	-1.601911000	4.704001000
1	-3.363669000	-2.714685000	3.940964000
6	-3.032979000	-0.634282000	-3.277199000
1	-1.993433000	-0.935358000	-3.149557000
1	-3.069596000	0.169564000	-4.015913000
1	-3.585202000	-1.483483000	-3.685030000
6	-5.092416000	0.302079000	-2.136302000
1	-5.725481000	-0.508647000	-2.501897000
1	-5.140263000	1.113004000	-2.866363000
1	-5.526486000	0.661828000	-1.200915000
1	-0.459767000	-1.298052000	-0.991502000
1	2.397859000	0.432225000	0.527842000
1	0.450171000	0.336811000	-1.658593000
1	1.389204000	-1.082881000	1.563797000

[PH_2BH_2·IDipp]

15	0.357432000	-1.443487000	2.849692000
7	1.044444000	0.062662000	-0.597908000
7	-1.112614000	-0.001761000	-0.589631000
6	-0.032796000	0.073377000	0.238769000
6	-2.506614000	0.039187000	-0.209022000
6	2.437590000	0.135080000	-0.218302000
6	-0.711712000	-0.046826000	-1.915697000
1	-1.419373000	-0.096355000	-2.722373000
6	0.634756000	-0.003626000	-1.920178000
1	1.336375000	-0.008384000	-2.733164000
6	-3.204928000	-1.169428000	-0.063370000
6	3.199242000	-1.046535000	-0.223165000
6	2.994254000	1.389901000	0.076763000
6	2.621918000	-2.401319000	-0.613522000
1	1.535265000	-2.330983000	-0.555999000
6	-3.125725000	1.290407000	-0.063434000
6	4.551250000	-0.940416000	0.100799000
1	5.165999000	-1.830236000	0.112251000
6	5.121615000	0.282395000	0.414430000
1	6.172424000	0.339129000	0.670040000
6	4.350331000	1.432704000	0.398108000
1	4.809447000	2.382968000	0.635891000
6	2.199942000	2.685277000	-0.001999000
1	1.142690000	2.429521000	-0.046686000
6	-2.545090000	-2.528434000	-0.245583000
1	-1.465036000	-2.380457000	-0.238725000
6	-4.565357000	-1.094224000	0.235121000
1	-5.133949000	-2.006595000	0.355836000
6	-2.381346000	2.606855000	-0.225362000
1	-1.328275000	2.381632000	-0.389552000
6	-5.201582000	0.127114000	0.385053000
1	-6.257912000	0.161274000	0.621094000
6	-4.486487000	1.304501000	0.237983000
1	-4.992540000	2.252893000	0.362744000
6	2.997239000	-2.759429000	-2.063100000
1	2.668731000	-1.999320000	-2.773021000
1	2.539215000	-3.708217000	-2.351118000
1	4.079473000	-2.863522000	-2.168336000
6	3.048781000	-3.534113000	0.330365000
1	4.117211000	-3.745484000	0.254288000
1	2.518084000	-4.451672000	0.068259000
1	2.819097000	-3.296628000	1.368076000
6	-2.868550000	-3.497925000	0.899919000
1	-2.623268000	-3.064303000	1.869101000
1	-2.287952000	-4.415377000	0.785185000
1	-3.923510000	-3.778698000	0.908676000
6	-2.922595000	-3.148224000	-1.602013000
1	-3.998163000	-3.328795000	-1.663622000
1	-2.413461000	-4.104782000	-1.739343000
1	-2.647387000	-2.498257000	-2.434508000
6	-2.460239000	3.468699000	1.043725000

1	-3.485821000	3.777648000	1.256295000
1	-1.863115000	4.374711000	0.918491000
1	-2.079527000	2.925220000	1.908134000
6	2.386209000	3.574477000	1.234680000
1	2.141042000	3.031676000	2.147167000
1	1.727488000	4.442981000	1.169451000
1	3.408684000	3.948238000	1.318783000
5	-0.066129000	0.214320000	1.821325000
6	2.547445000	3.455177000	-1.287951000
1	3.597731000	3.755138000	-1.294314000
1	1.939858000	4.359528000	-1.366025000
1	2.369103000	2.850780000	-2.179456000
6	-2.878634000	3.384338000	-1.454800000
1	-2.784868000	2.792969000	-2.367717000
1	-2.298039000	4.300297000	-1.584217000
1	-3.927855000	3.668092000	-1.348774000
1	-1.173004000	0.555869000	2.153558000
1	0.765346000	1.016007000	2.173994000
1	-0.183042000	-2.464773000	2.017378000
1	1.685691000	-1.693284000	2.413733000

$[HPH_2BH_2{\cdot}IDipp]^+$

15	1.241269000	-0.557142000	2.813432000
7	0.957570000	0.077936000	-0.710179000
7	-1.198373000	-0.001209000	-0.629727000
6	-0.092704000	0.076608000	0.144607000
6	-2.577237000	-0.039130000	-0.176608000
6	2.354047000	0.114972000	-0.330377000
6	-0.841836000	-0.037452000	-1.963465000
1	-1.577697000	-0.093892000	-2.744656000
6	0.507461000	0.011742000	-2.015712000
1	1.182619000	0.005234000	-2.851382000
6	-3.168108000	-1.291938000	0.048155000
6	3.065093000	-1.099247000	-0.282603000
6	2.943098000	1.360264000	-0.051942000
6	2.460878000	-2.434152000	-0.702581000
1	1.375536000	-2.322960000	-0.738651000
6	-3.266748000	1.173529000	-0.027468000
6	4.402258000	-1.036252000	0.110297000
1	4.986119000	-1.945160000	0.159271000
6	5.001743000	0.172936000	0.427514000
1	6.040943000	0.196027000	0.729721000
6	4.282591000	1.354859000	0.337891000
1	4.774006000	2.291858000	0.561596000
6	2.210007000	2.682678000	-0.228014000
1	1.143641000	2.473872000	-0.315974000
6	-2.427769000	-2.609900000	-0.129297000
1	-1.388009000	-2.388883000	-0.376557000
6	-4.504443000	-1.301326000	0.444832000
1	-4.997984000	-2.246486000	0.628234000
6	-2.637959000	2.532360000	-0.300478000
1	-1.575421000	2.384773000	-0.500435000
6	-5.213688000	-0.121742000	0.606401000
1	-6.250777000	-0.153812000	0.914660000
6	-4.600719000	1.098410000	0.371601000
1	-5.168908000	2.010247000	0.497618000
6	2.931685000	-2.814206000	-2.118722000
1	2.694915000	-2.039640000	-2.848996000
1	2.453257000	-3.740176000	-2.441896000
1	4.011886000	-2.968828000	-2.140571000
6	2.766232000	-3.576717000	0.276285000
1	3.829410000	-3.818116000	0.303866000
1	2.238472000	-4.480095000	-0.032482000
1	2.454082000	-3.341104000	1.294979000
6	-2.416471000	-3.438307000	1.164896000
1	-2.001868000	-2.870371000	1.999579000
1	-1.816095000	-4.340100000	1.030096000
1	-3.421447000	-3.754368000	1.448200000
6	-3.006741000	-3.425088000	-1.297077000
1	-4.045551000	-3.701586000	-1.109741000
1	-2.437864000	-4.346168000	-1.436770000
1	-2.977539000	-2.863917000	-2.232640000
6	-2.738808000	3.467955000	0.913740000
1	-3.775186000	3.719309000	1.143959000
1	-2.213735000	4.403075000	0.710855000
1	-2.298200000	3.015439000	1.802899000
6	2.384552000	3.631712000	0.965522000
1	2.077528000	3.163869000	1.901964000
1	1.772324000	4.523056000	0.821610000
1	3.417607000	3.964573000	1.075682000
5	-0.124870000	0.296565000	1.724129000
6	2.652839000	3.364282000	-1.535376000
1	3.714890000	3.614649000	-1.506680000
1	2.094283000	4.289284000	-1.687902000
1	2.486183000	2.722502000	-2.402219000
6	-3.249694000	3.183710000	-1.551830000
1	-3.146666000	2.544056000	-2.430328000
1	-2.756474000	4.133726000	-1.765488000
1	-4.313150000	3.385020000	-1.412428000
1	-1.130081000	-0.131208000	2.217623000
1	0.035586000	1.456540000	2.012300000
1	1.336345000	-1.956930000	2.813973000
1	2.584460000	-0.171583000	2.703553000
1	0.962144000	-0.287889000	4.159634000

$[Ni(CO)_3PH_2BH_2{\cdot}IDipp]$

28	-3.572621000	-1.713783000	-0.703811000
15	-1.859994000	-0.491381000	0.238947000
7	1.187295000	1.758854000	0.444384000
7	2.159832000	-0.166230000	0.472024000
8	-4.063198000	-0.453868000	-3.332994000
8	-5.838379000	-1.435923000	1.173094000
8	-2.553422000	-4.479813000	-0.916347000
6	1.019954000	0.459659000	0.074067000
6	2.497601000	-1.560448000	0.282969000
6	0.244538000	2.841093000	0.258377000
6	3.027882000	0.732728000	1.067948000
1	3.990665000	0.432299000	1.437732000
6	2.420219000	1.936421000	1.048407000
1	2.747005000	2.897283000	1.399393000
6	2.228830000	-2.465491000	1.321003000
6	-0.535620000	3.245413000	1.355768000
6	0.189525000	3.483823000	-0.988741000
6	-0.424155000	2.603106000	2.733037000
1	0.087268000	1.646489000	2.618043000
6	3.132832000	-1.940656000	-0.908734000
6	-1.408063000	4.315680000	1.161712000
1	-2.028605000	4.652204000	1.981192000
6	-1.499144000	4.954244000	-0.064245000
1	-2.189152000	5.778597000	-0.193858000
6	-0.706140000	4.544029000	-1.123263000
1	-0.782027000	5.058295000	-2.071766000
6	1.098617000	3.110340000	-2.150526000
1	1.521254000	2.128024000	-1.944877000
6	1.567238000	-2.051412000	2.627671000
1	1.141588000	-1.056970000	2.489554000
6	-3.872831000	-0.941173000	-2.317758000
6	2.618669000	-3.790938000	1.132085000
1	2.424455000	-4.518202000	1.908892000
6	3.439026000	-0.963769000	-2.034099000
1	3.025024000	0.007381000	-1.763141000
6	3.244845000	-4.196201000	-0.035368000

1	3.533920000	-5.231989000	-0.161664000
6	3.497393000	-3.279448000	-1.042615000
1	3.983874000	-3.608735000	-1.951497000
6	0.422399000	3.476942000	3.676478000
1	1.420130000	3.665355000	3.277997000
1	0.534649000	2.990219000	4.647648000
1	-0.056198000	4.444953000	3.839346000
6	-4.968067000	-1.549620000	0.441267000
6	-1.786353000	2.309587000	3.377274000
1	-2.320243000	3.226472000	3.632703000
1	-1.642977000	1.750939000	4.304241000
1	-2.423274000	1.717138000	2.721864000
6	0.411691000	-2.981377000	3.023551000
1	-0.315953000	-3.080702000	2.218282000
1	-0.103802000	-2.581934000	3.899095000
1	0.766353000	-3.980497000	3.282815000
6	2.600502000	-1.958952000	3.763574000
1	3.060681000	-2.931199000	3.952579000
1	2.122351000	-1.628529000	4.688258000
1	3.399807000	-1.254252000	3.527285000
6	-2.946843000	-3.410122000	-0.837036000
6	2.770072000	-1.381143000	-3.352254000
1	3.165204000	-2.329973000	-3.720882000
1	2.954486000	-0.627486000	-4.120917000
1	1.692439000	-1.485891000	-3.228680000
6	0.349680000	2.997915000	-3.484619000
1	-0.487699000	2.304618000	-3.409684000
1	1.025971000	2.628940000	-4.258192000
1	-0.031901000	3.963448000	-3.822073000
5	-0.175670000	-0.199784000	-0.749545000
6	2.268037000	4.104484000	-2.260538000
1	1.906784000	5.113426000	-2.471178000
1	2.939902000	3.812433000	-3.070556000
1	2.850251000	4.145805000	-1.337926000
6	4.954238000	-0.778470000	-2.214567000
1	5.429667000	-0.440927000	-1.291424000
1	5.156166000	-0.036757000	-2.990236000
1	5.435548000	-1.711819000	-2.513650000
1	0.172536000	-1.279238000	-1.147615000
1	-0.484863000	0.526785000	-1.661892000
1	-1.484150000	-0.938679000	1.529550000
1	-2.254833000	0.799242000	0.655617000

AsH_2BH_2·IDipp

33	0.337059000	-1.713823000	2.533771000
7	1.014839000	0.271731000	-0.786831000
7	-1.143017000	0.184927000	-0.766404000
6	-0.054809000	0.182496000	0.056730000
6	-2.533443000	0.172654000	-0.371722000
6	2.411851000	0.319645000	-0.418295000
6	-0.754222000	0.283900000	-2.092920000
1	-1.469119000	0.312662000	-2.894137000
6	0.591515000	0.341182000	-2.104695000
1	1.285220000	0.428912000	-2.919601000
6	-3.225106000	-1.048275000	-0.364689000
6	3.188774000	-0.842575000	-0.568250000
6	2.957790000	1.541412000	0.007331000
6	2.623038000	-2.154851000	-1.096111000
1	1.536811000	-2.109099000	-1.012486000
6	-3.157818000	1.394498000	-0.074850000
6	4.544832000	-0.753086000	-0.256362000
1	5.170956000	-1.629293000	-0.355941000
6	5.104866000	0.434823000	0.184171000
1	6.159393000	0.478261000	0.426844000
6	4.318434000	1.567830000	0.310567000
1	4.769308000	2.492588000	0.645366000
6	2.147313000	2.826940000	0.087587000
1	1.092776000	2.565768000	0.016437000
6	-2.563759000	-2.373637000	-0.714228000
1	-1.483887000	-2.225351000	-0.695561000
6	-4.583164000	-1.016454000	-0.047852000
1	-5.146120000	-1.940043000	-0.031868000
6	-2.422203000	2.725997000	-0.097312000
1	-1.365477000	2.524901000	-0.268614000
6	-5.223855000	0.174635000	0.251213000
1	-6.278250000	0.174563000	0.498215000
6	-4.515735000	1.365367000	0.238042000
1	-5.025573000	2.290004000	0.475855000
6	2.975761000	-2.346681000	-2.582468000
1	2.624359000	-1.518662000	-3.199239000
1	2.524345000	-3.264968000	-2.964518000
1	4.057008000	-2.423305000	-2.717647000
6	3.082316000	-3.377679000	-0.289930000
1	4.152018000	-3.562913000	-0.405365000
1	2.559777000	-4.268911000	-0.643461000
1	2.866272000	-3.258419000	0.770598000
6	-2.879427000	-3.474997000	0.307481000
1	-2.632203000	-3.160242000	1.320996000
1	-2.295206000	-4.369286000	0.082170000
1	-3.933321000	-3.759445000	0.285601000
6	-2.949483000	-2.826270000	-2.132840000
1	-4.025184000	-3.000174000	-2.208846000
1	-2.440048000	-3.758489000	-2.386525000
1	-2.680410000	-2.080947000	-2.883391000
6	-2.522982000	3.461025000	1.247187000
1	-3.552468000	3.745304000	1.474420000
1	-1.928133000	4.376646000	1.219346000
1	-2.151636000	2.837572000	2.060231000
6	2.332024000	3.562396000	1.421473000
1	2.098244000	2.910483000	2.262725000
1	1.664371000	4.425454000	1.465641000
1	3.351426000	3.933426000	1.544764000
5	-0.078985000	0.165906000	1.637432000
6	2.478173000	3.749239000	-1.098566000
1	3.525907000	4.057213000	-1.076577000
1	1.862841000	4.651123000	-1.063679000
1	2.297576000	3.254118000	-2.054678000
6	-2.912822000	3.612942000	-1.253176000
1	-2.801925000	3.112296000	-2.217043000
1	-2.341188000	4.542992000	-1.287930000
1	-3.966561000	3.873655000	-1.133578000
1	-1.178535000	0.470129000	2.018944000
1	0.776346000	0.890021000	2.078792000
1	-0.070362000	-2.673467000	1.408715000
1	1.812736000	-1.829923000	2.150946000

$[HAsH_2BH_2$·IDipp$]^+$

33	1.118281000	-1.020183000	2.586010000
7	0.858648000	0.273522000	-0.914628000
7	-1.292416000	0.123216000	-0.783043000
6	-0.166374000	0.168718000	-0.034115000
6	-2.658896000	0.011950000	-0.304477000
6	2.269023000	0.309672000	-0.582249000
6	-0.974546000	0.211627000	-2.123049000
1	-1.730918000	0.201939000	-2.886417000
6	0.371517000	0.304511000	-2.206289000
1	1.021854000	0.387832000	-3.057114000
6	-3.216917000	-1.269451000	-0.181867000
6	3.009302000	-0.882148000	-0.696082000
6	2.842681000	1.535320000	-0.204000000
6	2.413168000	-2.187734000	-1.209962000
1	1.324981000	-2.108617000	-1.166444000

6	-3.372252000	1.190253000	-0.038870000
6	4.364372000	-0.821174000	-0.371242000
1	4.970913000	-1.713103000	-0.448483000
6	4.952261000	0.365682000	0.038206000
1	6.005995000	0.388031000	0.285041000
6	4.201120000	1.527850000	0.113696000
1	4.681189000	2.450103000	0.410927000
6	2.072101000	2.848310000	-0.206812000
1	1.006865000	2.619366000	-0.245099000
6	-2.449443000	-2.548339000	-0.485712000
1	-1.423502000	-2.279001000	-0.742598000
6	-4.545672000	-1.345511000	0.233541000
1	-5.015366000	-2.314175000	0.341166000
6	-2.775974000	2.581754000	-0.193012000
1	-1.720248000	2.476739000	-0.448168000
6	-5.278357000	-0.201792000	0.508048000
1	-6.309191000	-0.285478000	0.827373000
6	-4.697087000	1.048567000	0.372692000
1	-5.283426000	1.931739000	0.588414000
6	2.799478000	-2.416796000	-2.682966000
1	2.495504000	-1.585611000	-3.320184000
1	2.326305000	-3.323541000	-3.063601000
1	3.879789000	-2.532859000	-2.786826000
6	2.810428000	-3.410769000	-0.370536000
1	3.876986000	-3.626124000	-0.442279000
1	2.279163000	-4.294005000	-0.728212000
1	2.570969000	-3.282230000	0.686229000
6	-2.381068000	-3.475217000	0.737848000
1	-1.963175000	-2.961311000	1.605622000
1	-1.759338000	-4.345791000	0.520002000
1	-3.369431000	-3.841295000	1.019135000
6	-3.039749000	-3.284067000	-1.699370000
1	-4.062717000	-3.610882000	-1.505999000
1	-2.447070000	-4.170573000	-1.932918000
1	-3.058068000	-2.646460000	-2.584818000
6	-2.843519000	3.381773000	1.117170000
1	-3.874729000	3.582816000	1.411458000
1	-2.345014000	4.344994000	0.994469000
1	-2.358701000	2.848798000	1.936065000
6	2.305979000	3.685299000	1.057992000
1	2.085352000	3.118103000	1.963087000
1	1.658418000	4.563255000	1.046385000
1	3.333815000	4.044623000	1.125549000
5	-0.148410000	0.282842000	1.553940000
6	2.413226000	3.661908000	-1.468420000
1	3.469088000	3.938402000	-1.482235000
1	1.825561000	4.581089000	-1.496203000
1	2.205111000	3.100895000	-2.381162000
6	-3.445552000	3.351228000	-1.343522000
1	-3.366807000	2.812117000	-2.289327000
1	-2.974537000	4.327560000	-1.470873000
1	-4.505606000	3.517489000	-1.144577000
1	-1.202616000	0.009677000	2.044532000
1	0.286486000	1.336173000	1.931055000
1	0.953865000	-2.509750000	2.452034000
1	2.611057000	-0.881439000	2.490110000
1	0.900878000	-0.843378000	4.060713000

[Ni(CO)$_3$AsH$_2$BH$_2$·IDipp]

28	-3.997488000	0.275289000	-0.797190000
33	-1.778305000	0.619415000	0.141833000
7	2.094119000	0.865250000	0.490440000
7	1.839255000	-1.277227000	0.560273000
8	-3.746661000	0.973195000	-3.657994000
8	-5.734179000	2.118857000	0.722845000
8	-4.608183000	-2.576585000	-0.337291000
6	1.262925000	-0.137232000	0.090516000
6	1.377963000	-2.633719000	0.357381000
6	1.931527000	2.280280000	0.235197000
6	3.016115000	-0.988340000	1.229170000
1	3.625514000	-1.758861000	1.663744000
6	3.176429000	0.349650000	1.182732000
1	3.955068000	0.979737000	1.569753000
6	0.587271000	-3.233575000	1.349647000
6	1.440296000	3.097533000	1.268367000
6	2.328927000	2.791728000	-1.010772000
6	1.082515000	2.563069000	2.649973000
1	0.959685000	1.481951000	2.571264000
6	1.791193000	-3.315560000	-0.797419000
6	1.331714000	4.463069000	1.007949000
1	0.952421000	5.122222000	1.776828000
6	1.696524000	4.991848000	-0.219355000
1	1.597159000	6.054739000	-0.400699000
6	2.192926000	4.164434000	-1.212990000
1	2.484143000	4.591977000	-2.162961000
6	2.948064000	1.928907000	-2.100828000
1	2.762301000	0.885260000	-1.851662000
6	0.164064000	-2.507622000	2.618660000
1	0.329723000	-1.440458000	2.466898000
6	-3.829976000	0.706078000	-2.551056000
6	0.209926000	-4.561433000	1.152384000
1	-0.402438000	-5.055942000	1.894193000
6	2.657994000	-2.679307000	-1.873952000
1	2.837942000	-1.641121000	-1.595576000
6	0.599124000	-5.258298000	0.020120000
1	0.289094000	-6.287022000	-0.114016000
6	1.380377000	-4.639846000	-0.942020000
1	1.674933000	-5.193761000	-1.823823000
6	2.218753000	2.835828000	3.652652000
1	3.166909000	2.405224000	3.328680000
1	1.973654000	2.412429000	4.629050000
1	2.370704000	3.909683000	3.781044000
6	-5.063095000	1.405961000	0.134306000
6	-0.236681000	3.127667000	3.195090000
1	-0.161791000	4.194314000	3.414046000
1	-0.494921000	2.623814000	4.128493000
1	-1.057432000	2.980890000	2.494579000
6	-1.327555000	-2.689019000	2.932586000
1	-1.952765000	-2.421547000	2.081048000
1	-1.610925000	-2.052342000	3.772857000
1	-1.561092000	-3.718033000	3.211755000
6	1.024465000	-2.944890000	3.816758000
1	0.894713000	-4.009833000	4.021257000
1	0.736553000	-2.393151000	4.714235000
1	2.086691000	-2.768073000	3.639027000
6	-4.363484000	-1.474658000	-0.515443000
6	1.950749000	-2.661785000	-3.237848000
1	1.772455000	-3.672871000	-3.609334000
1	2.569164000	-2.144521000	-3.974673000
1	0.991716000	-2.147990000	-3.175821000
6	2.323171000	2.172041000	-3.481057000
1	1.242205000	2.036918000	-3.453774000
1	2.734341000	1.464392000	-4.203701000
1	2.535399000	3.175999000	-3.853426000
5	-0.035062000	-0.052355000	-0.820135000
6	4.472896000	2.130619000	-2.147312000
1	4.724194000	3.161444000	-2.406169000
1	4.920522000	1.477315000	-2.899469000
1	4.938901000	1.906509000	-1.185821000
6	4.028800000	-3.367667000	-1.969127000
1	4.554525000	-3.348777000	-1.012444000
1	4.654856000	-2.864711000	-2.709197000

1	3.929527000	-4.411684000	-2.272920000
1	-0.305824000	-1.144422000	-1.236204000
1	0.121587000	0.750817000	-1.702003000
1	-1.647653000	0.164246000	1.590993000
1	-1.467656000	2.073780000	0.454123000

PH_2AlH_2·IDipp

6	0.532650000	0.247994000	-2.074865000
6	-0.814440000	0.173923000	-2.040872000
7	-1.173867000	0.081555000	-0.708549000
6	-0.079334000	0.096741000	0.098075000
7	0.969304000	0.195478000	-0.763759000
1	1.214303000	0.331404000	-2.900838000
1	-1.544354000	0.179828000	-2.829642000
6	2.374618000	0.220196000	-0.414307000
6	3.101667000	-0.979818000	-0.491954000
6	2.967232000	1.447540000	-0.075170000
6	4.461812000	-0.924589000	-0.191753000
6	4.329966000	1.437610000	0.220825000
6	5.069308000	0.267399000	0.167220000
1	5.052129000	-1.829833000	-0.233483000
1	4.819586000	2.361651000	0.495776000
6	-2.559729000	-0.008118000	-0.299231000
6	-3.142809000	-1.277472000	-0.179362000
6	-4.495667000	-1.331940000	0.152286000
6	-5.232182000	-0.176282000	0.354719000
1	-4.977706000	-2.294760000	0.260294000
6	-4.627156000	1.063892000	0.231792000
1	-5.211373000	1.959143000	0.400579000
6	-3.277597000	1.179626000	-0.097481000
6	-2.367457000	-2.570521000	-0.382335000
1	-1.324889000	-2.315436000	-0.572828000
6	-2.875789000	-3.348464000	-1.606583000
6	-2.391425000	-3.447278000	0.878965000
1	-2.024926000	-2.899844000	1.747319000
1	-3.401073000	-3.797347000	1.103091000
1	-1.760198000	-4.327019000	0.737355000
1	-3.914677000	-3.659011000	-1.477601000
1	-2.276688000	-4.248807000	-1.758861000
1	-2.819418000	-2.746811000	-2.515938000
6	-2.647923000	2.559722000	-0.215592000
1	-1.584382000	2.432197000	-0.417857000
6	-3.243075000	3.351475000	-1.390874000
6	-2.761116000	3.349365000	1.097539000
1	-3.802297000	3.566821000	1.344494000
1	-2.323591000	2.796560000	1.928794000
1	-2.236564000	4.303039000	1.007737000
1	-3.123042000	2.818681000	-2.336322000
1	-2.748893000	4.320871000	-1.484094000
1	-4.309826000	3.534475000	-1.246389000
6	2.478530000	-2.298725000	-0.930832000
1	1.394830000	-2.200101000	-0.857506000
6	2.822757000	-2.602302000	-2.400159000
6	2.880444000	-3.481506000	-0.038961000
1	3.942063000	-3.718133000	-0.132210000
1	2.665596000	-3.281009000	1.009488000
1	2.323894000	-4.372767000	-0.336141000
1	2.506865000	-1.800640000	-3.069369000
1	2.332516000	-3.523144000	-2.723540000
1	3.899711000	-2.733164000	-2.526506000
6	2.201286000	2.763372000	-0.089908000
1	1.139357000	2.533969000	-0.008861000
6	2.544135000	3.675094000	1.094294000
6	2.424774000	3.499196000	-1.423396000
1	3.477614000	3.760112000	-1.552699000
1	2.125614000	2.890481000	-2.278625000
1	1.843761000	4.423692000	-1.449181000
1	2.400597000	3.156353000	2.041330000
1	1.888291000	4.547967000	1.087379000
1	3.571258000	4.042384000	1.045213000
1	-6.281105000	-0.242508000	0.615404000
1	6.125559000	0.284860000	0.405255000
13	-0.091055000	0.165995000	2.200363000
1	-1.640871000	0.011213000	2.551824000
1	0.547197000	1.607878000	2.480819000
15	1.166460000	-1.549518000	3.290399000
1	2.384247000	-1.395655000	2.577390000
1	0.728748000	-2.648783000	2.501934000

$[HPH_2AlH_2$·IDipp$]^+$

6	0.401692000	0.012709000	-2.147267000
6	-0.948786000	-0.016524000	-2.060464000
7	-1.262120000	-0.018095000	-0.718432000
6	-0.137212000	0.009557000	0.034035000
7	0.885179000	0.027953000	-0.853701000
1	1.055068000	0.023588000	-3.000743000
1	-1.705554000	-0.034533000	-2.823399000
6	2.294665000	0.056714000	-0.523617000
6	2.984877000	-1.165921000	-0.437210000
6	2.916991000	1.304329000	-0.348123000
6	4.341628000	-1.106969000	-0.116406000
6	4.276627000	1.295704000	-0.033443000
6	4.979920000	0.107094000	0.088167000
1	4.910707000	-2.024057000	-0.043164000
1	4.794763000	2.234958000	0.106250000
6	-2.615989000	-0.030687000	-0.192570000
6	-3.229174000	-1.273262000	0.043822000
6	-4.534667000	-1.250652000	0.531073000
6	-5.194167000	-0.054304000	0.764623000
1	-5.044447000	-2.183805000	0.727996000
6	-4.565024000	1.153576000	0.510339000
1	-5.098767000	2.077005000	0.688533000
6	-3.260734000	1.200559000	0.019395000
6	-2.552676000	-2.605341000	-0.249007000
1	-1.488942000	-2.419807000	-0.408786000
6	-3.110320000	-3.224285000	-1.542689000
6	-2.662720000	-3.594139000	0.920345000
1	-2.290199000	-3.158309000	1.847652000
1	-3.692667000	-3.912964000	1.086217000
1	-2.078904000	-4.490759000	0.704669000
1	-4.173948000	-3.447221000	-1.441646000
1	-2.593238000	-4.157966000	-1.771638000
1	-2.992901000	-2.554993000	-2.396943000
6	-2.626348000	2.544154000	-0.314725000
1	-1.559490000	2.386667000	-0.483286000
6	-3.216909000	3.111525000	-1.617748000
6	-2.753433000	3.561797000	0.827716000
1	-3.792256000	3.841896000	1.007553000
1	-2.340605000	3.173177000	1.758955000
1	-2.213044000	4.474935000	0.572212000
1	-3.093984000	2.421574000	-2.454537000
1	-2.726006000	4.050611000	-1.879349000
1	-4.284316000	3.311104000	-1.508391000
6	2.337696000	-2.510888000	-0.744620000
1	1.265121000	-2.355330000	-0.866183000
6	2.870590000	-3.073010000	-2.074286000
6	2.516042000	-3.533962000	0.386086000
1	3.567220000	-3.761246000	0.569588000
1	2.076471000	-3.183152000	1.321264000
1	2.021983000	-4.470274000	0.122641000
1	2.721746000	-2.372386000	-2.897474000
1	2.356154000	-4.002160000	-2.324585000

1	3.938657000	-3.288671000	-2.012436000
6	2.193764000	2.631729000	-0.530276000
1	1.134590000	2.426671000	-0.689677000
6	2.295054000	3.530853000	0.710892000
6	2.707943000	3.363625000	-1.781944000
1	3.760796000	3.632503000	-1.680391000
1	2.607275000	2.748317000	-2.677605000
1	2.143301000	4.284041000	-1.938956000
1	1.883057000	3.043736000	1.596258000
1	1.733085000	4.452091000	0.550546000
1	3.327431000	3.811689000	0.925170000
1	-6.208253000	-0.063700000	1.143047000
1	6.035496000	0.127264000	0.327526000
13	-0.225448000	0.109235000	2.071987000
1	-0.937144000	-1.141834000	2.712604000
1	-0.412365000	1.597277000	2.561814000
15	2.060116000	-0.277426000	3.070212000
1	3.182381000	0.484155000	2.705800000
1	2.617935000	-1.565561000	3.097362000
1	2.005487000	-0.006105000	4.448864000

$[Ni(CO)_3PH_2AlH_2{\cdot}IDipp]$

6	2.526360000	2.322147000	0.396224000
6	3.380372000	1.276241000	0.393785000
7	2.621259000	0.144068000	0.166283000
6	1.306486000	0.456975000	0.024439000
7	1.263071000	1.807111000	0.171869000
1	2.696000000	3.373679000	0.537182000
1	4.445382000	1.230573000	0.529879000
6	0.081689000	2.643282000	0.131673000
6	-0.499152000	3.030722000	1.350724000
6	-0.398252000	3.080385000	-1.113705000
6	-1.613192000	3.866660000	1.291659000
6	-1.519475000	3.910005000	-1.107934000
6	-2.122742000	4.297205000	0.077517000
1	-2.092592000	4.180027000	2.209444000
1	-1.924922000	4.260533000	-2.047159000
6	3.208168000	-1.177625000	0.083558000
6	3.319180000	-1.935573000	1.258637000
6	3.928458000	-3.184722000	1.157689000
6	4.404452000	-3.655132000	-0.055450000
1	4.025120000	-3.801689000	2.041455000
6	4.281980000	-2.882194000	-1.198342000
1	4.654933000	-3.263591000	-2.139712000
6	3.682076000	-1.623937000	-1.159040000
6	2.811838000	-1.453367000	2.609497000
1	2.296324000	-0.504499000	2.459592000
6	3.974340000	-1.191641000	3.581018000
6	1.790516000	-2.426702000	3.216801000
1	0.970823000	-2.619018000	2.524526000
1	2.250020000	-3.384316000	3.469145000
1	1.375248000	-2.009359000	4.136612000
1	4.529001000	-2.108624000	3.790177000
1	3.596738000	-0.806812000	4.530769000
1	4.679651000	-0.462592000	3.176931000
6	3.586234000	-0.795326000	-2.432353000
1	2.975615000	0.083085000	-2.221984000
6	4.972793000	-0.294405000	-2.870252000
6	2.892548000	-1.557415000	-3.570764000
1	3.473894000	-2.425290000	-3.887851000
1	1.901586000	-1.899027000	-3.272547000
1	2.776789000	-0.905089000	-4.438672000
1	5.455796000	0.291943000	-2.085987000
1	4.886242000	0.335324000	-3.758206000
1	5.633794000	-1.128362000	-3.115307000
6	0.055348000	2.610084000	2.705580000
1	0.793787000	1.824669000	2.540765000
6	0.774298000	3.785074000	3.391183000
6	-1.020904000	2.026353000	3.631823000
1	-1.763612000	2.775112000	3.911952000
1	-1.543139000	1.194388000	3.160726000
1	-0.561089000	1.663054000	4.553134000
1	1.578503000	4.186830000	2.772338000
1	1.207510000	3.464661000	4.341018000
1	0.077908000	4.600312000	3.598229000
6	0.285218000	2.739150000	-2.430500000
1	0.947273000	1.891051000	-2.258368000
6	-0.700903000	2.313675000	-3.526099000
6	1.152024000	3.918406000	-2.907017000
1	0.537679000	4.799172000	-3.106164000
1	1.901902000	4.197335000	-2.164167000
1	1.673092000	3.657063000	-3.830445000
1	-1.322248000	1.480583000	-3.199923000
1	-0.149876000	1.990576000	-4.411203000
1	-1.352149000	3.134925000	-3.831007000
1	4.869328000	-4.631456000	-0.111079000
1	-2.994586000	4.938810000	0.054820000
13	-0.174211000	-0.904962000	-0.559700000
1	0.352113000	-2.322171000	-0.066841000
1	-0.266246000	-0.638847000	-2.131201000
15	-2.331275000	-0.560069000	0.432879000
1	-2.557851000	0.834424000	0.404796000
1	-2.070866000	-0.641041000	1.821092000
28	-4.178447000	-1.806818000	-0.230524000
8	-4.547850000	-1.264288000	-3.112811000
8	-3.552075000	-4.637229000	0.351957000
8	-6.386621000	-0.752630000	1.429021000
6	-4.392440000	-1.473316000	-2.000718000
6	-3.779168000	-3.541336000	0.125996000
6	-5.539892000	-1.167836000	0.784105000

$PH_2GaH_2{\cdot}IDipp$

6	0.678789000	0.339615000	-2.177551000
6	-0.670550000	0.340795000	-2.179188000
7	-1.070782000	0.195366000	-0.861767000
6	0.001618000	0.107268000	-0.032539000
7	1.076000000	0.193193000	-0.859370000
1	1.386461000	0.429607000	-2.980983000
1	-1.376174000	0.431439000	-2.984362000
6	2.470405000	0.169010000	-0.470690000
6	3.150946000	-1.058968000	-0.477884000
6	3.099903000	1.384038000	-0.159305000
6	4.506273000	-1.040209000	-0.150066000
6	4.456107000	1.340283000	0.159651000
6	5.153121000	0.143357000	0.166243000
1	5.062641000	-1.967456000	-0.140298000
1	4.972461000	2.257615000	0.410008000
6	-2.465556000	0.169345000	-0.475493000
6	-3.141675000	-1.061139000	-0.476120000
6	-4.497944000	-1.045631000	-0.152188000
6	-5.149987000	0.137679000	0.154363000
1	-5.050943000	-1.974865000	-0.137841000
6	-4.457374000	1.337147000	0.141845000
1	-4.977938000	2.254095000	0.384598000
6	-3.100432000	1.384078000	-0.173756000
6	-2.467498000	-2.372673000	-0.855258000
1	-1.389011000	-2.229970000	-0.782425000
6	-2.792111000	-2.752251000	-2.310756000
6	-2.827011000	-3.525816000	0.090943000
1	-2.626253000	-3.268250000	1.130190000
1	-3.877261000	-3.811490000	0.003533000
1	-2.228175000	-4.404659000	-0.153988000

1	-3.864406000	-2.915996000	-2.439394000
1	-2.275419000	-3.673751000	-2.587527000
1	-2.488666000	-1.973087000	-3.011863000
6	-2.381709000	2.725067000	-0.209736000
1	-1.313588000	2.532818000	-0.310339000
6	-2.818445000	3.550103000	-1.432126000
6	-2.569537000	3.524401000	1.087428000
1	-3.609461000	3.824837000	1.230218000
1	-2.258428000	2.940339000	1.953244000
1	-1.968667000	4.435842000	1.053593000
1	-2.646705000	3.010551000	-2.365505000
1	-2.260877000	4.488187000	-1.476915000
1	-3.881568000	3.795132000	-1.381535000
6	2.483727000	-2.370743000	-0.868586000
1	1.404412000	-2.232841000	-0.799376000
6	2.817533000	-2.738773000	-2.325086000
6	2.842254000	-3.528712000	0.071747000
1	3.897223000	-3.800886000	-0.000753000
1	2.616217000	-3.284537000	1.108983000
1	2.258151000	-4.411978000	-0.192586000
1	2.517861000	-1.954716000	-3.022452000
1	2.303519000	-3.658693000	-2.611955000
1	3.890721000	-2.900655000	-2.448642000
6	2.376436000	2.722755000	-0.186151000
1	1.309847000	2.528225000	-0.297936000
6	2.550841000	3.507080000	1.122101000
6	2.819915000	3.563624000	-1.395145000
1	3.881758000	3.811555000	-1.333526000
1	2.657199000	3.034394000	-2.336032000
1	2.259613000	4.500398000	-1.433336000
1	2.236465000	2.911078000	1.978519000
1	1.946274000	4.416292000	1.095129000
1	3.588446000	3.809883000	1.276304000
1	-6.203014000	0.124228000	0.406682000
1	6.205471000	0.132048000	0.421512000
31	0.000421000	-0.025184000	2.091896000
1	-1.325776000	0.741659000	2.494669000
1	1.374764000	0.654482000	2.490487000
15	-0.010902000	-2.375731000	2.598643000
1	-1.228874000	-2.369030000	3.327283000
1	0.787425000	-2.239448000	3.763977000

$[HPH_2GaH_2{\cdot}IDipp]^+$

6	0.921766000	-0.053500000	-2.201057000
6	-0.427793000	-0.019008000	-2.280357000
7	-0.904734000	0.015064000	-0.982701000
6	0.123736000	0.003171000	-0.104258000
7	1.244066000	-0.039141000	-0.859269000
1	1.674479000	-0.085027000	-2.967471000
1	-1.086650000	-0.015951000	-3.129549000
6	2.603291000	-0.051647000	-0.348426000
6	3.212505000	-1.293664000	-0.101960000
6	3.257897000	1.178114000	-0.163138000
6	4.525722000	-1.272203000	0.364284000
6	4.569574000	1.130909000	0.307738000
6	5.196111000	-0.076717000	0.569611000
1	5.032914000	-2.205671000	0.566736000
1	5.111092000	2.053824000	0.464112000
6	-2.313002000	0.051154000	-0.649676000
6	-3.009280000	-1.168034000	-0.563498000
6	-4.366440000	-1.102506000	-0.245575000
6	-4.999443000	0.114681000	-0.043528000
1	-4.939986000	-2.016802000	-0.172444000
6	-4.290020000	1.299779000	-0.164226000
1	-4.803908000	2.241538000	-0.026098000
6	-2.929632000	1.301520000	-0.475673000
6	-2.367919000	-2.516117000	-0.869637000
1	-1.293012000	-2.367232000	-0.978338000
6	-2.890470000	-3.068665000	-2.207506000
6	-2.565823000	-3.544116000	0.253224000
1	-2.136769000	-3.200446000	1.195783000
1	-3.620242000	-3.767396000	0.422201000
1	-2.073115000	-4.481441000	-0.009242000
1	-3.960748000	-3.276410000	-2.157446000
1	-2.380404000	-4.000639000	-2.456295000
1	-2.728025000	-2.366080000	-3.026417000
6	-2.199319000	2.624974000	-0.657234000
1	-1.137871000	2.415219000	-0.793531000
6	-2.687673000	3.344801000	-1.926208000
6	-2.321700000	3.537925000	0.571716000
1	-3.355764000	3.831867000	0.758159000
1	-1.937250000	3.055190000	1.471676000
1	-1.746462000	4.451697000	0.415710000
1	-2.569239000	2.720761000	-2.813617000
1	-2.119838000	4.263662000	-2.081008000
1	-3.742421000	3.614328000	-1.848120000
6	2.522229000	-2.625921000	-0.359377000
1	1.459487000	-2.434535000	-0.518470000
6	3.067122000	-3.282535000	-1.639666000
6	2.628932000	-3.586162000	0.834085000
1	3.657311000	-3.906523000	1.006434000
1	2.261751000	-3.125561000	1.751755000
1	2.038974000	-4.484259000	0.642710000
1	2.950847000	-2.633330000	-2.509414000
1	2.540394000	-4.216820000	-1.842827000
1	4.129244000	-3.512723000	-1.538954000
6	2.624052000	2.520912000	-0.501238000
1	1.555671000	2.364695000	-0.660933000
6	2.762385000	3.544133000	0.635111000
6	3.205326000	3.080920000	-1.811399000
1	4.274101000	3.278322000	-1.711923000
1	3.073574000	2.387374000	-2.643804000
1	2.714636000	4.020011000	-2.073421000
1	2.358446000	3.160751000	1.572600000
1	2.220971000	4.456951000	0.380662000
1	3.803212000	3.823138000	0.804788000
1	-6.055409000	0.140129000	0.193580000
1	6.216090000	-0.086655000	0.931827000
31	0.221517000	0.147781000	1.948467000
1	0.357216000	1.640292000	2.394194000
1	0.964037000	-1.061904000	2.597057000
15	-2.078883000	-0.290914000	2.918228000
1	-3.224597000	0.405435000	2.499214000
1	-2.070493000	0.037310000	4.285602000
1	-2.584150000	-1.599255000	2.989630000

$[Ni(CO)_3PH_2GaH_2{\cdot}IDipp]$

6	-2.597524000	-2.231810000	0.738551000
6	-3.392233000	-1.140989000	0.722304000
7	-2.601089000	-0.078818000	0.322501000
6	-1.326639000	-0.481968000	0.086998000
7	-1.335958000	-1.814111000	0.351679000
1	-2.808347000	-3.255266000	0.987885000
1	-4.434496000	-1.019876000	0.954287000
6	-0.204411000	-2.715325000	0.280618000
6	0.474701000	-3.027509000	1.470675000
6	0.132413000	-3.283596000	-0.958754000
6	1.540227000	-3.922435000	1.383459000
6	1.211051000	-4.167140000	-0.982996000
6	1.910211000	-4.481122000	0.171072000
1	2.092958000	-4.180295000	2.276799000
1	1.506747000	-4.617799000	-1.920335000

6	-3.122914000	1.264498000	0.184688000
6	-3.079201000	2.117344000	1.297162000
6	-3.632576000	3.388278000	1.150668000
6	-4.202809000	3.789132000	-0.046609000
1	-3.610675000	4.077043000	1.985068000
6	-4.231285000	2.923543000	-1.127836000
1	-4.674822000	3.251377000	-2.058811000
6	-3.692583000	1.640586000	-1.040689000
6	-2.457431000	1.717305000	2.627130000
1	-2.037453000	0.717079000	2.519289000
6	-3.512035000	1.649194000	3.743144000
6	-1.299825000	2.649892000	3.015128000
1	-0.548126000	2.695092000	2.226914000
1	-1.650852000	3.666422000	3.202627000
1	-0.819625000	2.292972000	3.928589000
1	-3.966587000	2.625855000	3.920657000
1	-3.053777000	1.321131000	4.678568000
1	-4.313666000	0.950344000	3.495876000
6	-3.750215000	0.716973000	-2.249064000
1	-3.186865000	-0.186451000	-2.014627000
6	-5.195276000	0.288818000	-2.553078000
6	-3.090517000	1.345727000	-3.485637000
1	-3.629039000	2.234516000	-3.819525000
1	-2.058186000	1.630124000	-3.282357000
1	-3.089240000	0.631860000	-4.311892000
1	-5.659269000	-0.199840000	-1.694053000
1	-5.216084000	-0.410267000	-3.391750000
1	-5.814056000	1.148065000	-2.819599000
6	0.066988000	-2.470960000	2.828928000
1	-0.605109000	-1.628434000	2.661809000
6	-0.703420000	-3.526546000	3.641662000
6	1.255270000	-1.939435000	3.642445000
1	1.932693000	-2.740424000	3.943740000
1	1.830114000	-1.205174000	3.079647000
1	0.893877000	-1.461334000	4.555103000
1	-1.586827000	-3.885066000	3.111210000
1	-1.029798000	-3.108848000	4.596422000
1	-0.070496000	-4.391176000	3.851938000
6	-0.667434000	-3.026024000	-2.228277000
1	-1.237182000	-2.108089000	-2.087243000
6	0.214342000	-2.811078000	-3.464608000
6	-1.671191000	-4.167936000	-2.468290000
1	-1.152606000	-5.115714000	-2.629128000
1	-2.346433000	-4.298398000	-1.620550000
1	-2.276958000	-3.961791000	-3.353291000
1	0.941320000	-2.016789000	-3.298968000
1	-0.407904000	-2.523106000	-4.314004000
1	0.749414000	-3.719033000	-3.749276000
1	-4.622536000	4.782963000	-0.138985000
1	2.747339000	-5.166287000	0.125430000
31	0.187311000	0.735504000	-0.760670000
1	-0.333133000	2.210974000	-0.565371000
1	0.307198000	0.172933000	-2.234814000
15	2.293293000	0.521059000	0.351705000
1	2.476861000	-0.872638000	0.492291000
1	1.961145000	0.759673000	1.706028000
28	4.186593000	1.652907000	-0.364370000
8	4.618829000	0.854985000	-3.178543000
8	3.614725000	4.536948000	-0.051184000
8	6.324692000	0.699169000	1.440880000
6	4.439643000	1.161507000	-2.093231000
6	3.823299000	3.421113000	-0.173919000
6	5.505242000	1.074542000	0.738932000

$PH^tBuBH_2{\cdot}NMe_3$

15	0.591546000	-0.914422000	0.096068000
7	-2.237994000	0.070097000	-0.010683000
6	-2.089976000	0.655863000	1.347782000
1	-3.044566000	0.620975000	1.877113000
1	-1.759308000	1.687321000	1.249983000
1	-1.339949000	0.089161000	1.894796000
6	-2.713374000	-1.333327000	0.111092000
1	-1.977438000	-1.906548000	0.670872000
1	-2.814951000	-1.755282000	-0.886019000
1	-3.675803000	-1.360550000	0.626811000
6	-3.245759000	0.857122000	-0.767075000
1	-4.204776000	0.843337000	-0.243787000
1	-3.356839000	0.426193000	-1.758669000
1	-2.891122000	1.879906000	-0.865737000
5	-0.802081000	0.134569000	-0.853757000
1	-0.534728000	1.310448000	-0.890672000
1	-1.076532000	-0.313588000	-1.938674000
1	0.922822000	-1.850499000	-0.915618000
6	2.182247000	0.119397000	-0.004405000
6	2.485847000	0.603062000	-1.428052000
6	3.335486000	-0.767017000	0.489755000
1	3.162297000	-1.114679000	1.509974000
1	3.462612000	-1.645768000	-0.146483000
1	4.277122000	-0.207645000	0.475979000
1	2.612979000	-0.238732000	-2.111674000
1	3.413320000	1.187711000	-1.442767000
1	1.685523000	1.233012000	-1.816698000
6	2.033588000	1.325198000	0.933958000
1	1.828291000	1.008733000	1.959495000
1	2.958405000	1.911028000	0.944885000
1	1.227471000	1.986463000	0.611109000

$[HPH^tBuBH_2{\cdot}NMe_3]^+$

15	-0.617884000	0.649511000	-0.003159000
7	2.347044000	-0.059213000	0.000230000
6	2.631369000	0.704007000	1.254056000
1	3.676024000	1.012759000	1.267240000
1	2.425344000	0.068259000	2.111163000
1	2.000163000	1.588756000	1.295706000
6	2.631398000	0.810227000	-1.182306000
1	2.017504000	1.706944000	-1.134336000
1	2.404111000	0.259610000	-2.091511000
1	3.681385000	1.100633000	-1.180883000
6	3.272982000	-1.240811000	-0.051181000
1	4.304353000	-0.890890000	-0.026945000
1	3.088930000	-1.794787000	-0.967501000
1	3.076622000	-1.881041000	0.804398000
5	0.853851000	-0.656623000	-0.024342000
1	0.687917000	-1.319853000	0.958909000
1	0.699210000	-1.265960000	-1.043842000
1	-0.621526000	1.550234000	-1.082208000
6	-2.313077000	-0.112163000	0.000454000
6	-2.465793000	-0.973046000	-1.264620000
6	-3.340223000	1.031962000	0.000698000
1	-3.251416000	1.664523000	0.885499000
1	-3.255563000	1.661035000	-0.886955000
1	-4.343585000	0.601390000	0.003951000
1	-2.341584000	-0.386960000	-2.177370000
1	-3.473974000	-1.391361000	-1.279752000
1	-1.760939000	-1.803700000	-1.286207000
6	-2.461564000	-0.969273000	1.268574000
1	-2.336121000	-0.380004000	2.179113000
1	-3.469129000	-1.388894000	1.287436000
1	-1.755681000	-1.799004000	1.291081000
1	-0.612896000	1.537820000	1.086448000

$[Ni(CO)_3PH^tBuBH_2{\cdot}NMe_3]$

28	1.358133000	-0.863827000	0.058582000
15	-0.152406000	0.764152000	-0.709811000
8	4.103057000	0.160428000	-0.369810000
8	0.848645000	-1.457172000	2.904058000
7	-2.840074000	-0.662031000	-0.042356000
8	1.029438000	-3.146425000	-1.786507000
6	-2.713109000	-0.338019000	1.403629000
1	-3.251180000	-1.076642000	2.000339000
1	-3.129416000	0.650080000	1.581208000
1	-1.663362000	-0.344718000	1.681517000
6	3.034419000	-0.199103000	-0.197793000
6	1.037216000	-1.222776000	1.799586000
6	-2.304284000	-2.030579000	-0.283189000
1	-1.259539000	-2.057530000	0.009869000
1	-2.387208000	-2.258839000	-1.342672000
1	-2.871904000	-2.757763000	0.300194000
6	-4.285367000	-0.655393000	-0.405293000
1	-4.818558000	-1.399250000	0.189711000
1	-4.383353000	-0.886478000	-1.462689000
1	-4.694422000	0.333850000	-0.219053000
6	1.138997000	-2.265305000	-1.067005000
5	-2.106376000	0.463100000	-0.996374000
1	-2.723397000	1.476709000	-0.798842000
1	-2.242329000	0.052107000	-2.119511000
1	0.189862000	1.020085000	-2.054389000
6	0.075046000	2.541637000	-0.063944000
6	-0.600583000	3.543772000	-1.012091000
6	1.573740000	2.863106000	0.005996000
1	2.087426000	2.237965000	0.735463000
1	2.063042000	2.727265000	-0.960615000
1	1.711840000	3.907507000	0.302568000
1	-0.152252000	3.511842000	-2.007092000
1	-0.475250000	4.560158000	-0.624735000
1	-1.667936000	3.353690000	-1.116447000
6	-0.532626000	2.664246000	1.339044000
1	-0.101318000	1.938795000	2.032409000
1	-0.334989000	3.661719000	1.742056000
1	-1.614809000	2.528879000	1.320351000

$AsH^tBuBH_2{\cdot}NMe_3$

33	-0.507902000	-0.789141000	-0.043426000
7	2.434244000	0.196436000	0.008692000
6	2.451178000	0.212325000	-1.478665000
1	3.451603000	-0.028041000	-1.844560000
1	2.161054000	1.203052000	-1.820158000
1	1.734552000	-0.516591000	-1.849221000
6	2.840700000	-1.150504000	0.490491000
1	2.143108000	-1.890333000	0.103976000
1	2.805212000	-1.158071000	1.577267000
1	3.851449000	-1.383364000	0.148808000
6	3.410752000	1.200458000	0.509128000
1	4.412031000	0.969428000	0.137971000
1	3.403674000	1.186212000	1.595782000
1	3.105961000	2.186303000	0.167709000
5	0.941898000	0.603774000	0.601046000
1	0.707143000	1.686461000	0.124636000
1	1.081780000	0.630600000	1.796023000
1	-0.755929000	-1.482250000	1.296142000
6	-2.206219000	0.333264000	0.005066000
6	-2.320678000	1.145232000	1.296533000
6	-3.389932000	-0.631873000	-0.111096000
1	-3.335556000	-1.226715000	-1.025130000
1	-3.429685000	-1.320827000	0.735433000
1	-4.333412000	-0.073431000	-0.128826000
1	-2.339210000	0.497016000	2.174701000
1	-3.249766000	1.729511000	1.293585000
1	-1.489310000	1.841056000	1.411187000
6	-2.179787000	1.268263000	-1.207720000
1	-2.111070000	0.708700000	-2.143729000
1	-3.099341000	1.863374000	-1.244024000
1	-1.338794000	1.962657000	-1.163006000

$[HAsH^tBuBH_2{\cdot}NMe_3]^+$

33	0.526338000	-0.585633000	-0.000258000
7	-2.541460000	0.153573000	0.000057000
6	-2.810233000	-0.658915000	1.226098000
1	-3.850897000	-0.980992000	1.231850000
1	-2.608020000	-0.052698000	2.105270000
1	-2.167246000	-1.536037000	1.231529000
6	-2.811312000	-0.677735000	-1.213059000
1	-2.170844000	-1.556686000	-1.203727000
1	-2.606724000	-0.086302000	-2.101716000
1	-3.852826000	-0.997098000	-1.214603000
6	-3.488625000	1.320509000	-0.008555000
1	-4.513286000	0.950859000	-0.004056000
1	-3.310782000	1.913680000	-0.901268000
1	-3.308419000	1.928695000	0.873524000
5	-1.066972000	0.784855000	-0.005261000
1	-0.902164000	1.413105000	0.998218000
1	-0.904491000	1.401665000	-1.016201000
1	0.568999000	-1.553180000	-1.156240000
6	2.334817000	0.278687000	0.000117000
6	2.437482000	1.135335000	-1.265899000
6	3.384031000	-0.836078000	0.001122000
1	3.315202000	-1.468303000	0.887685000
1	3.316106000	-1.469062000	-0.884966000
1	4.377344000	-0.379847000	0.001436000
1	2.339710000	0.540371000	-2.175890000
1	3.424141000	1.604269000	-1.288901000
1	1.693916000	1.932329000	-1.288246000
6	2.436405000	1.136556000	1.265378000
1	2.338223000	0.542412000	2.175863000
1	3.422913000	1.605793000	1.288578000
1	1.692611000	1.933368000	1.286459000
1	0.567066000	-1.549880000	1.158605000

$[Ni(CO)_3AsH^tBuBH_2{\cdot}NMe_3]$

28	1.483482000	-0.949011000	0.101382000
33	-0.191761000	0.694884000	-0.647185000
8	4.141147000	0.262244000	-0.368015000
8	1.005469000	-1.557382000	2.947608000
7	-2.885441000	-0.857905000	0.025904000
8	1.193753000	-3.243652000	-1.731292000
6	-2.650026000	-0.685675000	1.485583000
1	-3.118967000	-1.502112000	2.037272000
1	-3.075076000	0.263836000	1.800852000
1	-1.581198000	-0.686976000	1.678904000
6	3.103605000	-0.173446000	-0.182303000
6	1.180000000	-1.312440000	1.843309000
6	-2.313002000	-2.161457000	-0.412010000
1	-1.247206000	-2.167228000	-0.205043000
1	-2.474399000	-2.273356000	-1.481228000
1	-2.797928000	-2.978259000	0.125243000
6	-4.355765000	-0.881834000	-0.218552000
1	-4.809308000	-1.707248000	0.333458000
1	-4.533394000	-1.005379000	-1.283534000
1	-4.784081000	0.062727000	0.105963000
6	1.287045000	-2.353022000	-1.020854000
5	-2.277677000	0.392924000	-0.842135000
1	-2.859053000	1.368276000	-0.447666000
1	-2.504707000	0.133343000	-1.992827000
1	0.102468000	1.038270000	-2.095706000
6	0.006603000	2.584159000	0.085443000

6	-0.755352000	3.567467000	-0.807501000
6	1.491850000	2.949728000	0.103821000
1	2.060535000	2.302293000	0.771270000
1	1.938810000	2.887020000	-0.890449000
1	1.614165000	3.980204000	0.455169000
1	-0.353034000	3.579437000	-1.822254000
1	-0.662355000	4.581778000	-0.402780000
1	-1.817191000	3.329070000	-0.867119000
6	-0.554530000	2.613352000	1.508766000
1	-0.047486000	1.897903000	2.160102000
1	-0.414586000	3.608406000	1.943995000
1	-1.624437000	2.399179000	1.523524000

PH^tBuBH_2·IDipp

15	-0.083680000	-2.331204000	1.006537000
7	1.208115000	0.745306000	-0.857828000
7	-0.942856000	0.866281000	-0.940251000
6	0.081441000	0.393103000	-0.178009000
6	-2.354832000	0.775427000	-0.645397000
6	2.573628000	0.476711000	-0.466783000
6	-0.458323000	1.516132000	-2.063788000
1	-1.113079000	1.969879000	-2.784315000
6	0.886395000	1.441579000	-2.011632000
1	1.640787000	1.816808000	-2.677738000
6	-3.105908000	-0.244306000	-1.251083000
6	3.227510000	-0.633225000	-1.027379000
6	3.212833000	1.370324000	0.406692000
6	2.553793000	-1.573174000	-2.018486000
1	1.475492000	-1.432125000	-1.936197000
6	-2.931614000	1.748520000	0.186201000
6	4.562818000	-0.833610000	-0.677996000
1	5.098367000	-1.679219000	-1.087837000
6	5.216297000	0.028505000	0.187522000
1	6.252521000	-0.149632000	0.447061000
6	4.547147000	1.117582000	0.721442000
1	5.069839000	1.784202000	1.394635000
6	2.524077000	2.599656000	0.979919000
1	1.462071000	2.527701000	0.748921000
6	-2.498242000	-1.266391000	-2.202018000
1	-1.413861000	-1.215919000	-2.102672000
6	-4.475402000	-0.274024000	-0.987407000
1	-5.084949000	-1.047472000	-1.435006000
6	-2.134215000	2.884638000	0.809743000
1	-1.078023000	2.705543000	0.611826000
6	-5.069543000	0.666604000	-0.162216000
1	-6.134106000	0.620512000	0.031239000
6	-4.304014000	1.666657000	0.415217000
1	-4.780162000	2.397696000	1.055551000
6	2.964574000	-1.231068000	-3.461924000
1	2.725965000	-0.198602000	-3.721389000
1	2.447288000	-1.883229000	-4.168964000
1	4.039198000	-1.368470000	-3.601742000
6	2.830183000	-3.054169000	-1.727308000
1	3.878981000	-3.311996000	-1.887734000
1	2.236082000	-3.677772000	-2.397941000
1	2.562343000	-3.315042000	-0.704552000
6	-2.903802000	-2.707113000	-1.864951000
1	-2.612249000	-2.965304000	-0.847671000
1	-2.397046000	-3.399543000	-2.540378000
1	-3.977991000	-2.866225000	-1.978903000
6	-2.853600000	-0.930629000	-3.661111000
1	-3.932330000	-0.987131000	-3.823715000
1	-2.374778000	-1.638586000	-4.341071000
1	-2.529716000	0.074243000	-3.938624000
6	-2.297000000	2.940370000	2.335431000
1	-3.324582000	3.169900000	2.624384000
1	-1.657105000	3.721657000	2.751401000
1	-2.015625000	1.991578000	2.791318000
6	2.641744000	2.676584000	2.508389000
1	2.256283000	1.770200000	2.974502000
1	2.065593000	3.524730000	2.884446000
1	3.676105000	2.816525000	2.828745000
5	-0.015455000	-0.339750000	1.231737000
6	3.055162000	3.884156000	0.321515000
1	4.117926000	4.024502000	0.531062000
1	2.520997000	4.756782000	0.703971000
1	2.930835000	3.861108000	-0.762871000
6	-2.498788000	4.232563000	0.165634000
1	-2.338710000	4.217320000	-0.914210000
1	-1.886594000	5.033051000	0.586914000
1	-3.546457000	4.485515000	0.342228000
1	-1.068072000	-0.030748000	1.735319000
1	0.925749000	-0.001996000	1.904582000
1	1.299419000	-2.634105000	1.138202000
6	-0.587744000	-2.974800000	2.726754000
6	-0.306001000	-4.485091000	2.743694000
1	-0.633373000	-4.921677000	3.693846000
1	-0.833211000	-4.998817000	1.937062000
1	0.760654000	-4.692906000	2.632534000
6	-2.094854000	-2.742959000	2.904530000
1	-2.342556000	-1.680944000	2.878640000
1	-2.669751000	-3.243232000	2.121861000
1	-2.426331000	-3.141335000	3.869331000
6	0.177537000	-2.301585000	3.871372000
1	1.254267000	-2.453560000	3.770867000
1	-0.005342000	-1.227575000	3.898004000
1	-0.132653000	-2.722388000	4.835497000

$[HPH^tBuBH_2·IDipp]^+$

15	1.000596000	-2.024505000	1.128797000
7	0.796761000	1.022670000	-0.920763000
7	-1.342762000	0.750907000	-0.817801000
6	-0.182084000	0.409849000	-0.209054000
6	-2.683279000	0.352716000	-0.431272000
6	2.222540000	0.936911000	-0.673006000
6	-1.092036000	1.580213000	-1.893474000
1	-1.884840000	1.970380000	-2.504992000
6	0.246378000	1.751221000	-1.957645000
1	0.853662000	2.318624000	-2.638247000
6	-3.227836000	-0.804307000	-1.009323000
6	2.981631000	0.044818000	-1.452603000
6	2.790643000	1.781829000	0.295030000
6	2.387150000	-0.792652000	-2.579191000
1	1.301126000	-0.796216000	-2.467332000
6	-3.392568000	1.170417000	0.461014000
6	4.352378000	-0.011002000	-1.201179000
1	4.973378000	-0.680719000	-1.780331000
6	4.937330000	0.786050000	-0.229942000
1	6.003669000	0.725556000	-0.053443000
6	4.166006000	1.674548000	0.502141000
1	4.642608000	2.306081000	1.239300000
6	1.990745000	2.835106000	1.048284000
1	0.931570000	2.603783000	0.935537000
6	-2.475711000	-1.670158000	-2.010230000
1	-1.446368000	-1.312020000	-2.067060000
6	-4.532488000	-1.140717000	-0.650792000
1	-4.990838000	-2.023937000	-1.075434000
6	-2.819613000	2.444485000	1.064692000
1	-1.788029000	2.551373000	0.726387000
6	-5.256784000	-0.360796000	0.236692000
1	-6.268675000	-0.641251000	0.499607000
6	-4.692321000	0.780544000	0.782703000

1	-5.272852000	1.383041000	1.468522000
6	2.705712000	-0.163860000	-3.948073000
1	2.348083000	0.863959000	-4.019276000
1	2.238542000	-0.739422000	-4.749120000
1	3.782209000	-0.150918000	-4.127412000
6	2.850285000	-2.256628000	-2.556944000
1	3.916168000	-2.349330000	-2.768738000
1	2.319789000	-2.825400000	-3.322268000
1	2.662525000	-2.733563000	-1.593936000
6	-2.418365000	-3.141593000	-1.573222000
1	-2.006186000	-3.244233000	-0.567753000
1	-1.795826000	-3.716330000	-2.261683000
1	-3.408202000	-3.600055000	-1.570114000
6	-3.077906000	-1.542659000	-3.419448000
1	-4.109505000	-1.897794000	-3.440795000
1	-2.505433000	-2.136742000	-4.134319000
1	-3.077658000	-0.507182000	-3.763834000
6	-2.785984000	2.385088000	2.599571000
1	-3.790797000	2.321220000	3.020024000
1	-2.319685000	3.287165000	2.999959000
1	-2.218487000	1.523012000	2.952104000
6	2.287361000	2.852468000	2.553816000
1	2.142046000	1.869552000	3.003439000
1	1.618132000	3.553721000	3.054661000
1	3.308000000	3.175137000	2.764760000
5	-0.065562000	-0.397481000	1.165614000
6	2.226756000	4.225994000	0.432240000
1	3.272878000	4.523296000	0.525304000
1	1.618860000	4.974567000	0.943453000
1	1.968326000	4.248653000	-0.627901000
6	-3.584845000	3.685451000	0.576421000
1	-3.582301000	3.756633000	-0.512742000
1	-3.128298000	4.592846000	0.975827000
1	-4.625572000	3.665930000	0.904363000
1	-1.144907000	-0.769218000	1.529389000
1	0.480271000	0.268039000	2.006927000
1	2.366539000	-1.825723000	0.873683000
6	0.961220000	-3.047288000	2.679206000
6	1.908510000	-4.242016000	2.484842000
1	1.900306000	-4.855110000	3.388781000
1	1.600201000	-4.878635000	1.653446000
1	2.938077000	-3.923573000	2.312330000
6	-0.476791000	-3.535619000	2.915276000
1	-1.170213000	-2.707970000	3.060181000
1	-0.839686000	-4.151375000	2.089940000
1	-0.496574000	-4.150851000	3.817096000
6	1.433837000	-2.172123000	3.851611000
1	2.448486000	-1.798559000	3.699817000
1	0.773122000	-1.321318000	4.015906000
1	1.437742000	-2.774755000	4.762146000
1	0.666265000	-2.928161000	0.104928000

$[Ni(CO)_3PH^tBuBH_2{\cdot}IDipp]$

28	-2.782187000	1.768775000	-0.143992000
15	-1.665861000	0.016671000	-1.201368000
7	2.006399000	0.330412000	0.830199000
7	0.903241000	-1.509952000	1.089268000
8	-2.000482000	1.819156000	2.692951000
8	-5.672760000	1.149718000	-0.229257000
8	-2.069076000	4.231028000	-1.613956000
6	1.013368000	-0.421392000	0.275302000
6	0.082789000	-2.688762000	0.887148000
6	2.623322000	1.529428000	0.292885000
6	1.815904000	-1.432851000	2.127763000
1	1.889961000	-2.200687000	2.874677000
6	2.505401000	-0.287515000	1.964933000
1	3.305208000	0.141380000	2.538663000
6	-1.107603000	-2.826996000	1.620581000
6	2.317360000	2.771938000	0.871303000
6	3.577627000	1.390358000	-0.729296000
6	1.334236000	2.937973000	2.020647000
1	0.718926000	2.039899000	2.074108000
6	0.563724000	-3.697964000	0.034588000
6	2.985505000	3.892418000	0.376675000
1	2.768125000	4.865253000	0.795348000
6	3.916320000	3.786433000	-0.642422000
1	4.416937000	4.672266000	-1.012881000
6	4.208028000	2.546624000	-1.185278000
1	4.942185000	2.472544000	-1.976662000
6	3.977830000	0.049205000	-1.325616000
1	3.302511000	-0.711343000	-0.938705000
6	-1.590390000	-1.787289000	2.621525000
1	-1.077448000	-0.849132000	2.409700000
6	-2.271407000	1.799975000	1.578621000
6	-1.837347000	-4.002784000	1.444739000
1	-2.760921000	-4.138597000	1.990092000
6	1.911842000	-3.619633000	-0.666883000
1	2.245525000	-2.584283000	-0.641041000
6	-1.403340000	-4.998582000	0.586296000
1	-1.990285000	-5.900135000	0.462466000
6	-0.213009000	-4.846945000	-0.105223000
1	0.125883000	-5.638951000	-0.759294000
6	2.072832000	3.079716000	3.363681000
1	2.723352000	2.228074000	3.567780000
1	1.354852000	3.156936000	4.182602000
1	2.692638000	3.979195000	3.372230000
6	-4.555581000	1.388591000	-0.221600000
6	0.384613000	4.126852000	1.818949000
1	0.913802000	5.080238000	1.868866000
1	-0.371309000	4.131684000	2.604554000
1	-0.126657000	4.072517000	0.858633000
6	-3.096990000	-1.513976000	2.522198000
1	-3.388368000	-1.235568000	1.510153000
1	-3.365036000	-0.691735000	3.186348000
1	-3.687654000	-2.381102000	2.823315000
6	-1.227171000	-2.202666000	4.058926000
1	-1.732938000	-3.131146000	4.333475000
1	-1.536216000	-1.428434000	4.763827000
1	-0.154949000	-2.360701000	4.183522000
6	-2.341475000	3.271477000	-1.055906000
6	1.844238000	-4.025512000	-2.144597000
1	1.609361000	-5.084617000	-2.267331000
1	2.810690000	-3.851539000	-2.621985000
1	1.093268000	-3.445090000	-2.679551000
6	3.839274000	0.026089000	-2.854256000
1	2.825341000	0.284701000	-3.157475000
1	4.064322000	-0.972630000	-3.234599000
1	4.530513000	0.722132000	-3.333394000
5	0.314540000	-0.150641000	-1.136493000
6	5.401488000	-0.341089000	-0.893758000
1	6.138811000	0.370972000	-1.270235000
1	5.660128000	-1.327362000	-1.285190000
1	5.496086000	-0.373201000	0.193378000
6	2.958407000	-4.464823000	0.080689000
1	3.060018000	-4.152901000	1.121573000
1	3.936385000	-4.369042000	-0.396152000
1	2.684158000	-5.522002000	0.075273000
1	0.633453000	-1.078022000	-1.843978000
1	0.740492000	0.885184000	-1.574030000
1	-2.149323000	-1.229768000	-0.737978000
6	-2.110767000	-0.231188000	-3.037271000
6	-1.437942000	0.864799000	-3.875061000

1	-1.727428000	0.755280000	-4.924740000
1	-1.740263000	1.861888000	-3.551608000
1	-0.350953000	0.806456000	-3.817675000
6	-1.659095000	-1.612338000	-3.532733000
1	-1.951245000	-1.740898000	-4.580114000
1	-0.578709000	-1.731192000	-3.470432000
1	-2.124115000	-2.415612000	-2.957219000
6	-3.634282000	-0.129791000	-3.196119000
1	-4.003890000	0.859642000	-2.929283000
1	-3.908256000	-0.319839000	-4.238758000
1	-4.155709000	-0.864391000	-2.578261000

$[PMe_2BH_2{\cdot}IDipp]$

15	0.349107000	-1.592763000	2.369759000
7	0.987784000	0.301319000	-0.878338000
7	-1.165130000	0.232201000	-0.829709000
6	-0.068912000	0.218250000	-0.021917000
6	-2.546352000	0.150645000	-0.414745000
6	2.387593000	0.277466000	-0.522677000
6	-0.795394000	0.338915000	-2.160623000
1	-1.521652000	0.373316000	-2.951472000
6	0.551317000	0.383598000	-2.190671000
1	1.236847000	0.462720000	-3.013778000
6	-3.176659000	-1.102927000	-0.429211000
6	3.088209000	-0.933912000	-0.649076000
6	3.007734000	1.472519000	-0.124143000
6	2.442792000	-2.219737000	-1.150561000
1	1.362210000	-2.077079000	-1.155894000
6	-3.219556000	1.333075000	-0.071243000
6	4.448220000	-0.923045000	-0.339339000
1	5.018216000	-1.838830000	-0.422230000
6	5.081569000	0.237097000	0.074629000
1	6.137236000	0.220163000	0.315650000
6	4.367948000	1.420462000	0.176432000
1	4.876891000	2.321597000	0.492000000
6	2.271789000	2.803273000	-0.064521000
1	1.203730000	2.599818000	-0.128111000
6	-2.464950000	-2.385154000	-0.838821000
1	-1.401648000	-2.166904000	-0.935768000
6	-4.526593000	-1.145845000	-0.079734000
1	-5.044844000	-2.095699000	-0.078621000
6	-2.545011000	2.696949000	-0.072388000
1	-1.479636000	2.545957000	-0.243574000
6	-5.215969000	0.004646000	0.265931000
1	-6.263145000	-0.053085000	0.536012000
6	-4.567284000	1.229338000	0.268560000
1	-5.117032000	2.120619000	0.541964000
6	2.881133000	-2.517274000	-2.595547000
1	2.654185000	-1.688354000	-3.268464000
1	2.370670000	-3.406439000	-2.971747000
1	3.956524000	-2.700757000	-2.649200000
6	2.721858000	-3.424772000	-0.242431000
1	3.787294000	-3.656772000	-0.187527000
1	2.215089000	-4.307603000	-0.638110000
1	2.345570000	-3.251553000	0.765320000
6	-2.593218000	-3.490969000	0.217710000
1	-2.175524000	-3.172719000	1.172508000
1	-2.041835000	-4.376747000	-0.104137000
1	-3.632945000	-3.787218000	0.370968000
6	-2.964137000	-2.875376000	-2.208545000
1	-4.023785000	-3.137530000	-2.171427000
1	-2.410370000	-3.764299000	-2.518096000
1	-2.839083000	-2.113481000	-2.980472000
6	-2.680075000	3.408103000	1.281588000
1	-3.720901000	3.646285000	1.510303000
1	-2.123895000	4.347974000	1.267529000
1	-2.283396000	2.789595000	2.086372000
6	2.503499000	3.549198000	1.256004000
1	2.233336000	2.926166000	2.108142000
1	1.888240000	4.450900000	1.286304000
1	3.543603000	3.860834000	1.370919000
5	-0.059736000	0.202642000	1.570968000
6	2.648990000	3.685739000	-1.267024000
1	3.712139000	3.936118000	-1.253402000
1	2.084301000	4.620547000	-1.245273000
1	2.437761000	3.186256000	-2.214537000
6	-3.075404000	3.576865000	-1.216115000
1	-2.934801000	3.099295000	-2.187845000
1	-2.552577000	4.535737000	-1.232336000
1	-4.141886000	3.780190000	-1.097260000
1	-1.167286000	0.500607000	1.943148000
1	0.769719000	0.993026000	1.957549000
6	-0.738170000	-1.529487000	3.879377000
1	-1.782959000	-1.618305000	3.578589000
1	-0.504435000	-2.364831000	4.543560000
1	-0.620823000	-0.594529000	4.433788000
6	1.986554000	-1.288774000	3.206793000
1	1.958254000	-0.395967000	3.836676000
1	2.260137000	-2.148252000	3.823563000
1	2.766882000	-1.150358000	2.457393000

$[HPMe_2BH_2{\cdot}IDipp]^+$

15	0.733130000	-1.217074000	2.561250000
7	0.902557000	0.281215000	-0.917128000
7	-1.250263000	0.168218000	-0.815106000
6	-0.132384000	0.161932000	-0.048059000
6	-2.626658000	0.064323000	-0.367497000
6	2.315178000	0.293194000	-0.596081000
6	-0.916327000	0.301710000	-2.148130000
1	-1.664144000	0.334694000	-2.919041000
6	0.430456000	0.372960000	-2.212819000
1	1.092643000	0.478483000	-3.051944000
6	-3.214975000	-1.208390000	-0.317018000
6	3.046171000	-0.896144000	-0.771638000
6	2.908716000	1.503464000	-0.199694000
6	2.424948000	-2.188477000	-1.288533000
1	1.339049000	-2.090827000	-1.236690000
6	-3.323777000	1.243773000	-0.065691000
6	4.413869000	-0.849200000	-0.500946000
1	5.012751000	-1.740634000	-0.629404000
6	5.022987000	0.323049000	-0.080621000
1	6.086438000	0.335780000	0.121271000
6	4.278490000	1.482722000	0.064641000
1	4.772930000	2.394017000	0.372422000
6	2.145319000	2.818333000	-0.124148000
1	1.078726000	2.596086000	-0.154262000
6	-2.472293000	-2.486703000	-0.680182000
1	-1.427715000	-2.233423000	-0.868478000
6	-4.553835000	-1.275637000	0.066872000
1	-5.046302000	-2.237691000	0.116476000
6	-2.698179000	2.628397000	-0.150361000
1	-1.637549000	2.511779000	-0.377156000
6	-5.268975000	-0.130659000	0.379316000
1	-6.308142000	-0.206839000	0.672627000
6	-4.659772000	1.111922000	0.311702000
1	-5.233361000	1.996843000	0.553210000
6	2.796828000	-2.420325000	-2.764153000
1	2.501456000	-1.581775000	-3.395896000
1	2.305201000	-3.317592000	-3.144010000
1	3.874056000	-2.554746000	-2.877572000
6	2.807333000	-3.417461000	-0.450597000
1	3.872642000	-3.641102000	-0.517688000

1	2.269952000	-4.295614000	-0.812090000
1	2.562915000	-3.286069000	0.604735000
6	-2.488865000	-3.507202000	0.467806000
1	-2.097408000	-3.075585000	1.391051000
1	-1.881324000	-4.377083000	0.210982000
1	-3.498561000	-3.863875000	0.675543000
6	-3.027916000	-3.107595000	-1.972385000
1	-4.070226000	-3.407103000	-1.850797000
1	-2.455965000	-3.996516000	-2.245256000
1	-2.980913000	-2.405896000	-2.806833000
6	-2.790924000	3.383314000	1.184431000
1	-3.826637000	3.593751000	1.455640000
1	-2.271952000	4.340743000	1.110203000
1	-2.338736000	2.812989000	1.996508000
6	2.407633000	3.586006000	1.178436000
1	2.194513000	2.972690000	2.054580000
1	1.768916000	4.469396000	1.223512000
1	3.440456000	3.930502000	1.247927000
5	-0.139121000	0.200415000	1.550054000
6	2.467822000	3.695025000	-1.347527000
1	3.525547000	3.963898000	-1.369889000
1	1.888087000	4.619149000	-1.314294000
1	2.235147000	3.184780000	-2.283808000
6	-3.319143000	3.450211000	-1.292022000
1	-3.215973000	2.945998000	-2.254574000
1	-2.831343000	4.423774000	-1.366595000
1	-4.383056000	3.623757000	-1.121513000
1	-1.269124000	0.131369000	1.944659000
1	0.401629000	1.194352000	1.967650000
6	-0.121258000	-1.412968000	4.151385000
1	-1.154183000	-1.709711000	3.975400000
1	0.373710000	-2.158788000	4.772306000
1	-0.122672000	-0.453862000	4.670300000
6	2.490344000	-0.989777000	2.957950000
1	2.600505000	-0.055071000	3.508605000
1	2.856127000	-1.812412000	3.572048000
1	3.080756000	-0.925731000	2.045973000
1	0.668823000	-2.497653000	1.984168000

$[Ni(CO)_3PMe_2BH_2{\cdot}IDipp]$

15	-1.521777000	0.236483000	1.744293000
7	0.748570000	-1.539956000	-0.900905000
7	1.816723000	0.336438000	-0.837377000
6	0.917522000	-0.418434000	-0.142704000
6	2.457776000	1.569882000	-0.420801000
6	-0.021768000	-2.724532000	-0.579036000
6	2.200508000	-0.309934000	-1.999179000
1	2.914581000	0.118922000	-2.676781000
6	1.534639000	-1.479759000	-2.039133000
1	1.548160000	-2.274482000	-2.760881000
6	2.022170000	2.784418000	-0.973595000
6	-1.254164000	-2.929263000	-1.223584000
6	0.543545000	-3.677036000	0.287551000
6	-1.840409000	-1.952297000	-2.234194000
1	-1.341266000	-0.991083000	-2.108131000
6	3.557733000	1.489267000	0.449542000
6	-1.934521000	-4.114707000	-0.943484000
1	-2.887857000	-4.303900000	-1.417238000
6	-1.417322000	-5.053504000	-0.067378000
1	-1.968700000	-5.962433000	0.138606000
6	-0.190213000	-4.836006000	0.536397000
1	0.211807000	-5.586140000	1.203965000
6	1.934537000	-3.533679000	0.888009000
1	2.242440000	-2.495541000	0.783005000
6	0.876838000	2.880199000	-1.970360000
1	0.298570000	1.957958000	-1.912541000
6	2.712358000	3.940280000	-0.606963000
1	2.399586000	4.893711000	-1.009726000
6	4.088311000	0.177257000	1.007360000
1	3.396713000	-0.615522000	0.727876000
6	3.786814000	3.892673000	0.264588000
1	4.302787000	4.804616000	0.537964000
6	4.204123000	2.678111000	0.782763000
1	5.050347000	2.650518000	1.456452000
6	-1.579894000	-2.431272000	-3.674023000
1	-0.517153000	-2.566971000	-3.878581000
1	-1.968267000	-1.703092000	-4.388597000
1	-2.077029000	-3.385832000	-3.860831000
6	-3.342652000	-1.710835000	-2.032235000
1	-3.928889000	-2.610593000	-2.226750000
1	-3.685873000	-0.941681000	-2.724450000
1	-3.564295000	-1.369780000	-1.021592000
6	-0.083292000	4.035503000	-1.657720000
1	-0.444557000	3.987286000	-0.631387000
1	-0.946678000	3.988019000	-2.321956000
1	0.390279000	5.007647000	-1.806746000
6	1.407539000	3.009939000	-3.409340000
1	1.981566000	3.931568000	-3.529197000
1	0.576735000	3.035119000	-4.117188000
1	2.057584000	2.177885000	-3.684688000
6	4.159376000	0.183575000	2.541125000
1	4.883097000	0.913838000	2.908460000
1	4.470908000	-0.797711000	2.905476000
1	3.187341000	0.414561000	2.975656000
6	1.978275000	-3.857061000	2.387173000
1	1.261631000	-3.252050000	2.942015000
1	2.974246000	-3.647062000	2.781971000
1	1.766923000	-4.909492000	2.584521000
5	0.389868000	-0.094591000	1.331464000
6	2.945084000	-4.400082000	0.115572000
1	2.693207000	-5.459948000	0.193401000
1	3.950321000	-4.263437000	0.520286000
1	2.970929000	-4.141340000	-0.944470000
6	5.453716000	-0.170710000	0.391357000
1	5.400187000	-0.223633000	-0.697780000
1	5.802605000	-1.138046000	0.759735000
1	6.206799000	0.576138000	0.650856000
1	0.927916000	0.920758000	1.689537000
1	0.706352000	-1.020872000	2.046000000
6	-1.319717000	0.809190000	3.490254000
1	-0.827179000	1.780925000	3.498715000
1	-2.296227000	0.912028000	3.965267000
1	-0.712706000	0.106023000	4.064580000
6	-2.306822000	-1.407702000	2.062034000
1	-1.670555000	-2.022241000	2.702008000
1	-3.272802000	-1.267537000	2.549593000
1	-2.474715000	-1.942580000	1.129226000
28	-2.957173000	1.696336000	0.640315000
6	-2.566499000	3.313893000	1.355670000
8	-2.314434000	4.327831000	1.819551000
6	-4.602147000	1.119827000	1.129888000
8	-5.630395000	0.736884000	1.451066000
6	-2.701786000	1.639311000	-1.138301000
8	-2.553384000	1.618951000	-2.275832000

$PPh_2BH_2{\cdot}NMe_3$

15	0.056035000	-0.323023000	-0.663281000
7	2.588366000	-1.716231000	0.141065000
6	0.251486000	1.466149000	-0.229879000
6	0.356376000	2.387655000	-1.276752000
1	0.303390000	2.030253000	-2.298473000
6	-1.690016000	-0.687901000	-0.208272000

6	-2.136500000	-2.015235000	-0.278866000
1	-1.436293000	-2.802859000	-0.528593000
6	-2.630645000	0.298503000	0.104795000
1	-2.327178000	1.335064000	0.162182000
6	0.319991000	1.952596000	1.080866000
1	0.241668000	1.262158000	1.910242000
6	0.590771000	4.211402000	0.278737000
1	0.721539000	5.268204000	0.476721000
6	-4.385167000	-1.350719000	0.283658000
1	-5.420178000	-1.605307000	0.474358000
6	3.343744000	-0.479746000	-0.194742000
1	4.366907000	-0.731564000	-0.481731000
1	3.351168000	0.175035000	0.673183000
1	2.848006000	0.027920000	-1.018716000
6	-3.461789000	-2.343217000	-0.032626000
1	-3.776113000	-3.378644000	-0.089775000
6	0.486533000	3.309192000	1.333444000
1	0.533827000	3.663955000	2.356214000
6	0.524040000	3.747164000	-1.028924000
1	0.601392000	4.440958000	-1.857318000
6	2.525885000	-2.592873000	-1.059747000
1	1.967975000	-2.081630000	-1.840471000
1	2.009019000	-3.512089000	-0.795169000
1	3.535726000	-2.822257000	-1.406117000
6	-3.961052000	-0.030052000	0.347823000
1	-4.666760000	0.755527000	0.590783000
6	3.305010000	-2.439312000	1.224762000
1	4.304520000	-2.723581000	0.887991000
1	2.736299000	-3.326647000	1.491097000
1	3.375990000	-1.791854000	2.094729000
5	1.069489000	-1.349891000	0.700188000
1	1.256756000	-0.759882000	1.733625000
1	0.533811000	-2.415983000	0.860392000

$[HPPh_2BH_2NMe_3]^+$

15	-0.098649000	-0.329405000	-0.543759000
7	2.527425000	-1.796495000	0.013199000
6	0.345747000	1.373803000	-0.130365000
6	0.771581000	2.258339000	-1.125293000
1	0.820441000	1.940908000	-2.159994000
6	-1.859910000	-0.586628000	-0.232242000
6	-2.304402000	-1.580898000	0.642011000
1	-1.600074000	-2.225452000	1.147854000
6	-2.786678000	0.239087000	-0.879616000
1	-2.452995000	1.019259000	-1.552896000
6	0.271141000	1.807301000	1.198004000
1	-0.069620000	1.135635000	1.976601000
6	1.050990000	3.986173000	0.528218000
1	1.321657000	5.002052000	0.784635000
6	-4.583869000	-0.928133000	0.215492000
1	-5.643738000	-1.061811000	0.388654000
6	3.227570000	-0.646769000	0.665433000
1	4.302775000	-0.744335000	0.518426000
1	2.999775000	-0.653035000	1.727987000
1	2.884975000	0.286971000	0.228275000
6	-3.666763000	-1.745984000	0.863179000
1	-4.008793000	-2.516672000	1.541184000
6	0.621732000	3.109893000	1.521748000
1	0.556110000	3.444213000	2.548773000
6	1.125239000	3.561243000	-0.792580000
1	1.449964000	4.243738000	-1.566936000
6	2.858542000	-1.812369000	-1.443639000
1	2.566312000	-0.867011000	-1.894882000
1	2.322510000	-2.628448000	-1.921876000
1	3.931265000	-1.950482000	-1.574969000
6	-4.143489000	0.063924000	-0.656554000
1	-4.857541000	0.700561000	-1.161975000
6	3.044955000	-3.065690000	0.624749000
1	4.125431000	-3.114453000	0.492230000
1	2.571193000	-3.913602000	0.137981000
1	2.799741000	-3.073327000	1.683234000
5	0.938459000	-1.783196000	0.281692000
1	0.754097000	-1.691616000	1.463097000
1	0.469794000	-2.778038000	-0.196965000
1	0.017860000	-0.322285000	-1.944172000

$[Ni(CO)_3PPh_2BH_2{\cdot}NMe_3]$

28	0.305661000	-1.528845000	-1.249569000
15	-0.086403000	0.135807000	0.346034000
8	-1.907699000	-1.163594000	-3.185100000
8	2.952354000	-1.212423000	-2.511001000
7	2.455839000	-0.034404000	2.079527000
8	0.012587000	-4.071285000	0.226786000
6	0.075684000	1.860206000	-0.308896000
6	0.450947000	2.077997000	-1.635513000
1	0.624031000	1.228738000	-2.282855000
6	-1.858748000	0.051950000	0.855521000
6	-2.283566000	-0.948574000	1.737590000
1	-1.563679000	-1.629686000	2.169904000
6	-2.824959000	0.900732000	0.307562000
1	-2.533474000	1.677775000	-0.385795000
6	-0.155415000	2.977220000	0.504249000
1	-0.454058000	2.838022000	1.534620000
6	0.368399000	4.465152000	-1.319386000
1	0.479571000	5.469756000	-1.708169000
6	-4.575140000	-0.228439000	1.523806000
1	-5.620990000	-0.335587000	1.782625000
6	3.102109000	0.937279000	1.154389000
1	4.187573000	0.867635000	1.243160000
1	2.772118000	1.941351000	1.408273000
1	2.808715000	0.712818000	0.132976000
6	-3.625108000	-1.084771000	2.069553000
1	-3.927752000	-1.865132000	2.757065000
6	-1.054204000	-1.303709000	-2.442701000
6	-0.013994000	4.264896000	0.004427000
1	-0.203492000	5.114654000	0.649015000
6	0.599910000	3.368246000	-2.137870000
1	0.891912000	3.511107000	-3.170925000
6	1.926009000	-1.328245000	-2.016737000
6	2.846269000	-1.418621000	1.689120000
1	2.450123000	-1.635200000	0.701611000
1	2.420486000	-2.116831000	2.405035000
1	3.933961000	-1.507832000	1.683881000
6	-4.168245000	0.762319000	0.639638000
1	-4.897115000	1.432701000	0.200797000
6	2.956021000	0.220976000	3.460069000
1	4.034221000	0.053568000	3.498378000
1	2.451310000	-0.452933000	4.147625000
1	2.728146000	1.246550000	3.737336000
6	0.124985000	-3.086359000	-0.340757000
5	0.823868000	0.142444000	2.120689000
1	0.622484000	1.192683000	2.670920000
1	0.419575000	-0.796106000	2.751942000

$AsPh_2BH_2{\cdot}NMe_3$

33	0.035059000	-0.330296000	-0.785799000
7	2.575501000	-1.768197000	0.306211000
6	0.319687000	1.545397000	-0.207181000
6	0.597258000	2.499199000	-1.188675000
1	0.624867000	2.198626000	-2.229891000
6	-1.824721000	-0.619936000	-0.189173000
6	-2.320705000	-1.926055000	-0.132128000
1	-1.664292000	-2.762866000	-0.337075000

6	-2.703397000	0.432081000	0.075787000
1	-2.353055000	1.455050000	0.033066000
6	0.278887000	1.960851000	1.126647000
1	0.065749000	1.241126000	1.906668000
6	0.786108000	4.228944000	0.477720000
1	0.963969000	5.263702000	0.743765000
6	-4.512907000	-1.117349000	0.465293000
1	-5.547636000	-1.308820000	0.720952000
6	3.348979000	-0.511114000	0.118440000
1	4.400409000	-0.742678000	-0.063333000
1	3.250813000	0.099565000	1.012326000
1	2.944696000	0.036649000	-0.728956000
6	-3.648688000	-2.173095000	0.194292000
1	-4.008542000	-3.194310000	0.238434000
6	0.505935000	3.290049000	1.466577000
1	0.464712000	3.594295000	2.505881000
6	0.831627000	3.830576000	-0.852270000
1	1.043909000	4.554295000	-1.630147000
6	2.655547000	-2.585153000	-0.935100000
1	2.202425000	-2.033189000	-1.754725000
1	2.103035000	-3.508764000	-0.781035000
1	3.698239000	-2.810422000	-1.167451000
6	-4.033652000	0.185348000	0.402336000
1	-4.695870000	1.018026000	0.608311000
6	3.182516000	-2.540463000	1.424685000
1	4.219197000	-2.790625000	1.187740000
1	2.606271000	-3.449253000	1.577731000
1	3.142027000	-1.940039000	2.329536000
5	1.008402000	-1.448102000	0.716005000
1	1.063802000	-0.874259000	1.771476000
1	0.472976000	-2.524141000	0.781087000

$[HAsPh_2BH_2{\cdot}NMe_3]^+$

33	-0.054951000	-0.318714000	-0.522972000
7	2.672539000	-1.754009000	0.151766000
6	0.327532000	1.533212000	-0.115425000
6	0.661706000	2.425692000	-1.134107000
1	0.688806000	2.102482000	-2.167562000
6	-1.931235000	-0.625056000	-0.158422000
6	-2.359150000	-1.872476000	0.294472000
1	-1.654870000	-2.675386000	0.462541000
6	-2.847643000	0.405575000	-0.368011000
1	-2.519736000	1.378869000	-0.709828000
6	0.280016000	1.966496000	1.211015000
1	0.010683000	1.283490000	2.007579000
6	0.904971000	4.181982000	0.497262000
1	1.127087000	5.213770000	0.736157000
6	-4.628618000	-1.061970000	0.323337000
1	-5.680639000	-1.231949000	0.511655000
6	3.304054000	-0.528309000	0.731317000
1	4.384467000	-0.577864000	0.600007000
1	3.063950000	-0.475110000	1.789811000
1	2.917965000	0.354689000	0.228878000
6	-3.712278000	-2.085191000	0.534042000
1	-4.047133000	-3.051650000	0.887185000
6	0.567151000	3.291542000	1.512389000
1	0.523731000	3.629745000	2.539429000
6	0.951341000	3.750467000	-0.822886000
1	1.206052000	4.443543000	-1.613957000
6	3.015390000	-1.846257000	-1.299864000
1	2.668773000	-0.952545000	-1.813423000
1	2.532765000	-2.722638000	-1.724962000
1	4.095384000	-1.927368000	-1.417371000
6	-4.196834000	0.181564000	-0.126708000
1	-4.909579000	0.979316000	-0.289507000
6	3.249512000	-2.952889000	0.848420000
1	4.331362000	-2.957582000	0.718675000
1	2.819245000	-3.853906000	0.420132000
1	3.002336000	-2.900795000	1.905257000
5	1.088870000	-1.809381000	0.412421000
1	0.873456000	-1.660958000	1.579745000
1	0.660140000	-2.827117000	-0.047918000
1	0.051554000	-0.314799000	-2.029893000

$[Ni(CO)_3AsPh_2BH_2{\cdot}NMe_3]$

28	0.739421000	-1.525329000	-1.313073000
33	-0.104046000	0.095978000	0.316837000
8	-1.377368000	-1.629903000	-3.380516000
8	3.329171000	-0.594019000	-2.367852000
7	2.359615000	0.514433000	2.242814000
8	0.909377000	-4.062069000	0.188825000
6	-0.331949000	1.909245000	-0.435116000
6	0.040549000	2.164384000	-1.754035000
1	0.424586000	1.358790000	-2.366926000
6	-1.953380000	-0.351553000	0.825137000
6	-2.180956000	-1.386182000	1.735260000
1	-1.347339000	-1.892645000	2.204090000
6	-3.050222000	0.274433000	0.232789000
1	-2.901375000	1.073263000	-0.481707000
6	-0.838031000	2.960902000	0.333973000
1	-1.137826000	2.785788000	1.359125000
6	-0.585625000	4.480062000	-1.522269000
1	-0.685369000	5.473463000	-1.941748000
6	-4.564475000	-1.143872000	1.463686000
1	-5.573439000	-1.449484000	1.710719000
6	2.860049000	1.555961000	1.302689000
1	3.939576000	1.668811000	1.414659000
1	2.362553000	2.497513000	1.520880000
1	2.633308000	1.260322000	0.282204000
6	-3.476212000	-1.777767000	2.052992000
1	-3.633715000	-2.581036000	2.762452000
6	-0.564664000	-1.583190000	-2.582589000
6	-0.967473000	4.235007000	-0.206411000
1	-1.367083000	5.038029000	0.401181000
6	-0.081254000	3.442161000	-2.295004000
1	0.213605000	3.621013000	-3.321748000
6	2.321696000	-0.946101000	-1.953630000
6	2.983444000	-0.796448000	1.905108000
1	2.662465000	-1.099151000	0.912301000
1	2.651760000	-1.537109000	2.628235000
1	4.070715000	-0.708071000	1.934945000
6	-4.346403000	-0.117804000	0.552565000
1	-5.186159000	0.380030000	0.083119000
6	2.765416000	0.888909000	3.627500000
1	3.854342000	0.920591000	3.697391000
1	2.370121000	0.151532000	4.321414000
1	2.347792000	1.862923000	3.867228000
6	0.839865000	-3.076772000	-0.385006000
5	0.727644000	0.417210000	2.228612000
1	0.319906000	1.460662000	2.661398000
1	0.444100000	-0.530711000	2.908919000

$PPh_2BH_2{\cdot}IDipp$

15	0.375408000	1.927858000	0.224756000
7	-1.029215000	-1.881619000	0.224967000
7	1.067511000	-1.727876000	0.701814000
6	1.324959000	2.990195000	-0.950580000
6	0.057435000	-1.078764000	0.057866000
6	0.617379000	-2.920435000	1.241182000
1	1.270164000	-3.582307000	1.779018000
6	0.802739000	4.100016000	-1.621277000
1	-0.240202000	4.360698000	-1.502793000
6	-0.693110000	-3.017987000	0.942305000

1	-1.414210000	-3.781282000	1.167188000
6	1.603941000	4.882417000	-2.448808000
1	1.170317000	5.735330000	-2.957868000
6	-2.372765000	-1.646185000	-0.254725000
6	2.870753000	-0.653377000	1.971535000
6	2.684587000	2.699349000	-1.135074000
1	3.124461000	1.855305000	-0.617166000
6	-1.267787000	2.783631000	0.256957000
6	-2.691762000	-1.991909000	-1.577355000
6	2.945663000	4.573923000	-2.629030000
1	3.567740000	5.182760000	-3.273399000
6	2.448482000	-1.308093000	0.802384000
6	3.327267000	-1.635173000	-0.242909000
6	4.220130000	-0.311915000	2.061246000
1	4.580590000	0.198610000	2.943826000
6	1.938398000	-0.357504000	3.138395000
1	0.913430000	-0.438740000	2.775694000
6	-1.474531000	3.744998000	1.254619000
1	-0.681671000	3.942955000	1.966463000
6	-2.311576000	2.544152000	-0.641605000
1	-2.181832000	1.807831000	-1.422503000
6	-4.010292000	-1.804242000	-1.988920000
1	-4.290702000	-2.057605000	-3.002837000
6	-3.697108000	4.196127000	0.442457000
1	-4.632125000	4.738442000	0.512760000
6	3.482016000	3.473341000	-1.965557000
1	4.528804000	3.221659000	-2.090046000
6	-1.680497000	-2.594616000	-2.541347000
1	-0.692434000	-2.508915000	-2.091025000
6	2.890049000	-2.403530000	-1.481531000
1	1.801084000	-2.414953000	-1.503763000
6	-3.325117000	-1.146760000	0.648585000
6	-4.969287000	-1.304107000	-1.122718000
1	-5.987376000	-1.165709000	-1.465001000
6	-3.513221000	3.240064000	-0.550024000
1	-4.306542000	3.034883000	-1.259090000
6	4.663630000	-1.266018000	-0.097010000
1	5.367878000	-1.498129000	-0.884819000
6	-2.670224000	4.448446000	1.346007000
1	-2.801405000	5.189910000	2.125084000
6	-4.628671000	-0.983379000	0.180964000
1	-5.386544000	-0.595029000	0.847699000
6	-3.000592000	-0.830561000	2.102733000
1	-1.915464000	-0.785719000	2.204589000
6	-1.959658000	-4.091329000	-2.760694000
1	-1.953866000	-4.643297000	-1.818747000
1	-1.200002000	-4.527908000	-3.412866000
1	-2.933116000	-4.246913000	-3.230833000
6	2.125373000	-1.392682000	4.262097000
1	3.136822000	-1.343669000	4.671501000
1	1.959088000	-2.412887000	3.912065000
1	1.424342000	-1.199032000	5.077009000
6	2.102464000	1.065492000	3.687620000
1	1.345665000	1.253305000	4.452374000
1	1.972362000	1.801671000	2.895140000
1	3.078326000	1.212418000	4.154998000
6	-1.623985000	-1.844501000	-3.879357000
1	-2.562869000	-1.927287000	-4.430494000
1	-0.837464000	-2.265583000	-4.509076000
1	-1.405114000	-0.788187000	-3.725865000
6	5.106864000	-0.609329000	1.039543000
1	6.149071000	-0.329348000	1.130260000
6	-3.510663000	-1.947032000	3.031480000
1	-3.236213000	-1.734558000	4.067020000
1	-3.097096000	-2.921549000	2.767342000
1	-4.599019000	-2.025031000	2.982082000
6	-3.549515000	0.528584000	2.557739000
1	-4.640975000	0.535336000	2.585052000
1	-3.220893000	1.334615000	1.904086000
1	-3.199215000	0.746332000	3.568667000
5	0.177891000	0.241408000	-0.836677000
6	3.368265000	-3.864284000	-1.414399000
1	4.459056000	-3.921185000	-1.406861000
1	3.009888000	-4.422428000	-2.282230000
1	3.003806000	-4.367111000	-0.516526000
6	3.351960000	-1.736874000	-2.784479000
1	3.011218000	-0.703298000	-2.839179000
1	2.942904000	-2.275313000	-3.641988000
1	4.439282000	-1.746784000	-2.882831000
1	-0.747419000	0.283235000	-1.603852000
1	1.226869000	0.155141000	-1.423580000

$[HPPh_2BH_2{\cdot}IDipp]^+$

15	0.244105000	1.944878000	-0.059799000
7	-1.037864000	-1.891456000	0.227156000
7	1.069940000	-1.770474000	0.679986000
6	1.351130000	3.056896000	-0.974348000
6	0.058429000	-1.111296000	0.057825000
6	0.609637000	-2.957325000	1.214794000
1	1.258766000	-3.634538000	1.737981000
6	0.862712000	4.159601000	-1.674751000
1	-0.194013000	4.389617000	-1.668871000
6	-0.708143000	-3.033540000	0.930263000
1	-1.437040000	-3.788456000	1.159217000
6	1.738300000	4.974595000	-2.384092000
1	1.353324000	5.826924000	-2.928466000
6	-2.387782000	-1.624179000	-0.231453000
6	2.889946000	-0.676931000	1.913543000
6	2.721283000	2.776164000	-0.989608000
1	3.113671000	1.917656000	-0.458381000
6	-1.333787000	2.797457000	0.170863000
6	-2.728770000	-1.949077000	-1.554554000
6	3.099216000	4.698595000	-2.390312000
1	3.778844000	5.337497000	-2.939121000
6	2.458541000	-1.359573000	0.762102000
6	3.325579000	-1.721182000	-0.281794000
6	4.239475000	-0.330654000	1.979633000
1	4.613446000	0.193499000	2.848221000
6	1.970416000	-0.370545000	3.089534000
1	0.938887000	-0.407079000	2.731955000
6	-1.460429000	3.762473000	1.176647000
1	-0.632357000	3.969303000	1.843451000
6	-2.408829000	2.547337000	-0.685059000
1	-2.326101000	1.798008000	-1.460425000
6	-4.046736000	-1.715592000	-1.945281000
1	-4.350885000	-1.953614000	-2.955618000
6	-3.713474000	4.217327000	0.461531000
1	-4.637389000	4.769843000	0.573614000
6	3.589912000	3.600366000	-1.689993000
1	4.650303000	3.384321000	-1.691490000
6	-1.755380000	-2.593840000	-2.531257000
1	-0.750737000	-2.514886000	-2.115118000
6	2.881270000	-2.533730000	-1.489398000
1	1.791438000	-2.565120000	-1.497228000
6	-3.314554000	-1.122354000	0.697575000
6	-4.980161000	-1.201982000	-1.059102000
1	-5.999228000	-1.036976000	-1.385250000
6	-3.592976000	3.260393000	-0.538970000
1	-4.421568000	3.064077000	-1.206543000
6	4.663256000	-1.346567000	-0.156395000
1	5.362881000	-1.607359000	-0.938919000
6	-2.647838000	4.465571000	1.321837000

1	-2.741024000	5.208072000	2.103513000
6	-4.618236000	-0.915956000	0.247304000
1	-5.362944000	-0.532969000	0.931721000
6	-2.973864000	-0.862312000	2.159950000
1	-1.887241000	-0.873302000	2.265431000
6	-2.067387000	-4.092224000	-2.692681000
1	-2.036508000	-4.616727000	-1.735956000
1	-1.340576000	-4.561411000	-3.358411000
1	-3.059796000	-4.243499000	-3.121337000
6	2.116159000	-1.437524000	4.190269000
1	3.132340000	-1.442867000	4.588710000
1	1.900175000	-2.440120000	3.820532000
1	1.432416000	-1.229813000	5.015489000
6	2.196518000	1.024960000	3.689218000
1	1.416751000	1.245993000	4.419851000
1	2.182750000	1.808153000	2.929538000
1	3.151958000	1.092484000	4.210994000
6	-1.728936000	-1.892830000	-3.896533000
1	-2.678235000	-1.995515000	-4.424462000
1	-0.958457000	-2.338751000	-4.527755000
1	-1.508604000	-0.829795000	-3.795880000
6	5.115820000	-0.656691000	0.956320000
1	6.159912000	-0.380993000	1.032838000
6	-3.535916000	-1.979898000	3.057072000
1	-3.248494000	-1.813719000	4.096950000
1	-3.173814000	-2.965484000	2.761225000
1	-4.626235000	-2.002691000	3.010596000
6	-3.460056000	0.506919000	2.654632000
1	-4.549157000	0.565020000	2.677045000
1	-3.093778000	1.317583000	2.025752000
1	-3.108013000	0.678825000	3.673494000
5	0.209481000	0.170042000	-0.887706000
6	3.381629000	-3.984885000	-1.380524000
1	4.472458000	-4.026735000	-1.388693000
1	3.018590000	-4.574563000	-2.224193000
1	3.038769000	-4.464152000	-0.461832000
6	3.319624000	-1.905591000	-2.819988000
1	2.971014000	-0.876576000	-2.910939000
1	2.907328000	-2.477167000	-3.653236000
1	4.404922000	-1.908588000	-2.931956000
1	-0.680414000	0.235225000	-1.687871000
1	1.278643000	0.131672000	-1.429134000
1	0.785915000	1.945575000	1.235583000

$[Ni(CO)_3PPh_2BH_2{\cdot}IDipp]$

28	0.249989000	2.846083000	-1.296404000
15	-0.668814000	1.531775000	0.396660000
7	-0.262237000	-2.425482000	-0.448915000
7	1.801902000	-1.803302000	-0.337335000
8	2.994345000	3.424079000	-0.371296000
8	-1.205048000	5.421963000	-1.313088000
8	0.016359000	1.345219000	-3.822322000
6	0.533983000	-1.408420000	-0.011139000
6	3.059110000	-1.139303000	-0.048089000
6	-1.695426000	-2.582052000	-0.306658000
6	1.783610000	-3.047663000	-0.940001000
1	2.685158000	-3.542204000	-1.246424000
6	0.496891000	-3.434163000	-1.013428000
1	0.049734000	-4.328790000	-1.403756000
6	3.749708000	-0.512310000	-1.100409000
6	-2.515020000	-2.283582000	-1.407920000
6	-2.191576000	-3.158036000	0.874929000
6	-1.966215000	-1.763622000	-2.730168000
1	-0.978309000	-1.340030000	-2.544335000
6	3.590085000	-1.240855000	1.249351000
6	-3.878293000	-2.546897000	-1.279511000
1	-4.542007000	-2.320969000	-2.102577000
6	-4.398791000	-3.093843000	-0.118868000
1	-5.461447000	-3.288012000	-0.043315000
6	-3.563217000	-3.397607000	0.943126000
1	-3.981426000	-3.838678000	1.838154000
6	-1.295838000	-3.589744000	2.027884000
1	-0.315683000	-3.139041000	1.881272000
6	3.254985000	-0.509435000	-2.542514000
1	2.180575000	-0.699865000	-2.533076000
6	1.939987000	3.172985000	-0.733320000
6	4.978983000	0.074146000	-0.798015000
1	5.531606000	0.579936000	-1.577287000
6	2.923892000	-2.037843000	2.362338000
1	1.901045000	-2.255273000	2.060542000
6	5.504990000	0.027238000	0.481442000
1	6.456362000	0.499311000	0.692254000
6	4.820839000	-0.632372000	1.488758000
1	5.253237000	-0.681199000	2.479211000
6	-1.801959000	-2.912488000	-3.742569000
1	-1.151551000	-3.704117000	-3.369137000
1	-1.371787000	-2.536167000	-4.672889000
1	-2.770516000	-3.360452000	-3.975938000
6	-0.661733000	4.417907000	-1.302877000
6	-2.825136000	-0.651779000	-3.345658000
1	-3.791434000	-1.029660000	-3.685794000
1	-2.314077000	-0.231267000	-4.212384000
1	-3.006917000	0.153026000	-2.635744000
6	3.472932000	0.828502000	-3.260880000
1	3.061500000	1.662800000	-2.697989000
1	2.980800000	0.805095000	-4.234181000
1	4.532135000	1.023976000	-3.437322000
6	3.931811000	-1.629956000	-3.355473000
1	5.009974000	-1.464156000	-3.410388000
1	3.541689000	-1.643972000	-4.375281000
1	3.772850000	-2.617873000	-2.923677000
6	0.108242000	1.932263000	-2.842136000
6	2.837386000	-1.265700000	3.685229000
1	3.824544000	-1.072414000	4.109433000
1	2.277762000	-1.849319000	4.419038000
1	2.325376000	-0.313407000	3.552260000
6	-1.804566000	-3.107008000	3.392819000
1	-1.927224000	-2.024329000	3.409143000
1	-1.088062000	-3.374798000	4.171879000
1	-2.759078000	-3.565556000	3.657526000
5	0.159092000	-0.193051000	0.972915000
6	-1.110466000	-5.117274000	2.027275000
1	-2.062844000	-5.628552000	2.182877000
1	-0.432474000	-5.418925000	2.828631000
1	-0.693633000	-5.471492000	1.082820000
6	3.644297000	-3.383152000	2.561506000
1	3.667066000	-3.969087000	1.640639000
1	3.138186000	-3.976122000	3.326573000
1	4.676723000	-3.231216000	2.883583000
1	1.196279000	0.186708000	1.436526000
1	-0.546792000	-0.652877000	1.836968000
6	-0.522425000	2.505042000	1.969435000
6	-1.610778000	3.160889000	2.552077000
6	0.735434000	2.677925000	2.560882000
6	-1.451155000	3.948309000	3.688347000
6	0.894755000	3.461850000	3.695411000
6	-0.199622000	4.100905000	4.268854000
1	-2.597050000	3.064692000	2.120961000
1	1.604293000	2.201149000	2.129281000
1	-2.313876000	4.444366000	4.116551000
1	1.880654000	3.577183000	4.129440000
1	-0.075432000	4.713864000	5.152844000

6	-2.505566000	1.325429000	0.278617000
6	-3.212429000	0.516894000	1.174917000
6	-3.234603000	2.043273000	-0.671719000
6	-4.598036000	0.439017000	1.128597000
6	-4.623667000	1.968003000	-0.722023000
6	-5.310298000	1.167365000	0.180871000
1	-2.673220000	-0.044365000	1.925152000
1	-2.708941000	2.673261000	-1.375822000
1	-5.123463000	-0.190365000	1.836220000
1	-5.165302000	2.541101000	-1.464624000
1	-6.391475000	1.110793000	0.148671000

$AsPh_2BH_2$·IDipp

33	0.142830000	1.902522000	0.420900000
7	-0.805725000	-2.105571000	0.177632000
7	1.283611000	-1.784751000	0.611440000
6	1.001242000	3.148239000	-0.856161000
6	0.201882000	-1.201407000	0.019238000
6	0.955296000	-3.035871000	1.104690000
1	1.679044000	-3.661380000	1.592894000
6	0.326334000	4.153147000	-1.549664000
1	-0.744428000	4.262863000	-1.439287000
6	-0.349358000	-3.236988000	0.833611000
1	-0.992435000	-4.072068000	1.039363000
6	1.013009000	5.022936000	-2.393583000
1	0.466760000	5.793980000	-2.924455000
6	-2.174240000	-1.973623000	-0.269022000
6	3.014279000	-0.606789000	1.890303000
6	2.385826000	3.044230000	-1.025848000
1	2.938386000	2.278101000	-0.493546000
6	-1.717258000	2.587689000	0.326574000
6	-2.487199000	-2.294024000	-1.599618000
6	2.386961000	4.904314000	-2.559972000
1	2.919984000	5.580807000	-3.216686000
6	2.621222000	-1.242194000	0.700143000
6	3.495077000	-1.429402000	-0.383131000
6	4.325013000	-0.134963000	1.960595000
1	4.661319000	0.366323000	2.857785000
6	2.095565000	-0.470591000	3.097579000
1	1.069922000	-0.609870000	2.754035000
6	-2.101196000	3.527730000	1.287877000
1	-1.384804000	3.844410000	2.037429000
6	-2.661401000	2.190205000	-0.621347000
1	-2.390070000	1.461824000	-1.373673000
6	-3.824980000	-2.208826000	-1.982080000
1	-4.102049000	-2.445608000	-3.000916000
6	-4.315275000	3.657422000	0.347089000
1	-5.317114000	4.069398000	0.353286000
6	3.071743000	3.907846000	-1.870432000
1	4.144407000	3.805695000	-1.987432000
6	-1.445361000	-2.765797000	-2.603503000
1	-0.460164000	-2.603351000	-2.168167000
6	3.095604000	-2.178649000	-1.645642000
1	2.012562000	-2.292978000	-1.640510000
6	-3.149392000	-1.596516000	0.668746000
6	-4.807498000	-1.831365000	-1.080678000
1	-5.840362000	-1.771312000	-1.400657000
6	-3.949378000	2.719037000	-0.611436000
1	-4.667419000	2.397422000	-1.356659000
6	4.792425000	-0.935919000	-0.254324000
1	5.491074000	-1.057733000	-1.071292000
6	-3.385363000	4.062888000	1.298528000
1	-3.659767000	4.793137000	2.050540000
6	-4.471325000	-1.532924000	0.229270000
1	-5.247615000	-1.240124000	0.923086000
6	-2.825233000	-1.306113000	2.128122000
1	-1.746852000	-1.166238000	2.212602000
6	-1.589664000	-4.273496000	-2.871489000
1	-1.508762000	-4.854275000	-1.950599000
1	-0.809692000	-4.614770000	-3.555655000
1	-2.556470000	-4.502663000	-3.325031000
6	2.398336000	-1.564385000	4.137964000
1	3.414721000	-1.461161000	4.524611000
1	2.303666000	-2.567523000	3.719545000
1	1.708987000	-1.486068000	4.981421000
6	2.158567000	0.915652000	3.751581000
1	1.417164000	0.976591000	4.551197000
1	1.936793000	1.700172000	3.028946000
1	3.134310000	1.111409000	4.200683000
6	-1.486554000	-1.968059000	-3.913820000
1	-2.422797000	-2.121875000	-4.454270000
1	-0.674731000	-2.288220000	-4.570315000
1	-1.367531000	-0.901414000	-3.725718000
6	5.203949000	-0.292391000	0.901505000
1	6.215481000	0.086685000	0.978295000
6	-3.212391000	-2.498024000	3.021649000
1	-2.936914000	-2.300079000	4.059760000
1	-2.717403000	-3.419909000	2.712439000
1	-4.289958000	-2.673508000	2.988099000
6	-3.484173000	-0.019629000	2.644250000
1	-4.571010000	-0.111710000	2.691367000
1	-3.242905000	0.835754000	2.015480000
1	-3.133059000	0.192534000	3.656164000
5	0.176195000	0.157162000	-0.803478000
6	3.710681000	-3.588913000	-1.657916000
1	4.801704000	-3.540991000	-1.677188000
1	3.383644000	-4.139749000	-2.542641000
1	3.418869000	-4.163173000	-0.776449000
6	3.454199000	-1.414058000	-2.926932000
1	3.021882000	-0.413840000	-2.920650000
1	3.066142000	-1.946299000	-3.797918000
1	4.534311000	-1.322210000	-3.057043000
1	-0.749860000	0.153091000	-1.567123000
1	1.233655000	0.260605000	-1.367242000

$[HAsPh_2BH_2$·IDipp$]^+$

33	0.029828000	1.865701000	-0.035529000
7	-1.082005000	-2.007065000	0.491626000
7	1.074969000	-1.953811000	0.587004000
6	1.545511000	2.957247000	-0.584423000
6	-0.001674000	-1.285509000	0.100330000
6	0.668259000	-3.085839000	1.263899000
1	1.371534000	-3.760192000	1.716366000
6	1.439683000	4.347542000	-0.612292000
1	0.508981000	4.836641000	-0.357169000
6	-0.680980000	-3.119490000	1.203205000
1	-1.387727000	-3.828998000	1.591919000
6	2.536432000	5.114876000	-0.984964000
1	2.451830000	6.193568000	-1.008888000
6	-2.476693000	-1.719455000	0.214185000
6	3.113674000	-0.903944000	1.457594000
6	2.743746000	2.338195000	-0.935789000
1	2.831833000	1.260414000	-0.929860000
6	-1.548812000	2.931135000	-0.385630000
6	-3.024683000	-2.160731000	-1.000647000
6	3.735013000	4.499516000	-1.329599000
1	4.586411000	5.100315000	-1.622141000
6	2.472750000	-1.604628000	0.421802000
6	3.142000000	-2.047557000	-0.730942000
6	4.472270000	-0.632353000	1.296980000
1	5.003632000	-0.098036000	2.072562000
6	2.407829000	-0.489971000	2.742410000

1	1.330897000	-0.564902000	2.577691000
6	-2.032964000	3.818538000	0.576225000
1	-1.551355000	3.902512000	1.542636000
6	-2.179050000	2.832677000	-1.625535000
1	-1.815013000	2.142265000	-2.375167000
6	-4.379023000	-1.908024000	-1.214771000
1	-4.839598000	-2.232347000	-2.138145000
6	-3.770492000	4.508539000	-0.942693000
1	-4.635263000	5.121968000	-1.159918000
6	3.837363000	3.113900000	-1.305039000
1	4.766763000	2.631701000	-1.578648000
6	-2.228371000	-2.933878000	-2.042283000
1	-1.172097000	-2.877658000	-1.776903000
6	2.472576000	-2.874598000	-1.819256000
1	1.396506000	-2.864378000	-1.643286000
6	-3.233421000	-1.076134000	1.207044000
6	-5.149105000	-1.258787000	-0.263379000
1	-6.199392000	-1.076777000	-0.451995000
6	-3.287866000	3.623724000	-1.900830000
1	-3.775341000	3.546633000	-2.863953000
6	4.498688000	-1.741188000	-0.834613000
1	5.050533000	-2.065683000	-1.706472000
6	-3.144828000	4.604579000	0.295034000
1	-3.519879000	5.290911000	1.043144000
6	-4.582575000	-0.852979000	0.934052000
1	-5.201053000	-0.361327000	1.672614000
6	-2.660369000	-0.678679000	2.561372000
1	-1.571227000	-0.724073000	2.497301000
6	-2.624297000	-4.420651000	-2.034005000
1	-2.486343000	-4.870574000	-1.049161000
1	-2.017046000	-4.979258000	-2.748661000
1	-3.671687000	-4.549545000	-2.313252000
6	2.763359000	-1.446074000	3.894914000
1	3.831702000	-1.407041000	4.115331000
1	2.512522000	-2.480914000	3.658285000
1	2.223241000	-1.167679000	4.801708000
6	2.706364000	0.961210000	3.146515000
1	2.082041000	1.247434000	3.994807000
1	2.517462000	1.660166000	2.330719000
1	3.744577000	1.090286000	3.455047000
6	-2.365855000	-2.341337000	-3.451919000
1	-3.386139000	-2.424331000	-3.829297000
1	-1.718714000	-2.879617000	-4.146591000
1	-2.081563000	-1.288895000	-3.471429000
6	5.157139000	-1.041912000	0.164259000
1	6.212658000	-0.823292000	0.063881000
6	-3.098371000	-1.670571000	3.653575000
1	-2.648850000	-1.405749000	4.612474000
1	-2.806133000	-2.694419000	3.416247000
1	-4.182883000	-1.657554000	3.776684000
6	-3.029853000	0.754778000	2.967022000
1	-4.096909000	0.855447000	3.169808000
1	-2.773257000	1.473980000	2.188896000
1	-2.501155000	1.031587000	3.881078000
5	0.010911000	-0.049312000	-0.906414000
6	2.935100000	-4.340225000	-1.749717000
1	4.006801000	-4.423652000	-1.939569000
1	2.415621000	-4.937431000	-2.501240000
1	2.736447000	-4.781371000	-0.771360000
6	2.701399000	-2.296840000	-3.223501000
1	2.373072000	-1.259089000	-3.287464000
1	2.139817000	-2.875009000	-3.959238000
1	3.752490000	-2.338601000	-3.512996000
1	-0.990650000	-0.012633000	-1.557408000
1	1.004340000	-0.046017000	-1.570468000
1	0.088696000	1.925175000	1.474060000

[$Ni(CO)_3AsPh_2BH_2$·IDipp]

28	1.340686000	-2.674023000	-1.351857000
33	1.222562000	-0.979498000	0.417637000
7	-1.012953000	2.305332000	-0.637620000
7	-2.573420000	0.821311000	-0.473686000
8	-0.528505000	-4.769588000	-0.441599000
8	4.060379000	-3.828465000	-1.293497000
8	0.632145000	-1.409905000	-3.917382000
6	-1.282352000	1.078216000	-0.107419000
6	-3.400668000	-0.311914000	-0.107060000
6	0.192069000	3.097091000	-0.498554000
6	-3.093381000	1.880427000	-1.195254000
1	-4.104551000	1.878636000	-1.555257000
6	-2.119539000	2.804323000	-1.300147000
1	-2.108715000	3.768109000	-1.773223000
6	-3.655238000	-1.302255000	-1.070999000
6	1.119394000	3.103144000	-1.553943000
6	0.326531000	3.915860000	0.634901000
6	0.922649000	2.296289000	-2.830922000
1	0.225901000	1.484924000	-2.613849000
6	-3.994476000	-0.326697000	1.166526000
6	2.226772000	3.940850000	-1.425790000
1	2.968035000	3.964224000	-2.212100000
6	2.397585000	4.741129000	-0.308727000
1	3.268854000	5.379206000	-0.230396000
6	1.455236000	4.730604000	0.705889000
1	1.594333000	5.371267000	1.566517000
6	-0.728503000	3.995264000	1.729148000
1	-1.412872000	3.158063000	1.599977000
6	-3.100556000	-1.248438000	-2.489004000
1	-2.229126000	-0.591633000	-2.487332000
6	0.176948000	-3.940667000	-0.787944000
6	-4.501655000	-2.349212000	-0.704562000
1	-4.711883000	-3.135160000	-1.416450000
6	-3.816411000	0.792349000	2.182274000
1	-3.006000000	1.435217000	1.842644000
6	-5.076388000	-2.404834000	0.553799000
1	-5.724667000	-3.231673000	0.815693000
6	-4.829012000	-1.399957000	1.474050000
1	-5.295856000	-1.446148000	2.448891000
6	0.299025000	3.166020000	-3.938229000
1	-0.656328000	3.596954000	-3.637542000
1	0.129171000	2.567932000	-4.835729000
1	0.966224000	3.989369000	-4.203091000
6	3.022054000	-3.353821000	-1.304093000
6	2.216594000	1.655190000	-3.347046000
1	2.924229000	2.405489000	-3.705221000
1	1.989482000	0.994162000	-4.183703000
1	2.708595000	1.068437000	-2.573503000
6	-2.637231000	-2.616330000	-3.005794000
1	-1.952890000	-3.097670000	-2.310835000
1	-2.120419000	-2.493849000	-3.958311000
1	-3.479200000	-3.289567000	-3.176688000
6	-4.137275000	-0.660431000	-3.464742000
1	-5.022811000	-1.298155000	-3.512526000
1	-3.714717000	-0.595926000	-4.469505000
1	-4.464603000	0.338220000	-3.175320000
6	0.912725000	-1.889064000	-2.914979000
6	-3.415805000	0.276670000	3.571226000
1	-4.206503000	-0.323165000	4.025894000
1	-3.222929000	1.119343000	4.238305000
1	-2.510788000	-0.327608000	3.519839000
6	-0.137747000	3.869319000	3.139605000
1	0.433728000	2.947835000	3.247170000
1	-0.941034000	3.855071000	3.879025000

1	0.514879000	4.709234000	3.384928000
5	-0.432907000	0.237929000	0.954139000
6	-1.549819000	5.290072000	1.598357000
1	-0.918309000	6.170793000	1.733869000
1	-2.335254000	5.320711000	2.356666000
1	-2.024520000	5.369313000	0.618646000
6	-5.087851000	1.654998000	2.263061000
1	-5.357958000	2.066376000	1.288583000
1	-4.938582000	2.488740000	2.952709000
1	-5.937300000	1.070777000	2.623354000
1	-1.170299000	-0.568041000	1.443025000
1	-0.000961000	1.003603000	1.776564000
6	1.404425000	-1.969858000	2.123601000
6	2.621182000	-2.068131000	2.799354000
6	0.308525000	-2.678799000	2.621680000
6	2.735767000	-2.843390000	3.949732000
6	0.422535000	-3.452753000	3.770415000
6	1.637435000	-3.536927000	4.441808000
1	3.491619000	-1.540106000	2.434177000
1	-0.645304000	-2.632758000	2.112848000
1	3.690233000	-2.904734000	4.458764000
1	-0.440730000	-3.994143000	4.138481000
1	1.727229000	-4.140614000	5.336374000
6	2.842221000	0.153401000	0.534240000
6	2.986649000	1.122129000	1.529698000
6	3.894696000	-0.042623000	-0.358489000
6	4.155496000	1.866714000	1.633135000
6	5.065579000	0.704936000	-0.261406000
6	5.200123000	1.660033000	0.737533000
1	2.185519000	1.290510000	2.236794000
1	3.803993000	-0.790268000	-1.135299000
1	4.251217000	2.609029000	2.416384000
1	5.872807000	0.531819000	-0.962779000
1	6.112434000	2.237857000	0.821173000

PCy_2BH_2·IDipp

15	-0.080418000	1.780693000	0.367542000
7	1.035404000	-2.061378000	0.257729000
7	-1.114270000	-1.995314000	0.380041000
6	-3.097131000	-1.100141000	1.498710000
6	-2.503054000	-1.600564000	0.329138000
6	-0.035817000	-1.264590000	-0.021943000
6	3.164142000	-1.290315000	1.179427000
6	2.431726000	-1.742379000	0.069542000
6	0.624875000	-3.266647000	0.803547000
1	1.324889000	-4.031965000	1.082516000
6	-0.719334000	-3.224700000	0.880433000
1	-1.429738000	-3.946181000	1.239041000
6	3.018879000	-1.962814000	-1.186240000
6	-1.293405000	2.873500000	-0.592572000
1	-1.019565000	2.841090000	-1.653546000
6	-2.343245000	-0.946350000	2.813319000
1	-1.283360000	-1.106692000	2.616199000
6	1.876072000	3.006519000	-1.441310000
1	1.607403000	2.222765000	-2.151456000
1	1.230250000	3.862804000	-1.660074000
6	-3.222025000	-1.801411000	-0.860144000
6	-4.573417000	-1.460822000	-0.857659000
1	-5.157218000	-1.597015000	-1.758283000
6	1.625336000	2.520824000	-0.005698000
1	2.276263000	1.651045000	0.149222000
6	2.547382000	-1.118213000	2.561288000
1	1.463451000	-1.165617000	2.455617000
6	4.380910000	-1.694911000	-1.313056000
1	4.866587000	-1.848853000	-2.267547000
6	2.242213000	-2.517470000	-2.371135000
1	1.181124000	-2.461079000	-2.132132000
6	-1.278770000	4.340972000	-0.132546000
1	-1.490647000	4.378945000	0.942641000
1	-0.288760000	4.777497000	-0.265423000
6	-2.720190000	2.317042000	-0.458113000
1	-2.755902000	1.285920000	-0.808808000
1	-2.995636000	2.296484000	0.602611000
6	4.523727000	-1.040609000	0.993067000
1	5.118810000	-0.688720000	1.825115000
6	-5.184319000	-0.953375000	0.278428000
1	-6.235563000	-0.694112000	0.256524000
6	-4.453853000	-0.780331000	1.441980000
1	-4.943502000	-0.387556000	2.323352000
6	5.126517000	-1.236068000	-0.238628000
1	6.183052000	-1.032699000	-0.361719000
6	2.067479000	3.591414000	1.008813000
1	1.431064000	4.476568000	0.920221000
1	1.923493000	3.221466000	2.026984000
6	3.336566000	3.426988000	-1.654663000
1	3.980095000	2.544581000	-1.559659000
1	3.473206000	3.803361000	-2.673341000
6	-2.597257000	-2.411546000	-2.106381000
1	-1.515554000	-2.398914000	-1.979519000
6	3.527991000	4.009888000	0.796952000
1	3.800286000	4.796221000	1.507692000
1	4.181601000	3.155923000	1.011954000
6	-3.719003000	4.623140000	-0.777204000
1	-4.419271000	5.218753000	-1.370422000
1	-4.056719000	4.690382000	0.263933000
6	-3.749116000	3.159368000	-1.220250000
1	-3.538163000	3.102506000	-2.294767000
1	-4.749931000	2.740155000	-1.078109000
6	-2.305993000	5.197919000	-0.884468000
1	-2.283323000	6.223453000	-0.503268000
1	-2.020304000	5.253769000	-1.941602000
6	-3.031072000	-3.878281000	-2.270782000
1	-4.111481000	-3.955115000	-2.412454000
1	-2.767724000	-4.476599000	-1.396459000
1	-2.546162000	-4.323341000	-3.142523000
6	2.451016000	-1.697374000	-3.651027000
1	3.479976000	-1.758905000	-4.011452000
1	2.204887000	-0.648766000	-3.486481000
1	1.804743000	-2.077224000	-4.445127000
6	3.778576000	4.482109000	-0.637608000
1	4.835518000	4.727460000	-0.778216000
1	3.219119000	5.408687000	-0.813991000
6	2.588620000	-3.997799000	-2.604823000
1	1.996202000	-4.401793000	-3.428766000
1	2.388898000	-4.602437000	-1.717999000
1	3.643849000	-4.119397000	-2.859363000
6	2.868005000	0.241333000	3.195764000
1	2.346086000	0.336009000	4.150035000
1	2.545076000	1.061648000	2.557065000
1	3.935257000	0.358593000	3.393743000
6	-2.794048000	-2.014454000	3.825118000
1	-3.846730000	-1.888345000	4.087522000
1	-2.209166000	-1.936938000	4.744159000
1	-2.671435000	-3.025231000	3.430952000
6	-2.471490000	0.460773000	3.411480000
1	-2.066910000	1.210056000	2.731305000
1	-1.906203000	0.517423000	4.344427000
1	-3.508992000	0.712100000	3.640911000
5	-0.029946000	0.134028000	-0.797053000
6	2.976657000	-2.262433000	3.496249000
1	4.056378000	-2.248509000	3.660608000
1	2.717574000	-3.240494000	3.087520000

1	2.488311000	-2.163215000	4.468040000
6	-2.901265000	-1.607065000	-3.377217000
1	-2.360577000	-2.033657000	-4.224720000
1	-2.590402000	-0.568539000	-3.266293000
1	-3.963915000	-1.624924000	-3.627221000
1	0.973547000	0.160252000	-1.464872000
1	-1.013388000	0.146445000	-1.495278000

$[HPCy_2BH_2{\cdot}IDipp]^+$

15	0.235227000	1.804766000	0.011519000
7	0.730462000	-2.151340000	0.309859000
7	-1.405818000	-1.858102000	0.389196000
6	-3.300737000	-0.714170000	1.438494000
6	-2.747348000	-1.316360000	0.296024000
6	-0.248546000	-1.260759000	0.004770000
6	2.927780000	-1.600645000	1.237751000
6	2.158118000	-1.982639000	0.125372000
6	0.185801000	-3.294795000	0.860616000
1	0.796309000	-4.125696000	1.161549000
6	-1.150479000	-3.111073000	0.910763000
1	-1.938398000	-3.750503000	1.263336000
6	2.719475000	-2.283541000	-1.126318000
6	-0.877346000	3.102165000	-0.692766000
1	-0.745679000	2.997758000	-1.776580000
6	-2.564769000	-0.621986000	2.769839000
1	-1.513771000	-0.859636000	2.596289000
6	2.436832000	2.666504000	-1.521759000
1	2.119268000	1.911614000	-2.243579000
1	1.934271000	3.599016000	-1.794597000
6	-3.460772000	-1.483957000	-0.901570000
6	-4.762504000	-0.985145000	-0.940574000
1	-5.344966000	-1.092840000	-1.845551000
6	2.025758000	2.253169000	-0.094657000
1	2.512199000	1.292872000	0.116577000
6	2.336266000	-1.394227000	2.627121000
1	1.251157000	-1.327755000	2.530845000
6	4.101285000	-2.143345000	-1.252022000
1	4.573245000	-2.364579000	-2.199585000
6	1.901815000	-2.811059000	-2.296699000
1	0.847655000	-2.635085000	-2.081584000
6	-0.543871000	4.549593000	-0.290567000
1	-0.606261000	4.647189000	0.798687000
1	0.476495000	4.805697000	-0.573371000
6	-2.346406000	2.775177000	-0.354678000
1	-2.596361000	1.759157000	-0.659136000
1	-2.480415000	2.825482000	0.731069000
6	4.304743000	-1.481165000	1.049100000
1	4.933445000	-1.193990000	1.881137000
6	-5.330089000	-0.367321000	0.162415000
1	-6.345043000	0.005455000	0.108914000
6	-4.609064000	-0.240895000	1.338712000
1	-5.073936000	0.225095000	2.197049000
6	4.885028000	-1.741579000	-0.182024000
1	5.956544000	-1.646991000	-0.304113000
6	2.516637000	3.268787000	0.952744000
1	2.023277000	4.231412000	0.805355000
1	2.251228000	2.936023000	1.959343000
6	3.954000000	2.871289000	-1.610548000
1	4.454141000	1.907993000	-1.464934000
1	4.214581000	3.208216000	-2.616280000
6	-2.901316000	-2.225385000	-2.107475000
1	-1.831079000	-2.366696000	-1.954667000
6	4.034776000	3.461747000	0.846909000
1	4.356521000	4.211675000	1.572817000
1	4.537225000	2.527383000	1.119701000
6	-2.972381000	5.214289000	-0.637088000
1	-3.633106000	5.906234000	-1.163367000
1	-3.159288000	5.359281000	0.432801000
6	-3.303755000	3.771308000	-1.018303000
1	-3.246191000	3.655777000	-2.106036000
1	-4.329518000	3.526063000	-0.734435000
6	-1.512221000	5.543067000	-0.946489000
1	-1.268592000	6.554177000	-0.613099000
1	-1.357506000	5.528455000	-2.030930000
6	-3.537473000	-3.621531000	-2.224738000
1	-4.613223000	-3.549670000	-2.395089000
1	-3.384291000	-4.212706000	-1.320144000
1	-3.101520000	-4.168130000	-3.062931000
6	2.214146000	-2.093586000	-3.616824000
1	3.231030000	-2.292829000	-3.958237000
1	2.091559000	-1.014242000	-3.523191000
1	1.537229000	-2.443381000	-4.397997000
6	4.455898000	3.870829000	-0.566476000
1	5.542841000	3.958836000	-0.623376000
1	4.053058000	4.864590000	-0.791260000
6	2.095512000	-4.330822000	-2.444598000
1	1.473801000	-4.715077000	-3.255310000
1	1.826280000	-4.864255000	-1.531278000
1	3.134616000	-4.572506000	-2.675918000
6	2.807580000	-0.096581000	3.297266000
1	2.288328000	0.042618000	4.247077000
1	2.610027000	0.775288000	2.673453000
1	3.876472000	-0.114722000	3.513897000
6	-3.111443000	-1.659479000	3.766613000
1	-4.159312000	-1.461672000	3.999374000
1	-2.548232000	-1.624645000	4.701044000
1	-3.047676000	-2.674605000	3.372229000
6	-2.612129000	0.782942000	3.386587000
1	-2.230881000	1.538911000	2.699142000
1	-2.005933000	0.812972000	4.293713000
1	-3.626402000	1.070370000	3.666402000
5	-0.109828000	0.075825000	-0.866211000
6	2.645895000	-2.599434000	3.533373000
1	3.721379000	-2.702286000	3.688926000
1	2.284470000	-3.535356000	3.105554000
1	2.176312000	-2.472152000	4.510479000
6	-3.066203000	-1.439583000	-3.415858000
1	-2.577285000	-1.972310000	-4.233287000
1	-2.619414000	-0.447608000	-3.344296000
1	-4.115857000	-1.321002000	-3.689069000
1	0.829705000	-0.025491000	-1.607300000
1	-1.123332000	0.252294000	-1.479383000
1	-0.033940000	1.847162000	1.393419000

$[Ni(CO)_3PCy_2BH_2{\cdot}IDipp]$

15	-1.055124000	-1.169757000	-0.353436000
7	0.650232000	2.417801000	0.472684000
7	2.405372000	1.167915000	0.323430000
6	3.890564000	-0.681016000	0.977593000
6	3.393347000	0.164449000	-0.028706000
6	1.073301000	1.202610000	0.011318000
6	-1.513311000	3.084592000	1.425703000
6	-0.643634000	3.053472000	0.322208000
6	1.699043000	3.118178000	1.043358000
1	1.566429000	4.101324000	1.454144000
6	2.792133000	2.340615000	0.947111000
1	3.806801000	2.512734000	1.250995000
6	-0.917248000	3.742513000	-0.872886000
6	-1.114444000	-2.282425000	-1.885231000
1	-1.255236000	-1.600877000	-2.731895000
6	3.443549000	-0.602685000	2.431794000
1	2.482075000	-0.089829000	2.464534000

6	-3.145110000	0.174191000	-1.867906000
1	-2.330259000	0.648178000	-2.416532000
1	-3.405701000	-0.733980000	-2.417712000
6	3.902294000	0.154249000	-1.339423000
6	4.894451000	-0.777162000	-1.637889000
1	5.299880000	-0.816015000	-2.640049000
6	-2.684681000	-0.191567000	-0.445463000
1	-2.408070000	0.747076000	0.046299000
6	-1.185951000	2.430316000	2.760970000
1	-0.365257000	1.730625000	2.605966000
6	-2.123652000	4.436695000	-0.953046000
1	-2.367761000	4.972695000	-1.860365000
6	0.070134000	3.829622000	-2.027939000
1	0.837409000	3.073433000	-1.874726000
6	-2.286486000	-3.279253000	-1.867304000
1	-2.163308000	-3.955864000	-1.016022000
1	-3.236588000	-2.767463000	-1.716420000
6	0.192450000	-3.053798000	-2.133265000
1	1.041058000	-2.372683000	-2.162357000
1	0.370492000	-3.740309000	-1.302411000
6	-2.700654000	3.804440000	1.287885000
1	-3.392188000	3.849541000	2.118104000
6	5.377269000	-1.647959000	-0.674923000
1	6.145098000	-2.367334000	-0.930798000
6	4.885947000	-1.590382000	0.617637000
1	5.279511000	-2.265235000	1.364833000
6	-3.008051000	4.468087000	0.112492000
1	-3.936768000	5.018653000	0.028811000
6	-3.851770000	-0.787332000	0.357792000
1	-4.134912000	-1.760164000	-0.053670000
1	-3.533714000	-0.975477000	1.383354000
6	-4.371077000	1.096356000	-1.857427000
1	-4.095961000	2.059948000	-1.416459000
1	-4.684360000	1.301103000	-2.885774000
6	3.471041000	1.148720000	-2.407787000
1	2.564326000	1.642315000	-2.064416000
6	-5.080592000	0.130563000	0.357216000
1	-5.897205000	-0.348950000	0.904526000
1	-4.841401000	1.052491000	0.899596000
6	-1.049158000	-4.830553000	-3.450416000
1	-1.106426000	-5.351375000	-4.410556000
1	-0.891787000	-5.600674000	-2.686540000
6	0.133860000	-3.861434000	-3.435790000
1	0.049889000	-3.173212000	-4.285391000
1	1.072023000	-4.407531000	-3.570600000
6	-2.360399000	-4.098661000	-3.162395000
1	-3.187568000	-4.811705000	-3.099590000
1	-2.591138000	-3.428366000	-3.999004000
6	4.546392000	2.232193000	-2.601582000
1	5.480602000	1.797620000	-2.963805000
1	4.763108000	2.756290000	-1.668858000
1	4.214227000	2.970752000	-3.334610000
6	-0.573162000	3.535722000	-3.389364000
1	-1.312568000	4.290436000	-3.663877000
1	-1.060075000	2.561080000	-3.392892000
1	0.192527000	3.533254000	-4.167760000
6	-5.526779000	0.489003000	-1.060947000
1	-6.374218000	1.179971000	-1.030643000
1	-5.881172000	-0.415806000	-1.568527000
6	0.765016000	5.202605000	-2.040958000
1	1.506380000	5.245259000	-2.841764000
1	1.276322000	5.404324000	-1.098182000
1	0.044434000	6.006174000	-2.207540000
6	-2.359832000	1.627265000	3.337210000
1	-2.044579000	1.120491000	4.249484000
1	-2.709276000	0.868453000	2.638268000
1	-3.205060000	2.268854000	3.592672000
6	4.444353000	0.211709000	3.273425000
1	5.419391000	-0.280208000	3.294216000
1	4.088537000	0.296308000	4.302271000
1	4.592890000	1.220582000	2.887973000
6	3.245735000	-1.980703000	3.076628000
1	2.594993000	-2.615153000	2.479844000
1	2.792841000	-1.863445000	4.061987000
1	4.194757000	-2.502563000	3.214656000
5	0.316883000	0.161945000	-0.952443000
6	-0.717108000	3.479727000	3.784647000
1	-1.513451000	4.195273000	4.001481000
1	0.146623000	4.043144000	3.428849000
1	-0.437364000	2.992635000	4.720687000
6	3.126199000	0.479513000	-3.744705000
1	2.742272000	1.225030000	-4.444211000
1	2.362488000	-0.286322000	-3.614052000
1	4.000885000	0.019610000	-4.208442000
1	-0.223705000	0.827908000	-1.804497000
1	1.184731000	-0.505478000	-1.437961000
28	-0.816476000	-2.454148000	1.610911000
8	-3.324973000	-3.889838000	2.236757000
8	0.031898000	-0.707009000	3.822488000
8	1.171943000	-4.597129000	1.211191000
6	-2.381460000	-3.303706000	1.968088000
6	0.421168000	-3.740263000	1.316610000
6	-0.314073000	-1.360663000	2.945219000

$P(SiMe_3)_2BH_2$·IDipp

15	0.110426000	2.073991000	0.335899000
7	1.012589000	-1.803643000	0.269062000
7	-1.138512000	-1.762958000	0.211572000
6	-0.040299000	-1.003549000	-0.068068000
6	-2.532598000	-1.396286000	0.112357000
6	2.423761000	-1.491957000	0.237992000
6	-0.771601000	-3.008375000	0.691737000
1	-1.501640000	-3.748499000	0.961980000
6	0.573670000	-3.033395000	0.728257000
1	1.259782000	-3.800163000	1.036504000
6	-3.197300000	-1.015858000	1.289134000
6	3.043695000	-1.125112000	1.443450000
6	3.139361000	-1.684150000	-0.954526000
6	2.287371000	-0.973449000	2.757336000
1	1.224822000	-1.107048000	2.555644000
6	-3.193208000	-1.547942000	-1.116760000
6	4.425066000	-0.933521000	1.421923000
1	4.934563000	-0.644859000	2.331916000
6	5.154681000	-1.100865000	0.257240000
1	6.225695000	-0.941433000	0.262514000
6	4.516449000	-1.471442000	-0.916264000
1	5.099326000	-1.605047000	-1.817831000
6	2.482506000	-2.168154000	-2.239010000
1	1.404508000	-2.065893000	-2.123001000
6	-2.502264000	-0.904089000	2.640852000
1	-1.439424000	-1.095318000	2.495182000
6	-4.567071000	-0.768161000	1.200358000
1	-5.111364000	-0.469805000	2.086999000
6	-2.491197000	-2.042910000	-2.373042000
1	-1.417416000	-1.997456000	-2.197094000
6	-5.242252000	-0.894208000	-0.001641000
1	-6.305173000	-0.692746000	-0.048431000
6	-4.560795000	-1.280174000	-1.145292000
1	-5.102627000	-1.382252000	-2.076247000
6	2.704603000	-2.062365000	3.760346000
1	2.562350000	-3.065055000	3.352274000
1	2.112121000	-1.982007000	4.674157000

1	3.756568000	-1.964804000	4.036476000
6	2.446804000	0.425370000	3.368747000
1	3.491865000	0.654366000	3.586910000
1	1.892501000	0.484073000	4.308064000
1	2.053574000	1.190685000	2.700127000
6	-2.617496000	0.502086000	3.245918000
1	-2.149871000	1.246478000	2.602043000
1	-2.110544000	0.532690000	4.212765000
1	-3.658639000	0.787669000	3.409455000
6	-3.027971000	-1.966771000	3.620465000
1	-4.085585000	-1.812149000	3.843766000
1	-2.478481000	-1.917713000	4.562903000
1	-2.919580000	-2.976057000	3.218379000
6	-2.776519000	-1.162262000	-3.596641000
1	-3.828704000	-1.195293000	-3.886610000
1	-2.192049000	-1.512059000	-4.450094000
1	-2.504505000	-0.124802000	-3.404012000
6	2.877750000	-1.328346000	-3.460567000
1	2.656547000	-0.273691000	-3.299649000
1	2.318009000	-1.661385000	-4.336955000
1	3.939428000	-1.425217000	-3.696140000
5	0.010545000	0.409278000	-0.841372000
6	2.788263000	-3.656794000	-2.478946000
1	3.859104000	-3.820168000	-2.619398000
1	2.274575000	-4.010777000	-3.375526000
1	2.465042000	-4.275581000	-1.639710000
6	-2.855616000	-3.510222000	-2.657255000
1	-2.605751000	-4.157602000	-1.814427000
1	-2.314047000	-3.873861000	-3.533320000
1	-3.924372000	-3.619184000	-2.854484000
1	-0.979368000	0.466282000	-1.525633000
1	1.004081000	0.373054000	-1.522050000
14	-1.624066000	3.395693000	-0.299574000
6	-3.249880000	2.442250000	-0.225326000
1	-3.472203000	2.082761000	0.779100000
1	-4.066568000	3.104147000	-0.529326000
1	-3.248261000	1.583588000	-0.896631000
6	-1.778329000	4.829097000	0.927782000
1	-2.648714000	5.444685000	0.680260000
1	-1.911540000	4.455299000	1.945403000
1	-0.902317000	5.478759000	0.928119000
6	-1.540286000	4.131612000	-2.043024000
1	-2.476592000	4.654509000	-2.261834000
1	-0.728485000	4.851352000	-2.155949000
1	-1.407250000	3.354212000	-2.797932000
14	1.871124000	3.213959000	-0.532511000
6	1.850631000	5.018514000	0.041422000
1	1.033137000	5.592487000	-0.397285000
1	1.766331000	5.091687000	1.127790000
1	2.786335000	5.503466000	-0.252775000
6	1.997436000	3.202953000	-2.419751000
1	1.180597000	3.747852000	-2.892644000
1	2.937712000	3.669017000	-2.730538000
1	1.982971000	2.183100000	-2.806784000
6	3.483644000	2.473820000	0.113012000
1	4.331291000	3.029747000	-0.299521000
1	3.545933000	2.528759000	1.201063000
1	3.599802000	1.429952000	-0.178100000

$[HP(SiMe_3)_2BH_2{\cdot}IDipp]^+$

15	0.126155000	2.123524000	-0.030844000
7	1.003524000	-1.806665000	0.349149000
7	-1.149914000	-1.767650000	0.239296000
6	-0.042716000	-1.028477000	-0.039548000
6	-2.543949000	-1.402536000	0.083735000
6	2.420357000	-1.500529000	0.317528000
6	-0.794552000	-2.990282000	0.773071000
1	-1.530291000	-3.721535000	1.052166000
6	0.551838000	-3.014192000	0.842840000
1	1.228763000	-3.771014000	1.193267000
6	-3.243269000	-0.991952000	1.231340000
6	3.026235000	-1.068889000	1.510019000
6	3.146640000	-1.769932000	-0.853916000
6	2.257174000	-0.861474000	2.809282000
1	1.190361000	-0.918068000	2.587857000
6	-3.162753000	-1.590668000	-1.162610000
6	4.408383000	-0.883933000	1.492940000
1	4.912798000	-0.558216000	2.392922000
6	5.149795000	-1.120083000	0.346898000
1	6.222219000	-0.973051000	0.357923000
6	4.524224000	-1.556260000	-0.810535000
1	5.119370000	-1.752386000	-1.692080000
6	2.509820000	-2.342685000	-2.112035000
1	1.427599000	-2.254085000	-2.016345000
6	-2.598190000	-0.869102000	2.607276000
1	-1.523816000	-1.022609000	2.498095000
6	-4.607608000	-0.739386000	1.089897000
1	-5.184298000	-0.429127000	1.951237000
6	-2.432397000	-2.150521000	-2.375191000
1	-1.361476000	-2.107588000	-2.177159000
6	-5.241833000	-0.889163000	-0.132380000
1	-6.302330000	-0.689566000	-0.218300000
6	-4.526486000	-1.310163000	-1.242293000
1	-5.041567000	-1.441264000	-2.184312000
6	2.576771000	-1.975885000	3.820915000
1	2.361262000	-2.965745000	3.416299000
1	1.984995000	-1.846794000	4.729008000
1	3.630768000	-1.957666000	4.103561000
6	2.511258000	0.516227000	3.437780000
1	3.551084000	0.637611000	3.744430000
1	1.893198000	0.639725000	4.328884000
1	2.270927000	1.324133000	2.745751000
6	-2.787865000	0.521947000	3.229676000
1	-2.374307000	1.305761000	2.593741000
1	-2.281644000	0.571630000	4.195364000
1	-3.840833000	0.750439000	3.401427000
6	-3.121702000	-1.957789000	3.559787000
1	-4.191271000	-1.840355000	3.742252000
1	-2.610891000	-1.898768000	4.522624000
1	-2.965071000	-2.959082000	3.155790000
6	-2.683223000	-1.335668000	-3.651187000
1	-3.725331000	-1.388793000	-3.970229000
1	-2.074959000	-1.728595000	-4.467646000
1	-2.422044000	-0.286224000	-3.511961000
6	2.909431000	-1.577851000	-3.381160000
1	2.675383000	-0.516342000	-3.296072000
1	2.366782000	-1.974864000	-4.240678000
1	3.974303000	-1.675032000	-3.597654000
5	0.029365000	0.314524000	-0.918828000
6	2.840367000	-3.839277000	-2.251970000
1	3.914251000	-3.995247000	-2.370891000
1	2.342689000	-4.256713000	-3.129173000
1	2.517272000	-4.408629000	-1.378679000
6	-2.802642000	-3.628483000	-2.592072000
1	-2.579502000	-4.235021000	-1.712465000
1	-2.243895000	-4.039384000	-3.434971000
1	-3.866601000	-3.738831000	-2.809883000
1	-0.949507000	0.394651000	-1.605682000
1	1.027453000	0.278647000	-1.583276000
14	-1.738304000	3.507375000	-0.251211000
6	-3.289993000	2.474432000	-0.352454000
1	-3.488806000	1.911679000	0.557673000

1	-4.136900000	3.147068000	-0.517910000
1	-3.258634000	1.770335000	-1.184017000
6	-1.745292000	4.621833000	1.256181000
1	-2.586347000	5.317383000	1.187518000
1	-1.865279000	4.052106000	2.179511000
1	-0.834007000	5.214760000	1.340093000
6	-1.548916000	4.482227000	-1.842435000
1	-2.449748000	5.087056000	-1.980534000
1	-0.698343000	5.163472000	-1.836604000
1	-1.462129000	3.828278000	-2.711932000
14	2.013225000	3.292527000	-0.726595000
6	1.969499000	5.021939000	0.000041000
1	1.135258000	5.623447000	-0.361219000
1	1.932029000	5.003218000	1.090882000
1	2.890092000	5.540268000	-0.283532000
6	1.958118000	3.303311000	-2.598797000
1	1.120804000	3.877135000	-2.995507000
1	2.878206000	3.758089000	-2.976341000
1	1.900018000	2.291223000	-3.001941000
6	3.524290000	2.383308000	-0.109584000
1	4.413258000	2.891364000	-0.495064000
1	3.591839000	2.386155000	0.978599000
1	3.558060000	1.350060000	-0.452736000
1	0.290587000	2.050753000	1.368639000

$[Ni(CO)_3P(SiMe_3)_2BH_2{\cdot}IDipp]$

15	-1.581648000	-0.002045000	0.947002000
7	1.985366000	-1.078951000	-0.864247000
7	1.983415000	1.082831000	-0.863932000
6	1.401888000	0.001327000	-0.261394000
6	1.862753000	2.490647000	-0.529239000
6	1.867530000	-2.487077000	-0.529822000
6	2.900321000	0.675480000	-1.816637000
1	3.468620000	1.380498000	-2.393294000
6	2.901535000	-0.669657000	-1.816831000
1	3.471116000	-1.373488000	-2.393667000
6	1.153263000	3.336265000	-1.398154000
6	1.159525000	-3.333976000	-1.398700000
6	2.588195000	-2.978661000	0.574549000
6	0.468982000	-2.847079000	-2.664247000
1	0.408399000	-1.760838000	-2.624165000
6	2.582111000	2.983506000	0.575401000
6	1.146533000	-4.697492000	-1.101369000
1	0.604510000	-5.373822000	-1.748021000
6	1.809662000	-5.200924000	0.003182000
1	1.777758000	-6.261723000	0.218032000
6	2.525480000	-4.347649000	0.827024000
1	3.059763000	-4.754183000	1.675062000
6	3.491170000	-2.108546000	1.436644000
1	3.240925000	-1.067549000	1.245158000
6	0.464005000	2.848221000	-2.663928000
1	0.406222000	1.761798000	-2.624549000
6	1.137350000	4.699690000	-1.100575000
1	0.594043000	5.374985000	-1.747241000
6	3.486477000	2.115148000	1.437804000
1	3.239097000	1.073627000	1.245419000
6	1.799202000	5.204293000	0.004213000
1	1.765057000	6.264983000	0.219256000
6	2.516579000	4.352336000	0.828055000
1	3.049844000	4.759803000	1.676290000
6	1.286865000	-3.221859000	-3.913398000
1	2.305137000	-2.832114000	-3.871094000
1	0.810556000	-2.819343000	-4.809424000
1	1.353483000	-4.306328000	-4.025277000
6	-0.964820000	-3.375828000	-2.798970000
1	-0.988516000	-4.460247000	-2.920137000
1	-1.438232000	-2.937858000	-3.678523000
1	-1.566801000	-3.117667000	-1.929571000
6	-0.971132000	3.373387000	-2.798463000
1	-1.572131000	3.114498000	-1.928611000
1	-1.443658000	2.933249000	-3.677405000
1	-0.997558000	4.457636000	-2.920612000
6	1.280982000	3.225623000	-3.912894000
1	1.345160000	4.310296000	-4.024172000
1	0.805561000	2.822530000	-4.809135000
1	2.300135000	2.838146000	-3.870822000
6	3.286230000	2.344030000	2.941467000
1	3.598083000	3.343914000	3.249092000
1	3.885971000	1.629209000	3.508518000
1	2.243109000	2.208552000	3.224697000
6	3.293052000	-2.338777000	2.940374000
1	2.249833000	-2.206406000	3.224728000
1	3.891314000	-1.622524000	3.507178000
1	3.608079000	-3.337898000	3.247222000
5	0.468004000	0.000377000	1.048827000
6	4.965281000	-2.312968000	1.044947000
1	5.280745000	-3.341868000	1.231279000
1	5.609481000	-1.653194000	1.630381000
1	5.135103000	-2.099024000	-0.011746000
6	4.960444000	2.323523000	1.047719000
1	5.131833000	2.110765000	-0.008963000
1	5.605692000	1.664925000	1.633322000
1	5.273225000	3.353057000	1.235093000
1	0.757370000	0.989086000	1.668587000
1	0.759799000	-0.987482000	1.668805000
14	-2.126409000	1.804449000	2.245208000
6	-1.669163000	3.370999000	1.305034000
1	-2.235300000	3.470504000	0.378593000
1	-1.896100000	4.242570000	1.926298000
1	-0.607506000	3.404488000	1.061131000
6	-3.973414000	1.872861000	2.628762000
1	-4.197399000	2.834850000	3.099836000
1	-4.594574000	1.789569000	1.737368000
1	-4.277972000	1.090526000	3.324393000
6	-1.212817000	1.845354000	3.899420000
1	-1.333467000	2.834454000	4.351424000
1	-1.607865000	1.112166000	4.603233000
1	-0.145806000	1.656209000	3.781694000
14	-2.123201000	-1.810498000	2.243826000
6	-3.969732000	-1.880883000	2.629445000
1	-4.273566000	-1.101317000	3.328515000
1	-4.592129000	-1.794395000	1.739214000
1	-4.192783000	-2.844724000	3.097159000
6	-1.207835000	-1.852749000	3.897000000
1	-1.601013000	-1.119179000	4.601452000
1	-1.329302000	-2.841820000	4.348862000
1	-0.140707000	-1.665063000	3.778064000
6	-1.665714000	-3.375644000	1.301450000
1	-1.891281000	-4.248081000	1.921996000
1	-2.232751000	-3.474583000	0.375501000
1	-0.604283000	-3.408000000	1.056405000
28	-2.959727000	-0.001797000	-1.036935000
6	-1.929654000	-0.001573000	-2.510260000
8	-1.361955000	-0.001338000	-3.506650000
6	-4.001200000	-1.485214000	-1.012374000
8	-4.688375000	-2.395507000	-1.088013000
6	-4.001517000	1.481292000	-1.012424000
8	-4.689005000	2.391334000	-1.088327000

6.5.6 References

[1] A. J. Arduengo, R. Krafczyk, R. Schmutzler, H. A. Craig, J. R. Goerlich, W. J. Marshall, M. Unverzagt, *Tetrahedron* **1999**, *55*, 14523–14534.

[2] R. Szlosek, M. Seidl, G. Balázs, M. Scheer, *Chem. Eur. J.* **2023**, *29*, e202301752.

[3] M. T. Ackermann, M. Seidl, R. Grande, Y. Zhou, M. J. Ferguson, A. Y. Timoshkin, E. Rivard, M. Scheer, *Chem. Sci.* **2023**, *14*, 2313–2317.

[4] M. A. K. Weinhart, A. S. Lisovenko, A. Y. Timoshkin, M. Scheer, *Angew. Chem. Int. Ed.* **2020**, *59*, 5541-5545; *Angew. Chem.* **2020**, *132*, 5586-5590.

[5] C. Marquardt, T. Jurca, K.-C. Schwan, A. Stauber, A. V. Virovets, G. R. Whittell, I. Manners, M. Scheer, *Angew. Chem. Int. Ed.* **2015**, *54*, 13782–13786.

[6] L. Lochmann, J. Trekoval, *J. Organomet. Chem.* **1987**, *326*, 1–7.

[7] G. Brauer, *Handbuch der Präparativen Anorganischen Chemie,* 3. Aufl., **1975**.

[8] A. Tzschach, W. Lange, *Chem. Ber.* **1962**, *95*, 1360–1366.

[9] N. Auner, J. Grobe, *Z. Anorg. Allg. Chem.* **1982**, *489*, 23–41.

[10] R. Szlosek, M. T. Ackermann, C. Marquardt, M. Seidl, A. Y. Timoshkin, M. Scheer, *Chem. Eur. J.* **2023**, *29*, e202202911.

[11] O. V. Dolomanov, L. J. Bourhis, R. J. Gildea, J. A. K. Howard, H. Puschmann, *J. Appl. Crystallogr.* **2009**, *42*, 339–341.

[12] G. M. Sheldrick, *Acta Cryst. A* **2015**, *71*, 3–8.

[13] G. M. Sheldrick, *Acta Cryst. C* **2015**, *71*, 3–8.

[14] a) A. D. Becke, *J. Chem. Phys.* **1993**, *98*, 5648–5652; b) C. Lee, W. Yang, R. G. Parr, *Phys. Rev. B* **1988**, *37*, 785–789; c) F. Weigend, R. Ahlrichs, *Phys. Chem. Chem. Phys.* **2005**, *7*, 3297-305.

[15] Gaussian 09, Revision E.01, M. J. Frisch, G. W. Trucks, H. B. Schlegel, G. E. Scuseria, M. A. Robb, J. R. Cheeseman, G. Scalmani, V. Barone, G. A. Petersson, H. Nakatsuji, X. Li, M. Caricato, A. Marenich, J. Bloino, B. G. Janesko, R. Gomperts, B. Mennucci, H. P. Hratchian, J. V. Ortiz, A. F. Izmaylov, J. L. Sonnenberg, D. Williams-Young, F. Ding, F. Lipparini, F. Egidi, J. Goings, B. Peng, A. Petrone, T. Henderson, D. Ranasinghe, V. G. Zakrzewski, J. Gao, N. Rega, G. Zheng, W. Liang, M. Hada, M. Ehara, K. Toyota, R. Fukuda, J. Hasegawa, M. Ishida, T. Nakajima, Y. Honda, O. Kitao, H. Nakai, T. Vreven, K. Throssell, J. A. Montgomery, Jr., J. E. Peralta, F. Ogliaro, M. Bearpark, J. J. Heyd, E. Brothers, K. N. Kudin, V. N. Staroverov, T. Keith, R. Kobayashi, J. Normand, K. Raghavachari, A. Rendell, J. C. Burant, S. S. Iyengar, J. Tomasi, M. Cossi, J. M. Millam, M. Klene, C. Adamo, R. Cammi, J. W. Ochterski, R. L. Martin, K. Morokuma, O. Farkas, J. B. Foresman, and D. J. Fox, Gaussian, Inc., Wallingford CT, 2016.

[16] National InstituteRelease 22, May 2022, NIST Standard Reference Database 101, Internet: https://cccbdb.nist.gov/vibscalejust.asp of Standards and Technology, Computational Chemistry Comparison and Benchmark DataBase.

6.6 Author Contributions

- R. Szlosek – experimental work (syntheses of pnictogenyltrielanes, reproductions and analytical data for all compounds, acquisition and solution single-crystal X-ray structures), writing of original draft
- A. S. Niefanger – experimental work (syntheses and TEP determinations of Ni complexes) as part of her B.Sc. thesis ("Determination of Donor properties of Lewis Base stabilized Pentelyltrielanes") under the supervision of R. Szlosek
- G. Balázs – project management, conceptualization
- M. Seidl – finalization of single-crystal X-ray diffraction data
- A. Y. Timoshkin – quantum chemical calculations, acquisition of funding, co-writing of final manuscript
- M. Scheer – project supervision, acquisition of funding, co-writing of final manuscript

7 The parent GaH_2SbH_2 monomer stabilized by a N-heterocyclic carbene

R. Szlosek, K. Dollberg, G. Balázs, M. Seidl, C. von Hänisch and M. Scheer

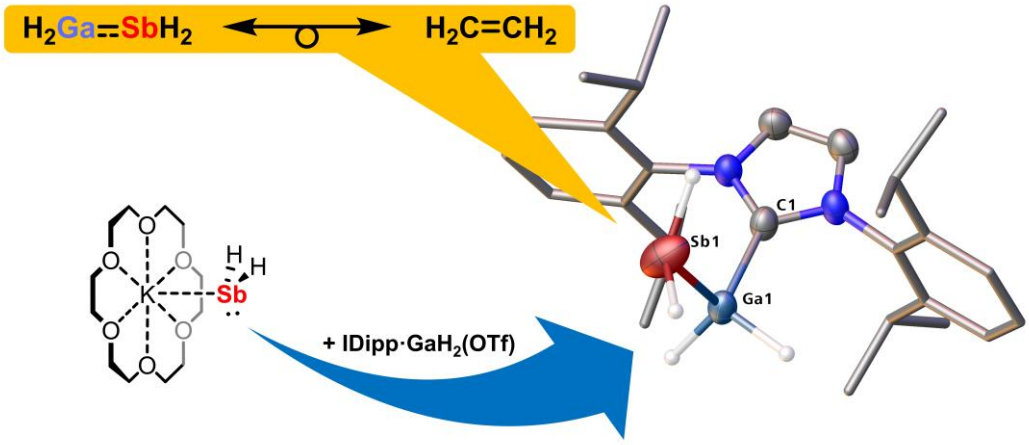

Abstract: The synthesis and characterization of the unprecedented heavy ethylene analogue IDipp·GaH_2SbH_2 is presented. The compound could be synthesized by salt metathesis reaction with the recently discovered reagent K(18c6)SbH_2 and characterized by ^{1}H NMR and IR spectroscopy, as well as single crystal X-ray structure determination and mass spectrometry. IDipp·GaH_2SbH_2 could only be obtained by this salt metathesis reaction, as ($SiMe_3$)/H exchange of IDipp·$GaH_2Sb(SiMe_3)_2$, prepared by the reaction of IDipp·GaH_2(OTf) with $KSb(SiMe_3)_2$, did not prove successful. IDipp·GaH_2SbH_2 is stable at -30 °C but decomposes readily in the presence of light, at room temperature or at air. The reaction of IDipp·$GaCl_3$ with K(18c6)SbH_2 yielded a product mixture, in which IDipp·GaH_2SbH_2 and IDipp·$GaH(SbH_2)_2$ could be identified, as well. Preliminary investigations on the reactivity of the compounds are also presented.

7.1 Introduction

Stibanes SbR_3 represent the heavier congeners of amines, phosphines and arsines. In comparison to their lighter homologs, tertiary stibanes display much higher senstivity towards air and display partially pyrophoric behaviour, except for aryl substituted stibanes.[1] Furthermore, stibanes can be considered as much weaker donors due to the increased *s* character of the lone pair as a consequence of poor *s*/*p* orbital mixing. The drastic sensitivity of stibanes is even more pronounced in primary stibanes $RSbH_2$. Stabilization can be achieved by using bulky residues R such as, for example, mesityl, terphenyl, triptycenyl or $CH(SiMe_3)_2$ (Figure 7.1, **I-V**).[2,3,4] Moreover primary stibanes carrying smaller alkyl substituents are known, they are difficult to handle due to their sensitivity towards air and light and rapid thermal decomposition.[3,5] Thus, examples for stable, isolable primary stibanes remain quite rare. This is surprising, given the fact, that these offer the potential for application in chemical vapor deposition (CVD) processes, e.g. for the deposition of thin GaSb layers, which is a highly relevant process in the production of semiconducting materials.[6,7,8] The synthesis of more complex functionalized stibanes is hampered by a low bonding stability and especially by the lack of suitable reagents. For example, $KSbH_2$ has been discovered several decades ago by the reaction of SbH_3 with elemental potassium in liquid ammonia but is reported to decompose already at temperatures above -78 °C, thus drastically limiting the synthetic value of the compound.[9] This drawback could only recently be overcome by a major breakthrough by the von Hänisch group, which could stabilize the alkali metal stibanide salts $M(crown)SbH_2$ (M = Li-Cs) by using crown-ethers as stabilization tools.[4,10] A very recent work by Liddle and von Hänisch demonstrated the enormous synthetic potential of the reagent by serving as an Sb source for compounds featuring covalent Th-Sb multiple bonding.[11] In general, element-pnictene multiple bonding has received quite of attention over the recent years. In this field, the popular *β*-deketiminate substituent (Nacnac) has served as a valuable platform towards the stabilization of such multiple bonded moieties.[12] Furthermore, von Hänisch and co-workers discovered that (Nacnac)Ga can oxidatively add SbH_3 affording the stibanylgallane (Nacnac)$GaHSbH_2$ (Figure 7.1, **VI**).

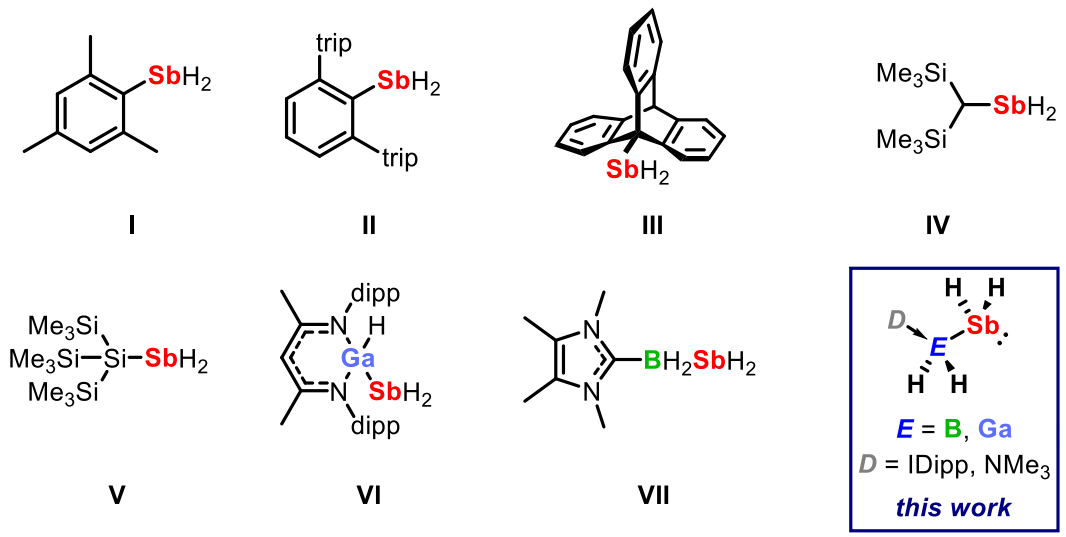

Figure 7.1: Selected examples of primary stibanes (trip = 2,4,6-triisopropylphenyl, dipp = 2,6-diisopropylphenyl, IDipp = 1,3-Bis-(2,6-diisopropylphenyl)-imidazolin-2-ylidene).

Despite these important results, primary stibanes with group 13 attachments are still barely described, especially due to the low bonding stability between group 13 elements and Sb.[13] Given the fact that compounds containing 13/15 element combinations represent important substrates for semiconductor

applications,[7,8] it is desirable to expand the library of these compounds, especially the lightweight hydrogen-bearing parent compounds. Previous results on phosphanyl- and arsanylboranes have shown that these compounds also display interesting reactivity not only as ligands in coordination chemistry,[14] but can also be functionalized by electrophiles,[15] nucleophiles[16] and oxidation.[17] Moreover, Lewis base stabilized monomeric phosphanylboranes can undergo controlled oligo- and polymerization towards inorganic 13/15 materials.[18] By methanolytic treatment of $IMe_4{\cdot}BH_2Sb(SiMe_3)_2$, it was also possible to obtain the parent monomeric stibanylborane $IMe_4{\cdot}BH_2SbH_2$ (Figure 7.1, **VII**), which represents the so far heaviest ethylene 13/15 analogue, but also the only isolable parent stibanyltrielane to this date.[19] In view of recent developments of new reagents, the question arose, if the synthesis of the parent stibanylboranes is possible by employing the novel reagent $K(18c6)SbH_2$ in salt metathesis reaction and if this also allowed for the preparation of the heavier stibanyltrielane homologs. Herein, the direct syntheses and characterizations of donor stabilized parent stibanyltrielanes are reported and their electronic properties are elucidated by quantum chemical calculations.

7.2 Results and Discussion

First, the previous approach for the synthesis of $IDipp{\cdot}GaH_2SbH_2$ by methanolytic cleavage of the silyl precursor monomers was tested for the respective heavier Ga derivative. As the corresponding compound $IDipp{\cdot}GaH_2Sb(SiMe_3)_2$ is unknown in literature, it was attempted to synthesize the compound by salt metathesis reaction of $IDipp{\cdot}GaH_2(OTf)$ (OTf = SO_3CF_3) with $KSb(SiMe_3)_2$. Thus, $KSb(SiMe_3)_2$ was reacted with $IDipp{\cdot}GaH_2(OTf)$ in diethylether under exclusion of light over the course of 16 hours (equation 1).

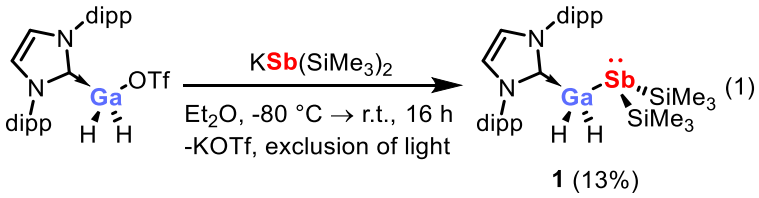

After extraction with toluene and subsequent filtration, $IDipp{\cdot}GaH_2Sb(SiMe_3)_2$ (**1**) was obtained in low yields as a brown microcrystalline solid. The ^1H NMR spectrum shows a characteristic peak at 0.42 ppm for the {$SiMe_3$} groups (C_6D_6, 18 H, $^2J_{HSi}$ = 6.72 Hz). Unfortunately, all attempts to gain single-crystals of **1** failed, so far. However, the presence of **1** could be confirmed by LIFDI-MS, in which the molecular ion peak at *m/z* = 728.35 was detected. Despite the poor accessibility of **1**, methanolytic cleavage of the {$SiMe_3$} groups was attempted. Inside an NMR tube, **1** was combined with an excess amount of MeOH in C_6D_6 and the reaction progress was monitored by ^1H NMR spectroscopy. However, except for thermal decomposition of **1**, no formation of the desired parent monomer $IDipp{\cdot}GaH_2SbH_2$ could be detected, even after prolonged time (cf. Supporting Information). According to DFT computations, the reaction is however predicted to be exergonic by -33.5 kcal mol^{-1}, indicating that rather a kinetic hinderance occurs preventing the cleavage of {$SiMe_3$} groups. However, numerous attempts to synthesize the corresponding silylated stibanylgallanes carrying smaller NHC donors have failed, so far, due to the even lower stability of the products.

As this approach did not prove fruitful, the use of the recently developed $K(18c6)SbH_2$ were attempted. To gain insight into whether the compound reacts smoothly in salt metathesis reactions with group 13

precursors, it was first tested on boranes. Hence, solid K(18c6)SbH_2 was added to a solution of IDipp·BH_2I in tetrahydrofuran at -80 °C in the dark and stirred for two hours (Equation 2).

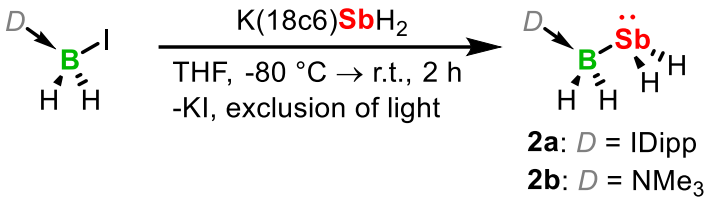

(2)

The ^{1}H and ^{11}B NMR spectra of the extracted solution showed full conversion of the starting material as well as the presence of IDipp·BH_2SbH_2 (**2a**) by a characteristic triplet at -0.81 ppm (2 H, $^3J_{HH}$ = 7.06 Hz). Furthermore, IDipp·BH_3 was detected as a side product of hydride transfer from $[SbH_2]^-$ under deposition of elemental antimony or as a result of thermal decomposition of **2a**. After removing all vo-latiles *in vacuo*, **2a** can be obtained in 78% yield although slightly contaminated with inseparable IDipp·BH_3. **2a** displays high sensitivity towards air, light and temperature and decomposes even at T=-30 °C. Hence, despite many attempts, it was not possible to grow single crystals of **2a** for X-ray structure determination. The IR spectrum (ATR diamond crystal) shows a weak B-H band at 2408 cm^{-1} (calc.: 2409 cm^{-1}) and a strong Sb-H vibration mode at 1834 cm^{-1} (calc.: 1829 cm^{-1}), which is in good agreement with values obtained by DFT computations (B3LYP-D3(BJ)/def2-TZVP, scaling factor 0.965).[20] The LIFDI-MS spectrum of a solution of **2a** in toluene does not show a molecular ion peak due to decomposition during the ionization process. Remarkably, the salt metathesis of Me_3N·BH_2I and K(18c6)SbH_2 in tetrahydrofuran proceeds smoothly, as well, affording the analogue trimethylamine stabilized Me_3N·BH_2SbH_2 (**2b**, equation 2). **2b** was already speculated to be an unstable intermediate in the methanolysis of Me_3N·$BH_2Sb(SiMe_3)_2$, which leads to Me_3N·BH_2SbHBH_2·NMe_3 under loss of SbH_3.[19] In contrast, salt metathesis affords isolable **2b**, although contaminated with small amounts of Me_3N·BH_3. **2b** is an extremely air, light sensitive and volatile compound, that readily decomposes at room temperature. Especially in solution, visible thermal decomposition is observed under deposition of elemental antimony. The ^{11}B NMR spectrum of a solution of **2b** in tetrahydrofuran shows a distinct triplet ($^1J_{HB}$ = 113 Hz) which merges into a singlet in the ^{11}B{^{1}H} NMR spectrum. In the ^{1}H NMR spectrum, a characteristic triplet at -1.11 ($^3J_{HH}$ = 5.43 Hz) is visible. Seeing that the direct synthesis of **2a**/**b** from K(18c6)SbH_2 was successful, the same methodology was investigated towards the heavier homolog gallium. Thus, solid K(18c6)SbH_2 was added to a solution of IDipp·GaH_2(OTf) in tetrahydrofuran at -80°C in the dark and stirred overnight (equation 3).

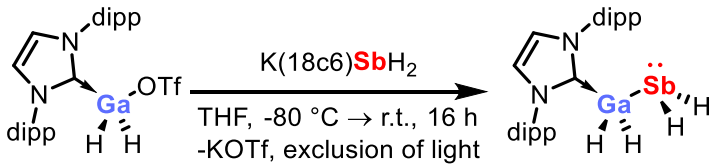

(3)

3

The ^{1}H NMR spectrum of the reaction mixture showed full conversion towards IDipp·GaH_2SbH_2 (**3**) with a characteristic triplet at -1.81 ppm (2 H, $^3J_{HH}$ = 3.94 Hz). After extraction and subsequent filtration, **3** was obtained in moderate yields as colourless solids within an inseparable mixture together with IDipp·GaH_3 and IDipp-H_2 as a consequence of hydride transfer and thermal decomposition. The IR spectrum (ATR diamond crystal) shows a Sb-H vibration mode of medium intensity at 1803 cm^{-1}, which agrees with a theoretically predicted value of 1824 cm^{-1} obtained by DFT computations (B3LYP-D3(BJ)/def2-TZVP, scaling factor 0.965).[20] In the LIFDI-MS mass spectrum, a molecular ion peak [M-H]$^+$ at m/z = 583.24 was detected. **3** displays high sensitivity towards air and light, but can be stored for

weeks at -30 °C. Thus, it was also possible to grow single crystals of **3** suitable for X-ray structure determination by storing a saturated *n*-hexane solution of **3** at -30 °C (Figure 7.2). **3** crystallizes in the triclinic space group $P\bar{1}$ as clear colourless block-shaped crystals. The asymmetric unit shows that **3** co-crystallizes with IDipp·GaH_3, causing structural and occupational disorder in the solid-state structure (cf. Supporting Information). The C-Ga (2.0345(4) Å) and Ga-Sb (2.6776(8) Å) bond lengths lie within the range of regular single bonds, although the Ga-Sb bond is elongated compared to (Nacnac)$GaHSbH_2$ (2.6189(19) Å)[21] and the C-Ga-Sb angle of 109.28(13)° indicates a tetrahedral geometry at the central core structure. **3** represents the first example of a parent compound containing the heavy ethylene analogue GaH_2SbH_2 stabilized by a Lewis base.

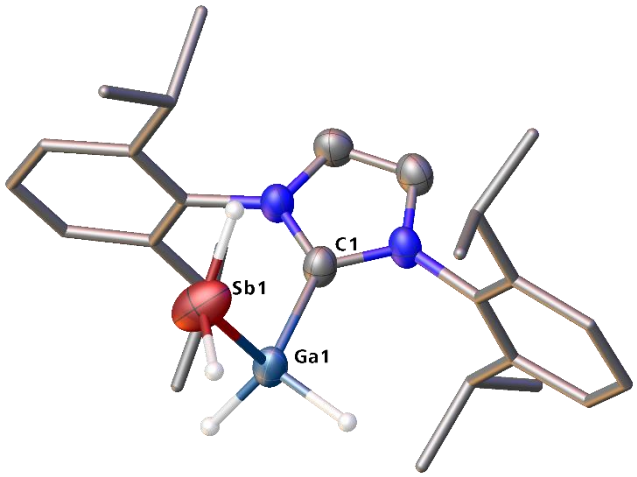

Figure 7.2: Molecular structure of **3** in the solid state. Anisotropic displacement ellipsoids are drawn at 50% probability. Dipp residues are displayed as stick models for clarity. Hydrogen atoms bound to carbon and disordered parts are omitted for clarity. Selected bond lengths [Å] and angles [°]: C1-Ga1 2.0345(4), Ga1-Sb1 2.6776(8), C1-Ga1-Sb1 109.28(13).

For closer inspection of the electronic situation of **3**, quantum chemical computations were carried out. NBO analysis confirms that the Ga-Sb bond can be considered as a regular 2c-2e bond with main contribution by the Sb atom (cf. Supporting Information). This is further supported by a comparably high Wiberg Bond Index (WBI) of 0.84 for the Ga-Sb bond (Table 7.1). According to the Natural Charges, the bonds within the core structural motif are highly polarized towards the H atoms bound to the Ga atom (Table 7.1, upper row). When compared to the corresponding arsanyl- and phosphanylgallane, the charge at Sb is significantly higher than for P and As, due to the higher metallic character of antimony. Similarly, the stibanylborane **2a** shows also a positive charge located on the antimony atom (Table 7.1, bottom row), which highlights the vastly different nature of the bonds between the chain atoms for the heavier congeners.

After examining the electronic properties of **3**, investigations on the reactivity of **3** were targeted. However, these studies were hampered by the low donor strength of the compound as the lone pair at the antimony atom is barely available. Thus, reactions with $W(CO)_5$(thf), IDipp·GaH_2(OTf), $Ni(CO)_4$, and BEt_3 did not prove fruitful. Only the addition of BH_3·SMe_2 to **3** resulted in the formation of a new compound as evident by the appearance of a quartet at -39.8 ppm ($^1J_{HB}$ = 95 Hz) in the ^{11}B NMR spectrum of the reaction mixture, but clear identification of the desired chain compound IDipp·$GaH_2SbH_2BH_3$ failed, as it was not possible to isolate a pure compound or to obtain single-crystals. Mass spectrometric analysis might confirm the presence of IDipp·$GaH_2SbH_2BH_3$, if the resulting molecular ion is stable under ionizing conditions and is currently ongoing.

Table 7.1: Calculated Natural Charges *q* and Wiberg Bond Indices (WBI) for compounds IDipp·EH_2PnH_2 (E = B, Ga; *Pn* = P, As, Sb) as calculated by NBO computations (B3LYP-D3(BJ)/def2-TZVP).

IDipp·EH_2PnH_2	*q*(E)	*q*(Pn)	*q*(H_E)	*q*(H_{Pn})	$WBI_{E\text{-}Pn}$
E = Ga *Pn* = P	+0.59	-0.37	-0.27	+0.01	0.72
E = Ga *Pn* = As	+0.56	-0.26	-0.27	-0.04	0.83
E = Ga *Pn* = Sb (**3**)	+0.46	+0.03	-0.27	+0.01	0.84
E = B *Pn* = P	-0.52	+0.08	+0.02	-0.05	0.96
E = B *Pn* = As	-0.51	+0.13	+0.01	-0.69	0.93
E = B *Pn* = Sb (**2a**)	+0.52	+0.36	+0.02	-0.16	0.88

During these investigations, the question arose, whether higher degrees of substitution on the Ga atom can be achieved by salt metathesis, as well, similar to reactions of IDipp·$GaCl_3$ with $NaPH_2$ or $KAsH_2$. Thus, a solution of IDipp·$GaCl_3$ in tetrahydrofuran was reacted with an excess of solid K(18c6)SbH_2 overnight at -80 °C. The ^{1}H NMR spectrum of the reaction mixture (Figure 7.3) confirmed the presence of a mixture of **3**, but also the di-substituted compound IDipp·$GaH(SbH_2)_2$ (**4**) by two separate distinct doublet of doublets at -0.42 ppm and -0.79 ppm (2 H, $^3J_{HH}$ = 3.12 Hz, $^2J_{HH}$ = 13.08 Hz) as a result of the diastereotopic {SbH_2} H atoms, which represents a characteristic splitting pattern already described for the homologs IDipp·$EH(AsH_2)_2$ (E = Ga, Al). Besides decomposition products, the spectrum also shows a singlet at 0.58 ppm, which is shifted equally downfield (+1.01 ppm) as the aforementioned doublet of doublets from **4** compared to the {SbH_2} signal of **3** (+1.10 ppm). This indicates that possibly IDipp·$Ga(SbH_2)_3$ could be present, but an unambiguous assignment was unfortunately not possible. Due to similar solubility, isolation of any components as well as separation from the decomposition products IDipp-H_2 and IDipp·GaH_xCl_{3-x} (x = 1-3) was not possible, regardless of numerous attempts. Analysis by mass spectrometry is still pending to further verify the presence of the compounds IDipp·GaH_xCl_{3-x}.

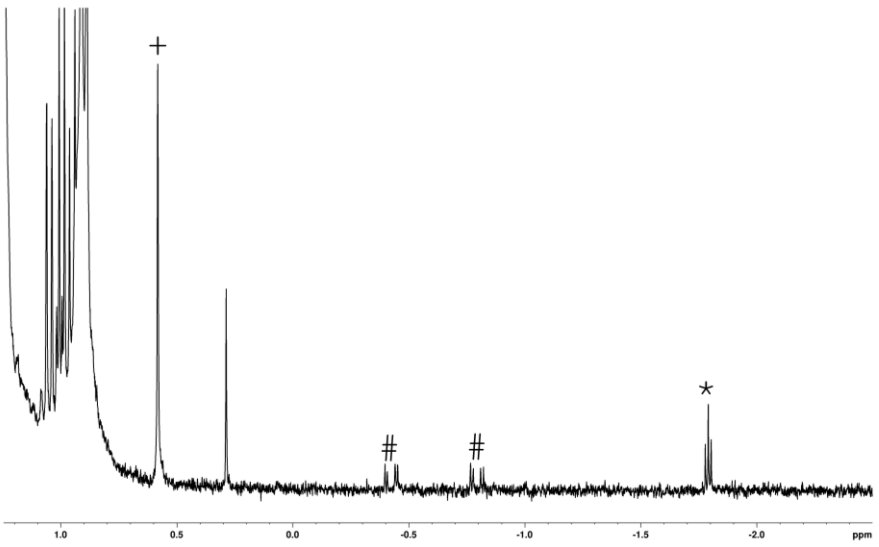

Figure 7.3: Section of the ^{1}H NMR spectrum in C_6D_6 of the reaction mixture of IDipp·$GaCl_3$ with K(18c6)SbH_2 (4 eq.; * = IDipp·GaH_2SbH_2, # = IDipp·$GaH(SbH_2)_2$, + = presumably IDipp·$Ga(SbH_2)_3$).

7.3 Conclusion

In summary, by using K(18c6)SbH_2 it was possible to synthesize the unprecedented ethylene analogue IDipp·GaH_2SbH_2 (**3**) and characterize it by NMR spectroscopy, LIFDI-MS, IR spectroscopy and single crystal X-ray structure determination. **3** remains inaccessible by methanolytic treatment of IDipp·$GaH_2Sb(SiMe_3)_2$ (**1**) obtained by the reaction of $KSb(SiMe_3)_2$ and IDipp·GaH_2(OTf), and thus the direct salt metathesis remains the most reliable way of obtaining **3**. Furthermore, the NMR spectroscopic elucidation of the reaction between IDipp·$GaCl_3$ and 4 eq. K(18c6)SbH_2 confirmed the existence of IDipp·$GaH(SbH_2)_2$ (**4**) during our investigations. Although stable at -30 °C, **3** still shows high lability and low nucleophilicity in chemical reactions, thus hampering investigations on its reactivity. Nevertheless, **3** represents the so far heaviest parent group 13/15 monomer known to this date and, so far, also the one of the rare examples of stable, isolable stibanes. Moreover, it could be shown that K(18c6)SbH_2 also reacts smoothly with iodoboranes to afford the parent stibanylboranes *D*·BH_2SbH_2 (**2a**: *D* = IDipp, **2b**: *D* = NMe_3). Future experiments will focus on further reactivity studies and possibly controlled decomposition towards thin layers.

7.4 References

[1] C. Elschenbroich, *Organometallchemie,* 6. Aufl., Teubner, Wiesbaden, **2008**.

[2] a) R. J. Baker, M. Brym, C. Jones, M. Waugh, *J. Organomet. Chem.* **2004**, *689*, 781–790; b) G. Balázs, H. J. Breunig, E. Lork, W. Offermann, *Organometallics* **2001**, *20*, 2666–2668; c) B. Twamley, C.-S. Hwang, N. J. Hardman, P. P. Power, *J. Organomet. Chem.* **2000**, *609*, 152–160.

[3] R. Waterman, T. D. Tilley, *Angew. Chem. Int. Ed.* **2006**, *45*, 2926–2929.

[4] K. Dollberg, S. Schneider, R.-M. Richter, T. Dunaj, C. von Hänisch, *Angew. Chem. Int. Ed.* **2022**, *61*, e202213098.

[5] a) K. Issleib, A. Balszuweit, *Z. Anorg. Allg. Chem.* **1975**, *418*, 158–166; b) A. L. Rheingold, P. Choudhury, M. F. El-shazly, *Synth. React. Inorg. Met.-Org. Chem.* **1978**, *8*, 453–465.

[6] a) A. C. Jones, P. O'Brien, *CVD of Compound Semiconductors: Precursor Synthesis Development and Applications*, VCH, Weinheim, **1996**; b) M. R. Leys, *Chemtronics* **1987**, *2*, 155–164; c) G. B. Stringfellow, *Rep. Prog. Phys.* **1982**, *45*, 469–525; d) S. Marchant, C. Y. Tang, A. J. Downs, T. M. Greene, H.-J. Himmel, S. Parsons, *Dalton Trans.* **2005**, 3281–3290; e) J. S. Foord, T. J. Whitaker, E. N. Downing, D. O'Hare, A. C. Jones, *Appl. Phys. Lett.* **1993**, *63*, 1270–1272; f) C. E. Housecroft, A. Sharpe, *Inorganic Chemistry,* 4. Aufl., Pearson, New York, **2012**.

[7] S. Schulz, *Adv. Organomet. Chem.* **2003**, *49*, 225–317.

[8] S. Schulz, *Coord. Chem. Rev.* **2001**, *215*, 1–37.

[9] E. Amberger, H. Boeters, *Angew. Chem. Int. Ed. Engl.* **1963**, *2*, 686.

[10] K. Dollberg, S. Schneider, C. von Hänisch, *Synlett* **2023**, *34*, 1777–1780.

[11] J. Du, K. Dollberg, J. A. Seed, A. J. Wooles, C. von Hänisch, S. T. Liddle, *Nat. Chem.* **2024**.

[12] a) J. Feld, D. W. N. Wilson, J. M. Goicoechea, *Angew. Chem. Int. Ed.* **2021**, *60*, 22057–22061; b) D. W. N. Wilson, J. Feld, J. M. Goicoechea, *Angew. Chem. Int. Ed.* **2020**, *132*, 21100–21104; c) A. Bücker, C. Wölper, G. Haberhauer, S. Schulz, *Chem. Comm.* **2022**, *58*, 9758–9761; d) C. Ganesamoorthy, C. Helling, C. Wölper, W. Frank, E. Bill, G. E. Cutsail, S. Schulz, *Nat. Comm.* **2018**, *9*, 87; e) S. Ghosh, E. Glöckler, C. Wölper, J. Linders, N. Janoszka, A. H. Gröschel, S. Schulz, *Eur. J. Inorg. Chem.* **2022**, *2022*; f) C. Helling, C. Ganesamoorthy, C. Wölper, S. Schulz, *Dalton Trans.* **2022**, *51*, 2050–2058; g) C. Helling, C. Wölper, Y. Schulte, G. E. Cutsail III, S. Schulz, *Inorg. Chem.* **2019**, *58*, 10323–10332; h) C. Helling, C. Wölper, S. Schulz, *J. Am. Chem. Soc.* **2018**, *140*, 5053–5056; i) C. Helling, C. Wölper, S. Schulz, *Eur. J. Inorg. Chem.* **2020**, *2020*, 4225–4235; j) C. Helling, C. Wölper, S. Schulz, *Dalton Trans.* **2020**, *49*, 11835–11842; k) J. Krüger, C. Ganesamoorthy, L. John, C. Wölper, S. Schulz, *Chem. Eur. J.* **2018**, *24*, 9157–9164; l) J. Krüger, C. Wölper, G. Haberhauer, S. Schulz, *Inorg. Chem.* **2022**, *61*, 597–604; m) J. Krüger, C. Wölper, S. Schulz, *Angew. Chem. Int. Ed.* **2021**, *60*, 3572–3575; n) B. Li, B. L. Geoghegan, H. M. Weinert, C. Wölper, G. E. Cutsail, S. Schulz, *Chem. Comm.* **2022**, *58*, 4372–4375; o) J. Schoening, L.

John, C. Wölper, S. Schulz, *Dalton Trans.* **2019**, *48*, 17729–17734; p) B. Li, C. Wölper, G. Haberhauer, S. Schulz, *Angew. Chem. Int. Ed.* **2021**, *133*, 2014–2019; q) M. K. Sharma, P. Dhawan, C. Helling, C. Wölper, S. Schulz, *Chem. Eur. J.* **2022**, *28*, e202200444; r) M. K. Sharma, C. Wölper, G. Haberhauer, S. Schulz, *Angew. Chem. Int. Ed.* **2021**, *60*, 6784–6790; s) M. K. Sharma, C. Wölper, S. Schulz, *Dalton Trans.* **2022**, *51*, 1612–1616; t) H. M. Weinert, C. Wölper, S. Schulz, *Chem. Sci.* **2022**, *13*, 3775–3786; u) A. D. Phillips in *Organometallic Chemistry* (Hrsg.: I. J. S. Fairlamb, J. M. Lynam), Royal Society of Chemistry, Cambridge, **2014**, S. 72–147.

[13] A. Y. Timoshkin, G. Frenking, *Inorg. Chem.* **2003**, *42*, 60–69.

[14] a) J. Braese, A. Schinabeck, M. Bodensteiner, H. Yersin, A. Y. Timoshkin, M. Scheer, *Chem. Eur. J.* **2018**, *24*, 10073–10077; b) M. Elsayed Moussa, J. Braese, C. Marquardt, M. Seidl, M. Scheer, *Eur. J. Inorg. Chem.* **2020**, *26*, 2501–2505; c) M. Elsayed Moussa, C. Marquardt, O. Hegen, M. Seidl, M. Scheer, *New J. Chem.* **2021**, *45*, 14916–14919; d) K.-C. Schwan, A. Adolf, M. Bodensteiner, M. Zabel, M. Scheer, *Z. Anorg. Allg. Chem.* **2008**, *634*, 1383–1387; e) R. Szlosek, M. T. Ackermann, C. Marquardt, M. Seidl, A. Y. Timoshkin, M. Scheer, *Chem. Eur. J.* **2023**, *29*, e202202911.

[15] a) M. T. Ackermann, M. Seidl, F. Wen, M. J. Ferguson, A. Y. Timoshkin, E. Rivard, M. Scheer, *Chem. Eur. J.* **2022**, *28*, e20210370; b) M. T. Ackermann, M. Seidl, R. Grande, Y. Zhou, M. J. Ferguson, A. Y. Timoshkin, E. Rivard, M. Scheer, *Chem. Sci.* **2023**, *14*, 2313–2317; c) C. Marquardt, G. Balázs, J. Baumann, A. V. Virovets, M. Scheer, *Chem. Eur. J.* **2017**, *23*, 11423–11429; d) C. Marquardt, C. Thoms, A. Stauber, G. Balázs, M. Bodensteiner, M. Scheer, *Angew. Chem. Int. Ed.* **2014**, *53*, 3727–3730; e) C. Marquardt, A. Adolf, A. Stauber, M. Bodensteiner, A. V. Virovets, A. Y. Timoshkin, M. Scheer, *Chem. Eur. J.* **2013**, *19*, 11887–11891; f) C. Marquardt, T. Kahoun, J. Baumann, A. Y. Timoshkin, M. Scheer, *Z. Anorg. Allg. Chem.* **2017**, *643*, 1326–1330; g) K.-C. Schwan, A. Y. Timoshkin, M. Zabel, M. Scheer, *Chem. Eur. J.* **2006**, *12*, 4900–4908.

[16] a) M. Elsayed Moussa, T. Kahoun, M. T. Ackermann, M. Seidl, M. Bodensteiner, A. Y. Timoshkin, M. Scheer, *Organometallics* **2022**, *41*, 1572–1578; b) C. Marquardt, T. Kahoun, A. Stauber, G. Balázs, M. Bodensteiner, A. Y. Timoshkin, M. Scheer, *Angew. Chem. Int. Ed.* **2016**, *55*, 14828–14832.

[17] a) O. Hegen, C. Marquardt, A. Y. Timoshkin, M. Scheer, *Angew. Chem. Int. Ed.* **2017**, *56*, 12783–12787; b) O. Hegen, A. V. Virovets, A. Y. Timoshkin, M. Scheer, *Eur. J. Inorg. Chem.* **2018**, *24*, 16521-16525; c) F. Lehnfeld, M. Seidl, A. Y. Timoshkin, M. Scheer, *Eur. J. Inorg. Chem.* **2022**, *3*, e202100930; d) C. Marquardt, O. Hegen, T. Kahoun, M. Scheer, *Chem. Eur. J.* **2017**, *23*, 4397–4404.

[18] a) M. Bodensteiner, A. Y. Timoshkin, E. V. Peresypkina, U. Vogel, M. Scheer, *Chem. Eur. J.* **2013**, *19*, 957–963; b) M. Bodensteiner, U. Vogel, A. Y. Timoshkin, M. Scheer, *Angew. Chem. Int. Ed.* **2009**, *48*, 4629–4633; c) J. Braese, F. Lehnfeld, V. T. Annibale, T. Oswald, R. Beckhaus, I. Manners, M. Scheer, *Chem. Eur. J.* **2023**, *29*, e202301741; d) A. V. Butlak, I. V. Kazakov, A. Stauber, O. Hegen, M. Scheer, A. V. Pomogaeva, A. Y. Timoshkin, *Eur. J. Inorg. Chem.* **2019**, *2019*, 3885–3891; e) C. Marquardt, T. Jurca, K.-C. Schwan, A. Stauber, A. V. Virovets, G. R. Whittell, I. Manners, M. Scheer, *Angew. Chem. Int. Ed.* **2015**, *54*, 13782–13786; f) C. Thoms, C. Marquardt, A. Y. Timoshkin, M. Bodensteiner, M. Scheer, *Angew. Chem. Int. Ed.* **2013**, *52*, 5150–5154.

[19] C. Marquardt, O. Hegen, M. Hautmann, G. Balázs, M. Bodensteiner, A. V. Virovets, A. Y. Timoshkin, M. Scheer, *Angew. Chem. Int. Ed.* **2015**, *54*, 13122–13125.

[20] National InstituteRelease 22, May 2022, NIST Standard Reference Database 101, Internet: https://cccbdb.nist.gov/vibscalejust.asp of Standards and Technology, Computational Chemistry Comparison and Benchmark DataBase.

[21] S. Schneider, S. Ivlev, C. von Hänisch, *Chem. Comm.* **2021**, *57*, 3781–3784.

7.5 Supporting Information

7.5.1 General Information

7.5.1.1 Working Techniques

All working steps were carried out under argon inert gas atmosphere using standard Schlenk and glovebox techniques. All reactions were conducted under exclusion of light. Glassware was dried in an oven at 170 °C and pre-conditioned in high vacuum (< 10^{-3} mbar, 650 °C) shortly before use. The protective gas was cleansed from traces of H_2O and O_2 by passing it through a BASF R 3-11 ($CuO/MgSiO_3$) catalyst, concentrated H_2SO_4, Orange Gel and Sicapent® supported on pumice stone. Prior to use, solvents were purified using an MBraun SPS-800 solvent purification system, degassed by freeze-pump-thaw cycles and stored over molecular sieves for at least 48 hours. C_6D_6 was dried over Na/K, distilled, degassed at room temperature, and stored over molecular sieves (4 Å). Elemental Analysis (CHNS) was performed by the in-house facility. Mass spectra were recorded on a Jeol AccuTOF GCX mass spectrometer (LIFDI-MS) mass spectrometer by the in-house facility or on a Waters Micromass LCT ESI-TOF mass spectrometer at the Scheer group.

$IDippGaH_2(OTf)$,[1] $KSb(SiMe_3)_2$,[2] $K(18c6)SbH_2$[3] were prepared according to literature procedures. $BH_3{\cdot}SMe_2$ was purchased from ABCR and used as received.

7.5.1.2 Spectroscopic Analysis

All NMR spectra were recorded on a BRUKER Avance 400 (frequencies: ^1H: 400.13 MHz, ^{11}B: 128.43) or Avance 300 (^1H: 300.13 MHz) spectrometers. Substances of reference are $Si(CH_3)_4$ (^1H) and $BF_3{\cdot}Et_2O$ (^{11}B). Chemical shifts δ are presented in ppm referring to the external standards and coupling constants J are given in Hz without consideration of absolute signs. IR spectra were recorded in the solid state using a ThermoFisher Nicolet iS5 FT-IR spectrometer on a Diamond ATR Crystal.

7.5.2 Experimental Details

7.5.2.1 Synthesis of IDipp·$GaH_2Sb(SiMe_3)_2$ (1)

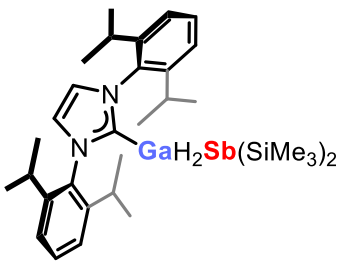

IDipp·$GaH_2(OTf)$ (122 mg, 0.20 mmol) was suspended in diethylether and suspension cooled to -80 °C. Then, solid $KSb(SiMe_3)_2$ (92 mg, 0.30 mmol) was added in one portion. The mixture was allowed to warm up to room temperature upon stirring overnight in the cooling bath. Subsequently, all volatiles were removed in vacuo and the product extracted with toluene and filtered through a P3 glass frit covered with Celite. The solvent was then removed *in vacuo*, yielding IDipp·$GaH_2Sb(SiMe_3)_2$ as a brown powder (19 mg, 13%).

^{1}H NMR (400.30 MHz, C_6D_6, 298 K): 7.22 (t, 2 H, 2 × aryl-C_{para}H, $^3J_{HH}$ = 7.74 Hz), 7.10 (d, 4 H, 4 × aryl-$C_{meta}H$, $^3J_{HH}$ = 7.74 Hz), 6.43 (s, 2 H, NC*H*C*H*N), 4.15 (s, broad, 2 H, GaH_2), 2.44 (sep, 4 H, 4 × ^{i}Pr-C*H*, $^3J_{HH}$ = 6.91 Hz), 1.45 (d, 12 H, 4 × ^{i}Pr-CH_3, $^3J_{HH}$ = 6.91 Hz), 0.97 (d, 12 H, 4 × ^{i}Pr-CH_3, $^3J_{HH}$ = 6.91 Hz). 0.42 (s, 18 H, $^2J_{HSi}$ = 6.72 Hz, 2 × Si(CH_3)$_3$).

LIFDI-MS (*m/z*): 728.35 ([M]$^+$, 100%).

Elemental Analysis ($C_{33}H_{56}GaSbN_2Si_2$) **[%]:** could not be performed, as it was not possible to completely separate **1a** from IDipp-H_2.

7.5.2.2 Synthesis of IDipp·BH_2SbH_2 (2a)

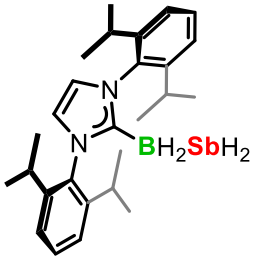

IDipp·BH_2I (265 mg, 0.5 mmol) was dissolved in tetrahydrofuran and the clear solution cooled to -80 °C. Then, solid K(18c6)SbH_2 (320 mg, 0.75 mmol) was added in one portion. The mixture was stirred at room temperature for two hours. Subsequently, all volatiles were removed *in vacuo* and the product extracted with toluene and filtered through a P3 glass frit covered with Celite. After removing the solvent *in vacuo*, IDipp·BH_2SbH_2 could be isolated as a brown powder (204 mg, 78%).

^{1}H NMR (400.30 MHz, C_6D_6, 298 K):): -0.81 (t, 2 H, SbH_2, $^3J_{HH}$ = 7.06 Hz), 1.06 (d, 12 H, 4×^{i}Pr-CH_3, $^3J_{HH}$ = 6.93 Hz), 1.30 (d, 12 H, superimposed, 4×^{i}Pr-CH_3, $^3J_{HH}$ = 6.93 Hz), 2.06 (q, very broad, 2 H (superimposed), BH_2, $^1J_{HB}$ ≈ 100 Hz), 2.86 (sep, 4 H, 4 × ^{i}Pr-C*H*, $^3J_{HH}$ = 6.93 Hz), 4.54 (s, broad, 2 H, GaH_2), 6.43 (s, 2 H, NC*H*C*H*N), 7.14 (d, 4 H, 4×aryl-$C_{meta}H$, $^3J_{HH}$ = 7.55 Hz), 7.23 (t, 2 H, 2×aryl-C_{para}H, $^3J_{HH}$ = 7.55 Hz).

^{11}B{^{1}H} NMR (128.43 MHz, C_6D_6, 298 K): -39.8 (s, broad).

^{11}B NMR (128.43 MHz, C_6D_6, 298 K): -39.8 (t, broad, $^1J_{HB}$ = 100 Hz).

IR (ATR) *ν* (cm^{-1}): 2960 (s), 2924 (m), 2865 (m), 2408 (w, B-H), 1834 (s, Sb-H), 1593 (w), 1558 (w), 1463 (s).

LIFDI-MS (*m/z*): 389.3 ([IDipp-H]$^+$, 23%), 401.3 ([IDipp·BH_2]$^+$, 100%). The mass spectrum does not show a molecular ion peak due to sample decomposition during the ionization process.

Elemental Analysis ($C_{27}H_{40}BSbN_2$) **[%]:** could not be performed, as it was not possible to separate the product from IDipp·BH_3.

7.5.2.3 Synthesis of Me_3N·BH_2SbH_2 (2b)

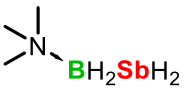

Me_3N·BH_2I (40 mg, 0.20 mmol) was suspended in tetrahydrofuran and cooled to -80 °C. Then, solid K(18c6)SbH_2 (128 mg, 0.30 mmol) was added. After stirring for two hours in the cooling bath, all volatiles were condensed into a separate Schlenk tube, affording Me_3N·BH_2SbH_2 alongside Me_3N·BH_3 as identified by multinuclear NMR spectroscopy.

^{1}H NMR (400.30 MHz, THF/C_6D_6-cap., 298 K):): -1.11 (t, SbH_2, $^3J_{HH}$ = 5.43 Hz). Other signals could not unambiguously be detected due to overlap with the solvent signals.

^{11}B{^{1}H} NMR (128.43 MHz, THF/C_6D_6-cap., 298 K): -8.07 (s, broad).

^{11}B NMR (128.43 MHz, THF/C_6D_6-cap., 298 K): -8.07 (t, broad, $^1J_{HB}$ = 113 Hz).

7.5.2.4 Synthesis of IDipp·GaH_2SbH_2 (3)

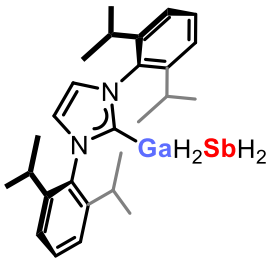

IDipp·GaH_2(OTf) (122 mg, 0.2 mmol) was dissolved in tetrahydrofuran and the clear solution cooled to -80 °C. Then, solid K(18c6)SbH_2 (128 mg, 0.3 mmol) was added in one portion. The mixture was allowed to warm up to room temperature upon stirring overnight in the cooling bath. Subsequently, all volatiles were removed *in vacuo* and the product extracted with *n*-hexane and filtered through a P3 glass frit covered with Celite. The solvent was then removed *in vacuo*, yielding IDipp·GaH_2SbH_2 as an off-white powder (28 mg, 24%). Storing a saturated solution of IDipp·GaH_2SbH_2 in *n*-hexane at -30 °C overnight yielded crystals suitable for single crystals X-ray structure determination.

^{1}H NMR (400.30 MHz, C_6D_6, 298 K): -1.81 (t, 2 H, SbH_2, 4×^{i}Pr-CH, $^3J_{HH}$ = 3.94 Hz), 0.98 (d, 12 H, 4×^{i}Pr-CH_3, $^3J_{HH}$ = 6.99 Hz), 1.30 (d, 12 H, superimposed, 4×^{i}Pr-CH_3, $^3J_{HH}$ = 6.99 Hz), 3.88 (sep, 4 H, 4 × ^{i}Pr-CH, $^3J_{HH}$ = 6.99 Hz), 4.54 (s, broad, 2 H, GaH_2), 6.45 (s, 2 H, superimposed, NCHCHN), 7.09 (d, 4 H, superimposed, 4×aryl-C$_{meta}H$, $^3J_{HH}$ = 7.82 Hz), 7.23 (t, 2 H, superimposed, 2×aryl-C$_{para}$H, $^3J_{HH}$ = 7.82 Hz). *Note: integration in the NMR spectrum is not quite fitting due to signal overlap.*

IR (ATR) *ν* (cm^{-1}): 2960 (m), 2926 (w), 2867 (w), 1803 (m, Sb-H), 1597 (w), 1463 (w).

LIFDI-MS (*m/z*): 389.4 ([IDipp-H]$^+$, 22%), 459.3 ([IDipp·GaH_2]$^+$, 100%), 583.24 ([M-H]$^+$, 5%).

Elemental Analysis ($C_{27}H_{40}GaN_2Sb$) **[%]:** could not be performed as **1b** could only be obtained within an inseparable mixture with IDipp·GaH_3 and IDipp-H_2.

7.5.2.5 Attempted methanolysis of IDipp·$GaH_2Sb(SiMe_3)_2$

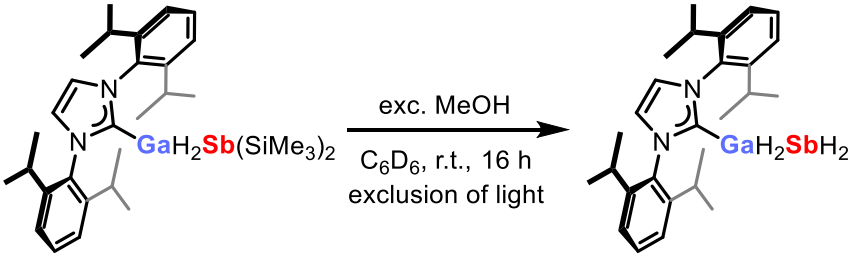

An NMR tube was charged with IDipp·$GaH_2Sb(SiMe_3)_2$ (15 mg, 0.02 mmol) and the solids dissolved in C_6D_6. Then, dry MeOH (0.03 mL, exc.) was added *via* syringe and the sample submitted to repeated NMR spectroscopic investigation. The ^{1}H NMR spectrum of the mixture showed exclusively unreacted starting material as well as decomposition products (cf. Figure S 7.9).

7.5.2.6 Reaction of IDipp·$GaCl_3$ with exc. K(18c6)SbH_2

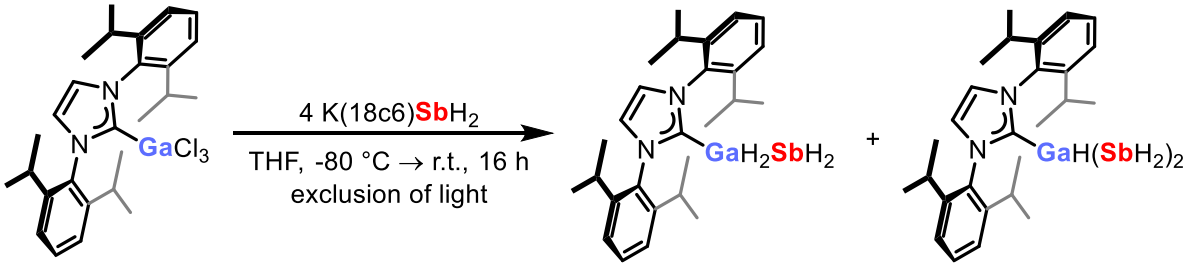

A Schlenk tube was charged with IDipp·$GaCl_3$ (56 mg, 0.1 mmol) and the solids dissolved in tetrahydrofuran. After cooling the solution to -80 °C, solid K(18c6)SbH_2 (171 mg, 0.4 mmol) was added. The mixture was stirred overnight in the cooling bath, resulting in a brown suspension. After removing all volatiles *in vacuo*, the products were extracted with *n*-hexane and separated by filtration through a P4 glass frit covered with Celite. The solvent was removed *in vacuo* and the residue submitted to NMR spectroscopic investigation (Figure S 7.10).

7.5.3 NMR Data

7.5.3.1 IDipp·$GaH_2Sb(SiMe_3)_2$

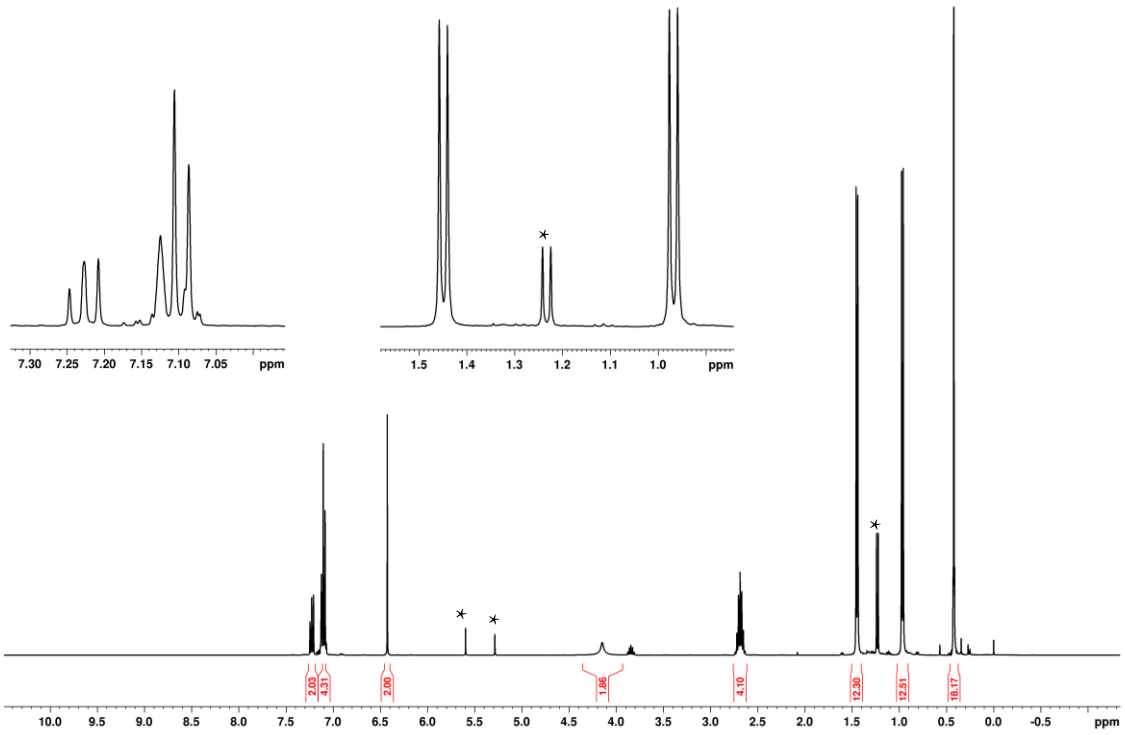

Figure S 7.1: ^1H NMR spectrum of IDipp $GaH_2Sb(SiMe_3)_2$ (C_6D_6, 298 K, * = IDipp-H_2).

7.5.3.2 IDipp·GaH_2SbH_2

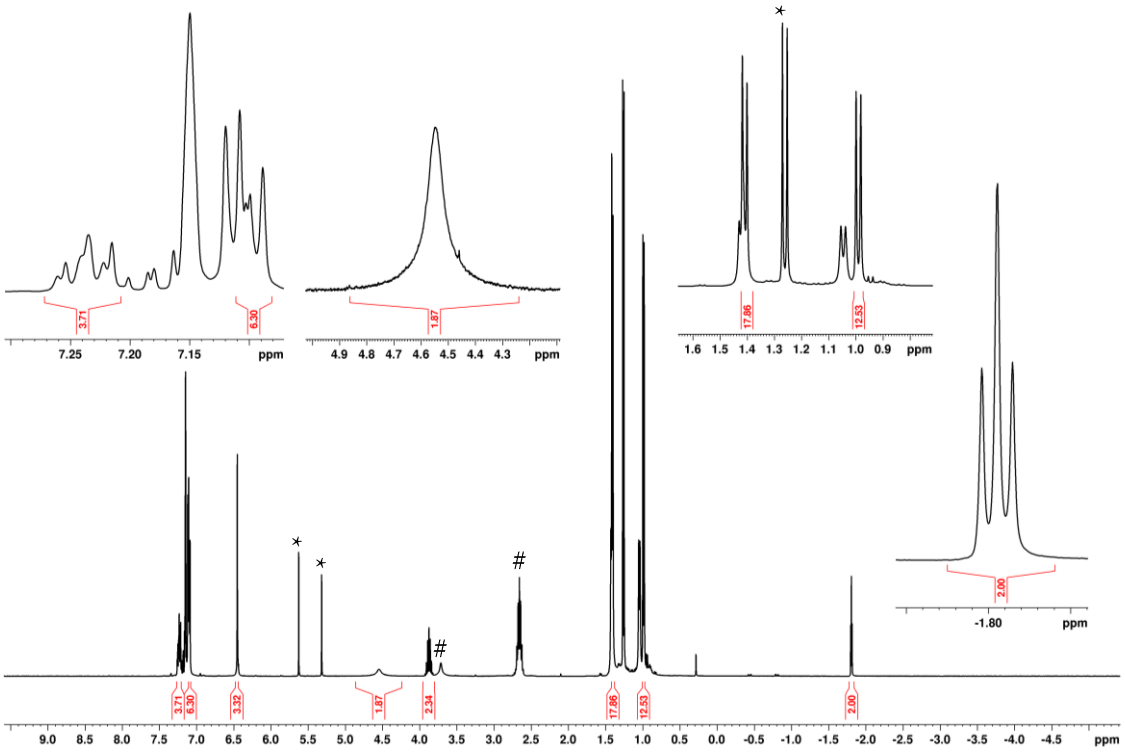

Figure S 7.2: ^1H NMR spectrum of IDipp·GaH_2SbH_2 (C_6D_6, 298 K; * = IDipp-H_2, # = IDipp·GaH_3).

7.5.3.3 IDipp·BH_2SbH_2

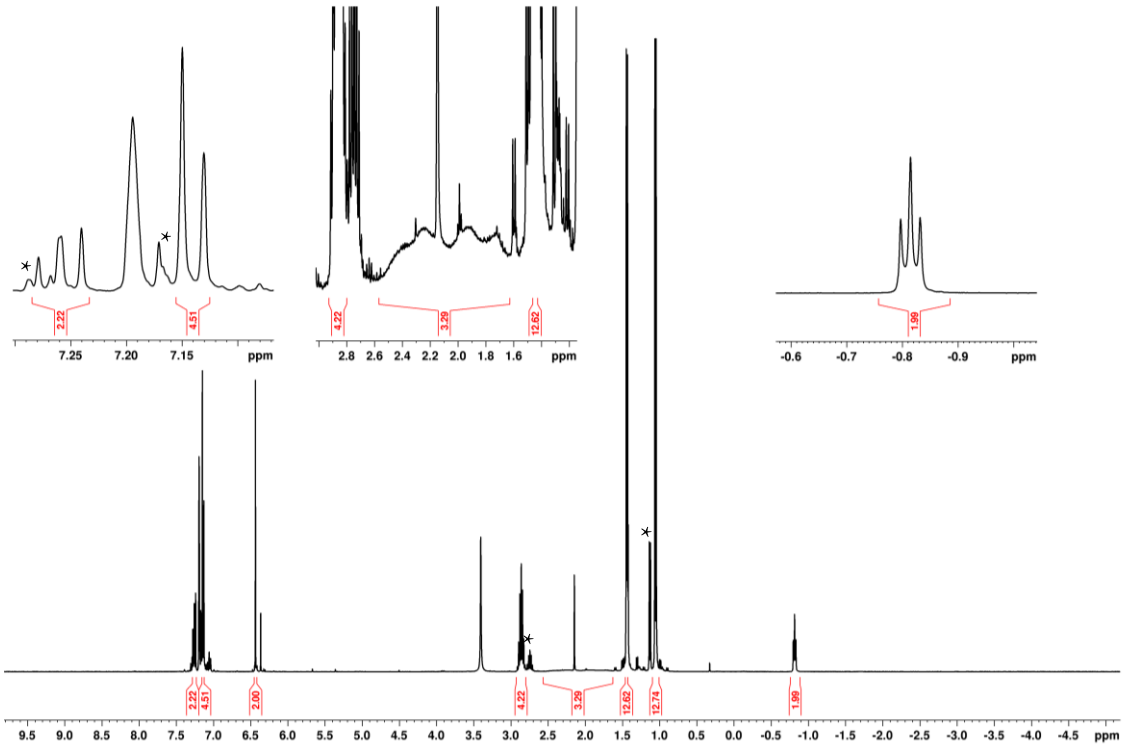

Figure S 7.3: ^{1}H NMR spectrum of IDipp·BH_2SbH_2 (C_6D_6, 298 K; * = IDipp·BH_3).

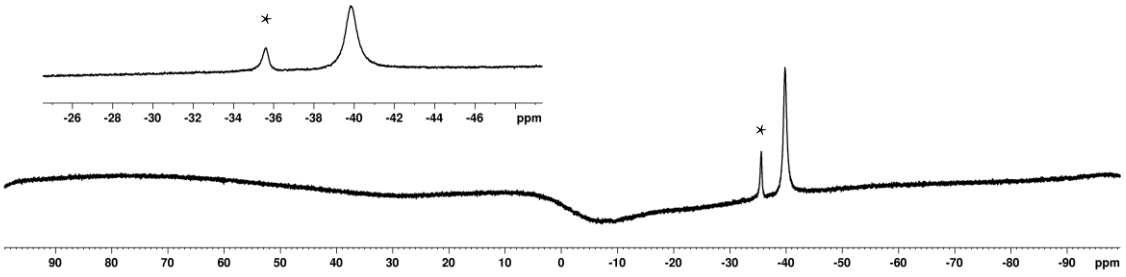

Figure S 7.4: $^{11}B\{^{1}H\}$ NMR spectrum of IDipp·BH_2SbH_2 (C_6D_6, 298 K; * = IDipp·BH_3).

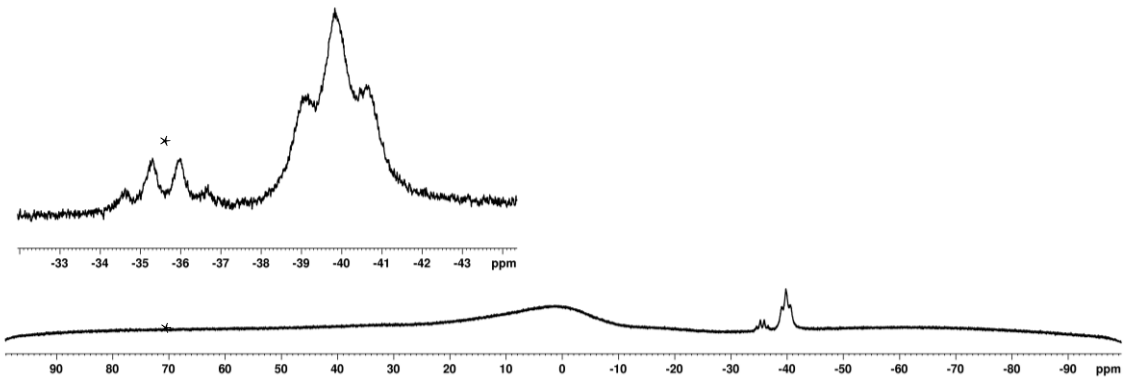

Figure S 7.5: ^{11}B NMR spectrum of IDipp·BH_2SbH_2 (C_6D_6, 298 K; * = IDipp·BH_3)

7.5.3.4 $Me_3N{\cdot}BH_2SbH_2$

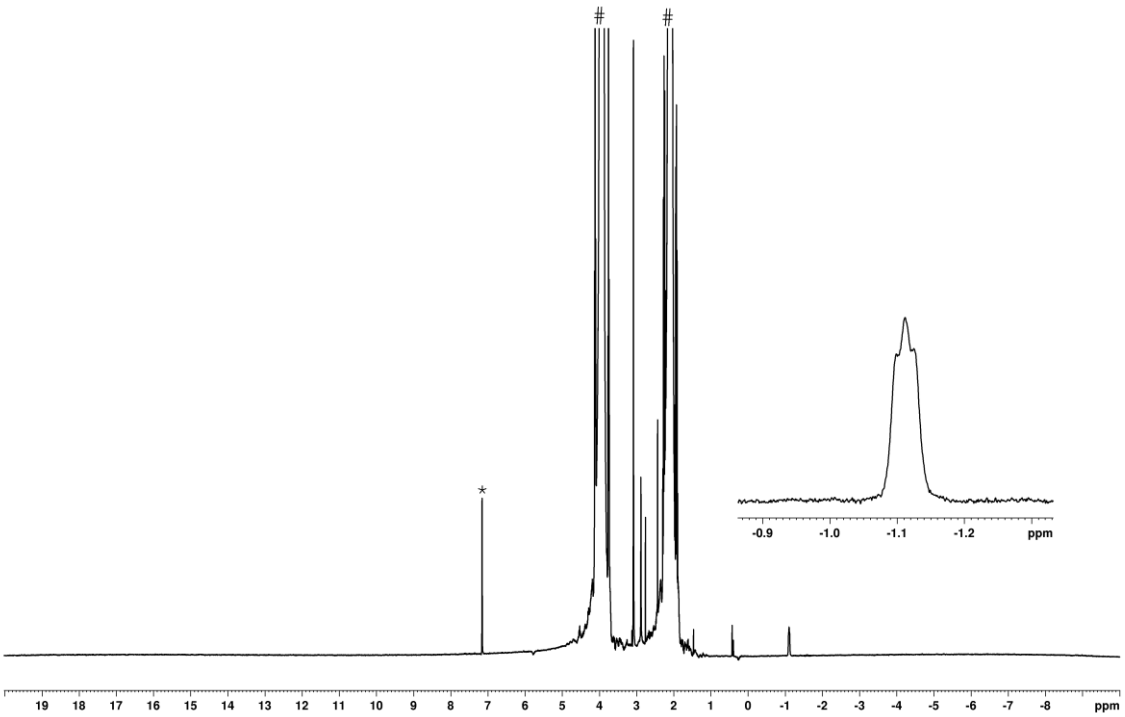

Figure S 7.6: ^1H NMR spectrum of a solution of $Me_3N{\cdot}BH_2SbH_2$ (C_6D_6-cap/THF, 298 K; * = C_6D_6, # = solvent).

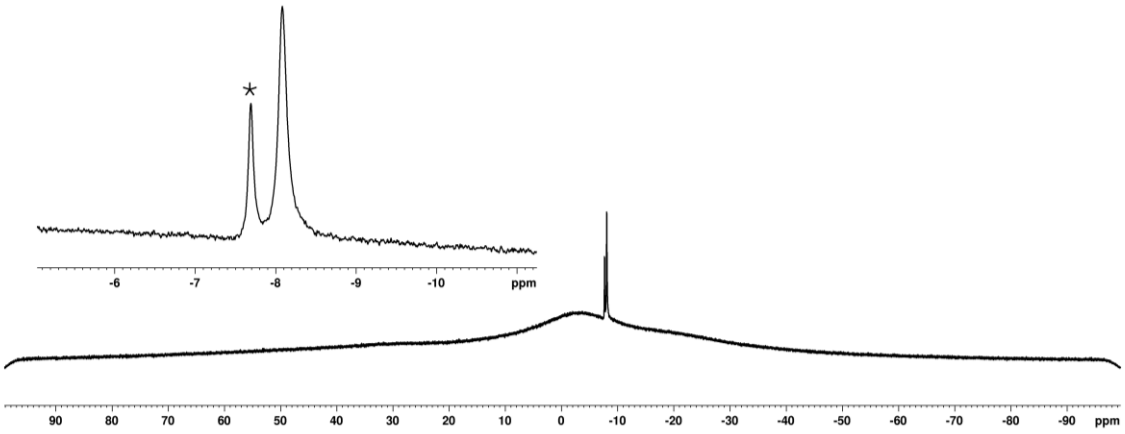

Figure S 7.7: $^{11}B\{^1H\}$ NMR spectrum of a solution of $Me_3N{\cdot}BH_2SbH_2$ (C_6D_6-cap/THF, 298 K; * = $Me_3N{\cdot}BH_3$).

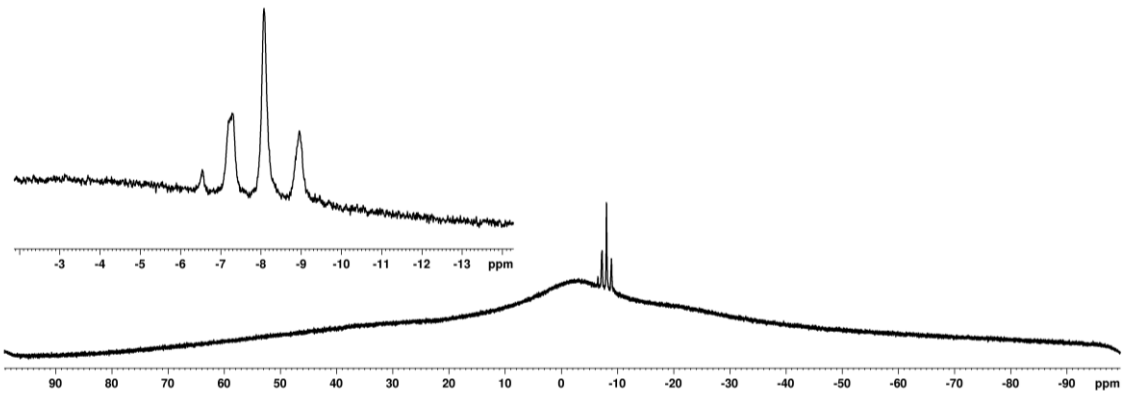

Figure S 7.8: $^{11}B\{^1H\}$ NMR spectrum of a solution of $Me_3N{\cdot}BH_2SbH_2$ (C_6D_6-cap/THF, 298 K).

7.5.3.5 Attempted methanolysis of IDipp·$GaH_2Sb(SiMe_3)_2$

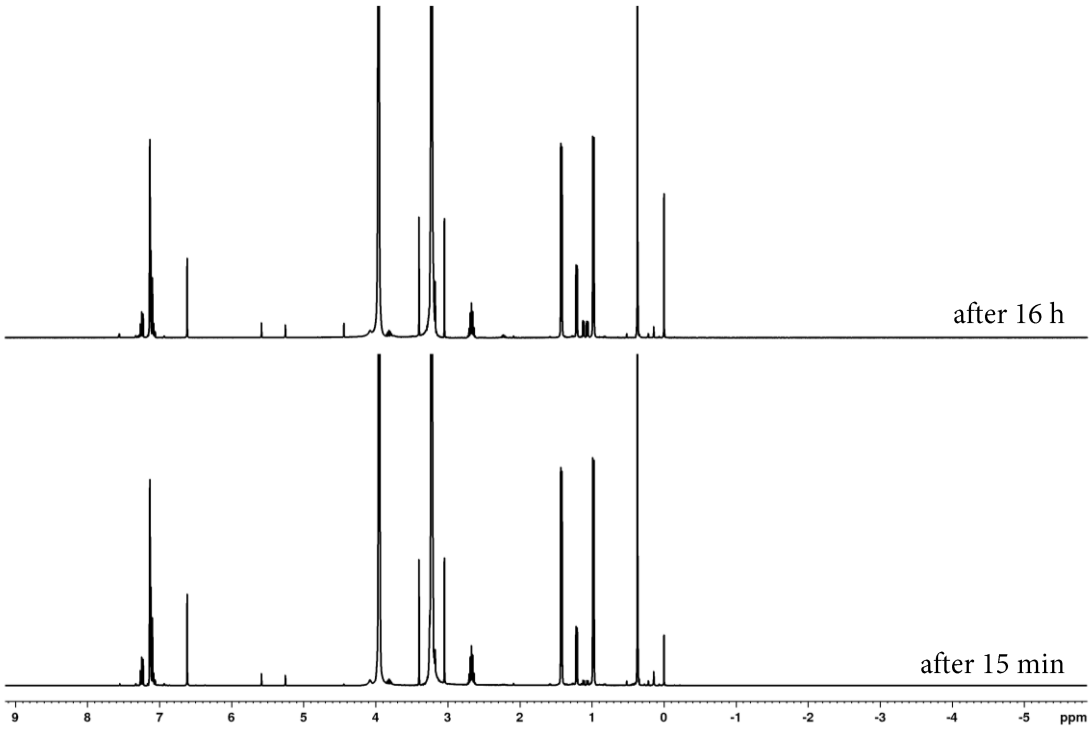

Figure S 7.9: ^{1}H NMR spectrum of the addition of MeOH to IDipp·$GaH_2Sb(SiMe_3)_2$ after 15 min (bottom) and 16 hours (top; C_6D_6, 298 K).

7.5.3.6 Reaction of IDipp·$GaCl_3$ with $K(18c6)SbH_2$ (4 eq.)

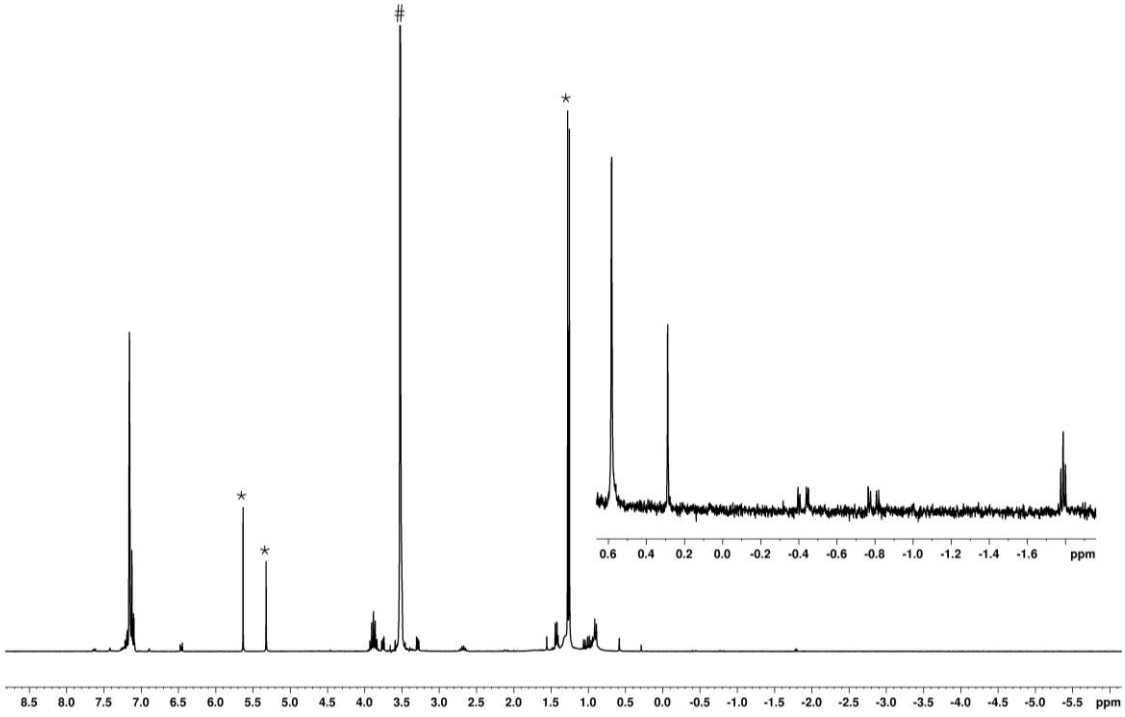

Figure S 7.10: ^{1}H NMR spectrum of the reaction mixture of $K(18c6)SbH_2$ (4 eq.) with IDipp·$GaCl_3$ (C_6D_6, 298 K; * = IDipp-H_2, # = 18c6).

7.5.4 Crystallographic Data

Single Crystal X-ray structure determination: Single-crystal X-ray diffraction data sets were collected using a XtaLAB Synergy R, DW system diffractometer (**1b**) equipped with a HyPix-Arc 150 detector operating at T = 123.01(10) K. Crystals were selected under mineral oil or perfluorinated Fomblin. Data reduction, scaling and absorption corrections were performed using CrysAlisPro (Rigaku, V1.171.41.90a, 2020). A gaussian absorption correction was performed using CrysAlisPro 1.171.41.90a (Rigaku Oxford Diffraction, 2020). Numerical absorption correction based on gaussian integration over a multifaceted crystal model. Empirical absorption correction using spherical harmonics, implemented in SCALE3 ABSPACK scaling algorithm. Using Olex2,[4] the structures were solved with ShelXT[5] and a least-squares refinement on $F2$ was carried out with ShelXL.[6] All non-hydrogen atoms were refined anisotropically. The hydrogen atoms at the carbon atoms have been located in idealized positions and refined isotropically according to the riding model. Figures were created with Olex2.

IDipp·GaH_2SbH_2 (1b)

1b crystallized by cooling a saturated solution of **1b** in *n*-hexane to -30 °C overnight as clear colourless block-shaped crystals in the triclinic space group *P*-1. **1b** co-crystallizes alongside IDipp·GaH_3. The structure of **1b** in the solid state is shown in Figure S 7.11.

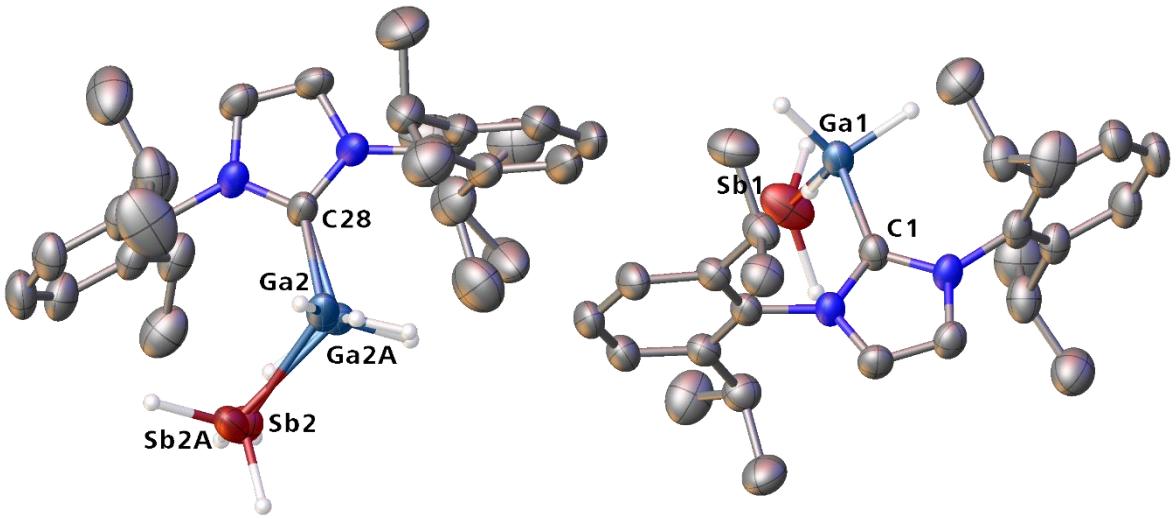

Figure S 7.11: Molecular structure of **1a** in the solid state. Anisotropic displacement ellipsoids are shown at 50% probability level. Hydrogen atoms bound to carbon are omitted for clarity. Selected bond lengths [Å] and angles [°]: C1-Ga1 2.0345(4), Ga-Sb1 2.6776(8), C28-Ga2 2.071(6), C28-Ga2A 2.057(6), Ga2-Sb2 2.615(5), Ga2A-Sb2A 2.604(7), C1-Ga1-Sb1 109.28(13), C28-Ga2-Sb2 110.0(2), C28-Ga2A-Sb2A 113.0(2).

The asymmetric unit contains two molecules of **1b** and two molecules of IDipp·GaH_3 with the individual components being disorder by position as well as occupation within the unit cell. The disorders were treated by applying SIMU, SADI and DANG restraints. Hydrogen atoms bound to Ga and Sb were fixed into idealized positions by applying DFIX and DANG restraints. One isopropyl arm displays positional disorder and was refined with SADI and SIMU restraints.

Table S 7.1: Crystallographic data for compounds **1b**.

Compound	**1b**
Formula	$C_{54}H_{79.58}Ga_2N_4Sb_{1.58}$
Dcalc	1.310
m/mm^{-1}	7.273
Formula Weight	1116.60
Colour	clear colourless
Shape	block-shaped
Size/mm^3	0.58×0.13×0.08
T/K	123.00(10)
Crystal System	triclinic
Space Group	P-1
a/Å	10.6757(3)
b/Å	14.3712(3)
c/Å	20.2914(4)
a/°	72.892(2)
b/°	75.891(2)
g/°	75.406(2)
V/Å^3	2830.56(12)
Z	2
Z'	1
Wavelength/Å	1.54184
Radiation type	Cu K_a
Q_{min}/°	2.318
Q_{max}/°	75.514
Measured Refl's.	57725
Indep't Refl's	11466
Refl's I≥2 s(I)	10355
R_{int}	0.0453
Parameters	644
Restraints	63
Largest Peak	0.783
Deepest Hole	-1.849
GooF	1.083
wR_2 (all data)	0.1543
wR_2	0.1517
R_1 (all data)	0.0655
R_1	0.0610

7.5.5 Computational Details

7.5.5.1 General Information

Quantum chemical calculations were performed using Gaussian 16.[7] Images of calculated structures were generated with ChemCraft.[8] Molecular geometries were optimized at the B3LYP/def2-TZVP[9] level of theory employing the D3(BJ) dispersion correction by Grimme and co-workers.[10] Subsequent analytical frequency analysis was carried out in order to determine the nature of stationary points on the potential energy surface. *Natural Bond Orbital* analysis (NBO 7.0)[11] was carried out at the same level of theory and used to describe electronic densities and to calculate the *Wiberg Bond Index* matrix (WBI) as well as the Natural Charges.

7.5.5.2 Cartesian coordinates and thermodynamic data of optimized structures

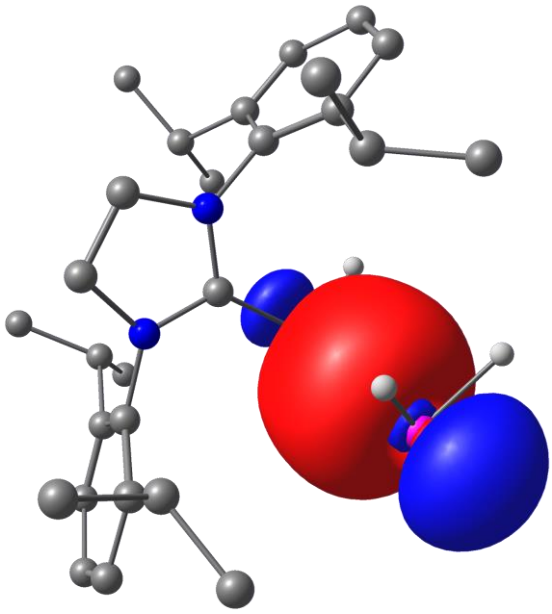

Figure S 7.12: Depiction of the NBO of the σ(Ga-Sb) bond orbital. Individual contributions: Ga (35%, 0.23 s, 0.77 p), Sb (65%, 0.13 s, 0.87 p).

IDipp·GaH_2PH_2							
15	0.4731670	-2.6316420	2.0178260	6	-3.1174240	-1.1558840	-0.3212950
31	-0.0413500	-0.2863870	1.9834690	6	3.2329140	-0.7746480	-0.5234880
7	1.0318610	0.2200820	-0.8972890	6	-3.1064290	1.3045040	-0.2788580
7	-1.1029050	0.0913700	-0.9184570	6	1.8792120	2.7796290	0.1045870
6	-0.0390010	0.0613860	-0.0850610	1	0.8586940	2.4013000	0.1223550
6	2.3934850	0.3416530	-0.4465330	6	2.7451880	-2.1131190	-1.0465680
6	0.6412990	0.3582410	-2.2193700	1	1.6627670	-2.1464930	-0.9154620
1	1.3515230	0.5098600	-3.0097690	6	-2.3937110	-2.4677680	-0.5542960
6	-0.7068250	0.2717190	-2.2337050	1	-1.3266990	-2.2889440	-0.4243210
1	-1.4166110	0.3325530	-3.0374460	6	2.8149680	1.5867470	0.0367750
6	-2.4787140	0.0747400	-0.4978720	6	5.0080490	0.6185760	0.3477570
				1	6.0383970	0.7271050	0.6615580

6	4.5556600	-0.6053500	-0.1181090
1	5.2356620	-1.4443470	-0.1577980
6	-2.3642400	2.6230940	-0.3976140
1	-1.4029180	2.4312950	-0.8733310
6	-4.4541460	-1.1272190	0.0681500
1	-4.9845010	-2.0566120	0.2197060
6	-4.4422290	1.2783900	0.1151570
1	-4.9606390	2.2084530	0.3052140
6	4.1456040	1.7010460	0.4287800
1	4.5095260	2.6444370	0.8106220
6	2.0290320	3.6544480	-1.1479880
1	1.8415960	3.0836780	-2.0586580
1	3.0379620	4.0673250	-1.2127520
1	1.3229720	4.4869830	-1.1188300
6	-5.1102470	0.0758090	0.2816070
1	-6.1474740	0.0747050	0.5914330
6	3.0506440	-2.2569340	-2.5450590
1	4.1283320	-2.2279950	-2.7196680
1	2.5966630	-1.4593040	-3.1328430
1	2.6715320	-3.2093830	-2.9203880
6	-2.6128890	-2.9592250	-1.9919640
1	-3.6719600	-3.1520900	-2.1769650
1	-2.0625480	-3.8859840	-2.1652430
1	-2.2738530	-2.2231800	-2.7226140
6	-3.1050020	3.6307250	-1.2820560
1	-2.5068290	4.5359390	-1.4017860
1	-4.0608880	3.9241140	-0.8452110
1	-3.3024940	3.2184050	-2.2730810
6	2.0583480	3.6051720	1.3799800
1	3.0231080	4.1150750	1.4046370
1	1.9744280	2.9724200	2.2629680
1	1.2834670	4.3718580	1.4340140
6	3.3260060	-3.3009330	-0.2750280
1	3.1802720	-3.1887120	0.7976230
1	4.3927800	-3.4256910	-0.4708180
1	2.8247970	-4.2191450	-0.5831980
6	-2.0749420	3.2050530	0.9925420
1	-3.0037290	3.4542250	1.5096300
1	-1.4806890	4.1171510	0.9059280
1	-1.5316250	2.4931920	1.6133120
6	-2.7803150	-3.5464700	0.4592380
1	-2.1166730	-4.4048470	0.3532650
1	-3.8041320	-3.8958890	0.3114400
1	-2.6868550	-3.1767720	1.4801700
1	-1.5328150	0.0054080	2.4206690
1	1.0914660	0.6610260	2.5490780
1	-0.3131140	-2.9193700	3.1631910
1	1.6769680	-2.5195830	2.7604000

IDipp·GaH_2AsH_2

33	-1.1552920	-2.4427330	-1.8223870
31	0.0871250	-0.2682520	-1.8297120
7	-0.8846950	0.5312170	1.0208280
7	1.2321930	0.2132590	1.0044210
6	0.1451890	0.2121400	0.2002390
6	-2.2440900	0.7335380	0.5899270
6	-0.4428140	0.7358100	2.3179790
1	-1.1115300	1.0135810	3.1098530
6	0.8920040	0.5294350	2.3093450
1	1.6279490	0.5882080	3.0894220
6	2.5905970	0.0555830	0.5575360
6	3.1412830	-1.2266190	0.5041910
6	-3.1928990	-0.2603800	0.8549250
6	3.2932830	1.2087500	0.1940630
6	-1.5104320	3.0135700	-0.2931920
1	-0.5429040	2.5240180	-0.3830200
6	-2.8429350	-1.5393270	1.5940430
1	-1.7696650	-1.7031340	1.4856430
6	2.3427960	-2.4578130	0.8834000
1	1.2888730	-2.1815960	0.8971050
6	-2.5539960	1.9346600	-0.0639900
6	-4.8399620	1.1582200	-0.2046160
1	-5.8612260	1.3228100	-0.5235840
6	-4.5023450	-0.0179150	0.4433380
1	-5.2625560	-0.7648010	0.6221520
6	2.6480190	2.5824340	0.1905080
1	1.6805550	2.5060900	0.6856720
6	4.4666500	-1.3334070	0.0895530
1	4.9296200	-2.3088140	0.0330970
6	4.6123890	1.0474940	-0.2219700
1	5.1865480	1.9136580	-0.5221850
6	-3.8758700	2.1226730	-0.4561880
1	-4.1547580	3.0308650	-0.9706130
6	-1.4459460	3.9626560	0.9126730
1	-1.2313510	3.4251950	1.8370120
1	-2.3951780	4.4870870	1.0415300
1	-0.6625500	4.7095070	0.7674270
6	5.1949420	-0.2094940	-0.2683550
1	6.2212070	-0.3152790	-0.5960610
6	-3.1567880	-1.4020990	3.0921390
1	-4.2269230	-1.2455270	3.2425680
1	-2.6326720	-0.5628450	3.5482920
1	-2.8689960	-2.3100250	3.6256990
6	2.7178550	-2.9351970	2.2926110
1	3.7695310	-3.2261800	2.3374040

1	2.1147060	-3.7999450	2.5760870
1	2.5570210	-2.1507160	3.0344850
6	3.4693270	3.6106040	0.9748680
1	2.9404490	4.5648230	1.0113380
1	4.4399550	3.7898340	0.5096050
1	3.6455630	3.2785450	1.9994510
6	-1.7207720	3.7942080	-1.5904050
1	-2.6167750	4.4167710	-1.5539400
1	-1.7960520	3.1177770	-2.4411350
1	-0.8712780	4.4580280	-1.7593200
6	-3.5526220	-2.7727730	1.0275050
1	-3.4094630	-2.8579850	-0.0484460
1	-4.6238920	-2.7489770	1.2357010
1	-3.1508570	-3.6736770	1.4940880
6	2.3873020	3.0540200	-1.2461910
1	3.3257850	3.1834000	-1.7888450
1	1.8646830	4.0128300	-1.2413720
1	1.7825910	2.3335080	-1.7962540
6	2.4896500	-3.5822210	-0.1448310
1	1.8118830	-4.4009800	0.1007490
1	3.5039860	-3.9852310	-0.1613840
1	2.2399320	-3.2284050	-1.1443650
1	1.6046930	-0.3713620	-2.2584150
1	-0.7717610	0.8755030	-2.5085020
1	-0.5519230	-2.9352010	-0.5057550
1	-0.0908380	-3.1779710	-2.6327270

IDipp·GaH_2SbH_2

51	-0.9734620	-2.7624240	-1.4276060
31	0.0384950	-0.2723630	-1.7001940
7	-0.8212570	0.8910220	1.0412070
7	1.2805090	0.4764800	1.0342990
6	0.1764130	0.4217500	0.2532830
6	-2.1770560	1.1176370	0.6120720
6	-0.3431810	1.2428580	2.2933960
1	-0.9836090	1.6497560	3.0524510
6	0.9812540	0.9791320	2.2899310
1	1.7353620	1.1117190	3.0427820
6	2.6228890	0.2228880	0.5806640
6	3.1534010	-1.0637390	0.7146550
6	-3.1646620	0.1981700	0.9795680
6	3.3323920	1.2914270	0.0244790
6	-1.3531060	3.2579920	-0.5079260
1	-0.4114050	2.7133660	-0.5352120
6	-2.8498360	-1.0395530	1.7986850
1	-1.7892630	-1.2609370	1.6729630
6	2.3537800	-2.1896270	1.3403650
1	1.2969940	-1.9686290	1.1894020
6	-2.4451200	2.2704270	-0.1390950
6	-4.7714210	1.6103600	-0.1484100
1	-5.7929380	1.8033250	-0.4501690
6	-4.4728380	0.4737150	0.5841230
1	-5.2636120	-0.2153190	0.8447450
6	2.7271230	2.6732250	-0.1407550
1	1.7414930	2.6717680	0.3225190
6	4.4583130	-1.2620090	0.2708320
1	4.9040090	-2.2432740	0.3491480
6	4.6325280	1.0395170	-0.4074230
1	5.2097290	1.8384080	-0.8534060
6	-3.7674250	2.4964620	-0.5087930
1	-4.0150640	3.3709760	-1.0931810
6	-1.2292660	4.3520890	0.5622340
1	-1.0311360	3.9291100	1.5477600
1	-2.1501400	4.9356710	0.6256970
1	-0.4118790	5.0335320	0.3171950
6	5.1899190	-0.2226900	-0.2845390
1	6.1998860	-0.4014830	-0.6306680
6	-3.1098400	-0.7878400	3.2914830
1	-4.1641970	-0.5606390	3.4624180
1	-2.5236510	0.0478250	3.6731680
1	-2.8544440	-1.6734950	3.8764030
6	2.6099060	-2.2585300	2.8529930
1	3.6611750	-2.4746500	3.0557060
1	2.0070490	-3.0486120	3.3048970
1	2.3600210	-1.3194710	3.3482140
6	3.5552170	3.7441950	0.5778780
1	3.0661400	4.7168190	0.4966620
1	4.5521480	3.8367490	0.1436970
1	3.6728990	3.5085520	1.6370380
6	-1.5390240	3.8687520	-1.8973980
1	-2.4050820	4.5317360	-1.9410650
1	-1.6556530	3.0890340	-2.6494070
1	-0.6615440	4.4633970	-2.1567410
6	-3.6288560	-2.2726760	1.3324110
1	-3.5337210	-2.4270700	0.2583370
1	-4.6904300	-2.1921440	1.5732990
1	-3.2452710	-3.1627790	1.8325100
6	2.5310140	3.0175040	-1.6222230
1	3.4899180	3.0762330	-2.1407870
1	2.0349970	3.9850910	-1.7228520
1	1.9263210	2.2626820	-2.1238710
6	2.6173940	-3.5461940	0.6857990
1	1.9111060	-4.2827430	1.0707030
1	3.6237480	-3.9119340	0.8991380
1	2.4861240	-3.4933960	-0.3940840

1	1.5144930	-0.2602890	-2.2586020
1	-1.0126000	0.6790090	-2.4021900
1	-0.6057330	-2.8885570	0.2482300
1	0.5067170	-3.5264260	-1.8371920

IDipp·BH_2AsH_2

33	-0.5328650	-1.9795760	-2.1636420
7	-0.9773850	0.2963460	0.8004320
7	1.1650910	0.1040140	0.8051330
6	0.0896700	0.1180200	-0.0261870
6	2.5394860	0.1052060	0.3867140
6	-2.3426510	0.4445540	0.3776370
6	0.7756800	0.2656140	2.1263590
1	1.4905910	0.2879820	2.9272130
6	-0.5669320	0.3919560	2.1215640
1	-1.2665440	0.5456020	2.9202800
6	3.2091290	-1.1126750	0.2509660
6	-3.2312980	-0.6185180	0.5775600
6	-2.7304670	1.6657700	-0.1890500
6	-2.8024640	-1.9216880	1.2272470
1	-1.7167240	-1.9866650	1.1538420
6	3.1492450	1.3422140	0.1490160
6	-4.5562570	-0.4266040	0.1904190
1	-5.2708970	-1.2262930	0.3260650
6	-4.9681070	0.7678370	-0.3770620
1	-6.0003520	0.8937630	-0.6779780
6	-4.0638830	1.8022630	-0.5648140
1	-4.4001890	2.7283160	-1.0092530
6	-1.7595370	2.8232200	-0.3350020
1	-0.7546470	2.4111880	-0.3755690
6	2.5210640	-2.4367760	0.5128330
1	1.4494110	-2.2504210	0.5666440
6	4.5497610	-1.0685030	-0.1261610
1	5.1009770	-1.9918440	-0.2410510
6	2.3873410	2.6507570	0.2512450
1	1.4242830	2.4468880	0.7181070
6	5.1830420	0.1406930	-0.3667660
1	6.2233790	0.1539820	-0.6657700
6	4.4880780	1.3332070	-0.2338180
1	4.9908080	2.2692910	-0.4366590
6	-3.1870660	-1.9375520	2.7146460
1	-2.7614250	-1.0937640	3.2574220
1	-2.8364330	-2.8560990	3.1893450
1	-4.2719840	-1.8902130	2.8293730
6	-3.3766750	-3.1575290	0.5280800
1	-4.4581520	-3.2278170	0.6575820
1	-2.9380260	-4.0600210	0.9572520
1	-3.1563670	-3.1469590	-0.5375250
6	2.7422660	-3.4372960	-0.6248790
1	2.4490430	-3.0113380	-1.5841610
1	2.1413370	-4.3322920	-0.4571520
1	3.7869530	-3.7466010	-0.6926140
6	2.9599280	-3.0201790	1.8622930
1	4.0319900	-3.2283630	1.8675100
1	2.4326970	-3.9546960	2.0640720
1	2.7507250	-2.3283200	2.6802710
6	2.1046530	3.2238760	-1.1438340
1	3.0359630	3.4731280	-1.6566630
1	1.5093060	4.1360610	-1.0645680
1	1.5614080	2.5066260	-1.7580110
6	-1.9548580	3.6117350	-1.6304140
1	-1.9213270	2.9501550	-2.4958740
1	-1.1575270	4.3491490	-1.7364180
1	-2.9027130	4.1529240	-1.6433260
5	0.1200210	-0.0448250	-1.5891970
6	-1.8376700	3.7428640	0.8918030
1	-2.8298740	4.1907200	0.9794040
1	-1.1065120	4.5500520	0.8104460
1	-1.6345540	3.1946160	1.8130350
6	3.1051690	3.6713150	1.1401160
1	3.2985570	3.2643520	2.1341450
1	2.4926290	4.5679650	1.2516120
1	4.0610760	3.9773150	0.7118000
1	1.2455590	0.0819280	-1.9894190
1	-0.6565760	0.7012760	-2.1265830
1	-0.3116360	-2.7471290	-0.8555220
1	-2.0136310	-1.7895190	-1.8471610

IDipp·BH_2PH_2

15	0.5722480	-1.7540560	2.5110960
7	1.0218550	0.0616090	-0.6415560
7	-1.1220170	-0.0845760	-0.6560820
6	-0.0571710	-0.0122420	0.1834860
6	-2.5023190	-0.0263630	-0.2606140
6	2.3855880	0.2178410	-0.2165230
6	-0.7150280	-0.0619870	-1.9817950
1	-1.4206860	-0.1042750	-2.7900580
6	0.6301040	0.0359290	-1.9713430
1	1.3428540	0.0943040	-2.7712560
6	-3.1833760	-1.2160320	0.0040160
6	3.2449860	-0.8847900	-0.2880340
6	2.8009980	1.4812890	0.2224870
6	2.7835160	-2.2387080	-0.7962250
1	1.6949240	-2.2594420	-0.7416770
6	-3.1049970	1.2339610	-0.1759780
6	4.5703230	-0.6891200	0.0950420

1	5.2631500	-1.5180980	0.0564380
6	5.0098990	0.5480260	0.5370420
1	6.0418770	0.6772430	0.8374020
6	4.1336920	1.6207710	0.6005860
1	4.4911740	2.5795920	0.9486430
6	1.8616110	2.6732110	0.2316140
1	0.8441630	2.2947320	0.2866300
6	-2.5013590	-2.5665480	-0.0771990
1	-1.4305250	-2.3944530	-0.1770370
6	-4.5299710	-1.1203890	0.3491870
1	-5.0901500	-2.0210060	0.5610920
6	-2.3250690	2.5163360	-0.4014940
1	-1.3713190	2.2570150	-0.8604310
6	-5.1574570	0.1121350	0.4366870
1	-6.2027280	0.1663430	0.7129660
6	-4.4501670	1.2773050	0.1810230
1	-4.9484660	2.2333720	0.2674660
6	3.1949140	-2.4347150	-2.2632690
1	2.8083760	-1.6433020	-2.9054560
1	2.8214460	-3.3888390	-2.6403080
1	4.2827100	-2.4355220	-2.3585890
6	3.2998620	-3.4045230	0.0525840
1	4.3816930	-3.5190620	-0.0352490
1	2.8452770	-4.3368450	-0.2869900
1	3.0519970	-3.2694230	1.1036810
6	-2.7047520	-3.3853740	1.2010860
1	-2.3842850	-2.8255850	2.0792110
1	-2.1181290	-4.3042470	1.1547050
1	-3.7511220	-3.6655350	1.3360900
6	-2.9652080	-3.3400340	-1.3180480
1	-4.0368590	-3.5452300	-1.2734960
1	-2.4415020	-4.2952870	-1.3904560
1	-2.7716960	-2.7754910	-2.2321180
6	-2.0155830	3.1990340	0.9378960
1	-2.9372610	3.5067250	1.4362660
1	-1.4054330	4.0904240	0.7765090
1	-1.4788570	2.5263950	1.6059350
6	2.0524620	3.5780730	1.4494650
1	1.9790670	3.0048940	2.3734810
1	1.2763120	4.3449960	1.4637980
1	3.0163040	4.0901840	1.4337130
5	-0.1063390	-0.0340790	1.7626460
6	1.9944020	3.4663590	-1.0761430
1	3.0012940	3.8758130	-1.1820730
1	1.2862960	4.2976450	-1.0915850
1	1.7954390	2.8366620	-1.9447770
6	-3.0360330	3.4719900	-1.3643890
1	-3.2563450	2.9852880	-2.3160670
1	-2.4054650	4.3405720	-1.5630760
1	-3.9765390	3.8381580	-0.9495270
1	-1.2469020	0.1083820	2.1201850
1	0.6164280	0.8161570	2.2230230
1	0.2664220	-2.6712830	1.4659090
1	1.9329700	-1.6585800	2.1240070

IDipp·BH_2SbH_2

51	0.4824980	-2.2510210	-1.8136440
5	-0.1268110	-0.0338720	-1.4477440
7	-1.1973980	0.3385880	0.9032080
7	0.9437940	0.5784950	0.8900120
6	-0.1129790	0.2817500	0.0810330
6	-2.5657590	0.2766060	0.4719440
6	-0.8220460	0.6613890	2.1987480
1	-1.5437960	0.7620300	2.9872400
6	0.5170890	0.8163350	2.1882870
1	1.2046330	1.0780900	2.9689360
6	2.3079080	0.7195720	0.4609620
6	3.2300860	-0.2794590	0.7945780
6	-3.2284550	-0.9533790	0.4878100
6	2.6619350	1.8769350	-0.2463730
6	-2.4341410	2.7889950	0.0259570
1	-1.4577540	2.6425240	0.4857520
6	-2.5397720	-2.2206280	0.9517290
1	-1.4656190	-2.0413920	0.9334180
6	2.8417240	-1.5069300	1.5986570
1	1.7613170	-1.6286480	1.5177440
6	-3.1785040	1.4672030	0.0653380
6	-5.1954690	0.1933180	-0.3278320
1	-6.2296230	0.1592200	-0.6460460
6	-4.5613200	-0.9692050	0.0825820
1	-5.1065100	-1.9029880	0.0807210
6	1.6550030	2.9750960	-0.5364960
1	0.6662840	2.5241980	-0.5497920
6	4.5520500	-0.0897770	0.3951080
1	5.2913210	-0.8421500	0.6313920
6	3.9935650	2.0129470	-0.6272200
1	4.3036780	2.8897690	-1.1777900
6	-4.5098610	1.3981570	-0.3375660
1	-5.0136890	2.2966760	-0.6680850
6	-3.1506860	3.8728100	0.8385330
1	-3.3070820	3.5546730	1.8707180
1	-4.1253900	4.1161270	0.4121940
1	-2.5567180	4.7886630	0.8499620
6	4.9298930	1.0402360	-0.3101470
1	5.9604780	1.1643240	-0.6175010

6	-2.9306240	-2.5497180	2.3988880
1	-4.0037750	-2.7362870	2.4787940
1	-2.6834480	-1.7287210	3.0740050
1	-2.4040080	-3.4420080	2.7430420
6	3.1977400	-1.3189210	3.0815420
1	4.2774770	-1.2105850	3.2037870
1	2.8767390	-2.1855810	3.6628190
1	2.7275870	-0.4336960	3.5090270
6	1.6734920	4.0262130	0.5823310
1	0.9163240	4.7917040	0.3990370
1	2.6471760	4.5177400	0.6376040
1	1.4693250	3.5755380	1.5546960
6	-2.1927580	3.2407870	-1.4198960
1	-3.1380950	3.4295300	-1.9327160
1	-1.6484560	2.4808030	-1.9792560
1	-1.6123390	4.1657320	-1.4346830
6	-2.8095440	-3.4085080	0.0251070
1	-2.5746340	-3.1624610	-1.0106680
1	-3.8519520	-3.7293760	0.0699420
1	-2.1890810	-4.2566410	0.3174230
6	1.8500340	3.6243830	-1.9069970
1	2.7774840	4.1972720	-1.9626360
1	1.0288790	4.3144070	-2.1076260
1	1.8600100	2.8717720	-2.6953600
6	3.4817660	-2.7948280	1.0722040
1	3.0606730	-3.6550010	1.5953500
1	4.5602330	-2.8063400	1.2405500
1	3.2960420	-2.9205310	0.0075760
1	0.7175930	0.5689080	-2.0513500
1	-1.2317590	0.0771440	-1.8994000
1	0.4079730	-2.8302800	-0.1911960
1	2.1721960	-1.9905810	-1.6584870

IDipp·$GaH_2Sb(SiMe_3)_2$

51	-2.1739200	-0.1728690	0.5034280
31	-0.0945760	0.0352000	-1.1461290
7	2.1557740	1.2751820	0.5727910
7	2.3638830	-0.8542310	0.5403040
6	1.5675430	0.1491570	0.1053290
6	1.6271840	2.6030660	0.4045450
6	3.3176610	0.9822280	1.2672170
1	3.9304070	1.7494420	1.7010510
6	3.4487040	-0.3620610	1.2478270
1	4.1971640	-1.0094690	1.6638310
6	2.1041030	-2.2570620	0.3537040
6	1.4384090	-2.9449920	1.3747930
6	0.7730210	3.1060710	1.3938690
6	2.5442850	-2.8695920	-0.8238980
6	2.9161350	2.7449310	-1.7873750
1	2.9245470	1.6621970	-1.6635390
6	0.4222720	2.3016150	2.6332110
1	0.4911740	1.2447910	2.3713320
6	0.9643330	-2.2472860	2.6374130
1	0.8844500	-1.1819120	2.4186760
6	1.9846040	3.3225100	-0.7392330
6	0.6273440	5.1403440	0.0935700
1	0.2276090	6.1384980	-0.0314200
6	0.2813240	4.3965010	1.2113340
1	-0.3902740	4.8196960	1.9440620
6	3.2679790	-2.0895240	-1.9046720
1	3.0039250	-1.0389060	-1.7870000
6	1.2496610	-4.3140240	1.2011010
1	0.7373160	-4.8824220	1.9642410
6	2.3217770	-4.2381910	-0.9511860
1	2.6407470	-4.7490030	-1.8486920
6	1.4691710	4.6095040	-0.8707860
1	1.7179050	5.1970050	-1.7434380
6	4.3490560	3.2506040	-1.5687110
1	4.7127590	3.0015630	-0.5705390
1	4.3965150	4.3358770	-1.6800620
1	5.0280240	2.8046690	-2.2982680
6	1.6885630	-4.9536790	0.0534120
1	1.5212110	-6.0162120	-0.0670000
6	1.4256480	2.5806980	3.7627540
1	1.3831280	3.6310800	4.0585980
1	2.4496170	2.3582850	3.4646560
1	1.1902430	1.9719390	4.6379470
6	1.9852110	-2.4237510	3.7709110
1	2.0900210	-3.4791960	4.0309020
1	1.6604280	-1.8851970	4.6632820
1	2.9702610	-2.0499130	3.4911370
6	4.7881770	-2.2129660	-1.7280130
1	5.3102640	-1.6203930	-2.4819690
1	5.1054040	-3.2525780	-1.8335730
1	5.1060080	-1.8644740	-0.7441970
6	2.4443420	3.0236040	-3.2163870
1	2.4978710	4.0857190	-3.4620950
1	1.4182560	2.6847630	-3.3551650
1	3.0810580	2.4927410	-3.9264970
6	-1.0041250	2.5431770	3.1282110
1	-1.7307070	2.3905390	2.3339400
1	-1.1291520	3.5511720	3.5283390
1	-1.2374430	1.8402510	3.9288700
6	2.8424320	-2.4954040	-3.3169710
1	3.1586340	-3.5110110	-3.5618320

1	3.3016480	-1.8268600	-4.0472950
1	1.7604660	-2.4295540	-3.4267370
6	-0.4219780	-2.7093140	3.0911470
1	-0.7525810	-2.1045670	3.9368450
1	-0.4172990	-3.7519270	3.4138590
1	-1.1563040	-2.5922590	2.2967380
1	0.1512890	-1.2753690	-1.9999580
1	-0.0330330	1.4072920	-1.9294970
14	-3.6044280	1.5710740	-0.7462880
14	-3.1011410	-2.2431870	-0.7174980
6	-3.4324470	-1.9785850	-2.5533740
1	-3.7334050	-2.9232000	-3.0166020
1	-4.2321870	-1.2560760	-2.7192720
1	-2.5372690	-1.6207330	-3.0638850
6	-1.8534720	-3.6449630	-0.5563370
1	-0.8842450	-3.3550720	-0.9627920
1	-1.7072980	-3.9366390	0.4840020
1	-2.2032520	-4.5249410	-1.1044100
6	-4.7118030	-2.7775380	0.1078470
1	-5.1127500	-3.6779770	-0.3670520
1	-4.5510410	-2.9949490	1.1657370
1	-5.4698760	-1.9952590	0.0428750
6	-3.2992640	3.2512650	0.0562550
1	-3.8794450	4.0249640	-0.4554400
1	-3.5889070	3.2539790	1.1085490
1	-2.2449460	3.5266300	-0.0057290
6	-5.4305460	1.1356870	-0.5524570
1	-5.6731620	0.2092710	-1.0759070
1	-5.6955100	1.0036290	0.4982590
1	-6.0613030	1.9282220	-0.9658270
6	-3.2210840	1.7564650	-2.5795360
1	-3.3788500	0.8277310	-3.1265290
1	-3.8678740	2.5237000	-3.0165200
1	-2.1833970	2.0574930	-2.7255410
MeOH			
6	-0.0465770	0.6639080	0.0000000
1	-1.0892040	0.9786020	0.0000000
1	0.4384260	1.0778710	0.8911160
1	0.4384260	1.0778710	-0.8911160
8	-0.0465770	-0.7565150	0.0000000
1	0.8644310	-1.0656720	0.0000000
$MeOSiMe_3$			
6	-2.3334160	-0.0009350	-0.2360670
1	-3.0835960	-0.0055900	-1.0276480
1	-2.4885540	-0.8862020	0.3902440
1	-2.4890610	0.8912000	0.3802940
8	-1.0543670	-0.0038900	-0.8354900
14	0.3761370	0.0000340	0.0030400
6	0.4905430	-1.5237660	1.0898040
1	-0.2947680	-1.5392840	1.8492500
1	0.4026720	-2.4371240	0.4973430
1	1.4498820	-1.5551110	1.6124920
6	0.4915240	1.5345520	1.0745410
1	1.4511550	1.5706040	1.5964110
1	0.4038700	2.4420360	0.4730850
1	-0.2933970	1.5580050	1.8341770
6	1.7092590	-0.0069130	-1.3015390
1	1.6281180	-0.8914970	-1.9363810
1	1.6326700	0.8740630	-1.9418900
1	2.7025760	-0.0080950	-0.8464500

7.5.6 References

[1] R. Szlosek, M. Seidl, G. Balázs, M. Scheer, *Chem. Eur. J.* **2023**, *29*, e202301752.

[2] C. Marquardt, O. Hegen, M. Hautmann, G. Balázs, M. Bodensteiner, A. V. Virovets, A. Y. Timoshkin, M. Scheer, *Angew. Chem. Int. Ed.* **2015**, *54*, 13122–13125.

[3] K. Dollberg, S. Schneider, R.-M. Richter, T. Dunaj, C. von Hänisch, *Angew. Chem. Int. Ed.* **2022**, *61*, e202213098.

[4] O. V. Dolomanov, L. J. Bourhis, R. J. Gildea, J. A. K. Howard, H. Puschmann, *J. Appl. Crystallogr.* **2009**, *42*, 339–341.

[5] G. M. Sheldrick, *Acta Cryst. A* **2015**, *71*, 3–8.

[6] G. M. Sheldrick, *Acta Cryst. C* **2015**, *71*, 3–8.

[7] Gaussian 16, Revision C.01, M. J. Frisch, G. W. Trucks, H. B. Schlegel, G. E. Scuseria, M. A. Robb, J. R. Cheeseman, G. Scalmani, V. Barone, G. A. Petersson, H. Nakatsuji, X. Li, M. Caricato, A. V. Marenich, J. Bloino, B. G. Janesko, R. Gomperts, B. Mennucci, H. P. Hratchian, J. V. Ortiz, A. F. Izmaylov, J. L. Sonnenberg, D. Williams-Young, F. Ding, F. Lipparini, F. Egidi, J. Goings, B. Peng, A. Petrone, T. Henderson, D. Ranasinghe, V. G. Zakrzewski, J. Gao, N. Rega, G. Zheng, W. Liang, M. Hada, M. Ehara, K. Toyota, R. Fukuda, J. Hasegawa, M. Ishida, T. Nakajima, Y. Honda, O. Kitao, H. Nakai, T. Vreven, K. Throssell, J. A. Montgomery, Jr., J. E. Peralta, F. Ogliaro, M. J. Bearpark, J. J. Heyd, E. N. Brothers, K. N. Kudin, V. N. Staroverov, T. A. Keith, R. Kobayashi, J. Normand, K. Raghavachari, A. P. Rendell, J. C. Burant, S. S. Iyengar,

J. Tomasi, M. Cossi, J. M. Millam, M. Klene, C. Adamo, R. Cammi, J. W. Ochterski, R. L. Martin, K. Morokuma, O. Farkas, J. B. Foresman, and D. J. Fox, Gaussian, Inc., Wallingford CT, 2016.

[8] "Chemcraft - graphical software for visualization of quantum chemistry computations. https://www.chemcraftprog.com".

[9] a) A. D. Becke, *J. Chem. Phys.* **1993**, *98*, 5648–5652; b) C. Lee, W. Yang, R. G. Parr, *Phys. Rev. B* **1988**, *37*, 785–789; c) F. Weigend, R. Ahlrichs, *Phys. Chem. Chem. Phys.* **2005**, *7*, 3297-305.

[10] S. Grimme, S. Ehrlich, L. Goerigk, *J. Comput. Chem.* **2011**, *32*, 1456–1465.

[11] A. E. Reed, L. A. Curtiss, F. Weinhold, *Chem. Rev.* **1988**, *88*, 899–926.

7.6 Author Contributions

- R. Szlosek – experimental work, writing of original draft, quantum chemical calculations
- K. Dollberg – preparation of $K(18c6)SbH_2$, conceptualization
- G. Balázs – project management, conceptualization
- M. Seidl – finalization of single-crystal X-ray data
- C. von Hänisch – acquisition of funding, project supervision
- M. Scheer – project supervision, acquisition of funding

8 Synthesis of Bismuthanyl-substituted monomeric Triel Hydrides

R. Szlosek, C. Marquardt, O. Hegen, G. Balázs, C. Riesinger, A. Y. Timoshkin and M. Scheer

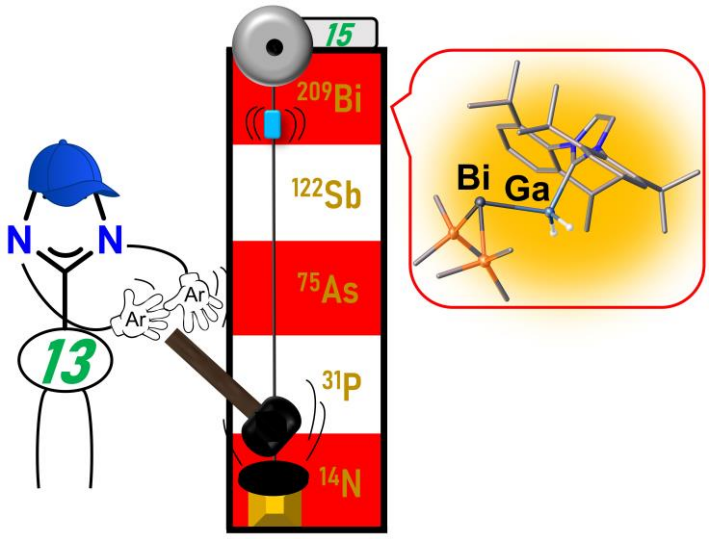

Abstract: The syntheses and characterizations of the first bismuthanylborane monomers stabilized only by a donor in D·$BH_2Bi(SiMe_3)_2$ (D = DMAP **1a**, IDipp **1b**, IMe_4 **1c**; DMAP = 4-dimethylaminopyridine, IDipp = 1,3-bis(2,6-diisopropylphenyl)-imidazolin-2-ylidene, IMe_4 = 1,3,4,5-tetramethylimidazol-2-ylidene) are presented. All compounds were synthesized by salt metathesis reactions between D·BH_2I and $KBi(SiMe_3)_2(THF)_{0.3}$ and represent some of the extremely rare compounds featuring a 2c-2e B-Bi bond in a molecular compound. The products display high sensitivity towards air and light and slowly decompose in solution even at -80 °C. By the reaction of IDipp·$GaH_2(SO_3CF_3)$ with $KBi(SiMe_3)_2(THF)_{0.3}$, the synthesis of the first bismuthanylgallane IDipp·$GaH_2Bi(SiMe_3)_2$ (**2**) stabilized only by a 2-electron donor was possible, as evident from single crystal X-ray structure determination, NMR spectroscopy and mass spectrometry. Computational studies shed light on the stability of the products and the electronic nature of the compounds.

8.1 Introduction

The attention paid to the chemistry of bismuth has increased tremendously within the last decade.[1,2–4] As bismuth can adopt all oxidation states from +V to -III and can often feature a stereoactive 6*s* atomic orbital, it is capable of an extraordinary structural diversity. What is more, strong spin-orbit coupling and relativistic effects influence the chemical and physical properties of bismuth compounds.[5] Prominent representatives for this flexibility are e.g. highly charged bismuth cluster anions.[2,6] The flexibility of binding modes makes organic and inorganic bismuth compounds very useful reagents. E.g. inorganic salts BiX_3 (X = Hal, OTf, NO_3; OTf = SO_3CF_3) have been commonly employed in organic transformations either stoichiometrically or catalytically.[7] In addition, more and more new bismuth-based catalyst systems have recently been developed, capable of impressive organic transformations.[3,8] For instance, the Cornella group has pushed the boundaries of bismuth-catalyzed organic transformations ranging from transfer hydrogenations and amide reductions to oxidative coupling reactions and many other applications.[4,9,10–12] Significantly, it could be demonstrated that bismuth-based catalysis not only relies on the Lewis acidic properties of Bi(III), but that the latter also displays a reaction behaviour similar to regular transition metals since important steps such as single-electron transfer can also be achieved.[10–12]

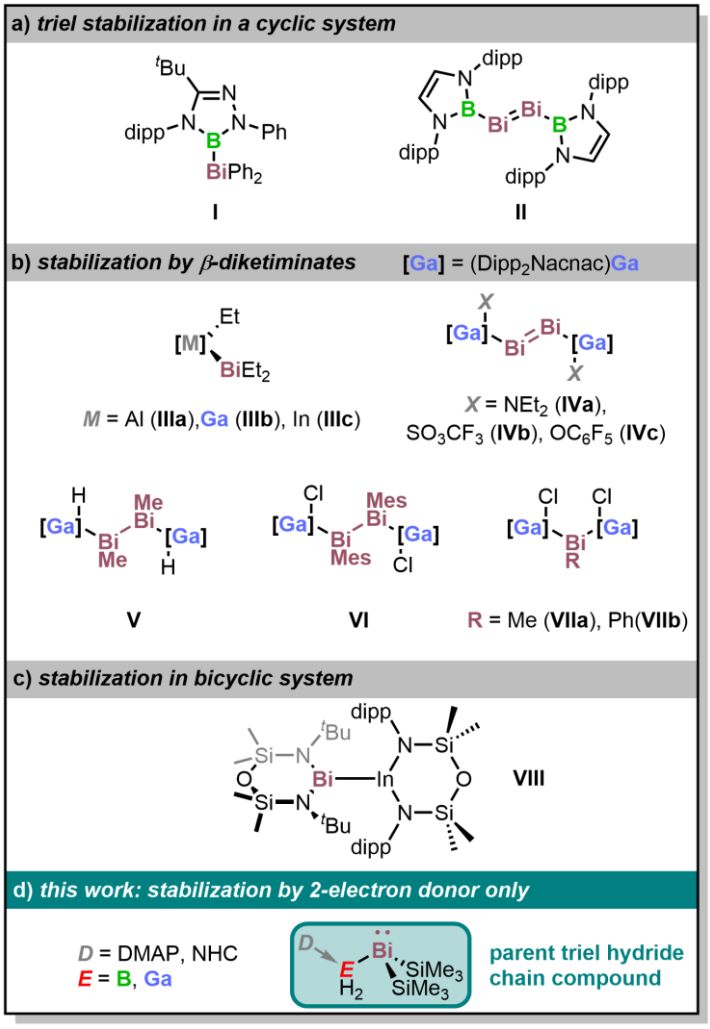

Figure 8.1: Selected examples of stabilization motifs of molecular 13/15 compounds featuring E-Bi bonds (Mes = 2,4,6-trimethylphenyl, dipp = 2,6-diisopropylphenyl, E = triel, Nacnac = bis(2,6-diaryl)-2,2'dimethyl-*β*-diketiminate).

Important contributions to the chemistry of trivalent bismuth were also attained by Chitnis and co-workers who exploited the geometric perturbation of planar trivalent bismuthanes to achieve an unusual reactivity thanks to the steric and electronic properties of these compounds.[13,14] Furthermore, planar Bi(III) complexes proved to act as tunable platforms for catalytic ring opening polymerizations of cyclic esters with good dispersity values and high molecular weights, with only low quantities of the corresponding bismuth triamide catalyst being needed.[14] The success of Bi in catalysis is based on rather strong Bi-C bonds, whereas Bi-triel bonds (triel = group 13 element) often suffer weak bonding because of rather low bond dissociation enthalpies. Thus, isolated examples of such compounds are quite rare, especially when heavy triels come into play. Therefore, such compounds are often unstable and difficult to isolate without prior decomposition.

To the best of our knowledge, the only examples of isolable compounds featuring covalent B-Bi compounds are found in a boryldiphenylbismuthane (Figure 8.1, **I**)[15] as well as in a boryl-dibismuthene (Figure 8.1, **II**).[16] Here, the B atom is incorporated in a stabilizing cycle. The von Hänisch group made important contributions to the field of covalent bismuth compounds and could obtain several highly sensitive interpnictogen chain compounds that include bismuth.[17] This group was recently also able to report on donor-free bismuth cations capable of intriguing reactivity.[18] The group of S. Schulz further advanced this field by the activation of bismuthanes with monovalent group 13 compounds of (Dipp$_2$Nacnac)M (dipp = 2,6 diisopropylphenyl, M = Al, Ga, In; Figure 8.1, **IIIa-c, IVa**).[19] R. A. Fischer and co-workers reported similar dibismuthenes supported by (Dipp$_2$Nacnac)Ga as well as (**IVb/c**).[20] Von Hänisch and co-workers were able to synthesize similar compounds by a related strategy (Figure 8.1, **V**, **VI, VIIa/b**).[21] Again, also in these compounds, the group 13 element is embedded in a cyclic system. Very recently, the groups of Coles and McMullin synthesized a unique bicyclic-like compound featuring a covalent 2c-2e In-Bi bond (Figure 8.1, **VIII**).[22] However, in all reports about Bi-triel bonded compounds, none of the mentioned examples contained parent H-substituted triel moieties and they were all embedded in chain compounds.

Our group is interested in the stabilization of parent group 13/15 element compounds stabilized only by Lewis acids or bases, which can be used e.g. as building blocks for selective oligo- and polymerization reactions.[23] These monomers are usually synthesized by salt metathesis or hydrogen elimination reactions and show interesting reactivities towards electrophiles and nucleophiles.[24] The group 15 element within such compounds also enables a broad range of coordination possibilities, even leading to promising luminescent materials.[25] By varying the group 15 element, the parent phosphanyl-, arsanyl- as well as stibanylboranes stabilized only by one donor molecule $D{\cdot}BH_2PnH_2$ (*Pn* = P, As, Sb) could be accessed.[26,27] The corresponding phoshanyl- and arsanylgallanes and -alanes IDipp·EH_2PnH_2 (E = Ga, Al; *Pn* = P, As) were also recently obtained, but only with the support of a bulky N-heterocyclic carbene (NHC) as donor.[28,29] Higher degrees of substitution at the group 13 entities could also be achieved by multiple salt metatheses, leading to the compounds IDipp·$EH_{3-x}(PnH_2)_x$ (x = 2, 3) and even the triphosphanylindiumane IDipp·$In(PH_2)_3$.[29,30]

Whereas phosphanyl-, arsanyl- and stibanylboranes have already been synthesized, the synthesis of the homologous bismuthanylboranes has so far not been realized. So, the question is whether such compounds are accessible and, if so, whether it is possible to synthesize even the parent compounds. Herein, we report on the synthesis of the first chain-like, donor-stabilized bismuthanylboranes featuring covalent 2c-2e electron B-Bi bonds which contain unique BH_2-moieties as well as on the isolation of an unprecedented bismuthanylgallane, making each of them the first representatives of their particular kinds.

8.2 Results and Discussion

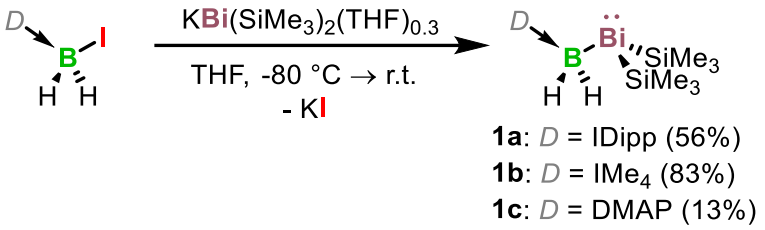

(1)

1a: *D* = IDipp (56%)
1b: *D* = IMe_4 (83%)
1c: *D* = DMAP (13%)

The first step was to target the synthesis of a suitable bismuth source to use it to prepare the donor-stabilized bismuthanylboranes. As salt metathesis presents a reliable pathway towards this type of 13/15 compounds, we started off by investigating the salt metathesis of *D*·BH_2I with an alkali metal bismuthanide. Unfortunately, $MBiH_2$ (M = alkali metal) remains inaccessible so that we decided to introduce $SiMe_3$ groups by using $MBi(SiMe_3)_2$, which offers the possibility towards future Bi-Si bond cleavage. $KBi(SiMe_3)_2(THF)_{0.3}$ was prepared by the reaction of $Bi(SiMe_3)_3$ with KO^{t}Bu in THF (cf. Supporting Information). Subsequently, this reagent was reacted with iodinated donor-stabilized boranes *D*·BH_2I (*D* = IDipp, IMe_4 (= 1,3,4,5-Tetramethylimidazol-2-ylidene), DMAP) by adding neat $KBi(SiMe_3)_2(THF)_{0.3}$ to a cold solution (-80 °C) of the corresponding boranes in THF under exclusion of light (equation 1). Upon reaching room temperature, full conversion of the starting materials is achieved according to NMR spectroscopy. After extraction with toluene, the donor-stabilized bismuthanylboranes *D*·$BH_2Bi(SiMe_3)_2$ (**1a**: *D* = IDipp, **1b**: *D* = IMe_4, **1c:** *D* = DMAP) were isolated in moderate to good yields. The compounds are obtained as grey powders, which display very high sensitivity towards air and light and decompose at room temperature under visible deposition of elemental bismuth. A very slow decomposition occurs even upon prolonged storage at -30 °C, complicating the storage of the solid products for longer than a month. Decomposition in solution happens even faster and at temperatures as low as -80 °C, with **1c** displaying the highest tendency towards decomposition. Presumably, the donor strength of NHCs significantly contributes to the overall better kinetic and thermodynamic stability of the compounds which keeps the molecules intact. This is further supported by quantum chemical calculations (*vide infra*), which show a higher dissociation energy for the NHC adducts **1a** and **1b**. Furthermore, this is in line with the isolated yields from the reactions (cf. equation 1). The NMR spectra of solutions of **1a-c** in C_6D_6 show characteristic triplet resonances in the ^{11}B NMR spectra and singlets ($Si(CH_3)_3$) as well as broadened quartets (BH_2) in the ^1H NMR spectra (cf. Table 8.1).

Table 8.1: Characteristic NMR signals of compounds **1a-2** [ppm] (C_6D_6, 298 K; s = singlet, t = triplet, br = broadened).

NMR spectrum	1a	1b	1c	2
^1H $Si(CH_3)_3$ signal	0.53, s	0.81, s	0.99, s	0.70, s
^1H EH_2 signal (*E* = B, Ga)	2.24, q, br $^1J_{BH}$ = 100 Hz	2.43, q, br $^1J_{BH}$ = 107 Hz	4.74, q, br $^1J_{BH}$ = 120 Hz	4.97, s, br
$^{11}B\{^1H\}$	-42.1, s, br	-39.5, s, br	-15.4, s, br	-
^{11}B	-42.1, t, br $^1J_{BH}$ = 100 Hz	-39.5, t, br $^1J_{BH}$ = 107 Hz	-15.2, t, br $^1J_{BH}$ = 120 Hz	-

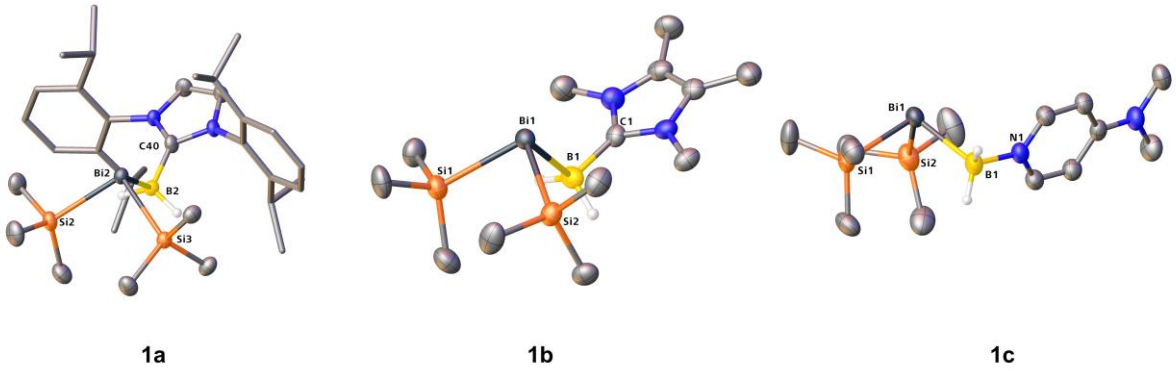

Figure 8.2: Molecular structures of **1a**, **1b** and **1c** in the solid state. Anisotropic displacement ellipsoids are shown at 50% probability level. Hydrogen atoms bound to carbon are omitted for clarity. Dipp groups are displayed as stick models for improved clarity. Selected bond lengths and angles: **1a** C40-B2 1.587(7), B2-Bi2 2.424(5), Bi2-Si2 2.639(4), Bi2-Si3 2.6494(15), C40-B2-Bi2 110.9(3), B2-Bi2-Si2 90.86(15), B2-Bi2-Si3 97.09(14). **1b** C1-B1 1.569(9), B1-Bi1 2.442(7), Bi1-Si1 2.6278(17), Bi1-Si2 2.6452(18), C1-B1-Bi1 107.2(4), B1-Bi1-Si1 89.12(18), B1-Bi1-Si2 97.05(19). **1c** N1-B1 1.578(5), B1-Bi1 2.424(5), Bi1-Si1 2.6331(9), Bi1-Si2 2.6322(11), N1-B1-Bi1 106.9(2), B1-Bi1-Si1 94.53(10), B1-Bi1-Si2 100.10(12).

Moreover, **1a** and **1b** could also be characterized by their molecular ion peaks at *m*/*z* = 756.44 (**1a**) and *m*/*z* = 492.20 (**1b**) in the LIFDI mass spectra. It was also possible to crystallize all bismuthanylboranes **1a-c** by storing saturated solutions in *n*-hexane (**1b**) or toluene (**1c**) at -30 °C overnight or slow evaporation (**1a**) of *n*-pentane at -30 °C. By single-crystal X-ray structure determination, the structures in the solid state could be elucidated (Figure 8.2). **1a** and **1b** show eclipsed conformations at the chain positions, whereas **1c** is arranged in a gauche conformation (cf. Figure 8.2, Figure 8.3). All atoms within the core structure motifs are bound in a (pseudo)tetrahedral manner, with the B-Bi-Si bond angles bent at almost 90° as a result of very poor *s*-*p* orbital mixing (**1a**: 90.83(13)° & 97.10(12)°; **1b**: 89.12(18)° & 97.05(19)°, **1c**: 94.53(10)° & 100.10(12)°), which is significantly lower than for the lighter homologs (cf. $Me_3N{\cdot}BH_2P(SiMe_3)_2$: Si-P-B 102.30(8)°).[27] The B-Bi bond distances of **1a-c** are between 2.423(4) Å and 2.442(7) Å and represent the first known examples of B-Bi 2c-2e bonds with tetracoordinate boron atoms within chain compounds. Compared to the B-Bi bonds in boryldiphenylbismuthane **I** (B-Bi: 2.343(6) Å)[15] and boryldibismuthene **II** (B-Bi: 2.326(7)/2.317(9) Å),[16] the bonds are significantly elongated due to the different electronic and steric environment of, especially, the boron atom.

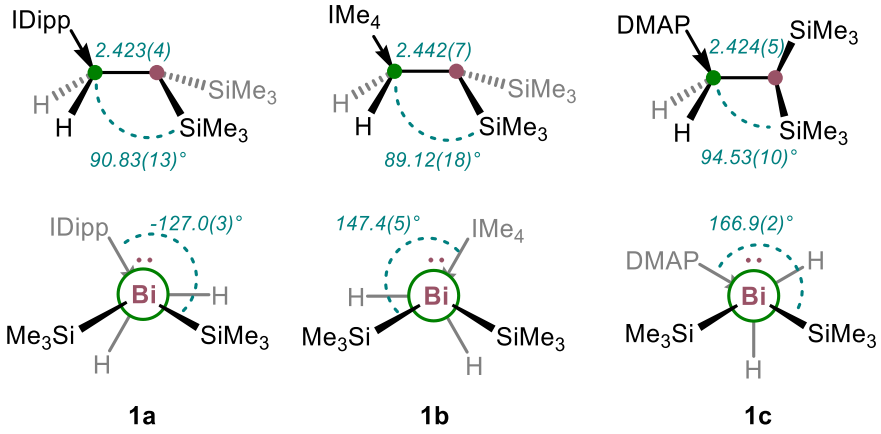

Figure 8.3: Structural features derived by X-ray crystallographic structure determination of **1a-c** including key bond distances [Å] and angles (top). Bottom: Newman projections along the B-Bi *σ*-bonds alongside the corresponding dihedral angles.

The $SiMe_3$ groups on the Bi atom of **1a-c** provided a possible opportunity to generate the only hydrogen-substituted parent compounds of **1a-c** $D{\cdot}BH_2BiH_2$ by cleavage of the $SiMe_3$ residues. Attempts at the

cleavage of the $SiMe_3$ groups were performed by the addition of MeOH, mixtures of MeOH/MeONa, hexanol or KF·HF. In all cases, however, only decomposition products or unreacted starting materials could be detected. The most promising attempt was the reaction of **1a** with 1,4-benzoquinone as a $\{SiMe_3\}$ scavenger in the presence of MeOH-d_4 in THF (cf. Supporting Information), which showed the cleavage of at least one $\{SiMe_3\}$ group at the bismuth atom in the ^{1}H NMR spectrum of the reaction mixture. Simultaneously, besides unreacted **1a**, IDipp·BH_2(OMe) and IDipp·BH_3, a new, broad signal at -31.4 ppm was detected in the ^{11}B NMR spectrum. The ^{2}H NMR spectrum shows a broad signal at 2.96 ppm but, unfortunately, a clear identification of the product was not possible. Conceivably, IDipp·$BH_2Bi(SiMe_3)_{2-x}D_x$ (x = 1-2) is formed as a transient species, but unequivocal evidence of this species could not be obtained. Hence, despite numerous efforts the parent compounds containing H_2Bi–BH_2 units have so far remained inaccessible.

After the successful synthesis of donor-stabilized bismuthanylboranes, the question arose as to whether it is also possible to synthesize the heavier gallium homolog. Thus, a reaction between IDipp·GaH_2(OTf) and $KBi(SiMe_3)_2(THF)_{0.3}$ was attempted. After cooling a solution of IDipp·GaH_2(OTf) in tetrahydrofuran to -80 °C, the solid bismuthide was added and the mixture was slowly warmed to room temperature over the course of 18 hours (equation 2). The ^{1}H NMR spectrum of the reaction mixture showed full conversion of the starting material (0.63 ppm, CD_3CN) with a characteristic singlet including ^{29}Si satellites at 0.71 ppm for the $\{SiMe_3\}$ residues (18 H, $^2J_{HSi}$ = 7.15 Hz).

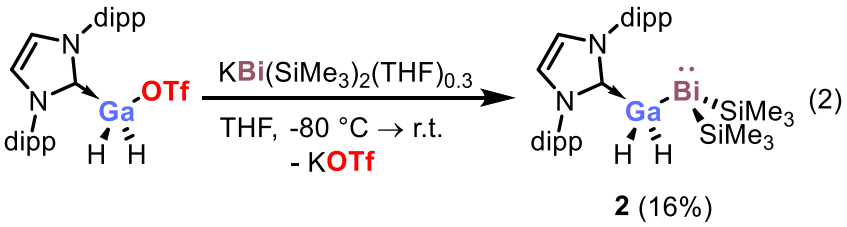

2 is extremely air-, light- and temperature-sensitive and decomposes very slowly in solution at -80 °C under deposition to elemental bismuth and other unidentified compounds. The ^{1}H NMR spectra of solutions of isolated **2** in C_6D_6 show characteristic signals at 0.70 ppm ($Si(CH_3)_3$) and 4.97 ppm (GaH_2; cf. Table 8.1). The sensitivity of **2** greatly complicates the handling of the product, but, fortunately, by slow evaporation of a solution of **2** in *n*-pentane under reduced pressure at -80 °C, it was possible to grow a few single crystals of **2**, which were of suitable quality for single crystal X-ray structure determination (Figure 8.4). **2** crystallizes in the orthorhombic space group *Pbca* as clear colorless plate-shaped crystals. The structure in the solid state shows (pseudo)tetrahedral geometries at the $[GaH_2Bi(SiMe_3)_2]$ unit with a Ga-Bi bond length of 2.7234(4) Å, which is only slightly elongated compared to the Ga-Bi bond distance of 2.7171(8) Å of $\{(Dipp_2NacNac)GaHBiMe\}_2$.[21] The C1-Ga1-Bi1 angle (110.10(8)°) indicates a tetrahedral geometry at the Ga atom while the Ga1-Bi1-Si1 (95.26(2)°) and Ga1-Bi1-Si2 (87.85(2)°) angles are significantly distorted from a regular tetrahedral binding situation. Similar to **1a** and **1b**, **2** is arranged in an eclipsed conformation (C1-Ga1-Bi1-Si1: 113.33(9)°). The presence of **2** could also be confirmed by mass spectrometry, as the LIFDI-MS spectrum of a solution of **2** in toluene shows a molecular ion peak at m/z = 814.34 besides the decomposition products $[IDipp\text{-}H]^+$ (m/z = 389.31) and $[IDipp\text{-}GaH_2]^+$ (m/z = 459.24).

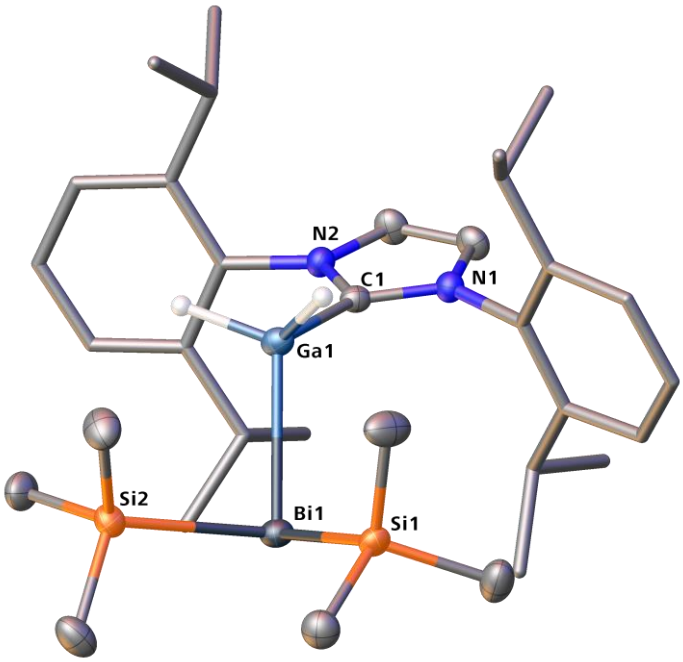

Figure 8.4: Molecular structure of **2** in the solid state. Anisotropic displacement ellipsoids are shown at 50% probability level. Hydrogen atoms bound to carbon are omitted for clarity. Dipp residues are depicted as stick models for better clarity. Selected bond lengths [Å] and angles [°]: N1-C1 1.352(4), N2-C1 1.357(4), C1-Ga1 2.061(3), Ga1-Bi1 2.7234(4), Bi1-Si1 2.6487(9), Bi1-Si2 2.6403(9), N1-B1-Bi1 106.9(2), N1-C1-N2 104.2(3), N1-C1-Ga1 129.2(2), C1-Ga1-Bi1 110.10(8), Ga1-Bi1-Si1 95.26(2), B1-Bi1-Si2 87.85(2).

To analyze the stability and electronic structure of all obtained products, quantum chemical calculations were performed on **1a**-**2** (B3LYP/def2-TZVP, ECP on Bi; cf. Supporting Information). The stability with respect to the dissociation of the Lewis acid/base adducts decreases in the order of IMe_4 > IDipp > DMAP and B > Ga, which is in line with the isolated yields and the observed stabilities in solution. The standard Gibbs energy for the dissociation of **2** into IDipp and $GaH_2Bi(SiMe_3)_2$ is endergonic by +27 kJ mol^{-1}, which makes this compound the least stable one within the synthesized series with respect to dissociation. Analyses of structural characteristics and Wiberg bond indices (WBIs) indicate that upon complex formation, the E-Bi bond distances increase by 0.1-0.2 Å and the WBIs of the E-Bi bonds decrease by 0.1-0.37, in line with the above-mentioned order of thermodynamic stability (cf. Supporting Information). The B-Bi bond in free $BH_2Bi(SiMe_3)_2$ has a partial double bond character (WBI 1.21) due to the π-interaction between the lone pair of Bi and the empty orbital of boron (see HOMO, cf. Supporting Information). In case of the gallium analog $GaH_2Bi(SiMe_3)_2$, the similar π-interaction is much less pronounced and the WBI value is close to one. Regarding the methanolysis reactions of **1a**-**1c**, the formation of IDipp·BH_2BiH_2, IMe_4·BH_2BiH_2 and DMAP·BH_2BiH_2, respectively, is predicted to be highly exothermic and exergonic by 187-206 kJ mol^{-1}, while the formed hydride compounds are predicted to be thermodynamically unstable with respect to the decomposition to LB·BH_3, H_2 and solid Bi (processes are exergonic by 120-150 kJ mol^{-1}) (cf. Supporting Information).

8.3 Conclusion

In summary, it could be shown that the synthesis of donor-stabilized bismuthanylboranes and gallanes can be achieved by salt metathesis with $KBi(SiMe_3)_2(THF)_{0.3}$, yielding IDipp·$BH_2Bi(SiMe_3)_2$ (**1a**),

$IMe_4{\cdot}BH_2Bi(SiMe_3)_2$ (**1b**), $DMAP{\cdot}BH_2Bi(SiMe_3)_2$ (**1c**), and $IDipp{\cdot}GaH_2Bi(SiMe_3)_2$ (**2**). All compounds could be characterized by multinuclear NMR spectroscopy and LIFDI-MS. Moreover, the crystal structures of **1b**, **1c** and **2** could be determined, representing the first solid-state structures of bismuthanyl-trielanes that contain parent $\{EH_2\}$ triel moieties and possess E-Bi σ-bonds in chain-like compounds. Specifically, **1a-c** represent the first examples of structures containing covalent B-Bi σ-bonds where the boron atom is not embedded in a cyclic system. All compounds display a very high sensitivity towards air and light. Desilylation attempts have been unsuccessful, which is likely to be also due to the extreme instability of the potentially formed $\{BH_2BiH_2\}$ moiety. Future investigations will focus on the reactivity of these compounds regarding catenation, coordination as well as deposition experiments.

8.4 References

[1] a) M. Kanatzidis, H. Sun, S. Dehnen, *Inorg. Chem.* **2020**, *59*, 3341–3343; b) P. Ondet, G. Lemière, E. Duñach, *Eur. J. Org. Chem.* **2017**, *2017*, 761–780; c) E. Lopez, S. C. Thorp, R. S. Mohan, *Polyhedron* **2022**, *222*, 115765.

[2] F. Pan, B. Peerless, S. Dehnen, *Acc. Chem. Res.* **2023**, *56*, 1018–1030.

[3] T. Ollevier, *Org. Biomol. Chem.* **2013**, *11*, 2740–2755.

[4] H. W. Moon, J. Cornella, *ACS Catal.* **2022**, *12*, 1382–1393.

[5] a) X. Gonze, J.-P. Michenaud, J.-P. Vigneron, *Phys. Scr.* **1988**, *37*, 785–789; b) A. Isaeva, M. Ruck, *Inorg. Chem.* **2020**, *59*, 3437–3451.

[6] a) J. Heine, B. Peerless, S. Dehnen, C. Lichtenberg, *Angew. Chem. Int. Ed.* **2023**, *62*, e202218771; b) F. Pan, S. Wei, L. Guggolz, A. R. Eulenstein, F. Tambornino, S. Dehnen, *J. Am. Chem. Soc.* **2021**, *143*, 7176–7188; c) A. R. Eulenstein, Y. J. Franzke, P. Bügel, W. Massa, F. Weigend, S. Dehnen, *Nat. Comm.* **2020**, *11*, 5122; d) A. R. Eulenstein, Y. J. Franzke, N. Lichtenberger, R. J. Wilson, H. L. Deubner, F. Kraus, R. Clérac, F. Weigend, S. Dehnen, *Nat. Chem.* **2021**, *13*, 149–155; e) B. Peerless, A. Schmidt, Y. J. Franzke, S. Dehnen, *Nat. Chem.* **2023**, *15*, 347–356.

[7] a) J. M. Bothwell, S. W. Krabbe, R. S. Mohan, *Chem. Soc. Rev.* **2011**, *40*, 4649–4707; b) R. Hua, *Curr. Org. Syn.* **2008**, *5*, 1–27.

[8] a) D. Janssen-Müller, M. Oestreich, *Angew. Chem. Int. Ed.* **2020**, *59*, 8328–8330; b) B. Jousseaume, C. Laporte, T. Toupance, J.-M. Bernard, *Tetrahedron Lett.* **2002**, *43*, 6305–6307; c) T. Kitanosono, T. Ollevier, S. Kobayashi, *Chem. Asian J.* **2013**, *8*, 3051–3062; d) C. Lichtenberg, *Chem. Commun.* **2021**, *57*, 4483–4495; e) H. Qin, N. Yamagiwa, S. Matsunaga, M. Shibasaki, *J. Am. Chem. Soc.* **2006**, *128*, 1611–1614; f) H. Qin, N. Yamagiwa, S. Matsunaga, M. Shibasaki, *Angew. Chem. Int. Ed.* **2007**, *46*, 409–413; g) J. Ramler, I. Krummenacher, C. Lichtenberg, *Angew. Chem. Int. Ed.* **2019**, *58*, 12924–12929; h) M. Rueping, B. J. Nachtsheim, W. Ieawsuwan, *Adv. Synth. Catal.* **2006**, *348*, 1033–1037; i) J. A. Salvador, S. M. Silvestre, *Tetrahedron Lett.* **2005**, *46*, 2581–2584; j) S. Vidal, *Synlett* **2001**, *2001*, 1194–1195; k) N. Worz, A. Brandner, P. Claus, *J. Phys. Chem. C* **2010**, *114*, 1164–1172; l) Z.-P. Zhang, N. Dong, X. Li, *Chem. Commun.* **2017**, *53*, 1301–1304; m) K. Zhou, W. Wang, Z. Zhao, G. Luo, J. T. Miller, M. S. Wong, F. Wei, *ACS Catal.* **2014**, *4*, 3112–3116; n) M. Pramanik, M. G. Guerzoni, E. Richards, R. L. Melen, *Angew. Chem. Int. Ed. Engl.* **2024**, *63*, e202316461; o) M. Mato, J. Cornella, *Angew. Chem. Int. Ed.* **2024**, *63*, e202315046.

[9] a) M. Magre, J. Cornella, *J. Am. Chem. Soc.* **2021**, *143*, 21497–21502; b) M. Magre, J. Kuziola, N. Nöthling, J. Cornella, *Org. Biomol. Chem.* **2021**, *19*, 4922–4929; c) Y. Pang, M. Leutzsch, N. Nöthling, J. Cornella, *J. Am. Chem. Soc.* **2020**, *142*, 19473–19479; d) Y. Pang, M. Leutzsch, N. Nöthling, F. Katzenburg, J. Cornella, *J. Am. Chem. Soc.* **2021**, *143*, 12487–12493; e) F. Wang, O. Planas, J. Cornella, *J. Am. Chem. Soc.* **2019**, *141*, 4235–4240; f) O. Planas, F. Wang, M. Leutzsch, J. Cornella, *Science* **2020**, *367*, 313–317; g) X. Yang, J. Kuziola, V. A. Béland, J. Busch, M. Leutzsch, J. Burés, J. Cornella, *Angew. Chem. Int. Ed.* **2023**, e202306447; h) X. Yang, E. J. Reijerse, K. Bhattacharyya, M. Leutzsch, M. Kochius, N. Nöthling, J. Busch, A. Schnegg, A. A. Auer, J. Cornella, *J. Am. Chem. Soc.* **2022**, *144*, 16535–16544; i) X. Yang, E. J. Reijerse, N. Nöthling, D. J. SantaLucia, M. Leutzsch, A. Schnegg, J. Cornella, *J. Am. Chem. Soc.* **2023**, *145*, 5618–5623; j) H. W. Moon, F. Wang, K. Bhattacharyya, O. Planas, M. Leutzsch, N. Nöthling, A. A. Auer, J. Cornella, *Angew. Chem. Int. Ed.* **2023**, e202313578; k) T. Tsuruta, D. Spinnato, H. W. Moon, M. Leutzsch, J. Cornella, *Journal of the American Chemical Society* **2023**, *145*, 25538–25544.

[10] M. Mato, D. Spinnato, M. Leutzsch, H. W. Moon, E. J. Reijerse, J. Cornella, *Nat. Chem.* **2023**, *15*, 1138-1145.

[11] O. Planas, V. Peciukenas, J. Cornella, *J. Am. Chem. Soc.* **2020**, *142*, 11382–11387.

[12] O. Planas, V. Peciukenas, M. Leutzsch, N. Nöthling, D. A. Pantazis, J. Cornella, *J. Am. Chem. Soc.* **2022**, *144*, 14489–14504.

[13] a) S. S. Chitnis, N. Burford, A. Decken, M. J. Ferguson, *Inorg. Chem.* **2013**, *52*, 7242–7248; b) S. S. Chitnis, A. P. M. Robertson, N. Burford, B. O. Patrick, R. McDonald, M. J. Ferguson, *Chem. Sci.* **2015**, *6*, 6545–6555; c) S. S. Chitnis, K. A. Vos, N. Burford, R. McDonald, M. J. Ferguson, *Chem. Commun.* **2016**, *52*, 685–688; d) T. Hynes, J. D. Masuda, S. S. Chitnis, *ChemPlusChem* **2022**, *87*; e) M. B. Kindervater, T. Hynes, K. M. Marczenko, S. S. Chitnis, *Dalton Trans.* **2020**, *49*, 16072–16076; f) M. B. Kindervater, K. M. Marczenko, U. Werner-Zwanziger, S. S. Chitnis, *Angew. Chem. Int. Ed.* **2019**, *58*, 7850–7855; g) K. M. Marczenko, S. S. Chitnis, *Chem. Commun.* **2020**, *56*, 8015–8018; h) K. M. Marczenko, J. A. Zurakowski, M. B. Kindervater, S. Jee, T. Hynes, N. Roberts, S. Park, U. Werner‐Zwanziger, M. Lumsden, D. N. Langelaan et al., *Chem. Eur. J.* **2019**, *25*, 16414–16424; i) K. M. Marczenko, S. Jee, S. S. Chitnis, *Organometallics* **2020**, *39*, 4287–4296.

[14] T. J. Hannah, W. M. McCarvell, T. Kirsch, J. Bedard, T. Hynes, J. Mayho, K. L. Bamford, C. W. Vos, C. M. Kozak, T. George et al., *Chem. Sci.* **2023**, *14*, 4549–4563.

[15] W. Lu, H. Hu, Y. Li, R. Ganguly, R. Kinjo, *J. Am. Chem. Soc.* **2016**, *138*, 6650–6661.

[16] D. Dange, A. Davey, J. A. B. Abdalla, S. Aldridge, C. Jones, *Chem. Commun.* **2015**, *51*, 7128–7131.

[17] a) T. Dunaj, K. Dollberg, C. von Hänisch, *Dalton Trans.* **2022**, *51*, 7551–7560; b) T. Dunaj, K. Dollberg, C. Ritter, F. Dankert, C. Hänisch, *Eur. J. Inorg. Chem.* **2021**, *2021*, 870–878; c) T. Dunaj, M. Egorycheva, A. Arebi, K. Dollberg, C. von Hänisch, *Z. Anorg. Allg. Chem.* **2023**, *649*; d) T. Dunaj, C. von Hänisch, *Chem. Eur. J.* **2022**, *28*, e202202932; e) C. Ritter, N. Michel, A. Rinow, B. Ringler, C. Hänisch, *Eur. J. Inorg. Chem.* **2021**, *2021*, 2514–2522; f) C. Ritter, F. Weigend, C. von Hänisch, *Chem. Eur. J.* **2020**, *26*, 8536–8540.

[18] T. Dunaj, J. Schwarzmann, J. Ramler, A. Stoy, S. Reith, J. Nitzsche, L. Völlinger, C. von Hänisch, C. Lichtenberg, *Chem. Eur. J.* **2023**, *29*, e202204012.

[19] a) C. Ganesamoorthy, D. Bläser, C. Wölper, S. Schulz, *Chem. Commun.* **2014**, *50*, 12382–12384; b) L. Tuscher, C. Helling, C. Wölper, W. Frank, A. S. Nizovtsev, S. Schulz, *Chem. Eur. J.* **2018**, *24*, 3241–3250.

[20] G. Prabusankar, C. Gemel, P. Parameswaran, C. Flener, G. Frenking, R. A. Fischer, *Angew. Chem. Int. Ed.* **2009**, *48*, 5526–5529.

[21] S. Schneider, C. von Hänisch, *Chem. Commun.* **2022**, *58*, 1522–1525.

[22] M. D. Anker, A. O'Reilly, C. L. McMullin, M. P. Coles, *Polyhedron* **2023**, *246*, 116695.

[23] a) C. Marquardt, O. Hegen, A. Vogel, A. Stauber, M. Bodensteiner, A. Y. Timoshkin, M. Scheer, *Chem. Eur. J.* **2018**, *24*, 360–363; b) M. Bodensteiner, A. Y. Timoshkin, E. V. Peresypkina, U. Vogel, M. Scheer, *Chem. Eur. J.* **2013**, *19*, 957–963; c) M. Bodensteiner, U. Vogel, A. Y. Timoshkin, M. Scheer, *Angew. Chem. Int. Ed.* **2009**, *48*, 4629–4633; d) C. Marquardt, T. Jurca, K.-C. Schwan, A. Stauber, A. V. Virovets, G. R. Whittell, I. Manners, M. Scheer, *Angew. Chem. Int. Ed.* **2015**, *54*, 13782–13786; e) C. Thoms, C. Marquardt, A. Y. Timoshkin, M. Bodensteiner, M. Scheer, *Angew. Chem. Int. Ed.* **2013**, *52*, 5150–5154.

[24] a) R. Szlosek, M. Seidl, G. Balázs, M. Scheer, *Chem. Eur. J.* **2023**, *29*, e202301752; b) O. Hegen, A. V. Virovets, A. Y. Timoshkin, M. Scheer, *Eur. J. Inorg. Chem.* **2018**, *24*, 16521-16525; c) F. Lehnfeld, M. Seidl, A. Y. Timoshkin, M. Scheer, *Eur. J. Inorg. Chem.* **2022**, *3*, e202100930; d) C. Marquardt, T. Kahoun, J. Baumann, A. Y. Timoshkin, M. Scheer, *Z. Anorg. Allg. Chem.* **2017**, *643*, 1326–1330; e) M. T. Ackermann, M. Seidl, F. Wen, M. J. Ferguson, A. Y. Timoshkin, E. Rivard, M. Scheer, *Chem. Eur. J.* **2022**, *28*, e20210370; f) C. Marquardt, G. Balázs, J. Baumann, A. V. Virovets, M. Scheer, *Chem. Eur. J.* **2017**, *23*, 11423–11429; g) C. Marquardt, C. Thoms, A. Stauber, G. Balázs, M. Bodensteiner, M. Scheer, *Angew. Chem. Int. Ed.* **2014**, *53*, 3727–3730; h) M. Elsayed Moussa, T. Kahoun, M. T. Ackermann, M. Seidl, M. Bodensteiner, A. Y. Timoshkin, M. Scheer, *Organometallics* **2022**, *41*, 1572–1578; i) C. Marquardt, T. Kahoun, A. Stauber, G. Balázs, M. Bodensteiner, A. Y. Timoshkin, M. Scheer, *Angew. Chem. Int. Ed.* **2016**, *55*, 14828–14832; j) C. Marquardt, O. Hegen, T. Kahoun, M. Scheer, *Chem. Eur. J.* **2017**, *23*, 4397–4404; k) U. Vogel, A. Y. Timoshkin, M. Scheer, *Angew. Chem. Int. Ed.* **2001**, *40*, 4409–4412; l) U. Vogel, P. Hoemensch, K.-C. Schwan, A. Y. Timoshkin, M. Scheer, *Chem. Eur. J.* **2003**, *9*, 515–519; m) F. Lehnfeld, M. Seidl, A. Y. Timoshkin, M. Scheer, *Eur. J. Inorg. Chem.* **2022**, *3*, e202100930; n) A. Adolf, M. Zabel, M. Scheer, *Eur. J. Inorg. Chem.* **2007**, *2007*, 2136–2143; o) F. Lehnfeld, M. Seidl, A. Timoshkin, M. Scheer, *Eur. J. Inorg. Chem.* **2023**, *26*, e202300338; p) R. Szlosek, A. S. Niefanger, G. Balázs, M. Seidl, A. Y. Timoshkin, M. Scheer, *Chem. Eur. J.* **2024**, *30*, e202303603.

[25] a) J. Braese, A. Schinabeck, M. Bodensteiner, H. Yersin, A. Y. Timoshkin, M. Scheer, *Chem. Eur. J.* **2018**, *24*, 10073–10077; b) M. Elsayed Moussa, J. Braese, C. Marquardt, M. Seidl, M. Scheer, *Eur. J. Inorg. Chem.* **2020**, *26*, 2501–2505; c) M. Elsayed Moussa, C. Marquardt, O. Hegen, M. Seidl, M. Scheer, *New J. Chem.* **2021**, *45*, 14916–14919; d) K.-C. Schwan, A. Adolf, M. Bodensteiner, M. Zabel, M. Scheer, *Z. Anorg. Allg. Chem.* **2008**, *634*, 1383–1387; e) R. Szlosek, M. T. Ackermann, C. Marquardt, M. Seidl, A. Y. Timoshkin, M. Scheer, *Chem. Eur. J.* **2023**, *29*, e202202911.

[26] a) K.-C. Schwan, A. Y. Timoskin, M. Zabel, M. Scheer, *Chem. Eur. J.* **2006**, *12*, 4900–4908; b) C. Marquardt, O. Hegen, M. Hautmann, G. Balázs, M. Bodensteiner, A. V. Virovets, A. Y. Timoshkin, M. Scheer, *Angew. Chem. Int. Ed.* **2015**, *54*, 13122–13125.

[27] C. Marquardt, A. Adolf, A. Stauber, M. Bodensteiner, A. V. Virovets, A. Y. Timoshkin, M. Scheer, *Chem. Eur. J.* **2013**, *19*, 11887–11891.

[28] M. A. K. Weinhart, A. S. Lisovenko, A. Y. Timoshkin, M. Scheer, *Angew. Chem. Int. Ed.* **2020**, *59*, 5541-5545; *Angew. Chem.* **2020**, *132*, 5586-5590.

[29] M. A. K. Weinhart, M. Seidl, A. Y. Timoshkin, M. Scheer, *Angew. Chem.* **2021**, *133*, 3850–3855; *Angew. Chem. Int. Ed.* **2021**, *60*, 3806–3811.

[30] R. Szlosek, M. A. K. Weinhart, G. Balázs, M. Seidl, L. Zimmermann, M. Scheer, *Chem. Eur. J.* **2023**, *29*, e202300340.

[31] a) N. Kuhn, G. Henkel, T. Kratz, J. Kreutzberg, R. Boese, A. H. Maulitz, *Chem. Ber.* **1993**, *126*, 2041–2045; b) G. Becker, M. Rößler, *Z. Naturforsch. B* **1982**, *37*, 91–96; c) F. Barth, F. Achrainer, A. M. Pütz, H. Zipse, *Chem. Eur. J.* **2017**, *23*, 13455–13464; d) O. V. Dolomanov, L. J. Bourhis, R. J. Gildea, J. A. K. Howard, H. Puschmann, *J. Appl. Crystallogr.* **2009**, *42*, 339–341; e) G. M. Sheldrick, *Acta Cryst. C* **2015**, *71*, 3–8; f) G. M. Sheldrick, *Acta Cryst. A* **2015**, *71*, 3–8; g) F. Weigend, R. Ahlrichs, *Phys. Chem. Chem. Phys.* **2005**, *7*, 3297-305; h) C. Lee, W. Yang, R. G. Parr, *Phys. Rev. B* **1988**, *37*, 785–789; i) A. D. Becke, *J. Chem. Phys.* **1993**, *98*, 5648–5652; j) Gaussian 09, Revision E.01, M. J. Frisch, G. W. Trucks, H. B. Schlegel, G. E. Scuseria, M. A. Robb, J. R. Cheeseman, G. Scalmani, V. Barone, G. A. Petersson, H. Nakatsuji, X. Li, M. Caricato, A. Marenich, J. Bloino, B. G. Janesko, R. Gomperts, B. Mennucci, H. P. Hratchian, J. V. Ortiz, A. F. Izmaylov, J. L. Sonnenberg, D. Williams-Young, F. Ding, F. Lipparini, F. Egidi, J. Goings, B. Peng, A. Petrone, T. Henderson, D. Ranasinghe, V. G. Zakrzewski, J. Gao, N. Rega, G. Zheng, W. Liang, M. Hada, M. Ehara, K. Toyota, R. Fukuda, J. Hasegawa, M. Ishida, T. Nakajima, Y. Honda, O. Kitao, H. Nakai, T. Vreven, K. Throssell, J. A. Montgomery, Jr., J. E. Peralta, F. Ogliaro, M. Bearpark, J. J. Heyd, E. Brothers, K. N. Kudin, V. N. Staroverov, T. Keith, R. Kobayashi, J. Normand, K. Raghavachari, A. Rendell, J. C. Burant, S. S. Iyengar, J. Tomasi, M. Cossi, J. M. Millam, M. Klene, C. Adamo, R. Cammi, J. W. Ochterski, R. L. Martin, K. Morokuma, O. Farkas, J. B. Foresman, and D. J. Fox, Gaussian, Inc., Wallingford CT, 2016; k) A. E. Reed, L. A. Curtiss, F. Weinhold, *Chem. Rev.* **1988**, *88*, 899–926.

8.5 Supporting Information

8.5.1 General Information

8.5.1.1 Working Techniques

All working steps were carried out under argon inert gas atmosphere using standard Schlenk and glovebox techniques under exclusion of light due to the sensitivity of the reagents and products. All glassware was dried in an oven at 150 °C and pre-conditioned in high vacuum ($p < 10^{-3}$ mbar, 650 °C) shortly before use. Traces of H_2O and O_2 were removed from argon gas by by passing it through a BASF R 3-11 ($CuO/MgSiO_3$) catalyst, concentrated H_2SO_4, Orange Gel and Sicapent® supported on pumice stone. Prior to use, solvents were purified using an MBraun SPS-800 solvent purification system, degassed at room temperature, and stored over molecular sieves for at least 48 hours. C_6D_6 was dried over Na/K, distilled, degassed at room temperature, and stored over molecular sieves (4 Å). CD_3CN was dried repeatedly over molecular sieves (3 Å). Elemental Analysis (CHNS) was performed by the in-house facility. Mass spectra were recorded on a Jeol AccuTOF GCX mass spectrometer (LIFDI-MS) mass spectrometer by the in-house facility.

IDipp·GaH_2(OTf),[1] IDipp·BH_2I,[1] IMe_4·BH_3,[2] and $Bi(SiMe_3)_3$[3] were prepared according to literature procedures. BH_3·SMe_2/BH_3·THF was purchased from ABCR and used as received. 1,4-benzoquinone was freshly sublimed prior to use. Preparation involving $KBi(SiMe_3)_2(THF)_{0.3}$ or the bismuth containing products were conducted under exclusion of light.

8.5.1.2 Spectroscopic Analysis

All NMR spectra were recorded on a BRUKER Avance 400 (frequencies: ^{1}H: 400.13 MHz, ^{11}B: 128.43 MHz) or Avance 300 (^{1}H: 300.13 MHz, ^{13}C: 75.47 MHz) spectrometers. Substances of reference are $Si(CH_3)_4$ (^{1}H, ^{13}C) and BF_3·Et_2O (^{11}B). Chemical shifts δ are presented in ppm referring to the external standards and coupling constants J are given in Hz without consideration of absolute signs.

8.5.2 Experimental Details

8.5.2.1 Synthesis of $KBi(SiMe_3)_2(THF)_{0.3}$

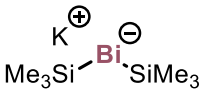

A round-bottom flask was charged with $Bi(SiMe_3)_3$ (18.0 g, 42.0 mmol) and the compound dissolved in tetrahydrofuran. The solution was cooled to -65 °C and solid KO^{t}Bu was added (4.8 g, 42.0 mmol). After stirring at room temperature for 1.5 hours, all volatiles were removed *in vacuo*, yielding a brown-greenish crude product. The solids were transferred onto a glass frit and washed three times with 30 mL of *n*-pentane each. The product was then dried *in vacuo* (16.8 g, 96%). According to ^{1}H NMR spectroscopy (*vide infra*), the content of tetrahydrofuran in the final product was determined.

^{1}H NMR (300.13 MHz, CD_3CN, 298 K): 0.63 (s, Si(CH_3)$_3$).

^{13}C{^{1}H} NMR (75.47 MHz, CD_3CN, 298 K): 12.1 (s).

8.5.2.2 Synthesis of IMe_4·BH_3

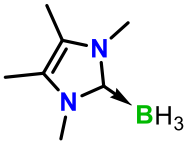

A Schlenk tube was charged with IMe_4 (1.27 g, 10.3 mmol) and the solids dissolved in toluene. After cooling the solution to -40 °C, neat BH_3·SMe_2 (1.45 mL, excess) was added *via* syringe. The mixture was stirred overnight at room temperature and then all volatiles were removed *in vacuo*, yielding IMe_4·BH_3 as a white powder (1.24 g, 87%).

^{1}H NMR (400.30 MHz, C_6D_6, 298 K): 1.20 (s, 6 H, 2 × CH_3), 2.03 (q, broad, 3 H, BH_3, $^{1}J_{HB}$ = 87 Hz), 3.13 (s, 6 H, 2 × NCH_3).

^{11}B{^{1}H} NMR (128.43 MHz, C_6D_6, 298 K): -35.8 (s, broad).

^{11}B NMR (128.43 MHz, C_6D_6, 298 K): -35.8 (q, broad, $^{1}J_{HB}$ = 87 Hz).

The NMR data are consistent with the literature values.[2]

8.5.2.3 Synthesis of DMAP·BH_3

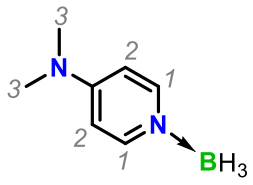

BH_3·THF (5 mL, 1.0 M in THF, 5.0 mmol) was added to a solution of DMAP (610 mg, 5.0 mmol) in toluene, resulting in an immediate precipitation of white solids. All volatiles are then removed *in vacuo* and the solids dried under reduced pressure. The residue is washed twice with *n*-hexane and dried under reduced pressure (355 mg, 52%).

^{1}H NMR (400.30 MHz, C_6D_6, 298 K): 1.89 (s, 6 H, C3*H*), 3.63 (q, 3 H, BH_3, $^{1}J_{HB}$ = 95 Hz), 5.49 (m, 2 H, C2*H*), 8.04 (m, 2 H, C1*H*).

^{11}B{^{1}H} NMR (128.43 MHz, C_6D_6, 298 K): -12.2 (s, broad).

^{11}B NMR (128.43 MHz, C_6D_6, 298 K): -12.2 (q, broad, $^{1}J_{HB}$ = 95 Hz).

The NMR data are consistent with the literature values.[4]

8.5.2.4 Synthesis of DMAP·BH_2I

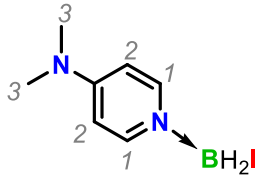

Solid I_2 (250 mg, 0.98 mmol) was slowly added to a solution of BH_3·DMAP (272 mg, 2.0 mmol) in benzene (gas evolution and precipitation of the product could be observed). After stirring for two hours at room temperature, all volatiles are

removed *in vacuo* in the residue is washed with *n*-hexane. After drying under reduced pressure, the product is obtained as white solids (425 mg, 81%).

^{1}H NMR (400.30 MHz, CD_2Cl_2, 298 K): 3.04 (s, 6 H, C3*H*), 3.54 (q, 2 H, BH_2, $^{1}J_{HB} \approx 130$ Hz), 6.52 (m, 2 H, C2*H*), 8.06 (m, 2 H, C1*H*).

^{11}B{^{1}H} NMR (128.43 MHz, CD_2Cl_2, 298 K): -11.7 (s, broad).

^{11}B NMR (128.43 MHz, CD_2Cl_2, 298 K): -11.7 (t, broad, $^{1}J_{HB} = 130$ Hz).

Elemental Analysis ($C_7H_{12}BIN_2$) **[%]:** calc. C 32.10, H 4.62, N 10.70; found C 32.82, H 4.55, N 10.83.

8.5.2.5 Synthesis of $IMe_4{\cdot}BH_2I$

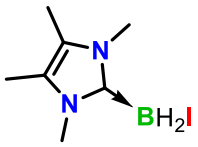

A Schlenk tube was charged with $IMe_4{\cdot}BH_3$ (272 mg, 1.97 mmol) and the solids dissolved in benzene. Then, a solution of I_2 (243 mg, 0.94 mmol) in benzene was added under cooling with a water bath (room temperature) and the reaction mixture stirred overnight at room temperature. Subsequently, all volatiles were removed *in vacuo*, yielding a slightly yellowish powder (511 mg, 97%).

^{1}H NMR (400.30 MHz, CD_2Cl_2, 298 K): 1.11 (s, 6 H, 2 × CH_3), 3.02 (s, 6 H, 2 × NCH_3), 3.10 (m, broad, 2 H, BH_2).

^{11}B{^{1}H} NMR (128.43 MHz, CD_2Cl_2, 298 K): -30.5 (s, broad).

^{11}B NMR (128.43 MHz, CD_2Cl_2, 298 K): -30.5 (t, broad, $^{1}J_{HB} = 102$ Hz).

Elemental Analysis ($C_7H_{14}BIN_2$) **[%]:** calc. C 31.86, H 5.35, N 10.61; found C 32.76, H 5.21, N 10.41.

8.5.2.6 Synthesis of $IDipp{\cdot}BH_2Bi(SiMe_3)_2$ (1a)

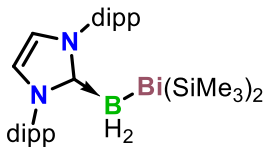

IDipp·BH_2I (212 mg, 0.4 mmol) was dissolved in tetrahydrofuran and cooled to -80 °C. Then, solid $KBi(SiMe_3)_2(THF)_{0.3}$ (250 mg, 0.6 mmol) was added. The solution was allowed to reach room temperature over 18 hours and the formation of a black suspension was observed. All volatiles were subsequently removed *in vacuo* and the residue suspended in toluene. The solution was filtered through a P4 glass frit covered with Celite and all volatiles removed *in vacuo*, yielding IDipp·$BH_2Bi(SiMe_3)_2$ as a black powder (169 mg, 56%).

^{1}H NMR (400.30 MHz, C_6D_6, 298 K): 0.53 (s, 18 H, 2 × Si(CH_3)$_3$, $^{2}J_{HSi} = 6.78$ Hz), 1.02 (d, 12 H, 4 × ^{i}Pr-CH_3, $^{3}J_{HH} = 6.92$ Hz), 1.47 (d, 12 H, 4 × ^{i}Pr-CH_3, $^{3}J_{HH} = 6.92$ Hz), 2.24 (q, broad, 2 H, BH_2, $^{1}J_{HB} \approx 100$ Hz), 2.28 (sep, 4 H, 4 × ^{i}Pr-C*H*, $^{3}J_{HH} = 6.92$ Hz), 6.34 (s, 2 H, NC*H*C*H*N), 7.14 (d, 4 H, 4 × aryl-C$_{meta}$*H*, $^{3}J_{HH} = 7.66$ Hz), 7.25 (t, 2 H, 2 × aryl-C$_{para}$H, $^{3}J_{HH} = 7.66$ Hz).

^{11}B{^{1}H} NMR (128.43 MHz, C_6D_6, 298 K): -42.1 (s, broad).

^{11}B NMR (128.43 MHz, C_6D_6, 298 K): -42.1 (t, very broad, $^{1}J_{HB} \approx 100$ Hz).

LIFDI-MS (*m/z*): 756.44 ([M]$^+$, 89%), 389.31 ([IDipp-H]$^+$, 100%).

Elemental Analysis ($C_{33}H_{56}BBiN_2Si_2$+ 0.1 Bi) **[%]:** calc. C 50.97, H 7.26, N 3.60; found C 50.37, H 7.07, N 3.55. Elemental bismuth results from sample decomposition at room temperature.

8.5.2.7 Synthesis of $IMe_4{\cdot}BH_2Bi(SiMe_3)_2$ (1b)

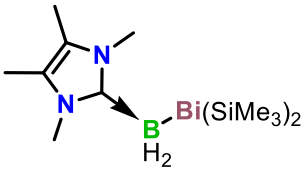

$IMe_4{\cdot}BH_2I$ (40 mg, 0.15 mmol) was dissolved in tetrahydrofuran and cooled to -80 °C. Then, solid $KBi(SiMe_3)_2(THF)_{0.3}$ (94 mg, 0.23 mmol) was added. The solution was allowed to reach room temperature over 18 hours and the formation of a black precipitate was observed. All volatiles were subsequently removed *in vacuo* and the residue suspended in *n*-hexane. The solution was filtered through a P4 glass frit covered with Celite. The black-brown solution was collected, and all volatiles were removed *in vacuo*, yielding the product as a sticky black-brown powder (61 mg, 83%). Single crystals suitable for X-ray structure determination were obtained by storing a saturated solution of $IMe_4{\cdot}BH_2Bi(SiMe_3)_2$ in *n*-hexane at -30 °C overnight.

^{1}H NMR (400.30 MHz, C_6D_6, 298 K): 0.81 (s, 18 H, 2 × Si(C*H*$_3$)$_3$, $^2J_{HSi}$ = 6.73 Hz), 1.09 (s, 6 H, 2 × C(C*H*$_3$)), 2.43 (q, very broad, 2 H, B*H*$_2$, $^1J_{HB} \approx$ 107 Hz), 2.90 (s, 6 H, 2 × N(C*H*$_3$)).

^{11}B{^{1}H} NMR (128.43 MHz, C_6D_6, 298 K): -39.5 (s, broad).

^{11}B NMR (128.43 MHz, C_6D_6, 298 K): -39.5 (t, broad, $^1J_{HB}$ = 107 Hz).

LIFDI-MS (*m/z*): 492.20 ([M]$^+$, 10%), 261.20 ([$(IMe_4)_2BH_2$]$^+$, 40%), 247.20 ([$(IMe_4)_2$-H]$^+$, 100%).

Elemental Analysis ($C_{13}H_{32}BBiN_2Si_2$) **[%]:** calc. C 31.69, H 6.55, N 5.69; found C 31.61, H 6.24, N 5.66.

8.5.2.8 Synthesis of $DMAP{\cdot}BH_2Bi(SiMe_3)_2$ (1c)

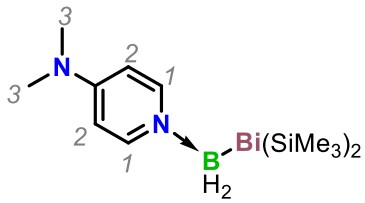

$DMAP{\cdot}BH_2I$ (39 mg, 0.15 mmol) was dissolved in toluene and cooled to -80 °C. Then, solid $KBi(SiMe_3)_2(THF)_{0.3}$ (75 mg, 0.18 mmol) was added to the solution. The mixture was stirred overnight in the cooling bath. Afterwards, the suspension was filtered through a P3 glass frit covered with Celite and the volatiles removed *in vacuo*, yielding $DMAP{\cdot}BH_2Bi(SiMe_3)_2$ as a brown powder (10 mg, 13%).

^{1}H NMR (400.30 MHz, C_6D_6, 298 K): 0.99 (s, 18 H, 2 × Si(C*H*$_3$)$_3$, $^2J_{HSi}$ = 6.98 Hz), 1.83 (s, 6 H, C3*H*), 4.86 (q, 2 H, $^1J_{BH} \approx$ 120 Hz, B*H*$_2$), 5.40 (m, 2 H, C2*H*), 8.05 (m, 2 H, C1*H*).

^{11}B{^{1}H} NMR (128.43 MHz, C_6D_6, 298 K): -15.4 (s, broad).

^{11}B NMR (128.43 MHz, C_6D_6, 298 K): -15.4 (t, very broad, $^1J_{HB} \approx$ 120 Hz).

LIFDI-MS (*m/z*): could not be performed due to too fast sample decomposition.

Elemental Analysis ($C_{13}H_{30}BBiN_2Si_2$) **[%]:** could not be performed, as it was not possible to prepare an analytically clean sample of **1c** due to its extreme sensitivity and electrostatic nature.

8.5.2.9 Synthesis of IDipp·GaH$_2$Bi(SiMe$_3$)$_2$ (2)

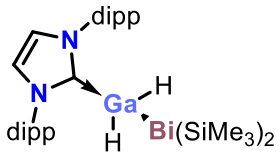

IDipp·GaH$_2$(OTf) (91 mg, 0.15 mmol) was dissolved in tetrahydrofuran and cooled to -80 °C. Then, solid KBi(SiMe$_3$)$_2$(THF)$_{0.3}$ (112 mg, 0.27 mmol) was added in one portion. The solution was allowed to reach room temperature over 18 hours and the formation of a black precipitate was observed. All volatiles were subsequently removed *in vacuo* and the residue suspended in *n*-hexane. The solution was filtered through a P4 glass frit covered with Celite. After removing the solvent *in vacuo*, IDipp·GaH$_2$Bi(SiMe$_3$)$_2$ could be obtained as a black powder (19 mg, 16%). Single crystals of **2** suitable for X-ray structure determination could be grown by slow evaporation of a solution of **2** in *n*-pentane at -80 °C under reduced pressure.

^{1}H NMR (300.13 MHz, C$_6$D$_6$, 298 K): 0.70 (s, 18 H, 2 × Si(C*H*$_3$)$_3$, $^2J_{HSi}$ = 7.15 Hz), 0.98 (d, 12 H, 4 × ^{i}Pr-C*H*$_3$, $^3J_{HH}$ = 6.89 Hz), 1.44 (d, 12 H, 4 × ^{i}Pr-CH$_3$, $^3J_{HH}$ = 6.89 Hz), 2.69 (sep, 4 H, 4 × ^{i}Pr-C*H*, $^3J_{HH}$ = 6.89 Hz), 4.97 (s, broad, 2 H, Ga*H*$_2$), 6.43 (s, 2 H, NC*H*C*H*N), 7.10 (d, superimposed, 4 H, 4 × aryl-C$_{meta}$*H*, $^3J_{HH}$ = 7.13 Hz), 7.25 (dd, 2 H, 2 × aryl-C$_{para}$H, $^3J_{HH}$ = 7.18 Hz, $^3J_{HH}$ = 8.56 Hz).

LIFDI-MS (*m/z*): 814.34 ([(M]$^+$, 46%), 459.24 ([IDipp-GaH$_2$]$^+$, 100%), 389.31 ([IDipp-H]$^+$, 31%).

Elemental Analysis ($C_{33}H_{56}GaBiN_2Si_2$) **[%]:** calc. C 48.59, H 6.92, N 3.43; found C 48.56, H 6.89, N 3.27.

8.5.2.10 Desilylation attempts of IDipp·BH$_2$Bi(SiMe$_3$)$_2$ with 1,4-benzoquinone/MeOH-*d*$_4$

Note: this experiment was conducted under exclusion of light to avoid decomposition of any forming Bi-D/Bi-H containing species.

A J.-Young tube was charged with IDipp·BH$_2$Bi(SiMe$_3$)$_2$ (83 mg, 0.12 mmol) and cooled to -80 °C. Then, a cold (-80 °C) solution of 1,4-benzoquinone (12 mg, 0.12 mmol) in 0.6 mL THF and 0.1 mL MeOH-*d*$_4$ was added to the tube. After vigorous shaking, the sample was submitted to variable-temperature NMR experiments. At $T < 0$ °C, no reaction was observed. Thus, the sample was warmed to room temperature and the NMR spectra were recorded subsequently (see below).

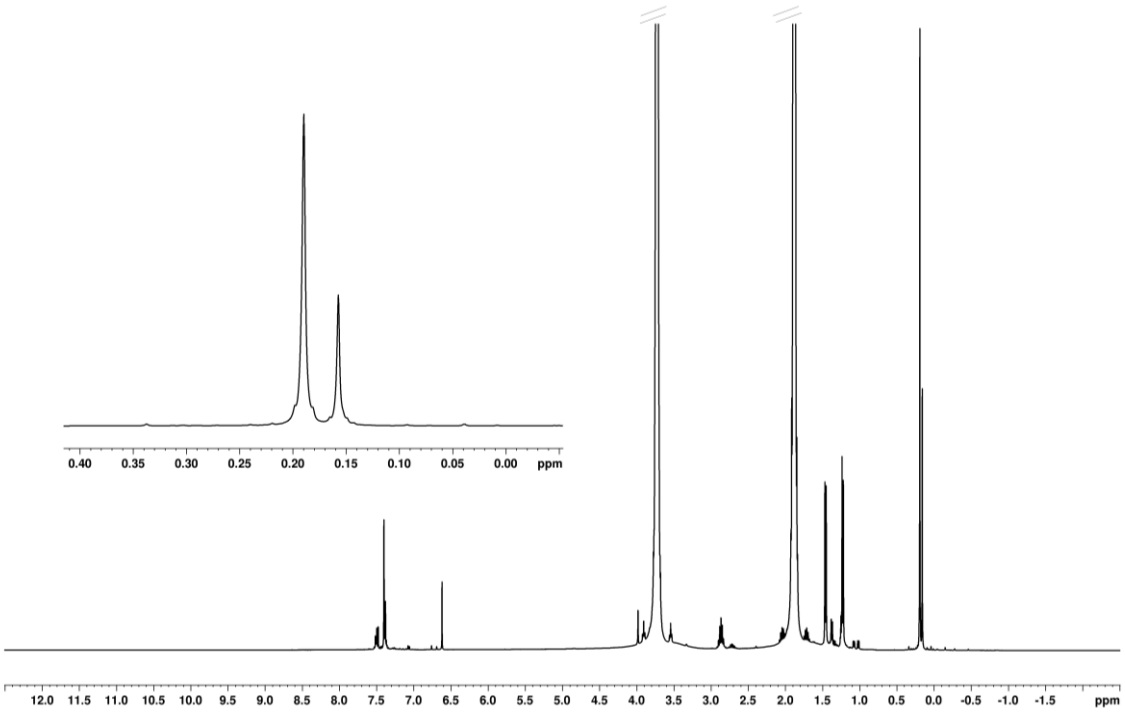

Figure S 8.1: ^{1}H NMR spectrum of the reaction mixture of IDipp·$BH_2Bi(SiMe_3)_2$ with 1,4-benzoquinone and MeOH-d_4 (298 K; truncated signals correspond to tetrahydrofuran). The zoomed region shows a second resonance of {$SiMe_3$} groups.

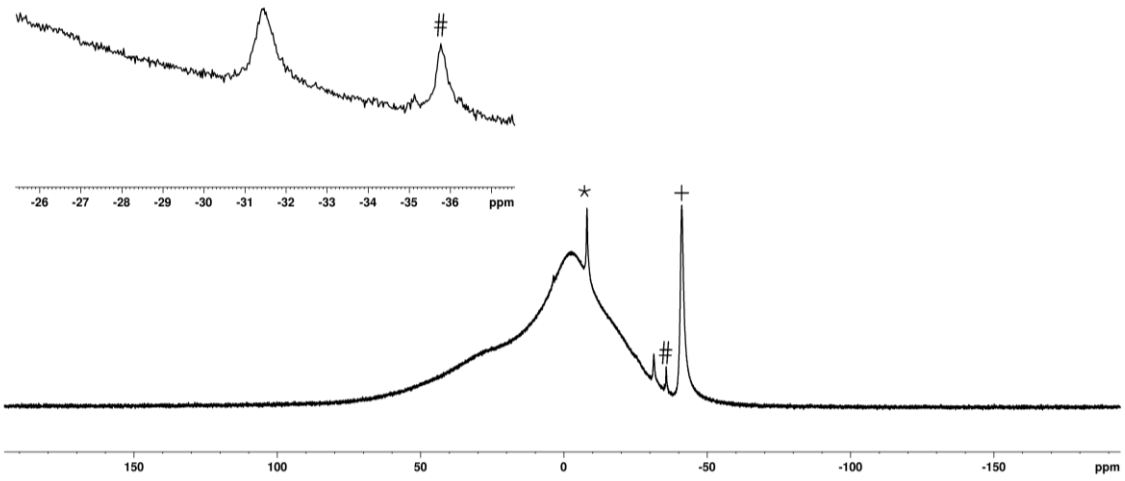

Figure S 8.2: $^{11}B\{^{1}H\}$ NMR spectrum of the reaction mixture of IDipp·$BH_2Bi(SiMe_3)_2$ with 1,4-benzoquinone and MeOH-d_4 (298 K, * = IDipp·BH_2OMe, # = IDipp·BH_3, + = starting material).

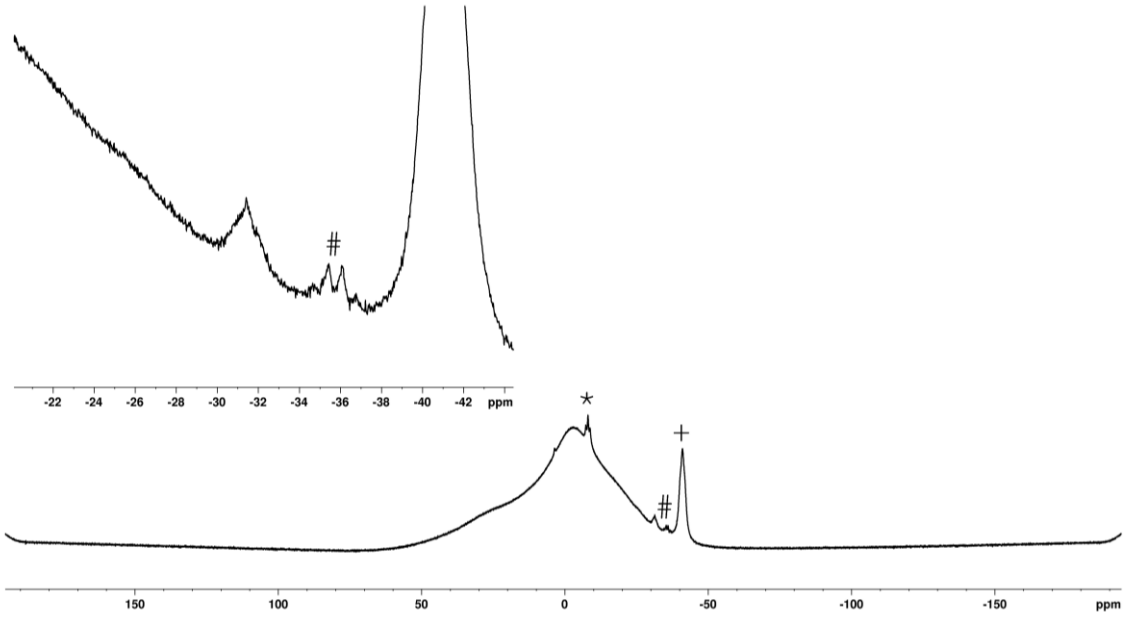

Figure S 8.3: ^{11}B NMR spectrum of the reaction mixture of IDipp·$BH_2Bi(SiMe_3)_2$ with 1,4-benzoquinone and MeOH-d_4 (298 K, * = IDipp·BH_2OMe, # = IDipp·BH_3, + = starting material).

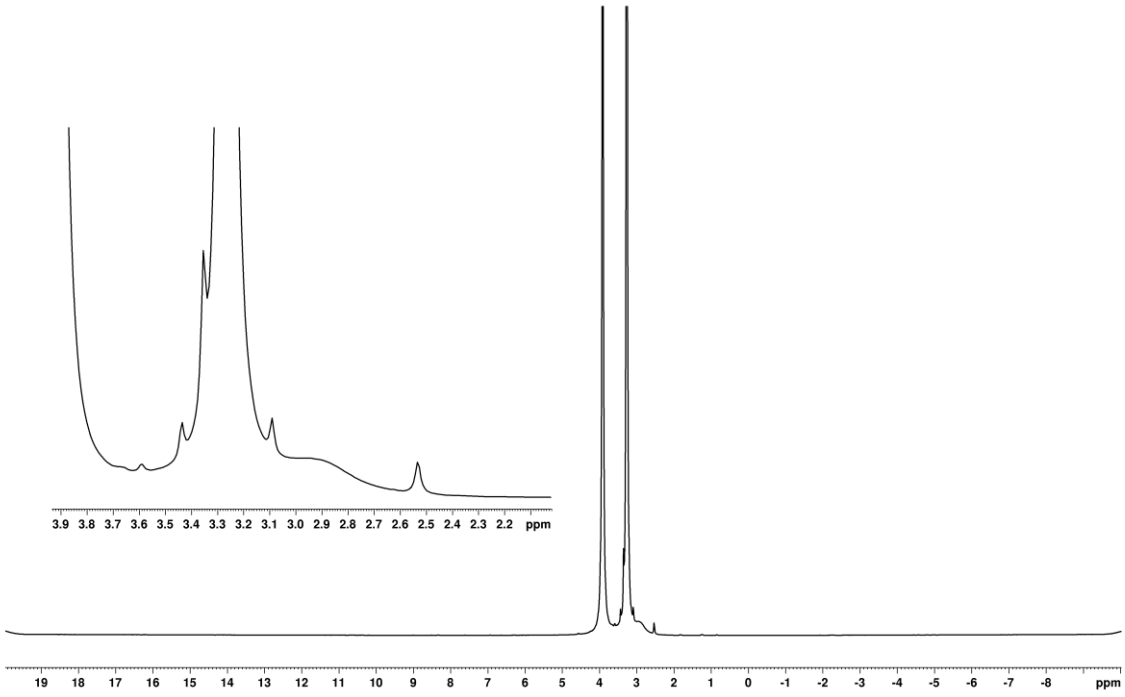

Figure S 8.4: ^{2}H NMR spectrum of the reaction mixture of IDipp·$BH_2Bi(SiMe_3)_2$ with 1,4-benzoquinone and MeOH-d_4 (298 K).

8.5.3 NMR Data

8.5.3.1 $KBi(SiMe_3)_2(THF)_{0.3}$

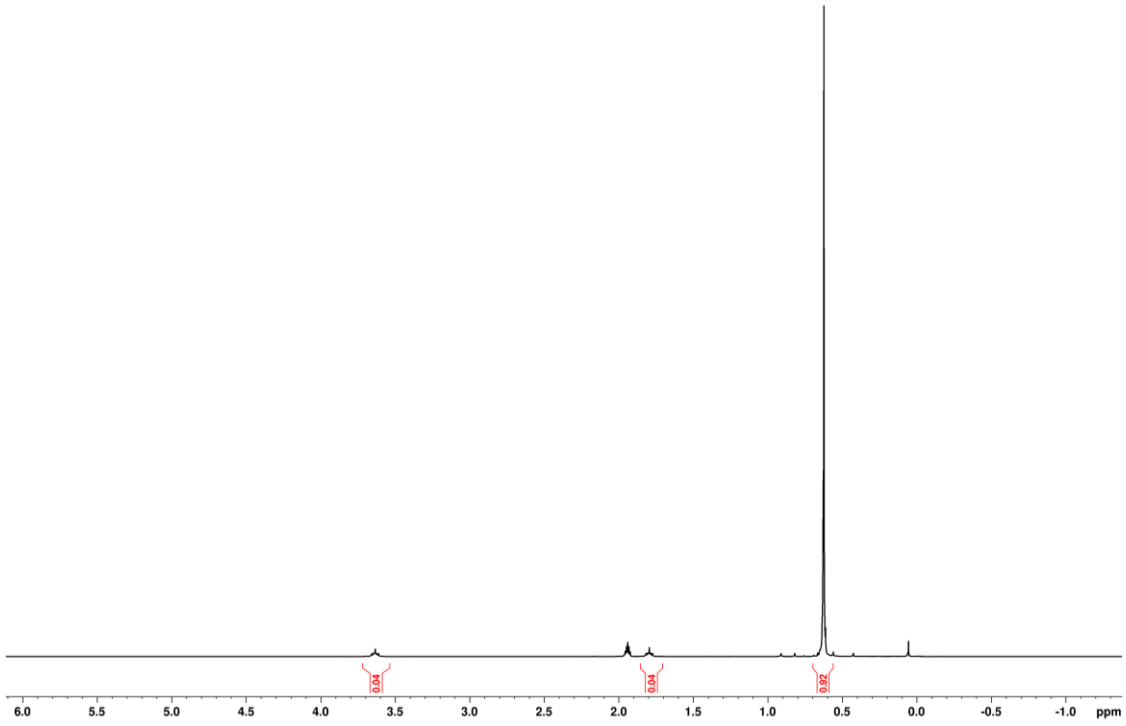

Figure S 8.5: ^{1}H NMR spectrum of $KBi(SiMe_3)_2(THF)_{0.3}$ (CD_3CN, 298 K).

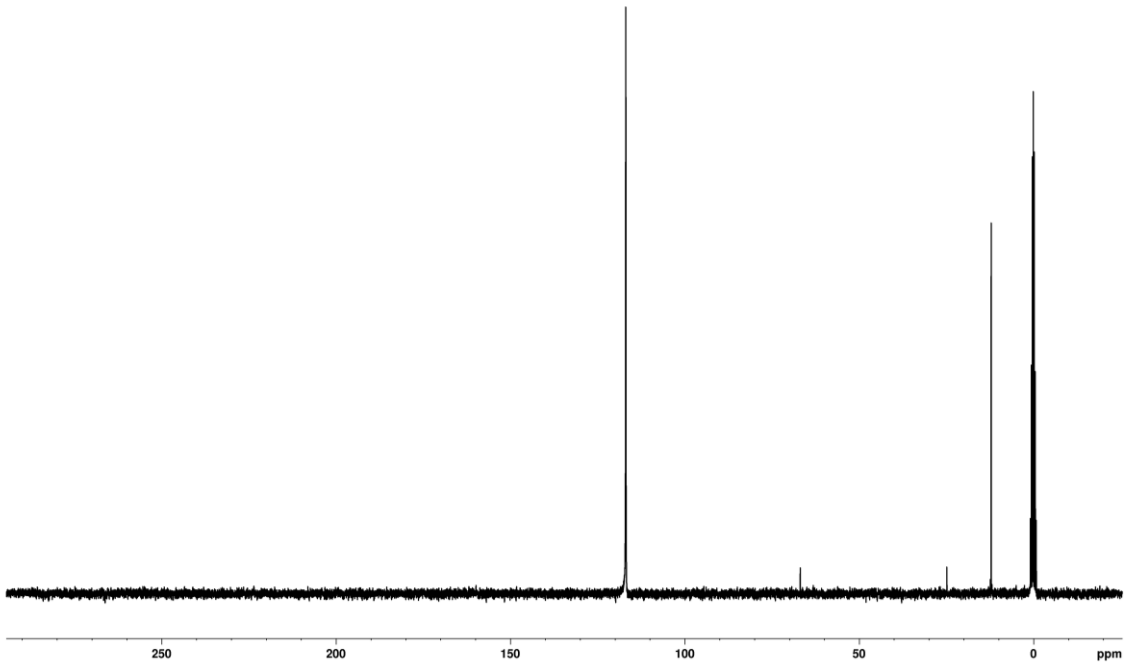

Figure S 8.6: $^{13}C\{^{1}H\}$ NMR spectrum of $KBi(SiMe_3)_2(THF)_{0.3}$ (CD_3CN, 298 K).

8.5.3.2 DMAP·BH_3

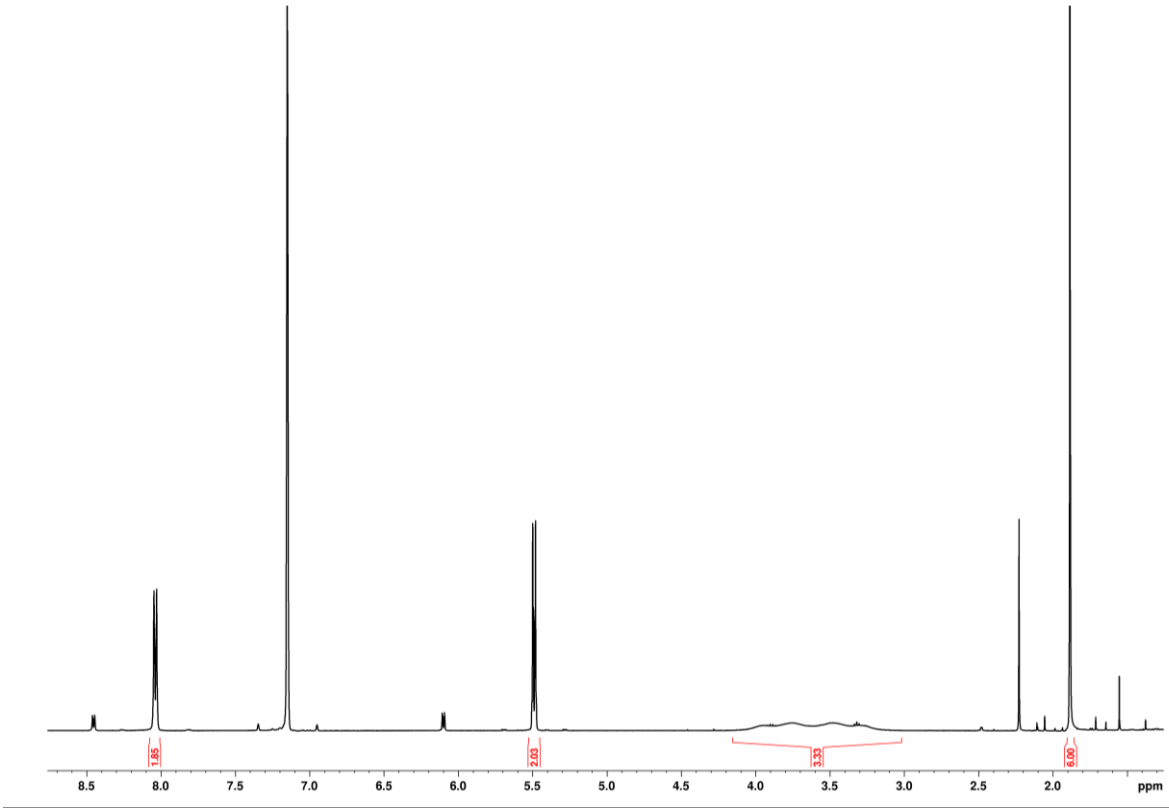

Figure S 8.7: ^{1}H NMR spectrum of DMAP·BH_3 (C_6D_6, 298 K).

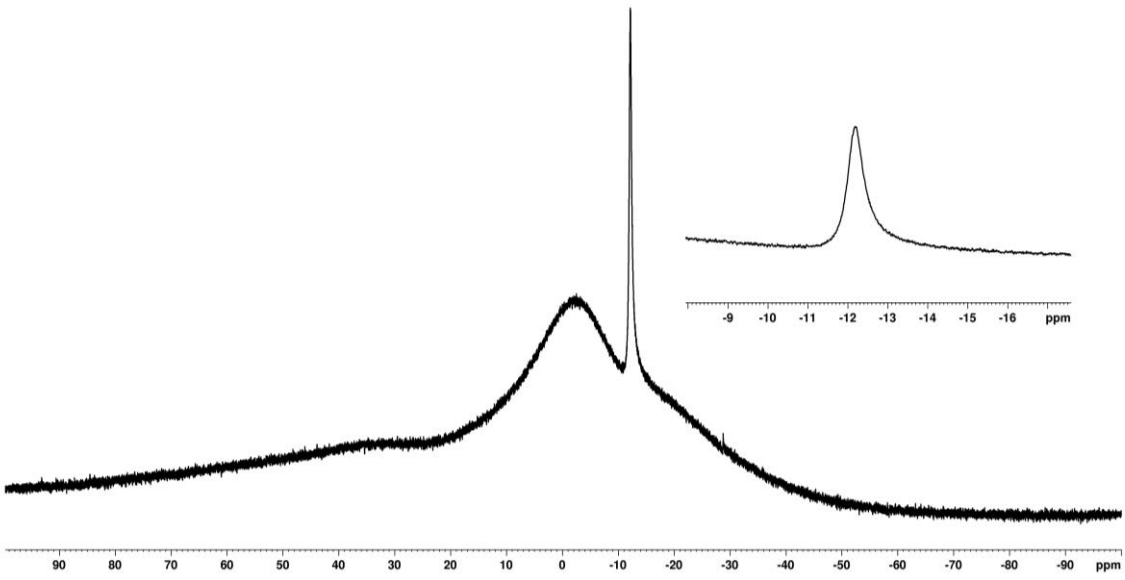

Figure S 8.8: $^{11}B\{^{1}H\}$ NMR spectrum of DMAP·BH_3 (C_6D_6, 298 K).

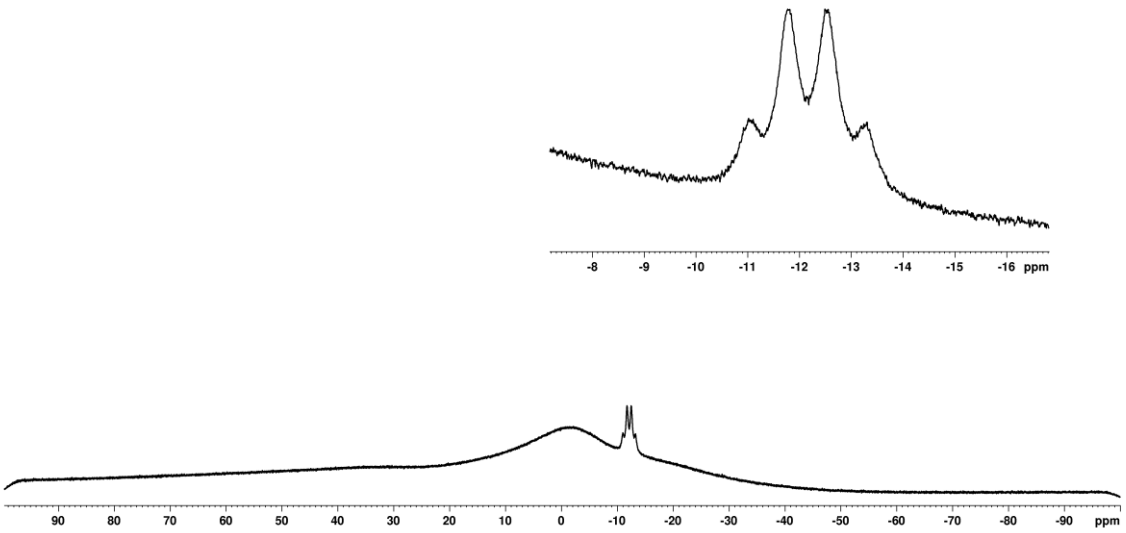

Figure S 8.9: ^{11}B NMR spectrum of DMAP·BH_3 (C_6D_6, 298 K).

8.5.3.3 $IMe_4{\cdot}BH_2I$

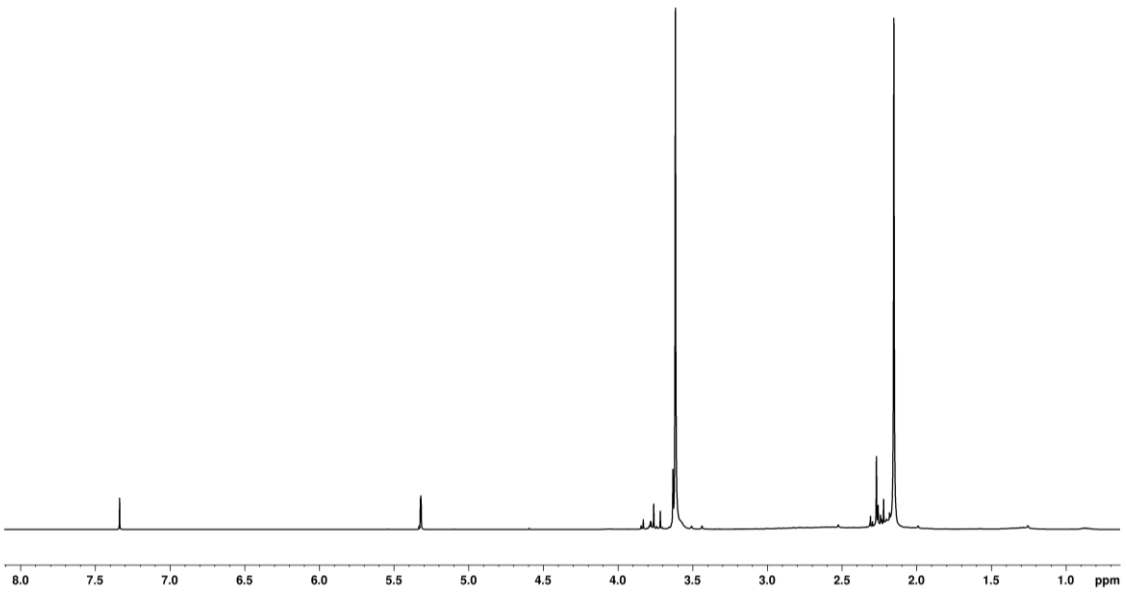

Figure S 8.10: ^1H NMR spectrum of $IMe_4{\cdot}BH_2I$ (CD_2Cl_2, 298 K).

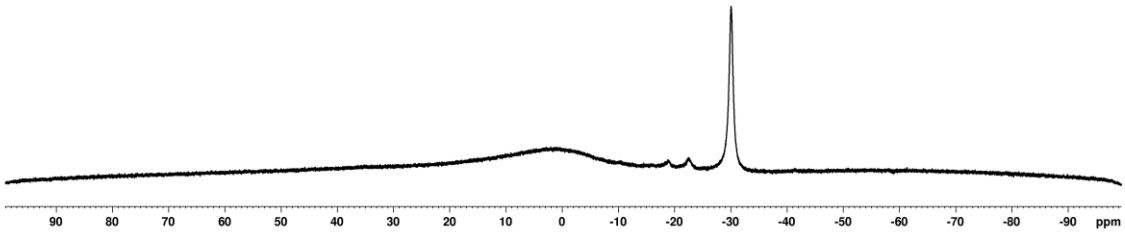

Figure S 8.11: $^{11}B\{^{1}H\}$ NMR spectrum of $IMe_4{\cdot}BH_2I$ (CD_2Cl_2, 298 K).

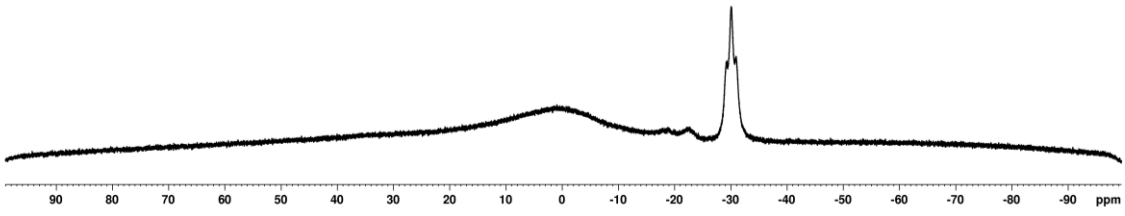

Figure S 8.12: ^{11}B NMR spectrum of $IMe_4{\cdot}BH_2I$ (CD_2Cl_2, 298 K).

8.5.3.4 DMAP·BH_2I

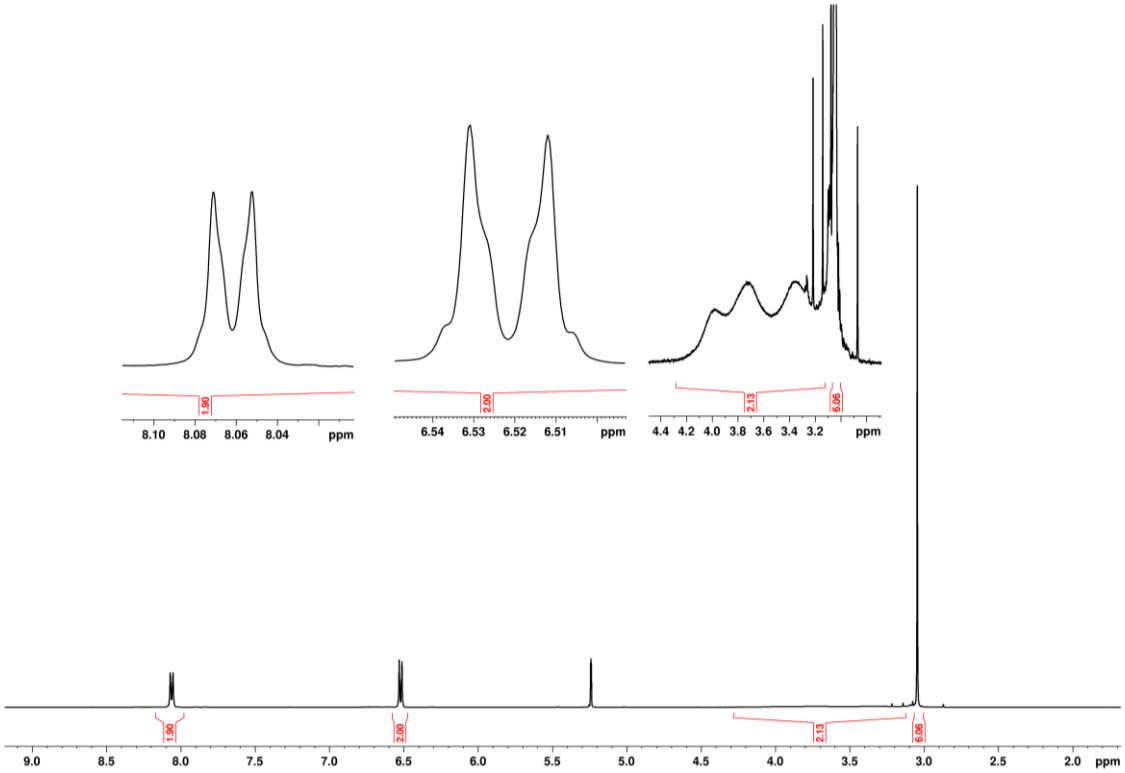

Figure S 8.13: ^{1}H NMR spectrum of DMAP·BH_2I (C_6D_6, 298 K).

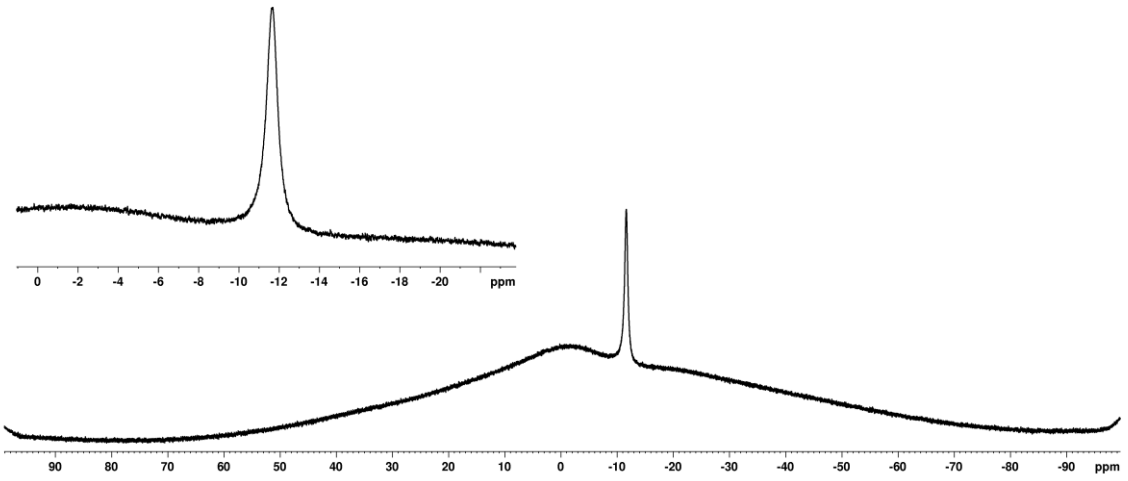

Figure S 8.14: $^{11}B\{^{1}H\}$ NMR spectrum of DMAP·BH_2I (CD_2Cl_2, 298 K).

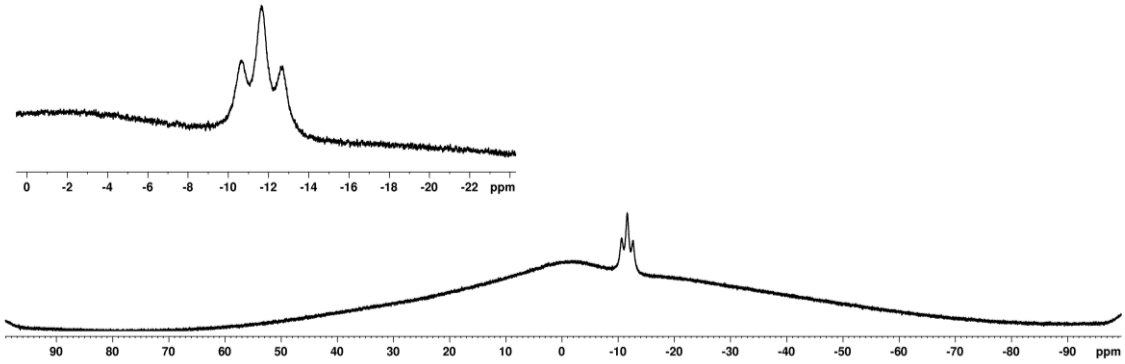

Figure S 8.15: ^{11}B NMR spectrum of DMAP·BH_2I (CD_2Cl_2, 298 K).

8.5.3.5 DMAP·$BH_2Bi(SiMe_3)_2$

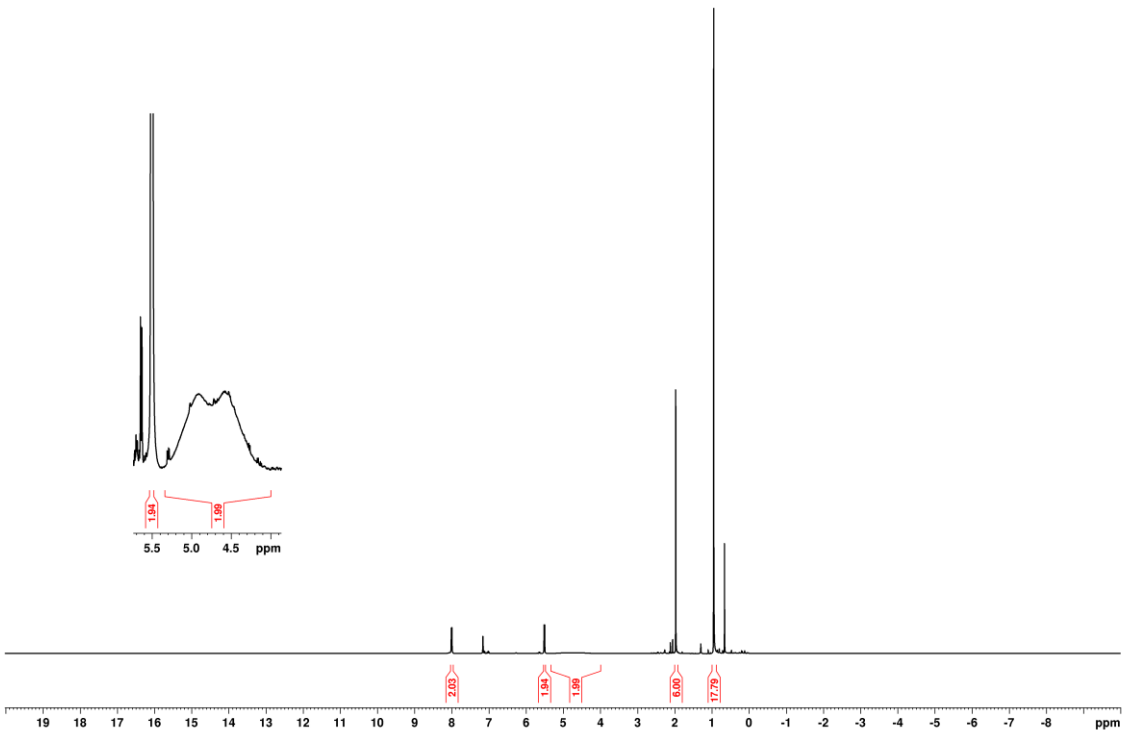

Figure S8.16: ^1H NMR spectrum of DMAP·$BH_2Bi(SiMe_3)_2$ (C_6D_6, 298 K).

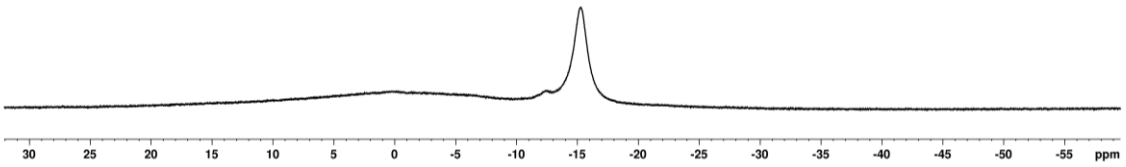

Figure S 8.17: $^{11}B\{^{1}H\}$ NMR spectrum of DMAP·$BH_2Bi(SiMe_3)_2$ (C_6D_6, 298 K).

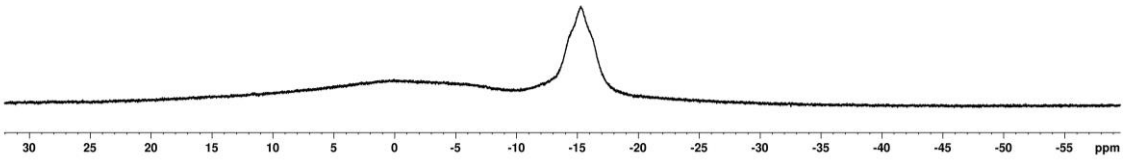

Figure S 8.18: ^{11}B NMR spectrum of DMAP·$BH_2Bi(SiMe_3)_2$ (C_6D_6, 298 K).

8.5.3.6 IDipp·$BH_2Bi(SiMe_3)_2$

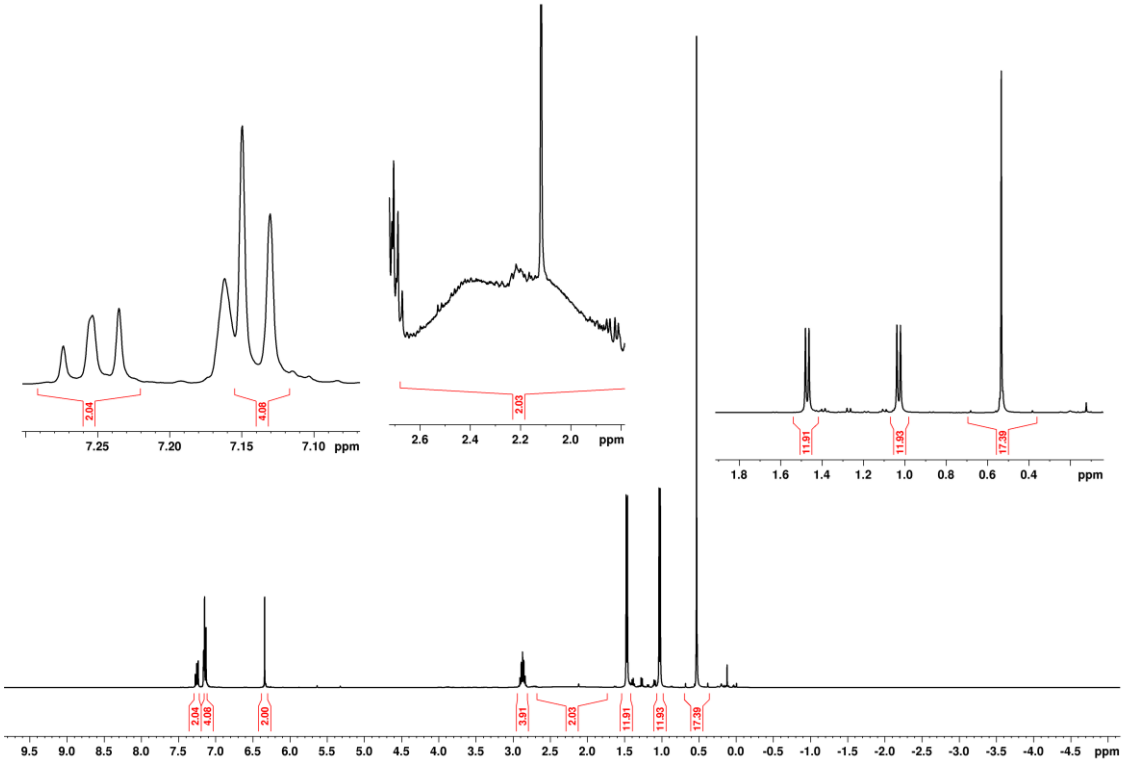

Figure S 8.19: ^{1}H NMR spectrum of IDipp·$BH_2Bi(SiMe_3)_2$ (C_6D_6, 298 K).

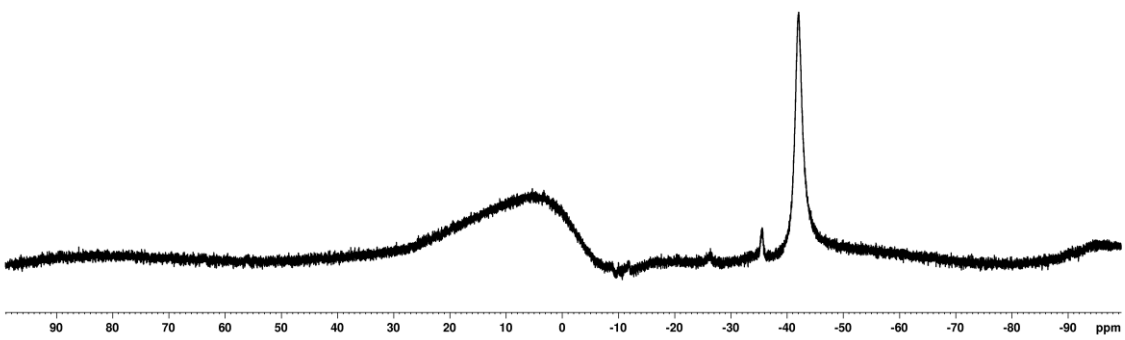

Figure S 8.20: $^{11}B\{^{1}H\}$ NMR spectrum of IDipp·$BH_2Bi(SiMe_3)_2$ (C_6D_6, 298 K).

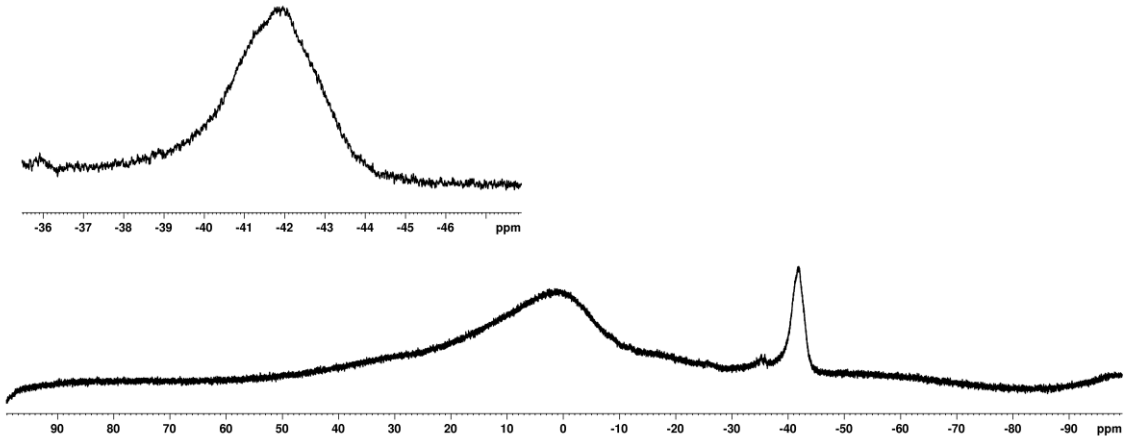

Figure S 8.21: ^{11}B NMR spectrum of IDipp·$BH_2Bi(SiMe_3)_2$ (C_6D_6, 298 K).

8.5.3.7 IMe_4·$BH_2Bi(SiMe_3)_2$

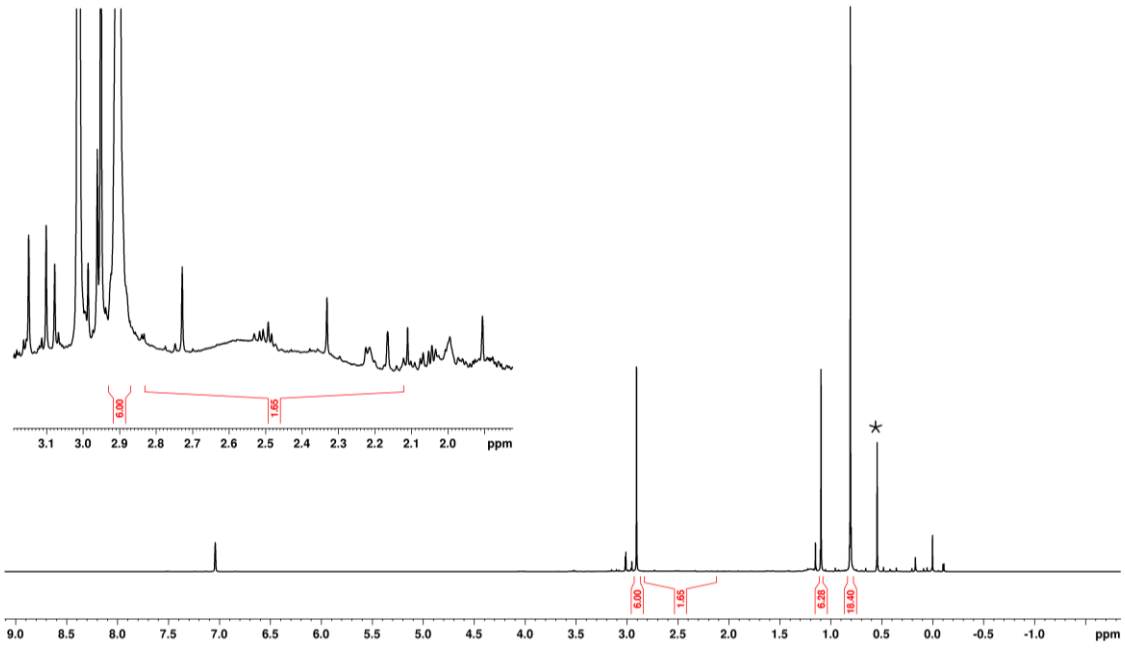

Figure S 8.22: ^{1}H NMR spectrum of IMe_4·$BH_2Bi(SiMe_3)_2$ (C_6D_6, 298 K, * = IMe_4·BH_3).

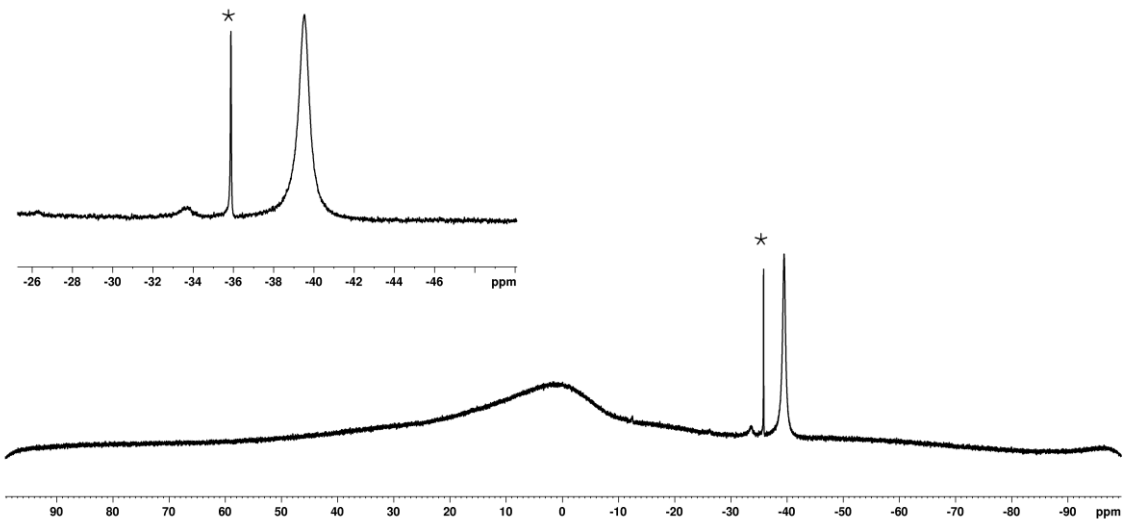

Figure S 8.23: $^{11}B\{^{1}H\}$ NMR spectrum of $IMe_4{\cdot}BH_2Bi(SiMe_3)_2$ (C_6D_6, 298 K, * = $IMe_4{\cdot}BH_3$).

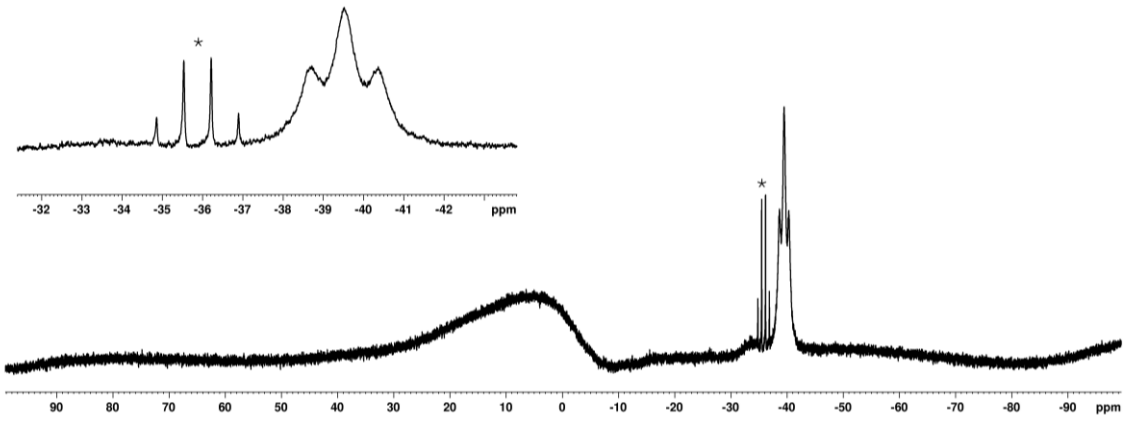

Figure S 8.24: ^{11}B NMR spectrum of $IMe_4{\cdot}BH_2Bi(SiMe_3)_2$ (C_6D_6, 298 K, * = $IMe_4{\cdot}BH_3$).

8.5.3.8 Crude NMR spectra of desilylation attempt

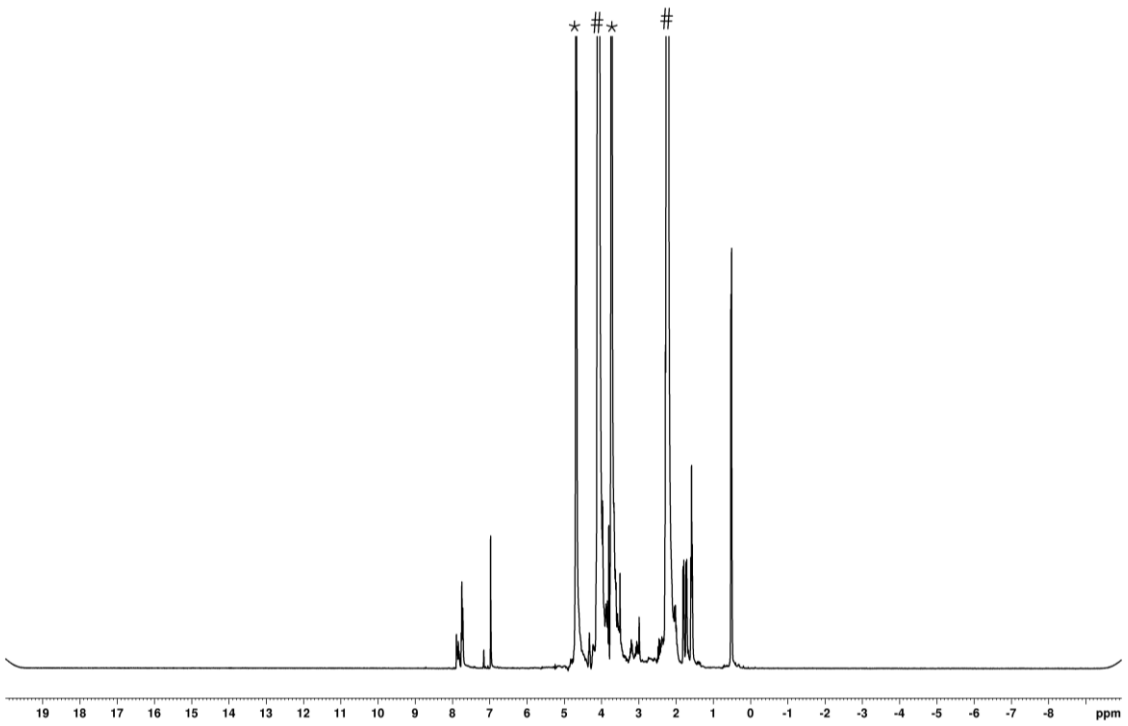

Figure S 8.25: ^{1}H NMR spectrum of the reaction mixture of IDipp·$BH_2Bi(SiMe_3)_2$ with benzoquinone in THF/MeOH (C_6D_6-cap., 298 K).

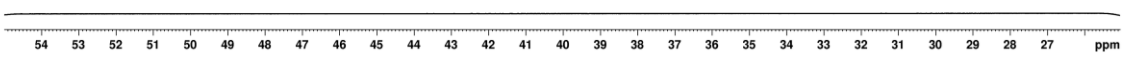

Figure S 8.26: Expanded ^{1}H NMR spectrum (> 20 ppm) of the reaction mixture of IDipp·$BH_2Bi(SiMe_3)_2$ with benzoquinone in THF/MeOH, showing no signs of Bi-H moieties (C_6D_6-cap., 298 K).

8.5.3.9 IDipp·GaH$_2$Bi(SiMe$_3$)$_2$

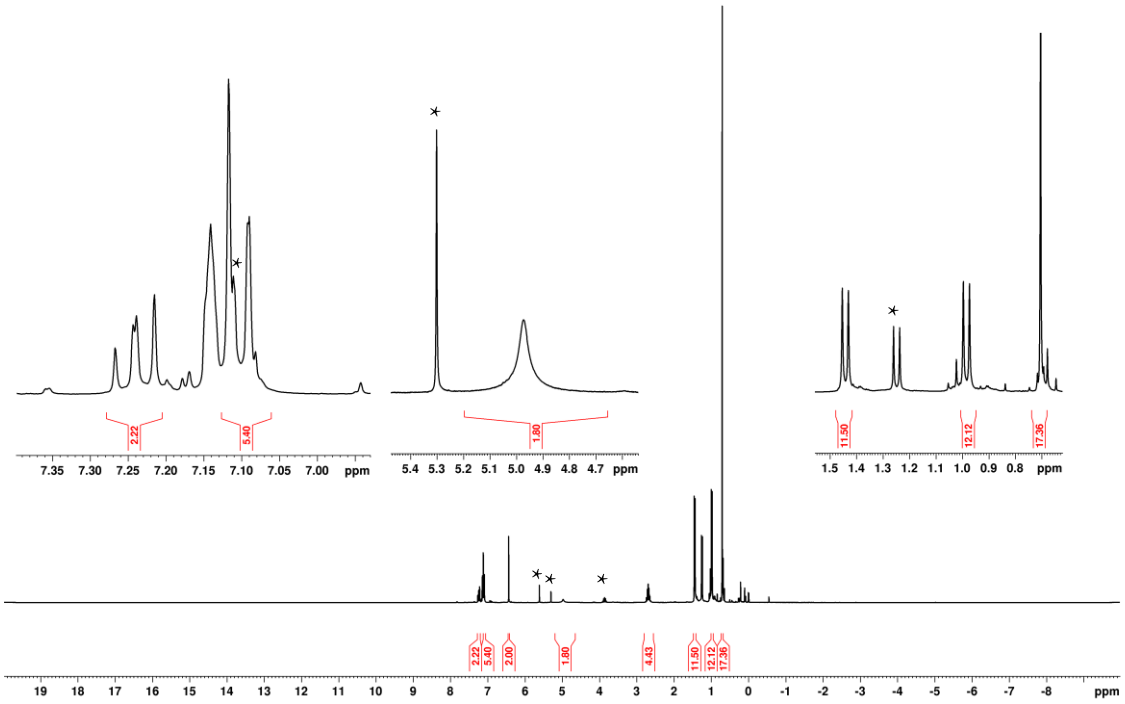

Figure S 8.27: ^{1}H NMR spectrum of IDipp·GaH$_2$Bi(SiMe$_3$)$_2$ (C$_6$D$_6$, 298 K, * = IDipp-H$_2$).

8.5.4 Mass spectra

8.5.4.1 IDipp·$BH_2Bi(SiMe_3)_2$

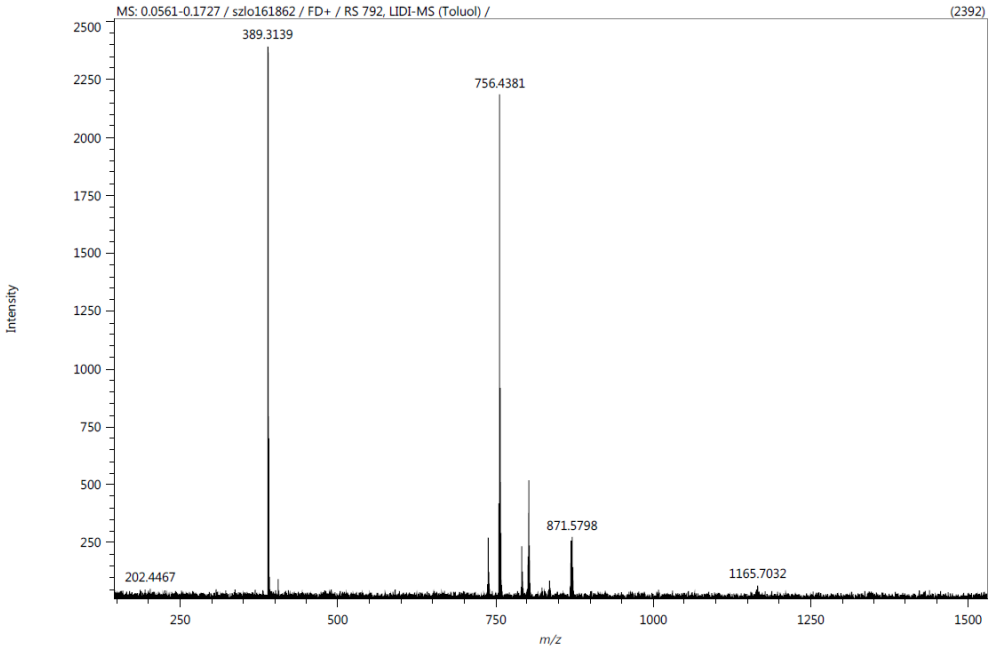

Figure S 8.28: LIFDI-MS spectrum of a solution of IDipp·$BH_2Bi(SiMe_3)_2$ in toluene.

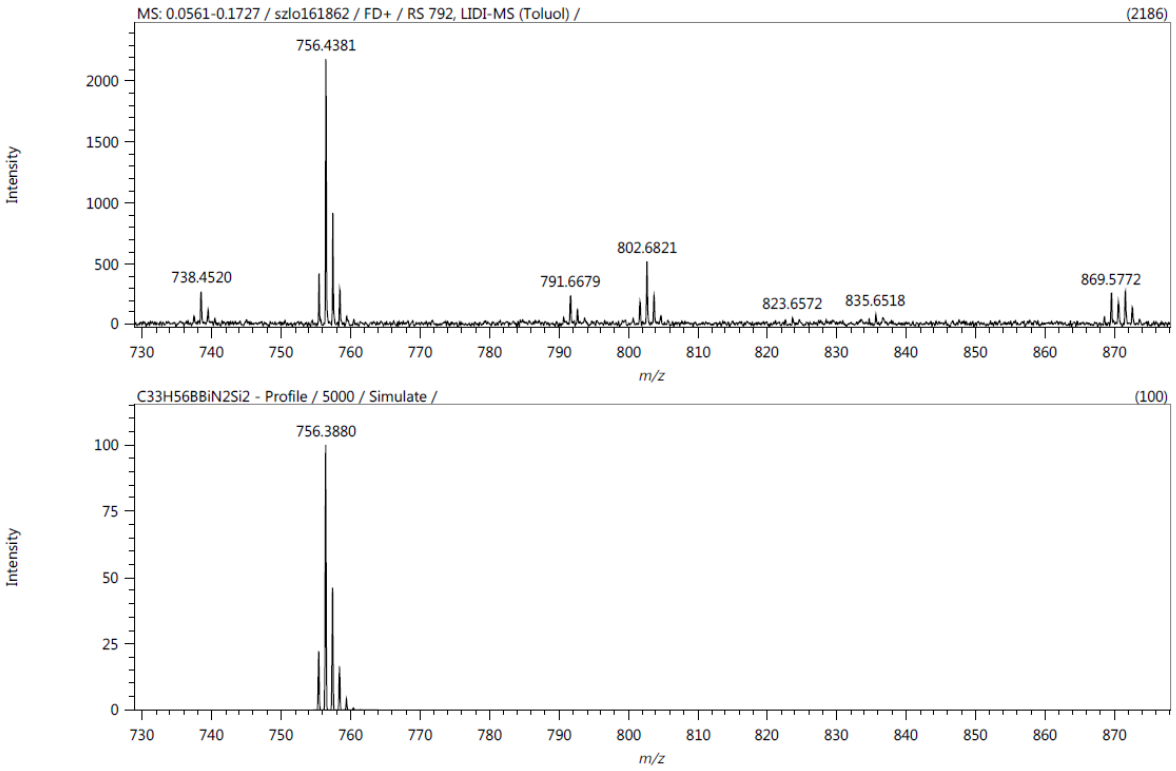

Figure S 8.29: Zoomed region within the LIFDI-MS spectrum of a solution of IDipp·$BH_2Bi(SiMe_3)_2$ in toluene (top: experiment, bottom: simulated product signal).

8.5.4.2 $IMe_4{\cdot}BH_2Bi(SiMe_3)_2$

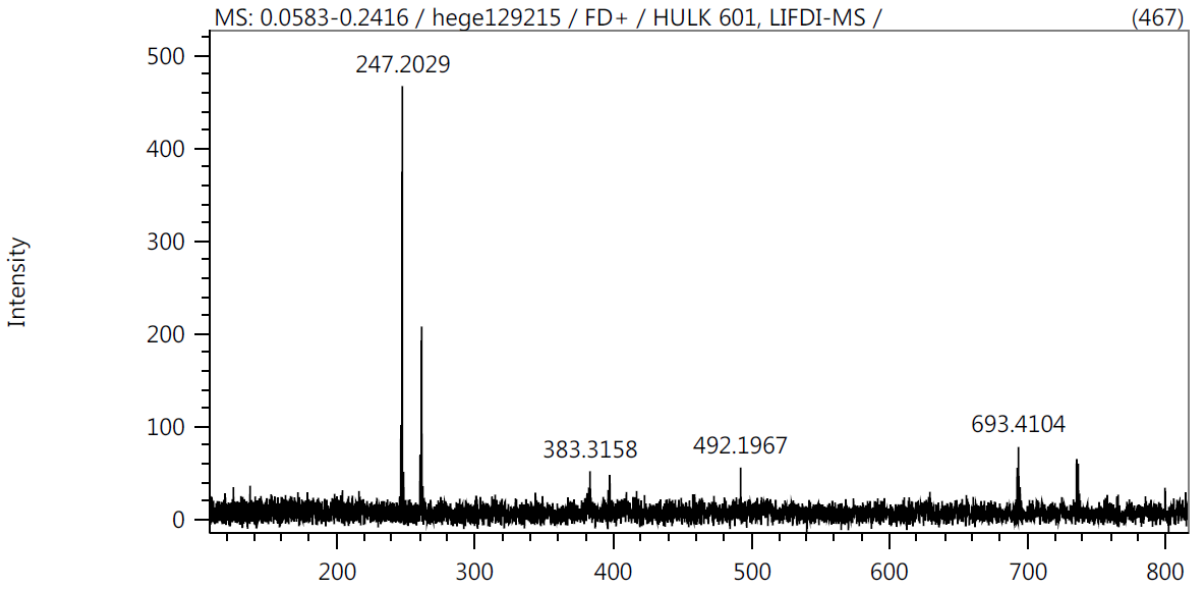

Figure S 8.30: LIFDI-MS spectrum of a solution of $IMe_4{\cdot}BH_2Bi(SiMe_3)_2$ in toluene.

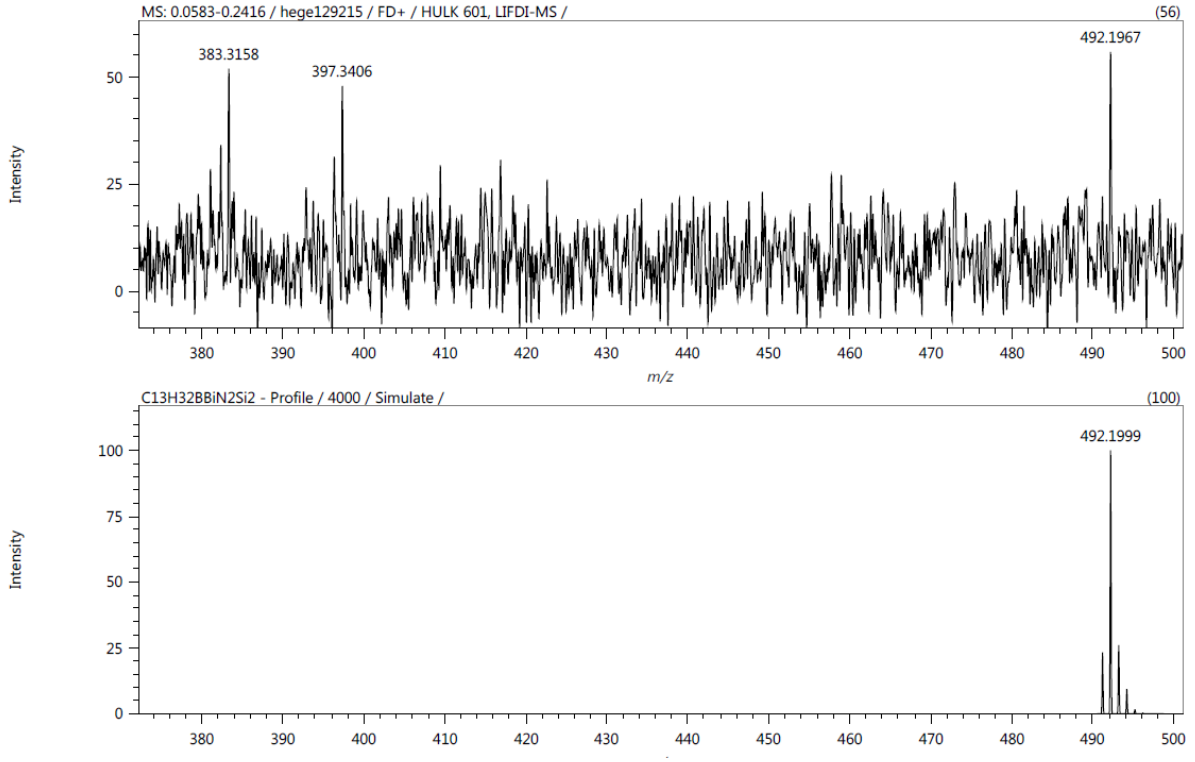

Figure S 8.31: Zoomed region within the LIFDI-MS spectrum of a solution of $IMe_4{\cdot}BH_2Bi(SiMe_3)_2$ in toluene (top: experiment, bottom: simulated product signal).

8.5.4.3 IDipp·GaH$_2$Bi(SiMe$_3$)$_2$

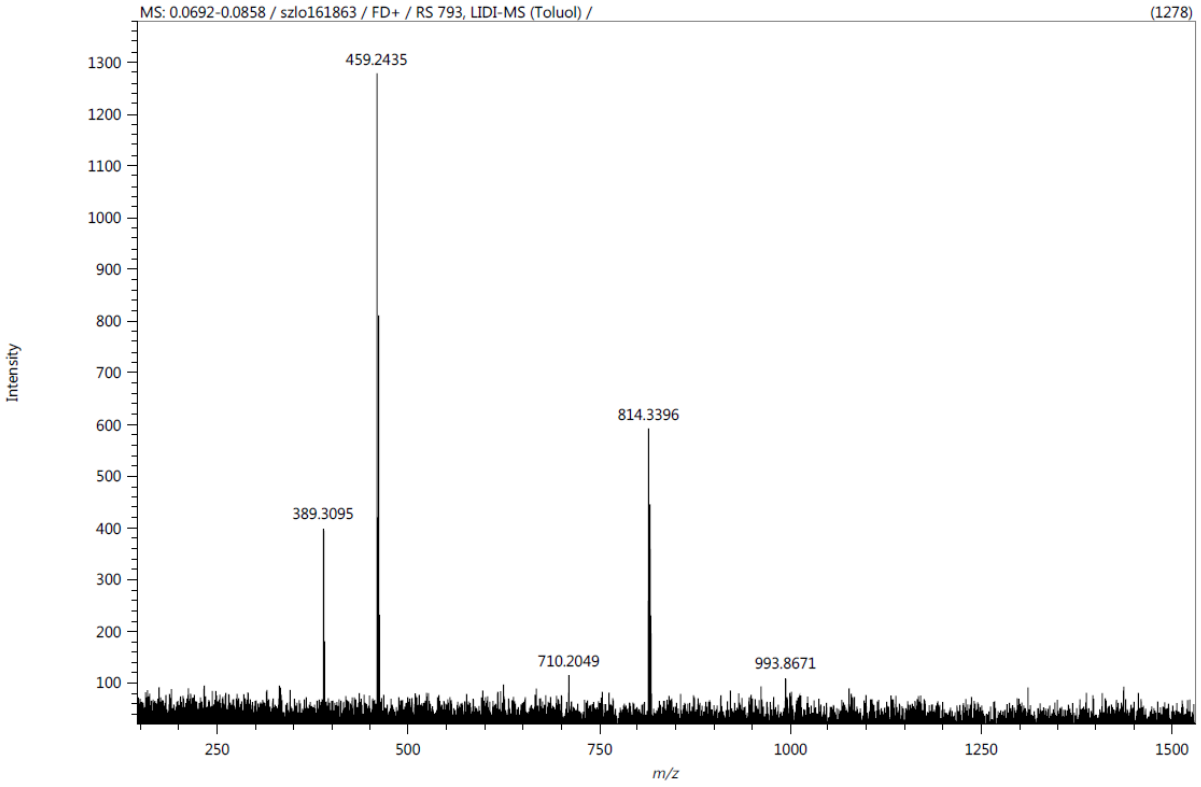

Figure S 8.32: LIFDI-MS spectrum of a solution of IDipp·GaH$_2$Bi(SiMe$_3$)$_2$ in toluene.

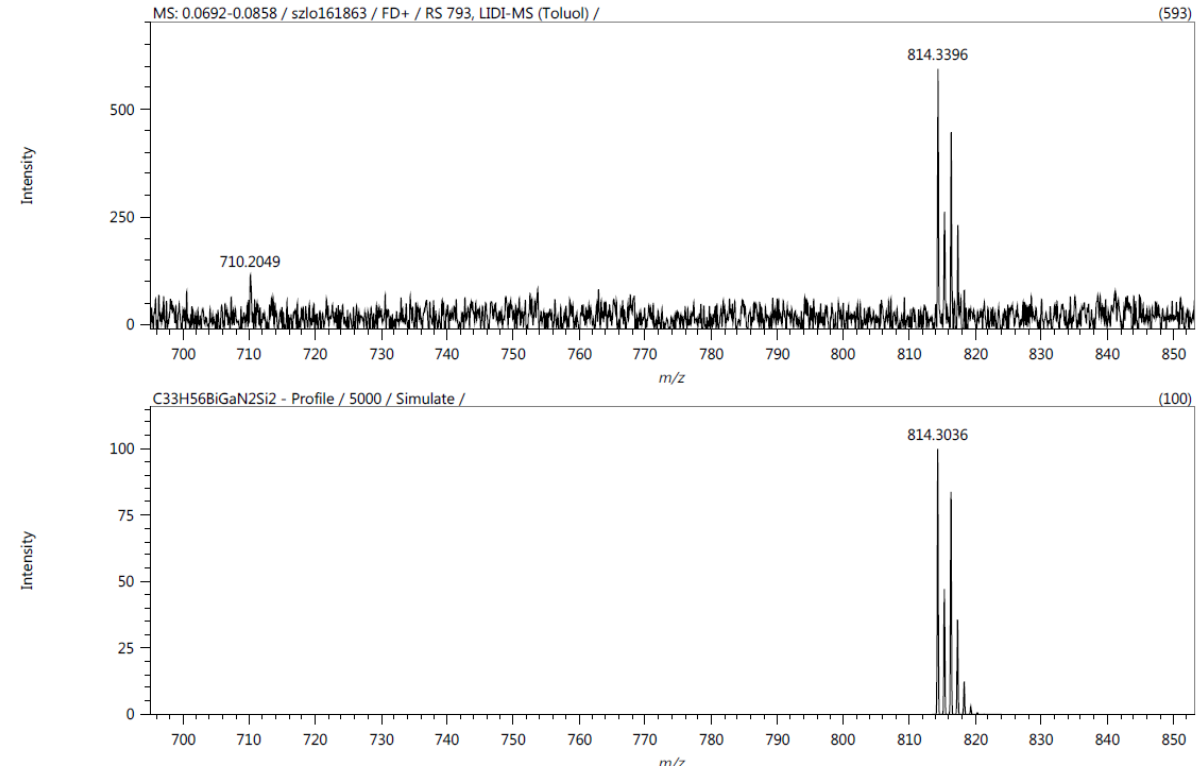

Figure S 8.33: Zoomed region within the LIFDI-MS spectrum of a solution of IDipp·GaH$_2$Bi(SiMe$_3$)$_2$ in toluene (top: experiment, bottom: simulated product signal).

8.5.5 Crystallographic Data

Single Crystal X-ray structure determination: Single-crystal X-ray diffraction data sets were collected using an Oxford Diffraction GV50 diffractometer (**1b**, **1c**) or a Rigaku XtaLAB Synergy R, DW system diffractometer (**1a**, **2**) equipped with a HyPix-Arc 150 detector operating at T = 123.01(10) K. Crystals were selected under mineral oil. Data reduction, scaling and absorption corrections were performed using CrysAlisPro (Rigaku, V1.171.41.90a, 2020). A gaussian absorption correction was performed using CrysAlisPro 1.171.41.90a (Rigaku Oxford Diffraction, 2020). Numerical absorption correction based on gaussian integration over a multifaceted crystal model. Empirical absorption correction using spherical harmonics, implemented in SCALE3 ABSPACK scaling algorithm. Using Olex2,[5] the structures were solved with ShelXT[6] and a least-squares refinement on $F2$ was carried out with ShelXL.[7] All non-hydrogen atoms were refined anisotropically. The hydrogen atoms at the carbon atoms have been located in idealized positions and refined isotropically according to the riding model. Figures were created with Olex2.

CCDC-2347535 (**1a**), CCDC-2340840 (**1b**), CCDC-2340841 (**1c**), and CCDC-2340842 (**2**), contain the supplementary crystallographic data for this paper. These data can be obtained free of charge at www.ccdc.cam.ac.uk/conts/retrieving.html (or from the Cambridge Crystallographic Data Centre, 12 Union Road, Cambridge CB2 1EZ, UK; Fax: +44-1223-336-033; e-mail: deposit@ccdc.cam.ac.uk).

Table S 8.1: Crystallographic data for compounds **1a** and **1b**.

Compound	**1a**	**1b**
CCDC	2347535	2340840
Formula	$C_{33}H_{56}BBiN_2Si_2$	$C_{13}H_{32}BBiN_2Si_2$
Dcalc	1.342	1.568
m/mm^{-1}	4.793	17.605
Formula Weight	756.76	492.37
Colour	clear light yellow	clear light yellow
Shape	plate-shaped	block
Size/mm^3	0.31×0.29×0.07	0.19×0.13×0.12
T/K	123.01(10)	123.00(10)
Crystal System	monoclinic	triclinic
Space Group	$P2_1/c$	P-1
a/Å	18.0837(3)	9.5403(4)
b/Å	10.2928(2)	9.8557(6)
c/Å	40.2707(12)	12.1971(4)
a/°	90	97.044(4)
b/°	91.900(2)	108.604(4)
g/°	90	101.577(4)
V/Å^3	7491.5(3)	1043.07(9)
Z	8	2
Z'	2	1
Wavelength/Å	0.71073	1.54184
Radiation type	MoK_a	CuK_α
Q_{min}/°	2.222	3.904
Q_{max}/°	25.123	74.073
Measured Refl's.	92561	6314
Indep't Refl's	13330	3974
Refl's I≥2 s(I)	11815	3703
R_{int}	0.0581	0.0365
Parameters	855	190
Restraints	241	0
Largest Peak	0.778	1.572
Deepest Hole	-1.762	-2.289
GooF	1.168	1.050
wR_2 (all data)	0.0696	0.0919
wR_2	0.0679	0.0891
R_1 (all data)	0.0436	0.0377
R_1	0.0362	0.0350

Table S 8.2: Crystallographic data for compounds **1c** and **2**.

Compound	**1c**	**2**
CCDC	2340841	2340842
Formula	$C_{13}H_{30}BBiN_2Si_2$	$C_{33}H_{56}BiGaN_2Si_2$
Dcalc	1.563	1.432
m/mm^{-1}	17.621	10.653
Formula Weight	490.36	815.67
Colour	brown	clear colourless
Shape	block-shaped	plate-shaped
Size/mm^3	0.22×0.12×0.10	0.50×0.31×0.14
T/K	123(1)	122.99(10)
Crystal System	triclinic	orthorhombic
Space Group	*P*-1	*Pbca*
a/Å	7.3161(2)	19.3792(3)
b/Å	9.8444(2)	19.2881(2)
c/Å	15.3209(3)	20.2475(2)
a/°	90.6300(10)	90
b/°	103.624(2)	90
g/°	103.085(2)	90
V/Å^3	1042.14(4)	7568.27(16)
Z	2	8
Z'	1	1
Wavelength/Å	1.54178	1.54184
Radiation type	CuK_a	CuK_a
Q_{min}/°	4.622	3.902
Q_{max}/°	66.582	73.674
Measured Refl's.	10095	26333
Indep't Refl's	3613	7278
Refl's I≥2 s(I)	3417	6764
R_{int}	0.0278	0.0513
Parameters	188	375
Restraints	0	1
Largest Peak	0.718	1.405
Deepest Hole	-0.543	-1.568
GooF	1.090	1.071
wR_2 (all data)	0.0532	0.0929
wR_2	0.0526	0.0916
R_1 (all data)	0.0221	0.0343
R_1	0.0202	0.0323

8.5.5.1 Crystal structures

IDipp·$BH_2Bi(SiMe_3)_2$ (1a)

1a crystallized by slow evaporation of a *n*-pentane solution at -30 °C as clear light-yellow plate shaped crystals in the monoclinic space group $P2_1/c$. The structure of **1a** is shown in Figure S 8.34.

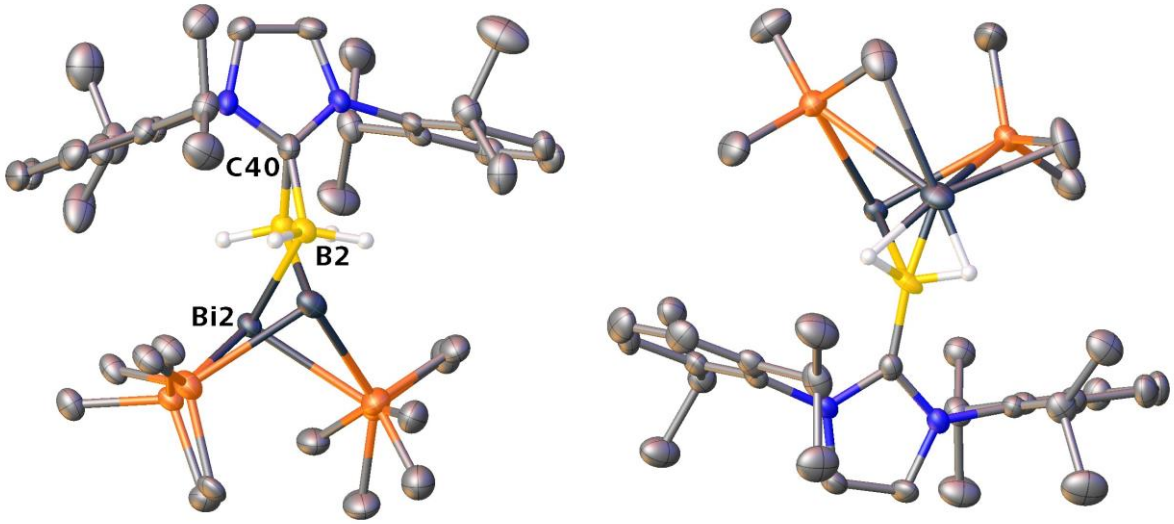

Figure S 8.34: Molecular structure of **1a** in the solid state (asymmetric unit). Anisotropic displacement ellipsoids are shown at 50% probability level. Hydrogen atoms bound to carbon are omitted for clarity. Selected bond lengths [Å] and angles [°]: C40-B2 1.587(7), B2-Bi2 2.424(5), C40-B2-Bi2 110.9(3).

The asymmetric unit contains two molecules of **1a** and had to be refined with further DANG, SADI and SIMU restraints due to disorder (right molecule: only the bismuth atom of the minor component could be located due to a small occupancy of 0.0377(7); left molecule: the chain structure is disordered by rotation of roughly 180° with an occupancy of the minor component of 0.1079(7)). Hydrogen atoms bound to B were fixed in idealized position using DFIX and DANG restraints.

IMe_4·$BH_2Bi(SiMe_3)_2$ (1b)

1b crystallized from a saturated *n*-hexane solution at -28 °C as clear light-yellow block-shaped crystals in the triclinic space group *P*-1. The structure of **1b** in the solid state is shown in Figure S 8.35.

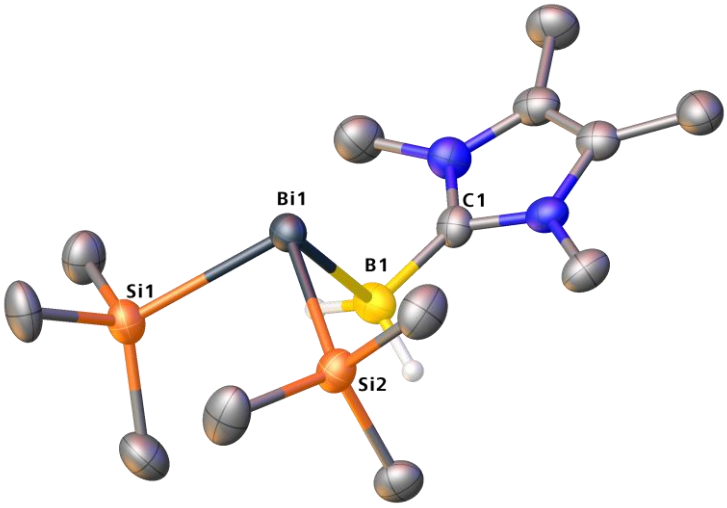

Figure S 8.35: Molecular structure of **1b** in the solid state. Anisotropic displacement ellipsoids are shown at 50% probability level. Hydrogen atoms bound to carbon are omitted for clarity. Selected bond lengths [Å] and angles [°]: C1-B1 1.569(9), B1-Bi1 2.442(7), Bi1-Si1 2.6278(17), Bi1-Si2 2.6452(18), C1-B1-Bi1 107.2(4), B1-Bi1-Si1 89.12(18), B1-Bi1-Si2 97.05(19).

The asymmetric unit contains one molecule of **1b** and was refined without further restrains/constraints. H-atoms bound to B were refined freely.

DMAP·$BH_2Bi(SiMe_3)_2$ (1c)

1c crystallized by storing a saturated solution of **1c** in toluene at-28 °C as brown block-shaped crystals in the triclinic space group *P*-1. The structure of **1c** in the solid state is shown in Figure S 8.36.

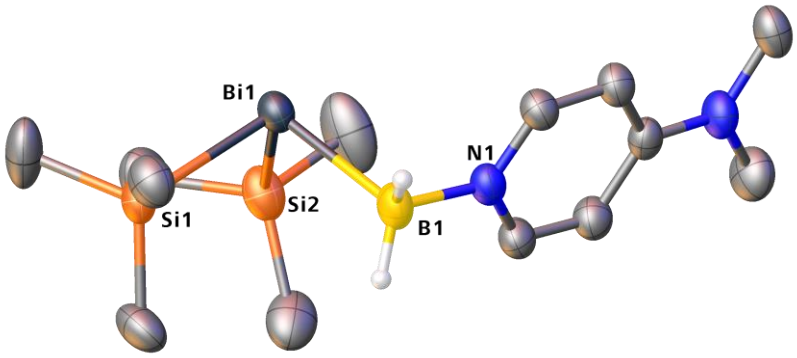

Figure S 8.36: Molecular structure of **1c** in the solid state. Anisotropic displacement ellipsoids are shown at 50% probability level. Hydrogen atoms bound to carbon are omitted for clarity. Selected bond lengths [Å] and angles [°]: N1-B1 1.578(5), B1-Bi1 2.424(5), Bi1-Si1 2.6331(9), Bi1-Si2 2.6322(11), N1-B1-Bi1 106.9(2), B1-Bi1-Si1 94.53(10), B1-Bi1-Si2 100.10(12).

The asymmetric unit contains one molecule of **1c** and was refined without further restrains/constraints. H-atoms bound to B were refined freely.

IDipp·GaH$_2$Bi(SiMe$_3$)$_2$ (2)

2 crystallized by slow evaporation of a *n*-pentane solution under reduced pressure at -80 °C over the course of two days as clear colourless plate-shaped crystals in the orthorhombic space group *Pbca*. The structure of **2** in the solid state is shown in Figure S 8.37.

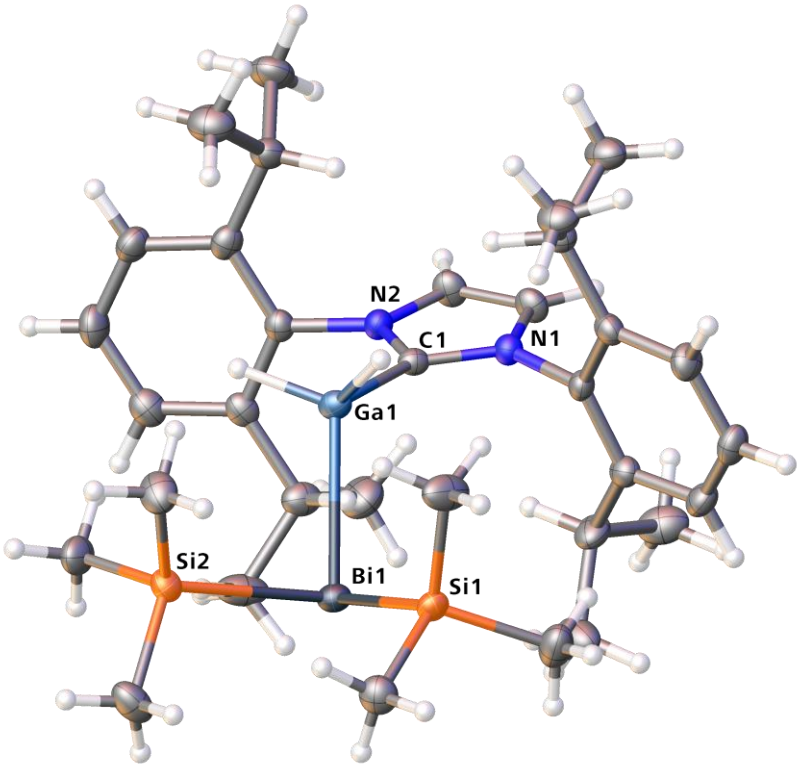

Figure S 8.37: Molecular structure of **2** in the solid state. Anisotropic displacement ellipsoids are shown at 50% probability level. Selected bond lengths [Å] and angles [°]: N1-C1 1.352(4), N2-C1 1.357(4), C1-Ga1 2.061(3), Ga1-Bi1 2.7234(4), Bi1-Si1 2.6487(9), Bi1-Si2 2.6403(9), N1-B1-Bi1 106.9(2), N1-C1-N2 104.2(3), N1-C1-Ga1 129.2(2), C1-Ga1-Bi1 110.10(8), Ga1-Bi1-Si1 95.26(2), B1-Bi1-Si2 87.85(2).

The asymmetric unit contains one molecule of **2**. H atoms bound to Ga were refined by applying a SADI restraint.

8.5.6 Computational Details

8.5.6.1 General Information

The geometries of the compounds have been fully optimized with gradient-corrected density functional theory (DFT) in form of Becke's three-parameter hybrid method B3LYP with def2-TZVP all electron basis set (ECP on Bi).[8] The Gaussian 09 programme package was used throughout.[9] All structures correspond to minima on their respective potential energy surfaces as verified by computation of second derivatives. Natural bond orbital analysis (NBO Version 3.1, E. D. Glendening, A. E. Reed, J. E. Carpenter, and F. Weinhold) was performed as implemented in Gaussian 09.[10]

8.5.6.2 Molecular Properties and Thermodynamics

Table S 8.3: Reaction energies ΔE, standard reaction enthalpies $\Delta H°_{298}$, Gibbs energies $\Delta G°_{298}$ (kJ mol^{-1}) and standard reaction entropies $\Delta S°_{298}$ (J mol^{-1} K^{-1}) for the considered gas phase processes). B3LYP/def2-TZVP(ECP on Bi) level of theory.

Process	ΔE	$\Delta H°_{298}$	$\Delta S°_{298}$	$\Delta G°_{298}$
1a = $BH_2Bi(SiMe_3)_2$ + IDipp	203.8	190.3	253.8	114.6
1b = $BH_2Bi(SiMe_3)_2$ + IMe_4	233.1	219.8	186.9	164.1
1c = $BH_2Bi(SiMe_3)_2$ + DMAP	139.7	130.2	176.0	77.8
2 = $GaH_2Bi(SiMe_3)_2$ + IDipp	109.9	99.5	242.1	27.4
1a + 2 MeOH = IDipp·BH_2BiH_2 + 2$MeOSiMe_3$	-170.6	-194.3	34.4	-204.6
1b + 2 MeOH = IMe_4·BH_2BiH_2 + 2$MeOSiMe_3$	-178.1	-201.8	13.6	-205.8
1c + 2 MeOH = DMAP·BH_2BiH_2 + 2$MeOSiMe_3$	-163.9	-184.4	8.0	-186.8
1a + 2 MeOH = IDipp·$BH_2Bi(OMe)_2$ + 2 $HSiMe_3$	-4.2	-24.0	5.5	-25.7
1b + 2 MeOH = IMe_4·$BH_2Bi(OMe)_2$ + 2 $HSiMe_3$	-25.5	-44.7	-14.1	-40.5
1c + 2 MeOH = DMAP·$BH_2Bi(OMe)_2$ + 2 $HSiMe_3$	-15.3	-31.8	-5.8	-30.1
IDipp·BH_2BiH_2 = 2 H_2 + $Bi_{(solid)}$ + $B_{(solid)}$ +IDipp		-8.9	239.5	-80.3
IMe_4·BH_2BiH_2 = 2 H_2 + $Bi_{(solid)}$ + $B_{(solid)}$ +IMe_4		28.1	193.3	-29.6
DMAP·BH_2BiH_2 = 2 H_2 + $Bi_{(solid)}$ + $B_{(solid)}$ + DMAP		-78.9	188.0	-135.0
IDipp·BH_2BiH_2 = ½ H_2 + $Bi_{(solid)}$ + IDipp·BH_3		-131.4	64.6	-150.7
IMe_4·BH_2BiH_2 = ½ H_2 + $Bi_{(solid)}$ + IMe·BH_3		-105.2	46.7	-119.1
DMAP·BH_2BiH_2 = ½ H_2 + $Bi_{(solid)}$ + DMAP·BH_3		-128.7	51.7	-144.1
$B_{(solid)}$ = $B_{(gas)}$[11]		561.6	147.5	517.6
$Bi_{(solid)}$ = $Bi_{(gas)}$[11]		208.4	130.0	169.6

Table S 8.4: Dipole moments μ in Debye, the E-Bi and E-LB bond distances in Å, the E-Bi and E-LB Wiberg bond indexes (WBI) and their changes upon complex formation. B3LYP/def2-TZVP(ECP on Bi) level of theory.

Compound	μ	R(E-Bi)	ΔR(E-Bi)	WBI(E-Bi)	ΔWBI(E-Bi)
$BH_2Bi(SiMe_3)_2$	1.51	2.291	-	1.208	-
$GaH_2Bi(SiMe_3)_2$	1.64	2.688	-	0.979	-
1a	6.61	2.484	0.193	0.845	-0.364
1b	7.62	2.501	0.210	0.841	-0.367
1c	10.9	2.463	0.172	0.890	-0.318
2	7.69	2.785	0.097	0.880	-0.099

Table S 8.5: Total energies E^o_0, sum of electronic and thermal enthalpies H^o_{298} (Hartree) and standard entropies S^o_{298} (cal mol^{-1}K^{-1}). B3LYP/def2-TZVP (ECP on Bi) level of theory.

Compound	E^o_0	H^o_{298}	S^o_{298}
DMAP	-382.4014129	-382.230446	91.131
IMe_4	-383.5797905	-383.386841	96.208
IDipp	-1160.4538534	-1159.854780	201.957
$BH_2Bi(SiMe_3)_2$	-1059.4617525	-1059.198250	152.893
$GaH_2Bi(SiMe_3)_2$	-2959.5435301	-2959.285449	157.331
1a	-2219.9932453	-2219.125522	294.179
1b	-1443.1303448	-1442.668822	204.426
1c	-1441.9163855	-1441.478291	201.97
2	-4120.0392468	-4119.178145	301.431
Bi ($^4S_{3/2}$)	-214.6848603	-214.6825	44.67
B ($^2P_{1/2}$)	-24.6639213	-24.661561	34.519
H_2	-1.1794826	-1.166608	31.223
$HSi(CH_3)_3$	-409.9478771	-409.821002	79.024
CH_3OH	-115.7756771	-115.72035	56.963
$CH_3OSi(CH_3)_3$	-524.5731799	-524.409144	98.141
$DMAP{\cdot}BH_2BiH_2$	-624.3838154	-624.170929	121.523
$DMAP{\cdot}BH_2Bi(OMe)_2$	-853.577813	-853.289115	156.463
$IDipp{\cdot}BH_2BiH_2$	-1402.46322	-1401.821945	220.033
$IDipp{\cdot}BH_2Bi(OMe)_2$	-1631.650437	-1630.933371	251.378
$IMe_4{\cdot}BH_2BiH_2$	-625.60319	-625.368077	125.327
$IMe_4{\cdot}BH_2Bi(OMe)_2$	-854.7956626	-854.484536	156.93
$DMAP{\cdot}BH_3$	-409.0805685	-408.874761	104.676
$IDipp{\cdot}BH_3$	-1187.160529	-1186.526817	206.272
$IMe_4{\cdot}BH_3$	-410.2905744	-410.062966	107.271

8.5.6.3 Frontier Molecular Orbitals

$BH_2Bi(SiMe_3)_2$	$GaH_2Bi(SiMe_3)_2$
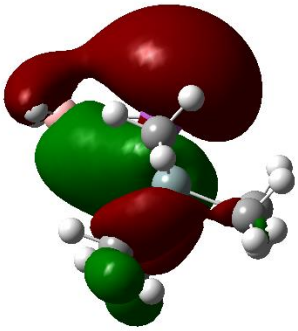	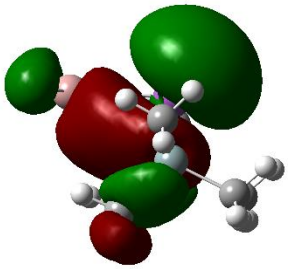
HOMO	HOMO
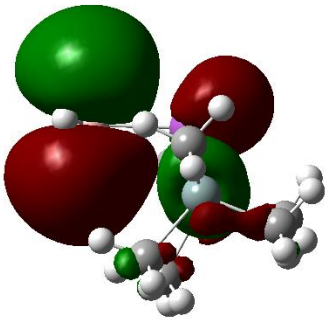	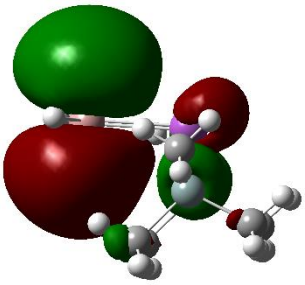
LUMO	LUMO

1a	**2**
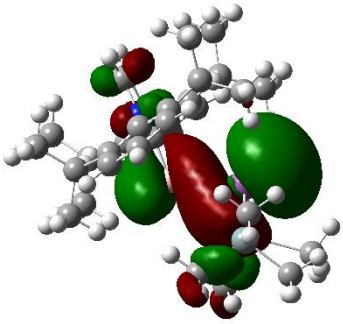	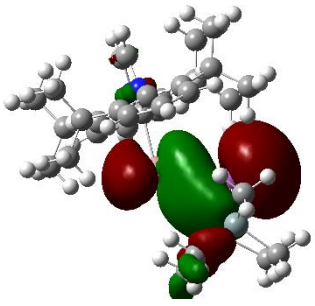
HOMO	HOMO
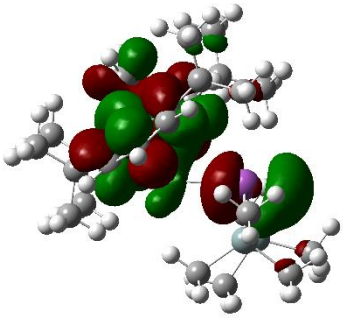	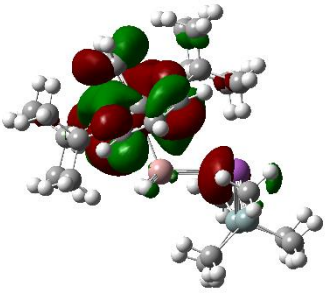
LUMO	LUMO

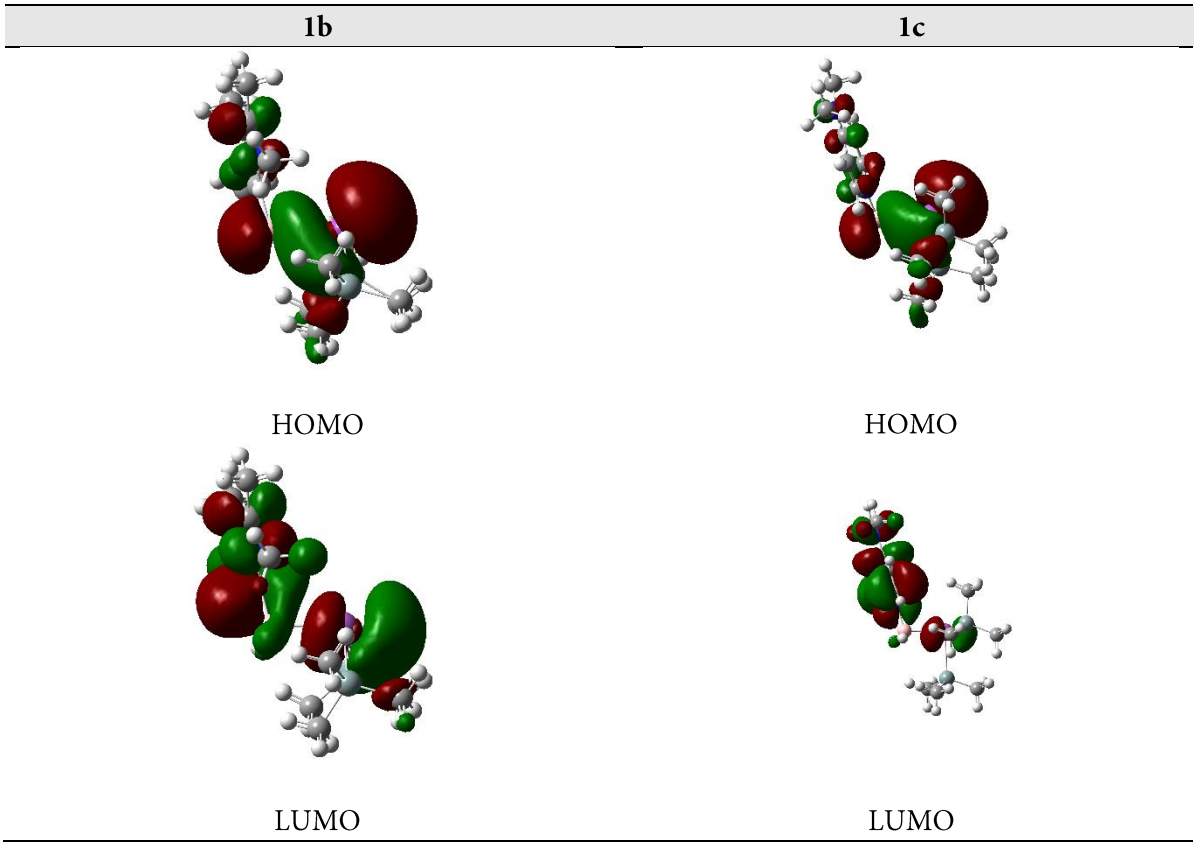

Figure S 8.38: Canonical frontier molecular orbitals of the studied compounds. B3LYP/def2-TZVP (ECP on Bi) level of theory.

8.5.6.4 Cartesian Coordinates of optimized Structures

Table S 8.6: Optimized geometries of the computationally studied compounds. Cartesian coordinates in Ångströms. B3LYP/def2-TZVP (ECP on Bi) level of theory.

DMAP			
7	-2.664387000	0.000007000	0.020859000
7	1.550059000	-0.000004000	-0.087102000
6	0.178850000	-0.000008000	-0.039012000
6	-0.570648000	-1.193118000	-0.015110000
1	-0.092052000	-2.160779000	-0.014376000
6	-0.570626000	1.193101000	-0.015123000
1	-0.092027000	2.160762000	-0.014397000
6	-1.953416000	-1.129170000	0.010031000
1	-2.524007000	-2.053033000	0.025352000
6	2.278814000	1.248571000	0.032671000
1	1.981164000	1.955653000	-0.745288000
1	3.341646000	1.053004000	-0.088174000
1	2.127967000	1.731534000	1.006166000
6	2.278866000	-1.248554000	0.032638000
1	2.128115000	-1.731511000	1.006152000
1	3.341679000	-1.052948000	-0.088300000
1	1.981188000	-1.955655000	-0.745289000
6	-1.953407000	1.129163000	0.009993000
1	-2.523974000	2.053042000	0.025331000

IMe_4			
7	1.058721000	-0.707717000	-0.000052000
7	-1.058756000	-0.707680000	0.000000000
6	0.679300000	0.636539000	0.000006000
6	-0.000044000	-1.561853000	-0.000050000
6	-0.679261000	0.636577000	0.000033000
6	-1.655840000	1.760614000	0.000062000
1	-2.304963000	1.737906000	-0.880115000
1	-1.135980000	2.718010000	-0.000517000
1	-2.304203000	1.738583000	0.880824000
6	2.431331000	-1.171720000	0.000087000
1	2.966486000	-0.825041000	-0.886935000
1	2.406417000	-2.257832000	0.000161000
1	2.966353000	-0.824873000	0.887114000
6	-2.431373000	-1.171667000	-0.000026000
1	-2.406491000	-2.257785000	0.000021000
1	-2.966428000	-0.824940000	-0.887085000
1	-2.966487000	-0.824864000	0.886967000
6	1.655912000	1.760560000	-0.000070000
1	2.304175000	1.738714000	0.880772000
1	1.136071000	2.717965000	-0.000936000
1	2.305141000	1.737636000	-0.880162000

IDipp			
7	-1.062433000	-0.000212000	0.517841000
7	1.062454000	-0.000280000	0.517849000
6	0.000014000	0.000056000	-0.342234000
6	2.435803000	-0.000119000	0.090083000
6	-2.435780000	0.000031000	0.090065000
6	0.674932000	-0.000753000	1.853545000
1	1.379330000	-0.001039000	2.666612000
6	-0.674922000	-0.000632000	1.853539000
1	-1.379327000	-0.000814000	2.666601000
6	3.085112000	-1.228217000	-0.111543000
6	-3.085203000	-1.228019000	-0.111480000
6	-3.084628000	1.228314000	-0.111866000
6	-2.381093000	-2.563361000	0.075298000
1	-1.394840000	-2.364457000	0.492766000
6	3.084766000	1.228118000	-0.111753000
6	-4.415996000	-1.199657000	-0.527711000
1	-4.940552000	-2.131324000	-0.697703000
6	-5.077330000	0.000517000	-0.734708000
1	-6.110261000	0.000711000	-1.060472000
6	-4.415425000	1.200441000	-0.528121000
1	-4.939541000	2.132307000	-0.698421000
6	-2.380115000	2.563426000	0.074960000
1	-1.393617000	2.364152000	0.491658000
6	2.380838000	-2.563492000	0.075097000
1	1.394747000	-2.364530000	0.492922000
6	4.415910000	-1.199950000	-0.527761000
1	4.940385000	-2.131651000	-0.697814000
6	2.380387000	2.563287000	0.075167000
1	1.393834000	2.364081000	0.491766000
6	5.077357000	0.000178000	-0.734668000
1	6.110292000	0.000298000	-1.060423000
6	4.415565000	1.200150000	-0.528000000
1	4.939772000	2.131978000	-0.698225000
6	-3.118372000	-3.476164000	1.065973000
1	-3.245495000	-2.990985000	2.035635000
1	-2.553854000	-4.398309000	1.220872000
1	-4.109001000	-3.755087000	0.701175000
6	-2.166931000	-3.265346000	-1.274824000
1	-3.119796000	-3.508481000	-1.750746000
1	-1.615644000	-4.198288000	-1.135832000
1	-1.599191000	-2.631234000	-1.956427000
6	2.166153000	-3.265043000	-1.275172000
1	1.598303000	-2.630639000	-1.956411000
1	1.614771000	-4.197947000	-1.136293000
1	3.118847000	-3.508169000	-1.751443000
6	3.118233000	-3.476719000	1.065286000
1	4.108667000	-3.755811000	0.700088000
1	2.553539000	-4.398763000	1.220140000
1	3.245805000	-2.991821000	2.035030000
6	2.167166000	3.266116000	-1.274636000
1	3.120312000	3.509567000	-1.749827000
1	1.615798000	4.198973000	-1.135410000
1	1.599859000	2.632440000	-1.957010000
6	-2.166707000	3.266069000	-1.274911000
1	-1.599409000	2.632249000	-1.957158000
1	-1.615255000	4.198886000	-1.135752000
1	-3.119789000	3.509558000	-1.750211000
6	-3.116700000	3.475804000	1.066580000
1	-4.107629000	3.754729000	0.702587000
1	-2.552150000	4.397934000	1.221440000
1	-3.243080000	2.990214000	2.036131000
6	3.117003000	3.475466000	1.066950000
1	3.243232000	2.989758000	2.036461000
1	2.552561000	4.397655000	1.221855000
1	4.108002000	3.754295000	0.703073000

$BH_2Bi(SiMe_3)_2$			
83	-0.002005000	-0.842442000	-0.281012000
14	2.143182000	0.756132000	0.081801000
14	-2.139361000	0.765344000	0.079266000
5	-0.025012000	-1.730894000	1.831002000
6	3.612625000	-0.383956000	0.394127000
1	3.755399000	-1.085611000	-0.430029000
1	3.480492000	-0.964611000	1.308907000
1	4.531038000	0.202042000	0.498447000
6	1.985881000	1.975008000	1.514032000
1	1.803127000	1.462275000	2.459817000
1	1.172525000	2.684840000	1.354118000
1	2.911961000	2.549962000	1.615895000
6	-3.658627000	-0.343099000	-0.063274000
1	-3.658370000	-1.120841000	0.702982000
1	-3.703860000	-0.833371000	-1.037642000
1	-4.572432000	0.246530000	0.059385000
6	2.423557000	1.720616000	-1.516209000
1	3.317501000	2.346296000	-1.431855000
1	1.579890000	2.375194000	-1.744258000
1	2.563005000	1.049505000	-2.365968000
6	-2.162591000	1.638769000	1.750685000
1	-1.282613000	2.268360000	1.890707000
1	-2.191510000	0.918529000	2.570375000
1	-3.048797000	2.276361000	1.831340000
6	-2.168970000	2.051884000	-1.301857000
1	-3.069313000	2.669292000	-1.224620000
1	-2.170353000	1.580055000	-2.286390000
1	-1.305521000	2.718163000	-1.252324000
1	0.994368000	-2.007128000	2.381649000
1	-1.059843000	-2.014723000	2.348495000

$GaH_2Bi(SiMe_3)_2$			
83	-0.000031000	-0.152184000	-0.862241000
14	2.111107000	0.943210000	0.427436000
14	-2.111313000	0.942877000	0.427520000
31	0.000364000	-2.384629000	0.635269000
6	3.648165000	0.157680000	-0.334777000
1	3.692132000	0.330294000	-1.411975000
1	3.672621000	-0.920744000	-0.166450000
1	4.551555000	0.586041000	0.110483000
6	2.151060000	0.670141000	2.295281000
1	2.224543000	-0.390811000	2.541672000
1	1.263340000	1.070947000	2.787042000
1	3.024481000	1.170970000	2.725340000
6	-3.648033000	0.157709000	-0.335771000
1	-3.671608000	-0.921048000	-0.169451000
1	-3.692422000	0.332275000	-1.412638000
1	-4.551622000	0.584541000	0.110543000
6	2.134421000	2.799735000	0.083026000
1	3.040776000	3.246149000	0.504122000
1	1.277273000	3.306564000	0.529977000
1	2.125199000	3.009689000	-0.988250000
6	-2.151714000	0.668590000	2.295171000
1	-1.264375000	1.069777000	2.787307000
1	-2.224581000	-0.392523000	2.541004000
1	-3.025588000	1.168636000	2.725233000
6	-2.134668000	2.799665000	0.084535000
1	-3.043439000	3.244816000	0.501727000
1	-2.120456000	3.010700000	-0.986466000
1	-1.280153000	3.306834000	0.536153000
1	1.352042000	-3.091638000	1.057199000
1	-1.350950000	-3.093061000	1.055878000

1a

83	0.607590000	1.771163000	0.507854000
7	0.275022000	-2.464525000	0.376229000
7	-1.772611000	-1.771262000	0.403114000
6	-0.516980000	-1.416110000	-0.012502000
6	-3.000654000	-1.034298000	0.221971000
6	1.700731000	-2.593511000	0.194580000
6	-1.754421000	-3.014606000	1.014408000
1	-2.648893000	-3.472206000	1.393868000
6	-0.479389000	-3.446336000	0.997049000
1	-0.038093000	-4.354238000	1.363648000
6	-3.502398000	-0.287901000	1.301301000
6	2.537993000	-2.353550000	1.296900000
6	2.193255000	-3.027728000	-1.047395000
6	2.008684000	-1.960726000	2.670209000
1	0.953989000	-1.705192000	2.566245000
6	-3.694129000	-1.164589000	-0.992112000
6	3.908896000	-2.538520000	1.115623000
1	4.583101000	-2.359674000	1.942653000
6	4.423126000	-2.944147000	-0.104475000
1	5.491439000	-3.074660000	-0.224221000
6	3.572201000	-3.188688000	-1.170914000
1	3.986672000	-3.516260000	-2.115032000
6	1.282356000	-3.385032000	-2.212939000
1	0.293182000	-2.982600000	-2.000653000
6	-2.780657000	-0.183562000	2.638735000
1	-1.755730000	-0.527158000	2.494954000
6	-4.735932000	0.340110000	1.130098000
1	-5.151500000	0.924258000	1.940096000
6	-3.187069000	-2.018380000	-2.144786000
1	-2.161224000	-2.308769000	-1.922784000
6	-5.437209000	0.234451000	-0.059464000
1	-6.390797000	0.735290000	-0.170995000
6	-4.919073000	-0.509107000	-1.107450000
1	-5.477923000	-0.587097000	-2.030714000
6	2.104666000	-3.143638000	3.649882000
1	1.573338000	-4.022588000	3.280733000
1	1.675819000	-2.872106000	4.616913000
1	3.145185000	-3.432108000	3.813882000
6	2.710427000	-0.726031000	3.251388000
1	3.771299000	-0.907793000	3.433453000
1	2.255137000	-0.458265000	4.207094000
1	2.618866000	0.132280000	2.586664000
6	-2.696691000	1.256731000	3.161378000
1	-2.230407000	1.918100000	2.432151000
1	-2.092252000	1.285714000	4.070050000
1	-3.680989000	1.658111000	3.410178000
6	-3.437218000	-1.094395000	3.691107000
1	-4.465178000	-0.782656000	3.889388000
1	-2.885136000	-1.046998000	4.632288000
1	-3.463642000	-2.136640000	3.369487000
6	-3.153220000	-1.250164000	-3.473166000
1	-4.155091000	-0.974236000	-3.808128000
1	-2.708022000	-1.872242000	-4.252529000
1	-2.557757000	-0.341956000	-3.383932000
6	1.735770000	-2.761956000	-3.539343000
1	1.823625000	-1.679297000	-3.454134000
1	1.004960000	-2.980708000	-4.320697000
1	2.696006000	-3.160912000	-3.872389000
5	-0.106740000	-0.168621000	-0.868691000
6	1.147110000	-4.912186000	-2.344413000
1	2.110506000	-5.373352000	-2.573337000
1	0.454658000	-5.164518000	-3.150612000
1	0.772143000	-5.364417000	-1.424266000
6	-4.015411000	-3.307692000	-2.277522000
1	-4.005862000	-3.888255000	-1.353052000
1	-3.614845000	-3.937038000	-3.075354000
1	-5.056902000	-3.084095000	-2.519083000
1	-1.047810000	0.255177000	-1.476282000
1	0.858738000	-0.408060000	-1.532092000
14	-0.811864000	3.594221000	-0.885163000
6	-2.660301000	3.281756000	-0.628534000
1	-2.939162000	3.358104000	0.424162000
1	-3.244510000	4.024805000	-1.181283000
1	-2.956596000	2.292958000	-0.981632000
6	-0.439364000	5.326590000	-0.214147000
1	-1.038499000	6.078691000	-0.737583000
1	-0.676509000	5.392115000	0.850166000
1	0.611748000	5.593716000	-0.333525000
6	-0.497837000	3.588049000	-2.750884000
1	-1.179705000	4.283714000	-3.250788000
1	0.522041000	3.889602000	-2.995391000
1	-0.662374000	2.593914000	-3.170139000
14	2.940573000	2.271932000	-0.770189000
6	3.313039000	4.130461000	-0.804461000
1	2.609231000	4.676862000	-1.434604000
1	3.274877000	4.568166000	0.195313000
1	4.317662000	4.300489000	-1.205064000
6	3.013164000	1.626226000	-2.545835000
1	2.245759000	2.080670000	-3.173822000
1	3.990041000	1.847202000	-2.988107000
1	2.864313000	0.546021000	-2.572795000
6	4.355976000	1.452250000	0.186608000
1	5.313280000	1.680053000	-0.293819000
1	4.407413000	1.811880000	1.216618000
1	4.248711000	0.366495000	0.214600000

1b

83	-0.662870000	-0.132254000	-0.615296000
14	-1.835879000	2.218612000	-0.028059000
14	-2.540410000	-1.758527000	0.414778000
7	3.083066000	0.855697000	0.754279000
7	2.989220000	-1.241553000	0.280171000
6	4.284492000	0.535800000	0.125449000
6	2.270684000	-0.230825000	0.837542000
6	4.223814000	-0.786765000	-0.176255000
6	5.213364000	-1.673454000	-0.845661000
1	5.564028000	-2.469930000	-0.183457000
1	6.084127000	-1.098067000	-1.154478000
1	4.795433000	-2.147043000	-1.737545000
6	-1.776243000	-3.487479000	0.550758000
1	-1.407952000	-3.839440000	-0.415636000
1	-2.520641000	-4.207238000	0.905810000
1	-0.942452000	-3.495489000	1.255387000
6	-1.968882000	2.612826000	1.816723000
1	-2.604668000	1.893550000	2.335138000
1	-2.397660000	3.609808000	1.961266000
1	-0.991792000	2.589208000	2.301597000
6	2.737786000	2.184800000	1.224478000
1	3.562983000	2.604579000	1.799040000
1	1.861634000	2.106719000	1.859137000
1	2.515358000	2.846565000	0.385649000
6	2.486298000	-2.593437000	0.107144000
1	1.824756000	-2.832344000	0.934292000
1	3.318051000	-3.293924000	0.095046000
1	1.924942000	-2.681430000	-0.825141000
6	5.359438000	1.538455000	-0.103952000
1	5.000878000	2.391546000	-0.685584000
1	6.184612000	1.088192000	-0.652523000
1	5.762300000	1.928360000	0.834994000
6	-0.804414000	3.590574000	-0.837473000
1	0.206997000	3.631370000	-0.427190000
1	-1.267424000	4.568783000	-0.672887000

1	-0.719105000	3.437234000	-1.915443000
6	-3.161714000	-1.264615000	2.130858000
1	-2.329643000	-1.134997000	2.825276000
1	-3.825469000	-2.036302000	2.534148000
1	-3.721453000	-0.327851000	2.100456000
6	-3.571925000	2.319209000	-0.779657000
1	-3.554475000	2.114071000	-1.852094000
1	-3.989284000	3.321113000	-0.636467000
1	-4.256238000	1.606185000	-0.315906000
6	-4.026610000	-1.882859000	-0.752534000
1	-4.523391000	-0.919036000	-0.878425000
1	-4.764517000	-2.591074000	-0.361976000
1	-3.722345000	-2.228564000	-1.742929000
5	0.809468000	-0.312187000	1.398733000
1	0.520480000	0.590008000	2.132081000
1	0.548312000	-1.400157000	1.834526000

1c

83	1.030644000	-0.303616000	-0.638716000
14	3.352036000	-1.145643000	0.417390000
14	1.195975000	2.312327000	-0.028633000
7	-1.821691000	-0.850789000	0.915255000
7	-5.817442000	-0.135276000	-0.122851000
6	-4.523098000	-0.371685000	0.220456000
5	-0.314191000	-1.096968000	1.265699000
6	-3.807627000	0.477927000	1.093757000
1	-4.265544000	1.349278000	1.534160000
6	3.289443000	-3.037766000	0.409398000
1	3.148360000	-3.426050000	-0.601794000
1	2.467495000	-3.406388000	1.026219000
1	4.221197000	-3.456863000	0.802481000
6	-3.804671000	-1.485717000	-0.270641000
1	-4.261091000	-2.202850000	-0.934266000
6	-2.499133000	0.207147000	1.406480000
1	-1.938328000	0.843420000	2.074901000
6	-6.511975000	-1.039368000	-1.025280000
1	-6.005130000	-1.108897000	-1.992010000
1	-7.516931000	-0.665425000	-1.199381000
1	-6.592826000	-2.047248000	-0.606520000
6	3.683033000	-0.581448000	2.193150000
1	2.841657000	-0.817337000	2.847193000
1	3.858266000	0.494850000	2.248176000
1	4.572126000	-1.083069000	2.589298000
6	-6.519151000	1.018188000	0.416878000
1	-6.580532000	0.979458000	1.508678000
1	-7.531711000	1.033900000	0.023788000
1	-6.031344000	1.955360000	0.133159000
6	-2.495749000	-1.679997000	0.089558000
1	-1.930238000	-2.522218000	-0.281360000
6	-0.337992000	3.155008000	-0.765237000
1	-1.259431000	2.748506000	-0.341087000
1	-0.385054000	3.014064000	-1.847327000
1	-0.324989000	4.231539000	-0.566390000
6	4.811032000	-0.603763000	-0.660826000
1	5.749154000	-1.015144000	-0.274534000
1	4.909459000	0.483279000	-0.688584000
1	4.690581000	-0.950991000	-1.689217000
6	1.222032000	2.712943000	1.822348000
1	2.126924000	2.334421000	2.300169000
1	0.372382000	2.266481000	2.342326000
1	1.185770000	3.795858000	1.980102000
6	2.718636000	3.117856000	-0.816327000
1	2.705951000	4.201565000	-0.661456000
1	2.756429000	2.932401000	-1.891788000
1	3.642618000	2.731112000	-0.381736000
1	-0.107024000	-2.279499000	1.295785000
1	-0.037570000	-0.495583000	2.264264000

2

83	2.247926000	0.100666000	0.512241000
7	-2.482864000	-1.178908000	0.485786000
7	-2.593426000	0.965284000	0.497739000
6	-1.804496000	-0.066574000	0.094613000
6	-2.332626000	2.377759000	0.325891000
6	-2.071898000	-2.554450000	0.307209000
6	-3.741193000	0.502898000	1.118125000
1	-4.491891000	1.170240000	1.499225000
6	-3.671664000	-0.844050000	1.110476000
1	-4.348530000	-1.589194000	1.485920000
6	-1.697893000	3.072956000	1.367287000
6	-1.399179000	-3.192528000	1.361161000
6	-2.424237000	-3.215515000	-0.880441000
6	-1.086042000	-2.501061000	2.681396000
1	-1.228865000	-1.428631000	2.544903000
6	-2.788011000	3.008335000	-0.842341000
6	-1.059302000	-4.533841000	1.185229000
1	-0.534578000	-5.057220000	1.973136000
6	-1.380808000	-5.207708000	0.018723000
1	-1.103090000	-6.247860000	-0.097794000
6	-2.058728000	-4.555219000	-0.998579000
1	-2.307394000	-5.096110000	-1.901662000
6	-3.219702000	-2.545942000	-1.991908000
1	-3.183328000	-1.468900000	-1.828604000
6	-1.262569000	2.399552000	2.662147000
1	-1.242503000	1.322468000	2.491272000
6	-1.512900000	4.445202000	1.200516000
1	-1.021354000	5.014069000	1.977968000
6	-3.524544000	2.265782000	-1.947876000
1	-3.397372000	1.196561000	-1.778192000
6	-1.944899000	5.093355000	0.054954000
1	-1.786850000	6.159047000	-0.054148000
6	-2.576831000	4.381703000	-0.951883000
1	-2.909952000	4.901408000	-1.840317000
6	-2.058796000	-2.963629000	3.780381000
1	-3.099485000	-2.789528000	3.501443000
1	-1.864656000	-2.426881000	4.711491000
1	-1.943379000	-4.031529000	3.978308000
6	0.366835000	-2.701479000	3.130609000
1	0.581570000	-3.746711000	3.360837000
1	0.559158000	-2.120951000	4.035053000
1	1.068234000	-2.368852000	2.366394000
6	0.149703000	2.805629000	3.101757000
1	0.878278000	2.626642000	2.311949000
1	0.449558000	2.219265000	3.972288000
1	0.201622000	3.858769000	3.384651000
6	-2.274917000	2.674926000	3.788046000
1	-2.328638000	3.743098000	4.009600000
1	-1.977233000	2.156872000	4.702277000
1	-3.279302000	2.340020000	3.523737000
6	-2.954931000	2.564179000	-3.341499000
1	-3.117237000	3.603790000	-3.632894000
1	-3.449760000	1.937039000	-4.086170000
1	-1.885600000	2.357948000	-3.377271000
6	-2.630629000	-2.802676000	-3.385370000
1	-1.583531000	-2.504221000	-3.426020000
1	-3.179830000	-2.224272000	-4.131276000
1	-2.704064000	-3.853614000	-3.671897000
31	-0.034602000	0.032382000	-1.081419000
6	-4.696097000	-2.975778000	-1.936960000
1	-4.796509000	-4.050118000	-2.106742000
1	-5.271958000	-2.459128000	-2.707950000
1	-5.148420000	-2.748762000	-0.969743000

6	-5.032560000	2.566334000	-1.897604000
1	-5.464859000	2.304903000	-0.929861000
1	-5.559777000	1.997740000	-2.666813000
1	-5.226819000	3.626742000	-2.072583000
1	-0.242456000	1.392522000	-1.872428000
1	-0.140280000	-1.299816000	-1.935273000
14	3.369809000	2.153857000	-0.825960000
6	2.448221000	3.734882000	-0.342936000
1	2.507028000	3.916104000	0.732488000
1	2.891412000	4.598158000	-0.850071000
1	1.393935000	3.687937000	-0.620687000
6	5.169915000	2.364314000	-0.273943000
1	5.612881000	3.241456000	-0.756823000
1	5.238069000	2.507179000	0.806684000
1	5.781287000	1.497730000	-0.531551000
6	3.341249000	2.022453000	-2.711149000
1	3.748668000	2.937024000	-3.154638000
1	3.941556000	1.184377000	-3.068937000
1	2.323441000	1.891579000	-3.082095000
14	3.517351000	-1.904117000	-0.770471000
6	5.383549000	-1.761237000	-0.479786000
1	5.801249000	-0.879089000	-0.968715000
1	5.618407000	-1.693223000	0.584417000
1	5.898144000	-2.639494000	-0.882876000
6	3.224001000	-2.028533000	-2.632745000
1	3.574845000	-1.140235000	-3.159648000
1	3.763283000	-2.892299000	-3.035766000
1	2.164395000	-2.154269000	-2.859985000
6	2.944796000	-3.532737000	0.007668000
1	3.459649000	-4.376122000	-0.463851000
1	3.163198000	-3.564813000	1.077271000
1	1.871324000	-3.682784000	-0.121749000

H_2

1	0.000000000	0.000000000	0.380000000
1	0.000000000	0.000000000	-0.380000000

$HSi(CH_3)_3$

6	1.545938000	-0.892548000	-0.221316000
14	0.000000000	0.000000000	0.374025000
6	0.000000000	1.785095000	-0.221316000
1	0.000000000	0.000000000	1.863245000
6	-1.545938000	-0.892548000	-0.221316000
1	0.000000000	1.838333000	-1.313166000
1	0.881763000	2.321263000	0.137266000
1	-0.881763000	2.321263000	0.137266000
1	-1.592043000	-0.919166000	-1.313166000
1	-2.451155000	-0.397002000	0.137266000
1	-1.569391000	-1.924261000	0.137266000
1	2.451155000	-0.397002000	0.137266000
1	1.592043000	-0.919166000	-1.313166000
1	1.569391000	-1.924261000	0.137266000

CH_3OH

8	-0.046596000	-0.756501000	0.000000000
6	-0.046596000	0.663615000	0.000000000
1	0.438484000	1.078506000	0.890984000
1	0.438484000	1.078506000	-0.890984000
1	-1.089053000	0.979408000	0.000000000
1	0.864424000	-1.066100000	0.000000000

$CH_3OSi(CH_3)_3$

6	-0.522153000	-1.535462000	1.078412000
14	-0.377723000	0.000016000	0.004045000
6	-1.680089000	0.003234000	-1.337530000
6	-0.520612000	1.531445000	1.084431000
1	-2.687101000	0.002876000	-0.912943000
1	-1.584433000	-0.877842000	-1.975698000
1	-1.583569000	0.886740000	-1.972211000
1	-1.491588000	1.563635000	1.585876000
1	-0.422622000	2.444218000	0.492065000
1	0.246563000	1.554117000	1.862466000
1	-0.427691000	-2.445955000	0.481953000
1	-1.492133000	-1.567424000	1.581804000
1	0.246622000	-1.563419000	1.854688000
8	1.069807000	0.000839000	-0.807514000
6	2.354798000	0.000152000	-0.220531000
1	3.096790000	0.000393000	-1.020411000
1	2.518811000	0.888706000	0.399095000
1	2.518353000	-0.889188000	0.398103000

DMAP·BH_2BiH_2

5	-0.833281000	0.302899000	1.625804000
1	-1.027624000	-0.578699000	2.411963000
1	-1.036667000	1.417374000	2.024942000
83	-2.333790000	-0.020341000	-0.281074000
7	0.637553000	0.208497000	1.093192000
6	3.279437000	0.014750000	0.096905000
6	1.323987000	1.300574000	0.697880000
6	1.271102000	-0.980676000	1.000577000
6	2.549510000	-1.118205000	0.525134000
6	2.605047000	1.250965000	0.206446000
1	0.796293000	2.238040000	0.796004000
1	0.695611000	-1.835260000	1.324772000
1	2.974082000	-2.108958000	0.489293000
1	3.074308000	2.177523000	-0.084215000
7	4.547591000	-0.080506000	-0.384959000
6	5.261558000	1.113738000	-0.805987000
6	5.200525000	-1.376418000	-0.476553000
1	6.250330000	0.831981000	-1.156800000
1	5.384122000	1.822203000	0.018795000
1	4.744906000	1.624846000	-1.623860000
1	5.302267000	-1.847964000	0.505530000
1	6.196078000	-1.244317000	-0.890782000
1	4.649738000	-2.059237000	-1.130066000
1	-1.716330000	-1.686417000	-0.637186000
1	-3.659149000	-0.701582000	0.727722000

DMAP·$BH_2Bi(OMe)_2$

5	0.536924000	-0.000206000	2.031996000
1	0.737618000	1.014161000	2.643269000
1	0.737668000	-1.014755000	2.642959000
83	2.066302000	-0.000026000	0.188652000
7	-0.888752000	-0.000155000	1.412075000
6	-3.447191000	-0.000017000	0.218352000
6	-1.518852000	-1.153723000	1.102154000
6	-1.518752000	1.153518000	1.102180000
6	-2.762762000	1.195812000	0.527201000
6	-2.762879000	-1.195903000	0.527144000
1	-0.973335000	-2.056174000	1.329077000
1	-0.973099000	2.055888000	1.329081000
1	-3.190084000	2.162687000	0.314352000
1	-3.190280000	-2.162748000	0.314320000
7	-4.686906000	0.000070000	-0.343978000
6	-5.345175000	-1.255485000	-0.663734000
6	-5.345221000	1.255698000	-0.663336000
1	-6.322930000	-1.046202000	-1.088643000
1	-5.489386000	-1.871932000	0.228450000
1	-4.775439000	-1.838149000	-1.394224000
1	-5.488858000	1.872112000	0.228956000
1	-6.323252000	1.046524000	-1.087664000
1	-4.775863000	1.838350000	-1.394138000
8	1.012355000	1.600883000	-0.729081000
6	1.353242000	2.039042000	-2.021971000
1	2.438824000	2.082988000	-2.190082000

1	0.923316000	1.397127000	-2.803337000
1	0.958124000	3.051454000	-2.169414000
8	1.012257000	-1.600687000	-0.729375000
6	1.353015000	-2.038716000	-2.022336000
1	0.922937000	-1.396783000	-2.803606000
1	2.438580000	-2.082551000	-2.190585000
1	0.957968000	-3.051153000	-2.169802000

IDipp·BH_2BiH_2

83	0.055659000	-2.315795000	-1.455897000
7	1.066288000	0.997391000	0.945083000
7	-1.097203000	0.990058000	0.933110000
6	2.572225000	-1.316990000	1.905430000
1	1.488348000	-1.255132000	1.796762000
6	2.278515000	3.147025000	-0.622724000
1	1.220193000	2.972948000	-0.433218000
6	-4.441879000	1.716391000	-0.505127000
1	-4.933937000	2.470482000	-1.105000000
6	-4.558671000	-0.336534000	0.733099000
1	-5.140686000	-1.175792000	1.088834000
6	-2.332685000	3.083332000	-0.694456000
1	-1.270558000	2.917400000	-0.520130000
6	4.406921000	1.808342000	-0.454724000
1	4.890551000	2.585790000	-1.031285000
6	3.190477000	-0.222867000	1.045197000
6	2.990931000	-2.728569000	1.472707000
1	2.787433000	-2.902341000	0.416333000
1	2.434209000	-3.472201000	2.046198000
1	4.052441000	-2.909572000	1.651974000
6	-3.086132000	1.852981000	-0.211194000
6	-0.697116000	1.538441000	2.140969000
1	-1.406389000	1.878350000	2.872205000
6	0.649872000	1.542624000	2.149105000
1	1.348856000	1.887361000	2.888066000
6	-2.913076000	-1.063799000	3.427690000
1	-2.585838000	-0.078042000	3.760656000
1	-2.429661000	-1.810044000	4.062082000
1	-3.990707000	-1.129243000	3.593397000
6	-5.171901000	0.634523000	-0.041285000
1	-6.223629000	0.547519000	-0.284249000
6	-2.745653000	4.327136000	0.110791000
1	-3.803366000	4.557066000	-0.034952000
1	-2.166947000	5.196994000	-0.207947000
1	-2.581096000	4.185569000	1.180741000
6	-0.010342000	0.659407000	0.169450000
6	-2.502055000	3.322849000	-2.200924000
1	-2.202834000	2.444251000	-2.772010000
1	-1.878925000	4.162294000	-2.516856000
1	-3.534090000	3.567764000	-2.459954000
6	3.048181000	1.917629000	-0.163004000
6	2.693855000	4.387309000	0.186426000
1	2.548098000	4.234730000	1.257573000
1	2.101704000	5.254146000	-0.115099000
1	3.746658000	4.629197000	0.025459000
6	2.459488000	0.884745000	0.584057000
6	4.547027000	-0.277077000	0.725220000
1	5.139802000	-1.116859000	1.061505000
6	5.150152000	0.723844000	-0.018743000
1	6.204132000	0.658516000	-0.258738000
6	-2.574903000	-1.317432000	1.947389000
1	-1.491415000	-1.245705000	1.838360000
6	-3.204439000	-0.255070000	1.055848000
6	2.905166000	-1.099232000	3.392482000
1	3.983079000	-1.155694000	3.559765000
1	2.428970000	-1.867342000	4.005788000
1	2.564555000	-0.126270000	3.749147000
6	-2.976925000	-2.745776000	1.554503000
1	-2.402598000	-3.466197000	2.140545000
1	-2.787915000	-2.937586000	0.498879000
1	-4.033085000	-2.937565000	1.753334000
5	0.005663000	0.128609000	-1.301052000
6	2.423787000	3.398832000	-2.129983000
1	3.451624000	3.646684000	-2.402711000
1	1.794861000	4.239879000	-2.429702000
1	2.116748000	2.524328000	-2.703223000
6	-2.486923000	0.849325000	0.566419000
1	1.039891000	0.399181000	-1.846337000
1	-0.984856000	0.437121000	-1.896518000
1	-1.733342000	-2.546452000	-1.531113000
1	0.124711000	-2.198061000	-3.248954000

IDipp·$BH_2Bi(OMe)_2$

83	-0.445418000	-2.277011000	-0.631940000
7	1.136728000	1.557046000	0.829378000
7	-1.027501000	1.553283000	0.866092000
6	2.674048000	-0.311826000	2.465480000
1	1.587457000	-0.243756000	2.391053000
6	2.301707000	3.061958000	-1.393432000
1	1.246967000	2.946968000	-1.146826000
6	-4.405477000	1.737601000	-0.663478000
1	-4.921855000	2.259473000	-1.458143000
6	-4.458294000	0.161787000	1.146631000
1	-5.016378000	-0.537660000	1.754098000
6	-2.335949000	3.035370000	-1.289093000
1	-1.267028000	2.942245000	-1.102485000
6	4.447876000	1.872423000	-0.818337000
1	4.916288000	2.416388000	-1.628011000
6	3.270669000	0.446558000	1.288026000
6	3.032731000	-1.804001000	2.448064000
1	2.750126000	-2.261591000	1.499655000
1	2.503297000	-2.319523000	3.253142000
1	4.100551000	-1.962830000	2.612725000
6	-3.052111000	1.991310000	-0.445375000
6	-0.604370000	2.448303000	1.835807000
1	-1.298705000	2.999377000	2.442072000
6	0.742394000	2.449096000	1.813335000
1	1.455976000	3.001115000	2.396158000
6	-2.798297000	0.389309000	3.914814000
1	-2.504245000	1.439247000	3.901006000
1	-2.290867000	-0.091048000	4.754120000
1	-3.873335000	0.348144000	4.102883000
6	-5.101806000	0.830120000	0.117783000
1	-6.151464000	0.645115000	-0.073361000
6	-2.758885000	4.454122000	-0.870760000
1	-3.825038000	4.614234000	-1.045922000
1	-2.208651000	5.200636000	-1.447610000
1	-2.564913000	4.635839000	0.188062000
6	0.046601000	0.998704000	0.219965000
6	-2.544683000	2.824444000	-2.794756000
1	-2.248683000	1.819841000	-3.095782000
1	-1.939858000	3.538856000	-3.357017000
1	-3.585377000	2.978462000	-3.087304000
6	3.091836000	2.063894000	-0.560058000
6	2.702624000	4.506054000	-1.047714000
1	2.556645000	4.720245000	0.012860000
1	2.102653000	5.215964000	-1.621568000
1	3.753361000	4.689881000	-1.281863000
6	2.525150000	1.334971000	0.497619000
6	4.623530000	0.296957000	0.984270000
1	5.226724000	-0.384241000	1.569071000
6	5.207310000	0.998510000	-0.057171000
1	6.258706000	0.862583000	-0.278171000

6	-2.448741000	-0.324471000	2.596201000
1	-1.366780000	-0.261189000	2.466487000
6	-3.105954000	0.375831000	1.412751000
6	3.087605000	0.332001000	3.800379000
1	4.170474000	0.285147000	3.935289000
1	2.623339000	-0.195332000	4.636757000
1	2.792466000	1.381273000	3.858037000
6	-2.809640000	-1.813138000	2.698177000
1	-2.222678000	-2.282559000	3.490050000
1	-2.607890000	-2.347782000	1.769417000
1	-3.862263000	-1.959100000	2.947346000
5	0.031928000	0.056369000	-1.024171000
6	2.436180000	2.800249000	-2.900079000
1	3.458083000	2.962185000	-3.248850000
1	1.789132000	3.481560000	-3.456846000
1	2.146971000	1.778928000	-3.146553000
6	-2.419152000	1.288688000	0.593119000
1	1.083071000	0.035285000	-1.593825000
1	-0.923104000	0.282241000	-1.721998000
8	1.577629000	-2.892427000	-0.446277000
6	1.864897000	-4.263506000	-0.611803000
1	1.308671000	-4.906300000	0.086859000
1	1.648062000	-4.612994000	-1.628617000
1	2.933350000	-4.419112000	-0.424470000
8	-0.648300000	-2.804142000	-2.656356000
6	0.110900000	-2.193761000	-3.676872000
1	-0.130913000	-1.131185000	-3.798446000
1	1.190480000	-2.275212000	-3.501078000
1	-0.118178000	-2.704828000	-4.618736000

$IMe_4{\cdot}BH_2BiH_2$

5	-0.267447000	0.000060000	1.566794000
6	1.132136000	0.000025000	0.871093000
1	-0.507731000	-1.007863000	2.175224000
1	-0.507717000	1.008034000	2.175144000
7	1.861052000	1.077238000	0.477567000
6	3.011883000	0.679147000	-0.198479000
6	3.011845000	-0.679187000	-0.198487000
7	1.861022000	-1.077223000	0.477605000
6	1.427481000	2.453277000	0.641654000
6	3.993581000	1.647263000	-0.758061000
6	3.993487000	-1.647351000	-0.758083000
6	1.427412000	-2.453244000	0.641735000
1	2.294984000	3.108117000	0.677046000
1	0.870978000	2.540872000	1.570104000
1	0.777697000	2.752198000	-0.183526000
1	2.294895000	-3.108109000	0.677145000
1	0.777620000	-2.752168000	-0.183438000
1	0.870906000	-2.540797000	1.570186000
1	3.528340000	-2.328648000	-1.474835000
1	4.458356000	-2.256630000	0.022188000
1	4.790077000	-1.116868000	-1.276380000
1	4.790132000	1.116743000	-1.276380000
1	4.458497000	2.256499000	0.022218000
1	3.528466000	2.328602000	-1.474793000
83	-1.961076000	0.000002000	-0.199406000
1	-1.180222000	-1.280894000	-1.218762000
1	-1.180195000	1.280792000	-1.218874000

$IMe_4{\cdot}BH_2Bi(OMe)_2$

5	0.153965000	0.000106000	1.868816000
6	1.472965000	-0.000074000	1.024796000
1	-0.025244000	-1.008299000	2.500962000
1	-0.025137000	1.008721000	2.500684000
7	2.149301000	1.077120000	0.559437000
6	3.228751000	0.679890000	-0.221654000
6	3.228517000	-0.680730000	-0.221607000
7	2.148919000	-1.077538000	0.559483000
6	1.735205000	2.454101000	0.796829000
6	4.144259000	1.642780000	-0.892057000
6	4.143783000	-1.643922000	-0.891910000
6	1.734232000	-2.454334000	0.796934000
1	2.532069000	3.124396000	0.486564000
1	1.542009000	2.596016000	1.858229000
1	0.826401000	2.663923000	0.232599000
1	2.530040000	-3.125038000	0.484857000
1	0.824335000	-2.663221000	0.234122000
1	1.542835000	-2.596743000	1.858606000
1	3.606724000	-2.299769000	-1.581771000
1	4.671007000	-2.278304000	-0.174200000
1	4.895694000	-1.106666000	-1.466954000
1	4.895701000	1.105303000	-1.467508000
1	4.672051000	2.276756000	-0.174401000
1	3.607248000	2.299031000	-1.581567000
83	-1.685931000	0.000423000	0.336615000
8	-0.923960000	1.604164000	-0.841355000
6	-1.621805000	2.032295000	-1.987639000
1	-1.381731000	1.420305000	-2.867635000
1	-2.713547000	2.015349000	-1.858965000
1	-1.336140000	3.066456000	-2.214211000
8	-0.925806000	-1.604803000	-0.840484000
6	-1.624438000	-2.033361000	-1.986126000
1	-2.716156000	-2.014014000	-1.857583000
1	-1.383066000	-1.423190000	-2.867028000
1	-1.340850000	-3.068449000	-2.211073000

DMAP·BH_3

7	-2.169417000	-0.000014000	-0.019902000
7	2.014287000	0.000006000	0.012820000
6	0.653412000	0.000006000	0.001103000
5	-3.782020000	0.000010000	0.034661000
6	-0.097883000	1.195933000	-0.007748000
1	0.379730000	2.162897000	-0.010841000
6	-0.097864000	-1.195930000	-0.007775000
1	0.379769000	-2.162884000	-0.010895000
6	-1.471837000	1.146592000	-0.018489000
1	-2.067533000	2.048204000	-0.028727000
6	2.746236000	-1.255778000	0.006196000
1	2.502836000	-1.868198000	0.879344000
1	3.811996000	-1.046219000	0.030180000
1	2.536434000	-1.842649000	-0.893412000
6	2.746253000	1.255781000	0.006152000
1	2.536359000	1.842676000	-0.893418000
1	3.812012000	1.046204000	0.030004000
1	2.502965000	1.868185000	0.879344000
6	-1.471821000	-1.146611000	-0.018512000
1	-2.067508000	-2.048227000	-0.028769000
1	-4.143517000	-1.010098000	-0.525992000
1	-4.143516000	1.009642000	-0.526855000
1	-4.083011000	0.000520000	1.210741000

IDipp·BH_3

5	0.000000000	-0.072951000	-1.921517000
1	1.008018000	0.449696000	-2.341361000
1	-1.008021000	0.449690000	-2.341361000
7	-1.075771000	0.004809000	0.501640000
7	1.075770000	0.004810000	0.501639000
6	0.000000000	-0.007258000	-0.329580000
6	-0.674309000	0.019790000	1.828965000
1	-1.381367000	0.031222000	2.638122000
6	0.674309000	0.019791000	1.828964000
1	1.381367000	0.031224000	2.638122000
6	-2.461291000	0.002435000	0.097868000
6	-3.114874000	1.232378000	-0.070557000

6	-4.466070000	1.202037000	-0.411664000
1	-4.999139000	2.133294000	-0.553155000
6	-5.136402000	0.001164000	-0.581757000
1	-6.185585000	0.000569000	-0.850151000
6	-4.463688000	-1.198573000	-0.416165000
1	-4.995224000	-2.130387000	-0.559461000
6	-3.111951000	-1.227863000	-0.074700000
6	-2.409230000	2.570081000	0.090350000
1	-1.362947000	2.373518000	0.322965000
6	-2.991932000	3.381738000	1.257845000
1	-2.439312000	4.315360000	1.383734000
1	-4.039072000	3.637152000	1.082447000
1	-2.938307000	2.827782000	2.197207000
6	-2.431792000	3.379974000	-1.215211000
1	-1.860882000	4.303443000	-1.094379000
1	-1.992784000	2.809932000	-2.033932000
1	-3.450319000	3.655737000	-1.497053000
6	-2.407372000	-2.565243000	0.093918000
1	-1.355511000	-2.369269000	0.299806000
6	-2.969951000	-3.350722000	1.289250000
1	-2.419401000	-4.284523000	1.422739000
1	-2.894437000	-2.778434000	2.216063000
1	-4.021824000	-3.603561000	1.140013000
6	-2.460062000	-3.400543000	-1.194138000
1	-1.893660000	-4.325471000	-1.064107000
1	-3.484982000	-3.674822000	-1.453204000
1	-2.028110000	-2.851447000	-2.030605000
6	2.461291000	0.002436000	0.097868000
6	3.114872000	1.232381000	-0.070560000
6	4.466068000	1.202040000	-0.411667000
1	4.999135000	2.133298000	-0.553160000
6	5.136402000	0.001168000	-0.581757000
1	6.185584000	0.000575000	-0.850152000
6	4.463689000	-1.198569000	-0.416164000
1	4.995227000	-2.130383000	-0.559458000
6	3.111952000	-1.227860000	-0.074698000
6	2.409226000	2.570083000	0.090345000
1	1.362943000	2.373518000	0.322957000
6	2.991925000	3.381741000	1.257842000
1	2.938297000	2.827784000	2.197203000
1	4.039064000	3.637155000	1.082446000
1	2.439303000	4.315362000	1.383729000
6	2.431790000	3.379976000	-1.215217000
1	1.860879000	4.303444000	-1.094385000
1	3.450318000	3.655741000	-1.497056000
1	1.992785000	2.809933000	-2.033939000
6	2.407376000	-2.565241000	0.093924000
1	1.355514000	-2.369268000	0.299810000
6	2.969955000	-3.350715000	1.289258000
1	2.419406000	-4.284517000	1.422750000
1	4.021828000	-3.603552000	1.140024000
1	2.894438000	-2.778424000	2.216070000
6	2.460069000	-3.400546000	-1.194129000
1	1.893668000	-4.325474000	-1.064096000
1	2.028117000	-2.851453000	-2.030599000
1	3.484990000	-3.674824000	-1.453193000
1	0.000003000	-1.258676000	-2.217371000

$IMe_4{\cdot}BH_3$

7	-0.858916000	0.750008000	-0.006097000
7	1.122481000	-0.067284000	-0.015043000
6	-1.003430000	-0.638215000	0.001148000
6	0.447016000	1.105663000	-0.012688000
6	0.252366000	-1.154236000	-0.002608000
6	0.729297000	-2.563581000	-0.000406000
1	1.294041000	-2.804198000	-0.905246000
1	-0.114851000	-3.248819000	0.052499000
1	1.378443000	-2.770363000	0.854402000
6	-1.974853000	1.681433000	0.001832000
1	-2.610956000	1.519265000	-0.869266000
1	-1.570593000	2.687607000	-0.025835000
1	-2.571047000	1.553355000	0.906416000
6	2.572041000	-0.162375000	0.008684000
1	2.977576000	0.820785000	-0.207142000
1	2.913971000	-0.871863000	-0.744681000
1	2.921433000	-0.486529000	0.990659000
6	-2.332559000	-1.306724000	0.005923000
1	-2.926962000	-1.026738000	0.879692000
1	-2.210066000	-2.388277000	0.023738000
1	-2.919162000	-1.055663000	-0.881969000
5	1.111675000	2.560699000	0.004661000
1	0.271353000	3.427622000	-0.079793000
1	1.891653000	2.626989000	-0.929720000
1	1.732565000	2.662470000	1.049603000

8.5.7 References

[1] R. Szlosek, M. Seidl, G. Balázs, M. Scheer, *Chem. Eur. J.* **2023**, *29*, e202301752.

[2] N. Kuhn, G. Henkel, T. Kratz, J. Kreutzberg, R. Boese, A. H. Maulitz, *Chem. Ber.* **1993**, *126*, 2041–2045.

[3] G. Becker, M. Rößler, *Z. Naturforsch. B* **1982**, *37*, 91–96.

[4] F. Barth, F. Achrainer, A. M. Pütz, H. Zipse, *Chem. Eur. J.* **2017**, *23*, 13455–13464.

[5] O. V. Dolomanov, L. J. Bourhis, R. J. Gildea, J. A. K. Howard, H. Puschmann, *J. Appl. Crystallogr.* **2009**, *42*, 339–341.

[6] G. M. Sheldrick, *Acta Cryst. A* **2015**, *71*, 3–8.

[7] G. M. Sheldrick, *Acta Cryst. C* **2015**, *71*, 3–8.

[8] a) A. D. Becke, *J. Chem. Phys.* **1993**, *98*, 5648–5652; b) C. Lee, W. Yang, R. G. Parr, *Phys. Rev. B* **1988**, *37*, 785–789; c) F. Weigend, R. Ahlrichs, *Phys. Chem. Chem. Phys.* **2005**, *7*, 3297-305.

[9] Gaussian 09, Revision E.01, M. J. Frisch, G. W. Trucks, H. B. Schlegel, G. E. Scuseria, M. A. Robb, J. R. Cheeseman, G. Scalmani, V. Barone, G. A. Petersson, H. Nakatsuji, X. Li, M. Caricato, A. Marenich, J. Bloino, B. G. Janesko, R. Gomperts, B. Mennucci, H. P. Hratchian, J. V. Ortiz, A. F. Izmaylov, J. L. Sonnenberg, D. Williams-Young, F. Ding, F. Lipparini, F. Egidi, J. Goings, B. Peng, A. Petrone, T. Henderson, D. Ranasinghe, V. G. Zakrzewski, J. Gao, N. Rega, G. Zheng, W. Liang, M. Hada, M. Ehara, K. Toyota, R. Fukuda, J. Hasegawa, M. Ishida, T. Nakajima, Y. Honda, O. Kitao, H. Nakai, T.

Vreven, K. Throssell, J. A. Montgomery, Jr., J. E. Peralta, F. Ogliaro, M. Bearpark, J. J. Heyd, E. Brothers, K. N. Kudin, V. N. Staroverov, T. Keith, R. Kobayashi, J. Normand, K. Raghavachari, A. Rendell, J. C. Burant, S. S. Iyengar, J. Tomasi, M. Cossi, J. M. Millam, M. Klene, C. Adamo, R. Cammi, J. W. Ochterski, R. L. Martin, K. Morokuma, O. Farkas, J. B. Foresman, and D. J. Fox, Gaussian, Inc., Wallingford CT, 2016.

[10] A. E. Reed, L. A. Curtiss, F. Weinhold, *Chem. Rev.* **1988**, *88*, 899–926.

[11] Thermal Constants of Substances database, Eds. V.S. Iorish and V.S. Yungman, https://www.chem.msu.ru/cgi-bin/tkv.pl?show=welcome.html/welcome.html

8.6 Author Contributions

- R. Szlosek – writing of original and final manuscript, experimental work (syntheses and characterizations of **1a** and **2**, reproductions and completion of analytical data of **1b/c**)
- C. Marquardt – original synthesis of **1c**
- O. Hegen – original synthesis of **1b**
- G. Balázs – project management, conceptualization
- C. Riesinger – finalization of single-crystal X-ray data for **1a**
- Y. Timoshkin – quantum chemical calculations, acquisition of funding, co-writing of final manuscript
- M. Scheer – project supervision, acquisition of funding, co-writing of final manuscript

9 NHC-stabilized Mixed Group 13/14/15 Element Hydrides

M. T. Ackermann, R. Szlosek, C. Riesinger, M. Seidl, A. Y. Timoshkin, E. Rivard and M. Scheer

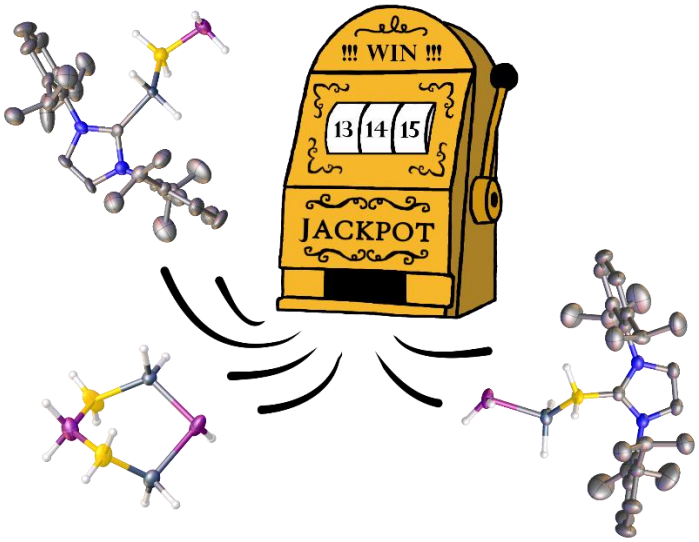

Abstract: The syntheses of novel N-heterocyclic carbene (NHC) adducts of group 13, 14 and 15 element hydrides are reported. Salt metathesis reactions between $NaPH_2$ and IDipp·GeH_2BH_2OTf (**1**) (IDipp = 1,3-bis(2,6-diisopropylphenyl)imidazol-2-ylidene) led to mixtures of the two isomers IDipp·$GeH_2BH_2PH_2$ (**2a**) and IDipp·$BH_2GeH_2PH_2$ (**2b**); by altering the reaction conditions an almost exclusive formation of **2b** was achieved. Attempts to purify mixtures of **2a** and **2b** by re-crystallization from THF afforded a salt [IDipp·GeH_2BH_2·IDipp][$PHGeH_2BH_2PH_2BH_2GeH_2$] (**4**) that contains the novel anionic cyclohexyl-like inorganic heterocycle [$PHGeH_2BH_2PH_2BH_2GeH_2$]$^-$. In addition, the borane adducts IDipp·$GeH_2BH_2PH_2BH_3$ (**3a**) and IDipp·$BH_2GeH_2PH_2BH_3$ (**3b**) as even longer chain compounds were obtained from reactions of **2a**/**2b** with H_3B·SMe_2 and were studied by NMR spectroscopy. Accompanying DFT computations give insight into the mechanism and energetics associated with **2a**/**2b** isomerization as well as their decomposition pathways.

9.1 Introduction

Hydrocarbons are an important class of compounds, representing the basis for the large-scale production of fuels as well as bulk and specialized chemicals. Due to the isolobal analogy between $TetH_2$, $E'H_2^-$, EH_2^+ and EH (Tet = Group 14 element; E' = Group 13 element; E = Group 15 element), combinations of such group 13 and group 15 element moieties (or additional group 14-based $TetH_2$ entities) can be considered as isoelectronic analogues of corresponding hydrocarbons. The pioneering work of Stock and Poland on the preparation of borazine $(HBNH)_3$ is just one of many examples for such group 13/15 analogues.[1a-e] Group 13/15 element compounds in general are investigated as valuable starting materials for the deposition of thin films in semiconductor processes and as building blocks for inorganic polymers.[1f-o] Moreover, the study of group 14/15 compounds[2] have only recently shifted to include heavier element homologues.[3] In contrast, heavier homologues of compounds consisting of combinations of group 13, group 14 (Tet ≠ C) and group 15 units remain scarce in the literature.[4]

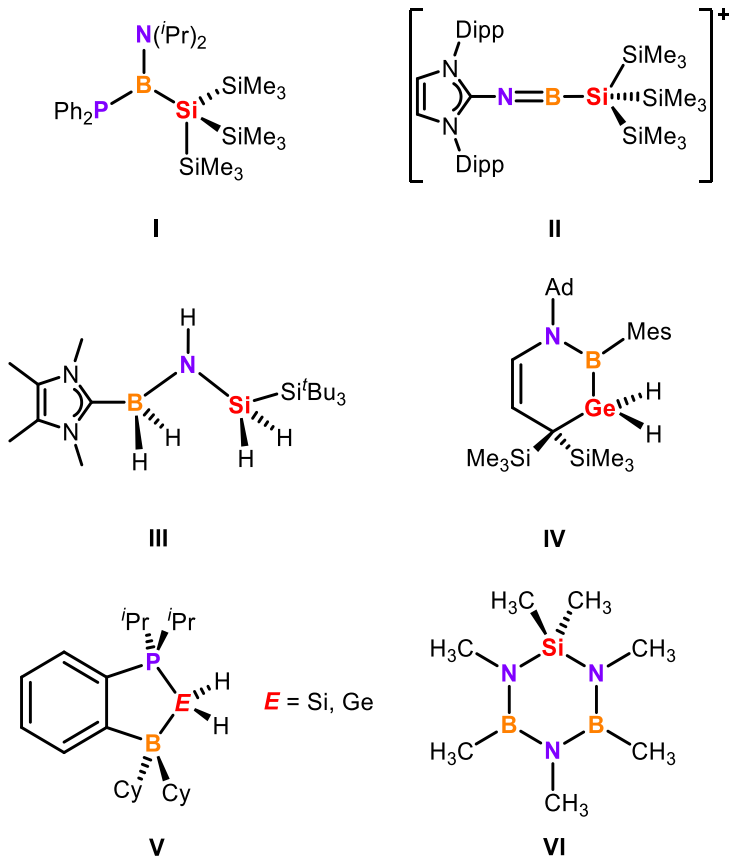

Figure 9.1: Selected examples of mixed group 13/14/15 chain and cyclic compounds.

One possible approach for synthesizing group 13/14/15 chains is via salt-metathesis, as used by Nöth in the synthesis of **I** (Figure 9.1),[5] and by Inoue to access the *N*-heterocyclic carbene (NHC)-stabilized borasilene **II**.[6] Also, Inoue reported on an alternative synthetic strategy resulting in the formation of **III**, which was obtained by the reaction of IMe_4·SiHSi*t*Bu_3 (IMe_4 = 1,3,4,5-tetra(methyl)imidazol-2-ylidene) with $H_3N{\cdot}BH_3$ by dehydrogenation to H_2NBH_2 and subsequent insertion/rearrangement processes.[7] Furthermore, two very recent examples of heterocycles that include group 13/14/15 element-based building blocks are: **IV**,[8] reported by Kinjo, and the Frustrated Lewis Pair (FLP)-stabilized adducts **V**, synthesized by the Rivard group; notably, compounds **V** can be used as precursors for the low-temperature deposition (< 100 °C) of elemental Si and Ge films from solution.[9] A rare example of a

heterocycle that consists exclusively of combinations of group 13, group 14 (Tet ≠ C) and group 15 elements is **VI**, reported by Nöth; however, the characterization of **VI** was limited to NMR spectroscopy.[10] Since most of the abovementioned compounds require some steric stabilization from organic substituents, the idea of an approach to access exclusively H-substituted (parent) compounds came to mind. While very few examples of the parent group 13/14/15 element chain compounds exist, including our recently introduced cationic species [IDipp·GeH_2BH_2·PH_3][OTf] and [IDipp·$GeH_2BH_2EH_2BH_2$·NMe_3][OTf] (E = P, As; IDipp = 1,3-bis(2,6-diisopropylphenyl)imidazol-2-ylidene), to our knowledge, no reports on corresponding parent heterocycles can be found.[11] Specifically, neutral group 13/14/15 element chain compounds bearing hydrogen substituents, which resemble their organic counterparts more closely, impose a synthetic challenge as the stability of such target compounds is reduced compared to their ionic derivatives. Furthermore, neutral mixed group 13/14/15 element hydrides (and their adducts) would be promising single-source precursors to novel ternary optoelectronic materials by MOCVD (Metal-Organic Chemical Vapor Deposition); thus, alternative synthetic strategies and a more versatile element selection for such compounds are desirable.[12] Within the last two decades, our group studied the synthesis and reactivity of only Lewis base (LB)-stabilized parent pnictogenyltrielanes $H_2EE'H_2$·LB (E = group 15 element, E' = group 13 element) in detail.[13,14] Since those compounds were mostly obtained through salt-metathesis, we wondered if the previously introduced NHC-stabilized H_2GeBH_2 precursor IDipp·GeH_2BH_2OTf (**1**) might serve as a starting reagent for the synthesis of novel neutral NHC-stabilized parent group 13/14/15 element compounds. Herein we report on the syntheses and reactivity of unprecedented neutral parent compounds consisting of elements of the group 13, 14 and 15 stabilized by the N-heterocyclic carbene IDipp.

9.2 Results and Discussion

The addition of a cold solution (−80 °C) of IDipp·GeH_2BH_2OTf (**1**) in THF to a suspension of $NaPH_2$ in THF at −80 °C, and subsequent stirring of the reaction mixture at room temperature leads to the formation of a mixture of the initially desired NHC-stabilized parent compound IDipp·$GeH_2BH_2PH_2$ (**2a**) and its unexpected isomer IDipp·$BH_2GeH_2PH_2$ (**2b**), in which the Ge and the B atoms have switched positions (Scheme 9.1, route **A**). The isomer mixture can be isolated in moderate yield as white powder with a ratio of **2a/2b** between 30-40:70-60. **2a/2b** mixtures are stable at ambient temperatures in an inert atmosphere. Unfortunately, all attempts to separate both isomers from each other failed due to their very similar solubility and the limited stability of **2a**. As NMR studies indicate no conversion of **2a** to **2b** in solution, altering the reaction conditions was the only possibility to increase the relative amount of one isomer over the other within a product mixture. Indeed, if both solid starting materials (**1** and $NaPH_2$) are combined in the same Schlenk tube and cold THF (-80 °C) is then added, the isolated white powder shows an isomer mixture with up to 93% of **2b** and only 7% of **2a** (Scheme 9.1, route **B**).

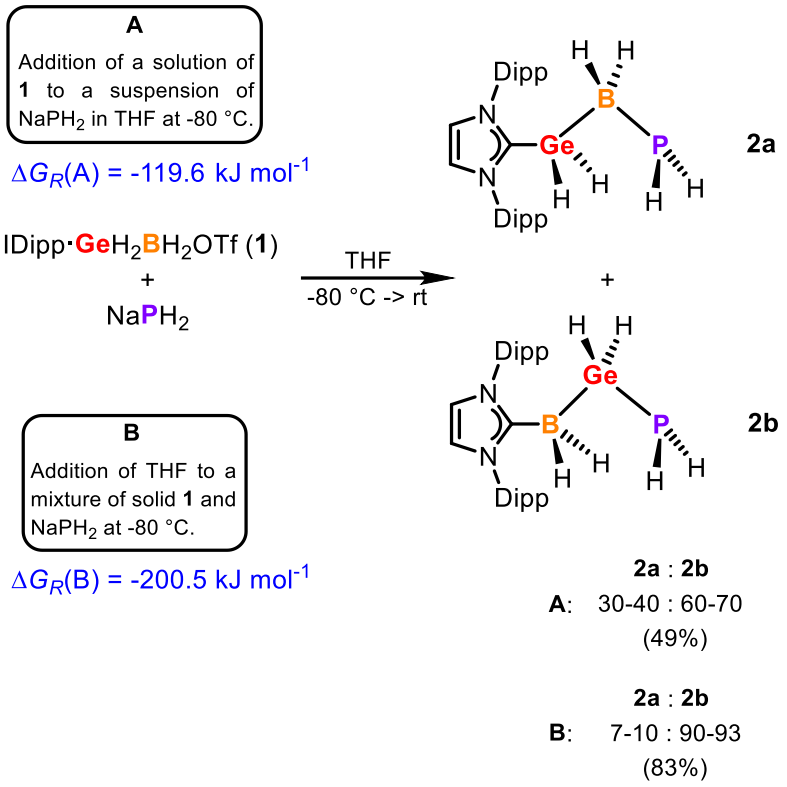

Scheme 9.1: Synthesis of the parent compounds **2a** and **2b**. Yields are given in parentheses. Calculated free enthalpy values ΔG_R of routes A and B were calculated at the B3LYP/def2-TZVP level of theory (cf. Supporting Information).

Interestingly, while changing the reaction temperature of route **B** to –60 °C does not affect the obtained **2a**/**2b** isomer ratio, an increased amount of **2a** with a product **2a**/**2b** ratio of 67:33 could be observed when employing route **A** at –60 °C (Scheme 9.1). Subsequently, numerous experiments applying different reaction conditions were carried out to solely obtain one isomer. For instance, an almost exclusive formation of **2b** with an isomer ratio of 97:3 was observed from the reaction of **1** with $LiPH_2$·DME in DME at –50 °C. However, the additional formation of the inseparable decomposition product IDipp·GeH_2BH_3[15] did not lead to an overall improvement compared to route **B** (Scheme 9.1). Similarly, all other attempts including different solvents (such as Et_2O or DME), alteration of the addition of the starting materials or addition of crown ethers and [2.2.2]cryptand, respectively, did not lead to the selective formation of one isomer over the other. Thus, route **B** was the optimal method to obtain samples enriched in isomer **2b**, while route **A** yields the best results for an increased amount of isomer **2a** (Scheme 9.1).

Computational studies reveal that the formation of both isomers **2a** and **2b** is exothermic and exergonic in the gas phase at room temperature (see Supporting Information for details). Since the formation of isomer **2b** is more exergonic by 80 kJ mol^{-1} (cf. Scheme 9.1), it represents the thermodynamically favored product, while isomer **2a** is feasible probably due to kinetic reasons. Furthermore, the experimental observation of significant amounts of **2a** (10–67%) indicates that a rearrangement process from **2a** to **2b** seems to be kinetically hindered. According to the ^{31}P NMR spectrum of a mixture of **2a**/**2b** in THF, no significant change of the ratio of **2a**:**2b** is observed over time, even after one week at room temperature. A possible reaction pathway in this case involves the nucleophilic attack of $[PH_2]^-$ at the germanium atom, resulting in the transition state **TS**, which then rearranges by a concerted mechanism to **2b** under elimination of the triflate group, $[OTf]^-$ (Scheme 9.2, Figure 9.2). This reaction pathway might also be favored at low temperatures since the resulting less labile B-O bond in **1** should lead to a higher probability of $[PH_2]^-$ to attack at the Ge atom and thus result in the formation of the thermodynamically more

stable product **2b**, which confirms the experimentally found isomer ratios. Also, our quantum chemical calculations were able to locate a corresponding transition state **TS** for the formation of **2b** (Scheme 9.2, Figure 9.2; cf. Supporting Information). This transition state features a bridging NHC that links both the Ge and B atoms, and the energy of this **TS** lies only 70 kJ mol^{-1} higher than the total energy of isolated **1** and $[PH_2]^-$, which helps explain the formation of **2b** even at low temperatures.

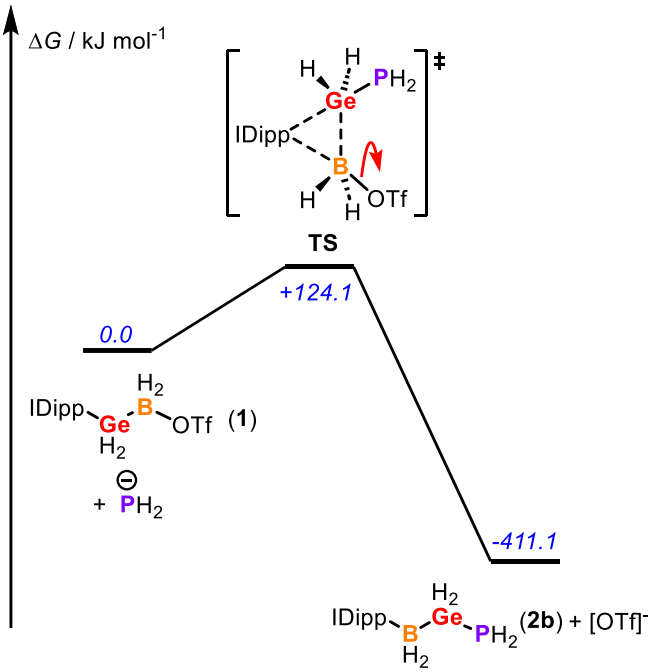

Scheme 9.2: Proposed reaction pathway for the formation of **2b**. Free enthalpy values were calculated at the B3LYP/def2-TZVP level of theory.

While only the decomposition by-product $[IDipp\text{-}H]^+$ of **2a** and **2b** could be detected by LIFDI-MS spectrometry, both isomers were successfully characterized by NMR spectroscopy and single-crystal X-ray structure analysis. The ^1H NMR spectra of **2a** and **2b** in C_6D_6 show a multiplet resonance for the GeH_2-moiety at δ = 3.85 ppm (**2a**) and a doublet of pseudo-quintets at δ = 3.46 ppm (**2b**; $^2J_{H,P}$ = 17.5 Hz, $^3J_{H,H}$ = 4.3 Hz). While the $^{31}P\{^1H\}$ NMR spectrum of **2a** (δ = −202.3 ppm) reveals a broad multiplet due to the coupling with the neighboring boron atom, a sharp singlet is found for **2b** (δ = −244.0 ppm). Both signals show further splitting in the corresponding ^{31}P NMR spectra into a broad triplet (**2a**, $^1J_{H,P}$ = 180 Hz) and a triplet of triplets (**2b**; $^1J_{H,P}$ = 176 Hz, $^2J_{H,P}$ = 17.5 Hz). Similarly, the ^{11}B NMR spectra reveal broad triplets at δ = −37.9 ppm (**2a**, $^1J_{H,B}$ = 104 Hz) and δ = −34.7 ppm (**2b**, $^1J_{H,B}$ = 97 Hz) that both collapse into a broad multiplet (**2a**) and a singlet (**2b**) within the respective $^{11}B\{^1H\}$ NMR spectra. Slow solvent evaporation of Et_2O solutions of mixtures of **2a** and **2b** afforded colorless single crystals with different ratios of the co-crystallized isomers (Figure 9.3).

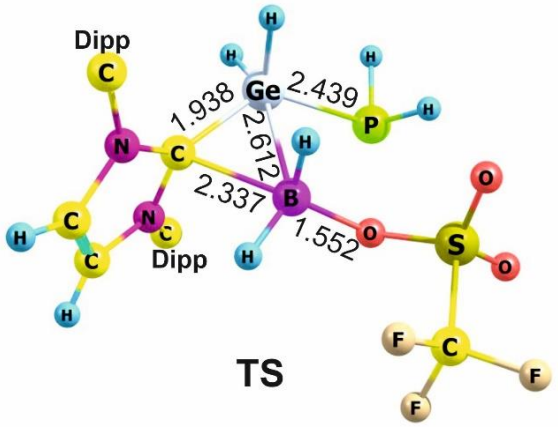

Figure 9.2: Optimized geometry of the transition state (Scheme 9.2, B3LYP/def2-TZVP). For clarity, only one carbon atom of each Dipp substituent is shown.

Interestingly, crystals that contain a higher amount of **2a** (≥ 63%) crystallize in the monoclinic space group $P2_1$ with two independent molecules in the asymmetric unit, while crystals containing a higher amount of **2b** (≥ 90%) crystallize in the orthorhombic space group *Pccn*, although co-crystallization of both isomers is observed in every case. For **2b** the H_2GePH_2 moiety shows slight disorder (see Supporting Information for details). In the solid state, the C-Ge distances [1.962(6) – 2.007(7) Å] as well as the Ge-B [2.031(15) – 2.076(19) Å] and B-P distances [1.93(2) – 2.07(2) Å] of **2a** are all in the expected range of single bonds. Analogously, the C-B [1.572(4) Å], B-Ge [2.047(4) Å] and Ge-P [2.320(3) Å] bond lengths within isomer **2b** are in the expected range of single bonds. The C-Ge-B-P torsion angles of **2a** in the asymmetric unit adopt values up to 169.9(5)°, while the C-B-Ge-P torsion angle of **2b** is 157.2(3)°.[16,20]

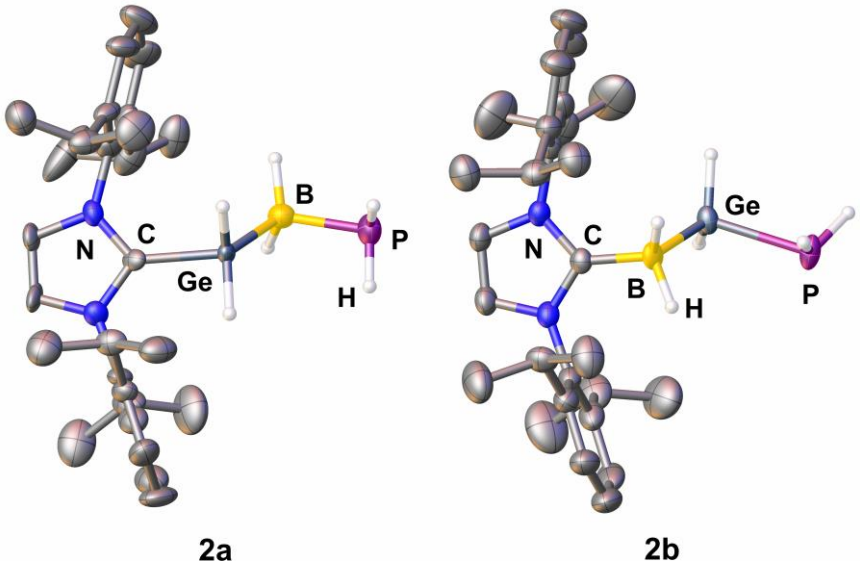

Figure 9.3: Molecular structure of one molecule of **2a** from a mixture containing largely **2a** (left) in the asymmetric unit with thermal ellipsoids at a 50% probability level. Hydrogen atoms bound to carbon are omitted for clarity. Selected bond lengths [Å] and angles [°] with metrical parameters for the second molecule listed in parentheses: C-Ge 1.962(6) [2.007(7)], Ge-B 2.076(19) [2.031(15)], B-P 1.93(2) [2.07(2)]; C-Ge-B 119.1(6) [115.3(6)], Ge-B-P 107.3(9) [103.7(9)]. Molecular structure of **2b** from a mixture containing mostly **2b** (right) in the solid state with thermal ellipsoids at a 50% probability level. Hydrogen atoms bound to carbon are omitted for clarity. Selected bond lengths [Å] and angles [°]: C-B 1.572(4), B-Ge 2.047(4), Ge-P 2.320(3); C-B-Ge 113.3(1), B-Ge-P 106.47(13).

As the lone pair at the phosphorus atoms within the isomers **2a** and **2b** should provide the opportunity for follow-up chemistry, we wondered if it would be possible to extend the group 13/14/15 moieties by combination with a main-group Lewis acid. In fact, the addition of $H_3B{\cdot}SMe_2$ to a toluene solution of

mixtures of **2a** and **2b** at −80 °C and subsequent stirring of the reaction mixture for 1.5 hours at room temperature affords the two borane adducts IDipp·$GeH_2BH_2PH_2BH_3$ (**3a**) and IDipp·$BH_2GeH_2PH_2BH_3$ (**3b**) (Scheme 9.3), which feature an extended hydrogen-substituted 13/14/15/13 element chain. Mixtures of **3a** and **3b** can be isolated as white powders in high yields, however, these isomers cannot be separated due to their similar solubilities. Both **3a** and **3b** are stable as solids at room temperature under an inert atmosphere but slowly decompose in solution with release of PH_3. While neither characterization of **3a** and **3b** by LIFDI-MS, nor crystallization of both isomers was successful (due to their very limited stability in solution), these isomers could be characterized by NMR spectroscopy.

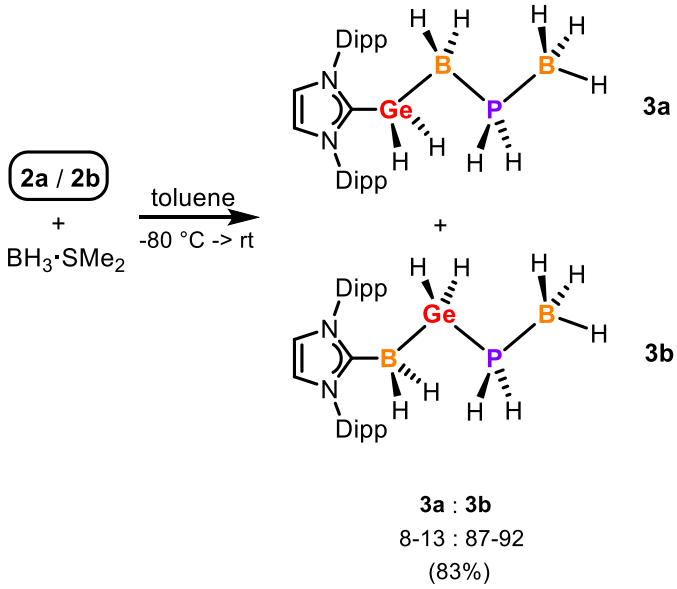

Scheme 9.3: Synthesis of the parent compounds **3a** and **3b**. Yields are given in parentheses.

The ^{1}H NMR spectra of **3a**/**3b** mixtures in C_6D_6 show two multiplet resonances for the respective GeH_2-moieties at δ = 3.84 ppm (**3a**) and δ = 3.45 ppm (**3b**), respectively. The ^{31}P NMR data assigned to **3a** shows a distinct triplet at δ = −104.2 ppm ($^1J_{H,P}$ = 311 Hz) and for **3b** a broad triplet at δ = −131.3 ppm ($^1J_{H,P}$ = 326 Hz) is observed; both resonances are significantly downfield-shifted in comparison to the signals from the starting materials (**2a**: δ = −202.3 ppm, **2b**: δ = −244.0 ppm; Figure 9.4). In addition, the ^{11}B NMR spectral data of **3b** yields a triplet for the BH_2 moiety at δ = −36.1 ppm ($^1J_{H,B}$ = 99 Hz) and a broad quartet for the terminal BH_3 moiety at δ = −38.7 ppm ($^1J_{H,B}$ = 100 Hz). The ^{11}B NMR signals for **3a** are superimposed by those of **3b** but can still be located as a broadened quartet at −39.5 ppm (BH_3) and a singlet at −40.4 ppm (BH_2, $^1J_{BH}$ coupling not resolved due to significant signal broadening). Furthermore, quantum chemical computations reveal that the formation of **3a** and **3b** are both exothermic and exergonic, which is in line with the experimental observations of the constant ratio between the isomers with respect to the isomer ratio of the starting mixture of **2a**/**2b** (cf. Supporting Information). According to the computational studies, **3b** is more stable than **3a** by −58.3 kJ mol^{-1} and can thus be considered as the thermodynamic product.

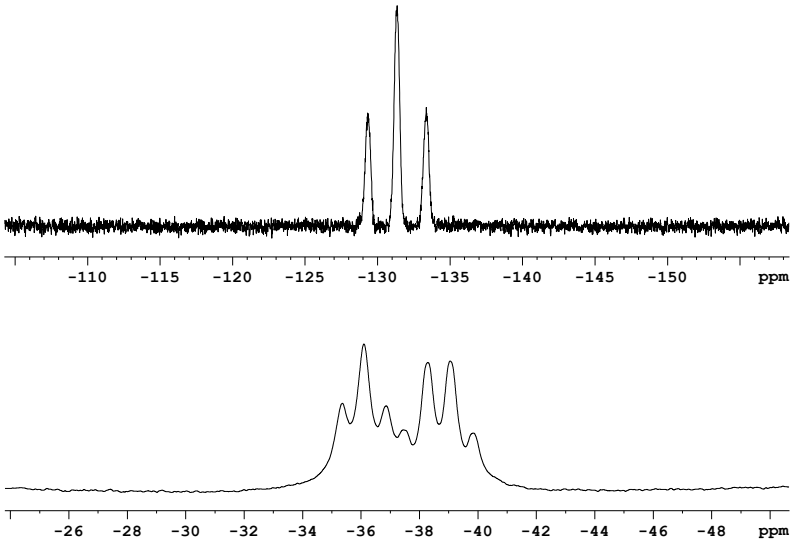

Figure 9.4: ^{31}P (top) and ^{11}B (bottom) NMR spectra of **3b** in C_6D_6 as sections of the overall spectra at 298 K.

Coming back to the initially introduced compounds **2a** and **2b**, which can be successfully crystallized either by slow evaporation of Et_2O or by cooling concentrated toluene/*n*-hexane solutions, to our surprise, the crystallization attempts by solvent diffusion of *n*-hexane into a THF solution of a mixture of **2a**/**2b** (4 °C, 9:91 ratio, Scheme 9.4) yielded a few colorless crystals of [IDipp·GeH_2BH_2·IDipp][$PHGeH_2BH_2PH_2BH_2GeH_2$] (**4**). **4** represents the first inorganic example of a heterocycle that exclusively consists of combinations of hydrogen-substituted (parent) group 13,14 and 15 moieties. In contrast, analogous layering/crystallization attempts where THF is substituted by CH_2Cl_2 only led to decomposition, as **2a**/**2b** show limited stability in CH_2Cl_2.

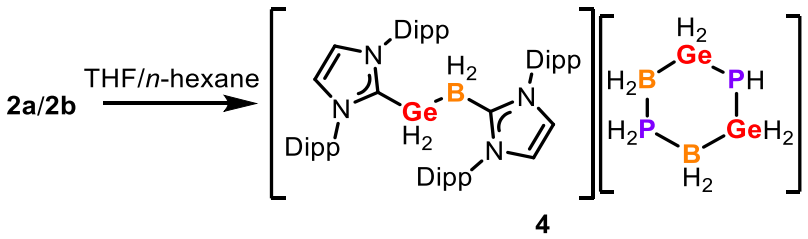

4

Scheme 9.4: Partial conversion of **2a**/**2b** to [IDipp·GeH_2BH_2·IDipp][$PHGeH_2BH_2PH_2BH_2GeH_2$] (**4**) by layering in THF/n-hexane.

While **4** is stable as a solid at ambient temperatures in an inert atmosphere, it slowly decomposes in solution under release of PH_3. In the mass spectra (ESI-MS) of a freshly prepared CH_2Cl_2 solution of **4**, the molecular ion peaks for the anionic heterocycle (negative mode) and the cation [IDipp·GeH_2BH_2·IDipp]$^+$ (positive mode) are detected (cf. Supporting Information for details). The ^1H NMR spectrum of **4** in CD_2Cl_2 shows two signals for the GeH_2-moieties of the anionic heterocycle due to the existence of axial and equatorial protons, which is comparable to the ^1H NMR spectrum of cyclohexane at low temperatures (see Supporting Information for details).[17] In the $^{31}P\{^1H\}$ NMR spectrum a broad multiplet is detected at δ = −98.1 ppm ($^1J_{P,B}$ = 64 Hz) and an additional sharp singlet is located at δ = −270.5 ppm. While the signal at δ = −98.1 ppm shows further splitting into a broad triplet (PH_2; $^1J_{H,P}$ = 320 Hz) in the ^{31}P NMR spectrum, the signal at δ = −270.5 ppm splits into a doublet (PH; $^1J_{H,P}$ = 163 Hz). In addition, the ^{11}B NMR spectrum reveals a doublet of triplets for the BH_2 moieties of the anionic heterocycle at δ = −40.3 ppm ($^1J_{P,B}$ = 64 Hz, $^1J_{H,B}$ = 102 Hz) and a triplet resonance from the counterion at δ = −37.7 ppm ($^1J_{H,B}$ = 100 Hz).

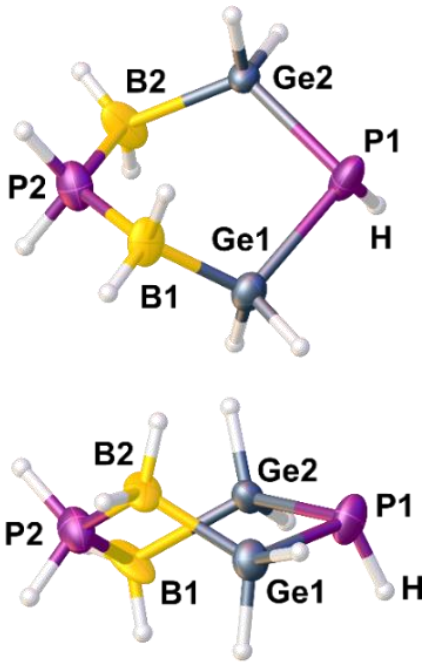

4

Figure 9.5: Top view (top) and side view (bottom) of the major part of the molecular structure of the anion in **4** in the solid state with thermal ellipsoids at a 50% probability level. Selected bond lengths [Å] and angles [°]: P-Ge 2.3264(15)-2.4284(18), Ge-B 1.952(6)-2.047(9), B-P 1.911(9)-1.965(5); Ge-P-Ge 99.42(6), B-P-B 122.8(4), B-Ge-P 110.8(2)-116.4(4), P-B-Ge 108.2(3)-109.6(4).

The solid-state structure of **4** shows a cation featuring a $[H_2BGeH_2]^+$ unit that is stabilized by two capping IDipp donors. The anion represents a cyclohexyl-like unit, which consists of two GeH_2 moieties, that enclose one PH entity, two BH_2 moieties and one PH_2 component (Figure 9.5). As a side note, a minor part (17%) of the inorganic heterocycle in **4** crystallized with an envelope conformation (cf. Supporting Information); the $B_2Ge_2P_2$ heterocycle is also distorted between several positions (see Supporting Information for details). The P-Ge distances [2.3264(15) – 2.4284(18) Å], the Ge-B bond lengths [1.952(6) – 2.047(9)Å] and the B-P distances [1.911(9) – 1.965(5) Å] of the heterocycle are all in the expected range of single bonds.[16] The cation shows a Ge-B bond length of 2.089(12) Å, which is also in range of a slightly elongated single bond. Moreover, computations for a possible isomer of the anionic heterocycle in **4** with the PH group placed in between two BH_2 moieties predict much longer Ge-P, Ge-B and B-P bond distances and a higher relative energy (145 kJ mol^{-1}) compared to the experimentally found isomer, proving support for the atom connectivity assigned via crystallography.[18]

9.3 Conclusion

In summary, we have shown that reactions of IDipp·GeH_2BH_2OTf (**1**) with $NaPH_2$ result in mixtures of the isomers IDipp·$GeH_2BH_2PH_2$ (**2a**) and IDipp·$BH_2GeH_2PH_2$ (**2b**), revealing unprecedented neutral NHC-stabilized parent group 13/14/15 compounds. The formation of **2b** was rather unexpected, however, tuning the reaction conditions enabled formation of **2b** with an isomer amount of over 90%. Both isomers were characterized by single-crystal X-ray diffraction and NMR spectroscopy. Furthermore, the corresponding isomer mixtures of the parent adducts IDipp·$GeH_2BH_2PH_2BH_3$ (**3a**) and

IDipp·$BH_2GeH_2PH_2BH_3$ (**3b**) could be obtained from reactions of **2a** and **2b** with $H_3B{\cdot}SMe_2$ and feature novel, even longer group 13/14/15 element chains with only hydrogen atom substituents. Computational results indicate that the isomers with a group 14 element occupying the central position of a chain are more energetically favorable and appear to be prospective synthetic targets. In addition, attempts to crystallize a mixture of **2a** and **2b** from THF solutions surprisingly afforded the anionic cyclohexyl-like ring $[PHGeH_2BH_2PH_2BH_2GeH_2]^-$ within the final product **4**, which represents the first example of an only hydrogen-substituted inorganic heterocycle consisting of group 13, 14 and 15 elements. Further investigations will be focused on the synthesis of comparable 13/14/15 element units with alternate congeners.

9.4 References

[1] a) A. Stock, E. Pohland, *Ber. Dtsch. Chem. Ges.* **1926**, *59*, 2215–2223; b) S. Schulz, *Coord. Chem. Rev.* **2001**, *215*, 1–37; c) S. Schulz, *Adv. Organomet. Chem.* **2003**, *49*, 225–317; d) B. Neumüller, E. Iravani, *Coord. Chem. Rev.* **2004**, *248*, 817–834; e) A. K. Swarnakar, C. Hering-Junghans, K. Nagata, M. J. Ferguson, R. McDonald, N. Tokitoh, E. Rivard, *Angew. Chem. Int. Ed.* **2015**, *54*, 10666–10669; *Angew. Chem.* **2015**, *127*, 10812–10816; f) A. H. Cowley, R. A. Jones, *Angew. Chem. Int. Ed.* **1989**, *28*, 1208-1215; *Angew. Chem.* **1989**, *101*, 1235-1243; g) J. F. Janik, R. L. Wells, V. G. Young, A. L. Rheingold, I. A. Guzei, *J. Am. Chem. Soc.* **1998**, *120*, 532–537; h) S. M. Stuczynski, R. L. Opila, P. Marsh, J. G. Brennan, M. L. Steigerwald, *Chem. Mater.* **1991**, *3*, 379–381; i) C. Marquardt, T. Jurca, K.-C. Schwan, A. Stauber, A. V. Virovets, G. R. Whittell, I. Manners, M. Scheer, *Angew. Chem. Int. Ed.* **2015**, *54*, 13782–13786; j) M. Bodensteiner, U. Vogel, A. Y. Timoshkin, M. Scheer, *Angew. Chem. Int. Ed.* **2009**, *48*, 4629–4633; *Angew. Chem.* **2009**, *121*, 4700-4704; k) M. Bodensteiner, A. Y. Timoshkin, E. V. Peresypkina, U. Vogel, M. Scheer, *Chem. Eur. J.* **2013**, *19*, 957–963; l) C. Marquardt, O. Hegen, A. Vogel, A. Stauber, M. Bodensteiner, A. Y. Timoshkin, M. Scheer, *Chem. Eur. J.* **2018**, *24*, 360–363; m) A. M. Belousova, A. Y. Timoshkin, *J. Phys. Chem. A* **2023**, *127*, 7353-7363; n) J. Braese, F. Lehnfeld, V. T. Annibale, T. Oswald, R. Beckhaus, I. Manners, M. Scheer, *Chem. Eur. J.* **2023**, *29*, e202301741; o) M. M. D. Roy, A. A. Omaña, A. S. S. Wilson, M. S. Hill, S. Aldridge, E. Rivard, *Chem. Rev.* **2021**, *121*, 12784–12965.

[2] a) D. P. Gates in *New Aspects in Phosphorus Chemistry V*, Springer, Berlin, Heidelberg, **2005**, vol. 250, pp. 107–126; b) A. Chirila, R. Wolf, J. C. Slootweg, K. Lammertsma, *Coord. Chem. Rev.* **2014**, *270-271*, 57–74.

[3] a) A. E. Seitz, M. Eckhardt, A. Erlebach, E. V. Peresypkina, M. Sierka, M. Scheer, *J. Am. Chem. Soc.* **2016**, *138*, 10433–10436; b) V. Nesterov, N. C. Breit, S. Inoue, *Chem. Eur. J.* **2017**, *23*, 12014–12039; c) M. Balmer, C. von Hänisch, *Z. Anorg. Allg. Chem.* **2018**, *644*, 1143–1148; d) V. Nesterov, R. Baierl, F. Hanusch, A. E. Ferao, S. Inoue, *J. Am. Chem. Soc.* **2019**, *141*, 14576–14580.

[4] a) I. Geisler, H. Nöth, *Chem. Commun.* **1969**, *13*, 775–776; b) K. Barlos, H. Nöth, *Z. Naturforsch.* **1980**, *35 b*, 415–420; c) T. Kajiwara, N. Takeda, T. Sasamori, N. Tokitoh, *Organometallics* **2004**, *23*, 4723–4734; d) R. J. Wilson, J. R. Jones, M. V. Bennett, *Chem. Commun.* **2013**, *49*, 5049–5051; e) M. Kapitein, M. Balmer, C. von Hänisch, *Phosphorus, Sulfur, Silicon Relat. Elem.* **2016**, *191*, 641–644; f) M. Fernández-Millán, L. K. Allen, R. García-Rodríguez, A. D. Bond, M. E. G. Mosquera, D. S. Wright, *Chem. Commun.* **2016**, *52*, 5993–5996; g) A. Rosas-Sánchez, I. Alvarado-Beltran, A. Baceiredo, D. Hashizume, N. Saffon-Merceron, V. Branchadell, T. Kato, *Angew. Chem. Int. Ed.* **2017**, *56*, 4814–4818; *Angew. Chem.* **2017**, *129*, 4892–4896; h) A. Rosas-Sánchez, I. Alvarado-Beltran, A. Baceiredo, N. Saffon-Merceron, S. Massou, V. Branchadell, T. Kato, *Angew. Chem. Int. Ed.* **2017**, *56*, 10481–10485; *Angew. Chem.* **2017**, *129*, 10685–10690; i) M. Köster, A. Kreher, C. von Hänisch, *Dalton Trans.* **2018**, *47*, 7875–7878; j) B. Rao, R. Kinjo, *Angew. Chem. Int. Ed.* **2020**, *59*, 3147–3150; *Angew. Chem.* **2020**, *132*, 3171–3174; k) R. J. Schwamm, M. P. Coles, M. S. Hill, M. F. Mahon, C. L. McMullin, N. A. Rajabi, A. S. S. Wilson, *Angew. Chem. Int. Ed.* **2020**, *59*, 3928–3932; *Angew. Chem.* **2020**, *132*, 3956–3960; l) S. Schneider, C. von Hänisch, *Eur. J. Inorg. Chem.* **2021**, 4655–4660; m) A. Bücker, C. Wölper, G. Haberhauer, S. Schulz, *Chem. Commun.* **2022**, *58*, 9758-9761.

[5] M. Fan, R. T. Paine, E. N. Duesler, H. Nöth, *Z. Anorg. Allg. Chem.* **2006**, *632*, 2443–2446.

[6] D. Franz, T. Szilvási, A. Pöthig, S. Inoue, *Chem. Eur. J.* **2019**, *25*, 11036–11041.

[7] G. Dübek, D. Franz, C. Eisenhut, P. J. Altmann, S. Inoue, *Dalton Trans.* **2019**, *48*, 5756–5765.

[8] B. Rao, R. Kinjo, *Angew. Chem. Int. Ed.* **2019**, *58*, 18150–18153; *Angew. Chem.* **2019**, *131*, 18318–18321.

[9] A. A. Omaña, R. K. Green, R. Kobayashi, Y. He, E. R. Antoniuk, M. J. Ferguson, Y. Zhou, J. G. C. Veinot, T. Iwamoto, A. Brown, E. Rivard, *Angew. Chem. Int. Ed.* **2021**, *60*, 228–231; *Angew. Chem.* **2021**, *133*, 230–233.

[10] W. Tinhof, H. Nöth, *Chem. Ber.* **1975**, *108*, 3109–3124.

[11] a) A. B. Burg, E. S. Kuljian, *J. Am. Chem. Soc.* **1950**, *72*, 3103–3107; b) J. E. Drake, J. Simpson, *Chem. Commun.* **1967**, *6*, 249–250; c) J. E. Drake, J. Simpson, *Inorg. Chem.* **1967**, *6*, 1984–1986; d) J. E. Drake, C. Riddle, *J. Chem. Soc.* **1968**, 1675–1678; e) N. Goddard, J. E. Drake, *J. Chem. Soc. A* **1969**, 662–665; f) M. T. Ackermann, M. Seidl, F. Wen, M. J. Ferguson, A. Y. Timoshkin, E. Rivard, M. Scheer, *Chem. Eur. J.* **2022**, *28*, e202103780; g) M. T. Ackermann, M. Seidl, R. Grande, Y. Zhou, M. J. Ferguson, A. Y. Timoshkin, E. Rivard, M. Scheer, *Chem. Sci.* **2023**, *14*, 2313–2317.

[12] a) A. G. Norman, J. M. Olson, J. F. Geisz, H. R. Moutinho, A. Mason, M. M. Al-Jassim, S. M. Vernon, *Appl. Phys. Lett.* **1999**, *74*, 1382–1384; b) T. Watkins, A. V. G. Chizmeshya, L. Jiang, D. J. Smith, R. T. Beeler, G. Grzybowski, C. D. Poweleit, J. Menéndez, J. Kouvetakis, *J. Am. Chem. Soc.* **2011**, *133*, 16212–16218; c) T. K. Purkait, A. K. Swarnakar, G. B. de Los Reyes, F. A. Hegmann, E. Rivard, J. G. C. Veinot, *Nanoscale* **2015**, *7*, 2241–2244; d) R. Jia, T. Zhu, V. Bulović, E. A. Fitzgerald, *J. Appl. Phys.* **2018**, *123*, 175101.

[13] a) U. Vogel, A. Y. Timoshkin, M. Scheer, *Angew. Chem. Int. Ed.* **2001**, *40*, 4409–4412; *Angew. Chem.* **2001**, *113*, 4541–4544; b) U. Vogel, P. Hoemensch, K.-C. Schwan, A. Y. Timoshkin, M. Scheer, *Chem. Eur. J.* **2003**, *9*, 515–519; c) K.-C. Schwan, A. Y. Timoskin, M. Zabel, M. Scheer, *Chem. Eur. J.* **2006**, *12*, 4900–4908; d) C. Thoms, C. Marquardt, A. Y. Timoshkin, M. Bodensteiner, M. Scheer, *Angew. Chem. Int. Ed.* **2013**, *52*, 5150–5154; *Angew. Chem.* **2013**, *125*, 5254–5259; e) C. Marquardt, C. Thoms, A. Stauber, G. Balázs, M. Bodensteiner, M. Scheer, *Angew. Chem. Int. Ed.* **2014**, *53*, 3727–3730; *Angew. Chem.* **2014**, *126*, 3801–3804; f) C. Marquardt, O. Hegen, M. Hautmann, G. Balázs, M. Bodensteiner, A. V. Virovets, A. Y. Timoshkin, M. Scheer, *Angew. Chem. Int. Ed.* **2015**, *54*, 13122–13125; *Angew. Chem.* **2015**, *127*, 13315–13318; g) C. Marquardt, T. Kahoun, A. Stauber, G. Balázs, M. Bodensteiner, A. Y. Timoshkin, M. Scheer, *Angew. Chem. Int. Ed.* **2016**, *55*, 14828–14832; *Angew. Chem.* **2016**, *128*, 15048–15052; h) O. Hegen, C. Marquardt, A. Y. Timoshkin, M. Scheer, *Angew. Chem. Int. Ed.* **2017**, *56*, 12783–12787; *Angew. Chem.* **2017**, *129*, 12959–12963; i) M. A. K. Weinhart, A. S. Lisovenko, A. Y. Timoshkin, M. Scheer, *Angew. Chem. Int. Ed.* **2020**, *59*, 5541–5545; *Angew. Chem.* **2020**, *132*, 5586–5590; j) M. A. K. Weinhart, M. Seidl, A. Y. Timoshkin, M. Scheer, *Angew. Chem. Int. Ed.* **2021**, *60*, 3806–3811; *Angew. Chem.* **2021**, *133*, 3850–3855.

[14] For examples of heavy element LB•H_2Tet-TetH_2•LA adducts, see: a) S. M. I. Al-Rafia, A. C. Malcolm, R. McDonald, M. J. Ferguson, E. Rivard, *Angew. Chem. Int. Ed.* **2011**, *50*, 8354–8357; *Angew. Chem.* **2011**, *123*, 8504–8507; b) S. M. I. Al-Rafia, M. R. Momeni, M. J. Ferguson, R. McDonald, A. Brown, E. Rivard, *Organometallics* **2013**, *32*, 6658–6665.

[15] K. C. Thimer, S. M. I. Al-Rafia, M. J. Ferguson, R. McDonald, E. Rivard, *Chem. Commun.* **2009**, 7119–7121.

[16] a) P. Pyykkö, M. Atsumi, *Chem. Eur. J.* **2009**, *15*, 12770–12779; b) Note: the torsion angles appear also with the opposite sign due to the chain appearing in a mirrored position in the solid state (cf. Supporting Information).

[17] N. C. Franklin, H. Feltkamp, *Angew. Chem. Int. Ed. Engl.* **1965**, *4*, 774–783; *Angew. Chem.* **1965**, *77*, 798–807.

[18] A possible mechanism under extrusion of PH_3 leading to the formation of **4** is described in the Supporting Information.

9.5 Supporting Information

9.5.1 Experimental section

9.5.1.1 General procedures

All working steps were carried out under argon inert gas atmosphere using standard Schlenk and glovebox techniques. Traces of H_2O and O_2 were removed from argon gas by passing it through a BASF R 3-11 ($CuO/MgSiO_3$) catalyst, concentrated H_2SO_4, and then Orange Gel and Sicapent® supported on pumice stone. Prior to use, solvents were purified using an MBraun SPS-800 solvent purification system, degassed at room temperature, and stored over molecular sieves for at least 48 hours. The NMR spectra were recorded on a Bruker Avance 400 spectrometer (^1H: 400.13 MHz, ^{31}P: 161.976 MHz, ^{11}B: 128.378 MHz) with δ [ppm] referenced to external $SiMe_4$ (^1H), H_3PO_4 (^{31}P), $F_3B{\cdot}Et_2O$ (^{11}B). Mass spectra were recorded on an Agilent Q-TOF 6540 UHD (ESI-MS) and a Jeol AccuTOF GCX spectrometer (LIFDI-MS). Elemental analyses were determined with a Vario Micro Cube apparatus.

The compounds IDipp·GeH_2BH_2OTf[1] and $NaPH_2$[2] were prepared according to literature procedures. $H_3B{\cdot}SMe_2$ was obtained from Sigma Aldrich and used as received.

9.5.1.2 Synthesis of IDipp·$GeH_2BH_2PH_2$ (2a) and IDipp·$BH_2GeH_2PH_2$ (2b)

Method A (2a : 2b / 30-40 : 60-70)

IDipp·GeH_2BH_2OTf (**1**) (610 mg, 0.97 mmol, 1 eq) and $NaPH_2$ (73 mg, 1.30 mmol, 1.3 eq) were each combined with 20 mL of THF in separate Schlenk flasks. After cooling both flasks to -80 °C, the solution of **1** was added to the $NaPH_2$ suspension. The reaction mixture was stirred for 3 hours at room temperature. The volatiles were then removed from the resulting colorless solution *in vacuo* and the remaining residue was suspended in 30 mL of toluene. After filtration through diatomaceous earth, the volatiles were removed from the filtrate *in vacuo* and the residue was washed with 5 mL of *n*-hexane. A product mixture containing of IDipp·$GeH_2BH_2PH_2$ (**2a**) and IDipp·$BH_2GeH_2PH_2$ (**2b**) (**2a** : **2b** / 30 : 70) was isolated as a white powder (250 mg, 49%). Colorless crystals of co-crystallized **2a** and **2b** could be obtained from a concentrated toluene/*n*-hexane solution at -30 °C.

Method B (2a : 2b / 7-10 : 90-93)

60 mL of THF were added to a mixture of solid IDipp·GeH_2BH_2OTf (**1**) (610 mg, 0.97 mmol, 1 eq) and $NaPH_2$ (73 mg, 1.30 mmol, 1.3 eq) at -80 °C. The reaction mixture was stirred for 3 hours at room temperature. The volatiles were then removed from the resulting colorless solution *in vacuo* and the remaining residue was suspended in 30 mL of toluene. After filtration through diatomaceous earth, the volatiles were removed from the filtrate *in vacuo* and the residue was washed with 5 mL of *n*-hexane. A product mixture containing IDipp·$GeH_2BH_2PH_2$ (**2a**) and IDipp·$BH_2GeH_2PH_2$ (**2b**) (**2a** : **2b** / 9 : 91) was be isolated as a white powder (415 mg, 83%). Colorless crystals of co-crystallized **2a** and **2b** could be obtained from a concentrated toluene/*n*-hexane solution at -30 °C.

IDipp·$GeH_2BH_2PH_2$ (**2a**)

^{1}H NMR (C_6D_6, 298 K): δ = 0.95 (d, 12H, $^3J_{H,H}$ = 6.9 Hz, CH(CH_3)$_2$), 1.34 (d,12H, $^3J_{H,H}$ = 6.8 Hz, CH(CH_3)$_2$), 1.57 (dm, 2H, $^1J_{H,P}$ = 180 Hz, PH_2), 1.32 (br, 2H, BH_2), 2.51 (h, 4H, $^3J_{H,H}$ = 6.9 Hz, CH(CH$_3$)$_2$), 3.85 (m, br, 2H, GeH_2), 6.41 (s, 2H, N-CH), 7.05 (d, 4H, $^3J_{H,H}$ = 7.8 Hz, ArH), 7.20 (t, 2H, $^3J_{H,H}$ = 7.8 Hz, ArH). **^{1}H{^{11}B} NMR** (C_6D_6, 298 K): δ = 0.95 (d, 12H, $^3J_{H,H}$ = 6.9 Hz, CH(CH_3)$_2$), 1.34 (d,12H, $^3J_{H,H}$ = 6.8 Hz, CH(CH_3)$_2$), 1.57 (dm, 2H, $^1J_{H,P}$ = 180 Hz, PH_2), 1.32 (br, 2H, BH_2), 2.51 (h, 4H, $^3J_{H,H}$ = 6.9 Hz, CH(CH$_3$)$_2$), 3.85 (m, 2H, GeH_2), 6.41 (s, 2H, N-CH), 7.05 (d, 4H, $^3J_{H,H}$ = 7.8 Hz, ArH), 7.20 (t, 2H, $^3J_{H,H}$ = 7.8 Hz, ArH). **^{1}H{^{31}P} NMR** (C_6D_6, 298 K): δ = 0.95 (d, 12H, $^3J_{H,H}$ = 6.9 Hz, CH(CH_3)$_2$), 1.34 (d,12H, $^3J_{H,H}$ = 6.8 Hz, CH(CH_3)$_2$), 1.57 (m, 2H, PH_2), 1.32 (br, 2H, BH_2), 2.51 (h, 4H, $^3J_{H,H}$ = 6.9 Hz, CH(CH$_3$)$_2$), 3.85 (m, br, 2H, GeH_2), 6.41 (s, 2H, N-CH), 7.05 (d, 4H, $^3J_{H,H}$ = 7.8 Hz, ArH), 7.20 (t, 2H, $^3J_{H,H}$ = 7.8 Hz, ArH). **^{31}P NMR** (C_6D_6, 298 K): δ = -202.3 (t, br, $^1J_{P,H}$ = 180 Hz, PH_2). **^{31}P{^{1}H} NMR** (C_6D_6, 298 K): δ = -202.3 (br, PH_2). **^{11}B NMR** (C_6D_6, 298 K): δ = -37.9 (t, br, $^1J_{H,B}$ = 104 Hz, BH_2). **^{11}B{^{1}H} NMR** (C_6D_6, 298 K): δ = -37.9 (s, br, BH_2).

IDipp·$BH_2GeH_2PH_2$ (**2b**)

^{1}H NMR (C_6D_6, 298 K): δ = 1.00 (d, 12H, $^3J_{H,H}$ = 6.8 Hz, CH(CH_3)$_2$), 1.37 (d,12H, $^3J_{H,H}$ = 6.8 Hz, CH(CH_3)$_2$), 1.42 (dt, 2H, $^1J_{H,P}$ = 176 Hz, $^3J_{H,H}$ = 5.1 Hz, PH_2), 1.63 (br, 2H, BH_2), 2.70 (h, 4H, $^3J_{H,H}$ = 6.8 Hz, CH(CH$_3$)$_2$), 3.46 (pseudo-dp, br, 2H, $^2J_{H,P}$ = 17.5 Hz, $^3J_{H,H}$ = 4.3 Hz, GeH_2), 6.36 (s, 2H, N-CH), 7.09 (d, 4H, $^3J_{H,H}$ = 7.8 Hz, ArH), 7.21 (t, 2H, $^3J_{H,H}$ = 7.8 Hz, ArH). **^{1}H{^{11}B} NMR** (C_6D_6, 298 K): δ = 1.00 (d, 12H, $^3J_{H,H}$ = 6.8 Hz, CH(CH_3)$_2$), 1.37 (d,12H, $^3J_{H,H}$ = 6.8 Hz, CH(CH_3)$_2$), 1.42 (dt, 2H, $^1J_{H,P}$ = 176 Hz, $^3J_{H,H}$ = 5.1 Hz, PH_2), 1.63 (s, br, 2H, BH_2), 2.70 (h, 4H, $^3J_{H,H}$ = 6.8 Hz, CH(CH$_3$)$_2$), 3.46 (pseudo-dp, 2H, $^2J_{H,P}$ = 17.5 Hz, $^3J_{H,H}$ = 4.3 Hz, GeH_2), 6.36 (s, 2H, N-CH), 7.09 (d, 4H, $^3J_{H,H}$ = 7.8 Hz, ArH), 7.21 (t, 2H, $^3J_{H,H}$ = 7.8 Hz, ArH). **^{1}H{^{31}P} NMR** (C_6D_6, 298 K): δ = 1.00 (d, 12H, $^3J_{H,H}$ = 6.8 Hz, CH(CH_3)$_2$), 1.37 (d,12H, $^3J_{H,H}$ = 6.8 Hz, CH(CH_3)$_2$), 1.42 (t, 2H, $^3J_{H,H}$ = 5.1 Hz, PH_2), 1.63 (br, 2H, BH_2), 2.70 (h, 4H, $^3J_{H,H}$ = 6.8 Hz, CH(CH$_3$)$_2$), 3.46 (p, br, 2H, $^3J_{H,H}$ = 4.3 Hz, GeH_2), 6.36 (s, 2H, N-CH), 7.09 (d, 4H, $^3J_{H,H}$ = 7.8 Hz, ArH), 7.21 (t, 2H, $^3J_{H,H}$ = 7.8 Hz, ArH). **^{31}P NMR** (C_6D_6, 298 K): δ = -244.0 (tt, $^1J_{P,H}$ = 176 Hz, $^2J_{P,H}$ = 17.5 Hz, PH_2). **^{31}P{^{1}H} NMR** (C_6D_6, 298 K): δ = -244.0 (s, PH_2). **^{11}B NMR** (C_6D_6, 298 K): δ = -34.7 (t, br, $^1J_{H,B}$ = 97 Hz, BH_2). **^{11}B{^{1}H}** NMR (C_6D_6, 298 K): δ = -34.7 (s, br, BH_2).

Elemental analysis (%) calculated for $C_{27}H_{42}BGeN_2P$(*n*-hexane/toluene)$_{0.25}$: C: 65.63, H: 8.65, N: 5.06; found: C: 65.62, H: 8.41, N: 5.41. (for **2a** : **2b** / 7 : 93)

9.5.1.3 Synthesis of IDipp·$GeH_2BH_2PH_2BH_3$ (3a) and IDipp·$BH_2GeH_2PH_2BH_3$ (3b) (3a : 3b / 8-13 : 87-92)

$H_3B{\cdot}SMe_2$ (15 mg, 0.20 mmol, 1 eq) in 0.4 mL toluene was added to solution of a mixture of IDipp·$GeH_2BH_2PH_2$ (**2a**) and IDipp·$BH_2GeH_2PH_2$ (**2b**) (**2a** : **2b** / 7 : 93) (102 mg, 0.200 mmol, 1 eq) in 20 mL of toluene at -80 °C. The reaction mixture was stirred for 1.5 hours at room temperature. The volatiles were removed *in vacuo* and the residue was washed with 5 mL of *n*-hexane. A mixture of IDipp·$GeH_2BH_2PH_2BH_3$ (**3a**) and IDipp·$BH_2GeH_2PH_2BH_3$ (**3b**) (**3a** : **3b** / 8 : 92) was isolated as a white powder (87 mg, 83%).

(3a : 3b / 75 : 25)

A solution of $H_3B{\cdot}SMe_2$ in toluene (0.22 mL, 0.11 mmol, 0.5 M) was added to solution of a mixture of IDipp·$GeH_2BH_2PH_2$ (**2a**) and IDipp·$BH_2GeH_2PH_2$ (**2b**) (**2a** : **2b** / 67 : 33) (51 mg, 0.10 mmol) in 10 mL of toluene at -80 °C. The reaction mixture was stirred for 1.5 hours at room temperature. The volatiles were removed from the reaction mixture *in vacuo* and the residue was washed with 5 mL of *n*-hexane. A product mixture containing IDipp·$GeH_2BH_2PH_2BH_3$ (**3a**) and IDipp·$BH_2GeH_2PH_2BH_3$ (**3b**) (**3a** : **3b** / 75 : 25) was isolated as a white powder (22 mg, 42%).

IDipp·$GeH_2BH_2PH_2BH_3$ (**3a**)

^{1}H NMR (C_6D_6, 298 K): δ = 0.95 (d, $^3J_{H,H}$ = 6.8 Hz, CH(CH_3)$_2$), 1.27 (d, $^3J_{H,H}$ = 6.8 Hz, CH(CH_3)$_2$), 2.41 (h, 4H, $^3J_{H,H}$ = 6.9 Hz, CH(CH$_3$)$_2$), 3.32 (dm, 2H, PH_2, $^1J_{H,P}$ = 311 Hz), 3.84 (m, 2H, GeH_2), 6.71 (s, 2H, N-CH), 7.04 (d, 4H, $^3J_{H,H}$ = 7.8 Hz, ArH), 7.21 (t, 2H, $^3J_{H,H}$ = 7.8 Hz, ArH). **^{1}H{^{11}B} NMR** (C_6D_6, 298 K): δ = 0.95 (d, $^3J_{H,H}$ = 6.8 Hz, CH(CH_3)$_2$), 1.27 (d, $^3J_{H,H}$ = 6.8 Hz, CH(CH_3)$_2$), 1.65 (m, 2H, BH_2), 2.41 (h, 4H, $^3J_{H,H}$ = 6.9 Hz, CH(CH$_3$)$_2$), 3.32 (dm, 2H, PH_2, $^1J_{H,P}$ = 311 Hz), 3.84 (m, 2H, GeH_2), 6.71 (s, 2H, N-CH), 7.04 (d, 4H, $^3J_{H,H}$ = 7.8 Hz, ArH), 7.21 (t, 2H, $^3J_{H,H}$ = 7.8 Hz, ArH). **^{1}H{^{31}P} NMR** (C_6D_6, 298 K): δ = 0.95 (d, $^3J_{H,H}$ = 6.8 Hz, CH(CH_3)$_2$), 1.27 (d, $^3J_{H,H}$ = 6.8 Hz, CH(CH_3)$_2$), 2.41 (h, 4H, $^3J_{H,H}$ = 6.9 Hz, CH(CH$_3$)$_2$), 3.32 (m, 2H, PH_2), 3.84 (m, 2H, GeH_2), 6.71 (s, 2H, N-CH), 7.04 (d, 4H, $^3J_{H,H}$ = 7.8 Hz, ArH), 7.21 (t, 2H, $^3J_{H,H}$ = 7.8 Hz, ArH). Due to signal overlap and strong signal broadening, the {BH_2} signals could not be assigned unambiguously in the ^{1}H NMR spectra. **^{31}P{^{1}H} NMR** (C_6D_6, 298 K): δ = -104.2 (s, br, PH_2). **^{31}P NMR** (C_6D_6, 298 K): δ = -104.2 (t, br, PH_2, $^1J_{H,P}$ = 311 Hz). **^{11}B NMR** (C_6D_6, 298 K): δ = -39.5 (q, br, BH_3), -40.4 (s, br, BH_2). **^{11}B{^{1}H}** NMR (C_6D_6, 298 K): δ = -39.5 (s, br, BH_3), -40.4 (s, br, BH_2).

IDipp·$BH_2GeH_2PH_2BH_3$ (**3b**)

^{1}H NMR (C_6D_6, 298 K): δ = 0.96 (d, 12H, $^3J_{H,H}$ = 6.8 Hz, CH(CH_3)$_2$), 1.30 (d,12H, $^3J_{H,H}$ = 6.8 Hz, CH(CH_3)$_2$), 1.52 (br, 2H, BH_2), 1.73 (br, 3H, BH_3), 2.52 (h, 4H, $^3J_{H,H}$ = 6.9 Hz, CH(CH$_3$)$_2$), 2.96 (dm, 2H, $^1J_{H,P}$ = 326 Hz, PH_2), 3.45 (m, 2H, GeH_2), 6.32 (s, 2H, N-CH), 7.05 (d, 4H, $^3J_{H,H}$ = 7.8 Hz, ArH), 7.19 (t, 2H, $^3J_{H,H}$ = 7.8 Hz, ArH). **^{1}H{^{11}B} NMR** (C_6D_6, 298 K): δ = 0.96 (d, 12H, $^3J_{H,H}$ = 6.8 Hz, CH(CH_3)$_2$), 1.30 (d,12H, $^3J_{H,H}$ = 6.8 Hz, CH(CH_3)$_2$), 1.52 (m, 2H, BH_2), 1.73 (dt, 3H, $^2J_{H,P}$ = 12.0 Hz, $^3J_{H,H}$ = 8.2 Hz, BH_3), 2.52 (h, 4H, $^3J_{H,H}$ = 6.9 Hz, CH(CH$_3$)$_2$), 2.96 (dm, 2H, $^1J_{H,P}$ = 326 Hz, PH_2), 3.45 (m, 2H, GeH_2), 6.32 (s, 2H, N-CH), 7.05 (d, 4H, $^3J_{H,H}$ = 7.8 Hz, ArH), 7.19 (t, 2H, $^3J_{H,H}$ = 7.8 Hz, ArH). **^{1}H{^{31}P} NMR** (C_6D_6, 298 K): δ = 0.96 (d, 12H, $^3J_{H,H}$ = 6.8 Hz, CH(CH_3)$_2$), 1.30 (d,12H, $^3J_{H,H}$ = 6.8 Hz, CH(CH_3)$_2$), 1.52 (br, 2H, BH_2), 1.73 (br, 3H, BH_3), 2.52 (h, 4H, $^3J_{H,H}$ = 6.9 Hz, CH(CH$_3$)$_2$), 2.96 (m, 2H, PH_2), 3.45 (m, 2H, GeH_2), 6.32 (s, 2H, N-CH), 7.05 (d, 4H, $^3J_{H,H}$ = 7.8 Hz, ArH), 7.19 (t, 2H, $^3J_{H,H}$ = 7.8 Hz, ArH). **^{31}P NMR** (C_6D_6, 298 K): δ = -131.3 (t, br, $^1J_{P,H}$ = 326 Hz, PH_2). **^{31}P{^{1}H} NMR** (C_6D_6, 298 K): δ = -131.3 (br, PH_2). **^{11}B NMR** (C_6D_6, 298 K): δ = -36.1 (t, br, $^1J_{H,B}$ = 99 Hz, BH_2), -38.7 (q, br, $^1J_{H,B}$ = 100 Hz, BH_3). **^{11}B{^{1}H}** NMR (C_6D_6, 298 K): δ = -36.1 (s, br, BH_2), -38.7 (s, br, BH_3).

Elemental analysis (%) calculated for $C_{27}H_{45}B_2GeN_2P$: C: 62.02, H: 8.67, N: 5.36; found: C: 62.49, H: 9.01, N: 5.29. (for **3a** : **3b** / 8 : 92)

9.5.1.4 Synthesis of [IDipp·BH_2GeH_2·IDipp][$PHGeH_2BH_2PH_2BH_2GeH_2$] (4)

A solution of a mixture of IDipp·$GeH_2BH_2PH_2$ (**2a**) and IDipp·$BH_2GeH_2PH_2$ (**2b**) (**2a** : **2b** / 9 : 91) (200 mg, 0.392 mmol, 1 eq) in 5 mL of THF was layered with a 3-fold amount of *n*-hexane at 4 °C. A few colorless crystals of [IDipp·BH_2GeH_2·IDipp][$PHGeH_2BH_2PH_2BH_2GeH_2$] (**4**) were be obtained.

^{1}H NMR (CD_2Cl_2, 298 K): δ = 0.55 (br, 2H, BH_2), 0.62 (dm, 1H, $^1J_{H,P}$ = 163 Hz, PH), 0.55 (br, 4H, 2 x BH_2), 0.99 (d, 24H, $^3J_{H,H}$ = 6.9 Hz, CH(C*H*$_3$)$_2$), 1.04 (d, 24H, $^3J_{H,H}$ = 6.9 Hz, CH(C*H*$_3$)$_2$), 2.10 (h, 4H, $^3J_{H,H}$ = 6.8 Hz, C*H*(CH$_3$)$_2$), 2.18 (h, 4H, $^3J_{H,H}$ = 6.8 Hz, C*H*(CH$_3$)$_2$), 2.91 (m, 2H, GeH_2), 3.14 (m, br, 2H, GeH), 3.40 (m, br, 2H, GeH), 3.83 (dm, 2H, $^1J_{H,P}$ = 320 Hz, PH_2), 7.03 (s, 2H, N-C*H*), 7.18 (d, 4H, $^3J_{H,H}$ = 7.8 Hz, ArH), 7.20 (d, 4H, $^3J_{H,H}$ = 7.8 Hz, ArH), 7.28 (s, 2H, N-C*H*), 7.43 (t, 2H, $^3J_{H,H}$ = 7.8 Hz, ArH), 7.48 (t, 2H, $^3J_{H,H}$ = 7.8 Hz, ArH). **^{1}H{^{11}B} NMR** (CD_2Cl_2, 298 K, ^{11}B decoupled at -37.7 ppm): δ = 0.55 (m, 2H, BH_2), 0.62 (dm, 1H, $^1J_{H,P}$ = 163 Hz, PH), 0.55 (m, br, 4H, BH_2), 0.99 (d, 24H, $^3J_{H,H}$ = 6.9 Hz, CH(C*H*$_3$)$_2$), 1.04 (d, 24H, $^3J_{H,H}$ = 6.9 Hz, CH(C*H*$_3$)$_2$), 2.10 (h, 4H, $^3J_{H,H}$ = 6.8 Hz, C*H*(CH$_3$)$_2$), 2.18 (h, 4H, $^3J_{H,H}$ = 6.8 Hz, C*H*(CH$_3$)$_2$), 2.91 (m, 2H, GeH_2), 3.14 (m, br, 2H, GeH), 3.40 (m, br, 2H, GeH), 3.83 (dm, 2H, $^1J_{H,P}$ = 320 Hz, PH_2), 7.03 (s, 2H, N-C*H*), 7.18 (d, 4H, $^3J_{H,H}$ = 7.8 Hz, ArH), 7.20 (d, 4H, $^3J_{H,H}$ = 7.8 Hz, ArH), 7.28 (s, 2H, N-C*H*), 7.43 (t, 2H, $^3J_{H,H}$ = 7.8 Hz, ArH), 7.48 (t, 2H, $^3J_{H,H}$ = 7.8 Hz, ArH). **^{1}H{^{11}B} NMR** (CD_2Cl_2, 298 K, ^{11}B decoupled at -40.0 ppm): δ = 0.55 (m, 2H, BH_2), 0.62 (dm, 1H, $^1J_{H,P}$ = 163 Hz, PH), 0.55 (m, br, 4H, BH_2), 0.99 (d, 24H, $^3J_{H,H}$ = 6.9 Hz, CH(C*H*$_3$)$_2$), 1.04 (d, 24H, $^3J_{H,H}$ = 6.9 Hz, CH(C*H*$_3$)$_2$), 2.10 (h, 4H, $^3J_{H,H}$ = 6.8 Hz, C*H*(CH$_3$)$_2$), 2.18 (h, 4H, $^3J_{H,H}$ = 6.8 Hz, C*H*(CH$_3$)$_2$), 2.91 (m, 2H, GeH_2), 3.14 (m, br, 2H, GeH), 3.40 (m, br, 2H, GeH), 3.83 (dm, 2H, $^1J_{H,P}$ = 320 Hz, PH_2), 7.03 (s, 2H, N-C*H*), 7.18 (d, 4H, $^3J_{H,H}$ = 7.8 Hz, ArH), 7.20 (d, 4H, $^3J_{H,H}$ = 7.8 Hz, ArH), 7.28 (s, 2H, N-C*H*), 7.43 (t, 2H, $^3J_{H,H}$ = 7.8 Hz, ArH), 7.48 (t, 2H, $^3J_{H,H}$ = 7.8 Hz, ArH). **^{1}H{^{31}P} NMR** (CD_2Cl_2, 298 K, ^{31}P decoupled at -98.7 ppm): δ = 0.55 (br, 2H, BH_2), 0.62 (dm, 1H, $^1J_{H,P}$ = 163 Hz, PH), 0.55 (br, 4H, BH_2), 0.99 (d, 24H, $^3J_{H,H}$ = 6.9 Hz, CH(C*H*$_3$)$_2$), 1.04 (d, 24H, $^3J_{H,H}$ = 6.9 Hz, CH(C*H*$_3$)$_2$), 2.10 (h, 4H, $^3J_{H,H}$ = 6.8 Hz, C*H*(CH$_3$)$_2$), 2.18 (h, 4H, $^3J_{H,H}$ = 6.8 Hz, C*H*(CH$_3$)$_2$), 2.91 (m, 2H, GeH_2), 3.14 (m, br, 2H, GeH), 3.40 (m, br, 2H, GeH), 3.83 (m, 2H, PH_2), 7.03 (s, 2H, N-C*H*), 7.18 (d, 4H, $^3J_{H,H}$ = 7.8 Hz, ArH), 7.20 (d, 4H, $^3J_{H,H}$ = 7.8 Hz, ArH), 7.28 (s, 2H, N-C*H*), 7.43 (t, 2H, $^3J_{H,H}$ = 7.8 Hz, ArH), 7.48 (t, 2H, $^3J_{H,H}$ = 7.8 Hz, ArH). **^{1}H{^{31}P} NMR** (CD_2Cl_2, 298 K, ^{31}P decoupled at -271 ppm): δ = 0.55 (br, 2H, BH_2), 0.62 (m, 1H, PH), 0.55 (br, 4H, BH_2), 0.99 (d, 24H, $^3J_{H,H}$ = 6.9 Hz, CH(C*H*$_3$)$_2$), 1.04 (d, 24H, $^3J_{H,H}$ = 6.9 Hz, CH(C*H*$_3$)$_2$), 2.10 (h, 4H, $^3J_{H,H}$ = 6.8 Hz, C*H*(CH$_3$)$_2$), 2.18 (h, 4H, $^3J_{H,H}$ = 6.8 Hz, C*H*(CH$_3$)$_2$), 2.91 (m, 2H, GeH_2), 3.14 (m, br, 2H, GeH), 3.40 (m, br, 2H, GeH), 3.83 (dm, 2H, $^1J_{H,P}$ = 320 Hz, PH_2), 7.03 (s, 2H, N-C*H*), 7.18 (d, 4H, $^3J_{H,H}$ = 7.8 Hz, ArH), 7.20 (d, 4H, $^3J_{H,H}$ = 7.8 Hz, ArH), 7.28 (s, 2H, N-C*H*), 7.43 (t, 2H, $^3J_{H,H}$ = 7.8 Hz, ArH), 7.48 (t, 2H, $^3J_{H,H}$ = 7.8 Hz, ArH). **^{31}P NMR** (CD_2Cl_2, 298 K): δ = -98.1 (t, br, $^1J_{P,H}$ = 320 Hz, PH_2), -270.5 (d, $^1J_{P,H}$ = 163 Hz, PH). **^{31}P{^{1}H} NMR** (CD_2Cl_2, 298 K): δ = -98.1 (m, br, $^1J_{P,B}$ = 64 Hz, PH_2), -270.5 (s, PH). **^{11}B NMR** (CD_2Cl_2, 298 K): δ = -37.7 (t, br, $^1J_{H,B}$ = 100 Hz, BH_2), -40.3 (dt, $^1J_{P,B}$ = 64 Hz, $^1J_{H,B}$ = 102 Hz, BH_2). **^{11}B{^{1}H}** NMR (CD_2Cl_2, 298 K): δ = -37.7 (m, br, BH_2), -40.3 (d, $^1J_{P,B}$ = 64 Hz, BH_2).

ESI-MS (neg. mod., CH_2Cl_2): *m/z* = 240.9 (100%, [$PHGeH_2BH_2PH_2BH_2GeH_2$]$^-$); **ESI-MS** (pos. mod., CH_2Cl_2): *m/z* = 865.5 (100%, [IDipp·BH_2GeH_2·IDipp]$^+$).

9.5.2 NMR data

IDipp·$GeH_2BH_2PH_2$ (**2a**)

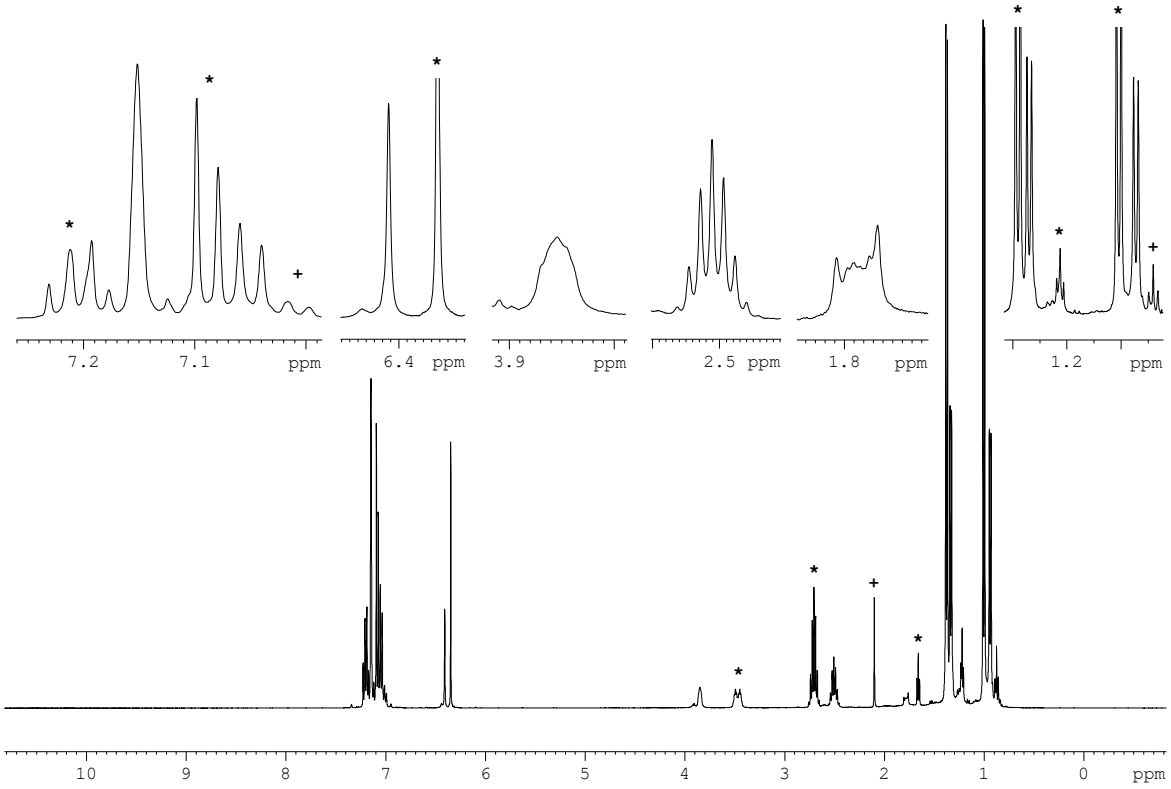

Figure S 9.1: ^{1}H NMR spectrum of **2a** in C_6D_6 at 298 K. * = **2b**. + = residual solvents (toluene, *n*-hexane).

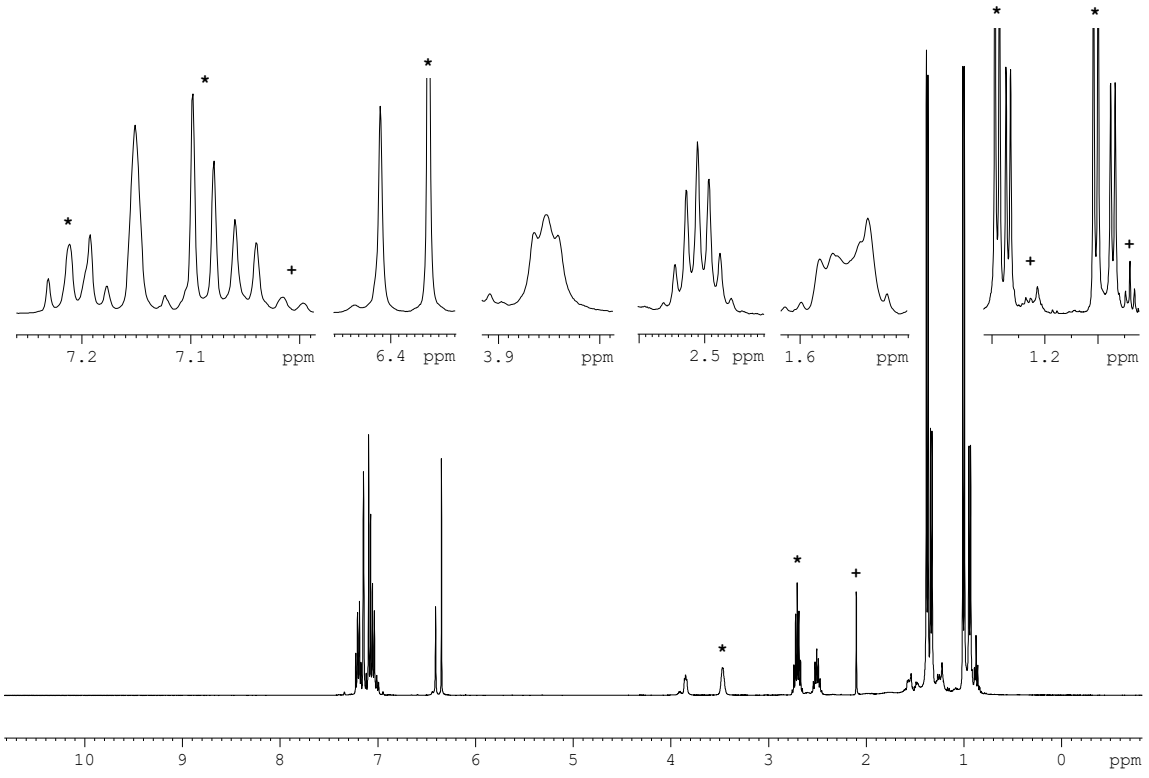

Figure S 9.2: $^{1}H\{^{31}P\}$ NMR spectrum of **2a** in C_6D_6 at 298 K. * = **2b**. + = residual solvents (toluene, *n*-hexane).

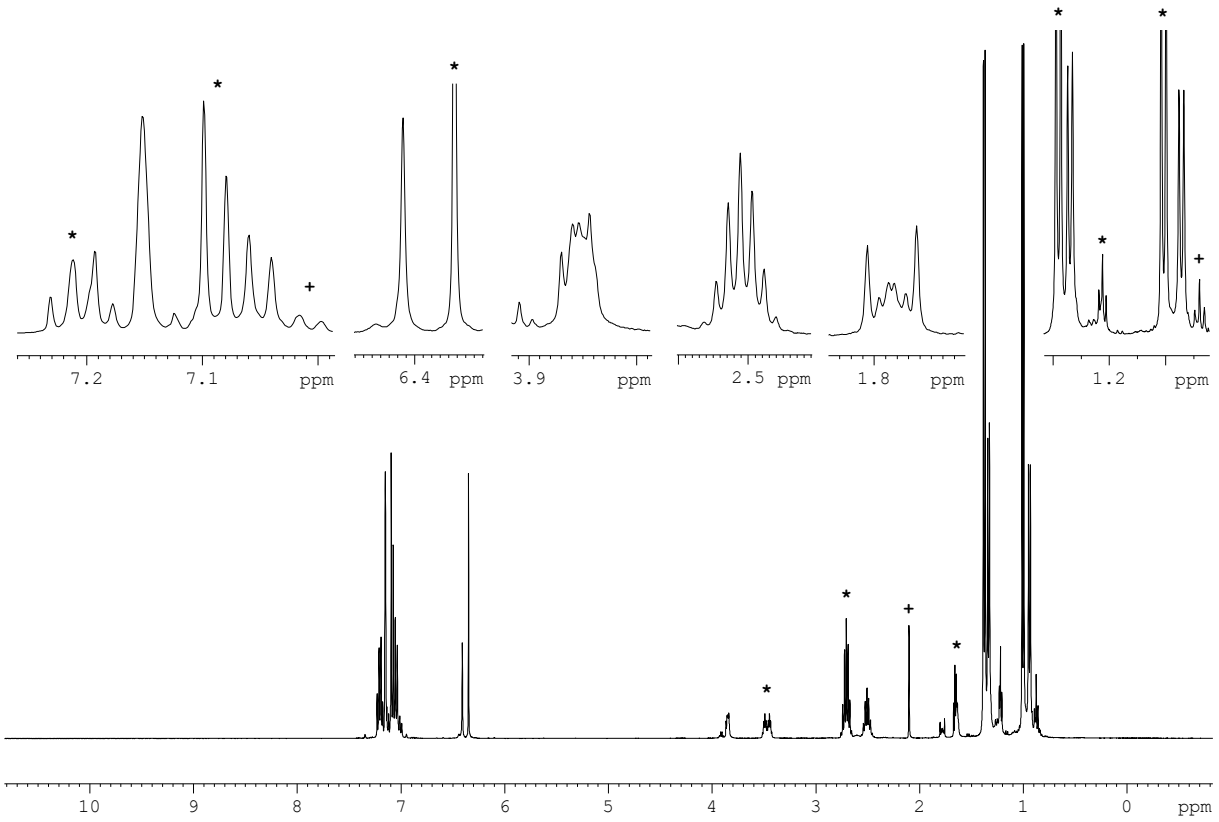

Figure S 9.3: $^{1}H\{^{11}B\}$ NMR spectrum of **2a** in C_6D_6 at 298 K. * = **2b**. + = residual solvents (toluene, *n*-hexane).

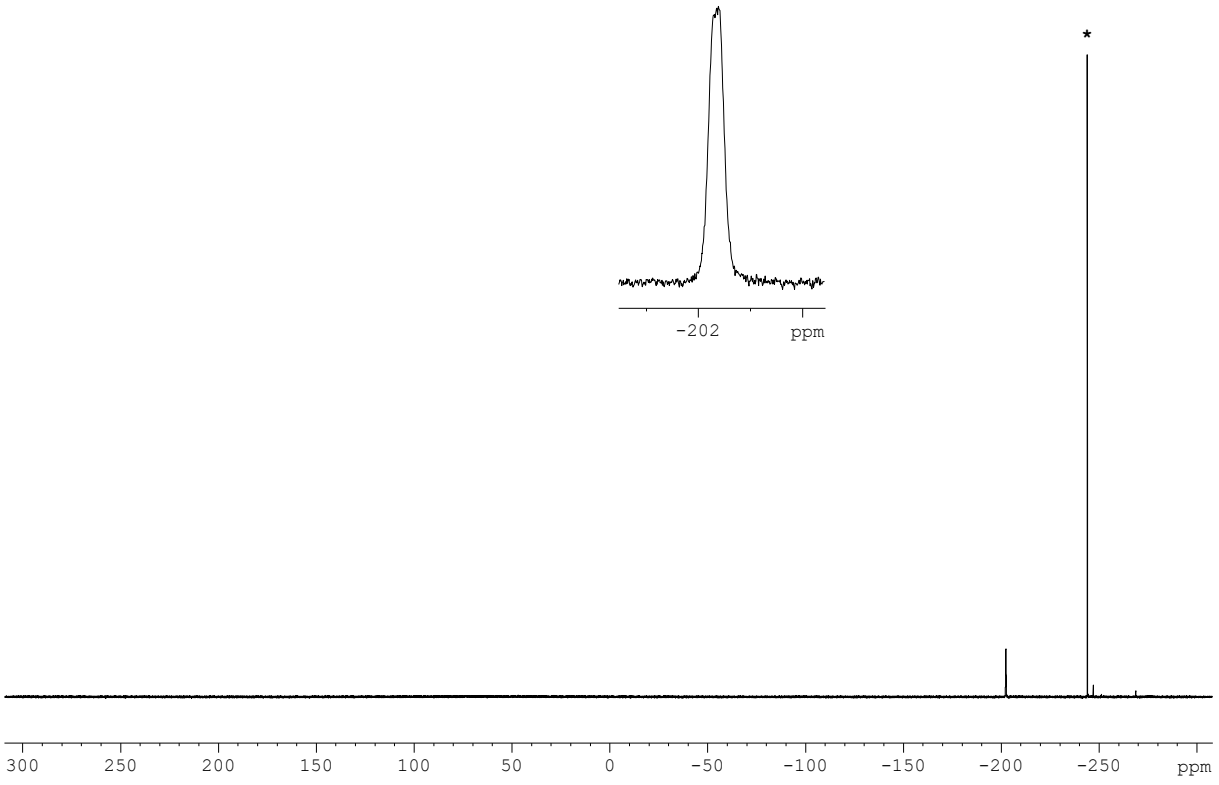

Figure S 9.4: $^{31}P\{^{1}H\}$ NMR spectrum of **2a** in C_6D_6 at 298 K. * = **2b**.

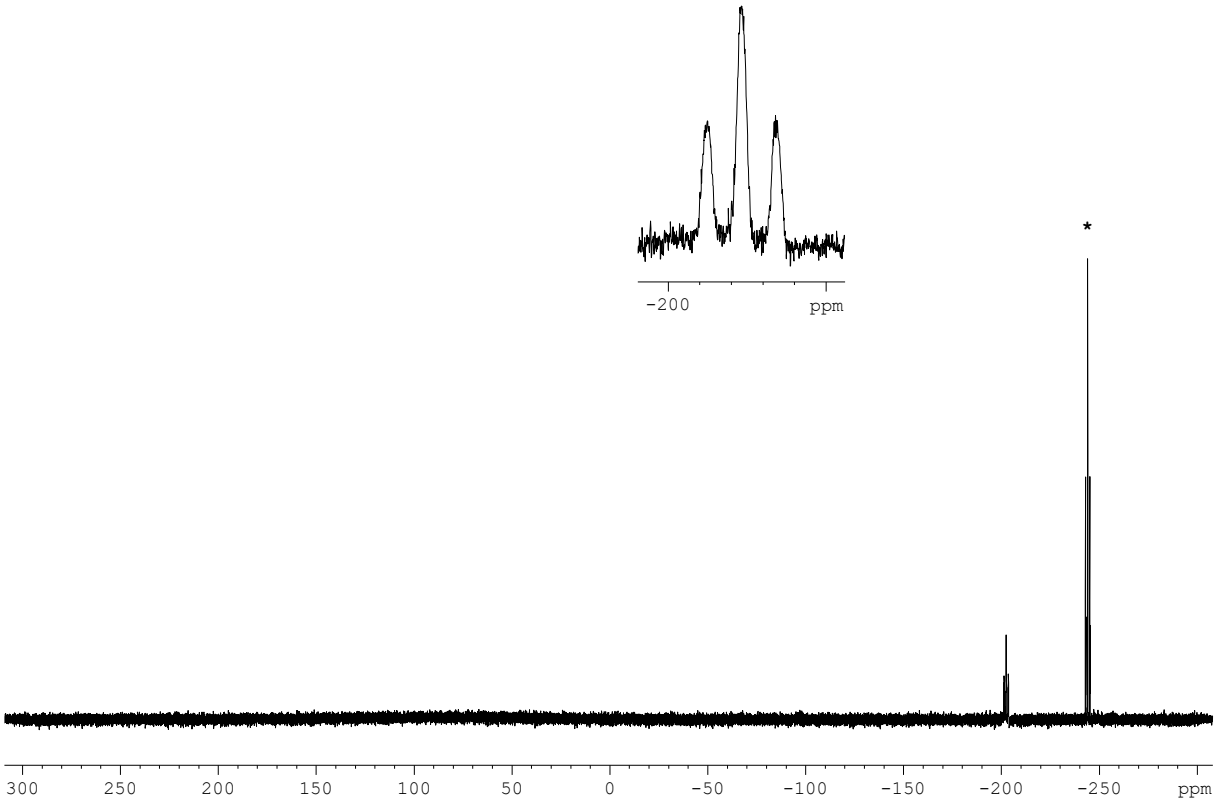

Figure S 9.5: ^{31}P NMR spectrum of **2a** in C_6D_6 at 298 K. * = **2b**.

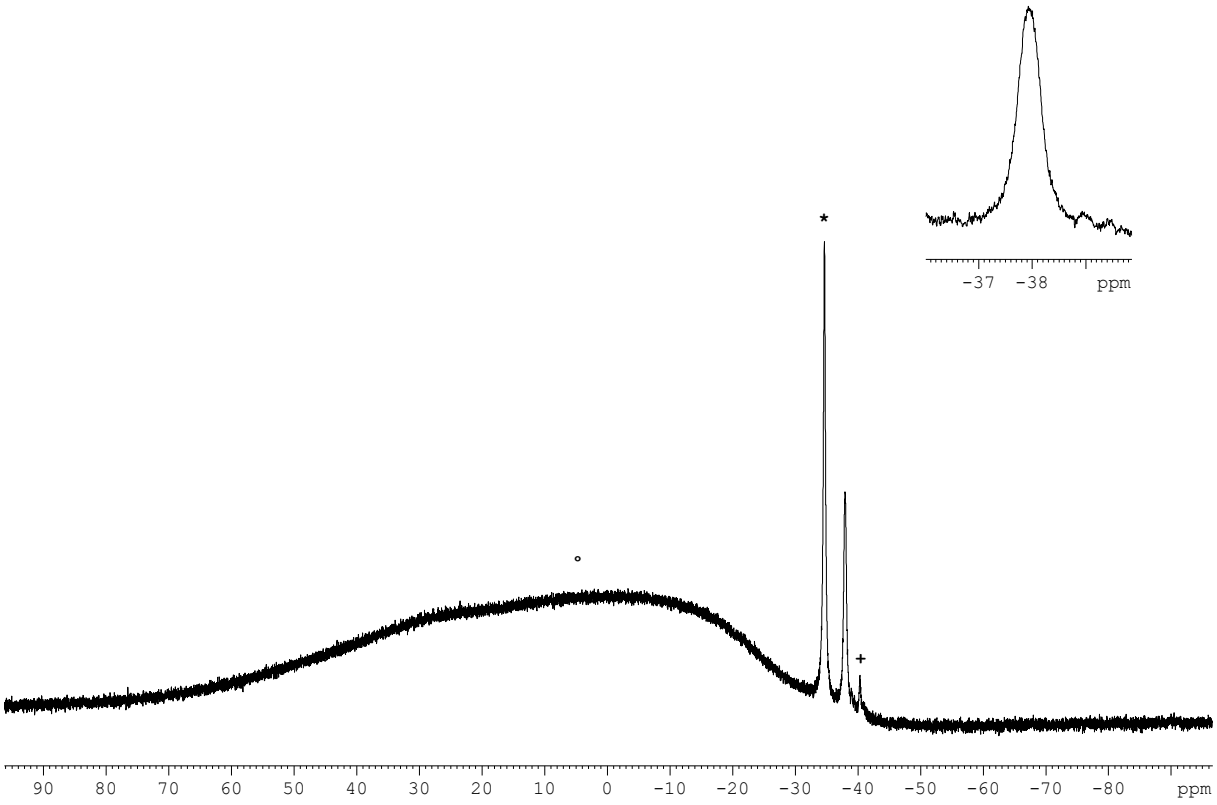

Figure S 9.6: $^{11}B\{^1H\}$ NMR spectrum of **2a** in C_6D_6 at 298 K. ° = signal from the NMR probe. * = **2b**. + = IDipp·GeH_2BH_3.

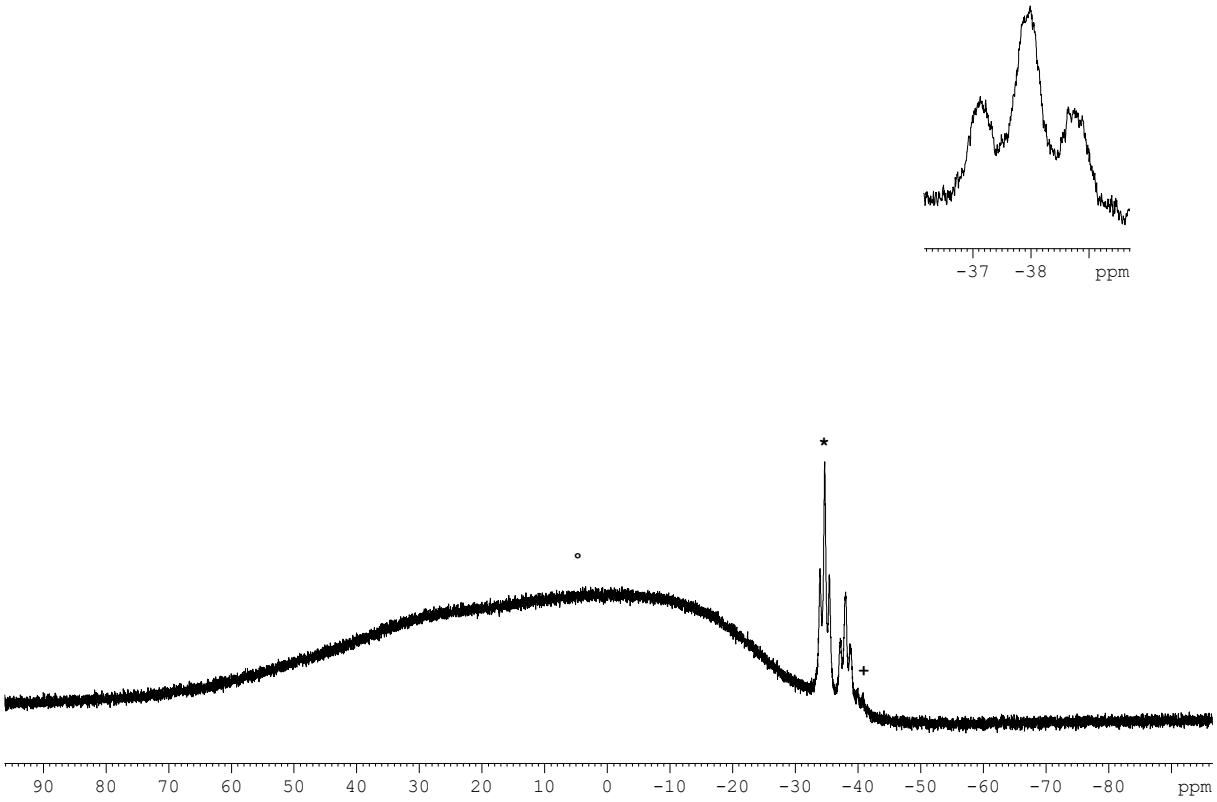

Figure S 9.7: ^{11}B NMR spectrum of **2a** in C_6D_6 at 298 K. ° = signal from the NMR probe. * = **2b**. + = IDipp·GeH_2BH_3.

IDipp·$BH_2GeH_2PH_2$ (**2b**)

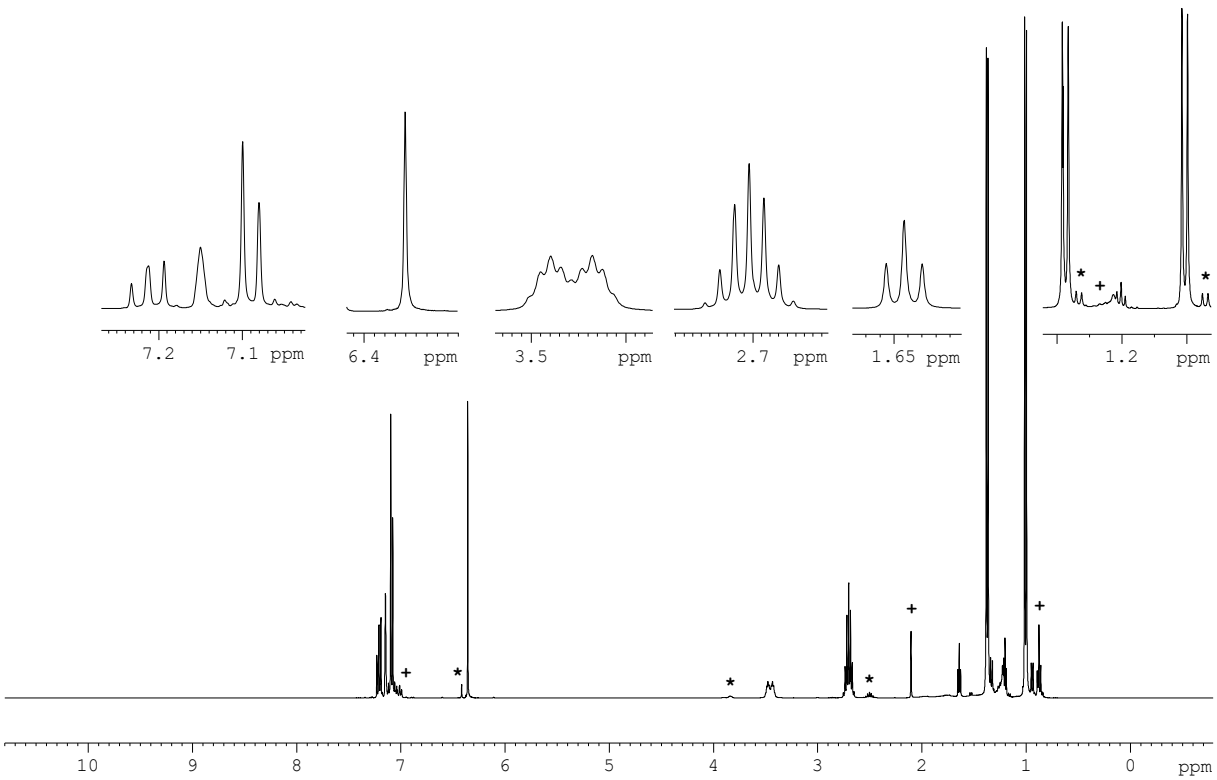

Figure S 9.8: ^{1}H NMR spectrum of **2b** in C_6D_6 at 298 K. * = **2a**. + = residual solvents (toluene, *n*-hexane).

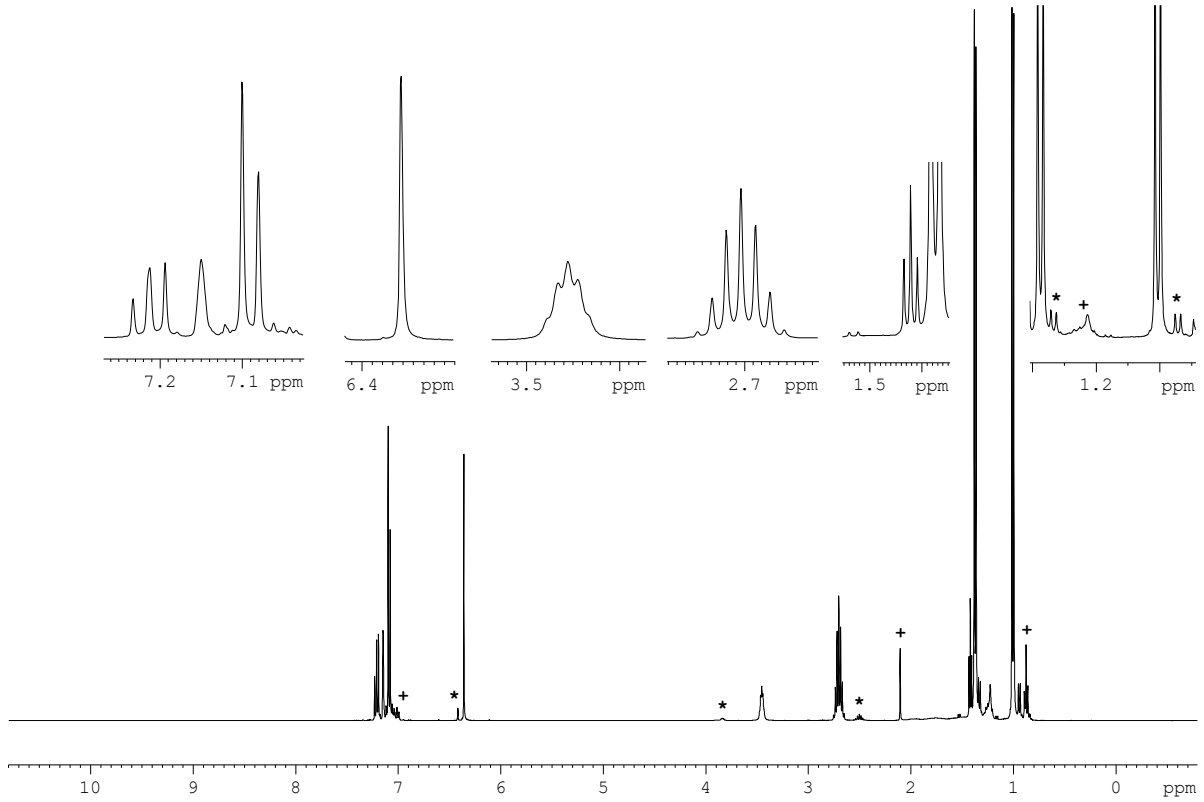

Figure S 9.9: $^{1}H\{^{31}P\}$ NMR spectrum of **2b** in C_6D_6 at 298 K. * = **2a**. + = residual solvents (toluene, *n*-hexane).

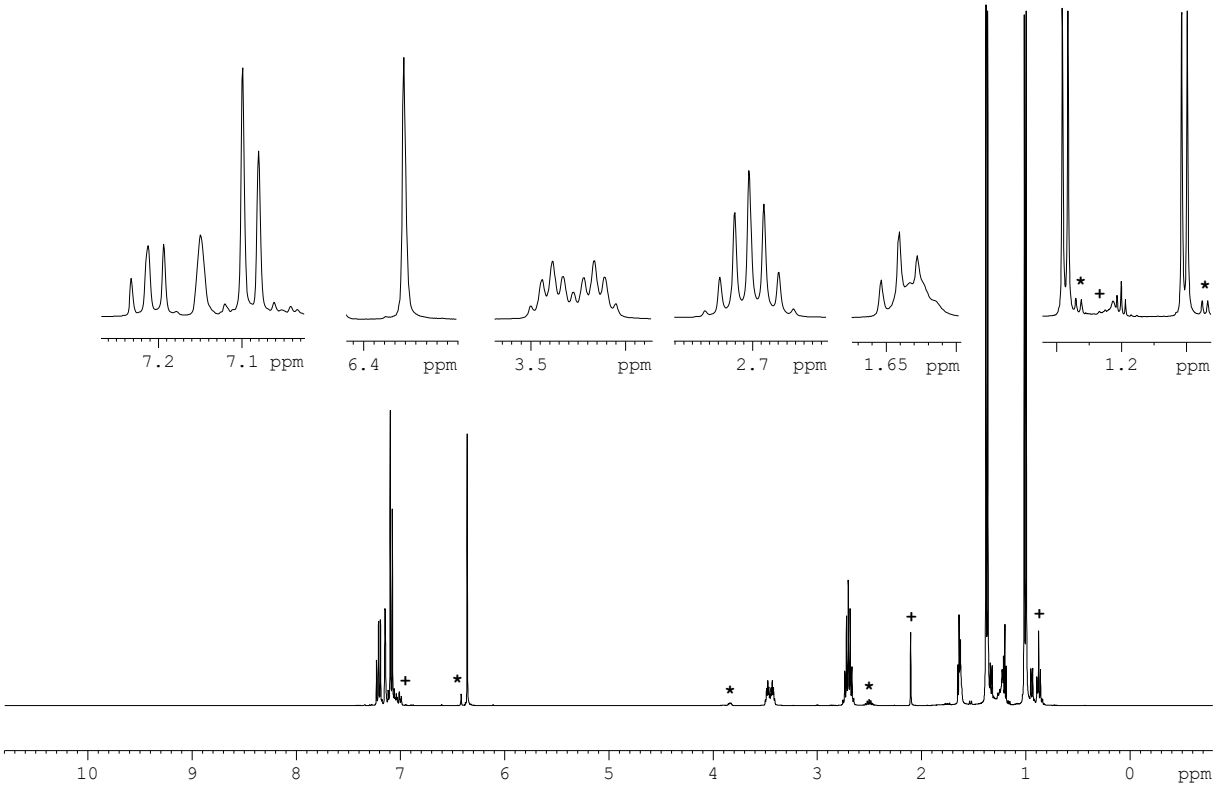

Figure S 9.10: $^{1}H\{^{11}B\}$ NMR spectrum of **2b** in C_6D_6 at 298 K. * = **2a**. + = residual solvents (toluene, *n*-hexane).

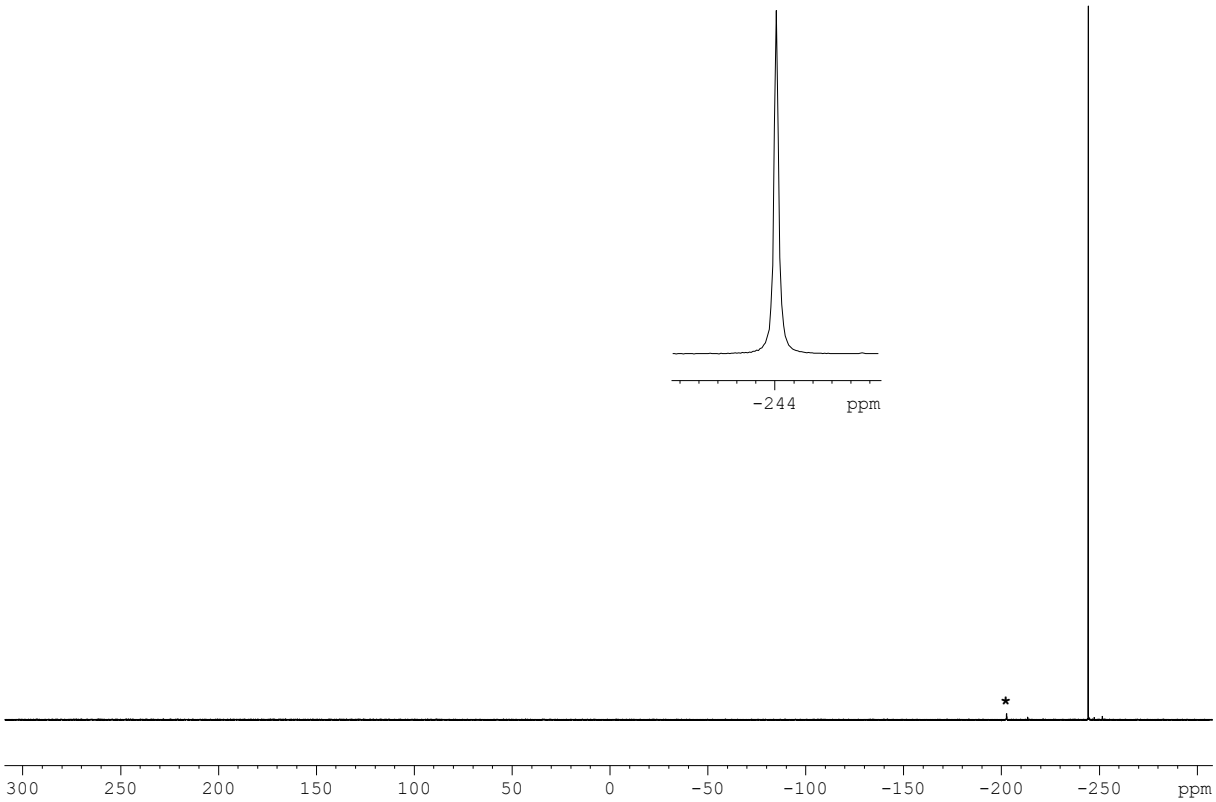

Figure S 9.11: $^{31}P\{^{1}H\}$ NMR spectrum of **2b** in C_6D_6 at 298 K. * = **2a**.

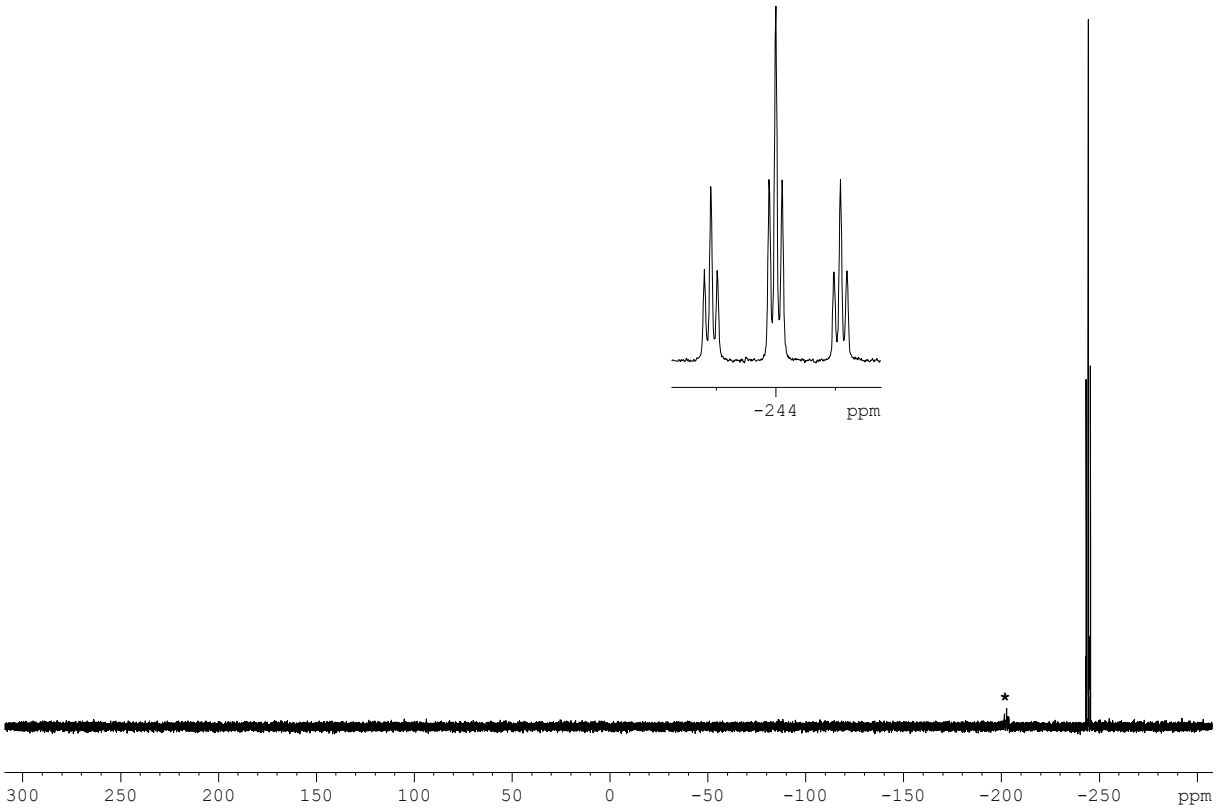

Figure S 9.12: ^{31}P NMR spectrum of **2b** in C_6D_6 at 298 K. * = **2a**.

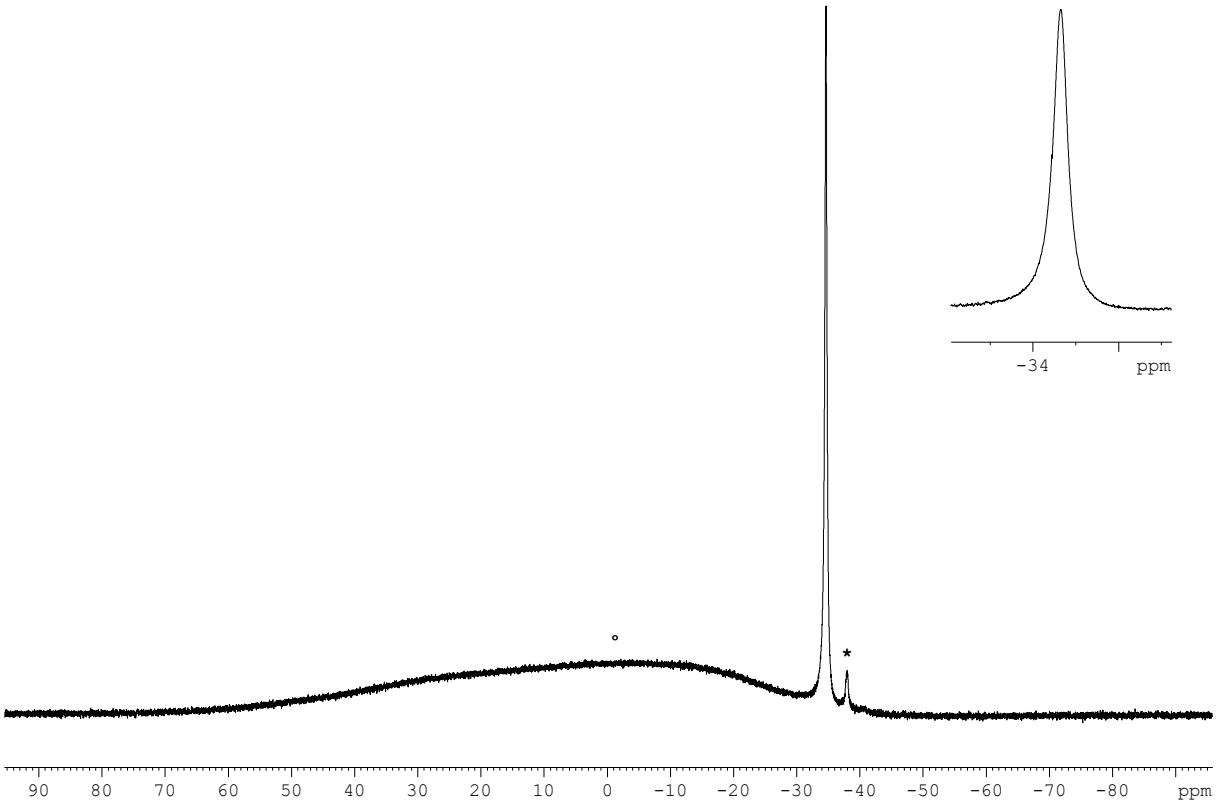

Figure S 9.13: $^{11}B\{^1H\}$ NMR spectrum of **2b** in C_6D_6 at 298 K. ° = signal from the NMR probe. * = **2a**.

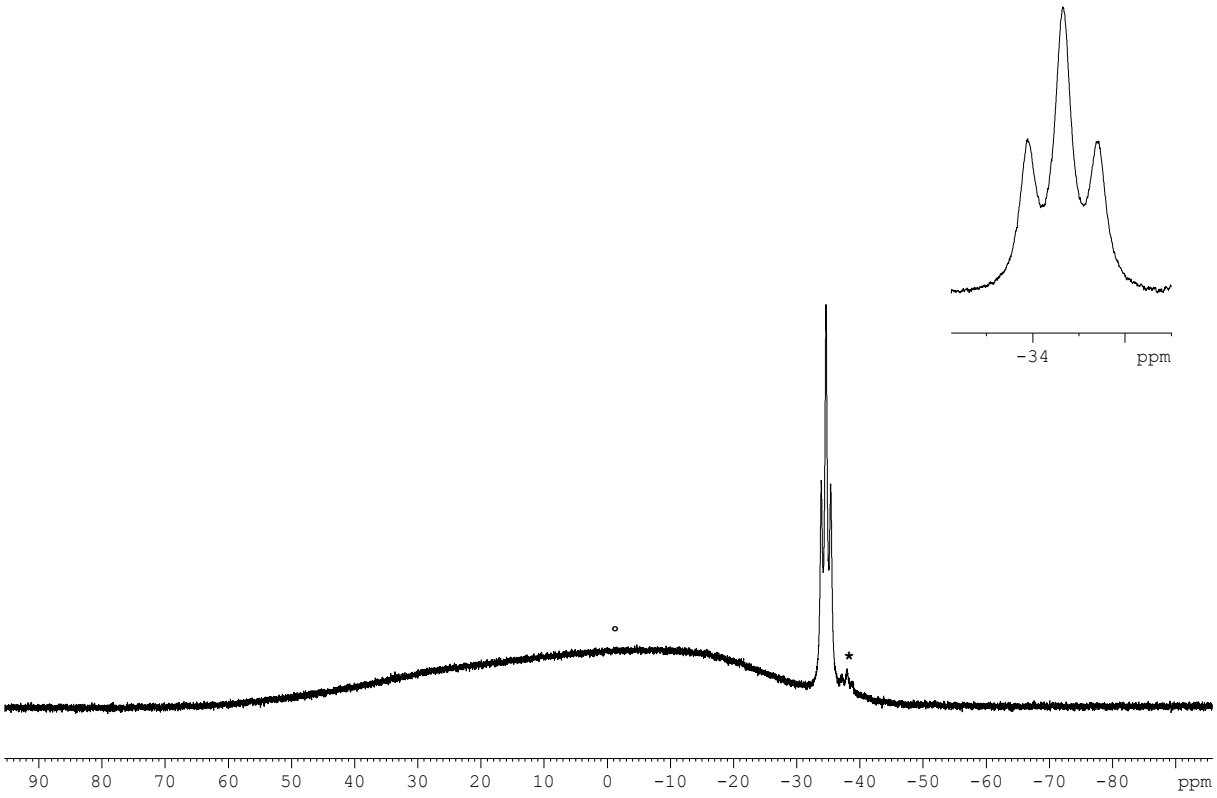

Figure S 9.14: $^{11}B\{^1H\}$ NMR spectrum of **2b** in C_6D_6 at 298 K. ° = signal from the NMR probe. * = **2a**.

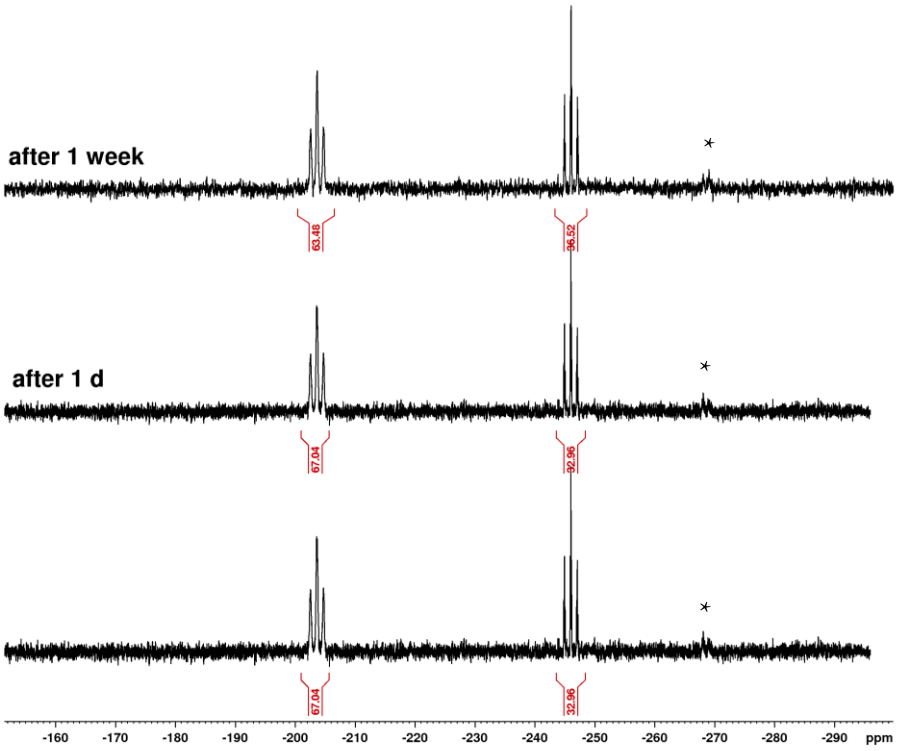

Figure S 9.15: ^{31}P NMR spectra of a mixture of **2a/b** (67:33) recorded over the course of one week (THF/C_6D_6-cap., 298 K; * = trace amounts of compound **4**).

0.75 IDipp·$GeH_2BH_2PH_2BH_3$ (**3a**) + 0.25 IDipp·$BH_2GeH_2PH_2BH_3$ (**3b**)

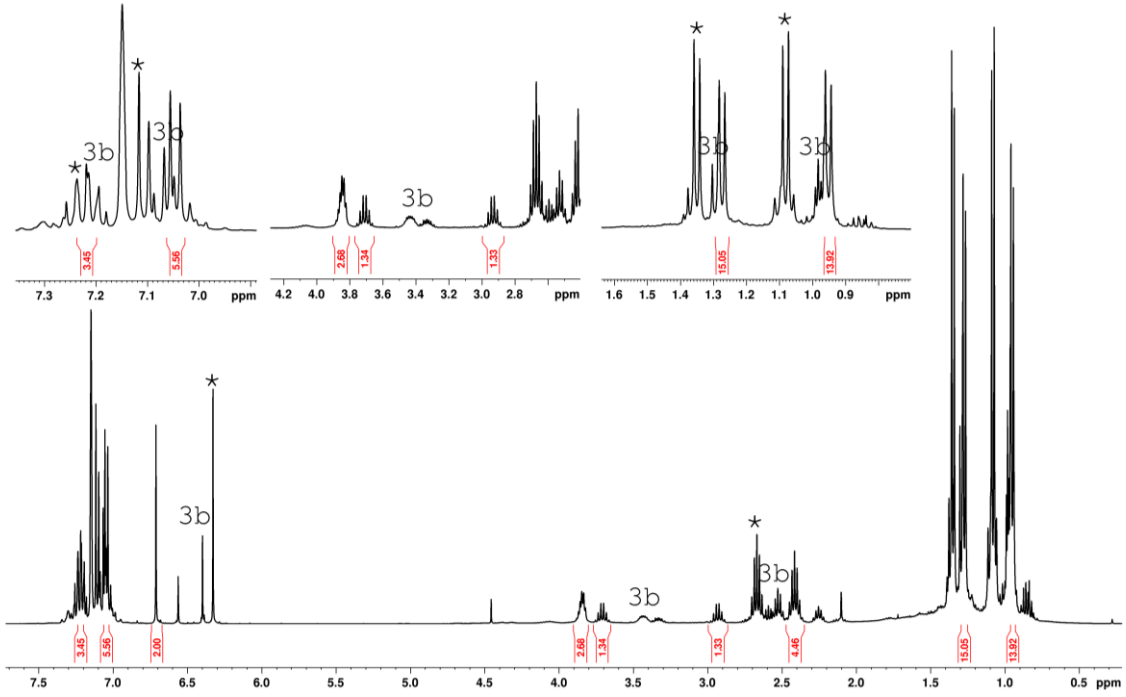

Figure S 9.16: ^{1}H NMR spectrum of a mixture of **3a/b** (75:25) in C_6D_6 at 298 K (* = IDipp·BH_3).

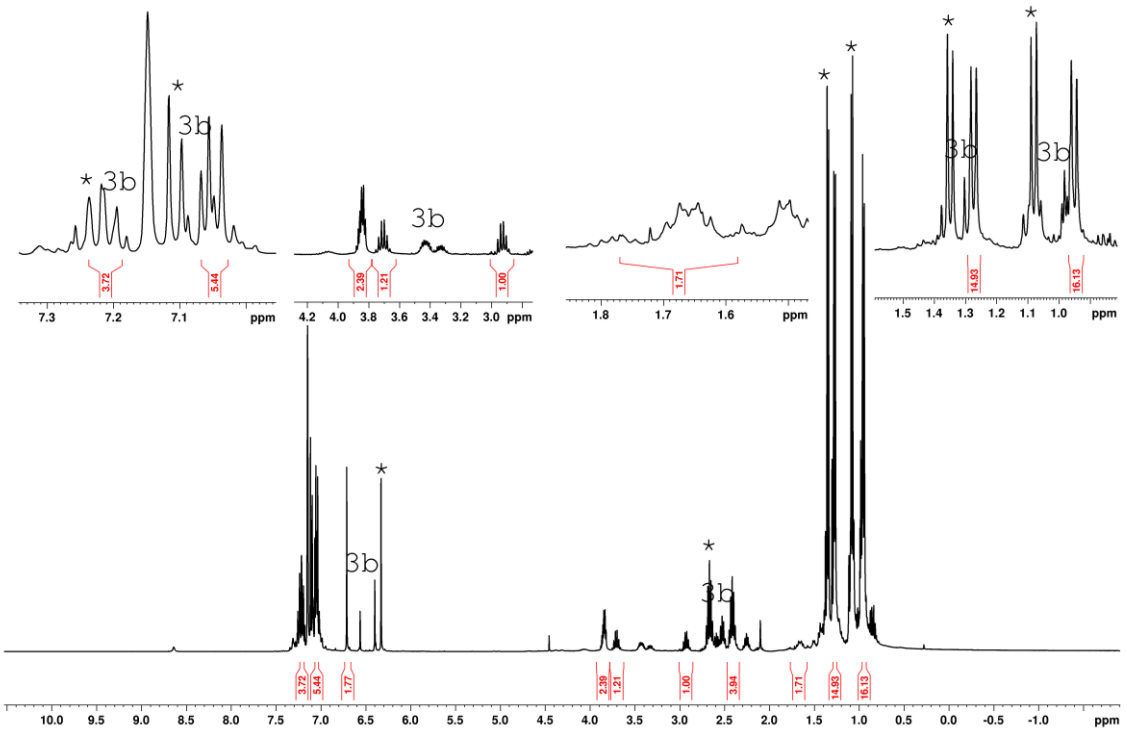

Figure S 9.17: $^{1}H\{^{11}B\}$ NMR spectrum of a mixture of **3a/b** (75:25) in C_6D_6 at 298 K (* = IDipp·BH_3).

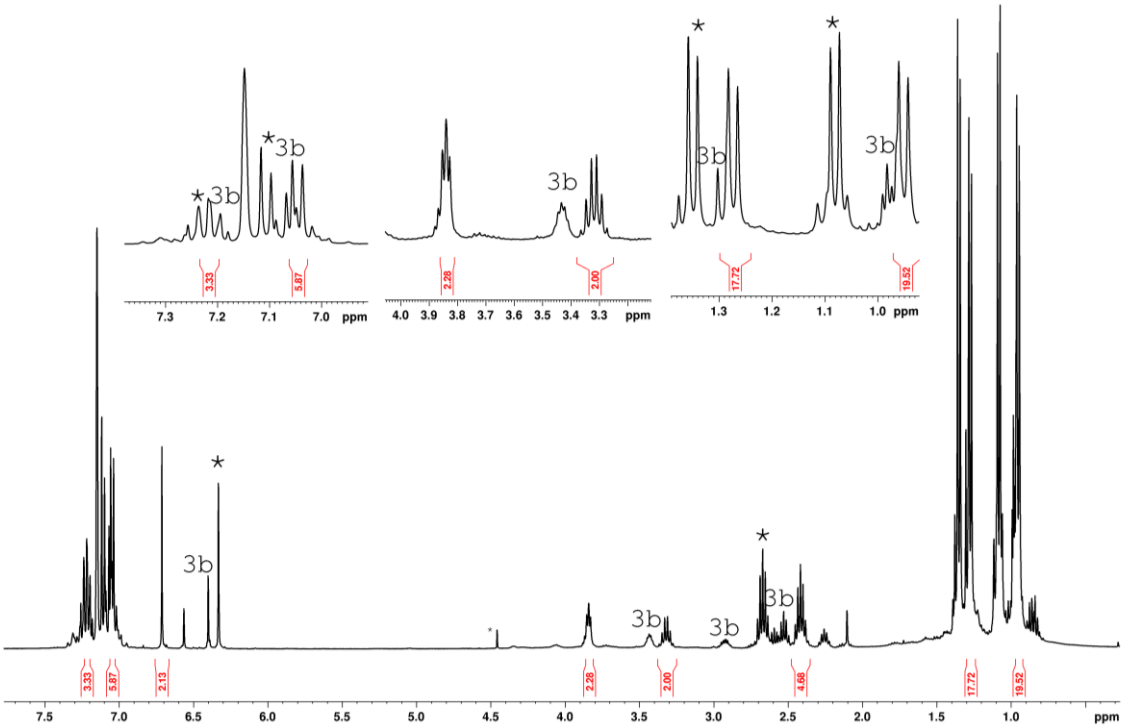

Figure S 9.18: $^{1}H\{^{31}P\}$ NMR spectrum of a mixture of **3a/b** (75:25) in C_6D_6 at 298 K (* = IDipp·BH_3).

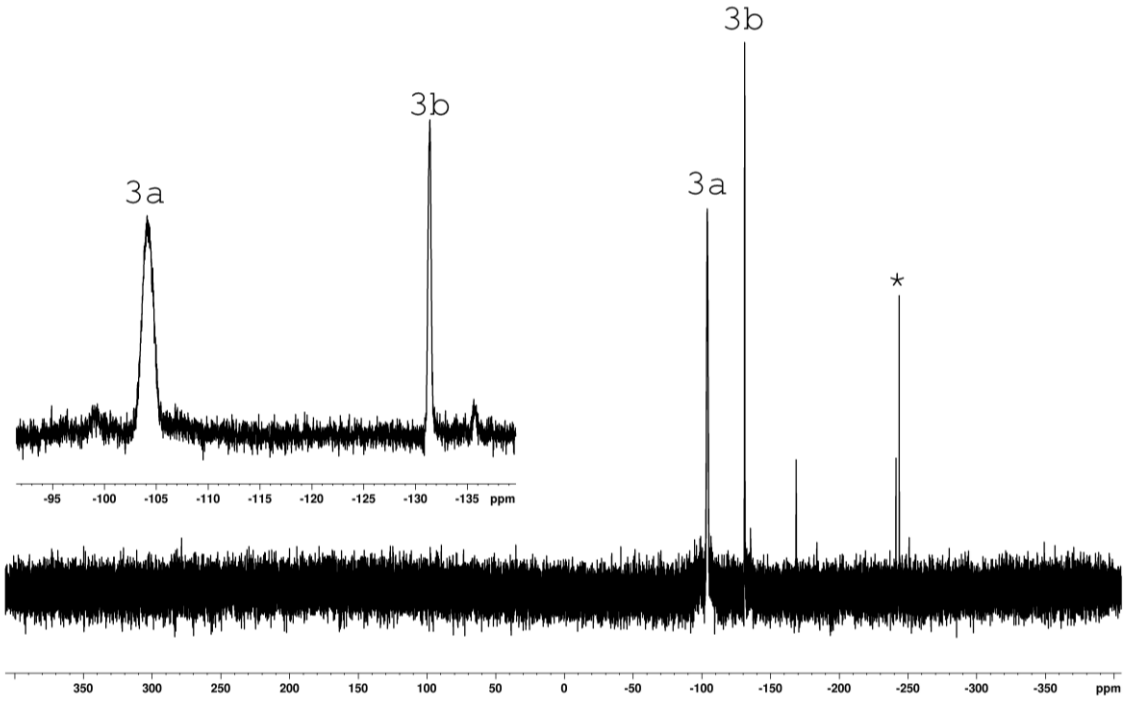

Figure S 9.19: $^{31}P\{^{1}H\}$ NMR spectrum of a mixture of **3a**:**3b** (75:25) in C_6D_6 at 298 K (* = PH_3).

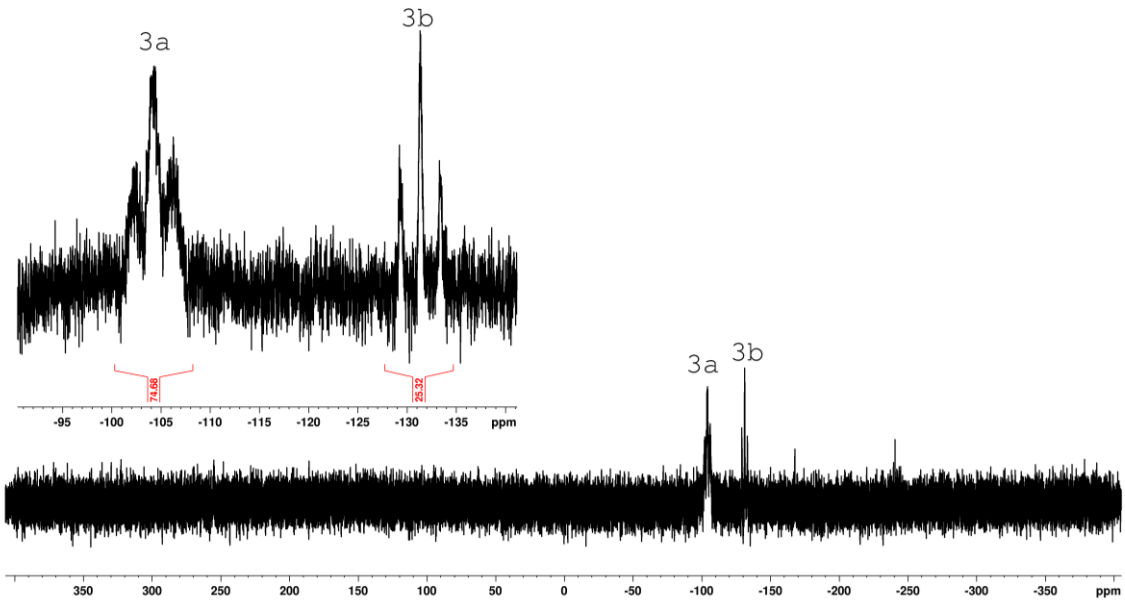

Figure S 9.20: ^{31}P NMR spectrum of a mixture of **3a**:**3b** (75:25) in C_6D_6 at 298 K.

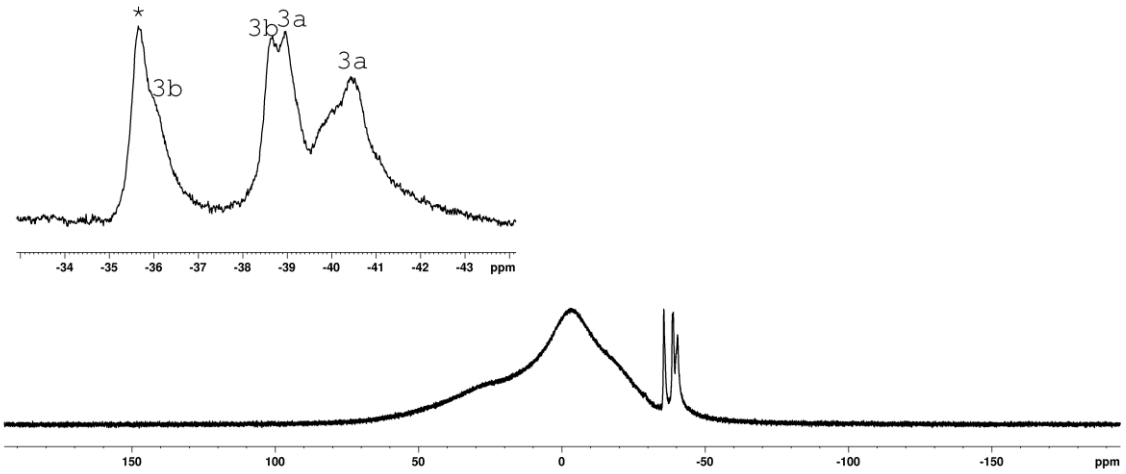

Figure S 9.21: $^{11}B\{^1H\}$ NMR spectrum of a mixture of **3a**:**3b** (75:25) in C_6D_6 at 298 K (* = IDipp·BH_3).

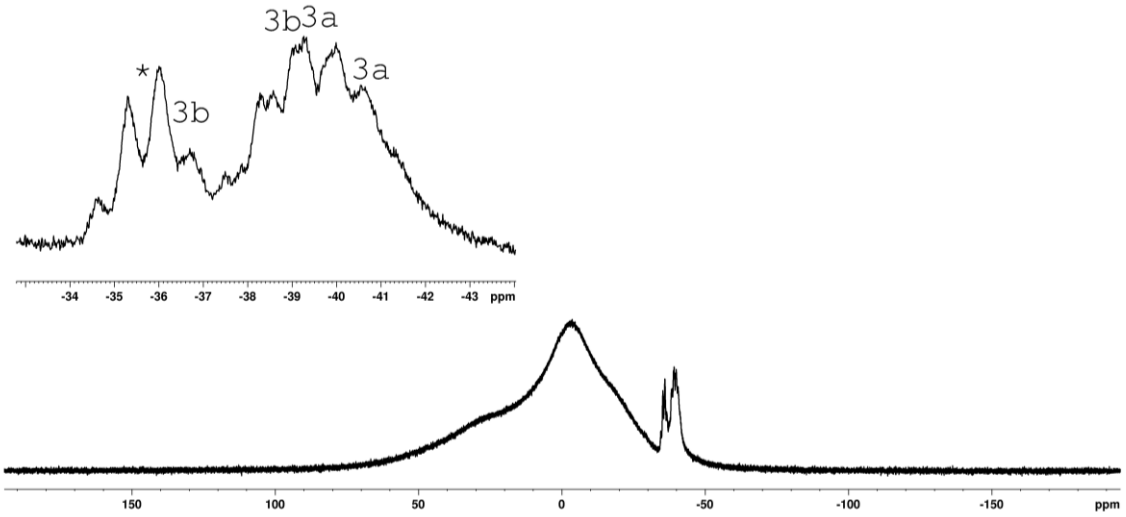

Figure S 9.22: $^{11}B\{^1H\}$ NMR spectrum of a mixture of **3a**:**3b** (75:25) in C_6D_6 at 298 K (* = IDipp·BH_3).

IDipp·$BH_2GeH_2PH_2BH_3$ (**3b**)

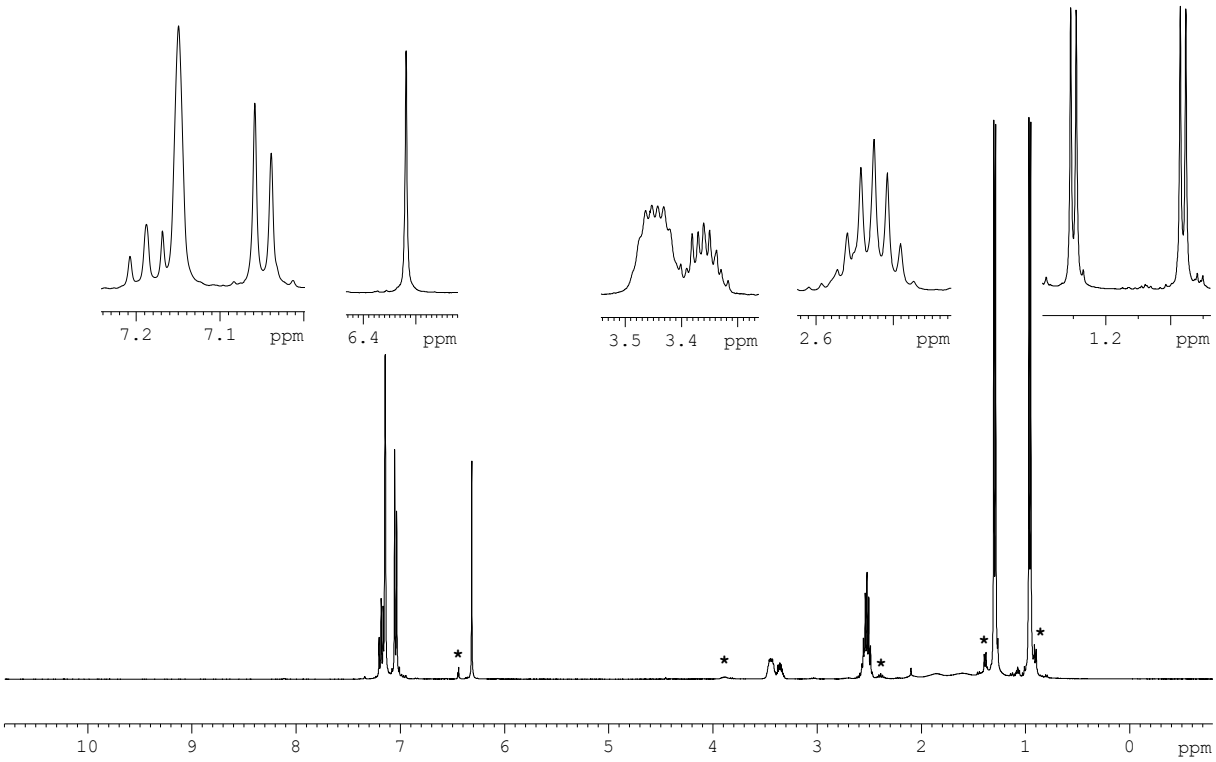

Figure S 9.23: ^1H NMR spectrum of **3b** in C_6D_6 at 298 K. * = **3a**.

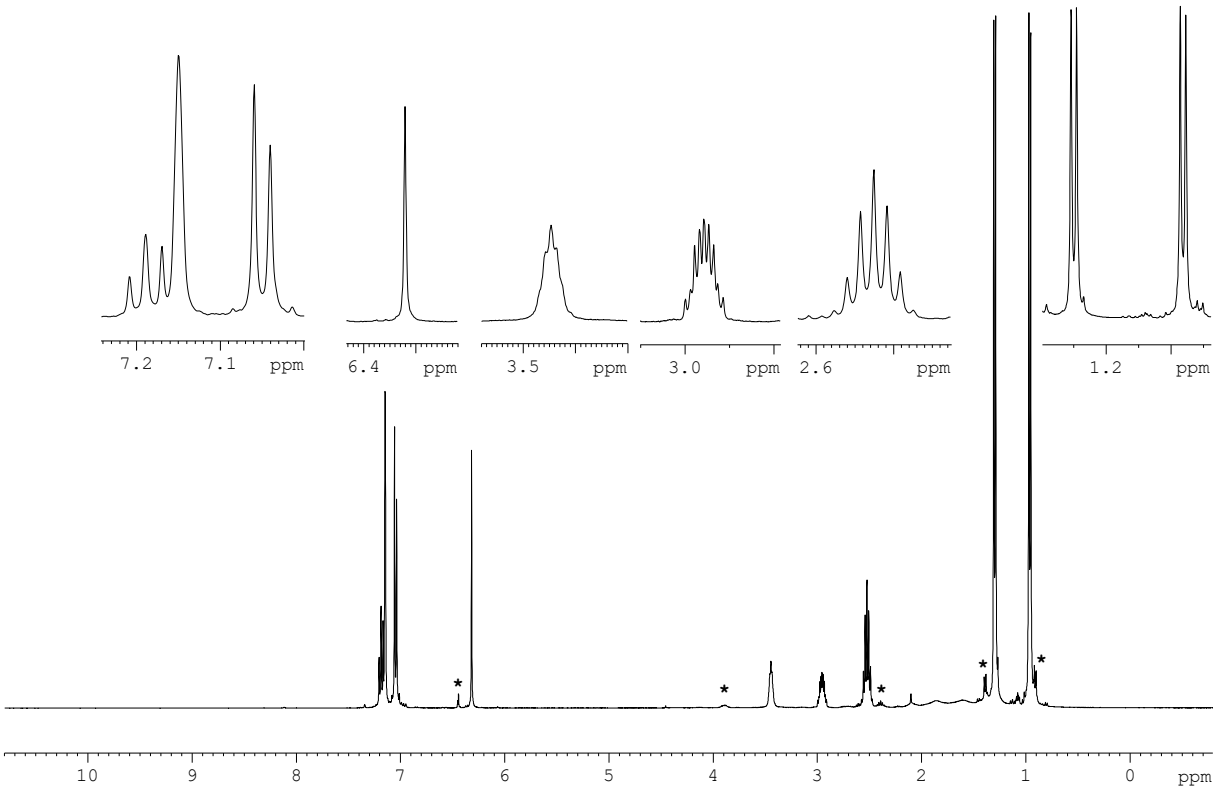

Figure S 9.24: $^1H\{^{31}P\}$ NMR spectrum of **3b** in C_6D_6 at 298 K. * = **3a**.

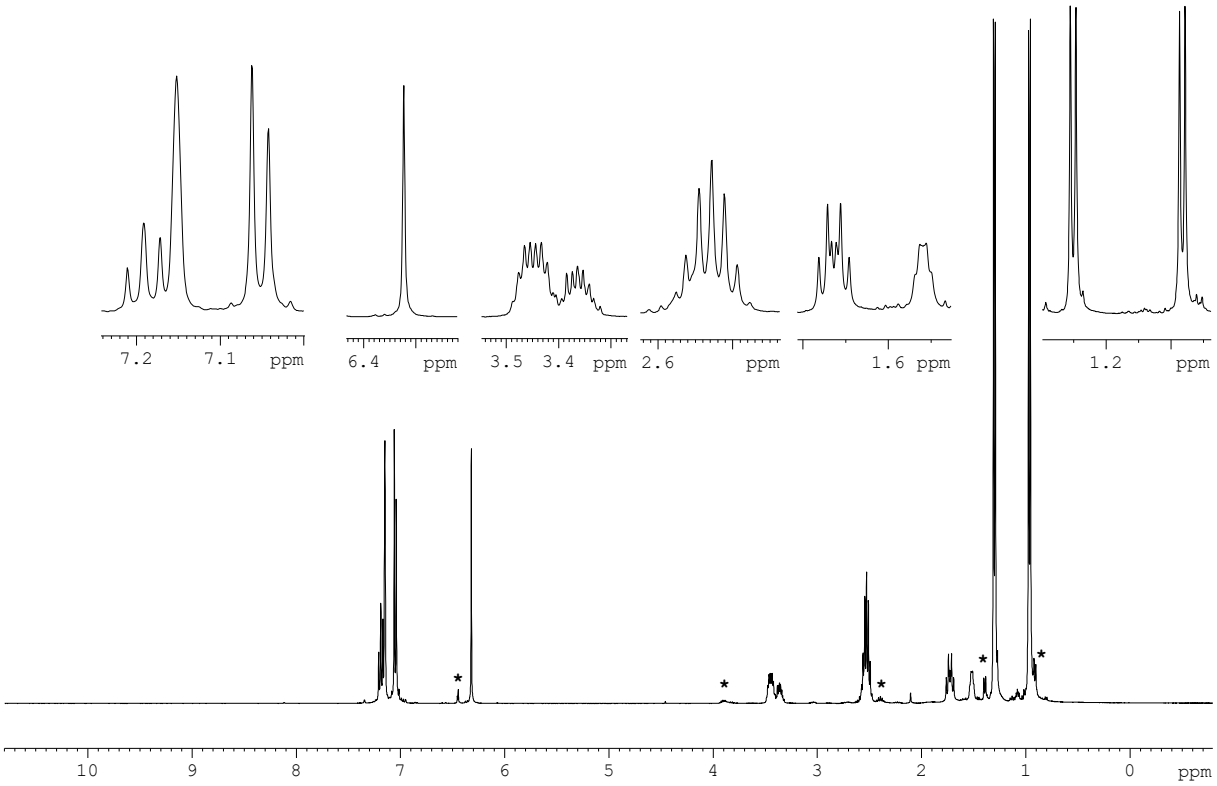

Figure S 9.25: $^{1}H\{^{11}B\}$ NMR spectrum of **3b** in C_6D_6 at 298 K. * = **3a**.

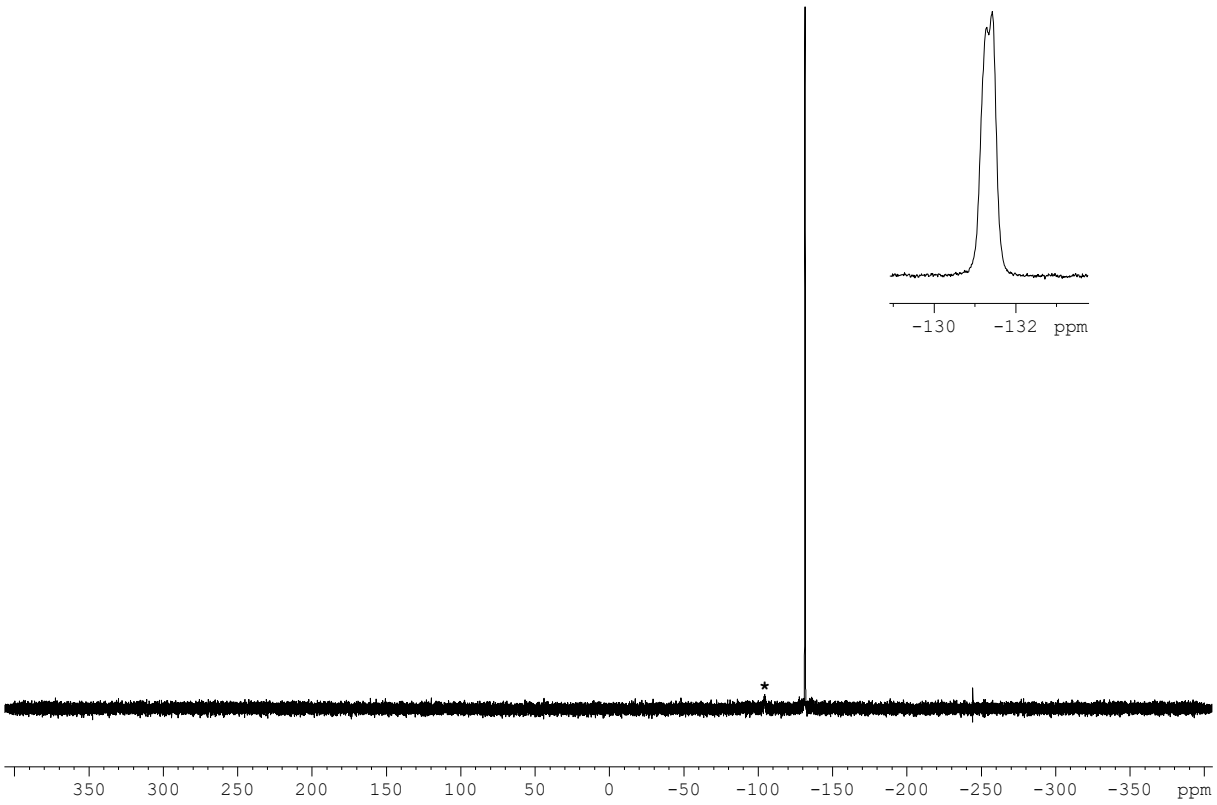

Figure S 9.26: $^{31}P\{^{1}H\}$ NMR spectrum of **3b** in C_6D_6 at 298 K. * = **3a**.

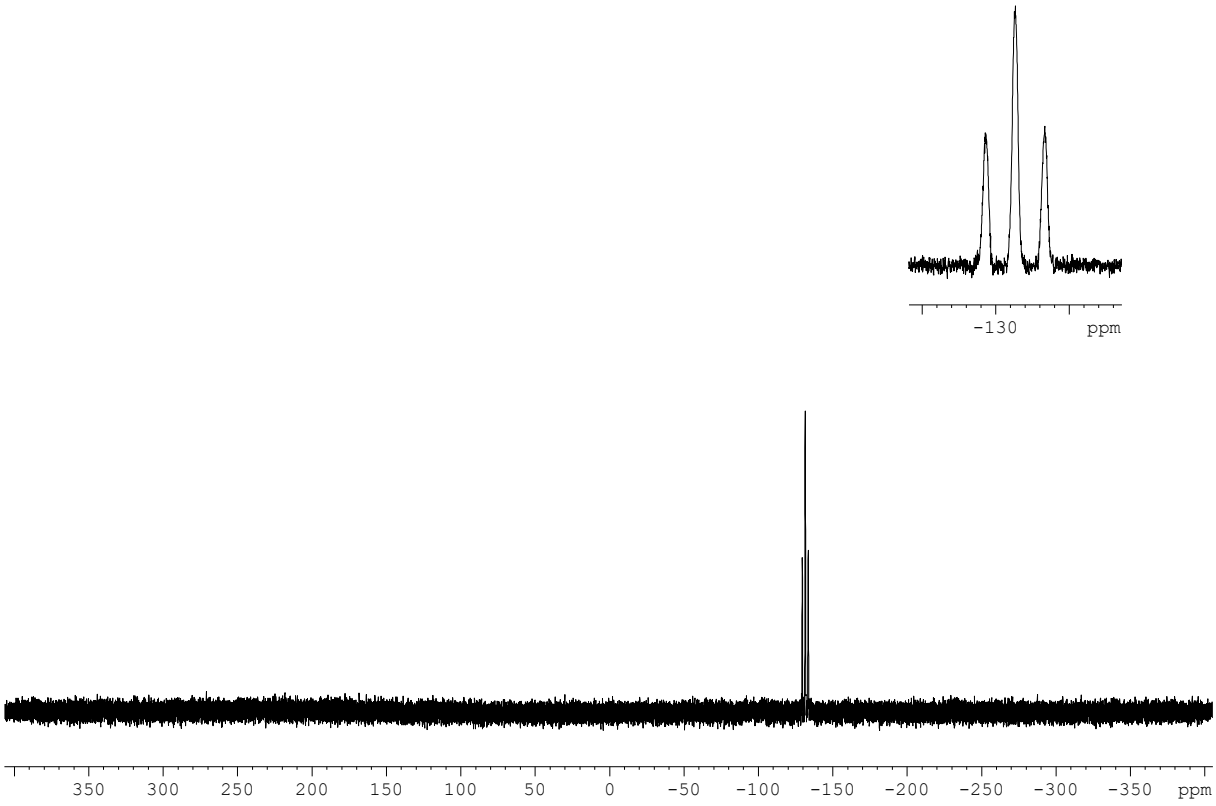

Figure S 9.27: ^{31}P NMR spectrum of **3b** in C_6D_6 at 298 K.

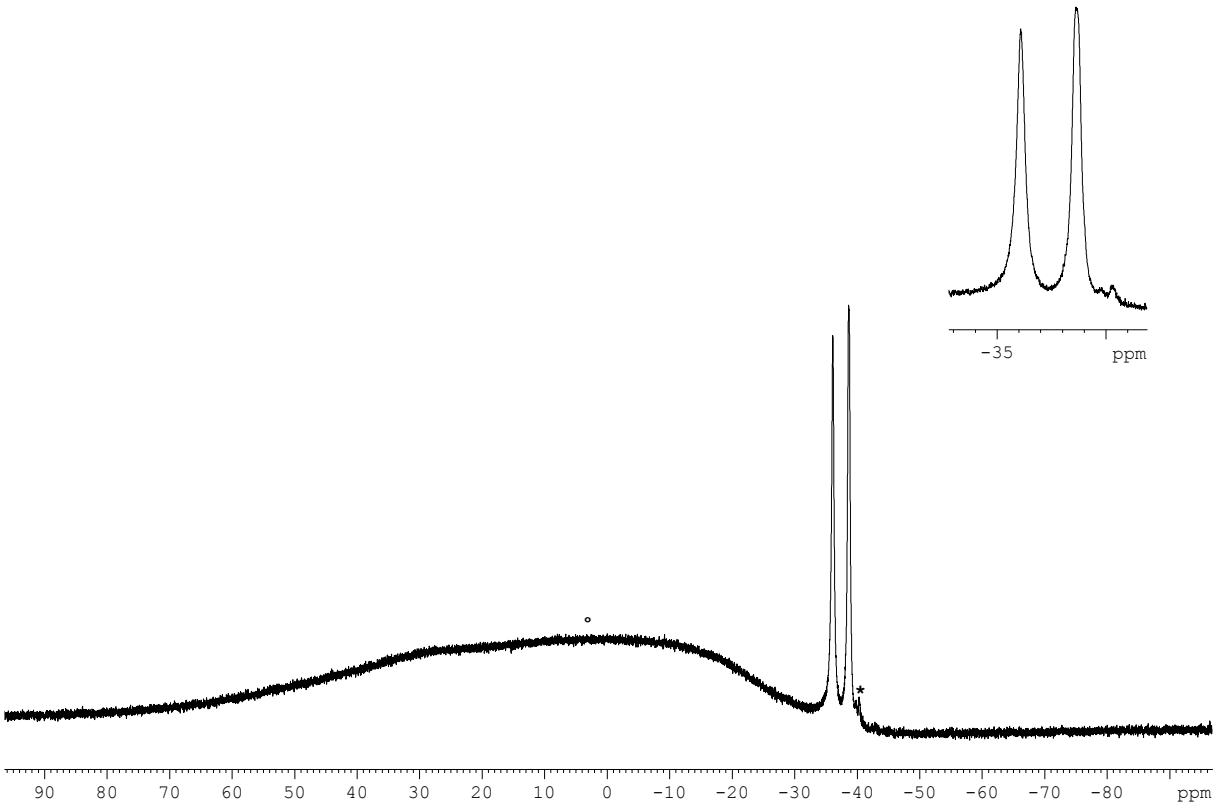

Figure S 9.28: $^{11}B\{^1H\}$ NMR spectrum of **3b** in C_6D_6 at 298 K. ° = signal from the NMR probe. * = **3a**.

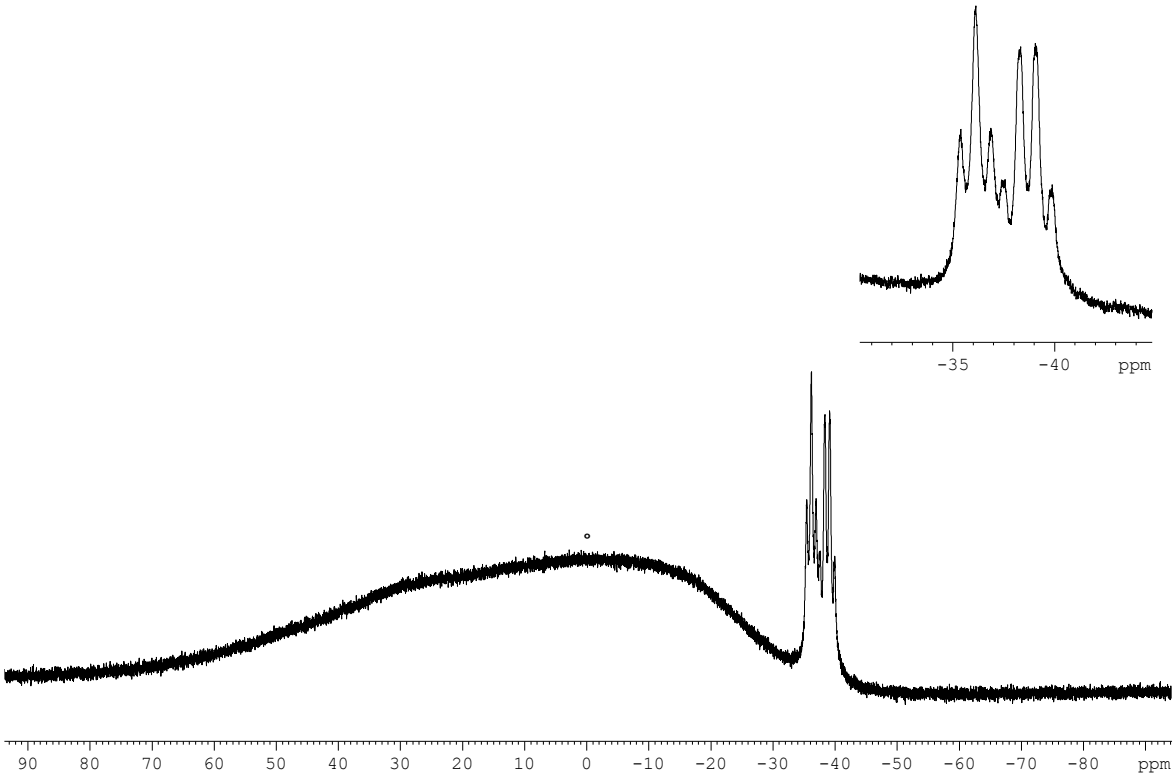

Figure S 9.29: ^{11}B NMR spectrum of **3b** in C_6D_6 at 298 K. ° = signal from the NMR probe.

$[PHGeH_2BH_2PH_2BH_2GeH_2][IDipp{\cdot}BH_2GeH_2{\cdot}IDipp]$ (**4**)

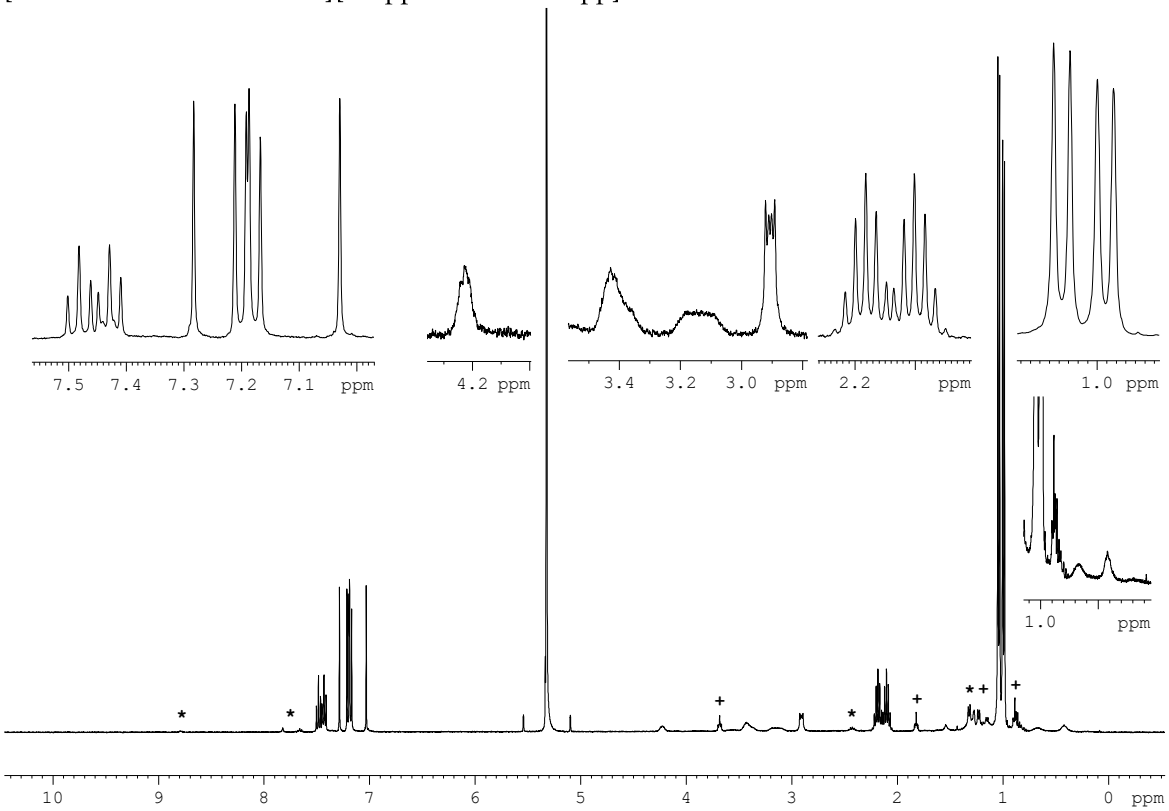

Figure S 9.30: ^1H NMR spectrum of **4** in CD_2Cl_2 at 298 K. * = $[IDippH]^+$. + = residual solvents (thf, *n*-hexane).

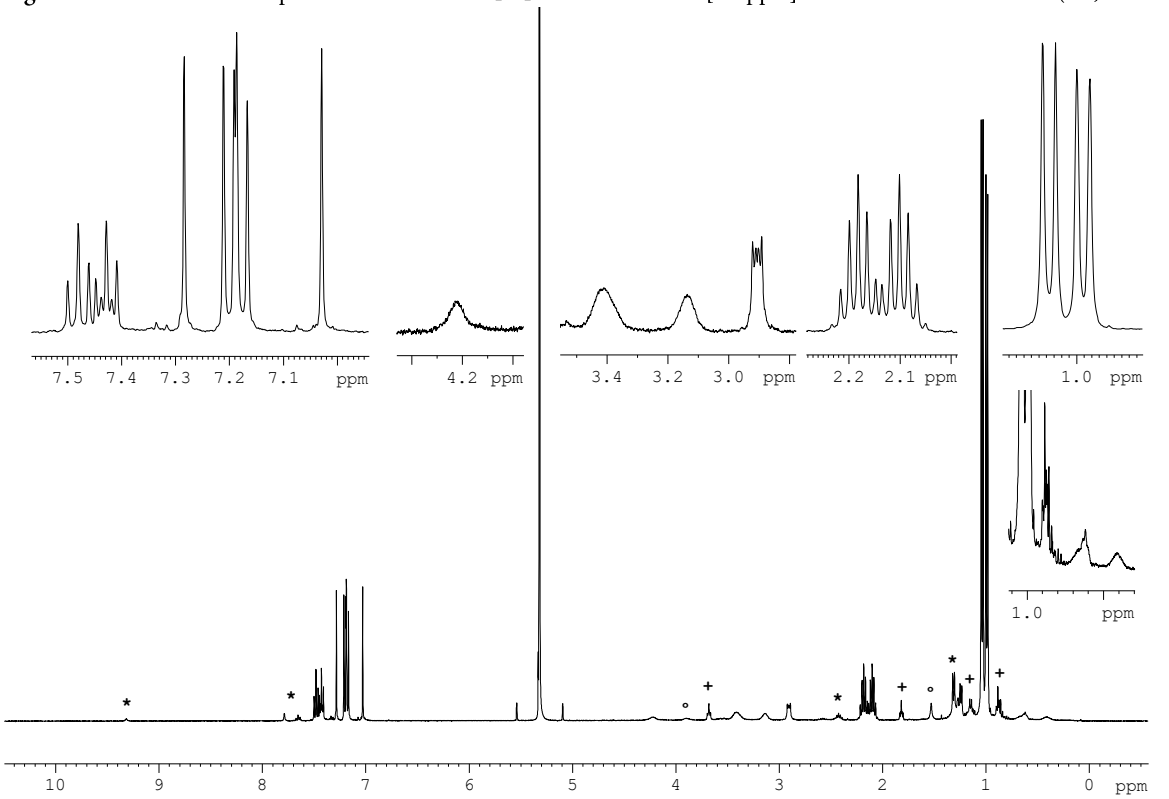

Figure S 9.31: $^1H\{^{31}P\}$ NMR spectrum of **4** in CD_2Cl_2 at 298 K (^{31}P decoupled at -271 ppm). * = $[IDippH]^+$. + = residual solvents (thf, *n*-hexane). ° = unidentified decomposition product.

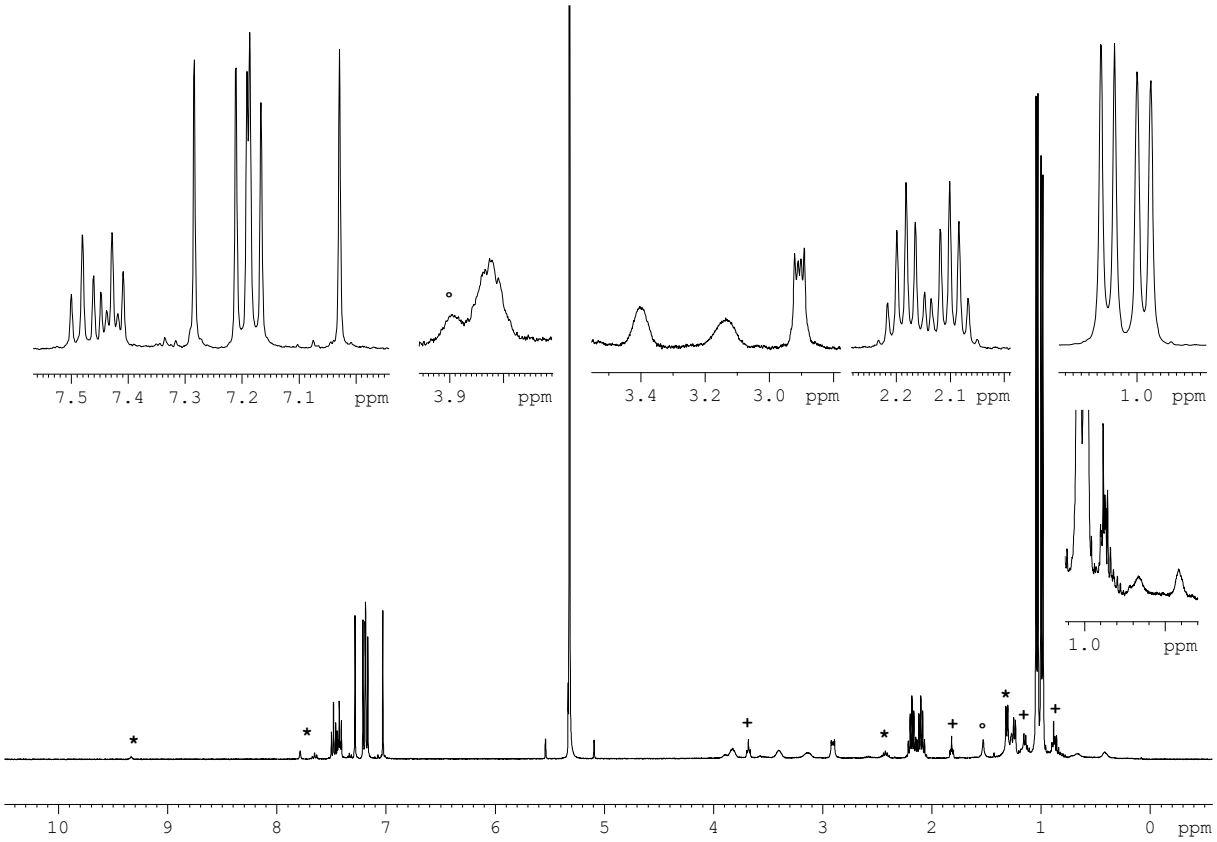

Figure S 9.32: $^{1}H\{^{31}P\}$ NMR spectrum of **4** in CD_2Cl_2 at 298 K (^{31}P decoupled at -98.7 ppm). * = $[IDippH]^+$. + = residual solvents (thf, *n*-hexane). ° = unidentified decomposition product.

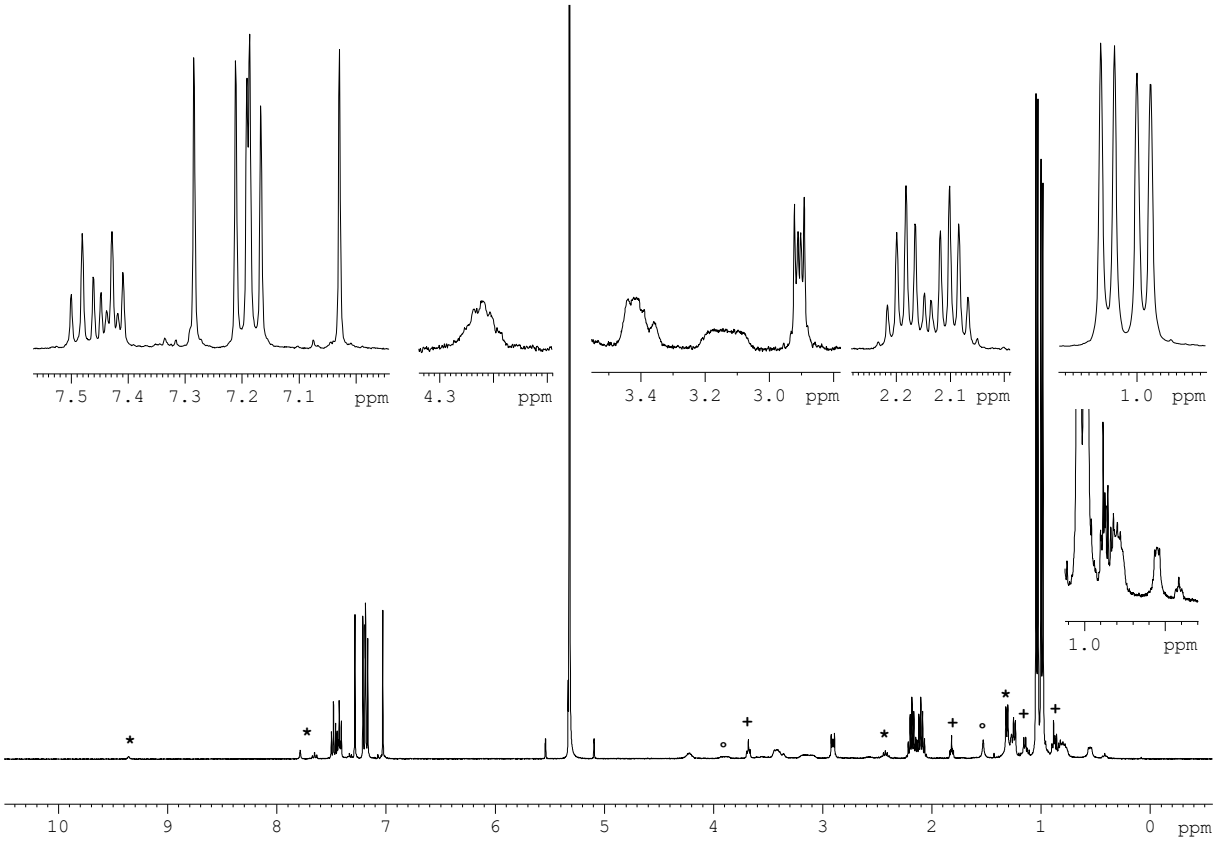

Figure S 9.33: $^{1}H\{^{11}B\}$ NMR spectrum of **4** in CD_2Cl_2 at 298 K (^{11}B decoupled at -40.0 ppm). * = $[IDippH]^+$. + residual solvents (thf, *n*-hexane). ° = unidentified decomposition product.

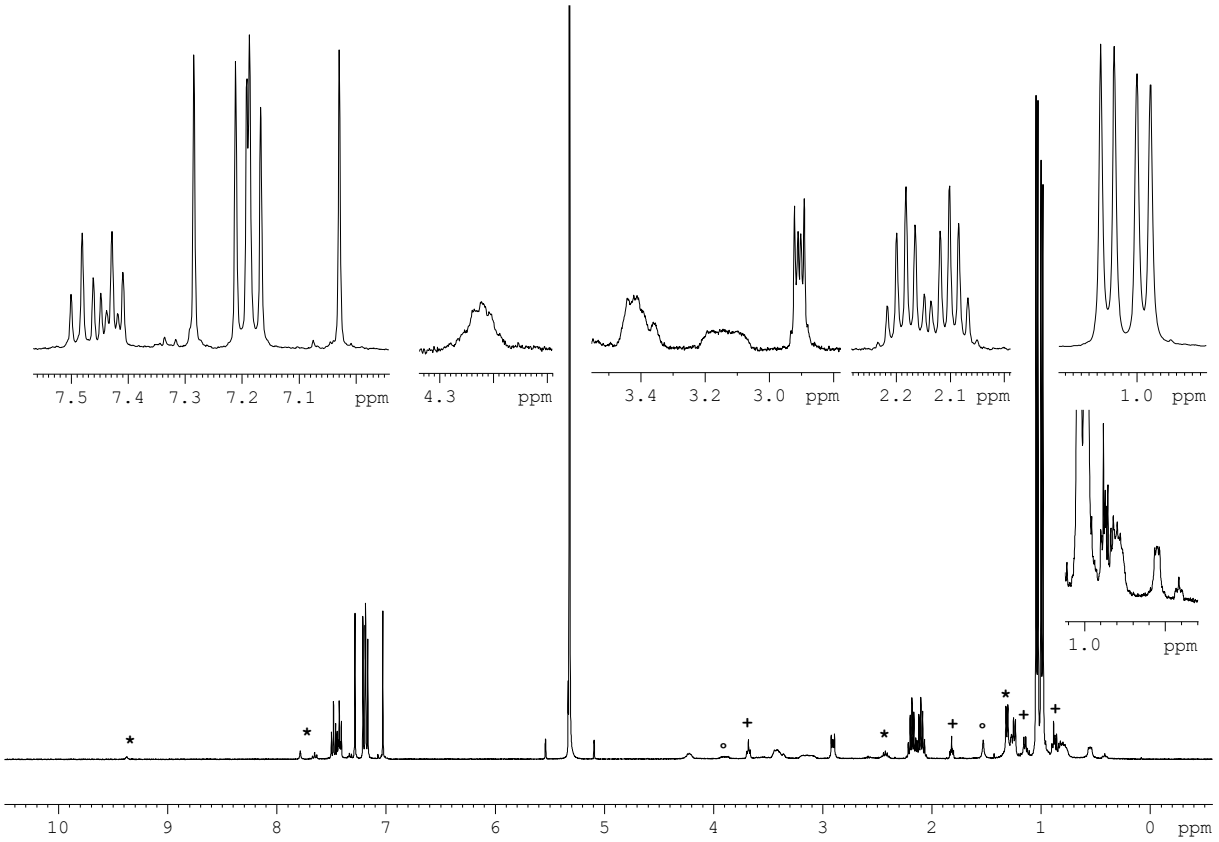

Figure S 9.34: $^{1}H\{^{11}B\}$ NMR spectrum of **4** in CD_2Cl_2 at 298 K (^{11}B decoupled at -37.7 ppm). * = $[IDippH]^+$. + = residual solvents (thf, *n*-hexane). ° = unidentified decomposition product.

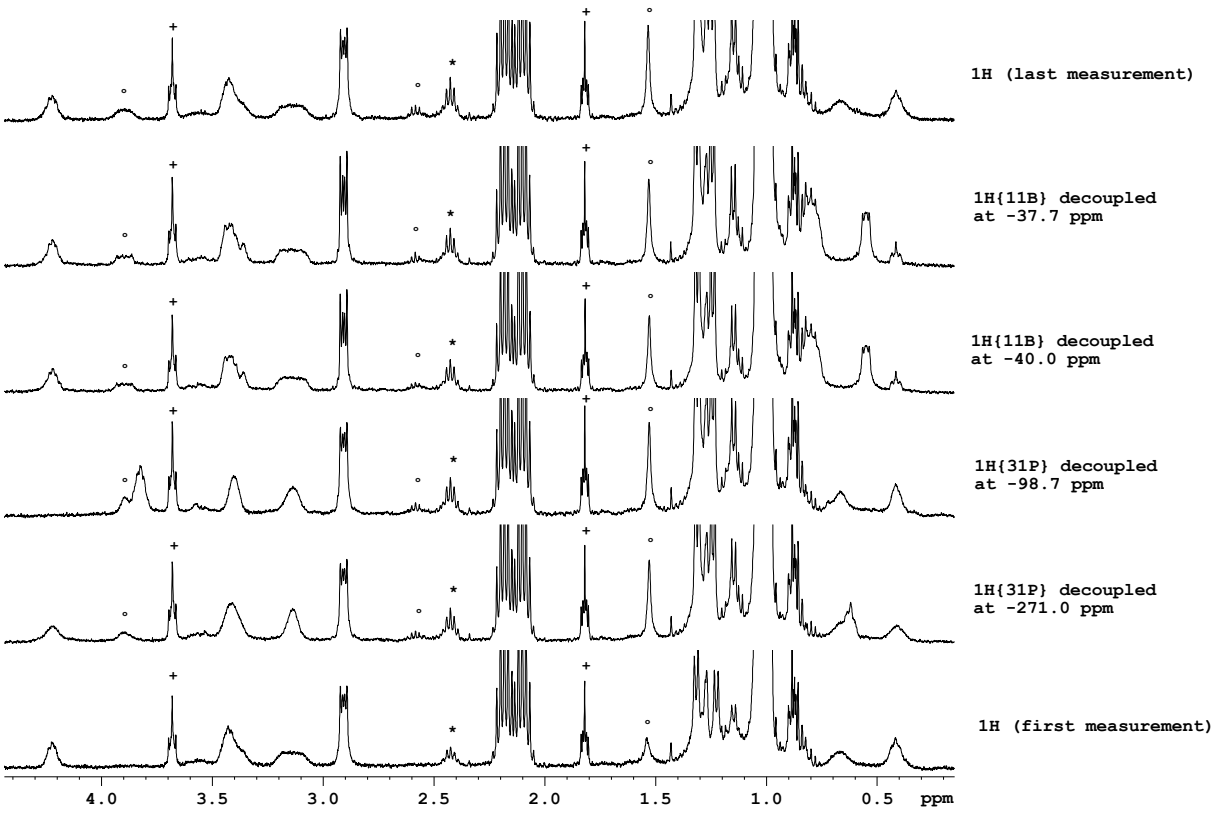

Figure S 9.35: Combined ^{1}H NMR spectra of **4** in CD_2Cl_2 at 298 K. * = $[IDippH]^+$. + = residual solvents (thf). ° = unidentified decomposition product.

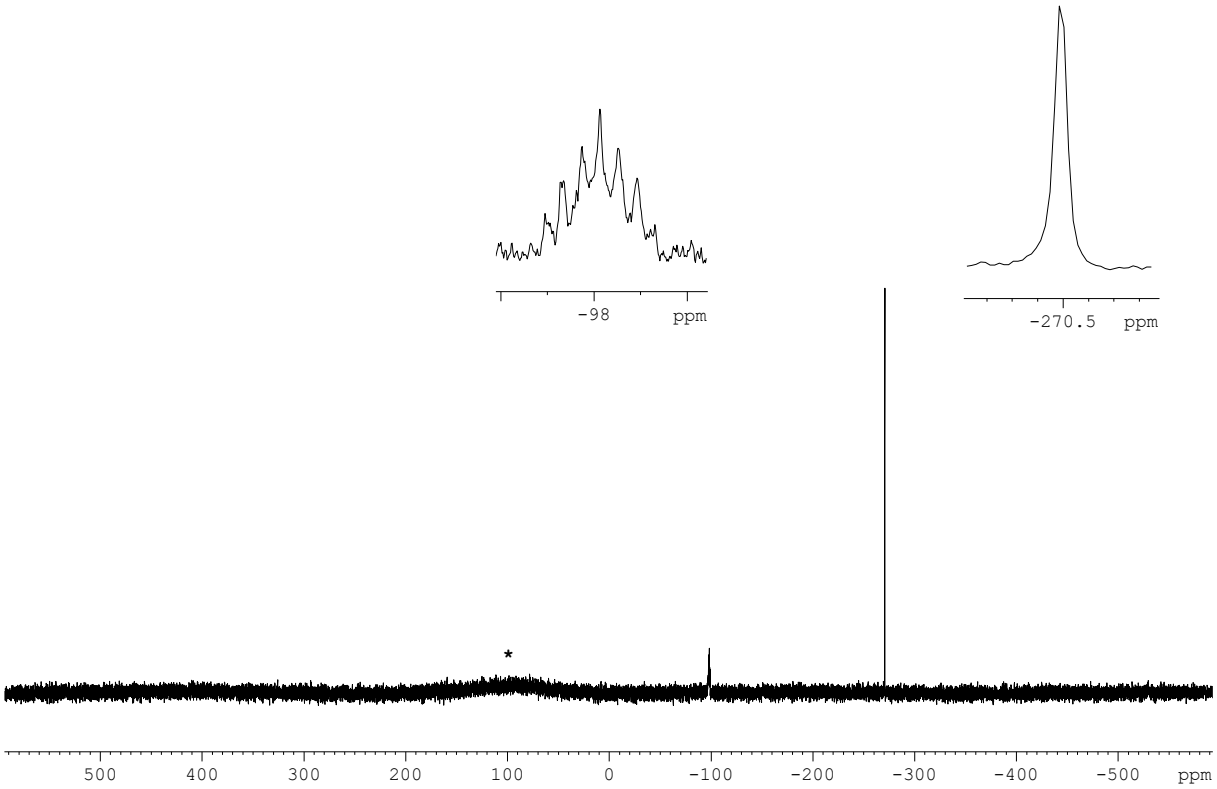

Figure S 9.36: $^{31}P\{^{1}H\}$ NMR spectrum of **4** in CD_2Cl_2 at 298 K. * = unidentified signal.

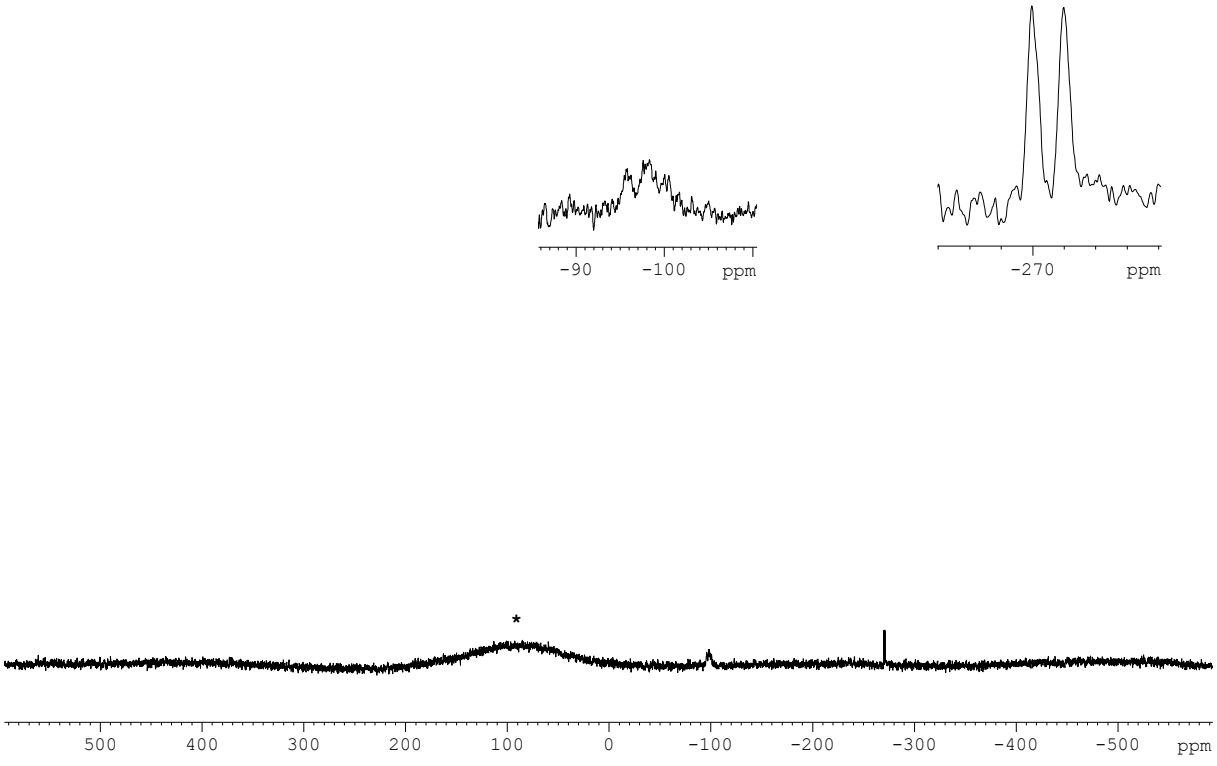

Figure S 9.37: ^{31}P NMR spectrum of **4** in CD_2Cl_2 at 298 K. * = unidentified signal.

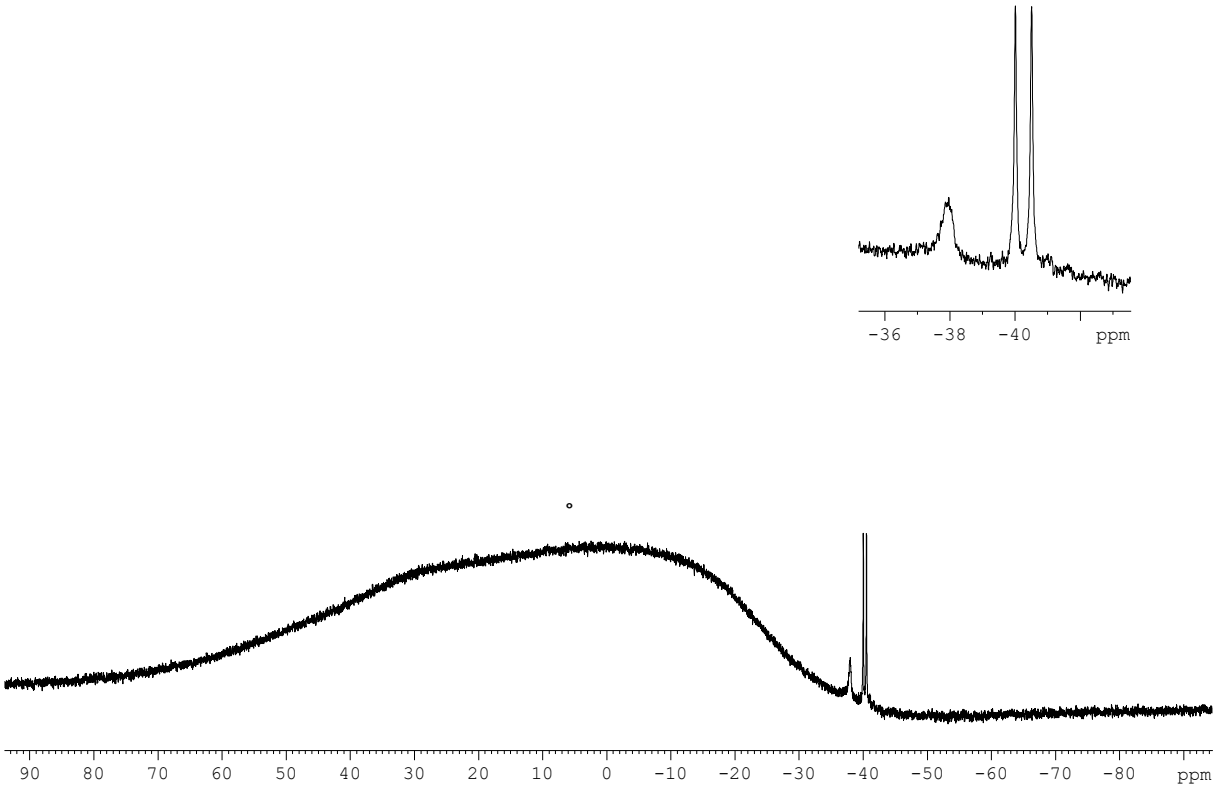

Figure S 9.38: $^{11}B\{^{1}H\}$ NMR spectrum of **4** in CD_2Cl_2 at 298 K. ° = signal from the NMR probe.

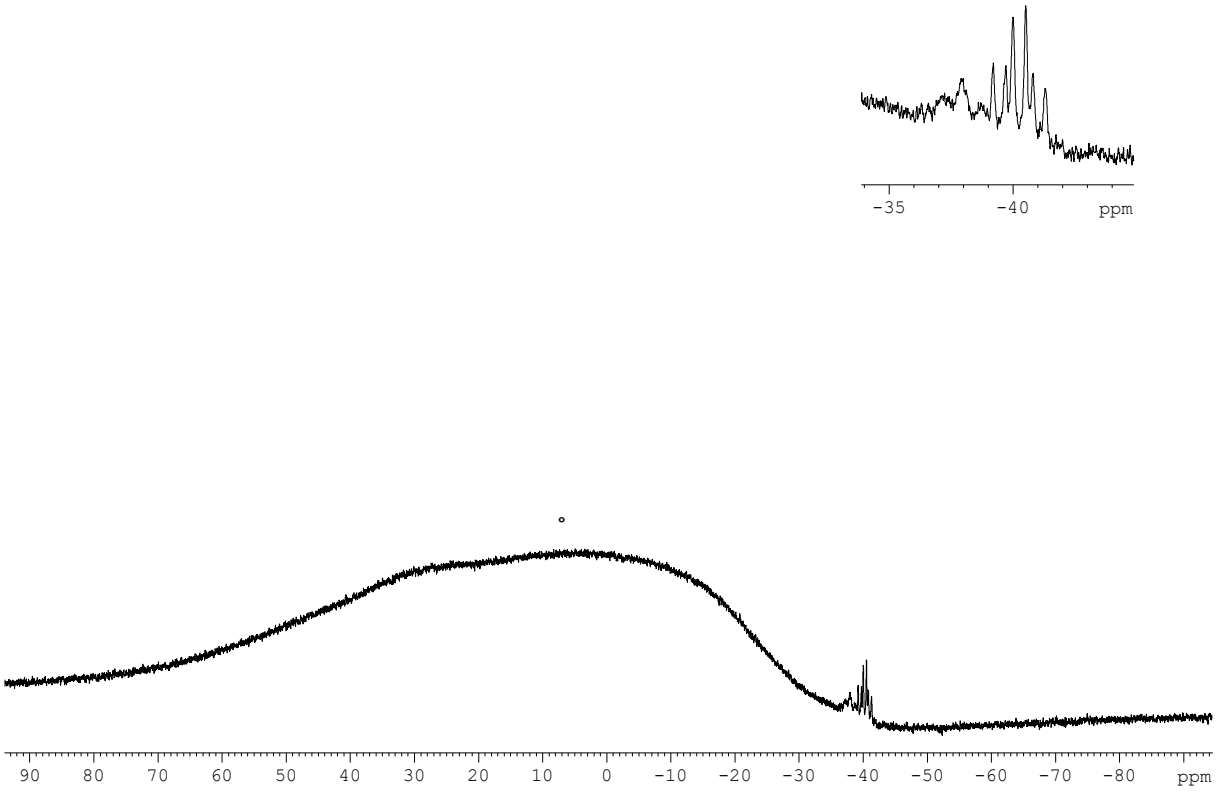

Figure S 9.39: ^{11}B NMR spectrum of **4** in CD_2Cl_2 at 298 K. ° = signal from the NMR probe.

NMR spectra of the solution after layering a mixture of 2a:2b (67:33) in THF/*n*-hexane (4 °C, two weeks)

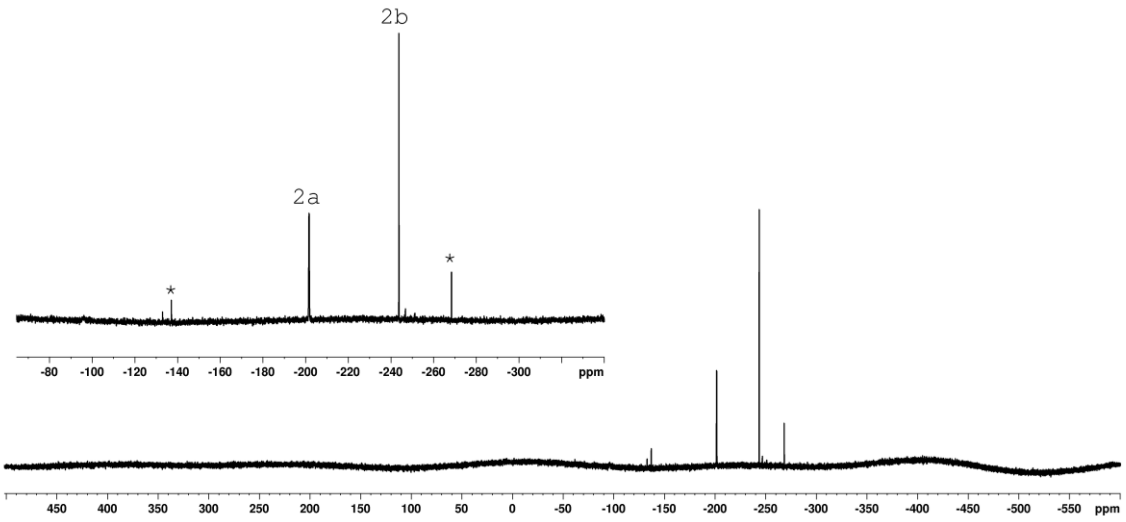

Figure S 9.40: $^{31}P\{^{1}H\}$ NMR spectrum of a solution of **2a**:**2b** (67:33) in THF layered with n-hexane at 4 °C for two weeks (C_6D_6-cap.).

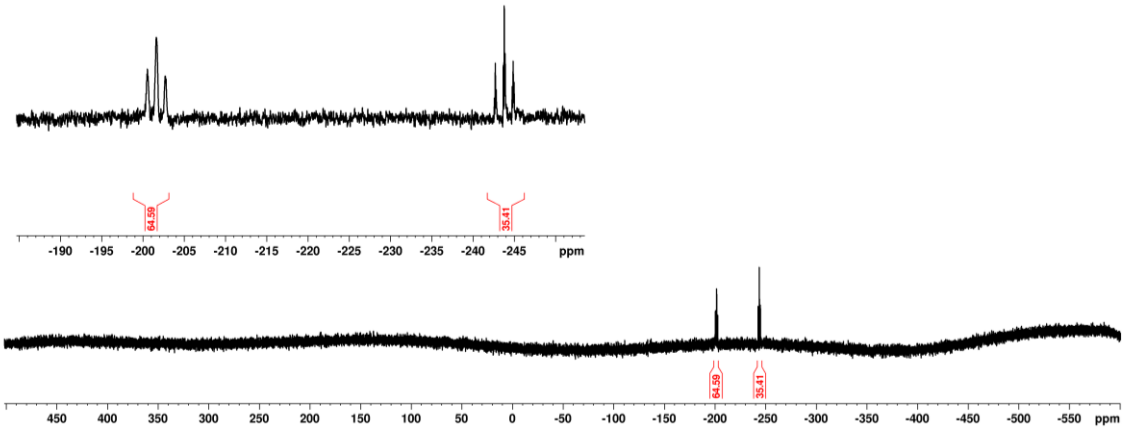

Figure S 9.41: ^{31}P NMR spectrum of a solution of **2a**:**2b** (67:33) in THF layered with n-hexane at 4 °C for two weeks (C_6D_6-cap.).

9.5.3 Crystallographic data

Single-crystal X-ray diffraction experiments were performed on a Xcalibur, AtlasS2, Gemini ultra diffractometer (**2b**, **4**) and on a XtaLAB Synergy R DW system (Rigaku) equipped with a HyPix-Arc 150 detector (**2a**). Data were collected using Cu-K_α radiation (λ = 1.54178 Å). Data reduction, scaling and absorption corrections were performed using CrysAlisPro[3] (Rigaku). A numerical absorption correction based on Gaussian integration over a multifaceted crystal model (**2a**), an analytical numeric absorption correction using a multifaceted crystal model based on expressions derived by *Clark* and *Reid*[4] (**2b**, **4**) and an empirical absorption correction using spherical harmonics as implemented in SCALE3/ABSPACK was applied. Using Olex2,[5] all structures were solved with ShelXT[6] and a least-square refinement on F^2 was carried out with ShelXL[7]. All non-hydrogen atoms were refined anisotropically. Most hydrogen atom positions were calculated geometrically and refined using the riding model, but some hydrogen atoms were refined freely.

Crystallographic data and details of the experiments are given in Table S 9.1 .

CIF files with comprehensive information on the details of the diffraction experiments and full tables of bond lengths and angles are deposited in Cambridge Crystallographic Data Centre under the deposition codes CCDC 2301528 – 2301530. These data can be obtained free of charge at www.ccdc.cam.ac.uk/conts/retrieving.html (or from the Cambridge Crystallographic Data Centre, 12 Union Road, Cambridge CB2 1EZ, UK; Fax: + 44-1223-336-033; e-mail: deposit@ccdc.cam.ac.uk).

Table S 9.1: Crystallographic data for compounds **2a**, **2b** and **4**.

Compound	**2a**	**2b**	**4**
Formula	$B_2C_{58}Ge_2H_{94}N_4OP_2$	$BC_{30.5}GeH_{45.1}N_2P$	$C_{56.5}H_{93}B_3Ge_3N_4P_2$
Dcalc	1.143	1.167	1.206
μ/mm^{-1}	1.922	1.931	2.437
Formula Weight	1092.11	554.15	1140.48
Color	clear colorless	colorless	clear colorless
Shape	block-shaped	block-shaped	plate-shaped
Size/mm^3	0.26×0.17×0.08	0.38×0.15×0.12	0.27×0.17×0.10
T/K	123.01(10)	123(1)	293(2)
Crystal System	monoclinic	orthorhombic	triclinic
Flack Parameter	0.50(4)		
Hooft Parameter	0.194(6)		
Space Group	$P2_1$	*Pccn*	*P*-1
a/Å	12.50930(10)	16.9117(3)	12.4055(3)
b/Å	20.2374(2)	19.8556(3)	12.5438(4)
c/Å	12.53640(10)	18.7920(3)	23.3620(6)
α/°	90	90	82.747(3)
β/°	91.0900(10)	90	77.991(2)
γ/°	90	90	62.128(3)
V/Å^3	3173.09(5)	6310.20(18)	3141.59(18)
Z	2	8	2
Z'	1	1	1
Wavelength/Å	1.54184	1.54184	1.54184
Radiation type	Cu K$_a$	Cu K$_a$	Cu K$_a$
θ_{min}/°	3.526	3.433	3.871
θ_{max}/°	73.634	71.583	71.703
Measured Refl's.	51867	18158	29890
Indep't Refl's	12283	6029	11573
Refl's I≥2 σ(I)	11174	4672	10558
R_{int}	0.0353	0.0314	0.0282
Parameters	680	373	784
Restraints	199	151	287
Largest Peak	0.524	0.524	0.722
Deepest Hole	-0.642	-0.287	-0.586
GooF	1.061	1.040	1.150
wR_2 (all data)	0.1524	0.1277	0.1281
wR_2	0.1481	0.1189	0.1253
R_1 (all data)	0.0511	0.0569	0.0574
R_1	0.0473	0.0443	0.0523

9.5.4 Molecular structures

IDipp·$GeH_2BH_2PH_2$ (2a)

A mixture of **2a** and **2b** (**2a** : **2b** / 37 : 63) was crystallized from an Et_2O solution by slow solvent evaporation at room temperature as clear colorless blocks in the monoclinic space group $P2_1$. The structure of **2a** in the solid state is shown in Figure S 9.42.

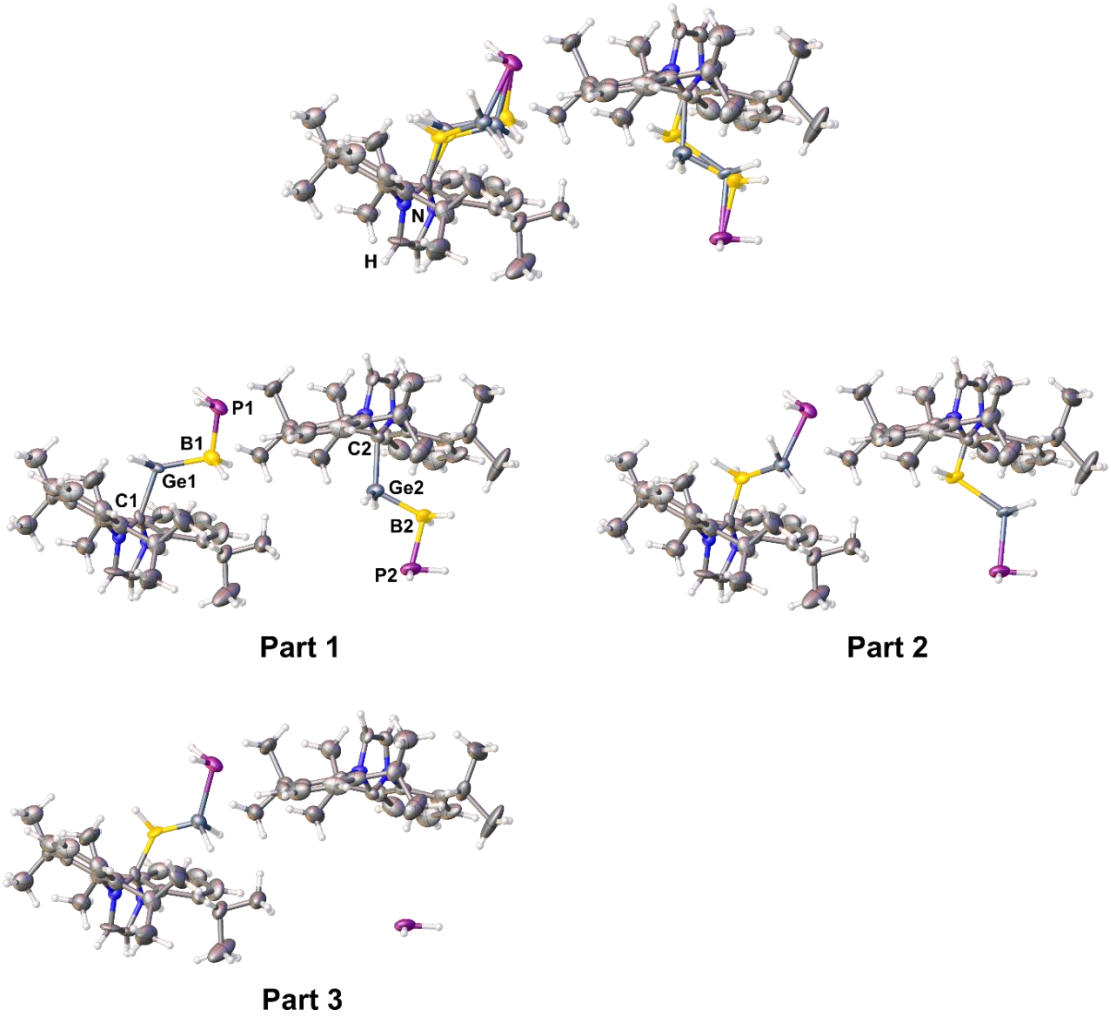

Figure S 9.42: Molecular structures of co-crystallized **2a** and **2b** in the solid state. Anisotropic displacement parameters are set to 50% probability level. Top: Combined disordered parts; middle left: part 1 (occupancy left molecule: 68%; occupancy right molecule: 88%) middle right: part 2 (occupancy left molecule: 13%; occupancy right molecule: 12%) bottom left: part 3 (occupancy left molecule: 19%). Selected bond lengths [Å] and angles [°] for part 1: C1-Ge1 1.962(6), Ge1-B1 2.076(19), B1-P1 1.93(2), C1-Ge1-B1 119.1(6), Ge1-B1-P1 107.3(9); C2-Ge2 2.007(7), Ge2-B2 2.031(15), B2-P2 2.07(2), C2-Ge2-B2 115.3(6), Ge2-B2-P2 103.7(9).

Within the measured crystal, compound **2a** co-crystallized with 22% of **2b**. The asymmetric unit contains two molecules of **2a**/**2b**. A solvent mask was calculated and 84 electrons were found in a volume of 500 $Å^3$ in 1 void per unit cell. This is consistent with the presence of 1 Et_2O per asymmetric unit which account for 84 electrons per unit cell. Furthermore, the H_2BGeH_2 moiety of **2b** of the left molecule in the asymmetric unit is disordered over two positions (occupancies: 0.13:0.19). The DFIX, DANG, ISOR and SIMU restraints were applied to model this disorder and co-crystallized **2b**.

IDipp·$BH_2GeH_2PH_2$ (2b)

A mixture of **2a** and **2b** (**2a** : **2b** / 10 : 90) was crystallized from an Et_2O solution by slow solvent evaporation at room temperature as clear colorless blocks in the orthorhombic space group *Pccn*. The structure of **2b** in the solid state is shown in Figure S 9.43.

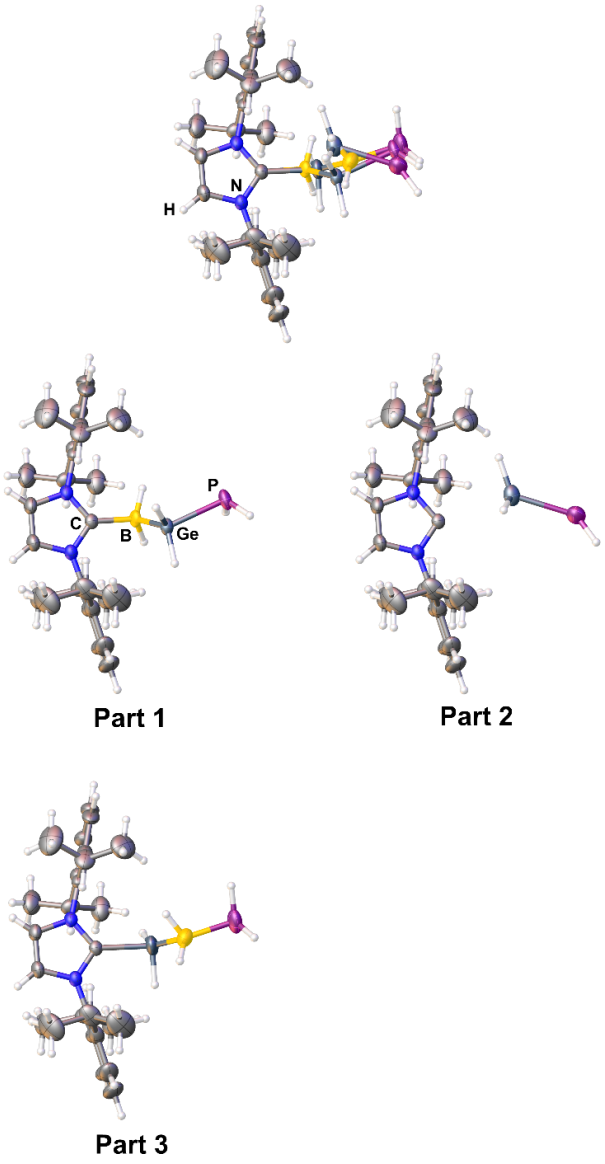

Figure S 9.43: Molecular structures of co-crystallized **2a** and **2b** in the solid state. Anisotropic displacement parameters are set to 50% probability level. Top: Combined disordered parts; middle left: part 1 (occupancy: 76%) middle right: part 2 (occupancy: 14%) bottom left: part 3 (occupancy: 10%). Selected bond lengths [Å] and angles [°] for part 1: C-B 1.572(4), B-Ge 2.047(4), Ge-P 2.320(3), C-B-Ge 113.3(1), B-Ge-P 106.47(13).

Within the measured crystal, compound **2b** co-crystallized with 10% of **2a**. A solvent mask was calculated, and 184 electrons were found in a volume of 912 $Å^3$ in 1 void per unit cell. This is consistent with the presence of 0.5 C_7H_8 per asymmetric unit which account for 200 electrons per unit cell. Furthermore, the H_2GePH_2 moiety of **2b** is disordered over two positions (occupancies: 0.76:0.14). The DFIX, DANG, ISOR and SIMU restraints were applied to model this disorder and co-crystallized **2a**.

[PHGeH$_2$BH$_2$PH$_2$BH$_2$GeH$_2$][IDipp·BH$_2$GeH$_2$·IDipp] (4)

A THF solution of a mixture of **2a** and **2b** (**2a** : **2b** / 9 : 91) was layered with three times the amount of *n*-hexane at 4 °C. **4** crystallized as clear colorless plates in the triclinic space group *P*-1. The structure of **4** in the solid state is shown in Figure S 9.44.

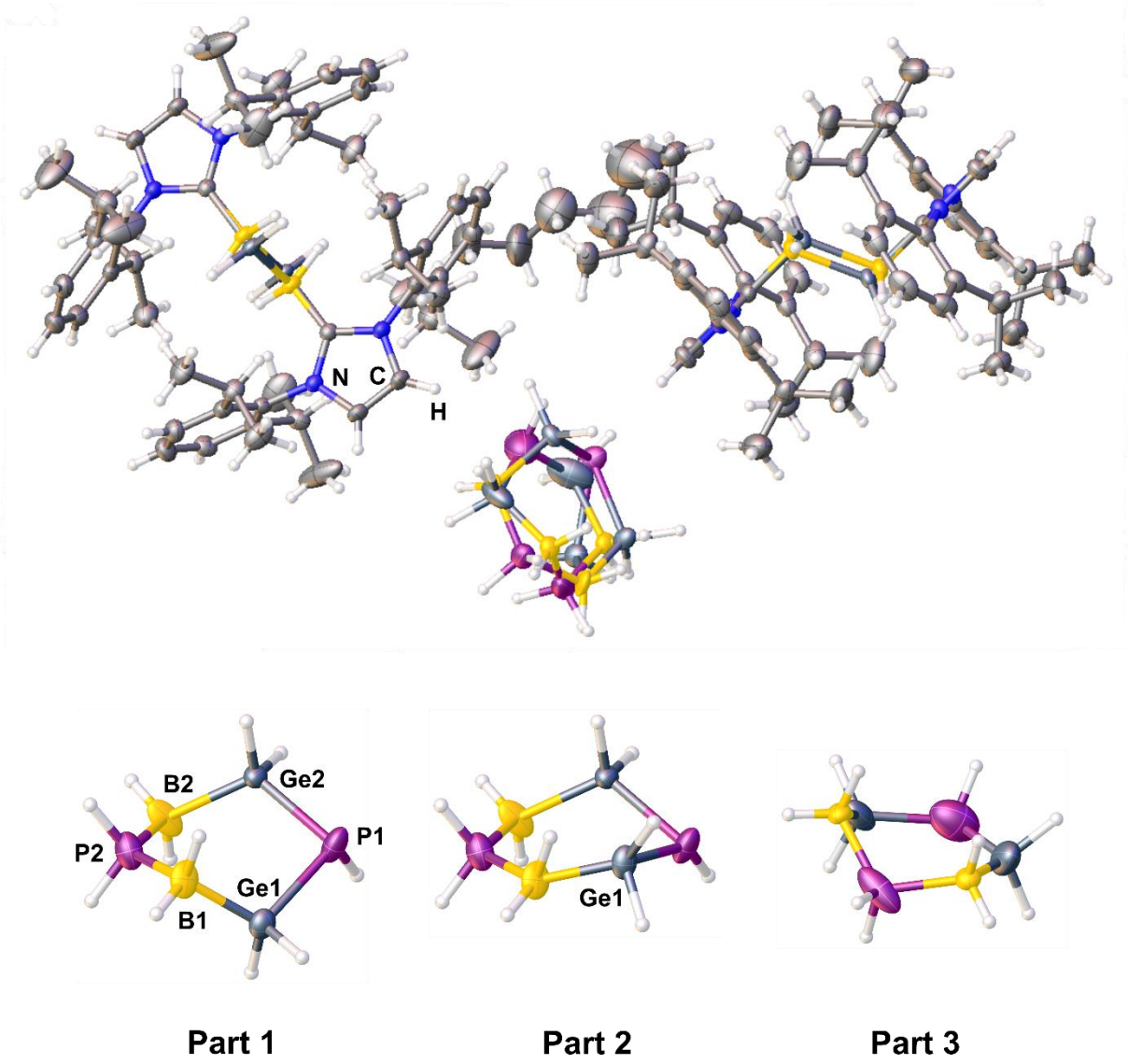

Figure S 9.44: Molecular structure of **4** in the solid state. Anisotropic displacement parameters are set to 50% probability level. Top: Combined disordered parts of grown structure; bottom left: part 1 of the anion (occupancy P1B1P2Ge2B2: 83%; occupancy Ge1: 41.5%) bottom middle: part 2 of the anion (occupancy P1B1P2Ge2B2: 83%; occupancy Ge1: 41.5%) bottom right: part 3 of the anion (occupancy: 17%). Selected bond lengths [Å] and angles [°] for part 1: P-Ge 2.3264(15)-2.4284(18), Ge-B 1.952(6)-2.047(9), B-P 1.911(9)-1.965(5), Ge-P-Ge 99.42(6), B-P-B 122.8(4), B-Ge-P 110.8(2)-116.4(4), P-B-Ge 108.2(3)-109.6(4).

The H_2BGeH_2 moiety of the cation [IDipp·BH_2GeH_2·IDipp]$^+$ is disordered over two positions (occupancies: 0.5:0.5). The presence of 0.5 C_5H_{12} per asymmetric unit is found in the measured crystal, which most likely originates from traces of *n*-pentane in *n*-hexane. The anion [PHGeH$_2$BH$_2$PH$_2$BH$_2$GeH$_2$]$^-$ is distorted and disordered over three positions (occupancies: 0.415:0.415:17). The EADP constraint and the DFIX, DANG, ISOR, SADI and SIMU restraints were applied to model these disorders.

9.5.5 Computational details

The geometries of the compounds have been fully optimized with gradient-corrected density functional theory (DFT) in form of Becke's three-parameter hybrid method B3LYP[8] with def2-TZVP all electron basis set. [9] The Gaussian 09 program package[10] was used throughout. All structures correspond to minima on their respective potential energy surfaces as verified by computation of second derivatives. Basis sets were obtained from the EMSL basis set exchange database.[11]

Relative energies of the isomers

The interaction of the $GeH_2BH_2^+$ monomer with IDipp is highly exothermic (by 430-470 kJ mol^{-1}). Two isomers are possible: coordination of IDipp to the Ge atom or to the B atom (Figure S 9.46, top). Quantum chemical computations predict that the isomer with the C-B bond is by 39 kJ mol^{-1} more stable than the isomer with the C-Ge bond, which can be explained by the smaller radii of B. In addition, the more stable isomer features one H atom bridging the B and Ge atoms, featuring an elongated B-H distance of 1.300 Å and H-Ge distance of 1.892 Å (Figure S 9.46, middle).

When the interaction of IDipp with the $GeH_2BH_2PH_2$ monomer is considered, three isomers are possible (Figure C1, bottom). The isomer IDipp·$BH_2GeH_2PH_2$ (**2b**) is the most stable, while the isomer IDipp·$BH_2PH_2GeH_2$ is by 53 kJ mol^{-1}, and the isomer IDipp·$GeH_2BH_2PH_2$ (**2a**) by 83 kJ mol^{-1} higher in energy. The formation of **2a** and **2b** from **1** and $NaPH_2$ are both exothermic and exergonic in the gas phase (Table S 9.2), which is in line with experimental observations in solution. However, computational results predict that **2b** is thermodynamically much more stable in the gas phase than **2a**. This excludes the real equilibrium between the isomers (**2a** should almost completely rearrange to **2b**), so the experimental evidence of the existence of **2a** can be attributed to the fact that the rearrangement process from **2a** to **2b** is kinetically hindered.

Interactions of **2a** and **2b** with BH_3·SMe_2 and the resulting formation of **3a** and **3b** are both exothermic and exergonic (Table S 9.2), which is also in line with experimental observations. Isomer **3b** is by 57 kJ mol^{-1} more stable than **3a**, which indicates that the addition of BH_3 stabilizes the C-Ge-B-P bonding pattern by 25 kJ mol^{-1} more than the C-B-Ge-P bonding pattern.

Formation of 4

In addition, computational studies reveal that the process for the formation of **4** from **2a** (Figure S 9.45, upper pathway) under release of PH_3 and free IDipp is exothermic by - 71 kJ mol^{-1}, but the analogous reaction starting from **2b** (Figure S 9.45, lower pathway) is highly endothermic (by + 177 kJ mol^{-1}). This would indicate that the formation of **4** according to this pathway most likely correlates with the presence of the less stable isomer **2a**.

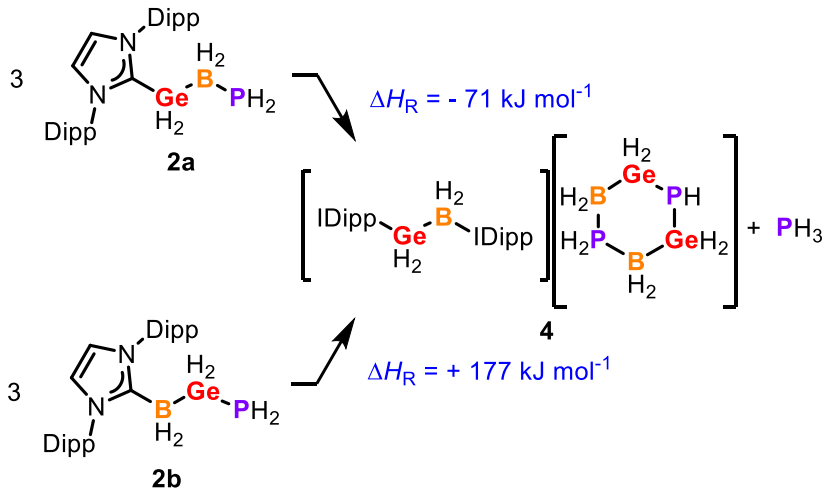

Figure S 9.45: Formation of **4** by decomposition of **2a** or **2b** under release of PH_3.

Table S 9.2: Reaction energies ΔE°_0, standard reaction enthalpies ΔH°_{298}, Gibbs energies ΔG°_{298} (kJ mol^{-1}) and standard reaction entropies ΔS°_{298} (J mol^{-1} K^{-1}) for the considered gas phase processes. B3LYP/def2-TZVP level of theory.

Process	ΔE°_0	ΔH°_{298}	ΔS°_{298}	ΔG°_{298}
IDipp·GeH_2BH_2OTf + $NaPH_2$ = **2a** + NaOTf	-119.6	-120.0	-1.4	-119.6
IDipp·GeH_2BH_2OTf + $NaPH_2$ = **2b** + NaOTf	-202.6	-201.4	-2.9	-200.5
IDipp·GeH_2BH_2OTf + THF = $[IDipp{\cdot}GeH_2BH_2(THF)]^+$ + $[OTf]^-$	277.2	281.0	-3.5	282.1
IDipp·GeH_2BH_2OTf + $[PH_2]^-$ = **2a** + $[OTf]^-$	-204.5	-203.5	8.4	-206.0
IDipp·GeH_2BH_2OTf + $[PH_2]^-$ = **2b** + $[OTf]^-$	-287.4	-284.9	6.9	-286.9
IDipp·GeH_2BH_2OTf + $[PH_2]^-$ = **TS**	69.9	67.4	-190.2	124.1
TS = **2b** + $[OTf]^-$	-357.3	-352.3	197.2	-411.1
$[IDipp{\cdot}GeH_2BH_2]^+$ = $[IDipp{\cdot}BH_2GeH_2]^+$	-39.0	-38.4	11.3	-41.7
IDipp·GeH_2BH_2OTf = IDipp·BH_2GeH_2OTf	-45.9	-47.8	-22.2	-41.1
$[IDipp{\cdot}GeH_2BH_2(THF)]^+$ = $[IDipp{\cdot}BH_2GeH_2(THF)]^+$	-28.8	-29.4	1.9	-30.0
IDipp·$GeH_2BH_2PH_2$ = IDipp·$BH_2GeH_2PH_2$ (**2a** = **2b**)	-82.9	-81.4	-1.5	-80.9
IDipp·$GeH_2BH_2PH_2BH_3$ = IDipp·$BH_2GeH_2PH_2BH_3$ (**3a** = **3b**)	-56.7	-56.2	7.3	-58.3
2a + $BH_3{\cdot}SMe_2$ = **3a** + SMe_2	-40.6	-39.0	-4.3	-37.7
2b + $BH_3{\cdot}SMe_2$ = **3b** + SMe_2	-14.4	-13.8	4.5	-15.1
$[IDippGeH_2BH_2IDipp]^+$ + $[PH(GeH_2)_2(BH_2)_2PH_2]^-$ = $[IDippGeH_2BH_2IDipp]^+\ldots[PH(GeH_2)_2(BH_2)_2PH_2]^-$	-188.7			
3 **2a** = $[IDippGeH_2BH_2IDipp]^+\ldots$ $[PH(GeH_2)_2(BH_2)_2PH_2]^-$ + IDipp + PH_3	-71.3			
3 **2b** = $[IDippGeH_2BH_2IDipp]^+\ldots$ $[PH(GeH_2)_2(BH_2)_2PH_2]^-$ + IDipp + PH_3	177.5			

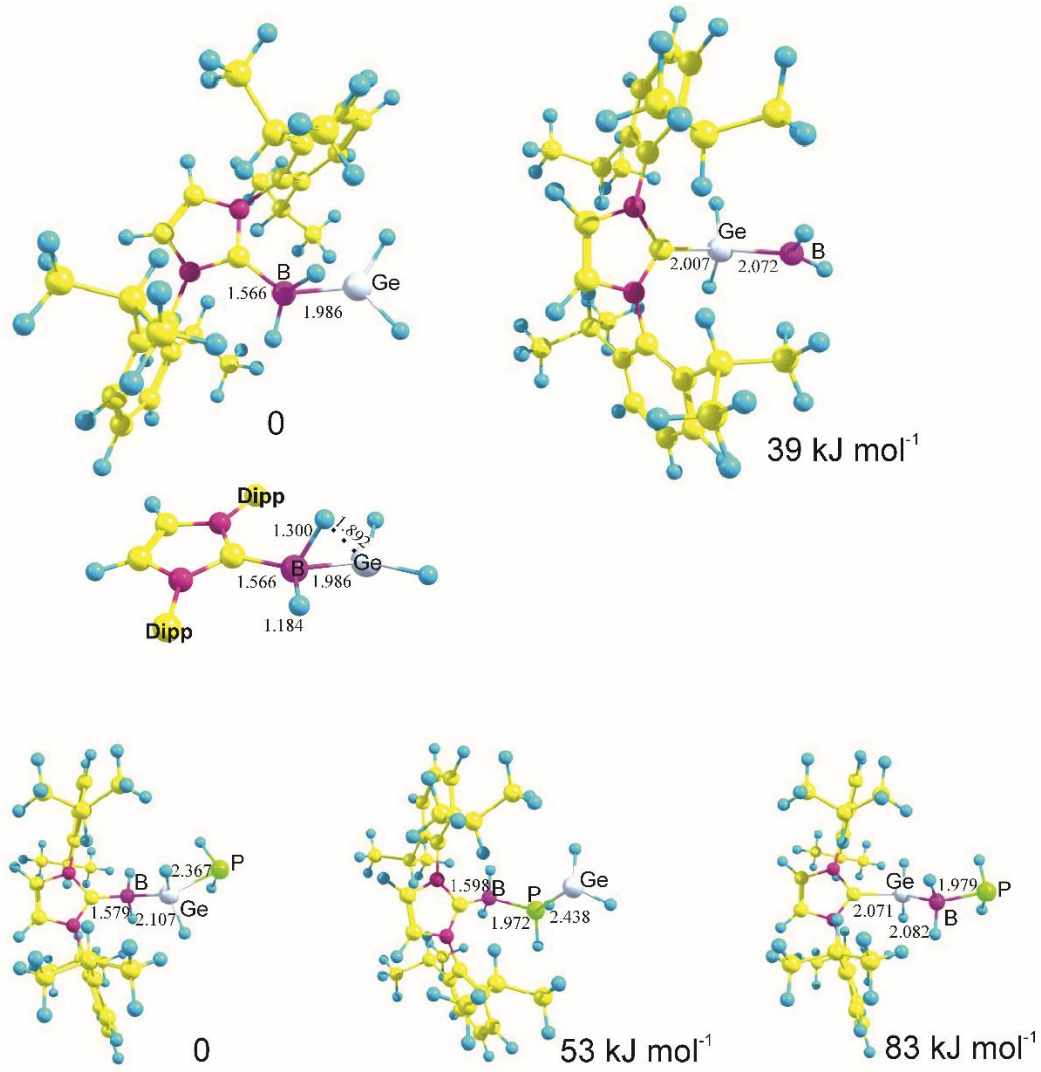

Figure S 9.46: Optimized geometries and relative energies of isomers of $[IDipp{\cdot}GeH_2BH_2]^+$ (top) and $IDipp{\cdot}GeH_2BH_2PH_2$ (bottom).

Formation of the cyclic anion

Optimized geometries of two possible isomers of the cyclic $[(GeH_2)_2(BH_2)_2PH_2PH]^-$ anion are shown in Figure S 9.47. The isomer with the PH group between the two GeH_2 moieties is the most stable. The alternative isomer with the PH group between the two BH_2 moieties shows much longer Ge-P, Ge-B and B-P bond distances and lies 145 kJ mol^{-1} higher in energy. These computational predictions agree well with the experimental observation, which only show the formation of the $[PH(GeH_2)_2(BH_2)_2PH_2]^-$ isomer in **4**.

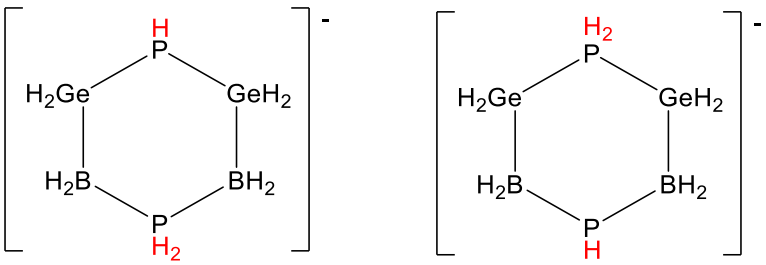

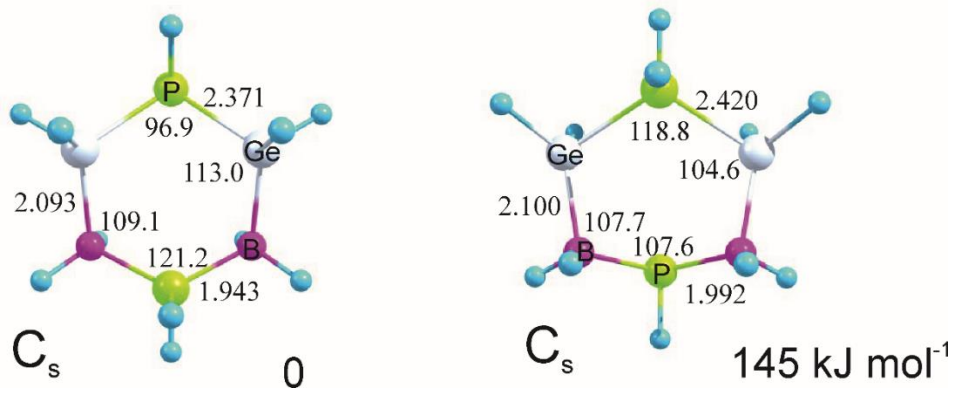

Figure S 9.47: Optimized geometries and relative energies of the isomers of the cyclic $[(GeH_2)_2(BH_2)_2PH_2PH]^-$ anion.

The interaction between the $[IDipp{\cdot}GeH_2BH_2GeH_2{\cdot}IDipp]^+$ cation and the $[PH(GeH_2)_2(BH_2)_2PH_2]^-$ anion with the formation of a contact ion pair in the gas phase is exothermic by 189 kJ mol^{-1}. The overall reaction, leading to this contact ion pair, can be written as follows:

$$3\ \mathbf{2a} = [IDipp{\cdot}GeH_2BH_2{\cdot}IDipp]^+\ldots[PH(GeH_2)_2(BH_2)_2PH_2]^- + IDipp + PH_3$$

$$3\ \mathbf{2b} = [IDipp{\cdot}GeH_2BH_2{\cdot}IDipp]^+\ldots[PH(GeH_2)_2(BH_2)_2PH_2]^- + IDipp + PH_3$$

Interestingly, only the first reaction (starting from **2a**) is exothermic by 71 kJ mol^{-1}, while the same reaction starting from **2b** is highly endothermic by 178 kJ mol^{-1} (Table S 9.2). This indicates that the formation of **4** most likely correlates with the presence of the less stable isomer **2a**, which is also in line with the experimentally found low yield of **4**.

Table S 9.3: Total energies E^{o}_{0}, sum of electronic and thermal enthalpies H^{o}_{298} (Hartree) and standard entropies S^{o}_{298} (cal mol^{-1}K^{-1}). B3LYP/def2-TZVP level of theory.

Compound	E^{o}_{0}	H^{o}_{298}	S^{o}_{298}
SMe_2	-478.0786627	-477.997492	67.801
THF	-232.5434651	-232.421132	70.441
$BH_3{\cdot}SMe_2$	-504.7394515	-504.624627	78.925
$NaPH_2$	-504.8907533	-504.870409	63.816
NaOTf	-1124.1483316	-1124.109655	94.941
$[PH_2]^-$	-342.5706559	-342.554141	49.472
$[OTf]^-$	-961.8605337	-961.825199	82.953
IDipp	-1160.453853	-1159.854780	201.948
IDippGeH_2BH_2OTf (**1**)	-4226.5937589	-4225.911610	264.687
IDippBH_2GeH_2OTf	-4226.6112229	-4225.929801	259.373
$[GeH_2BH_2]^+$	-2103.9594069	-2103.920182	63.834
$[IDipp{\cdot}GeH_2BH_2]^+$	-3264.5777383	-3263.934434	216.57
$[IDipp{\cdot}BH_2GeH_2]^+$	-3264.592577	-3263.949052	219.259
$[IDipp{\cdot}GeH_2BH_2(THF)]^+$	-3497.1711025	-3496.400507	251.338
$[IDipp{\cdot}BH_2GeH_2(THF)]^+$	-3497.1820563	-3496.411703	251.783
IDipp $GeH_2BH_2PH_2$ (**2a**)	-3607.381753	-3606.718073	233.217
IDipp BH_2 GeH_2PH_2 (**2b**)	-3607.413342	-3606.749058	232.863
$[IDipp{\cdot}BH_2PH_2GeH_2]^+$	-3607.393131	-3606.728393	226.700
$IDipp{\cdot}GeH_2BH_2PH_2BH_3$ (**3a**)	-3634.058010	-3633.360061	243.311
$IDipp{\cdot}BH_2GeH_2PH_2BH_3$ (**3b**)	-3634.079605	-3633.381450	245.058
TS $[PH_2GeH_2(\mu\text{-IDipp})BH_2OTf]^-$	-4569.137791	-4568.440070	268.696
$[PH(GeH_2)_2(BH_2)_2PH_2]^-$	-4893.327288	-4893.211810	104.130
$[PH_2(GeH_2)_2(BH_2)_2PH]^-$	-4893.271902	-4893.158409	107.479
$[IDipp{\cdot}GeH_2BH_2{\cdot}IDipp]^+$	-4425.142951	-4423.895035	365.483
$[IDippGeH_2BH_2IDipp]^+\ldots[PH(GeH_2)_2(BH_2)_2PH_2]^-$	-9318.542122		

Table S 9.4: Optimized geometries of theoretically studied compounds. *xyz* coordinates are given in Ångstroms (B3LYP/def2-TZVP level of theory).

SMe_2

6	0.000000000	1.386738000	-0.509955000
16	0.000000000	0.000000000	0.656752000
6	0.000000000	-1.386738000	-0.509955000
1	-0.891591000	1.375383000	-1.138358000
1	0.891591000	1.375383000	-1.138358000
1	0.000000000	2.301130000	0.082432000
1	-0.891591000	-1.375383000	-1.138358000
1	0.000000000	-2.301130000	0.082432000
1	0.891591000	-1.375383000	-1.138358000

THF

8	0.000000000	0.000000000	1.248613000
6	0.000000000	1.174023000	0.428631000
6	-0.303342000	0.703687000	-0.993447000
6	0.303342000	-0.703687000	-0.993447000
6	0.000000000	-1.174023000	0.428631000
1	0.984587000	1.653957000	0.485246000
1	-0.743080000	1.872623000	0.818962000
1	-1.382475000	0.651360000	-1.156313000
1	0.122081000	1.359338000	-1.753452000
1	1.382475000	-0.651360000	-1.156313000
1	-0.122081000	-1.359338000	-1.753452000
1	0.743080000	-1.872623000	0.818962000
1	-0.984587000	-1.653957000	0.485246000

BH_3SMe_2

16	-0.525363000	0.018393000	0.000000000
6	0.277188000	-0.813774000	-1.388537000
1	1.356095000	-0.682688000	1.319783000
1	0.008956000	-1.868987000	1.395727000
1	-0.089833000	-0.335261000	2.294290000
1	1.356095000	-0.682688000	-1.319783000
1	-0.089833000	-0.335261000	-2.294290000
1	0.008956000	-1.868987000	-1.395727000
5	0.277188000	1.807039000	0.000000000
1	-0.162919000	2.296195000	1.009836000
1	1.469020000	1.617276000	0.000000000
1	-0.162919000	2.296195000	-1.009836000

$NaPH_2$

11	0.070711000	1.606231000	0.000000000
15	0.070711000	-1.039854000	0.000000000
1	-0.919237000	-1.035364000	1.028458000
1	-0.919237000	-1.035364000	-1.028458000

NaOTf

16	-0.342153000	0.669492000	0.000042000
8	0.113922000	2.025783000	-0.000004000
9	0.858080000	-1.686790000	-0.000397000
9	1.936250000	-0.143911000	1.084421000
9	1.936110000	-0.142978000	-1.084072000
8	-1.058518000	0.202404000	-1.201995000
8	-1.058897000	0.202745000	1.201970000
6	1.196885000	-0.379023000	-0.000033000
11	-2.568444000	-0.920190000	0.000017000

$[OTf]^-$

16	0.000000000	0.000000000	0.933210000
8	0.000000000	1.419124000	1.243406000
9	0.000000000	-1.252108000	-1.449323000
9	1.084357000	0.626054000	-1.449323000
9	-1.084357000	0.626054000	-1.449323000
8	-1.228998000	-0.709562000	1.243406000
8	1.228998000	-0.709562000	1.243406000
6	0.000000000	0.000000000	-0.940232000

IDipp

6	0.674960000	-0.000061000	1.853488000
6	-0.674915000	0.000151000	1.853504000
7	-1.062430000	0.000181000	0.517812000
6	-0.000003000	-0.000008000	-0.342280000
7	1.062444000	-0.000158000	0.517787000
1	1.379343000	-0.000152000	2.666568000
1	-1.379279000	0.000280000	2.666601000
6	2.435809000	-0.000373000	0.090009000
6	3.085267000	1.227701000	-0.111259000
6	3.084594000	-1.228644000	-0.112192000
6	4.416080000	1.199376000	-0.527433000
6	4.415415000	-1.200728000	-0.528378000
6	5.077373000	-0.000779000	-0.734658000
1	4.940696000	2.131057000	-0.697180000
1	4.939506000	-2.132569000	-0.698867000
6	-2.435805000	0.000376000	0.090067000
6	-3.084599000	1.228638000	-0.112164000
6	-4.415430000	1.200704000	-0.528315000
6	-5.077391000	0.000746000	-0.734534000
1	-4.939527000	2.132537000	-0.698825000
6	-4.416091000	-1.199400000	-0.527282000
1	-4.940708000	-2.131088000	-0.696980000
6	-3.085267000	-1.227707000	-0.111139000
6	-2.379919000	2.563741000	0.074073000
1	-1.393576000	2.364550000	0.491176000
6	-3.116585000	3.476910000	1.064890000
6	-2.165994000	3.265466000	-1.276204000
1	-1.598665000	2.631072000	-1.957893000
1	-3.118903000	3.508866000	-1.751899000
1	-1.614358000	4.198245000	-1.137505000
1	-4.107294000	3.755953000	0.700388000
1	-2.551805000	4.398959000	1.219408000
1	-3.243448000	2.991921000	2.034677000
6	-2.381271000	-2.563037000	0.076099000
1	-1.394748000	-2.364031000	0.492864000
6	-3.118247000	-3.474983000	1.067808000
6	-2.167978000	-3.266026000	-1.273622000
1	-3.121111000	-3.509351000	-1.748906000
1	-1.600472000	-2.632523000	-1.955991000
1	-1.616794000	-4.198969000	-1.134232000
1	-3.244707000	-2.989116000	2.037209000
1	-2.553925000	-4.397197000	1.223016000
1	-4.109161000	-3.753816000	0.703698000
6	2.381278000	2.563038000	0.075947000
1	1.394759000	2.364048000	0.492731000
6	3.118270000	3.475011000	1.067620000
6	2.167970000	3.265989000	-1.273791000
1	3.121097000	3.509298000	-1.749094000
1	1.600454000	2.632467000	-1.956135000
1	1.616789000	4.198937000	-1.134421000
1	3.244740000	2.989172000	2.037034000
1	2.553955000	4.397232000	1.222809000
1	4.109181000	3.753828000	0.703489000
6	2.379915000	-2.563739000	0.074108000
1	1.393589000	-2.364532000	0.491243000
6	2.165939000	-3.265500000	-1.276141000
6	3.116612000	-3.476885000	1.064923000
1	4.107306000	-3.755945000	0.700393000
1	3.243515000	-2.991870000	2.034692000
1	2.551832000	-4.398925000	1.219489000
1	1.598586000	-2.631124000	-1.957827000
1	1.614307000	-4.198275000	-1.137397000
1	3.118831000	-3.508913000	-1.751864000
1	-6.110357000	0.000889000	-1.060192000
1	6.110332000	-0.000936000	-1.060341000

IDippGeH$_2$BH$_2$OTf (**1**)

32	0.383125000	-0.303497000	-0.865870000
1	0.613011000	1.026251000	-1.620510000
1	-0.304536000	-1.241328000	-1.887035000
16	4.031879000	-0.234705000	-0.964603000
9	6.110626000	-1.674070000	-1.680756000
9	4.577327000	-2.823802000	-0.665242000
9	5.867243000	-1.500174000	0.469515000
8	3.167892000	-0.293934000	0.294043000
8	4.849261000	0.938134000	-0.928470000
8	3.288082000	-0.571877000	-2.146871000
7	-2.321823000	-0.524380000	0.571202000
7	-1.544502000	1.481590000	0.708059000
6	-1.288736000	0.260183000	0.181309000
6	-3.221390000	0.205275000	1.328073000
1	-4.115698000	-0.235578000	1.727948000
6	-2.733828000	1.461555000	1.414116000
1	-3.117905000	2.337620000	1.903134000
6	5.216426000	-1.651895000	-0.687456000
6	-2.524274000	-1.918769000	0.231315000
6	-3.212013000	-2.221803000	-0.954954000
6	-3.431952000	-3.568592000	-1.238542000
1	-3.954198000	-3.842298000	-2.145540000
6	-2.991140000	-4.563285000	-0.380938000
1	-3.169191000	-5.603300000	-0.623927000
6	-2.321607000	-4.232221000	0.785587000
1	-1.983110000	-5.019984000	1.444258000
6	-2.071712000	-2.902695000	1.125100000
6	-3.744975000	-1.156504000	-1.902715000
1	-3.326671000	-0.195172000	-1.603803000
6	-5.275288000	-1.043886000	-1.795331000
1	-5.644931000	-0.247512000	-2.444717000
1	-5.759382000	-1.974607000	-2.098228000
1	-5.592716000	-0.822050000	-0.774694000
6	-3.315490000	-1.395402000	-3.357349000
1	-3.643549000	-0.563547000	-3.983864000
1	-2.231932000	-1.477701000	-3.441980000
1	-3.758337000	-2.305389000	-3.766078000
6	-1.379377000	-2.572262000	2.440158000
1	-1.021188000	-1.543692000	2.385794000

6	-2.373096000	-2.660027000	3.612366000
1	-1.881508000	-2.382672000	4.547028000
1	-3.229531000	-1.997688000	3.473572000
1	-2.755110000	-3.677300000	3.722620000
6	-0.152432000	-3.453877000	2.708016000
1	0.363434000	-3.101750000	3.602906000
1	-0.430697000	-4.495167000	2.881692000
1	0.555468000	-3.415357000	1.881409000
6	-0.749982000	2.682457000	0.535171000
6	-1.037553000	3.515719000	-0.557523000
6	-0.288875000	4.684589000	-0.682901000
1	-0.476869000	5.349605000	-1.515363000
6	0.697284000	5.005939000	0.235185000
1	1.273009000	5.914701000	0.113307000
6	0.954234000	4.165229000	1.305647000
1	1.731003000	4.427207000	2.010346000
6	0.237130000	2.982981000	1.487289000
6	-2.126718000	3.209162000	-1.575784000
1	-2.498839000	2.202277000	-1.384644000
6	-3.315523000	4.172074000	-1.419190000
1	-3.732619000	4.136325000	-0.410933000
1	-3.015480000	5.203081000	-1.616987000
1	-4.109671000	3.914311000	-2.123129000
6	-1.596782000	3.222433000	-3.017212000
1	-2.385708000	2.918213000	-3.708231000
1	-1.266669000	4.218796000	-3.316280000
1	-0.756341000	2.538711000	-3.136757000
6	0.511312000	2.106691000	2.701460000
1	0.104801000	1.114688000	2.501813000
6	-0.204736000	2.664548000	3.944685000
1	-0.034674000	2.012450000	4.803879000
1	0.172886000	3.657868000	4.197022000
1	-1.282789000	2.747898000	3.794180000
6	2.008877000	1.921945000	2.980599000
1	2.144218000	1.189649000	3.778328000
1	2.541909000	1.559005000	2.102981000
1	2.477414000	2.851229000	3.310570000
5	1.854989000	-1.080134000	0.459153000
1	1.490964000	-0.882769000	1.587096000
1	1.985659000	-2.241179000	0.185343000

IDipp·BH_2GeH_2OTf

7	2.398023000	0.061761000	0.132307000
6	3.389653000	-0.892261000	-0.019785000
6	2.773252000	-2.085113000	-0.145438000
7	1.411376000	-1.847159000	-0.065601000
6	2.675365000	1.472473000	0.288970000
1	4.431769000	-0.632393000	-0.020982000
1	3.168921000	-3.075297000	-0.275598000
6	0.433783000	-2.912863000	-0.113794000
6	-1.333537000	-5.028150000	-0.207409000
6	-0.014693000	-3.359496000	-1.366096000
6	0.017696000	-3.495759000	1.093015000
6	-0.876189000	-4.562484000	1.014517000
6	-0.905869000	-4.431939000	-1.382395000
6	0.448403000	-2.745166000	-2.679219000
6	0.504393000	-3.024559000	2.455123000
1	-1.220426000	-5.034087000	1.925555000
1	-1.273289000	-4.802596000	-2.329902000
1	-2.028855000	-5.857334000	-0.244196000
6	3.277465000	4.147837000	0.584777000
6	2.718262000	2.013386000	1.584242000
6	2.943354000	2.234457000	-0.861071000
6	3.243374000	3.584268000	-0.679847000
6	3.020999000	3.368998000	1.701247000
6	2.504850000	1.177122000	2.837304000
6	2.970410000	1.639427000	-2.263596000
1	3.450946000	4.204118000	-1.541535000
1	3.056350000	3.822414000	2.682673000
1	3.506045000	5.199745000	0.701071000
1	1.121375000	-2.138245000	2.308335000
6	1.387114000	-4.087893000	3.128929000
6	-0.659343000	-2.610977000	3.368263000
1	-1.275301000	-1.845290000	2.897304000
1	-0.273285000	-2.208324000	4.307027000
1	-1.299490000	-3.460657000	3.614070000
1	2.243119000	-4.353975000	2.505546000
1	0.824375000	-5.002338000	3.327190000
1	1.766399000	-3.716809000	4.083413000
1	0.963225000	-1.810620000	-2.452906000
6	-0.722726000	-2.397286000	-3.609146000
6	1.454090000	-3.663469000	-3.394562000
1	2.321872000	-3.879201000	-2.768535000
1	1.809883000	-3.195459000	-4.314915000
1	0.991732000	-4.616454000	-3.660573000
1	-1.452335000	-1.758245000	-3.112358000
1	-1.240218000	-3.291845000	-3.960408000
1	-0.354418000	-1.866775000	-4.489318000
6	4.418757000	1.406405000	-2.729364000
6	2.216359000	2.492568000	-3.293781000
1	2.477946000	0.666084000	-2.229764000
6	3.849891000	0.873337000	3.519748000
1	2.066303000	0.225865000	2.537924000
6	1.524721000	1.825429000	3.824381000
1	4.968172000	0.758273000	-2.045208000
1	4.960306000	2.352324000	-2.795561000
1	4.431337000	0.941526000	-3.717413000
1	2.720023000	3.443125000	-3.477357000
1	1.197777000	2.711565000	-2.974413000
1	2.165422000	1.963385000	-4.247136000
1	4.336368000	1.792433000	3.853300000
1	4.537585000	0.359092000	2.845453000
1	3.696990000	0.238184000	4.394897000
1	1.927146000	2.745224000	4.253054000
1	1.326606000	1.141472000	4.651948000
1	0.575152000	2.058427000	3.343279000
6	1.167964000	-0.521390000	0.115036000
5	-0.240872000	0.153432000	0.378250000
32	-0.974092000	1.297691000	-1.197653000
1	-0.166348000	0.915222000	1.305615000
1	-1.073745000	-0.695725000	0.537020000
8	-2.889269000	1.260193000	-1.070861000
1	-0.915436000	0.770524000	-2.657016000
1	-0.718320000	2.819073000	-1.290864000
16	-3.799180000	2.171841000	-0.248337000
8	-4.825557000	2.741211000	-1.065353000
8	-3.051986000	2.994508000	0.659743000
6	-4.659765000	0.894102000	0.802447000
9	-5.547217000	1.503586000	1.593230000
9	-3.784638000	0.238744000	1.570990000
9	-5.304698000	0.006038000	0.041133000

$[GeH_2BH_2]^+$

32	0.000000000	0.000000000	-0.336436000
5	0.000000000	0.000000000	1.718666000
1	1.050042000	0.000000000	2.267014000
1	-1.050042000	0.000000000	2.267014000
1	0.000000000	1.279896000	-1.180707000
1	0.000000000	-1.279896000	-1.180707000

$[IDipp·GeH_2BH_2]^+$

32	0.071736000	-0.255934000	1.999686000
1	-1.205786000	0.428526000	2.508021000

1	1.292286000	0.570704000	2.418157000
7	1.067930000	0.070273000	-0.811775000
7	-1.094045000	0.118761000	-0.773088000
6	-0.000827000	0.004899000	0.011078000
6	0.644618000	0.225771000	-2.115765000
1	1.339534000	0.301103000	-2.932249000
6	-0.708342000	0.259459000	-2.090525000
1	-1.426565000	0.375235000	-2.881336000
6	2.465012000	0.033420000	-0.417363000
6	3.143819000	1.254738000	-0.272040000
6	4.492867000	1.190614000	0.074012000
1	5.053203000	2.107816000	0.195394000
6	5.130856000	-0.024448000	0.265439000
1	6.179316000	-0.046839000	0.533005000
6	4.432155000	-1.210822000	0.112124000
1	4.946398000	-2.151269000	0.259263000
6	3.082163000	-1.214130000	-0.237292000
6	2.486528000	2.611530000	-0.483683000
1	1.419593000	2.455675000	-0.651158000
6	3.045557000	3.310188000	-1.734424000
1	2.530975000	4.258086000	-1.900233000
1	4.109908000	3.524425000	-1.624628000
1	2.922728000	2.697909000	-2.629620000
6	2.618279000	3.513955000	0.753072000
1	2.075887000	4.447353000	0.593710000
1	2.214096000	3.034750000	1.645937000
1	3.658794000	3.771758000	0.954966000
6	2.355102000	-2.540725000	-0.403185000
1	1.322497000	-2.338479000	-0.691213000
6	2.971702000	-3.397258000	-1.521068000
1	2.399443000	-4.316982000	-1.653191000
1	2.976497000	-2.861904000	-2.471508000
1	4.000790000	-3.676637000	-1.291391000
6	2.317210000	-3.322495000	0.916440000
1	1.720686000	-4.229010000	0.822994000
1	3.315137000	-3.603691000	1.256435000
1	1.897890000	-2.709385000	1.733637000
6	-2.479603000	0.150268000	-0.332687000
6	-3.026627000	1.388977000	0.040296000
6	-4.364723000	1.395446000	0.432521000
1	-4.826589000	2.327278000	0.729144000
6	-5.116445000	0.231955000	0.441948000
1	-6.153774000	0.263208000	0.749383000
6	-4.549471000	-0.970749000	0.051234000
1	-5.155147000	-1.866221000	0.054525000
6	-3.216436000	-1.045831000	-0.351063000
6	-2.251643000	2.698724000	-0.011950000
1	-1.197984000	2.470141000	-0.181343000
6	-2.724129000	3.562868000	-1.194178000
1	-2.627680000	3.035624000	-2.144966000
1	-3.771427000	3.846920000	-1.078308000
1	-2.134294000	4.479199000	-1.254139000
6	-2.332711000	3.485750000	1.304390000
1	-1.696825000	4.370807000	1.249134000
1	-3.347746000	3.828428000	1.509070000
1	-2.005181000	2.885952000	2.154575000
6	-2.642514000	-2.370003000	-0.837303000
1	-1.552810000	-2.297251000	-0.817315000
6	-3.060538000	-2.642160000	-2.293888000
1	-2.616319000	-3.573553000	-2.649434000
1	-4.145007000	-2.735701000	-2.373838000
1	-2.748162000	-1.842271000	-2.966891000
6	-3.031558000	-3.556169000	0.056145000
1	-2.490470000	-4.450156000	-0.257903000
1	-2.798094000	-3.369527000	1.104599000
1	-4.095598000	-3.784791000	-0.014356000
5	0.079795000	-2.258378000	2.531499000
1	-0.507012000	-3.053578000	1.880294000
1	0.533260000	-2.557751000	3.585678000

$[IDipp{\cdot}BH_2GeH_2]^+$

5	-0.142838000	0.064714000	1.512712000
7	-1.322037000	0.057794000	-0.784372000
7	0.833946000	0.144404000	-0.948251000
6	-2.682198000	-0.002285000	-0.276730000
6	-0.181171000	0.078484000	-0.052774000
6	-3.355724000	1.204511000	-0.035074000
6	-3.268304000	-1.263600000	-0.093661000
6	2.249534000	0.156375000	-0.638703000
6	0.329844000	0.168012000	-2.228806000
1	0.970353000	0.219413000	-3.090183000
6	-5.279922000	-0.115542000	0.615837000
1	-6.302530000	-0.160063000	0.967710000
6	-4.671012000	1.113469000	0.418520000
1	-5.227551000	2.019295000	0.618528000
6	-1.020345000	0.111019000	-2.125348000
1	-1.786378000	0.104024000	-2.879175000
6	-4.586145000	-1.287673000	0.361218000
1	-5.077310000	-2.239029000	0.516232000
6	2.941171000	-1.067091000	-0.651813000
6	4.305563000	-1.024834000	-0.366785000
1	4.878270000	-1.942473000	-0.369426000
6	-2.728151000	2.573774000	-0.254089000
1	-1.688856000	2.432363000	-0.555935000
6	2.870493000	1.390764000	-0.383202000
6	-2.546003000	-2.573156000	-0.376776000
1	-1.521100000	-2.344019000	-0.673822000
6	2.282563000	-2.395993000	-0.999087000
1	1.203187000	-2.243847000	-1.045741000
6	4.236245000	1.364343000	-0.101503000
1	4.755866000	2.291379000	0.098691000
6	4.944938000	0.173126000	-0.089034000
1	6.005407000	0.179966000	0.127765000
6	-3.428249000	3.333904000	-1.392451000
1	-3.412041000	2.767002000	-2.325022000
1	-2.933788000	4.290686000	-1.569356000
1	-4.471716000	3.539954000	-1.148803000
6	-2.711932000	3.407487000	1.036633000
1	-3.722323000	3.640370000	1.375816000
1	-2.197243000	4.354772000	0.866115000
1	-2.202236000	2.882809000	1.846166000
6	2.137617000	2.722886000	-0.467222000
1	1.064717000	2.523956000	-0.481206000
6	2.484519000	3.445250000	-1.781419000
1	3.547499000	3.688920000	-1.824782000
1	1.923246000	4.377728000	-1.861186000
1	2.248891000	2.833713000	-2.654058000
6	2.535509000	-3.477147000	0.061704000
1	3.592692000	-3.733867000	0.138649000
1	1.996050000	-4.389169000	-0.198065000
1	2.195651000	-3.160928000	1.050142000
32	1.324858000	-0.529339000	2.711744000
6	-3.196423000	-3.328985000	-1.546909000
1	-4.221311000	-3.619556000	-1.310760000
1	-2.636417000	-4.239264000	-1.768475000
1	-3.225550000	-2.720446000	-2.452510000
6	-2.463536000	-3.460810000	0.874773000
1	-1.988175000	-2.937209000	1.705682000
1	-1.883944000	-4.360662000	0.660797000
1	-3.453013000	-3.779531000	1.205679000
6	2.736023000	-2.882856000	-2.386376000
1	2.525086000	-2.145168000	-3.162394000

1	2.221184000	-3.807926000	-2.650975000
1	3.809100000	-3.080937000	-2.402363000
6	2.409868000	3.633374000	0.738484000
1	2.179544000	3.137344000	1.682725000
1	1.793658000	4.531199000	0.672452000
1	3.450420000	3.957964000	0.776929000
1	2.836590000	-0.390600000	2.462195000
1	1.051307000	-0.341354000	4.215414000
1	0.557131000	1.046309000	1.999386000
1	-1.187643000	0.035924000	2.069728000

[IDipp·GeH_2BH_2(THF)]$^+$

7	-0.600526000	-1.641637000	0.639093000
6	0.090869000	-2.578503000	1.380779000
6	1.392143000	-2.212422000	1.366980000
7	1.478948000	-1.057728000	0.614570000
6	-2.036065000	-1.694690000	0.424772000
1	-0.404453000	-3.411225000	1.844620000
1	2.258719000	-2.662924000	1.815143000
6	2.734228000	-0.376293000	0.357490000
6	5.148012000	0.863192000	-0.096860000
6	3.162183000	0.603608000	1.266729000
6	3.485247000	-0.767551000	-0.762059000
6	4.701649000	-0.118139000	-0.967142000
6	4.388317000	1.215489000	1.007062000
6	2.381606000	0.976279000	2.519787000
6	3.049950000	-1.869234000	-1.718398000
1	5.311524000	-0.387771000	-1.818960000
1	4.757593000	1.974979000	1.682745000
1	6.097288000	1.351614000	-0.276152000
6	-4.757113000	-1.852614000	0.054794000
6	-2.516811000	-2.340836000	-0.726727000
6	-2.876641000	-1.152222000	1.411516000
6	-4.250449000	-1.243465000	1.191129000
6	-3.900424000	-2.398520000	-0.887746000
6	-1.605712000	-3.022723000	-1.738728000
6	-2.355047000	-0.550166000	2.710124000
1	-4.933919000	-0.836717000	1.923458000
1	-4.314012000	-2.885219000	-1.760132000
1	-5.827937000	-1.911553000	-0.092827000
1	2.027038000	-2.156394000	-1.470013000
6	3.927595000	-3.120769000	-1.547424000
6	3.040399000	-1.402694000	-3.181772000
1	2.415767000	-0.518637000	-3.315332000
1	2.650465000	-2.194851000	-3.823368000
1	4.043819000	-1.161720000	-3.535803000
1	3.903008000	-3.494213000	-0.522105000
1	4.968641000	-2.908140000	-1.796718000
1	3.582570000	-3.919556000	-2.206419000
1	1.378185000	0.555056000	2.438144000
6	2.214963000	2.493674000	2.683011000
6	3.036051000	0.365014000	3.770964000
1	3.118274000	-0.720576000	3.695785000
1	2.447898000	0.597966000	4.660521000
1	4.041419000	0.763093000	3.920122000
1	1.760419000	2.941999000	1.799051000
1	3.169893000	2.989253000	2.862914000
1	1.571970000	2.706674000	3.538704000
6	-2.472363000	-1.566476000	3.861105000
6	-3.052053000	0.763307000	3.090044000
1	-1.295654000	-0.321649000	2.579487000
6	-1.554150000	-4.539555000	-1.480666000
1	-0.595107000	-2.633844000	-1.604664000
6	-2.002683000	-2.739199000	-3.193874000
1	-1.949561000	-2.498709000	3.642288000
1	-3.518042000	-1.812857000	4.054921000
1	-2.050276000	-1.151718000	4.778330000
1	-4.100799000	0.606058000	3.346497000
1	-3.002901000	1.490998000	2.281143000
1	-2.568695000	1.195828000	3.967900000
1	-2.539508000	-4.990548000	-1.612037000
1	-1.217601000	-4.769147000	-0.468291000
1	-0.868701000	-5.021170000	-2.180515000
1	-2.960093000	-3.194760000	-3.450416000
1	-1.255505000	-3.158809000	-3.869506000
1	-2.073200000	-1.668823000	-3.389810000
6	0.253457000	-0.707648000	0.162325000
32	-0.206020000	0.853051000	-1.037563000
5	-1.254511000	2.379608000	-0.037792000
1	-0.914626000	0.111458000	-2.195204000
1	1.194331000	1.214905000	-1.578671000
8	-1.137175000	3.694574000	-0.912617000
1	-0.704307000	2.627436000	0.995977000
1	-2.421159000	2.116888000	0.063582000
6	-1.905007000	3.807400000	-2.158140000
6	-1.771089000	5.270008000	-2.523439000
6	-1.826159000	5.964372000	-1.154744000
6	-1.088686000	5.008325000	-0.226006000
1	-2.932913000	3.510425000	-1.943533000
1	-1.459710000	3.114538000	-2.868397000
1	-0.816203000	5.453440000	-3.018426000
1	-2.568087000	5.594099000	-3.190708000
1	-2.861042000	6.083924000	-0.832434000
1	-1.361941000	6.949006000	-1.165709000
1	-1.554109000	4.883438000	0.747695000
1	-0.032425000	5.240043000	-0.105932000

[IDipp·BH_2GeH_2 (THF)]$^+$

7	-0.287395000	-1.818608000	0.031608000
6	0.516559000	-2.924632000	0.245705000
6	1.789951000	-2.480256000	0.296968000
7	1.748822000	-1.110533000	0.109914000
6	-1.730871000	-1.876745000	-0.043159000
1	0.110267000	-3.914372000	0.340443000
1	2.715778000	-3.004164000	0.448193000
6	2.938819000	-0.283669000	0.102679000
6	5.255408000	1.205671000	0.108731000
6	3.401818000	0.229194000	1.323922000
6	3.604783000	-0.078333000	-1.114643000
6	4.774147000	0.680709000	-1.079845000
6	4.575830000	0.981080000	1.295363000
6	2.694307000	-0.009156000	2.650357000
6	3.123787000	-0.660658000	-2.435735000
1	5.318893000	0.859555000	-1.997336000
1	4.966918000	1.392827000	2.216512000
1	6.167196000	1.789264000	0.111023000
6	-4.480255000	-2.026405000	-0.174579000
6	-2.339752000	-1.944345000	-1.307843000
6	-2.461268000	-1.917630000	1.160965000
6	-3.851339000	-1.986209000	1.059468000
6	-3.732060000	-2.012717000	-1.340896000
6	-1.546930000	-2.015410000	-2.605340000
6	-1.799162000	-1.971956000	2.533224000
1	-4.449327000	-2.021474000	1.959746000
1	-4.238640000	-2.066768000	-2.295015000
1	-5.560063000	-2.082690000	-0.227318000
1	2.149551000	-1.122070000	-2.270474000
6	4.073809000	-1.762684000	-2.933081000
6	2.929169000	0.423393000	-3.506041000
1	2.242160000	1.197793000	-3.162882000
1	2.518319000	-0.017730000	-4.416077000
1	3.873462000	0.901245000	-3.772221000

1	4.187509000	-2.559073000	-2.195360000
1	5.067344000	-1.362790000	-3.143976000
1	3.691366000	-2.207434000	-3.853745000
1	1.778209000	-0.567710000	2.453873000
6	2.281983000	1.309751000	3.321662000
6	3.551537000	-0.863816000	3.597801000
1	3.818295000	-1.820147000	3.144704000
1	3.007905000	-1.067689000	4.522295000
1	4.478752000	-0.353441000	3.863832000
1	1.655107000	1.910937000	2.661349000
1	3.151825000	1.909352000	3.594621000
1	1.720787000	1.109207000	4.236343000
6	-1.785720000	-3.416679000	3.065986000
6	-2.451812000	-1.040054000	3.564079000
1	-0.761316000	-1.651783000	2.424021000
6	-1.545875000	-3.453108000	-3.154101000
1	-0.512922000	-1.748867000	-2.387505000
6	-2.050371000	-1.027134000	-3.666130000
1	-1.283963000	-4.101741000	2.381853000
1	-2.803083000	-3.783803000	3.213360000
1	-1.269462000	-3.462202000	4.026469000
1	-3.466914000	-1.353348000	3.811771000
1	-2.495308000	-0.008156000	3.214249000
1	-1.875876000	-1.055570000	4.490762000
1	-2.556873000	-3.778270000	-3.406653000
1	-1.140807000	-4.161160000	-2.429012000
1	-0.938741000	-3.512758000	-4.059206000
1	-3.060514000	-1.268341000	-4.000843000
1	-1.401735000	-1.062136000	-4.542946000
1	-2.051734000	-0.003733000	-3.289266000
6	0.470433000	-0.696955000	-0.063688000
5	0.032872000	0.784147000	-0.451534000
32	-1.735528000	1.490021000	0.364540000
1	-0.171107000	0.848013000	-1.641219000
1	0.872205000	1.571727000	-0.110050000
8	-1.748520000	3.383913000	-0.320885000
1	-1.923109000	1.878393000	1.855615000
1	-3.152471000	1.205620000	-0.177714000
6	-2.952731000	4.222304000	-0.215054000
6	-2.517544000	5.556476000	-0.788342000
6	-1.049150000	5.650010000	-0.352416000
6	-0.543462000	4.223089000	-0.495952000
1	-3.225949000	4.286008000	0.839660000
1	-3.739844000	3.719762000	-0.771730000
1	-2.600794000	5.549253000	-1.876198000
1	-3.124053000	6.375787000	-0.405671000
1	-0.979314000	5.978676000	0.685612000
1	-0.471179000	6.340600000	-0.964347000
1	0.183031000	3.927447000	0.256133000
1	-0.153314000	4.000447000	-1.487255000

IDipp·$GeH_2BH_2PH_2$ (**2a**)

32	0.018582000	-0.490103000	1.740820000
15	0.400903000	-2.929004000	3.912501000
7	-1.141530000	0.425808000	-0.975698000
7	1.010385000	0.518516000	-0.998468000
6	2.410406000	0.443647000	-0.632147000
6	-0.046878000	0.232516000	-0.198832000
6	3.128599000	-0.714414000	-0.972998000
6	-3.202927000	1.382280000	-0.062680000
6	5.089704000	0.327932000	-0.006752000
1	6.141181000	0.278609000	0.247105000
6	3.000269000	1.551108000	-0.001653000
6	-4.548772000	1.218503000	0.260773000
1	-5.102785000	2.053801000	0.668672000
6	-5.188348000	0.003585000	0.074422000
1	-6.233786000	-0.102120000	0.335830000
6	-4.492744000	-1.077621000	-0.441465000
1	-5.003731000	-2.021169000	-0.578257000
6	4.482387000	-0.743021000	-0.641122000
1	5.067489000	-1.621131000	-0.877094000
6	-2.421104000	-2.176615000	-1.373360000
1	-1.354631000	-1.951957000	-1.402023000
6	4.356975000	1.461583000	0.305531000
1	4.847082000	2.291143000	0.796787000
6	-3.144687000	-0.974431000	-0.783763000
6	-2.537418000	2.733986000	0.151756000
1	-1.479697000	2.635224000	-0.092783000
6	-2.525907000	0.268570000	-0.582487000
6	-0.770320000	0.839472000	-2.243497000
1	-1.495986000	1.050207000	-3.007407000
6	0.578112000	0.900576000	-2.255899000
1	1.265720000	1.175743000	-3.033906000
6	-2.617468000	3.184506000	1.618241000
1	-3.649616000	3.358271000	1.928530000
1	-2.070946000	4.120217000	1.753640000
1	-2.185731000	2.437531000	2.284569000
6	-2.876319000	-2.434483000	-2.819922000
1	-3.938642000	-2.684957000	-2.858716000
1	-2.319620000	-3.270013000	-3.249160000
1	-2.718076000	-1.561048000	-3.455779000
6	2.237975000	2.834800000	0.296231000
1	1.171761000	2.614697000	0.241372000
6	2.506232000	-1.885732000	-1.721277000
1	1.421954000	-1.800347000	-1.639211000
6	-2.585079000	-3.437856000	-0.513737000
1	-2.245598000	-3.270078000	0.507736000
1	-1.988316000	-4.250762000	-0.931122000
1	-3.623219000	-3.774279000	-0.482980000
5	0.754879000	-2.415521000	2.034208000
6	-3.123373000	3.801021000	-0.786913000
1	-3.030871000	3.508357000	-1.834622000
1	-2.601937000	4.751268000	-0.653932000
1	-4.182334000	3.971022000	-0.582353000
6	2.545367000	3.905901000	-0.765068000
1	3.603654000	4.175377000	-0.751807000
1	1.965577000	4.811291000	-0.572520000
1	2.303979000	3.558783000	-1.771443000
6	2.869655000	-1.826285000	-3.216195000
1	2.563139000	-0.886012000	-3.677939000
1	2.383446000	-2.640967000	-3.756962000
1	3.948048000	-1.927232000	-3.356831000
6	2.888461000	-3.249838000	-1.131814000
1	3.952339000	-3.461657000	-1.256438000
1	2.339541000	-4.038463000	-1.650510000
1	2.641060000	-3.304961000	-0.073091000
6	2.505664000	3.376748000	1.706560000
1	2.308310000	2.619410000	2.465049000
1	1.856191000	4.231912000	1.904106000
1	3.535627000	3.718747000	1.823304000
1	-0.974429000	-2.588841000	4.056477000
1	0.188467000	-3.174968000	1.286518000
1	0.842223000	-1.772801000	4.617240000
1	1.945985000	-2.379602000	1.852798000
1	0.793559000	0.706970000	2.365063000
1	-1.461696000	-0.178138000	2.094877000

IDipp·$BH_2GeH_2PH_2$ (**2b**)

5	-0.069017000	-0.133171000	1.364358000
15	-0.522184000	-3.117495000	3.614083000
7	-1.092727000	0.637874000	-0.934506000
7	1.065738000	0.677316000	-0.894406000

6	2.452815000	0.569565000	-0.502578000
6	-0.023007000	0.359462000	-0.135612000
6	3.194121000	-0.537966000	-0.948548000
6	-3.104196000	1.622169000	0.056415000
6	5.127600000	0.410433000	0.159953000
1	6.175481000	0.344934000	0.425179000
6	3.023489000	1.605711000	0.254166000
6	-4.467344000	1.522739000	0.330712000
1	-4.970293000	2.342715000	0.826663000
6	-5.189009000	0.393069000	-0.018276000
1	-6.247144000	0.336506000	0.204961000
6	-4.557960000	-0.666332000	-0.649825000
1	-5.132757000	-1.543521000	-0.914589000
6	4.542650000	-0.590878000	-0.597396000
1	5.142673000	-1.431404000	-0.918494000
6	-2.540951000	-1.794730000	-1.666145000
1	-1.460668000	-1.691391000	-1.560879000
6	4.375112000	1.496089000	0.577210000
1	4.846103000	2.274432000	1.162671000
6	-3.195644000	-0.624710000	-0.945694000
6	-2.353835000	2.888068000	0.442296000
1	-1.299950000	2.741975000	0.208005000
6	-2.490437000	0.533175000	-0.581810000
6	-0.673429000	1.132123000	-2.159542000
1	-1.370708000	1.422868000	-2.923112000
6	0.673409000	1.158644000	-2.133100000
1	1.386865000	1.475364000	-2.870574000
6	-2.441343000	3.168441000	1.949870000
1	-3.467658000	3.373445000	2.261299000
1	-1.839506000	4.043783000	2.203921000
1	-2.071323000	2.320786000	2.526141000
6	-2.868285000	-1.768985000	-3.169313000
1	-3.942449000	-1.876443000	-3.336104000
1	-2.364756000	-2.590976000	-3.682774000
1	-2.551414000	-0.835739000	-3.637916000
6	2.246175000	2.843307000	0.677681000
1	1.186873000	2.645081000	0.521380000
6	2.599037000	-1.632099000	-1.825767000
1	1.512583000	-1.569693000	-1.750056000
6	-2.919909000	-3.151570000	-1.057565000
1	-2.717770000	-3.178381000	0.012644000
1	-2.335691000	-3.944830000	-1.527374000
1	-3.974586000	-3.386733000	-1.213443000
32	0.366326000	-2.177793000	1.631615000
6	-2.839759000	4.095825000	-0.375292000
1	-2.739694000	3.919886000	-1.448129000
1	-2.257177000	4.984408000	-0.122603000
1	-3.889485000	4.317303000	-0.171572000
6	2.626868000	4.049725000	-0.197738000
1	3.681329000	4.306956000	-0.075490000
1	2.034151000	4.924167000	0.080013000
1	2.454754000	3.848138000	-1.256779000
6	2.978415000	-1.416864000	-3.302201000
1	2.658972000	-0.441210000	-3.670743000
1	2.514204000	-2.181263000	-3.929104000
1	4.060305000	-1.483656000	-3.436814000
6	2.999951000	-3.045714000	-1.381830000
1	4.063777000	-3.233210000	-1.540178000
1	2.450455000	-3.785147000	-1.967665000
1	2.775220000	-3.213549000	-0.329580000
6	2.419381000	3.171018000	2.166746000
1	2.150842000	2.317666000	2.789004000
1	1.772944000	4.007372000	2.440727000
1	3.444811000	3.461436000	2.403712000
1	-1.827331000	-2.586951000	3.429537000
1	-0.129518000	-3.166984000	0.529828000
1	-0.124185000	-2.035525000	4.444405000
1	1.880354000	-2.519286000	1.753927000
1	0.777684000	0.430745000	2.011173000
1	-1.175481000	0.028980000	1.805533000

IDipp·$BH_2PH_2GeH_2$

7	0.986676000	-0.686090000	0.789605000
6	0.547410000	-1.002512000	2.063228000
6	-0.798627000	-0.935097000	2.044977000
7	-1.169483000	-0.577197000	0.760486000
6	2.387254000	-0.740349000	0.420588000
1	1.230645000	-1.249392000	2.853884000
1	-1.525040000	-1.115389000	2.815012000
6	-2.561029000	-0.522837000	0.355462000
6	-5.242702000	-0.488467000	-0.288696000
6	-3.147158000	-1.691500000	-0.155037000
6	-3.284131000	0.663981000	0.557585000
6	-4.637856000	0.648727000	0.221867000
6	-4.503302000	-1.643862000	-0.475048000
6	-2.382034000	-2.991105000	-0.358520000
6	-2.659128000	1.923799000	1.140564000
1	-5.225515000	1.546064000	0.354398000
1	-4.985216000	-2.525710000	-0.876686000
1	-6.294508000	-0.471608000	-0.545845000
6	5.077815000	-0.903960000	-0.172845000
6	3.208148000	0.365235000	0.705035000
6	2.885175000	-1.930429000	-0.136419000
6	4.246950000	-1.980952000	-0.431606000
6	4.562654000	0.250947000	0.392240000
6	2.690471000	1.636834000	1.365107000
6	2.025124000	-3.164045000	-0.371157000
1	4.663127000	-2.880460000	-0.865014000
1	5.223378000	1.083054000	0.590977000
1	6.132512000	-0.964941000	-0.410709000
1	-1.587628000	1.898577000	0.932737000
6	-2.844436000	1.980982000	2.667952000
6	-3.199157000	3.210464000	0.503510000
1	-3.145533000	3.174088000	-0.583847000
1	-2.596767000	4.057856000	0.832072000
1	-4.232847000	3.406529000	0.797140000
1	-2.404117000	1.119862000	3.172063000
1	-3.905168000	2.013157000	2.928128000
1	-2.371640000	2.879552000	3.069477000
1	-1.337330000	-2.816733000	-0.103808000
6	-2.412669000	-3.449626000	-1.824243000
6	-2.898397000	-4.095398000	0.578017000
1	-2.837070000	-3.793125000	1.625246000
1	-2.308493000	-5.006058000	0.453413000
1	-3.940212000	-4.342218000	0.364284000
1	-2.021282000	-2.676113000	-2.484550000
1	-3.426885000	-3.693432000	-2.146582000
1	-1.802558000	-4.346832000	-1.949715000
6	2.308276000	-4.234298000	0.697150000
6	2.194470000	-3.743915000	-1.781963000
1	0.980570000	-2.872479000	-0.274822000
6	2.905551000	1.593640000	2.889225000
1	1.617222000	1.705258000	1.179209000
6	3.320856000	2.912923000	0.791583000
1	2.141348000	-3.851135000	1.705530000
1	3.342197000	-4.581336000	0.640552000
1	1.656285000	-5.098461000	0.552363000
1	3.199321000	-4.139491000	-1.941404000
1	1.997922000	-2.989549000	-2.543519000
1	1.493156000	-4.567227000	-1.931934000
1	3.970089000	1.535881000	3.128073000
1	2.414237000	0.738032000	3.353701000

1	2.505525000	2.498775000	3.350467000
1	4.371768000	3.008497000	1.073076000
1	2.793744000	3.785256000	1.178113000
1	3.252179000	2.946863000	-0.295057000
6	-0.071437000	-0.430305000	-0.027117000
32	0.138550000	3.665425000	-1.348423000
5	-0.069520000	-0.186261000	-1.605954000
15	0.781950000	1.482464000	-2.222988000
1	1.031219000	4.356410000	-2.475110000
1	-1.165536000	3.596638000	-2.264472000
1	-1.202708000	-0.121008000	-2.000666000
1	0.532013000	-1.091868000	-2.131223000
1	2.174574000	1.332613000	-2.055540000
1	0.748869000	1.322090000	-3.624551000

IDipp·$GeH_2BH_2PH_2BH_3$ (**3a**)

32	0.027651000	0.672890000	-1.538341000
15	0.343671000	3.818796000	-2.585781000
7	-1.178106000	-0.757190000	0.888600000
7	0.970675000	-0.937110000	0.887453000
6	2.375643000	-0.853425000	0.535127000
6	-0.069695000	-0.434770000	0.180349000
6	3.154644000	0.158777000	1.120583000
6	-3.263306000	-1.420646000	-0.209622000
6	5.054414000	-0.736017000	-0.087809000
1	6.105834000	-0.682677000	-0.340817000
6	2.904620000	-1.821181000	-0.334717000
6	-4.598570000	-1.141613000	-0.496016000
1	-5.178159000	-1.850925000	-1.072169000
6	-5.195622000	0.029916000	-0.059312000
1	-6.233339000	0.227916000	-0.296574000
6	-4.468446000	0.950333000	0.677731000
1	-4.947251000	1.861408000	1.009715000
6	4.506553000	0.193291000	0.780925000
1	5.137795000	0.964865000	1.198884000
6	-2.372929000	1.741954000	1.842878000
1	-1.308959000	1.510873000	1.782831000
6	4.263027000	-1.733193000	-0.634134000
1	4.707633000	-2.455597000	-1.305014000
6	-3.129308000	0.726900000	0.997425000
6	-2.646382000	-2.723002000	-0.699622000
1	-1.589960000	-2.723508000	-0.430325000
6	-2.553631000	-0.466949000	0.536311000
6	-0.832655000	-1.465008000	2.025771000
1	-1.572298000	-1.816899000	2.721136000
6	0.512639000	-1.580673000	2.022175000
1	1.182518000	-2.055924000	2.714171000
6	-2.719686000	-2.851813000	-2.228825000
1	-3.752650000	-2.913652000	-2.576040000
1	-2.207990000	-3.759965000	-2.554102000
1	-2.249494000	-2.000213000	-2.721121000
6	-2.787482000	1.635981000	3.320778000
1	-3.845245000	1.876447000	3.447693000
1	-2.209557000	2.336345000	3.926922000
1	-2.625301000	0.631880000	3.717725000
6	2.078054000	-2.969166000	-0.898104000
1	1.023662000	-2.717912000	-0.780101000
6	2.599077000	1.154645000	2.130381000
1	1.514925000	1.185867000	2.012068000
6	-2.541844000	3.179916000	1.333164000
1	-2.262134000	3.268380000	0.284227000
1	-1.898746000	3.852505000	1.902455000
1	-3.568266000	3.533322000	1.447053000
5	0.794981000	2.567497000	-1.166851000
6	-3.289978000	-3.938359000	-0.012725000
1	-3.204329000	-3.877438000	1.073886000
1	-2.804563000	-4.860320000	-0.339322000
1	-4.351082000	-4.016007000	-0.257472000
6	2.336461000	-4.261836000	-0.103827000
1	3.380054000	-4.571109000	-0.192150000
1	1.712038000	-5.073937000	-0.482550000
1	2.117176000	-4.135047000	0.957892000
6	2.904091000	0.690479000	3.567010000
1	2.504924000	-0.303514000	3.775281000
1	2.469687000	1.385222000	4.288688000
1	3.981786000	0.656461000	3.740732000
6	3.109305000	2.585921000	1.918548000
1	4.176169000	2.672980000	2.133996000
1	2.587975000	3.262668000	2.597956000
1	2.927136000	2.927757000	0.901660000
6	2.313593000	-3.199431000	-2.396756000
1	2.155215000	-2.285004000	-2.968311000
1	1.620624000	-3.956653000	-2.768804000
1	3.324066000	-3.558121000	-2.600098000
1	-1.045065000	3.707460000	-2.824161000
1	0.311409000	2.966161000	-0.137847000
1	0.783797000	3.251681000	-3.802899000
1	1.992031000	2.465175000	-1.117737000
1	0.815247000	-0.332419000	-2.421306000
1	-1.444299000	0.489035000	-1.992841000
5	0.884805000	5.687863000	-2.414822000
1	0.497656000	6.249122000	-3.414141000
1	0.336604000	6.068862000	-1.403817000
1	2.090406000	5.657132000	-2.311765000

IDipp·$BH_2GeH_2PH_2BH_3$ (**3b**)

5	0.074867000	-0.303963000	-1.203101000
15	0.693101000	-3.597084000	-2.681490000
7	1.040964000	1.056868000	0.834352000
7	-1.116156000	1.013836000	0.768143000
6	-2.492563000	0.755793000	0.406800000
6	-0.006654000	0.549526000	0.127794000
6	-3.197277000	-0.236370000	1.109819000
6	3.047442000	1.813246000	-0.348232000
6	-5.145274000	0.323559000	-0.216110000
1	-6.184562000	0.149471000	-0.465223000
6	-3.088552000	1.546926000	-0.588528000
6	4.416283000	1.679943000	-0.576289000
1	4.910488000	2.362650000	-1.255119000
6	5.154626000	0.688498000	0.048707000
1	6.216667000	0.602190000	-0.143976000
6	4.536040000	-0.195145000	0.918345000
1	5.124445000	-0.965585000	1.397866000
6	-4.535874000	-0.432426000	0.771601000
1	-5.108547000	-1.191243000	1.287056000
6	2.528255000	-1.077961000	2.169660000
1	1.447611000	-1.032702000	2.029785000
6	-4.428752000	1.302858000	-0.884478000
1	-4.919480000	1.890409000	-1.648817000
6	3.169291000	-0.112056000	1.183171000
6	2.277360000	2.926636000	-1.042744000
1	1.222413000	2.817142000	-0.792790000
6	2.447433000	0.902452000	0.534861000
6	0.587830000	1.834768000	1.887245000
1	1.264169000	2.333907000	2.555969000
6	-0.759130000	1.809330000	1.844168000
1	-1.493816000	2.280796000	2.469629000
6	2.386168000	2.831277000	-2.571844000
1	3.413252000	2.978723000	-2.911502000
1	1.771099000	3.602610000	-3.040322000
1	2.044751000	1.859646000	-2.928364000
6	2.827247000	-0.661051000	3.620389000

1	3.900325000	-0.693768000	3.821313000
1	2.333784000	-1.338577000	4.320429000
1	2.480700000	0.351922000	3.831883000
6	-2.352135000	2.672307000	-1.300409000
1	-1.288209000	2.561837000	-1.094876000
6	-2.576574000	-1.050380000	2.238223000
1	-1.491708000	-0.963629000	2.159169000
6	2.948938000	-2.534763000	1.933365000
1	2.772851000	-2.841138000	0.902746000
1	2.372631000	-3.197601000	2.581079000
1	4.004467000	-2.694970000	2.160613000
32	-0.322799000	-2.351953000	-0.953436000
6	2.723178000	4.309706000	-0.540971000
1	2.606601000	4.400460000	0.540723000
1	2.127632000	5.094521000	-1.012190000
1	3.771796000	4.499579000	-0.778923000
6	-2.790744000	4.040841000	-0.751155000
1	-3.852346000	4.216890000	-0.937658000
1	-2.228075000	4.843008000	-1.233684000
1	-2.626179000	4.113933000	0.325566000
6	-2.989764000	-0.487013000	3.610079000
1	-2.713466000	0.562064000	3.723643000
1	-2.508798000	-1.050190000	4.412599000
1	-4.070542000	-0.561672000	3.748374000
6	-2.916232000	-2.545537000	2.161570000
1	-3.973946000	-2.730602000	2.357669000
1	-2.347377000	-3.092148000	2.915967000
1	-2.673602000	-2.965683000	1.186516000
6	-2.516458000	2.617127000	-2.825152000
1	-2.210062000	1.648028000	-3.218390000
1	-1.896784000	3.384477000	-3.293551000
1	-3.548103000	2.801436000	-3.130829000
1	2.002192000	-3.073608000	-2.709577000
1	0.212421000	-3.084312000	0.307781000
1	0.202298000	-2.962333000	-3.841299000
1	-1.796564000	-2.815332000	-1.078756000
1	-0.762086000	0.068429000	-1.985348000
1	1.187643000	-0.239353000	-1.653353000
5	0.613163000	-5.550224000	-2.732782000
1	1.147764000	-5.896612000	-1.705642000
1	-0.566518000	-5.806999000	-2.770213000
1	1.217375000	-5.863847000	-3.731036000

$[PH(GeH_2)_2(BH_2)_2PH_2]^-$

1	-0.513334000	-2.753839000	0.000000000
15	-1.183381000	-1.499162000	0.000000000
5	0.032396000	1.589864000	1.692676000
5	0.032396000	1.589864000	-1.692676000
15	0.796913000	2.161301000	0.000000000
32	0.032396000	-0.501495000	-1.774385000
32	0.032396000	-0.501495000	1.774385000
1	-1.110093000	1.983131000	1.706511000
1	-1.110093000	1.983131000	-1.706511000
1	2.178334000	1.863202000	0.000000000
1	1.451931000	-1.162064000	-1.800315000
1	1.451931000	-1.162064000	1.800315000
1	0.697084000	2.033039000	2.600659000
1	0.697084000	2.033039000	-2.600659000
1	0.919840000	3.573214000	0.000000000
1	-0.631500000	-1.062911000	-3.073799000
1	-0.631500000	-1.062911000	3.073799000

$[PH_2(GeH_2)_2(BH_2)_2PH]^-$

5	-0.004959000	1.642052000	1.607212000
5	-0.004959000	1.642052000	-1.607212000
32	-0.004959000	-0.420705000	-2.003261000
32	-0.004959000	-0.420705000	2.003261000
1	-1.180021000	1.929264000	1.521677000
1	-1.180021000	1.929264000	-1.521677000
1	1.288739000	-1.299327000	-2.077544000
1	1.288739000	-1.299327000	2.077544000
1	0.513322000	2.103730000	2.604898000
1	0.513322000	2.103730000	-2.604898000
1	-0.929399000	-1.130423000	-3.059233000
1	-0.929399000	-1.130423000	3.059233000
15	-0.914135000	-1.427850000	0.000000000
1	-2.280552000	-1.087858000	0.000000000
1	-1.052278000	-2.835875000	0.000000000
15	1.131048000	1.950940000	0.000000000
1	1.060833000	3.375503000	0.000000000

$[IDipp{\cdot}GeH_2BH_2{\cdot}IDipp]^+$

7	-3.324405000	0.887230000	0.364475000
6	-4.437495000	0.509058000	1.090044000
6	-4.205666000	-0.741017000	1.544236000
7	-2.954104000	-1.109462000	1.091783000
6	-3.225992000	2.192822000	-0.259923000
1	-5.280204000	1.163658000	1.215179000
1	-4.805829000	-1.398327000	2.145578000
6	-2.362848000	-2.394318000	1.418325000
6	-1.352609000	-4.857425000	2.110442000
6	-1.718386000	-2.527196000	2.659182000
6	-2.545194000	-3.465080000	0.527629000
6	-2.012840000	-4.697533000	0.902549000
6	-1.214035000	-3.787334000	2.978885000
6	-1.616264000	-1.393936000	3.671531000
6	-3.349729000	-3.344390000	-0.759407000
1	-2.127706000	-5.548210000	0.245228000
1	-0.712605000	-3.934577000	3.925752000
1	-0.954029000	-5.826659000	2.382107000
6	-3.173759000	4.701487000	-1.387512000
6	-3.689400000	2.342493000	-1.576863000
6	-2.752299000	3.262723000	0.514985000
6	-2.733523000	4.521268000	-0.086634000
6	-3.646765000	3.624764000	-2.121273000
6	-4.263959000	1.191428000	-2.390463000
6	-2.320930000	3.112432000	1.967495000
1	-2.376744000	5.373825000	0.475406000
1	-3.995144000	3.784795000	-3.132687000
1	-3.155213000	5.688769000	-1.831335000
1	-3.421054000	-2.287166000	-1.017836000
6	-4.782632000	-3.866762000	-0.550362000
6	-2.688652000	-4.050848000	-1.950198000
1	-1.657983000	-3.723142000	-2.087508000
1	-3.241868000	-3.829739000	-2.864681000
1	-2.687309000	-5.135321000	-1.829755000
1	-5.298117000	-3.332100000	0.249157000
1	-4.775901000	-4.926886000	-0.290025000
1	-5.366983000	-3.748771000	-1.464854000
1	-1.883425000	-0.462711000	3.169895000
6	-0.195209000	-1.211796000	4.221131000
6	-2.617458000	-1.602651000	4.821567000
1	-3.643496000	-1.690344000	4.460397000
1	-2.576530000	-0.762593000	5.517532000
1	-2.386450000	-2.511359000	5.380593000
1	0.522772000	-1.056427000	3.416911000
1	0.125852000	-2.074123000	4.807764000
1	-0.163439000	-0.342806000	4.880956000
6	-3.360997000	3.736506000	2.913907000
6	-0.926904000	3.696883000	2.228661000
1	-2.266292000	2.048094000	2.199629000
6	-5.797292000	1.290643000	-2.469832000
1	-4.023803000	0.258841000	-1.877625000

6	-3.652376000	1.097542000	-3.795499000
1	-4.351007000	3.298088000	2.775964000
1	-3.449432000	4.811515000	2.745984000
1	-3.066800000	3.584206000	3.954023000
1	-0.908294000	4.777797000	2.081655000
1	-0.176785000	3.253559000	1.574469000
1	-0.630082000	3.503545000	3.260992000
1	-6.104604000	2.203083000	-2.984386000
1	-6.254555000	1.299369000	-1.478896000
1	-6.205207000	0.441523000	-3.021437000
1	-3.917896000	1.957897000	-4.411679000
1	-4.025473000	0.207026000	-4.304338000
1	-2.564640000	1.034291000	-3.752853000
6	-2.407120000	-0.109641000	0.359507000
32	-0.648441000	-0.166063000	-0.675461000
1	-0.941978000	0.967796000	-1.687779000
1	-0.918330000	-1.470043000	-1.462156000
5	1.078062000	-0.071766000	0.513188000
1	0.928281000	0.863234000	1.251190000
6	2.441845000	0.091533000	-0.300641000
1	1.088272000	-1.122779000	1.099029000
7	3.255872000	1.181224000	-0.306850000
6	4.426598000	0.910815000	-0.992537000
6	4.342177000	-0.361357000	-1.429177000
7	3.120159000	-0.854088000	-1.008138000
6	3.027079000	2.468450000	0.314936000
1	5.203358000	1.645215000	-1.098124000
1	5.031911000	-0.960501000	-1.993582000
6	2.685915000	-2.201096000	-1.314107000
6	2.757343000	4.969862000	1.441011000
6	2.513801000	3.508922000	-0.475674000
6	3.420784000	2.649417000	1.649537000
6	3.266728000	3.924012000	2.193694000
6	2.387188000	4.762714000	0.122025000
6	2.153134000	3.330780000	-1.944119000
6	4.033198000	1.541188000	2.493079000
1	3.560006000	4.102597000	3.219695000
1	2.001301000	5.591288000	-0.456592000
1	2.655677000	5.953214000	1.882536000
6	1.952594000	-4.782626000	-1.942952000
6	2.901491000	-3.211231000	-0.362330000
6	2.148396000	-2.456365000	-2.587699000
6	1.781536000	-3.771184000	-2.873911000
6	2.512114000	-4.504904000	-0.706031000
6	3.603937000	-2.955851000	0.963396000
6	2.032680000	-1.389079000	-3.669616000
1	1.365220000	-4.008721000	-3.843503000
1	2.661348000	-5.310202000	0.000111000
1	1.663393000	-5.796592000	-2.189040000
1	2.131773000	-0.411135000	-3.195124000
6	0.681609000	-1.404033000	-4.398186000
6	3.177695000	-1.527469000	-4.689836000
1	-0.153935000	-1.332036000	-3.702685000
1	0.550626000	-2.311825000	-4.989200000
1	0.624723000	-0.560067000	-5.088043000
1	4.158448000	-1.477940000	-4.215777000
1	3.122823000	-0.730434000	-5.433821000
1	3.113438000	-2.482336000	-5.215202000
6	2.920375000	-3.646916000	2.149883000
1	3.572692000	-1.884841000	1.161262000
6	5.083934000	-3.369474000	0.875248000
1	5.179805000	-4.440549000	0.685783000
1	5.597744000	-3.147336000	1.812680000
1	5.604788000	-2.842802000	0.073874000
1	3.004717000	-4.733571000	2.092489000
1	1.862820000	-3.389339000	2.204380000
1	3.395636000	-3.336535000	3.082221000
6	3.210579000	3.980516000	-2.853316000
6	0.754188000	3.866224000	-2.277176000
1	2.144956000	2.262157000	-2.163311000
1	0.696767000	4.949472000	-2.158604000
1	-0.009340000	3.417048000	-1.642373000
1	0.506326000	3.640015000	-3.315968000
1	4.207949000	3.579192000	-2.667110000
1	3.253474000	5.059784000	-2.694259000
1	2.968378000	3.806735000	-3.903664000
6	5.522374000	1.812413000	2.764587000
1	3.970341000	0.610372000	1.929412000
6	3.267380000	1.321880000	3.805560000
1	3.331311000	2.192440000	4.460825000
1	3.689953000	0.473768000	4.347677000
1	2.214222000	1.114532000	3.616119000
1	5.658162000	2.725004000	3.348125000
1	6.087035000	1.924427000	1.837320000
1	5.961314000	0.987616000	3.329319000

$[IDippGeH_2BH_2IDipp]^+ \ldots [PH(GeH_2)_2(BH_2)_2PH_2]^-$

7	-4.986972000	1.076396000	-0.284000000
6	-6.263371000	0.760750000	0.142240000
6	-6.224986000	-0.512106000	0.589427000
7	-4.925967000	-0.956220000	0.432425000
6	-4.655019000	2.385447000	-0.811608000
1	-7.069311000	1.469202000	0.089966000
1	-6.991291000	-1.139520000	1.005127000
6	-4.509581000	-2.288586000	0.828246000
6	-3.839310000	-4.838031000	1.617353000
6	-4.166076000	-2.503636000	2.172929000
6	-4.549056000	-3.316649000	-0.127740000
6	-4.197592000	-4.595377000	0.301250000
6	-3.828682000	-3.805567000	2.540504000
6	-4.208448000	-1.406238000	3.228354000
6	-5.012255000	-3.097595000	-1.561509000
1	-4.207808000	-5.414410000	-0.404564000
1	-3.553817000	-4.013236000	3.565531000
1	-3.569296000	-5.839871000	1.926334000
6	-4.150775000	4.908059000	-1.789051000
6	-4.756093000	2.598520000	-2.195481000
6	-4.322516000	3.400392000	0.098492000
6	-4.069555000	4.667244000	-0.427734000
6	-4.491599000	3.885400000	-2.660329000
6	-5.171988000	1.509745000	-3.174995000
6	-4.273811000	3.185373000	1.604753000
1	-3.805561000	5.475825000	0.240490000
1	-4.553634000	4.090517000	-3.720535000
1	-3.947750000	5.899088000	-2.174685000
1	-4.958552000	-2.029402000	-1.774854000
6	-6.479192000	-3.531815000	-1.729340000
6	-4.121213000	-3.803550000	-2.592354000
1	-3.071154000	-3.544713000	-2.457454000
1	-4.417974000	-3.509330000	-3.600789000
1	-4.213790000	-4.889407000	-2.532784000
1	-7.142892000	-2.996406000	-1.048225000
1	-6.592736000	-4.599718000	-1.532162000
1	-6.818397000	-3.340487000	-2.749501000
1	-4.254290000	-0.443850000	2.716700000
6	-2.956820000	-1.378591000	4.114970000
6	-5.476479000	-1.534477000	4.091676000
1	-6.386808000	-1.505877000	3.490336000
1	-5.525742000	-0.719183000	4.816191000
1	-5.476084000	-2.475400000	4.645614000
1	-2.050975000	-1.283508000	3.518285000
1	-2.874403000	-2.277029000	4.729045000

1	-3.006823000	-0.526267000	4.795159000
6	-5.471925000	3.863922000	2.290850000
6	-2.951665000	3.657552000	2.223848000
1	-4.350392000	2.115143000	1.800143000
6	-6.618653000	1.725900000	-3.651293000
1	-5.139850000	0.552579000	-2.652890000
6	-4.216415000	1.396686000	-4.371068000
1	-6.423760000	3.502904000	1.896436000
1	-5.443864000	4.946000000	2.148067000
1	-5.454596000	3.667912000	3.364735000
1	-2.823767000	4.737054000	2.130192000
1	-2.093110000	3.174928000	1.758597000
1	-2.934625000	3.418512000	3.288629000
1	-6.714575000	2.667163000	-4.196289000
1	-7.320088000	1.754006000	-2.815386000
1	-6.923347000	0.918820000	-4.320582000
1	-4.248585000	2.286936000	-5.001455000
1	-4.499611000	0.546552000	-4.994614000
1	-3.186888000	1.250015000	-4.044630000
6	-4.157802000	0.018871000	-0.110897000
32	-2.198110000	-0.134833000	-0.685556000
1	-2.194497000	1.017764000	-1.720466000
1	-2.367707000	-1.413845000	-1.540788000
5	-0.823495000	-0.145473000	0.901528000
1	-1.115718000	0.788228000	1.599409000
6	0.700622000	-0.044515000	0.436001000
1	-1.021878000	-1.201638000	1.444439000
7	1.552701000	0.989255000	0.663336000
6	2.833435000	0.667282000	0.246669000
6	2.781884000	-0.581585000	-0.256705000
7	1.469855000	-1.006640000	-0.141996000
6	1.256687000	2.271361000	1.260406000
1	3.663669000	1.344489000	0.339132000
1	3.568270000	-1.189379000	-0.678790000
6	1.043844000	-2.311582000	-0.594410000
6	0.878885000	4.763190000	2.384120000
6	1.039723000	3.367582000	0.410670000
6	1.305786000	2.394086000	2.657777000
6	1.104521000	3.664010000	3.197184000
6	0.848995000	4.614121000	1.007324000
6	1.056176000	3.256539000	-1.107433000
6	1.611198000	1.224784000	3.582310000
1	1.144411000	3.796498000	4.270471000
1	0.691211000	5.482668000	0.381435000
1	0.739548000	5.742417000	2.825484000
6	0.330934000	-4.824865000	-1.479845000
6	0.990906000	-3.362898000	0.334894000
6	0.795997000	-2.497832000	-1.965662000
6	0.428849000	-3.777646000	-2.381509000
6	0.617364000	-4.619508000	-0.139799000
6	1.408565000	-3.193760000	1.788131000
6	1.000424000	-1.397153000	-2.998829000
1	0.235814000	-3.960873000	-3.430045000
1	0.570490000	-5.454204000	0.546586000
1	0.052315000	-5.812157000	-1.827458000
1	1.028553000	-0.440292000	-2.474680000
6	-0.130526000	-1.313402000	-4.033886000
6	2.353402000	-1.573088000	-3.713429000
1	-1.109385000	-1.217396000	-3.563482000
1	-0.152054000	-2.192515000	-4.680655000
1	0.025043000	-0.445470000	-4.677617000
1	3.192509000	-1.600711000	-3.018699000
1	2.523555000	-0.748636000	-4.408704000
1	2.365111000	-2.503997000	-4.285072000
6	0.436107000	-3.857205000	2.771551000
1	1.412281000	-2.128510000	2.015909000
6	2.841040000	-3.715422000	1.998125000
1	2.899273000	-4.787117000	1.794815000
1	3.157471000	-3.550090000	3.029904000
1	3.556734000	-3.213638000	1.346754000
1	0.449044000	-4.945648000	2.685289000
1	-0.586857000	-3.515133000	2.610867000
1	0.722093000	-3.611935000	3.796331000
6	2.316637000	3.911925000	-1.696626000
6	-0.211335000	3.841469000	-1.746060000
1	1.086230000	2.198577000	-1.370353000
1	-0.284346000	4.918661000	-1.583515000
1	-1.114334000	3.379288000	-1.345953000
1	-0.195213000	3.675070000	-2.825197000
1	3.231948000	3.473716000	-1.298382000
1	2.336475000	4.982600000	-1.481013000
1	2.333942000	3.788758000	-2.781504000
6	3.011515000	1.361179000	4.202894000
1	1.608116000	0.312390000	2.986603000
6	0.540799000	1.054442000	4.669872000
1	0.527178000	1.901686000	5.358520000
1	0.748470000	0.159030000	5.259280000
1	-0.453666000	0.952794000	4.233879000
1	3.084950000	2.264829000	4.812167000
1	3.791662000	1.401475000	3.442406000
1	3.223332000	0.505131000	4.846762000
1	7.035365000	-2.342886000	-2.079580000
15	6.174448000	-1.458860000	-1.380641000
5	6.817783000	0.344587000	1.785919000
5	6.504992000	2.211216000	-0.980954000
15	7.334084000	1.901637000	0.747619000
32	6.937590000	0.608129000	-2.254232000
32	7.288975000	-1.387130000	0.711632000
1	5.616505000	0.407376000	1.924090000
1	5.310191000	2.253026000	-0.784423000
1	8.736941000	1.927699000	0.602094000
1	8.444481000	0.427737000	-2.608893000
1	8.804873000	-1.618631000	0.431644000
1	7.407504000	0.339281000	2.838412000
1	6.924893000	3.233856000	-1.463639000
1	7.203518000	3.064351000	1.543991000
1	6.238170000	0.719193000	-3.644585000
1	6.838069000	-2.698507000	1.426771000

TS $[PH_2GeH_2(\mu\text{-IDipp})BH_2OTf]^-$

8	-2.475313000	0.406504000	-0.702771000
5	-1.315688000	-0.493266000	-0.197754000
32	0.619670000	0.200653000	-1.809536000
1	-1.363527000	-0.473425000	0.997802000
6	0.956926000	-0.027888000	0.084905000
1	-1.311353000	-1.555492000	-0.741755000
1	1.927410000	0.928780000	-2.361027000
1	0.700793000	-1.210179000	-2.427243000
15	-0.813449000	1.783661000	-2.987937000
7	1.073019000	1.000942000	1.058406000
6	1.071735000	0.424438000	2.327738000
6	1.135147000	-0.907034000	2.196258000
7	1.178543000	-1.227233000	0.829753000
6	1.254502000	2.399815000	0.825848000
1	1.051219000	1.022392000	3.221121000
1	1.172156000	-1.663941000	2.956455000
6	1.470192000	-2.541198000	0.359617000
6	1.621409000	5.139699000	0.435719000
6	0.176768000	3.287161000	1.038581000
6	2.523961000	2.892543000	0.452415000
6	2.676900000	4.262201000	0.246646000
6	0.391420000	4.651908000	0.841154000

6	-1.192560000	2.815355000	1.502147000
6	3.748297000	1.995725000	0.374645000
1	3.644587000	4.651414000	-0.044327000
1	-0.428207000	5.342048000	0.993242000
1	1.759668000	6.202049000	0.272000000
6	2.086399000	-5.154024000	-0.471276000
6	0.652017000	-3.628676000	0.761086000
6	2.616667000	-2.786435000	-0.438158000
6	2.886091000	-4.087155000	-0.851587000
6	0.992601000	-4.914120000	0.339720000
6	-0.592723000	-3.480905000	1.628597000
6	3.629667000	-1.700158000	-0.765988000
1	3.759212000	-4.275130000	-1.462773000
1	0.367075000	-5.745129000	0.640915000
1	2.319505000	-6.160184000	-0.798630000
6	-2.337952000	3.429150000	0.685262000
6	-1.398530000	3.104248000	2.999970000
1	-1.234678000	1.736920000	1.364599000
6	4.631116000	2.188043000	1.620473000
6	4.564026000	2.196971000	-0.908598000
1	3.400188000	0.966554000	0.385071000
1	-0.801440000	-2.420959000	1.745710000
6	-0.382873000	-4.087868000	3.027049000
6	-1.836288000	-4.097285000	0.969262000
1	3.126021000	-0.741055000	-0.683774000
6	4.185427000	-1.781007000	-2.193438000
6	4.772027000	-1.722012000	0.264860000
1	-2.431130000	4.504107000	0.862397000
1	-3.284037000	2.966172000	0.967752000
1	-2.196827000	3.267315000	-0.382272000
1	-1.380032000	4.179746000	3.198027000
1	-0.625701000	2.639498000	3.614813000
1	-2.366138000	2.717819000	3.328906000
1	4.998287000	3.198264000	-0.962610000
1	3.943364000	2.044232000	-1.791932000
1	5.391194000	1.483704000	-0.944849000
1	5.017640000	3.209210000	1.675721000
1	5.483780000	1.504517000	1.595462000
1	4.069034000	1.992276000	2.535195000
1	-2.719630000	-3.893704000	1.578656000
1	-1.747484000	-5.181773000	0.866546000
1	-2.008780000	-3.666942000	-0.016113000
1	-1.259560000	-3.907742000	3.654617000
1	0.486894000	-3.664677000	3.534094000
1	-0.230249000	-5.168992000	2.969528000
1	3.379967000	-1.799667000	-2.928070000
1	4.810121000	-2.664570000	-2.346137000
1	4.804971000	-0.905463000	-2.398819000
1	4.391688000	-1.593607000	1.279657000
1	5.488039000	-0.920185000	0.066304000
1	5.311373000	-2.672332000	0.226538000
1	-1.799551000	0.875821000	-3.445829000
1	0.004964000	1.610872000	-4.139313000
16	-3.848934000	-0.008892000	-1.199508000
6	-4.759540000	-0.387360000	0.392652000
8	-3.859350000	-1.248159000	-1.920722000
8	-4.533593000	1.133785000	-1.730247000
9	-6.051559000	-0.632608000	0.120316000
9	-4.707941000	0.649448000	1.242090000
9	-4.258169000	-1.459460000	1.014139000

9.5.6 References

[1] M. T. Ackermann, M. Seidl, F. Wen, M. J. Ferguson, A. Y. Timoshkin, E. Rivard, M. Scheer, *Chem. Eur. J.* **2022**, *28*, e202103780.

[2] H. Jacobs, K. M. Hassiepen, *Z. Anorg. Allg. Chem.* **1985**, *531*, 108–118.

[3] CrysAlisPro (ROD), Rigaku Oxford Diffraction, Poland (2021).

[4] R. C. Clark, J. S. Reid, *Acta Cryst.* **1995**, *A51*, 887–897.

[5] O. V. Dolomanov, L. J. Bourhis, R. J. Gildea, J. A. K. Howard, H. Puschmann, *J. Appl. Cryst.* **2009**, *42*, 339–341.

[6] G. M. Sheldrick, *Acta Cryst.* **2015**, *A71*, 3–8.

[7] G. M. Sheldrick, *Acta Cryst.* **2015**, *C71*, 3–8.

[8] a) A. D. Becke, *J. Chem. Phys.* **1993**, *98*, 5648-5652; b) C. Lee, W. Yang, R. G. Parr, *Phys. Rev. B, Condensed Matter* **1988**, *37*, 785-789.

[9] F. Weigend, R. Ahlrichs, *Phys. Chem. Chem. Phys.* **2005**, *7*, 3297-3305.

[10] M. J. Frisch, G. W. Trucks, H. B. Schlegel, G. E. Scuseria, M. A. Robb, J. R. Cheeseman, G. Scalmani, V. Barone, B. Mennucci, G. A. Petersson, H. Nakatsuji, M. Caricato, X. Li, H. P. Hratchian, A. F. Izmaylov, J. Bloino, G. Zheng, J. L. Sonnenberg, M. Hada, M. Ehara, K. Toyota, R. Fukuda, J. Hasegawa, M. Ishida, T. Nakajima, Y. Honda, O. Kitao, H. Nakai, T. Vreven, J. A. Montgomery, Jr., J. E. Peralta, F. Ogliaro, M. Bearpark, J. J. Heyd, E. Brothers, K. N. Kudin, V. N. Staroverov, T. Keith, R. Kobayashi, J. Normand, K. Raghavachari, A. Rendell, J. C. Burant, S. S. Iyengar, J. Tomasi, M. Cossi, N. Rega, J. M. Millam, M. Klene, J. E. Knox, J. B. Cross, V. Bakken, C. Adamo, J. Jaramillo, R. Gomperts, R. E. Stratmann, O. Yazyev, A. J. Austin, R. Cammi, C. Pomelli, J. W. Ochterski, R. L. Martin, K. Morokuma, V. G. Zakrzewski, G. A. Voth, P. Salvador, J. J. Dannenberg, S. Dapprich, A. D. Daniels, O. Farkas, J. B. Foresman, J. V. Ortiz, J. Cioslowski, D. J. Fox, in *Gaussian 09, Vol. Revision E.01*, Gaussian Inc., Wallingford CT, **2013**.

[11] a) K. L. Schuchardt, B. T. Didier, T. Elsethagen, L. Sun, V. Gurumoorthi, J. Chase, J. Li, T. L. Windus, *J. Chem. Inf. Model.* **2007**, *47*, 1045-1052; b) D. Feller, *J. Comput. Chem.* **1996**, *17*, 1571-1586.

9.6 Author Contributions

M. T. Ackermann – writing of the original draft, experimental work (syntheses and characterizations of all compounds)

R. Szlosek – writing of the final manuscript, experimental work (reproductions and acquisition of missing analytical data for **2a/b** and **3**, NMR studies on the stabilities on solution)

C. Riesinger – finalization of single-crystal X-ray data for **4**

M. Seidl – finalization of single-crystal X-ray data for **2a/b**

A. Y. Timoshkin – quantum chemical calculations, acquisition of funding, co-writing of final manuscript

E. Rivard – project management, conceptualization, co-writing of final manuscript

M. Scheer – project supervision, acquisition of funding, co-writing of final manuscript

10 Electrophilic functionalization of Donor stabilized Phosphanylboranes – a new Pathway towards heavy 13/14/15 parent hydride containing Compounds

R. Szlosek, M. Seidl, C. Riesinger, L. Zimmermann, A. S. Niefanger, C. Marquardt and M. Scheer

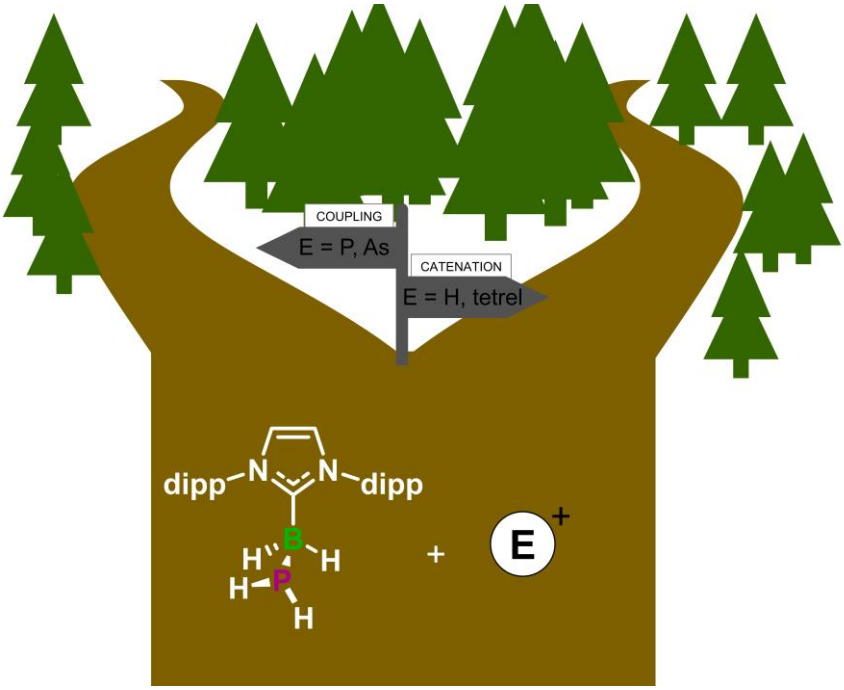

Abstract: A novel method for the functionalization of donor stabilized 13/15 compounds is presented. Reacting the IDipp (1,3-bis(2,6-diisopropylphenyl)-imidazolin-2-ylidene) stabilized parent phosphanylborane IDipp·BH_2PH_2 with (*in situ* generated) main group electrophiles resulted in mixed 13/14/15 compounds containing the complete series from carbon to tin [IDipp·BH_2PH_2E][WCA] (WCA = weakly coordinating anion, E = CH_3 (**2**), $SiEt_3$ (**3**), $Ge(SiMe_3)_3$ (**4**), $SnMe_3$ (**5**)). Reactions with the group 15 electrophiles [Cy_2E][PF_6] (E = P, As) yielded an intriguing P-P coupling reaction, affording [IDipp·$BH_2PH_2PHBH_2$·IDipp][PF_6] (**6**). The protonated phosphanylboranes reveal acidic protons at the phosphorus atom and this could be exploited by reactions with $LiGaH_4$ and $LiAlH_4$, resulting in either deprotonation to the parent phosphanylborane or chain extension to yield *D*·$BH_2PH_2GaH_3$ (*D* = IDipp (**7a**), Me_3N (**7b**)), the first examples of a {GaH_3} unit bound to a primary phosphine. The compounds could be isolated and characterized by multinuclear NMR spectroscopy and single-crystal X-ray structure determination.

10.1 Introduction

The chemistry of materials consisting of elements of groups 13/15 (13/15 compounds) has thrived within the last two decades. With modern stabilization tools such as N-heterocyclic carbenes (NHCs),[1] cyclic(alkyl)(amino)carbenes (CAACs)[2] and β-diketiminates,[3] the structural molecular motifs obtained have increased tremendously across the *p*-block elements. More recently, embedding elements from group 14 in mixed 13/14/15 compounds has found numerous applications, most importantly for chemical vapor deposition (CVD) processes, which can be used for the deposition of thin material layers.[4,5]

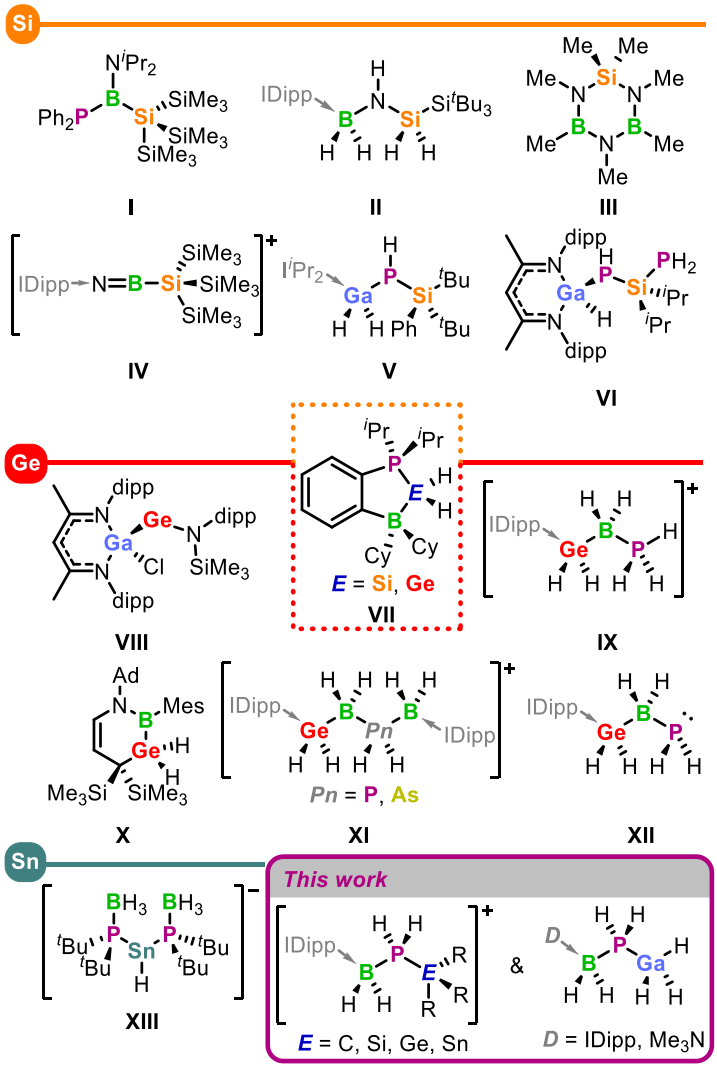

Figure 10.1: Selected examples for 13/14/15 mixed compounds ranging from Si to Sn (IDipp = 1,3-bis(2,6-diisopropylphenyl)-imidazolin-2-ylidene, dipp = 2,6-diisopropylphenyl, I^iPr_2 = 1,3-diisopropyl-imidazolin-2-ylidene).

By now, the area of known mixed 13/14/15 compounds covers a broad range of the periodic table, though reports on the heavier congeners of group 14 are still quite limited. Silicon containing 13/14/15 compounds can be prepared in manifold ways as charged neutral chain or cyclic compounds (Figure 10.1, **I**-**VI**).[6] By using Frustrated Lewis Pair (FLP)[7] chelation, Rivard and co-workers were able to trap

the parent tetrelenes {*Tet*H_2} (*Tet* = Si, Ge) in a cyclic system (Figure 10.1, **VII**), capable of depositing thin *Tet* layers on wafers under very mild conditions.[4] Furthermore, Schulz and co-workers isolated [(Dipp$_2$Nacnac)GaCl{GeN(Ar)(SiMe$_3$)}] (**VIII**) by the oxidative addition of a heteroleptic germylene to (Dipp$_2$NacNac)Ga.[8] By ring expansion of a cyclic(alkyl)(amino)germylene followed by addition of H_2, Kinjo and co-workers isolated a cyclic dihydrogermane with a boryl substitutent **X** (Figure 10.1).[9] More recently, the parent Ge/B/P combinations substituted only by hydrogen atoms could be realized by stabilization with N-heterocyclic carbenes (Figure 10.1, **IX**, **XI**, **XII**).[10,11] However, examples for molecular 13/14/15 combinations including tin are extremely rare.[8,12] The most prominent example is featured by [Li(HNMe$_2$)$_2$][HSn(P^{t}Bu$_2$BH$_3$)$_2$] (Figure 10.1, **XIII**), prepared by the reaction between LiSn(NMe$_2$)$_3$ and ^{t}Bu$_2$PH·BH$_3$.[12]

Still, the field of parent hydride containing compounds remains underdeveloped, especially for compounds containing the heavier group 14 congeners. An important molecular building block for this type of chemistry consists of Lewis base (LB) stabilized parent pnictogenyltrielanes *LB*·EH_2*Pn*H_2 (E = B, Al, Ga; *Pn* = P, As).[13–17] While the stabilization by tertiary amines is enough to obtain stable monomers for the pnictogenylboranes (*E* = B), the heavier group 13 homologs require a stronger and bulkier donor such as an NHC due to the weaker E-*Pn* bond.[15–17] These compounds have shown to display intriguing possibilities for reactivity. Besides classic coordination chemistry,[18,19,20] pnictogenyltrielanes serve as capable building blocks for the formation of inorganic oligo- and polymeric 13/15 materials.[21] More importantly, mixed 13/15 compounds can be obtained by reactions with electrophiles or nucleophiles.[10,11,13,20,22,23]

However, a general molecular basis for the formation of mixed 13/14/15 parent hydride compounds for the whole of group 14 is not reported to the best of our knowledge. Based on their high stability and previous reports on the reactivity of phosphanylboranes, it seemed likely that these compounds would represent suitable platforms towards the formation of stable molecular 13/14/15 hydride containing chain compounds. Specifically, tetrylium cations [R_3Tet]$^+$ (Tet = Si, Ge, Sn, Pb), have gained a lot of attention in the recent years due to their interesting chemical properties in chemical transformations, especially in catalysis and small molecule activation.[24] This type of cations represents a suitable candidate for conversions with phosphanylboranes towards new mixed 13/14/15 compounds. Herein, we report on the functionalization of the parent NHC stabilized phosphanylborane with cationic group 14 electrophiles ranging from carbon to tin, leading to unique mixed 13/14/15 chain structures. Furthermore, functionalization by protonation leads to a substantial change in reactivity of the phosphanylborane which could be exploited by reactions with $LiGaH_4$ and $LiAlH_4$. Similarly, reactions with group 15 electrophiles are presented, which surprisingly led to a P-P coupling reactions.

10.2 Results and Discussion

As the P-E bond strength can be quite low, especially for heavy group 14 elements E, the phosphanylborane of choice for our investigation was the NHC-stabilized IDipp·BH_2PH_2 (**A**), which profits drastically from the stabilization by the bulky NHC.[22] Our initial study focused on the smallest possible electrophile, the proton H^+. Thus, **A** was protonated with [H(OEt$_2$)$_2$][BAr^F][25] in *o*-DFB (Scheme 10.1, [BAr^F] = [B(C$_6$F$_5$)$_4$]$^-$), affording [IDipp·BH_2PH_3][BAr^F] (**1a**) as identified by multinuclear NMR spectroscopy. The ^{31}P NMR spectrum of the reaction mixture shows a highly broadened quartet at -122.6 ppm with a scalar coupling (large $^1J_{PH}$ = 394 Hz) and a broad doublet of triplets at -36.65 ppm in the ^{11}B

NMR spectrum ($^{1}J_{BH}$ = 106 Hz, $^{1}J_{BP}$ = 52 Hz), thus confirming the connectivity of **1a**. It was also possible to crystallize the product and determine its structure in the solid state by single-crystal X-ray structure determination (Figure 10.2, *vide infra*).

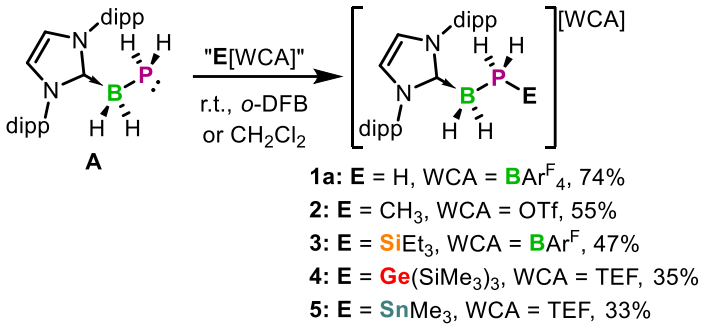

Scheme 10.1: Reactions of IDipp·BH_2PH_2 (A) with main group electrophiles.

Whereas protonation of the NHC stabilized phosphanylborane proceeds smoothly, the analogue reaction with $Me_3N{\cdot}BH_2PH_2$ is prone to protonation of the amine and requires a different approach. Inspired by works of Grützmacher and co-workers,[26] $H_3P{\cdot}AlCl_3$ was reacted with $Me_3N{\cdot}BH_2Cl$, resulting in $[Me_3N{\cdot}BH_2PH_3][AlCl_4]$ (**1b**, Scheme 10.2). The compound can be isolated in medium yields as an air sensitive colorless powder, that decomposes slowly at room temperature under release of PH_3.

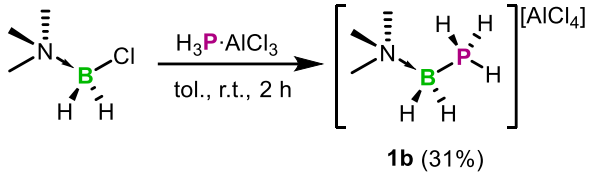

Scheme 10.2: Synthesis of $[IDipp{\cdot}BH_2PH_3][AlCl_4]$ (1b) by reaction of $Me_3N{\cdot}BH_2Cl$ with $H_3P{\cdot}AlCl_3$.

1b can be stored for at least several weeks at -30 °C under inert conditions, though. Characteristic NMR spectroscopic data are given in Table 10.1. It was also possible to crystallize **1b** and determine its structure in the solid state by X-ray structure determination (Figure 10.2). Next, it was targeted to react **A** with cationic main group electrophiles of group 14 to extend the chain structure towards mixed 13/15/14 compounds. **A** cleanly reacts with Me(OTf) (OTf = $[SO_3CF_3]^-$) to give the methylated parent compound $[IDipp{\cdot}BH_2PH_2CH_3][OTf]$ (**2**) as evident by multinuclear NMR spectroscopy and single-crystal X-ray diffraction (cf. Table 10.1, Figure 10.2) in a crystalline yield of 55%. Since suitable cationic electrophiles of the heavier group 14 homologs are difficult to obtain in stable form, ER_3X precursors (E = tetrel, X = halide or hydride) were reacted *in situ* with the abstracting agents Tl[TEF][27] or $[Ph_3C][BAr^F]$ (TEF = $[Al\{OC(CF_3)_3\}_4]^-$)[28] in the presence of **A** (Scheme 10.1). For all reactions, the corresponding cationic 13/15/14 chain compounds $[IDipp{\cdot}BH_2PH_2E][WCA]$ (**3**: E = $SiEt_3$, WCA = BAr^F, **4**: E = $Ge(SiMe_3)_3$, WCA = TEF, **5**: E =$SnMe_3$, WCA = TEF) could be obtained in moderate isolated yields as stable solids when stored under inert conditions. The lowered yield can be attributed to the very high sensitivity to air, especially of the heavier congeners, which also react readily with untreated glass surfaces to form $[IDipp{\cdot}BH_2PH_3]^+$. This requires all experiments to be carried out using silanized glassware. This is especially relevant for the silylated product **3**, which also decomposes readily into **1a** in most common organic solvents except 1,2-difluorobenzene. Characteristic ^{11}B and ^{31}P NMR data for the products **1-5** are given in Table 10.1. Moreover, **4** shows a sharp doublet resonance at 38.5 ppm ($^{1}J_{PSn}$ = 280 Hz) in the $^{119}Sn\{^{1}H\}$ NMR spectrum. Solutions of **3** in 1,2-difluorobenzene give a characteristic doublet resonance in the $^{29}Si\{^{1}H\}$ NMR spectrum at 16.1 ppm ($^{1}J_{SiP}$ = 17 Hz), which is in the range of previously reported silyliumphosphine cations.[29–31] The small $^{1}J_{SiP}$ coupling constant is also typical for such compounds.[29–

[31] The connectivity could further be confirmed by ^{29}Si, ^{1}H HMBC (cf. Supporting Information). By layering solutions of **1,2** and **4**-**6** in *o*-DFB with *n*-hexane, it was possible to obtain single-crystals of these products suitable for X-ray structure determination (Figure 10.2).

Table 10.1: Summary of characteristic heteronuclear NMR data in solution (cf. Supporting Information) for the obtained compounds **1**-**7b**.

	$^{31}P\{^{1}H\}$	^{31}P	$^{11}B\{^{1}H\}$	^{11}B
1a (CD_2Cl_2)	q, -115.9 $^{1}J_{BP}$ = 56 Hz	qm, -115.9 $^{1}J_{HP}$ = 409 Hz	s, -16.9 d, -36.7 $^{1}J_{BP}$ = 56 Hz	s, -16.9 m, -36.7
1b (CD_2Cl_2)	q, -119.3 $^{1}J_{BP}$ = 48 Hz	qq, -119.3 $^{1}J_{BP}$ = 48 Hz $^{1}J_{HP}$ = 418 Hz	d, -13.1 $^{1}J_{BP}$ = 48 Hz	td $^{1}J_{BP}$ = 48 Hz $^{1}J_{HB}$ = 118 Hz
2 (CD_2Cl_2)	q, -75.4 $^{1}J_{BP}$ = 59 Hz	tm, -75.4 $^{1}J_{HP}$ = 405 Hz	d, -34.5 $^{1}J_{BP}$ = 59 Hz	dt, -34.5 $^{1}J_{BP}$ = 59 Hz
3 (oDFB/C_6D_6-cap.)	q, -150.4 $^{1}J_{BP}$ = 59 Hz	tq, -150.4 $^{1}J_{HP}$ = 350 Hz	m, -36.5	dt, -36.5 $^{1}J_{BP}$ = 59 Hz
4 (CD_2Cl_2)	m, -146.7	tm, -146.7 $^{1}J_{HP}$ = 339 Hz	m, -34.2	m, -34.2
5 (CD_2Cl_2)	q, -160.8 $^{1}J_{BP}$ = 54 Hz	tq, -160.8 $^{1}J_{BP}$ = 54 Hz $^{1}J_{HP}$ = 353 Hz	d, -35.8 $^{1}J_{BP}$ = 54 Hz	td, -35.8 $^{1}J_{BP}$ = 54 Hz $^{1}J_{HB}$ = 103 Hz
6 (CD_2Cl_2)	dm, -76.1 $^{1}J_{PP}$ = 263 Hz dm, -186.7 $^{1}J_{PP}$ = 263 Hz	dt, -76.1 $^{1}J_{PP}$ = 263 Hz $^{1}J_{PH}$ = 374 Hz dd, -186.7 $^{1}J_{PP}$ = 263 Hz $^{1}J_{PH}$ ≈ 248 Hz	m, -31.0 d, -33.8 $^{1}J_{BP}$ = 56 Hz	t, -31.0 $^{1}J_{HB}$ ≈ 95 Hz dt, -33.8 $^{1}J_{BP}$ = 56 Hz $^{1}J_{HB}$ ≈ 106 Hz
7a (C_6D_6)	m, -165.1	m, -165.1	m, -35.1	m, -35.1
7b (Et_2O/C_6D_6-cap.)	m, -176.7	tm, -176.7 $^{1}J_{HP}$ ≈ 300 Hz	d, -8.9 $^{1}J_{BP}$=56 Hz	td, -8.9 $^{1}J_{BP}$ = 56 Hz $^{1}J_{HB}$ ≈ 113 Hz

Selected structural parameters of the crystal structures of **1a/b**, **2**, **4** and **5** are depicted in Table 10.2. Whereas the B-P bond length remains nearly constant throughout all structures between 1.90-1.94 Å, the P-E distances reveal an increase when moving down the group 14, as to be expected. Still, the P-E bond distances (Table 10.2) lie within the range of regular single bonds (e.g. P-C 1.85 Å, P-Ge 2.38, P-Sn 2.52 Å).[32] The C-B-P (113-120°) and B-P-E (108-112°) bond angles indicate the pseudotetrahedral environment of the chain atoms. All compounds feature a sterically favored antiperiplanar configuration as evident by the CB-PE torsion angles (Table 10.2). Structures **4** and **5** represent the first examples of parent phosphanylboranes coordinated to the heavier group 14 homologs Ge and Sn.

Table 10.2: Selected structural parameters of **1a**, **1b**, **2**, **4**, **5** and **7a** derived by single-crystal X-ray structure determination. Bond lengths are given in [Å] and angles in [°].

	B-P	P-E	C-B-P	B-P-E	CB-PE
1a	1.896(5)	-	119.7(7)	-	-
1b	1.987(9)	-	113.2(5)	-	-
2	1.924(3)	1.795(3)	120.4(2)	108.52(14)	-172.0(3)
4	1.948(3)	2.3417(8)	118.2(2)	112.45(10)	166.88(18)
5	1.943(6)	2.5455(13)	120.3(3)	107.69(17)	178.7(4)
7a	1.916(9)	2.425(3)	114.1(5)	112.0(3)	163.48(17)

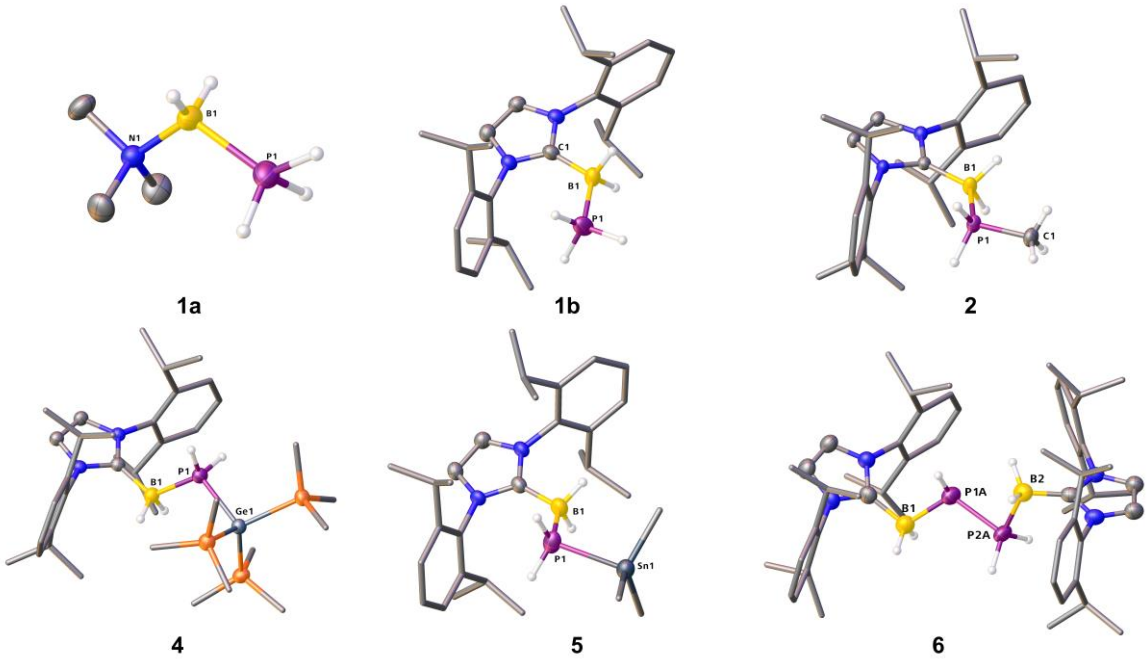

Figure 10.2: Molecular structures of the cations of **1a/b**, **2**, **4**, **5** and **6** in the solid state. Anisotropic displacement ellipsoids are drawn at 50% probability. Counterions and hydrogen atoms bound to carbon are omitted for clarity. Dipp groups are displayed as stick models for improved clarity.

After the successful functionalization by group 14 electrophiles, the question arose, if a similar reaction can be achieved with suitable group 15 electrophiles. Similar to the other conversions, reactions of **A** with *in situ* generated pnictogenium ions from $Cy_2PnBr/Tl[PF_6]$ (*Pn* = P, As) were performed, potentially leading to 13/15/15 cationic chain compounds. Surprisingly, these compounds cannot be detected but instead P-P coupling yielding $[IDipp{\cdot}BH_2PH_2\text{-}PHBH_2{\cdot}IDipp][PF_6]$ (**6**, Scheme 10.3) under extrusion of Cy_2PnH. A similar P-P coupling reaction for phosphanylboranes has already been reported by reaction of $Me_3N{\cdot}BH_2PH_2$ with Tl[TEF][27] in dichloromethane.[19] In accordance, the $^{31}P\{^1H\}$ NMR spectra of both reaction solutions (Scheme 10.3) show two broadened doublets at -76.1 ppm and -186.7 ppm coupled by $^1J_{PP}$ = 263 Hz.

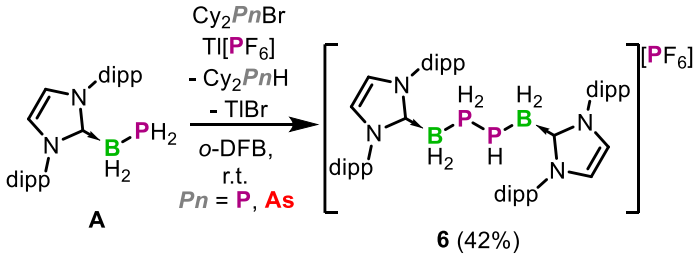

Scheme 10.3: Reaction of A with *in situ* generated pnictogenium ions.

Whereas the reported analogue $[Me_3N{\cdot}BH_2PH_2\text{-}PH_2BH_2{\cdot}NMe_3]^+$ cation could only be characterized by multinuclear NMR spectroscopy and MS, it was now possible to grow single-crystals of **6** suitable for X-ray structure determination (Figure 10.2). The structure in the solid-state shows a zigzag chain structure, albeit heavily disordered (cf. Supporting Information), which impedes a detailed discussion of the bond parameters.

Intrigued by the obtained structural motifs, the question arose, if such compounds display interesting patterns of reactivity. Especially, the focus relied on the protonated phosphanylboranes **1a** and **1b**, which offered the possibility for further reactions with main group hydrides under elimination of hydrogen. Thus, possible conversion with $LiAlH_4$ and $LiGaH_4$, respectively, were targeted.

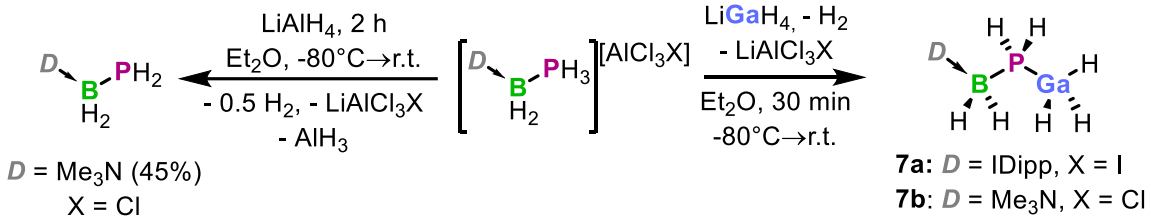

Scheme 10.4: Reactions of protonated parent phosphanylboranes with $LiGaH_4$ and $LiAlH_4$.

Reacting **1a/b** with $LiGaH_4$ in diethylether at -80 °C (Scheme 10.4, right) shows the clean formation of a new product each according to ^{31}P NMR spectra of the reaction mixture. In both cases, downfield shifted signals at -211.2 ppm (*D* = IDipp, broad s, $\omega_{1/2} \approx 603$ Hz) and -176.7 ppm (*D* = Me_3N, t, $^1J_{PH} = 294$ Hz), respectively, are observed with significantly enlarged $^1J_{PH}$ coupling constants compared to the substrates which overall indicates the formation of the desired hydride chain compounds $D{\cdot}BH_2PH_2GaH_3$ (**7a**: *D* = IDipp; **7b**: *D* = Me_3N). It was also possible to obtain single-crystals of $IDipp{\cdot}BH_2PH_2GaH_3$ (**7a**) suitable for X-ray structure determination, which confirm the structural assignment (Figure 10.3). **7a** crystallizes in the orthorhombic space group *Cmce* as clear colorless plates contains 0.5 molecules of **7a** as a mirror plane runs straight through the center of the molecule (through C2-B1-Ga; cf. Supporting Information). All atoms of the central chain motif are bound in (pseudo)tetrahedral fashion. The B1-P1 bond (1.916(9) Å) lies within the range of regular B-P single bonds (cf. $Me_3N{\cdot}BH_2PH_2$: B-P 1.976(2) Å)[13] and the Ga1-P1 bond (2.425(3) Å) is significantly longer than a regular Ga-P single bond (cf. $IDipp{\cdot}GaH_2PH_2$: Ga-P 2.3373(6) Å).[15] So far, it was not possible to grow suitable single-crystals of **7b** to determine its structure in the solid state.

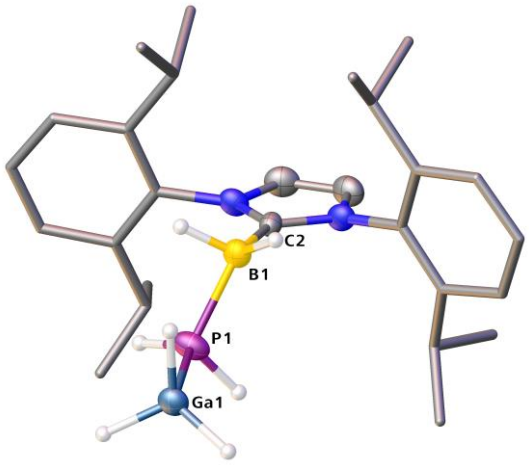

Figure 10.3: Molecular structure of $IDipp{\cdot}BH_2PH_2GaH_3$ (**7a**) in the solid-state. Anisotropic displacement ellipsoids are drawn at 50% probability. Disordered parts and hydrogen atoms bound to carbon are omitted for clarity. Dipp groups are displayed as stick models for improved clarity.

Reproductions and isolation of clean **7a/b** are still undergoing. Both compounds would not only represent rare examples of 13/15/13 parent hydride compounds containing a heavy group 13 element, but

also the first molecules with a terminal {GaH_3} unit bound to a primary phosphine. On the other side, performing the same reaction with $LiAlH_4$ (Scheme 10.4, left) or any other suitable base instead yields deprotonation and the parent phosphanylborane is obtained instead, which provides a, new alternative preparation of these type of compounds, opposed to salt metathesis or methanolytic pathways.

10.3 Conclusion

In summary, it was possible to synthesize a plethora of new cationic 13/15 compounds functionalized by main group electrophiles. Besides protonation of IDipp·BH_2PH_2 (**A**) yielding [*D*·BH_2PH_3][WCA] (**1a**: *D* = IDipp, WCA = X; **1b**: *D* = NMe_3, WCA = $AlCl_4$), a library of novel mixed 13/14/15 cationic chain compounds [IDipp·BH_2PH_2E][WCA] (**2**: E = CH_3, WCA = OTf; **3**: E = $SiEt_3$, WCA = TEF; **4**: E = $Ge(SiMe_3)_3$, WCA = TEF; **5**: E = $SnMe_3$, WCA = TEF) featuring the entire range from C-Sn could be synthesized and characterized by multinuclear NMR spectroscopy, ESI-MS and single-crystal X-ray structure determination. The compounds are highly sensitive to air and the heavier congeners (Si-Sn) will readily decompose upon contact with unsilylated glass surfaces. Reactions of **A** with the *in situ* generated pnictogenium ions [Cy_2Pn][PF_6] (*Pn* = P, As) unexpectedly resulted in a P-P coupling reaction instead, leading to [IDipp·BH_2PH_2-$PHBH_2$·IDipp][PF_6] (**6**) as verified by NMR spectroscopy, ESI-MS and single-crystal X-ray structure determination. Closer examination of the underlying mechanism by computational methods is still pending. Furthermore, the protonated compounds **1a/b** can react with other main group hydrides under elimination of H_2. Thus, exposing **1a/b** to $LiAlH_4$ resulted in deprotonation resulting in the parent phosphanylborane, which represents an alternative synthetic access towards this type of compounds. On the contrary, the reaction of **1a/b** with $LiGaH_4$ produced the unprecedented parent hydride containing neutral 13/15/13 chain compounds *D*·$BH_2PH_2GaH_3$ (**7a**: *D* = IDipp; **7b**: *D* = Me_3N) which represent the first examples of isolable compounds containing a terminal {GaH_3} unit bound to a primary phosphine. Future work will focus on the reactivity of the protonated moieties and exploring their potential as building blocks for the formation of novel 13/14/15 neutral element hydride chain compounds. Moreover, the chemistry of the unique donor stabilized *D*·$BH_2PH_2GaH_3$ element hydrides offer plenty of possibilities for subsequent studies regarding hydride abstraction etc. and will be investigated, as well.

10.4 References

[1] a) A. J. Arduengo, R. L. Harlow, M. Kline, *J. Am. Chem. Soc.* **1991**, *113*, 361–363; b) H.-W. Wanzlick, H.-J. Schönherr, *Angew. Chem. Int. Ed. Engl.* **1968**, *7*, 141–142; c) S. Würtemberger-Pietsch, U. Radius, T. B. Marder, *Dalton Trans.* **2016**, *45*, 5880–5895; d) A. Doddi, M. Peters, M. Tamm, *Chem. Rev.* **2019**, *119*, 6994–7112; e) M. N. Hopkinson, C. Richter, M. Schedler, F. Glorius, *Nature* **2014**, *510*, 485–496; f) V. Nesterov, D. Reiter, P. Bag, P. Frisch, R. Holzner, A. Porzelt, S. Inoue, *Chem. Rev.* **2018**, *118*, 9678–9842; g) Y. Wang, G. H. Robinson, *Inorg. Chem.* **2014**, *53*, 11815–11832; h) P. Bellotti, M. Koy, M. N. Hopkinson, F. Glorius, *Nat. Rev. Chem.* **2021**, *5*, 711–725.

[2] a) U. S. D. Paul, U. Radius, *Eur. J. Inorg. Chem.* **2017**, *2017*, 3362–3375; b) V. Lavallo, Y. Canac, C. Präsang, B. Donnadieu, G. Bertrand, *Angew. Chem. Int. Ed.* **2005**, *44*, 5705–5709; c) M. Soleilhavoup, G. Bertrand, *Acc. Chem. Res.* **2015**, *48*, 256–266; d) M. Melaimi, R. Jazzar, M. Soleilhavoup, G. Bertrand, *Angew. Chem. Int. Ed.* **2017**, *56*, 10046–10068.

[3] a) C. Camp, J. Arnold, *Dalton Trans.* **2016**, *45*, 14462–14498; b) A. D. Phillips in *Organometallic Chemistry* (Hrsg.: I. J. S. Fairlamb, J. M. Lynam), Royal Society of Chemistry, Cambridge, **2014**, S. 72–147; c) Y.-C. Tsai, *Coord. Chem. Rev.* **2012**, *256*, 722–758; d) J. R. Khusnutdinova, D. Milstein, *Angew. Chem. Int. Ed.* **2015**, *54*, 12236–12273; e) N. Govil, B. Jana, *Inorg. Chim. Acta* **2021**, *515*, 120037.

[4] A. A. Omaña, R. K. Green, R. Kobayashi, Y. He, E. R. Antoniuk, M. J. Ferguson, Y. Zhou, J. G. C. Veinot, T. Iwamoto, A. Brown et al., *Angew. Chem. Int. Ed.* **2021**, *60*, 228–231.

[5] a) J. Sinclair, G. Dai, R. McDonald, M. J. Ferguson, A. Brown, E. Rivard, *Inorg. Chem.* **2020**, *59*, 10996–11008; b) J. Bykowski, J. Sinclair, J. Trach, M. J. Ferguson, E. Rivard, *Dalton Trans.* **2023**, *52*, 1602–1607; c) W. Del Medroa Pino, A. A. Ferero Pico, M. Gupta, E. Rivard, *Chem. Commun.* **2023**, *59*, 6849–6852; d) S. Schulz, *Coord. Chem. Rev.* **2001**, *215*, 1–37; e) R. L. Wells, W. L. Gladfelter, *J. Clust. Sci.* **1997**, *8*, 217–238; f) S. Schulz, *Adv. Organomet. Chem.* **2003**, *49*, 225–317.

[6] a) M. Balmer, M. Kapitein, C. von Hänisch, *Dalton Trans.* **2017**, *46*, 7074–7081; b) G. Dübek, D. Franz, C. Eisenhut, P. J. Altmann, S. Inoue, *Dalton Trans.* **2019**, *48*, 5756–5765; c) D. Franz, T. Szilvási, A. Pöthig, S. Inoue, *Chem. Eur. J.* **2019**, *25*, 11036–11041; d) S. Schneider, C. Hänisch, *Eur. J. Inorg. Chem.* **2021**, *2021*, 4655–4660; e) M. Fan, R. T. Paine, E. N. Duesler, H. Nöth, *Z. Anorg. Allg. Chem.* **2006**, *632*, 2443–2446; f) H. Nöth, W. Tinhof, *Chem. Ber.* **1975**, *108*, 3109–3124.

[7] a) F.-G. Fontaine, D. W. Stephan, *Philos. Trans. R. Soc. A.* **2017**, *375*; b) A. R. Jupp, D. W. Stephan, *Trends Chem.* **2019**, *1*, 35–48; c) D. W. Stephan, *J. Am. Chem. Soc.* **2015**, *137*, 10018–10032; d) D. W. Stephan, *Acc. Chem. Res.* **2015**, *48*, 306–316; e) D. W. Stephan, *Science* **2016**, *354*; f) D. W. Stephan, G. Erker, *Angew. Chem. Int. Ed.* **2010**, *49*, 46–76; g) D. W. Stephan, G. Erker, *Angew. Chem. Int. Ed.* **2015**, *54*, 6400–6441.

[8] A. Bücker, C. Wölper, G. Haberhauer, S. Schulz, *Chem. Comm.* **2022**, *58*, 9758–9761.

[9] B. Rao, R. Kinjo, *Angew. Chem. Int. Ed.* **2019**, *58*, 18150–18153.

[10] M. T. Ackermann, M. Seidl, F. Wen, M. J. Ferguson, A. Y. Timoshkin, E. Rivard, M. Scheer, *Chem. Eur. J.* **2022**, *28*, e20210370.

[11] M. T. Ackermann, M. Seidl, R. Grande, Y. Zhou, M. J. Ferguson, A. Y. Timoshkin, E. Rivard, M. Scheer, *Chem. Sci.* **2023**, *14*, 2313–2317.

[12] M. Fernández-Millán, L. K. Allen, R. García-Rodríguez, A. D. Bond, M. E. G. Mosquera, D. S. Wright, *Chem. Commun.* **2016**, *52*, 5993–5996.

[13] K.-C. Schwan, A. Y. Timoshkin, M. Zabel, M. Scheer, *Chem. Eur. J.* **2006**, *12*, 4900–4908.

[14] C. Marquardt, O. Hegen, M. Hautmann, G. Balázs, M. Bodensteiner, A. V. Virovets, A. Y. Timoshkin, M. Scheer, *Angew. Chem. Int. Ed.* **2015**, *54*, 13122–13125.

[15] M. A. K. Weinhart, A. S. Lisovenko, A. Y. Timoshkin, M. Scheer, *Angew. Chem. Int. Ed.* **2020**, *59*, 5541-5545; *Angew. Chem.* **2020**, *132*, 5586-5590.

[16] M. A. K. Weinhart, M. Seidl, A. Y. Timoshkin, M. Scheer, *Angew. Chem.* **2021**, *133*, 3850–3855; *Angew. Chem. Int. Ed.* **2021**, *60*, 3806–3811.

[17] R. Szlosek, M. A. K. Weinhart, G. Balázs, M. Seidl, L. Zimmermann, M. Scheer, *Chem. Eur. J.* **2023**, *29*, e202300340.

[18] a) J. Braese, A. Schinabeck, M. Bodensteiner, H. Yersin, A. Y. Timoshkin, M. Scheer, *Chem. Eur. J.* **2018**, *24*, 10073–10077; b) M. Elsayed Moussa, J. Braese, C. Marquardt, M. Seidl, M. Scheer, *Eur. J. Inorg. Chem.* **2020**, *26*, 2501–2505; c) M. Elsayed Moussa, C. Marquardt, O. Hegen, M. Seidl, M. Scheer, *New J. Chem.* **2021**, *45*, 14916–14919; d) K.-C. Schwan, A. Adolf, M. Bodensteiner, M. Zabel, M. Scheer, *Z. Anorg. Allg. Chem.* **2008**, *634*, 1383–1387.

[19] R. Szlosek, M. T. Ackermann, C. Marquardt, M. Seidl, A. Y. Timoshkin, M. Scheer, *Chem. Eur. J.* **2023**, *29*, e202202911.

[20] M. Elsayed Moussa, T. Kahoun, M. T. Ackermann, M. Seidl, M. Bodensteiner, A. Y. Timoshkin, M. Scheer, *Organometallics* **2022**, *41*, 1572–1578.

[21] a) C. Thoms, C. Marquardt, A. Y. Timoshkin, M. Bodensteiner, M. Scheer, *Angew. Chem. Int. Ed.* **2013**, *52*, 5150–5154; b) C. Marquardt, T. Jurca, K.-C. Schwan, A. Stauber, A. V. Virovets, G. R. Whittell, I. Manners, M. Scheer, *Angew. Chem. Int. Ed.* **2015**, *54*, 13782–13786; c) A. V. Butlak, I. V. Kazakov, A. Stauber, O. Hegen, M. Scheer, A. V. Pomogaeva, A. Y. Timoshkin, *Eur. J. Inorg. Chem.* **2019**, *2019*, 3885–3891; d) J. Braese, F. Lehnfeld, V. T. Annibale, T. Oswald, R. Beckhaus, I. Manners, M. Scheer, *Chem. Eur. J.* **2023**, *29*, e202301741; e) M. Bodensteiner, U. Vogel, A. Y. Timoshkin, M. Scheer, *Angew. Chem. Int. Ed.* **2009**, *48*, 4629–4633; f) M. Bodensteiner, A. Y. Timoshkin, E. V. Peresypkina, U. Vogel, M. Scheer, *Chem. Eur. J.* **2013**, *19*, 957–963.

[22] R. Szlosek, M. Seidl, G. Balázs, M. Scheer, *Chem. Eur. J.* **2023**, *29*, e202301752.

[23] a) O. Hegen, C. Marquardt, A. Y. Timoshkin, M. Scheer, *Angew. Chem. Int. Ed.* **2017**, *56*, 12783–12787; b) O. Hegen, A. V. Virovets, A. Y. Timoshkin, M. Scheer, *Eur. J. Inorg. Chem.* **2018**, *24*, 16521-16525; c) F. Lehnfeld, M. Seidl, A. Y. Timoshkin, M. Scheer, *Eur. J. Inorg. Chem.* **2022**, *3*, e202100930; d) C. Marquardt, A. Adolf, A. Stauber, M. Bodensteiner, A. V. Virovets, A. Y. Timoshkin, M. Scheer, *Chem. Eur. J.* **2013**, *19*, 11887–11891; e) C. Marquardt, T. Kahoun, J. Baumann, A. Y. Timoshkin, M. Scheer, *Z. Anorg. Allg. Chem.* **2017**, *643*, 1326–1330; f) C. Marquardt, G. Balázs, J. Baumann, A. V. Virovets, M. Scheer, *Chem. Eur. J.* **2017**, *23*, 11423–11429; g) C. Marquardt, C. Thoms, A. Stauber, G. Balázs, M. Bodensteiner, M. Scheer, *Angew. Chem. Int. Ed.* **2014**, *53*, 3727–3730; h) C. Marquardt, T. Kahoun, A. Stauber, G. Balázs, M. Bodensteiner, A. Y. Timoshkin, M. Scheer, *Angew. Chem. Int. Ed.* **2016**, *55*, 14828–14832.

[24] a) I. Fernández, G. Frenking, *Faraday Discuss.* **2007**, *135*, 403-421; b) *Tin chemistry. Fundamentals, frontiers, and applications*, Wiley, Chichester, West Sussex, **2008**; c) M. Janssen, S. Mebs, J. Beckmann, *Chem. Commun.* **2023**, *59*, 7267–7270; d) P. M. Keil, T. J. Hadlington, *Z. Anorg. Allg. Chem.* **2022**, *648*; e) H. F. T. Klare, L. Albers, L. Süsse, S. Keess, T.

Müller, M. Oestreich, *Chem. Rev.* **2021**, *121*, 5889–5985; f) V. Y. Lee (Hrsg.) *Organogermanium Compounds*, Wiley, **2023**; g) S. Stigler, S. Fujimori, A. Kostenko, S. Inoue, *Chem. Sci.* **2024**, *15*, 4275–4291.

[25] M. Brookhart, B. Grant, A. F. Volpe, *Organometallics* **1992**, *11*, 3920–3922.

[26] H. Grützmacher, M. Bispringhoff, WO 2019/175319 A1.

[27] M. Gonsior, I. Krossing, *Z. Anorg. Allg. Chem.* **2002**, *628*, 1821–1830.

[28] I. Krossing, H. Brands, R. Feuerhake, S. Koenig, *J. Fluor. Chem.* **2001**, *112*, 83–90.

[29] T. J. Herrington, B. J. Ward, L. R. Doyle, J. McDermott, A. J. P. White, P. A. Hunt, A. E. Ashley, *Chem. Commun.* **2014**, *50*, 12753–12756.

[30] M. H. Holthausen, J. M. Bayne, I. Mallov, R. Dobrovetsky, D. W. Stephan, *J. Am. Chem. Soc.* **2015**, *137*, 7298–7301.

[31] K. M. Riley, A. L. Wierschen, S. J. Lee, M. R. Gagné, *Organometallics* **2020**, *39*, 1683–1687.

[32] a) S. Pelzer, B. Neumann, H.-G. Stammler, N. Ignat'ev, B. Hoge, *Angew. Chem. Int. Ed.* **2016**, *55*, 6088–6092; b) O. Fuhr, D. Fenske, *Z. Anorg. Allg. Chem.* **2004**, *630*, 244–246; c) P. Pyykkö, M. Atsumi, *Chem. Eur. J.* **2009**, *15*, 186–197.

10.5 Supporting Information

10.5.1 General Information

10.5.1.1 Working Techniques

All working steps were carried out under argon (4.6) inert gas atmosphere using standard Schlenk and glove-box techniques. Glassware was dried in an oven at 150 °C and pre-conditioned in high vacuum ($p < 10^{-3}$ mbar, 650 °C) shortly before use. The protective gas was purified from traces of H_2O and O_2 by passing it through a BASF R 3-11 ($CuO/MgSiO_3$) catalyst, concentrated H_2SO_4, Orange Gel and Sicapent® supported on pumice stone. Prior to use, solvents were purified using an MBraun SPS-800 solvent purification system, degassed by freeze-pump-thaw cycles, and stored over molecular sieves for at least 48 hours. C_6D_6 was dried over Na/K, distilled, degassed at room temperature, and stored over molecular sieves (4 Å). CD_2Cl_2 was dried over CaH_2, distilled, and degassed by freeze-pump-thaw. Elemental Analysis (CHN) was performed by the in-house facility. Mass spectra were recorded on a Jeol AccuTOF GCX mass spectrometer (LIFDI-MS) or Agilent Q-TOF 6540 UHD (ESI-MS) by the in-house facility. Glassware was silanized by heating neat TMSCl to reflux for one hour (subsequent rinsing with toluene and drying *in vacuo*).

$LiGaH_4$,[1] IDipp·BH_2PH_2,[2] Tl[TEF],[3] [Ph_3C][TEF],[4] Me_3N·BH_2Cl,[5] IDipp·BH_2I,[2] Cy_2AsBr,[6] and [$H(OEt_2)_2$][$B(C_6F_5)_4$][7] were prepared according to literature procedures. H_3P·$AlCl_3$ was prepared according to a slightly modified literature procedure.[8] Me(OTf), Me_3SnBr and $HGe(SiMe_3)_3$ were purchased from Sigma Aldrich and used as received. Tl[PF_6] was purchased from ABCR and used as received. $LiAlH_4$ was purified by extraction with diethylether from the crude reagent.

10.5.1.2 Spectroscopic Analysis

All NMR spectra were recorded on a BRUKER Avance 400 (frequencies: ^{1}H: 400.13 MHz, ^{29}Si: 79.49 MHz, ^{31}P: 161.98 MHz, ^{19}F: 376.50 MHz, ^{11}B: 128.43, ^{119}Sn: 149.21) or Avance 300 (^{1}H: 300.13 MHz) spectrometers. Substances of reference are $Si(CH_3)_4$ (^{1}H, ^{29}Si), 85 % H_3PO_4 (^{31}P), $CFCl_3$ (^{19}F), 90% Me_4Sn in C_6D_6 (^{119}Sn) and BF_3·Et_2O (^{11}B). Chemical shifts δ are presented in ppm referring to the external standards and coupling constants J are given in Hz without consideration of absolute signs.

10.5.2 Experimental Details

10.5.2.1 Preparation of $H_3P{\cdot}AlCl_3$ (stock solution in toluene)

Warning: PH_3 is an extremely pyrophoric and toxic gas that should only be handled at utmost care. It is vital to use only high quality tubings and glassware. It is recommended to secure every tube connection from an unexpected pop-off and wear appropriate personal protective equipment at all times. The stock solution of $H_3P{\cdot}AlCl_3$ is also highly sensitive towards air and reacts vigorously with traces of oxygen or water.

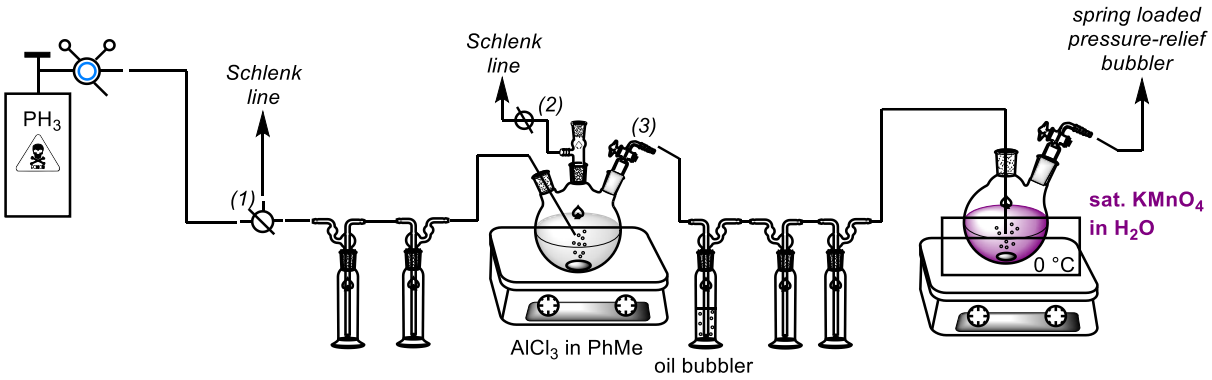

Figure S 10.1: Schematic apparatus for the preparation of a stock solution of $H_3P{\cdot}AlCl_3$ under inert conditions. Individual description: (1) 3-way connection, (2) ground glass attachment for the addition of solvents, (3) outlet for quenching excess PH_3.

A 100 mL two-necked round-bottom flask (as displayed in Figure S 10.1) was charged with $AlCl_3$ (3.333 g, 0.025 mol) and the solids suspended in roughly 50 mL of toluene. Then, the apparatus was assembled by cycling the individual parts (left: PH_3 bottle + two washing bottles, middle: round-bottom flask, right: three washing bottles + empty round bottom flask) separately onto the Schlenk line and then each part was connected. Subsequently, a saturated solution of $KMnO_4$ was prepared and filled into the corresponding round-bottom flask (Figure S 10.1) under a stream of inert gas and the solution cooled using an ice-bath. Stopcocks (*1*)+(*2*) were closed from the Schlenk line and (*3*) opened for the release of excess PH_3 gas. Then, a gently stream of PH_3 is introduced from (*1*)→(*3*) until the $AlCl_3$ has dissolved completely and a clear colourless solution was obtained. The flow of PH_3 was then stopped and the apparatus purged from (1)→(3) with inert gas for at least 10 min (and also for a few minutes from (2)→(3)). The tubing between the PH_3 bottle and (*1*) cannot be purged effectively, but any residual PH_3 can be removed here by repeated vacuum/Ar cycles on the Schlenk line (*care needs to be taken when the cooling traps of the Schlenk line are disassembled after the experiment*!). The stock solution can now be transferred to e.g., a Teflon tapped ampoule for long term storage and the concentration can be determined by NMR spectroscopy.

^{1}H NMR (400.30 MHz, PhMe-d_8-cap., 298 K): 1.74/2.69 (d, $^1J_{HP}$ = 374 Hz).

^{31}P{^{1}H} NMR (161.98 MHz, PhMe-d_8-cap., 298 K): -169.0 (s).

^{31}P NMR (161.98 MHz, PhMe-d_8-cap., 298 K): -169.0 (q, $^1J_{HP}$ = 374 Hz).

The NMR data agree with literature values.[8]

10.5.2.2 Synthesis of [IDipp·BH_2PH_3][BAr^F] (1a)

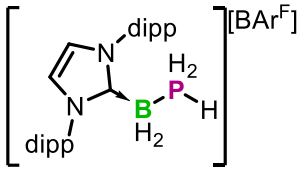

A mixture of IDipp·BH_2PH_2 (217 mg, 0.5 mmol) and [$H(OEt_2)_2$][$B(C_6F_5)_4$] (414 mg, 0.5 mmol) was dissolved in *ortho*-difluorobenzene and the solution stirred for one hour at room temperature. The product was precipitated by the addition of the fourfold amount of *n*-pentane and the supernatant decanted. The crude oily product was washed twice with *n*-pentane and subsequently dried *in vacuo*, yielding [IDipp·BH_2PH_3][BAr^F] as white solids (415 mg, 74%).

^{1}H NMR (400.30 MHz, CD_2Cl_2, 298 K): 1.22 (d, 12 H, 4 × ^{i}Pr-CH_3, $^3J_{HH}$ = 6.81 Hz), 1.28 (d, 12 H, 4 × ^{i}Pr-CH_3, $^3J_{HH}$ = 6.81 Hz), 1.68 (q, broad, 2 H, $^3J_{HB}$ = 113 Hz), 2.37 (sep, 4 H, 4 × ^{i}Pr-CH, $^3J_{HH}$ = 6.81 Hz), 3.26/4.28 (dt, 3 H, $^1J_{PH}$ = 408.44 Hz, PH_2, $^3J_{HH}$ = 8.14 Hz), 7.43 (s superimposed with d, 2 H, NCHCHN), 7.44 (d superimposed with s, 4 H, 4 × aryl-C$_{meta}H$, $^3J_{HH}$ = 7.99 Hz), 7.65 (t, 2 H, 2 × aryl-C$_{para}$H, $^3J_{HH}$ = 7.99 Hz).

^{31}P{^{1}H} NMR (161.98 MHz, CD_2Cl_2, 298 K): -116.2 (q, broad, $^1J_{PB}$ = 56 Hz).

^{31}P NMR (161.98 MHz, CD_2Cl_2, 298 K): -116.2 (qm, broad, $^1J_{HP}$ = 409 Hz).

^{11}B{^{1}H} NMR (128.38 MHz, CD_2Cl_2, 298 K): -16.9 (s, $B(C_6F_5)_4$), -36.7 (d, $^1J_{PB}$ = 56 Hz).

^{11}B NMR (128.38 MHz, CD_2Cl_2, 298 K): -16.9 (s, $B(C_6F_5)_4$), -36.7 (td, broad, $^1J_{PB}$ = 56 Hz, $^3J_{HB}$ = 113 Hz).

^{19}F{^{1}H} NMR (376.50 MHz, CD_2Cl_2, 298 K): -133.0 (s, 2 F, broad, *ortho*-F), -163.6 (t, 1 F, $^3J_{FF}$ = 20.5 Hz, *para*-F), - 167.5 (t, slightly broad, 2 F, $^3J_{FF}$ = 20.5 Hz, *meta*-F).

ESI-MS (*m/z*, 1,2-difluorobenzene, pos. mod.): *m/z* = 389.2963 (81%, [IDipp-H]$^+$), 401.3252 (66%, [IDipp·BH_2]$^+$), 435.3114 (100%, [IDipp·BH_2PH_3]$^+$), 835.6186 (1%, [IDipp·$BH_2PH_2BH_2$·IDipp]$^+$).

Elemental Analysis ($C_{51}H_{41}B_2F_{20}N_2P$) **[%]:** calcd. C 54.96, H 3.71, N 2.51; found C 54.67, H 3.97, N 2.61.

10.5.2.3 Synthesis of [Me_3N·BH_2PH_3][$AlCl_4$] (1b)

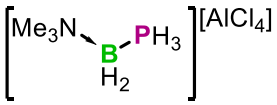

H_3P·$AlCl_3$ (1.5 mL, 2.7 M in toluene, 4.06 mmol) was added *via* syringe to a solution of Me_3N·BH_2Cl (218 mg, 2.03 mmol) in toluene, upon which the mixture instantly turned cloudy by partial precipitation of the product. After stirring for two hours at room temperature, the remaining dissolved product was precipitated by the addition of *n*-hexane and the supernatant was decanted off. The solids were washed twice with *n*-hexane. Subsequently, the product was dried *in vacuo*, yielding [Me_3N·BH_2PH_3][$AlCl_4$] as a colourless powder (202 mg, 31%).

^{1}H NMR (400.30 MHz, CD_2Cl_2, 298 K): 2.93 (s, N(CH_3)$_3$, 9 H), 2.07-2.91 (qm, broad, $^1J_{BH}$ = 118 Hz), 4.51/5.56 (dt, $^1J_{HP}$ = 418 Hz, $^3J_{HH}$ = 6.74 Hz).

^{31}P{^{1}H} NMR (161.98 MHz, CD_2Cl_2, 298 K): -119.3 (q, $^1J_{PB}$ = 48 Hz).

^{31}P NMR (161.98 MHz, CD_2Cl_2, 298 K): -119.3 (qq, broad, $^1J_{HP}$ = 418 Hz, $^1J_{PB}$ = 48 Hz).

^{11}B{^{1}H} NMR (128.38 MHz, CD_2Cl_2, 298 K): -13.1 (d, $^1J_{PB}$ = 48 Hz).

^{11}B NMR (128.38 MHz, CD_2Cl_2, 298 K): -13.1 (td, $^1J_{PB}$ = 26 Hz, $^1J_{BH}$ = 118 Hz).

ESI-MS (*m/z*, 1,2-difluorobenzene, pos. mod.): *m/z* = 209.1681 (100%, $[Me_3N{\cdot}BH_2PH_2PHBH_2{\cdot}NMe_3]^+$), 317.0814 (62%, unassignable ion peak). No molecular ion peak for **1b** could be observed.

Elemental Analysis ($C_3H_{14}AlBCl_4NP$ + 0.2 $[Me_3N\text{-}H][AlCl_4]$) **[%]:** calcd. C 13.49, H 5.03, N 5.24; found C 14.61, H 5.21, N 5.21. $[Me_3N\text{-}H][AlCl_4]$ is produced by thermal decomposition of the compound and remains as an inseparable impurity.

10.5.2.4 Synthesis of [IDipp·$BH_2PH_2CH_3$][OTf] (2)

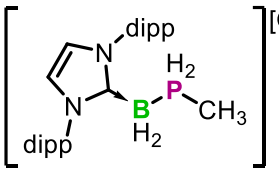

To a solution of IDipp·BH_2PH_2 (43 mg, 0.1 mmol) in toluene, neat Me(OTf) (0.5 mL, 0.2 M stock solution in toluene, 0.1 mmol) was added *via* syringe. After a few minutes, the solution slowly turned cloudy. The mixture was stirred overnight, and the solution decanted. The remaining precipitate washed once with toluene and once with *n*-hexane. The residue was dissolved in THF and layered with *n*-hexane at -30 °C, yielding colourless blocks of [IDipp·$BH_2PH_2CH_3$][OTf] (33 mg, 55%).

^{1}H NMR (400.30 MHz, CD_2Cl_2, 298 K): 1.12 (dt, superimposed, C*H*$_3$, 3 H, $^3J_{HH}$ = 6.67 Hz, $^2J_{HP}$ = 13.56 Hz), 1.22 (d, 12 H, 4 × ^{i}Pr-C*H*$_3$, $^3J_{HH}$ = 6.91 Hz), 1.28 (d, 12 H, 4 × ^{i}Pr-C*H*$_3$, $^3J_{HH}$ = 6.91 Hz), 1.48 (superimposed q, broad, $^1J_{BH}$ = 88.6 Hz, B*H*$_2$), 2.39 (sep, 4 H, 4 × ^{i}Pr-C*H*, $^3J_{HH}$ = 6.91 Hz), 3.90 (dm, 2 H, $^1J_{PH}$ = 403.6 Hz, P*H*$_2$), 7.42 (d, 4 H, 4 × aryl-C$_{meta}$*H*, $^3J_{HH}$ = 7.90 Hz), 7.45 (s, 2 H, NC*H*C*H*N), 7.64 (t, 2 H, 2 × aryl-C$_{para}$H, $^3J_{HH}$ = 7.90 Hz).

^{31}P{^{1}H} NMR (161.98 MHz, CD_2Cl_2, 298 K): -75.4 (q, $^1J_{PB}$ = 59 Hz).

^{31}P NMR (161.98 MHz, CD_2Cl_2, 298 K): -75.4 (tm, broad, $^1J_{HP}$ = 405 Hz).

^{11}B{^{1}H} NMR (128.38 MHz, CD_2Cl_2, 298 K): -34.5 (d, $^1J_{PB}$ = 59 Hz).

^{11}B NMR (128.38 MHz, CD_2Cl_2, 298 K): -34.5 (superimposing dt, $^1J_{PB} \approx$ 60 Hz, $^1J_{BH} \approx$ 100 Hz).

^{19}F{^{1}H} NMR (376.50 MHz, CD_2Cl_2, 298 K): -78.8 (s).

ESI-MS (*m/z*, 1,2-difluorobenzene, pos. mod.): *m/z* = 449.4087 (100%, $[IDipp{\cdot}BH_2PH_2CH_3]^+$).

Elemental Analysis ($C_{29}H_{43}BF_3N_2O_3PS$) **[%]:** calcd. C 58.20, H 7.24, N 4.68, S 5.36; found C 58.18, H 7.13, N 4.54, S 5.31.

10.5.2.5 Synthesis of [IDipp·$BH_2PH_2SiEt_3$][BAr^F] (3)

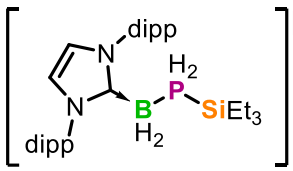

A mixture of IDipp·BH_2PH_2 (80 mg, 0.18 mmol) and [Et_3SiH-Et_3Si][BAr^F] (164 mg, 0.14 mmol) was dissolved in *ortho*-difluorobenzene and the reaction mixture was stirred for one hour at room temperature, resulting in a clear colourless solution. The volatiles were removed *in vacuo* and the residue washed twice *n*-pentane. Drying the product *in vacuo* yielded [IDipp·$BH_2PH_2SiEt_3$][BAr^F] as a colourless, highly electrostatic powder (94 mg, 43%).

^{1}H NMR (400.30 MHz, 1,2-difluorobenzene/C_6D_6-cap., 298 K): 0.49 (q, Et-CH_2, 6 H, $^3J_{HH}$ = 7.50 Hz), 0.62 (t, Et-CH_3, 9 H, $^3J_{HH}$ = 7.50 Hz), 1.03 (d, 12 H (partially superimposed), 4 × ^{i}Pr-CH_3, $^3J_{HH}$ = 6.84 Hz), 1.18 (d, 12 H, 4 × ^{i}Pr-CH_3, $^3J_{HH}$ = 6.84 Hz), 1.54 (superimposed q, 2 H, broad, $^1J_{BH} \approx$ 95 Hz, BH_2), 2.39 (sep, superimposed by PH_2 signal, 4 H, 4 × ^{i}Pr-CH, $^3J_{HH}$ = 7.50 Hz), 2.78 (dm, superimposed, 2 H, $^1J_{PH}$ = 350 Hz, PH_2), 7.16 (d, 4 H, 4 × aryl-C$_{meta}H$, $^3J_{HH}$ = 7.74 Hz), 7.20 (s, 2 H, NCHCHN), 7.31 (t, 2 H, 2 × aryl-C$_{para}$H, $^3J_{HH}$ = 7.74 Hz).

^{31}P{^{1}H} NMR (161.98 MHz, 1,2-difluorobenzene/C_6D_6-cap., 298 K): -150.4 (q, broad, $^1J_{PB}$ = 59 Hz).

^{31}P NMR (161.98 MHz, 1,2-difluorobenzene/C_6D_6-cap., 298 K): -150.4 (tm, broad, $^1J_{HP}$ = 350 Hz).

^{11}B{^{1}H} NMR (128.38 MHz, 1,2-difluorobenzene/C_6D_6-cap., 298 K): -16.5 (s, $B(C_6F_5)_4$), -36.5 (m, broad, BH_2).

^{11}B NMR (128.38 MHz, 1,2-difluorobenzene/C_6D_6-cap., 298 K): -16.5 (s, $B(C_6F_5)_4$), -36.5 (dt, superimposed, broad, $^1J_{HB}$ = 103 Hz, BH_2).

^{29}Si{^{1}H} NMR (79.49 MHz, 1,2-difluorobenzene/C_6D_6-cap., 298 K): 16.1 (d, $^1J_{SiP}$ = 17 Hz). *For ^{1}H, ^{29}Si HMBC: cf. section "NMR data".*

^{19}F{^{1}H} NMR (376.50 MHz, 1,2-difluorobenzene/C_6D_6-cap., 298 K): -133.0 (s, 2 F, broad, *ortho*-F), -164.0 (t, 1 F, $^3J_{FF}$ = 19.8 Hz, *para*-F), - 167.8 (t, slightly broad, 2 F, $^3J_{FF}$ = 19.8 Hz, *meta*-F).

ESI-MS (*m/z*, 1,2-difluorobenzene, pos. mod.): *m/z* = 401.3142 (41%, [IDipp·BH_2]$^+$), 435.3118 (100%, [IDipp·BH_2PH_3]$^+$). Does not show a molecular ion peak due to decomposition of the compound within the mass spectrometer.

10.5.2.6 Synthesis of [IDipp·$BH_2PH_2Ge(SiMe_3)_3$][TEF] (4)

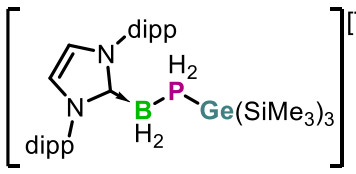

$HGe(SiMe_3)_3$ (0.2 mL, 0.487 M in PhMe, 0.1 mmol) was added to a solution of [Ph_3C][TEF] (121 mg, 0.1 mmol) in diethylether, resulting in a discoloration of the solution. After stirring for 15 min at room temperature, a solution of IDipp·BH_2PH_2 (43 mg, 0.1 mmol) in diethylether was added and the mixture stirred for 1.5 hours at room temperature. Subsequently, all volatiles were removed *in vacuo* and the solids dissolved in dichloromethane. The solution was layered with *n*-hexane and left to crystallize at -30 °C, resulting in

large colourless block-shaped crystals. The mother liquor was decanted off, the crystals washed with *n*-hexane repeatedly and dried *in vacuo* (60 mg, 35%).

^{1}H NMR (400.30 MHz CD_2Cl_2, 298 K): 1.12 (s, Si(CH_3)$_3$, ~ 18 H (superimposed)), 1.21 (d, superimposed, 12 H, 4 × ^{i}Pr-CH_3, $^{3}J_{HH}$ = 6.93 Hz), 1.29 (d, superimposed, ^{i}Pr-CH_3, $^{3}J_{HH}$ = 6.93 Hz), 2.37 (sep, superimposed, ^{i}Pr-C*H*, $^{3}J_{HH}$ = 6.93 Hz), 2.51/3.36 (dm, 2 H, $^{1}J_{PH}$ = 339 Hz, PH_2), 7.36 (s, 2 H, NC*H*C*H*N), 7.39 (d, 4 H, 4 × aryl-C$_{meta}$*H*, $^{3}J_{HH}$ = 7.87 Hz), 7.73 (t, 2 H, 2 × aryl-C$_{para}$H, $^{3}J_{HH}$ = 7.87 Hz). Note: signals partially overlap with resonances of inseparable [IDipp·BH_2PH_3]$^{+}$. The signal of the {BH_2} moiety could not be unambiguously assigned due to strong broadening and signal overlap.

^{31}P{^{1}H} NMR (161.98 MHz, CD_2Cl_2, 298 K): -146.7 (m, broad).

^{31}P NMR (161.98 MHz, CD_2Cl_2, 298 K): -146.7 (tm, broad, $^{1}J_{HP}$ = 339 Hz).

^{11}B{^{1}H} NMR (128.38 MHz, CD_2Cl_2, 298 K): -34.2 (m, broad).

^{11}B NMR (128.38 MHz, CD_2Cl_2, 298 K): -34.2 (m, broad).

^{19}F{^{1}H} NMR (376.50 MHz, CD_2Cl_2, 298 K): -75.6 (s).

ESI-MS (*m/z*, 1,2-difluorobenzene, pos. mod.): *m/z* = 401.3252 (66%, [IDipp·BH_2]$^{+}$), 435.3228 (100%, [IDipp·BH_2PH_3]$^{+}$), 727.3678 (20%, [IDipp·BH_2PH_2Ge($SiMe_3$)$_3$]$^{+}$).

Elemental Analysis ($C_{52}H_{67}AlBF_{36}GeN_2O_4PSi_3$) **[%]:** could not be performed as the product co-crystallizes with inseparable amounts of [IDipp-H][TEF] and [IDipp·BH_2PH_3][TEF] (cf. NMR and ESI-MS data).

10.5.2.7 Synthesis of [IDipp·$BH_2PH_2SnMe_3$][TEF] (5)

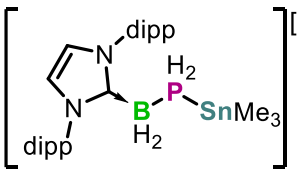

A mixture of IDipp·BH_2PH_2 (43 mg, 0.1 mmol) and Tl[TEF] (117 mg, 0.1 mmol) was dissolved in 1,2-difluorobenzene. Then, neat Me_3SnBr (0.02 mL, 0.1 mmol) was added *via* syringe. Immediately upon addition, white solids precipitated from the solution. The reaction mixture was stirred for two hours at room temperature and filtered through a glass fibre filter. After removing all volatiles *in vacuo*, the oily residue was washed once with toluene and three times with *n*-hexane. Drying in vacuo yielded the final product as greyish solids (52 mg, 33%). For crystallization, the solid residue was dissolved in dichloromethane, filtered and layered with *n*-hexane at -30 °C to give colourless blocks of [IDipp·$BH_2PH_2SnMe_3$][TEF].

^{1}H NMR (400.30 MHz, CD_2Cl_2, 298 K): 0.43 (d + dd(^{119}Sn satellites, $^{2}J_{HSn}$ = 58.56 Hz), Sn(CH_3)$_3$, 9 H, $^{3}J_{HP}$ = 5.28 Hz), 1.1 (d, 12 H, 4 × ^{i}Pr-CH_3, $^{3}J_{HH}$ = 6.93 Hz), 1.27 (d, 12 H, 4 × ^{i}Pr-CH_3, $^{3}J_{HH}$ = 6.93 Hz), 1.47 (superimposed q, broad, 2 H, $^{1}J_{HB}$ ≈100 Hz, BH_2), 2.21/3.07 (dm, 2 H, $^{1}J_{PH}$ = 353 Hz, PH_2), 2.40 (sep, 4 H, 4 × ^{i}Pr-C*H*, $^{3}J_{HH}$ = 6.93 Hz), 7.33 (s, 2 H, NC*H*C*H*N), 7.90 (d, 4 H, 4 × aryl-C$_{meta}$*H*, $^{3}J_{HH}$ = 7.88 Hz), 7.61 (t, 2 H, 2 × aryl-C$_{para}$H, $^{3}J_{HH}$ = 7.88 Hz).

^{1}H{^{11}B} NMR (400.30 MHz, CD_2Cl_2, 298 K): 0.43 (d + dd(^{119}Sn satellites, $^{2}J_{HSn}$ = 58.56 Hz), Sn(CH_3)$_3$, 9 H, $^{3}J_{HP}$ = 5.28 Hz), 1.1 (d, 12 H, 4 × ^{i}Pr-CH_3, $^{3}J_{HH}$ = 6.93 Hz), 1.27 (d, 12 H, 4 × ^{i}Pr-CH_3, $^{3}J_{HH}$ = 6.93 Hz), 1.47 (s, broad, 2 H, BH_2), 2.21/3.07 (dm, 2 H, $^{1}J_{PH}$ = 353 Hz, PH_2), 2.40 (sep, 4 H, 4 × ^{i}Pr-C*H*, $^{3}J_{HH}$ =

6.93 Hz), 7.33 (s, 2 H, NC*H*C*H*N), 7.90 (d, 4 H, 4 × aryl-C$_{meta}$*H*, $^{3}J_{HH}$ = 7.88 Hz), 7.61 (t, 2 H, 2 × aryl-C$_{para}$H, $^{3}J_{HH}$ = 7.88 Hz).

^{31}P{^{1}H} NMR (161.98 MHz, CD_2Cl_2, 298 K): -160.8 (q, $^{1}J_{PB}$ = 54 Hz).

^{31}P NMR (161.98 MHz, C_6D_6, 298 K): -160.8 (tq, very broad, $^{1}J_{HP}$ = 353 Hz, $^{1}J_{PB}$ = 54 Hz).

^{11}B{^{1}H} NMR (128.38 MHz, CD_2Cl_2, 298 K): -35.8 (d, broad, $^{1}J_{PB}$ = 54 Hz).

^{11}B NMR (128.38 MHz, CD_2Cl_2, 298 K): -35.8 (td, broad, $^{1}J_{PB}$ = 54 Hz, $^{1}J_{HB}$ = 103 Hz).

^{119}Sn{^{1}H} NMR (149.21 MHz, CD_2Cl_2, 298 K): 38.5 (d, $^{1}J_{PSn}$ = 280 Hz).

^{19}F{^{1}H} NMR (376.50 MHz, CD_2Cl_2, 298 K): -75.6 (s).

ESI-MS (*m/z*, 1,2-difluorobenzene, pos. mod.): *m/z* = 389.4161 (64%, [IDipp-H]$^+$), 401.4228 (100%, [IDipp·BH_2]$^+$), 436.4758 (97%, [IDipp·BH_2PH_3]$^+$), 599.5961 (1%, [IDipp·$BH_2PH_2SnMe_3$]$^+$).

Elemental Analysis ($C_{46}H_{49}AlBF_{36}N_2O_4PSn$) **[%]:** could not successfully be performed as the product co-crystallizes with inseparable amounts of [IDipp-H][TEF] and [IDipp·BH_2PH_3][TEF] (cf. ESI-MS data).

10.5.2.8 Reaction of IDipp·BH_2PH_2 with *in situ* generated [Cy_2E][PF_6] (E = P, As)

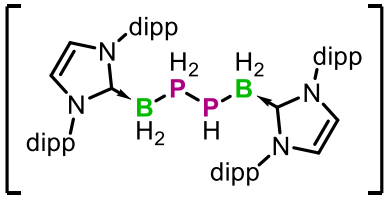

Reaction with Cy_2AsBr/Tl[PF_6]

A mixture of IDipp·BH_2PH_2 (65 mg, 0.15 mmol) and Tl[PF_6] was dissolved in *o*-DFB. Then, Cy_2AsBr (30 µL, 0.15 mmol) was added *via* syringe, resulting in an instant precipitation of TlBr. The mixture was stirred for 16 hours at room temperature and filtered through a glass fibre filter. The product was then precipitated by the addition of *n*-hexane and the solution decanted. The solids were subsequently washed twice with *n*-hexane and dried *in vacuo* to give [IDipp·$BH_2PH_2PHBH_2$·IDipp][PF_6] as a white powder (32 mg, 42%).

Reaction with Cy_2PBr/Tl[PF_6]

A mixture of IDipp·BH_2PH_2 (52 mg, 0.12 mmol) and Tl[PF_6] was dissolved in *o*-DFB. Then, Cy_2PBr (0.09 mL, 1.33 M in PhMe, 0.12 mmol) was added *via* syringe, resulting in an instant precipitation of TlBr. The mixture was stirred for 16 hours at room temperature and filtered through a glass fibre filter. The product was then precipitated by the addition of *n*-hexane and the solution decanted. The solids were subsequently washed twice with *n*-hexane and dried *in vacuo* to give [IDipp·$BH_2PH_2PHBH_2$·IDipp][PF_6] as a white powder (25 mg, 41%).

^{1}H NMR (400.30 MHz, CD_2Cl_2, 298 K): 0.49/1.11 (dm, ~ 1 H, $^{1}J_{PH} \approx$ 248 Hz, *P*H)1.09-1.19 (superimposing doublets, 48 H, ^{i}Pr-C*H*$_3$) 1.28 (d, 12 H, 4 × ^{i}Pr-C*H*$_3$, $^{3}J_{HH}$ = 6.91 Hz), 2.25 (sep, 4 H, 4 × ^{i}Pr-C*H*, $^{3}J_{HH}$ = 6.75 Hz), 2.34 (sep, 4 H, 4 × ^{i}Pr-C*H*, $^{3}J_{HH}$ = 7.01 Hz), 3.55/2.62 (dm, 1 H, $^{1}J_{PH}$ = 373.9 Hz, one diastereotopic proton of P*H*$_2$), 3.69/2.75 (dm, 1 H, $^{1}J_{PH}$ = 373.9 Hz, one diastereotopic proton of P*H*$_2$), 7.12 (s, 2 H, NC*H*C*H*N), 7.24 (s, 2 H, NC*H*C*H*N), 7.26 (d, superimposed, 4 × aryl-C$_{meta}$*H*, $^{3}J_{HH}$ = 7.79 Hz), 7.29 (d, 4 H, 4 × aryl-C$_{meta}$*H*, $^{3}J_{HH}$ = 7.74 Hz), 7.49 (t, 2 H, 2 × aryl-C$_{para}$H, $^{3}J_{HH}$ = 7.74 Hz), 7.49 (t, 2 H, 2 ×

aryl-C*para*H, $^{3}J_{HH}$ = 7.79 Hz). Due to strong signal overlap and line broadening, the signals of the {B*H*$_2$} protons could not unambiguously be assigned.

^{31}P{^{1}H} NMR (161.98 MHz, CD_2Cl_2, 298 K): -76.1 (dm, broad, $^{1}J_{PP}$ = 263 Hz, *P*H$_2$), -143.9 (sep, *P*F$_6$, $^{1}J_{PF}$ = 710 Hz), -186.7 (dm, broad, $^{1}J_{PP}$ = 263 Hz, *P*H).

^{31}P NMR (161.98 MHz, CD_2Cl_2, 298 K): -76.1 (dt, superimposed, broad, $^{1}J_{PP}$ = 263 Hz, $^{1}J_{PH}$ ≈ 374 Hz, *P*H$_2$), -143.9 (sep, *P*F$_6$, $^{1}J_{PF}$ = 710 Hz), -186.7 (dd, broad, $^{1}J_{PP}$ = 263 Hz, $^{1}J_{PH}$ ≈ 248 Hz, *P*H).

^{11}B{^{1}H} NMR (128.38 MHz, CD_2Cl_2, 298 K): -31.0 (m, broad, *B*H$_2$), -33.8 (d, broad, $^{1}J_{BP}$ ≈ 55 Hz, *B*H$_2$).

^{11}B NMR (128.38 MHz, CD_2Cl_2, 298 K): -31.0 (t, broad, $^{1}J_{BH}$ ≈ 95 Hz, *B*H$_2$), -33.8 (superimposed dt, broad, $^{1}J_{BH}$ ≈ 106 Hz, $^{1}J_{BP}$ ≈ 55 Hz *B*H$_2$).

^{19}F{^{1}H} NMR (376.50 MHz, CD_2Cl_2, 298 K): -73.5 (d, $^{1}J_{PF}$ = 710 Hz, P*F*$_6$).

ESI-MS (*m/z*, 1,2-difluorobenzene, pos. mod.): *m/z* = 867.6055 (100%, [IDipp·BH$_2$PH$_2$PHBH$_2$·IDipp]$^+$).

Elemental Analysis ($C_{54}H_{79}B_2F_6N_4P_3$+0.3 *n*-hexane C_6H_{14}) **[%]:** calcd. C 64.53, H 8.07, N 5.39; found C 64.97, H 7.94, N 5.37.

10.5.2.9 Synthesis of $Me_3N{\cdot}BH_2PH_2$ (deprotonation of $[Me_3N{\cdot}BH_2PH_3][AlCl_4]$)

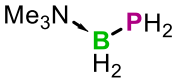

$LiAlH_4$ (7 mg, 0.18 mmol) was dissolved in dimethoxyethane (4.0 mL) and cooled to -80 °C. Then, a solution of $[Me_3N{\cdot}BH_2PH_3][AlCl_4]$ in dimethoxyethane (48 mg, 0.15 mmol) was added to the solution of $LiAlH_4$. After stirring at room temperature for two hours, full conversion to $Me_3N{\cdot}BH_2PH_2$ can be observed by multinuclear NMR spectroscopy. The product was isolated as a stock solution by condensation of all volatiles into a separate Schlenk tube under reduced pressure (Yield acc. to NMR spectroscopic determination with internal standard PPh_3: 45%)

^{31}P{^{1}H} NMR (161.98 MHz, C_6D_6-cap./Et_2O, 298 K): -217.6 (q, $^{1}J_{PB}$ = 28 Hz).

^{31}P NMR (161.98 MHz, C_6D_6-cap./Et_2O, 298 K): -217.6 (tq, broad, $^{1}J_{HP}$ = 187 Hz, $^{1}J_{PB}$ = 28 Hz).

^{11}B{^{1}H} NMR (128.38 MHz, C_6D_6-cap./Et_2O, 298 K): -6.1 (d, $^{1}J_{PB}$ = 28 Hz).

^{11}B NMR (128.38 MHz, C_6D_6-cap./Et_2O, 298 K): -6.1 (td, $^{1}J_{PB}$ = 26 Hz, $^{1}J_{BH}$ = 106 Hz).

The NMR data agrees with literature values.[9]

10.5.2.10 Synthesis of IDipp·$BH_2PH_2GaH_3$ (7a)

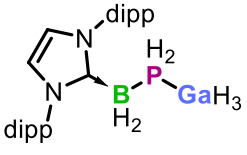

[IDipp·BH_2PH_3][BAr^F] (100 mg, 0.09 mmol) was dissolved in diethylether and cooled to -80 °C. Then, a solution of $LiGaH_4$ (7 mg, 0.09 mmol) in diethylether was added. The mixture was stirred for one hour at room temperature, resulting in a grey suspension. Then, all volatiles were removed *in vacuo* and the product

extracted with toluene and filtration through a glass fibre filter. The solvent was removed *in vacuo* and the residue washed with *n*-hexane, yielding IDipp·$BH_2PH_2GaH_3$ as a colourless, highly electrostatic solid residue. Single-crystals suitable for X-ray structure determination were obtained by storing a saturated solution of IDipp·$BH_2PH_2GaH_3$ in diethylether overnight at -30 °C.

$^{31}P\{^1H\}$ NMR (161.98 MHz, C_6D_6, 298 K): -165.1 (m, broad).

^{31}P NMR (161.98 MHz, C_6D_6, 298 K): -165.1 (m, broad, $^1J_{PH}$ = 323 Hz).

$^{11}B\{^1H\}$ NMR (128.38 MHz, C_6D_6, 298 K): -35.1 (m, very broad).

^{11}B NMR (128.38 MHz, C_6D_6, 298 K): -35.1 (m, very broad).

10.5.2.11 Synthesis of $Me_3N{\cdot}BH_2PH_2GaH_3$ (7b)

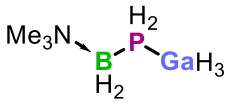

$[Me_3N{\cdot}BH_2PH_3][AlCl_4]$ (32 mg, 0.10 mmol) was suspended in diethylether and cooled to - 80 °C. Then, a solution of $LiGaH_4$ (10 mg, 0.12 mmol) in diethylether was added. After stirring for one hour at room temperature, the solution was analysed by multinuclear NMR spectroscopy.

$^{31}P\{^1H\}$ NMR (161.98 MHz, C_6D_6-cap./Et_2O, 298 K): -176.7 (m, broad).

^{31}P NMR (161.98 MHz, C_6D_6-cap./Et_2O, 298 K): -176.7 (tm, broad, $^1J_{HP} \approx$ 300 Hz).

$^{11}B\{^1H\}$ NMR (128.38 MHz, C_6D_6-cap./Et_2O, 298 K): -8.9 (d, $^1J_{PB}$ = 56 Hz).

^{11}B NMR (128.38 MHz, C_6D_6-cap./Et_2O, 298 K): -8.95 (td, $^1J_{PB}$ = 56 Hz, $^1J_{BH}$ = 113 Hz).

10.5.3 NMR Data

10.5.3.1 $H_3P{\cdot}AlCl_3$ stock solution

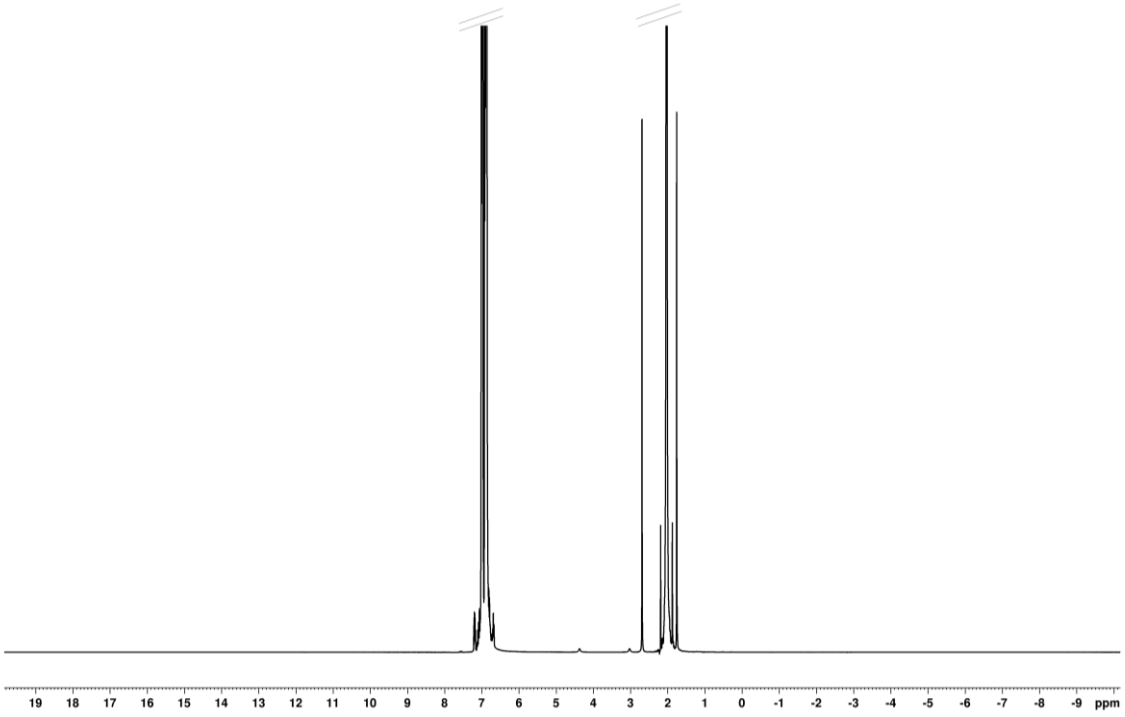

Figure S 10.2: ^{1}H NMR spectrum of the $H_3P{\cdot}AlCl_3$ stock solution (PhMe-d_8-cap., 298 K).

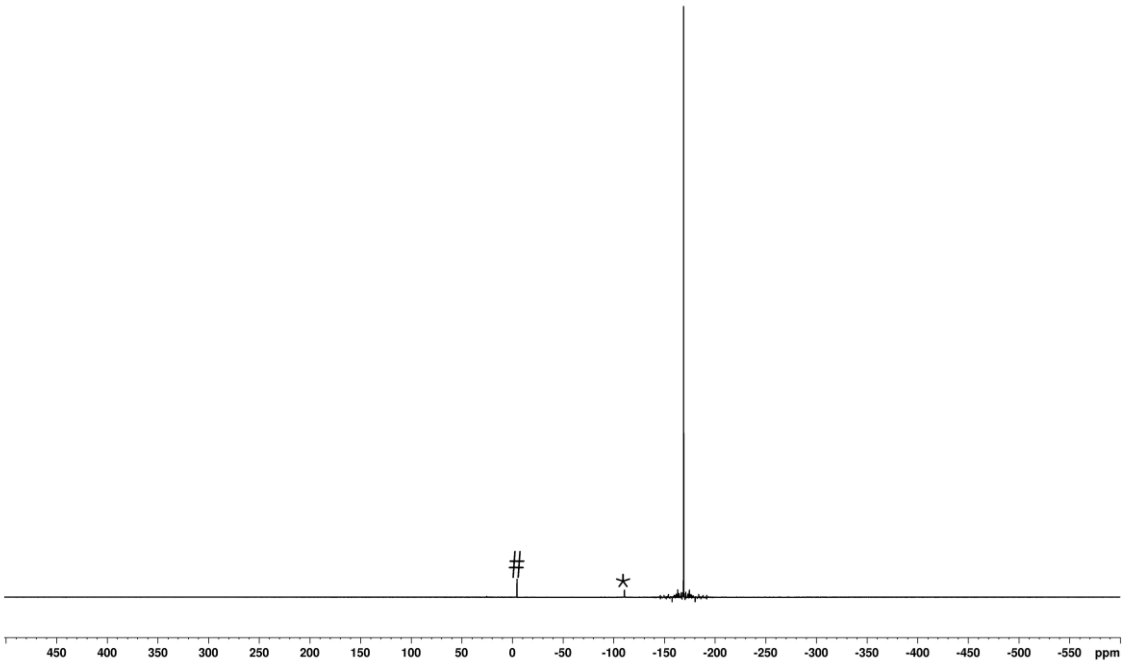

Figure S 10.3: $^{31}P\{^{1}H\}$ NMR spectrum of the $H_3P{\cdot}AlCl_3$ stock solution (PhMe-d_8-cap., 298 K, + $[H_4P][AlCl_4]$, # = PPh_3 from capillary).

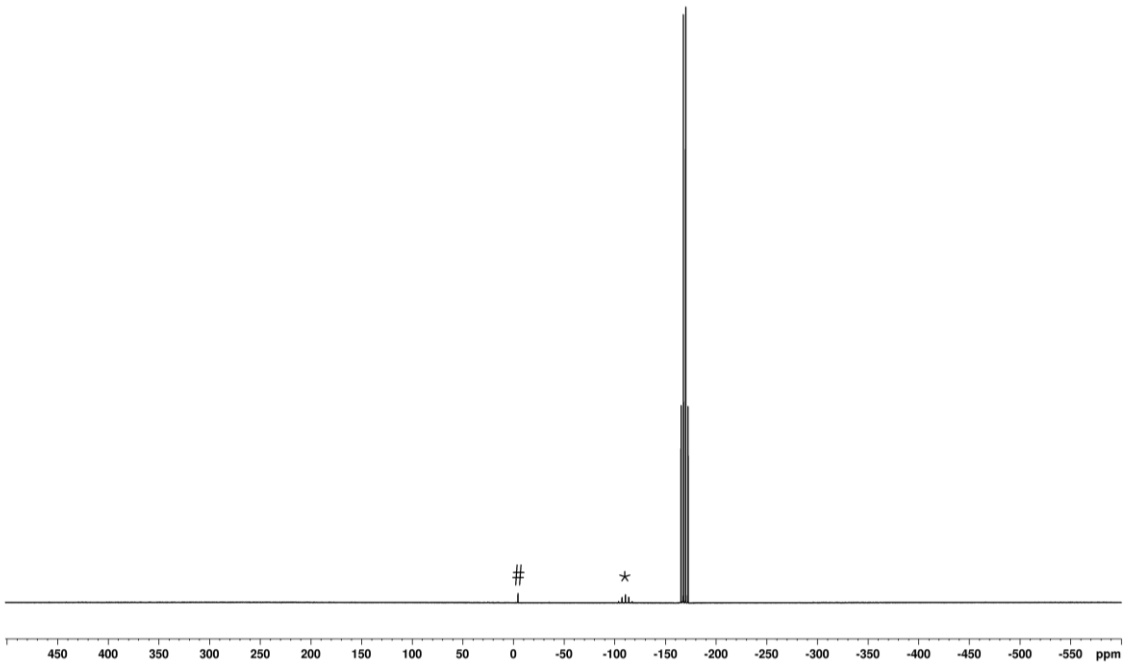

Figure S 10.4: ^{31}P NMR spectrum of the $H_3P{\cdot}AlCl_3$ stock solution (PhMe-d_8-cap., 298 K, + $[H_4P][AlCl_4]$, # = PPh_3 from capillary).

10.5.3.2 [IDipp·$BH_2PH_2CH_3$][OTf]

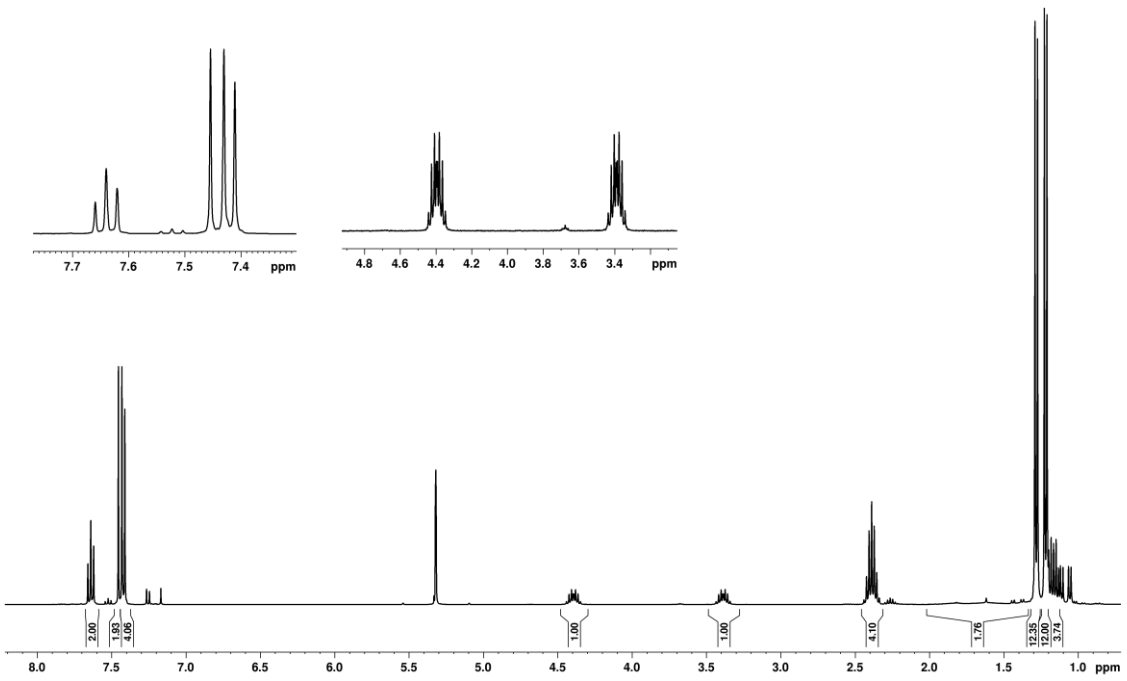

Figure S 10.5: ^1H NMR spectrum of $[IDipp{\cdot}BH_2PH_2CH_3][OTf]$ (CD_2Cl_2, 298 K).

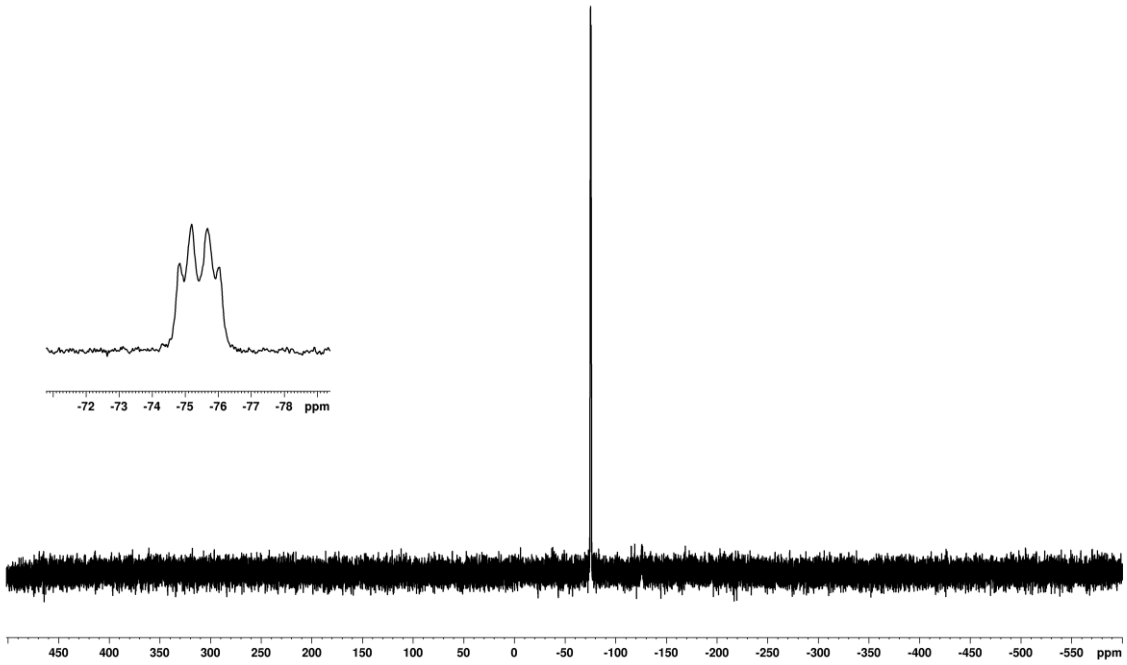

Figure S 10.6: $^{31}P\{^{1}H\}$ NMR spectrum of [IDipp·$BH_2PH_2CH_3$][OTf] (CD_2Cl_2, 298 K).

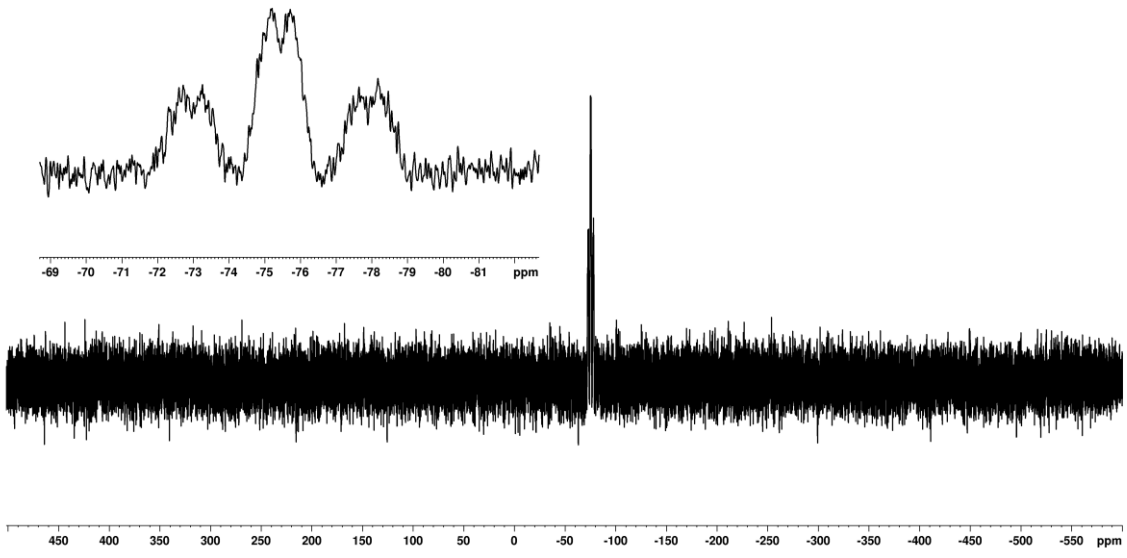

Figure S 10.7: ^{31}P NMR spectrum of [IDipp·$BH_2PH_2CH_3$][OTf] (CD_2Cl_2, 298 K).

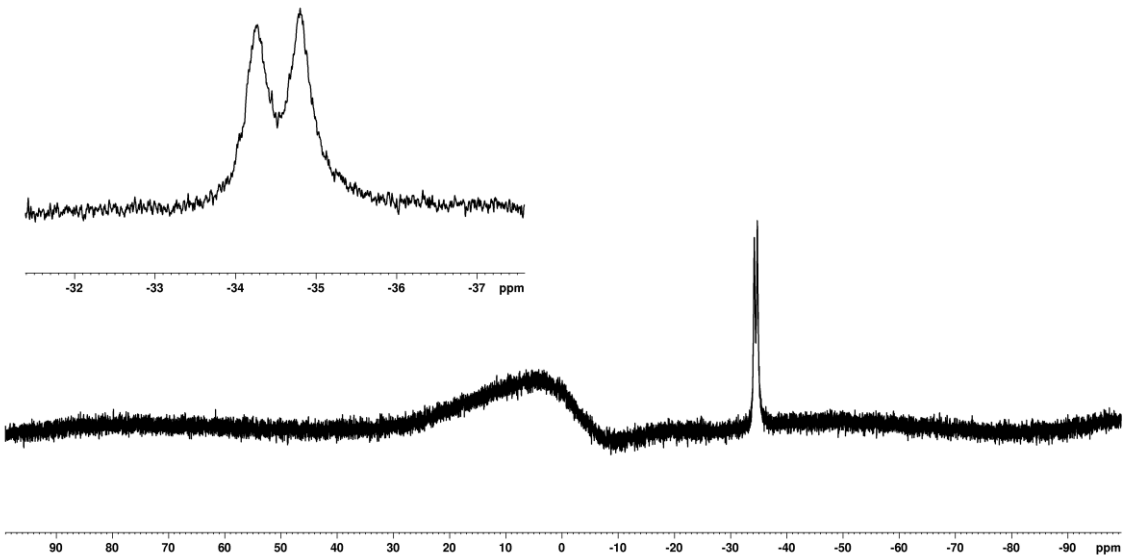

Figure S 10.8: $^{11}B\{^{1}H\}$ NMR spectrum of [IDipp·$BH_2PH_2CH_3$][OTf] (CD_2Cl_2, 298 K).

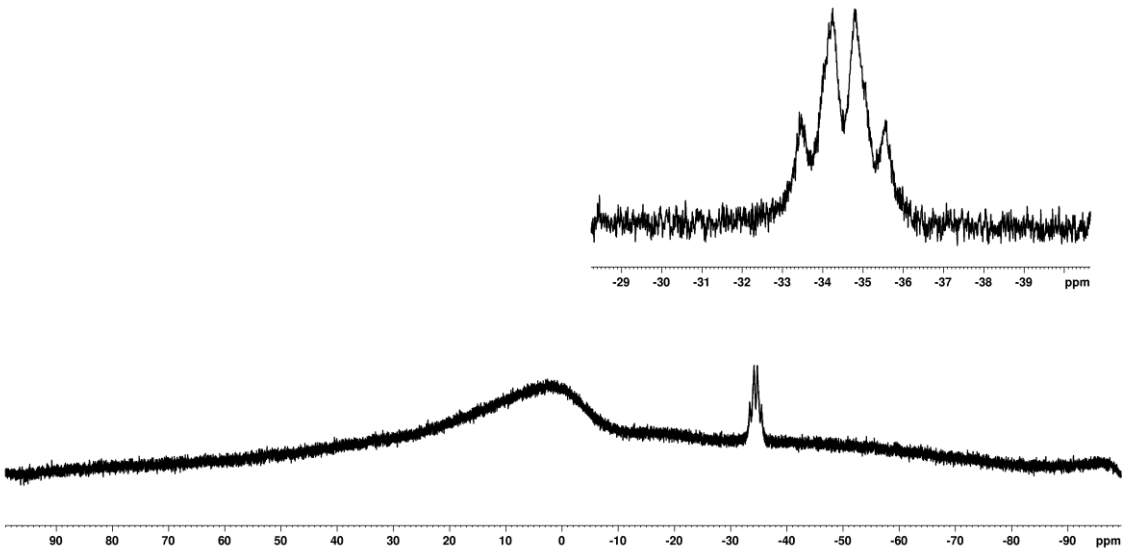

Figure S 10.9: ^{11}B NMR spectrum of [IDipp·$BH_2PH_2CH_3$][OTf] (CD_2Cl_2, 298 K).

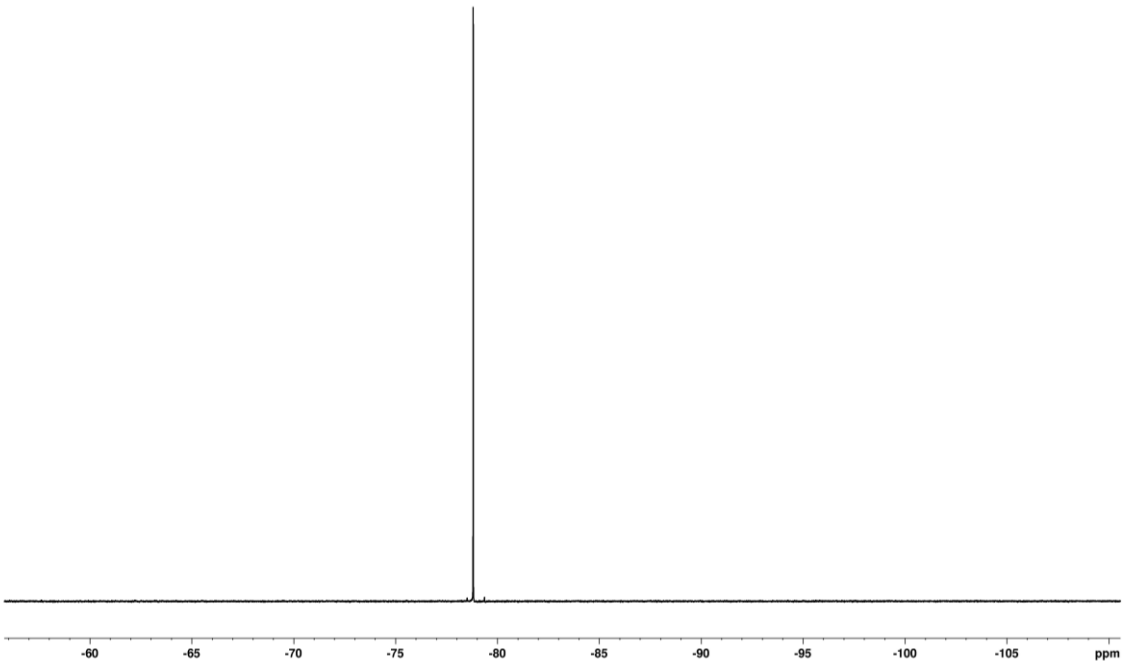

Figure S 10.10: $^{19}F\{^{1}H\}$ NMR spectrum of [IDipp·$BH_2PH_2CH_3$][OTf] (CD_2Cl_2, 298 K).

10.5.3.3 [IDipp·$BH_2PH_2SiEt_3$][BAr^F]

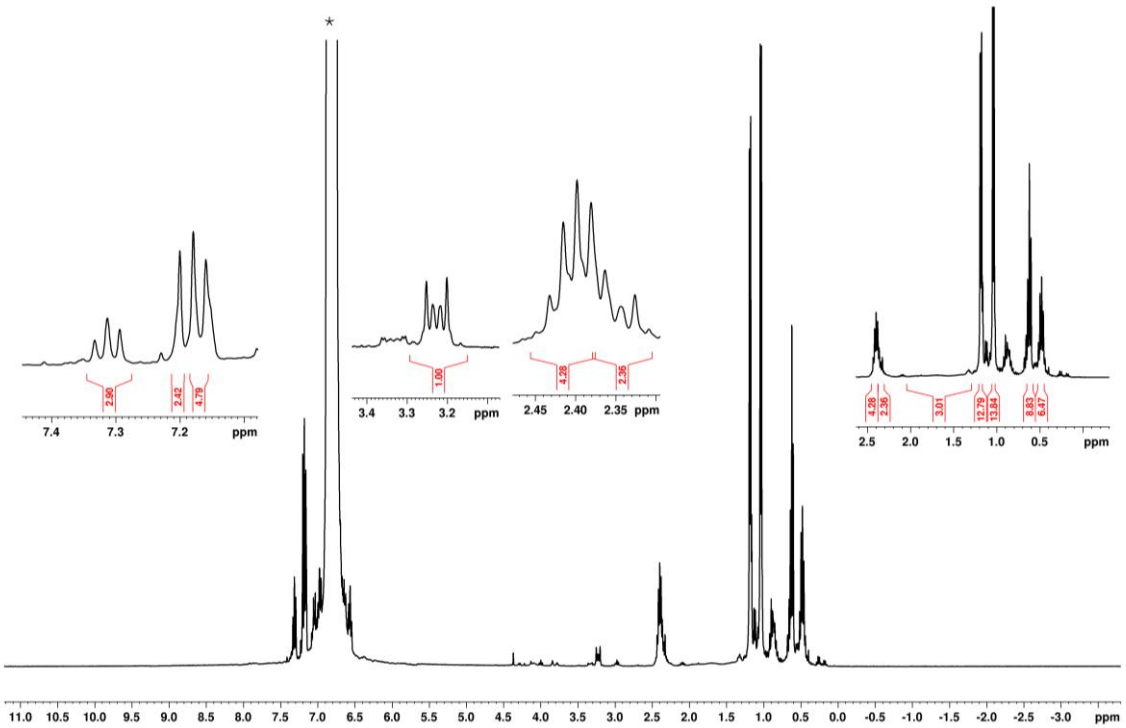

Figure S 10.11: ^{1}H NMR spectrum of [IDipp·$BH_2PH_2SiEt_3$][BAr^F] (1,2-difluorobenzene/C_6D_6-cap., 298 K; * = solvent signal).

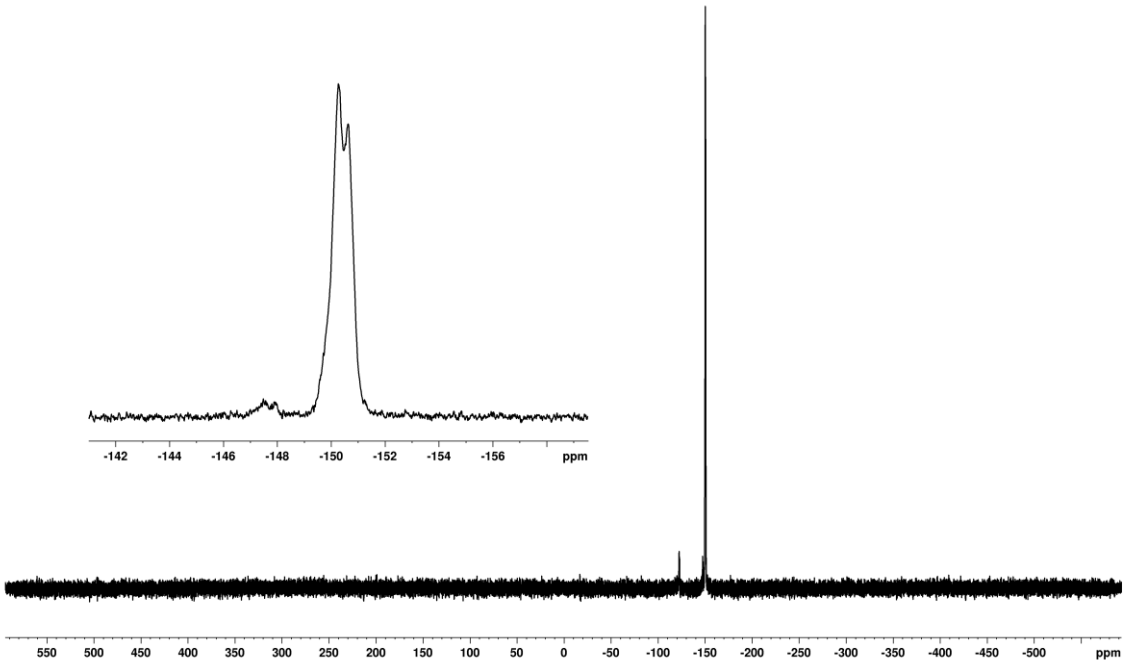

Figure S 10.12: $^{31}P\{^{1}H\}$ NMR spectrum of [IDipp·$BH_2PH_2SiEt_3$][BAr^F] (1,2-difluorobenzene/C_6D_6-cap., 298 K).

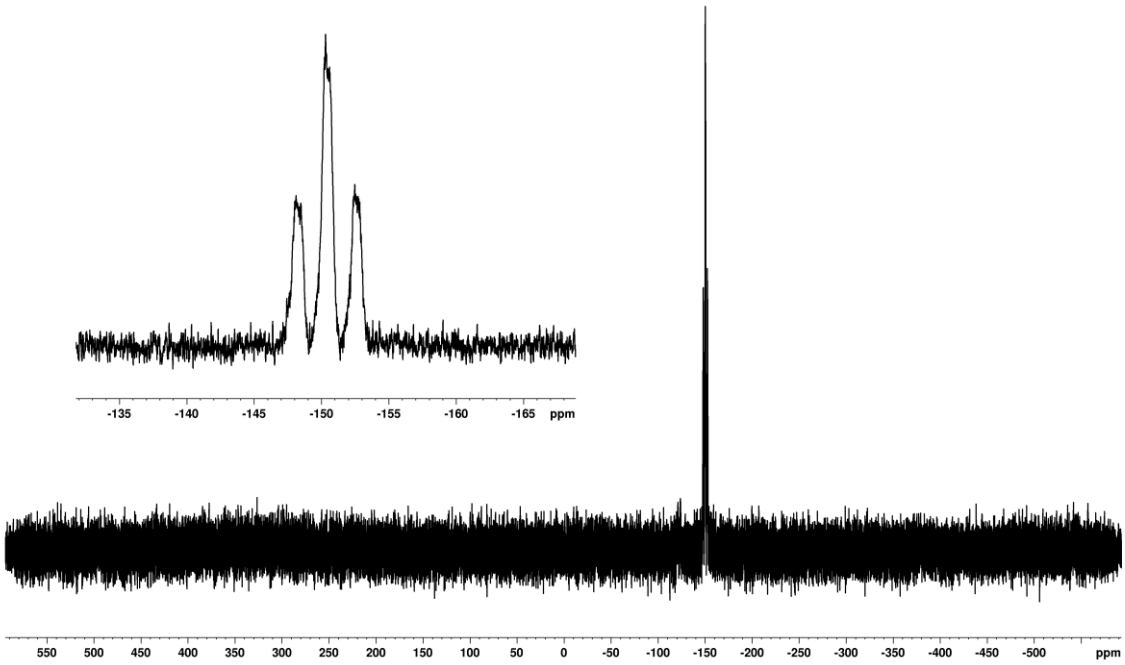

Figure S 10.13: ^{31}P NMR spectrum of [IDipp·$BH_2PH_2SiEt_3$][BAr^F] (1,2-difluorobenzene/C_6D_6-cap., 298 K).

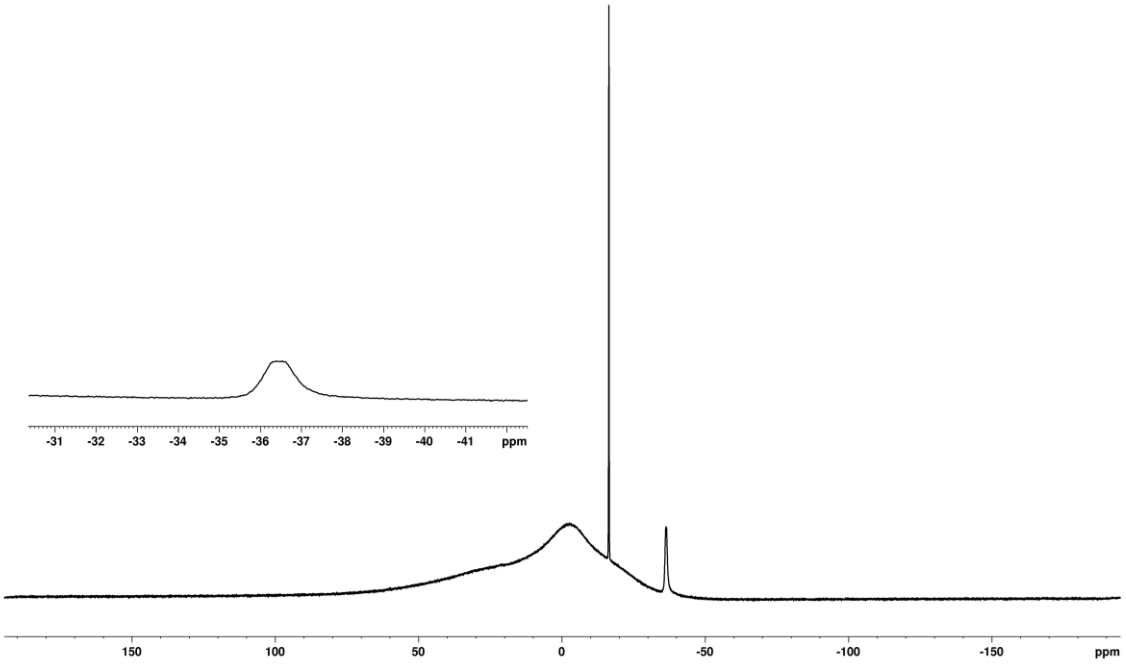

Figure S 10.14: $^{11}B\{^{1}H\}$ NMR spectrum of [IDipp·$BH_2PH_2SiEt_3$][BAr^F] (1,2-difluorobenzene/C_6D_6-cap., 298 K).

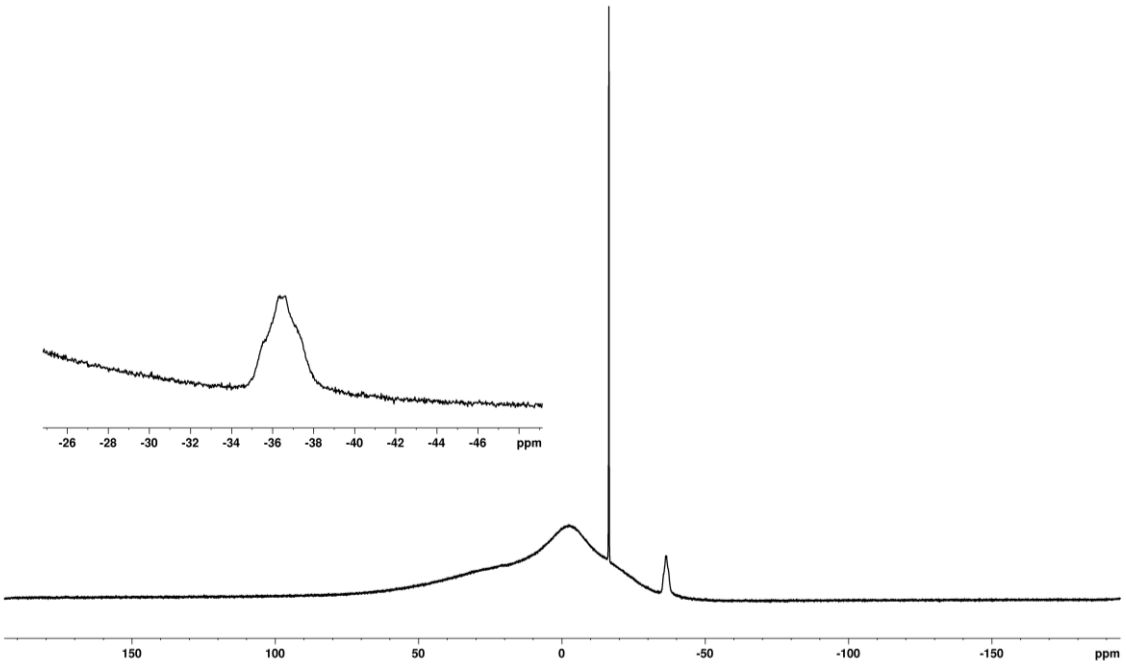

Figure S 10.15: ^{11}B NMR spectrum of [IDipp·$BH_2PH_2SiEt_3$][BAr^F] (1,2-difluorobenzene/C_6D_6-cap., 298 K).

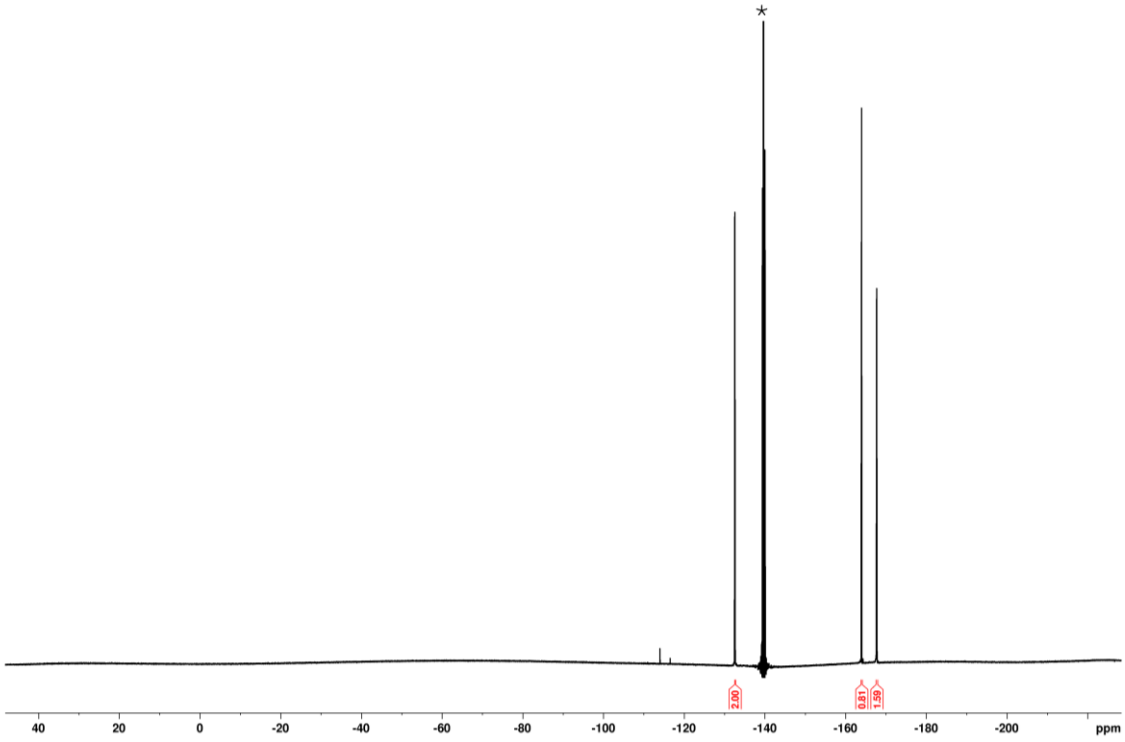

Figure S 10.16: $^{19}F\{^{1}H\}$ NMR spectrum of [IDipp·$BH_2PH_2SiEt_3$][BAr^F] (1,2-difluorobenzene/C_6D_6-cap., 298 K; * = solvent signal).

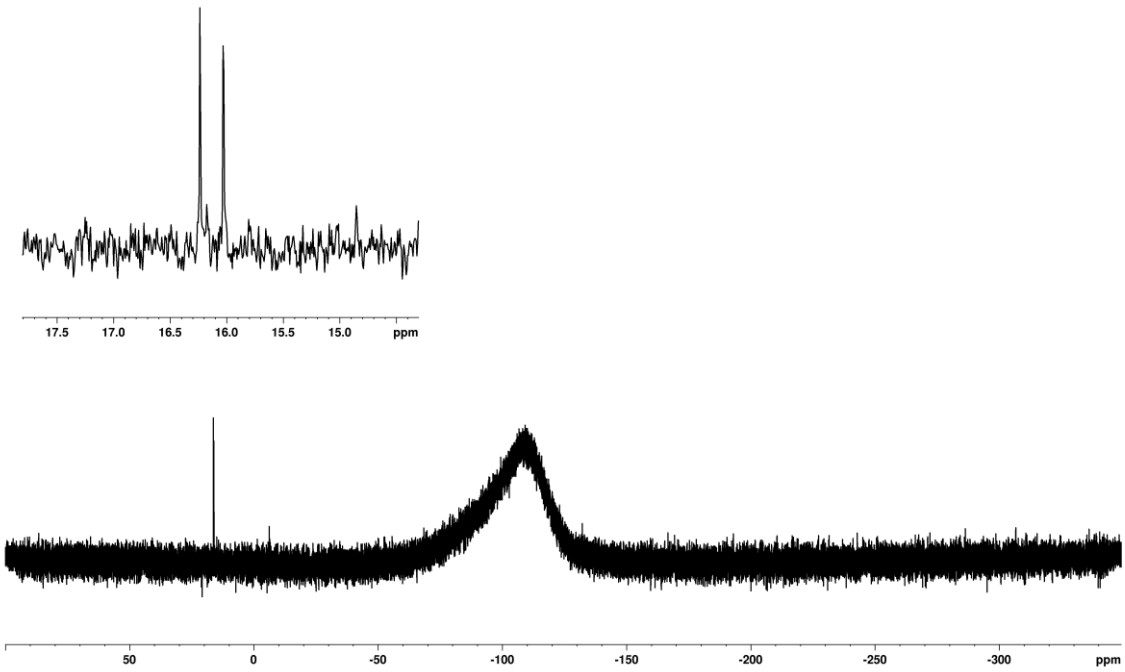

Figure S 10.17: $^{29}Si\{^{1}H\}$ NMR spectrum of [IDipp·$BH_2PH_2SiEt_3$][BAr^F] (1,2-difluorobenzene/C_6D_6-cap., 298 K).

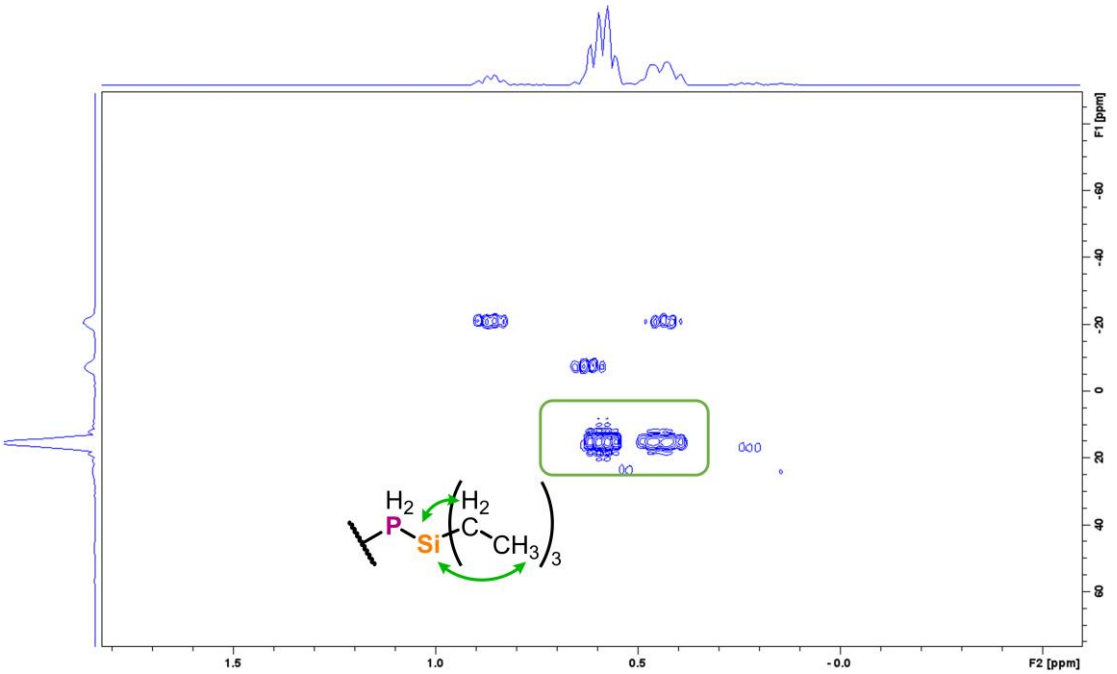

Figure S 10.18: ^{29}Si, ^{1}H HMBC NMR spectrum of [IDipp·$BH_2PH_2SiEt_3$][BAr^F] (1,2-difluorobenzene/C_6D_6-cap., 298 K).

10.5.3.4 [IDipp·$BH_2PH_2SnMe_3$][TEF]

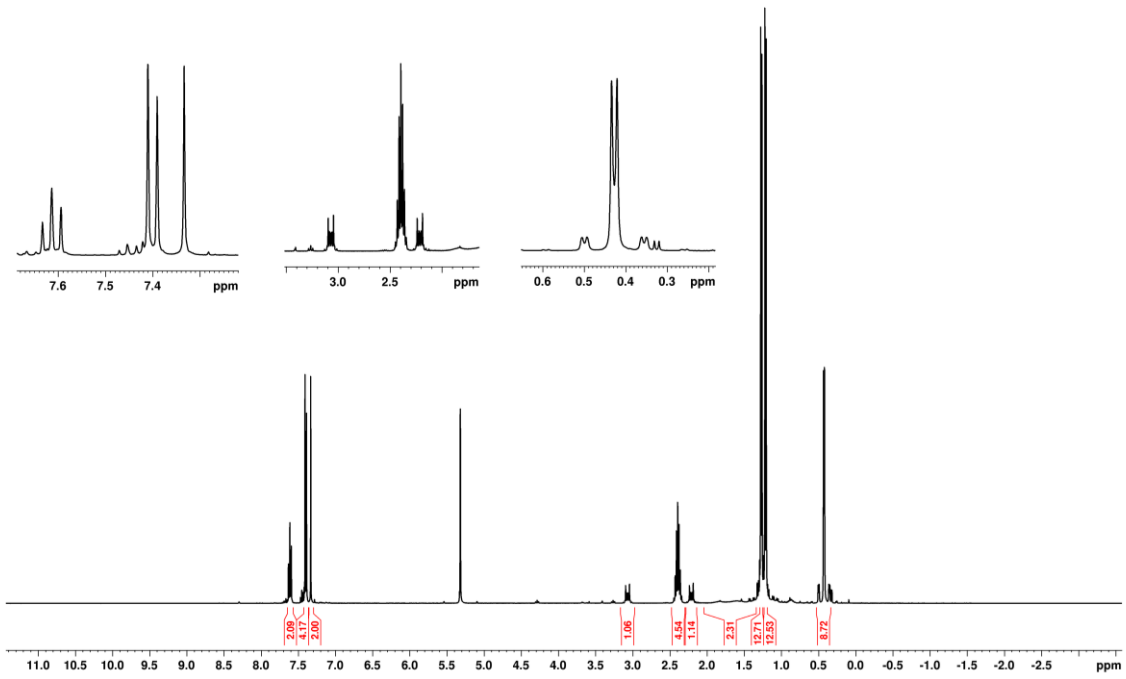

Figure S 10.19: ^{1}H NMR spectrum of [IDipp·$BH_2PH_2SnMe_3$][TEF] (CD_2Cl_2, 298 K).

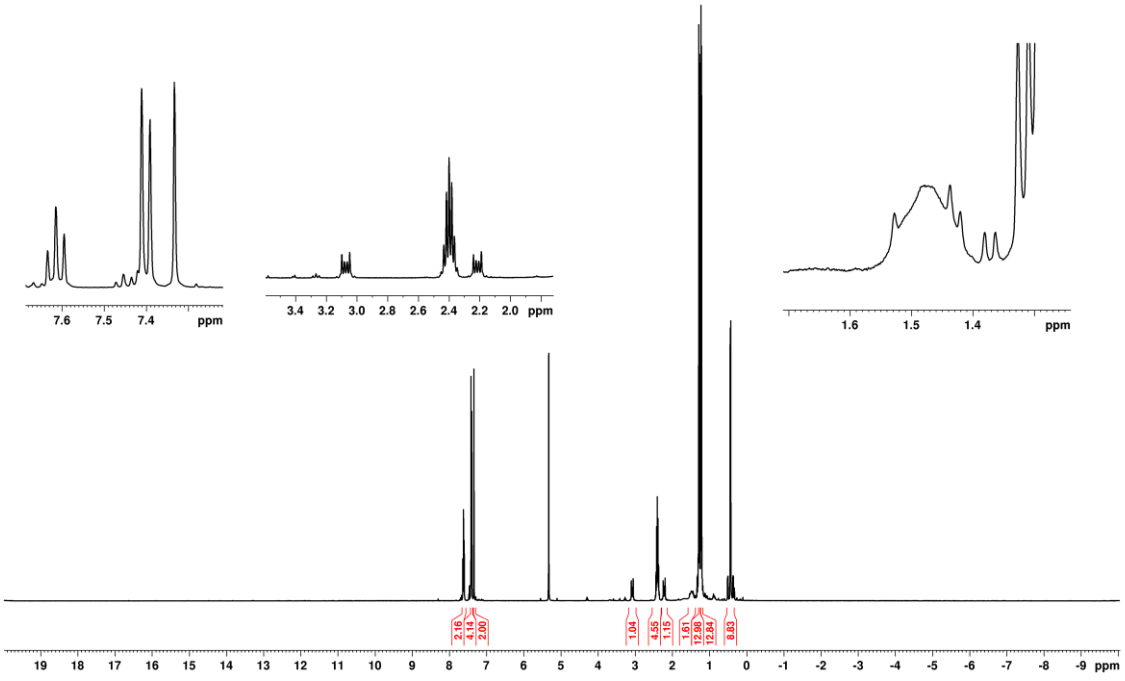

Figure S 10.20: $^{1}H\{^{11}B\}$ NMR spectrum of [IDipp·$BH_2PH_2SnMe_3$][TEF] (CD_2Cl_2, 298 K).

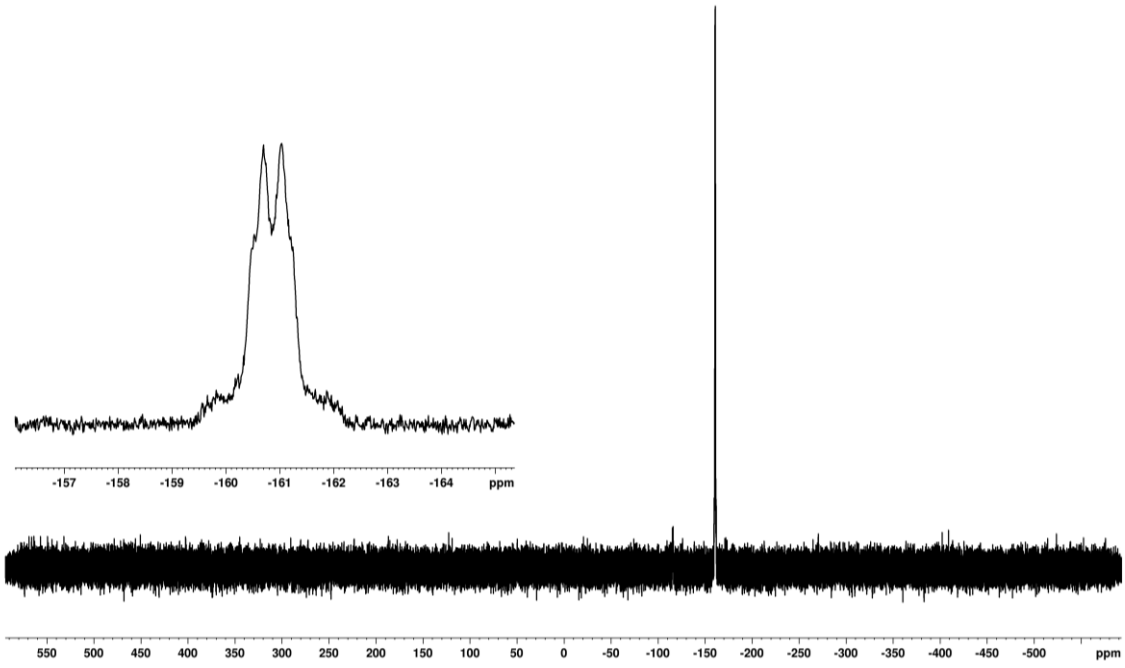

Figure S 10.21: $^{31}P\{^{1}H\}$ NMR spectrum of [IDipp·$BH_2PH_2SnMe_3$][TEF] (CD_2Cl_2, 298 K).

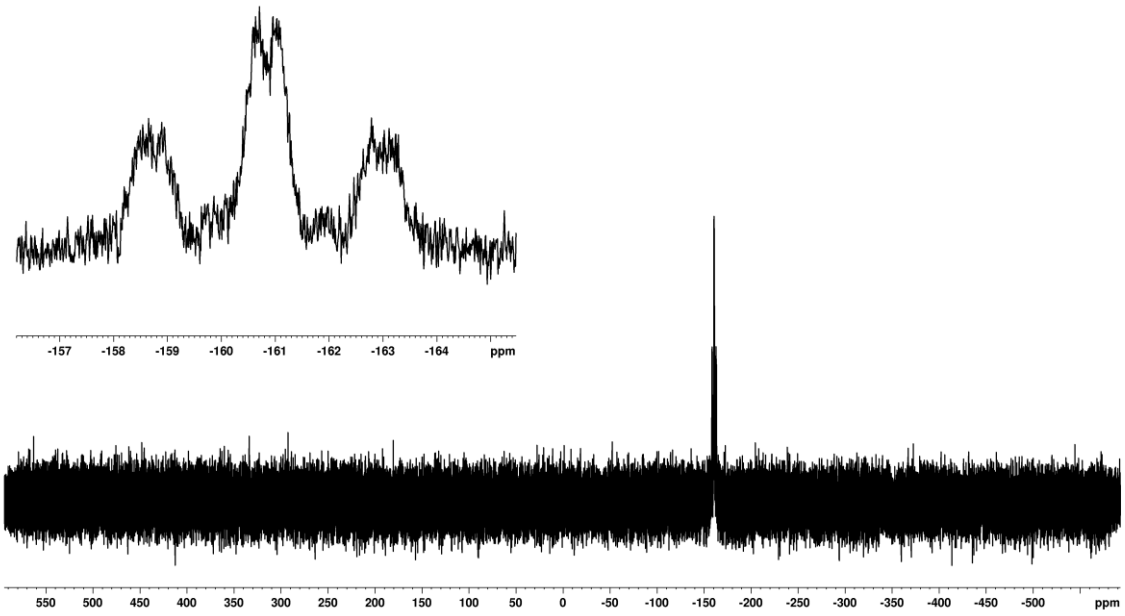

Figure S 10.22: ^{31}P NMR spectrum of [IDipp·$BH_2PH_2SnMe_3$][TEF] (CD_2Cl_2, 298 K).

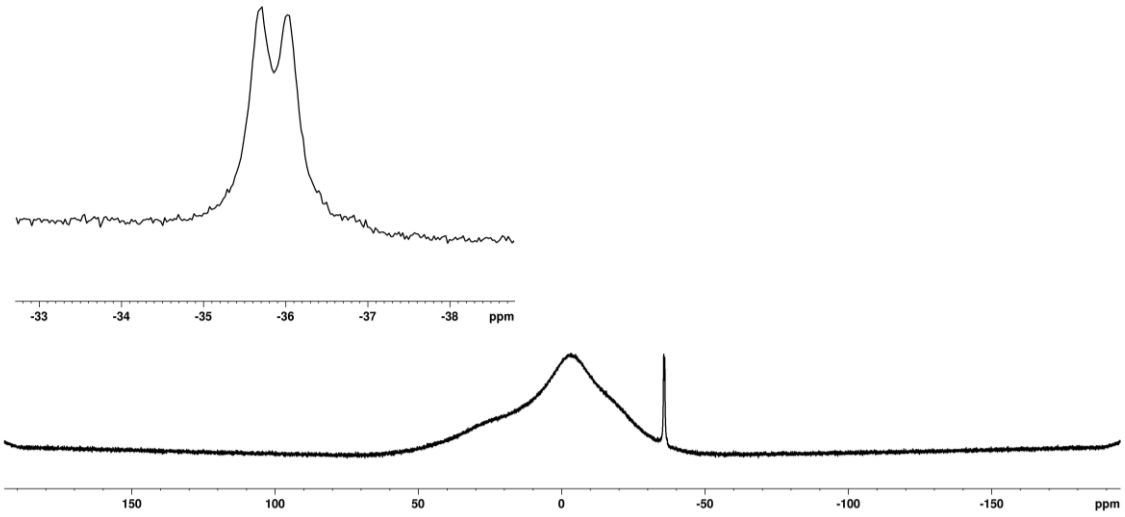

Figure S 10.23: $^{11}B\{^1H\}$ NMR spectrum of [IDipp·$BH_2PH_2SnMe_3$][TEF] (CD_2Cl_2, 298 K).

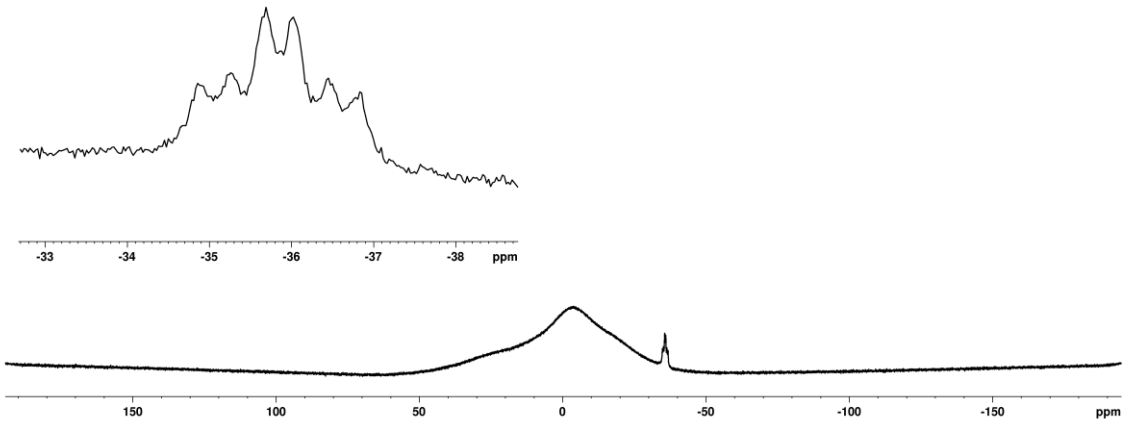

Figure S 10.24: ^{11}B NMR spectrum of [IDipp·$BH_2PH_2SnMe_3$][TEF] (CD_2Cl_2, 298 K).

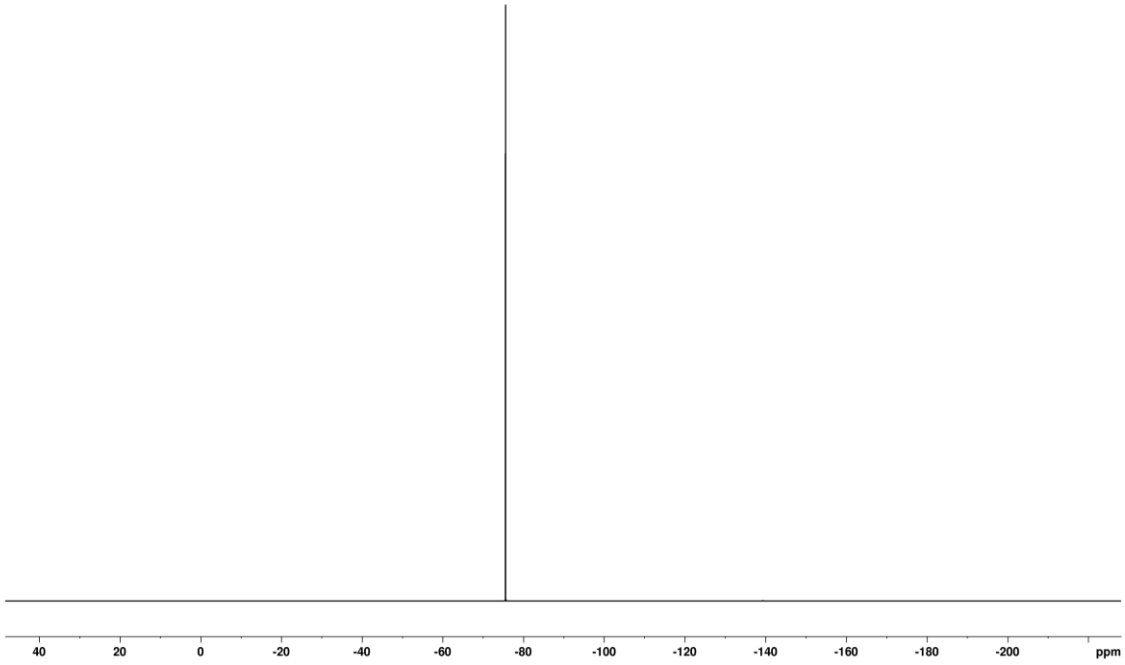

Figure S 10.25: $^{19}F\{^1H\}$ NMR spectrum of [IDipp·$BH_2PH_2SnMe_3$][TEF] (CD_2Cl_2, 298 K).

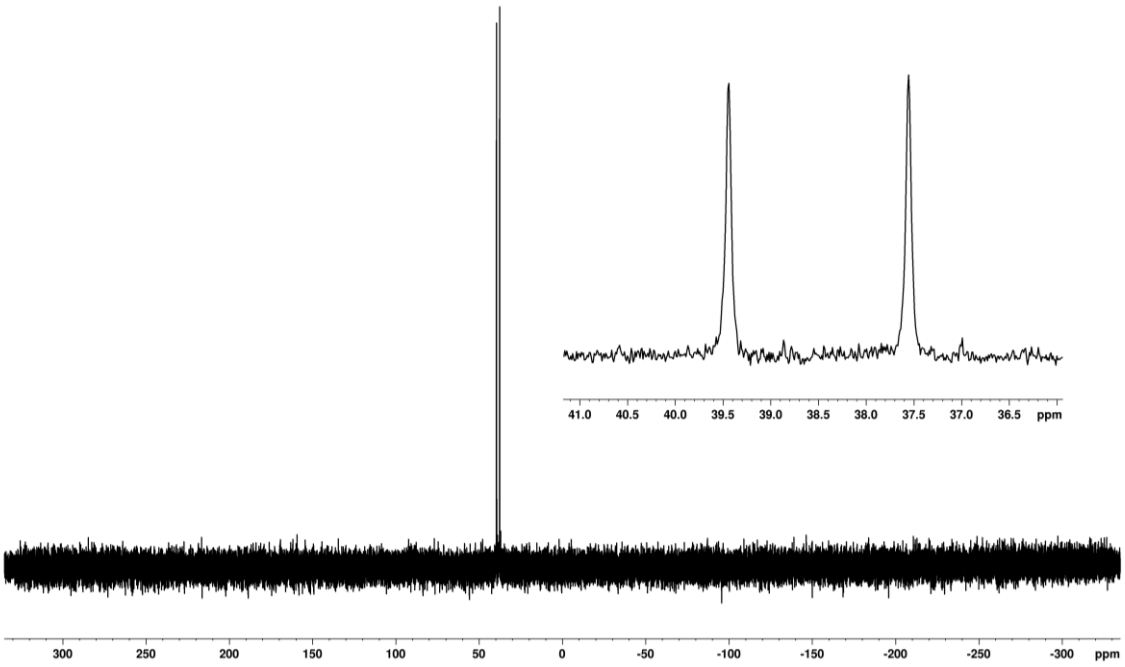

Figure S 10.26: $^{119}Sn\{^{1}H\}$ NMR spectrum of [IDipp·$BH_2PH_2SnMe_3$][TEF] (CD_2Cl_2, 298 K).

10.5.3.5 [IDipp·$BH_2PH_2Ge(SiMe_3)_3$][TEF]

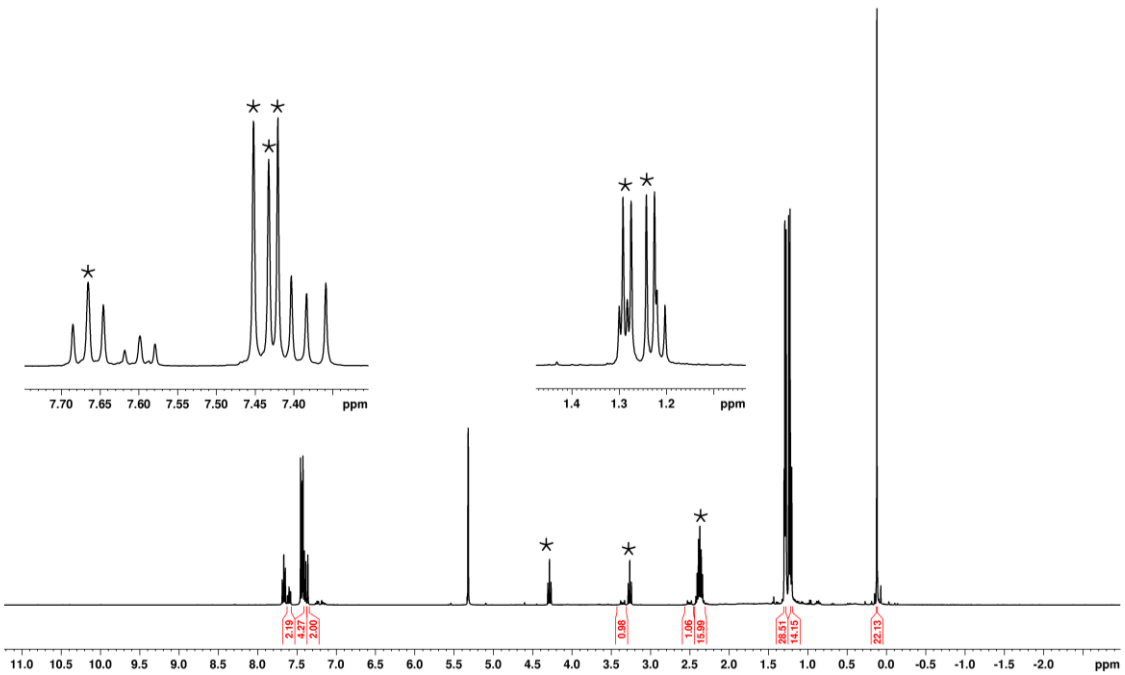

Figure S 10.27: ^{1}H NMR spectrum of [IDipp·$BH_2PH_2Ge(SiMe_3)_3$][TEF] (CD_2Cl_2, 298 K; * = [IDipp·BH_2PH_3]$^+$).

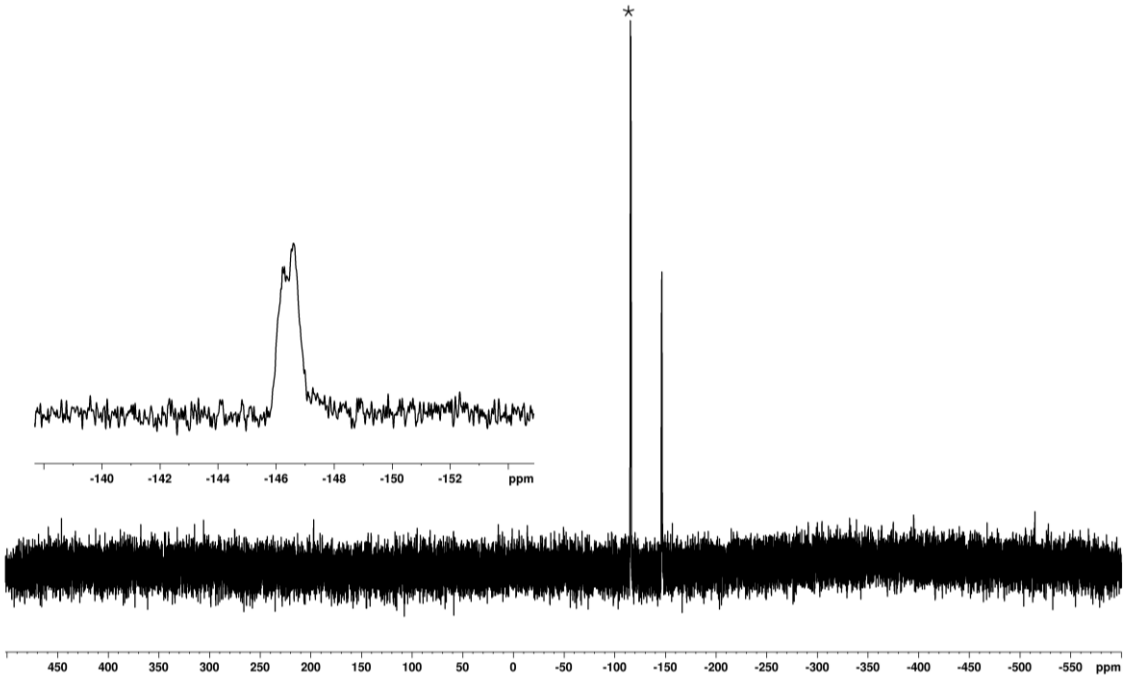

Figure S 10.28: $^{31}P\{^{1}H\}$ NMR spectrum of [IDipp·$BH_2PH_2Ge(SiMe_3)_3$][TEF] (CD_2Cl_2, 298 K; * = [IDipp·BH_2PH_3]$^+$).

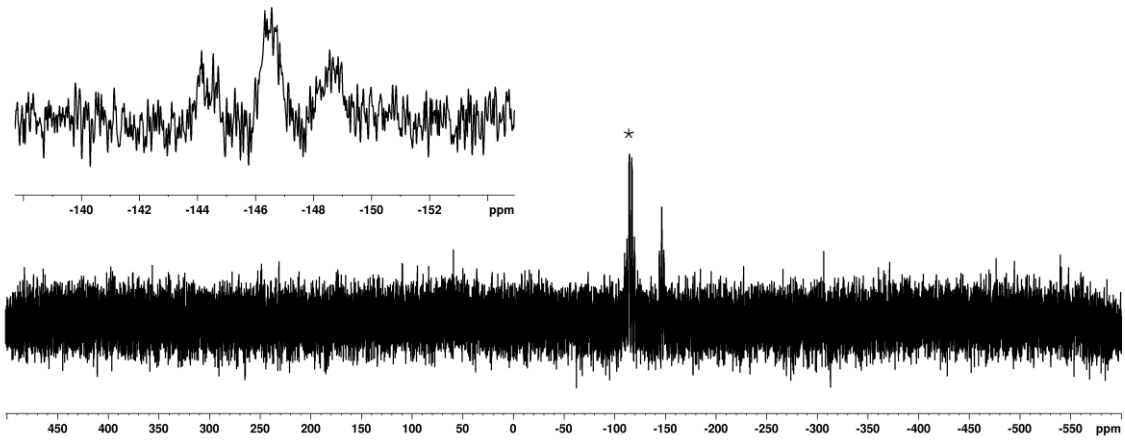

Figure S 10.29: ^{31}P NMR spectrum of [IDipp·$BH_2PH_2Ge(SiMe_3)_3$][TEF] (CD_2Cl_2, 298 K; * = [IDipp·BH_2PH_3]$^+$).

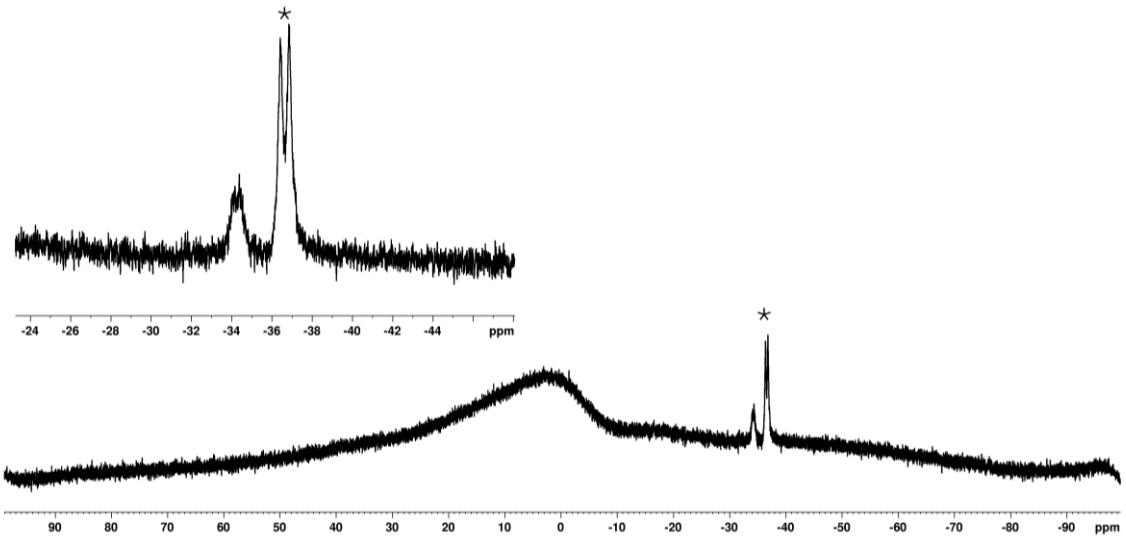

Figure S 10.30: $^{11}B\{^{1}H\}$ NMR spectrum of [IDipp·$BH_2PH_2Ge(SiMe_3)_3$][TEF] (CD_2Cl_2, 298 K; * = [IDipp·BH_2PH_3]$^+$).

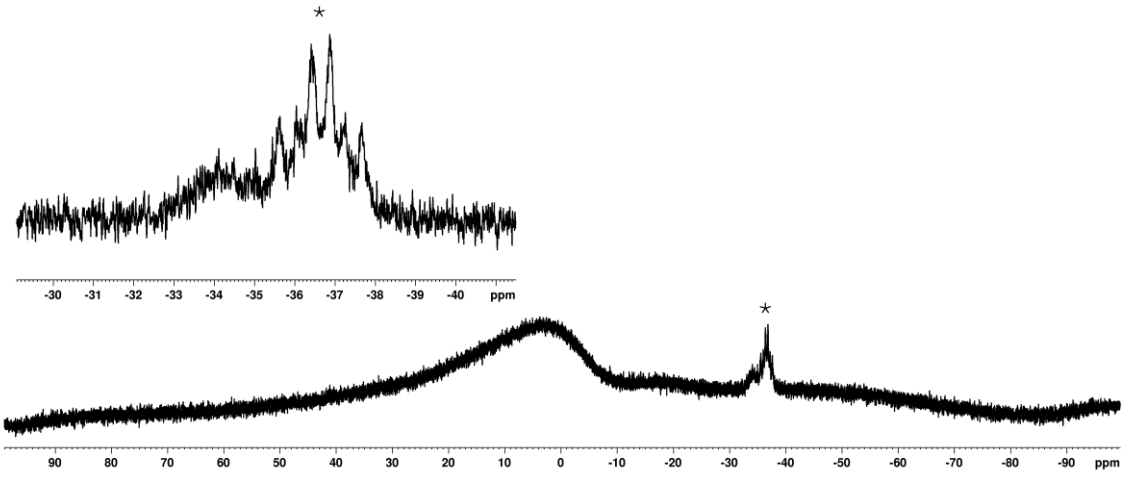

Figure S 10.31: ^{11}B NMR spectrum of [IDipp·$BH_2PH_2Ge(SiMe_3)_3$][TEF] (CD_2Cl_2, 298 K; * = [IDipp·BH_2PH_3]$^+$).

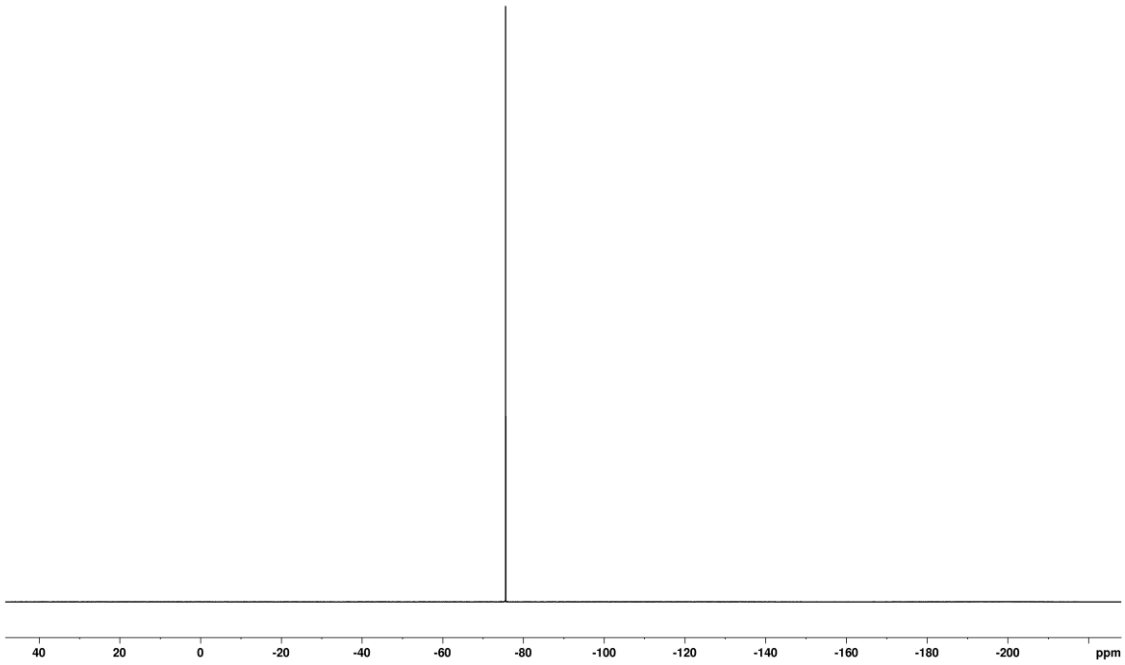

Figure S 10.32: $^{19}F\{^{1}H\}$ NMR spectrum of [IDipp·$BH_2PH_2Ge(SiMe_3)_3$][TEF] (CD_2Cl_2, 298 K).

10.5.3.6 [IDipp·BH_2PH_3][BAr^F]

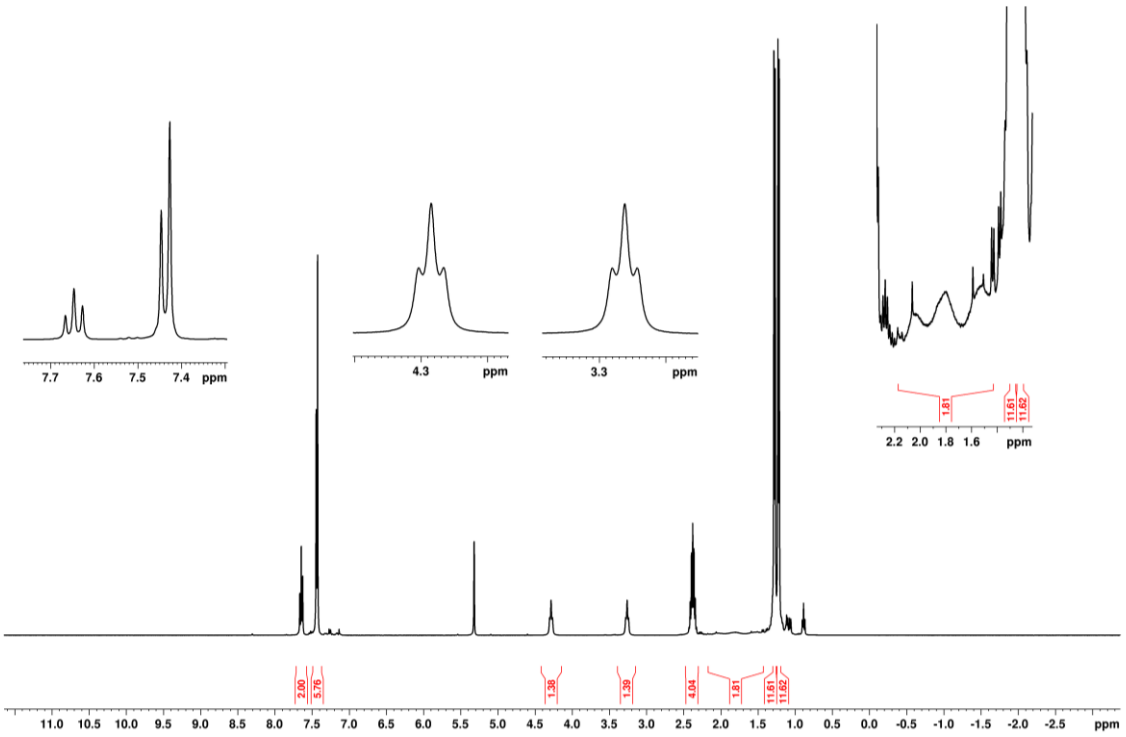

Figure S 10.33: ^{1}H NMR spectrum of [IDipp·BH_2PH_3][$B(C_6F_4)_4$] (CD_2Cl_2, 298 K).

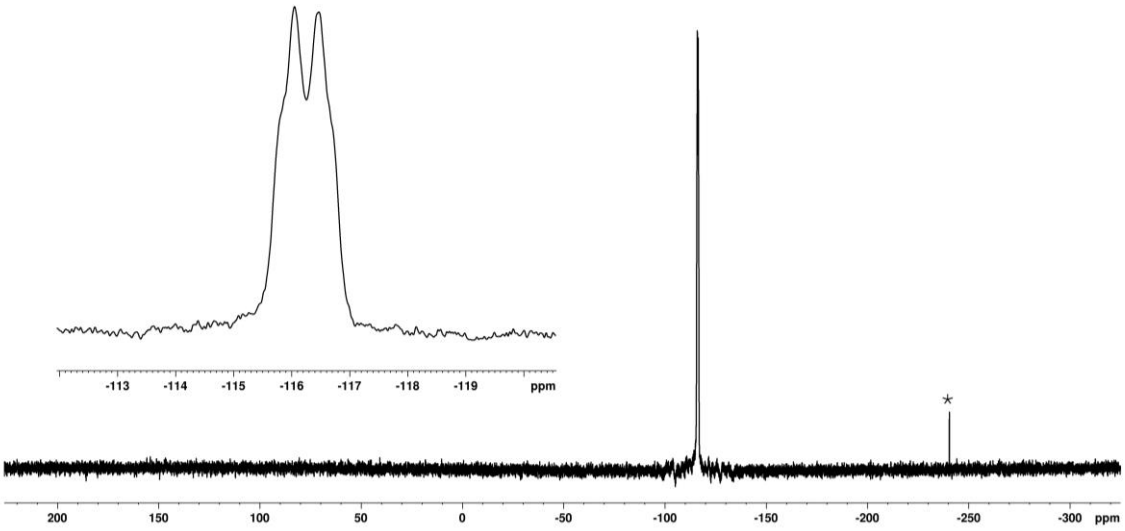

Figure S 10.34: $^{31}P\{^{1}H\}$ NMR spectrum of $[IDipp{\cdot}BH_2PH_3][B(C_6F_4)_4]$ (CD_2Cl_2, 298 K; * = PH_3).

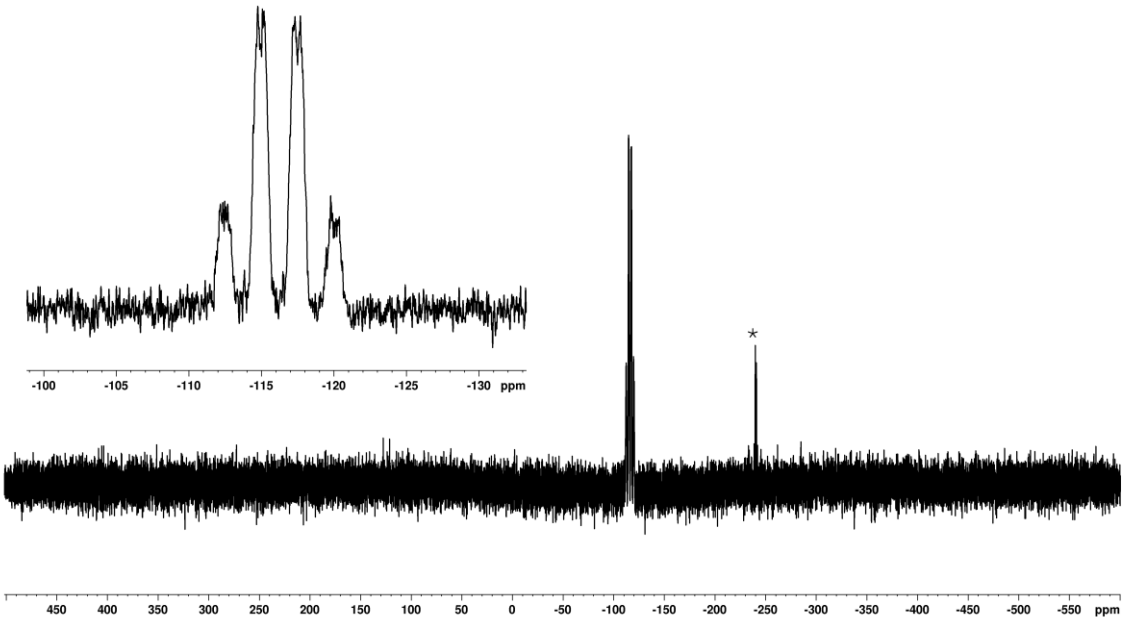

Figure S 10.35: ^{31}P NMR spectrum of $[IDipp{\cdot}BH_2PH_3][B(C_6F_4)_4]$ (CD_2Cl_2, 298 K; * = PH_3).

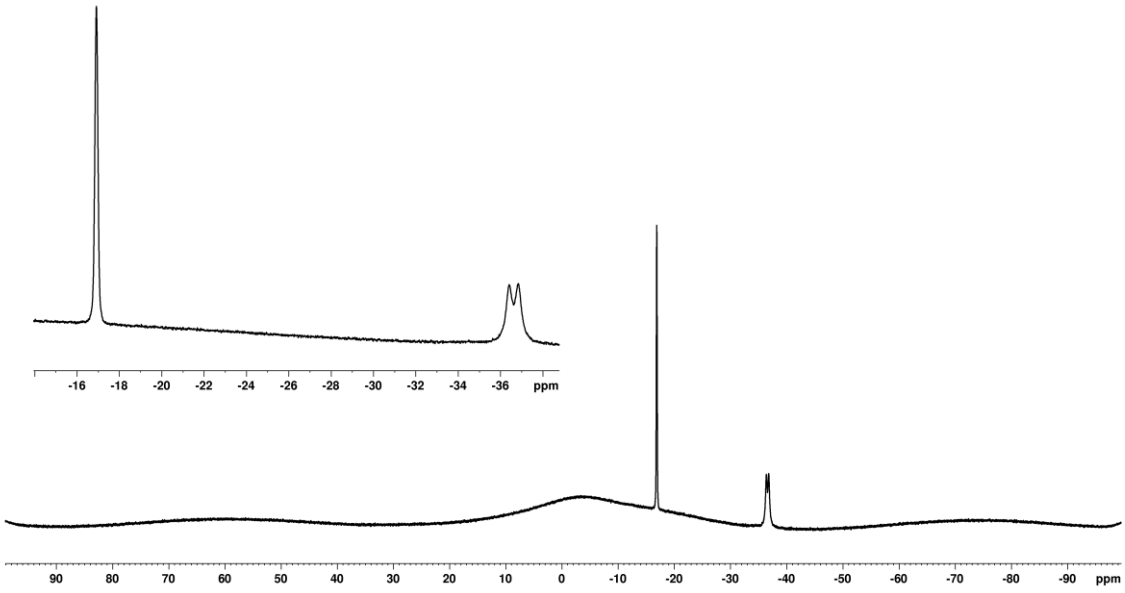

Figure S 10.36: $^{11}B\{^{1}H\}$ NMR spectrum of $[IDipp{\cdot}BH_2PH_3][B(C_6F_4)_4]$ (CD_2Cl_2, 298 K).

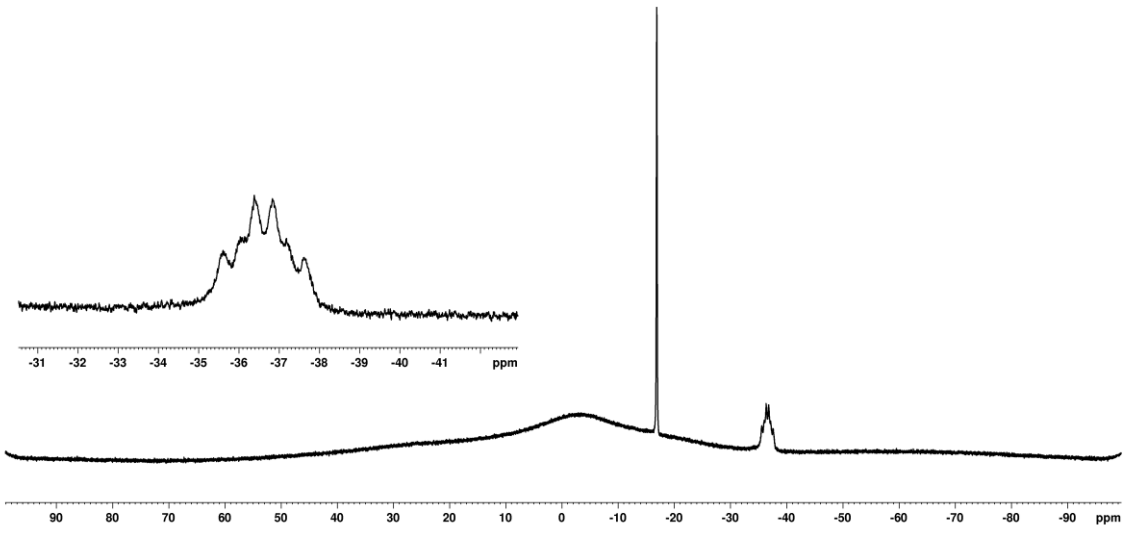

Figure S 10.37: ^{11}B NMR spectrum of $[IDipp{\cdot}BH_2PH_3][B(C_6F_4)_4]$ (CD_2Cl_2, 298 K).

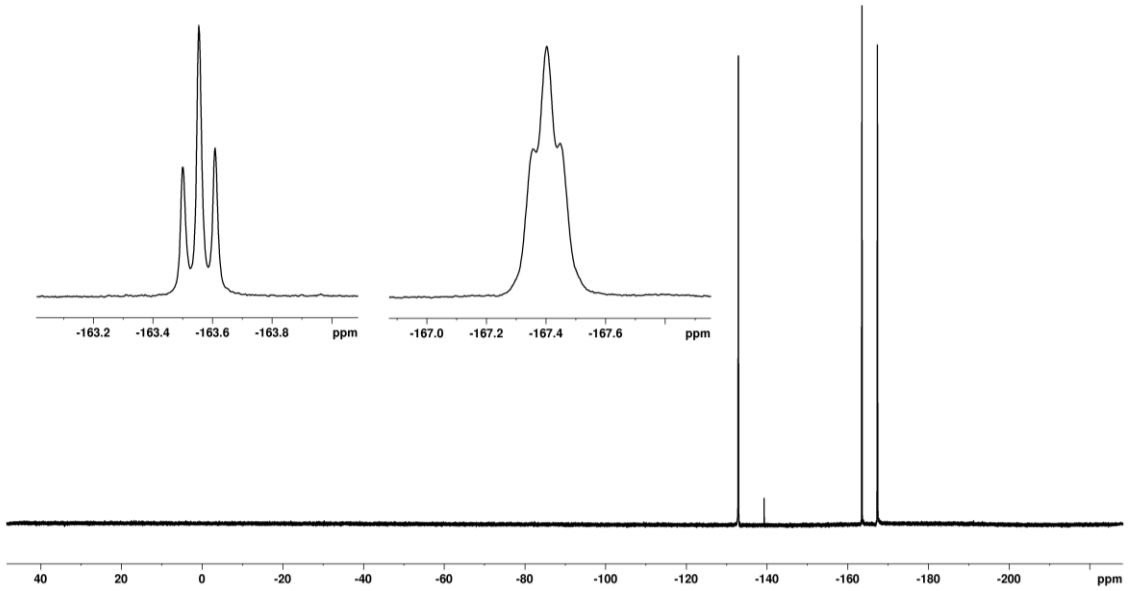

Figure S 10.38: $^{19}F\{^{1}H\}$ NMR spectrum of $[IDipp{\cdot}BH_2PH_3][B(C_6F_4)_4]$ (CD_2Cl_2, 298 K).

10.5.3.7 [IDipp·$BH_2PH_2PHBH_2$·IDipp][PF_6]

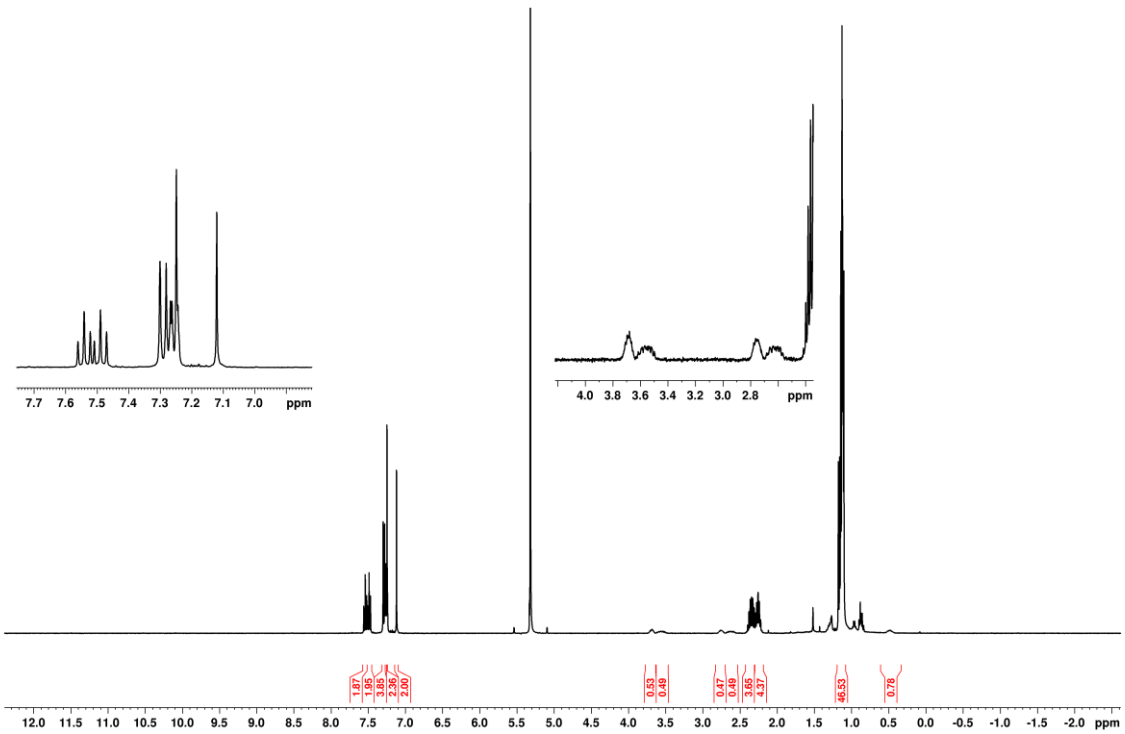

Figure S 10.39: ^{1}H NMR spectrum of $[IDipp{\cdot}BH_2PH_2PHBH_2{\cdot}IDipp][PF_6]$ (CD_2Cl_2, 298 K).

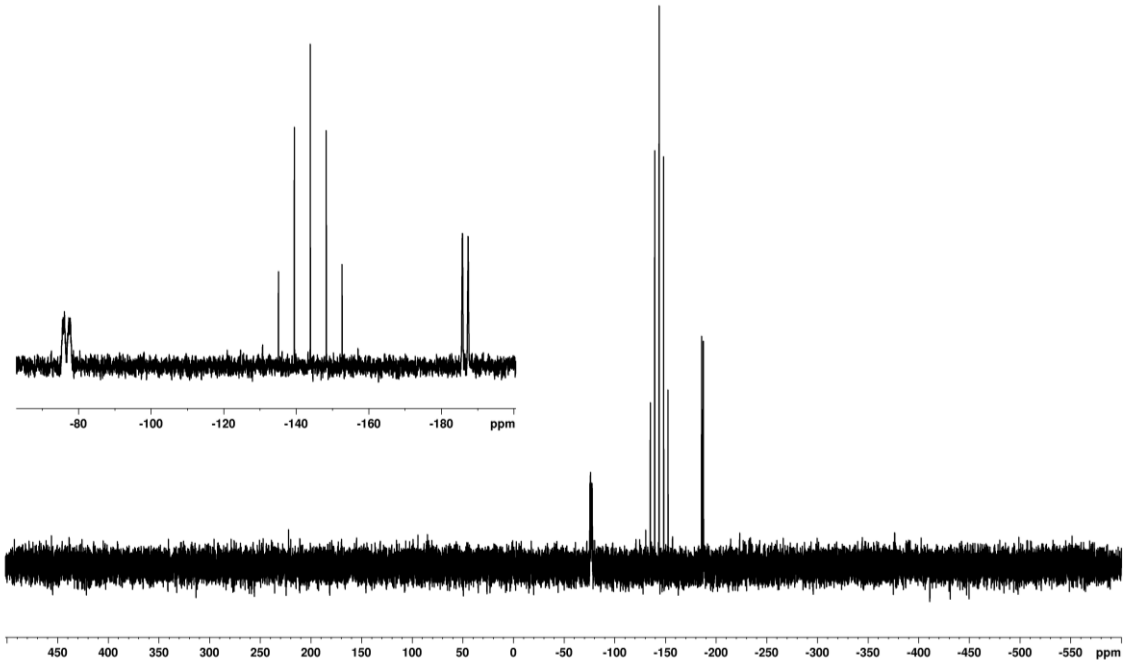

Figure S 10.40: $^{31}P\{^{1}H\}$ NMR spectrum of [IDipp·$BH_2PH_2PHBH_2$·IDipp][PF_6] (CD_2Cl_2, 298 K).

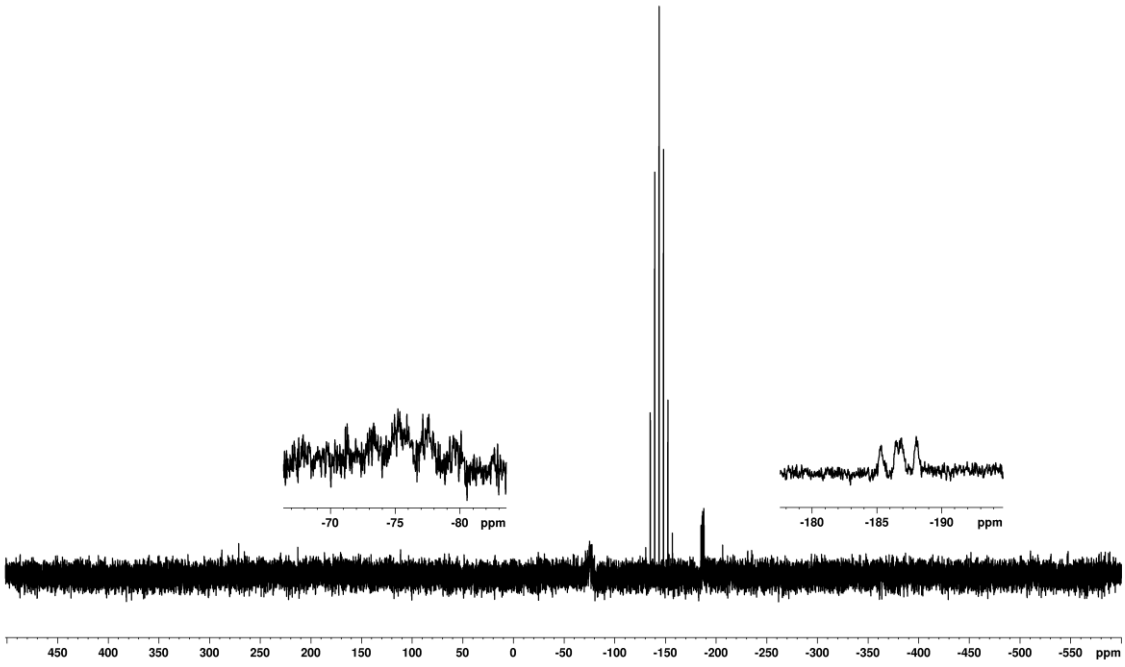

Figure S 10.41: ^{31}P NMR spectrum of [IDipp·$BH_2PH_2PHBH_2$·IDipp][PF_6] (CD_2Cl_2, 298 K).

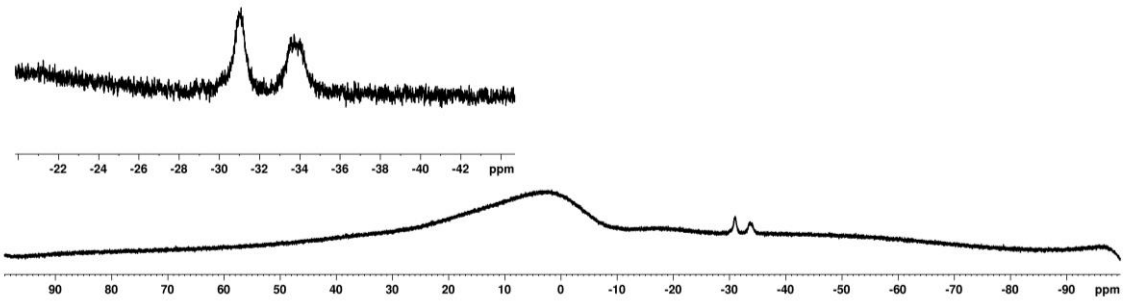

Figure S 10.42: $^{11}B\{^{1}H\}$ NMR spectrum of [IDipp·$BH_2PH_2PHBH_2$·IDipp][PF_6] (CD_2Cl_2, 298 K).

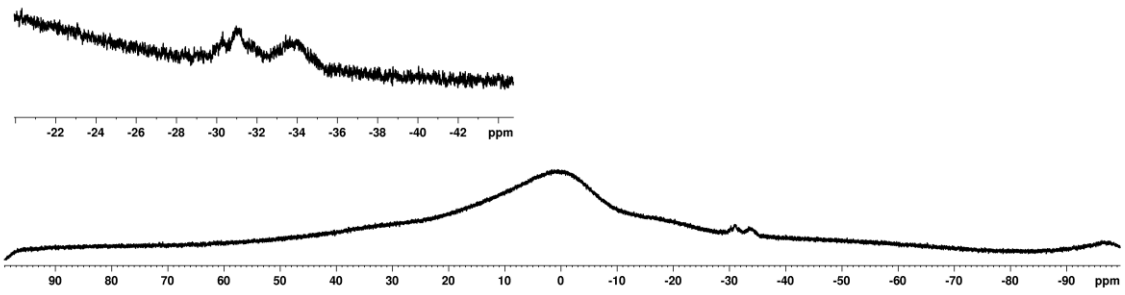

Figure S 10.43: ^{11}B NMR spectrum of [IDipp·$BH_2PH_2PHBH_2$·IDipp][PF_6] (CD_2Cl_2, 298 K).

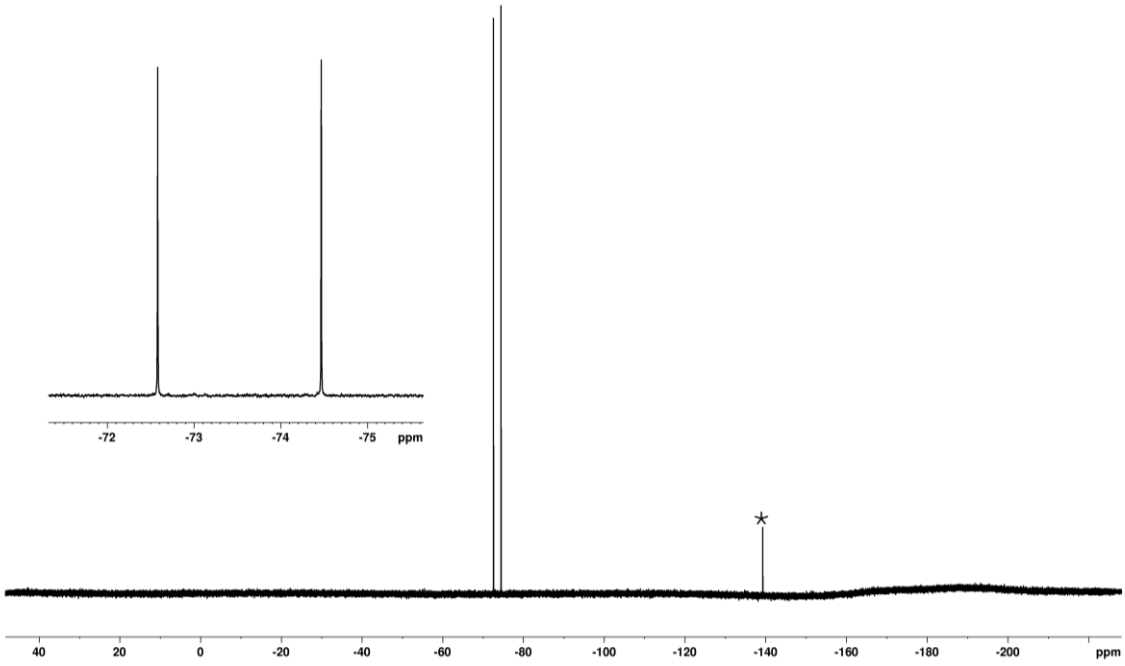

Figure S 10.44: $^{19}F\{^{1}H\}$ NMR spectrum of [IDipp·$BH_2PH_2PHBH_2$·IDipp][PF_6] (CD_2Cl_2, 298 K; * = residual o-DFB).

10.5.3.8 [IDipp·$BH_2PH_2PHBH_2$·IDipp][PF_6] by the reaction of IDipp·BH_2PH_2 with Tl[PF_6]/Cy_2PBr

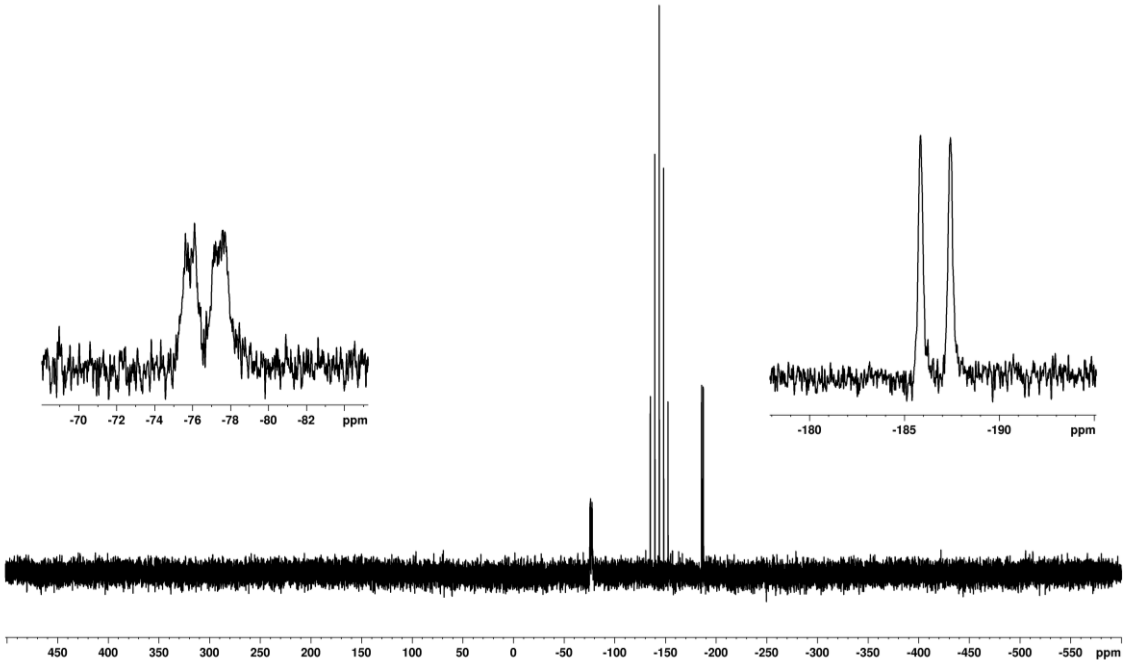

Figure S 10.45: $^{31}P\{^{1}H\}$ NMR spectrum of [IDipp·$BH_2PH_2PHBH_2$·IDipp][PF_6] obtained by the reaction of IDipp·BH_2PH_2 with Tl[PF_6]/Cy_2PBr (CH_2Cl_2/C_6D_6-cap., 298 K).

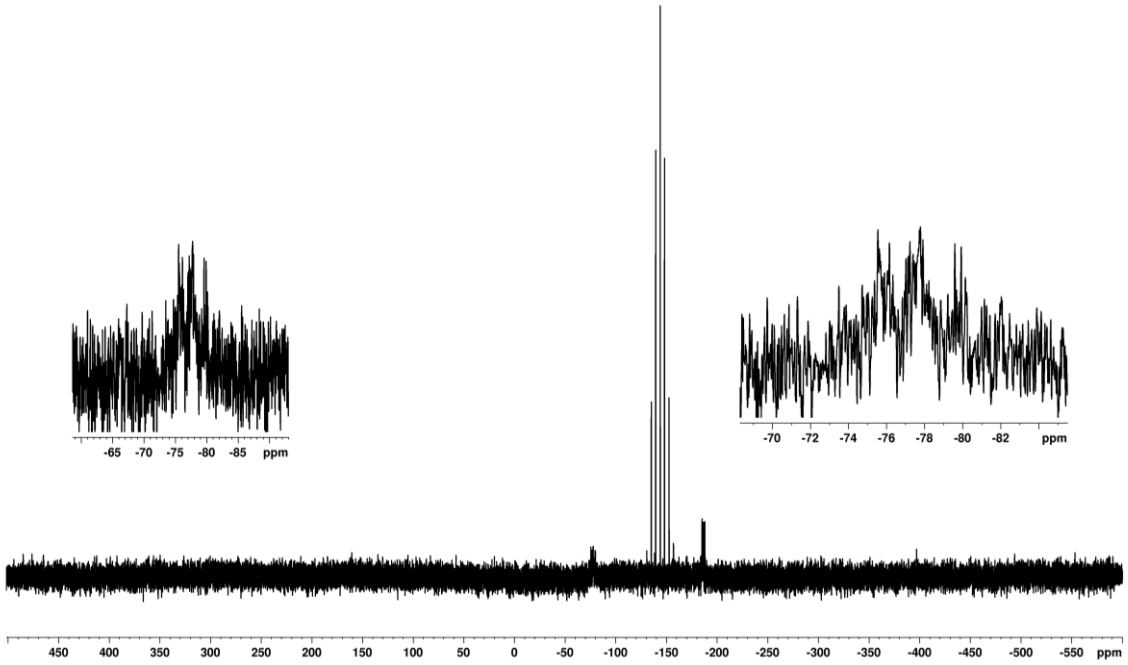

Figure S 10.46: ^{31}P NMR spectrum of [IDipp·$BH_2PH_2PHBH_2$·IDipp][PF_6] obtained by the reaction of IDipp·BH_2PH_2 with Tl[PF_6]/Cy_2PBr (CH_2Cl_2/C_6D_6-cap., 298 K).

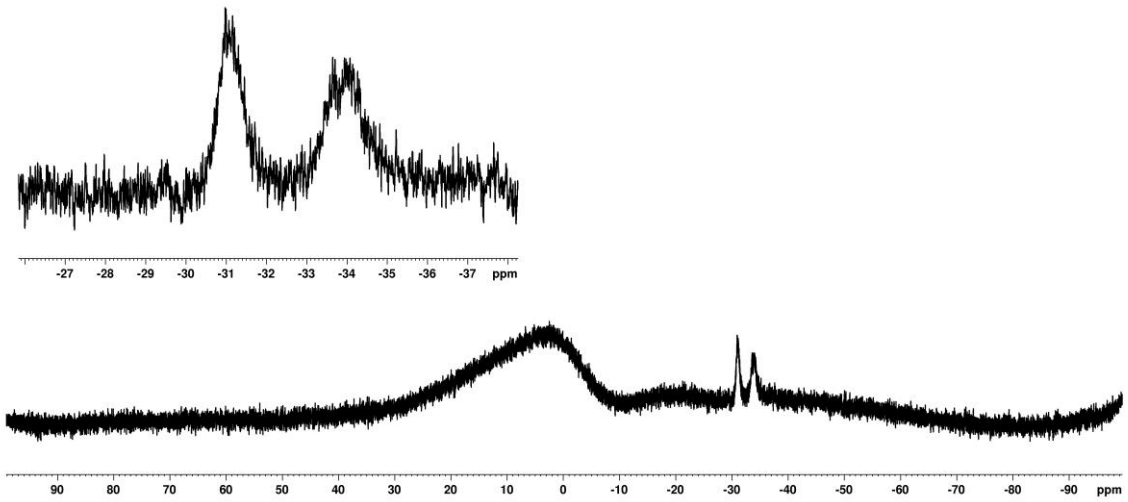

Figure S 10.47: $^{11}B\{^1H\}$ NMR spectrum of [IDipp·$BH_2PH_2PHBH_2$·IDipp][PF_6] obtained by the reaction of IDipp·BH_2PH_2 with Tl[PF_6]/Cy_2PBr (CH_2Cl_2/C_6D_6-cap., 298 K).

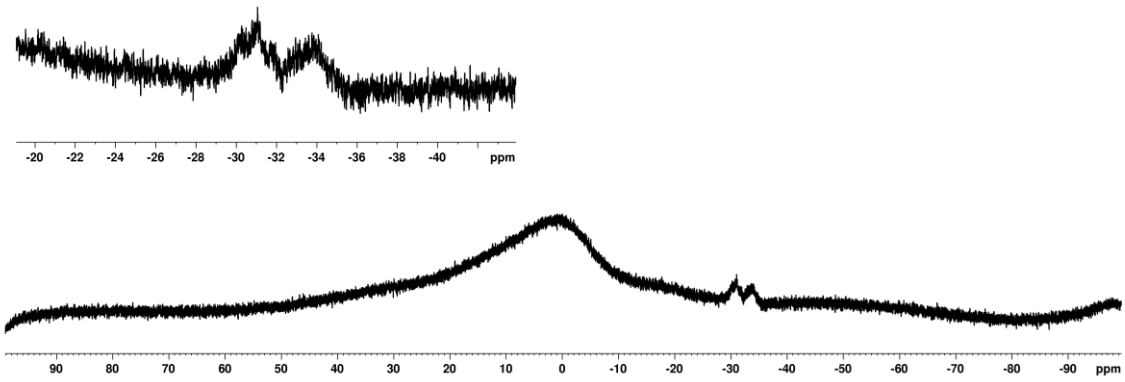

Figure S 10.48: ^{11}B NMR spectrum of [IDipp·$BH_2PH_2PHBH_2$·IDipp][PF_6] obtained by the reaction of IDipp·BH_2PH_2 with Tl[PF_6]/Cy_2PBr (CH_2Cl_2/C_6D_6-cap., 298 K).

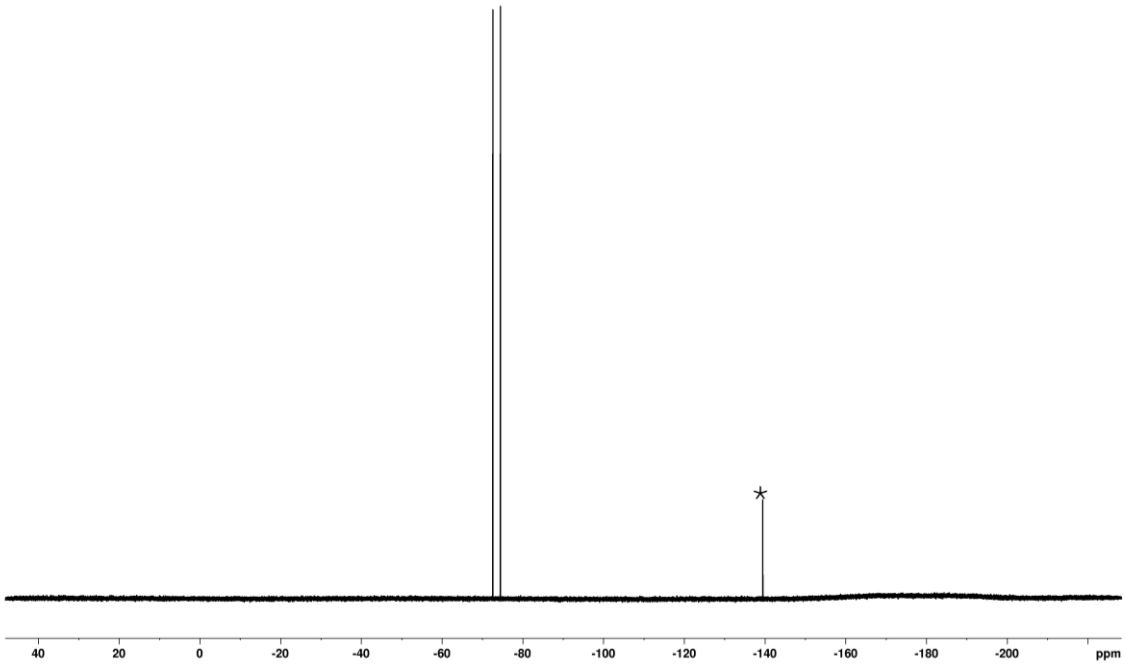

Figure S 10.49: $^{19}F\{^1H\}$ NMR spectrum of [IDipp·$BH_2PH_2PHBH_2$·IDipp][PF_6] obtained by the reaction of IDipp·BH_2PH_2 with Tl[PF_6]/Cy_2PBr (CH_2Cl_2/C_6D_6-cap., 298 K; * = residual o-DFB).

10.5.3.9 NMR spectra of the reaction mixture of IDipp·BH_2PH_2 (2 eq.) with Tl[PF_6]

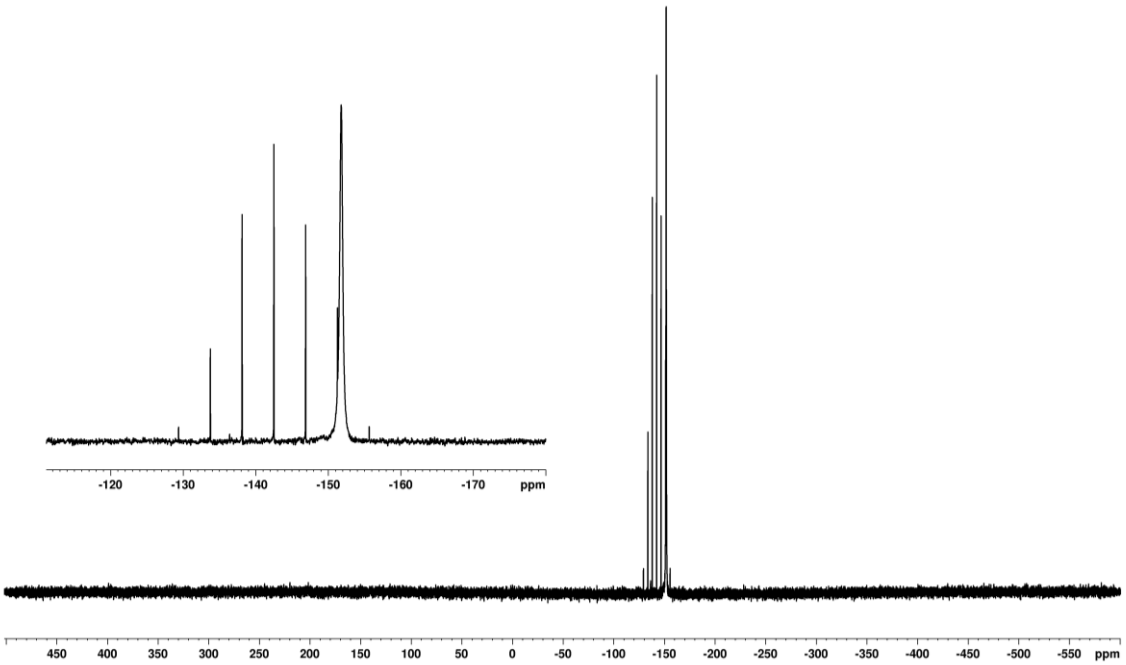

Figure S 10.50: $^{31}P\{^1H\}$ NMR spectrum of the reaction mixture of IDipp·BH_2PH_2 (43 mg, 0.1 mmol, 2 eq.) with Tl[PF_6] (17 mg, 0.05 mmol)(o-DFB/C_6D_6-cap., 298 K).

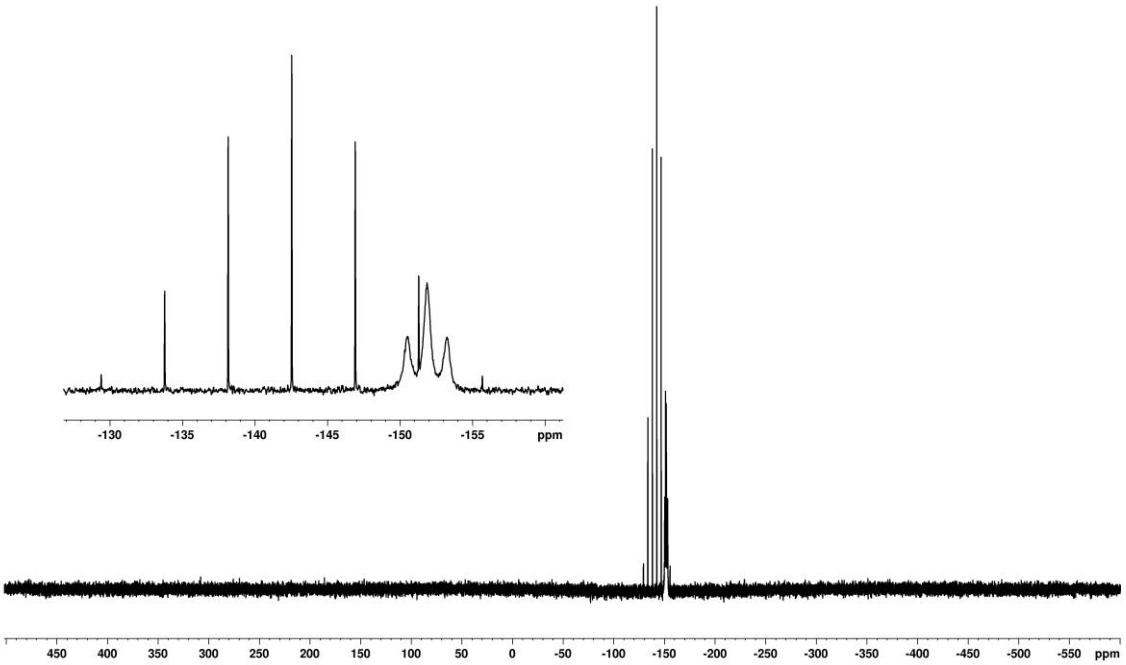

Figure S 10.51: ^{31}P NMR spectrum of the reaction mixture of IDipp·BH_2PH_2 (43 mg, 0.1 mmol, 2 eq.) with Tl[PF_6] (17 mg, 0.05 mmol)(o-DFB/C_6D_6-cap., 298 K).

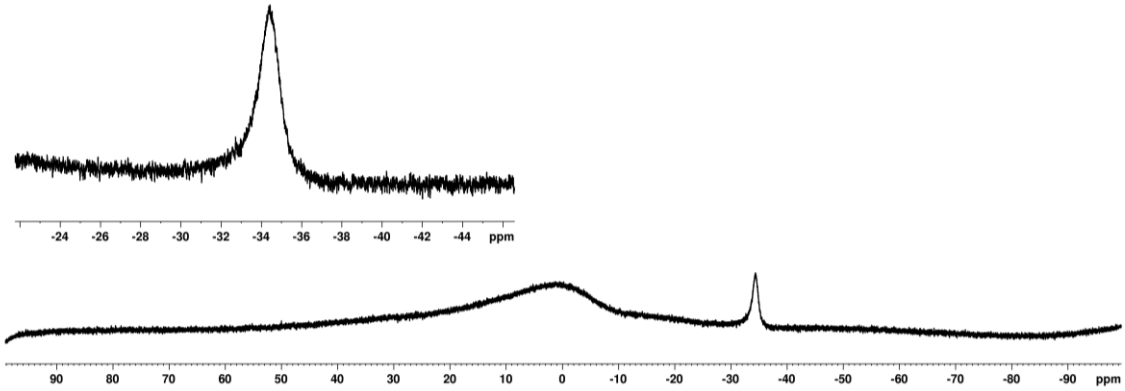

Figure S 10.52: $^{11}B\{^{1}H\}$ NMR spectrum of the reaction mixture of IDipp·BH_2PH_2 (43 mg, 0.1 mmol, 2 eq.) with $Tl[PF_6]$ (17 mg, 0.05 mmol)(o-DFB/C_6D_6-cap., 298 K).

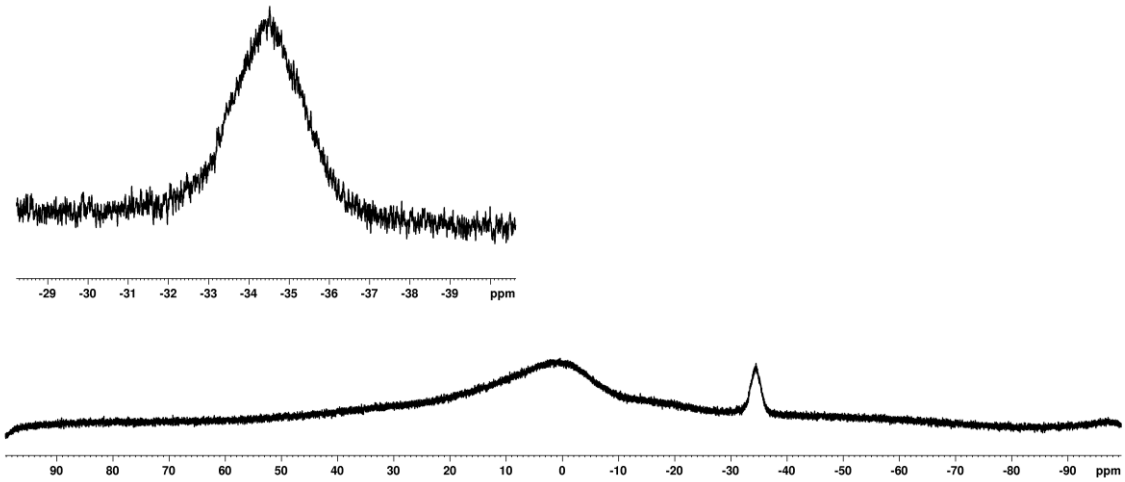

Figure S 10.53: ^{11}B NMR spectrum of the reaction mixture of IDipp·BH_2PH_2 (43 mg, 0.1 mmol, 2 eq.) with $Tl[PF_6]$ (17 mg, 0.05 mmol)(o-DFB/C_6D_6-cap., 298 K).

10.5.3.10 $[Me_3N{\cdot}BH_2PH_3][AlCl_4]$

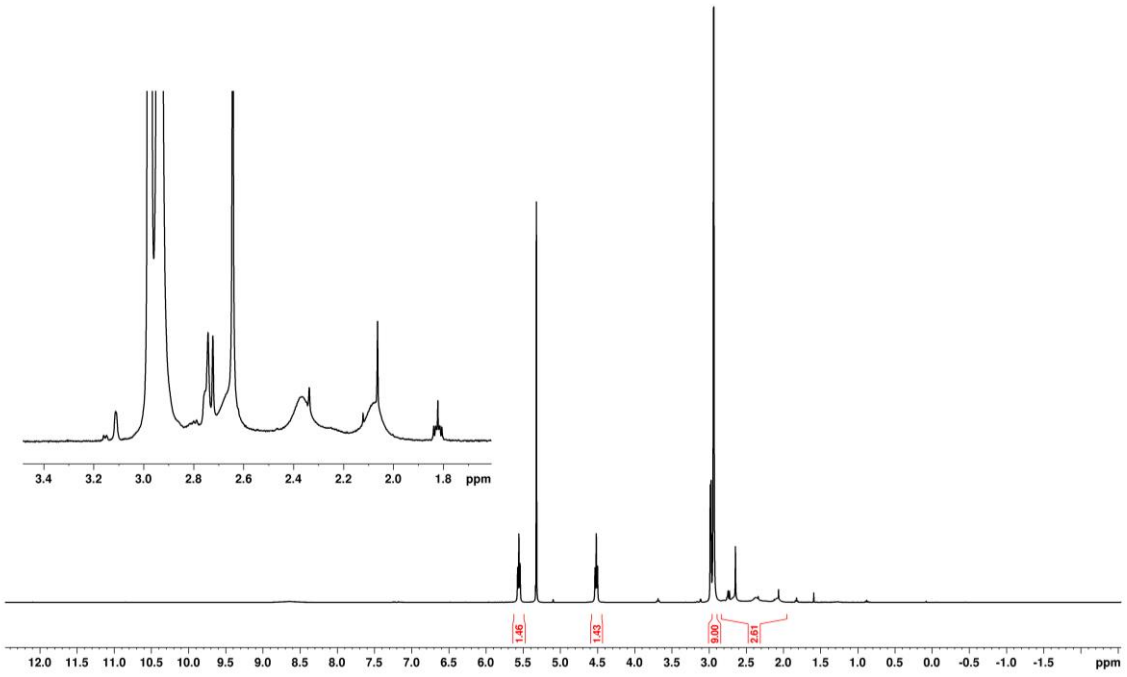

Figure S 10.54: ^{1}H NMR spectrum of $[Me_3N{\cdot}BH_2PH_3][AlCl_4]$ (CD_2Cl_2, 298 K).

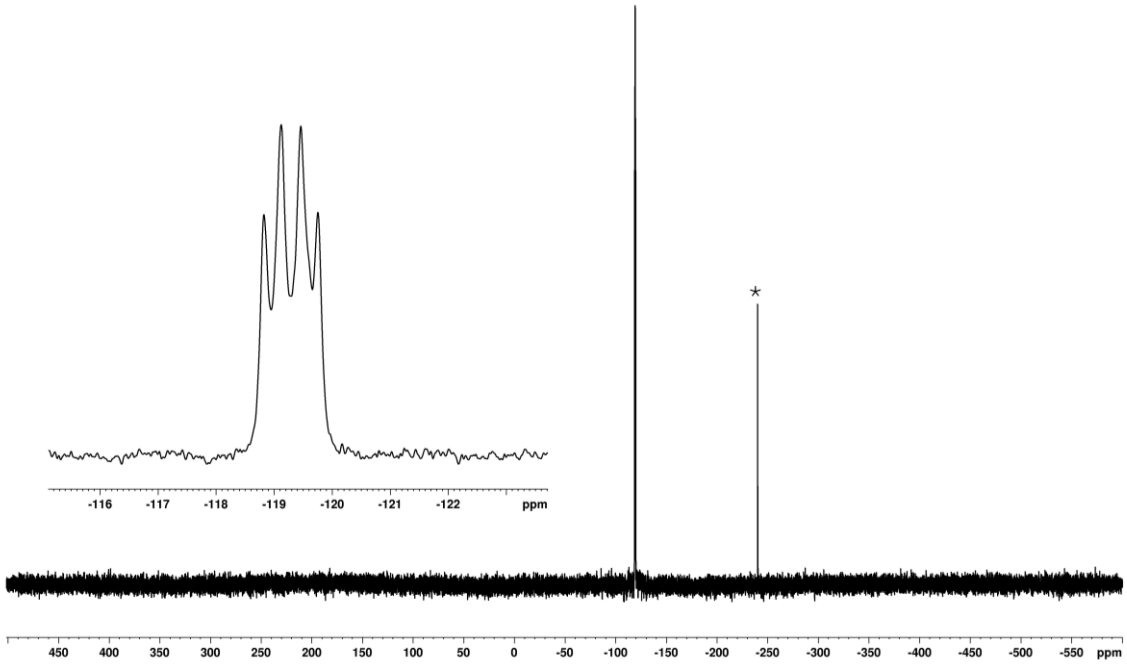

Figure S 10.55: $^{31}P\{^{1}H\}$ NMR spectrum of $[Me_3N{\cdot}BH_2PH_3][AlCl_4]$ (CD_2Cl_2, 298 K; * = PH_3).

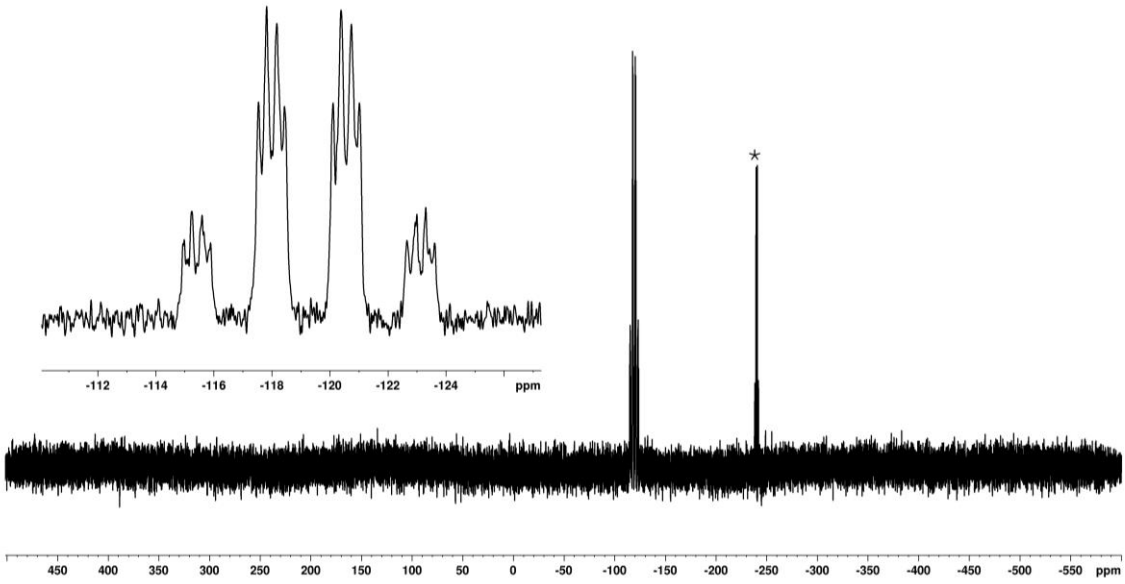

Figure S 10.56: ^{31}P NMR spectrum of $[Me_3N{\cdot}BH_2PH_3][AlCl_4]$ (CD_2Cl_2, 298 K; * = PH_3).

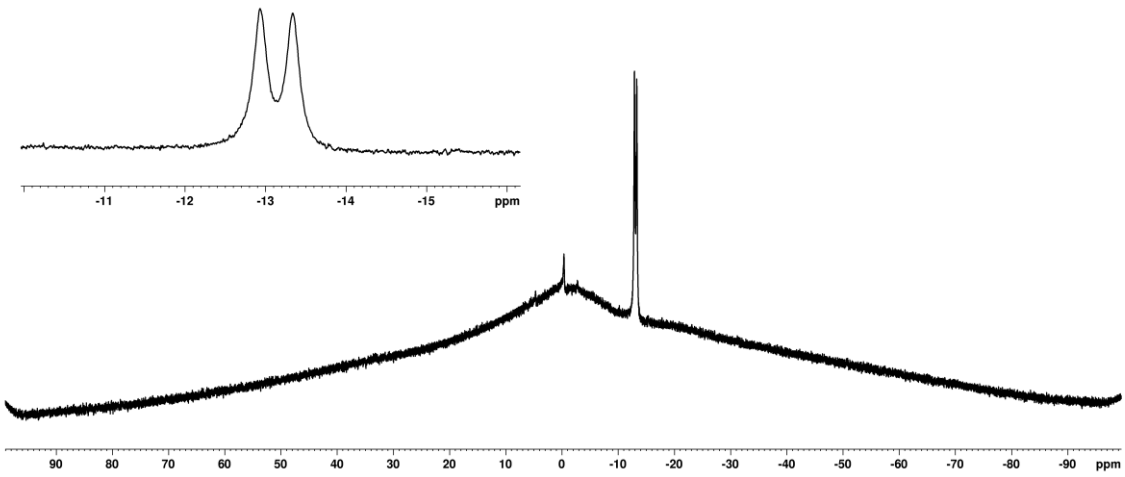

Figure S 10.57: $^{11}B\{^1H\}$ NMR spectrum of $[Me_3N{\cdot}BH_2PH_3][AlCl_4]$ (CD_2Cl_2, 298 K).

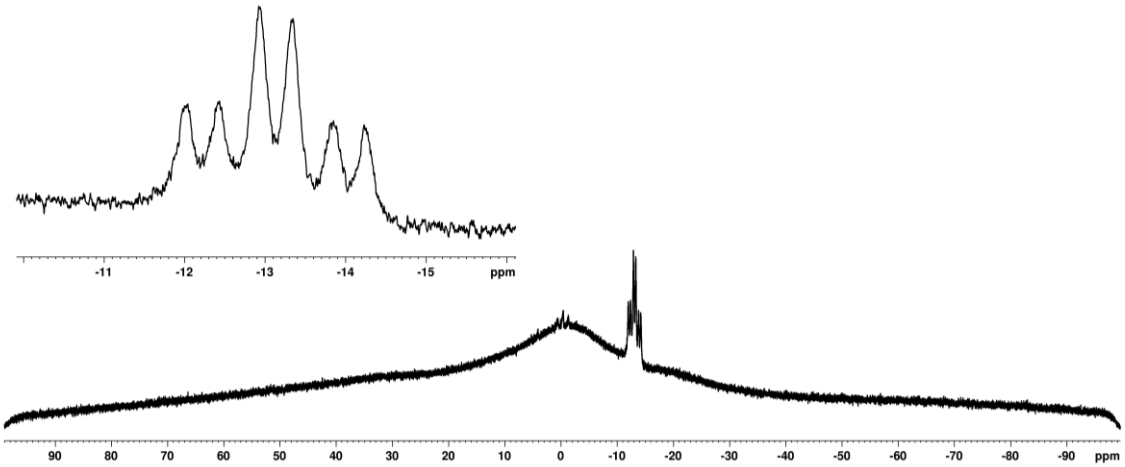

Figure S 10.58: ^{11}B NMR spectrum of $[Me_3N{\cdot}BH_2PH_3][AlCl_4]$ (CD_2Cl_2, 298 K).

10.5.3.11 $Me_3N{\cdot}BH_2PH_2$ (by deprotonation of $[Me_3N{\cdot}BH_2PH_3][AlCl_4]$)

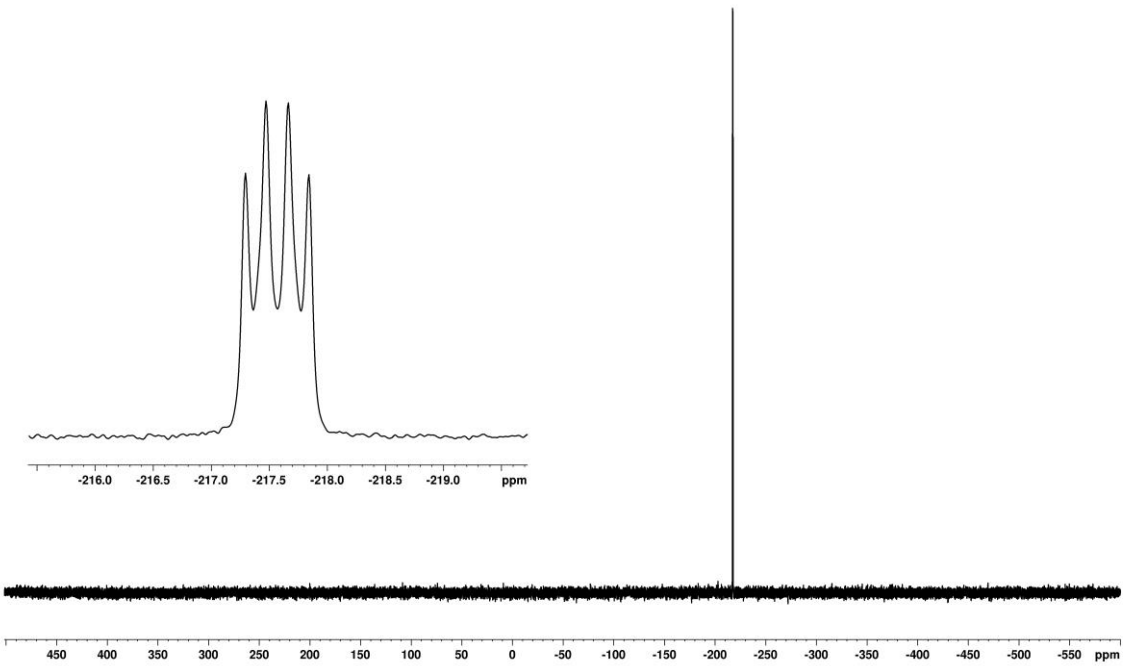

Figure S 10.59: $^{31}P\{^1H\}$ NMR spectrum of $Me_3N{\cdot}BH_2PH_2$ obtained by the deprotonation of $[Me_3N{\cdot}BH_2PH_3][AlCl_4]$ (Et_2O/C_6D_6-cap., 298 K).

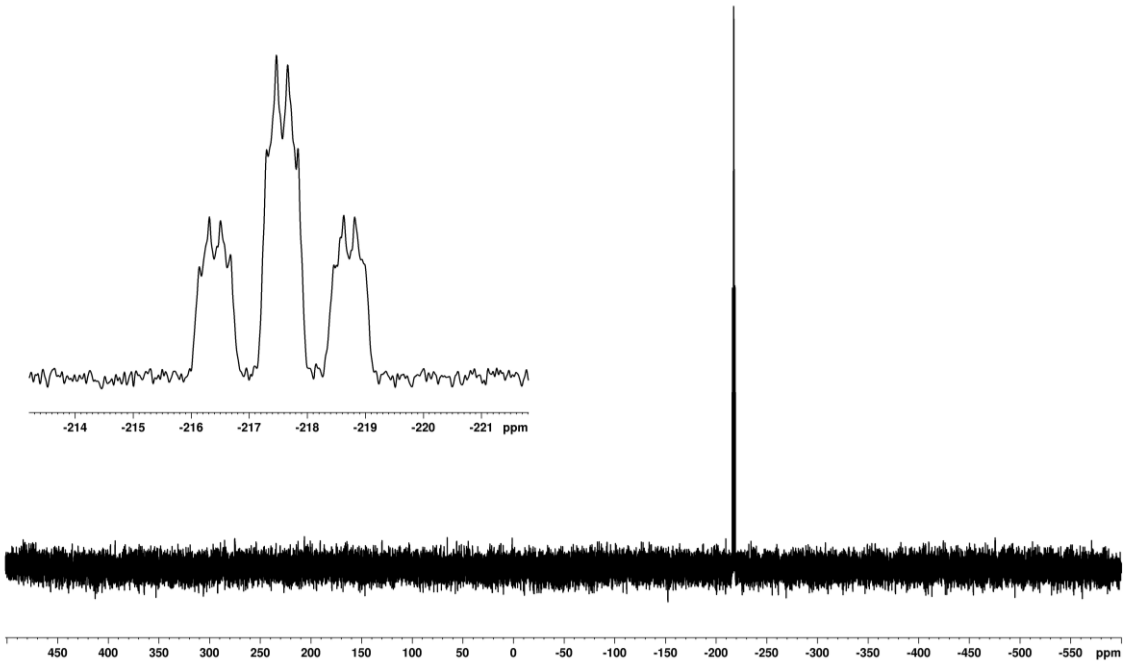

Figure S 10.60: ^{31}P NMR spectrum of $Me_3N{\cdot}BH_2PH_2$ obtained by the deprotonation of $[Me_3N{\cdot}BH_2PH_3][AlCl_4]$ (Et_2O/C_6D_6-cap., 298 K).

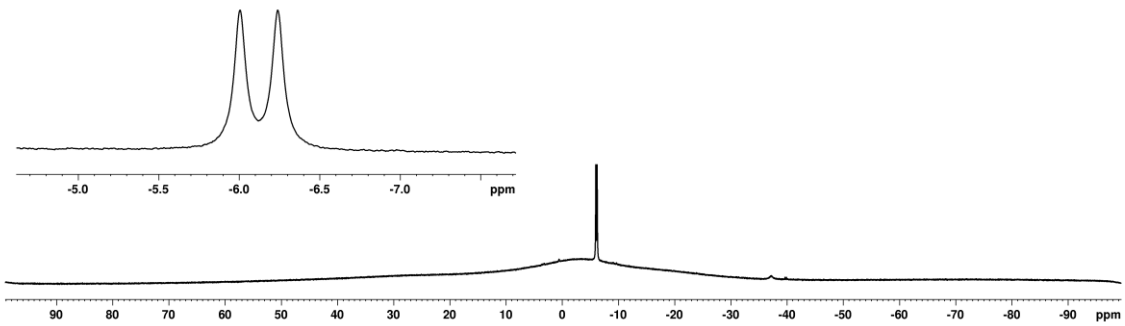

Figure S 10.61: $^{11}B\{^1H\}$ NMR spectrum of $Me_3N{\cdot}BH_2PH_2$ obtained by the deprotonation of $[Me_3N{\cdot}BH_2PH_3][AlCl_4]$ (Et_2O/C_6D_6-cap., 298 K).

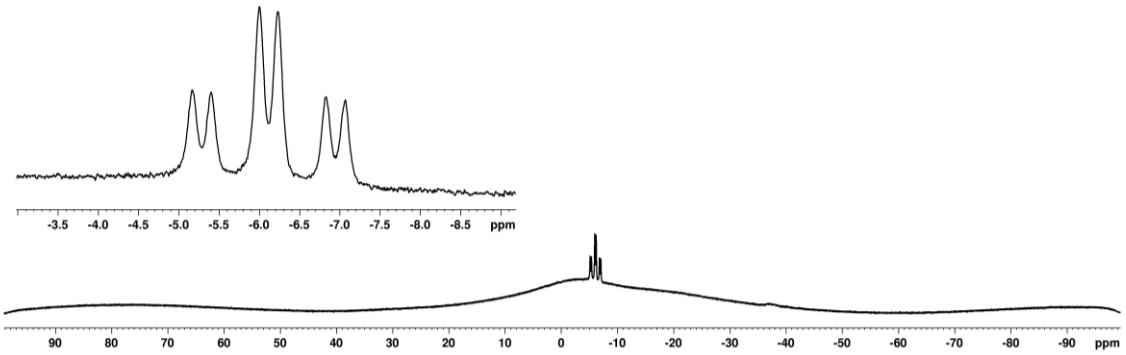

Figure S 10.62: ^{11}B NMR spectrum of $Me_3N{\cdot}BH_2PH_2$ obtained by the deprotonation of $[Me_3N{\cdot}BH_2PH_3][AlCl_4]$ (Et_2O/C_6D_6-cap., 298 K).

10.5.3.12 IDipp·$BH_2PH_2GaH_3$

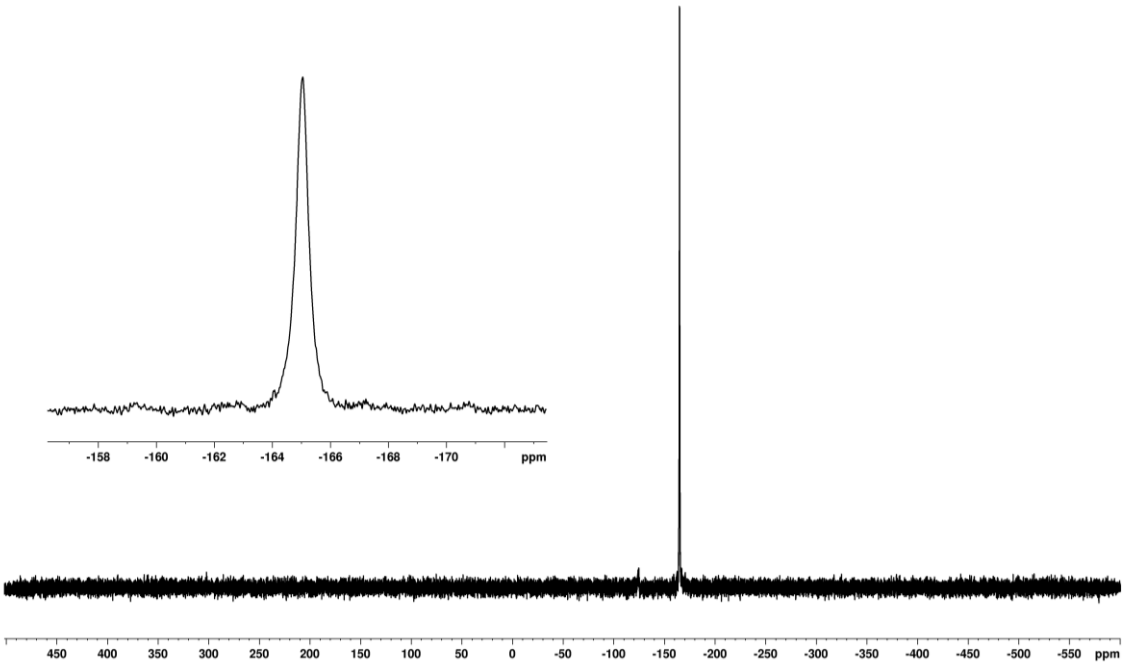

Figure S 10.63: $^{31}P\{^1H\}$ NMR spectrum of IDipp·$BH_2PH_2GaH_3$ (C_6D_6, 298 K).

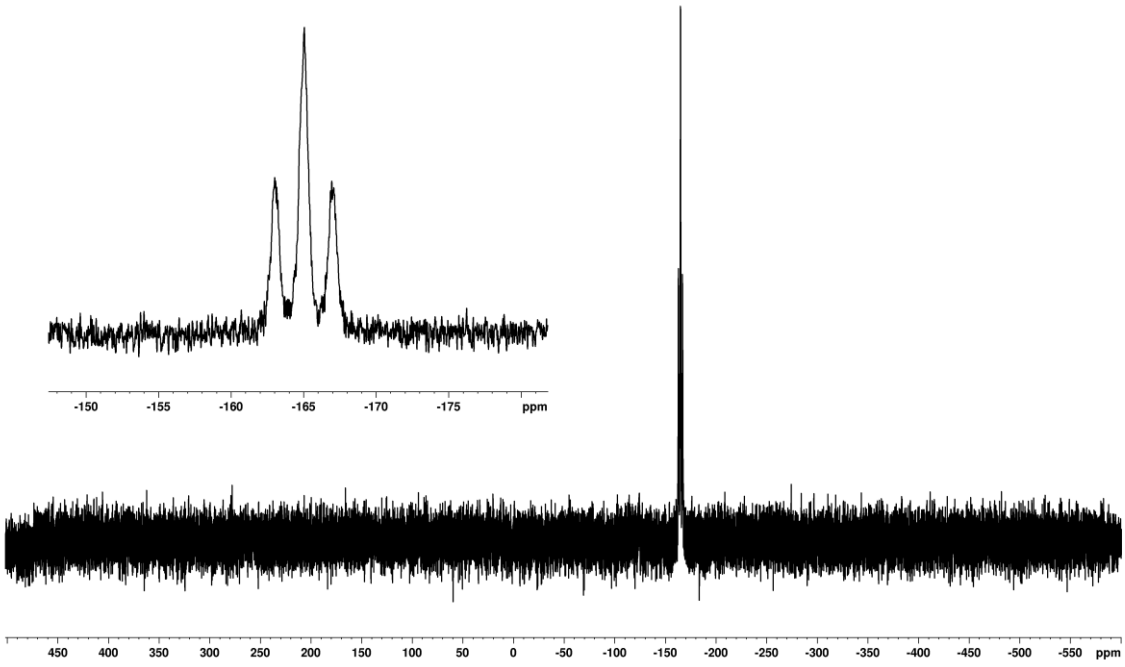

Figure S 10.64: ^{31}P NMR spectrum of IDipp·$BH_2PH_2GaH_3$ (C_6D_6, 298 K).

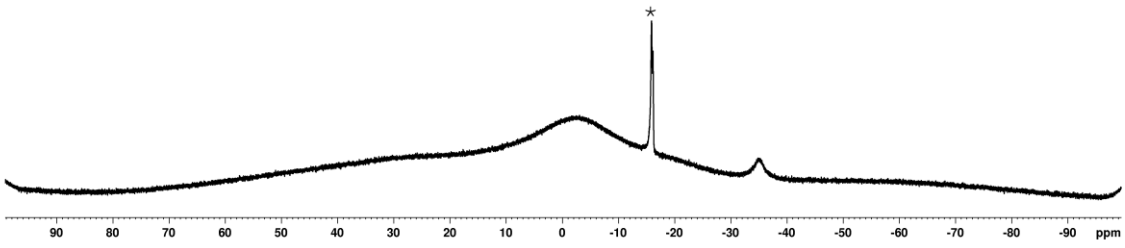

Figure S 10.65: $^{11}B\{^1H\}$ NMR spectrum of IDipp·$BH_2PH_2GaH_3$ (C_6D_6, 298 K; * = residual $[B(C_6F_5)_4]^-$ which remained inseparable).

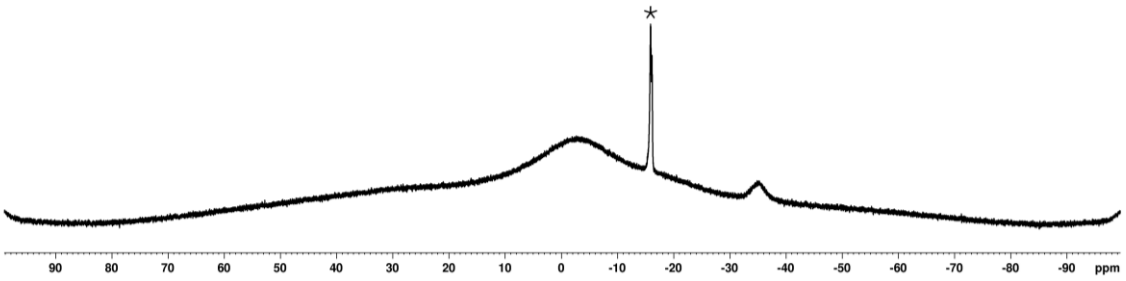

Figure S 10.66: ^{11}B NMR spectrum of IDipp·$BH_2PH_2GaH_3$ (C_6D_6, 298 K; * = residual $[B(C_6F_5)_4]^-$ which remained inseparable).

10.5.3.13 $Me_3N{\cdot}BH_2PH_2GaH_3$

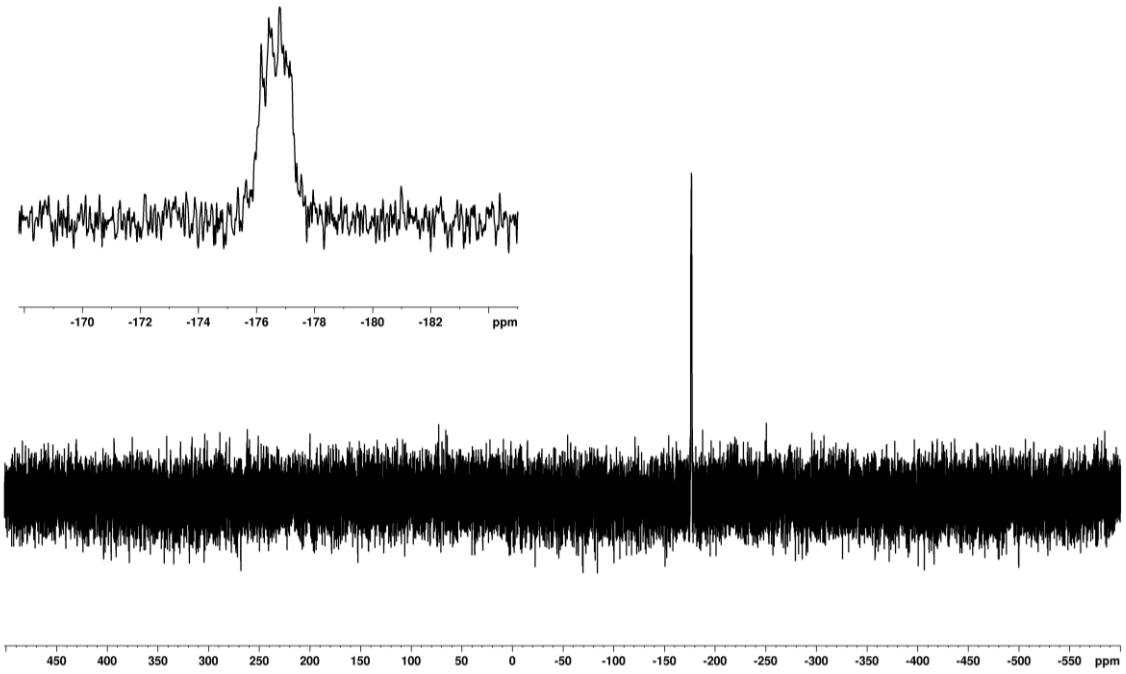

Figure S 10.67: $^{31}P\{^1H\}$ NMR spectrum of $Me_3N{\cdot}BH_2PH_2GaH_3$ (C_6D_6-cap./Et_2O, 298 K).

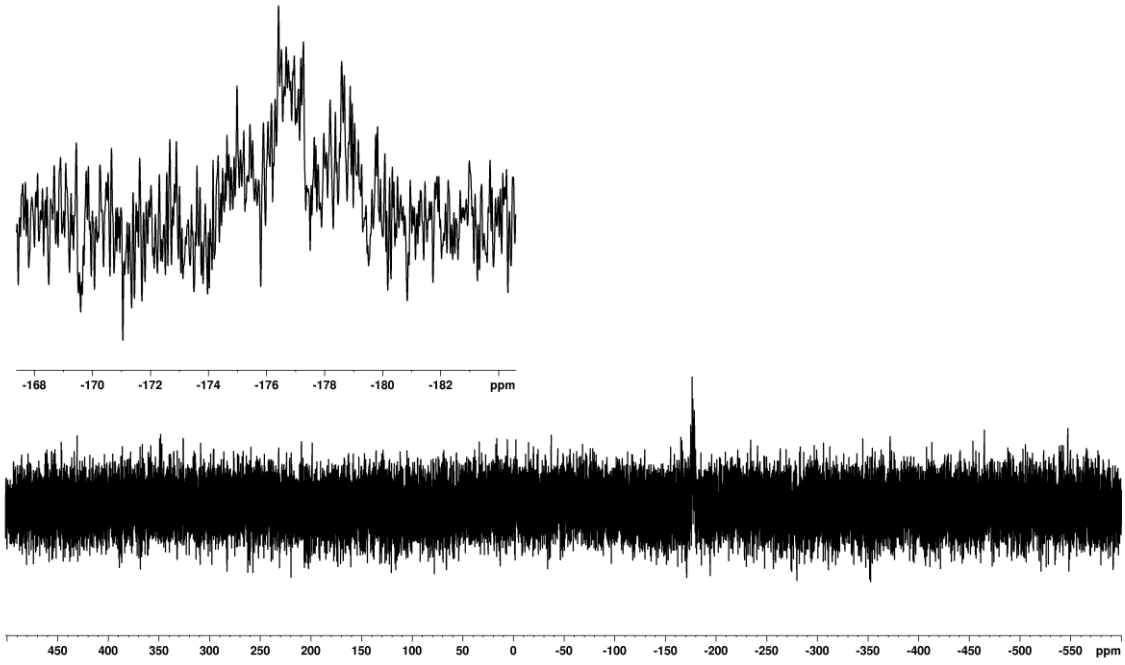

Figure S 10.68: ^{31}P NMR spectrum of $Me_3N{\cdot}BH_2PH_2GaH_3$ (C_6D_6-cap./Et_2O, 298 K).

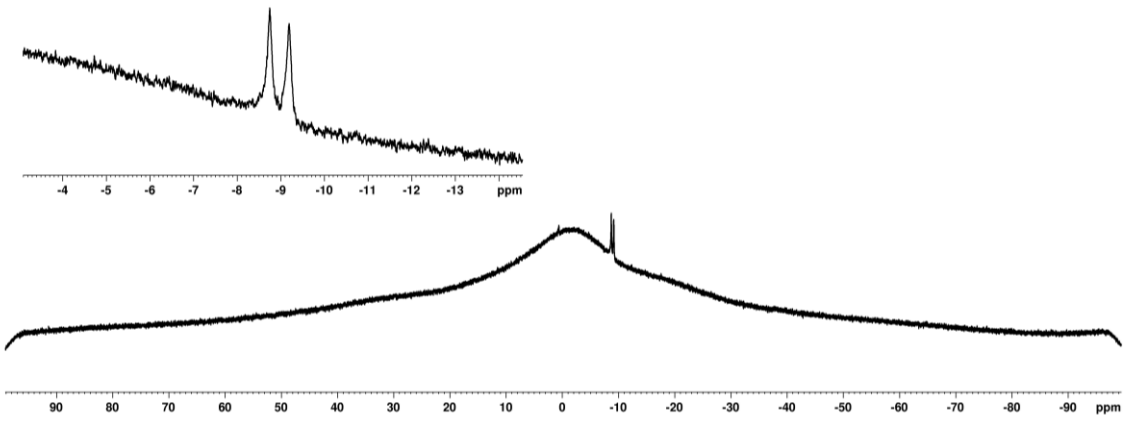

Figure S 10.69: $^{11}B\{^1H\}$ NMR spectrum of $Me_3N{\cdot}BH_2PH_2GaH_3$ (C_6D_6-cap./Et_2O, 298 K).

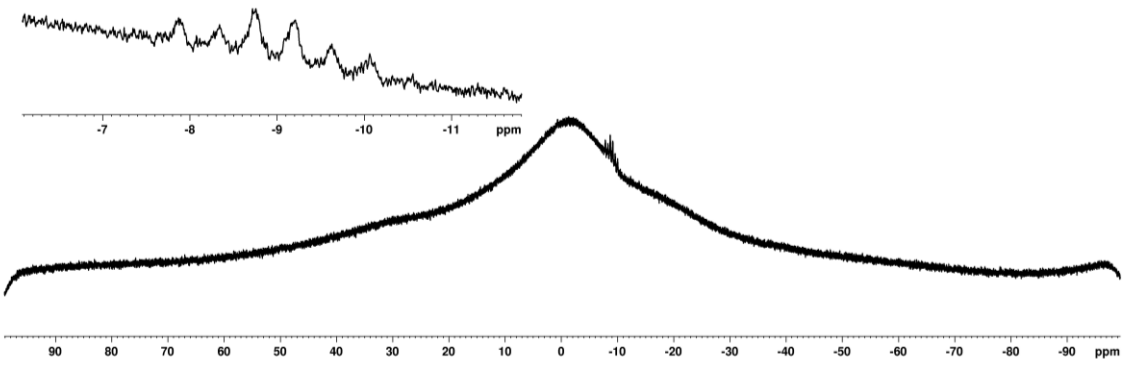

Figure S 10.70: ^{11}B NMR spectrum of $Me_3N{\cdot}BH_2PH_2GaH_3$ (C_6D_6-cap./Et_2O, 298 K).

10.5.4 Crystallographic Data

Single Crystal X-ray structure determination: Single-crystal X-ray diffraction data sets were collected using a XtaLAB Synergy R, DW system diffractometer (**1a**, **2**, **4**, **5**, **6**, **7a**) equipped with a HyPix-Arc 150 detector or a Xcalibur, Gemini ultra diffractometer (**1b**) operating at T = 123.01(10) K. Crystals were selected under mineral oil or perfluorinated Fomblin. Data reduction, scaling and absorption corrections were performed using CrysAlisPro (Rigaku, V1.171.41.90a, 2020). A gaussian absorption correction was performed using CrysAlisPro 1.171.41.90a (Rigaku Oxford Diffraction, 2020). Numerical absorption correction based on gaussian integration over a multifaceted crystal model. Empirical absorption correction using spherical harmonics, implemented in SCALE3 ABSPACK scaling algorithm. Using Olex2,[10] the structures were solved with ShelXT[11] and a least-squares refinement on $F2$ was carried out with ShelXL.[12] All non-hydrogen atoms were refined anisotropically. The hydrogen atoms at the carbon atoms have been located in idealized positions and refined isotropically according to the riding model. Figures were created with Olex2.

Table S 10.1: Crystallographic data for compounds **1a**, **1b** and **2**.

Compound	**1a**	**1b**	**2**
Formula	$C_{44.4}H_{43.8}AlBCl_{2.8}F_{36}N_2O_4P$	$AlPCl_4BC_3NH_{14}$	$C_{29}H_{43}BF_3N_2O_3PS$
Dcalc	1.632	1.395	1.213
μ/mm^{-1}	3.043	9.647	1.743
Formula Weight	1521.43	274.71	598.49
Colour	clear colourless	clear colourless	clear colourless
Shape	block-shaped	needle-shaped	block-shaped
Size/mm^3	0.70×0.49×0.13	0.15×0.12×0.10	0.53×0.13×0.08
T/K	123.00(10)	122.9(5)	122.99(10)
Crystal System	monoclinic	orthorhombic	orthorhombic
Flack Parameter	-	0.01(2)	-0.004(10)
Hooft Parameter	-	-	-0.015(7)
Space Group	$P2_1/n$	$Pna2_1$	$P2_12_12_1$
a/Å	16.80710(10)	12.64740(10)	11.40270(10)
b/Å	22.0708(2)	10.24600(10)	14.52680(10)
c/Å	17.26610(10)	10.09640(10)	19.7863(2)
α/°	90	90	90
β/°	104.7550(10)	90	90
γ/°	90	90	90
V/Å^3	6193.58(8)	1308.34(2)	3277.50(5)
Z	4	4	4
Z'	1	1	1
Wavelength/Å	1.54184	1.54178	1.54184
Radiation type	Cu K_a	Cu K_a	Cu K_a
Θ_{min}/°	3.276	3.494	4.469
Θ_{max}/°	75.131	66.593	75.294
Measured Refl's.	73048	6699	29668
Indep't Refl's	12564	2187	6657
Refl's I≥2 ⍰(I)	10768	2106	6297
R_{int}	0.0916	0.0276	0.0561
Parameters	987	124	450
Restraints	588	5	166
Largest Peak	1.472	1.574	0.245
Deepest Hole	-0.457	-0.391	-0.338
GooF	1.044	1.043	1.087
wR_2 (all data)	0.1727	0.1223	0.1071
wR_2	0.1674	0.1203	0.1058
R_1 (all data)	0.0645	0.0458	0.0423
R_1	0.0584	0.0445	0.0403

Table S 10.2: Crystallographic data for compounds **4**, and **5**.

Compound	**4**	**5**
Formula	$C_{52}H_{67}BN_2O_4F_{36}AlSi_3PGe$	$C_{46}H_{49}AlBF_{36}N_2O_4PSn$
Dcalc	1.543	1.673
μ/mm^{-1}	2.604	5.047
Formula Weight	1693.69	1565.32
Colour	clear dark colourless	clear yellow
Shape	plate-shaped	block-shaped
Size/mm^3	0.45×0.41×0.16	0.26×0.09×0.08
T/K	123.00(10)	123.00(10)
Crystal System	triclinic	triclinic
Space Group	*P*-1	*P*-1
a/Å	12.8761(2)	12.3364(4)
b/Å	17.3604(2)	16.0278(4)
c/Å	17.4272(2)	16.4471(5)
α/°	71.6530(10)	79.553(2)
β/°	80.5080(10)	80.284(3)
γ/°	85.2080(10)	78.805(3)
V/Å^3	3644.85(9)	3107.04(16)
Z	2	2
Z'	1	1
Wavelength/Å	1.54184	1.54184
Radiation type	Cu K_a	Cu K_a
Θ_{min}/°	2.683	2.758
Θ_{max}/°	75.381	73.786
Measured Refl's.	86425	12598
Indep't Refl's	14803	12598
Refl's I≥2 ⊠(I)	13799	10664
R_{int}	0.0391	.
Parameters	1107	857
Restraints	550	1
Largest Peak	0.679	1.567
Deepest Hole	-0.838	-1.256
GooF	1.075	1.071
wR_2 (all data)	0.1469	0.1759
wR_2	0.1452	0.1658
R_1 (all data)	0.0552	0.0707
R_1	0.0527	0.0601

Table S 10.3: Crystallographic data for compounds **6** and **7a**.

Compound	**6**	**7a**
Formula	$C_{63}H_{90}B_2F_8N_4P_3$	$C_{29}H_{48}BGaN_2O_{0.5}P$
Dcalc	1.167	1.138
μ/mm^{-1}	1.329	1.794
Formula Weight	1169.91	544.19
Colour	clear colourless	clear colourless
Shape	block-shaped	plate-shaped
Size/mm^3	0.23×0.17×0.13	0.17×0.14×0.07
T/K	123.00(10)	123.01(10)
Crystal System	monoclinic	orthorhombic
Space Group	*C*2/*c*	*Cmce*
a/Å	28.0943(2)	16.9221(4)
b/Å	18.88230(10)	18.7080(3)
c/Å	25.5940(2)	20.0673(4)
α/°	90	90
β/°	101.2440(10)	90
γ/°	90	90
V/Å^3	13316.62(16)	6352.9(2)
Z	8	8
Z'	1	0.5
Wavelength/Å	1.54184	1.54184
Radiation type	Cu K_a	Cu K_a
Θ_{min}/°	2.837	4.155
Θ_{max}/°	73.729	73.501
Measured Refl's.	53323	21656
Indep't Refl's	12977	3234
Refl's I≥2 *s*(I)	10770	3073
R_{int}	0.0219	0.0271
Parameters	812	204
Restraints	742	75
Largest Peak	0.666	0.557
Deepest Hole	-0.370	-0.723
GooF	1.068	1.123
wR_2 (all data)	0.1518	0.1986
wR_2	0.1460	0.1978
R_1 (all data)	0.0586	0.0965
R_1	0.0507	0.0943

10.5.4.1 Crystal structures

[IDipp·BH_2PH_3][TEF] (1a)

1a crystallized from a CH_2Cl_2 solution layered with *n*-hexane at -30 °C as clear colourless block-shaped crystals in the monoclinic space group $P2_1/n$. The structure of **1a** in the solid state is shown in Figure S 10.71.

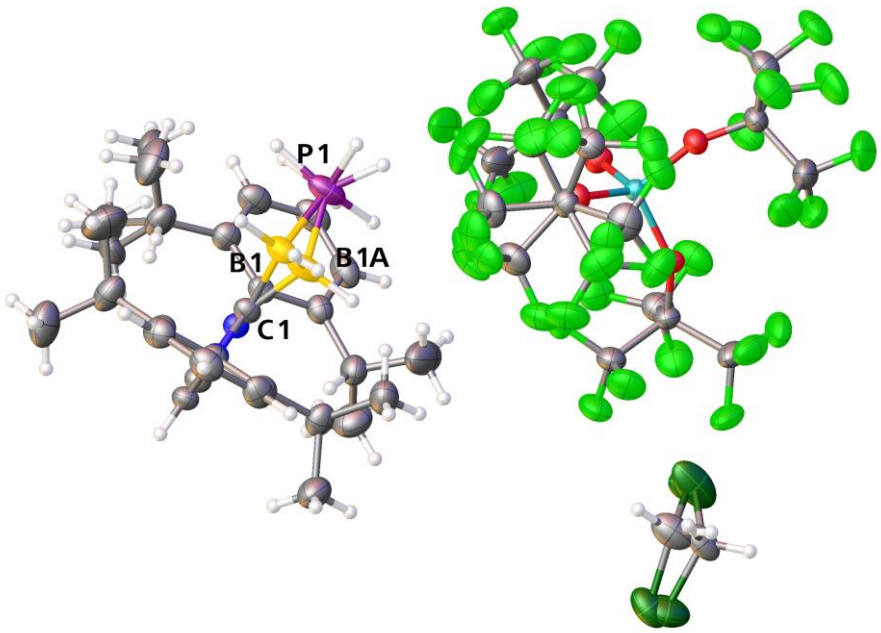

Figure S 10.71: Molecular structure of **1a** in the solid state. Anisotropic displacement ellipsoids are shown at 50% probability level. Dipp moieties are displayed in a stick model for improved overall clarity. Selected bond lengths [Å] and angles [°]: C1-B1 1.622(5), C1-B1A 1.595(10), B1-P1 1.896(5), B1A-P1 1.902(9), C1-B1-P1 118.6(3), C1-B1A-P1 119.7(7).

The asymmetric unit contains one molecule of **1a** and 0.9 CH_2Cl_2, which displays disorder at the chain atom position, the solvent and the anion. These were modelled by applying SIMU and SADI restraints. H atoms bound to B and P were fixed in idealized positions.

[Me_3N·BH_2PH_3][$AlCl_4$] (1b)

1b crystallized by from a dichloromethane solution layered by *n*-hexane as clear colourless needle-shaped crystals in the orthorhombic space group $Pna2_1$. The structure of **1b** in the solid state is shown in Figure S 10.72. The asymmetric unit contains one molecule of **1b**. Hydrogen atoms bound to B and P were refined by applying DFIX restraints.

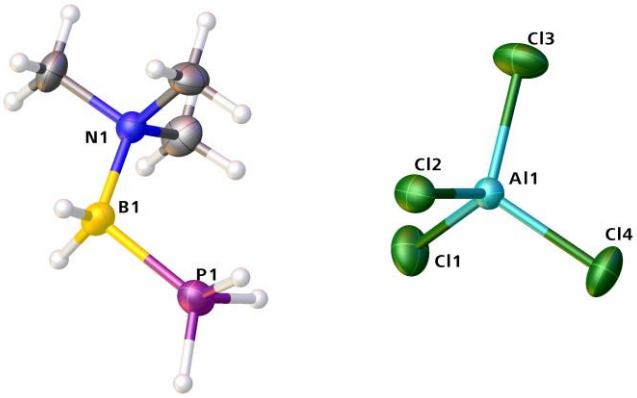

Figure S 10.72: Structure of **1b** in the solid state (asymmetric unit). Anisotropic displacement ellipsoids are displayed with 50% probability. Selected bond lengths [Å] and angles [°]: N1-B1 1.581(7), B1-P1 1.987(9), N1-B1-P1 113.2(5).

[IDipp·$BH_2PH_2CH_3$][OTf] (2)

2 crystallized by layering a THF solution of **2** with n-hexane at -30 °C as clear colourless block-shaped crystals in the orthorhombic space group $P2_12_12_1$. The structure of **2** in the solid state is shown in Figure S 10.73. The asymmetric unit contains one molecule of **2**. The triflate anion displays minor disorder and was refined with SIMU and SADI restraints.

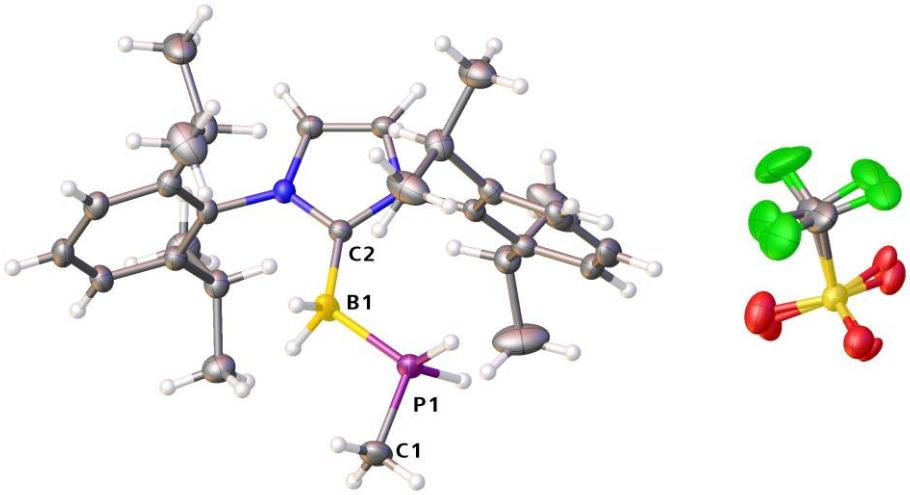

Figure S 10.73: Molecular structure of **2** in the solid state. Anisotropic displacement ellipsoids are shown at 50% probability level. Selected bond lengths [Å] and angles [°]: C2-B1 1.594(4), B1-P1 1.923(3), P1-C1 1.794(3), C1-B1-P1 120.4(2), B1-P1-C1 108.54(14).

[IDipp·$BH_2PH_2Ge(SiMe_3)_3$][TEF] (4)

4 crystallized from a *o*-DFB solution layered with *n*-hexane at -30 °C as clear colourless block-shaped crystals in the triclinic space group *P*-1. The structure of **4** in the solid state is shown in Figure S 10.74. The asymmetric unit contains one molecule of **4**. Hydrogen atoms bound to B and P were refined freely. The $[TEF]^-$ anion displays minor disorder and was refined by applying DFIX, SADI and SIMU restraints.

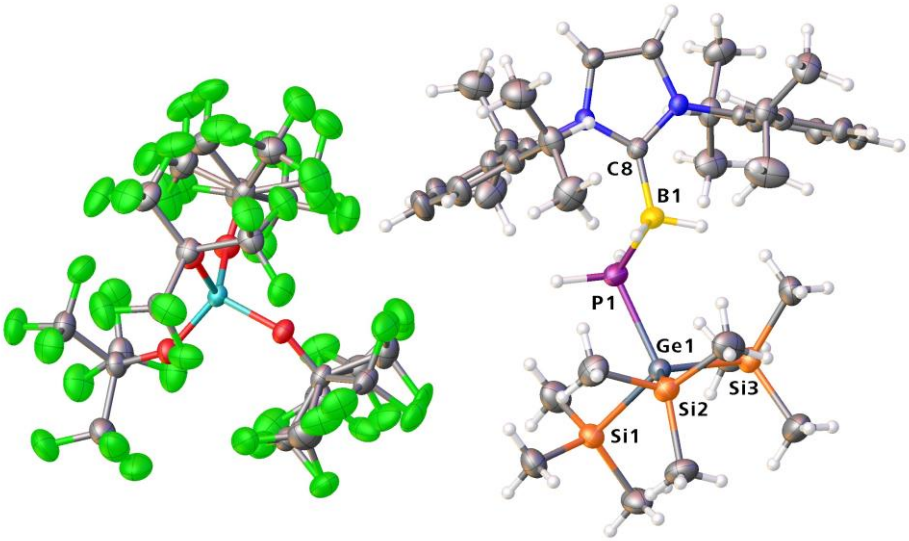

Figure S 10.74: Molecular structure of **4** in the solid state. Anisotropic displacement ellipsoids are shown at 50% probability level. Selected bond lengths [Å] and angles [°]: C8-B1 1.593(4), B1-P1 1.948(3), P1-Ge1 2.3417(8), Ge1-Si1 2.3853(8), Ge1-Si2 2.3983(8), Ge1-Si3 2.4021(8), C8-B1-P1 118.2(2), B1-P1-Ge1 112.45(10).

[IDipp·$BH_2PH_2SnMe_3$][TEF] (5)

5 crystallized from a *o*-DFB solution layered with *n*-hexane at -30 °C as clear colourless block-shaped crystals in the triclinic space group *P*-1. The structure of **5** in the solid state is shown in Figure S 10.75.

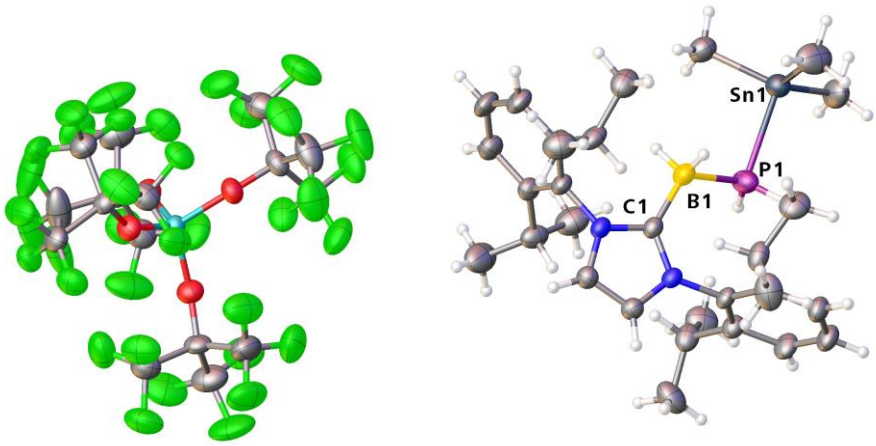

Figure S 10.75: Molecular structure of **5** in the solid state. Anisotropic displacement ellipsoids are shown at 50% probability level. Selected bond lengths [Å] and angles [°]: C1-B1 1.598(7), B1-P1 1.943(6), P1-Sn1 2.5455(13), C1-B1-P1 120.3(3), B1-P1-Sn1 107.69(17).

The compound crystallized as twinned crystals and had to be refined with respect to the individual twin components. The asymmetric unit contains one molecule of **5**. Hydrogen atoms bound to P were refined by applying a SADI restraint.

[IDipp·$BH_2PH_2PHBH_2$·IDipp][PF_6] (6)

6 crystallized from a *o*-DFB solution layered with *n*-hexane at room temperature as clear colourless block-shaped crystals in the triclinic space group *C*2/*c*. The structure of **6** in the solid state is shown in **Figure S 10.76**.

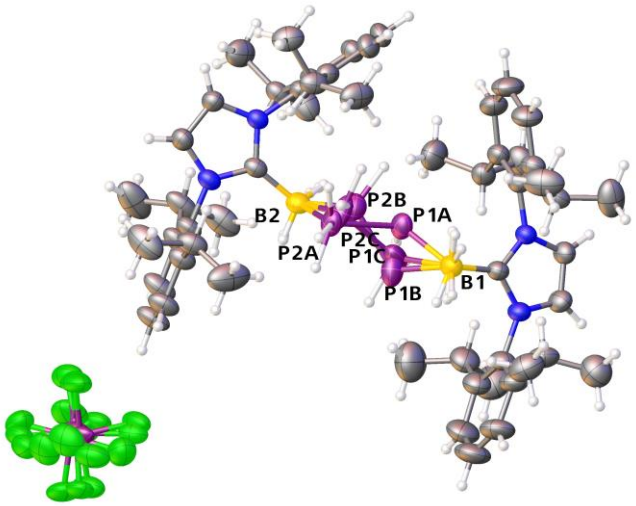

Figure S 10.76: Molecular structure of **4g** in the solid state. Anisotropic displacement ellipsoids are shown at 50% probability level.

The compound displays threefold disorder in the chain P atom positions and the anion and had to be refined by applying DFIX, DANG, SIMU and SADI restraints. Hydrogen atoms bound to B and P were fixed in idealized positions.

IDipp·$BH_2PH_2GaH_3$ (7a)

7a crystallized from a concentrated diethylether solution at -30 °C as clear colourless plate-shaped crystals in the orthorhombic space group *Cmce*. The structure of **7a** in the solid state is shown in Figure S 10.77.

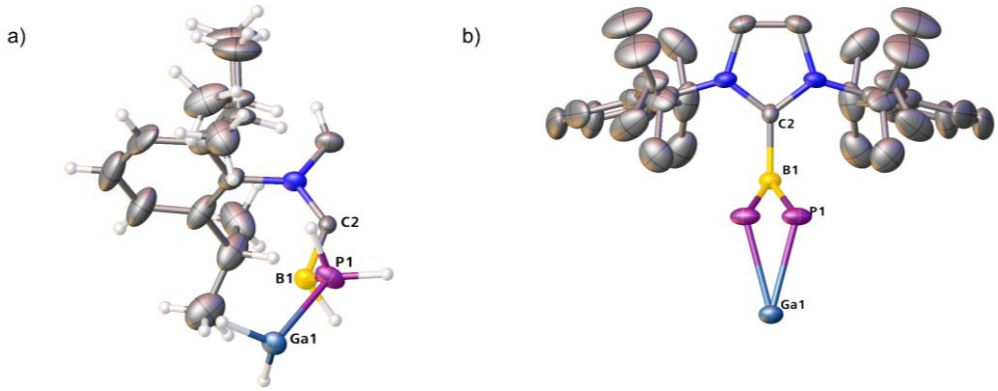

Figure S 10.77: Molecular structure of **7a** in the solid state (a: asymmetric unit, b: grown molecular structure). Anisotropic displacement ellipsoids are shown at 50% probability level. Hydrogen atoms bound to carbon are omitted for clarity in Fig. b.

Selected bond lengths [Å] and angles [°]: C2-B1 1.607(10), B1-P1 1.916(9), P1-Ga1 2.425(3), C2-B1-P1 114.1(5), B1-P1-Ga1 112.0(3).

The asymmetric unit shows 0.5 molecules of **7a** as a mirror plane cuts directly through the centre of the molecule (cf. Figure S 10.77b). and was refined without further restrains/constraints. H-atoms bound to B were refined freely. Disordered ^{i}Pr groups were refined with additional SADI and SIMU restraints. Hydrogen atoms bound to heteroatoms were fixed in idealized positions with DFIX and DANG restraints.

10.5.5 References

[1] L. I. Zakharkin, V. V. Gavrilenko, Y. N. Karaksin, *Synth. React. Inorg. Met.-Org. Chem.* **1971**, *1*, 37–43.
[2] R. Szlosek, M. Seidl, G. Balázs, M. Scheer, *Chem. Eur. J.* **2023**, *29*, e202301752.
[3] M. Gonsior, I. Krossing, *Z. Anorg. Allg. Chem.* **2002**, *628*, 1821–1830.
[4] I. Krossing, H. Brands, R. Feuerhake, S. Koenig, *J. Fluor. Chem.* **2001**, *112*, 83–90.
[5] G. E. Rysciikewitscii, J. W. Wiggins, R. L. Sneath, L. J. Todd in *Inorganic Syntheses* (Hrsg.: R. W. Parry), Wiley, **1970**, S. 116–126.
[6] W. Steinkopf, H. Dudek, S. Schmidt, *Ber. dtsch. Chem. Ges. A/B* **1928**, *61*, 1911–1918.
[7] Z. M. Heiden, S. Chen, M. T. Mock, W. G. Dougherty, W. S. Kassel, R. Rousseau, R. M. Bullock, *Inorg. Chem.* **2013**, *52*, 4026–4039.
[8] H. Grützmacher, M. Bispringhoff, WO 2019/175319 A1.
[9] U. Vogel, P. Hoemensch, K.-C. Schwan, A. Y. Timoshkin, M. Scheer, *Chem. Eur. J.* **2003**, *9*, 515–519.
[10] O. V. Dolomanov, L. J. Bourhis, R. J. Gildea, J. A. K. Howard, H. Puschmann, *J. Appl. Crystallogr.* **2009**, *42*, 339–341.
[11] G. M. Sheldrick, *Acta Cryst. A* **2015**, *71*, 3–8.
[12] G. M. Sheldrick, *Acta Cryst. C* **2015**, *71*, 3–8.
[13] a) A. D. Becke, *J. Chem. Phys.* **1993**, *98*, 5648–5652; b) C. Lee, W. Yang, R. G. Parr, *Phys. Rev. B* **1988**, *37*, 785–789; c) F. Weigend, R. Ahlrichs, *Phys. Chem. Chem. Phys.* **2005**, *7*, 3297-305.
[14] Gaussian 09, Revision E.01, M. J. Frisch, G. W. Trucks, H. B. Schlegel, G. E. Scuseria, M. A. Robb, J. R. Cheeseman, G. Scalmani, V. Barone, G. A. Petersson, H. Nakatsuji, X. Li, M. Caricato, A. Marenich, J. Bloino, B. G. Janesko, R. Gomperts, B. Mennucci, H. P. Hratchian, J. V. Ortiz, A. F. Izmaylov, J. L. Sonnenberg, D. Williams-Young, F. Ding, F. Lipparini, F. Egidi, J. Goings, B. Peng, A. Petrone, T. Henderson, D. Ranasinghe, V. G. Zakrzewski, J. Gao, N. Rega, G. Zheng, W. Liang, M. Hada, M. Ehara, K. Toyota, R. Fukuda, J. Hasegawa, M. Ishida, T. Nakajima, Y. Honda, O. Kitao, H. Nakai, T. Vreven, K. Throssell, J. A. Montgomery, Jr., J. E. Peralta, F. Ogliaro, M. Bearpark, J. J. Heyd, E. Brothers, K. N. Kudin, V. N. Staroverov, T. Keith, R. Kobayashi, J. Normand, K. Raghavachari, A. Rendell, J. C. Burant, S. S. Iyengar, J. Tomasi, M. Cossi, J. M. Millam, M. Klene, C. Adamo, R. Cammi, J. W. Ochterski, R. L. Martin, K. Morokuma, O. Farkas, J. B. Foresman, and D. J. Fox, Gaussian, Inc., Wallingford CT, 2016.
[15] National InstituteRelease 22, May 2022, NIST Standard Reference Database 101, Internet: https://cccbdb.nist.gov/vibscalejust.asp of Standards and Technology, Computational Chemistry Comparison and Benchmark DataBase.

10.6 Author Contributions

R. Szlosek – writing of original and final manuscript, experimental work (syntheses/reproductions and characterization of all compounds)

M. Seidl – finalization of single-crystal X-ray data

C. Riesinger – conceptualization, provision of reagents

L. Zimmermann – conceptualization, provision of reagents

A. S. Niefanger – synthesis of compound **6** as part of her B. Sc. thesis ("Determination of Donor properties of Lewis base stabilized Pentelyltrielanes") under supervision of R. Szlosek

C. Marquardt – acquisition of single-crystal X-ray data for **1b**

M. Scheer – project supervision, acquisition of funding, co-writing of final manuscript

11 Thesis Treasury

This chapter is composed of preliminary results and the compounds described are not fully characterized. Nevertheless, the results provide a basis for subsequent investigations and thus all acquired information of these reactions and their outcomes is presented.

11.1 Synthesis and Reactivity of an NHC stabilized Triphosphanylborane

The synthesis of the parent tripentelyltrielanes has been described in detail in a previous chapter. However, the corresponding triphosphanylboranes were not discussed, so far. The synthesis of the parent triphosphanylborane by triple salt metathesis has proven to be less clean than in the case of the gallanes or alanes, as more side reactions are observed by multinuclear NMR spectroscopy. While many reactions using NHC·BX_3 (NHC = IDipp, IPr_2Me_2, X = halide) precursors and $LiPH_2$·DME have been performed, the cleanest outcome was so far achieved with IPr_2Me_2·BBr_3. When solid $LiPH_2$·DME is added to a solution of IPr_2Me_2·BBr_3 in tetrahydrofuran at -80 °C and the mixture stirred for two hours at room temperature, the parent triphosphanylborane IPr_2Me_2·$B(PH_2)_3$ can be identified by multinuclear NMR spectroscopy (equation 1).

$$IPr_2Me_2{\cdot}BBr_3 \xrightarrow[\text{THF, -80°C} \rightarrow \text{r.t., 2 h}]{\text{3.3 Li}PH_2{\cdot}\text{DME}} IPr_2Me_2{\cdot}B(PH_2)_3 \quad \textbf{55\%} \qquad (1)$$

The ^{31}P NMR spectrum of a solution of IPr_2Me_2·$B(PH_2)_3$ in C_6D_6 shows a triplet of multiplets ($^1J_{HP}$ = 180 Hz) which collapses to a well resolved quartet ($^1J_P{}^{11}_B$ = 26 Hz) upon proton decoupling. This signal is superimposed with a rarely observed 7-line shaped signal of equal intensity distribution by coupling to the ^{10}B nucleus ($^1J_P{}^{10}_B$ = 14 Hz). The high symmetry at the boron atom results also in a sharp quartet in the $^{11}B\{^1H\}$ NMR spectrum ($^1J_P{}^{11}_B$ = 26 Hz), which is split into a sharp quartet of septets in the ^{11}B NMR spectrum ($^2J_{BH}$ = 3 Hz). It was also possible to grow single crystals suitable for X-ray structure determination by layering a solution of IPr_2Me_2·$B(PH_2)_3$ in tetrahydrofuran with *n*-hexane (Figure 11.1).

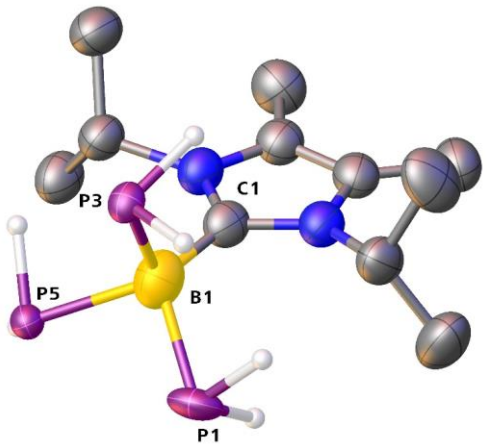

Figure 11.1: Molecular structure of IPr_2Me_2·$B(PH_2)_3$ in the solid state. Atomic displacement ellipsoids are displayed at 50% probability level. Disordered parts and hydrogen atoms bound to carbon are omitted for clarity. Selected bond distances [Å]

and angles [°]: C1-B1 1.622(9), B1-P1 1.921(13), B1-P3 1.951(12), B1-P5 2.062(10), C1-B1-P1 118.1(5), C1-B1-P3 112.4(5), C1-B1-P5 118.7(5).

The structure in the solid-state shows a disordered (pseudo)tetrahedral geometry at the core {BP_3} motif (C1-B1-P1 118.1(5)°, C1-B1-P3 112.4(5)°, C1-P1-P5 118.7(5)°) with bond lengths in the range of classic B-P single bonds (1.921(13)-2.148(10) Å). All attempts to prepare the corresponding triarsanylborane by reaction of $KAsH_2$ with $IPr_2Me_2{\cdot}BBr_3$ have failed, so far. According to ^1H NMR spectroscopy of the reaction mixture, only an intractable product mixture is obtained, and extraction attempts did not result in the isolation of any identifiable species.

With three available pnictogen lone pairs, the triphosphanylborane represents a promising candidate towards further functionalization by coordination to transition metals or towards main group electrophiles. However, all attempted reactions at coordination of $IPr_2Me_2{\cdot}B(PH_2)_3$ with $[W(CO)_3(MeCN)_3]$, $[Mo(CO_3)(MeCN)_3]$ or $Ni(CO)_4$ led mostly to intractable product mixtures. It is likely, that the NHC stabilized triphosphanylborane displays a reactivity pattern which significantly differs from a triphosphine. This further illustrated by the reaction of $IPr_2Me_2{\cdot}B(PH_2)_3$ with an excess amount of $BH_3{\cdot}SMe_2$, which led serendipitously to the formation of the cyclic dimer $[IPr_2Me_2{\cdot}B(PH_2BH_3)(\mu\text{-}PHBH_3)]_2$ (Figure 11.2). Reproducibility and further analytical data of the compound still need to be verified, however.

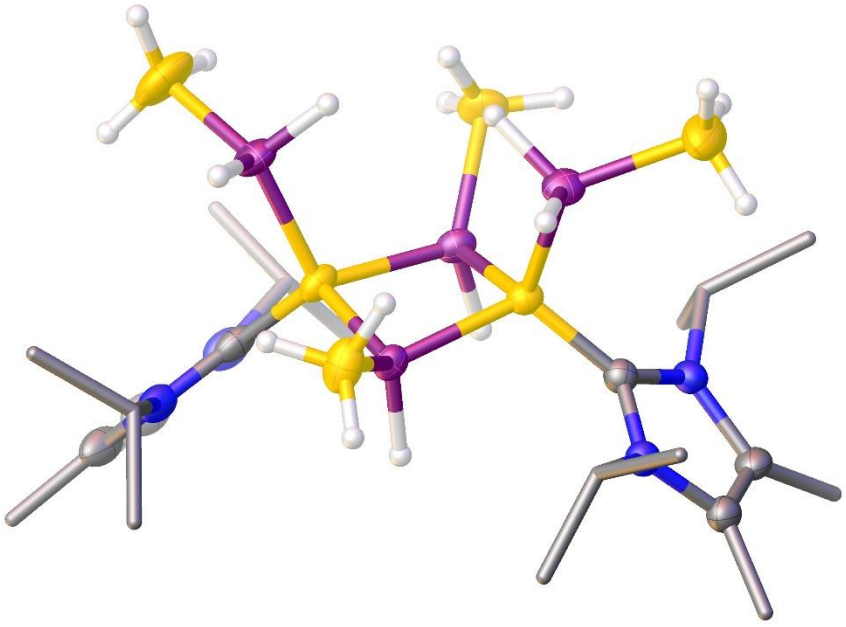

Figure 11.2: Preliminary molecular structure of $[IPr_2Me_2{\cdot}B(PH_2BH_3)(\mu\text{-}PHBH_3)]_2$ in the solid state. Anisotropic displacement ellipsoids are drawn at 50% probability. Hydrogen atoms bound to carbon are omitted for clarity.

Synthesis of $IPr_2Me_2{\cdot}B(PH_2)_3$

$IPr_2Me_2{\cdot}BBr_3$ (129 mg, 0.3 mmol) was dissolved in tetrahydrofuran and cooled to -80 °C. Then, solid $LiPH_2{\cdot}DME$ (115 mg, 0.99 mmol) was added. The solution was then stirred for two hours at room temperature, upon which a yellowish suspension formed. Subsequently, all volatiles were removed *in vacuo* and the product extracted with toluene. Insoluble solids were separated by filtration through a P4 glass frit. After removing the solvent *in vacuo*, the final product was washed once with cold *n*-hexane (-60 °C) and dried *in vacuo*, yielding $IPr_2Me_2{\cdot}B(PH_2)_3$ as a white-yellowish powder (48 mg, 55%).

^{1}H NMR (400.30 MHz, C_6D_6, 298 K): 6.59 (sep, ^{i}Pr-C*H*, $^{3}J_{HH}$= 302 Hz, $^{3}J_{HH}$ = 7.05 Hz, 2 H), 2.68 (dm, PH_2, $^{1}J_{HP}$ = 180 Hz, 6 H, broad), 1.45 (s, CH_3, 6 H), 1.08 (d, ^{i}Pr-C*H*$_3$, $^{3}J_{HH}$ = 7.05 Hz, 12 H).

^{31}P{^{1}H} NMR (161.98 MHz, C_6D_6, 298 K): -147.4 (q superimposed with sep, $^{1}J_{P}{}^{11}{}_{B}$ = 26 Hz, $^{1}J_{P}{}^{10}{}_{B}$ = 14 Hz).

^{31}P NMR (161.98 MHz, C_6D_6, 298 K): -147.4 (tm, $^{1}J_{HP}$ = 180 Hz).

^{11}B{^{1}H} NMR (128.38 MHz, C_6D_6, 298 K): -27.9 (q, $^{1}J_{P(11)B}$ = 26 Hz, $^{1}J_{P(10)B}$ = 13 Hz satellite).

^{11}B NMR (128.38 MHz, C_6D_6, 298 K): -37.6 (qsep, $^{1}J_{PB}$ = 26 Hz, $^{2}J_{BH}$ = 3 Hz).

^{13}C{^{1}H} NMR (100.61 MHz, C_6D_6, 298 K): 9.88 (s, *C*H_3), 20.5 (s. iPr-*C*H_3), 50.9 (s, iPr-*C*H). The signal of $C_{carbene}$ could not be reliably detected due to low intensity of the corresponding peak.

IR (ATR) *ν* (cm^{-1}): 2973, 2931, 2246 (PH), 1632, 1551, 1454, 1370, 1314, 1206, 1109, 1065, 903, 827, 762, 686, 649, 600.

Reaction of $IPr_2Me_2{\cdot}B(PH_2)_3$ with $BH_3{\cdot}SMe_2$ (exc.)

$IPr_2Me_2{\cdot}B(PH_2)_3$ (29 mg, 0.,1 mmol) was dissolved in toluene. Then, $BH_3{\cdot}SMe_2$ (0.05 mL, exc.) was added *via* syringe. After stirring for two hours at room temperature, excess $BH_3{\cdot}SMe_2$ was removed *in vacuo*. The solid residue was dissolved in tetrahydrofuran and layered with *n*-pentane which yielded single-crystals suitable for X-ray structure determination of $[IPr_2Me_2{\cdot}B(PH_2BH_3)(\mu\text{-}PHBH_3)]_2$.

NMR data

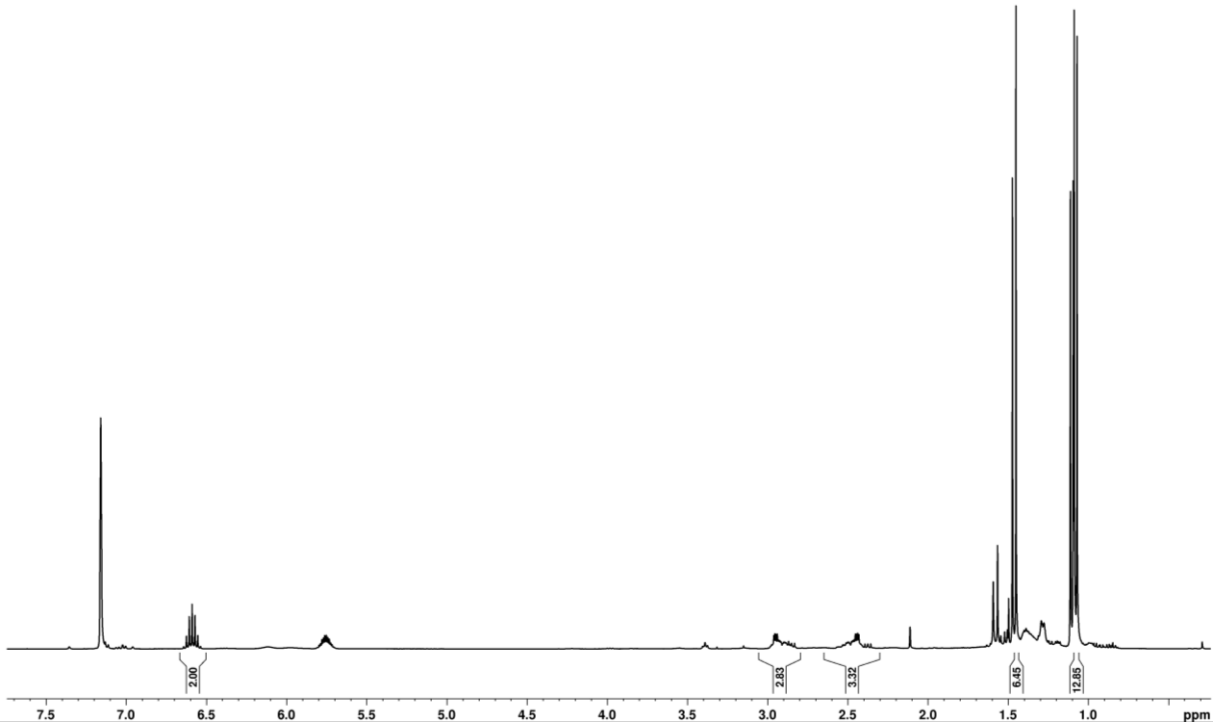

Figure 11.3: ^{1}H NMR spectrum of $IPr_2Me_2{\cdot}B(PH_2)_3$ (C_6D_6, 298 K).

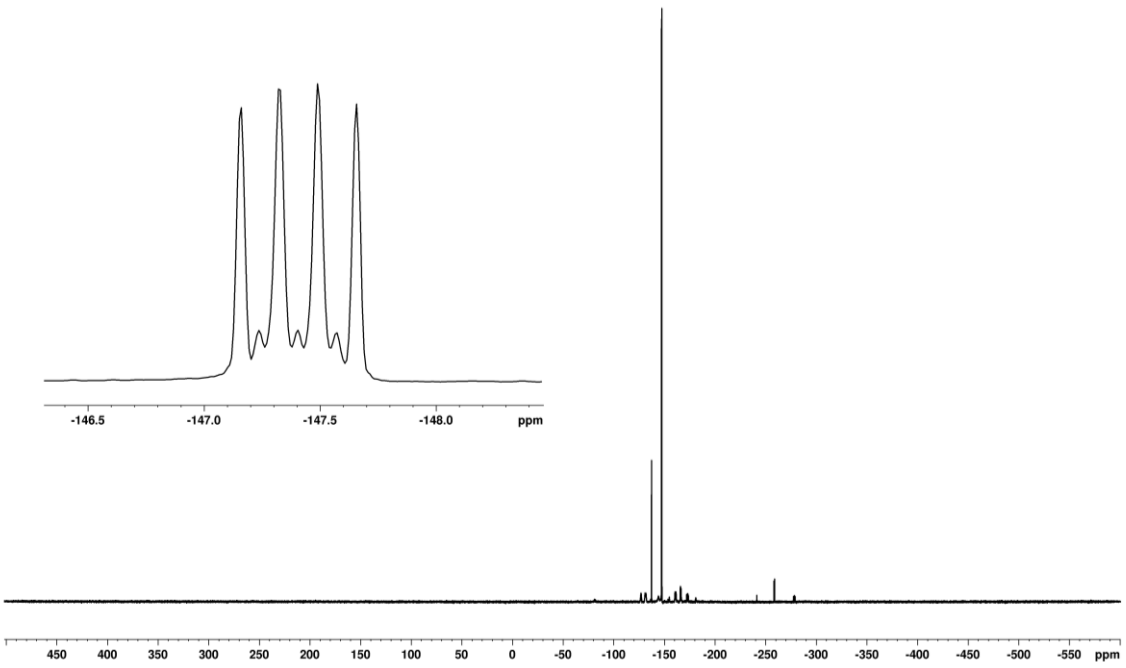

Figure 11.4: $^{31}P\{^{1}H\}$ NMR spectrum of $IPr_2Me_2{\cdot}B(PH_2)_3$ (C_6D_6, 298 K).

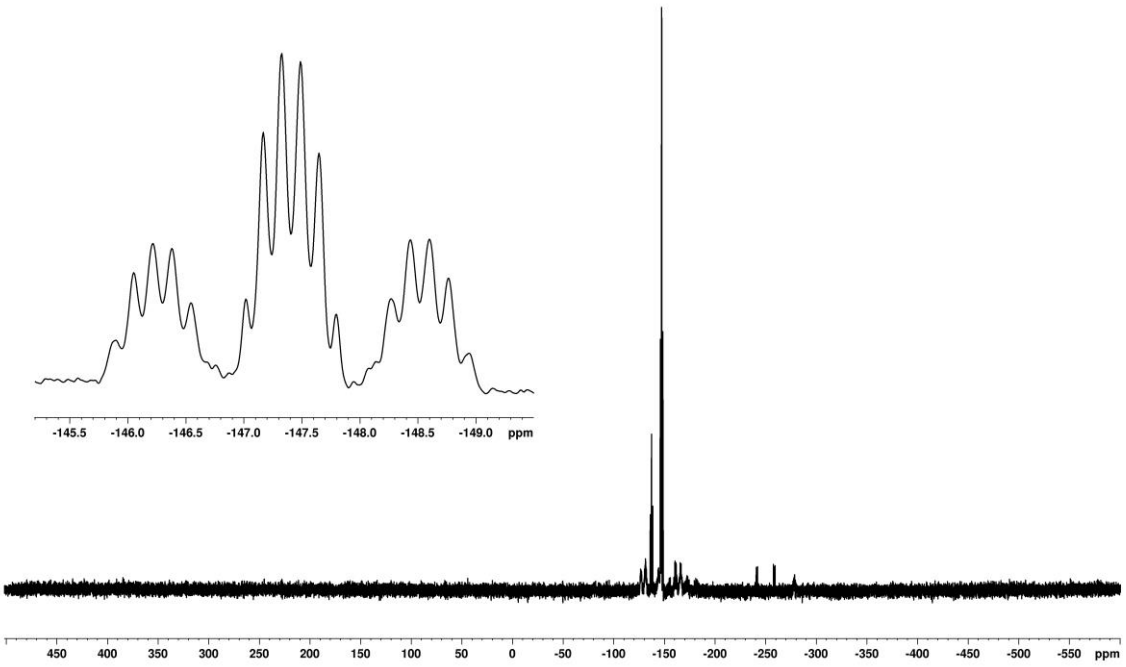

Figure 11.5: ^{31}P NMR spectrum of $IPr_2Me_2{\cdot}B(PH_2)_3$ (C_6D_6, 298 K).

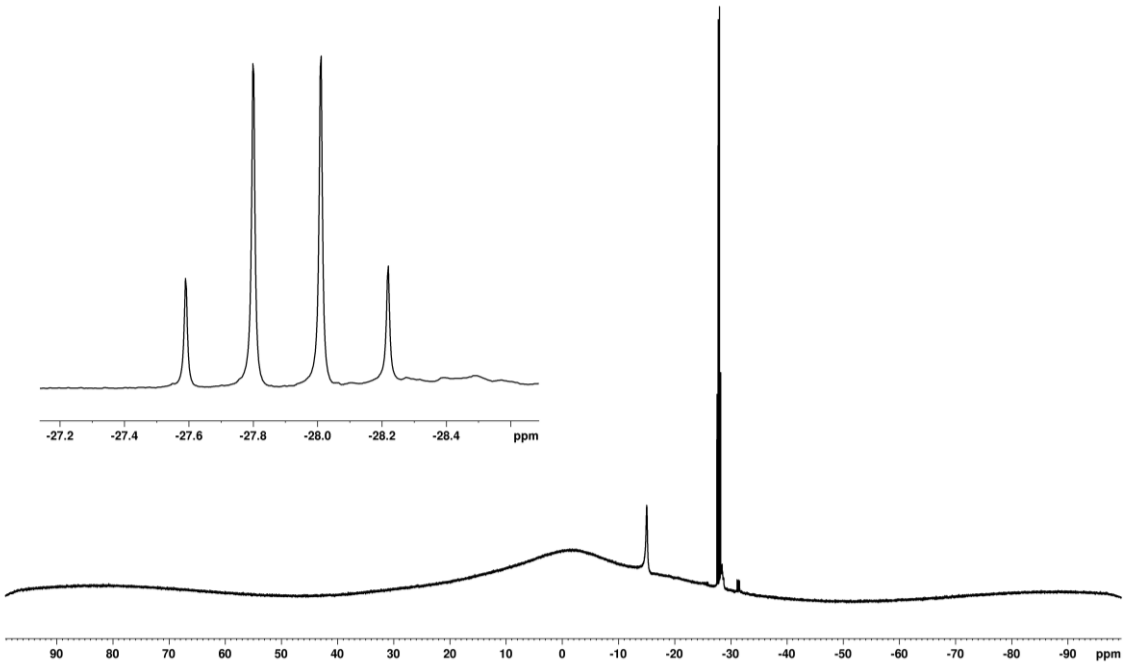

Figure 11.6: $^{11}B\{^{1}H\}$ NMR spectrum of $IPr_2Me_2{\cdot}B(PH_2)_3$ (C_6D_6, 298 K).

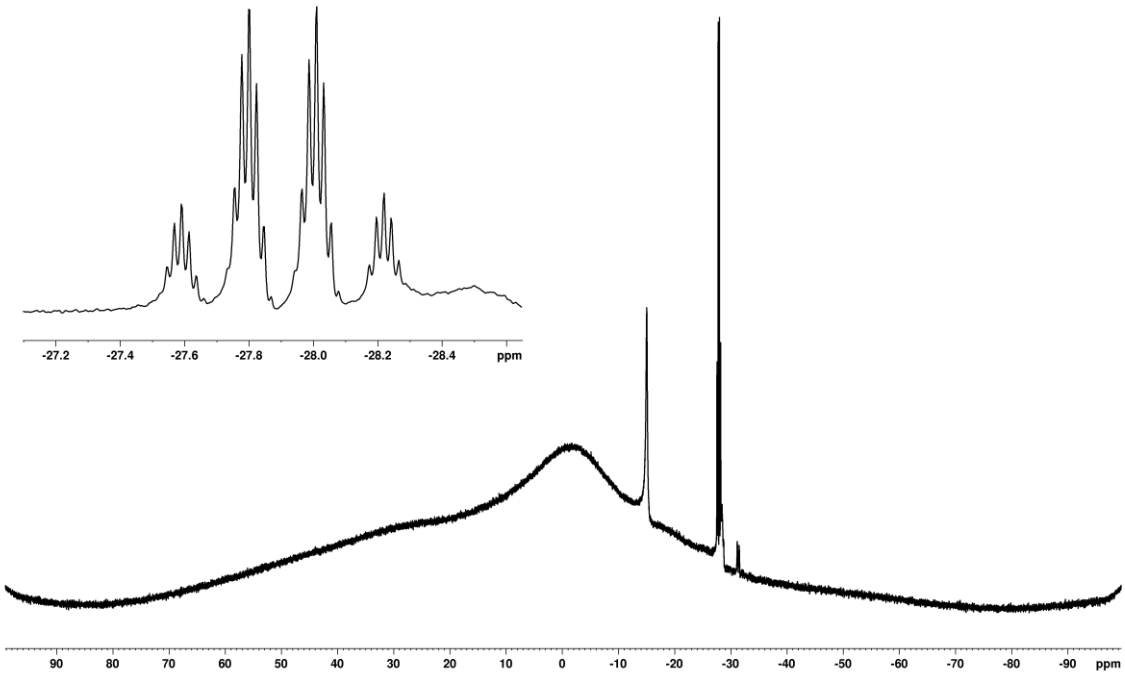

Figure 11.7: ^{11}B NMR spectrum of $IPr_2Me_2{\cdot}B(PH_2)_3$ (C_6D_6, 298 K).

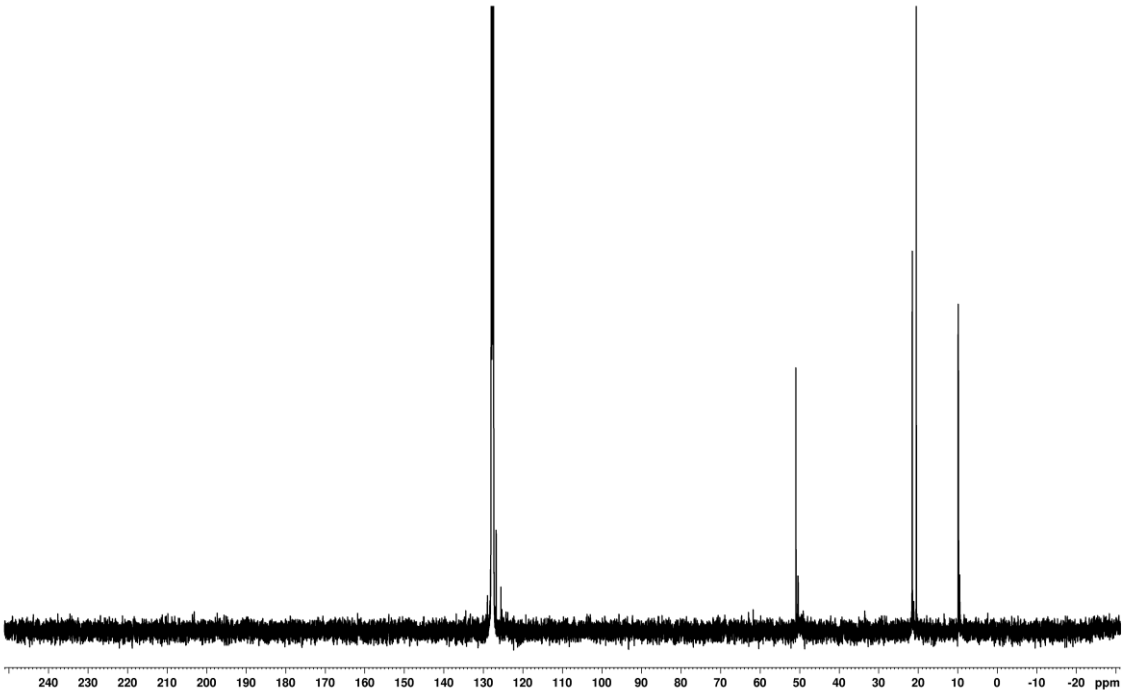

Figure 11.8: $^{13}C\{^{1}H\}$ NMR spectrum of $IPr_2Me_2{\cdot}B(PH_2)_3$ (C_6D_6, 298 K).

X-ray data of $IPr_2Me_2{\cdot}B(PH_2)_3$

Table 11.1: Finalized crystallographic data for $IPr_2Me_2{\cdot}B(PH_2)_3$.

Compound	**rs_600_abs1**
Formula	$C_{11}H_{26}BN_2P_3$
$D_{calc.}$/ g cm^{-3}	1.211
m/mm^{-1}	3.277
Formula Weight	290.06
Colour	clear colourless
Shape	plate-shaped
Size/mm^3	0.28×0.14×0.06
T/K	123.00(10)
Crystal System	triclinic
Space Group	P-1
a/Å	8.7690(6)
b/Å	9.5099(5)
c/Å	11.4216(7)
a/°	69.632(5)
b/°	79.366(5)
g/°	63.045(6)
V/Å^3	795.51(10)
Z	2
Z'	1
Wavelength/Å	1.54184
Radiation type	CuK_a
Q_{min}/°	4.131
Q_{max}/°	66.634
Measured Refl's.	9935
Indep't Refl's	2810
Refl's I≥2 s(I)	2501
R_{int}	0.0568
Parameters	187
Restraints	54
Largest Peak	0.650
Deepest Hole	-0.703
GooF	1.076
wR_2 (all data)	0.2509
wR_2	0.2418
R_1 (all data)	0.0870
R_1	0.0807

11.2 Deprotonation of parent Phosphanylboranes

The parent donor stabilized phosphanylboranes $D{\cdot}BH_2PH_2$ (D = donor) in principle offer the opportunity for deprotonation towards a phosphanide anion. This 13/15 anion should hold remarkable synthetic value as this would allow for a completely new way of functionalizing phosphanylboranes, especially by salt metathesis. However, adding a strong base to $D{\cdot}BH_2PH_2$ will usually result in the substitution of the donor molecule instead of deprotonation of the P-H acidic bond. This reaction behaviour can be avoided by using N-heterocyclic carbenes (NHCs) as donor, which are not easily replaced in the presence of a strong base. Still, attempts to deprotonate IDipp·BH_2PH_2 (IDipp = 1,3-Bis-(2,6-diisopropylphenyl)-imidazolin-2-ylidene) with ^{n}BuLi led to a product mixture as presumably the backbone of the NHC takes part in side reactions. NHCs containing a saturated backbone structure are usually inert at those positions and thus it was targeted to deprotonate SIDipp·BH_2PH_2 (SIDipp = 1,3-bis(2,6-diisopropylphenyl)-imidazolidin-2-ylidene). And indeed, the reaction of SIDipp·BH_2PH_2 with ^{n}BuLi in diethylether (equation 2) showed full conversion after stirring at room temperature for two hours according to multinuclear NMR spectroscopy. The connectivity of the deprotonated phosphanylborane could be confirmed by a broad doublet of multiplets at -129.3 ppm ($^1J_{PH}$ = 224 Hz) in the ^{31}P NMR spectrum and a triplet of doublets in the ^{11}B NMR spectrum at -27.4 ppm ($^1J_{BP}$ = 42 Hz, $^1J_{BH}$ = 96 Hz). Nevertheless, all attempts to isolate the anionic species have failed. All attempts resulted in oily residues of the product. Exchanging ^{n}BuLi for KBn did not provide any improvement. Instead, very likely double deprotonation towards SIDipp·BH_2PK_2 possibly takes place, as the ^{31}P NMR spectrum of the reaction solution only shows a broadened quartet ($^1J_{BP}$ = 46 Hz) without any scalar H-P coupling. The ^{11}B NMR spectrum of this solution confirms the presence of a {BH_2P} moiety by broad triplet of doublets ($^1J_{BP}$ = 46 Hz, $^1J_{BH}$ = 97 Hz). Further investigations on this matter are still pending, though.

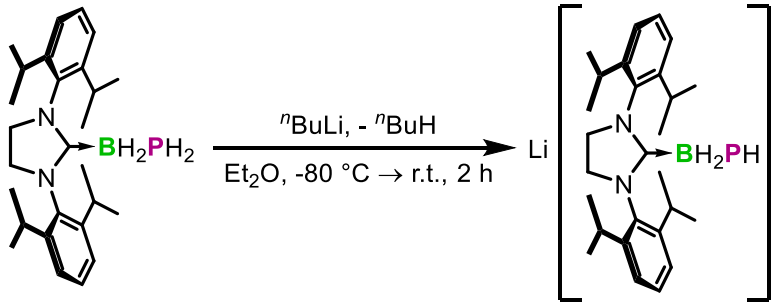

(2)

Furthermore, a crystallization attempt by adding 12-crown-4 to a freshly prepared solution of SIDipp·BH_2PHLi and subsequent layering with *n*-hexane (storage at 8 °C) surprisingly resulted in decomposition by intramolecular rearrangement of one dipp group at the NHC. This yielded a highly aggregated coordination compound, as seen by X-ray structure determination of single-crystals grown from this solution (Figure 11.9).

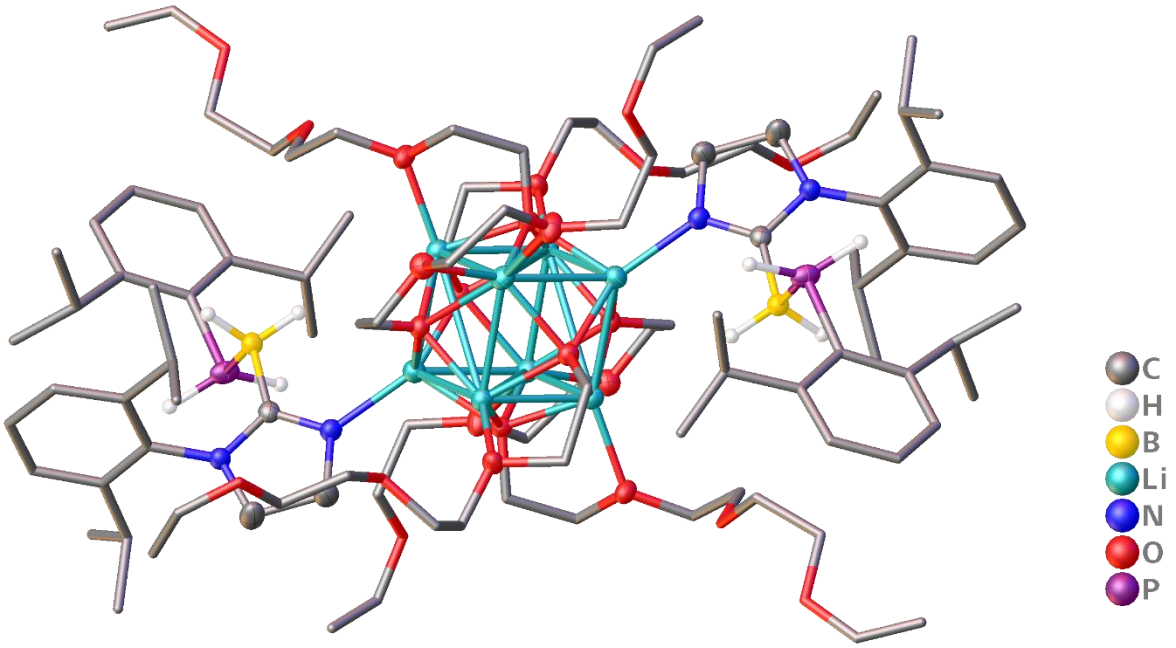

Figure 11.9: Preliminary molecular structure of the product resulting by reaction of IDipp·BH_2PHLi with 12-crown-4 in the solid state. Anisotropic displacement ellipsoids are displayed at 50% probability. Hydrogen atoms bound to carbon are omitted for clarity. Dipp groups and hydrocarbon chains are displayed as stick models for improved clarity.

Attempts to quench *in situ* generated solutions of SIDipp·BH_2PHLi with MeI, $^{i}Pr_3SiCl$ or $Me_3N{\cdot}BH_2I$ proved unsuccessful as only unidentifiable product mixtures are obtainable this way. Likely, the reactivity of this highly electron rich phosphanide is so high that side reactions occur. Moreover, the resulting phosphanylborane from the salt metathesis might be reactive enough under the reaction conditions to react with another equivalent of SIDipp·BH_2PHLi or the electrophile itself.

Deprotonation of SIDipp·BH_2PH_2

SIDipp·BH_2PH_2 (70 mg, 0.16 mmol) was dissolved in diethylether and cooled to -80 °C. Then, ^{n}BuLi (0.1 mL, 1.6 M stock solution in hexanes, 0.16 mmol) was added via syringe and the mixture allowed to warm up to room temperature. Upon warming up, the solution gradually turned bright red. After stirring for two hours at room temperature, full conversion is observed according to ^{31}P NMR spectroscopy. All attempts to isolate the phosphanide anion were unsuccessful due to its extremely high reactivity and limited stability in solution.

^{31}P{^{1}H} NMR (161.98 MHz, Et_2O/C_6D_6-cap., 298 K): δ = -129.3 (q, broad, $^{1}J_{BP}$ = 42 Hz).

^{31}P NMR (161.98 MHz, Et_2O/C_6D_6-cap., 298 K): δ = -129.3 (dm, broad, $^{1}J_{PH}$ = 224 Hz).

^{11}B{^{1}H} NMR (128.38 MHz, Et_2O/C_6D_6-cap., 298 K): -27.4 (d, broad, $^{1}J_{BP}$ = 42 Hz).

^{11}B NMR (128.38 MHz, Et_2O/C_6D_6-cap., 298 K): -27.4 (td, $^{1}J_{BP}$ = 42 Hz, $^{1}J_{BH}$ = 96 Hz).

NMR data of SIDipp·BH_2PH_2

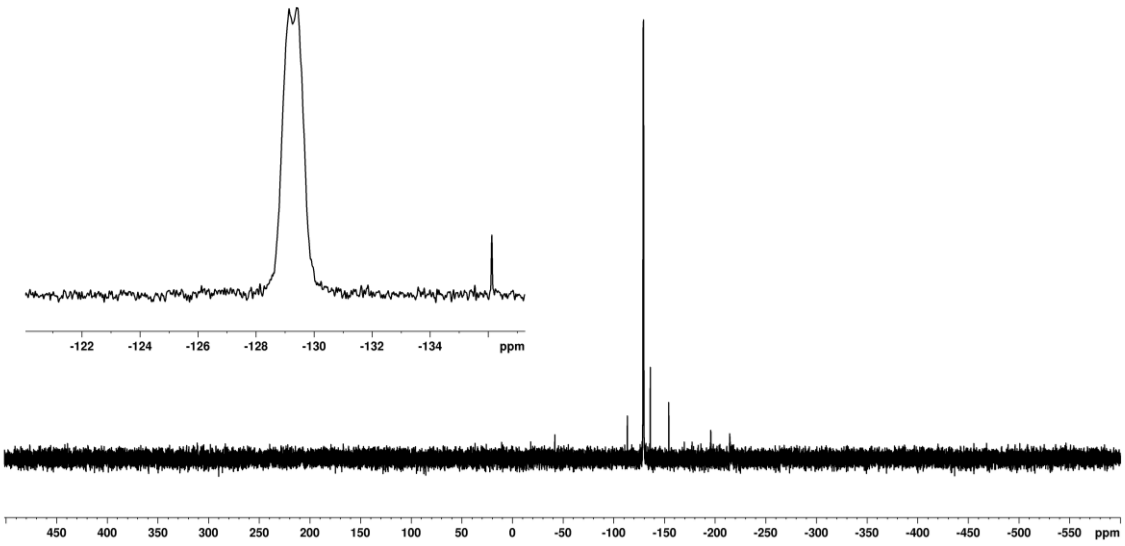

Figure 11.10: $^{31}P\{^1H\}$ NMR spectrum of SIDipp·BH_2PHLi (Et_2O/C_6D_6-cap.).

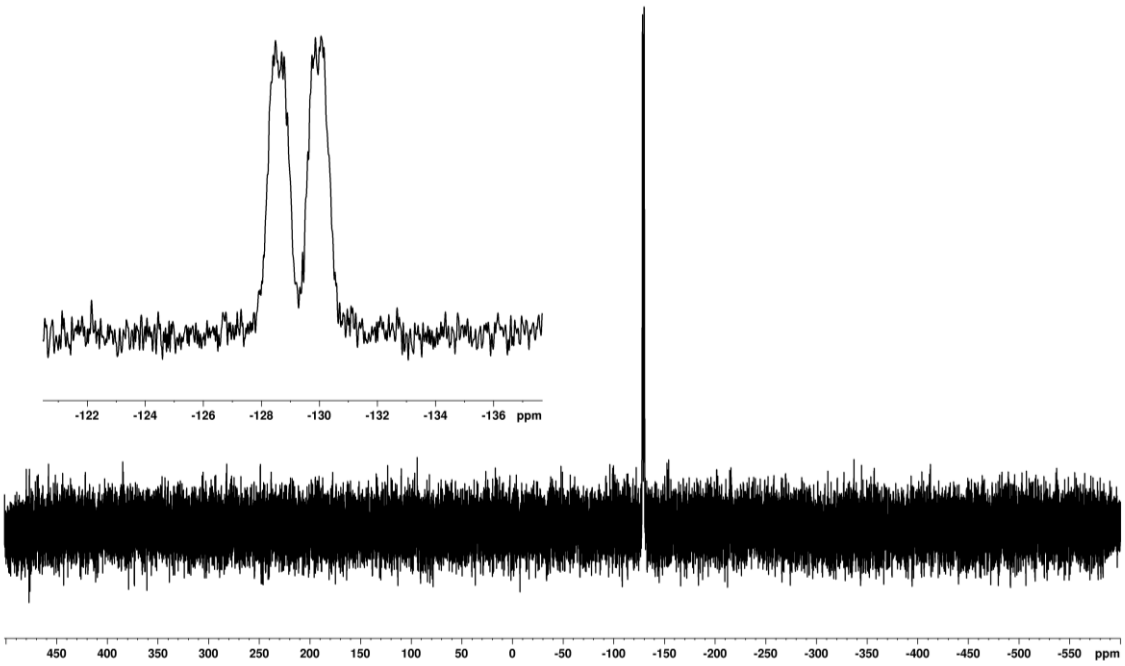

Figure 11.11: ^{31}P NMR spectrum of SIDipp·BH_2PHLi (Et_2O/C_6D_6-cap.).

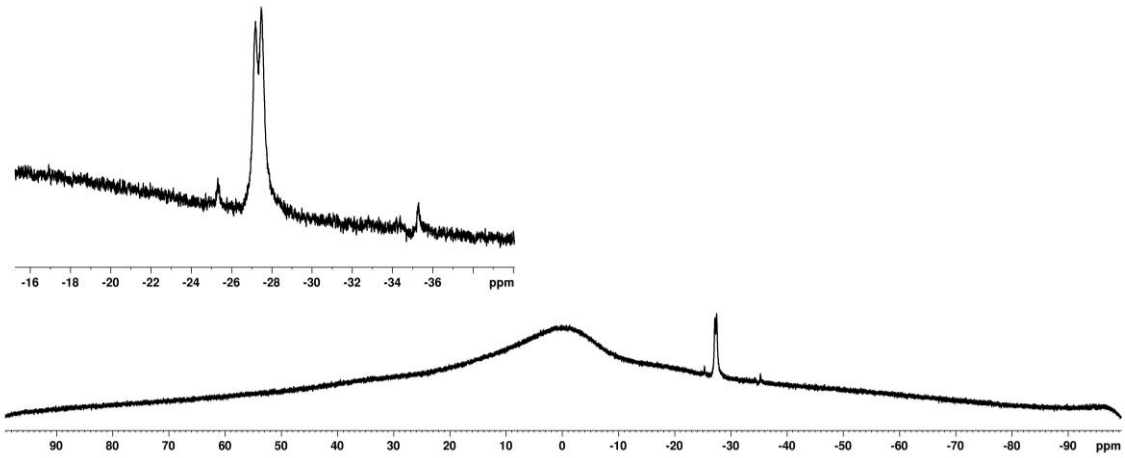

Figure 11.12: $^{11}B\{^{1}H\}$ NMR spectrum of SIDipp·BH_2PHLi (Et_2O/C_6D_6-cap.).

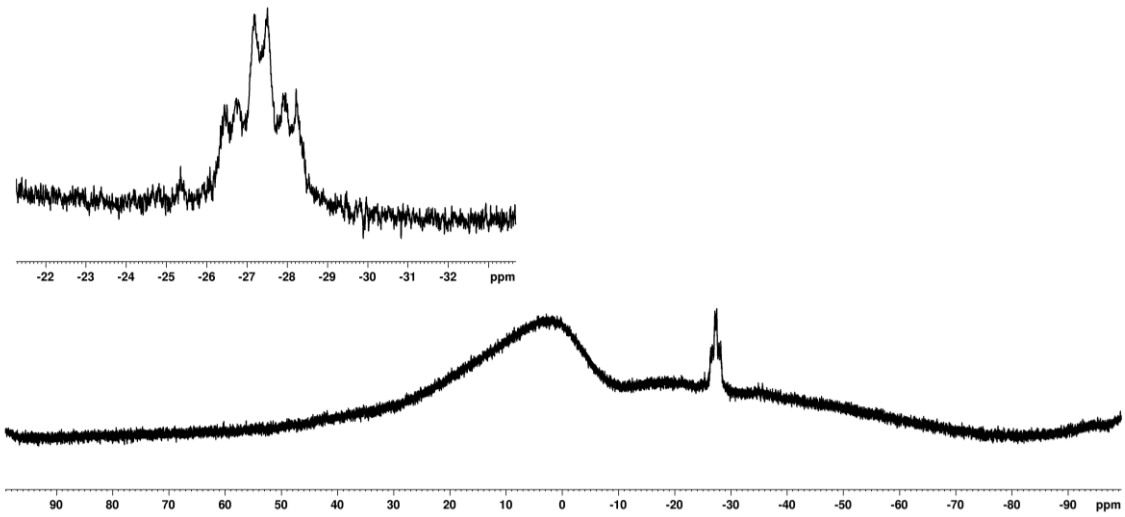

Figure 11.13: ^{11}B NMR spectrum of SIDipp·BH_2PHLi (Et_2O/C_6D_6-cap.).

11.3 Synthesis of an NHC stabilized Phosphanylborane Au(I) complex

Au(I) complexes of pnictogenylboranes have already been reported in the past. These compounds displayed interesting structural features and emission properties. However, the reported examples have so far been limited to trimethylamine stabilized pnictogenylboranes. Exchanging the amine for, e.g., an N-heterocyclic carbene (NHC) has a drastic influence on the steric and electronic nature of the pnictogenylborane has shown in a different chapter of this work. Thus, the question arises if Au(I) complexes of NHC stabilized phosphanylboranes show similar or different characteristics. In the following, the preparation of the first NHC stabilized phosphanylborane Au(I) complex is described. Reaction of IDipp·BH_2PH_2 with AuCl(tht) (tht = tetrahydrothiophene) cleanly results in the formation of the mononuclear complex IDipp·BH_2PH_2AuCl, which could be isolated in a crystalline yield of 12%. The ^{31}P NMR spectrum of a solution of the isolated complex shows a characteristic, strongly downfield shifted triplet of quartets at -141.6 ppm ($^1J_{BP}$ = 60 Hz, $^1J_{PH}$ = 335 Hz). The large coupling constant is further indicative of the phosphorus lone pair being coordinated to the metal. The structure of IDipp·BH_2PH_2AuCl could further be elucidated by single-crystal X-ray diffraction structure determination (Figure 11.14). The structure in the solid state shows a linear coordination mode of IDipp·BH_2PH_2 towards AuCl (P1-Au1-Cl1 177.76(4)°) with a B-P bond length of 1.944(4) Å, indicative of a regular single-bond. With a C1-B1-P1-Au1 dihedral angle of -174.99(19)°, the central core is arranged in antiperiplanar manner. Further experiments regarding substituents at the pnictogen, NHC size and the use of arsanylboranes are pending. Moreover, abstraction of the chloride in the presence of another donor molecule is desirable, potentially leading to aggregation by aurophilic interactions.

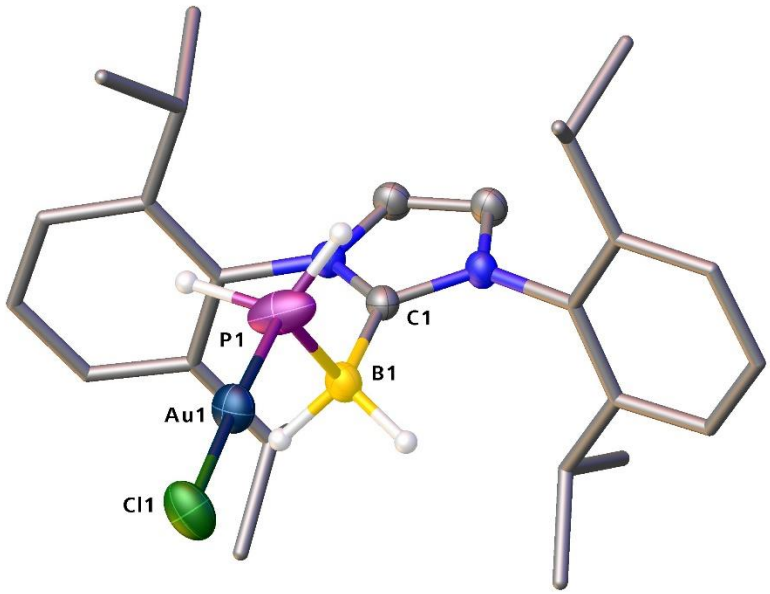

Figure 11.14: Molecular structure of IDipp·BH_2PH_2AuCl in the solid state. Anisotropic displacement ellipsoids are drawn with 50% probability. Hydrogen atoms bound to carbon are omitted for clarity. Dipp groups are displayed as stick models for improved clarity.

Synthesis of IDipp·BH_2PH_2AuCl

AuCl(tht) (48 mg, 0.15 mmol) was dissolved in dichloromethane and cooled to -80 °C. Then, a solution of IDipp·BH_2PH_2 (65 mg, 0.15 mmol) in toluene was added. The mixture was stirred for one hour at room temperature, resulting in a clear, slightly yellowish solution. Subsequently, the threefold amount of *n*-hexane was added, and the solution stored at -30 °C overnight, yielding large single-crystals of IDipp·BH_2PH_2AuCl. The supernatant was decanted, and the crystals washed twice with *n*-hexane. After drying *in vacuo*, the product was obtained as a highly electrostatic off-white powder (12 mg, 12%).

^{1}H NMR (400.30 MHz, CD_2Cl_2, 298 K): 1.16 (d, 12 H, 4 × ^{i}Pr-CH_3, $^{3}J_{HH}$ = 6.87 Hz), 1.32 (d, 12 H, 4 × ^{i}Pr-CH_3, $^{3}J_{HH}$ = 6.87 Hz), 1.45 (q, broad, 2 H, $^{1}J_{BH}$ ≈ 80 Hz, BH_2), 2.50 (sep, 4 H, 4 × ^{i}Pr-CH, $^{3}J_{HH}$ = 6.87 Hz), 2.54/3.39 (dt, 2 H, $^{1}J_{PH}$ = 335 Hz, $^{3}J_{HH}$ = 7.97 Hz, PH_2), 7.23 (s, 2 H, NCHCHN), 7.35 (d, 4 H, 4 × aryl-C$_{meta}H$, $^{3}J_{HH}$ = 7.88 Hz), 7.55 (t, 2 H, 2 × aryl-C$_{para}$H, $^{3}J_{HH}$ = 7.88 Hz).

^{31}P{^{1}H} NMR (161.98 MHz, CD_2Cl_2, 298 K): δ = -141.6 (q, broad, $^{1}J_{BP}$ = 60 Hz).

^{31}P NMR (161.98 MHz, CD_2Cl_2, 298 K): δ = -141.6 (tq, broad, $^{1}J_{BP}$ = 60 Hz, $^{1}J_{PH}$ = 335 Hz).

^{11}B{^{1}H} NMR (128.38 MHz, CD_2Cl_2, 298 K): -33.4 (d, broad, $^{1}J_{BP}$ = 60 Hz).

^{11}B NMR (128.38 MHz, CD_2Cl_2, 298 K): -33.4 (superimposing dt).

NMR data of IDipp·BH_2PH_2AuCl

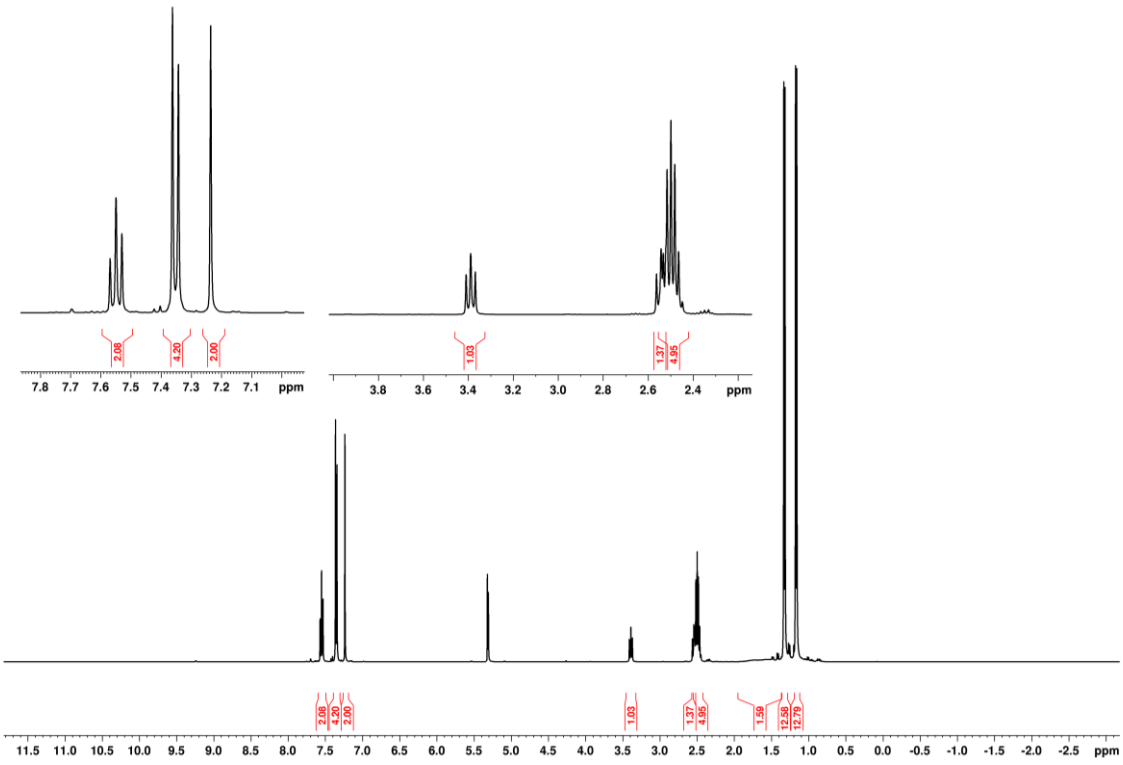

Figure 11.15: ^{1}H NMR spectrum of IDipp·BH_2PH_2AuCl (CD_2Cl_2, 298 K).

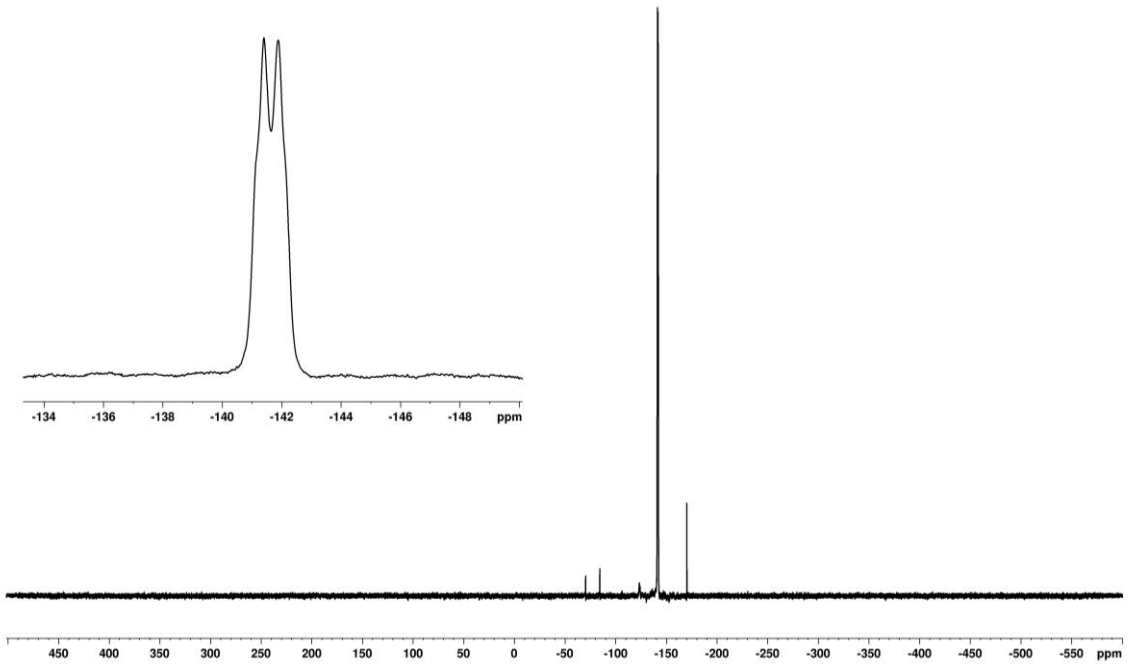

Figure 11.16: $^{31}P\{^{1}H\}$ NMR spectrum of IDipp·BH_2PH_2AuCl (CD_2Cl_2, 298 K).

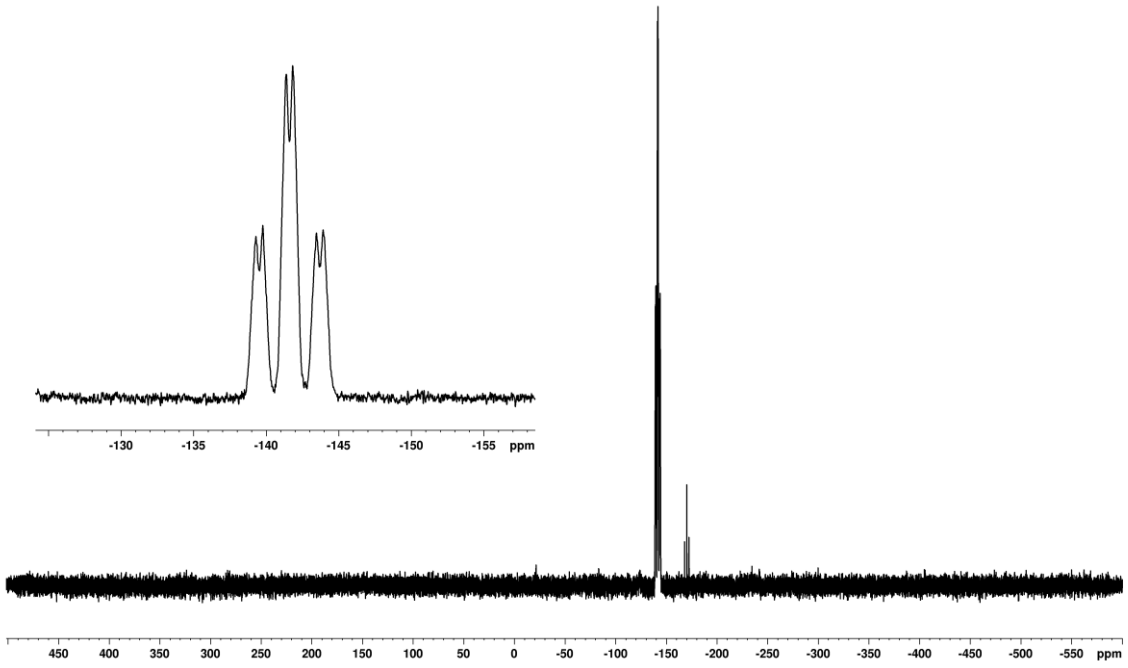

Figure 11.17: ^{31}P NMR spectrum of IDipp·BH_2PH_2AuCl (CD_2Cl_2, 298 K).

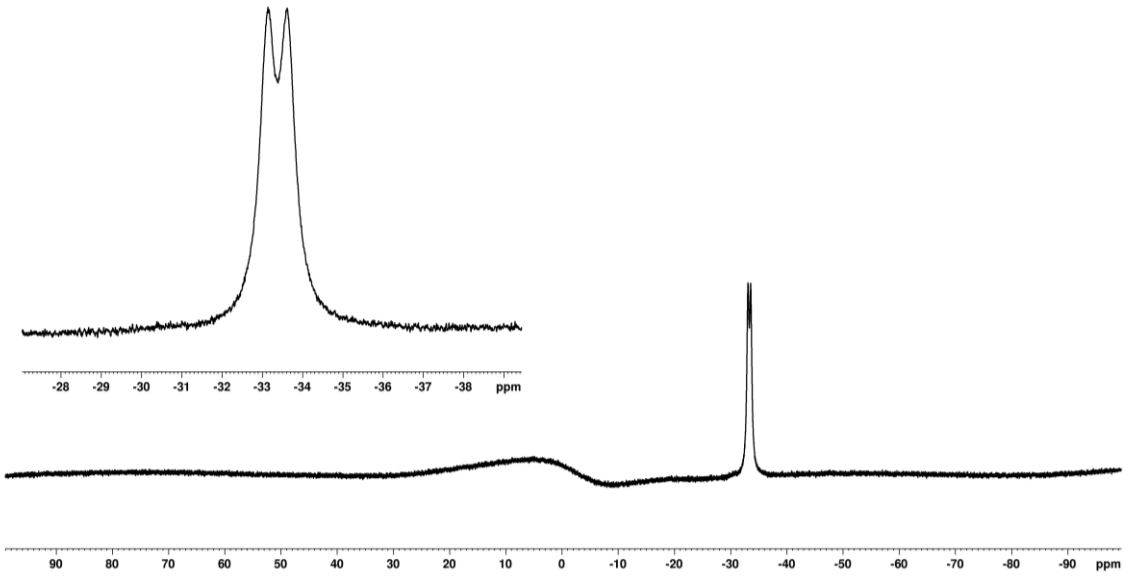

Figure 11.18: $^{11}B\{^{1}H\}$ NMR spectrum of IDipp·BH_2PH_2AuCl (CD_2Cl_2, 298 K).

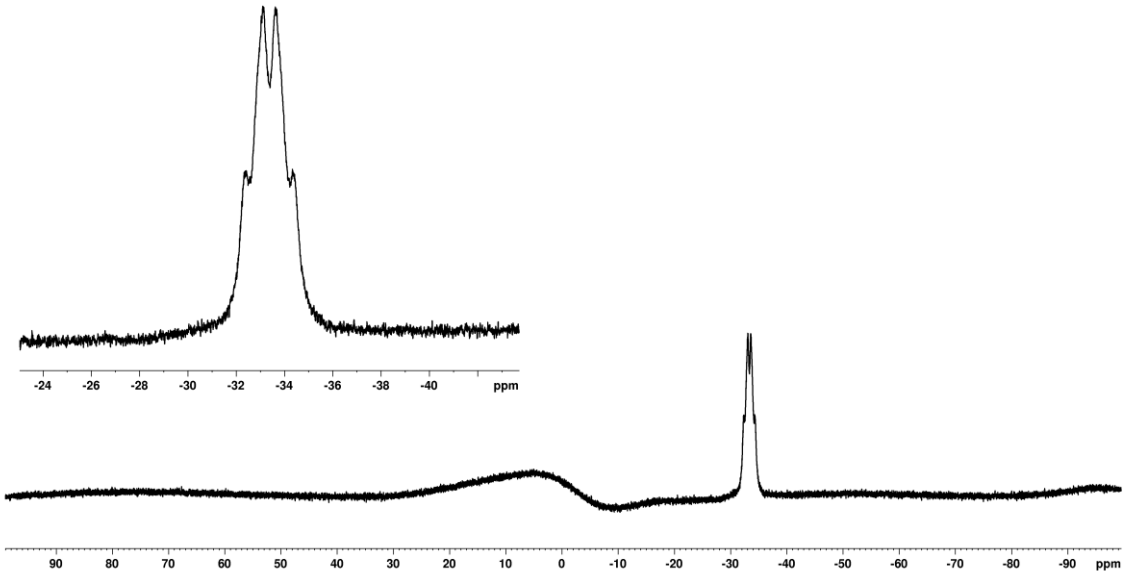

Figure 11.19: ^{11}B NMR spectrum of IDipp·BH_2PH_2AuCl (CD_2Cl_2, 298 K).

X-ray data of IDipp·BH_2PH_2AuCl

Table 11.2: Finalized X-ray data for IDipp·BH_2PH_2AuCl.

Compound	RS832_Cua_abs
Formula	$C_{28}H_{42}AuBCl_3N_2P$
$D_{calc.}$/ g cm^{-3}	1.567
m/mm^{-1}	11.601
Formula Weight	751.73
Colour	clear colourless
Shape	plate-shaped
Size/mm^3	0.34×0.18×0.09
T/K	123.00(10)
Crystal System	monoclinic
Space Group	$P2_1/c$
a/Å	12.1411(2)
b/Å	24.9356(2)
c/Å	12.1502(2)
a/°	90
b/°	119.957(2)
g/°	90
V/Å^3	3186.98(10)
Z	4
Z'	1
Wavelength/Å	1.54184
Radiation type	Cu K_a
Q_{min}/°	3.545
Q_{max}/°	73.728
Measured Refl's.	25419
Indep't Refl's	6260
Refl's I≥2 s(I)	6001
R_{int}	0.0347
Parameters	349
Restraints	7
Largest Peak	2.406
Deepest Hole	-1.758
GooF	1.066
wR_2 (all data)	0.1067
wR_2	0.1055
R_1 (all data)	0.0387
R_1	0.0376

12 Conclusion

This work investigated the synthesis and reactivity of heavy group 13/15 element combinations with the focus on monomeric 13/15 parent compounds stabilized by N-heterocyclic carbenes. In the following, the individual results of the chapters presented in this work are presented and the most important findings discussed.

12.1 Coordination of Pnictogenylboranes Towards Tl(I) Salts and a Tl-mediated P-P coupling

The chemistry of Tl(I) phosphine complexes remained underdeveloped throughout the literature, as only a handful of examples are known. One objective within this work was to extend this library by complexation of Tl(I) with pnictogenylboranes. By reaction of donor stabilized pnictogenylboranes with Tl(I) salts of weakly coordinating anions (WCAs), unprecedented Tl(I) coordination compounds could be synthesized (Scheme 12.1). Depending on the counter ion and the stoichiometry, monovalent $[Tl(EH_2BH_2{\cdot}NMe_3)][BAr^{Cl}]$ (**1a**: E = P, **1b**: E = As) or three-valent Tl(I) phosphine and arsine complexes $[Tl(EH_2BH_2{\cdot}NMe_3)_3][WCA]$ (**2a**: E = P, WCA = TEF^{Cl}; **2b**: E = As, WCA = TEF) were prepared and comprehensively characterized. Unexpectedly, at a stoichiometry of two equivalents of phosphanylborane to one Tl[WCA] a P-P coupling with involvement of the solvent dichloromethane takes place, leading to $[Me_3N{\cdot}BH_2PH_2PHBH_2{\cdot}NMe_3][WCA]$ (**3a**: WCA = TEF, **3b**: WCA = BAr^{Cl}, **3c**: WCA = TEF^{Cl}) independently of the used WCA.

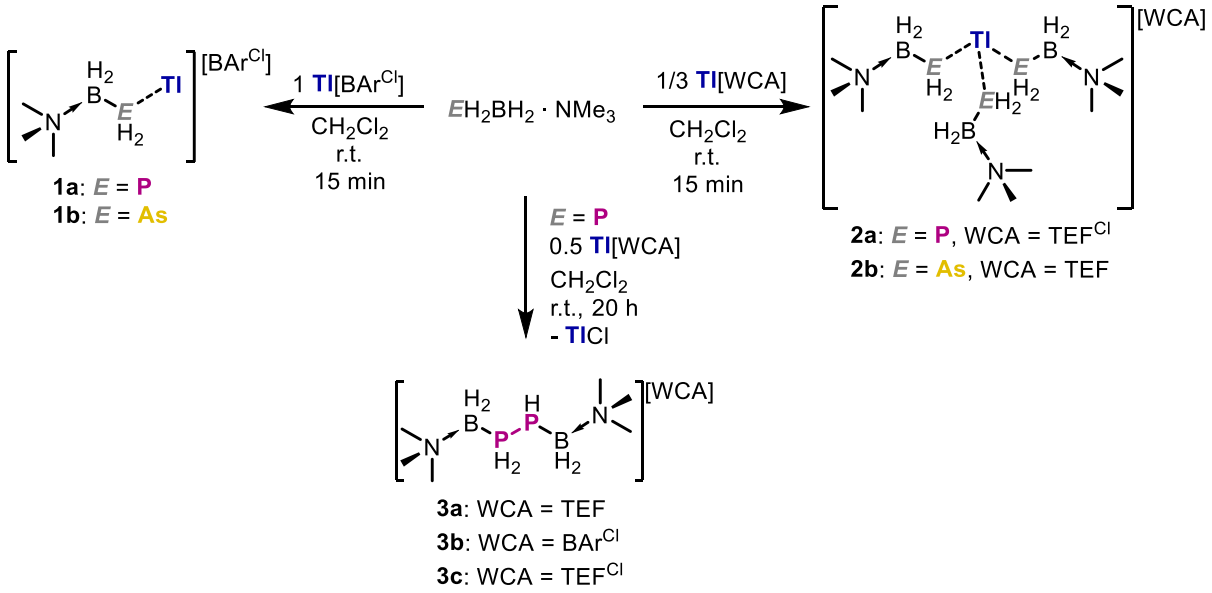

Scheme 12.1: Overview of the coordination products by the reaction of pnictogenylboranes with Tl[WCA] salts.

As verified by powder X-ray diffraction measurements, elimination of TlCl leads to the formation of **3a-c**. The coupling only takes place in dichloromethane and cannot be induced by, e.g. hydride abstracting agents such as $[Ph_3C][TEF]$, which simply leads to coordination of the phosphanylborane to $[Ph_3C]^+$, as in $[Me_3N{\cdot}BH_2PH_2CPh_3][TEF]$ (**4**). According to quantum chemical calculations, a concerted mechanism

at the intermediate $[Tl(PH_2BH_2{\cdot}NMe_3)_2(CH_2Cl_2)]^+$ takes place in the coupling process rather than a stepwise pathway. The analogue reactions with arsanylboranes did not result in As-As bond formation, so far. The obtained complexes **1a**-**2b** represent rare examples of phosphine thallium complexes, which are surprisingly scarce throughout the literature.

12.2 NHC-Stabilized Parent Tripentelyltrielanes

Based on previous results, the synthesis and isolation of heavy NHC stabilized parent tripentelyltrielanes appeared to be possible, which would fill an important gap in the literature as last missing type of compounds featuring a E(*Pn*H_2) substitution pattern. Thus, it was targeted to prepare these compounds by triple salt metathesis of NHC stabilized trichloride precursors IDipp·ECl_3 (E = Ga, Al, In) with $LiPH_2$·DME or $KAsH_2$, affording the tripentelyltrielanes IDipp·E(*Pn*H_2)$_3$ (**1a**: E/*Pn* = Ga/P, **1b**: Ga/As, **2a**: Al/P, **2b**: Al/As, **3**: In/P; cf. Scheme 12.2). The compounds display extreme sensitivity to air and decompose slowly at room temperature. Regarding the triphosphanylindiumane, the isolation proved highly difficult, but the existence could be unambiguously proven by multinuclear NMR spectroscopy.

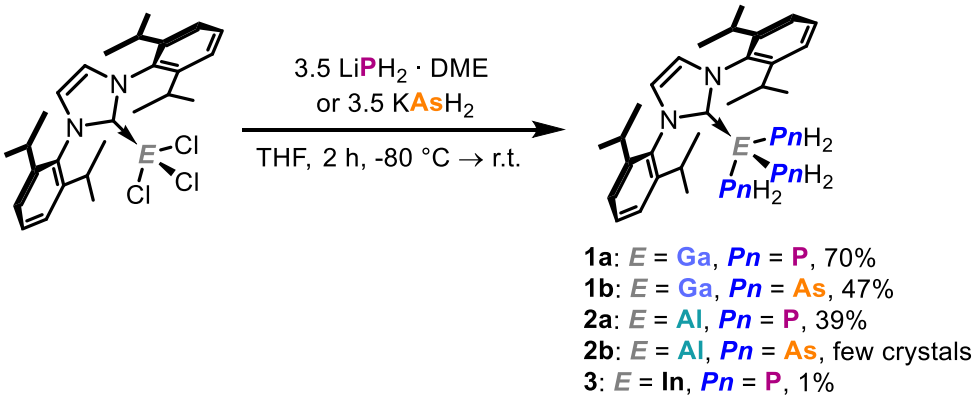

Scheme 12.2: Obtained NHC-stabilized tripentelyltrielanes by triple salt metathesis reactions.

Investigation on the reactivity of the tripentelyltrielanes has shown, that in many cases E-*Pn* bond fission is observed rather than coordination. With a very soft acceptor such as $(HgC_6F_4)_3$, coordination can still be achieved, however (Scheme 12.3). Reaction of IDipp·$Ga(PH_2)_3$ with $(HgC_6F_4)_3$ in *o*-DFB led to the very air sensitive compound $[IDipp{\cdot}Ga(PH_2)_2(\mu_3\text{-}PH_2\{HgC_6F_4\}_3)]$, which could be characterized by multinuclear NMR spectroscopy as well as single-crystal X-ray diffraction structure determination. Besides slow decomposition at room temperature, the compound displayed high lability and even CH_2Cl_2 is strong enough to substitute IDipp·$Ga(PH_2)_3$ from $(HgC_6F_4)_3$. The bonding situation of $[IDipp{\cdot}Ga(PH_2)_2(\mu_3\text{-}PH_2\{HgC_6F_4\}_3)]$ could be characterized by quantum chemical calculations which revealed, that electrostatic binding of the ligand rather than covalent bonding takes place at the $\{Hg\}_3$ unit.

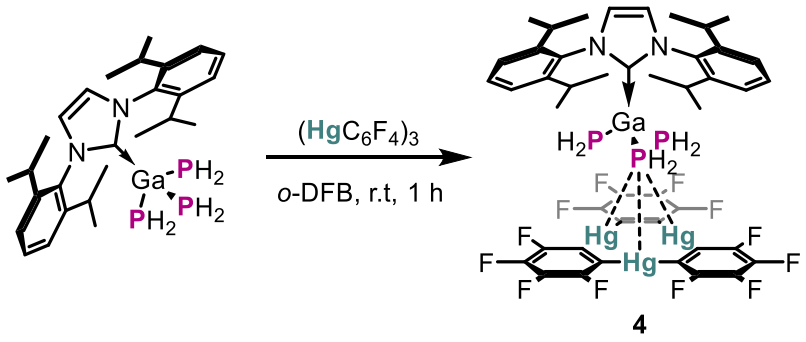

Scheme 12.3: Coordination of IDipp·Ga(PH$_2$)$_3$ to (HgC$_6$F$_4$)$_3$.

In subsequent studies, the homologue NHC stabilized triphosphanylboranes could be synthesized, as well, though the triple salt metathesis reactions do not proceed as cleanly as in the other cases. Nevertheless, IPr$_2$Me$_2$·B(PH$_2$)$_3$ (**5**) could be accessed (Scheme 12.4), and the structure elucidated by multinuclear NMR spectroscopy and single-crystal X-ray diffraction structure determination. The triarsanylborane however could not be obtained by this pathway as only intractable product mixtures occur and thus this compound remains elusive, so far.

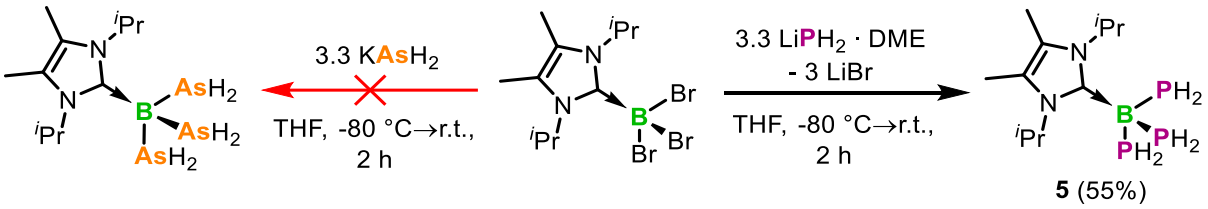

Scheme 12.4: Synthesis of the first NHC-stabilized triphosphanylborane IPrMe·B(PH$_2$)$_3$ (**5**) and attempted synthesis of the corresponding triarsanylborane.

12.3 A general Pathway towards NHC·GaH$_2$(OTf) adducts – The key for the Synthesis of NHC-stabilized cationic 13/15 Chain Compounds of Gallium

As pnictogenylboranes show a remarkable reactivity behaviour towards cationic chain elongation by the reaction with group 13 electrophiles, the question arose, whether this concept also applies to their heavier Ga containing congener. However, the formation of cationic chain compounds of gallium starting from the parent compound IDipp·GaH$_2$PH$_2$ has proven to be unsuccessful due to the low nucleophilicity of the reactant and low stability of the Ga-P bond. By reversing the reaction principle and adding phosphanylboranes to NHC stabilized galliummonotriflates, the formation of cationic chain compounds was successful. The galliummonotriflates themselves could be synthesized in high purity in excellent yields by the reaction of NHC·GaH$_3$ with Me(OTf) (**1a**: NHC = IDipp, **1b**: NHC = IPr$_2$Me$_2$, **1c**: NHC = IMes; Scheme 12.5).

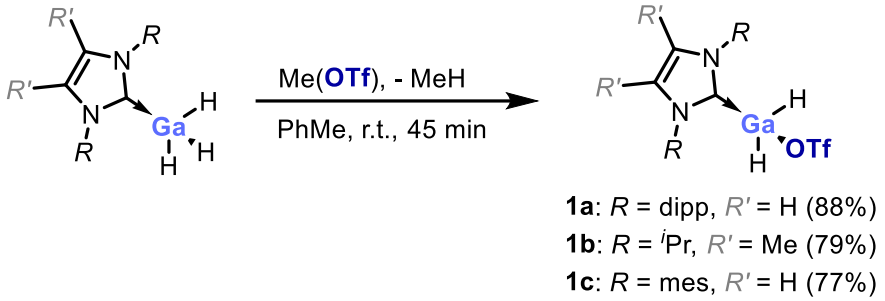

Scheme 12.5: Synthesis of NHC-stabilized galliummonotriflates starting from NHC·GaH_3.

By addition of *D*·BH_2PR_2 to IDipp·GaH_2(OTf), the unprecedented mixed chain compounds [IDipp·$GaH_2PR_2BH_2$·*D*][OTf] (**3a**: *D* = IDipp, R = H; **3b**: *D* = NMe_3, R = H, **3c**: *D* = NMe_3, R = Ph) could be obtained (Scheme 12.6). All chain compounds display high sensitivity towards air and decompose slowly at room temperature in solution or in the solid state. The compounds could be characterized by multinuclear NMR spectroscopy, ESI-MS and by single crystal X-ray structure determination. However, reactions with any arsanylboranes have failed in producing the desired chain compounds, so far. Surprisingly though, when the phosphanylgallanes IDipp·GaH_2PH_2 was reacted with IDipp·GaH_2(OTf), the parent chain compound [IDipp·$GaH_2PH_2GaH_2$·IDipp][OTf] (**3d**, Scheme 12.6) was obtained and characterized. **3d** displays extreme sensitivity towards air and decomposes quickly at room temperature as solids or in solution. Furthermore, the compound could only be dissolved in *ortho*-difluorobenzene, as any other suitable solvent will result in re-conversion back into the starting materials, due to the low nucleophilicity of IDipp·GaH_2PH_2.

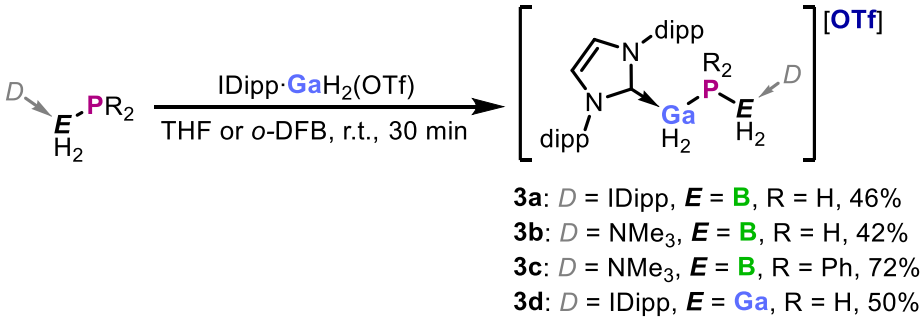

Scheme 12.6: Cationic chain compounds obtained by the substitution reactions at IDipp·GaH_2(OTf).

The chain compounds presented here represent the first examples of catena extension of the parent phosphanylboranes/gallanes by a heavy [*D*·GaH_2]$^+$ synthon. It yet remains to be tested, if a similar strategy can be applied to obtain the corresponding aluminium chain compounds.

12.4 Characterization of the Ligand Properties of Donor stabilized Pnictogenyltrielanes

Despite being known for almost two decades, the donor strength of Lewis base stabilized pnictogenyltrielanes has not been classified, so far. A classification of this type of compound regarding their steric and electronic properties would fill an important gap in this field and was a central task within this thesis. In this work, the library of NHC stabilized alkyl substituted phosphanylboranes has been extended

(Scheme 12.7) by salt metathesis reactions of NHC·BH_2I with alkalimetalpnictogenides and the donor strength of the phosphanyl- and arsanylboranes, as well as of the parent phosphanylgallane IDipp·GaH_2PH_2 was evaluated by experimental comparison of the Tolman Electronic Parameter (TEP).

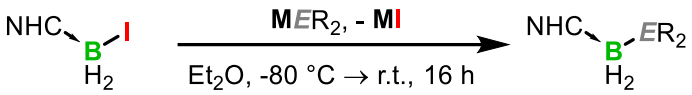

1a: NHC = SIDipp, *E* = P, R = H (62%)
1b: NHC = IDipp, *E* = P, R = Ph (72%)
1c: NHC = IDipp, *E* = P, R = Me (57%)
1d: NHC = IDipp, *E* = P, R_2 = H^{t}Bu (54%)
1e: NHC = IDipp, *E* = P, R = Cy (60%)
1f: NHC = IDipp, *E* = P, R = $SiMe_3$ (15%)
2: NHC = IDipp, *E* = As, R = Ph (37%)

Scheme 12.7: Preparation of novel NHC stabilized alkyl substituted pnictogenylboranes.

Therefore, the compounds were reacted with $Ni(CO)_4$ in order to obtain [$Ni(CO)_3$(*D*·EH_2PnR_2)] complexes (Scheme 12.8). The scope of the investigations focussed on the influence of the applied donor *D* at the triel moiety (NMe_3 vs. IDipp), the triel atom itself (B vs. Ga) and the pnictogen atom (P vs. As). The reactions of the NHC-stabilized pnictogenylboranes with $Ni(CO)_4$ (Scheme 12.8) selectively led to the substitution of one CO ligand, while the reactions with NMe_3 stabilized pnictogenylboranes (Scheme 12.8, left) partially led to the substitution of multiple CO ligands, which can be avoided by short reaction times. Reacting IDipp·GaH_2PH_2 with $Ni(CO)_4$ (Scheme 12.8, bottom) also selectively led to the formation of the desired [$Ni(CO)_3$(IDipp·GaH_2PH_2)] complex, which to this date remains the only example of successful coordination of IDipp·GaH_2PH_2 to a metal centre without Ga-P bond fission.

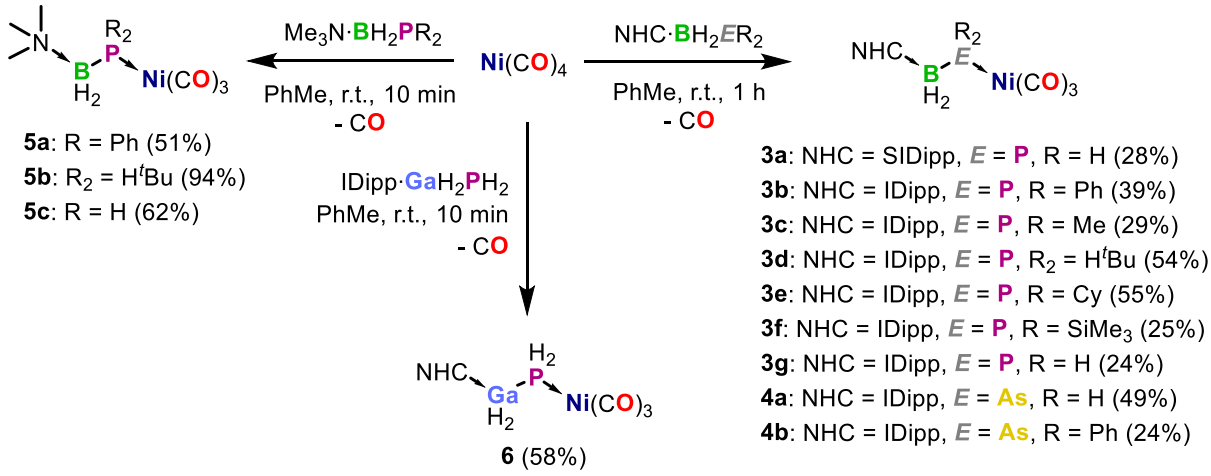

5a: R = Ph (51%)
5b: R_2 = H^{t}Bu (94%)
5c: R = H (62%)

6 (58%)

3a: NHC = SIDipp, *E* = P, R = H (28%)
3b: NHC = IDipp, *E* = P, R = Ph (39%)
3c: NHC = IDipp, *E* = P, R = Me (29%)
3d: NHC = IDipp, *E* = P, R_2 = H^{t}Bu (54%)
3e: NHC = IDipp, *E* = P, R = Cy (55%)
3f: NHC = IDipp, *E* = P, R = $SiMe_3$ (25%)
3g: NHC = IDipp, *E* = P, R = H (24%)
4a: NHC = IDipp, *E* = As, R = H (49%)
4b: NHC = IDipp, *E* = As, R = Ph (24%)

Scheme 12.8: Syntheses of [$Ni(CO)_3L$] complexes (*L* = pnictogenyltrielane) by substitution reactions at $Ni(CO)_4$.

All complexes could be isolated in medium yields and the TEPs were recorded by IR spectroscopic measurements. Comparison of the TEPs showed that the pnictogenyltrielanes can be considered as of similar donor strength than commonly used NHCs (Scheme 12.9), which underlines the unique donor properties of 13/15 compounds compared to regular phosphines. The donor atom D contributes strongly to the donor strength of the pnictogen with the trend being IDipp > NMe_3 in general for all compounds. Moreover, it can be concluded that the donor strength decreases by Ga > B for the triel, P > As for the pnictogen and overall R > H as substituents at the pnictogen atom. According to the percent buried volumes %V_{bur} and Tolman Cone Angles (TCA). The steric demand can be considered comparably low,

with the parent compounds displaying a similar demand as PH_3. Quantum chemical calculations could show that the Tolman Electronic Parameter depends on the HOMO energies of the pnictogenyltrielanes. A similar correlation could be observed for the proton affinities of the 13/15 compounds. The study overall fills an important gap in the studies of monomeric 13/15 compounds by providing an overview of the electronic and steric nature of these compounds.

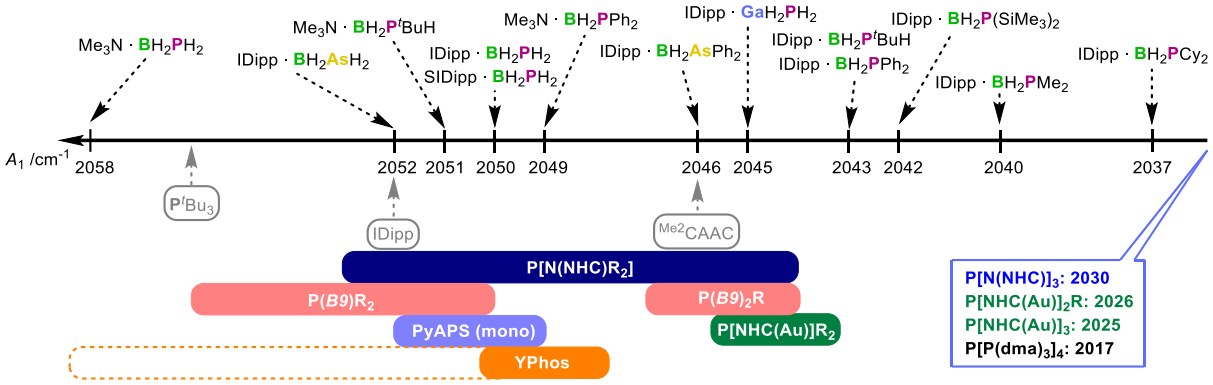

Scheme 12.9: Experimentally determined TEPs of donor stabilized pnictogenyltrielanes and the comparison to other commonly used superbasic phosphines and NHCs.

12.5 The parent GaH_2SbH_2 monomer stabilized by a N-heterocyclic carbene

As the pnictogenylgallane monomers IDipp·GaH_2PH_2 and IDipp·GaH_2AsH_2 were described previously, the question remained, if the even heavier homolog IDipp·GaH_2SbH_2 can be prepared, as well, which would represent the heaviest parent ethylene analogue of a group 13/15 element combination. By using the novel reagent K(18c6)SbH_2 by von Hänisch and co-workers, direct salt metathesis leading to parent stibanyltrielanes has been discovered. Beforehand, this class of compounds could only be accessed by the methanolytic treatment of the corresponding silylated precursor compounds. Although the reaction of $KSb(SiMe_3)_2$ with IDipp·GaH_2(OTf) afforded the stibanylgallane IDipp·$GaH_2Sb(SiMe_3)_2$ (**1**), conversion to the parent compound by methanolysis was unsuccessful, as no reaction occurred (Scheme 12.10). In contrast, the analogue reaction of IDipp·GaH_2(OTf) with K(18c6)SbH_2 led to the, so far, heaviest parent donor stabilized 13/15 element combination, IDipp·GaH_2SbH_2 (**3**). **3** shows high sensitivity and decomposes and room temperature, under light and at air. **3** could be crystallized alongside the inseparable side product IDipp·GaH_3. Furthermore, K(18c6)SbH_2 could be reacted with *D*·BH_2I (*D* = NMe_3, IDipp) to directly yield the corresponding stibanylboranes *D*·BH_2SbH_2 (**2a**: *D* = NMe_3, **2b**: *D* = IDipp), which display extreme sensitivity towards air and light and decompose slowly in solution even at -30°C. **2b** could previously only be observed detected as an intermediate during the reaction of Me_3N·$BH_2Sb(SiMe_3)_2$ with MeOH and the salt metathesis reaction presented in this work represents the first direct synthetic pathway towards **2b**. The obtained compounds are rare examples for primary stibanes and compound **3** represents the heaviest parent ethylene analogue up to this date.

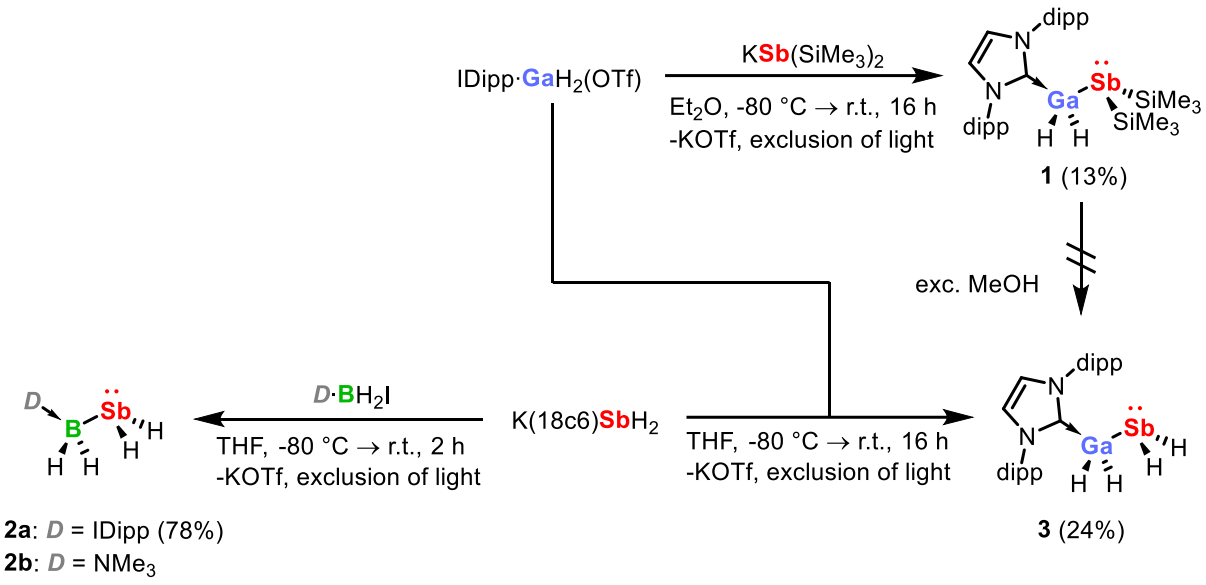

Scheme 12.10: Synthesis of donor stabilized stibanyltrielanes by salt metathesis.

Investigations on the reactivity of **2a** and **3** were hampered by the low nucleophilicity and low stability of these primary stibanes. Reactions with $Ni(CO)_4$, $W(CO)_5(thf)$, BEt_3 and IDipp·$GaH_2(OTf)$ either yielded intractable mixtures as a result of side reactions or no reaction was observed. Only the reaction of **3** with BH_3·SMe_2 towards catenation seems promising according to NMR spectroscopic investigation, but clear determination of the resulting product is still pending. To address the question, whether di- and tristibanylgallanes can be prepared by salt metathesis, as well, IDipp·$GaCl_3$ was reacted with an excess amount of K(18c6)SbH_2 (Scheme 12.11). According to ^{1}H NMR spectroscopy, a mixture of IDipp·$GaH_x(SbH_2)_{3-x}$ (x = 1-3) can likely be seen as a result of hydride transfer from the stibanide salt, though only **1** and IDipp·$GaH(SbH_2)_2$ can clearly be identified.

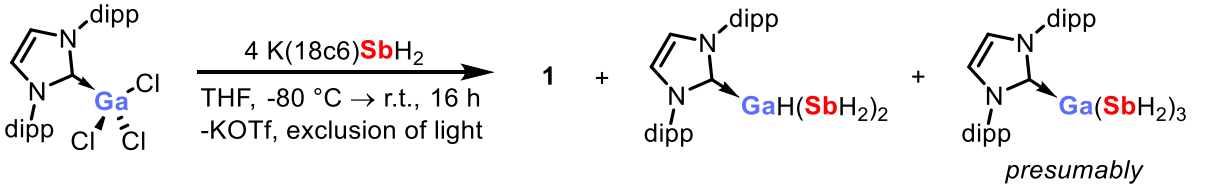

Scheme 12.11: Reaction of IDipp·$GaCl_3$ with 4 eq. K(18c6)SbH_2.

12.6 Synthesis of Bismuthanyl-substituted monomeric Triel Hydrides

Throughout the literature, Lewis base stabilized parent phosphanyl-, arsanyl- and even stibanylboranes have been reported. However, the missing link in this perspective still remained the bismuthylboranes, which represent the combination of the lightest group 13 and heaviest group 15 element. Together with the experimental works by Marquardt and Hegen, a new class of 13/15 compounds stabilized only by a Lewis base containing the heavy group 15 element bismuth (bismuthanyltrielanes) could be prepared and characterized. Salt metathesis reactions of $KBi(SiMe_3)_2(THF)_{0.3}$ with IDipp·BH_2I, IMe_4·BH_2I, DMAP·BH_2I and IDipp·$GaH_2(OTf)$ (IDipp = 1,3-Bis-(2,6-diisopropylphenyl)-imidazolin-2-ylidene,

IMe_4 = 1,3-Bis-(dimethyl)-4,6-dimethyl-imidazolin-2-ylidene, Scheme 12.12) led to the formation of the unprecedented bismuthyltrielanes IDipp·$BH_2Bi(SiMe_3)_2$ (**1a**), IMe_4·$BH_2Bi(SiMe_3)_2$ (**1b**), DMAP·$BH_2Bi(SiMe_3)_2$ (**1c**) and IDipp·$GaH_2Bi(SiMe_3)_2$ (**2**).

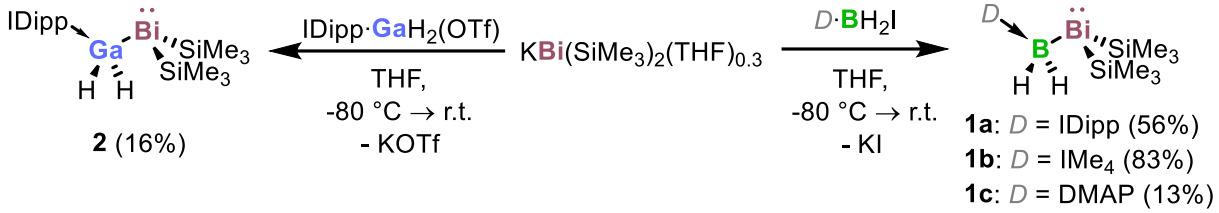

Scheme 12.12: Reactions of $KBi(SiMe_3)_2(THF)_{0.3}$ with Lewis base stabilized group 13 precursors.

All compounds could be characterized by multinuclear NMR spectroscopy, single-crystal X-ray structure determination and partially by LIFDI-MS. **1a**-**2** display drastic sensitivity towards air and light and decompose as solids and in solution at temperatures above -30 °C. Even below -30 °C, slow decomposition of **1a**-**2** in solution is observed under deposition of elemental bismuth. Compounds **1a**-**2** represent the first examples of B-Bi bonds where the boron atom is not stabilized within a cyclic system. The stability of the Lewis acid/base adducts decreases according to IMe_4 > IDipp > DMAP, which is in line with calculated dissociation enthalpies and isolated yields. The obtained compounds represent the first examples of molecules containing triel-bismuth σ-bonds in chain-like compounds. Unfortunately, any desilylation attempts have not been successful and the parent bismuthylborane remains elusive, so far. However, it cannot be excluded that such a transient species was formed during the attempts, but any attempt at isolating or spectroscopic observation did not prove fruitful. The most promising reaction of all attempts was the conversion of IDipp·$BH_2Bi(SiMe_3)_2$ with MeOH-d_4 in the presence of 1,4-benzoquinone, which resulted in the partial consumption of the starting material and presumably cleavage of at least one {$SiMe_3$} group. However, clear identification of any Bi-D/H containing species was not possible.

12.7 Electrophilic Functionalization of Donor stabilized Phosphanylboranes

The functionalization of phosphanylboranes by electrophiles has been investigated in the past. However, these investigations were mostly limited towards group 13 electrophiles. A study towards catenation by main group electrophiles other than group 13 has not yet been reported in the literature and this was a further aim of this work. The possible scope of functionalization of phosphanylboranes by main group electrophiles could be successfully expanded to a broader range of the periodic table. First, protonation of IDipp·BH_2PH_2 with $[H(OEt_2)_2][BAr^F]$ ($[BAr^F]$ = $[B(C_6F_5)_4]^-$) selectively led to $[IDipp{\cdot}BH_2PH_3][BAr^F]$ (**1a**, Scheme 12.13). While this method works for NHC stabilized phosphanylboranes, the amine stabilized analogues required a different approach. Reacting $Me_3N{\cdot}BH_2Cl$ with $H_3P{\cdot}AlCl_3$ results in the very sensitive compound $[Me_3N{\cdot}BH_2PH_3][AlCl_4]$ (**1b**, Scheme 12.14), which slowly decomposes at room temperature under release of PH_3. When **A** was reacted with main group electrophiles from group 14, a plethora of novel cationic 13/15/14 chain compounds [IDipp·BH_2PH_2E][WCA] (**2**: E = CH_3, WCA = OTf; **3**: E = $SiEt_3$, WCA = TEF; **4**: E = $Ge(SiMe_3)_3$, WCA = TEF; **5**: E = $SnMe_3$, WCA = TEF) could be obtained, ranging from the group 14 elements C to Sn.

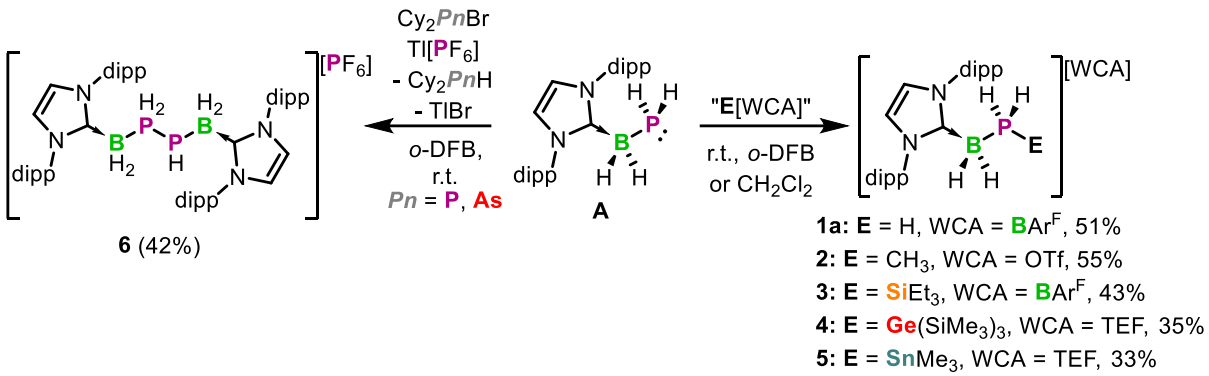

Scheme 12.13: Reactions of IDipp·BH_2PH_2 (**A**) with main group electrophiles.

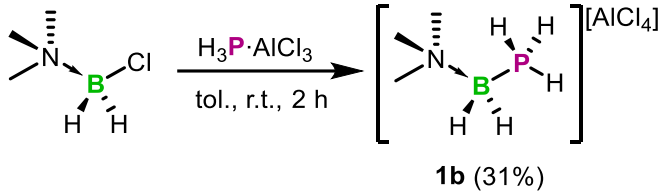

Scheme 12.14: Synthesis of $[Me_3N{\cdot}BH_2PH_3][AlCl_4]$ from $Me_3N{\cdot}BH_2Cl$ and $H_3P{\cdot}AlCl_3$.

The heavier group 14 homologs **3**-**5** display very high sensitivity towards air and decompose upon contact with untreated glass surfaces due to the lability of the P-E bond. Interestingly, reactions of **A** with *in situ* generated $[Cy_2Pn][PF_6]$ (*Pn* = P, As) did not yield the corresponding phosphinophosphonium cation, but rather a P-P coupling reaction took place. Both reactions exclusively resulted in the formation of $[IDipp{\cdot}BH_2PH_2PHBH_2{\cdot}IDipp][PF_6]$ (**6**, Scheme 12.13) as evident by single-crystal X-ray structure determination, NMR spectroscopy and ESI-MS. To probe the reactivity of the obtained products, **1a** and **1b** were reacted with the main group hydrides $LiGaH_4$ and $LiAlH_4$ (Scheme 12.15). The reaction with $LiAlH_4$ yielded simple deprotonation towards the parent phosphanylboranes, which represents an alternative synthetic approach towards this class of compounds. However, when **1a/b** are reacted with $LiGaH_4$, catenation occurs leading to the neutral elongated chain compounds $D{\cdot}BH_2PH_2GaH_3$ (**7a**: *D* = IDipp, **7b**: *D* = Me_3N). These compounds represent the first known examples of compounds containing terminal $\{GaH_3\}$ units bound to a primary phosphine.

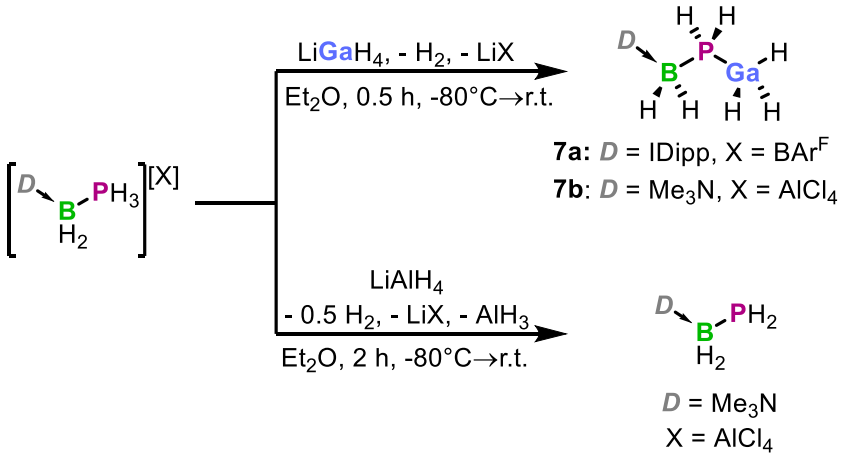

Scheme 12.15: Reactivity of protonated **1a/b** towards main group hydrides.

13 Appendices

13.1 Alphabetic List of Abbreviations

18c6	18-crown-6 ether (1,4,7,10,13,16-Hexaoxacyclooctadecane)
Å	Angström (1 Å = $1 \cdot 10^{-3}$ m)
°	degrees (angle)
°C	degree Celsius
$\%V_{bur}$	percent buried volume
B3LYP	Becke-3-Parameter Lee-Yang-Parr functional
BP86	GGA functional by Becke and Perdew
btmsa	bis(trimethylsilyl)acetylene
c	speed of light in vacuum (299792458 m s^{-1})
CAAC	Cyclic Alkyl Amino Carbene
CCSD(T)	Coupled cluster theory with singles, doubles and (perturbative) triples excitation
cf.	confer
COSY	correlated spectroscopy (2D NMR experiment)
CPCM	Conductor-like Polarizable Continuum Model
CVD	Chemical Vapour Deposition
Cy	cyclohexyl
d	days (reaction time)
d	doublet (NMR multiplicity)
d_{AB}	distance between atoms A and B
Δ	heat (reaction condition)
δ	chemical shift (NMR)
D3(BJ)	D3 dispersion correction incl. Becke-Johnson dampening
D4	D4 dispersion correction
DAC	N,N'-diamidocarbene
def2-TZVP	triple-ζ basis set by Ahlrichs (redefined)
def2-QZVP	quadruple-ζ basis set by Ahlrichs (redefined)
DFT	density functional theory
Dipp	2,6-diisopropylphenyl
DLPNO	Domain-based local pair natural orbital (coupled cluster approximation)
DMAP	4-dimethylaminopyridine
DME	1,2-dimethoxyethane
$E°_0$	total energy
e.g.	*exempli gratia*
ECP	effective core potential
ESI-MS	electron-spray ionization mass spectrometry
Et	ethyl
et al.	*et alia*
eq.	equivalents
Exc.	excess
Exp.	experimental
Fig.	figure
FLP	frustrated Lewis pair

$G°_{298}$	standard Gibbs free energy (298 K)
GGA	generalized gradient approximation
h	Planck's constant ($6.62607015 \cdot 10^{-34}$ J s)
$H°_{298}$	standard enthalpy (298 K)
HF	Hartree-Fock
HOMO	highest occupied molecular orbital
±I	positive/negative inductive effect
IBO	intrinsic bond orbital
IDipp	1,3-Bis-(2,6-diisopropylphenyl)-imidazolin-2-ylidene
IPrMe/IPr_2Me_2	1,3-Diisopropyl-4,5-dimethylimidazolin-2-ylidene
IMe_4	1,3,4,5-Tetramethylimidazolin-2-ylidene
IMes	1,3-Bis-(2,4,6-trimethylphenyl)-imidazolin-2-ylidene
incl.	including
J	scalar coupling value
K	Kelvin
k	rate constant (kinetics)
λ	wavelength
LA	Lewis acid
LB	Lewis base
LED	light-emitting diode
LIFDI-MS	Liquid Injection Field Desorption Ionization mass spectrometry
m (NMR)	multiplet
M	metal
±M	positive/negative mesomeric effect
Me	methyl
M06-2X	Minnesota '06 global hybrid functional (double amount of HF exchange)
Mes	mesityl
MOCVD	metal-organic chemical vapour deposition
Nacnac	β-diketiminate ligand
NBO	natural bond orbital
nbd	norbornadiene
NCI	non-covalent interaction
NEB	nudged elastic band
nm	nanometer ($1 \cdot 10^{-9}$ m)
NPA	natural population analysis
NHC	N-heterocyclic carbene
NLMO	natural localized molecular orbital
NMR	nuclear magnetic resonance
$\omega_{1/2}$	half-linewidth (NMR)
o-DFB	*ortho*-difluorobenzene
OTf	triflate anion
PA	proton affinity
PES	potential energy surface
Ph	phenyl
Pn	pnictogen
ppm	parts per million
PWPB95	double-hybrid-*meta* GGA functional with reparameterized PW and B95 parts
q(X)	charge of atom X

QTAIM	quantum theory of atoms in molecules
Quin	quinuclidine
qt	quintet (NMR)
r.t.	room temperature
RIJ	resolution of identity (IJ) approximation
RIJCOSX	resolution of identity (IJ) + chain of spheres (X) approximation
s	singlet (NMR)
$S°_{298}$	standard entropy (298 K)
SARC	Segmented All-electron Relativistically Contracted basis set
Sep	septet (NMR)
SIDipp	1,3-bis(2,6-diisopropylphenyl)-imidazolidin-2-ylidene
t	triplet (NMR)
T	temperature
TS	transition state
^{t}Bu	*t*-butyl
TEF	teflonate anion $[Al\{OC(CF_3)_3\}_4]^-$
TEF^{Cl}	chloroteflonate anion $[Al\{(OC(CF_3)_2(CCl_3)\}_4]^-$
TEP	Tolman Electronic Parameter
Tet	tetrel
THF	tetrahydrofuran
tht	tetrahydrothiophene
TMEDA	*N*,*N*,*N*',*N*'-Tetramethylethane-1,2-diamine
TMS	trimethylsilyl
TPSSh	Tao-Perdew-Staroverov-Scuseria *meta* hybrid functional
USD	US-dollar
WBI	Wiberg Bond Index
WCA	Weakly Coordinating Anion
ZORA	Zeroth-Order Regular Approximation

13.2 Acknowledgements

At the end of this work, I would briefly take the chance to thank all people who accompanied and supported me during my PhD. Specifically, I would like to thank:

- Prof. Dr. Manfred Scheer for providing excellent working conditions to work on these intriguing topics and the freedom to develop my own ideas in the lab, no matter the topic. Further, I am highly grateful for all support in going abroad including my stay in Berkeley and the attendance of numerous conferences all around the world.
- The Fonds der Chemischen Industrie for funding my PhD by a very generous and unbureaucratic PhD scholarship.
- Dr. Gábor Balázs for all his motivation and advice no matter the topic 😊. Major parts of this work would not have been possible without his input and it has been a privilege to work with him.
- Prof. Dr. Alexey Timoshkin for his supporting quantum chemical calculations and contributions to many of the topics.
- Prof. Dr. Don Tilley and Rosemary Tilley for being excellent hosts during my internship in Berkeley.
- Our lab technicians Lukas, Petra, Martina, Sophie and Schotti for all their hard work and support during my PhD, which I am very grateful for.
- Our secretaries Mina and Barbara for managing all the paperwork and formalities.
- All staff of the Central Analytical Services of the University of Regensburg: X-ray (Birgit Hischa, Sabine Stempfhuber), Mass Spectrometry (Wolfgang Söllner, Josef Kiermaier), and especially the NMR (Tuan-Anh Nguyen, Fritz Kastner, Annette Schramm) and elemental analysis departments (Barbara Baumann, Helmut Schüller) for their reliable services, no matter how difficult the problem. Special thanks go out to Tuan-Anh Nguyen who spent a lot of time measuring even the craziest and complicated compounds/reactions without any hesitation.
- The glassblowing and manufacturing facilities (Markus Lindner, Carl-Heinz Hierl, Helena Ackermann, Romy Knop) for their excellent and fast work, as well as their friendly service.
- My dear friend and expert crystallographer Dr. Michael Seidl for solving even the most uncomfortable crystal structures, for all his advice, for our board game rounds and our friendship.
- Kevin Dollberg (von Hänisch group, Marburg) for the bold preparations and deliveries of K(18c6)SbH_2.
- My former and present lab mates Nase, Max, Spezi and Tania for the relaxed and very enjoyable atmosphere.
- The core of the board game group Nicoló, Michi, Julian, Lukas and Witzi for all the joyous evenings that I will definitely miss a lot.
- My fellow climbers Lisa, Sabrina and Christoph for introducing me to this wonderful sport and all the shared adventures!
- The whisky tasters Lisa, Sabrina and Christoph for some highly enjoyable whisky tastings.
- My former interns Tania (now PhD student in the group), Sophia Vogler and Thomas Tiefel for their hard work during their internships.
- Amelie Sophie Niefanger for her excellent work and great lab atmosphere during her Bachelor`s thesis.
- Max for his jokes and hard-fought chess battles, which I sadly lose most of by now…
- Sabrina for the combined "Hausstand" and support throughout my entire studies. Thank you!

- Spezi for the great lab atmosphere, advices and fun board game rounds. It has been my pleasure!
- My family for their enduring love and support over all those years. Thank you for everything!
- And especially to you, my dear Lisa! Thanks to you, the past 4 years have been the most special time of my life. Unfortunately, I cannot dedicate additional 100 pages of this work to thank you for everything. No matter what, you have always been there for me. You are my family and my home and I look forward to everything that's to come in the future 😊